



# EUROCLAY

## Edinburgh 2015

5TH — 10TH JULY



## Programme & Abstracts

[www.euroclay2015.org](http://www.euroclay2015.org)

Thank you to those who have supported our conference

 APPLIED MINERALS



 **BYK**  
Additives & Instruments



**Ian Wilson**



WILLAMETTE GEOLOGICAL SERVICE



Dr. J. Reed Glasmann  
31191 Peterson Rd.  
Philomath, OR 97370  
(503) 929-3607 PH/FAX

Clay Mineral Analysis, Sedimentary Petrology, Pedology



**Thiele**  
*Tailoring kaolin to your needs*



# contents

---

Contents	1
Instructions to Session Chairs and to Oral and Poster Presenters	2
Welcome	3
Social Programme	4
Programme at a Glance	5
Plenary Lecturers	
R. James Kirkpatrick (CMS Bailey Awardee)	18
S. Krivovichev (CMG George Brown Lecturer I)	36
R. Kleeberg (CMS Pioneer in Clay Science Lecturer)	99
N. Skipper (Mineralogical Society Hallimond Lecturer)	110
B. Singh (CMS Jackson Awardee; CMG George Brown Lecturer II)	271
S. Mills (Mineralogical Society Max Hey Medallist)	460
Oral sessions – <b>Monday</b>	<b>10</b>
<i>Lecture room 5: General (1)</i>	19
<i>Lecture room 5: Natural zeolites environmental biomedical and industrial applications</i>	27
<i>Lecture room 4: Asian Clay Minerals Group Research in Progress II (1)</i>	37
<i>Lecture room 3: Computational chemistry studies of clay minerals - bridging length and time-scales</i>	51
<i>Lecture room 2: Halloysite a unique, diverse and widely useful natural nanomaterial</i>	65
<i>Lecture room 1: From microscopic pore structures to transport properties in shales (workshop follow on session)</i>	77
<i>Lecture room 1: General (2)</i>	88
Oral Sessions – <b>Tuesday</b>	<b>92</b>
<i>Lecture room 5: General (3)</i>	100
<i>Lecture room 4: Clay mineral indices in palaeo-geothermal studies hydrocarbon and geothermal prospection – third Frey-Kübler symposium</i>	118
<i>Lecture room 3: Bioreactive clay minerals impacts on environmental and human health</i>	131
<i>Lecture room 3: Asian Clay Minerals Group Research in Progress II (2)</i>	144
<i>Lecture room 2: Clay and fine particle based materials for environmental technologies and clean up</i>	147
<i>Lecture room 1: Developments and applications of quantitative analysis to clay bearing materials incorporating The Reynolds Cup School</i>	161
Poster session – <b>Tuesday</b>	<b>177</b>
Oral Sessions – <b>Thursday</b>	<b>264</b>
<i>Lecture room 5: The many faces of chlorite</i>	272
<i>Lecture room 5: Structural characterization of lamellar compounds (1)</i>	283
<i>Lecture room 4: Industry perspectives in clay and fine-particle science (1)</i>	292
<i>Lecture room 3: Bentonites linking clay science with technology</i>	310
<i>Lecture room 2: Clay and fine particle based materials for environmental technologies and clean up (2)</i>	328
<i>Lecture room 1: Clays in the Critical Zone soils, weathering and elemental cycling</i>	342
Poster session – <b>Thursday</b>	<b>361</b>
Oral Sessions – <b>Friday</b>	<b>437</b>
<i>Lecture room 5: Structural characterization of lamellar compounds (2)</i>	444
<i>Lecture room 5: General (4)</i>	461
<i>Lecture room 4: Clays in the Critical Zone soils, weathering and elemental cycling (2)</i>	463
<i>Lecture room 3: Beyond smectite-based nanocomposites</i>	469
<i>Lecture room 2: Industry perspectives in clay and fine-particle science (2)</i>	485
<i>Lecture room 1: Clay minerals in the oil and gas industry</i>	494
Delegate list	512
Author Index	526

---

# instructions to session chairs and to oral and poster presenters

Oral presentations are limited to 15 minutes maximum plus 5 minutes discussion period, giving a total of 20 minutes for each paper.

## 1. Responsibilities of Session Chairs

Session Chairs will introduce the presenters and are responsible for the smooth running of the individual sessions. To facilitate this they should:

- a) Be on location at the lecture room at least 10 minutes before the session is to begin.
- b) Check with the computer assistant that all talks have been loaded in advance and that all are working appropriately.
- c) Determine that the speakers are present. Speak to the presenters to ensure that you know how to introduce them. There are awards for best student oral presentations, so please indicate to the audience when a student is presenting and, as with all speakers, do your best to make them feel at ease.
- d) Ensure that the session starts on time and that the individual speakers stay within their allotted time; being on schedule is essential for those who wish to move from one session to another. Speakers should not be allowed to overrun into the next speaker's allocated time.
- e) Facilitate questions and discussion when individual speakers have discussion time available.
- f) If for any reason a presenter is not available to deliver his/her talk, the order must not be modified and the time slot should be used for a break or discussion.

## 2. Responsibilities of Oral Presenters

- a) Deliver the appropriately named file (e.g. Surname\_Session.pptx) of their presentation to the computer assistant well before the session begins.
- b) Check with the computer assistant that the presentation loads and displays correctly.
- c) Arrive at the scheduled lecture room at least 10 minutes before the session begins and introduce yourself to the Session Chairs.
- d) Be ready when the time for your paper comes and most importantly, keep to time; leave time for questions.

## 3. Computers

The computers running the presentations will be using Microsoft-PC based Powerpoint v. 2013 software. Please ensure that your presentation will work correctly with this software. It is possible to use other computers but ensure that you bring appropriate adapters with you. Test the changeover routine before the session begins.

## 4. Poster Session Instructions

There are two poster sessions: one running on Monday and Tuesday, and the other on Thursday and Friday. Authors may place their posters on the allocated board (each board will be marked with the title of the poster), from early on Monday (for Mon-Tue) and early on Thursday (Thu-Fri) as detailed in the programme, and are requested to be present at their posters between 17:00 and 19:00 during the official poster sessions on Tuesday and Thursday, respectively. Delegates will also be free to visit posters at other times. The poster boards will be A0 (841 x 1189 mm) portrait orientation only. Velcro will be provided. No pins or tape to be used.

# welcome



It is a great pleasure and honour to welcome you all to Edinburgh and to this conference – a fusion of Euroclay and The Clay Minerals Society 52<sup>nd</sup> annual meeting. The International Natural Zeolite Association also joined us and The Year of Mud from The Geological Society was mixed in along with support from the International Union of Soil Science in the International Year of Soils. The blending together of all of these parts and the success of this conference is now down to you - the 500+ delegates who have assembled together in Edinburgh representing some 48 different countries. More than 100 of our number are students; the clay community has always been good at integrating students into our fold and I have no doubt that you will all join me in making our students most welcome.

We have an exciting programme lined up, including 16 themed sessions, general sessions, field trips and social events. Our convened sessions are aligned with the themes of Energy, Materials, and Environment and Health, and in that framework our students should recognise that mankind's future, and the challenges it will bring, will be entwined, inevitably, with Clay Science and all its strands.

On behalf of the conference organising committees I hope you enjoy the conference and that when we are done you will leave enthused with new knowledge and ideas. Now it's over to you to make the most of the conference and all that Edinburgh and Scotland have to offer.

**Steve Hillier**

**The James Hutton Institute, Aberdeen**

## **Programme and Abstracts**

Clearly we have a very large book of abstracts. We reproduced this at A5 size, to avoid delegates having to carry around a back-breaking load every day. (Note that the electronic version is also available at the conference website.) The abstracts are divided up by day and then by lecture room. The table of contents will guide you to the first page of each session block listing. The session listing includes page numbers for each abstract. So, choose a day, choose a session and choose an abstract(s). Alternatively, you can find a colleague's name in the Author Index at the back and go straight to his/her abstract. We have also provided a delegate list, with contact details.

## **Acknowledgements**

- Thanks to the session convenors and session chairs; they are largely responsible for putting together the great programme. A full list of all those who helped to convene sessions etc. is available at the website.
- The Mineralogical Society staff: Anna Lofts, Martin Hughes, Russell Rajendra and especially Kevin Murphy (with contributions by Aideen Murphy) have done great work to help make this conference tick – thank you.
- The team of volunteers who agreed to review/edit abstracts is acknowledged: D. Bain, R. Ferrell, P. Ryan, D. Wray, B. Singh, S. Mills, K. Murphy, W. Huff, N. Tosca, H. Shaw, J. Walker and S. Hillier.
- Liaison between the Clay Minerals Group committee, representing ECGA, and The CMS has been handled ably by the conference team, and in particular through Derek Bain and Paul Schroeder. Derek has also led our Social Programme team.
- The Field Trip leaders: Jeff Wilson, Chris Jeans, Simon Kemp and Linda Campbell and Stuart Monro and their respective teams, have done a great job organizing the Field Trips. We hope that the weather will be kind!
- The staff at Edinburgh University have been thoroughly professional in terms of their organization of this event – we are grateful to them.
- Finally, sincere thanks to The James Hutton Institute for my time to be involved in the organization of this conference.

# social and accompanying persons' programme

## **Sunday 5th July**

- Icebreaker reception 18.30-20.30 at the Playfair Library Hall

## **Monday 6th July**

- Day trip to Stirling Castle departing Appleton Tower at 09.00, returning at 17.00.
- Student reception (all delegates welcome to attend) 17.00-19.00 – Appleton Tower

## **Tuesday 7th July**

- Afternoon visit to Rosslyn Chapel at Roslin, Midlothian, departing Appleton Tower at 13.00, returning at 17.00.
- Beer and posters 17.00-19.00 – Appleton Tower

## **Wednesday 8th July**

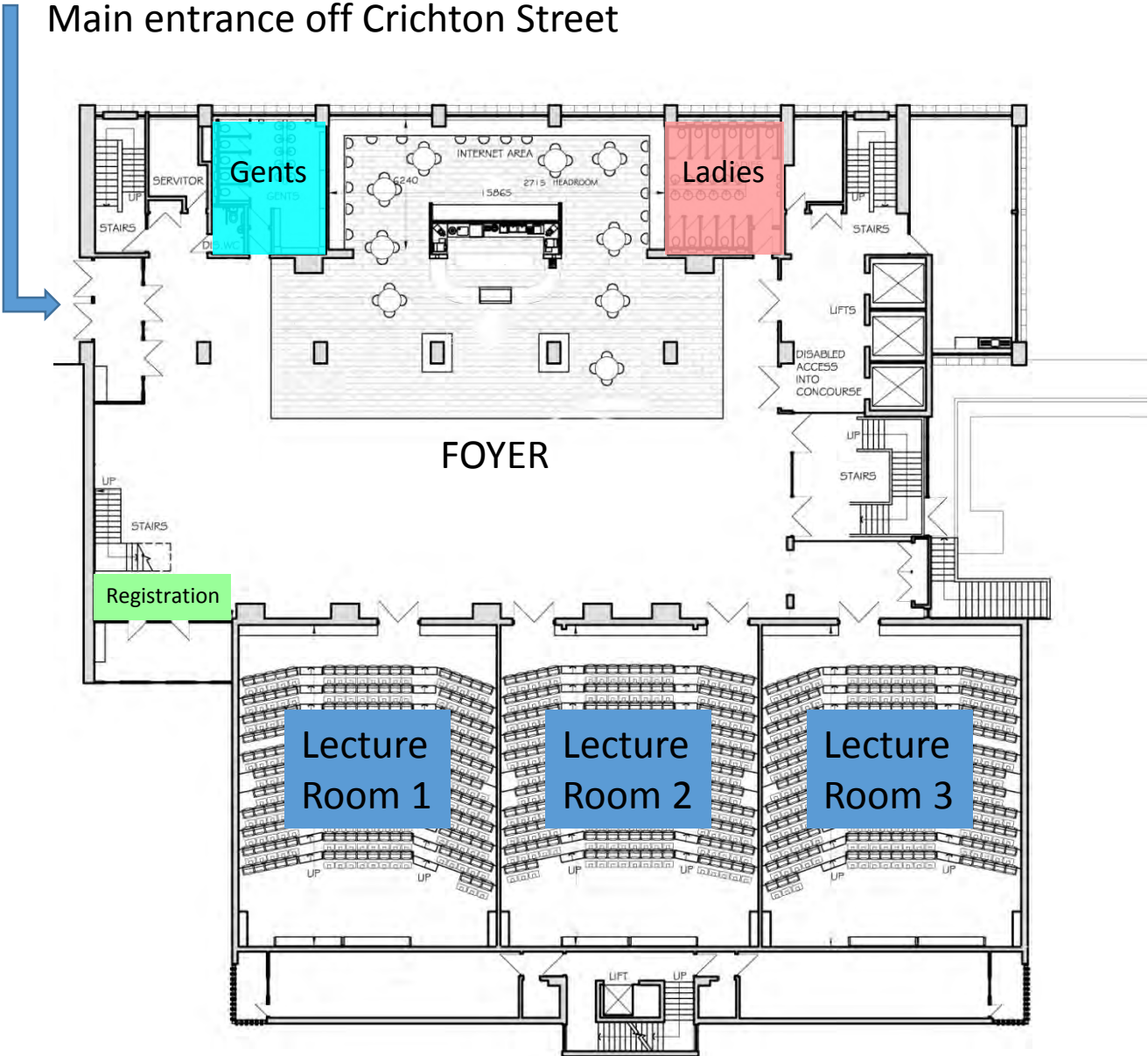
- Arthur's Seat: a 2–3 hour walking trip around the spectacular city centre Volcano Geology of Edinburgh; departs Pollock Halls at 09.30, returning at ~12.30.
- Whisky tasting at the Scotch Whisky Experience – 19.30-21.30

## **Thursday 9th July**

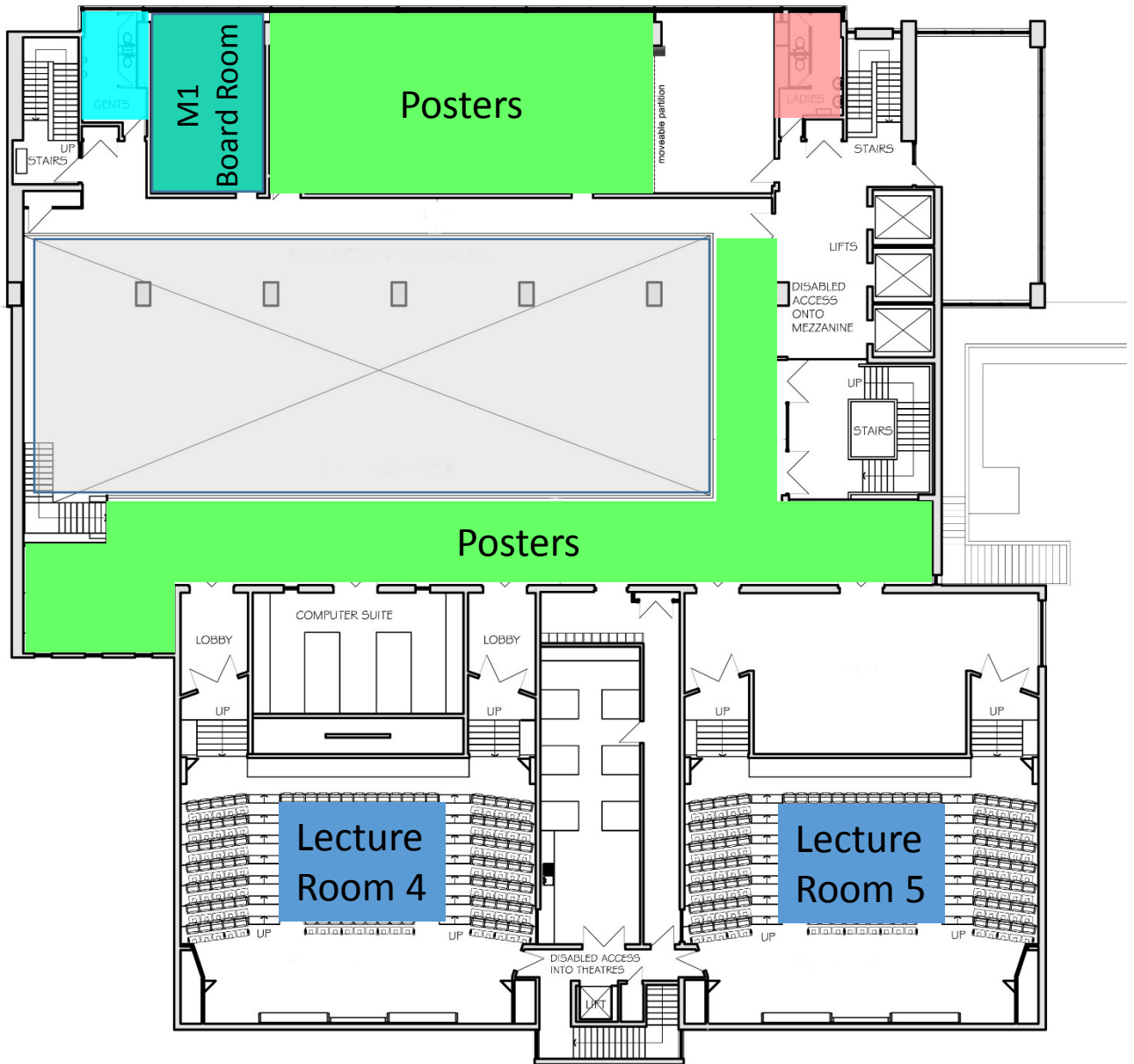
- Morning visit to the Royal Yacht Britannia, departing Appleton Tower at 09.30, returning at 13.00
- Beer and posters 17.00-19.00 – Appleton Tower
- Conference Dinner and Céilidh 19.30 (doors open at 19.00) for 20.00 – at 'Our Dynamic Earth'

# Ground Floor Appleton Tower

Main entrance off Crichton Street



# Mezzanine level Appleton Tower





# Programme at a Glance

Monday, 6th July 2015

Lecture Room 5	Lecture Room 4	Lecture Room 3	Lecture Room 2	Lecture Room 1	M1 board room
Registration 07:30 onwards					
08:20-08:30 Opening					
08:30-09:10 Plenary Lecture R. James Kirkpatrick p 18					
09:10-11:30 General Session (1) p 20	09:50-11:10 Asian Clay Minerals Group Research in Progress II (1) p 38	09:10-11:50 Computational chemistry studies of clay minerals - bridging length and time-scales p 52	09:30-10:40 Halloysite: a unique, diverse and widely useful natural nanomaterial  <i>Keynote</i> 09:30-10:00 Stefano Loporatti p 66	09:10-10:40 From microscopic pore structures to transport properties in shales  <i>Keynote</i> 09:10-09:40 Thorsten Schäfer p 78	
Break					
11:50-12:40 Natural zeolites – environmental, biomedical and industrial applications  <i>Keynote</i> 11:50-12:20 Piergiulio Cappelletti p 28	11:30-12:50 Asian Clay Minerals Group Research in Progress II (1) p 42	11:10-13:00 Computational chemistry studies of clay minerals - bridging length and time-scales  <i>Keynote</i> 12:30-13:00 Peter Coveney p 57	11:00-12:30 Halloysite: a unique, diverse and widely useful natural nanomaterial  <i>Keynote</i> 12:00-12:30 M. Liu p 69	11:00-13:10 Shales  <i>Keynote</i> 12:40-13:10 Wen-An Chiou p 82	
Lunch					
13:40-14:40 Natural zeolites – environmental, biomedical and industrial applications p 30	14:00-15:50 Asian Clay Minerals Group Research in Progress II (1)  <i>Keynote</i> 15:20-15:50 Toshihiro Kogure p 46	14:00-15:00 Computational chemistry studies of clay minerals - bridging length and time-scales p 62	13:30-14:50 Halloysite: a unique, diverse and widely useful natural nanomaterial p 73	14:15-15:15 General Session (2) p 89	
Break					
15:00-16:00 Natural zeolites – environmental, biomedical and industrial applications p 33					
16:00-16:40 Plenary Lecture Sergey Krivovichev p 36					
17:00-19:00 Student reception					16:40-18:00 ECGA council
19:30-10:30 CMS Presidents' and Sustainers dinner					

General session
Energy theme
Materials theme
Environment and Health theme

# Programme at a Glance

Tuesday 7th July 2015

Lecture Room 5	Lecture Room 4	Lecture Room 3	Lecture Room 2	Lecture Room 1
08:30-09:10 Plenary Lecture Reinhard Kleeberg p 99				
09:10-10:50 General Session (3) p 101	9:40-11:10 Clay mineral indices in palaeo-geothermal studies, hydrocarbon and geothermal prospection - third Frey-Kübler symposium  <i>Keynote</i> 09:40-10:10 <i>I. Tonguç Uysal</i> p 119	09:10-10:40 Bioreactive clay minerals: impacts on environmental and human health  <i>Keynote</i> 10:10-10:40 <i>C. Viseras</i> p 132	09:30-11:00 Clay and fine particle based materials for environmental technologies and clean up  <i>Keynote</i> 09:30-10:00 <i>Giora Rytwo</i> p 148	09:10-10:30 Developments and applications of quantitative analysis to clay bearing materials, incorporating 'The Reynolds Cup School'  <i>Keynote</i> 09:10-09:30 <i>Jan Srodon</i> p 162
Break				
11:10-12:30 General Session (3) p 106	11:30-12:30 Clay mineral indices in palaeo-geothermal studies, hydrocarbon and geothermal prospection - third Frey-Kübler symposium p 123	11:00-12:20 Bioreactive clay minerals: impacts on environmental and human health p 136	11:20-12:20 Clay and fine particle based materials for environmental technologies and clean up (1) p 152	10:50-12:30 Developments and applications of quantitative analysis to clay bearing materials, incorporating 'The Reynolds Cup School' p 166
Lunch				
13:40-14:20 Plenary Lecture Neal Skipper p 110				
14:20-15:20 General Session (3) p 111	14:20-15:50 Clay mineral indices in palaeo-geothermal studies, hydrocarbon and geothermal prospection - third Frey-Kübler symposium p 126	14:20-15:40 Bioreactive clay minerals: impacts on environmental and human health p 140	14:20-15:20 Clay and fine particle based materials for environmental technologies and clean up (1) p 155	14:20-15:35 Developments and applications of quantitative analysis to clay bearing materials, incorporating 'The Reynolds Cup School' p 171
Break				
15:40-17:00 General Session 3 p 114		16:00-16:40 Asian Clay Minerals Group Research in Progress II (2) p 144	15:40-16:50 Clay and fine particle based materials for environmental technologies and clean up (1)  <i>Keynote</i> 16:20-16:50 <i>David Laird</i> p 158	15:55-17:10 Developments and applications of quantitative analysis to clay bearing materials, incorporating 'The Reynolds Cup School' p 174
17:15-18:00 Pre field trip meeting			17:00-18:00 CMS business meeting	
17:00-19:00 Poster Session 1				
19:30 for 20.00 Editorial Boards Dinner				

General session
Energy theme
Materials theme
Environment and Health theme

# Wednesday, 8<sup>th</sup> July

## The Chemistry of Clay–Polymer Reactions

A one day short course on the Chemistry of Clay Polymer Reaction will be delivered from 09.00-17.00 on Wednesday the 8th of July at the Appleton Tower venue. The course will be delivered by Benny K.G. Theng, Landcare Research, Palmerston North, New Zealand

### Morning session

- the basic structures, compositions, and colloid chemical properties of some clay minerals
- the theoretical aspects of the clay-polymer interaction
- the interactions of clay minerals with uncharged and negatively charged polymers

### Afternoon session

- the interactions of clay minerals with positively charged polymers
- some applications of the clay-polymer interaction in agriculture and industry
- the synthesis, properties, and applications of polymer-clay nanocomposites

## Field Trips

- Dob's Linn and Grey Mare's Tail – Southern Uplands, to be led by Simon Kemp (with co-leaders Hugh Barron and Maxine Akhurst).  
Departs from Appleton Tower at 09.30.
- The Devonian – Carboniferous upland – acid coal swamp transition 325 – 350 million years ago exposed in the sea cliffs of S.E. Scotland, to be led by Christopher Jeans, Jennifer Huggett, Elena Kuznetsova and David Wray (with co-leader Euan Clarkson).  
Departs from Appleton Tower at 08.30.
- Soils and geological time along The James Hutton trail, to be led by Jeff Wilson (with co-leaders Allan Lilly and Helen Pendlowski).  
Departs from Appleton Tower at 08.30.

# Programme at a Glance

Thursday 9th July 2015

Lecture Room 5	Lecture Room 4	Lecture Room 3	Lecture Room 2	Lecture Room 1	M1 board room
08:30-09:10 Plenary Lecture Balwant Singh p 271					
09:10-10:50 The many faces of chlorite p 273	09:10-11:00 Industry perspectives in clay and fine-particle science (1)  <i>Keynote</i> 09:10-09:40 Jarrod Hart p 293	09:10-10:50 Bentonites: linking clay science with technology p 311	09:10-10:30 Clay and fine particle based materials for environmental technologies and clean up (2) p 329	09:10-10:40 Clays in the Critical Zone: soils, weathering and elemental cycling (1)  <i>Keynote</i> 09:10-09:40 Daniel deB. Richter p 343	
Break					
11:10-13:00 The many faces of chlorite  <i>Keynote</i> 11:30-12:00 O. Vidal p 278	11:20-13:00 Industry perspectives in clay and fine-particle science (1) p 298	11:20-12:40 Bentonites: linking clay science with technology p 316	10:50-12:30 Clay and fine particle based materials for environmental technologies and clean up (2) p 333	11:00-12:20 Clays in the Critical Zone: soils, weathering and elemental cycling (1) p 347	
Lunch					
14:00-15:30 Structural characterization of lamellar compounds (1)  <i>Keynote</i> 14:00-14:30 Bruno Lanson p 284	14:00-15:20 Industry perspectives in clay and fine-particle science (1) p 303	13:40-14:20 Bentonites: linking clay science with technology p 321	13:30-14:50 Clay and fine particle based materials for environmental technologies and clean up (2) p 338	13:20-14:40 Clays in the Critical Zone: soils, weathering and elemental cycling (1) p 351	13:00-14:00 CMG Meeting
Break					
15:50-17:10 Structural characterization of lamellar compounds (1) p 288	15:40-16:40 Industry perspectives in clay and fine-particle science (1) p 307	14:40-16:30 Bentonites: linking clay science with technology  <i>Keynote</i> 14:40-15:10 Will P. Gates p 327		15:00-17:00 Clays in the Critical Zone: soils, weathering and elemental cycling (1) p 355	
17:00-19:00 Poster Session 2					
19:00-24:00 Conference Dinner and Céilidh at 'Our Dynamic Earth'					

General session
Energy theme
Materials theme
Environment and Health theme

# Programme at a Glance

Friday 10th July 2015

Lecture Room 5	Lecture Room 4	Lecture Room 3	Lecture Room 2	Lecture Room 1
08:40-10:20 Structural characterization of lamellar compounds (2)  p 445	09:00-10:40 Clays in the Critical Zone: soils, weathering and elemental cycling (2)  p 464	08:50-10:40 Beyond smectite-based nanocomposites  <i>Keynote</i> 08:50-09:20 Eduardo Ruiz-Hitzky p 470	09:10-10:50 Industry perspectives in clay and fine-particle science (2)  p 486	08:30-10:20 Clay minerals in the oil and gas industry  <i>Keynote</i> 08:30-09:00 Paul Nadeau p 495
Break				
10:40-12:20 Structural characterization of lamellar compounds (2)  p 450		11:00-12:50 Beyond smectite-based nanocomposites  <i>Keynote</i> 12:20-12:50 Jin-Ho Choy p 475	11:10-12:10 Industry perspectives in clay and fine-particle science (2)  p 491	10:40-12:20 Clay minerals in the oil and gas industry  p 500
Lunch				
14:10-15:50 Structural characterization of lamellar compounds (2)  p 455		13:50-15:30 Beyond smectite-based nanocomposites  <i>Martin Vivaldi Award</i> 13:50-14.10 Bernd Wicklein p 480		13:30-15:50 Clay minerals in the oil and gas industry  p 505
15:50-16:30 Plenary Lecture Stuart Mills p 460				
16:30-16:50 General Session (4) <i>Keynote</i> 16:30-16:50 Edward Grew p 462				
16:50-18:10 Awards and Closing				

General session
Energy theme
Materials theme
Environment and Health theme

**MONDAY**

**ORAL**

**SESSIONS**

Monday, 6th July: PROGRAMME

Time	Title + Authors	Page No.
	<b>MONDAY</b>	
08.20	<b>Opening and welcome</b> <i>S. Hillier, P. Komadel and W.C. Elliott</i>	
08.30	<b>PLENARY:</b> NMR Spectroscopy and Computational Molecular Modelling of Clay Minerals <u>R. James Kirkpatrick</u> ( <i>Marilyn and Sturges W. Bailey Awardee of The Clay Minerals Society</i> ) Introduced by Prof. P. Komadel	18
	<b>Lecture room 5: General (1)</b> <i>Session chairs: Jana Madejová and Jakub Matusik</i>	
09.10	Structure and photoresponse of azobenzene-smectite intercalation compounds to UV radiation <u>Anna Koteja</u> and Jakub Matusik	20
09.30	Competitive adsorption of sulfamethoxazole-trimethoprim and sulfamethoxazole-cadmium(II) on organobentonite from aqueous solution <u>Roberto Leyva-Ramos</u> and Jesus I. Martinez-Costa	21
09.50	Near-infrared spectroscopy as a tool to monitor the conformation of surfactants in montmorillonite interlayer <u>Jana Madejová</u> , <u>Ľudmila Sekeráková</u> and <u>Ľuboš Jankovič</u>	22
10.10	Organo-kaolinite: 50 Å intercalation compound with azobenzene <u>Jakub Matusik</u> and Anna Koteja	23
10.30	Intercalation of organoamines into acidic clay from Tsunagi mine, Niigata, Japan <u>Makoto Ogawa</u> , Takayuki Hayakawa, Makoto Minase <sup>1</sup> and Ken-ichi Fjuita	24
10.50	Dispersion stability of layered materials in the presence of polyelectrolytes <u>Istvan Szilagyí</u> , Endre Horvath, Laszlo Forro and Vanessa Prevot	25
11.10	Effect of an "in situ" hydrous perturbation on the structural changes of Ba modified montmorillonite: Quantitative XRD analysis Marwa Ammar, <u>Walid Oueslati</u> and Nejmeddine Chorfi	26
11.30	<b>BREAK</b>	

Monday, 6th July: PROGRAMME

	<b>Lecture room 5: Natural zeolites environmental biomedical and industrial applications</b> <i>Session chairs: Alessio Langella and Linda Campbell</i>	
11.50	<b>KEYNOTE:</b> Natural zeolites in pharmaceutical applications <u>Piergiulio Cappelletti</u> , Bruno de Gennaro, Alessio Langella and Mariano Mercurio	28
12.20	Zeolite identification, proper nomenclature and regulatory issues <u>Kristina Pourtabib</u> and Mickey Gunter	29
12.40	<b>LUNCH</b>	
13.40	Ethiopian Natural Zeolite: An unusual occurrence of zeolitic volcanoclastic sediment <u>Peter J. Leggo</u> Simon R. Passey and Giulio L. Lampronti	30
14.00	Comparative analysis of the physic-chemical and oil sorption properties of zeolites (clinoptilolites) from Turkey and the USA <u>Ali Riza Demirkiran</u> , Michael A. Fullen and Craig D. Williams	31
14.20	Pozzolanic activity of the zeolitic tuffs of Western Turkey Neogene deposits: Examination of hydration products <u>S. Ozen</u> , M. C. Goncuoglu, F. Iucolano, B. Liguori, B. de Gennaro, G.D. Gatta, C. Colella	32
14.40	<b>BREAK</b>	
15.00	Amine binding capacity of natural Cuban zeolite and its medical applications <u>Wilfried Dathe</u> , Thangaraj Selvam, Wilhelm Schwieger and Richard P. Baum	33
15.20	The utilization of zeolite tuffs originating from Italy and Greece in agricultural and environmental applications <u>Michael G. Stamatakis</u> , Spiridoula Giannatou, Charalampos Vasilatos, Ioannis Mitsis, Foteini Drakou, Katerina Xinou and Stefania Stamataki	34
15.40	Preparation and characterisation of nanocomposite membranes composed of ZSM-5 zeolite and cellulose nanofibrils <u>Madhuri Lakhane</u> , Rajendra Khairnar, Megha Mahabole and Vanja Kokol	35
15.50	<b>PLENARY:</b> Structural complexity of zeolites Sergey Krivovichev ( <i>George Brown Lecture of the Clay Minerals Group of the Mineralogical Society</i> ) Introduced by C. Greenwell	36



Monday, 6th July: PROGRAMME

	<b>Lecture Room 4: Asian Clay Minerals Group Research in Progress II (1)</b> <i>Session Chairs: Hyen-Goo Cho, Jae-Min Oh and Jinwook Kim</i>	
9.50	Synthesis of layered siloxane-imidazoline hybrids and their optical properties <u>Kazuko Fujii</u> , Hideo Hashizume, Shuichi Shimomura and Toshihiro Ando	38
10.10	Distribution of radioactive cesium in soil and practical approach to decontamination in Fukushima <u>Kenichi Ito</u> , Tatsuro Matsuda, Masaya Suzuki, Tamao Hatta, and Hirohisa Yamada	39
10.30	Controlling Mg(II)/Al(III) metal ratio in hydrotalcite type anionic clays <u>Hyoung-Mi Kim</u> , Ji-Yeong Lee, Jae-Min Oh	40
10.50	Biogeochemical process in the secondary phase mineral formation by extremophiles in Norris Geyser Basin, Yellowstone National Park, USA <u>Tae-hee Koo</u> , Jee-Young Kim, Kyong Ryang Park, Da Hee Jung, Gill Geesey, and Jin-wook Kim	41
11.10	<b>BREAK</b>	
11.30	Clay minerals as proxies for tracing sediment provenance and transport process in the South China Sea <u>Zhifei Liu</u> , Yulong Zhao, Christophe Colin, Karl Stattegger, Martin G. Wiesner, Yanwei Zhang, Xiajing Li	42
11.50	DOM-Affected Transformation of Contaminants on Mineral Surfaces: a Review <u>Tamara Polubesova</u> and Benny Chefetz	43
12.10	Adsorption characteristic of arsenate on delaminated layered double hydroxides Yu Takaki, Paulmanickam Koilraj, Tsuyoshi Hirajima, <u>Keiko Sasaki</u>	44
12.30	Kinetics of smectite dissolution at high pH conditions for long-term safety assessment of radioactive waste disposal: effect of Gibbs free energy and secondary minerals <u>Tsutomu Sato</u> and Chie Oda	45
12.50	<b>LUNCH</b>	
14.00	Cesium adsorption behavior of vermiculite and its application to the column method. Part II <u>Noriko Suizuki</u> , Yuri Amano, Kotaro Ochi, and Toshiyuki Chikuma	46
14.20	Reversible fluorescent color change of dyes intercalated in a synthetic saponite <u>Makoto Tominaga</u> , Yudai Oniki, Yasutaka Suzuki and Jun Kawamata	47
14.40	The formation of smectite and its redox reaction in deep subsea floor sediment, South Pacific Gyre: IODP expedition 329 <u>Kiho Yang</u> , Toshihiro Kogure, Bryce Hoppie, Robert Harris, Hionsuck Baik <sup>5</sup> , Hailiang Dong, IODP Expedition 329 shipboard scientists, and Jinwook Kim	48
15.00	Flame retardancy enhancement of ethylene-vinyl acetate(EVA) loaded with mica, Laponite® (registered trademark of BYK Additives) and MgAl layered double hydroxide <u>J. Yoon Choi</u> , Minjae Kwon, Jae-Hun Yang, Jin-Ho Choy and Hyun-Joong Kim	49
15.20	<b>KEYNOTE:</b> Fukushima nuclear disaster and clay <u>Toshihiro Kogure</u> and Tsuyoshi Yaita	50

Monday, 6th July: PROGRAMME

	<p><b>Lecture Room 3: Computational chemistry studies of clay minerals - bridging length and time-scales</b></p> <p><i>Session chairs: Randy Cygan, Chris Greenwell and Richard Anderson</i></p>	
09.10	<p>Molecular dynamics simulations of Cs<sup>+</sup> adsorption on hydrated surfaces of illite, smectite, and interstratified illite/smectite clays</p> <p><u>Andrey G. Kalinichev</u>, Narasimhan Loganathan, Brice F. Nguouana Wakou, Zongyuan Chen and Gilles Montavon</p>	52
09.30	<p>Influence of layer charge, hydration state and cation nature on the collective dynamics of interlayer water in tetrahedrally charged swelling clay minerals</p> <p><u>Laurent Michot</u>, Eric Ferrage, Alfred Delville and Monica Jimenez-Ruiz</p>	53
09.50	<p>Molecular Dynamics Simulations of the Structure and Dynamics of H<sub>2</sub>O and Metal ions on Hydrated Hectorite Surfaces</p> <p><u>Narasimhan Loganathan</u>, A. Ozgur Yazaydin, Geoffrey M. Bowers, R. James Kirkpatrick, and Andrey G. Kalinichev</p>	54
10.10	<p>Molecular simulation of structure and diffusion at smectite-water interfaces: Using expanded clay interlayers as model nanopores</p> <p><u>Jeffery A. Greathouse</u>, David B. Hart, Geoffrey M. Bowers, R. James Kirkpatrick, Randall T. Cygan</p>	55
10.30	<p>Improving the description of the structure and dynamics of clay surfaces at the classical level using DFT calculations</p> <p><u>Maxime Pouvreau</u> and Andrey Kalinichev</p>	56
10.50	<b>BREAK</b>	
11.10	<p>Studies of cations and water molecules dynamics in montmorillonites with a Polarizable Force Field</p> <p><u>S. Tesson</u>, M. Salanne, S.Tazi, B.Rotenberg, V. Marry</p>	57
11.30	<p>Structure and behavior of water and carbon dioxide on clay mineral surfaces</p> <p><u>Randall T. Cygan</u> and Craig M. Tenney</p>	58
11.50	<p>Modeling the transport of water and ions tracers in a micrometric sample of clay</p> <p><u>Pauline Bacle</u>, Benjamin Rotenberg, Jean-François Dufrêche, Virginie Marry</p>	59
12.10	<p>Amino acids, layered double hydroxides and origins of Life.</p> <p><u>Valentina Erastova</u>, H. Christopher Greenwell</p>	60
12.30	<p><b>KEYNOTE:</b> Modelling clay-polymer nanocomposites using a multiscale approach</p> <p><u>Peter Coveney</u>, University College London</p>	61
13.00	<b>LUNCH</b>	
14.00	<p>μ-oxo-Fe<sup>+3</sup>-phenanthroline complexes intercalated in montmorillonite: molecular structures and properties</p> <p><u>C. Ignacio Sainz-Dia</u>, Fabrizio Bernini, Elena Castellini, Daniele Malferrari, Marco Borsari, and M. Franca Brigatti</p>	62
14.20	<p>Experimental and theoretical insights into the interaction of methylene blue with kaolinite</p> <p><u>Cliff T. Johnston</u>, Robert A. Schoonheydt,, Jeffery A. Greathouse, Dawn L. Geatches, Darin Q. Pike, H. Christopher Greenwell, Jennifer Wilcox and Randall T. Cygan</p>	63
14.40	<p>MD Simulations of Low-Salinity Enhanced Oil Recovery</p> <p><u>Thomas Underwood</u>, Valentina Erastova, Pablo Cubillas and H. Chris Greenwell</p>	64

Monday, 6th July: PROGRAMME

	<b>Lecture room 2: Halloysite a unique, diverse and widely useful natural nanomaterial</b> <i>Session chairs: Pooria Pasbakhsh and Stephen Hillier</i>	
09.30	<b>KEYNOTE:</b> Halloysite clay nanotubes as novel carriers for drug delivery Chiara Dionisi, Nemany A.N. Hanafy, Viviana Vergaro, Yuri M. Lvov and <u>Stefano Loporatti</u>	66
10.00	Global occurrence and geology of halloysite <u>Ian Wilson</u>	67
10.20	Water, pH and iron: Are these the keys to selecting halloysites for applications as nanotubes? Jock Churchman, <u>Pooria Pasbakhsh</u> , David Lowe and Benny Theng	68
10.40	<b>BREAK</b>	
11.00	Functionalisation of halloysite nanotubes for sustainable nanocomposites <u>Giuseppe Lazzara</u> , Giuseppe Cavallaro, Stefana Milioto and Filippo Parisi	69
11.20	Correlations among mineralogical and physical properties of halloysite nano-tubes (HNTs) <u>Stephen Hillier</u> , Helen Pendlowski, Tony Fraser, Jean Robertson, Evelyne Delbos, Ian Phillips, Nia Gray and Ian Wilson	70
11.40	A comprehensive analysis of the structure of imogolite nanotubes M.S. Amara, S. Rouzière, E. Paineau and <u>P. Launois</u>	71
12.00	<b>KEYNOTE:</b> Hallosyite nanotubes for biomedical application: Opportunities and challenges <u>Mingxian Liu</u> , Rui He, Jing Yang, Changren Zhou	72
12.30	<b>LUNCH</b>	
13.30	An investigation into the pH effects on the CEC of halloysite <u>Nia Gray</u> , David Lumsdon, Stephen Hillier	73
13.50	Structure of halloysite by electron microscopy: a review <u>Toshihiro Kogure</u> and Victor A. Drits	74
14.10	Halloysite nanotubes as additives and carriers: Prospects and challenges <u>Pooria Pasbakhsh</u> and Jock Churchman	75
14.30	Polymer nanocomposites for medical applications: effect of magnetic halloysite on structure and properties <u>Viera Khunová</u> , Ivo Šafařík, Martin Škrátek, and Katarína Tomanová	76

Monday, 6th July: PROGRAMME

	<p><b>Lecture room 1: From microscopic pore structures to transport properties in shales (workshop follow on session)</b>  <i>Session Chairs: R. Dohrmann and T. Schaefer</i></p>	
09.10	<p><b>KEYNOTE:</b> Workshop summary: from microscopic pore structures to transport properties in shales: Which gaps are filled?  Thorsten Schäfer</p>	78
09.40	<p>A combined macroscopic and microscopic approach to describe the diffusion of cations in the interlayer of swelling clay minerals  <u>Emmanuel Tertre, Alfred Delville, Frederick Delay, Dimitri Prêt, Fabien Hubert and Eric Ferrage</u></p>	79
10.00	<p>A comparison of porewater natural tracers in low-permeability sedimentary rocks characterized using two methods  <u>Magda Celejewski, Tom Al, Ian Clark</u></p>	80
10.20	<p>Cation exchange capacity in black shales  <u>Arkadiusz Derkowski and Leszek Marynowski</u></p>	81
10.40	<b>BREAK</b>	
11.00	<p>Percolation Characteristics of Carboniferous Shale Gas in the Eastern Qaidam Basin  <u>Gao Jun, Xia Lu, Li Yingjie and Yu Qingchun</u></p>	82
11.20	<p>Porosity evolution in the chalk: an example from the chalk-type source rocks of the Outer Carpathians (Poland)  <u>Katarzyna Górniak</u></p>	83
11.40	<p>3D imaging of pore networks using FIB-SEM microscopy in Posidonia organic-rich shales  <u>Georg H. Grathoff, Markus Peltz and Stephan Kaufhold</u></p>	84
12.00	<p>Whitby Mudstone Formation its microstructure, porosity and permeability  <u>M.E. Houben, A. Barnhoorn, J. Lie-A-Fat, T. Ravenstein, C.J. Peach and M.R. Drury</u></p>	85
12.20	<p>Nano-micro scale characterization of pore space and microstructure of an overmature organic-rich shale  <u>Jop Klaver, Guillaume Desbois, Jens-Oliver Schwarz and Janos L. Urai</u></p>	86
12.40	<p><b>KEYNOTE:</b> Microstructure of clay assembly – from clay particles to shale  <u>Wen-An Chiou, Stephan Kaufhold and Reiner Dohrmann</u></p>	87
13.10	<b>LUNCH</b>	

Monday, 6th July: PROGRAMME

	<b>Lecture Room 1: General (2)</b> <i>Session Chair: George Grathoff</i>	
14.15	Timing and source of paleofluid pulses in the North Anatolian Keirogen <u>Austin Boles</u> and Ben van der Pluijm	89
14.35	Alteration of Ordovician black slates at Retortillo-Santidad uranium mine (Salamanca) induced by acidic leaching solutions <u>F. Javier Huertas</u> and Fernando Gervilla	90
14.55	Using chemical element ratios for 3D modeling of advanced and intermediate argillic alterations based on their correlation with clay mineral-Biely Vrch porphyry gold deposit <u>Michal Jánošík</u> , Jana Brčeková, Andrej Bíroň, Peter Uhlík, Peter Koděra and Ľubica Puškelová	91

## **NMR spectroscopy and computational molecular modeling of clay minerals**

R. James Kirkpatrick

College of Natural Science, Michigan State University, East Lansing, MI USA 48824

The combination of nuclear magnetic resonance spectroscopy (NMR) and computational molecular modeling using molecular dynamics (MD) and related methods is an effective approach to understanding the structure, dynamics and energetics of surface and interlayer species in clays and other layer-structure materials. This presentation will describe the mutually reinforcing capabilities of experimental NMR and computational MD, briefly review early high-field NMR structural studies of clays and related materials, and discuss several examples of combined NMR/MD studies of the interlayers and surfaces of smectite and layered double hydroxides (LDHs). For interlayers and surfaces near ambient temperature and pressure, dynamical processes with characteristic frequencies of kHz and greater are critical to understanding the structure. NMR is a unique, element specific probe of processes at relatively low frequencies, but it is often difficult to ascribe a specific structure and type of molecular motion to the observed data. The smectite and LDH examples will illustrate how the results of MD calculations can help do this.

Monday  
6<sup>th</sup> July

Lecture room 5

General (1)

## Structure and photoresponse of azobenzene-smectite intercalation compounds to UV radiation

Anna Koteja and Jakub Matusik\*

Department of Mineralogy, Petrography and Geochemistry, Faculty of Geology, Geophysics and Environmental Protection, AGH University of Science and Technology, al. Mickiewicza 30 30-059 Krakow, Poland. \*jakub\_matusik@wp.pl

Organically modified smectites are of great interest, as they exhibit specific properties that are used in a broad area of industrial and environmental protection applications. The large cation exchange capacity of smectites permits the introduction of organic or inorganic cations into their interlayer space and facilitates further modifications of the organo-smectite precursors. Intercalation of layered minerals with photoactive organic compounds, especially azobenzene, was observed in several previous studies (Fujita et al., 2003; Heinz et al., 2008; Ogawa et al., 2003). Under UV radiation the azobenzene molecule changes its conformation from *trans* to *cis*, which is coupled with a change of the molecule dimensions. This transformation, when it occurs in the mineral's interlayer space, may be translated to a change of the  $d_{001}$  value. Such photo-activated materials are useful in nanotechnology as photo-controlled nanoswitches. This study shows the effect of ultraviolet radiation on organo-smectites modified with a quaternary ammonium salt and intercalated with azobenzene.

Four smectites were chosen for study: Na-montmorillonite (SWy), Ca-montmorillonite (STx), beidellite (Bld) and synthetic Laponite® (*registered trademark of BYK Additives*) (SynL). The minerals were pretreated with hexadecyltrimethylammonium bromide (abbreviated C16) in an amount equal to the minerals' CEC. The smectite/C16 suspension (20 g/L) was stirred for 2 h at 60°C. Oriented mounts on glass slides of the obtained organo-smectites were prepared and reacted with azobenzene in a closed teflon vessel at ~100°C for 24 h. The azobenzene/smectite weight ratio was equal to 0.2. The functionalized azobenzene organo-smectites were characterized with X-ray diffraction (XRD) and infrared spectroscopy (FTIR). The amount of intercalated ammonium salt and azobenzene was calculated from the nitrogen content of the tested samples. The materials were treated with UV radiation and shortly after characterized with the XRD in order to describe the materials' response.

The infrared spectra of modified materials confirmed the presence of intercalated ammonium salt and azobenzene. Two distinct bands appeared at ~2924  $\text{cm}^{-1}$  and ~2851  $\text{cm}^{-1}$ , which stand for C-H stretching vibrations. A series of bands at ~3061  $\text{cm}^{-1}$ , ~1581  $\text{cm}^{-1}$ , ~1455  $\text{cm}^{-1}$ , ~1302  $\text{cm}^{-1}$  is derived from the vibrations within the azobenzene molecule. The CHN analysis showed the presence of organic molecules as the amount of carbon and nitrogen increased, compared to the raw minerals. The XRD patterns of C16-smectites showed an increase of the basal spacing value by ~3.5-6.0 Å, as compared to the raw minerals. This suggests a monolayer arrangement of C16 molecules in the interlayer space. Intercalation of azobenzene caused an additional increase of  $d_{001}$  value by 7.0 Å, 15.0 Å, 21.7 Å and 23.5 Å for SWy, STx, Bld and SynL samples, respectively. The significant differences between samples are derived from the different arrangement of azobenzene molecules in the interlayer space, which undoubtedly influences the photoresponse of obtained materials upon UV-radiation.

This project was supported by the National Science Centre, Poland under research project no. 2014/13/B/ST10/01326.

Fujita, T. et al., 2003. Materials Research Bulletin, 38(15): 2009-2017.

Heinz, H., Vaia, R.A., Koermer, H., Farmer, B.I., 2008. Chemistry of Materials(20): 6444-6456.

Ogawa, M., Ishii, T., Miyamoto, N., Kuroda, K., 2003. Applied Clay Science, 22(4): 179-185.



## Competitive adsorption of sulfamethoxazole-trimethoprim and sulfamethoxazole-cadmium(II) on organobentonite from aqueous solution

Roberto Leyva-Ramos and Jesus I. Martinez-Costa

Centro de Investigación y Estudios de Posgrado, Facultad de Ciencias Químicas, Universidad Autónoma de San Luis Potosí, México, rlr@uaslp.mx

Industrial and population growth has led to high consumption of pharmaceuticals and personal-care products and generation of wastes containing heavy metals. The presence of these compounds in water resources is a serious problem that affects directly and indirectly the environment and human health. The antibiotics sulfamethoxazole (SMX) and trimethoprim (TMP) are harmful organic compounds commonly detected in the effluents of wastewater treatment plants. These antibiotics are prescribed together to treat bacterial infections. Cadmium is considered the second most toxic metal, and exposure to it leads to central nervous, immune and reproductive health problems and DNA alterations [3]. In recent years, adsorption has been successfully applied for removing both organic and inorganic harmful contaminants present in aqueous solution. Organoclays are novel adsorbents prepared by adsorbing a cationic surfactant on the negatively charged surface of the natural clay. The cationic surfactant is an organic molecule consisting of a hydrophilic and positively charged quaternary ammonium group and a hydrophobic alkyl chain. The competitive adsorption of two pharmaceutical compounds and a pharmaceutical with a metal cation on organoclays has not been investigated in previous works. The aim of this work is to study the competitive adsorption of SMX-TMP and SMX-Cd(II) on an organoclay prepared from bentonite and hexadecyltrimethylammonium bromide. The bentonite and organobentonite were characterized by thermogravimetric analysis (TGA), X-ray diffraction (XRD), Small-angle X-ray scattering (SAXS) and infrared spectroscopy (FTIR). The single and binary adsorption equilibrium data were obtained in a batch adsorber. The experimental single component adsorption equilibrium data of SMX, TMP and Cd(II) were interpreted using the Langmuir and Freundlich isotherms, and the Langmuir provided a better fit to the experimental data. The competitive adsorption equilibrium data of SMX-TMP and SMX-Cd were analyzed using several binary adsorption isotherms reported in the literature. The results revealed that the modified Langmuir multicomponent isotherm (MLMI) with an interaction factor and the dual-site Langmuir (DSM) best fitted the binary adsorption data of SMX-TMP and SMX-Cd, respectively. The interaction factor of the MLMI isotherm incorporates the interactions between SMX adsorbed and TMP adsorbed on the organobentonite. The effect of SMX on the adsorption of TMP is very similar to the effect of TPM on the adsorption of SMX. Thus, the presence of the TMP did not affect the adsorption capacity of the organobentonite towards SMX and vice versa. The adsorption capacity of the organobentonite towards Cd(II) was enhanced six times when the SMX was adsorbed on the organobentonite, and the pi-cation interactions between the pi electrons of the aromatic rings of the SMX adsorbed and Cd<sup>2+</sup> cations in solution were responsible for this synergistic effect.

## Near-infrared spectroscopy as a tool to monitor the conformation of surfactants in montmorillonite interlayer

Jana Madejová<sup>1</sup>, Ľudmila Sekeráková<sup>1</sup> and Ľuboš Jankovič<sup>1</sup>

<sup>1</sup> Institute of Inorganic Chemistry, Slovak Academy of Sciences, Bratislava, Slovakia

jana.madejova@savba.sk

Near-infrared (NIR) spectroscopy is experiencing dynamic development and spreading into many areas of science and technology, however, its utilization in organoclay studies is not very extensive. These inorganic/organic hybrid materials can be utilized in different applications such as in the removal of organic pollutants, as reinforcing filler for plastics, or host structures for direct intercalation of polymers. In this study detailed analysis of the IR spectra of organo-montmorillonites was performed to show the advantages of the NIR region in probing the arrangement of surfactants in montmorillonite interlayers. The samples were prepared from a sodium-saturated <2 μm fraction of bentonite Jelšovský Potok (JP, Slovakia) and trimethylalkylammonium (C<sub>N</sub>-TMA<sup>+</sup>) and alkylammonium (C<sub>N</sub>-NH<sub>3</sub><sup>+</sup>) cations with increasing alkyl chain length from C6 to C18. The XRD patterns showed consecutive transition of the alkyl chains arrangement from monolayer to bilayer and pseudotrimolecular configuration with increasing alkyl chain length. Higher *d*<sub>001</sub> values for C<sub>N</sub>-TMA-JP in comparison to C<sub>N</sub>-NH<sub>3</sub>-JP for surfactants containing the same number of methylene groups indicated the influence of hydrogen bonds between primary ammonium head groups (C<sub>N</sub>-NH<sub>3</sub><sup>+</sup>) and oxygen on the silicate surface. The conformation of alkyl chains was examined by vibrations of CH<sub>2</sub> groups observed in the middle (MIR) and near (NIR) regions. While it is well known that the positions of fundamental CH<sub>2</sub> stretching bands are very sensitive to the ordering of carbon chains, the changes of the vibrational modes of methylene groups appearing in the NIR region were not studied previously in detail. The MIR spectrum of C<sub>6</sub>-TMA-JP showed the asymmetric (*v*<sub>as</sub>CH<sub>2</sub>) and symmetric (*v*<sub>s</sub>CH<sub>2</sub>) stretching bands at 2930 cm<sup>-1</sup> and 2862 cm<sup>-1</sup>, respectively. For C<sub>18</sub>-TMA-JP the bands were shifted to 2922 and 2852 cm<sup>-1</sup>, indicating decreasing number of disordered (*gauche*) conformers in favour of more ordered (*all-trans*) conformers. A similar trend was observed for C<sub>N</sub>-NH<sub>3</sub>-JP samples; the CH<sub>2</sub> stretching bands shifted to lower wavenumbers by 8 cm<sup>-1</sup>. The NIR spectra of organo-montmorillonites showed a complex band in the 6100-5600 cm<sup>-1</sup> region related to 2*v*CH vibrations of CH<sub>3</sub> and CH<sub>2</sub> groups. The position of the most intense component related to 2*v*<sub>as</sub>CH<sub>2</sub> was shifted from 5811 cm<sup>-1</sup> for C<sub>6</sub>-TMA-JP to 5784 cm<sup>-1</sup> for C<sub>18</sub>-TMA-JP confirming creation of more ordered structure with the increasing alkyl chain length. Similarly, the CH<sub>2</sub> overtone band of C<sub>N</sub>-NH<sub>3</sub>-JP samples changed from 5827 cm<sup>-1</sup> (C6) to 5789 cm<sup>-1</sup> (C18), i.e. by 38 cm<sup>-1</sup>. The NIR spectra also revealed that due to the different mode of head group bonding, namely N-H...O-Si hydrogen bonds of C<sub>N</sub>-NH<sub>3</sub><sup>+</sup> versus flexible bonding of C<sub>N</sub>-TMA<sup>+</sup> head groups, the C<sub>N</sub>-NH<sub>3</sub><sup>+</sup> surfactants adopted a less ordered conformation than their C<sub>N</sub>-TMA<sup>+</sup> counterparts. The magnitude of the 2*v*<sub>as</sub>CH<sub>2</sub> shift was clearly higher than observed in the MIR region for CH<sub>2</sub> stretching modes confirming the benefits of NIR spectroscopy for probing the conformation of alkyl chains.

Acknowledgment: The authors gratefully acknowledge the financial support of the Slovak Research and Development Agency under the Contract No. APVV-0291-11.

## Organo-kaolinite: 50 Å intercalation compound with azobenzene

Jakub Matusik\* and Anna Koteja

Department of Mineralogy, Petrography and Geochemistry, Faculty of Geology, Geophysics and Environmental Protection, AGH University of Science and Technology,  
al. Mickiewicza 30, Krakow, 30 059, Poland, \*e-mail: jakub\_matusik@wp.pl

Molecules showing a change in conformation upon exposure to UV radiation include azobenzene (AzBz). The insertion of AzBz into layered structures opens the possibility to control inter-atomic distances using UV radiation [1]. The key to this is the change of molecule conformation, from *trans* to *cis* which affects the whole crystal structure. Up to now photoactive nanocomposites, involving layered structures, were obtained on the basis of synthetic micas and montmorillonite [2,3]. There are no data on the use of 1:1 layered structure in such studies. Recently it was shown that kaolinite can be intercalated with selected organic molecules including quaternary ammonium salts [4,5]. Such modification changes the interlayer environment to hydrophobic and subsequently enables insertion of other hydrophobic molecules. Thus, the research objective was to investigate the possibility of using organo-kaolinite derivatives for insertion of AzBz for further studies involving photomechanical properties.

For the experiments a well ordered kaolinite (M sample) from the Polish Maria III deposit was used with Hinckley index equal to 1.31. The M sample was pre-intercalated with dimethyl sulphoxide (DMSO) and further grafted with -OCH<sub>3</sub> methoxyl groups through repeated washing with methanol (MM sample). Afterwards, the MM sample was intercalated with selected organic chlorides: benzyltrimethylammonium (BTA) or benzyldimethylhexadecylammonium (BC<sub>16</sub>A). For this purpose the MM sample was mixed in 1.0 mol/L methanol solution of BTA or BC<sub>16</sub>A in 200 mg/5 ml ratio at room temperature for 24 h. The obtained materials: MBTA and MBC<sub>16</sub>A were dried at 70°C and powdered. The intercalates were reacted with AzBz in a closed teflon vessel at ~100°C for 24 h using a weight ratio of AzBz/intercalate equal to 0.2.

As revealed from the XRD patterns the basal spacing of MM (8.7 Å) increased to 13.9 Å and 33.3 Å for the MBTA and MBC<sub>16</sub>A intercalates, respectively. In accordance with earlier studies, the  $d_{001}$  values indicated that the BTA molecules formed a monolayer in the kaolinite interlayer space, while the BC<sub>16</sub>A molecules were tilted with respect to the kaolinite layers. The FTIR spectra confirmed the presence of ammonium salts in the interlayer space as C-H stretching bands (3100-2800 cm<sup>-1</sup>) were found. Also the vibrations of kaolinite OH hydroxyls were altered in 3700-3600 cm<sup>-1</sup> region. The intercalation of AzBz shifted the basal spacing of MBTA and MBC<sub>16</sub>A to 23.1 Å and ~50.8 Å, respectively. For both intercalates the presence of AzBz was confirmed by C-H stretching ring vibrations in FTIR spectra. The longest axis of the AzBz molecule is equal to ~13.1 Å. Thus, for the MBTA the increase of  $d_{001}$  by ~9.2 Å indicates a tilted arrangement of AzBz molecules. In turn, for the MBC<sub>16</sub>A a large increase by ~17.5 Å was observed. This may be due to agglomeration of AzBz molecules. However, also a perpendicular arrangement of BC<sub>16</sub>A (longest axis ~30.6 Å) and AzBz, which interact through benzene rings, could be proposed. The 50.8 Å distance is very close to the sum of molecule dimensions and MM sample  $d$  spacing: 30.6 Å, 13.1 Å and 8.7 Å. It is assumed that the change of interlayer distance induced by UV radiation will be influenced by the type of co-intercalated molecule. Future experiments will explore the design of hybrids showing different changes in the interlayer space upon exposure to UV-Vis radiation.

This project was supported by the National Science Centre, Poland under research project no. 2014/13/B/ST10/01326.

[1] Russew, M.M., Hecht, S. (2010) *Advanced Materials*, 22, 3348-3360.

[2] Fujita, T., Iyi, N., Kłapyta, Z. (2001) *Materials Research Bulletin*, 36, 557-571.

[3] Ogawa, M., Ishii, T., Miyamoto, N. and Kuroda, K. (2003) *Applied Clay Science*, 22, 179-185.

[4] Matusik, J. and Kłapyta, Z. (2013) *Applied Clay Science*, 83-84, 433-440.

[5] Matusik, J., Kłapyta, Z. and Olejniczak, Z. (2013) *Applied Clay Science*, 83-84, 426-432.

## Intercalation of organoamines into acidic clay from Tsunagi mine, Niigata, Japan

Makoto Ogawa<sup>1,2\*</sup>, Takayuki Hayakawa<sup>1</sup>, Makoto Minase<sup>1</sup> and Ken-ichi Fjuita<sup>1</sup>

<sup>1</sup> Laboratory of Applied Clay Technology, Hojun Co., Ltd., An-naka, Gunma 379-0133, Japan.

(waseda.ogawa@gmail.com)

<sup>2</sup> Vidyasirimedhi Institute of Science and Technology, Rayong 21210, Thailand

Incorporation of organic molecular species into the interlayer space of layered clay minerals (smectites, kaolinite, etc.) as well as the micropores of nanoporous silica and silicates (zeolites, sepiolite, etc.) has been investigated extensively from the viewpoints of adsorption itself and as a way of constructing functional hybrid materials.<sup>[1-4]</sup> The incorporation has generally been done by means of the reactions between host nanoporous materials (smectites, zeolite, etc.) and solutions or neat liquids of the guest. The adsorption of vapors is also possible. We have been interested in the incorporation of guest species into the interlayer space of smectites by solid-solid reactions, where host and guest are mixed together in the solid-state at room temperature.<sup>[5-8]</sup> As a synthetic mean, the solid-solid reactions have such advantages as solvent free synthesis (cost efficient and environmentally benign) and simple process (no solid-liquid separation is required). Accordingly, the application of the solid-solid reaction for the preparation of functional hybrid materials based on nanoporous materials.

Here, we report the solid-state intercalation of organoamines into the interlayer space of acid clays. Intercalation of organoamines into the interlayer space of layered materials has been extensively investigated. In the present study, acid clay was used as the host so that the reaction may include acid-base reaction to lead organoammonium-clays. The samples were prepared by the solid-solid reaction between acid clay, obtained from Tsunagi mine, Niigata, Japan, and organoamines and were characterized by XRD and TG-DTA. The reactions took only a few minutes at room temperature by manual mixing using mortar and pestle, suggesting the possible application of the present solid-state reaction for the preparation of organophilic-clays.

1. T. Okada, Y. Ide, M. Ogawa, Organic-inorganic hybrids based on ultrathin oxide layers - Designed nanostructures for molecular recognition, *Chem. Asian J.* **7** (2012) 1980-1992.
2. T. Okada, Y. Seki, M. Ogawa, Designed nanostructures of clay for controlled adsorption of organic compounds, *J. Nanosci. Nanotech.* **14** (2014) 2121-2134.
3. M. Ogawa, K. Saito, M. Sohmiya, A controlled spatial distribution of functional units in the two dimensional nanospace of layered silicates and titanates, *Dalton Trans.* **43** (2014) 10340-10354.
4. M. Ogawa, K. Saito, M. Sohmiya, Possible roles of the spatial distribution of organic guest species in mesoporous silicas to control the properties of the hybrids, *European J. Inorg. Chem.* (2015) 1126-1136.
5. N. Khaorapong, M. Ogawa, Solid-state intercalation of organic and inorganic substances in smectites, *Clay Sci.* **15** (2011) 147-159.
6. M. Ogawa, T. Handa, K. Kuroda, C. Kato, Formation of organoammonium-montmorillonites by solid-solid reactions, *Chem. Lett.* (1990) 71-74.
7. M. Ogawa, K. Kuroda, C. Kato, Preparation of montmorillonite-organic intercalation compounds by solid-solid reactions, *Chem. Lett.* (1989) 1659-1662.
8. M. Ogawa, K. Kuroda, C. Kato, Preparation of montmorillonite-alkylamine intercalation compounds by solid-solid reactions, *Clay Sci.* **8** (1990) 31-36.

## Dispersion stability of layered materials in the presence of polyelectrolytes

Istvan Szilagyi<sup>1</sup>, Endre Horvath<sup>2</sup>, Laszlo Forro<sup>2</sup> and Vanessa Prevot<sup>3</sup>

<sup>1</sup> Department of Inorganic and Analytical Chemistry, University of Geneva, 1205 Geneva, Switzerland; email: istvan.szilagyi@unige.ch; <sup>2</sup> Laboratory of Physics of Complex Matter, École Polytechnique Fédérale de Lausanne, 1015 Lausanne, Switzerland

<sup>3</sup> Institut de Chimie de Clermont-Ferrand, Université Clermont Auvergne, Université Blaise Pascal, CNRS, UMR 6296, BP 80026, 63171 Aubière, France

Inorganic nanoparticles of lamellar structure have been the focus of investigations worldwide due to their growing applications ranging from development of sensors to catalysts. In many applications, these nanomaterials are used in dispersions where aggregation of the particles is an important issue. For instance in catalysis performed in a liquid medium, stable dispersions are required during the catalytic run, however, the catalysts can be removed by aggregation and subsequent sedimentation after the reaction terminated. Despite the substantial importance of aggregation in dispersions, only a limited number of quantitative studies have been reported so far. Therefore, we have recently focused on formulation of layered double hydroxide (LDH) and titanate nanowire (TiONW) dispersions using polyelectrolytes which have proved to be powerful aggregating agents for charged particles suspended in an aqueous medium.

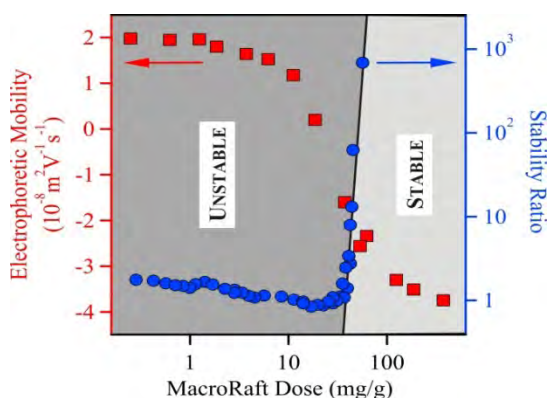


Figure 1. Electrophoretic mobility (square) and stability ratio (circle) values of LDH particles as a function of the MacroRaft dose. Stability ratios close to unity indicate fast aggregation, while

Electrophoretic mobility measurements were carried out with Mg,Al-LDH particles containing carbonate interlayer anions in the presence of negatively charged MacroRaft polyelectrolyte. MacroRaft adsorbs strongly on the oppositely charged LDHs leading to charge neutralization and subsequent overcharging at high doses (Figure 1). Aggregation processes were followed in time-resolved dynamic light scattering experiments to probe the dispersion stability of the system. Stability ratios close to unity indicated fast aggregation at doses lower than the charge neutralization point. However, the samples were stable at higher MacroRaft concentrations where the particles possessed negative charge. No aggregation was observed under the latter condition even at high ionic strength. This fact confirms that the stabilization forces are of non-electrostatic origin.

Similar observations were produced in dispersions of layered TiONWs in the presence of oppositely charged polyelectrolytes. Poly(styrene sulfonate) was used to stabilize the nanowires at low pH where they are positively charged [1], while poly(diallyldimethylammonium) was used for negatively charged TiONWs at a pH higher than the point of zero charge which occurred at pH 4.1 [2]. For instance, adding an appropriately high amount of poly(styrene sulfonate) to the nanowire dispersions led to 75-times more stable samples than with the bare TiONWs, indicating the enormous stabilizing effect of the polyelectrolyte. In summary, colloid stability of aqueous dispersions of layered materials can be well tuned by polyelectrolytes. Accordingly, the particles can be aggregated, but highly stable dispersions can be also obtained if one applies the appropriate dose.

[1] E. Horvath, L. Grebikova, P. Maroni, T. Szabo, A. Magrez, L. Forro, I. Szilagyi: Dispersion Characteristics and Aggregation in Titanate Nanowire Colloids *ChemPlusChem* **79**, 592-600 (2014)

[2] T. Szabo, V. Toth, E. Horvath, L. Forro, I. Szilagyi: Tuning the Aggregation of Titanate Nanowires in Aqueous Dispersions *Langmuir* **31**, 42-92 (2015)

## Effect of an “in situ” hydrous perturbation on the structural changes of Ba-modified montmorillonite: Quantitative XRD analysis

Marwa Ammar<sup>1</sup>, Walid Oueslati<sup>1,2</sup> and Nejmeddine Chorfi<sup>3</sup>

<sup>1</sup> UR05/13-01: Physique des Matériaux Lamellaires et Nanomatériaux Hybrides (PMLNMH), Faculté des Sciences de Bizerte, Zarzouna 7021, Tunisia

<sup>2</sup> Technical and Vocational Training Corporation, College of Electronics & Communications, General Studies Department, TV Street, P.O. Box 2816, Jeddah 21461, Saudi Arabia

<sup>3</sup> Department of Mathematics, College of Science, King Saud University, P.O. Box 2455, Riyadh 11451, Saudi Arabia

E-mail: walidoueslati@gmail.com

This work characterises the hydration performance of Ba-exchanged montmorillonite under environmental solicitation created "in situ" during two hydration–dehydration cycles resulting in various relative humidities (i.e. %RH). These goals are achieved using the X-ray diffraction (XRD) profile modeling approach that consists of the comparison between experimental and theoretical patterns calculated from structural models. This indirect method allows defining changes in structural parameters along the  $c^*$  axis related to the organisation and position of both exchangeable cation and the water molecules in the interlamellar space. Furthermore, the evolution of the contributions of the hydration states and the interlayer water quantities as a function of the %RH are derived from the quantitative investigation. All proposed theoretical models are heterogeneous, suggesting that the main structure contains various proportions of layer types at different RH ranges. The hydration behaviour and structural changes of the sample (i.e. Swy-2-Ba) depend on the sequence orientation of the applied cycles. Furthermore, the structural fluctuation and the hydrous perturbation strongly affect the interlayer water molecule amounts that led to the appearance of a logic hydration hysteresis.

Monday  
6<sup>th</sup> July

Lecture room 5

Natural zeolites  
environmental  
biomedical and  
industrial applications

## Natural zeolites in pharmaceutical applications

Piergiulio Cappelletti<sup>1</sup>, Bruno de Gennaro<sup>2</sup>, Alessio Langella<sup>3</sup> and Mariano Mercurio<sup>3</sup>

<sup>1</sup> Dip. di Scienze della Terra, dell'Ambiente e delle Risorse, Università Federico II, Via Mezzocannone 8, 80134, Napoli (Italy) piergiulio.cappelletti@unina.it

<sup>2</sup> Dip. di Ingegneria chimica, dei Materiali e della Produzione Ind., Università Federico II, P. Tecchio 80, 80125, Napoli (Italy)

<sup>3</sup> Dip. di Scienze e Tecnologie, Università del Sannio, Via dei Mulini 59A, 82100 Benevento (Italy)

Georesources have long been widely used in the pharmaceutical and cosmetic sector for different purposes (excipients, carriers). For many years, biomedical industries directed their interest mainly to clays and clay minerals, such as kaolins and bentonites, to take advantage of the physical-chemical properties of these materials [1 and references therein]. Lately, proposals for the use of zeolitized materials are opening new scenarios for these georesources in the biomedical sphere. Literature shows that the alkaline composition of zeolites and their molecular absorption and cationic exchange properties (external and internal), have induced positive therapeutic effects [2,3]. These minerals have been used as antibacterial agents, antidiarrheal agents, anticancer adjuvants, biosensors, and in decontaminant and detoxification systems for vaccines and adjuvants for the preparation of release-modified pharmaceutical forms (PF). The use of zeolite-rich materials in the pharmaceutical sector, as carriers of pharmacologically active molecules, concerns both preparation of PF for topical uses in the treatment of superficial wounds and their use as active ingredients in antacid preparations [4]. More recent studies have concerned their use as potential systems for unconventional PF preparation, taking account of the special property of zeolites, allowing drug adsorption in the zeolitic matrix and ensuring, therefore, a control of release kinetics [5]. Natural zeolite functionalization is a promising approach for the design of materials with innovative surface properties. Properties such as hydrophobicity, hydrophilicity and the ability to complex specific molecules, can be controlled through functionalization with organic molecules of the external and/or internal surfaces of minerals, making them suitable for applications in specific areas. Surface functionalization of these materials is commonly performed through exchange-based surfactants with long chain quaternary amines [6]. Examples in the biomedical sphere are presented and related to surface modified system characterization, mainly clinoptilolite-based, focusing on the choice of the optimal surfactant, both from the point of view of its interaction with the zeolitic substrate and its biological compatibility towards the selected system [7]. For this reason, the use of natural zeolites in the biomedical field cannot be separated from a preliminary and accurate mineralogical characterization, which intends to ensure the essential quality level and standardization of the final product.

[1] Carretero M I, Pozo M. (2009) Clay and non-clay minerals in the pharmaceutical industry: Part I. Excipients and medical applications. *App. Clay Sci.*, 46, 1, 73-80

[2] Pavelic K, Hadzija M. (2003). Medical applications of zeolites. In: Auerbach SM, Carrado KA, Dutta PK, eds. *Handbook of zeolite science and technology*. New York: Marcel Dekker, 1143-1174.

[3] Andronikashvili T., Pagava K., Kurashvili T., Eprikashvili L. (2009). Possibility of application of natural zeolites for medicinal purposes. *Bulletin of the Georgian National Academy of Science*, 3, 158-167

[4] Rodríguez-Fuentes G., Denis A.R., Barrios Álvarez M.A., Iraizoz A.C. (2006). Antacid drug based on purified natural clinoptilolite. *Microp. Mesop. Mater.*, 94, 200-207.

[5] Bonferoni M.C., Cerri G., de' Gennaro M., Juliano C., Caramella C. (2007) Zn<sup>2+</sup>-exchanged clinoptilolite-rich rock as active carrier for antibiotics in anti-acne topical therapy. In-vitro characterization and preliminary formulation studies. *App. Clay Sci.*, 36 (1-3), 95-102.

[6] Li Z., Bowman R. S. (1998). Sorption of Perchloroethylene by Surfactant-Modified Zeolite as Controlled by Surfactant Loading. *Environ. Sci. Technol.*, 32, 2278-2282.

[7] de Gennaro B., Catalanotti L., Cappelletti P., Langella A., Mercurio M., Serri C., Biondi M., Mayol L. (2015) Surface modified natural zeolite as a carrier for sustained diclofenac release: a preliminary study. *Colloids Surf., B*, 130, 101-109. Zeolite identification, proper nomenclature and regulatory issues



## Zeolite identification, proper nomenclature and regulatory issues

Kristina Pourtabib<sup>1</sup> and Mickey Gunter<sup>2</sup>

<sup>1</sup>875 Perimeter Drive, Moscow, ID, U.S.A. 83844, pour1824@vandals.uidaho.edu

<sup>2</sup>mgunter@uidaho.edu

The need for a correct identification method for the fibrous/acicular zeolite erionite has become more critical due to erionite's ties to mesothelioma in Turkey, and now in the western USA. The regulatory community still struggles to correctly identify potentially asbestiform minerals when they occur in the natural rather than synthetic environments due to the similar cation content and poorly understood differences in crystal structure between these zeolite species. Erionite presents a unique challenge because there is no regulatory method for the correct identification of these fibrous/acicular particles in nature. Correct zeolite identification is possible utilizing some of the common analytical instrumentation found in most laboratory settings.

By definition zeolites are framework silicates with "open" structures composed of channels and cages that house extraframework cations and water. Two components are needed for the correct identification of zeolites based first on structure type and second on composition. To further complicate matters there are three general methods to describe the structure: 1) framework codes, 2) secondary building units and 3) a combination of secondary building units and historical context. For instance, erionite can form with a fibrous habit but is not part of the fibrous zeolite subgroup ( $T_5O_{10}$ ). Simplified identification techniques for the zeolites can be obtained largely by the use of SAED on the TEM and indirect identification can be determined by the PLM. When studying zeolites it is essential to note the associated environments of formation, mainly altered volcanic tuffs vs. vesicles. Although erionite can be found throughout the western USA, erionite present in the vesicles of basaltic rocks are in very small, isolated quantities compared to volcanic tuff where the rock is widespread and easily erodible and thus erionite is more likely to be airborne and have an increased potential for exposure through inhalation.

The use of TEM and PLM for the identification of these fibrous and acicular zeolites is largely scale-dependent. Due to the morphology of these elongate zeolites, the  $c$  crystallographic axes will lie in the plane of view, making particle orientation simpler. The TEM-scale provides direct structural data in the form of diffraction patterns, and gives compositional data in the form of EDS (i.e. diffraction patterns of erionite along  $uv0$  will show constraints of  $00l = 2n$  along  $c^*$  due to space group symmetry, while offretite will show no diffraction constraints along  $c^*$ ). At the larger PLM-scale, zeolites can be distinguished based on their low birefringence and refractive index values (i.e. there is no refractive index overlap for erionite and offretite, and erionite is one of the only length slow fibrous/acicular zeolites). Fibrous and acicular zeolite identification does not need to be overcomplicated. By using scale dependent identification methods such as TEM and PLM, these zeolites can be easily distinguished from one another.

## Ethiopian Natural Zeolite: An unusual occurrence of zeolitic volcaniclastic sediment

Peter J. Leggo<sup>1</sup> Simon R. Passey<sup>2</sup> and Giulio L. Lampronti<sup>1</sup>

<sup>1</sup> Department of Earth Sciences, University of Cambridge. Pjl46@cam.ac.uk

<sup>2</sup> CASP West Building, Department of Earth Sciences, University of Cambridge, UK

A recent discovery of clinoptilolite in the North West Highlands of Ethiopia is a new locality for this mineral. The North West Highlands occur in the north of the East African Rift Zone. In this area diatomaceous sediments were found in 1968. These rocks occur over a wide area and are known to be of lacustrine origin of Tertiary to Pleistocene age. The Main Ethiopian Rift is known for its widespread silicic volcanism and it is thought that the presence of lacustrine basins containing high concentrations of silica favour the accumulation of diatomaceous oozes (Ministry of Mines, Geological Survey Of Ethiopia). Powder XRD analysis of some of these rocks show clinoptilolite to be present as a well formed crystalline phase, whereas the siliceous exoskeletons of the diatoms, being made of amorphous silica, scatter x-rays and do not show well defined reflections. The occurrence of clinoptilolite presents the question of whether the zeolite occurs by the alteration of volcanic glass falling into the lacustrine basins or is formed from the alteration of diatomite during compaction. Recent laboratory studies have shown that relatively little energy is required to synthesise a zeolite from diatomite without an organic template, which raises the controversial question as to its origin.

Further fieldwork is being undertaken to map the location of the natural zeolite bearing rocks. However, at this time as the clinoptilolite bearing diatomite is only known to occur in some localities it would appear that the alteration of volcanic glass falling into water and undergoing alteration is the most likely explanation. It is important to realise that the presence of clinoptilolite in the East African Rift Zone has major implications on food security and sustainability as clinoptilolitic tuff together with organic waste is a highly efficient plant fertilizer. ( Leggo and Ledésert, 2009).

Key words: North West Ethiopia, silicic volcanism, clinoptilolite, plant fertilizer

### References:

Ministry of Mines Geological Survey of Ethiopia , Geoscience Data Centre, Addis Ababa 2010. Opportunities for diatomite resources development in Ethiopia.

Leggo,P.J and Ledésert,B. Organo-Zeolitic Soil Ststems: A New Approach to Plant Nutrition. Chapter X In: Fertilizers: Properties, Applications and Effects, L.R. Elsworth et al.,(eds). Nova Science Publishers, Inc., New York, 223 – 239.

## Comparative analysis of the physico-chemical and oil sorption properties of zeolites (clinoptilolites) from Turkey and the USA

Ali Riza Demirkiran<sup>1,2</sup>, Michael A. Fullen<sup>2</sup> and Craig D. Williams<sup>2</sup>

<sup>1</sup> University of Bingol, Faculty of Agriculture, Department of Soil Science and Plant Nutrition  
Bingol, Turkey

<sup>2</sup> University of Wolverhampton, Faculty of Science and Technology, Wolverhampton WV1 1LY, UK

This study reports the oil sorption and re-use efficiency of the zeolite, clinoptilolite. Three clinoptilolite samples from Turkey were analysed, including samples from the Aegean, Rota and Teknomin Mines. Analyses were compared with clinoptilolite from New Mexico, USA. Samples were tested in replicated laboratory analyses in terms of their ability to sorb automobile oil (AO). Analyses included:

(i) Clinoptilolite samples were prepared for oil sorption, using both hydrated (HC) and dehydrated (DHC) samples.

(ii) Buchner funnels were lined with Whatman filter paper and batch sorption experiments were conducted by adding 10 ml oil to 10 g samples of clinoptilolite. The oil infiltrating through samples was measured, thus enabling calculation of the amount of sorbed oil. There were five replicates of each treatment.

(iii) Oil was removed from the clinoptilolite samples by heat treatment in a muffle furnace. Treatments were 500, 700 and 900°C for 1 h. The oil sorption experiments were repeated on the ignited samples (four replicates).

Results showed that DHC samples generally sorbed more AO than HC after the 900°C treatment. The sorption capacities of the HC and DHC were 44.10-49.71% and 43.00-48.70%, respectively. The sorption capacities of HC and DHC were 31.27-46.09% and 47.71-54.70%, respectively, after ignition at 700 °C. The sorption capacities of HC and DHC were 68.92-80.9% and 65.57-78.94%, respectively, after the 500 °C treatment. Overall, the amount of oil re-cycled by clinoptilolite varied between 39.01-82.78%. The results show that Turkish clinoptilolites had similar oil sorption properties to the US clinoptilolite and they could potentially be re-used for AO sorption after the clinoptilolite-oil mix was ignited.

**Key words:** Natural Zeolite, Clinoptilolite, Hydrated and Dehydrated Clinoptilolite, Automobile Oil, Turkish Clinoptilolite.

## **Pozzolanic activity of the zeolitic tuffs of Western Turkey Neogene deposits: Examination of hydration products**

S. Ozen<sup>1</sup>, M. C. Goncuoglu<sup>2</sup>, F. Iucolano<sup>3</sup>, B. Liguori<sup>3</sup>, B. de Gennaro<sup>3</sup>, G.D. Gatta<sup>4</sup>, C. Colella<sup>3</sup>

<sup>1</sup> Department of Industrial Design Engineering, Recep Tayyip Erdogan University, Rize, Turkey; E-mail: sevgi.ozen@erdogan.edu.tr

<sup>2</sup> Department of Geological Engineering, Middle East Technical University, Ankara, Turkey

<sup>3</sup> Dipartimento di Scienze della Terra, Università Federico II, Naples, Italy

<sup>4</sup> Dipartimento di Scienze della Terra, Università Degli Studi di Milano, Milan, Italy

Morphological, chemical and microstructural properties of crystalline hydration products of hardened pastes and compressive strength behavior of blended cement mortars containing zeolitic tuffs in place of Portland cement were examined. Decreasing intensity of zeolitic peaks on XRD and FTIR patterns confirms the dissolution of zeolites and their involvement in pozzolanic reactions. Although FTIR results are in good agreement with XRD, the X-ray technique has proved to be more sensitive for the investigation of the hydration products [1]. All blended cements exhibit lower compressive strength than the control Portland cement mortar at 7 days of age. This behavior is typical for supplementary cementitious materials (SCMs), which often reduce the initial strength development [2]. The compressive strength of clinoptilolite-rich tuff from Bigadiç (CLI-B) exhibited excellent strength performance, which is approximately 10% higher than that of control Portland cement at 28 days of hydration. MOR and CLI-G, however, lead to similar strength values if compared to the reference Portland cement mortar, while those of CLI-A and ANA are lower. Furthermore, the comparison between the compressive strength analysis and the thermogravimetric analysis (TG) shows that the ability of lime fixation does not always lead to a better mechanical behavior [2, 3]. In fact, particle size distribution of material, which indeed controls the water requirement, is one of the main factors that govern the development of mechanical strength of blended cements.

[1] S. Ozen, M.C. Goncuoglu, 2013. Pozzolanic activity of natural zeolites: mineralogical, chemical and physical characterization and examination of hydration products. PhD thesis, Middle East Technical University, Turkey, 135 pp.

[2] F. Massazza, 1992. Pozzolana and pozzolanic cements, in: P.C. Hewlett (Ed.) *Lea's Chemistry of Cement and Concrete*, 4th Edition, Elsevier Ltd., London.

[3] B. Uzal, L. Turanlı, H. Yücel, M.C. Göncüoğlu, A. Çulfaz, 2010. Pozzolanic activity of clinoptilolite: A comparative study with silica fume, fly ash and a non-zeolitic natural pozzolan, *Cement and Concrete Research* 40, 398 -404.

## Amine binding capacity of natural Cuban zeolite and its medical applications

Wilfried Dathe<sup>1</sup>, Thangaraj Selvam<sup>2</sup>, Wilhelm Schwieger<sup>2</sup> and Richard P. Baum<sup>3</sup>

<sup>1</sup> Heck Bio-Pharma GmbH, Karlstraße 5, D-73650 Winterbach, Germany; daweidoc@gmx.de

<sup>2</sup> Friedrich-Alexander-Universität Erlangen-Nürnberg, Institute of Chemical Reaction Engineering, Egerlandstraße 3, D-91058 Erlangen, Germany

<sup>3</sup> Zentralklinik Bad Berka GmbH, Clinic for Molecular Radiotherapy and Molecular Imaging, Robert-Koch-Allee 9, D-99437 Bad Berka, Germany

The use of natural zeolites as medical products for patients requires a very detailed analysis of their chemical composition, phase purity, ion-exchange properties and microstructural harmlessness as described earlier for the natural Cuban zeolite (Selvam et al. 2014). This natural zeolite contains both clinoptilolite and mordenite as major phases (ca. 80%) in a ratio of 1:1 and exhibits high BET surface area ( $140 \text{ m}^2\text{g}^{-1}$ ). Furthermore, its histamine binding capacity amounts to about 12 mg (pH 1) and 15 mg (pH 7) per gram of zeolite. It has been found that the adsorbed histamine is strongly bound to zeolite and its leaching is negligible. Histamine, an endogenous amine derived from the amino acid histidine, plays an important role in the production of gastric acid and is also involved in numerous immunological reactions. In gastritis, the positive experience of clinoptilolite zeolite application (Potgieter et al. 2014) was confirmed by several German general practitioners, who prescribe the natural Cuban zeolite (Dickreiter and Weitsch).

Another important biogenic amine is serotonin, which is derived from the amino acid tryptophan. It is well known as the 'hormone for fortune' in the brain, but excessive peripheral blood levels (produced by neuroendocrine tumors, usually known as "carcinoids") cause severe diarrhea and flushing as well as bronchial obstruction, wheezing and carcinoid heart disease (tricuspid valve insufficiency). As a zeolite product has been proven to be an effective anti-diarrheic drug (Rodríguez-Fuentes et al. 1997), it has been applied by us for the first time to patients suffering from the above mentioned clinical symptoms (mainly severe diarrhea). In the present study, we have investigated the serotonin binding capacity of natural zeolite at different pH values. In addition, we have analyzed the binding capacity of zeolite for both histamine and serotonin separately as well as histamine loading (pH 1) followed by serotonin (pH 5). We found that histamine is nearly irreversibly bound to zeolite, while serotonin shows initially a much higher binding affinity to zeolite that declines gradually over time.

The regular use of zeolite in patients suffering from carcinoid syndrome due to serotonin-producing neuroendocrine tumors seems to reduce significantly the number of bowel movements, thereby improving the quality of life in these patients.

The binding capacity of Cuban zeolite to biogenic amines, which are important regulators in many physiological processes, promises to become an effective application in different clinical formulations. Furthermore, the type of galenics has to be modified, possibly according to the mode of desired application.

### References

Dickreiter, B. and K.-H. Weitsch, personal communications.

Potgieter, W., C. S. Samuels & J. R. Snyman (2014) *Clinical and Experimental Gastroenterology* **7**, 215-220.

Rodríguez-Fuentes, G., M.A. Barrios, A. Iraizoz, I. Perdomo & B. Cedré (1997) *Zeolites* **19**, 441-448.

Selvam, T., W. Schwieger, & W. Dathe (2014) *Clay Minerals* **49**, 501-512.

## The utilization of zeolite tuffs originating from Italy and Greece in agricultural and environmental applications

Michael G. Stamatakis<sup>1</sup>, Spiridoula Giannatou<sup>1</sup>, Charalampos Vasilatos<sup>1</sup>, Ioannis Mitsis<sup>1</sup>, Foteini Drakou<sup>1</sup>, Katerina Xinou<sup>2</sup> and Stefania Stamatakis<sup>3</sup>

<sup>1</sup> University of Athens, Panepistimiopolis 15784 Athens, Greece, [stamatakis@geol.uoa.gr](mailto:stamatakis@geol.uoa.gr)

<sup>2</sup> TITAN Cement Company S.A. Kamari, Viotia Plant, 19200 Elefsis, Greece

<sup>3</sup> Via Corridoni 12, Florence, Italy

Zeolite tuffs are currently used in construction, animal feeding, agriculture and certain environmental applications. Since 1994, the UoA (University of Athens) and the TITAN Cement Company have been involved in research and characterization of zeolite tuffs across Europe, mainly for the construction industry. In Italy, zeolite deposits of commercial grade occur near Naples, Rome and Lake Bolsena. In Greece, significant deposits are located in Kimolos Island and in Pentalofos and Metaxades in NE Greece. Even though, the Italian zeolite tuffs have been utilized in agriculture applications, the Greek deposits are only occasionally used for such purposes.

The aim of the present study is to characterize and to test Italian and Greek zeolite tuffs of diverse chemistry and mineralogy, in order to identify the behavior of such multifunctional micro-porous materials alone and in mixtures, as soil amendments and controlled-released fertilizers. Five representative bulk rock samples were studied: two from central Italy [Viterbo and Sorano], and three from Greece [Kimolos Island and NE Greece]. XRD analysis revealed that the Italian samples are mostly composed of chabasite, whereas the Greek samples contain clinoptilolite or mordenite. The most siliceous samples are from Metaxades and Kimolos, due to their silica polymorphs content. SEM analysis revealed the presence of cubic chabasite in the Italian samples, tabular clinoptilolite in Metaxades and Pentalofos, whereas in Kimolos sample needle-like mordenite predominates, followed by opal-CT lepispheres [Figure 1]. Grain size analysis has shown that the Metaxades sample is the coarser [20 % < 58 $\mu$ m], whereas the Viterbo sample is the finest [50% < 58 $\mu$ m]. The highest pH values were measured in the Italian samples, whereas the highest CEC values were reported in the Italian and the Kimolos samples. The relatively high CEC value of Kimolos sample is attributed to the action of smectite and micro-silica, besides mordenite. The highest amount of K, Mg, Ca and Fe was measured in the Italian samples and the lowest in Kimolos sample which is rich in Na. The Pb content of all samples is below the upper limit of 100ppm for agricultural uses, with the Greek samples having lower values than the Italian ones. The Cr+Ni content of the samples is low [<10ppm], with the lowest values measured in Kimolos <1ppm and in Sorano <5ppm. These two materials were selected to produce mixtures of: 30/70, 50/50 and 70/30 chabasite/mordenite tuff. In such way, the pH and specific element content of the final products can be adjusted, whereas their total CEC is close to the original materials. The combinations of these zeolitic materials are suitable for agricultural and environmental applications.

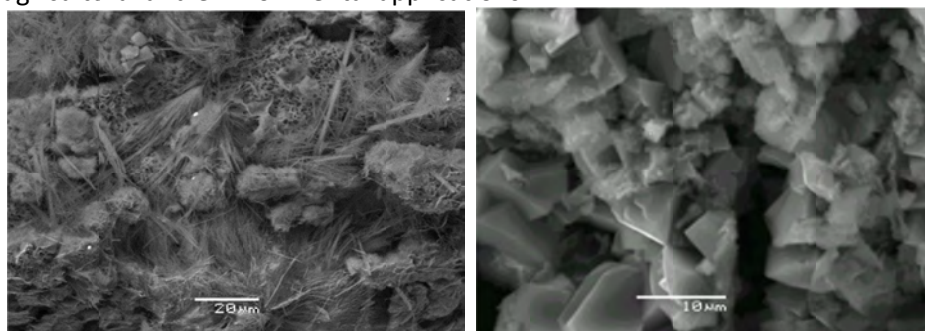


Figure1: SEM images of mordenite/opal-CT-rich tuff, Kimolos [L] and chabasite-rich tuff, Sorano, [R]

## Preparation and characterisation of nanocomposite membranes composed of ZSM-5 zeolite and cellulose nanofibrils

Madhuri Lakhane<sup>1</sup>, Rajendra Khairnar<sup>2</sup>, Megha Mahabole<sup>2</sup> and Vanja Kokol<sup>1,\*</sup>

<sup>1</sup> Institute of Mechanical Engineering, Faculty of Mechanical Engineering, University of Maribor, Slovenia

<sup>2</sup> School of Physical Sciences, Swami Ramanand Teerth Marathwada University, Nanded (MS), India  
Email: madhurilakhane@gmail.com

Zeolites are microporous crystalline aluminosilicates with uniform pore size, and are chemically and thermally stable. They possess a permanent negative charge in the framework, which is balanced by non-framework exchangeable cations. Due to their unique properties they are widely used in adsorption, separation of gases, ion-exchange, catalysis and sensing. Being biocompatible and bioactive they can also be applied in biomedical applications like antitumor, drug-carrier, hemostatic material etc.

Based on green and safe nanotechnology which is the requirement for today and the future, the aim of this study was to develop new bio-based and nano-structured film-forming materials by using nanocellulose fibrils (CNFs), another biorenewable and biodegradable material, and differently formulated nano-zeolites. Their nano-scale dimensions and ability to form a strong entangled nanoporous network have been studied by dispersing zeolite into the CNF matrix using different approaches and conditions. The films have been characterised by various analytical techniques like FTIR, RAMAN, XRD, TG/DSC, BET, SEM and AFM analysis, and evaluated relative to the water content and selected solvent stability. These results reveal that the prepared nanocomposite films can have prospective and high added-value applications like gas adsorption, separation and sensing, oxygen-impermeable packaging, water and solvent filtration membranes, and drug-delivery biomedical matrices.

**Keywords:**- zeolite, cellulose nanofibrils (CNF), FTIR, RAMAN, X-RD, TG/DSC, BET, SEM and AFM.

1. M.Soheilmoghaddam, M.U.Wahit, W.T. Whye, N.I. Akos,R.H.Pour, A.A.Yusuf, "Bionanocomposites of regenerated cellulose/zeolite prepared using environmentally benign ionic liquid solvent", *Carbohydrate Polymers* 106 , 326-334 (2014).
2. M. Čolić, D.Mihajlović, A. Mathew, N. Naseri, V.Kokol, "Cytocompatibility and immunomodulatory properties of wood based nanofibrillated cellulose", *Cellulose*, 22 (1), 763-778 (2015).
3. M.Mahabole,M.Lakhane,A.Choudhari,R.Khairnar, "Comparative study of natural calcium stilbite and magnesium exchanged stilbite for ethanol sensing", *J.Porous Materials*, 20 (4), 607-617 (2013).
4. M.P.Pina,R,Mallada,M.Arrueo, M.Urbiztondo, N.Navascues, O.de la Lgesia, J.Santamaria, "Zeolite films an membranes,emerging applications", *Microporous Mesoporous Materials* , 144, 19-27 (2010).

## Structural complexity of zeolites: fundamental approach and applications

Sergey V. Krivovichev<sup>1,2</sup>

<sup>1</sup>Department of Crystallography, St. Petersburg State University, University Emb. 7/9, 199034 St. Petersburg, Russia

<sup>2</sup>Institute of Silicate Chemistry, Russian Academy of Sciences, Makarova Emb. 6, 199034 St. Petersburg, Russia

It is usually implied that the crystal structures of zeolites are complex, but the very notion of complexity and its quantitative evaluation remained subjective till the recent time. The application of the Shannon information theory allowed to formulate quantitative measures of topological and structural complexity of zeolite frameworks (Krivovichev, 2013). Within this approach, the content of the reduced unit cell volume is considered as a message with atoms as symbols. Two atoms are considered equivalent, if they belong to the same crystallographic orbit. The framework complexity is characterized by its total topological information content. Topological complexity parameters are calculated for the 201 zeolite structure types listed in the International Zeolite Association Zeolite Structure Database. On the basis of the proposed complexity measures, zeolite frameworks can be classified into very simple, simple, intermediate, complex, and very complex. The six most complex zeolite frameworks are [in bits/cell]: SFV [19557.629], ITV [2825.097], IMF [2614.111], CLO [2413.449], and LTN [2285.985]. The six simplest zeolite frameworks are: SOD [16.529], BCT [19.020], ABW [23.020], NPO [28.529], EDI and NAB [32.603]. The topological complexity measures can be used to investigate evolution of complexity during crystallization and transformation of zeolites.

Chipera and Apps (2001) provided thermodynamic modeling of the zeolite parageneses in silicic-rock hydrothermal environments that contained a representative suite of zeolites (analcime, chabazite, clinoptilolite, erionite, heulandite, laumontite, mordenite, phillipsite, stilbite, and wairakite). Analysis of the behaviour of the average topological complexity of the phase diagrams at different temperatures revealed that the temperature dependencies of the average topological complexity parameters are almost linear: the topological complexity of the system decreases almost linearly with the increasing temperature. The very general empirical rule that describes the complexity behaviour can be formulated as follows: structural and topological complexity of the chemically isolated system consisting of  $n$  crystalline phases decreases with the increase of temperature. This rule reflects the fact that both configurational and vibrational entropies of crystalline materials are increasing with the increasing temperature. Though the exact relations between these two kinds of entropies and information-based complexity parameters are not yet clear, it is very probable that they both have positive correlation.

Krivovichev, S.V. (2013): Structural and topological complexity of zeolites: an information-based approach. *Microporous and Mesoporous Materials*, **171**, 223-229.

Chipera SJ, Apps JA (2001): Geochemical stability of natural zeolites. *Reviews in Mineralogy and Geochemistry*, **45**, 117-161.



Monday  
6<sup>th</sup> July

Lecture Room 4

Asian Clay Minerals  
Group Research in  
Progress II (1)

## Synthesis of layered siloxane-imidazoline hybrids and their optical properties

Kazuko Fujii, Hideo Hashizume, Shuichi Shimomura and Toshihiro Ando

National Institute for Materials Science (NIMS), 1-1 Namiki, Tsukuba, Ibaraki 305-0044, Japan,  
FUJII.Kazuko@nims.go.jp

Layered inorganic-organic composites have attracted much attention due to their interesting properties. Fukushima and Tani reported organic/inorganic hybrid layered polymers.<sup>1)</sup> The inorganic and organic moieties bond covalently with each other in the hybrids. The organic moieties are located between the layers. Many subsequent studies have reported syntheses of this type of layered inorganic-organic hybrids with the covalent bonds between the inorganic and organic moieties.<sup>2, 3)</sup> In particular, Richard-Plouet and her co-workers have reported interesting hybrids with the covalent bonds.<sup>2)</sup> The interlayer space of the hybrids with the covalent bonds provides attractive solid-state two-dimensional nanospace. For example, energy transfer occurs between dyes immobilized within the solid-state two-dimensional nanospace in one of the reported hybrids.<sup>4)</sup> Imidazolines have been studied in order to develop novel adsorbents. Sepiolite has been modified with an imidazoline derivative.<sup>5)</sup> The aims of the present study are to provide layered siloxane-imidazoline hybrids and to develop the attractive solid-state two-dimensional nanospace.

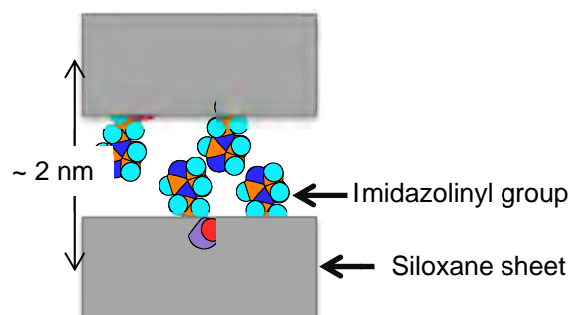
Imidazoline derivative was added slowly to aqueous solutions or suspensions of metallic salts or metallic hydroxides under continuous stirring at room temperature (RT). After sufficient stirring at RT, starting mixtures were obtained. Other starting mixtures were prepared with using tetraethoxysilane ( $\text{Si}(\text{OC}_2\text{H}_5)_4$ ) instead of the imidazoline derivative for reference. These starting mixtures were reacted in Morey-type pressure vessel at  $\sim 80\text{--}170^\circ\text{C}$  for 10 h to 1 week. Samples after the heat treatments were characterized by X-ray diffraction (XRD), and Fourier transform infrared (FT-IR) and ultraviolet-visible (UV-vis) spectroscopies.

XRD showed several reflection peaks in the low angle range ( $2\theta \leq 20^\circ$ ). The  $d$  value corresponded to  $\sim 2$  nm for the reflection peak which appeared at the lowest angle. Other reflections in the low-angle range were due to higher order reflections. A reflection was also observed  $\sim 60^\circ 2\theta$ . There was no reflection assigned to the starting reagents. These results suggest that the starting reagents reacted with each other and a new layered compound was obtained.

We now propose a model for a structure of the synthesized sample (Scheme) based on the experimental results by XRD, FT-IR and so on. In the proposed model, siloxane sheets are stacked with interlayer space of  $\sim 2$  nm. The imidazolyl group is located between the stacked siloxane sheets and bonds covalently with the siloxane sheet.

UV-vis spectra showed an absorption band attributed to the imidazolyl group of the synthesized layered hybrid. The absorption depended on the synthesis conditions.

- 1) Fukushima, Y. and Tani, M., *J. Chem. Soc., Chem. Commun.*, 241(1995)
- 2) Richard-Plouet, M. et al., *New J. Chem.*, 1073(2004)
- 3) Fujii, K. et al, *Appl. Clay Sci.*, 88(2015)
- 4) Fujii, K. et al, *J. Photochem. Photobio. A: Chem.*, 125(2011)
- 5) Turhan, Y. et al., *Ind. Eng. Chem. Res.*, 1883(2008)



**Scheme.** Schematic representation of the proposed model for layered siloxane-imidazoline hybrids

## Distribution of radioactive cesium in soil and practical approach to decontamination in Fukushima

Kenichi Ito<sup>1</sup>, Tatsuro Matsuda<sup>1</sup>, Masaya Suzuki<sup>2</sup>, Tamao Hatta<sup>3</sup>, and Hirohisa Yamada<sup>4</sup>

<sup>1</sup>University of Miyazaki, 1-1, Gakuen Kibanadai-nishi, Miyazaki-shi, Miyazaki 889-2192, Japan,  
itoken@cc.miyazaki-u.ac.jp

<sup>2</sup>National Institute of Advanced Industrial Science and Technology, <sup>3</sup>Japan International Research Center for  
Agricultural Sciences, <sup>4</sup>National Institute for Materials Science

Four years have elapsed since the 2011 Tohoku earthquake and tsunami. After the natural disaster, the Tohoku area has gradually been revived. On the other hand, decontamination of radioactive cesium that was spread by the accident in the Fukushima Daiichi Nuclear Power Station caused by the disaster is continues throughout Fukushima prefecture, Japan. Moreover, the huge amount of radioactive waste, as typified by the amount of contaminated soil removed, has been increasing on a daily basis. In order to decide on interim storage facilities, various kinds of volume-reduction methods have been suggested by scientists, researchers and engineers. The classification method is one feasible prospect. Research and identification of the distribution of radioactive cesium in the soil and in the general area are required to optimize a classification of contaminated soil for the volume reduction. The present study focuses on the distribution of radioactive cesium in contaminated soil, and the relations between radioactive cesium and soil particles. Previous studies have reported that clay minerals can specifically adsorb cesium. Wet classification tests have proved that the fine particles containing clay minerals that were classified from the contaminated soil in Fukushima clearly accumulated radioactive cesium. Radioactive cesium exceeding tolerance levels have remained in the large particles (>0.5 mm). After floatation treatment of these particles, they were sorted and hand-picked by the difference in optical characters such as color and shape. The observation of sorted particle groups showed differences of radiation quantity and minerals. The particle groups of clear, white and orange, mainly including quartz and feldspar contained a small amount of radioactive cesium. However, floating substances, organic matter, and soil aggregation showed significant radiation. Furthermore, the group of tabular particles including clay minerals, such as mica and vermiculite showed the largest quantity of radiation. These results demonstrated that the main soil particles retaining radioactive cesium consist of clay minerals such as mica and vermiculite in the case of the contaminated soil in Fukushima. For the future, it is suggested that the classification method for the volume reduction should be improved with a focus on the clay minerals mineralogically, not mechanically.

1) Fukushima, Y. and Tani, M., *J. Chem. Soc., Chem. Commun.*, 241(1995)

2) Richard-Plouet, M. et al., *New J. Chem.*, 1073(2004)

3) Fujii, K. et al, *Appl. Clay Sci.*, 88(2015)

4) Fujii, K. et al, *J. Photochem. Photobio. A: Chem.*, 125(2011)

5) Turhan, Y. et al., *Ind. Eng. Chem. Res.*, 1883(2008)

## Controlling Mg(II)/Al(III) metal ratio in hydrotalcite type anionic clays

Hyung-Mi Kim<sup>1</sup>, Ji-Yeong Lee<sup>1</sup>, Jae-Min Oh<sup>1\*</sup>

<sup>1</sup>Department of Chemistry and Medical Chemistry, College of Science and Technology, Yonsei University,  
Wonju, Korea

\*Email: jaemin.oh@yonsei.ac.kr

We controlled the Mg(II)/Al(III) metal ratio in hydrotalcite-type anionic clays, with the chemical formula  $Mg_{1-x}Al_x(OH)_2(CO_3)_{x/2} \cdot mH_2O$ , by means of coprecipitation and isomorphous substitution. For coprecipitation reaction, aqueous solutions with various Mg(II)/Al(III) ratios were titrated with NaOH solution and the reaction pH was controlled systematically. The Mg(II)/Al(III) ratio of hydrotalcite was found to be controlled to 2/1, 5/1 and 12/1 when an appropriate pH condition was applied. The crystallinity and surface charge of the anionic clays synthesized thus were characterized using X-ray diffraction and light scattered electrophoresis, respectively, and showed decrease in both properties with increasing Mg(II)/Al(III) ratio. For isomorphous substitution, a brucite ( $Mg(OH)_2$ ) suspension was mixed with Al(III) aqueous solution under hydrothermal condition at 150°C. Isomorphous substitution resulted in anionic clays with Mg(II)/Al(III) ratios of 2/1, 3/1 and 5/1 with high crystallinity compared with coprecipitation. The present authors observed that the brucite transformed to anionic clays after 5 h through the temporary formation of boehmite when the brucite/Al(III) ratio was 3/1; on the other hand, lower or higher ratios required more time for the complete formation of hydrotalcite. We also found that, in isomorphous substitution, the starting materials brucite was not fully transformed to anionic clay when the Mg(II)/Al(III) ratio of > 10/1 was applied during synthesis.

## Biogeochemical process in the secondary phase mineral formation by extremophiles in Norris Geyser Basin, Yellowstone National Park, USA

Tae-hee Koo<sup>1\*</sup>, Jee-Young Kim<sup>1,2</sup>, Kyong Ryang Park<sup>3</sup>, Da Hee Jung<sup>3</sup>, Gill Geesey<sup>4</sup>, and Jin-wook Kim<sup>1, §</sup>

<sup>1</sup>Department of Earth System Sciences, Yonsei University, Seoul, Korea; \*ktaehee@yonsei.ac.kr;  
§correspondence: jinwook@yonsei.ac.kr

<sup>2</sup>Environmental Infrastructure Research Department, Environmental Measurement & Analysis Center, National Institute of Environmental Research, Korea

<sup>3</sup>Department of Biological Science and Biotechnology, Hannam University, Daejeon, Korea

<sup>4</sup>Department of Microbiology, Montana State University, Bozeman, Montana, USA

Redox reaction associated with microbial elemental respiration is a ubiquitous process in sediments as well as suspended particles in water, regardless of temperature or pH/Eh conditions. Particularly, changes in elemental redox states (both structural form in the mineral or dissolved elemental form in the water) induced by microbial respiration result in the unexpected biogeochemical reactions in the light of biotic/abiotic mineralization. The objective of the present study is to investigate the microbe-mineral interaction in the acido-hyperthermal Norris Geyser Basin in Yellowstone National Park, USA to understand the mechanism of biogeochemical process in extreme environment.

The experiments were designed in two sets with control in order to distinguish the biotic and abiotic process with the natural sediment and hot-spring water collected from the active acidic hot-spring (pH=3.5 and temperature=78 °C) of the Yellowstone National Park. The first set is the mimic of the natural environment which contains only clay slurry and the hot-spring water (Natural set). The other set contains carbon source, yeast extract and other ingredient to enhance the microbial activity (Enrichment set). The consequences of changes in mineralogy and chemistry were compared with the original sample and control set. The control was prepared in the same condition except adding glutaraldehyde to eliminate the microbial activity. Whole samples were prepared in the serum bottle and N<sub>2</sub> gas purged to maintain the anaerobic condition. Then samples were incubated at 78 °C for each time point (0, 6, and 12 months).

X-ray diffraction (XRD), scanning electron microscopy with energy dispersive x-ray spectroscopy (SEM-EDS), and X-ray absorption near edge structure (XANES) were applied to study the changes in the solid phases. The changes in water chemistry of experiments were measured by inductively coupled plasma-atomic emission spectrometry (ICP-AES) and liquid chromatography with ICP-mass spectrometry (LC-ICP-MS) with filtrated supernatant.

The secondary phase mineral formation with elemental compositions of the oxidative phase of Fe and As, and K was identified as pharmacosiderite only in the enrichment after 6-month incubation suggesting a major role of biotic process in the mineral formation. The considerable population of Fe-oxidizer (*Metallosphaera yellowstonensis*) and As-oxidizer (*Sulfurihydrogenibium* sp.) was detected by Phylogenetic analysis supporting the major role of extremophiles in biotic mineral process. The possible biotic/abiotic mechanism or process in mineral alteration/formation in extreme environment will be discussed.

## Clay minerals as proxies for tracing sediment provenance and transport process in the South China Sea

Zhifei Liu<sup>1</sup>, Yulong Zhao<sup>1</sup>, Christophe Colin<sup>2</sup>, Karl Stattegger<sup>3</sup>, Martin G. Wiesner<sup>4</sup>, Yanwei Zhang<sup>1</sup>,  
Xiajing Li<sup>1</sup>

<sup>1</sup> State Key Laboratory of Marine Geology, Tongji University, Shanghai 200092, China

<sup>2</sup> UMR 8148 CNRS-GEOPS, Université de Paris-Sud, Orsay 91405, France

<sup>3</sup> Institute of Geosciences, University of Kiel, Kiel 24118, Germany

<sup>4</sup> Institute of Geology, University of Hamburg, Hamburg 20146, Germany

The South China Sea offers an excellent case for studying source-to-sink transport process of terrigenous sediments among the global marginal seas. Clay minerals have been realized as effective tools to trace the fine-grained terrigenous sediment provenance and the transport process from the estuary to the continental shelf and then to the abyssal basin. This study synthesizes almost all the existing clay mineralogical data from ~1500 seafloor and surrounding river surface samples to obtain the basin-wide distribution of clay mineral assemblages. The results show that provenance control pattern and differential settlement effect are two critical controlling mechanisms for the source-to-sink transport processes in the South China Sea. Three significant features are summarized: (1) strong provenance control on clay mineral distribution commonly on the seafloor adjacent to the drainage systems with prevailing clay mineral species; (2) strong differential settling occurring at least for kaolinite and smectite during their transport from fluvial estuary to abyssal basin; and (3) high homogeneity with moderate contents of four clay mineral species in the western and southern South China Sea. By combining clay mineralogical distribution on the seafloor with observed oceanic current systems, the modern transport processes can be well illustrated: in the north, smectite derived from Luzon is transported mainly by surface current with significant influence of the Kuroshio intrusion, illite and chlorite from Taiwan are mainly carried by deepwater Contour Current, while kaolinite from the Pearl River is affected obviously by the eastward Guangdong Coastal Current; in the east, the distinguishable smectite content is suggested to be produced through chemical weathering on the seafloor; while in the west and south, the transport pathway of clay minerals is difficult to identify because it is highly homogenized or mixed by surface current systems.

## **DOM-affected transformation of contaminants on mineral surfaces: a review**

Tamara Polubesova<sup>1</sup> and Benny Chefetz<sup>2</sup>

<sup>1,2</sup> Department of Soil and Water Sciences, Faculty of Agriculture, Food and Environment, The Hebrew University of Jerusalem, P.O. Box 12, Rehovot 76100, Israel. E-mail: tamara.polubesova@mail.huji.ac.il

This review analyzes the role and reactivity of dissolved organic matter (DOM) in oxidation, reduction, hydrolysis and photochemical reactions of contaminants occurring on mineral surfaces. DOM affects transformation via competition for adsorption sites on the mineral surface, dissolution of minerals and exposing new reactive surface sites on the mineral surface, and by electron shuttling. Most of the data suggest that DOM reduces oxidation and hydrolysis, and increases reduction of contaminants by minerals. Alternatively, mineral surfaces can enhance redox transformations of contaminants due to interactions with DOM. DOM impact on transformation of contaminants varies as a function of its molecular composition and chemical properties. In some cases, the influence of dissolved small organic molecules on the transformation of contaminants by minerals might be opposite to the bulk DOM effect. In addition, fractionation of DOM on the mineral surface can also influence the contaminant-mineral interactions.

Based on the vast reviewed data, we suggest that the evaluation of DOM effects on contaminant transformations needs to be based on the chemistry and concentration of the DOM functional groups and the overall physico-chemical properties of the DOM. Moreover, the self-fractionation of the DOM upon interactions with minerals must be considered in order to elucidate the holistic effect of DOM in the contaminant-mineral system. In addition, we suggest that “natural DOM” should be used to elucidate DOM impact on the mineral surface reactions and not dissolved humic acids which exhibit quite different chemical structure and properties.

## Adsorption characteristic of arsenate on delaminated layered double hydroxides

Yu Takaki, Paulmanickam Koilraj, Tsuyoshi Hirajima, Keiko Sasaki\*  
Department of Earth Resources Engineering, Kyushu University, Fukuoka, 819-0395, Japan  
\*keikos@mine.kyushu-u.ac.jp

Synthesis of delaminated layered double hydroxides (LDHs) is targeted to provide the efficient sorbent for immobilization of arsenate.  $Mg_2Al-NO_3$  LDH was produced by co-precipitation at pH 10.0 following by ageing at 65 °C. Delamination was successfully performed by a sonication method. In brief, the wet cake after filtration was dispersed in water and treated ultrasonically for 12 hrs and centrifuged at 2500 rpm for 30 min to obtain delaminated LDH. The delaminated LDH was characterized by different physicochemical techniques such as XRD, TEM and measurement of zeta potentials. The colloidal suspension showed a large amount of suspended solid around 8.85 g/L LDH, and is stable for more than 2 months. Delaminated LDH showed a small amount suspended solid around 1.48 g/L, but is stable for more than 1 month.

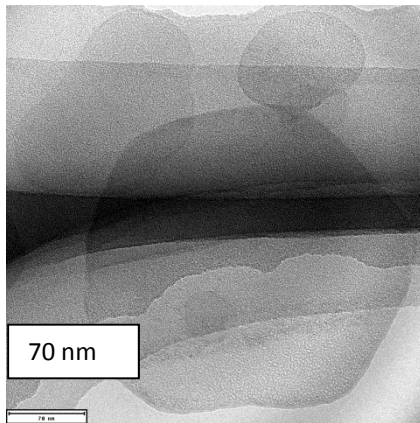


Fig.1 TEM image of delaminated LDH.

TEM images of colloidal LDH showed the presence of separated hexagonal host layers confirming the delamination of LDH in nano-sheets [1].

For comparison, sorption capacities of arsenate were investigated on both delaminated and crystalline  $Mg_2Al$ -LDH.

The results revealed that sorption (Fig.1 TEM image of delaminated LDH) capacity of delaminated LDH was 3.09 mmol/g corresponding to around four times higher than the sorption capacity of crystalline  $Mg_2Al-NO_3$ -LDH (0.784 mmol/g). Moreover, the solid residues after sorption of arsenate using delaminated LDH showed sharp XRD peaks with  $d_{003}$  spacing of 8.65 Å corresponding to the interlayer  $HAO_4^{2-}$  anion [2]. This confirms that the sorption of arsenate occurs by stacking of host layers with arsenate. In conclusion, the delaminated LDH showed more rapid and higher arsenate uptake than that of parent  $Mg_2Al-NO_3$ -LDH indicating the usefulness of the nano-materials for aqueous arsenate remediation.

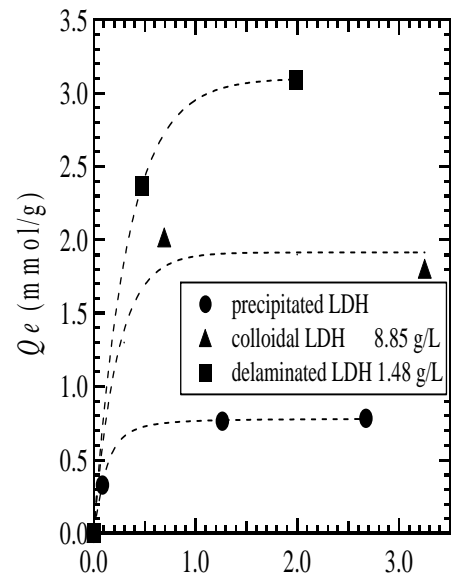


Fig. 2 Adsorption isotherms of arsenate on precipitated, colloidal and delaminated LDHs at 25 °C.

### References

- [1] Z.P. Xu, G. Stevenson, C.-Q. Lu, G.Q. Lu, The Journal of Physical Chemistry B, 2006. 110(34): p. 16923-16929.
- [2] S.-L. Wang, C.H. Liu, M.K. Wang, Y.H. Chuang, P.N. Chiang, Applied Clay Science, 2009.



## **Kinetics of smectite dissolution at high pH conditions for long-term safety assessment of radioactive waste disposal: effect of Gibbs free energy and secondary minerals**

<sup>1</sup>Tsutomu Sato and <sup>2</sup>Chie Oda

<sup>1</sup> Faculty of Engineering, Hokkaido University, Sapporo, Japan: tomsato@eng.hokudai.ac.jp

<sup>2</sup> Japan Atomic Energy Agency, Ibaraki, Japan

Bentonite-cement fluid interaction has been a key research issue in long-term safety assessment of radioactive waste disposal. The dissolution rate of smectite, the main constituent mineral of bentonite, has therefore been investigated under hyperalkaline conditions using batch and flow-through experiments with high fluid/solid weight ratios. Previous studies of smectite dissolution have contributed to the derivation of a kinetic model to account for differences in the pH of the reactive fluid, temperature and deviation of the system from equilibrium. The experimental conditions in such studies were, however, completely different from the expected conditions in an actual radioactive waste disposal system. For quantitative understanding, dissolution experiments of compacted bentonite have also been conducted. These studies show that the dissolution rate for compacted bentonite was significantly lower than that obtained from batch and flow-through experiments. Differences in the dissolution rate due to compaction cannot be fully explained by only considering the associated changes in reactive surface area. According to the results of reactive transport modeling, the Gibbs free energy of reaction ( $\Delta Gr$ ) should also be taken into account to describe fully the dissolution rate.

In this context, a review of the effect of  $\Delta Gr$  on the dissolution kinetics of smectite was conducted, and a dissolution rate equation of smectite applicable to  $pH = 7-13$  and  $t = 25-80^\circ C$  was proposed. The rate equation was used in reactive-transport model analyses to elucidate the consequences of coupled changes in the porewater chemistry, mineralogy and, ultimately, the mass transport properties of the bentonite buffer. The reactive-transport model analyses were conducted for bentonite alteration test cases with the use of different combinations of secondary minerals that will likely form in the bentonite buffer. Calculations of the temporal and spatial changes of kinetic smectite dissolution were interpreted as a consequence of  $\Delta Gr$  and porewater chemistry. Furthermore, the bentonite porewater chemistry was also affected by the stoichiometry and thermodynamic stability of the secondary minerals. Except in the close proximity of the cement interface, it was found that regardless of the choice of secondary minerals, the effective diffusion coefficient and hydraulic conductivity remained largely unchanged after 100,000 years.

## Cesium adsorption behavior of vermiculite and its application to the column method. Part II

Noriko Suzuki, Yuri Amano, Kotaro Ochi, and Toshiyuki Chikuma  
Showa Pharmaceutical University, Machida, Tokyo 194-8543, JAPAN  
\* n-suzuki@ac.shoyaku.ac.jp

### Introduction

Radioactive Cs was dispersed in all directions as a result of the Fukushima Daiichi Nuclear Power Plant accident. A huge amount of contaminated water was generated by decontamination before evacuated residents could return to their houses. Most clay minerals adsorb radioactive material such as  $^{137}\text{Cs}$ , including vermiculite which has a layer structure with interlamellar  $\text{Mg}^{2+}$  which can exchange with other cations. When the column method is considered for the application, it is important to know which grain size is the most effective for Cs uptake, because cohesion of small particles, like a powder, will be a serious problem.

The purpose of this study is to examine suitable particle diameters of vermiculite for adsorbing Cs when used in the column method.

### Experimental

The essential ion-exchange required was investigated by a batch method. 0.2 g of vermiculite of each particle size was put into the plastic container, 20 cm<sup>3</sup> of CsCl solution of the desired concentration added and the container placed on a rotary shaker for 24 h (expect time-dependent test). After filtration, the concentration of Cs in the supernatant solution was measured by atomic absorption and the adsorptive capacities were calculated. In addition, reaction time was set to 1 h, 2 h, 4 h, 8 h, 16 h, and 24 h in a time-dependent test. Two different types of column method were examined.

### Results and Discussion

Figure 1 shows the relationship between grain size and percentage of Cs uptake from pure aqueous solutions. Because of cation exchange capacity, at the high concentration of CsCl, the adsorption rate was low, and small differences among the particle sizes were observed. In contrast, the adsorption rate was distinct between the size of 500/599  $\mu\text{m}$  and 1400/1699  $\mu\text{m}$  at low CsCl concentration. Although the total amount of Cs adsorbed is the same, the adsorption rates might be different. To elucidate this, the time dependence of Cs uptake in different sizes of vermiculite was examined and it was found that the smaller the particle size was, the quicker the uptake of Cs.

From these results, the grain size of 500/600  $\mu\text{m}$  was applied for column method.

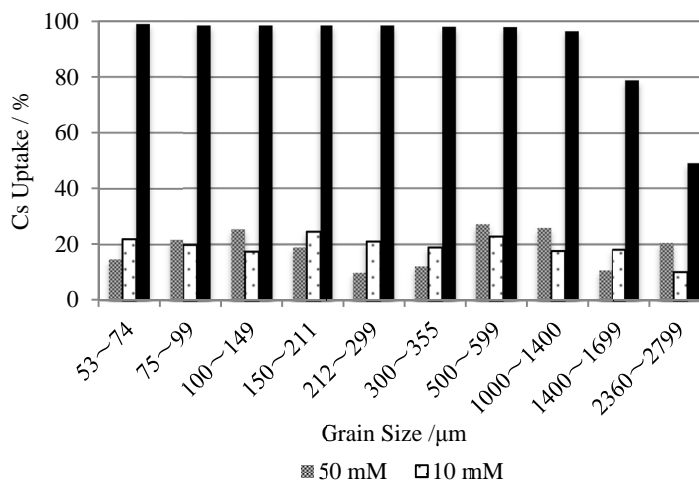


Fig. 1 Effect of grain size for Cs uptake. Abscissa axis A/B means that the grain passed through the sieve of opening size A and gathered on the sieve of opening size B.

## Reversible fluorescent color change of dyes intercalated in a synthetic saponite

Makoto Tominaga<sup>1</sup>, Yudai Oniki<sup>2</sup>, Yasutaka Suzuki<sup>1,2</sup> and Jun Kawamata<sup>1,2</sup>

<sup>1</sup>Graduate School of Medicine, Yamaguchi University, 1677-1, Yoshida, Yamaguchi, 753-8512, Japan

E-mail: t030uh@yamaguchi-u.ac.jp

<sup>2</sup>Department of Chemistry, Faculty of Science, Yamaguchi University, 1677-1, Yoshida, Yamaguchi, 753-8512, Japan

The gallery height of a clay mineral changes dynamically by swelling. The gallery height of a synthetic saponite (SSA) in the dry state is 0.3 nm which is similar to the thickness of  $\pi$ -electron system of a cationic dye with high planarity. Such a situation is realized at low dye loadings of SSA-dye hybrid system. This fact indicates that the cationic dye exists as a monomer state in the interlayer space of SSA in the dry state. On the other hand, the gallery height of SSA increases up to 1.0 nm from 0.3 nm when dimethylsulfoxide (DMSO) is introduced into the interlayer space of SSA, namely swelling of SSA. This extended gallery height allows formation of a dimer of rod-like cationic dyes due to  $\pi$ - $\pi$  stacking.

In this study, we have attempted to switch monomer and dimer due to  $\pi$ - $\pi$  stacking by swelling. The fluorescent color of rod-like cationic dyes is drastically changed by formation of a dimer called excimer. Therefore, a switchable fluorescent color change material should be obtained by employing rod-like fluorescent dye as a guest.

We fabricated hybrid films consisting of SSA and seven rod-like cationic dyes shown in Fig. 2. The

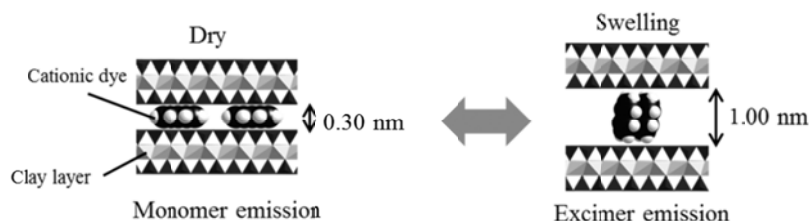


Fig. 1 Mechanism of monomer and excimer emission in hybrid films

fluorescent color of the obtained film was monitored during the swelling and drying procedure. A remarkable red-shift of fluorescent color which is attributed to the formation of excimer was observed for all dyes. The fluorescent color could easily be restored to the original one by drying. The reversible color change was observed for at least 50 cycles.

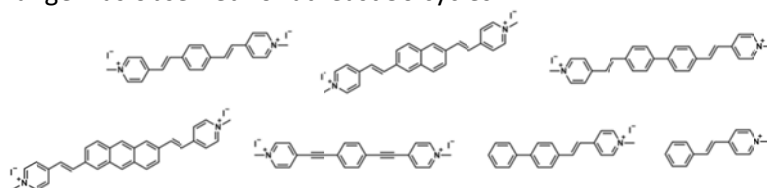


Fig. 2 Chemical structure of rod-like cationic dyes

## The formation of smectite and its redox reaction in deep subsea floor sediment, South Pacific Gyre: IODP expedition 329

Kiho Yang<sup>1</sup>, Toshihiro Kogure<sup>2</sup>, Bryce Hoppie<sup>3</sup>, Robert Harris<sup>4</sup>, Hionsuck Baik<sup>5</sup>, Hailiang Dong<sup>6</sup>, IODP Expedition 329 shipboard scientists<sup>7</sup>, and Jinwook Kim<sup>1\*</sup>

<sup>1</sup>Department of Earth System Sciences, Yonsei University, Seoul, Korea;

khyang@yonsei.ac.kr; \*Correspondence to jinwook@yonsei.ac.kr

<sup>2</sup>Department of Earth and Planetary Sciences, Graduate School of Science, The University of Tokyo, Tokyo, Japan;

<sup>3</sup>Department of Chemistry and Geology, Minnesota State University, Mankato, MN, USA;

<sup>4</sup>College of Oceanic and Atmospheric Sciences, Oregon State University, OR, USA;

<sup>5</sup>Korea Basic Science Institute (KBSI), Seoul, Korea;

<sup>6</sup>Department of Geology and Environmental Science, Miami University, Oxford, OH, USA;

<sup>7</sup>IODP Expedition 329 shipboard scientists

Subsea floor sediment in the South Pacific Gyre (SPG) was recovered for the first time by the Integrated Ocean Drilling Program (IODP) Expedition 329 (2010.10.10-2010.12.13). Clay mineralogy from two sites (U1369 and U1365) was investigated and comparisons made of clay mineralogy and formation from the sites U1365 (margin of SPG), and site U1369 (center of SPG close to the East Pacific Rise). The sediment at the site U1369 has a young crustal age of 13.5 Ma compared with the site U1365 (84-120 Ma).

Fine clay fractions less than 1  $\mu\text{m}$  were analyzed by X-ray diffractometry (XRD), transmission electron microscopy (TEM) with selected area electron diffraction (SAED), and electron dispersive X-ray spectrometry (EDS). The saturation index (SI) with respect to smectite was modeled based on the pore water chemistry.

The dominant clay minerals in the investigated sediments are smectite and illite. The higher ordering of the illite polytype ( $1M$ ,  $2M_1$ , and  $3T$ ) at U1369 was distinctly different to the disordered  $1M_d$  illite at U1365 suggesting that hydrothermal alteration influences the smectite mineral formation at U1369. The lower heat flow measurement comparing to the lithospheric cooling reference also supports the hydrothermal activity at U1369. Smectites of hydrothermal origin such as Al-rich beidellite, and saponite were observed at U1369 whereas Fe-rich montmorillonite that is likely to be associated with the basalt-seawater interaction at ambient temperature was dominant at U1365. Fe-rich smectite (nontronite) was detected at both sites. The measurement of saturation indices with respect to smectite phases, and muscovite using pore water chemistry showed an oversaturated condition. The red-brown to yellow-brown semi-opaque oxide minerals (RSO) were widely distributed with Fe-rich smectite near the basaltic crust at U1365. The presence of K-nontronite at the basalt-sediment interface at both sites indicates an oxidative basalt alteration; however, the variations in oxidation state of structural Fe in nontronite measured by EELS may indicate that the reductive environment may persist locally at the basalt/sediment interface.

**Flame retardancy enhancement of ethylene-vinyl acetate(EVA) loaded with mica, Laponite® (*registered trademark of BYK Additives*) and MgAl layered double hydroxide**

J. Yoon Choi<sup>1,\*</sup>, Minjae Kwon<sup>1</sup>, Jae-Hun Yang<sup>2</sup>, Jin-Ho Choy<sup>2</sup> and Hyun-Joong Kim<sup>3</sup>

<sup>1</sup>Fire & Safety Evaluation Technology Center, Korea Conformity Laboratories,  
73, Yangcheong 3-gil, Cheongwon-gu, Cheongju-si, Chungcheongbuk-do, 363-883 South Korea  
(j.yoon.choi@kcl.re.kr)

<sup>2</sup>Center for Intelligent Nano Bio Materials (CINBM), Department of Chemistry and Nanoscience, Ewha  
Womans University, Seoul 120-750, South Korea

<sup>3</sup>Lab. of Adhesion and Bio-Composites, Program in Environmental Materials Science, Seoul National  
University, Seoul 151-921, Republic of Korea

The usage of polymers can be found nearly everywhere in our lives but their intrinsic flammability and subsequent fire safety concerns require their products to meet national/international regulations in every country. To meet the level of fire retardancy, either chemical compositions of the polymer concerned are modified or flame retarding agents are added. In general, the latter method is preferred due to simplicity and convenience.

Conventionally, flame retardants such as hydroxides and halogenated organic compounds have been used widely but relatively high amounts of loading to meet the fire safety guides would often causes detrimental effects of physical properties. Also concerns of toxicity for environments and accumulation within the human body have caused some to be taken out of use and others to be avoided [1].

Many attempts to overcome the current limitations of flame retardants have been under investigation. Some of the promising candidates include high molecular weight halogenated polymer flame retardants and nanomaterials such as clays, carbonic fiber and graphene[2-4]. Synergetic effects between these flame retardants along with conventional ones have been another important research area[5].

Comparing with other flame retardants, the application of nanoclay as a flame retardant has received much attention due to various possible benefits over a wide range of applications including environmental and economic. Particle size dependent flame retardancy for nanoclays has been of particular interest.

The most accepted mechanism of nanoclay flame retardancy is based on the barrier effect caused by nanodispersion of clays within a polymer matrix. Using mica, Laponite® (*registered trademark of BYK Additives*) and MgAl layered double hydroxide clays (w/o intercalated), clay particles varying in size from approximately one micrometer to several tens of nanometers were introduced into ethylene vinyl acetate (EVA). Flame retardancy changes were investigated from various aspects including heat release rate, thermal decomposition weight changes and burning behaviors. The probable size limitation of the above mentioned mechanism is discussed.

J.L. Lyche *et al.* Human health risk associated with brominated flame-retardants (BFRs). *Environment International*. 74 (2015) 170–180.

K. Chrissafis *et al.* Can nanoparticles really enhance thermal stability of polymers? Part I: An overview on thermal decomposition of addition polymers. *Thermochimica Acta*. 523 (2011) 1-24.

K. Chrissafis *et al.* Can nanoparticles really enhance thermal stability of polymers? Part II: An overview on thermal decomposition of polycondensation polymers. *Thermochimica Acta* 523 (2011) 25-45.

Beyer, G. Short communication: Carbon nanotubes as flame retardants for polymers. *Fire Mater.* 26 (2002) 291–293.

Xin Wang *et al.* Synergistic Effect of Graphene on Antidripping and Fire Resistance of Intumescent Flame Retardant Poly (butylene succinate) Composites. *Ind. Eng. Chem. Res.* 50 (9) (2011) 5376–5383

## Fukushima nuclear disaster and clay

Toshihiro Kogure<sup>1\*</sup> and Tsuyoshi Yaita<sup>2</sup>

<sup>1</sup>Dept. of Earth and Planetary Science, Graduate School of Science, The University of Tokyo, Tokyo, 113-0033, Japan

<sup>2</sup>Atomic Energy Agency (JAEA), Hyogo, 679-5148. Japan  
\*kogure@eps.s.u-tokyo.ac.jp

Four years after the Fukushima nuclear accident, Cs-137 is now the main source of radioactive contamination of the land, due to its abundance and relatively long half-life. Though there have been a number of researches into the state and behavior of radioactive cesium in the soil, microscopic results to investigate the adsorption sites of radioactive cesium in the actual soil are few. For example, it is expected that radioactive cesium is fixed to clay minerals in the soil, but the actual mineral species involved have not been specified. Recently we have reported, using autoradiography with micro-processed imaging plates (IPs) and various electron microscopic techniques, that weathered biotite is a major adsorbent in the actual soil of Fukushima (Mukai et al., 2014). Structurally, the weathered biotite is an interstratification of the original biotite layers with the potassium-occupied interlayer and vermiculite layers with hydrated-magnesium/calcium replacing potassium in the interlayer. Such weathered biotite is abundant in the Fukushima soil as the mountains and hillsides in this area are covered with weathered granite soil a few tens of meters thick.

Several laboratory experiments indicated that vermiculite efficiently incorporates Cs from solutions. On the other hand, the adsorption experiments to survey the Cs-adsorption ability of various clay minerals indicated that weathered biotite or vermiculite is not superior to other clay minerals such as smectite and illite in the adsorption ability of Cs, at a very low contamination level similar to that at Fukushima. This discrepancy should be compromised for understanding the behavior of Cs in the soil. We speculated that the actual adsorption of Cs in the soil was controlled by kinetics among multi-mineral phases and solution, rather than by simple equilibrium between mono-mineral and solution. Therefore, we conducted a new Cs-adsorption experiment, in which various clay minerals were immersed together in dilute Cs-137 radioisotope solutions and the amount of Cs-137 adsorbed in each mineral was measured by autoradiography using an IP, instead of chemical analyses of solutions or minerals. This revealed that weathered biotite predominantly adsorbed the Cs-137 among the clay minerals investigated, proving the observation made in the actual soil.

Monday  
6<sup>th</sup> July

Lecture Room 3

Computational  
chemistry studies of  
clay minerals - bridging  
length and time-scales

## Molecular dynamics simulations of Cs<sup>+</sup> adsorption on hydrated surfaces of illite, smectite, and interstratified illite/smectite clays

Andrey G. Kalinichev, Narasimhan Loganathan, Brice F. Ngouana Wakou, Zongyuan Chen and Gilles Montavon

Laboratoire SUBATECH (UMR 6457), Ecole des Mines de Nantes, 44307 Nantes Cedex 3, France

\*E-mail: kalinich@subatech.in2p3.fr

Callovo-Oxfordian clay (COx) is under investigation as a host rock for long-term nuclear waste repository in France. For that purpose, safety assessment models must account for interaction of radionuclides with repository materials over time- and distance-scales spanning many orders of magnitude. The clayey component of COx consists mostly of illite, smectite and interstratified illite/smectite (I/S) minerals, and the radionuclide sorption on COx is usually predicted considering an “additivity rule”, e.g., averaging between their behavior with respect to illite and smectite separately.

Indeed, experimental studies of cation exchange indicate that in some cases I/S behaves more like a mixture of illite and smectite for the following reasons: (i) Cs<sup>+</sup> sorption on I/S can be quantitatively explained by two sub-models describing the sorption on illite and smectite; (ii) the measured value of I/S cation exchange capacity (CEC) is very close to the value calculated by the CECs of illite and smectite according to their ratio in I/S. However, this conclusion cannot be further verified because the cation exchange selectivity coefficients for illite and smectite are similar. Therefore, more detailed understanding and description of the adsorption and transport properties of radionuclides in I/S clay becomes an important issue.

We have applied molecular dynamics (MD) computer simulations in order to quantify the molecular scale mechanisms responsible for the adsorption of Cs<sup>+</sup> cations at the basal surfaces of illite, smectite, and I/S. A set of new structural models of illite and smectite have been constructed to more accurately account for the natural disorder in the structural isomorphic Al/Si and Mg/Al substitutions in the tetrahedral and octahedral clay sheets, respectively. In addition, an atomistic structural model of I/S clay has been developed for the first time according to the atomic composition of the ISCz1 type of illite/smectite, the composition used in experiments and closely resembling that of COx.

The newly developed models allowed us to identify several structurally different energetically favorable adsorption sites at the basal surfaces of all three clay substrates. Canonical ensemble (NVT) MD simulations were carried out by systematically constraining one Cs<sup>+</sup> cation at different distances from the clay surface (potential of mean force calculations using an umbrella sampling algorithm). The results are quantitatively analyzed in terms of Cs<sup>+</sup> adsorption free energy profiles above each individual adsorption site on each clay surface. Cs<sup>+</sup> sorption properties for the three clay mineral surfaces are compared in terms of preferable sorption sites and their surface distributions, most stable adsorption distances and free energies of adsorption. The resulting equilibrium constants for surface adsorption and ion exchange are then calculated and compared with available experimental data.



## Influence of layer charge, hydration state and cation nature on the collective dynamics of interlayer water in tetrahedrally charged swelling clay minerals

Laurent Michot<sup>1</sup>, Eric Ferrage<sup>2</sup>, Alfred Delville<sup>3</sup> and Monica Jimenez-Ruiz<sup>4</sup>

<sup>1</sup> Physicochimie des Electrolytes et Nanosystèmes Interfaciaux (Phenix) CNRS-UPMC-Sorbonne Université UMR 8234, 4 place Jussieu case courrier 51, 75005 Paris (laurent.michot@upmc.fr); <sup>2</sup> Institut de Chimie des Milieux et Matériaux de Poitiers, IC2MP-HydrASA, UMR7285-CNRS, Université de Poitiers, 86022 Poitiers Cedex, France

<sup>3</sup> Interfaces, Confinement, Matériaux et Nanostructures (ICMN), CNRS, Université d'Orléans, UMR 7374, 45071 Orléans Cedex 2, France, <sup>4</sup> Institut Laue Langevin (ILL), 6 Rue Jules Horowitz, BP. 156, F-38042 Grenoble Cedex 9, France

Upon water adsorption, swelling clay minerals expand stepwise. Their apparent interlamellar distance ( $d_{001}$ ) then increases step by step from a value around 10 Å for the dry state to roughly 12.5 Å for the so-called monolayer state and then to around 15.5 Å for the bilayer state. In such systems, the dynamical and structural properties of water can be considered as those of a bidimensional confined fluid. Indeed, the system displays strong confinement in the direction perpendicular to the clay layers, inducing a specific structuration of water molecules. This structuration in turn impacts water organization in the parallel direction, and early molecular simulations studies have revealed that it is significantly different from that of bulk water. Such anisotropic organization is also revealed by measurements and simulations of water diffusion at the molecular scale that yield anisotropic diffusion coefficients significantly lower than that of bulk water. Most of these studies rely on the use of neutron-based techniques (Martins *et al.*, 2014) mainly quasi-elastic neutron scattering (QENS) or neutron spin-echo (NSE). In contrast, much less work has been devoted to the investigation of collective motions measured by coherent inelastic neutron scattering (INS) on deuterated samples. The study of these collective motions is different from both self motions of individual molecules obtained by incoherent QENS and slow collective motions obtained by NSE. In a recent study (1), we analyzed the INS signal of an oriented synthetic Na-saponite clay sample with a layer charge of 0.7 per unit-cell in the bihydrated state. We could evidence a clear anisotropy of the low-energy excitation of the collective dynamics of interlayer water that display a behavior significantly different from that of bulk water, this difference being stronger in the direction perpendicular to the clay layer. Molecular dynamics simulations of the system could reproduce qualitatively the experimental results that could be assigned to the presence of cations in the interlayer space and/or confinement effects. To get a further understanding of the observed features, it was then necessary to vary the cation nature, layer charge and hydration state. The present study therefore combines inelastic neutron scattering measurements and molecular dynamics simulations carried out on a low-charge Ca-saponite in the bihydrated state and on a high-charge Na-saponite in the monohydrated state at different temperatures. The data obtained confirm the strong anisotropy of collective motions and, in the perpendicular direction, a dispersive behavior is observed for  $Q$  values  $\geq 0.5 \text{ \AA}^{-1}$  in contrast with what is observed for bulk water and in the parallel direction. Such a behavior must somehow be linked to a correlation between the motions of water molecules located in the adjacent interlayer space that is likely transmitted through the solid clay layer. Unfortunately, molecular dynamics simulations are, in their present state, unable to account for such an effect, as they do not satisfactorily describe vibrations of the clay layers. In the parallel direction, experimental results and molecular dynamics simulations show that the features of the low-energy excitation and in particular, the energy corresponding to the non dispersive component, are linked to the structuration and rigidity of the interlayer water network. Indeed, this position displays an upward energy shift with increasing confinement and decreasing temperature. Jimenez-Ruiz *et al.* (2012). **J.Phys. Chem. A**, 116, 2379-2387.

## Molecular dynamics simulations of the structure and dynamics of H<sub>2</sub>O and metal ions on hydrated hectorite surfaces

Narasimhan Loganathan<sup>1</sup>, A. Ozgur Yazaydin<sup>2</sup>, Geoffrey M. Bowers<sup>3</sup>, R. James Kirkpatrick<sup>4</sup>, and Andrey G. Kalinichev<sup>5</sup>

<sup>1</sup>Department of Chemistry, Michigan State University, East Lansing, Michigan 48824, USA <sup>2</sup>Dept. of Chemical Engineering, Univ College London, Torrington Place, London WC1E7JE, UK

<sup>3</sup>Division of Chemistry, Alfred University, Alfred, New York 14802, USA

<sup>4</sup>College of Natural Science, Michigan State University, East Lansing, Michigan 48824, USA

<sup>5</sup>Lab. SUBATECH, Ecole des Mines de Nantes, 4 Rue Alfred Kastler, 44307 Nantes, France

The investigation of mineral-water interfaces plays a pivotal role in the study of a wide variety of environmental and scientific issues, including CO<sub>2</sub> sequestration<sup>1</sup> and long-term containment of radioactive waste in geological formations<sup>2</sup>. Ion-water-mineral interactions, for instance, greatly influence such geochemical phenomena as clay mineral swelling, dispersion, element diffusion, and mineral alteration. These interactions can be different for different surface cations and are strongly influenced by the composition of the clay substrate structure. Recent experimental studies using XRD and NMR techniques provide vital information regarding the interlayer spacing and the structure and dynamics of hydrated metal ions in the interlayers and on the basal surfaces of the smectite mineral hectorite<sup>3,4</sup>. The results indicate that metal cations with higher hydration energies and smaller ionic radii are less strongly coordinated with the hectorite surface than those with lower hydration energies and larger ionic radii. In parallel, computational molecular simulations have become one of the most important tools in the study of such mineral-fluid interfacial systems and by providing invaluable atomistic information about the underlying physical and chemical processes.<sup>5-7</sup> We present here the results of classical molecular dynamics (MD) computer simulations of the fluid and solute structure on the basal surfaces of hectorite that connect directly to experimental results. The simulations used the CLAYFF<sup>8</sup> force field parameters and were performed for the adsorption of Na<sup>+</sup>, Cs<sup>+</sup> and Ca<sup>2+</sup> ions at the hydrated hectorite surface. The structural charge in hectorite results from isomorphous substitution of Li<sup>+</sup>/Mg<sup>2+</sup> in the octahedral sheet, and in this study a new model of hectorite structure is developed using a disordered distribution of Li<sup>+</sup>/Mg<sup>2+</sup> substitutions over a significantly larger substrate surface area in order to represent the natural situation more realistically than in the earlier studies.<sup>6</sup> Atomic density profiles and the hydrogen bonding structure were analyzed in detail for the three systems, which represent a range of cation hydration energies. The results indicate that Na<sup>+</sup> and Ca<sup>2+</sup> are predominantly adsorbed as outer sphere surface complexes whereas Cs<sup>+</sup> ions are adsorbed as inner sphere surface complexes. A small fraction of the Na<sup>+</sup> ions (~1%) are adsorbed at the center of ditrigonal cavities as inner sphere surface complex. The distributions of H<sub>2</sub>O molecular orientations at the hectorite surface provide a quantitative picture of the H-bonding structure at this hydrophilic interface. The dynamics of water molecules were examined by self diffusion coefficients and residence time correlation functions for H<sub>2</sub>O molecules in the solvation shell of metal cations. Results obtained from the simulations are compared with the available experimental data and also with other simulation studies in order to provide a reliable comprehensive molecular-scale image of the structure and dynamics of ions and water molecules on the hectorite surface.

<sup>1</sup> Shao, H.; Ray, J. R.; Jun, Y. S. *Environ. Sci. Tech.* 2010, **44**, 5999

<sup>2</sup> Ngouana, B.; Kalinichev, A. G. *J. Phys. Chem. C* 2014, **118**, 12758

<sup>3</sup> Bowers, G. M.; Singer, J. W.; Bish, D. L.; Kirkpatrick, R. J. *J. Phys. Chem. C* 2011, **115**, 23395

<sup>4</sup> Bowers, G. M.; Bish, D. L.; Kirkpatrick, R. J. *J. Phys. Chem. C* 2008, **112**, 6430

<sup>5</sup> Cygan, R. T.; Greathouse, J. A.; Heinz, H.; Kalinichev, A. G. *J. Mater. Chem.* 2009, **19**, 2470.

<sup>6</sup> Morrow, C. P.; Yazaydin, A. Ö.; Krishnan, M.; Bowers, G. M.; Kalinichev, A. G.; Kirkpatrick, R. J. *J. Phys. Chem. C* 2013, **117**, 5172.

<sup>7</sup> Narasimhan, L.; Ngouana Wakou, B. F.; Kalinichev, A. G., *Mineralogical Magazine* 2013, **77**, 1636.

<sup>8</sup> Cygan, R. T.; Liang, J. J.; Kalinichev, A. G. *J. Phys. Chem. B* 2004, **108**, 1255.

## Molecular simulation of structure and diffusion at smectite-water interfaces: using expanded clay interlayers as model nanopores

Jeffery A. Greathouse<sup>1</sup>, David B. Hart<sup>1</sup>, Geoffrey M. Bowers<sup>2</sup>, R. James Kirkpatrick<sup>3</sup>, Randall T. Cygan<sup>1</sup>

<sup>1</sup> Geochemistry Department, Sandia National Laboratories, Albuquerque, New Mexico, USA.

jagreat@sandia.gov

<sup>2</sup> Division of Chemistry, Alfred University, Alfred, New York, USA.

<sup>3</sup> College of Natural Science, Michigan State University, East Lansing, Michigan USA.

Nanopores bounded by clay mineral surfaces play a critical role in the transport of aqueous species through geologic formations relevant to a number of energy extraction and potential waste sequestration processes. Using expanded clay interlayers as models of nanopores, we implemented molecular dynamics simulations to investigate the structure and diffusion of aqueous solutions in smectite nanopores approximately 6 nm thick, comparing the effect of clay composition with model Na-hectorite and Na-montmorillonite surfaces.

In addition to structural properties at the interface, water and ion diffusion coefficients were calculated for each aqueous layer at the interface, as well as the central bulk-like region of the nanopore. The results show similar solution structure and diffusion properties at each surface, with striking differences in sodium adsorption complexes and water structure in the first adsorbed layer due to different arrangements of layer hydroxyl groups in the two clay models. Interestingly, the extent of surface disruption on bulk-like solution structure and diffusion extends to only a few water layers (Figure 1). A comparison of sodium ion residence times confirms similar behavior of inner-sphere and outer-sphere surface complexes at each clay surface, but approximately 1 % of sodium ions adsorb in ditrigonal cavities on the hectorite surface. The presence of these anhydrous ions is consistent with highly immobile anhydrous ions observed in previous nuclear magnetic resonance spectroscopic measurements of hectorite pastes.

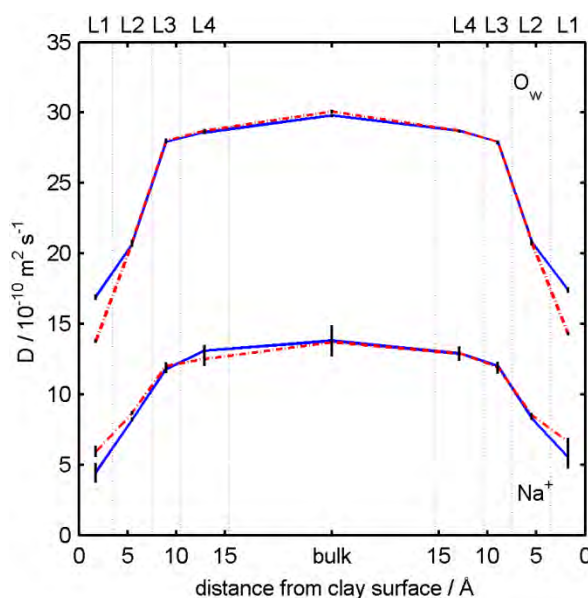


Figure 1. Diffusion coefficients for water molecules ( $O_w$ , top) and sodium ions (bottom) for each adsorption layer in Na-hectorite (blue) and Na-montmorillonite (red) nanopores, for translational motion parallel to the basal surfaces.

This work is supported by the U.S. Department of Energy, Office of Science, Office of Basic Energy Sciences, Geosciences Research Program. Sandia National Laboratories is a multi-program laboratory managed and operated by Sandia Corporation, a wholly owned subsidiary of Lockheed Martin Corporation, for the U.S. Department of Energy's National Nuclear Security Administration under Contract DE-AC04-94AL85000.

## Improving the description of the structure and dynamics of clay surfaces at the classical level using DFT calculations

Maxime Pouvreau<sup>1</sup> Andrey Kalinichev<sup>2</sup>

<sup>1,2</sup> Subatech - 4 rue Alfred Kastler - La Chantrerie - BP 20722 44307 Nantes cedex 3 France

E-mail: Maxime.Pouvreau@subatech.in2p3.fr

Clay minerals consist of layered tetrahedral silicate sheets and octahedral hydroxide sheets. In many cases, various isomorphic substitutions are possible on both tetrahedral (e.g., Al<sup>3+</sup> for Si<sup>4+</sup>) and octahedral (e.g., Mg<sup>2+</sup> for Al<sup>3+</sup>; Fe<sup>2+</sup> for Al<sup>3+</sup>, etc.) sites. This leads to a very significant compositional and structural diversity of clays. The substitutions create a negative charge on the clay layer, which is usually compensated by various interlayer cations (alkali metals, alkaline earths, etc.) which can be easily hydrated. Because of the potential large-scale use of clay minerals as host rocks for radioactive waste repository, good understanding of the molecular mechanisms controlling radionuclide sorption and mobility in clays is necessary.

Clay surfaces interacting with ions can be divided into two types: basal surfaces (parallel to the layering), and edge surfaces. When the cleavage of the clay crystal is imperfect, the sites can be heterogeneously protonated. Therefore, in addition to the ability of all surfaces to offer sites for complexation with various aqueous species, edge surfaces are also the place of active proton transfers. While molecular simulations involving the current classical force fields can be used to study the stable basal surfaces, quantum chemical calculations are necessary to fully describe the dynamics and reactivity of the edge surfaces. However, quantum methods are computationally much more demanding by many orders of magnitude than the classical modeling methods. Therefore, they are much more limited by the time scale and the sizes of the simulated systems and processes, and cannot fully describe the true compositional and structural complexity of clays. Consequently, it is still necessary to use classical molecular modeling methods for larger-scale simulations. This requires improvements in the description of edge surfaces at the classical level with the help of higher level quantum modelling methods such as DFT.

A new three-body term (3B) for the ClayFF force field has recently been introduced by Zeitler et al. [1] for dry brucite surfaces, using a vibrational analysis. As an extension of that work, we present here: (i) a detailed quantitative assessment of the capacity of ClayFF-3B to describe a wider range of brucite surfaces (fully coordinated edge surfaces, hydrated basal and edge surfaces); (ii) further development of the ClayFF-3B model to include the description of the surfaces of other similarly structured minerals (gibbsite, portlandite) and, later, to clays. To that end, DFT calculations were performed for these systems using the GGA approximation and the Gaussian and plane waves method [2]. The metal–O–H angular bending term was fitted for bulk, basal, and edge models of the hydroxyls using a vibrational analysis. To measure the contribution of the 3B term to the description of surface hydroxyls, DFT, ClayFF and ClayFF-3B molecular dynamics are compared in terms of the metal–O–H angle distributions, metal–O pair distribution functions and power spectra of hydrogen atoms.

[1] Zeitler, T. R.; Greathouse, J. A.; Gale, J. D.; Cygan, R. T. Vibrational Analysis of Brucite Surfaces and the Development of an Improved Force Field for Molecular Simulation of Interfaces. *J. Phys. Chem. C* **2014**, *118*, 7946–7953.

[2] VandeVondele, J.; Krack, M.; Mohamed, F.; Parrinello, M.; Chassaing, T.; Hutter, J. Quickstep: Fast and Accurate Density Functional Calculations Using a Mixed Gaussian and Plane Waves Approach. *Computer Physics Communications* **2005**, *167*, 103–128.

## Studies of cations and water molecules dynamics in montmorillonites with a polarizable force field

S. Tesson<sup>1</sup>, M. Salanne<sup>2</sup>, S.Tazi<sup>2</sup>, B.Rotenberg<sup>2,3</sup>, V. Marry<sup>2</sup>

<sup>1</sup>Sorbonne Universités, UPMC Univ Paris 06, UMR 8234, PHENIX, F-75005, Paris, France  
stephane.tesson@upmc.fr

<sup>2</sup>Sorbonne Universités, UPMC Univ Paris 06, UMR 8234, PHENIX, F-75005, Paris, France  
3CNRS, UMR 8234, PHENIX, F-75005, Paris, France

The extensive use of clay minerals in industrial applications (catalysis, formulation), energy and ecological engineering (oil recovery, ground water remediation, geological barrier for radioactive waste and CO<sub>2</sub>) is partly due to their remarkable properties of retention at the mineral surface. In environmental engineering, the role of water on clay permeability and retention properties is crucial. Indeed, the water is the vector of the motion of the species present in the medium, hazardous elements for instance.

Clays are lamellar inorganic materials composed of layers piled on top of each other to form particles. Clays show different behaviors towards water, depending on the value of the negative structural charge carried by the mineral layers. In particular, clays swell or not, depending on the hydration property of the counter-ions located between the layers.

Molecular simulations allow a detailed picture of the structure, thermodynamics and dynamics of the fluid at the interface<sup>[1,2]</sup>. Unfortunately, the numerical results do not always reproduce quantitatively the experimental results, which casts, consequently, a doubt on the validity of simulations interpretations<sup>[3]</sup>. In particular, the polarizability, which is not taken into account, could play a significant role especially when an electric field is present at the interface<sup>[4]</sup>.

Therefore we developed a polarizable force field based on DFT calculations. The dry structures of two uncharged clays (pyrophyllite and talc) and montmorillonites with different types of counter ions (Na<sup>+</sup>, Cs<sup>+</sup>, Ca<sup>2+</sup> and Sr<sup>2+</sup>) were simulated and compared with diffraction data. The polarizable force field was then used to study the diffusion of cations and water molecules in montmorillonite. Our results were compared with those given by non polarizable force-fields and with the available experimental data.

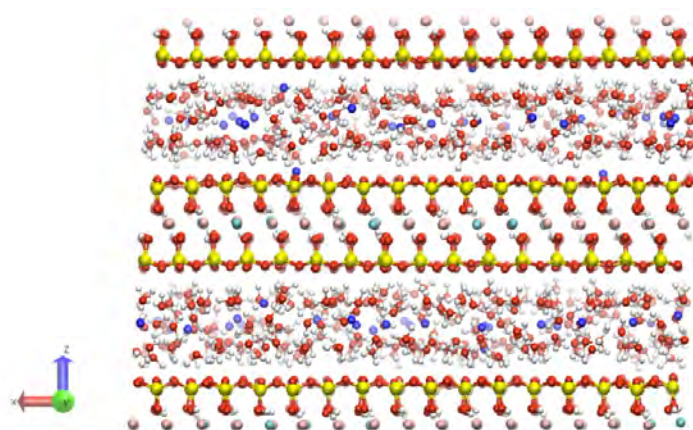


Figure : Structure of Na-montmorillonite

[1] Rotenberg, B. et al., J. Am. Chem. Soc., 2011, 133, 20521

[2] Botan, A. et al., J. Phys. Chem. C., 2013, 117, 978-985

[3] Marry, V. et al., J. Phys. Chem. C., 2013, 117, 15106-15115

[4] Kamath, G. et al., J. Phys.: Condens. Matter, 2013, 25, 305003

## Structure and behavior of water and carbon dioxide on clay mineral surfaces

Randall T. Cygan and Craig M. Tenney

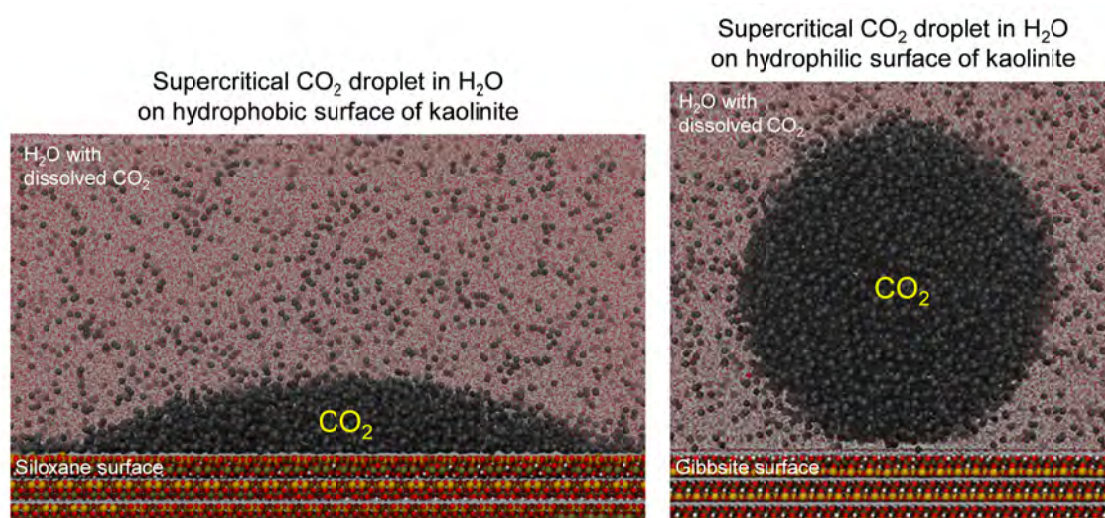
Geochemistry Department, Sandia National Laboratories

Albuquerque, New Mexico, 87185-0754, USA; rtcygan@sandia.gov

Structure and reactivity of minerals in aqueous environments control many important geochemical processes. Basal surfaces and interlayers of clay minerals, in particular, provide constrained interfacial environments to better evaluate these complex processes. We have used large-scale classical molecular dynamics simulations to examine the interfacial structure and adsorption behavior associated with kaolinite and smectite phases. The models provide insights into the wettability of different fluids—water, electrolyte solutions, and supercritical carbon dioxide—on silicate mineral surfaces.

Large-scale molecular dynamics simulations were used to study the behavior of aqueous fluids and supercritical carbon dioxide on both hydrophilic and hydrophobic basal surfaces of common clay minerals. In the presence of a bulk aqueous phase, supercritical carbon dioxide forms a non-wetting droplet above the hydrophilic surface of kaolinite. This carbon dioxide droplet is separated from the mineral surface by distinct layers of water, which prevent the carbon dioxide droplet from interacting directly with the mineral surface. Conversely, both carbon dioxide and water molecules interact directly with the hydrophobic surface of kaolinite. Simulation results suggest the influence of clay mineral composition and adsorbed species on interfacial structure, interfacial tension, contact angle, and related properties. Molecular simulations of water and hydrated cations within the clay interlayer of smectites reveal a dynamic between cation hydration and the adsorption of the cation at the clay surface. Analysis of librational modes of water molecules derived from power spectra and by inelastic neutron scattering experiments indicates the influence of hydration state, interlayer cation, and location of layer charge on water dynamics.

This work is supported by the U.S. Department of Energy, Office of Basic Energy Sciences. Sandia National Laboratories is a multi-program laboratory managed and operated by Sandia Corporation, a wholly owned subsidiary of Lockheed Martin Corporation, for the U.S. Department of Energy's National Nuclear Security Administration under contract DE-AC04-94AL85000.



## Modeling the transport of water and ions tracers in a micrometric sample of clay

Pauline Bacle<sup>1</sup>, Benjamin Rotenberg<sup>1</sup>, Jean-François Dufrêche<sup>3</sup>, Virginie Marry<sup>1</sup>

<sup>1</sup>UMR 8234 PHENIX, CNRS, UPMC Univ. Paris 06, 4 place Jussieu, 75005 PARIS, France

<sup>2</sup>Institut de Chimie Séparative de Marcoule (ICSM), UMR 5257, CEA-CNRS-Université Montpellier, France

Clay minerals have a significant role in many environmental applications because of their properties such as cation exchange, swelling behavior, retention and low permeability. Numerous experimental and theoretical studies have focused on predicting the performances of clay as barrier materials in the containment of high-level radioactive waste by evaluating the diffusion of mobile species in compacted, water-saturated Na-bentonites<sup>[1]</sup>. Conceptual models<sup>[2,3]</sup> and simulations<sup>[4]</sup> have been developed to understand the transport of tracers in clay samples. One difficulty arises from the complex, multi-porosity structure of clay materials since particles of clay consist of stacks of parallel negatively-charged layers separated by nanopores while particles are themselves separated by larger pores.

Here we present a simple model which enables us to investigate the transport of water and ionic ( $\text{Na}^+$ ,  $\text{Cl}^-$ ) tracers in a micrometric sample of clay. In our model, the clay particles are modeled by cylindrical platelets the dimensions of which are calculated according to the density of clay  $\rho_b$ . Furthermore, the cylinders can intersect each other, allowing us to reach high densities and thus investigate the diffusion in highly compacted porous media. We use Brownian dynamics to describe the diffusion of the tracer in the sample. The diffusion coefficients of the species vary with regard to the location of the tracer within the porous medium. The diffusion outside the platelets (e.g. in the interparticle pores) is the same as in the bulk solution but the diffusion inside the platelets is slowed by confinement and depends on the charge of the tracer. The concentrations and the diffusion coefficients in the interparticle pores and the platelets are used as simulation parameters and are calculated based on experimental values<sup>[5,6]</sup> and/or determined from molecular dynamics simulations<sup>[2,7]</sup>. We evaluated the global diffusion coefficients of three tracers (water,  $\text{Na}^+$  and  $\text{Cl}^-$ ) for various densities and salinities from the trajectories of the tracer and compared the simulations results with experimental data from tracer diffusion experiments<sup>[1]</sup>.

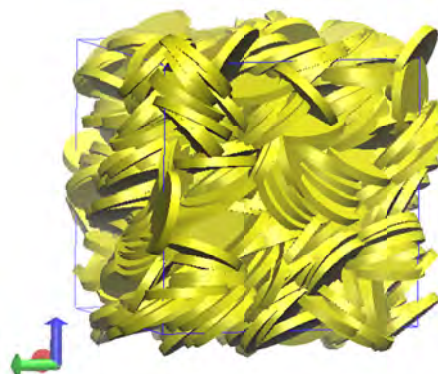


Fig. 1. Simulation box (length  $\sim 1.9\mu\text{m}$ ) representing a sample of clay at  $\rho_b = 0.7\text{kg/L}$ . The box contains 922 platelets with a radius of  $2500\text{\AA}$  and a height of  $688\text{\AA}$ .

[1] Bourg, I.C. and Tournassat, C. Self-diffusion of water and ions in clay barriers. In : Natural and Engineered Clay Barriers (Tournassat, C., Steefel, C. I., Bourg, I. C. and Bergaya, F., eds.), vol. 6 of *Developments in Clay Science*, chap. 6. Elsevier, 1st edition ed., 2015.

[2] Bourg, I. C. and Sposito, G. Connecting the molecular scale to the continuum scale for diffusion processes in smectite-rich porous media. *Environ. Sci. Technol.*, 44(6):2085–2091, **2010**.

[3] Birgersson, M. and Karnland, O. Ion equilibrium between montmorillonite interlayer space and an external solution - consequences for diffusional transport. *Geochim. Cosmochim. Ac.*, 73:1908–1923, **2009**.

[4] Churakov, S. V. and Gimmi, T. Up-scaling of molecular diffusion coefficients in clays: A two-step approach. *J. Phys. Chem. C*, 115:6703–6714, **2011**.

[5] Holmboe, M., Wold, S. and Jonsson, M. Porosity investigation of compacted bentonite using XRD profile modeling. *J. Contam. Hydrol.*, 128:19–32, **2012**.

[6] Malikova, N., Cadène, A., Marry, V., Dubois, E., and Turq, P. Diffusion of Water in Clays on the Microscopic Scale: Modeling and Experiment. *J. Phys. Chem. B*, 110(7):3206–3214, **2006**.

[7] Marry, V. and Turq, P. Microscopic simulations of interlayer structure and dynamics in bihydrated heteroionic montmorillonites. *J. Phys. Chem. B*, 107:1832–1839, **2003**.

## Amino acids, layered double hydroxides and the origins of life

Valentina Erastova<sup>1</sup>, H. Christopher Greenwell<sup>1</sup>

<sup>1</sup>Department of Earth Sciences, Durham University, South Road, Durham, DH1 3LE UK  
E-mail: valentina.erastova@durham.ac.uk

The role of mineral surfaces in concentrating and facilitating the polymerisation of simple protobiomolecules in the early Earth has been the subject of much research. Layered double hydroxides (LDH) provide a favourable environment for amino acid concentration and the occurrence of the first prebiotic chemical reactions that may have led to the origins of life.

With molecular dynamics and quantum mechanics we study the intercalation of amino acids and simple peptides in LDH. We show how LDH can concentrate, align and order amino acids, such as by favouring the co-alignment for a peptide forming condensation reaction. We observe how a mineral surface can provide attractive-dispersive forces that could assist the simple peptide accumulation and folding. As such, our findings support the hypothesis of life having originated via clay-assisted peptide formation.

**Keywords:** MD, DFT, origins of life, clay, amino acids, peptides

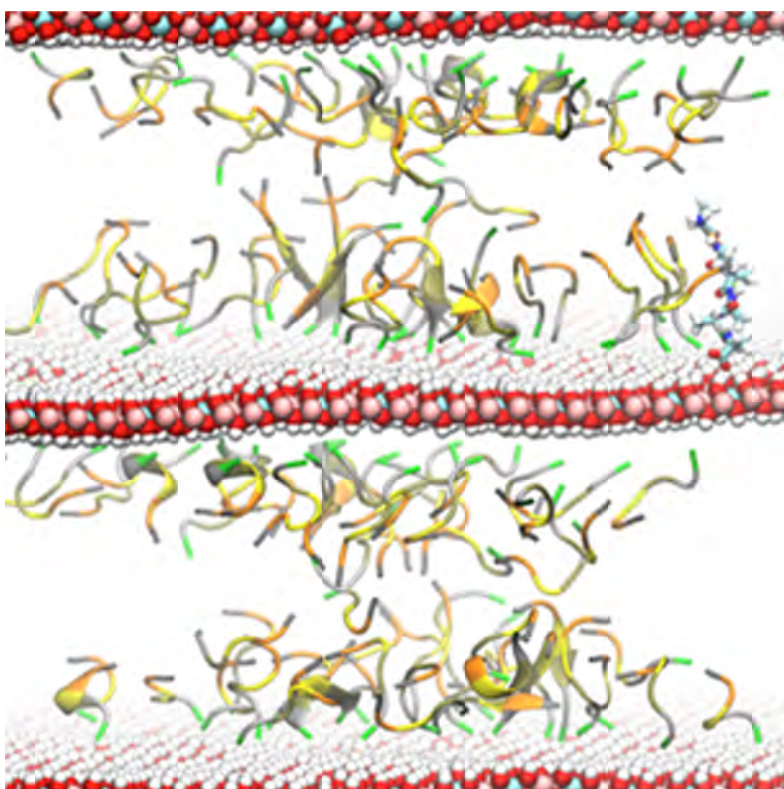


Figure 1: LDH intercalated with hexa-alanine peptides in water. C-termini (green) maintain a contact with the surface



## Modelling clay-polymer nanocomposites using a multiscale approach

Peter Coveney, University College London

We have developed an advanced multiscale simulation system to predict the properties of polymer-clay nanocomposites based on their molecular structures and composition. These methods could have applications in modelling a wide range of materials and it is our aim to create a “virtual lab” to compute the properties of new soft materials based simply on knowledge of their chemical composition, molecular structure and processing conditions [1]. Here we will present our findings from modelling chemically specific combinations of clay and polymers, where we use our multiscale methods and tools to take us from a parameter free quantum description to atomistic and coarse-grained simulations, ultimately leading to predictions of the materials properties of these nanocomposites. Our simulations approach realistic sizes of clay platelets (diameter 100 Å) at low clay volume fractions (5%). These systems exhibit property enhancements compared to the pristine polymer (elastic properties, gas permeation) but homogenous dispersion of the clay sheets is required.

Our multiscale approach provides us with predictions of the melt intercalation behaviour and final morphologies of montmorillonite clay – polyvinyl-alcohol and montmorillonite clay – polyethylene-glycol systems, and associated organic-treated clays. Many hitherto unobserved phenomena come into view as a result of this study, including the dynamical process of polymer intercalation into pristine and organo-treated clay tactoids and the ensuing aggregation of polymer-entangled tactoids into larger structures. We observe the role of surfactants and are able to elucidate how it facilitates polymer intercalation and ultimately clay sheet exfoliation, which is driven by attraction to the clay surfaces.

From our multiscale simulations, we can compute various characteristics of these nanocomposites, including clay-layer spacings, out-of-plane clay sheet bending energies, X-ray diffractograms and materials properties, which we relate to the system's final morphology.

[1] J.L. Suter, D Groen, P.V. Coveney, *Adv. Mater.* 2015, 27, 966–984

## $\mu$ -oxo-Fe<sup>+3</sup>-phenanthroline complexes intercalated in montmorillonite: molecular structures and properties

C. Ignacio Sainz-Diaz<sup>1</sup>, Fabrizio Bernini<sup>2</sup>, Elena Castellini<sup>2</sup>, Daniele Malferrari<sup>2</sup>, Marco Borsari<sup>2</sup>, and M. Franca Brigatti<sup>2</sup>

<sup>1</sup> Instituto Andaluz de Ciencias de la Tierra (CSIC-UGR), Av. De las Palmeras, 4, 18100-Armilla, Granada (Spain), ignacio.sainz@iact.ugr-csic.es

<sup>2</sup> Dipartimento di Scienze Chimiche e Geologiche, Universita' degli Studi di Modena e Reggio Emilia, Via Campi 183, I-41125 Modena (Italy)

Smectites are good candidates for nanofunctionalized materials due to their high adsorption properties. The high cation exchange capacity and swelling properties of 2:1 phyllosilicates allow the formation of organoclays where the behavior of water in the nanospace of interlayer is important. The Fe complexes with phenanthroline and other diimine derivatives have interesting analytical and catalytic applications. The  $\mu$ -oxo bridged binuclear Fe complexes have a special interest due to the critical role of  $\mu$ -oxo bridged binuclear center in the catalytic activity of some iron proteins, such as, hemerythrin and ribonucleotide reductase (Bernini et al., 2015).

The complexation of Fe<sup>3+</sup> with a neutral ligand allows the complexes to retain the positive charge despite the  $\mu$ -oxo bridge and this property is essential to immobilize iron<sup>+3</sup> on the negative surfaces of clay minerals. In this work, we study the interactions of  $\mu$ -oxo bridged binuclear iron complexes of 1,10-phenanthroline in the interlayer of montmorillonite. The experimental research has been complemented with computational modelling work at quantum mechanical level based on density functional theory (DFT) and periodical boundary conditions. This combination has allowed the identification of the geometrical disposition of the complexes, the hydration coordination of the water molecules and the explanation of the physico-chemical properties of these nanofunctionalized materials.

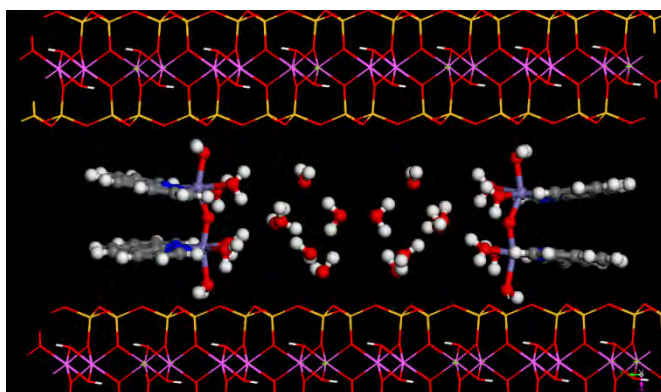


Figure. Complexes of  $\mu$ -oxo-bis[Fe<sup>+3</sup>-1,10-phenanthroline] in the interlayer of montmorillonite.

Bernini, F., Castellini, E., Malferrari, D., Borsari, M., Brigatti, M.F. (2015). Stepwise structuring of the adsorbed layer modulates the physico-chemical properties of hybrid materials from phyllosilicates interacting with the  $\mu$ -oxo Fe<sup>+3</sup>-phenanthroline complex. *Microporous and Mesoporous Materials* (in press). DOI: 10.1016/j.micromeso.2015.02.039.

## Experimental and theoretical insights into the interaction of methylene blue with kaolinite

Cliff T. Johnston<sup>1</sup>, Robert A. Schoonheydt<sup>2</sup>, Jeffery A. Greathouse<sup>3</sup>, Dawn L. Geatches<sup>4</sup>, Darin Q. Pike<sup>5</sup>,  
H. Christopher Greenwell<sup>6</sup>, Jennifer Wilcox<sup>7</sup> and Randall T. Cygan<sup>3</sup>

<sup>1</sup>Crop, Soil and Environmental Sciences, Purdue University, 915 W State St., West Lafayette, IN 47907  
(USA)

<sup>2</sup>Center for Surface Chemistry and Catalysis, KU Leuven, Kasteelpark Arenberg 23, 3000 Leuven  
(Belgium)

<sup>3</sup>Geochemistry Department, Sandia National Laboratories, P.O. Box 5800, MS 0754, Albuquerque,  
NM 87185-0754, USA

<sup>4</sup>Hartree Centre, Daresbury Laboratory (STFC), Warrington, WA4 4AD, UK

<sup>5</sup>Chemical and Biological Systems Department, Sandia National Laboratories, P.O. Box 5800, MS  
0734, Albuquerque, NM 87185-0734, USA

<sup>6</sup>Department of Earth Sciences, Durham University, South Road, Durham DH1 3LE, UK

<sup>7</sup>Energy Resources Engineering, Earth Sciences, Stanford University, CA 94305-2220,

Cationic dyes are a group of 'classic' molecular probes that have been used extensively in the mineral processing industry for the past 65 years. Of these cationic dyes, methylene blue (MB) has been used the most extensively in both applied mining and laboratory research. The interaction of methylene blue, a cationic organic dye, with clay minerals has been studied for many years using a wide range of spectroscopic, sorption and theoretical methods. For clay minerals, much of this work has focused on the interaction of methylene blue with expandable 2:1 clay minerals where sorption, orientation and optical properties of sorbed methylene blue have been clearly related to structure, charge density and charge location. Despite wide-scale adoption and utility in kaolin-related fields, surprisingly little is known about the mechanisms of interaction between methylene blue and kaolinite. The interaction of methylene blue with a suite of kaolins of varying size, aspect ratio, and structural disorder is examined in the present study using a combination of spectroscopic, quantum and classical molecular simulation methods. The spectral signature of methylene blue sorbed to kaolinite reveals interesting spectral features related to the unique types of surfaces found on kaolinite. In addition, a combination of quantum (density functional theory) and classical molecular simulation methods were used to provide molecular detail of such adsorption processes, specifically the adsorption of methylene blue onto kaolinite basal surfaces. The structure and energetics of adsorbed methylene blue at infinite dilution are consistent with the gas-phase binding results, which indicate that monomer adsorption is driven by strong interfacial forces rather than by the hydration properties of the dye.

## MD simulations of low-salinity enhanced oil recovery

Thomas Underwood<sup>1</sup>, Valentina Erastova<sup>1</sup>, Pablo Cubillas<sup>1</sup> and H. Chris Greenwell<sup>1</sup>

<sup>1</sup>Department of Earth Sciences, Durham University

E-mail: thomas.underwood@durham.ac.uk

### Introduction

In an age of increasing energy demand it is clear that we must utilise our energy resources as efficiently as possible. Current oil extraction methods only recover in the region of a third of the oil in a reservoir. Presently oil is recovered through primary methods (pressure differentials) and secondary methods (water flooding). However, it has been shown that incremental oil recovery beyond secondary methods can be achieved via using water floods of decreased salinity [1]. The aim of this research is to bring clarity to the fundamental mechanisms behind low-salinity enhanced oil recovery (EOR), a technique where sea water, partially desalinated, is used to push increasing amounts of crude oil from existing, and future, oil reservoirs, increasing the reservoir lifetime and overall production.

### Background theory

The phenomenon of low-salinity enhanced oil recovery is thought to be due to the complex interactions between the organic oil compounds, inorganic colloid clay particles and the simple salt ions within the reservoir. Many theories have been hypothesised to describe the phenomenon, from the electric double layer expansion of charged clay particles [2], to divalent cation bridging between clay and organic [2], and pH effects of the local system surrounding the clay [3].

### Conclusions

Using large-scale classical molecular simulations, Figure 1, our research shows that it is neither the effect of double layer expansion nor divalent cation bridging that explains the phenomenon of low-salinity enhanced oil recovery [4]. Rather, the results show that it is the pH level surrounding the clay, and thus it is the altered charge of the organic molecules that is the determining factor driving the titular effect.

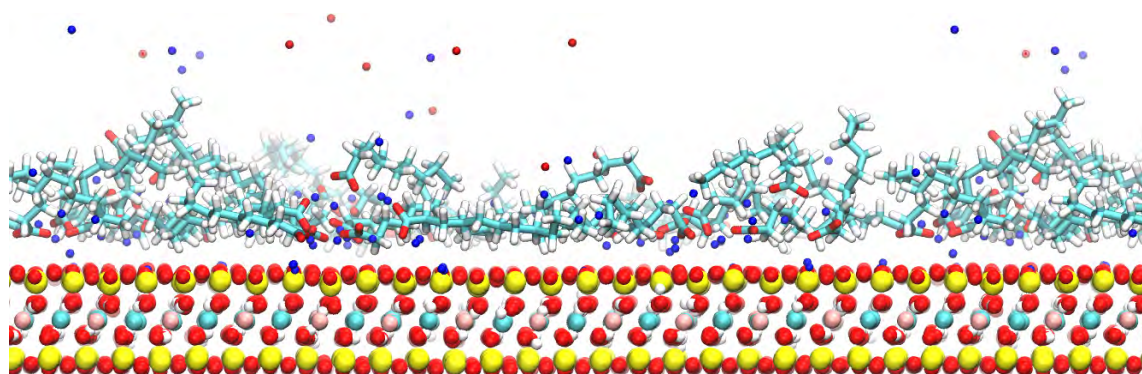


Figure 2: A snapshot presenting the interaction between an initially oil-wet montmorillonite clay particle, charged decanoate organics, and a salt concentration of 5 parts NaCl per thousand water molecules (water molecules not represented)

Monday  
6<sup>th</sup> July

Lecture room 2

Halloysite a unique,  
diverse and widely  
useful natural  
nanomaterial

## Halloysite clay nanotubes as novel carriers for drug delivery

Chiara Dionisi<sup>1,2</sup>, Neman A.N. Hanafy<sup>2,3</sup>, Viviana Vergaro<sup>2</sup>, Yuri M. Lvov<sup>4</sup> and Stefano Leporatti<sup>2</sup>

<sup>1</sup> University of Pisa, Lungarno Pacinotti, 43, 56126 Pisa (PI), Italy

<sup>2</sup> CNR NANOTEC - Istituto di Nanotecnologia, Polo di Nanotecnologia, c/o Campus Ecotekne, via Monteroni - 73100 Lecce, Italy stefano.leporatti@nano.cnr.it

<sup>3</sup> Department of Mathematics and Physics "E. De Giorgi" University of Salento, Via Monetrone 73100 Lecce (LE), Italy

<sup>4</sup> Institute for Micromanufacturing (IfM), Louisiana Tech University, Ruston (USA)

The increasing interest in nanoscience and nanotechnology has led to the development of advanced materials with unique chemical and physical properties, such as liposomes, nanocapsules or carbon nanotubes, and also to the investigation of nanostructured natural materials. Halloysite is a clay mineral, chemically similar to kaolinite, which has a predominantly hollow tubular structure, in the submicrometer range<sup>1</sup>. Halloysite has found an important role as nanocarrier for encapsulation, delivery and controlled release of biologically active molecules and drugs<sup>2-4</sup>. Halloysite nanotubes (HNTs) sizes varies between 0.5 – 5 micrometers in length and their external diameter is of  $50 \pm 10$  nm and their lumen is around 15 nm, when they are completely rolled<sup>3</sup>. The use of halloysite nanotubes offers significant advantages over other systems: they are naturally occurring, easily available and not expensive, and the loading procedure is quite simple. In this work, we characterize HNTs, in terms of both structure and biocompatibility, and use them for loading and controlled release of polyphenols such as Resveratrol or Curcumin. Curcumin is a naturally occurring yellow compound, found as the main constituent in the rhizome of the plant *Curcuma Longa*, grown in tropical Southeast Asia. It exhibits anti-oxidative, anti-inflammatory and anti-cancer properties<sup>5</sup>, but its therapeutic potential is hindered by its low water solubility and bioavailability, whence the need for suitable carriers.

The structure of HNTs has been analyzed with a combination of Transmission Electron Microscopy (TEM), Scanning Electron Microscopy (SEM) and Scanning Force microscopy (SFM) imaging. The loading efficiency of polyphenols has been determined by TEM analysis and absorbance measurements, while the release kinetics have been studied photometrically. To provide an additional control over the drug release rate, HNTs have been coated with polyelectrolyte multilayers by the Layer-by-Layer (LbL) technique. The stability of naked and coated HNTs in solution has been evaluated by Dynamic Light Scattering measurements. MTT assay has also been used to investigate the biocompatibility of HNTs and the anti-cancer activity of naked polyphenol and drug-loaded halloysite, at different concentrations and upon different time intervals against the breast cancer cell line MCF-7 whereas confocal fluorescence microscopy imaging has been used to monitor the intracellular localization of both HNTs and polyphenols. Our results envisage the use of Halloysite Nanotubes as efficient carriers for polyphenols delivery to tumor cells.

R. Price, B. Gaber, Y. Lvov (2001) Release Characteristics of Tetracycline, Khellin and NAD from Halloysite; a Cylindrical Mineral for Delivery of Biologically Active Agents. *J. Microencapsulation* 18, pp. 713-723.

Y. Lvov, D. Shchukin, H. Mohwald, R. Price (2008) Clay Nanotubes for Controlled Release of Protective Agents. *ACS Nano Journal*, v.2, pp. 814-820.

V. Vergaro, E. Abdullayev, Y.M. Lvov, A. Zeitoun, R. Cingolani, R. Rinaldi and S. Leporatti (2010) Cytocompatibility and Uptake of Halloysite Clay Nanotubes *Biomacromolecules* 11, 820–826.

V. Vergaro, Y. M. Lvov and S. Leporatti (2012) Halloysite Clay Nanotubes for Resveratrol Delivery to Cancer Cells *Macromolecules Bioscience* 12, 9, pp. 1265-1271.

S. Shishodia, G. Sethi and B. B. Aggarwal, (2005) Curcumin: Getting Back to the Roots, *Annals of the New York Academy of Sciences*, Vol. 1056, No. 1, pp. 206-217.

## Global occurrence and geology of halloysite

Ian Wilson

Consultant Geologist, Withielgoose Farmhouse, Withiel, Bodmin, Cornwall, PL30 5NW, UK  
ian.r.wilson@btinternet.com

Halloysite is an aluminosilicate clay mineral with formula  $\text{Al}_2\text{Si}_2\text{O}_5(\text{OH})_4$  and was named after Belgian geologist Jean Baptise Julien d'Omalius d'Halloy from an occurrence of the mineral near Liège in Belgium.

The tubular morphology of halloysite is formed in a wide range of geological environments from the alteration of various rock types. Intrusive acidic coarse-grained rock types, such as granites, pegmatites and anorthosite, cooled slowly with potash and sodic feldspars subsequently being altered to kaolinite, halloysite and other clay minerals by a combination of hydrothermal and meteoric fluids. In mixed kaolinite and halloysite the length of the tubes are up to 20 microns or more and these clays are used as fillers and ceramics from deposits in Brazil, China and Thailand.

In New Zealand at Kerikeri-Matauri Bay area of Northland, North Island, an acidic volcanic rhyolite was extruded and cooled rapidly with fine-grained feldspar being altered to halloysite. The mine and processing plant are currently operated by Imerys supplying halloysite mainly for porcelain and bone china.

The Dragon mine of Applied Minerals Inc. is now producing halloysite from the Tintic district of Utah 75 miles southwest of Salt Lake City. Geologically in the Dragon Mine area the host rocks consist of Tintic quartzite aged about 513 Ma, Ajax-Opex dolomite from around 500-488 Ma, and the Silver City monzonite about 33.6 Ma. Iron Ore was later introduced into the monzonite with coeval volcanic activity of andesite and latite.

Zones of up to 100% white halloysite with dominantly cylindrical and some polygonal morphology tubes up to 50-500 nm in length are adjacent to goethite-hematite iron ore. The pureness of the halloysite is attributed to precipitation from Al-Si solutions. Applied Minerals Inc. now offers Dragonite™ products based on the tubular nature of the halloysite for various markets.

Smaller occurrences of tubular halloysite are encountered in China, Turkey and elsewhere.

## Water, pH and iron: Are these the keys to selecting halloysites for applications as nanotubes?

Jock Churchman<sup>1</sup>, Pooria Pabakhsh<sup>2</sup>, David Lowe<sup>3</sup> and Benny Theng<sup>4</sup>

<sup>1</sup> School of Agriculture, Food & Wine, University of Adelaide, SA 5005, Australia (jock.churchman@adelaide.edu.au), <sup>2</sup> School of Engineering, Monash University Malaysia, Bandar Sunway, 47500 Selangor, Malaysia, <sup>3</sup> Earth and Ocean Sciences, University of Waikato, Private Bag 3105, Hamilton, New Zealand, <sup>4</sup> Landcare Research, Private Bag 11052, Palmerston North, New Zealand

Halloysite has long fascinated clay mineralogists and many questions remain about its peculiar properties and even about its mode of formation. Nonetheless, only a few papers were published on this mineral until 2006. Its main use was as a raw material for ceramics, in place of kaolinite. The approximately 1000 papers published in the 8-9 years since then attest to recognition that its often nanotubular nature makes it a very promising nanomaterial. As such it has proven widely useful, as reinforcing fillers in plastics, as carriers for the controlled internal release of medicines – and of pesticides – and also for immobilizing catalysts.

The various uses of halloysite nanotubes (HNTs) require different properties for their optimum application. Long and uniform tubes with high aspect ratios, giving high surface areas provide the best fillers while large internal diameters (lumen) enable the most effective tubes for carriers and templates for catalysts and chemical reactions. Most studies of the applications of HNTs have used a sample from a single source although a few have compared examples from a small number of sources. Even so, no rational basis has been established for selecting HNTs in relation to the requirements of their intended applications. Through a survey of the literature as well as a presentation of previously unpublished data, this paper aims to provide indicators of the suitability of occurrences or of syntheses of halloysite for the different types of applications of HNTs as well as to identify gaps in knowledge. It has been found that:

1. Continuous hydration is needed to form halloysite rather than kaolinite in nature. This is essential for interlayer water, itself the reason why many halloysites occur as nanotubes.

2. A polar driving force is needed to attract water to the interlayer. Possibilities include tetrahedral Al –or Fe(II) in octahedra: these help provide a higher negative layer charge attracting water to the interlayer surface. It may also arise from the contrasting variable charge behaviours of the Al octahedral and Si tetrahedral sheets in kaolins. Octahedral sheets are positively charged up to pH 8.5 but tetrahedral sheets are always negatively charged. Positive charges on the octahedral sheets increase with decreasing pH, providing a driving force for the uptake of water.

3. Kaolinites can be converted to nanotubes by either washing out an intercalate (of potassium acetate or DMSO, etc) with water or by dissolving an organic intercalate in an organic solvent; Kaolinites converted to nanotubes via organic solvents have very small lumen and only a water route leads to a hydrated halloysite.

4. Ordering in their organic complexes show that some halloysites, at least, are fundamentally different from kaolinite: they have a 2-layer structure similar to dickite.

5. Not all halloysites are tubular. In tubular halloysites, Fe content seems to relate to tube length. It is not known if there is any relation between Fe content and lumen size. The determinants of lumen size require more research.



## Functionalisation of halloysite nanotubes for sustainable nanocomposites

Giuseppe Lazzara, Giuseppe Cavallaro, Stefana Milioto and Filippo Parisi  
University of Palermo, Department of Physics and Chemistry, Viale delle Scienze Pad. 17, Italy  
giuseppe.lazzara@unipa.it

Halloysite nanoclays (HNTs) are promising nanomaterials because of their versatile properties, such as hollow tubular morphology and tunable surface chemistry. HNTs are biocompatible, not toxic and abundantly available at low cost. Due to these characteristics HNTs are suitable for development of hybrid sustainable materials, which are suitable for wastewater remediation, green packaging and drug delivery. HNTs are quite polydisperse in size with a length of ca. 1  $\mu\text{m}$ , while the external diameter and the lumen range between 50-80 nm and 10-15 nm, respectively. Chemically, halloysite is composed of gibbsite-like octahedral sheet with (Al-OH) groups on the inner surface and siloxane (Si-O-Si) groups on the external surface. This different chemistry allows the selective modification of HNTs surfaces. We performed several chemical functionalizations of HNTs to confer properties valuable in specific applications. The HNTs inner lumen was modified to generate an hydrophobic microenvironment for the solubilization of compounds sparingly soluble in water (aromatic and aliphatic oils).<sup>1,2</sup> In contrast, outer surface hydrophobization was employed to create reverse inorganic micelles to be used as dispersants for hydrophilic compounds (such as  $\text{CuSO}_4 \cdot 5\text{H}_2\text{O}$ ) in a confined environment within an organic solvent.

Pristine and modified HNTs were dispersed in biopolymeric matrices to obtain functional nanocomposites. The morphology as well as physico-chemical properties such as mechanical, thermal, wettability were affected by specific interactions between the polymer and the filler.<sup>3,4</sup>

1. Cavallaro, G.; Lazzara, G.; Milioto, S.; Parisi, F.; Sanzillo, V. *ACS Appl. Mater. Interfaces* **2014**, *6*, 606–612.
2. Cavallaro, G.; Lazzara, G.; Milioto, S. *J. Phys. Chem. C* **2012**, *116*, 21932–21938.
3. Cavallaro, G.; Donato, D. I.; Lazzara, G.; Milioto, S. *J. Phys. Chem. C* **2011**, *115*, 20491–20498.
4. Cavallaro, G.; Lazzara, G.; Konnova, S.; Fakhrullin, R.; Lvov, Y. *Green Materials* **2014**, *2*, 232-242.

## Correlations among mineralogical and physical properties of halloysite nano-tubes (HNTs)

Stephen Hillier<sup>1,2</sup>, Helen Pendlowski<sup>1</sup>, Tony Fraser<sup>1</sup>, Jean Robertson<sup>1</sup>, Evelyne Delbos<sup>1</sup>, Ian Phillips<sup>1</sup>,  
Nia Gray<sup>1</sup> and Ian Wilson<sup>3</sup>

<sup>1</sup>The James Hutton Institute, Craigiebuckler, Aberdeen, AB15 8QH  
stephen.hillier@hutton.ac.uk

<sup>2</sup>Department of Soil and Environment, Swedish University of Agricultural Sciences, Box  
7014, Uppsala SE-750 07, Sweden

<sup>3</sup>Consultant, Withielgoose Farmhouse, Withiel, Bodmin, Cornwall, PL30 5NW

The kaolin sub group mineral halloysite may occur in a variety of morphological forms but the tubular form is undoubtedly the most common and well known variety. As a naturally occurring nano-tube (HNT) interest in technological uses for halloysite has increased dramatically over recent years. These range from its incorporation into polymers to the controlled release or containment of compounds by its nano-tubular form. Here we review the mineralogical characteristics of tubular halloysite based on a set of samples of diverse provenance. It will be shown how X-ray diffraction, infrared-spectroscopy and electron microscopy observations are related in terms of some of the characteristics and properties of tubular halloysite. For some technological applications these different characteristics of tubular halloysites may have important influences on their function.

## A comprehensive analysis of the structure of imogolite nanotubes

M.S. Amara, S. Rouzière, E. Paineau and P. Launois

Laboratoire de Physique des Solides, UMR CNRS 8502, Université Paris Sud, 91405, Orsay, France

Imogolites, ‘tubular clays’ with a diameter on the order of a nanometer, discovered as early as 1962 in volcanic soils [1], can now be synthesized through controllable pathways. They thus appear as most promising candidates for molecular recognition applications taking advantage of their one-dimensional porosity (catalysis, molecular sieves, sensors, etc) [2]. In 1972, natural imogolite nanotubes (INT) were proposed to have nominal composition  $(\text{OH})_3\text{Al}_2\text{O}_3\text{SiOH}$  and to be formed of a curved gibbsite-like layer whose vacancies are bonded by isolated  $[\text{Si}(\text{Ge})\text{O}_4]$  tetrahedra [3] (figure (a)). It was shown later that silicon can be substituted by germanium [4]. Different studies corroborated the structural proposal of Cradwick and co-workers [3] but, to the best of our knowledge, more than forty years after their seminal article, no complete determination of INT structure has been achieved based on experimental data. We present here the first comprehensive X-ray scattering study, from small angles to wide angles, of three sorts of INT, in solution: natural and synthetic  $(\text{OH})_3\text{Al}_2\text{O}_3\text{SiOH}$  nanotubes, with different diameters despite their similar composition, and synthetic  $(\text{OH})_3\text{Al}_2\text{O}_3\text{GeOH}$  nanotubes [5]. We will explain the strategy we have developed to minimize interatomic distortions and to account for both small and wide angle X-ray scattering data (figure (b)). The refined atomic structures will be discussed with respect to energetical minimizations proposed recently [6]. It is of special interest since these numerical approaches are used as guides to predict new imogolite-like structures [7]. Our methodology should also be applied in the near future to newly-discovered imogolite-type nanotubes (double-walled nanotubes or functionalized nanotubes [2,8]).

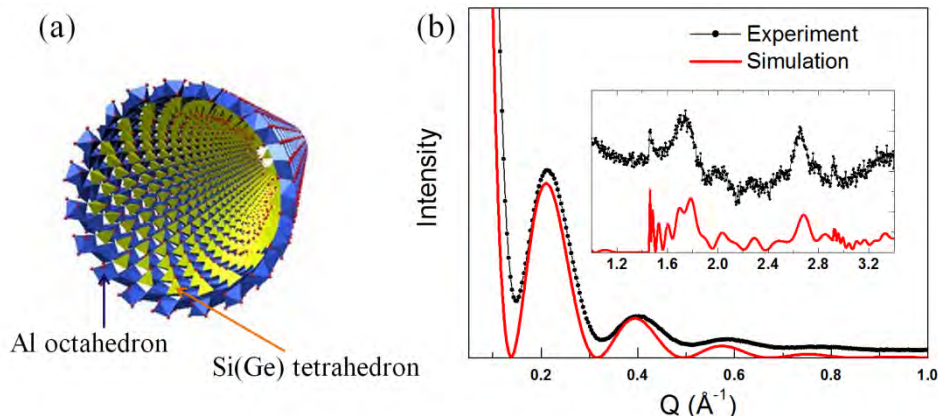


Figure. (a) Schematic representation of an imogolite nanotube, with its curved gibbsite-like wall formed of Al octahedra and with Si(Ge) tetrahedra inside; (b) X-ray scattering pattern of  $(\text{OH})_3\text{Al}_2\text{O}_3\text{GeOH}$  nanotubes, together with its simulation for the refined structure, showing the good agreement between experiment and simulation.

- [1] N. Yoshinaga, S. Aomine, *Soil Sci. Plant Nutr.* **8**, 22 (1962)
- [2] D. Y. Kang et al, *Nat. Comm.* **5**, 3342 (2014) ; M.S. Amara et al., *Chem. Mater.*, DOI: 10.1021/cm503428q
- [3] P. Cradwick et al, *Nature* **240**, 187 (1972)
- [4] S. Wada and K. Wada, *Clays and Clay Minerals* **30**, 123 (1982)
- [5] M.S. Amara, S. Rouzière, E. Paineau, P. Launois, article in preparation
- [6] K. Tamura, K. Kawamura, *J. Phys. Chem. B* **106**, 271 (2002); S. Konduri et al, *Phys. Rev. B* **74**, 033401 (2006); L. Guimarães et al, *ACS Nano* **1**, 362 (2007); M. Zhao et al, *J. Phys. Chem. C* **113**, 14834 (2009) ; M. P. Lourenço et al, *J. Phys. Chem. C* **118**, 5945 (2014)
- [7] L. Guimarães et al, *Phys. Chem. Chem. Phys.* **15**, 4303 (2013)
- [8] P. Maillot et al, *JACS* **132**, 1208 (2010) ; M.S. Amara et al, *Chem. Comm.* **49**, 11284 (2013)

## Halloysite nanotubes for biomedical application: Opportunities and challenges

Mingxian Liu, Rui He, Jing Yang, Changren Zhou

Department of Materials Science and Engineering, Jinan University, Guangzhou 510632, China;

Email: liumx@jnu.edu.cn

As tube-like natural nanomaterials, halloysite nanotubes (HNTs) have potential applications for improved tracking of cells, sensing of microenvironments, delivering of transfection agents, and scaffolding for incorporating with the host's body<sup>1</sup>. HNTs exhibit high mechanical strength, good biocompatibility, hemostatic property, and wound healing ability as reported recently. The structure of HNTs is shown in Figure 1(a).

Firstly, HNTs can be incorporated into polymer scaffolds providing structural reinforcement as well as imparting novel properties such as promoting cell growth<sup>2</sup>. The incorporation of HNTs can also enhance blood clotting, platelet activation ability, and wound healing ability of chitosan<sup>3</sup>. Bio-functionalization has made HNTs able to generate a new class of bioactive nanocarriers which are conjugated with drug, proteins, carbohydrates, or nucleic acids for controlled delivery<sup>4</sup>. HNTs coatings on a microscale flow system can promote increased capture of leukemic and epithelial cancer cells from flow<sup>5</sup>. All of these current research topics aims at translating these biotechnology modified nanotubes into potential novel therapeutic approaches. Figure 1(b) shows the biomedical applications of HNTs.

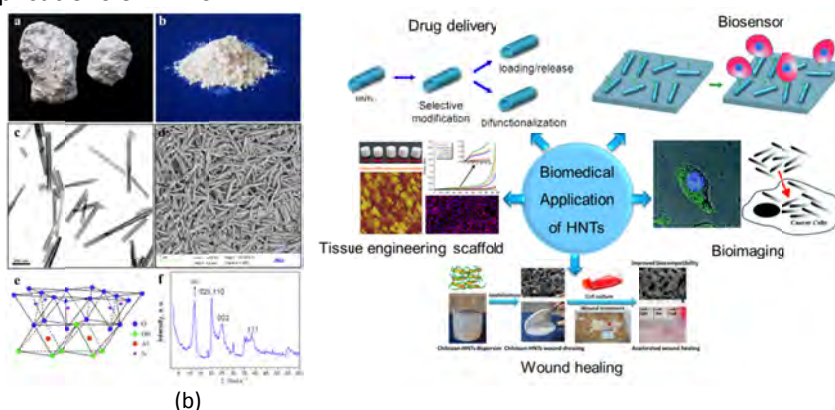


Figure 1 The structure and biomedical application of HNTs

However, major gaps in basic knowledge remain, with the major obstacles confronting the HNT field being the lack of a detailed understanding of the nanotube dimension with biocompatibility. How to separate the tubes by diameter and length is unknown. Also, it is highly desirable to achieve surface patterns of HNTs with well-controlled spatial arrangements for cell growth supporting materials. Additionally, a method of assessing the body distribution and biodegradation behavior of HNTs in vivo needs to be created. Based on potential research advances, we believe that the nanotechnology-derived products on the nanotube can assist in the improvement of people health.

1. Lvov Y and Abdullayev E. Functional polymer-clay nanotube composites with sustained release of chemical agents. *Progress in Polymer Science*. 2013; 38: 1690-719.
2. Liu M, Jia Z, Jia D and Zhou C. Recent advance in research on halloysite nanotubes-polymer nanocomposite. *Progress in Polymer Science*. 2014; 39: 1498-525.
3. Liu M, Shen Y, Ao P, Dai L, Liu Z and Zhou C. The improvement of hemostatic and wound healing property of chitosan by halloysite nanotubes. *RSC Advances*. 2014; 4: 23540-53.
4. Yah WO, Takahara A and Lvov YM. Selective Modification of Halloysite Lumen with Octadecylphosphonic Acid: New Inorganic Tubular Micelle. *Journal of the American Chemical Society*. 2012; 134: 1853-9.
5. Hughes AD and King MR. Use of naturally occurring halloysite nanotubes for enhanced capture of flowing cells. *Langmuir*. 2010; 26: 12155-64.

## An investigation into the pH effects on the CEC of halloysite

Nia Gray, David Lumsdon, Stephen Hillier  
The James Hutton Institute, Craigiebuckler, Aberdeen AB15 8QH (nia.gray@hutton.ac.uk)

Halloysite is a tubular aluminosilicate belonging to the kaolin sub-group of minerals with the ideal chemical composition of  $\text{Al}_2(\text{OH})_4\text{Si}_2\text{O}_5(\text{nH}_2\text{O})$  ( $\text{n}=0-2$ ). Halloysite in its hollow nano-tubular form (HNT) accounts for a diverse set of characteristics which have resulted in a wide range of both industrial and research applications. This study uses cation exchange capacity (CEC) measurements by cobalt hexamine trichloride over a pH range to study both pH dependent and pH independent contributions to the CEC from edge and basal sites. The cobalt hexamine trichloride method is employed since this has been shown to be an analytically accurate method for CEC determination (1), especially where basal exchange sites are dominant.

Computational modelling of the data obtained using a two site Constant Capacitance Model (CCM) can be used to determine whether the exchange reaction occurs at edge or basal sites on the clay surface, where the two site model considers the permanently charged basal sites ( $\equiv\text{X}^-$ ) and edge hydroxyl groups ( $\equiv\text{SOH}$ ). It has been suggested that the permanently charged basal sites are unaffected by changes in pH whilst the variable edge sites display pH dependant adsorption (2). A range of halloysites are used in the study to determine whether the physical characteristics of the halloysites, can be related to the exchange reactions on the surface of the clay.

Dohrmann et al, *Clays and Clay Minerals*, Vol. 57, No. 3, 338–352, 2009.

Gu and Evans, *Geochimica et Cosmochimica, Acta* 72, 267-276, 2008

## Structure of halloysite by electron microscopy: a review

Toshihiro Kogure<sup>1</sup> and Victor A. Drits<sup>2</sup>

<sup>1</sup>Department of Earth and Planetary Science, Graduate School of Science, The University of Tokyo, Tokyo, 113-0033, Japan, kogure@eps.s.u-tokyo.ac.jp

<sup>2</sup>Geological Institute of the Russian Academy of Sciences, Pyzhevsky per 7, Moscow, Russia

Halloysite,  $\text{Al}_2\text{Si}_2\text{O}_5(\text{OH})_4 \cdot n\text{H}_2\text{O}$ , is one of the most common and ubiquitous clay minerals on the terrestrial surface. It belongs to kaolin group minerals or dioctahedral 1:1 aluminous phyllosilicates, but the structure of halloysite has not been fully understood yet despite a number of researches devoted to this mineral. Because information derived from X-ray diffraction is so limited, the structure of halloysite has been investigated mainly using electron diffraction, from which many workers proposed that halloysite has a two-layer structure but the origin of the “two-layer” was not explained except for Chukhrov and Zvyagin (1966).

As demonstrated by the analysis of stacking faults in kaolinite (e.g., Kogure and Inoue, 2005), direct observation and determination of the stacking structure by high-resolution transmission electron microscopy (HRTEM) is the most promising way also for halloysite, but this mineral is far more beam-sensitive than kaolinite and HRTEM analysis for halloysite has not been successful to date. However, a new TEM with computer-assisted minimal-dose system first recorded HRTEM images of halloysite with sufficient resolution to analyze its stacking structure (Kogure et al., 2011). In the images, two-layer periodicity was never observed, but rather one-layer periodicity with dense stacking faults. Their group further investigated the structure of “prismatic” halloysite (Kogure et al., 2013). HRTEM imaging showed stacking of most dioctahedral 1:1 layers with their pseudo-mirror plane perpendicular to the prism axis, and almost random, or rather alternating lateral stagger to the right or left from the preceding layer, which corresponds to the interlayer displacements of  $\tau_+$  and  $\tau_-$  in Zvyagin symbols or layer displacements of  $t_1$  and  $t_2$  used to describe the stacking in kaolinite. Based on these results, it is proposed that tubular halloysite initially forms as a hydrated form, then dehydrates with, possibly, partially hydrogen-bonded interlayers, and finally transforms to a prismatic one consisting of sectorized flat layers with the complete hydrogen-bonded interlayers. During this transformation, stacking with comparable ratio and frequent alternation of  $\tau_+$  and  $\tau_-$  is formed, to minimize morphological change of the tubes.

## Halloysite nanotubes as additives and carriers: Prospects and challenges

Pooria Pasbakhsh<sup>1</sup> and Jock Churchman<sup>2</sup>

<sup>1</sup> School of Engineering, Monash University Malaysia, Bandar Sunway, 47500 Selangor, Malaysia (Pooria.pasbakhsh@monash.edu). <sup>2</sup> School of Agriculture, Food & Wine, University of Adelaide, SA 5005, Australia

There is increasing research interest in potential applications of halloysite as fillers for polymer composites, controlled drug delivery, carriers for the supply and sustained release of active agents for anticorrosion coatings, in nanoreactors or nanotemplates, for the uptake of contaminants or pollutants and for the support and enhancement of catalysts. Our recent findings about the prospects and challenges arising from the use of halloysite nanotubes in different polymeric matrices for a range of applications will be discussed and elaborated. The compositions have included chitosan/halloysite membranes as bone tissue scaffolds, polylactic acid (PLA)/halloysite membranes for food packaging applications and their antimicrobial activities, instrumented impact properties of epoxy/halloysite nanocomposites and the role of halloysite in the self-healing of epoxy composites as well as the use of polyacronitrile (PAN)/halloysite membranes in water filters.

Halloysite has become a promising nanofiller due to its hollow lumen space, which ranges from 5-70 nm (depending on the deposit), distribution of hydroxyl groups and different charges on its outer and inner surfaces as well as a high aspect ratio and surface area. The hollow lumen space of halloysite makes them capable of uses as nanofillers for applications such as drug delivery and the sustained release of various agents. In this study the lumen space of halloysite nanotubes (HNTs) was used for the deposition of an antimicrobial agent (ZnO) to enhance the food packaging applications of its PLA composites. ZnO deposited into the lumen and surface of HNTs (Fig.1(a)) made an active packaging film where the ZnO can strongly influence the antimicrobial activity of the used HNTs. Results revealed that HNTs alone do not have any antimicrobial ability.

Using halloysite as a filler in polymer composites has brought new insights to this research area due to the good ability of HNTs to disperse throughout many types of polymers. However when halloysites are used simultaneously as carriers and for reinforcement, especially when they are mixed with other polymer nanofibers, having a well dispersed mixture of tubes along and/or inserted into the nanofibers in an electrospun membrane has remained challenging during our recent efforts at fabrication of biopolymer/halloysite membranes with the electrospinning method. Fig 1 (b) shows an individual halloysite nanotube alongside a PAN nanofibre while Fig.1 (c) shows an agglomeration of tubes in a matrix of PAN electrospun membrane with 3 wt% halloysite. Prospects and challenges presented by the use of halloysite as carriers and additives in other polymer matrices will be also be discussed.

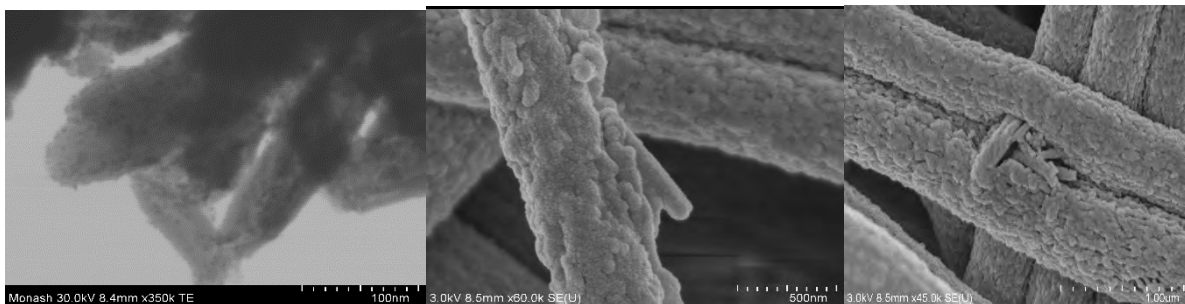


Fig.1. (a) ZnO deposited on the surface and into the lumen of HNTs; (b) Halloysite nanotube alongside the PAN nanofibers; (c) Agglomeration of halloysite nanotubes between two PAN nanofibers.

## Polymer nanocomposites for medical applications: effect of magnetic halloysite on structure and properties

Viera Khunová<sup>1</sup>, Ivo Šafařík<sup>2</sup>, Martin Škrátek<sup>3</sup> and Katarína Tomanová<sup>1</sup>

<sup>1</sup>Institute of Polymer Materials, Slovak University of Technology, FCHPT, Radlinského 9, 812 37 Bratislava, Slovakia, viera.khunova@stuba.sk

<sup>2</sup>Department of Nanobiotechnology, Institute of Nanobiology and Structural Biology of GCRC, České Budejovice, Czech Republic

<sup>3</sup>Institute of Measurement Science, Slovak Academy of Sciences, Dúbravská cesta 9, 841 04 Bratislava, Slovakia

In this work, we report the production of polymer nanocomposites based on magnetic halloysite and polycaprolactone for medical applications. Magnetic halloysite has been prepared by two different methods. In the first procedure halloysite suspended in methanol was magnetically modified with perchloric acid stabilized magnetic fluid; the suspension was mixed for two hours, and then magnetically modified halloysite was separated (1). Alternatively halloysite was modified using magnetic iron oxides nano- and microparticles prepared by microwave assisted procedure from ferrous sulphate at high pH (2).

Hysteresis loops and achieved magnetic properties confirmed that whilst PCL nanocomposites based on untreated HNT are diamagnetic, by application of magnetic HNT into PCL soft magnetic nanocomposite materials were prepared. The most significant effect on magnetic properties has been observed when perchloric acid stabilized magnetic fluid was applied. Structure and morphology investigations revealed that MHNT nanoparticles do not create agglomerates and are uniformly dispersed in PCL matrix.

Achieved results confirmed that the combination of polycaprolactone and magnetic halloysite enable generate a new advanced environmentally friendly polymer nanocomposites suitable for tissue engineering and other biomedical applications.

**Acknowledgement:** This work was supported by Slovak Scientific Grant Agency VEGA (1/0361/14). The authors thank Imerys Table Ware New Zealand Ltd. for the supply of halloysite.

Š is work was supported by Slovak Scientific Grant Agency VEGA (1/0361/14). The authors thank Imerys

Š is work was supported by Slovak Scientific Grant Agency VEGA (1/0361/14). The authors thank Imerys



Monday  
6<sup>th</sup> July

Lecture room 1

From microscopic pore  
structures to transport  
properties in shales  
(workshop follow on  
session)

## Workshop summary: from microscopic pore structures to transport properties in shales: which gaps are filled?

Thorsten Schäfer<sup>1,2</sup>

<sup>1</sup> Institute for Nuclear Waste Disposal (INE), Karlsruhe Institute of Technology (KIT), D-76021 Karlsruhe, GER

<sup>2</sup> Institute of Applied Geosciences (AGW), Environmental Geology, KIT, D-76021 Karlsruhe, GER

A wide spectrum of argillaceous media are being considered in Nuclear Energy Agency (NEA) member countries as potential host rocks for the final, safe, disposal of radioactive waste, and/or as major constituents of repository systems in which waste will be emplaced. In this context, the NEA established in 1990 a Working Group on Argillaceous Media, known informally as the "Clay Club". The Clay Club examines those various argillaceous rocks that are being considered for the deep disposal of radioactive waste, ranging from soft clays to indurated shales. These rocks exhibit a wide spectrum of characteristics which make them useful as barriers to the movement of water and solutes and as repository construction materials. Studies include clay media characterization and modeling. For further details refer to: <http://www.nea.fr/rwm/clayclub.html>. This workshop is a follow-up of the 1<sup>st</sup> workshop organized in Karlsruhe in 2011 (NEA, 2013) and is intended to document the progress made over the last four years.

Additionally, the shale gas and oil community is interested in the characterization of sediments and black shales from the core- to nano-scale, focusing on clay/brine/organic interfaces and understanding how pore space evolves and affects the transport and production potential of the shale system.

Through characterizing fundamental properties such as nano-/micropore connectivity, all the way up to understanding transport and mechanical fracture properties of whole rock units, both communities (radioactive waste disposal community and shale gas and oil community) are studying the geological materials with a shared set of tools, from quantum mechanics computer simulations, through advanced microscopy and diffraction methods, up to triaxial mechanical tests and large-scale transport models.

Very generally speaking, these clay rocks are composed of fine-grained minerals showing pore sizes from < 2nm (micropores) up to > 50 nm (macropores). The water flow, solute and gas transport and mechanical properties are largely determined by this microstructure, the spatial arrangement of the minerals and the chemical pore water composition. Examples include anion accessible ("geochemical") porosity and macroscopic membrane effects (chemical osmosis, hyperfiltration), geomechanical properties and the characteristics of two-phase flow properties (relevant for gas transport). In shale oil/gas systems, the role of clay minerals in creating porosity and controlling organic matter distribution is of key interest, as well as larger scale phenomena such as how diagenesis affects the mechanical properties of the shale gas unit. At the current level of knowledge, there is a strong need to improve the nanoscale description of the phenomena observed at a more macroscopic scale. However, based on the scale of individual clay minerals and pore sizes, for most of the imaging techniques this resolution is a clear challenge. Furthermore, the gap between scales accessible to direct observation and those that are subject to molecular / Monte Carlo modeling providing valuable information on the porous media described on a lattice (1 clay surface; Å-scale) will be addressed. Only the interplay between experimentalists providing inter alia geometrical data on the 10-100nm scale and modeling groups will provide information on the interplay between geometry and electrostatics and e.g. the effective diffusion coefficient of ions at this scale.

This lecture will give an overview of the outcome of the one-day pre-conference workshop discussing the current state-of-the-art of different spectro-microscopic methods and will point out new developments in the field in order to address the above mentioned knowledge gaps in clays.

## A combined macroscopic and microscopic approach to describe the diffusion of cations in the interlayer of swelling clay minerals

Emmanuel Tertre<sup>1</sup>, Alfred Delville<sup>2</sup>, Frederick Delay<sup>3</sup>, Dimitri Prêt<sup>1</sup>, Fabien Hubert<sup>1</sup> and Eric Ferrage<sup>1</sup>

<sup>1</sup> Institut de Chimie des Milieux et Matériaux de Poitiers, UMR 7285 Université de Poitiers/CNRS, équipe HydrASA, Bat. B8 rue Albert Turpain - 86073 Poitiers Cedex 9, France; Email : emmanuel.tertre@univ-poitiers.fr

<sup>2</sup> Interfaces, Confinement, Matériaux et Nanostructure, UMR 7374 CNRS Université d'Orléans, 45071 Orléans cedex 2, France

<sup>3</sup> Laboratoire d'Hydrologie et de Géochimie de Strasbourg, UMR 7517 Université de Strasbourg/EOST – CNRS, 1 rue Blessig, 67000 Strasbourg, France

Diffusion is the main transport process occurring in compacted geological systems such as shales and engineered barriers considered for the storage of nuclear wastes. Due to the high compaction of these environments, water and cations mainly diffuse in the interlayer spaces of the swelling clay minerals present in these systems. In the framework of constraining macroscopic models predicting diffusion in porous media rich in swelling clays, the aim of this study was to investigate the specific diffusion of calcium cations confined in the interlayer space of 5 mm sized disks of vermiculite during Na-for-Ca exchange process. Vermiculite material was chosen as the model swelling clay because this mineral does not show any osmotic swelling in water saturated conditions, as compared to low-charge montmorillonite generally considered in literature.

Diffusion experiments were performed by immersing disks of Ca-saturated vermiculite in aqueous reservoirs characterized by different NaCl salinities ( $3 \cdot 10^{-3}$ ,  $5 \cdot 10^{-2}$ , 0.1 and 1 M). Experimental data were obtained by analysis of aqueous calcium concentrations released in the solution and Ca-profiles obtained in the solid using scanning electron microscopy. Then, a set of molecular and Brownian dynamics simulations was used to quantitatively interpret experimental data obtained from analysis of both aqueous and solid phases (Tertre et al., 2015).

Microscopic simulations allow us to quantitatively determine that the dynamical properties of calcium in the interlayer of vermiculite during the Na-for-Ca exchange process was driven by both the external gradient between the solid and the solution related to the salinity of the solution, and also by the internal calcium gradient in the solid. These simulations highlighted the role played by the ionic flux existing at the disk/solution interface, and which can limit the global diffusion process in the case of a low salinity reservoir. Then, a macroscopic model based on differential equations and the gradients evidenced by Brownian dynamics simulations was proposed to interpret the aqueous and the solid profile data obtained experimentally. These findings should contribute to the improvement of diffusion models used to describe the diffusion of cations/pollutants in compacted swelling clay minerals.

Tertre, E. et al. (2015). *Geochim. Cosmochim. Acta* **149**, 251-267.

## A comparison of porewater natural tracers in low-permeability sedimentary rocks characterized using two methods

Magda Celejewski<sup>1</sup>, Tom Al<sup>2</sup>, Ian Clark<sup>2</sup>

<sup>1</sup> Department of Earth Sciences, University of New Brunswick, Fredericton, New Brunswick, E3B 5A3, Canada, m.celejewski@unb.ca

<sup>2</sup> Department of Earth Sciences, University of Ottawa, Ottawa, Ontario, K1N 6N5, Canada

Measurements of the spatial variability of naturally-occurring anionic tracers (e.g. Cl and Br) in porewater from low-permeability argillaceous rocks can provide insight into porewater residence time and the nature of solute transport. These system characteristics, in turn, are required to assess the long-term stability of geologic systems for waste management. However, extraction of porewater for chemical and isotopic composition measurements is challenging because of small fluid volumes and low permeability. It is also necessary to consider where the solutes originate from within porewater that can be distributed among fractions commonly defined as a) interlayer water which is contained in the interlayer spaces of swelling clay minerals, b) diffuse double-layer (DDL) water which is immediately adjacent to mineral surfaces and contains an excess of cations to balance negative surface charge, and c) mobile, or bulk water which is far enough from mineral surfaces as to be beyond the influence of the DDL. Anions are excluded from the interlayer water and from the near-surface regions of the DDL so their transport occurs dominantly in the mobile water.

The objective of this work was to compare methods for determining Cl<sup>-</sup> and Br<sup>-</sup> distributions in the porewater of low-permeability shale. Solutes were extracted using a crush and leach method and a new absorption method that draws porewater from the rock into hydrophilic cellulosic membranes. The crush and leach method aims to extract all of the available solutes from the rock, while the absorption method targets solutes in the mobile water fraction.

Trials were conducted on paired samples of low-permeability ( $K < 10^{-12}$  m/s, porosity  $< 10\%$ ) shale drill cores from the Michigan Basin at the Bruce nuclear site in southwest Ontario, Canada. The crush and leach method is susceptible to artefacts from ion exchange and mineral precipitation/dissolution, but both methods provide precise measures of the extractable Cl<sup>-</sup> and Br<sup>-</sup> mass. Dissimilarities in Cl<sup>-</sup>:Br<sup>-</sup> ratios between the two methods suggest differences in the anion exclusion effect on Cl<sup>-</sup> versus Br<sup>-</sup> (Figure 1) resulting in a larger accessible porosity for Cl<sup>-</sup> than for Br<sup>-</sup> in these low-permeability formations.

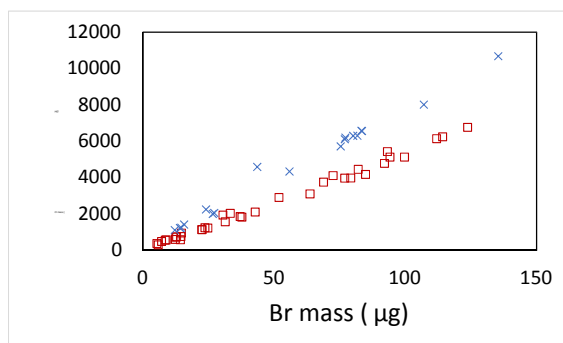


Figure 1. Cl:Br mass ratios in porewater extracted using the absorption method (□) and a crush and leach method (x) for shales and limestones from the Michigan Basin.

## Cation exchange capacity in black shales

Arkadiusz Derkowski<sup>1</sup> and Leszek Marynowski<sup>2</sup>

<sup>1</sup> Institute of Geological Sciences, Polish Academy of Sciences, Senacka 1, 31-002 Krakow, Poland; ndderkow@cyf-kr.edu.pl

<sup>2</sup> Faculty of Earth Sciences, University of Silesia, Będzińska 60, PL-41-200 Sosnowiec, Poland

Terrigenous and marine recent sediments contain the two most abundant types of constituents that control their potential for binding chemical compounds from water: clay minerals and organic matter (OM). Because of weakly bonded hydrogen on carboxyl and phenolic hydroxyl groups, soil OM potential to adsorb cationic species can be even greater than that for smectite and vermiculite. In ancient sediments where OM was subjected to thermal transformation and hydrocarbon generation, a common paradigm assumes that the OM surface has become chemically inactive because all exchangeable sites in functional groups are considered to have been polymerized during burial. Kerogen, however, usually contains substantial quantities of oxygen that forms numerous polar groups. Their content decreases strongly with OM maturation, but these groups have never been considered as contributing to the bulk rock cation exchange capacity (CEC).

CEC determination *via* exchange with complex cation of Hexamminecobalt(III) (ISO 23470 normalization) is a fast and accurate technique most widely used in geotechnical studies and oil and gas exploration, including oil- and gas-shale that are, by definition, OM rich.

Applying numerous CEC tests combined with bulk rock mineral quantification and detailed clay minerals studies, using a large series of shales with variable OM content and degree of diagenesis, we have found that CEC measured using Hexamminecobalt(III) is much greater than theoretical CEC estimated from clay minerals structure, composition, and content. The excess CEC correlates with the S3 parameter (CO<sub>2</sub> evolved during OM pyrolysis) analyzed using Rock Eval 6 apparatus. Carboxyl and carbonyl groups, either naturally occurring in the OM or produced by thermal oxidation, are responsible for binding excess Hexamminecobalt(III). Small, hydrated, non-complex cations, like Na<sup>+</sup>, do not bind to carboxyl groups on OM surface and represent the portion of the bulk CEC contributed by clay minerals. Samples that underwent bitumen removal with dichloromethane / methanol solvent treatment showed the same behavior toward [Co(NH<sub>3</sub>)<sub>6</sub>]<sup>3+</sup> and Na<sup>+</sup> cations as the untreated samples, proving that it is the kerogen that is responsible for the excess CEC.

Partially hydrophobic OM in the studied samples bind the anhydrous [Co(NH<sub>3</sub>)<sub>6</sub>]<sup>3+</sup> cation *via* positively charged ammine groups either by substituting carboxylic hydrogen or by weak hydrogen bonding to the double-bonded oxygen. Fully hydrated Na<sup>+</sup> cations seem not to be able to exchange the carboxylic H either because hydrated Na<sup>+</sup> cannot approach the OM hydrophobic surface or because under the pH of the NaCl solution used for the CEC<sub>Na</sub> determination (5.5-6.0), -COOH dissociation could not occur.

Because in petrophysics CEC is linked to immobile, adsorbed water of particular properties, CEC determination by Hexamminecobalt(III) vastly overestimates the clay-bound water content, leading to effective porosity underestimation. CEC determination with [Co(NH<sub>3</sub>)<sub>6</sub>]<sup>3+</sup> cation can serve, however, as a useful probe for interactions in sedimentary OM.

## Percolation characteristics of Carboniferous shale gas in the Eastern Qaidam Basin

Gao Jun<sup>1</sup>, Xia Lu<sup>2</sup>, Li Yingjie<sup>2</sup>, Yu Qingchun<sup>2</sup>

<sup>1</sup>School of Water Resources and Environment, China University of Geosciences(Beijing), Beijing 100083, China E-mail: gjun@cugb.edu.cn

<sup>2</sup>School of Water Resources and Environment, China University of Geosciences(Beijing), Beijing 100083, China

Shale gas is one kind of unconventional gas resource with a rich potential, and has multi-scale porosity structures and a variety of seepage patterns. Study of the porosity structures and seepage law of shale gas can be used as a theoretical support for the exploration and development of shale gas. The mass flow model of shale gas considering gas slippage and diffusion behavior are established based on the complex pore structure and multi-scale flow patterns of shale gas, and a quadratic function relation which is between the apparent permeability and the reciprocal average pressure is concluded. Shale samples from the Carboniferous Hurleg and Huaitoutala Formations in Eastern Qaidam Basin were collected for focused ion beam-scanning electron microscopy and pore-size distribution testing, etc. Through simulating methane displacing shale samples with no irreducible water under 25<sup>0</sup>C and different environmental pressures (between 0.1MPa to 4.0MPa), the pressure and flux change with time were observed and the apparent permeability was measured. The parameters were obtained in the apparent permeability formula by quadratic regression analysis of the apparent permeability and the reciprocal average pressure, and the shale gas flow characteristics affected by the slippage and the diffusion were analyzed. Results show that the slippage and diffusion behavior in the whole seepage weakens along with the increase of the formation pressure. The seepage pattern of shale gas is mainly diffusion flow under low pressure (when the pressure is less than 2MPa). However, when the pressure is greater than 2 MPa, the Darcy flow mainly influences the seepage, slippage and diffusion behavior is not obvious, and moreover the greater the Darcy permeability of shale samples, the smaller the contribution of diffusion and gas slippage to the seepage. The relationship between the Darcy permeability and pore-volume distribution coefficients of micropore, mesopore and macropore were analyzed. Results show that there is a good correlation between the Darcy permeability and mesopore volume distribution coefficient; the size and distribution of mesopores may influence the major seepage network of shale.

## Porosity evolution in the chalk: an example from the chalk-type source rocks of the Outer Carpathians (Poland)

Katarzyna Górniak

AGH University of Science and Technology, Faculty of Geology, Geophysics and Environmental Protection,  
al. Mickiewicza 30, Kraków, 30-059, Poland, e-mail: gorniak@agh.edu.pl

Chalk became a seal, a reservoir or source rock by a combination of fortunate circumstances related to the depositional environment, composition of sediments and their diagenetic pathways. This paper deals with pore-space evolution in the Eocene chalk-type deposits called the Grybów Marls, which are thought to be source rocks for the Outer Carpathian oil and gas deposits. The region where the Grybów Marl outcrops are located (Grybów Tectonic Unit) shows complicated tectonics. The strata were subject to strong folding, overthrusting, thrust faulting and uprooted during the closing stage of the Carpathian basin (Miocene). Analyses have been performed on samples from the outcrop to the microscopic scale to obtain a better knowledge of the pore system in the rocks studied and also their geological history.

The Grybów Marls represent synorogenic chalk facies re-deposited by mass flow from a shelf-related area into deeper parts of the basin. The thickness of the marls is estimated to be up to 400 m. Based on the X-ray data of these marls, carbonates constitute 19 - 48%, clay minerals occur in amounts that range from 31 - 50%, quartz varies from 8 - 18%, and feldspars vary from 3 - 8%. Pyrite content ranges from 7 - 10% and organic matter averages about 2%.

The XRD patterns of < 0.2  $\mu\text{m}$  carbonate-free particle-size fractions in homoionic-saturated states are similar to those of high-illitic ordered illite-smectite referred to as about 82% illite in I-S. The structural formulae reveal a dioctahedral composition with similar octahedral Mg and  $\text{Fe}^{+3}$  contents.

As revealed by the FESEM/BS/CCI study, the Grybów Marls have a wackstone texture with groundmass composed mostly of coccoliths and clay, so that these rocks can be classified as dirty chalk.

Deposition and diagenesis: because coccolith shields with calcite overgrowths are cemented by clay, the clay postdates the formation of coccolith overgrowths, i.e. overgrown coccoliths were re-deposited along with clay (pore-filling clay) and starting material for clay neoformation (pore-lining clay).

Compaction: there occur broken foraminifer chambers, some coccolith shields altered by pressure-solution and crushed, and slightly flattened pyrite framboids. In the majority of clay aggregates clay flakes are in close contact and consist of nearly face-face association.

The pore-space evolution in the Grybów Marls is postulated to result from a combination of: (1) origin of components (minute bioclasts and volcanogenic smectite altered during diagenesis to high-illitic I-S); (2) organic acids-rich sedimentary environment (re-distribution of calcite); (3) tectonic-induced clogging of pore space and reducing porosity within clay aggregates (lamellar clay).

A possible pathway for the evolution of porosity in the Grybów Marls is as follows: (1) the deposition of coccoliths in oxygen-depleted conditions of a sedimentary basin with limited water circulation; (2) the dissolution and recrystallization of coccolith shields due to calcite re-distribution in organic matter-rich environment; (3) periodic deposition of volcanic material and scarce terrigenous particles to the biogenic mud followed by the initial alteration of volcanic glass shards to clay; (4) the re-deposition of overgrown coccolith shields along with siliciclastic material, which subsequently acted as pore-filling cement; (5) the burial-induced compaction, which brought about closer relationships between coccolith shields, and the formation of pore-lining clay along with scarce pore-filling micro-quartz cements originated from the dissolution of disseminated volcanic glass fragments, as well as the smectite-to-illite alteration accompanied by the re-organization of clay flakes into less porous aggregates; (6) the tectonically-induced micro-cracks mostly created in foraminiferal tests, because the majority of coccoliths shields were protected against crushing by the presence of clay cement, which underwent re-organization by stress-creating lamellar aggregates.

The pore space accessible for fluid and gas migration, which can be seen by using the FESEM, in the chalk-type rocks studied is: (1) within pyrite framboids, (2) in the central part of interstices partially cemented by pore-lining clay, and (3) in fractures observed on allochems.

Funding was provided by Grant no 11.11.140.319 of the AGH University of Science and Technology, Faculty of Geology, Geophysics and Environmental Protection.

## 3D imaging of pore networks using FIB-SEM microscopy in Posidonia organic-rich shales

Georg H. Grathoff<sup>1</sup>, Markus Peltz<sup>1</sup> & Stephan Kaufhold<sup>2</sup>

<sup>1</sup>Dept. of Geogr. & Geology, EMA Univ. of Greifswald, FL Jahnstr. 17a, D-17489 Greifswald, Germany

<sup>2</sup>BGR, Bundesanstalt für Geowissenschaften und Rohstoffe, Stilleweg 2, D-30655 Hannover, Germany

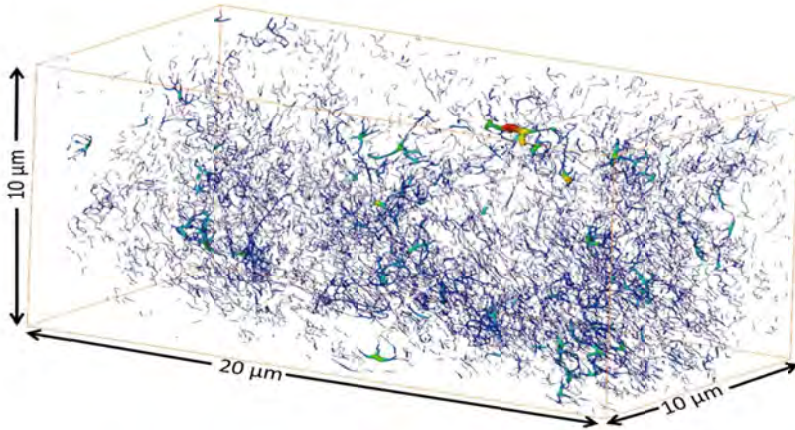
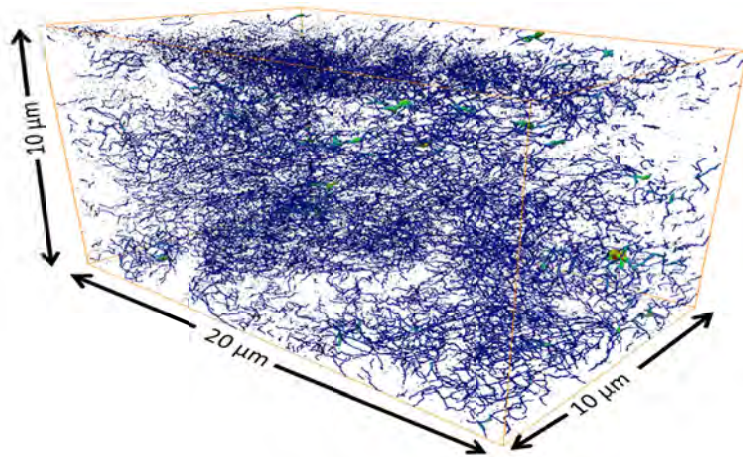


Figure 1: Pore network of Wickensen sample (0.53 % R0), colors represent radius of pores, blue to red: smallest to largest

The goal of this study is to understand better the porosity development in shales in order to improve modelling of fluid and gas flow related to shale diagenesis. The samples investigated are Mid Jurassic Posidonia shales from central Germany. The method we used was focused ion beam (FIB) microscopy coupled with SEM and EDX.

The results show that the quantity and distribution of pores ( $\geq 40\text{nm}$ ) are somewhat similar. The largest pores are located within carbonates and clays. The pore space that can be visualized within silicate mineral grains and the immature organics is small. The pore networks vary significantly as a function of organic maturity. With increasing organic maturity small pores with a complex pore network develop as seen by comparing Figure 1 and 2. Figure 1 shows the pore network of the Wickensen sample, which has not reached the gas window and has a FIB porosity of 2.4%. Figure 2 shows the pore network of the Haddessen sample which has reached the gas window and has a FIB porosity of 3.0%. Both samples have little to no axis connectivity on the scale of 10s of micrometers, but do show connectivity on the micrometer scale. With increasing maturity the connectivity increases. We find that the volume of the connected pore space in organic matter can be very large, of the order of  $\mu\text{m}^3$ . Using these data we will discuss how porosity changes in relation to thermal activation, hydraulic fracturing, and supercritical  $\text{CO}_2$ .



represent radius of pores.



## Whitby Mudstone Formation: its microstructure, porosity and permeability

M.E. Houben<sup>1,\*</sup>, A. Barnhoorn<sup>2</sup>, J. Lie-A-Fat<sup>2</sup>, T. Ravenstein<sup>2</sup>, C.J. Peach<sup>1</sup>, M.R. Drury<sup>1</sup>

1. Department of Earth Sciences, Utrecht University, NL, \*m.e.houben@uu.nl.

2. Department of Geoscience & Engineering, Delft University, NL.

The Whitby Mudstone Formation is an analogue for the Dutch Posidonia Shale which was deposited during the early Toarcian, and is a possible unconventional gas source in Northern Europe. The microstructure, porosity and permeability of the Jet Dogger section of the Whitby Mudstone Formation (UK) were characterized using a combination of methods including microscopy, gas adsorption, and Ar gas permeametry. The aim of this study was to investigate gas storage and potential gas flow through the rock by studying microstructure, porosity and permeability in the undeformed state, before further research on ways to improve gas productivity..

Using high resolution scanning electron microscope (SEM) images of representative areas for the mineralogically different layers (area > 150x150  $\mu\text{m}$ ) we have found a mineralogy in the upper half of the section that is characterized by a clay matrix content of ca. 65%, 21% of carbonates, 3% of silicates, 7% of organic matter and 4% of pyrite. The lower half of the section is more heterogeneous where the clay matrix content varies between 68 and 75%, furthermore we found on average 3-4% of pyrite, 2-6% carbonates, 8-14% silicates, and 3-9% organic matter. The Jet section (circa 8 meters thick) has been subdivided into a carbonat- (fossil) rich upper half and a laminated lower half of the section. The porosity visible in the SEM images is of the order of 0.5-2.5% and shows a non-connected pore network in 2D (pore diameter > 100 nm), where overall 40-80% of the porosity is situated in the clay matrix. Furthermore, flow through these rocks will probably depend on the porosity and pore network present in the clay matrix since all larger porous and non-porous minerals (> 2  $\mu\text{m}$ ) present are embedded within this matrix. Gas adsorption techniques (N<sub>2</sub>, Ar, He) have been used to measure the porosity and size distributions of pores in the connected pore network. Ar and N<sub>2</sub> porosities are in the range 0.5-6% and He porosities go up to 7% for the different samples measured. Porosity values depend on the method used, the sample shape, the sample preparation and the actual sample measured, where sub-samples from the same block show a range of porosity values even when measured using the same method. An Ar-gas-permeametry set-up has been used to measure the permeability on 1-inch diameter cores. Permeability has been measured at a confining pressure of 0.8 MPa and the permeability for different samples was in the range  $2 \cdot 10^{-19}$  –  $1 \cdot 10^{-17}$  m<sup>2</sup>, where no systematic relationships between permeability, porosity and mineralogy were found.

Comparing porosity and microstructures to other (producing) gas shales shows that mineralogically the Whitby Mudstone has a high clay matrix content and has a relatively low porosity. Overall the Whitby Mudstone is less carbonate rich than the Posidonia Shale, where microstructurally the Posidonia Shale is comparable to the upper half of the Whitby Mudstone section [1]. Permeability values measured on the other hand fall within the same range of values for the Posidonia, Evie and Muskwa shales [2,3].

[1] Klaver, J., Desbois, G., Urai, J.L., Littke, R. (2012). BIB-SEM study of the pore space morphology in early mature Posidonia Shale from the Hils area, Germany, *International Journal of Coal Geology*, 103, 12-25.

[2] Chalmers, G.R., Ross, D.J.K., Bustin, R.M. (2012). Geological controls on matrix permeability of Devonian Gas Shales in the Horn River and Liard basins, northeastern British Columbia, Canada, *International Journal of Coal Geology*, 103, 120-131.

[3] Ghanizadeh, A., Amann-Hildenbrand, A., Gasparik, M., Gensterblum, Y., Krooss, B.M., Littke, R. (2013). Experimental study of fluid transport processes in the matrix system of European organic-rich shales: II. Posidonia Shale, *International Journal of Coal Geology*, 123, 20-33.

## Nano – Micro scale characterization of pore space and microstructure of an overmature organic-rich shale

Jop Klaver<sup>1</sup>, Guillaume Desbois<sup>1</sup>, Jens-Oliver Schwarz<sup>2</sup> and Janos L. Urai<sup>1</sup>

<sup>1</sup> Structural Geology, Tectonics and Geomechanics, EMR, RWTH Aachen University, Lochnerstr. 4-20, D-52056 Aachen, Germany, jop.klaver@emr.rwth-aachen.de

<sup>2</sup> Institute of Geosciences, Johannes Gutenberg University Mainz, J.-J.-Becher-Weg 21, D-55128 Mainz, Germany

It is generally found that organic-matter porosity controls to a large extent the storage capacity and in that sense enhances the permeability in organic-rich shales (Jarvie et al., 2007; Loucks et al., 2009). We endeavored to capture and visualize the microstructures relevant for storage and transport in an overmature organic-rich shale sample from the Haynesville Shale formation (Klaver et al., 2015) by applying a range of imaging techniques. Broad ion beam (BIB) milling and scanning electron microscopy (SEM) imaging indicates porous organic matter and carbonate aggregates. Wood's metal injection (WMI) followed by BIB-SEM indicates that these organic-matter and carbonate aggregates phases have the relatively highest degree of connectivity. This is verified by focused ion beam (FIB) milling and SEM tomography showing the largest pores in these phases. Micro computed tomography ( $\mu$ CT) demonstrated pervasive distribution of the organic-matter phase throughout a mm-size sub-sample. We infer that in this shale the organic matter and the carbonate aggregates host the pore space relevant for transport as found by the preliminary WMI-BIB-SEM results.

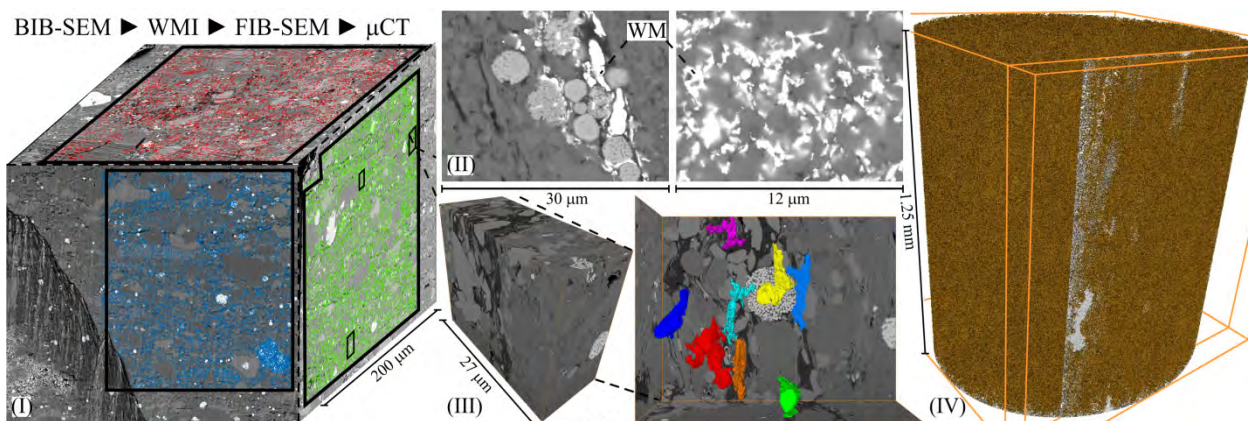


Fig. 1 Multiscale characterization of pore space and microstructure of an overmature organic-rich shale by using: (I) BIB-SEM; (II) Wood's metal injection followed by BIB-SEM; (III) FIB-SEM; and (IV) Segmented organic matter in MicroCT sample.

Jarvie, D.M., Hill, R.J., Ruble, T.E., Pollastro, R.M., 2007. Unconventional shale-gas systems: The Mississippian Barnett Shale of north-central Texas as one model for thermogenic shale-gas assessment. AAPG Bulletin 91, 475-499.

Klaver, J., Desbois, G., Littke, R., Urai, J.L., 2015. BIB-SEM characterization of pore space morphology and distribution in postmature to overmature samples from the Haynesville and Bossier Shales. Marine and Petroleum Geology 59, 451-466.

Loucks, R.G., Reed, R.M., Ruppel, S.C., Jarvie, D.M., 2009. Morphology, Genesis, and Distribution of Nanometer-Scale Pores in Siliceous Mudstones of the Mississippian Barnett Shale. Journal of Sedimentary Research 79, 848-861.

## Microstructure of clay assembly – from clay particles to shale

Wen-An Chiou<sup>1</sup>, Stephan Kaufhold<sup>2</sup> and Reiner Dohrmann<sup>2</sup>

<sup>1</sup> NISP Lab, Nanocenter, University of Maryland, College Park, MD 20742, USA, wachiou@umd.edu

<sup>2</sup> Federal Institute for Geosciences and Natural Resources, State Authority of Mining, Energy and Geology, GEOZENTRUM HANNOVER, Stilleweg 2, D-30655 Hannover, Germany

The spatial distribution, orientation, and particle-to-particle relationships of < 4  $\mu\text{m}$  solid particles (mainly clay minerals) or as an assembly in fine-grained sediment determines the properties and behavior of sediments/soils, and provides pore space for interstitial water, gas, and organic matter in both living organisms and their products. Recent interest in oil shale due to energy needs and the enormous economic potential has sputtered the interest in the study of clay microstructure. However, advancements in this area of research have been slow due to the lack of a high-resolution instrument. This paper introduces unique novel methods and technologies of studying individual clay particle/assembly and its applications to geological, mineralogical, biogeochemical, soil science, and civil engineering research.

High-resolution characterization of clay particle size, mineralogy, shape (morphology), and texture is important for understanding clay microstructure. Historical difficulties of measuring individual clay particles (domains/assemblies) due to minute size have been overcome by recent technological developments in electron and ion microscopy and microanalysis, such as high-resolution scanning/transmission electron microscopy (S/TEM) with different analytical techniques, wet environmental TEM (WETEM) and focus ion beam (FIB). Other techniques, such as 3D SEM image reconstruction, 3D TEM tomography and 3D tomography using FIB have also recently provided excellent characterization of the fundamental characteristics of clay particles, small clay assemblages, and hard shale.

Samples from various depositional environments depicting individual clay particles have been studied. Traditionally, researchers believed that smectite was characterized by a platy fluffy morphology. Through WETEM, it was discovered that different shapes (spherical-like, platy, elongated rod-like, needle, triangular, and polygon shape) of nano-size clay particles exist. Recent studies revealed that almost all of smectite particles are < 500 nm in equivalent diameter with a mode between 30 to 125 nm and a mean between 90 to 180 nm regardless of the clay fraction obtained by the settling method. The thinnest individual smectite particles range 4 to 10 nm with a mode of 5 to 6 nm. This thickness corresponds to  $\sim$  4 to 5 unit cell layers and is unique to the development of smectitic clay microstructure.

TEM observation of clay particles/assemblies in marine sediments from the Mississippi Delta, Middle-America Trench, Pacific Basin, California Continental Slope, and Baltic Sea reveals many characteristics of the depositional environment. Clay aggregates observed in both conventional TEM, WETEM, and SEM showed many interesting features. With advanced hard- and soft-wares, surface 3-D images and 3-D tomography can be constructed by images obtained from SEM, TEM and FIB. Using advanced FIB technique and 3D tomography software, microstructure (such as particle orientation) of highly compacted shale, particle to particle relationships, and micropores can be clearly observed and volume fraction of pore space or solids and porosity can thus be calculated. The application of 3-D analysis of clays and their assembly promises to increase our understanding and improve the application of clays.

Depositional environment, pore-water geochemistry, and biological/organic interactions play important roles in the formation and diagenesis of clay fabric and ultimately the fundamental sediment properties. Investigation of clay assembly and its microstructure synthesized in the laboratory contributes to the understanding of the developmental history of clay microstructure in natural environments, and also provides useful and important applications in materials science/engineering and related disciplines.

Monday

6th July

Lecture Room 1

General (2)

## Timing and source of paleofluid pulses in the North Anatolian Keirogen

Austin Boles<sup>1</sup> and Ben van der Pluijm<sup>1</sup>

<sup>1</sup>Department of Earth and Environmental Sciences, University of Michigan, 1100 North University Ave., Ann Arbor, MI, 48109, USA (aboles@umich.edu)

Hydrogen isotopic and  $^{40}\text{Ar}/^{39}\text{Ar}$  geochronological investigation of clay-gouge fault rocks collected from the surface trace of the modern North Anatolian Fault (NAF) give insight into the deformation history of this historically active region of Northern Turkey known as the North Anatolian Keirogen. A newly-developed approach permits the identification of geofluid activity in the upper several kilometers of the crust, with the ability to characterize the  $\delta\text{D}$  composition and constrain the  $^{40}\text{Ar}/^{39}\text{Ar}$  age of fluid activity. We identify several fluid pulses.  $\delta\text{D}$  values of detrital material from several locations spanning more than 750 km of the NAF are  $-45\pm 13\text{‰}$ ,  $-60\pm 6\text{‰}$ , and  $-64\pm 6\text{‰}$  for samples KSL, G1G2, and RES4-1, respectively. Fluid values above  $300^\circ\text{C}$  are  $-26$  to  $-45\text{‰}$ . Detrital material ages are as follows: sample G2 (western Turkey) is  $95.8\pm 7.7$  Ma, and sample RES4-1 (eastern Turkey) is  $96.5\pm 3.8$  Ma. This closely matches ages and fluid compositions of the metamorphic soles of ophiolites coincident with Neo-Tethyan closure and the Anatolide-Pontide block accretion to Eurasia. Authigenic population  $\delta\text{D}$  values are  $-89\pm 3\text{‰}$ ,  $-90\pm 2\text{‰}$ , and  $-97\pm 2\text{‰}$  for samples KSL, RES4-1, and G1G2, respectively. With temperature constrained by illite crystallinity at  $125^\circ\text{C} \pm 25^\circ$ , corresponding fluid values are  $-62$  to  $-85\text{‰}$ , which are indistinguishable from modern meteoric values in the region. Authigenesis timing is determined by sample G2 as  $41.4 \pm 3.4$  Ma and by sample RES4-1 as  $24.6 \pm 1.6$  Ma. These results indicate that the formation of weak fault rock material within the modern shear zone pre-dates movement, and that meteoric fluid with compositions indistinguishable from modern values has been circulating in the upper crust of this region since the early Cenozoic.

## Alteration of Ordovician black slates at Retortillo-Santidad uranium mine (Salamanca) induced by acidic leaching solutions

F. Javier Huertas<sup>1</sup> and Fernando Gervilla<sup>1,2</sup>

<sup>1</sup> Instituto Andaluz de Ciencias de la Tierra (CSIC-Univ. Granada), Granada, Spain - javierhuertas@ugr.es

<sup>2</sup> Department of Mineralogía y Petrología (Univ. Granada) Granada, Spain

The Ordovician gray/black slates of the Retortillo-Santidad area crop out in a NW-SE-trending synform, above a thick quartzite formation (Armorican Quartzite). They show millimeter to centimeter banding and near vertical foliation. This Ordovician sequence is intruded by a late Variscan, coarse-grained granite (the Bañobarez granite). The granite itself and the associated black slates are intruded by variably thick (from centimeters to tens of centimeters) pegmatite, aplite and quartz veins. The slates are locally tourmalinized and host uranium mineralization. Most slates contain quartz-sulfide ( $\pm$ carbonate) veins of variable thickness. Sulfides mainly consist of pyrite and/or pyrrhotite, with minor amounts of marcasite. Pyrite and pyrrhotite also occur disseminated in the rock and pyrite forms narrow veins parallel to the foliation.

Alteration is relatively heterogeneous but tends to increase to the surface. Deep samples tend to preserve the primary, metamorphic assemblage, mainly made up of quartz, muscovite, biotite, andalusite and cordierite (locally, potassium feldspar and plagioclase become abundant), with pyrrhotite in veins and disseminated in the slate. Below 15 m and from 40-115 m (the lower level varies with the presence of fault zones), the slates show moderate alteration, characterized by the presence of: i) dark red to greenish brown biotite caused by its strong alteration to chlorite/berthierine and to a lesser extent to muscovite; ii) cordierite transformed into ovoid-shaped, fine-grained aggregates of pinnite (consisting mainly of fine-grained kaolinite) giving rise to a characteristic mottling, or to kaolinite-rich bands parallel to the foliation; iii) muscovite partly replaced by kaolinite; iv) some andalusite crystals (associated with kaolinite-rich bands) showing fracture fillings and grain-boundary alteration to Al-rich smectite; v) pyrite with very minor amounts (mainly inclusions) of marcasite, chalcopyrite, and pyrrhotite (textural relationships suggest that pyrite forms by replacement of pyrrhotite). Shallow samples (<15 m) exhibit a typical red color caused by the dissemination of Fe hydroxides (mainly goethite). The most characteristic features of these samples are the strong alteration of cordierite (rarely andalusite) to fine-grained kaolinite (pinnite), the alteration of biotite to Fe-rich chlorite, berthierine, kaolinite and/or smectite, the partial replacement of muscovite by kaolinite and the complete alteration of Fe sulfides to Fe hydroxides.

The observed alteration zoning can be explained by the interaction of downward percolation of meteoric water with the black/gray slates. Alteration progressed through sub-vertical foliation planes and fractures, as well as through porous, quartz-rich bands. These percolating solutions should be saturated in atmospheric oxygen, which promoted the alteration of Fe sulfides to Fe hydroxides, supplying  $\text{SO}_4^{2-}$  and  $\text{H}^+$  ions to the solutions, thus contributing to an increase in their acidity. As these solutions percolated downward their reaction with the host gave rise to the described alteration assemblages until they become neutralized. Consequently, deep slates tended to remain unaltered. Textural relations suggest that whereas kaolinite+smectite-bearing assemblages formed during the described process, chlorite should form during a previous, near-neutral alteration event.

The acid alteration process contributed to remobilize and concentrate a pre-existing, low-grade uranium mineralization. The percolating acid-oxidizing solutions oxidized uranium minerals and transported uranium in the form of  $\text{UO}_2\text{SO}_4^0$ . As percolation/reaction progressed, solutions became reduced and partly neutralized, causing reduction of uranyl sulfate complexes and the precipitation of uranium mineral (mainly pitchblende and coffinite). The downward percolating solutions tended to become neutralized and uranium-free with depth.

## Using chemical element ratios for 3D modeling of advanced and intermediate argillic alterations based on their correlation with clay minerals – Biely Vrch porphyry gold deposit

Michal Jánošík<sup>1</sup>, Jana Brčeková<sup>1</sup>, Andrej Bíroň<sup>2</sup>, Peter Uhlík<sup>1</sup>, Peter Koděra<sup>1</sup>, Ľubica Puškelová<sup>3</sup>

1 Department of Economic Geology, Faculty of Natural Sciences, Comenius University in Bratislava, Mlynská dolina G, 842 15 Bratislava, Slovakia, mjanosik1@gmail.com

2 Geological Institute, Slovak Academy of Sciences, Detached branch Banská Bystrica, Ďumbierska 1, Banská Bystrica, Slovakia

3 Geological Institute, Slovak Academy of Sciences, Dúbravská cesta 9, Bratislava 845 03, Slovakia

The Biely Vrch deposit is a new economic Au-porphyry mineralization discovered in Slovakia. The deposit is located in the central zone of the Neogene Javorie stratovolcano, situated in the eastern part of the Central Slovakian Volcanic Field.

Zones of advanced argillic alteration are the uppermost part of the porphyry system and the youngest alteration. They occur from the surface to depths of several hundred metres in the shape of ledges. Kaolinite was the main clay mineral from the studied samples. Pyrophyllite accompanies kaolinite as the second clay mineral in the upper part of advanced argillic alteration. Dickite, another index mineral of advanced argillic alteration, occurred with kaolinite more frequently than pyrophyllite but in a smaller amount. Intermediate argillic alteration is the most widespread alteration in the deposit and is situated immediately adjacent to the advanced argillic alteration. The main clay minerals of this alteration are illite, illite/smectite and chlorite. Smectite and chlorite/smectite are also present in smaller amounts.

Oxygen and hydrogen isotopic composition of fluids in equilibrium with the alteration minerals indicates their magmatic-hydrothermal origin.

Characterization of the mineral composition of the alteration zones was performed by X-Ray diffraction analysis (oriented clay fraction and randomly oriented bulk fraction).

Using chemical element ratios rather than separate elements, used in previous research, proved to be better for 3D modeling of alteration zones. Consequently we were able to improve our previous models and eliminate their shortcomings.

The authors are grateful to the Slovak Research and Development Agency for the support of the projects APVV-0537-10 and APVV-0993-12, EMED Mining, Ltd. for providing samples and data, and ARANZ Geo Limited for providing 3D modeling software LeapFrog Geo.

# TUESDAY ORAL SESSIONS



Time	Title + Authors	Page No.
08.30	<b>PLENARY:</b> The application of the Rietveld method X-ray diffraction analysis of clays <u>Reinhard Kleeberg</u> ( <i>Pioneer in Clay Science Lecturer of the Clay Minerals Society</i> ) Introduced by Prof. S. Hillier	99
	<b>Lecture room 5: General (3)</b> <i>Session Chairs: Jeff Wilson, Sabine Petit and Selahattin Kadir</i>	
09.10	Compression behaviour of natural and remoulded clays under monotonous and cyclic loading considering micro-structural evolution <u>Nina Müthing, Wolfgang Lieske and Tom Schanz</u>	101
09.30	A sinking scenario which may require examinations on FEPs in bentonite <u>Koichi Shin</u>	102
09.50	The structure of opal-CT revisited <u>M J Wilson</u>	103
10.10	Study of a synthetic (IV)Fe <sup>3+</sup> -nontronite series with a wide range of tetrahedral charge <u>Fabien Baron and Sabine Petit</u>	104
10.30	Searching for nontronite in Eemian interglacial lake deposits <u>Christian Bender Koch and Takeshi Kasama</u>	105
10.50	<b>BREAK</b>	
11.10	NH <sub>4</sub> -bearing smectite as a nitrogen conveyer to deep Earth: An experimental approach <u>Daniel Grings Cedeño, Rommulo Vieira Conceição, Márcio R. W. de Souza, Larissa C. Carniel</u>	106
11.30	Fraipontite/sauconite – a new interstratified clay mineral from the oxidation zone of the Zn-Pb-deposit Preguiça, Southern Portugal <u>Patrizia Will, Frank Friedrich, Georg Grathoff, Rupert Hochleitner and H. Albert Gilg</u>	107
11.50	Implications of Cation occupation from the adsorption and desorption experiment of chromium for montmorillonite <u>Y. Cai, N. Meidina, T. Maierdan, H. Wang and Y. Pan</u>	108
12.10	Interpretation of the infrared spectra of synthetic silicate clays of the lizardite-nepouite series <u>Sabine Petit and Fabien Baron</u>	109
12.30	<b>LUNCH</b>	
13.40	<b>PLENARY:</b> Neutron scattering studies of clay minerals <u>Neal Skipper</u> ( <i>Hallimond Lecturer of the Mineralogical Society</i> ) Introduced by C. Greenwell	110
14.20	Iron-oxides in the hyper-saline environment of the Dead-Sea area <u>Nurit Taitel-Goldman, Vladimir Ezersky and Dmitry Mogilyanski</u>	111
14.40	Clay mineralogy as a reflection of parent material and processes <u>Georgina Holbeche and Robert Gilkes</u>	112
15.00	Preliminary approach to mineralogy and geochemistry of clay minerals intercalated with coal seams in the Neogene lacustrine Seyitömer Basin, Kütahya, western Turkey <u>Hülya Erkoyun, Selahattin Kadir and Tacit Külâh</u>	113
15.20	<b>BREAK</b>	
15.40	Mineralogy, geochemistry and genesis of sepiolite and palygorskite in Neogene lacustrine sediments at the northern Eskişehir area, NW Turkey <u>Selahattin Kadir, Hülya Erkoyun, Muhsin Eren and Nergis Önalgil</u>	114
16.00	Palaeoenvironmental meaning of clay minerals assemblages across the Late Pliensbachian-Early Toarcian (Early Jurassic) of Iberian Peninsula: Lusitanian, Algarve and Subbetic basins <u>Ana Caniço, Luís Vitor Duarte, Fernando Rocha, Matías Reolid and Denise Terroso</u>	115
16.20	Diagenesis and reservoir development in the Triassic Bunter Sandstone of Structure 5/42, Southern North Sea: evaluation for purposes of CO <sub>2</sub> storage <u>Graham Blackbourn, Alastair Brown, Steve Furnival, Peter Rowbotham, Iulia Wright and Rohan De Silva</u>	116
16.40	Is there a connection between early tetrapods and clay mineralogy in the coastal floodplain sediments of the Old Red Sandstone–Carboniferous of S.E. Scotland? <u>Christopher Jeans and Giulio Lampromnti</u>	117

	<p><b>Lecture room 4: Clay mineral indices in palaeo-geothermal studies hydrocarbon and geothermal prospecting – third Frey-Kübler symposium</b>  <i>Session Chair: Hans Albert Gilg, Rafael Ferreiro Mählmann</i></p>	
09.40	<p><b>KEYNOTE:</b> Geochronology and isotope geochemistry of clay minerals to study thermal and fluid flow events  <u>Tonguç Uysal</u></p>	119
10.10	<p>Age constraints of low-temperature alteration using K-Ar dating of celadonite in the Proterozoic basaltic North Shore Volcanic Group, Minnesota  <u>Susanne Th. Schmidt</u> and Klaus Wemmer</p>	120
10.30	<p>XRD and K-Ar of illite-smectite as basin history tools: verification by apatite fission tracks and (U-Th)/He in zircon  <u>Jan Šrodoň</u>, Aneta A. Anczkiewicz, István Dunkl, Igor Vlahović, Ivo Velić<sup>4</sup>, Bruno Tomljenović, Tadeusz Kawiak, Michał Banaś and Hilmar von Eynatten</p>	121
10.50	<p>Deformation controlled low-grade metamorphism in the Patagonian fold-and-thrust belt in the Torres del Paine area, Chile (51° 30' S): Combining K/Ar, XRD and O isotopic data  <u>Annette Süssenberger</u> and Susanne Th. Schmidt</p>	122
11.10	<p><b>BREAK</b></p>	
11.30	<p>Applying clay mineral and organic matter indices to determine rock maturity and grade of diagenesis to incipient metamorphism focused on correlation problems  <u>Rafael Ferreiro Mählmann</u></p>	123
11.50	<p>Temperature determination between 50 and 270°C through fluid inclusion microthermometry and vitrinite reflectance values in the external parts of the Central Alps  <u>Josef Mullis</u>, Monika Wolf and Rafael Ferreiro Mählmann</p>	124
12.10	<p>Reliability of very low-grade metamorphic methods to decipher basin evolution: case studies from basins of the Southern Vosges (NE France)  <u>Sébastien Potel</u>, Marine Maillot, Anta-Clarisse Sarr, Michael-Patrick Doublier, Tatiana Maison and Rafael Ferreiro Mählmann</p>	125
12.30	<p><b>LUNCH</b></p>	
14.20	<p>Illitization sequence controlled by temperature on hydrothermal altered volcanic rocks from the Tinguiririca Geothermal Field (Andean Cordillera, Central Chile)  <u>Blanca Bauluz</u>, Mercedes Vazquez, Fernando Nieto and Diego Morata</p>	126
14.40	<p>Hydrothermal clays in Fe oxide deposits of Norrbotten County, northern Sweden  <u>H. Albert Gilg</u>, Adrian M. Hall, Anthony E. Fallick, Frank Friedrich and Ulf B. Andersson</p>	127
15.00	<p>Hydrothermal alteration of chlorite to interlayered chlorite/smectite: geological evidence from the Oligocene Smrekovec Volcanic Complex, Slovenia  <u>Polona Kralj</u></p>	128
15.20	<p>Clay mineral signature in geothermal environments related to subduction zones  <u>Patricia Patrier</u>, Daniel Beaufort, Delphine Guisseau, Photinie Papapanagiotou, and Antoine Mas</p>	129
15.30	<p>Evolution of out-of-equilibrium clay mineral assemblages in the Tolhuaca geothermal field, Southern Chile  <u>Mercedes Vázquez</u>, Diego Morata, Martin Reich, Gloria Arancibia, Pablo Sánchez and Fernando Nieto</p>	130

	<b>Lecture room 3: Bioreactive clay minerals impacts on environmental and human health</b> <i>Session Chairs: Tim Jones, Fernando Rocha and Lynda Williams</i>	
09.10	Characterization of clays used in the pharmaceutical industry <u>John A. Smoliga</u>	132
09.30	Antimicrobial activity of Ag-treated clay-based nano-composites <u>Dimitrios Papoulis</u> , Eleni Koutra Michalis Kornaros Andreas Rapsomanikis Dionisios Panagiotaras and Elias Stathatos	133
09.50	Synthesis of europium doped layered double hydroxide by rapid-mixing method and its cellular uptake behavior <u>Sumio Aisawa</u> , Satsuki Shinohara, Hidetoshi Hirahara, Eiichi Narita, Tsugio Sato	134
10.10	<b>KEYNOTE:</b> Safety assessment of clays used in health care products <u>C. Viseras</u>	135
10.40	<b>BREAK</b>	
11.00	Chemical modifications and diatom community development on volcanic clayey sediments during <i>indoor</i> and <i>in situ</i> maturation processes <u>F. Rocha</u> , A. Quintela, S. Almeida and D. Terroso	136
11.20	The bioreactivity of 'red clays' from basaltic terrains <u>Timothy Jones</u> , Kelly Berube, Anna Wlodarczyk, Zoe Prytherch, Yusuf, Hassan, Stephen Potter, Rachel Adams	137
11.40	The anatomy of an antibacterial clay mine <u>Lynda. B Williams</u> , Keith D. Morrison, Dennis D. Eberl and Stanley N. Williams	138
12.00	Unearthing the antibacterial activity of medicinal clays <u>Keith D. Morrison</u> and Lynda B. Williams	139
12.20	<b>LUNCH</b>	
14.20	Mechanistic considerations on the healing properties of clays and related minerals <u>Javiera Cervini-Silva</u> , Antonio Nieto-Camacho, María Teresa Ramírez-Apán, Eduardo Palacios, Paz del Angel, Esmeralda Juárez-Carbajal, Eduardo Terres, Virginia Gómez-Vidales, Elba Ronquillo de Jesús, Kristian Üfer, Stephan Kaufhold, Martin Pentrak, Linda Pentrakova, Ascención Montoya, Joseph W. Stucki and Benny Theng	140
14.40	Peptide bond formation in layered double hydroxides - implications for abiological life-precursors Brian Gregoire, H. Christopher Greenwell and <u>Donald G. Fraser</u>	141
15.00	Nano-structured multi-enzymatic @LDH bio-hybrid as a one-pot biocatalyst for polyalcohol synthesis <u>Claude Forano</u> , Rima Mahdi, Suraj Charan, Ulla Gro Nielsen, Vanessa Prevot, Christine Guérard-Hélaine, and Marielle Lemaire	142
15.20	Formation of adenosine from adenine and ribose in the presence of montmorillonite after repeated wetting and drying <u>Hideo Hashizume</u> , Sjerry van der Gaast and Benny K.G. Theng	143
15.40	<b>BREAK</b>	

Tuesday, 7th July

	<b>Lecture room 3: Asian Clay Minerals Group Research in Progress II (2)</b> <i>Session Chairs: Hyen-Goo Cho, Jae-Min Oh and Jinwook Kim</i>	
16.00	Layered silicate adsorbent as an excellent partner of a TiO <sub>2</sub> photocatalyst for highly efficient green fine-chemical syntheses <u>Yusuke Ide</u> , Masato Torii and Tsuneji Sano	145
16.20	Organoclays in water cause interlayer expansion that facilitates caffeine adsorption <u>Tomohiko Okada</u> , Junpei Oguchi, Ken-ichiro Yamamoto, Takashi Shiono, Masahiko Fujit and Taku Iiyama	146

	<p><b>Lecture room 2: Clay and fine particle based materials for environmental technologies and clean up (1)</b>  <i>Session Chairs: Anke Neumann and Binoy Sarkar</i></p>	
09.30	<p><b>KEYNOTE:</b> The “magic” in environmental applications of clay based materials  Giora Rytwo</p>	148
10.00	<p>Reaction kinetics of molecular aggregation of laser xanthene dye in colloids of synthetic saponite nanoparticles  <u>Juraj Bujdák</u> and Timea Baranyaiová</p>	149
10.20	<p>Mechanisms of atenolol and metoprolol adsorption on Ca-montmorillonite (SAz-2)  <u>Po-Hsiang Chang</u>, Wei-Teh Jiang, Zhaohui Li, Jiin-Shuh Jean</p>	150
10.40	<p>Removal of Diclofenac from a sandy soil by clay particle injection: a preliminary laboratory study  <u>Jean-Frank Wagner</u> and Alessandro Santin</p>	151
11.00	<b>BREAK</b>	
11.20	<p>Application of waste ceramics in environmental protection  <u>Barbora Dousova</u>, David Kolousek, Miloslav Lhotka, Lenka Holcova and Martin Keppert</p>	152
11.40	<p>Kinetic experiments and XPS study of uranyl adsorption onto montmorillonite-at pH = 4  <u>Vanessa Guimarães</u>, Enrique Rodríguez-Castellón, Fernando Rocha, Manuel Algarra and Luliu Bobos</p>	153
12.00	<p>Simulation of Zn(II) transport in a soil column considering sorption properties of clay minerals  <u>Christelle Latrille</u>, Catherine Beaucaire and Aubéry Wissocq</p>	154
12.20	<b>LUNCH</b>	
14.20	<p>Adsorption of organic acids on clay rock. Desorption study using isotopic exchange  <u>Sabrina Rasamimanana</u>, R. Dagnelie and G. Lefèvre</p>	155
14.40	<p>Inverse Gas Chromatography, <sup>13</sup>C and <sup>19</sup>F solid state NMR as powerful tools to study the interactions between a fluorinated fungicide and raw or organically modified Patagonian montmorillonites  <u>Jocelyne Brendlé</u>, Rosa Maria Torres Sanchez, Federico Manuel Flores, Eric Brendlé and Séverinne Rigolet</p>	156
15.00	<p>Viability of bacteria in the presence of modified clay minerals: Perspective of polyaromatic hydrocarbon (PAH) biodegradation  <u>Bhabananda Biswas</u>, Binoy Sarkar, Asit Mandal and Ravi Naidu</p>	157
15.20	<b>BREAK</b>	
15.40	<p>From spent clay minerals to functional materials  <u>Ruanliang Zhu</u>, Qingze Chen, Minwang Laipan, Tianyuan Xu and Hongping He</p>	158
16.00	<p>The effect of diatomite addition on the pore characteristics of a pyrophyllite-diatomite composite support layer  <u>Jang-Hoon Ha</u>, Jongman Lee, and In-Hyuck Song</p>	159
16.20	<p><b>KEYNOTE:</b> Biochar Effects on Nutrient Leaching in Soils  <u>David Laird</u> and Natalia Rogovska</p>	160

	<b>Lecture room 1: Developments and applications of quantitative analysis to clay bearing materials incorporating The Reynolds Cup School</b> <i>Session Chairs: Mark Raven, Michael Plötze and Helen Pendlowski</i>	
09.10	<b>KEYNOTE:</b> The background, motivation and history of the Reynolds Cup <u>Jan Środoń</u>	162
09.30	Preliminary results of an inter-laboratory study on quantitative phase analysis <u>M. Suárez</u> , P. Aparicio, J. Fernández Barrenechea, J. Cuevas, R. Delgado, A.M. Fernández, F.J. Huertas, M.T. García-González, E. García-Romero, I. González, R. Fernández, L. León-Reina, A. López Galindo, J. Párraga, M. Pelayo, E. Pozo, M. Pozo, J.M. Martín-García, F. Nieto, A. Sánchez-Bellón, J. Santaren, A.I. Ruiz, E. and D. Terroso	163
09.50	PyXRD; a FOSS model to quantify disordered, layered minerals using multi-specimen X-ray diffraction profile fitting <u>Mathijs Dumon</u> and Eric Van Ranst	164
10.10	Geological interpretations of clay mineral content enhanced by discriminant function analysis (DFA) <u>Ray E. Ferrell</u> , George F. Hart, and Mohamed Agha	165
10.30	<b>BREAK</b>	
10.50	Quantitative clay mineralogy as provenance indicator for recent muds in the North Sea <u>Rieko Adriaens</u> , Edwin Zeelmaekers, Michaël Fettweis, Noël Vandenberghe and Jan Elsen	166
11.10	In-situ XRD studies of the clay mineralogy of Gale Crater, Mars <u>David Bish</u> and Ralph Milliken	167
11.30	Quantitative mineralogy of clay-rich silicoclastic rocks by using XRD and XRD/XRF methods <u>M. Cesarano</u> , D.L. Bish, P. Cappelletti, C. Belviso, F. Cavalcante and S. Fiore	168
11.50	Quantification of Soil Mineralogy by X-ray Powder Diffraction (XRPD) Full Pattern Fitting <u>Helen A. Pendlowski</u> and Stephen Hillier	169
12.10	Latest breakthrough of sub-micron SEM-EDS analysis discussed within the context of the 2014 Reynolds Cup participation <u>David Haberlah</u> , Dirk Sandmann and Michael Owen	170
12.30	<b>LUNCH</b>	
14.20	Outcomes of 12 years of the Reynolds Cup quantitative mineral analysis round robin <u>Mark D Raven</u>	171
14.45	Sample preparation suitable for quantitative XRD and procedures for identification of clay minerals <u>Michael Plötze</u>	172
15.10	Multi-specimen computer modelling: Examples of illite-smectite mixed-layered structural characterization <u>Marek Szczerba</u> and <u>Douglas K. McCarty</u>	173
15.35	<b>BREAK</b>	
15.55	X-ray powder diffraction full-pattern summation methods for quantitative analysis of clay bearing samples <u>Stephen Hillier</u>	174
16.20	The application of the Rietveld method in the Reynolds Cup contest <u>Kristian Ufer</u> and Mark Raven	175
16.45	Supporting methods for mineral quantification in clay-bearing rocks <u>Arkadiusz Derkowski</u> and Stephan Kaufhold	176

## The application of the Rietveld method in X-ray diffraction analysis of clays

Reinhard Kleeberg

Institute of Mineralogy, TU Bergakademie Freiberg, Brennhausgasse 14, D-09596 Freiberg, Germany.

kleeberg@mineral.tu-freiberg.de

The Rietveld method was originally developed to perform the refinement of crystal structure parameters from powder diffraction data (Rietveld, 1967). The principle consists in the fitting of a calculated diffraction pattern to a measured pattern by variation of structural, profile, and other parameters in a least-squares procedure. The complete diffraction profile must be calculated, and due to this the full information of the pattern (including crystal and microstructure, texture and phase abundance) is in principle obtainable and should be described in the model. The talk summarizes the success of the application of the Rietveld technique in clay science since the review of Bish (1993).

Just a few examples of successful clay crystal structure analysis by the Rietveld method have been published until now, because the general crystal structures of the most common clay minerals have been already solved and refined by using single crystals, by manual powder pattern modelling, or by combined techniques. Similarly, the majority of information about layer stacking and disorder is still derived from manual pattern fitting techniques, often by one-dimensional patterns measured from oriented samples. However, a boom of applications came up in the field of mineral quantification since the early 1990s. As the Rietveld method calculates the intensity from the scattering power of the content of the elementary cell, there is no calibration necessary (Hill & Howard, 1987), and the use of the full powder pattern minimizes some sources of errors which occur in classical XRD single peak mineral quantification. The challenge of the application to clay minerals consists in an adequate modelling of the complicated broadening of XRD peaks caused by the disorder of layer stacking of the clay minerals. Already the introduction of compromise models like the use of "observed" (calibrated) *hkl* files (Taylor & Matulis, 1994) or the formulation of empirical *hkl* dependent line broadening models (Bergmann & Kleeberg, 1998) significantly improved the results of clay mineral quantification and gave rise to a broad application of the Rietveld method in the daily practice. Further improvements in Rietveld phase analysis were reached by the development of the "single layer approach" suitable to model the patterns of turbostratically disordered clay minerals like smectites (Ufer et al., 2004). This approach allows phase quantification of smectites simultaneously with the refinement of structural parameters like the average site occupation factors and lattice parameters. More complex types of stacking faults like translational and rotational layer displacement or interstratification can hardly be treated in traditional Rietveld programs. Therefore, the integration of the recursive calculation (Treacy et al., 1991) into a Rietveld software code (Ufer et al., 2008) was necessary to formulate and refine a physically based model of stacking disorder of clay minerals. To a certain degree, classical structure analysis of interstratified clay minerals from oriented samples may be performed now within an automatic refinement (Ufer et al., 2012). Further improvements of models and software are to be expected and will probably cause a growing spread of Rietveld applications in clay science.

Bergmann, J. & Kleeberg, R. (1998) *Mat. Sci. Forum*, **278-281** (1), 300-305.

Bish, D.L. (1993) pp. 80-121 in: (R.C. Reynolds, Jr. and J.R. Walker, editors). CMS workshop lectures **5**, The Clay Minerals Society, Boulder CO.

Hill, R.J. & Howard, C.J. (1987) *J. Appl. Cryst.*, **20**, 467-474.

Rietveld, H.M. (1967) *Acta Cryst.*, **22** (1), 151-152.

Taylor J.C. & Matulis C.E. (1994) *Powder Diffraction* **9** (2) pp. 119-123.

Treacy, M.J., Newsam, J.M. & Deem, M.W. (1991) *Proc. R. Soc. London*, **A433**, 499-520.

Ufer, K., Roth, G., Kleeberg, R., Stanjek, H., Dohrmann, R. & Bergmann, J. (2004) *Z. Kristallogr.* **219**, 519-527.

Ufer, K., Kleeberg, R., Bergmann, J., Curtius, H. & Dohrmann, R. (2008) *Z. Kristallogr. Suppl.*, **27**, 151-158.

Ufer, K., Kleeberg, R., Bergmann, J. & Dohrmann, R. (2012) *Clays and Clay Minerals*, **60**, (5), 507-534.

Tuesday

7th July

Lecture Room 5

General (3)



## **Compression behaviour of natural and remoulded clays under monotonous and cyclic loading considering micro-structural evolution**

Nina Müthing, Wolfgang Lieske and Tom Schanz

Chair of Foundation Engineering, Soil and Rock Mechanics, Ruhr-Universität Bochum, Bochum, Germany,  
Nina.Muething@rub.de

Clays show a strongly time dependent material behaviour depending on the initial void ratio and stress conditions as well as on their microstructure, namely fabric (spatial particle arrangement) and bonding of the clay particles. The compression behaviour of a natural clay sample thus differs significantly from the behaviour of a mineralogical equivalent but destructured or remoulded sample. In engineering practice this difference in compression behaviour plays a significant role for many geotechnical applications such as tunnelling processes, where due to cyclic loading the soil is changed in its microstructure and experiences a transformation from natural to destructured state.

To analyse the microstructure-dependent compression behaviour, in the present study experiments on natural and remoulded clay material from a marine clay site in Onsøy, Norway are conducted. First of all the material is characterized considering its sensitivity, the plasticity characteristics as well as the intrinsic structure and salt content of the marine soil. In a series of oedometer tests the compression behaviour of natural and remoulded samples is studied. These tests results are analysed to study the influence of soil destructure on the compression behaviour of clays under static and cyclic loading. Furthermore, the influence of microstructural changes during the on-going consolidation process on the macroscopic compression behaviour is analysed. To do so, different methods for the analysis of the soil structure are evaluated and used to study the evolution of soil structure and pore size distribution during the on-going compression. For the cyclic compression tests a modified oedometer cell is used allowing measurements of the complete stress state (axial and radial total stresses) and pore water pressures.

## A sinking scenario which may require examinations on FEPs in bentonite

Koichi Shin

CRIEPI, Abiko 1646, Abiko-c. Chiba, Japan, shin@criepi.denken.or.jp

In some of the engineering barrier concepts for radioactive waste disposal, the waste container is surrounded and supported by a bentonite buffer. Since the container is heavy, the scenario of a container sinking in the bentonite buffer has been examined because excessive sinking may result in too-short distance between the container and the rock. In the previous considerations of a container sinking scenario and related 'Features, Events and Processes' FEPs, it seems only mechanical deformation of the bentonite buffer is considered.

This paper brings up another mechanism for the container sinking scenario, which has seemingly not been considered in the previous safety cases of rad-waste disposal. The FEPs are pressure dissolution of minerals at the stressed region in the bentonite buffer, followed by transportation to a less stressed region by diffusion and precipitation or flowing out. The container sinking by this mechanism will continue without ceasing because of the stress gradient caused by the container weight.

Pressure dissolution is enhanced dissolution of minerals by the stress. The process of pressure dissolution, diffusion and precipitation has come to be recognized as a predominant mechanism in many aspects of geological deformation and phenomena such as stylolite formation, diagenetic compaction and folding. This paper reviews the previous works on pressure dissolution of minerals and tries to convince readers that a pressure dissolution facilitated container sinking scenario exists.

The purpose of this paper is to contribute to making the safety cases robust from the viewpoint of container sinking. The safe disposal of rad-waste is considered as the responsibility of the current generation. The bases of the safety are to be described in safety case documents and transferred to the future generation as our message. The container sinking, which is a matter in the time frame of more than tens of thousands of years, should be evaluated not only from a mechanical point of view (such as soil mechanics and others which have dealt with mechanical deformation in the time frame of a few tens of years at most), but also from chemical point of view. Chemical deformation of bentonite through the process of pressure dissolution, diffusion and precipitation in the time frame of geological span should be addressed in a safety case and duly handled because we the current generation know chemical deformation of rocks and minerals exists.

The problem to be solved for the design and safety assessment of the engineered barrier is the estimation of the time-scale in which the sinking scenario proceeds. If the time is long enough compared to the safety assessment period, the scenario may not be important. If the time is not so long enough, then some adjustments to the design may be needed. But presently it seems detailed mechanism clarification and data about the scenario are lacking. It is hoped that science communities provide information to those responsible for compiling and reviewing the safety cases.

## The structure of opal-CT revisited

M J Wilson

James Hutton Institute, Aberdeen, AB15 8QH, UK, jeff.wilson@hutton.ac.uk

There is a conflict of evidence with regard to the structure of the silica polymorph known as opal-CT. The current widely accepted interpretation of the structure views opal-CT as made up essentially of a disordered interlayering of crystalline cristobalitic and tridymitic stacking units, in about equal proportions where the  $d$  spacing of the diffraction maximum is close to  $4.11\text{\AA}$ , but becoming progressively more ordered and cristobalitic as this spacing decreases in value and approaches the  $d_{(101)}$  reflection at  $4.04\text{\AA}$  of  $\alpha$ -cristobalite. The most compelling evidence for this interpretation comes from matching calculated and experimental XRD profiles, HRTEM lattice images and SAED patterns. This interpretation is here described as the “crystalline” model. However, the crystalline model is not supported by a variety of spectroscopic techniques that can be used to probe both long-range and short-range order. In general, these techniques which include FTIR, Raman, NMR and XANES spectroscopies are more consistent with a structure, especially where the diffraction maximum approaches  $4.11\text{\AA}$ , as being dominated by disordered material similar to amorphous opal (opal-A) but containing a small volume of crystalline stacking units which are mainly (sometimes exclusively) of a tridymitic nature. This interpretation is referred to as the “paracrystalline” model. From a critical review of the literature, suggestions are made as to how these two conflicting strands of evidence can be reconciled, as well as matters concerning appropriate nomenclature of opaline materials.

References.

M.J.Wilson, J.D. Russell, J.M. Tait, A new interpretation of the structure of disordered  $\alpha$ -cristobalite, *Contrib. Mineral. Petrol.* 47 (1974) 1–6.

M J Wilson. The structure of opal-CT revisited. *Journal of Non-Crystalline Solids.* 405 (2014) 68-75

## Study of a synthetic (IV)Fe<sup>3+</sup>-nontronite series with a wide range of tetrahedral charge

Fabien Baron and Sabine Petit

Université de Poitiers, CNRS-UMR 7285 IC2MP, HydrASA, Bât. 35, 4 rue Michel Brunet, 86073 Poitiers Cedex 9,  
France - fabien.baron@univ-poitiers.fr

Fe-rich dioctahedral smectites are ubiquitous at Earth surface, and exhibit large chemical variability in both tetrahedral and octahedral sheets. The common octahedral cations in natural dioctahedral smectite are Al<sup>3+</sup>, Fe<sup>3+</sup> and Mg<sup>2+</sup>, while Al<sup>3+</sup>, and sometimes Fe<sup>3+</sup>, can substitute Si<sup>4+</sup> in tetrahedral sheet. Due to the Fe<sup>3+</sup>/Al<sup>3+</sup> partitioning between tetrahedral and octahedral sites in dioctahedral smectite, and the strong preference of Al<sup>3+</sup>-for-Si<sup>4+</sup> substitutions (Decarreau and Petit, 2014), natural smectites with a high Fe<sup>3+</sup>-for-Si<sup>4+</sup> tetrahedral substitutions are uncommon. Pure Fe<sup>3+</sup>- nontronites can be useful to study the specific role of tetrahedral Fe<sup>3+</sup> on smectite reactivity, especially for redox experiments, and can also be used as reference minerals for spectroscopic techniques.

Clay synthesis is essential to obtain dioctahedral smectites free from Al<sup>3+</sup> and Mg<sup>2+</sup> and with a mastered amount of Fe<sup>3+</sup>-for-Si<sup>4+</sup> substitutions. A chemical series of strictly ferric nontronites with various tetrahedral Fe<sup>3+</sup> amount ((Si<sub>4-x</sub>Fe<sup>3+</sup><sub>x</sub>)Fe<sup>3+</sup><sub>2</sub>O<sub>10</sub>(OH)<sub>2</sub>Na<sub>x</sub>) are obtained from a coprecipitated gel under hydrothermal conditions at 150°C during six days. The interest of these synthetic nontronites is that the permanent layer charge due to Fe<sup>3+</sup>-for-Si<sup>4+</sup> substitutions only is localized in the tetrahedral sheet.

Experimental syntheses were performed under alkali conditions and clearly revealed that one of the key parameters controlling the tetrahedral Fe<sup>3+</sup>-for-Si<sup>4+</sup> substitutions is the pH of the contact solutions. The chemical analyses performed on synthetic nontronites by energy dispersive X-ray spectroscopy (EDS) suggest a tetrahedral Fe<sup>3+</sup> amount (x) ranging from about 0.35 to as high as 1.55 per half formula unit. The spectroscopic and X-ray diffraction data reveal a progressive incorporation of Fe<sup>3+</sup> in the tetrahedral sheet with increasing pH. The high incorporation of Fe<sup>3+</sup> in the tetrahedral sheet modifies drastically the b-parameter of the nontronite unit-cell. The b-parameter varies from 9.16 Å (d(06-33) = 1.529 Å) to 9.37 Å (d(06-33) = 1.56 Å) for x = 0.35 and 1.55, respectively. This very high d(06-33) value at 1.56 Å for a dioctahedral smectite was not previously reported and reveals a great flexibility of the smectite structure. The layer expandability moves from smectitic to vermiculite behavior with the increase of tetrahedral Fe<sup>3+</sup>-substitutions. These synthetic nontronites were used as reference minerals to calibrate spectroscopic techniques in order to better assign the Fe<sup>3+</sup> distribution in the crystallographic site of natural clay minerals. Another use of these synthetic nontronites could be the study of electron transfers processes in redox experiments.

Decarreau, A., and Petit, S. (2014) Fe<sup>3+</sup>/Al<sup>3+</sup> partitioning between tetrahedral and octahedral sites in dioctahedral smectites. *Clay Minerals*, 49, 657–665.

## Searching for nontronite in Eemian interglacial lake deposits

Christian Bender Koch<sup>1</sup> and Takeshi Kasama<sup>2</sup>

<sup>1</sup> Department of Chemistry, University of Copenhagen, Universitetsparken 5, DK-2100 Copenhagen Ø, Denmark  
(cbk@chem.ku.dk)

<sup>2</sup> Center for Electron Nanoscopy, Technical University of Denmark, DK-2800 Kgs. Lyngby, Denmark

The relatively recent Eemian interglacial in Scandinavia represents an approximately 100 kyear period of weathering and biological activity on land and in lake environments. During this period carbonates and sulphides were dissolved and leached from the surficial part of the glacial sediments into springs and lakes, where they reprecipitated as calcite and iron oxides. Within the lakes the primary productivity was high, adding silica (in the form of diatome frustules) and organic matter to the sediment. Decomposition of the organic matter potentially could induce recrystallization processes within the sediments. To investigate the possibility of such new mineral formation, we have sampled the only known interglacial lake deposit dominated by mixtures of calcium carbonate/iron oxide/silica in Denmark. In terms of bulk chemistry the lake sediment varies between 1 and 53 %wt. CaO, 0 and 60 %wt. Fe<sub>2</sub>O<sub>3</sub>, and 0.5 and 45 %wt. SiO<sub>2</sub>. The content of Al<sub>2</sub>O<sub>3</sub> is below 1 %wt. throughout the approximately 5 m thick deposit.

The purpose of this study is to investigate the possible new formation of minerals with emphasis on layer silicates using a combination of XRD, TEM and spectroscopies. The presentation includes the evidence obtained for the formation of nontronite, commonly together with Si-substituted iron oxides.

## NH<sub>4</sub>-bearing smectite as a nitrogen conveyor to deep Earth: An experimental approach

Daniel Grings Cedeño<sup>1</sup>, Rommulo Vieira Conceição<sup>2</sup>, Márcio R. W. de Souza<sup>3</sup> and Larissa C. Carniel<sup>4</sup>

<sup>1</sup>Universidade Federal do Rio Grande do Sul, Porto Alegre, Brazil/ daniel.gringscedeno@gmail.com

<sup>2</sup>Universidade Federal do Rio Grande do Sul, Porto Alegre, Brazil/ rommulo.conceicao@ufrgs.br

<sup>3</sup>Universidade Federal do Rio Grande do Sul, Porto Alegre, Brazil/ rwsmarcio@gmail.com

<sup>4</sup>Münster Universität, Münster, Germany/ larissageo@gmail.com

Nitrogen is one of the most important elements for life on Earth. It is an active participant in many biochemical and geochemical cycles in the upper crust. However, its role in deep Earth geochemical cycles and on a planetary scale is yet not fully understood. It is known by experimental research and chemical analyses in UHP (ultra high-pressure) minerals (mainly diamonds) that nitrogen is a relatively abundant component in the deep Earth, especially in the nucleus (Roskosz *et al.*, 2013). New research is trying to find out how the nitrogen found in the lower mantle is connected to the surface nitrogen cycle. A possible theory is that nitrogen could descend to deep Earth through a subduction mechanism (Sadofsky & Bebout, 2004) and in such a case, we suggest that nitrogen could enter in the clay minerals structure as an interchangeable cationic complex (NH<sub>4</sub><sup>+</sup>, for example). Previous studies showed that potassic smectite is stable at high pressure and moderate temperature (Carniel *et al.*, 2014), the similar conditions of cold subduction setting. Based on this, and the great capability of smectite to exchange its interlayer cation, we conducted experiments at high pressure and high temperature (HPHT) conditions on previously modified Ca-montmorillonite samples, in which we replaced the original Ca<sup>+2</sup> from by NH<sub>4</sub><sup>+</sup>, in order to verify its stability on such conditions. Ammonium is a good candidate to act as the cationic species that transport nitrogen into the mantle due to its similarities with K<sup>+</sup> (same charge and similar ionic radius), its reduced state, and its participation in biochemical cycles closely related to benthonic organic activity. In subduction zones, with increasing pressure and temperature, previous studies from our group (Carniel *et al.*, 2014) have shown that Ca<sup>+2</sup>-, La<sup>+3</sup>- and K<sup>+</sup>-smectite exposed to (HPHT) changes its structure at a certain temperature to illite-like or muscovite-like structures without losing any of these interlayered cations. This behavior is observed in nature, where smectites normally evolve to illites and later to muscovites in deep sedimentary basins or low to medium-grade metamorphic environments. In order to test this hypothesis we developed a series of experiments in which we simulated the exposure of pelagic sediments (smectites) with significant amounts of ammonium to the conditions found on a subducting oceanic plate. For that, we performed HPHT experiments conducted at pressures between 2,5 and 7,7 GPa and temperatures between 200 to 700 °C, on a high-pressure toroidal chamber (HPTC); and between ~1 to 12 GPa at room temperature, on the diamond anvil cell (DAC) apparatus. The samples were analyzed by different techniques such as Fourier Transform Infrared Spectroscopy (FTIR), *in situ* FTIR in a DAC and X-Ray Diffraction (XRD). We have observed that pressure and temperature modifies the structure in different ways, *i.e.* when pressure is applied at room temperature all the modifications that the mineral suffers are reversible (at least until 8 GPa). On the other hand, experiments of <1 atm shows that the structure changes irreversibly (to a dehydrated smectite) at about 600°C. But when applied together with pressure, the changes in the structure are anticipated to lower temperatures (approximately 300°C). These changes in the structure are generally confirmed with XRD analysis, as the variations of the 001 plane on the X-ray diffractogram are easily noticed. So far, all the changes in the crystal structure caused by both the increment of pressure and temperature helped to retain the ammonium inside the smectite lattice, as FTIR data indicates by the presence of nitrogen and hydrogen bonds (typical of ammonium) in all the samples.

**Keywords:** Experimental Petrology; Nitrogen; Mantle; Smectite; Subduction Zone.

Carniel L.C.; Conceição R.V.; Dani N.; Stefani V.F.; Balzaretto N.M.; dos Reis R. *Structural changes of potassium-saturated smectite at high pressures and high temperatures: Application for subduction zones.* Applied Clay Science, 2014, v. 102, pp. 164-171.

Roskosz M.; Bouhifd M.A.; Jephcoat A.P.; Marty B.; Mysen B.O. *Nitrogen solubility in molten metal and silicate at high pressure and temperature.* Geochimica et Cosmochimica Acta, 2013, v. 121, pp. 15-28.

Sadofsky S.J.; Bebout G.E. *Nitrogen geochemistry of subducting sediments: New results from the Izu-Bonin-Mariana margin and insights regarding global nitrogen subduction.* Geochemistry Geophysics Geosystems, 2004, v. 5, n. 3.

## Fraipontite/sauconite – a new interstratified clay mineral from the oxidation zone of the Zn-Pb-deposit Preguiça, Southern Portugal

Patrizia Will<sup>1,\*</sup>, Frank Friedrich<sup>2</sup>, Georg Grathoff<sup>3</sup>, Rupert Hochleitner<sup>4</sup> and H. Albert Gilg<sup>1</sup>

<sup>1</sup>Technische Universität München, Lehrstuhl für Ingenieurgeologie, Arcisstr. 21, 80333 München, Germany  
(\* patrizia.will@mytum.de)

<sup>2</sup>Karlsruhe Institute of Technology, Institute for Nuclear Waste Disposal, Hermann-von-Helmholtz-Platz 1, 76344  
Eggenstein-Leopoldshafen, Germany

<sup>3</sup>Ernst-Moritz-Arndt Universität Greifswald, Institute for Geography and Geology, Friedrich-Ludwig-Jahn-Str. 17A,  
17487 Greifswald, Germany

<sup>4</sup>Mineralogische Staatssammlung München (SNSB), Theresienstr. 41, 80333 München, Germany

The Zn-rich clay minerals sauconite and fraipontite are known from the oxidation zones of carbonate-hosted Zn-Pb deposits. While fraipontite is a rather rare serpentine mineral, some large and economically important occurrences of the smectite mineral sauconite exist. Interstratified clay minerals of the trioctahedral Zn-rich sheet silicates, however, have not been described so far.

The Preguiça mine is a carbonate-hosted Zn-Pb-deposit located in the Ossa-Morena-Zone in Southern Portugal close to the Spanish frontier. In the near-surface parts of the oxidation zone remarkably large amounts of white Zn-rich clays occur that have previously been reported as a fraipontite-bearing clay mineral association (Will et al. 2014). Detailed clay mineralogical investigations using XRD, FTIR spectroscopy, SEM and TEM both combined with EDX prompted by inconsistencies in the results of mineralogical investigations identified the hitherto unknown interstratified clay mineral fraipontite/sauconite. In most of the samples, fraipontite/sauconite is associated with tubular 7Å-halloysite. Accessory minerals are opal-A, APS-minerals, goethite and hematite as well as very minor amounts of calcite and descloizite. Additionally, detrital quartz and in some samples muscovite 2M<sub>1</sub> is present.

Fraipontite/sauconite from the Preguiça mine is a Zn-rich, irregular, two-component, interstratified clay mineral with fraipontite contents of about 70 to 90 % that was identified using XRD. Diagnostic properties for XRD identification are the intercalation of ethylene glycol that for instance expands the basal distance of fraipontite(0,70)/sauconite from 7,25 Å to 7,49 Å and the selective intercalation of sodium acetate (NaOAc) that could only be achieved by dry grinding, whereas KOAc, NH<sub>4</sub>OAc and NaCl, KCl, NH<sub>4</sub>Cl were not intercalated. The presence of fraipontite and sauconite in the mixed-layer structure was confirmed by ATR-FTIR-spectroscopy. The most characteristic peaks are at 3592 cm<sup>-1</sup>, 1066 cm<sup>-1</sup>, 610 cm<sup>-1</sup> and 566 cm<sup>-1</sup> for fraipontite and at 3635 cm<sup>-1</sup> for sauconite.

Fraipontite/sauconite forms platy to wavy sheets that are in most samples present in random orientation together with the halloysite tubes. Samples with higher sauconite content of up to 30 % in the mixed-layer structure exhibit characteristic smectite-like honeycomb structures.

Will P, Friedrich F, Hochleitner R, Gilg HA (2014) Fraipontite in the hydrothermally overprinted oxidation zone of the Preguiça mine, Southern Portugal. Programme and abstractbook, 7<sup>th</sup> Mid-European Clay Conference, 16-19 september 2014, Dresden, Germany, p. 133.

## Implications of cation occupation from the adsorption and desorption experiment of chromium for montmorillonite

Y. Cai<sup>1,\*</sup>, N. Meidina<sup>1</sup>, T. Maierdan<sup>1</sup>, H. Wang<sup>2</sup> and Y. Pan<sup>1</sup>

<sup>1</sup>State Key Laboratory of Metal Ore Deposits, School of Earth Sciences and Engineering, Nanjing University

\*caiyf@nju.edu.cn

<sup>2</sup> Key Laboratory of Surficial Geochemistry, Ministry of Education. School of Earth Sciences and Engineering, Nanjing University

Purified montmorillonite with trace amounts of quartz was equilibrated with different concentration chromium sulphate solutions for one week cation exchange to obtain chromium bearing montmorillonite (Cr-M), and then was subjected to desorption in solutions with different pHs. The pure montmorillonite, chromium bearing ones and desorbed ones were verified and tested using powder X-ray diffractometry (XRD), X-ray Fluorescence (XRF), Electron Spin Resonance (ESR) spectrometry and Fourier Transform Infrared (FTIR) spectroscopy to explore the occupation site of chromium. Based on the XRD analysis and the theoretical calculation of the size of the interlayer space, two types of hydration cations, such as  $[\text{Cr}(\text{H}_2\text{O})_6]^{3+}$  and  $[\text{Cr}(\text{H}_2\text{O})_3\text{O}_3]^{3+}$ , were inferred to be present in 0.2 M chromium sulphate solution-exchanged clays. And ESR spectra strongly differ before and after chromium exchange and desorption, where the new signals, such as  $g=1.976$ , 2.362, 2.510 and 3.055 in the second derivative spectrum of Cr-M3, suggest several occupational sites for chromium. Among them, the  $g=1.976$  and 2.510 were assigned to  $[\text{Cr}(\text{H}_2\text{O})_6]^{3+}$  (Zheng, 1991), and  $\text{Cr}^{3+}$  in tetrahedral site (Henning et al., 1967<sup>1</sup>), respectively. Then, the  $g=2.362$  and 3.055 may be assigned to the  $[\text{Cr}(\text{H}_2\text{O})_3\text{O}_3]^{3+}$  and the one present in the hexagonal cavity of the tetrahedron sheet which bounded with oxygen by van der Waals' force. Furthermore, the substitution of chromium for octahedral aluminium or daughter products with the  $(\text{Cr}, \text{Al})_2\text{OH}$  octahedron was suggested by the shift of  $\text{Al}_2\text{OH}$  bands comparing to the persistence of the  $\text{Mg}_2\text{OH}$  bands at  $845\text{ cm}^{-1}$ . And a  $\sim 20\text{ cm}^{-1}$  shift to a lower band sides of the Si-OH vibrations in the FTIR spectra of chromium bearing montmorillonite could be attributed to the substitution of Si or Al in tetrahedral site (Farmer, 1974). After desorption, this band revert to the original one (M0). This may suggest that the  $\text{Cr}^{3+}$  was entrapped in the easy accessible site, such as the edge of the TOT or near the surface of in the hexagonal cavities of TOT. This may suggest that the species of hydration cation is constrained by the concentration of the chromium solution. After desorption, the  $g=2.362$ , 2.510 and 3.055 disappeared in the ESR spectrum. This may imply the  $\text{Cr}^{3+}$  present in these three sites were leached out from the chromium bearing montmorillonite. In summary, the results comprehensively suggested that  $\text{Cr}^{3+}$  can exchange for cations in octahedral sites, such as  $\text{Al}^{3+}$  in octahedron,  $\text{Al}^{3+}$  in tetrahedron, and the cation entrapped in the hexagonal cavities and adsorbed on the surface of clay grains, as well as the cations in the interlayer space of montmorillonite, such as  $[\text{Cr}(\text{H}_2\text{O})_6]^{3+}$  and  $[\text{Cr}(\text{H}_2\text{O})_3\text{O}_3]^{3+}$  etc.

**Acknowledgements:** This study was supported by NSFC Project (41272055) and grant (G1210284013) from the ability of innovating and Entrepreneurship training programme (Nanjing University).

Farmer, V.C., 1974. Infrared Spectra of Minerals. Mineralogical Society monograph. Mineralogical Society of Great Britain & Ireland 539 pp.

Henning, J.C.M., Liebertz, J. and van Staple, R.P., 1967. Evidence for  $\text{Cr}^{3+}$  in four-coordination: ESR- and optical investigations of Cr-doped  $\text{AlPO}_4$  crystals. J. Phys. Chem. Solids, 28: 1109-1114.

Zheng, W.C., 1991. Determination of the Local Compressibility of the  $(\text{Al}_6\text{H}_2\text{O})^{3+}$  Group in  $\text{AlCl}_3 \cdot 6\text{H}_2\text{O}$  from the Pressure and Stress Dependences of Epr-Spectra for Substituting  $\text{Cr}^{3+}$  and  $\text{Fe}^{3+}$  Ions. Journal of Physics and Chemistry of Solids, 52(7): 871-874.



## Interpretation of the infrared spectra of synthetic silicate clays of the lizardite-nepouite series

Sabine Petit and Fabien Baron

Université de Poitiers, CNRS-UMR 7285 IC2MP, HydrASA, Bât. 35, 4 rue Michel Brunet, 86073 Poitiers Cedex 9,  
France - [sabine.petit@univ-poitiers.fr](mailto:sabine.petit@univ-poitiers.fr)

Nepouite and lizardite are the Ni- and Mg- end-members of the 1:1 layer silicates, respectively. These minerals are generally present in garnierites. Garnierites are weathering products of ultramafic rocks and constitute important Ni ore deposits in the world. Garnierites are composed of intimate and complex mixtures of 2:1 and 1:1 layer silicates whose compositions range from low to high Ni contents and the degree of structural order exhibits considerable variations. Due to this occurrence, pure samples of the –lizardite-nepouite series are rare. Consequently, there is a lack of spectroscopic reference data. Notably, Fourier Transform Infrared (FTIR) spectra of the –lizardite-nepouite series in the near infrared (NIR) region are not available in literature. Such spectral data are of interest, especially for field studies and Ni-mining companies. In order to obtain clear spectroscopic fingerprints, samples from the lizardite-nepouite series ( $\text{Si}_2\text{Mg}_{3-x}\text{Ni}_x\text{O}_5(\text{OH}_4)$  with  $x = 0, 0.5, 1, 1.5, 2, 2.5,$  and  $3$ ) were synthesized at  $220^\circ\text{C}$  during 7 days from coprecipitated gels in hydrothermal conditions. X-Ray Diffraction (XRD) confirms that pure 1:1 silicate clays were synthesized for all samples. A clear relationship between the  $d(06-33)$  and the Ni/Mg ratio of the synthesized samples followed a Vegard's law and suggested a rather random distribution of octahedral cations. IR spectra of this series were measured in both near and mid IR spectral regions ( $250 - 7500 \text{ cm}^{-1}$ ). The IR features for both Ni-nepouite and Mg-lizardite end-members were attributed. Notably, in the NIR region, the combination bands observed for both end-members could be attributed thanks to combinations of two or three vibration bands observed in the MIR region. The improvement in band attributions, especially in the near infrared range, contributes to development of infrared analyses in field geology and remote sensing.

## Neutron scattering studies of clay minerals

Neal Skipper

Department of Physics & Astronomy, UCL, Gower Street, London WC1E 6BT

Neutron scattering techniques can provide definitive information regarding both the molecular structure and dynamics within swelling clay minerals. In this lecture the focus will be on the interlayer region of these materials, and in particular our understanding of the role played by water as a solvent and the concomitant mechanisms of clay swelling and interlayer molecular diffusion. Results of experiments from the ISIS pulsed neutron source at the Rutherford Appleton Laboratory and the Institut Laue-Langevin reactor source will be discussed. We note that these facilities provide intense beams of neutrons whose wavelengths and energies are very well matched to the relevant length-scales and molecular excitation spectra. In the context of structure determination, a key advantage of neutron diffraction is that the atomic scattering lengths are isotope dependent. Isotopic labelling of samples via exchange of species including H/D,  $^6\text{Li}/^7\text{Li}$  and  $^{25}\text{Mg}/^* \text{Mg}$  can therefore be used in conjunction with difference analysis to obtain detailed information centred on the interlayer water and cations. This has allowed us to investigate the structural origins of hydrogen bonding, cation solvation, and the electric double-layer. In the context of interlayer dynamics, we are able to exploit the fact that, of all the elements, hydrogen has by far the largest incoherent neutron scattering cross-section. Measurements of interlayer diffusion by quasi-elastic neutron scattering are therefore dominated by the signal from any hydrogenated species. This has been applied to water itself, and, through selective deuteration, to study the dynamics of molecules such as aromatic pollutants and hydrogen  $\text{H}_2$ . Future opportunities will be reviewed, including those arising from direct time-resolved neutron imaging.

## Iron-oxides in the hyper-saline environment of the Dead-Sea area

Nurit Taitel-Goldman<sup>1</sup>, Vladimir Ezersky<sup>2</sup> and Dmitry Mogilyanski<sup>2</sup>

<sup>2</sup>The Open University P.O. Box 808 Raanana, Israel; nuritg@openu.ac.il

<sup>2</sup>Ilse Katz Institutes for Nanoscale Science and Technology, Ben-Gurion University of the Negev, Beer-Sheva, Israel

Iron oxides precipitated from the discharging Ca-chloride hyper-saline brines close to the Dead Sea or from Ein-Ashlag located on the eastern flanks of Mount Sedom diapir. Apart from Fe<sup>2+</sup> the brines are enriched with Mn, Zn and P. Initially formed iron oxides occur as inclusions within halite crystals, hence their initial composition is preserved and recrystallization processes are hindered.

By using XRD and HRTEM, hydrated iron-oxides were identified: initially formed due to oxidation of Fe<sup>2+</sup> at pH<5 and in the presence of Si is short-range ordered ferrihydrite - Fe<sub>5</sub>HOg\*4H<sub>2</sub>O (2-5nm) with Si/Fe 0.05-0.26, Mn/Fe=0.02-0.06 and P/Fe=0.02 impurities.

Acicular crystals of goethite  $\alpha$ -FeOOH (<100nm) are usually formed in the presence of carbonate, yet, at elevated Na concentration, multi-domain crystals were formed. Mn in goethite crystals had elevated concentrations (Mn/Fe 0.3) indicating a possible solid solution of goethite-groutite due to similar ionic radii. On the other hand, transformations of other phases into goethite in Ein Ashlag lead to more pure goethite crystals.

Rod-shaped akaganéite  $\beta$ -FeOOH (10-50 nm) precipitated in the presence of Cl. It crystallized either directly from the discharging brine or via dissolution/precipitation that preserved the morphology of the ferrihydrite precursor. Transformation of akaganéite into hematite was probably hindered due to Mn impurity (Mn/Fe=0.02-0.06) within the crystals.

Lepidocrocite  $\gamma$ -FeOOH (20-100nm) crystallized at a relatively fast oxidation rate having impurities of Si and Mn that reached the values of Si/Fe 0.06 and Mn/Fe 0.06.

Tiny hematite ( $\alpha$ -Fe<sub>2</sub>O<sub>3</sub>) crystallites were found in a recently formed crust covering limestone pebbles close to a discharging spring. The morphology of the hematite crystallites that are formed by a process of dehydration and rearrangement of ferrihydrite preserve the morphology of their precursor.

The most common impurity is Si, detected in all phases (Si/Fe 0.07-0.08). Zn, P and Pb probably adsorb on ferrihydrite, akaganéite and goethite surfaces.

## Clay mineralogy as a reflection of parent material and processes

Georgina Holbeche<sup>1</sup> and Robert Gilkes<sup>2</sup>

<sup>1</sup> School of Earth and Environment (M087), University of Western Australia, 35 Stirling Highway, Crawley, WA 6009, Australia. georgina.holbeche@uwa.edu.au

<sup>2</sup> School of Earth and Environment (M087), University of Western Australia, 35 Stirling Highway, Crawley, WA 6009, Australia

The south west of Western Australia is a landscape demarcated most significantly by geological stability, several major climatic shifts and a long history of weathering. Of low relief, this ancient landscape was formed under humid conditions however has experienced a semi-arid climate for the past million years. The region is largely underlain by the Archean granitic and gneissic rocks of the Yilgarn Craton. These materials have weathered to deep laterite profiles that are now highly dissected by erosion.

Although initially dominated by quartz and kaolinite of lateritic regolith; the landscape has experienced a long and complex weathering history during the dry climates of the last million years. Most regolith materials have experienced alteration by solute-rich ground water. Carbonates, gypsum and other evaporite minerals are now present in the regolith, having accumulated in valley floors during the current semi-arid climate. In addition, valley floors contain complex mixtures of alluvium, colluvium and saprolite as well as showing evidence of the impact of localised climatic, geological and groundwater conditions. Figure one shows their stratigraphic organisation, and some of the processes that have taken place in this complex landscape.

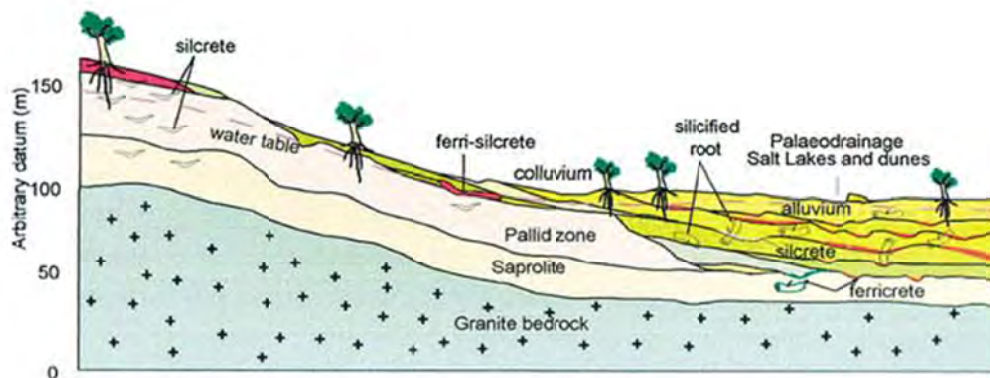


Figure one: An example of the complexity of materials formed in the Western Australian landscape (Gilkes et al. 2003).

A combination of detailed sampling and field observations has been used along with XRD (mineralogy), ICP-MS/XRF (chemistry) and SEM (image analysis) to identify materials and processes associated with this landscape. Features such as angular quartz or other primary minerals were identified in hand specimens and supported by SEM images. Similarly, XRD allowed identification of a variety of minerals including palygorskite and illite while SEM-EDS could detect rare earth minerals such as cerium phosphate. A combination of element mapping and imaging helped identify processes and sequences of events. Variations in iron concentration for example can be seen as fronts in SEM images, suggesting sequential episodes of inundation by iron-rich groundwater. In areas where XRD shows kaolinite is not the dominant matrix mineral, imaging shows where these sediments have been replaced or impregnated by calcite and dolomite; with illite, palygorskite or smectite now the dominant clay minerals in a carbonate matrix.

Gilkes R., Lee S. and Singh, B. (2003). The imprinting of aridity upon a lateritic landscape: an illustration from south western Australia C.R. Geoscience 335 (2003) 1207 - 1218

## **Preliminary approach to mineralogy and geochemistry of clay minerals intercalated with coal seams in the Neogene lacustrine Seyitömer Basin, Kütahya, western Turkey**

Hülya Erkoyun<sup>1</sup>, Selahattin Kadir<sup>1</sup> and Tacit Külah<sup>1</sup>

<sup>1</sup>Eskişehir Osmangazi University, Department of Geological Engineering, TR-26480 Eskişehir, Turkey, herkoyun@ogu.edu.tr

The Late Miocene-Pliocene units comprise bituminous shale, bituminous marl, marl, coal seam, siltstone, and sandstone which were deposited in lacustrine environment and associated with volcanic materials such as tuff and tuffite, and continue upward into Pliocene age andesite and basalt. Miocene and Pliocene units are affected by NW-SE and E-W trending faults. The geological, petrographical, mineralogical (XRD, SEM), and geochemical analyses were performed on the A19, S49 and Ayvalı panels at the Seyitömer basin. The fine grained pyrite and gypsum crystals occur in silicified levels and coal-bituminous units, respectively. Abundant smectite, illite-smectite and kaolinite is associated with quartz, accessory feldspar, olivine, gypsum and pyrite. The serpentinite and tuffaceous host rocks are partly to completely argillized and bearing stockwork type silica in-fill fissures. Micromorphologically, association of oriented flaky illite with irregular outlined kaolinite and edge feldspar, and smectite flakes associated with glass shard and feldspar suggest authigenic precipitation via dissolution and precipitation mechanism. The association of subrounded microorganism on resorbed feldspar indicate that biological processes produced organic acid which may have resulted in alteration of feldspar and volcanic glass. Enrichment of large ion lithophile elements, and light rare earth elements relative to middle rare earth elements and heavy rare earth elements with respect to primitive mantle and chondrite and distinct negative Eu anomalies reflect fractional crystallization of feldspar and amphibole. Increases in leaching of Na, K, Sr, Ba, Rb, and Fe with increasing degree of alteration reveal that hydration of feldspar, biotite, serpentine and volcanic glass in a basic environment resulted in precipitation of smectite and illite, in contrast kaolinite under acidic condition. Increase of Sr+Ba and Ni in altered units also suggest that Si, Al+Fe, Mg, and K required for smectite, illite, and kaolinite formation are presumed supplied from volcanic and ophiolitic basement units and precipitated under various pH conditions. Association of argillization and silicification with coal, microorganism, pyrite, and gypsum may indicate swampy environment and presence of hydrothermal activities.

**Keywords:** Smectite, Illite, Kaolinite, Coal seam, Neogene, Seyitömer coal deposit, Turkey.

**Acknowledgments:** This study was supported financially by the Scientific Research Projects Fund of Eskişehir Osmangazi University in the framework of Project 2014-368.

## Mineralogy, geochemistry and genesis of sepiolite and palygorskite in Neogene lacustrine sediments at the northern Eskişehir area, NW Turkey

Selahattin Kadir<sup>1</sup>, Hülya Erkoyun<sup>1</sup>, Muhsin Eren<sup>2</sup> and Nergis Önalgil<sup>1</sup>

<sup>1</sup> Eskişehir Osmangazi University, Department of Geological Engineering, TR–26480 Eskişehir, Turkey

skadir.euroclay@gmail.com

<sup>2</sup> Mersin University, Department of Geological Engineering, TR–33343, Mersin, Turkey

Sepiolite and palygorskite deposits are common in the Neogene lacustrine sediments at the northern Eskişehir area. They appear as layer or nodule of different color within the sediments. Sepiolites and palygorskite layers in the lacustrine sediments are associated with dolomite, sepiolite-palygorskite-bearing dolomite, marl and argillaceous limestone in Kepeztepe, Yukarı Dudaş, Karageyikli and Yunusemre regions. White nodular sepiolite crops out in the Upper Miocene reddish-brown conglomerates close to the stockwork-type magnesite deposits in the Nemli and Türkmentokat regions. X-ray diffraction (XRD) analysis reveals that sepiolite is dominant in the samples and associated with palygorskite. Both sepiolite and palygorskite are rarely associated with abundant dolomite and accessory magnesite, quartz, feldspar, and amphibole. Petrographic studies indicate that the carbonate rock samples are predominantly micrite, and partly converted to microsparite. In some samples, ostracods and dacycladecean algae are observed, and indicate restricted environmental conditions. Micromorphologically, development of sepiolite and palygorskite fibers as oriented platy fan- and interwoven hairlines-shapes and absence of dolomite, indicate direct precipitation from supersaturated solution, whereas fibers bridging dolomite crystals, indicate that both sepiolite and palygorskite formed post-dated dolomite via dissolution-precipitation mechanism under semi-arid to arid climatic conditions. Enrichment of large-ion lithophile elements and light rare earth elements relative to middle rare earth elements and heavy rare earth elements, and depletion in high-field-strength elements (except Th) with respect to primitive mantle and chondrite, and distinct negative Eu anomalies reflect fractional crystallization of feldspar and amphibole in claystone, limy claystone, argillaceous carbonate and carbonate. The sepiolite and palygorskite structural formulae are:  $(\text{Si}_{10.08}\text{Al}_{0.02})(\text{Fe}_{0.02}\text{Mg}_{11.43})(\text{Ca}_{0.36})$  and  $(\text{Si}_{7.32}\text{Al}_{0.68})(\text{Al}_{0.91}\text{Fe}_{0.77}\text{Mg}_{2.27}\text{Ti}_{0.06}\text{Mn}_{0.01})(\text{Ca}_{0.26}\text{Na}_{0.02}\text{K}_{0.3})$ , respectively.

The layered sepiolite deposits formed by direct precipitation from Si-supersaturated alkaline lake water. In contrast, sepiolite nodules occurred from diagenetic replacement of magnesite pebbles in shallow burial under alkaline environmental condition. The Si, Mg, Al+Fe and Ca required for sepiolite and palygorskite formation were supplied in solution(s) from the Paleozoic metamorphic and Upper Cretaceous ophiolitic rocks and locally Late Miocene-Early Pliocene volcanic, volcanoclastic and fluvio-lacustrine sedimentary rocks.

**Keywords:** Palygorskite, Sepiolite, Neogene, Argillaceous carbonate, dolomite, Eskişehir, Turkey

**Acknowledgments:** This study was supported financially by the Scientific Research Projects Fund of Eskişehir Osmangazi University in the framework of Project 2014-487.

## **Palaeoenvironmental meaning of clay minerals assemblages across the Late Pliensbachian-Early Toarcian (Early Jurassic) of Iberian Peninsula: Lusitanian, Algarve and Subbetic basins**

Ana Caniço<sup>1</sup>, Luís Vitor Duarte<sup>1</sup>, Fernando Rocha<sup>2</sup>, Matías Reolid<sup>3</sup> and Denise Terroso<sup>2</sup>

1 MARE – Marine and Environmental Sciences Centre, Faculdade de Ciências e Tecnologia, Universidade de Coimbra, Departamento de Ciências da Terra, Coimbra, Portugal; canico.ana@gmail.com

2 Departamento de Geociências and Centro Geobiotec, Universidade de Aveiro, Portugal

3 Departamento de Geología y Centro de Estudios Avanzados en Ciencias de la Tierra. Universidad de Jaén, Jaén, Spain

In the Iberian Peninsula, the Pliensbachian and Toarcian are characterized by marine carbonate deposits (mainly marly limestones). This interval shows important changes in depositional palaeoenvironment such as the cases of the Pliensbachian-Toarcian transition and the early Toarcian oceanic anoxic event. In this work we developed a mineralogical analysis (whole-rock mineralogy and clay minerals) across the upper Pliensbachian – lower Toarcian in three reference sections of western and southern parts of the Iberian Peninsula, which represent distinct palaeogeographic contexts, namely: Ponta do Trovão section (Lusitanian Basin), Armação Nova section (Algarve Basin) and Cueva del Agua section (Subbetic Basin). Our aims are to demonstrate the stratigraphic mineralogical variability in each sector, correlate its evolution in the three stratigraphic successions and highlight the important contribution that the clay minerals assemblages can give pertaining to the palaeoenvironmental changes and depositional conditions for this time. We analyzed about 90 samples by X-ray diffraction and semi-quantification was calculated using MacDiff 4.2.6. Besides the clear domain of calcite in the series, the whole-rock mineralogy demonstrates an increase of phyllosilicates above the Pliensbachian-Toarcian transition, which becomes more evident at the base of Levisoni Zone, with a quite regular evolution along the stratigraphic succession of quartz, potassium feldspar and dolomite. This mineralogical variation is corroborated by marly deposition dominated in the base of the lower Toarcian of the three basins. The clay minerals assemblages identified in all sectors are always dominated by illite+illite-smectite mixed-layers, with different contributions of kaolinite and chlorite, and with smectite occurring in trace amounts, except in Cueva del Agua section where its quantitative expression is more significant. In the Pliensbachian-Toarcian transition of Ponta do Trovão and Cueva del Agua sections, the decrease of the illite+illite-smectite mixed-layers with an increase of kaolinite and chlorite is particularly evident. The base of Levisoni/Serpentinum chronozone, correlatable with the Early Toarcian oceanic anoxic event, is generally marked in Cueva del Agua by a clear decrease of kaolinite, showing this mineral at Peniche the same kind of expression observed in the previous chronozone (Polymorphum).

## Diagenesis and reservoir development in the Triassic Bunter Sandstone of Structure 5/42, Southern North Sea: evaluation for purposes of CO<sub>2</sub> storage

Graham Blackburn<sup>1</sup>, Alastair Brown<sup>2</sup>, Steve Furnival<sup>2</sup>, Peter Rowbotham<sup>2</sup>, Iulia Wright<sup>2</sup> and Rohan De Silva<sup>3</sup>

<sup>1</sup> Blackburn Geoconsulting, 26 East Pier Street, Bo'ness, EH51 9AB, UK, graham@blackbourn.co.uk

<sup>2</sup> AGR TRACS International Ltd, 3<sup>rd</sup> Floor, Union Plaza, 1 Union Wynd, Aberdeen, AB10 1SL. UK

<sup>3</sup> National Grid Carbon, 1<sup>st</sup> Floor East, 31 Homer Road, Solihull, B91 3LT, UK

National Grid Carbon are in the process of assessing the suitability of a large anticline within the Triassic Bunter Sandstone, the 5/42 structure, located in UKCS quadrants 42 and 43, for CO<sub>2</sub> storage. The structure forms part of an extensive Bunter Sandstone saline aquifer. Appraisal well 42/25d-3 was drilled on the western margin of the structure during the summer of 2013. Cores were cut representing a section 631.6 ft (192.51 m) thick covering the lower part of the Rot Halite and underlying Rot Clay, and much of the underlying Bunter Sandstone reservoir sequence.

Bunter Sandstone detrital grains are dominated by quartz and feldspar, with granitic fragments and altered volcanic material. Small volumes of mica and heavy minerals occur. An extensive bed of reworked ooids from the underlying Rogenstein Member forms a distinct calcareous horizon several feet thick. Authigenic cements include dolomite and anhydrite, precipitated shortly after deposition and during burial. Minor quartz and feldspar overgrowths are observed.

The Rot Clay, deposited in an extensive playa lake in which the succeeding Rot Halite was also precipitated, comprises red mudstones with anhydrite nodules and finely crystalline dolomite cement. The Rot Halite comprises coarsely crystalline halite, with thin laminae, pods, and beds up to 3-ft (1 m) thick of finely crystalline anhydrite. These deposits would form the top-seal for CO<sub>2</sub> storage.

Burial modelling indicates that the Bunter in 42/25d-3 reached a maximum depth of around 2500 m during the Late Cretaceous, with maximum temperatures of up to around 115-130° C during episodes of crustal heating in the Late Jurassic and Early Tertiary. The smectite→illite transition appears to have been completed during these episodes. Subsequent Tertiary cooling to <70° C resulted from a combination of reduced basal heat flow and substantially lower surface temperatures.

Evidence for the former presence of substantial halite cement includes abundant halite in other Bunter Sandstone successions in the region, undercompaction of the sediment despite previous deeper burial, and the presence of a seismic phase reversal at top-Bunter level, interpreted as resulting from the presence of halite cements at greater depth. A model is proposed for halite removal from the 5/42 structure by circulating groundwaters in the form of thermohaline convection cells related to Zechstein salt diapirs. Similar convection cells have been demonstrated within laterally equivalent deposits in the Northeast German Basin. The Bunter Sandstone reaches the sea bed over a salt diapir to the ESE of the 5/42 structure. Halite-bearing fluids may have been expelled here since at least the Early Tertiary. Meteoric fluids may also have entered the Bunter during periods of uplift, and there are indications of the action of such fluids during diagenesis. Stable isotope results are ambiguous, and neither disprove nor support the presence of meteoric fluids.

Reservoir quality within the Bunter Sandstone is influenced by grain size, grain sorting, authigenic cements and detrital clay volumes. Much of the existing porosity probably results from dissolution of former halite cements which would have been patchily developed, imparting an essentially random element to the porosity at the local scale, preventing accurate prediction. On a larger scale the Bunter sandstone is moderately uniform, with almost no barriers to horizontal flow. Beds of mudstone and mud rip-up clasts, layers of anhydrite and the ooid-bearing horizon will all act as baffles to vertical flow, but the presence of substantial barriers to flow in any direction in the 42/25d-3 area is considered to be very unlikely.



## **Is there a connection between early tetrapods and clay mineralogy in the coastal floodplain sediments of the Old Red Sandstone–Carboniferous of S.E. Scotland?**

Christopher Jeans and Giulio Lampromnti

Department of Geography, University of Cambridge, Cambridge, CB2 3EQ, cj302@cam.ac.uk

Department of Earth Sciences, University of Cambridge, Cambridge CB2 3EQ

There is in progress a large research project [TW:eed] based around Roemer's Gap — a 15 million year period [approx. 360 to 345 million years ago] named after this famous American vertebrate palaeontologist— where there is little or no evidence in the fossil record about the evolutionary development of vertebrates. Missing are links between fish and tetrapods and the splitting off of the amphibians and amniotes. Recent fossil finds suggest that intermediary links may occur in the Cementstones [now referred to as the Ballagan Formation]. The Cementstones represent deposits of coastal plain environments and mark the transition from the sediments of the Old Red Sandstone— deposited on the continent under arid conditions in valleys, flood plains and lakes by rivers draining the Lower Palaeozoic sediments of the rising Southern Uplands after they had been lightly metamorphosed during the Caledonian orogeny— and the overlying Carboniferous sediments of limestone, mudstone, sandstone and coals representing the lushly vegetated coastal plain, swamps and river deltas and the marine reefal environments of a tropical region. Preliminary investigation in S. E. Scotland, unrelated to the TW:eed Project, of the clay mineralogy of the upper part of the Old Red Sandstone, the transition zone [Cementstones/Ballagan Formation], and the overlying Carboniferous sediments has suggested a complicated pattern of clay mineral assemblages quite unlike those associated with either the underlying Old Red Sandstone or the overlying Carboniferous.

Tuesday  
7<sup>th</sup> July

Lecture room 4

Clay mineral indices in  
palaeo-geothermal studies  
hydrocarbon and  
geothermal prospection –  
third Frey-Kübler  
symposium

## Geochronology and isotope geochemistry of clay minerals to study thermal and fluid flow events

I. Tonguç Uysal<sup>1, 2</sup>

<sup>1</sup>Queensland Geothermal Energy Centre of Excellence, The University of Queensland, Queensland 4072, Australia

<sup>2</sup>Department of Geological Engineering, Hacettepe University, Beytepe, Ankara TR 06800, Turkey

E-mail: t.uysal@uq.edu.au

Combined application of geochronology (Rb–Sr and Ar–Ar), isotope ( $\delta^{18}\text{O}$  and  $\delta\text{D}$ ), and trace element geochemistry of potassium-bearing authigenic clay minerals is a powerful tool in recording episodic fluid flow events initiated by tectonics. Illite can particularly provide useful information on ore-forming hydrothermal processes, geothermal systems, and hydrocarbon maturation and migration in sedimentary basins. In this contribution, key findings of previous and current studies are presented on geochronology and isotope geochemistry of illitic clay minerals to reconstruct the evolution of some Australian sedimentary basins with energy and metal resources, deformation history for plate-boundary fault systems, and hydrothermal processes in relation to meteorite impact events.

The thermal history and fluid flow events of eastern and post-depositional extensional tectonic processes largely dominated the central Australian sedimentary basins. One of the largest hydrocarbon-bearing basins in the world is the Bowen Basin in eastern Australia, which experienced significant extensional tectonics in the late Triassic and early Jurassic. This tectonic regime was more effective in the northern part of the basin with the development of a meteoric hydrothermal system. Significant differences are evident in the clay mineralogy and isotope compositions of clays for samples from the northern and southern Bowen Basin, although the investigated samples are from similar stratigraphic levels and similar lithology. The Gunnedah Basin, which is the central part of the Bowen-Gunnedah-Sydney Basin system, has a different thermal and fluid flow history than the Bowen Basin, despite similar depositional and basin history. Episodic meteoric hydrothermal fluid flow events occurred in the Gunnedah Basin during the mid-Cretaceous in association with Gondwana rifting accompanied by alkaline magmatism. The Cooper, Warburton, Galilee, Drummond, and Eromanga Basins in central-eastern Australia are endowed with significant metal and energy resources. Integrated analyses of authigenic illite from these basins provide evidence for three periods of elevated thermal regime associated with regional tectonism during the Carboniferous, Late Triassic-Jurassic, and Cretaceous. The present geothermal regime in Australia is related to Cretaceous extensional tectonic episodes that control the creation and distributions of fracture zones being reactivated neo-tectonically and hence allowing heat and volatile release from the mantle.

Besides regional geological implications, direct dating of brittle faulting using illite-bearing fault gouge is a relatively new and exciting field in tectonics and offers a prolific approach for determining the absolute timing of tectonic events in areas that have largely relied on indirect information. For example, Rb–Sr and Ar–Ar geochronology of fault gouge illites from plate boundary fault zones and regional-scale intra-plate fault systems in Turkey and Australia determine the timing of tectonic plate movements and interactions. Stable isotope data of fault gouge illites suggest that clays precipitated from metamorphic fluids mobilised from lower crust in plate boundary deep fault zones and from evolved basinal fluids in the upper crust in intra-plate fault systems.

The combination of geochronology and clay mineralogy has also been used to investigate the evolution of Woodleigh impact structure in Western Australia, as information on physico-chemical conditions of post-impact hydrothermal alteration processes are recorded in clay minerals.

## **Age constraints of low-temperature alteration using K-Ar dating of celadonite in the Proterozoic basaltic North Shore Volcanic Group, Minnesota**

Susanne Th. Schmidt<sup>1</sup> and Klaus Wemmer<sup>2</sup>

<sup>1</sup> Sciences de la Terre et de l'environnement, Uni Genève, Rue des Maraîchers 13 CH 1205 Genève,

<sup>2</sup> Geowissenschaftliches Zentrum der Georg-August-Universität, Goldschmidtstr. 3 DE 37077 Göttingen

Susanne.Schmidt@unige.ch

Determining onset and duration of low-temperature alteration in burial or hydrothermal environments in basaltic sequences is not a straightforward task due to the lack of minerals suitable for dating. In general, it is considered that low-temperature alteration following the deposition of lava flows is a short-termed event spanning some millions of years. Celadonite occurring in amygdules of the low-temperature altered Proterozoic basaltic North Shore Volcanic Group (NSVG) in Minnesota established a time window for the alteration in zeolite and lower greenschist facies conditions.

The North Shore Volcanic Group is part of the Midcontinent Rift System in North America. Initiation of the Midcontinent Rift magmatism is attributed to an upwelling mantle plume at an early magmatic stage at ca. 1109-1106 Ma. A main stage of Midcontinent Rift evolution is dated at ca. 1100-1094 Ma during which the voluminous North Shore Volcanic Group was deposited.

During burial conditions the ca. 8000 m thick North Shore Volcanic Group was overprinted at lower greenschist to zeolite facies conditions. Celadonite is part of low-temperature assemblages occurring in amygdules together with laumontite or stilbite and interstratified smectite-chlorite. In the stratigraphically lower part of the NSVG at prehnite-pumpellyite facies conditions, celadonite formation occurred between  $1062 \pm 16.1$  Ma. A second sample from the same lava flow but at a distance of ca 0.8 km was dated at  $1039.4 \pm 14.5$  Ma. Another sample is located higher in the stratigraphic pile and overprinted at upper zeolite facies conditions (stilbite-heulandite-smectite assemblage). It was dated at  $955.0 \pm 12.4$  Ma. The dates allow us to postulate that low-temperature alteration occurred well after lava deposition and was a long-lasting process spanning a period of ca. 100 Ma related to hydrothermal activity during burial.

## **XRD and K-Ar of illite-smectite as basin history tools: verification by apatite fission tracks and (U-Th)/He in zircon**

Jan Środoń<sup>1</sup>, Aneta A. Anczkiewicz<sup>1</sup>, István Dunkl<sup>2</sup>, Igor Vlahović<sup>3</sup>, Ivo Velić<sup>4</sup>, Bruno Tomljenović<sup>3</sup>, Tadeusz Kawiak<sup>1</sup>, Michał Banaś<sup>1</sup> and Hilmar von Eynatten<sup>2</sup>

<sup>1</sup>Institute of Geological Sciences, Polish Academy of Sciences, Research Centre in Kraków, Senacka St. 1, PL-31002 Kraków, Poland

<sup>2</sup>Sedimentology & Environmental Geology, Geoscience Center, University of Göttingen Goldschmidtstrasse 3, D-37077 Göttingen, Germany

<sup>3</sup>University of Zagreb, Faculty of Mining, Geology and Petroleum Engineering, Pierottijeva 6, HR-10000 Zagreb, Croatia

<sup>4</sup>Geolog d.o.o. and Croatian Geological Summer School, Pančićeva 5, HR-10000 Zagreb, Croatia

Among clay minerals, illite-smectite is a unique source of information on the thermal history of a sedimentary basin: both on the maximum paleo-temperatures and the timing of these paleo-temperatures. The maximum paleo-temperatures can be evaluated from the illite:smectite ratio measured by XRD for shales and mudstones, and the timing can be estimated from the K-Ar dates of the clay fractions of bentonite layers. The abundance of illite-smectite makes this approach quite universal, particularly in oxidized sedimentary sequences devoid of organic matter.

This approach requires verification, as it is based on the assumption that temperature is by far the dominant factor controlling the illite:smectite ratio, so the other factors can be safely ignored. Such verification is provided by the products of natural radioactive decay of <sup>238</sup>U, present in the structures of apatite and zircon: fission tracks and atoms of He. The concentrations of these reaction products and of the un-reacted uranium serve as isotopic clocks. The fission tracks anneal and He diffuses out of the crystal grain at specific temperatures, characteristic of these crystals, so the isotopic clocks are totally reset if the rocks enter elevated temperatures. The ages obtained by these techniques for such reset rocks date the last crossing of a given isotherm (100-120 °C for AFT – apatite fission tracks, and 170–190 °C for ZHe – (U-Th)/He in zircon) during the cooling segment of thermal history.

The combined XRD, K-Ar, AFT, and ZHe study was conducted for the Carboniferous, Permian, and Triassic clastic rocks exposed in several tectonic structural domains of the Karst Dinarides in Croatia. All these rocks contain illite and/or illite-smectite as the dominant clay minerals. The most illitic composition in a given area was used as the measure of the maximum paleo-temperatures and these values were evaluated from a calibration curve (Środoń, 2007). They decrease between 250 and 156°C from west to east. The K-Ar dates of the finest clay fractions of bentonites indicate roughly the beginning of illitization: 99–76 Ma, and of the coarsest - the end of the process, i.e. age of the maximum paleo-temperatures: 84–49 Ma. This significant spread of K–Ar dates is consistent with a complex and long burial history: slow sedimentary burial in a carbonate platform, followed by tectonic burial.

In all areas with illite–smectite maximum palaeo-temperatures >180 °C the ZHe ages are totally reset and range from 82 to 34 Ma. In the locality with the maximum paleo-temperature below the ZHe reset range, the ZHe age is much higher (213 Ma), close to the stratigraphic age, which indicates low level of reset. Thus the ZHe dates support the estimates of the maximum paleo-temperatures based on the illite–smectite composition. The reset ZHe ages, representing ca. 190 °C period are close or substantially lower than the corresponding K–Ar ages, representing the maximum paleo-temperature period.

All AFT ages are totally reset and range from 80 to 24 Ma, which means they are at least 120 Ma younger than the stratigraphic ages. This is consistent with the maximum temperatures for these samples being >156°C.

Based on this and previous studies of the authors, illite paleo-thermometry works well, at least for the Miocene-Silurian time range.

## Deformation controlled low-grade metamorphism in the Patagonian fold-and-thrust belt in the Torres del Paine area, Chile (51° 30' S): Combining K/Ar, XRD and O isotopic data

Annette Süssenberger<sup>1</sup> and Susanne Th. Schmidt<sup>1</sup>

<sup>1</sup> Section of Earth and Environmental Sciences, University of Geneva, Rue de Maraichers 13, 1205 Genève, Switzerland  
(annette.suessenberger@unige.ch)

The deformation-controlled low-grade metamorphism of the Late Jurassic to Cretaceous sedimentary sequence of the Patagonian fold-and-thrust belt deposited in the westernmost Ultima Esperanza Precordillera (southern Chile) was determined using a dating approach that combines K/Ar chronology, XRD quantification and stable isotope geochemistry (H,O) on diagenetic and syn-kinematic illites.

The studied area is located east of the Patagonian Cordillera and is part of the Patagonian fold-and-thrust belt which forms the western part of the Magallanes retro-arc basin. In this basin structure a >4000 m thick marine sequence of turbidites, sandstones and shales was deposited during the late Cretaceous (Turonian to Campanian). A compressional deformation along the foreland basin margin resulted in an intense folding and thrust faulting of the Upper Cretaceous Punta Barrosa and the lowermost Cerro Toro Formations. Further east, the Upper Cerro Toro and overlying basin formations are lacking this metamorphic overprint. Crosscutting relationships reveal that folding and thrust faulting of the Punta Barrosa Formation occurred before 17 Ma (Fosdick et al. 2011) as well as before the plutonic phase of the Torres del Paine intrusion (12.5 Ma, Leuthold et al.).

Clay-rich samples were selected within the Cretaceous Zapata, Punta Barrosa and Cerro Toro Formations. Kübler Index (KI) values of the <0.2 µm and <2 µm fractions were determined and range from 0.23 to 0.58 °2θ in the <0.2 µm and 0.28 to 0.46 °2θ in the <2 µm fraction. Diagenetic values are observed in the East, where they reflect burial conditions. In the West, KI values seem to correlate best with the regional deformation intensity and any contact-metamorphism by the post-kinematic Torres del Paine intrusive complex can be excluded. Oxygen isotope values (δ<sup>18</sup>O) vary between 11.09 and 15.19 ‰ and hydrogen isotope values (δD) between -76 and -113 ‰. Minor variations within different grain sizes indicate an isotopic equilibration between different illite generations. At present, these values can be interpreted either as a result of burial or hydrothermal origin caused by a deformation or a magmatic event.

K-Ar ages obtained from the <0.2 µm and <2 µm fractions vary between 46.2±0.7 and 62.1±0.1 Ma in the <0.2 µm fraction and between 55.3±0.9 and 80.8±1.2 Ma in the <2 µm fraction. Samples in the East show ages of around 80 Ma in the <2 µm fraction and confirm a late Cretaceous burial peak which is close to the stratigraphic age of 80-86 Ma. Ages in the <0.2 µm fraction are significantly younger (ca.60 Ma) and indicate a weak thermal event which likely corresponds to the deformational event. The resetted <2 µm fraction of samples in the West suggest an onset of compressional deformation at around 60 Ma which continued until 46 Ma in the westernmost part of the study area. The age data indicate a continuous regression of deformation intensity and a regional low-grade metamorphic overprint from west to east related to deformational shortening.

Fosdick, J.C., Romans, B., W., Fildani, A., Bernhardt, A., Calderon, M., Graham, S., A. 2011: Kinematic evolution of the Patagonian retroarc fold-and-thrust belt and Magallanes foreland basin, Chile and Argentina, 51°30, Geol. Soc. Am. Bull., 123, no. 9-10, 1679-1698.

Leuthold, J., Müntener, O. Baumgartner, L.P., Putlitz, B., Ovtcharova, M., Schaltegger, U. (2012) Time resolved construction of a bimodal laccolith (Torres del Paine, Patagonia) Earth and Planetary Science Letters 325-326, 85-92.

## Applying clay mineral and organic matter indices to determine rock maturity and grade of diagenesis to incipient metamorphism focused on correlation problems

Rafael Ferreira Mählmann

Technische- u. Niedrigtemperatur Petrologie, Technische Universität Darmstadt, Germany (Ferreiro@geo.tu-darmstadt.de)

It is widely accepted that many clay minerals are useful to determine the grade of diagenesis as some of their properties are temperature dependent. The most frequently applied methods are the 10 Å illite Kübler-Index (KI), the 7 Å and 14 Å chlorite Árkai-Index (ÁI), the smectite (montmorillonite) – illite reaction progress (I-S), the decrease in expandable clay minerals, but also the evolution of clay mineral paragenesis, polytype transformations, and the neo-formation of micas. When using these methods, however, kinetic control of the reactions during early and late diagenesis to incipient metamorphism is mostly not considered. The temperature of thermal events can be determined, but also pressure estimates are feasible for example by illite  $b_0$ -values or Si (pfu) in micas. These clay mineral geo-thermometers and geo-barometers are rarely compared with clay-mineral evolution independent processes as organic matter indices or organo-mineralogical and geochemical parameters like vitrinite reflectance (VR), vitrinite like bituminite reflectance (VIBR), bituminite reflectance (BR), organic matter (OM) fluorescence, methyl-phenanthrene index (MPI), pristine-phytane index, HC/TOC ratio; and also fluid inclusion micro-thermometry (FI), index mineral or facies-critical paragenesis to estimate equilibrium levels to better decipher peak thermal or pressure conditions.

The study focuses on the comparison between KI, I-S, VR, BR and VIBR using samples from different geodynamic settings. The BR (VIBR) of the homogeneous isotropic (low grade diagenesis) and anisotropic bituminite (at higher grade) shows a highly significant and robust correlation with VR, I-S or KI if autochthonous. This can be used as a rank-indicator for the grade of diagenesis and metamorphism. Therefore, it is recommended to use both methods as a mutual controlling technique for further correlation.

The correlation between clay mineral content (discrete phase analysis), facies-critical paragenesis (bulk rock analysis) optical coal-petrology (discrete maceral characterization) and organochemical (bulk organic analysis) parameters mostly show a poor correlation due to the different scales analysed (composition of the mineral phase, bulk rock, OM). The best correlation between a clay mineral method and OM method is found if the metamorphic event is iso-chemical, syn-kinematic, monophasic and synchronous. Under polyphase or pluri-facies conditions this is of course very different. Nevertheless HC/TOC, MPI, OM Raman data, I-S plus KI and ÁI should be combined with pressure, temperature, time, and heat flow dependent as shown by VR, VIB and BR. This will be shown in a simple visualization using a P-T geothermal gradient plot. The need for accurate kinetic models is evident. Finally these results will be evaluated with regard to recent discussions on KI calibration.

## Temperature determination between 50 and 270°C through fluid inclusion microthermometry and vitrinite reflectance values in the external parts of the Central Alps

Josef Mullis<sup>1</sup>, Monika Wolf<sup>2</sup>, Rafael Ferreiro Mählmann<sup>1,3</sup>

<sup>1</sup>Mineralogisch-Petrographisches Institut, Bernoullistr. 30, 4056 Basel, Switzerland (Josef.Mullis@unibas.ch)

<sup>2</sup>Mergelskull 29, 47802 Krefeld, Germany

<sup>3</sup>Technische- u. Niedrigtemperatur Petrologie, Technische Universität Darmstadt, Germany

Fluid inclusion homogenization temperatures in prismatic and fibrous quartz from 40 Alpine fissures formed synkinematically during orogenic metamorphism in external parts of the Central Alps were compared with maturation rank determined by vitrinite reflectance  $\%R_f / \%R_{max}$  of the host rocks and with fluid inclusion composition. As the measured higher hydrocarbon- (HHC) and methane-bearing water-rich fluid inclusions are related to water-bearing higher hydrocarbon- and methane-rich fluid inclusions due to fluid immiscibility, their homogenization temperatures reveal entrapping formation temperatures.

Earliest prismatic and fibrous quartz (without decrepitated and reequilibrated fluid inclusions) in diagenetic and anchimetamorphic rocks crystallized close to maximum heating temperatures. Thus, the homogenization temperatures of hydrocarbon saturated water-rich fluid inclusions can be used as a geothermometer between 50 and 270 °C (Mullis, 1979; Mullis et al., 2002).

The process of vitrinite maturation is irreversible and the level of organic maturity is basically the product of temperature and time. Based on experimental data, numerical kinetic models and maturity inversion techniques, it is possible to derive thermal histories from vitrinite reflectance data in sedimentary basins and also in orogenic belts. The main premise is the use of a petrological calibrated VR model (Ferreiro Mählmann, 2001). Currently all available VR modeling packages are questionable because they neglect pressure (Le Bayon et al. 2011; Ferreiro Mählmann & Le Bayon, 2015). Thus, temperatures determined by fluid inclusion microthermometry give a much higher and direct temperature control to maturity models. Precondition is the syngenetic and synchronous peak of temperature of vitrinite maturation and fluid inclusion entrapment.

In the temperature range from 50 to 270 °C, the following relationships between fluid inclusion homogenization temperatures, vitrinite reflectance and fluid composition for an orogenic belt like the external parts of the Central Alps have been established:

~150°C	VR = 1.3 ± 0.2 %	End of the oil window; transition light oil/wet gas
200°C	VR = 2.4 ± 0.4 %	Transition: higher hydrocarbon (wet gas)/methane (dry gas), with ≤ 1 mol% of wet gas
240 °C	VR = 3.8 ± 0.5 %	Transition diagenesis/anchizone, Kübler Index $\Delta^{\circ}2\theta$ (KI) = 0.42
270 °C	VR = 6.0 ± 0.8 %	End of the methane stability by red-ox reactions (Tarantola et al., 2007, 2009).

Lowest anchizone/epizone limit, KI  $\Delta^{\circ}2\theta$  = 0.25.

Using the KI/VR correlations published in a review by Ferreiro Mählmann et al. (2012) these temperatures are crucial for normal thermal conditions at moderate pressures (1 – 6 kbar).

Ferreiro Mählmann, R. (2001): *Tectonophysics* 334, 1-33.

Ferreiro Mählmann, R., Bozkaya, Ö., Potel, S., Le Bayon, R., Šegvić, B. & Nieto, F. (2012): *Swiss Journal of Geosciences* 105/2, 121-152.

Ferreiro Mählmann, R. & Le Bayon, R. (2015): *International Journal of Coal Geology*, in press.

Le Bayon, R., Brey, G.P., Ernst, W.G. & Ferreiro Mählmann, R. (2011): *Organic Geochemistry* 42, 340-355.

Mullis, J. (1979): *Bulletin de Minéralogie* 102, 526-536.

Mullis, J., Rahn, M.K., Schwer, P., de Capitani, Ch., Stern, W.B. & Frey, M. (2002): *Schweizerische Mineralogische und Petrographische Mitteilungen* 82/2, 325-340.

Tarantola, A., Mullis, J., Vennemann, T., Dubessy, J. & de Capitani, Ch. (2007): *Chemical Geology* 237, 329-357.

Tarantola, A., Mullis, J., Guillaume, D., Dubessy, J. de Capitani, Ch. & Abdelmoula, M. (2009): *Lithos* 122, 497-510.



## Reliability of very low-grade metamorphic methods to decipher basin evolution: case studies from basins of the Southern Vosges (NE France)

Sébastien Potel<sup>1</sup>, Marine Maillat<sup>1</sup>, Anta-Clarisse Sarr<sup>1</sup>, Michael-Patrick Doublie<sup>2</sup>, Tatiana Maison<sup>2</sup> and Rafael Ferreira Mählmann<sup>(3)</sup>

B2R, Institut Polytechnique LaSalle Beauvais, Geosciences Department, 19 Rue Pierre Waguet, F-60026 Beauvais (sebastien.potel@lasalle-beauvais.fr)

Geoscience Australia, Resources Division, Cnr Jerrabomberra Avenue and Hindmarsh Drive, Symonston 2609, ACT, Australia

Technische Universität Darmstadt, Institut für Angewandte Geowissenschaften, Schnittspahnstraße 9, D-64287 Darmstadt, Germany

Low-grade metamorphic studies involving clay mineral alteration and reaction progress help to decipher the thermal evolution of sedimentary and inverted meta-sedimentary basins. Sheet silicates such as illite and chlorite are very common in sedimentary basin sequences. Therefore, they are used for determining the grade of diagenesis and low-temperature metamorphism: the illite Kübler Index (KI) and the chlorite *Á*rkai Index (*Á*I), respectively. Although the *Á*I method is considered to be slightly less sensitive than the KI method, a reliable correlation between both methods exists in some metamorphic domains where a uniform heat-flow history and minor structural imprint occur. Complementary to these methods, the illite-muscovite b cell dimension determination provides a robust estimate of maximum pressure reached in low-temperature domains and in polyphase metamorphic history settings.

Here, we present a study of Markstein and Giromagny basins located in the Southern Vosges, and characterized by different lithostratigraphic units composed of deep marine turbidites of Upper Devonian to Upper Visean age (Krecher 2005) and volcano-clastic sediments, respectively. The Markstein basin is surrounded by granitic intrusions with an intrusion ages between 340 and 326 Ma. The previous study of Petrini & Burg (1998) showed orogenic deformation characterized by regional folding and a contact metamorphism found in an outer halo up to 1500 m away from the contact (based on the occurrence of biotite). Preliminary results of the recent study combining mineralogical assemblages, "crystallinity indices" of clay minerals, and illite-muscovite b-cell dimension determinations better constrained the metamorphic zonation and differentiated between burial and contact metamorphism. The contact metamorphic zone is characterized by the occurrence of biotite and/or actinolite and low illite-muscovite b cell dimensions, and the burial zone yields KI and *Á*I values of the high diagenetic zone and intermediate illite-muscovite b cell dimensions. In the south, in the Giromagny basin, no influence of contact metamorphism is observed, but rather syn-sedimentary burial conditions with intermediate illite-muscovite b cell dimensions at diagenetic conditions without thermal overprint are recognized.

Krecher (2005), PhD thesis, Freiburg / Br., Germany.

Petrini & Burg (1998) Geol France, 2.

## Illitization sequence controlled by temperature on hydrothermal altered volcanic rocks from the Tinguiririca Geothermal Field (Andean Cordillera, Central Chile)

Blanca Bauluz<sup>1</sup>, Mercedes Vazquez<sup>2</sup>, Fernando Nieto<sup>3</sup> and Diego Morata<sup>2</sup>

<sup>1</sup> Departamento de Ciencias de la Tierra. Universidad de Zaragoza, Zaragoza (Spain). bauluz@unizar.es

<sup>2</sup> Department of Geology and Andean Geothermal Center of Excellence, Facultad de Ciencias Físicas y Matemáticas, Universidad de Chile, Santiago (Chile). mvazquez@ing.uchile.cl, dmorata@cec.uchile.cl

<sup>3</sup> Departamento de Mineralogía y Petrología and Instituto Andaluz de Ciencias de la Tierra, Universidad de Granada-CSIC. Granada (Spain), nieto@ugr.es

The formation of the sequential distribution from smectite to illite, via interstratified I/S, in hydrothermal systems has been frequently described. This distribution is mainly controlled by temperature and chemical composition of the hydrothermal fluid, but also the fluid/rock ratio and the composition of the precursor seem to be important factors controlling illitization.

In this research we have investigated (XRD, SEM and HR-TEM techniques) the illitization process developed on Quaternary volcanic and volcanoclastic rocks in the active Tinguiririca Geothermal field (Andean Cordillera, Central Chile), previously described by Vazquez et al. (2014). SAnalyzed samples were collected from through a 815 m depth slim hole core in which the in situ temperature was measured (up to 230°C on the bottom of drill core) and estimated by means of chlorite composition. The volcanic rocks are calc-alkaline basaltic andesite to andesites, porphyritic in texture, with some pyroclastic levels. Ca-rich plagioclase ( $Ab_{52} An_{44} Or_3$ ) and pyroxene are the main phenocryst phases in an intersertal to hyalopilitic groundmass.

Textural information (SEM images) shows that the dioctahedral clays have replaced most of the vitreous components. In contrast, plagioclase phenocrysts have been only partially and patchily albitized. The observed replacements imply dissolution – crystallization processes. The illitization sequence detected by XRD is apparently continuous from smectite to R3 I/S through R0 and R1 stages with a progressive increase in illite layers, as commonly described in literature. HRTEM data show a similar illitization trend. However, the high resolution images reflect reveal that the analyzed clays are more heterogeneous than deduced from XRD patterns deduced, with the coexistence of different types of dioctahedral clays at the sample level. They also indicate that the most abundant dioctahedral clays are smectite, R1 I/S and illite. Thus, the XRD patterns probably are the result of the mixture of these phases plus accessory I/S mixed layers with higher ordering ( $R>1$ ). Therefore, the illitization sequence is not as continuous as XRD patterns seem to indicate. Increasing temperature with depth would enhance the kinetic conditions necessary for illitization progress. Moreover, this increase in temperature also favors the dissolution of the vitreous component and also the albitization of plagioclases. Both processes release K, thus the concomitant increase in temperature enhances the crystallization of clays progressively richer in K being with illite being the more stable phase at higher temperatures. Therefore, at  $T \leq 85^\circ\text{C}$  smectite crystallizes, at  $T > 85^\circ\text{C}$  the conditions are appropriate for the crystallization of R1 I/S (with minor smectite+R0 I/S), and at  $T \geq 175^\circ\text{C}$  illite is the most abundant and relatively stable phase.

### Acknowledgements

This research has been funded by Chilean Fondap-Conicyt 15090013 project “Andean Geothermal Center of Excellence (CEGA)”, the 1140629 Chilean Fondecyt Project, the University of Zaragoza project (UZ2012-CIE-05), the Gobierno de Aragón and the European Social Fund (“Grupos Consolidados”).

### References

Vazquez et al. (2014). Journal of Volcanology and Geothermal Research 28, 43–59.

## Hydrothermal clays in Fe oxide deposits of Norrbotten County, northern Sweden

H. Albert Gilg<sup>1</sup>, Adrian M. Hall<sup>2</sup>, Anthony E. Fallick<sup>3</sup>, Frank Friedrich<sup>4</sup> and Ulf B. Andersson<sup>5</sup>

<sup>1</sup>Lehrstuhl für Ingenieurgeologie, Technische Universität München, Arcisstr. 21, D-80333 Munich, Germany, agilg@tum.de

<sup>2</sup>Department of Physical Geography and Quaternary Geology, Stockholm University, S-106 91 Stockholm, Sweden

<sup>3</sup>Scottish Universities Environmental Research Centre, East Kilbride, Glasgow G75 0QF, Scotland, UK

<sup>4</sup>IFG, Karlsruhe Institute of Technology, 76344 Eggenstein-Leopoldshafen, Germany

<sup>5</sup>Luossavaara-Kiirunavaara AB, 981 86 Kiruna, Sweden

Europe's largest Fe oxide deposits are hosted in Palaeoproterozoic supracrustal rock of the Fennoscandian Shield in the northern Norrbotten province, Sweden. Significant clay alteration zones occur at the present land surface and at depth in the Kiirunavaara, Malmberget, Gruvberget, Leveäniemi and Mertainen iron oxide-apatite deposits that are hosted in Svecofennian, mostly intermediate to acid volcanic and subvolcanic rocks, but also in the vicinity of skarn-rich iron formations in the upper part of the older Karelian Greenstone group.

A whitish, up to 30 m thick, soft clay alteration zone below glacial till was discovered in 1977 to 1979 by geophysical survey, trenching and drilling in the Vathanvaara area that hosts several prospects in skarn-rich iron formations. The <6 µm fractions of the altered rocks consist predominantly of a dioctahedral Mg-bearing, Al-rich, but Fe-free sodium smectite with minor amounts of an interstratified chlorite-smectite mineral, chlorite, zeolite minerals of the stilbite group and residual albite and actinolite. Whitish to greenish clay alteration zones that can reach a thickness of at least 50 m are encountered in association with the southern part of the Kiirunavaara ore body at a depth of more than 1 km. In part, alteration is pervasive, in part it occurs along multiple fractures or near breccias. The clays can be soft and hard. They occur within the ores and along the contacts with the ore, but also as isolated masses in the hanging wall and the footwall several tens of meters away from the ore. The clay fractions consist mainly of Mg-bearing, Al-rich sodium smectites that shows no signs of interstratification. At the contact, or within the ore, additionally residual green Fe-rich chlorite, phlogopite, talc, albite, sulfides (pyrite and chalcopyrite), and rare calcite in the altered rocks was observed.

Stable hydrogen and oxygen isotope data of sodium smectites from Vathanvaara clearly indicate a low-temperature hydrothermal origin of the expandable clay mineral consistent with their close association with stilbite group minerals. The Na-smectite ± stilbite group mineralization at Vathanvaara and Kiirunavaara may be related to regional post-metamorphic hydrothermal events that overprinted Fe ores in the northern Norrbotten area and that have been dated between ~1.62 and ~1.73 Ga. At Kiirunavaara, the earliest clays may even date back to the time of ore emplacement, at ~1.88 Ga.

## Hydrothermal alteration of chlorite to interlayered chlorite/smectite: geological evidence from the Oligocene Smrekovec Volcanic Complex, Slovenia

Polona Kralj

Dimiceva 14, 1000 Ljubljana, Slovenia, e-mail: polona.kralj@geo-zs.si

The Oligocene submarine composite stratovolcano of Smrekovec, Slovenia hosted a geothermal/hydrothermal system as evidenced by a complex rock alteration involving zeolites and phyllosilicate minerals. The study area of about 3 km<sup>2</sup> encompasses a succession of andesitic and dacitic lavas, autoclastic, pyroclastic, resedimented volcanoclastic and mixed volcanoclastic-siliciclastic deposits attaining a thickness of over 500 m. The succession overlies a sill (termed the Kramarica sill) that extends and grows thinner (150-50 m) over a distance of 2400 m. The alteration occurring above the Kramarica sill is characterised by the assemblage of prehnite, laumontite, albite, quartz, sphene, chlorite and randomly interstratified chlorite/smectite with 80-90% of chlorite layers. Retrograde replacement of prehnite by laumontite is common. Yugawaralite is rare and occurs as interstitial cement and vein mineral, and postdates (and replaces) prehnite. Analcime formed in the latest-stage of hydrothermal activity and locally replaces prehnite, yugawaralite and laumontite.

In highly fractured zones and coarse-grained layers with high original porosity, laumontite amounts to 20-32 wt% of the bulk rock composition. It occurs in association with randomly interstratified chlorite/smectite (Fig. 1A) with 70-50% of smectite layers representing 30-55 wt% of the bulk rock. Chlorite/smectite possibly formed by retrograde hydrothermal alteration of chlorite. In oriented samples saturated with ethylene glycol, typical displacements of reflections occur (Fig. 1B). In x-ray diffraction patterns the peak at about 14.3 Å in untreated samples shifts to about 15.3 Å in glycolated samples. The reaction from chlorite to interstratified chlorite/smectite was accompanied by extensive leaching of quartz as its modal content decreases from 18-26 wt% to 2-5 wt%. Chemical composition of the bulk rock does not show a comparable decrease in SiO<sub>2</sub> and indicates that at least a part of the dissolved silica must have been involved in the formation of smectite layers.

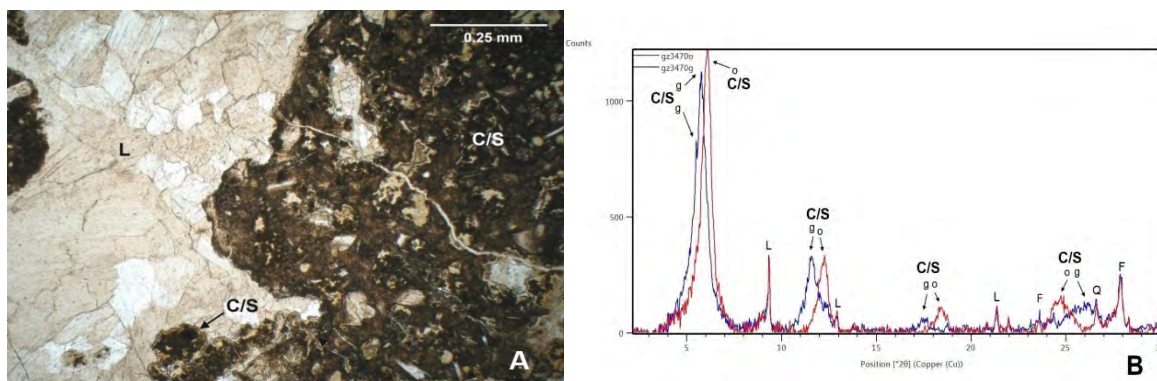


Fig. 1. A, Laumontite (L) and randomly interstratified chlorite/smectite (C/S) in plane polarised light, semi-crossed nicols; B, The displacement of peak positions in X-ray diffraction pattern of oriented sample - (o) untreated and (g) glycolated. L-laumontite, F – feldspars, Q – quartz, C/S interstratified chlorite/smectite.

## Clay mineral signature in geothermal environments related to subduction zones

Patricia Patrier, Daniel Beaufort, Delphine Guisseau, Photinie Papapanagiotou, and Antoine Mas  
Université de Poitiers, UMR 7285 CNRS, IC2MP, équipe HydrASA, rue Michel Brunet, Bat. 35, TSA 51106, 86073  
POITIERS cedex 9, France, patricia.patrier@univ-poitiers.fr

Clay minerals are widespread alteration products in most of the active and fossil hydrothermal systems and the availability of these minerals to record the hydrothermal history in their crystal properties has been intensively investigated. Many studies have considered the sequence from smectite to non-expandable di- or trioctahedral phyllosilicates as a unique function of the thermal conditions since the mixed-layer minerals in fossil hydrothermal settings shows a nearly systematic variation in proportion of interstratified components and degree of structural ordering with increasing temperature. In many active geothermal fields, however, the clay distribution appears much more complex as mixed-layered minerals and sometimes smectites are observed at unusually high temperatures, in association with non-expandable clays. At least three different reasons could explain such complex clay distributions: 1) hydrothermal systems generally evolve during several stages and information provided by clay mineralogy is therefore a “multi-stage picture” with incomplete reaction processes; 2) a geothermal system is composed of a network of narrow highly permeable path ways developed within a large mass of low permeability host rocks. So the material extracted from drilling consists of a mixture in variable proportions of secondary clay minerals crystallized in both the host rocks and the permeable fractures which constitute the geothermal reservoirs; and 3) the assumption that a clay phase systematically formed within a specific range of temperatures because it crystallized under thermodynamic equilibrium condition needs to be reevaluated with respect to kinetic considerations. Indeed, the functioning of geothermal systems (successive opening stages in relation with the tectono-magmatic activity) is generally associated with temporally strong disequilibrium (e.g. phreatic eruptions, mixing of fluids), which can produce explosive nucleation of metastable phases.

Investigations of the geothermal fields of Milos (Greece) and Chipilapa (Salvador) where smectites crystallized in high temperature aquifers in which the hydrodynamic conditions promoted the crystallization processes (i.e. boiling and mixing of fluids with contrasting temperatures) demonstrate that the clay distribution must be considered as a sequence of incomplete or non-equilibrium mineral reactions. The transformation series and the intermediate products are then kinetically controlled following the Ostwald Step Rule. This results in the formation of heterogeneous clay assemblages including both stable and metastable phases resulting from the incomplete transformations. From these observations, the clay alteration zoning usually observed in fossil systems has to be reinterpreted as the result of a long lasting post-crystallization cooling history during which the thermal gradient is mostly controlled by diffusive heat transfer.

The data provided by the study of several geothermal fields, Milos (Greece), Chipilapa (Salvador), and Bouillante (Lesser Antilles) confirm that clay minerals, through their structure (coherent domain size in the c-axis, polytypism, mixed-layering), composition (e.g. cation site occupancy, oxygen isotope composition) and texture (particle size, morphology) can be considered as good markers of the thermal history in geothermal systems (i.e. the temporal and spatial evolution of temperature).

## Evolution of out-of-equilibrium clay mineral assemblages in the Tolhuaca geothermal field, Southern Chile

Mercedes Vázquez<sup>1,2</sup>, Diego Morata<sup>1,2</sup>, Martin Reich<sup>1,2</sup>, Gloria Arancibia<sup>2,3</sup>, Pablo Sánchez<sup>1,2</sup> and Fernando Nieto<sup>4</sup>

<sup>1</sup>Department of Geology, Universidad de Chile, Santiago (Chile). mvazquez@ing.uchile.cl;dmorata@ing.uchile.cl;

<sup>2</sup>Andean Geothermal Center of Excellence (CEGA), Universidad de Chile, Santiago (Chile)

<sup>3</sup>Departamento de Ing. Estructural y Geotécnica, Pontificia Universidad Católica Chile, and Andean Geothermal Center of Excellence, Santiago, Chile. garancibia@ing.puc.cl

<sup>4</sup>Departamento de Mineralogía y Petrología and Instituto Andaluz de Ciencias de la Tierra, Universidad de Granada-CSIC. Granada (Spain). nieto@ugr.es

Clay minerals are alteration products in most of active and fossil geothermal systems. Many studies have considered both the sequential distribution from smectites to non-expandable di- or trioctahedral phyllosilicates as a function of the past or present thermal conditions. However, the fluid/rock ratio, the mechanism of alteration and the composition of precursor phases seem to be important factors controlling the properties and nature of clay minerals.

This study focuses on the clay minerals within the high-enthalpy Tolhuaca geothermal system (Southern Chile), strongly controlled by the nature of the Liquiñe-Ofqui Fault System and hosted in the Holocene Tolhuaca volcano. A continuous 1100 m deep drill core (Tol-1) has been used to study hydrothermal alteration in this active geothermal system. A systematic vertical sampling and subsequent XRD study offers the opportunity to elucidate how the clay mineral assemblages vary spatially as a function of intensity of hydrothermal alteration and how this alteration is controlled by the structural domains defined. Basaltic andesite lava flows and minor intercalated volcanoclastic layers dominate the corewell lithology. Three main structural domains controlling the intensity and nature of alteration mineralogy have been defined. Three main hydrothermal alteration zones have been also proposed: (1) argillic zone (0-300 m), rich in clay minerals and Fe-oxides and with steeply dipping veins and normal faults; (2) subpropylitic zone (300-670 m), with a pervasive alteration to clay minerals filling open spaces and discrete reverse faults; and (3) propylitic zone (670-1100 m), where chlorite and epidote dominate in veins and minor fault-veins. Temperatures obtained from fluid inclusions studies are concordant with present-day, in situ temperature measurements along within the well. In terms of clay mineral assemblages, four main clay mineral alteration zones can be defined: zone I (20-160°C) dominated by smectite and coincident with the argillic zone; zone II (160-220°C) with heterogeneous phyllosilicate assemblages (corrensite, smectite, chlorite and I-S R1); zone III (220-245°C) with chlorite, I-S R1 and I-S R3; and zone IV (245-270°C) dominated by chlorite with the absence of smectite.

The vertical distribution of clay minerals shows a pattern of transformation from smectite at the top to illite at the bottom, with the progressive formation of corrensite and chlorite. Smectite is the dominant phyllosilicate in the argillic zone, where the temperature reaches values around 160°C. Subpropylitic zone is characterised by the occurrence of heterogeneous mineral assemblages. Clay mineral assemblage indicates that the mineral reactions took place far from the chemical equilibrium with nucleation of metastable phases, possibly representing various nucleation conditions (i.e., coexistence of smectite and I-S R1). These mineral assemblages could result from the structural compartmentalization of the geothermal system that controls the fluid/rock ratio. In fact, the proposed model for alteration in this geothermal system defines an early hydrothermal event that sealed the fractures and preserved it from further alteration processes. Hydrothermal alteration in the propylitic zone appears to be temperature-dependent. However, reaction of I-S R1 to R3 should occur between 150-190°C, lower than present-day temperatures along the well.

### Acknowledgements

This research has been funded by Chilean Fondap-Conicyt 15090013 project "Andean Geothermal Center of Excellence (CEGA)" and the 1130030 and 1140629 Chilean Fondecyt Projects.

Tuesday  
7<sup>th</sup> July

Lecture room 3

Bioreactive clay minerals  
impacts on environmental  
and human health

## Characterization of clays used in the pharmaceutical industry

John A. Smoliga

Boehringer Ingelheim Pharmaceuticals, Inc., 900 Ridgebury Rd., Ridgefield, Connecticut 06877 USA,  
john.smoliga@boehringer-ingelheim.com

Well over 50 minerals from both natural and synthetic sources are utilized within the pharmaceutical industry for various purposes. These include active pharmaceutical ingredients (API's), excipients (non-active ingredients), and coloring agents along with fillers used in polymeric packaging materials. Clays, in particular kaolinite, are versatile minerals which can be used as an API, a functional excipient or as filler in packaging materials. Talc is utilized both as a functional excipient and filler in packaging components. Regulatory agencies such as the FDA require that these minerals be controlled for quality and purity. As is typical in mineralogical laboratories, characterization and analyses of these mineral phases are conducted using a variety of analytical techniques such as polarized light microscopy, scanning electron microscopy, energy dispersive x-ray fluorescence spectroscopy, x-ray powder diffraction, Fourier transform infrared spectroscopy and Raman spectroscopy. This paper will review the specific functions of clay minerals and talc used in the pharmaceutical industry, along with the typical methods utilized for characterization and control.



## Antimicrobial activity of Ag-treated clay-based nano-composites

Dimitrios Papoulis<sup>1</sup>, Eleni Koutra<sup>2</sup>, Michalis Kornaros<sup>2</sup>, Andreas Rapsomanikis<sup>3</sup>, Dionisios Panagiotaras<sup>4</sup> and Elias Stathatos<sup>3</sup>

<sup>1</sup> Geology Department, University of Patras, 26504

<sup>2</sup> Chemical Engineering Department, University of Patras, 26504 Greece

<sup>3</sup> Electrical Engineering Dept., Tech. Educational Institute (TEI) of Western Greece, 263 34 Patras, Greece

<sup>4</sup> Mechanical Engineering Dept., Tech. Educational Institute (TEI) of Western Greece, 263 34 Patras, Greece

papoulis@upatras.gr

Photocatalytic – antimicrobial activity of seven Ag-doped agents, TiO<sub>2</sub>-Ag, Halloysite-Ag, Palygorskite-Ag, Al<sub>2</sub>O<sub>3</sub>-Ag, Halloysite-TiO<sub>2</sub>-Ag, Palygorskite-TiO<sub>2</sub>-Ag and Al<sub>2</sub>O<sub>3</sub>-TiO<sub>2</sub>-Ag, was investigated using two pathogenic bacteria cultured in Mueller Hinton Broth, the Gram negative bacterium *Escherichia coli* (DSM 1103) and the Gram positive, *Bacillus subtilis* sub. *spizizenii* (DSM 347).

To prepare the composite-TiO<sub>2</sub> powders, each material was placed into an alkoxide solution. A sample of Palygorskite from Grevena, Greece and one of halloysite from Utah, USA were added to the titanium isopropoxide precursor solution. High purity powders were obtained after thermal treatment at 500 °C. The antimicrobial activities of bare palygorskite, halloysite without titanium dioxide were also tested. All powders were immersed in 1mM Ag(NO<sub>3</sub>)<sub>3</sub> aqueous solution for 15min and then rinsed with Millipore water. Afterwards, they were exposed to a black light (UV source) for 2min which caused their color to turn brown, indicating that the adsorbed Ag ions were reduced and converted to zero valence silver particles.

The minimum inhibitory concentration (MIC) of the agents was determined according to a modified broth micro-dilution method of CLSI (M7-A7). Ten different concentrations of the agents were tested ranging between 1025 µg/ml and 2 µg/ml. 50 µL of sample were placed into each sterile microtiter plate well and 50 µL of bacterial inoculum, standardized by 0.5 McFarland, were added. Gentamicin was used as standard antibacterial agent. Plates were incubated for 15 h in the dark and then 10 µL of resazurin indicator (0.18%) were added and plates were incubated for 2-3 more hours (Amornpitoksuk et al., 2012). Each test was performed in triplicate. It was found that all the agents tested had an inhibitory activity against the two pathogens, with Pal-Ag exhibiting the strongest antibacterial activity and Al<sub>2</sub>O<sub>3</sub>-Ag being the least effective against the two bacteria.

## Synthesis of europium doped layered double hydroxide by rapid-mixing and its cellular uptake behavior

Sumio Aisawa<sup>1</sup>, Satsuki Shinohara<sup>1</sup>, Hidetoshi Hirahara<sup>1</sup>, Eiichi Narita<sup>1</sup>, Tsugio Sato<sup>2</sup>

<sup>1</sup>Dept. Frontier Materias and Function Engineering, Iwate Univ. 4-3-5 Ueda, Morioka 020-8551 Japan

<sup>2</sup> Inst. Multi. Res. for Advanced Materials, Tohoku University, 2-1-1 Katahira, Aoba, Sendai 980-8577, Japan

Mg–Al layered double hydroxide (LDH) is tantalizing as a material for drug delivery because of properties such as low toxicity, controllable particle size and good water-soluble drug loading capacity. To investigate cellular uptake behavior and intracellular traffic of LDH, a fluorescent LDH is required to visualize and define in cell; therefore, the synthesis of rare earth ion doped LDH and fluorescence dye intercalated LDH have been studied<sup>1</sup>. In this study, we report that the fabrication of Eu<sup>3+</sup>-doped Mg–Al LDH (Eu<sub>x</sub>-LDH) carried out by a rapid-mixing method which produces well-dispersed and nano-sized LDH particles. We also investigated the effect of synthesis conditions on crystal structure, particle size and dispersion in water or cell culture medium of LDH.

The synthesis of the Eu<sub>x</sub>-LDH was undertaken according to the procedure below: a 10.0 mL mixed solution of 0.30 M MgCl<sub>2</sub> and 0.10 M AlCl<sub>3</sub>–EuCl<sub>3</sub> (molar ratio Mg : Al : Eu = 3.0 : 1.0–x : x, x = 0.00, 0.10, 0.20, 0.30, 0.50, 1.0) and 10 mL of 0.80 M NaOH solutions were simultaneously added within 10 sec, using a syringe, into 100 mL of stirred 0.15

M NaCl solution under normal laboratory conditions. After aging for 24 hrs, the LDH slurry was centrifuged, washed with distilled water and lyophilized for 24 hrs. The solid products were characterized using XRD, FT-IR, SEM and photoluminescence spectrum. To observe the cellular uptake behavior of the Eu<sub>x</sub>-LDH in a mammalian cell line we used L929 (mouse, connective tissue). This was incubated in a cell culture medium containing the Eu<sub>x</sub>-LDH. Fluorescence images of cell were taken by CLSM using live-cell imaging and fixed-cell cross section images were observed by TEM.

XRD patterns of the Eu<sub>x</sub>-LDH and the assignment diffraction peaks (003), (006), (009) and (110) are shown in Fig. 1, indicating that solid products have a primitive LDH structure. The *a*- and *c*-lattice constants of the Eu<sub>x</sub>-LDH (Table 1) increased with increasing amount of doped Eu<sup>3+</sup>, suggesting that Eu<sup>3+</sup> was internalized into the crystal lattice of LDH basal layer. The average particle size of the Eu<sub>x</sub>-LDH, was 60.1 nm for x=0.00, 74.5 nm for x=0.10, 382 nm for x=0.20 and 981 nm for x=0.30, showing an increase with the amount of Eu-doping; however, the Eu<sub>x</sub>-LDH is more dispersible water than that made by the more usual coprecipitation method. The excitation spectra (λ<sub>ex</sub> = 395 nm) of the Eu<sub>x</sub>-LDH (x > 0.00) displays four characteristic emissions at 594, 615, 652 and 720 nm, which can be assigned to the <sup>5</sup>D<sub>0</sub>–<sup>7</sup>F<sub>J</sub> (J = 1, 2, 3, 4) transitions of the substituted Eu<sup>3+</sup> in the LDH basal layer. The cellular uptake of the Eu<sub>x</sub>-LDH particle and subsequently to dissolution in early endosome was demonstrated in the live-cell imaging and TEM images.

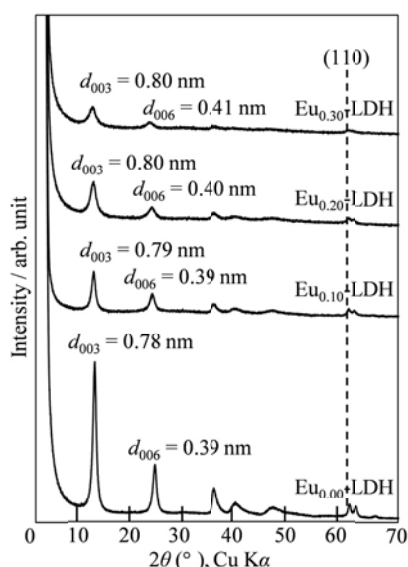


Fig. 1 XRD patterns of Eu<sub>x</sub>-LDH.

Table 1 Lattice constants *a* and *c* of Eu<sub>x</sub>-LDH

Sample	<i>a</i> (nm)	<i>c</i> (nm)
Eu <sub>0.00</sub> -LDH	0.3056	2.330
Eu <sub>0.10</sub> -LDH	0.3064	2.356
Eu <sub>0.20</sub> -LDH	0.3066	2.372
Eu <sub>0.30</sub> -LDH	0.3078	2.401

<sup>1</sup>Wei et al., *J. Mater. Chem.*, **22**, 5503 (2012)

<sup>2</sup>Sun et al., *J. Nanopart. Res.*, **16**, 2597 (2014)

## Safety assessment of clays used in health care products

C. Viseras<sup>1,2</sup>

<sup>1</sup> Department of Pharmacy and Pharmaceutical Technology, School of Pharmacy, University of Granada, Campus of Cartuja, 18071 s/n, Granada, Spain

<sup>2</sup> Andalusian Institute of Earth Sciences, CSIC-University of Granada, Avda. de Las Palmeras 4, 18100, Armilla (Granada), Spain  
cviseras@ugr.es

Clays are raw materials that once controlled and, if necessary, purified and/or modified are used as ingredients of many industrial and natural health care products, including pharmaceutical and cosmetics products. To be used, it is necessary to ascertain the quality attributes of the candidate clays, including their identity, purity, richness and safety (López-Galindo et al., 2007). In particular, clays are used in patent medicinal products both as pharmacologically inactive ingredients (Viseras et al., 2007) and as pharmacologically active substances (López-Galindo et al., 2011). Together with these allopathic uses, clays are also employed in natural health care formulations and complementary medicines, including for example, balneotherapy (Carretero et al., 2006). Simultaneously, clays are used in cosmetic formulations as additives with different functions (López-Galindo and Viseras, 2004). The presence of mineral impurities naturally associated with clay minerals and the particle size distribution, speciation and physicochemical state of elemental impurities presented in the clay as well as the possible microbiological impurities are important factors in considering the toxicity associated with the use of a clay in health care products. Differences (or even absence) in legislation regarding the allowed limits of particular clays depending on country and type of health care product (cosmetics, pharmaceuticals, natural health and others) will be presented, together with the necessity to harmonize the quality attributes and limits that sustain the safe use of these recognized health care ingredients.

### References

Carretero, M.I., Gomes, C.S.F., Tateo, F., 2006. Clays and human health. In: Bergaya, F., Theng, B.K.G., Lagaly, G. (Eds.), Handbook of Clay Science, Elsevier, Amsterdam, pp. 717-741. Chap. 11.5. Developments in Clay Science, Vol. 1

López Galindo, A. and Viseras, C., 2004. Pharmaceutical and cosmetic applications of clays. In: Wypych, F., Satyanarayana, K.G. (Eds.), Clay Surfaces. Fundamentals and Applications. Elsevier, Amsterdam, pp. 267–289.

López-Galindo, A., Viseras, C., Cerezo, P., 2007. Compositional, technical and safety specifications of clays to be used as pharmaceutical and cosmetic products. Applied Clay Science 36, 51-63.

López-Galindo, A., Viseras, C., Aguzzi, C., Cerezo, P., 2011. Pharmaceutical and Cosmetics Uses of Fibrous Clays. In: Galán, E., Singer, A. (Eds.), Handbook of Clay Science,

Developments in Clay Science, vol. 3. Elsevier, Amsterdam, pp. 299-324. Viseras, C., Aguzzi, C., Cerezo, P., Lopez-Galindo, A., 2007. Uses of clay minerals in semisolid health care and therapeutic products. Applied Clay Science 36, 37-50.

## Chemical modifications and diatom community development on volcanic clayey sediments during *indoor* and *in situ* maturation processes

F. Rocha<sup>1</sup>, A. Quintela<sup>1</sup>, S. Almeida<sup>1</sup> and D. Terroso<sup>1</sup>

<sup>1</sup>Univ. of Aveiro, GeoBioTec Research Center, Universitario de Santiago 3810-193 Aveiro, Portugal  
tavares.rocha@ua.pt

*Indoor* maturation experiments of volcanic mud samples with mineral water were performed over 120 days at constant room temperature (20 °C) in order to track geochemical modifications induced by the process and, eventually, the development of diatom communities. Different abiotic conditions were tested during the experiments. Mud samples were collected in the Azores and Madeira Archipelagos (Portugal) and the biological inoculum collected from the edge of a fumarole from the Azores (Portugal). The assemblages of diatoms were dominated by *Nitzschia* species both in the inoculum and on matured muds. While one of the samples from São Miguel island (Azores) was dominated by *Nitzschia* cf. *thermalis* var. *minor*, the mud sample from Porto Santo (Madeira) allowed the development mainly of *Nitzschia* communities during maturation experiments.

Associations between chemical composition and a samples mineralogical signature were established by cluster analysis. Slight enrichment of Na<sup>+</sup> and Ca<sup>2+</sup> was detected in samples after maturation and the exchangeable cations content were improved by the process. This research includes a multidisciplinary approach that contributes to the understanding of interactions between volcanic substrates and specific diatom species and geochemical modifications induced by maturation of volcanic materials.

Ribeira Grande caldera, São Miguel Island (Azores Archipelago, Portugal) is a particular case of maturation *in situ* where sediments and mineral-rich pluvial waters are constantly mixed in a pool. The peloids extracted from this boiling-mud pool are used in a local thermal center, which has existed since 1811, especially for the relief of pain associated with rheumatic diseases and for the treatment of skin disorders.

This work aims to study the mineralogical and geochemical characterization of the peloids from the pool and, secondly, establish a diagenetic mineralogical evolution. Sediments from 11 sampling sites were collected inside the pool and segmentation was performed on samples that show clear granulometric and color heterogeneities. Sampling sites are highly “diluted” and continuously affected by thermal gases originating from the geothermal systems. Mineralogical analysis of samples was performed by X-ray Diffraction and geochemical characterization was carried out using X-ray Fluorescence. Results point to an authigenic formation of phyllosilicates based on trachytic rocks as the outcome of the maturation process.

## The bioreactivity of 'red clays' from basaltic terrains

Timothy Jones<sup>1</sup>, Kelly BeruBe<sup>2</sup>, Anna Wlodarczyk<sup>2</sup>, Zoe Prytherch<sup>2</sup>, Yusuf, Hassan<sup>2</sup>, Stephen Potter<sup>3</sup>, Rachel Adams<sup>3</sup>

<sup>1</sup>School of Earth and Ocean Sciences, Cardiff University, Main Building, Park Place, Cardiff, CF10 3YE UK

<sup>2</sup>School of Biosciences, Cardiff University, Museum Avenue, Cardiff, CF10 3US, UK

<sup>3</sup>Cardiff School of Health Science, Cardiff Metropolitan University, Western Avenue, Cardiff, CF5 2YB UK

JonesTP@cardiff.ac.uk

For over 50 years an epidemiological correlation has been recognised between specific human health issues and basaltic terrains with 'red clays'. This correlation has been seen worldwide, including counties along the African Great Rift, Central America, India and others. The health effects are due to the internalisation of the clay minerals into the body's circulatory systems, resulting in skin discolouration and 'mossy' textures, and disruption of the balance of interstitial fluids resulting in oedema in lower limbs. These health issues are invariably seen in the poorer communities in these countries, and millions of people are affected worldwide. The basaltic terrains of concern are also usually characterised by high elevations, relatively warm average temperatures, and significant amounts of rainfall. We have collected 'red clays' from a number of such locations and compared their bioreactivity with characterised 'non-red clays'; and a consistent result is the enhanced bioreactivity of red clays with high iron content. All the results in this presentation relate to 'red clay' samples collected from the Atlantic island of Madeira, which was our most bioreactive clay. These Madeira clays are dominated by kaolinite and resemble spheroidal halloysite under SEM. Once collected the clays were not subjected to any pre-treatment other than size sorting by suspension in double-distilled water, which allowed the separation of clay grains of 2 microns or less. These extremely small grains are the ones capable of translocation around the human body via the circulatory system.

The plasmid scission assay uses the bacterio-phage  $\Phi$ X174, which is susceptible to damage by Reactive Oxygen Species (ROS) and metals. The lack of a cell or its components makes it suitable to study the effect of ROS directly on DNA. The general principle of the assay is that free radicals on the surface of the mineral grains cause damage to the super coiled DNA, leading to single strand breaks, double strand breaks, or complete DNA fragmentation. The relative proportion of damage can be measured and quantified by gel electrophoresis. The bacterio-phage was exposed to a range of Madeira clay concentrations in aqueous suspension from 50 to 1000  $\mu$ g/ml. A clear dose response is seen with the highest doses causing 35% DNA damage.

*Vibrio fischeri* is a bioluminescent marine bacteria. Toxicity tests using *Vibrio fischeri* have been used extensively to monitor environmental contamination of soils, with the reduction of bioluminescence being indicative of toxicity. Incubation of *Vibrio fischeri* with Madeira clay resulted in a significant drop of 70% in viability within the first minutes, almost mirroring the response to the positive control.

The haemolysis assay monitors the lysis of human red blood cells (erythrocytes) that are susceptible to damage by ROS and metals. Blood samples were collected from three donors and were centrifuged to separate the erythrocytes, which were then exposed to a range of concentrations of Madeira clay. The degree of lysis is determined by the optical density of samples. There was a clear dose response with 1000  $\mu$ g/ml causing between 1% and 2% erythrocyte lysis.

The effect of clays on oxidative stress in immune cells was determined by measurement of intracellular  $H_2O_2$  production by THP-1, cultured monocyte cells. Cells incubated for 1 hour with 0.5 mg/ml of Madeira clay produced more  $H_2O_2$  (MFI=262) than cells incubated with control Kaolin (MFI=189). Incubation of THP-1 cells with Madeira clay for 24 hours increased secretion of all cytokines.

The bioreactivity of 'red clays' from basaltic terrains is clearly demonstrated. The 'red clays' have the potential of cause damage to DNA, reduce cell viability and cause haemolysis. In addition 'red clays' have immunological effects which include increased oxidative burst and production of a range of inflammatory cytokines in immune cells.

## The anatomy of an antibacterial clay mine

Lynda. B Williams<sup>1</sup>, Keith D. Morrison<sup>1</sup>, Dennis D. Eberl<sup>2</sup> and Stanley N. Williams<sup>1</sup>

<sup>1</sup>Arizona State University, School of Earth & Space Exploration, Tempe AZ 85287-1404, USA

<sup>2</sup>US Geological Survey, 3215 Marine St., Boulder, CO 80303. USA

Lynda.Williams@asu.edu

Clays are used to benefit human health by treatment of various ailments, i.e., indigestion, arthritis (pelotherapy), and in wound healing and drug delivery. Antibacterial clays have been recognized and used historically (Williams and Hillier, 2014), but few studies of their formation have been reported. Here we identify the development of an antibacterial clay deposit formed in hydrothermally altered andesite porphyry from the western Cascade Mountains, Oregon (USA). Blue clay from one alteration zone of this deposit is effective in killing 100% a broad spectrum of human pathogens, including antibiotic resistant strains such as methicillin resistant *Staphylococcus aureus* (MRSA).

The clay is in an epithermal sulfide deposit located along a right lateral transverse fault (NW-SE) in 30Ma volcanics ~20km west of modern day Crater Lake. The deposit is ~1800 km<sup>2</sup>, with maximum thickness ~600m. Topped by basaltic lava flows, the underlying andesite was decomposed by hydrothermal fluids that produced four major clay alteration zones identified by oxidation state and reflected by color. From top to bottom, the recognized sequence is a red clay (highly oxidized), white clay (bleached zone), blue clay (reduced Fe-rich), and black clay (highly sulfidic). Elemental sulfur crystals up to hand size are associated with the black clay, and pyrite concentrations are as high as 15%. Pyrite morphology is crystalline in the >2µm fraction, but pyrite spheres (amorphous FeS?) are common in the <1µm fraction that may provide easily soluble toxic metals. FeS appears to replace environmental bacteria that are 0.5µm in length. Metabolically active acidophilic microbes (e.g., Burkholdaria sp.) were identified via RNA extraction from the blue clay.

Hydrothermal quartz is ubiquitous throughout this deposit, so the O-isotopes of quartz separated from each alteration zone was measured to estimate alteration temperatures and fluid composition. Using published meteoric water  $\delta^{18}\text{O}$  of the Cascades (Kohn et al., 2002) 30 Ma ago (-5‰) to today (-15‰), and the temperature stability of major minerals (illite, sulfur), the alteration history was deduced. Quartz associated with black clay ( $\delta^{18}\text{O}$  +20 to +25‰) shows evidence of dissolution; therefore igneous primary quartz may have been hydrothermally altered by fluid with  $\delta^{18}\text{O}$  of +5 to +10‰, at ~200-300°C. However, the presence of S<sup>0</sup> crystals in this zone, stable <115°C, indicates the water  $\delta^{18}\text{O}$  became gradually lighter (0‰) by mixing with meteoric water. The antibacterial blue clay contains porous quartz nodules with inclusions of plagioclase, supporting dissolution/precipitation. The blue clay is primarily illitic, so temperatures were ~150-200°C, consistent with a 0‰ water  $\delta^{18}\text{O}$ . The white clay formed along a fault surface through the blue clay, and contains kaolinite and smectite supporting lower temperatures. The quartz replacement texture and  $\delta^{18}\text{O}$  (+1 to +10‰) is consistent with precipitation from meteoric water at temperatures as low as 70°C.

Clay alteration conditions are important for defining antibacterial potential in natural deposits. It is clear that the hydrothermally altered zones (blue and black) associated with high sulfidation have the highest antibacterial effect against human pathogens. Hot meteoric water, while effective at forming clays, does not contain the essential antibacterial elements derived from magmatic sources. The oxidation state of the fluids is also important, as only clays containing reduced metals are antibacterial while oxidized clays (red clay) are not.

Kohn, M.J., Miselis, J.L., Fremd, T.J. (2002) Oxygen isotope evidence for progressive uplift of the Cascade Range, Oregon, Earth & Planetary Science Letters 204: 151-165

Williams, L. B. and Hillier, S. (2014) Kaolins and Health: From first grade to first aid. Elements Magazine 10: 207-211.

## Unearthing the antibacterial activity of medicinal clays

Keith D. Morrison<sup>1</sup> and Lynda B. Williams<sup>1</sup>

<sup>1</sup>School of Earth & Space Exploration, Arizona State University, Tempe, AZ 85287-1404 USA

keith.morrison@asu.edu

Recent evidence reveals that certain clay mineral deposits containing sub-micron iron sulfides have the ability to prevent pathogenic bacterial growth. These antibacterial clays have been shown to prevent the growth of a broad spectrum of bacteria, including *methicillin-resistant Staphylococcus aureus* MRSA and *extended-spectrum beta lactamase (ESBL) Escherichia coli* (antibiotic resistant strains) when tested *in vitro*. This research tests the hypothesis that mixed-layered illite-smectite clay minerals associated with sub-micron iron sulfides, act as a reservoir to store and release Fe<sup>2+</sup> at low pH, while generating reactive oxygen species (ROS) resulting in membrane and DNA damage.

*E. coli* (ATCC 25922) was reacted with clay suspensions and clay leachates (aqueous solutions equilibrated with clays for 24 hrs). Inductively coupled plasma mass spectrometry (ICP-MS) was used to measure the elements leaching from the clays. Scanning transmission X-ray microscopy (STXM) imaging was performed on bacteria reacting with leachates to map the redox state of Fe adsorbed to membranes. NanoSIMS (secondary ion mass spectrometry) Al maps were measured to determine if cytoplasmic uptake occurs. Scanning transmission electron microscopy-electron energy loss spectroscopy (STEM-EELS) was used to investigate the precipitation of intracellular mineral particles. ROS generated by minerals and mineral leachates were measured using a spectrophotometric hydrogen peroxide assay (H<sub>2</sub>O<sub>2</sub>) assay. Protein oxidation (carbonyl content) was measured in membrane and soluble fractions. Genetic responses to leachates were measured using two *lacZ* fusion strains, *sulA::lacZ* for genotoxicity and *rpoHP3::lacZ* for membrane damage.

Antibacterial susceptibility testing and ICP-MS elemental analysis of the leachates reveals that samples containing mM levels of soluble Fe and Al are antibacterial. Elemental mapping using STXM and nanoSIMS reveal Fe<sup>2+</sup> and Al<sup>3+</sup> adsorption to bacterial membranes. The hydrogen peroxide assay of the mineral leachates indicates that H<sub>2</sub>O<sub>2</sub> is being generated in the presence of Fe<sup>2+</sup>, ultimately generating hydroxyl radicals. Intracellular particles observed upon cell death were determined to be Fe<sup>3+</sup>-oxides by STEM-EELS, supporting a mechanism of intracellular oxidation. Protein oxidation measurements show that cell membranes are most oxidized, allowing the gradual oxidation of intracellular proteins. Results from the *lacZ* fusions indicate that Fe<sup>2+</sup> and Al<sup>3+</sup> synergistically damage membranes, while Fe<sup>2+</sup> floods the cell generating ROS that cause DNA damage. Results from this research should lead to the design of new antibacterial agents involving the mechanisms exhibited by these natural minerals.

## Mechanistic considerations on the healing properties of clays and related minerals

Javiera Cervini-Silva<sup>1</sup>, Antonio Nieto-Camacho<sup>2</sup>, María Teresa Ramírez-Apán<sup>2</sup>, Eduardo Palacios<sup>3</sup>, Paz del Angel<sup>3</sup>, Esmeralda Juárez-Carbajal<sup>4</sup>, Eduardo Terres<sup>3</sup>, Virginia Gómez-Vidales<sup>5</sup>, Elba Ronquillo de Jesús<sup>1</sup>, Kristian Üfer<sup>6</sup>, Stephan Kaufhold<sup>6</sup>, Martin Pentrak<sup>7</sup>, Linda Pentrakova<sup>7</sup>, Ascención Montoya<sup>8</sup>, Joseph W. Stucki<sup>7</sup>, Benny Theng<sup>9</sup>

<sup>1</sup>Departamento de Procesos y Tecnología, Universidad Autónoma Metropolitana, Unidad Cuajimalpa, México City, México; Av. Vasco de Quiroga 4871, Cuajimalpa de Morelos, Col. Santa Fe, México, D.F., México (jcervini@correo.cua.uam.mx, elba\_ronquillo@hotmail.com)

<sup>2</sup> Laboratorio de Pruebas Biológicas, Instituto de Química, Universidad Nacional Autónoma de México, Ciudad Universitaria México City, México, (anieto\_camacho@yahoo.com.mx; mtrapan@yahoo.com.mx)

<sup>3</sup> Departamento de Microscopía Electrónica, Dirección de Investigación y Posgrado, Instituto Mexicano del Petróleo, México (epalacio@imp.mx, jamontoyadela fuente@gmail.com)

<sup>4</sup> Departamento de Investigación en Microbiología, Instituto Nacional de Enfermedades Respiratorias, Ismael Cosío Villegas (esmeraldajc@yahoo.com)

<sup>5</sup> Laboratorio de Resonancia Paramagnética Electrónica, Instituto de Química, Universidad Nacional Autónoma de México, Ciudad Universitaria, México City, México (gomvidal@gmail.com)

<sup>6</sup>BGR Bundesanstalt für Geowissenschaften und Rohstoffe, Stilleweg 2, D-30655, Hannover, Germany (Stephan.Kaufhold@bgr.de; Kristian.Ufer@bgr.de)

<sup>7</sup> Department of Natural Resources and Environmental Sciences, University of Illinois at Urbana-Champaign, Urbana, IL, United States (martin.pentrak@gmail.com; jstucki@illinois.edu);

<sup>8</sup> Dirección de Investigación y Posgrado, Instituto Mexicano del Petróleo, Mexico City, México (amontoya@imp.mx); <sup>9</sup> Landcare Research, Private Bag 11052, Palmerston North 4442, New Zealand (Thengb@landcareresearch.co.nz)

Healing properties of minerals is a thriving research area that remains by enlarge unexplored. Here we study the biological reactivity of clays and refractory minerals by using an array of molecular biology and high resolution microscopic and spectroscopic techniques. We present data on clay materials (kaolins, homites, allophanes, bentonites; [1-3]) on infiltration and migration of inflammatory and immune effector cells, viability of cancer cells, oxidative stress *via* lipid peroxidation (the oxidative degradation of lipids in cell membranes). Histological cuts of mice ears (NOM-062-ZOO-1999) were used for quantifying and differentiating among cells found in the epidermis; assessing the formation of neutrophil extracellular traps (NETs); and conducting elemental mapping using high resolution electron microscopy. Microstructural analysis and modeling of surface binding sites provide evidence to show specificity of mineral surface/cell interactions, whereby it is possible to identify controls for enzymatic vs non-enzymatic mechanisms of action.

[1] In *Natural Mineral Nanotubes*. Pasbakhsh P and Churchman J (Eds.). New York: CRC Press, **2015**, Ch.25; [2] *Coll. Surf. B* **2015**, 129, 1-6; [3] *Appl. Clay Sci.* **2015**, 105-106, 48-51.



## Peptide bond formation in layered double hydroxides - implications for abiological life-precursors

Brian Gregoire<sup>1</sup>, H. Christopher Greenwell<sup>2</sup> and Donald G. Fraser<sup>1</sup>

<sup>1</sup>Department of Earth Sciences, University of Oxford, South Parks Road, Oxford, OX1 3AN, U.K.

<sup>2</sup>Department of Earth Sciences, Durham University, South Road, Durham, DH1 3LE, U.K.

gregoirb@gmail.com

Understanding the interaction of biomolecules such as amino acids with hydrated mineral surfaces is key to unravelling the origins of life on Earth. It also has potentially important applications in the increasing medical demand for 100% pure D- or L- pharmaceuticals (Fraser et al 2011). Amino acids are well-known products of Urey-Miller spark discharges in reducing early-Earth atmospheres and a wide range of extra-terrestrial amino acids has also been observed to exist in some primitive, hydrated meteorites. Here we present new results that show that peptide-forming reactions can take place abiologically in layered double hydroxides without using highly concentrated solutions of Cu(II) as usually required by the Salt-Induced Peptide Formation (SIPF) reaction.

The formation of peptides from amino acid precursors has been demonstrated under possible primitive earth conditions using the SIPF reaction (Rode and Suwannachot, 1999). In the presence of NaCl and Cu ions, amino acids condense to form oligomers. These SIPF reactions exhibit selectivity toward the formation of alpha-amino acids, and even enantioselectivity, favouring L-forms of some amino acids (Plankensteiner et al., 2004). Although glycine can polymerise up to Gly<sub>6</sub>, the SIPF reaction generally forms small peptides, limited to AA<sub>2</sub> or AA<sub>3</sub>. However, these small peptides can undergo further evolution pathways via chain elongation and stabilisation on mineral surfaces Budjkák and Rode, 1999; Li et al., 2010).

One of the drawbacks of the SIPF reaction in nature is the requirement for free Cu<sup>2+</sup>. We have therefore explored the possibility that some minerals may have acted as heterogeneous catalysts for the formation of peptides in the ancient environment. In this study, we report studies of alanine in layered hydroxides and demonstrate that the elemental composition of the mineral has a strong influence on the yield of dialanine. Brucite, Mg(OH)<sub>2</sub> was used as model starting material and can easily be modified to form a variety of isostructural materials with different properties. These are described by the formula : [M<sup>II</sup><sub>1-x</sub>M<sup>III</sup><sub>x</sub>(OH)<sub>2</sub>] (A<sup>n-</sup>)<sub>x/n</sub>·mH<sub>2</sub>O, where M<sup>II</sup> and M<sup>III</sup> are di- and trivalent cations, A<sup>n-</sup> is an exchangeable interlayer anion with charge n, and x represents the M<sup>II</sup>/(M<sup>III</sup>+M<sup>II</sup>) molar fraction. Since they can be synthesised in the laboratory the possibility of contamination by biological systems or other molecules is decreased. Secondly, LDH phases exhibit a large range of composition, since pure phases can be obtained with different types of cation (Grégoire et al., 2012).

We present results for the formation of Alanine peptides for M<sup>II</sup>-M<sup>III</sup> LDH material where (M<sup>II</sup> = Mg<sup>II</sup>, Zn<sup>II</sup>, Ni<sup>II</sup>, and M<sup>III</sup> = Al<sup>III</sup> and Fe<sup>III</sup> and for ternary Mg<sup>II</sup>-Cu<sup>II</sup>-Al<sup>III</sup> LDH with different copper contents, submitted to wetting/drying cycles. Dialanine yields vary from 0.1% to around 7% after only 14 cycles depending on the nature of the cation. The influence of these structures on peptide bond catalysis is discussed and provides a new mechanism for forming early peptides on Earth.

## Nano-structured multi-enzymatic @LDH bio-hybrid as a one-pot biocatalyst for polyalcohol synthesis

Claude Forano<sup>1</sup>, Rima Mahdi,<sup>1</sup> Suraj Charan,<sup>2</sup> Ulla Gro Nielsen,<sup>2</sup> Vanessa Prevot,<sup>1</sup> Christine Guérard-Hélaine,<sup>1</sup> and Marielle Lemaire<sup>1</sup>

<sup>1</sup>Université Clermont Auvergne, Université Blaise Pascal, Institut de Chimie de Clermont-Ferrand, CNRS, UMR 6296, BP 80026, F-63171 Aubière, France

<sup>2</sup> Department of Physics, Chemistry, and Pharmacy, University of Southern Denmark, 5230 Odense M, Denmark  
claude.forano@univ-bpclermont.fr

Layered Double Hydroxides (LDH) ( $M^{II}_{1-x}M^{III}_xX_{q/x}\cdot nH_2O$ ), also called anionic clays, display suitable opened 2D host structures and chemical surface properties (biocompatible chemical composition, positive layers with exchange anions, high hydration rate) for the design of novel enzyme based bio-hybrid nanomaterials with expected promising development for drug delivery, gene therapy, biofuel cells, biosensors and biocatalysis<sup>1,2</sup>. More recently, LDH have been used for the design of novel enzyme-based nano-bioreactors for the synthesis of molecules of interests for medical applications. Enzyme@LDH biohybrid materials display improved catalytic activity and stability that facilitates their storage and re-use. For instance, Fructose-6-phosphate aldolase (FSA) from *Escherichia coli* was successfully immobilised on  $Mg_2Al$  layered double hydroxide (LDH) and reused without any loss of activity<sup>3</sup>. FSA is a selective enzyme which catalyzes asymmetric synthesis of poly-hydroxylated compounds stereo-selectively such as aldol condensation of dihydroxyacetone (DHA)<sup>4</sup>.

We have developed an appropriate strategy to immobilize mono- or multi-enzyme systems with preservation of the bio-catalytic activity through a soft chemical process based on the self-assembling of enzymes and Layered Double Hydroxides (LDH) nano-platelets. Co-precipitation and adsorption of FSA and  $Mg_RAl$  LDH ( $R=2, 4$ ) were first performed under various synthesis conditions. Enzyme-LDH nano-structures were closely investigated using XRD and FTIR. Influence of the FSA on the  $Mg_RAl$  LDH formation was studied by SSNMR. The bio-catalytic activity was found to be strongly dependent on both the amount of loaded FSA and method of assembling. 100% of the free FSA was retained once immobilized by co-precipitation.

From the study of the FSA@ $Mg_RAl$  mono-enzyme system, optimised preparation conditions were used to design a multi-enzyme@LDH nanobioreactor. The design cascade system is the first nanobioreactor involving 4 enzymes with various catalytic activities. As a proof of concept kinases, an isomerase and an aldolase for C-C bond formation were selected. The separate immobilisation of the different enzymes as well as the optimisation of the synthetic biocatalytic pathway were studied. Finally, reusable nanobioreactors were designed and applied for the synthesis of interesting metabolites like D- or L-phosphorylated sugars. This novel nanobioreactor can be considered as an artificial metabolism system.

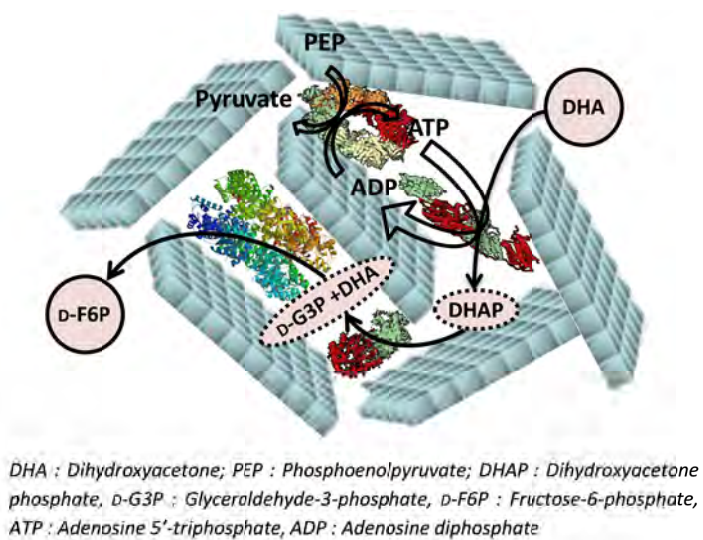


Fig. 1. Multi-enzymatic /LDH nanobioreactor.

<sup>1</sup>V. Prevot, C. Mousty, C. Forano, *Advances in Chemistry Research*, 2013, 17, 35-83.

<sup>2</sup>C. Forano, V. Prevot, *Bio-Inorganic Hybrid Nanomaterials*. Ed. By: E. Ruiz-Hitzky, K. Ariga, Y. Lvov (2008), 443-484.

<sup>3</sup>C. Guérard-Hélaine, B. Legeret, C. Fernandes, V. Prevot, C. Forano, M. Lemaire, *New J. Chem.* 2011, 35, 776-779.

<sup>4</sup>A. L. Concia, C. Lozano, J. A. Castillo, T. Parella, J. Joglar and P. Clapes, *Chem. Eur. J.*, 2009, 15, 3808-3816.

## Formation of adenosine from adenine and ribose in the presence of montmorillonite after repeated wetting and drying

Hideo Hashizume<sup>1</sup>, Sjerry van der Gaast<sup>2</sup> and Benny K.G. Theng<sup>3</sup>

<sup>1</sup>National Institute for Materials Science, 1-1 Namiki, Tsukuba 305-0044, Japan

<sup>2</sup>Hugo de Grootstraat 37, 2311XK Leiden, The Netherlands

<sup>3</sup>Landcare Research, Private Bag 11-052, Palmerston North 4442, New Zealand.

HASHIZUME.Hideo@nims.go.jp

Clay minerals have characteristics such as a small particle size, a large surface area and a particular charge. Clay minerals can adsorb various organic molecules and catalyze their reaction and polymerization. On the early earth, clay minerals might have adsorbed amino acids, purine or pyrimidine bases and concentrated them. Organic molecules might have reacted with each other via a clay mineral catalyst. Clay minerals might have played important roles in the origins of life. Ribonucleic acids (RNA) are one of important biopolymers. Some of RNA have enzymatic and genetic functions. Gilbert (1986) proposed one of the hypotheses of origins of life<sup>1</sup> called "RNA world". Adsorption of RNA components by clay minerals has been investigated<sup>2</sup>. The polymerization of nucleotides has been studied by using montmorillonite<sup>3</sup>. The synthesis of nucleosides and nucleotides has not been well studied when compared to polynucleotides. We attempt the formation of adenosine from adenine and ribose in the presence of montmorillonite by repeated wetting and drying.

We use montmorillonite (Mt) purified from Wyoming bentonite (Supplied by Hojun Co. Ltd). Interlayer cations were exchanged with Mg<sup>2+</sup> cations. We prepared 5 mmol·dm<sup>3</sup> of mixed solution of adenine and ribose. For wetting and drying treatments 5 cm<sup>3</sup> Mg-montmorillonite (Mg-Mt) was added to a glass beaker. The beakers were put in a chamber filled by N<sub>2</sub> gas or in an oven in a normal atmosphere. We carried out 30 repeats of wetting and drying at 40, 50 and 60 °C. We also undertook the same experiments using non-cation exchanged Mt, and also without clay (Mg-Mt or Mt). Moreover, the mixed solution with either or neither Mg-M or Mt was put in the sealed container and treated at 40, 50 and 60 °C. After the treatments, about 10 cm<sup>3</sup> of water was added to the beaker and the beaker and container were left for one night at room temperature. The suspension of the beaker and container were centrifuged. The supernatants were analyzed by HPLC and LC-MS.

We found a component with molecular weight 268 (mass/charge) in the samples with Mg-Mt and Mt at 40 °C by the wetting and drying repeat. The molecular weight of 268 is the same as that of adenosine plus H<sup>+</sup>. The abundance of the component was too small to measure by other instruments. Other treatments did not show the component with a molecular weight 268.

Gilbert, W. (1986) *Nature* **319**, 618.

Hashizume, H, S.van der Gaast and B.K.G.Theng (2010) *Clay Miner.*, **45**, 469-475.

Ferris, J.P. (2002) *Orig. Life Evol. Biosph.* **32**, 311-332.

Tuesday  
7<sup>th</sup> July

Lecture room 3

Asian Clay Minerals Group  
Research in Progress II (2)

## Layered silicate adsorbent as an excellent partner with a TiO<sub>2</sub> photocatalyst for highly efficient green fine-chemical syntheses

Yusuke Ide<sup>1</sup>, Masato Torii<sup>2</sup> and Tsuneji Sano<sup>2</sup>

<sup>1</sup>International Center for Materials Nanoarchitectonics (MANA), National Institute for Materials Science (NIMS), 1-1 Namiki, Tsukuba 305-0044, Japan E-mail: IDE.Yusuke@nims.go.jp

<sup>2</sup>Graduate School of Engineering, Department of Applied Chemistry, Hiroshima University, 1-4-1 Kagamiyama, Higashi-Hiroshima 739-8527, Japan

Selective oxidation of organic molecules by photocatalysis has great potential for fine chemical synthesis in an economically and environmentally benign fashion. Due to its abundance, non-toxicity and high stability, titanium dioxide (TiO<sub>2</sub>) is a promising photocatalyst for the purpose. However, organic substrates tend to be overoxidized to undesired by-products (e.g. CO<sub>2</sub>) on TiO<sub>2</sub> due to the presence of highly oxidizing species. The design of novel photocatalysts, including those based on precious metals, has been investigated extensively. Low-cost photocatalysts are preferred for practical purposes.

One of the most desired selective oxidations in the chemical industry is the selective oxidation of benzene to phenol. When this reaction is conducted using TiO<sub>2</sub> in the presence of a layered silicate (a proton-exchanged layered alkali silicate, magadiite (H-mag)) which recognizes phenol precisely, phenol can be recovered effectively.<sup>1</sup> When phenol forms it is captured rapidly, selectively and efficiently by the adsorbent, after which the captured phenol can be eluted easily by simple washing (Fig. 1). Furthermore, using TiO<sub>2</sub> as a photocatalyst and layered silicates as adsorbents to capture desired partially oxidized products, we successfully expanded the approach to other important selective oxidations, like benzene to catechol.<sup>2</sup> As a wide variety of abundant layered silicates with specific adsorption abilities for organic molecules is available,<sup>3</sup> we anticipate that layered silicate adsorbents as additives to TiO<sub>2</sub> photocatalysts are key ingredients in the effort to develop realistic and 'green' fine chemical syntheses.

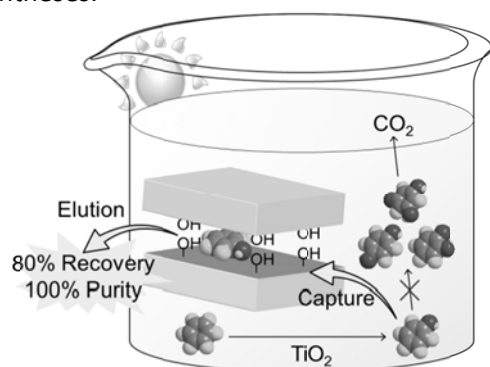


**Fig. 1** Effective and selective recovery of phenol by a phenol-philic adsorbent (H-mag) during the photocatalytic oxidation of benzene by TiO<sub>2</sub>.

1 Y. Ide, M. Torii, T. Sano, *J. Am. Chem. Soc.* 2013, 135, 11784-11786.

2 Y. Ide and T. Sano, manuscript to be submitted.

3 T. Okada, Y. Ide, M. Ogawa, *Chem. Asian J.* 2012, 7, 1980-1992.

## Organoclays in water cause interlayer expansion that facilitates caffeine adsorption

Tomohiko Okada,<sup>1</sup> Junpei Oguchi,<sup>1</sup> Ken-ichiro Yamamoto,<sup>2</sup> Takashi Shiono,<sup>2</sup> Masahiko Fujita<sup>3</sup> and Taku Iiyama<sup>3</sup>  
Department of Chemistry and Material Engineering, Shinshu University, Wakasato 4-17-1, Nagano 380-8553, Japan  
(tomohiko@shinshu-u.ac.jp)

Kirin Company, Ltd., Namamugi 1-17-1, Tsurumi-ku, Yokohama 230-8628, Japan

Department of Chemistry, Faculty of Science, Shinshu University, Asahi 3-1-1, Matsumoto 390-0802, Japan

Adsorption of specific molecular species onto solid surfaces is currently exploited in a wide range of scientific and practical applications such as removing toxic compounds and recovering desired substances. Precisely controlled nanostructures are important in producing smart adsorbents (Okada et al., 2012). The smectite group of clay minerals has long been investigated in such applications because they possess cation-exchange ability, large surface area, and structural versatility. Cation-exchange reactions with the a relatively small of organoammonium cations, such as tetramethylammonium and trimethylphenylammonium ions, create nanospaces surrounded by cation–silicate layer structures. In nanospace engineering, the structure of the pillaring agents and negative layer charge density of the smectites are the factors responsible for determining the adsorption equilibrium constants for nonionic aromatic compounds (Okada et al., 2014). Although it has been pointed out that the nanostructures affect the adsorption behavior of organic molecules in organoclay series, the interlayer structures of the adsorbents in aqueous media have not been fully understood. We expect that chemical species occluded in the interlayer space will be rearranged in the presence of both adsorbate and solvent, potentially enhancing the adsorption (intercalation) of the target molecules.

Here we analyze the adsorption of caffeine in water on organoclays (Okada et al., 2015). Two smectites, a natural montmorillonite and a synthetic saponite, were used as the host materials. The organoclays were prepared by cation-exchange reactions of benzylammonium (BA) and neostigmine (CONH) with interlayer exchangeable cations. The commercially available hydrophobic smectites containing long-chain alkylammonium ions are less effective the at caffeine adsorption. Results indicate that less caffeine was sorbed to CONH-modified clays than on untreated smectites; however, uptake was increased by adding BA to the smectites. The adsorption equilibrium constant was considerably larger on BA-modified saponite (containing small amounts of intercalated BA) than on its montmorillonite counterpart. These observations suggest that decreasing the size and number of intercalated cations increases the available surface area of siloxane, thus enhancing caffeine adsorption. When the BA–smectite powders were immersed in water, the intercalated water molecules expanded the interlayer space (revealed by using a transmission-based XRD measurement). Addition of caffeine to the aqueous dispersion resulted in further expansion of the interlayer space of BA–montmorillonite, and showed no effect on BA–saponite. Intercalated water molecules were thought to be exchanged with caffeine molecules. By intercalating BA into smectites, an adaptable two-dimensional nanospace that sequesters caffeine from aqueous media was provided.

Okada, T., Ide, Y. and Ogawa, M. (2012): Chem. Asian-J., 7, 1980.

Okada, T., Seki, Y. and Ogawa, M. (2014): J. Nanosci. Nanotechnol., 14, 2121.

Okada, T., Oguchi, J., Yamamoto, K., Shiono, T., Fujita, M. and Iiyama, T. (2015): Langmuir, 31, 180.

Tuesday  
7<sup>th</sup> July

Lecture room 2

Clay and fine particle  
based materials for  
environmental  
technologies and clean up

## The “magic” in environmental applications of clay based materials

Giora Rytwo<sup>1,2</sup>

<sup>1</sup> Environmental Physical Chemistry Lab., MIGAL Galilee Research Center, Kiryat Shmona, Israel

<sup>2</sup> Environmental Sciences Dept., Tel Hai College, Israel, rytwo@telhai.ac.il

There are over a hundred documented industrial applications of clay materials<sup>1</sup>: Clays can be found in industrial processes, agricultural applications, engineering and construction, geology, pharmaceutical and cosmetics, and also in environmental oriented applications or remediation processes.

The so called "environmental applications" of clay based materials may be traced since dawn of history<sup>2</sup>: removal of polluting oil from wool, fining and purification of oils and wines, direct use as cheap and efficient construction materials or useful containers, and even "advanced photo-stabilization" as in the case of palygorskite and indigo in "Maya Blue"<sup>3</sup>. In recent decades, additional new applications seem to arise from the need for water purification, better and less hazardous formulations of pest management compounds, and remediation treatments of polluted areas.

In water environments most clays behave as colloids due to their small size that results in high surface area that in most cases is charged and exhibits six different interaction sites<sup>4</sup>: neutral siloxane surfaces, isomorphic substitution sites, metal cations occupying cation exchange sites, water molecules surrounding exchangeable cations, hydrophobic sites and edge sites exposing silanol or aluminol groups. Such sites can act directly — or in combination with — inorganic ions, organic ions or chemicals, and even polymers. Modified surfaces offer new and versatile additional options of interaction, making the spectrum of possibilities almost infinite. The result of such interactions is a broad range of nanomaterial that are, based on clays which have been specifically modified and functionalized to perform their task.

This presentation aims to elucidate the different aspects that enable such a broad spectrum of applications in the environment. It will summarize the main physico-chemical characteristics (such as large and charged surfaces, specific 3D structure, thermodynamic properties, specific interactions) that lead to a series of physico-chemical processes that include adsorption/desorption, catalyzed degradation or stabilization of chemicals, flocculation and dispersion of colloidal suspensions, influence on redox behavior, buffer capacity and rheological behavior). These processes make clays, organoclays and nanocomposites so versatile and useful. Applying such understanding of the reactions and processes that occur in the interface between clay and the surroundings might yield interesting novel applications that might improve technological, industrial or commercial processes, minimizing their environmental hazard. Some examples of such "clean-tech" applications of natural and modified clay minerals — for example, to treatment of wastewater and industrial polluted effluents<sup>5</sup>, formulation of environmentally oriented pesticides<sup>6</sup>, applications in the gaseous phase<sup>7</sup>, and even as biocides<sup>8</sup> — will be presented .

1. Murray, H. H. *Applied Clay Mineralogy - Occurrences, Processing and Application of Kaolins, Bentonites, Palygorskite-Sepiolite, and Common Clays*. *Developments in Clay Science* **2**, 1–6 (Elsevier, 2006).
2. Robertson, R. H. S. *Fuller's Earth—A History of Calcium Montmorillonite*. 421pp. (Volturna Press, 1986).
3. Sánchez del Río, M. et al. in *Developments in Clay Science* (ed. Singer, E. G. and A.) **Vol. 3**, 453–481 (Elsevier, 2011).
4. Johnston, C. T. in *CMS Workshop Lectures, Vol. 8* (ed. Sahwney, B.) pp. 1–44 (The Clay Mineral Society, 1996).
5. Rytwo, G. et al. *Sci. Total Environ.* **442**, 134–142 (2013).
6. Margulies, L. et al. *Arch. Insect Biochem. Physiol.* **22**, 467–486 (1993).
7. Hashemifard, S. A., Ismail, A. F. & Matsuura, T. *Chem. Eng. J.* **170**, 316–325 (2011).
8. Bruna, J. E., Peñaloza, A., Guarda, A., Rodríguez, F. & Galotto, M. J. *Development of MtCu<sub>2</sub>+LDPE nanocomposites with antimicrobial activity for potential use in food packaging*. *Appl. Clay Sci.* **58**, 79–87 (2012).



## Reaction kinetics of molecular aggregation of laser xanthene dye in colloids of synthetic saponite nanoparticles.

Juraj Bujdák<sup>1,2</sup> and Timea Baranyaiová<sup>1</sup>

<sup>1</sup>Department of Physical and Theoretical Chemistry, Faculty of Natural Sciences, Comenius University, Bratislava, Slovakia

<sup>2</sup>Institute of Inorganic Chemistry, Slovak Academy of Sciences, Bratislava, Slovakia, bujdak@fns.uniba.sk

Assembly of organic molecules at inorganic surfaces plays an important role for the design and formation of hybrid materials and nanomaterials. Especially for organic dyes, the formation of dye molecular aggregates at the surface of inorganic solids leads to significant changes of dye electronic properties. The main objective of this work was detailed analysis of molecular aggregation kinetics of rhodamine 123 in the colloid of saponite. For this purpose, a spectrophotometer with fast data sampling equipped with diode array detector was applied in combination with a stopped-flow device. Recorded data were analyzed using chemometry methods: principal component analysis (PCA) and multivariate curve resolution-alternating least squares (MCR-ALS). Concentration profiles obtained by MCR were then analyzed using non-linear fitting verifying relevant reaction kinetics models.

Dye molecular aggregation represents a complex reaction proceeding in two main steps: 1. Dye adsorption and formation of metastable assemblies, which was very fast and could not be analyzed in detail; 2. Rearrangement of the initially formed species, which was characterized as formation of J-aggregates. PCA identified only two main spectral components, dye monomers and oblique J-aggregates in the colloids. Detailed analysis of reaction kinetics revealed partial changes in the structure of the aggregates with time. The positions of the H- and J-bands were unchanged, but partial changes of absorbance ratio of the bands occurred, indicating slight structural changes with time. The analysis of reaction kinetics confirmed the relatively complicated nature of the formation of dye assemblies. Possibly non-equivalent reaction sites of variable properties were present. Indeed, two parallel reactions characterized by a function based on two exponential decays or growths described well the concentration profiles of reactants and products, respectively. A fractal kinetics model based on a time-dependent rate constant was also considered due to sterically confined space for the reaction. Stretched exponential function was employed for this model.

Dye molecular aggregation in clay mineral colloids proceeds as a template-controlled reaction. Reaction kinetics parameters are useful for the characterization of the activity of the mineral surface. If general theory is developed and a suitable model is verified for clay minerals, it could be expanded to the characterization of similar colloidal systems and nanomaterials.

Acknowledgement: This work was supported by the Slovak Research and Development Agency under the contract No. APVV-0291-11 and Grant Agency VEGA (2/0107/13, 1/0943/13).

## Mechanisms of atenolol and metoprolol adsorption on Ca-montmorillonite (SAz-2)

Po-Hsiang Chang<sup>1</sup>, Wei-Teh Jiang<sup>2,\*</sup>, Zhaohui Li<sup>3,\*</sup>, Jiin-Shuh Jean<sup>4</sup>

<sup>1,2,4</sup> Department of Earth Sciences, National Cheng Kung University, 1 University Road, Tainan 70101, Taiwan  
tectonicion@gmail.com

<sup>3</sup> Department of Geosciences, University of Wisconsin – Parkside, 900 Wood Road, Kenosha, WI 53144, USA

Adsorption of atenolol (AT) and metoprolol (MT) from aqueous solution by Ca-montmorillonite (SAz-2) was investigated in batch studies under different physicochemical conditions. AT adsorption on SAz-2 obeyed the Freundlich isotherm with a capacity of 170 mmol/kg at pH 10 without pH adjustment, while the Langmuir isotherm was followed with a capacity of 300 mmol/kg at pH 7 for the MT adsorption. The kinetics for AT adsorption were slow and the equilibrium time was 16 h. In contrast, MT adsorption was fast and reached equilibrium within 0.5 h. The amount of exchangeable cations desorbed from SAz-2 was linearly correlated with the amounts of adsorbed AT and MT, having slopes of 0.43 and 1.12, respectively, which implies an adsorption mechanism dominated by cation exchange but complicated by surface complexation. AT and MT adsorption decreased at low pH and under high ionic strength when solution pH was below the pKa values of 9.6 and 9.7, respectively. Intercalation of AT and MT into the interlayer of SAz-2 was confirmed by larger  $d_{001}$  after adsorption compared to that of the SAz-2 raw material after being heated to 400 °C. Prominent interaction between the pharmaceutical molecules and SAz-2 was evidenced by apparent shifts of the FTIR absorption bands before and after adsorption. Thermodynamic parameters based on partitioning coefficients measured at 25, 45, and 60 °C suggested that the AT and MT adsorption on SAz-2 was exothermic in nature at pH < pKa, but endothermic physisorption enhanced by temperature increase occurred at pH > pKa. The results suggest that montmorillonite is a good candidate to remove AT and MT from wastewater and could be an important sink for them in soil and groundwater.

**Keywords:** Atenolol, Metoprolol, Adsorption, Cation Exchange, Montmorillonite

## **Removal of Diclofenac from a sandy soil by clay particle injection: a preliminary laboratory study**

Jean-Frank Wagner and Alessandro Santin  
Geology Department, Trier University  
ICEA Department, Padova University, Italy

A new remediation technique for soils contaminated with Diclofenac was tested by the injection of different clay suspensions into sandy soils. In a preliminary laboratory study its feasibility was investigated with bentonite, kaolin and illitic clay. In the first part of the experiments the infiltration properties of the different clays injected into different sands were evaluated to find the optimum clay concentration of the injected suspension. The tests showed that bentonite had to be discarded because of its high viscosity. Despite its high sorption capacity for Diclofenac it was not possible to inject a bentonite suspension without clogging the pores of the sands. A clay concentration with 80 g clay/l was found suitable for kaolin as well as the illitic clay suspensions and chosen for the subsequent investigations, which assessed the sorption properties in batch and column tests. Batch tests with Diclofenac concentrations of 1, 5 and 10 mg/l respectively were performed to construct sorption isotherms. The results obtained from the batch tests were then compared with the sorption results in column test. Here suspensions with 80 g clay/l were injected for both clays into coarse sand contaminated with different concentrations of diclofenac (0.26, 1.32, 2.63  $\mu\text{g/g}$ ). The results showed that a significant amount of diclofenac was removed only by injection and the movement of water by some kind of physical soil flushing. Only small amounts were really adsorbed by the clay (up to 17% in the case of illitic clay for a concentration of 0.26  $\mu\text{g/g}$ ). In general illitic clay showed a better remediation capacity compared to kaolin, especially for the lowest Diclofenac concentration.

## Application of waste ceramics in environmental protection

Barbora Dousova<sup>1</sup>, David Kolousek<sup>1</sup>, Miloslav Lhotka<sup>1</sup>, Lenka Holcova<sup>1</sup> and Martin Keppert<sup>2</sup>

<sup>1</sup> University of Chemistry and Technology Prague, Technicka 5, 166 28 Prague 6, Czech Republic,  
barbora.dousova@vscht.cz

<sup>2</sup> Faculty of Civil Engineering, Czech Technical University in Prague, Thakurova 7, 166 29 Prague 6, Czech Republic

Waste ceramics represent chemically stable, available and environmentally friendly silicate material which, analogous to other aluminosilicates, can function as effective sorbents in natural and technological processes. Favourable adsorption properties result from chemical composition (e.g. variation in Al, Si, Fe content), surface hydration of aluminosilicate structure and a high specific surface area ( $S_{BET}$ ). In this study, waste brick dust was tested as a potential sorbent of cationic and anionic contaminants, including radioactive residues.

Table 1. Characterization of waste brick dust

chemical composition (% wt)						mineralogical composition
SiO <sub>2</sub>	Al <sub>2</sub> O <sub>3</sub>	Fe <sub>2</sub> O <sub>3</sub>	TiO <sub>2</sub>	CaO	MgO	illite, feldspar, quartz, micas, hematite
49.5	19.7	6.1	0.8	13.5	4.8	

For adsorption experiments, highly toxic and/or ecologically risky cations (Cd, Pb, Cs) and anions (As, Sb, Cr, U) were selected according to their current environmental concern in the international scale. The study proceeded in two directions – (i) adsorption of cationic/anionic particles from aqueous solution for the determination of optimal sorption parameters, and (ii) verification of the stability of fixed particles in saturated sorbent. The preliminary study with Pb<sup>2+</sup>, As<sup>V</sup> and As<sup>III</sup>, resp. (Fig. 1) indicated a wide sorption selectivity of waste brick dust for both cationic and anionic contaminants. The approximate mass consumption of sorbent per 1 g of toxic element in highly

contaminated aqueous systems ( $\approx 40 \text{ mg L}^{-1}$ ) was found from  $<70 \text{ g}$  (Pb<sup>2+</sup>) to  $>400 \text{ g}$  (As<sup>III</sup>) which predicated possible technological applications. The adsorption efficiency was also high, 90% for As<sup>V</sup>,  $<60\%$  for As<sup>III</sup> and 95% for Pb<sup>2+</sup>.

The stability of cations/anions in saturated brick dust and the type of surface complexation will be evaluated by leaching tests according to the International norms. A coherent study will be focused on possible fixation of saturated brick dust in building materials, such as cements and concretes.

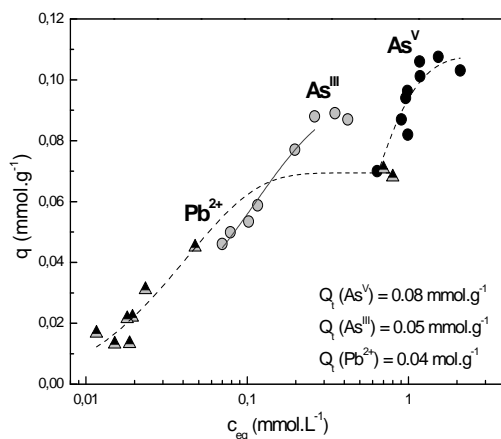


Fig. 1. Langmuir adsorption isotherms ( $Q_t$  – theoretical sorption capacity)

**Acknowledgements:** This work was the part of the project 13-24155S (Grant Agency of Czech Republic).

## Kinetic experiments and XPS study of uranyl adsorption onto montmorillonite at pH = 4

Vanessa Guimarães<sup>1</sup>, Enrique Rodríguez-Castellón<sup>2</sup>, Fernando Rocha<sup>1</sup>, Manuel Algarra<sup>2</sup> and Iuliu Bobos<sup>3</sup>

<sup>1</sup>Geobiotec. Departamento de Geociências da Universidade de Aveiro, Campo Universitário de Santiago. 3810-193 Aveiro, Portugal. vsguima@fc.up.pt

<sup>2</sup>Departamento de Química Inorgánica, Facultad de Ciencias, Universidad de Málaga. Campus de Teatino s/n, 29071 Málaga, Spain; <sup>3</sup>DGAOT, Faculdade de Ciências, Universidade do Porto. Rua do Campo Alegre 687. 4169-007 Porto, Portugal.

High- and low-charge montmorillonite (S1 and S2) and randomly interstratified illite/smectite (S3) were used in adsorption experiments with uranyl. Kinetic experiments were carried out in a continuous flow stirred-tank reactor at a pH=4, low ionic strength ( $[\text{NaCH}_3\text{COO}]=0.1 \text{ mM}$ ) and a concentration of 0.15 mM of uranyl acetate. Adsorption experiments were run for 42 hours followed by 10 hours of desorption. The breakthrough curves suggest that more than one sorption mechanism occurred, associated with two different adsorption rates (before and after 4 hours), for each case. Moreover, the decrease of pH during the first 4 hours of adsorption may be indicative of possible complexes formed in the edge sites ( $\Delta\text{pH}=0.40$ ). Higher adsorption capacity after 42 hours was found for S2 [adsorbed 67.98 mg( $\text{UO}_2^{2+}$ )/g], which adsorbed 28% more than S1 and 176% more than S3. After the desorption process, S1 and S2 have shown the highest retention capacities (~86%) whereas S3 retained 79% of adsorbed  $\text{UO}_2^{2+}$ . XPS results revealed the existence of two binding energies at ( $\text{U}4f_{7/2}$ ) 382.2 and 383.3 eV, assigned to the presence of  $\text{UO}_2^{2+}$  mononuclear species onto aluminol edge sites and into the interlayer space, respectively [Drot et al. 2007; Catalano et al. 2005]. Also, a new binding energy at 380.8 eV was identified for the three samples studied. The binding energy at 380.8 eV was correlated with high charge montmorillonite layers interstratified with low-charge montmorillonite. The same low binding energy (380.8 eV) was found for quartz samples in contact with highly acidic solutions, where  $\text{UO}_2^{2+}$  mononuclear species were dominant in solution. It suggests that the position of charge on the tetrahedral sheet may have contributed to the increase in attractive forces between hydrated  $\text{UO}_2^{2+}$  on interlayer and silanol groups.

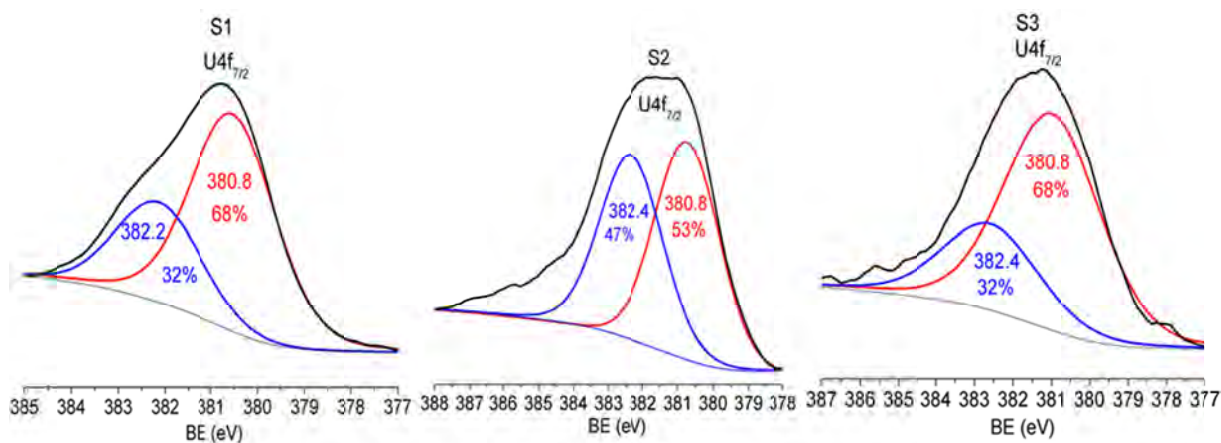


Fig.1: XPS results of S1, S2 and S3 obtained from flow-through experiments.

[1] [5] R. Drot et al., C. R. Chimie 10, 1078-1091 (2007).

[2] J.G. Catalano and G.E. Brown Jr., Geochimica et Cosmochimica Acta 69, 2995-3005 (2005).

## Simulation of Zn(II) transport in a soil column considering sorption properties of clay minerals

Christelle Latrille, Catherine Beaucaire and Aubéry Wissocq

CEA, DEN,DANS,DPC, Laboratory of Radionuclides Migration Measurements and Modeling,  
F-91191 Gif-sur-Yvette, France. christelle.latrille@cea.fr

To evaluate the impact of nuclear facilities on the soil environment, the ability to predict the behavior of contaminants in more or less complex physico-chemical contexts is required. This prediction requires consideration of both transport processes and physico-chemical conditions. Moreover, a dissemination of contaminants in soil will depend on the retention properties of soil components, usually attributed to clay minerals, organic matter and metallic oxides. The choice of coupled transport and thermodynamic models is important therefore. This study is focused on Zn reactive transport in a soil column filled with a soil Bt horizon (Lamy et al., 2006). The sandy clay Bt horizon contains 20.4 wt% clay and 0.34 wt% organic matter. Clay minerals identified using XRD are kaolinite, illite, and illite/smectite mixed layers. They represent the major reactive components of this soil. The behavior of Zn(II) in the column was then simulated by considering, in particular, the sorption reactions on clay mineral surfaces towards major and trace cations and transport processes defined in the HP1 code, coupling HYDRUS-1D and PHREEQC.

Intrinsic charges in clay minerals are known to have their origin in isomorphous substitution in the octahedral and tetrahedral sheets as well as surface protonation - deprotonation charge related to sites on layer edges (silanols or aluminols) or frayed edge sites. In a soil sample, the clay minerals proportion is easily evaluable but the involvement of each clay sorption site on the global sorption properties of the soil is difficult to evaluate. Considering that clay minerals are cation exchangers containing multiple sorption sites, it is possible to interpret the sorption of Zn(II), as well as competitor cations, by ion-exchange equilibria with the clay minerals for which no mineralogical or structural assignment is possible (Tertre et al. 2009). This approach is applied to interpret the experimental data by assimilating soil to an illite and smectite mixture and using the retention parameters (site concentrations and selectivity parameters of Zn(II) and  $\text{Ca}^{2+}$  versus  $\text{H}^+$ ) previously determined separately on pure illite and smectite phases.

Simulations are compared to experimental data. In this study, we bring out the role played by some parameters, such as flow velocity, dispersivity, major element concentration, and number of sites of sorption in order to evaluate the sensitivity of each of these parameters on the Zn breakthrough curves. Simulations show that the residence time of Zn in the soil column depends principally on the flow velocity and major Ca concentration. The arrival time and Zn spreading in time are sensitive to dispersivity and the number of sorption sites considered describing the exchanger. Comparing simulations with experimental data, the arrival time and the maximum value of the breakthrough curve are well matched using the measured flow velocity and our retention model, which reveals the major contribution of the sorption site accounting for the highest concentration. The tail may be attributed to the contribution of other type of sites.

Lamy I., van Oort F., Dère C. and Baize D. 2006. DOI: 10.1111/j.1365-2389.2005.00765.x

Tertre E., Beaucaire C., Coreau N. and Juery A. 2009. DOI: 10.1016/j.apgeochem.2009.06.006

## Adsorption of organic acids on clay rock: Desorption study using isotopic exchange

Sabrina Rasamimanana<sup>1\*</sup> and R. Dagnelie<sup>1</sup>, G. Lefèvre<sup>2</sup>

<sup>1</sup> CEA, DEN, DPC, Laboratory of Radionuclides Migration Measurements and Modelling, 91191 Gif-sur-Yvette, France.

\* Email: sabrina.rasamimanana@cea.fr

<sup>2</sup> Institut de Recherche de Chimie Paris, CNRS – Chimie ParisTech, 11 rue Pierre et Marie Curie, 75005 Paris.

The Callovo-Oxfordian clay rock (COx) is investigated by the French radioactive waste management agency (Andra) in the context of the underground retrievable nuclear waste repository project (*Cigéo*). There is already a large dataset on ion diffusion in COx clay rock [1, 2]. Cation transport is limited by adsorption on argillaceous minerals while inorganic anions display an “anionic exclusion” from the porosity of the rock. Recent results obtained on small carboxylic acids have shown intermediate behaviour dealing with diffusion of organic anions [3]. Furthermore, strong reactivity and desorption hysteresis are observed as well as differences between adsorption data obtained by diffusion and adsorption experiments.

In order to improve transport modelling of organic molecules in sedimentary rocks, we use <sup>14</sup>C-radiolabelled tracers to study adsorption/desorption kinetics and processes using a classical method and an isotopic exchange method [4]. Complementary protocols were performed to assess the stability of the solid phase during these experiments. This presentation will focus on the adsorption/desorption of five anthropogenic acids (acetate, phthalate, citrate, isosaccharinate, ethylenediaminetetraacetate) on COx clay rock. The different experimental adsorption protocols evidenced an apparent equilibrium regardless of volume/mass ratio, equilibration step, or organic concentration. Still, a desorption hysteresis was quantified by isotope exchange. Similar tests were then performed during the desorption step (figure 1). These results will be presented in order to illustrate the interest in this isotopic technique to make a mechanistic study of desorption and the difficulty to measure desorption on a natural sample without perturbation of the system.

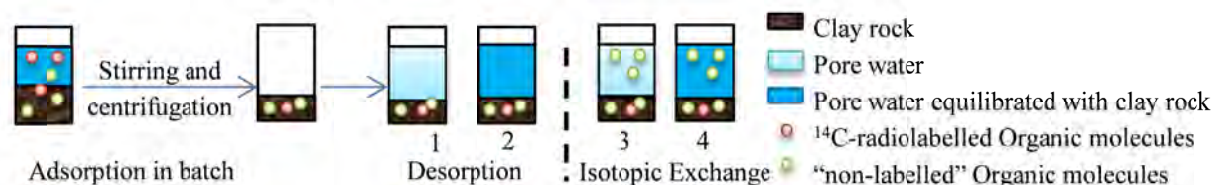


Fig. 1: Experimental protocols possible for desorption. 1&2 - Desorption using pore water, 3&4 - Isotopic exchange with organic solution. Renewal solutions are synthetic (1&3) or equilibrated with clay rock (2&4).

The data acquired provide macroscopic clues on the mineralogical phases which drive the adsorption of small soluble organic molecules on clay rocks. These results are useful to estimate the adsorption parameters of organic complexes in sedimentary rocks. They should help to consolidate the reactive-transport modelling and specify their field of validity.

This work was partially financed by CEA and Andra.

[1] Melkior, T. et al. *Physics and Chemistry of the Earth* 32, 453–462 (2007).

[2] Descostes, M., et al. *Applied Geochemistry* 23, 655–677 (2008).

[3] Dagnelie R.V.H., et al. *Journal of Hydrology* 511, 619–627 (2014).

[4] Sander M., & Pignatello J. *Environmental Science & Technology* 39, 7476–7484 (2005).

## **Inverse Gas Chromatography, $^{13}\text{C}$ and $^{19}\text{F}$ solid state NMR as powerful tools to study the interactions between a fluorinated fungicide and raw or organically modified Patagonian montmorillonites**

Jocelyne Brendlé<sup>1</sup>, Rosa Maria Torres Sanchez<sup>2</sup>, Federico Manuel Flores<sup>2</sup>, Eric Brendlé<sup>3</sup> and Séverinne Rigolet<sup>1</sup>

<sup>1</sup> Pôle Matériaux à Porosité Contrôlée, Institut de Science des Matériaux de Mulhouse, UMR CNRS 7361, Université de Strasbourg-Université de Haute-Alsace, 3b rue A. Werner, 68093 Mulhouse Cedex, France,

Jocelyne.Brendle@uha.fr

<sup>2</sup> Center of Technological Mineral Resources and Ceramic (CETMIC-CCT), La Plata, Camino Centenario y 506, (1897) M. B. Gonnet, La Plata, Argentina

<sup>3</sup>Adscientis, Parc Sécoia, 10 rue A. Kastler, 68310 Wittelsheim, France

Fungicides such as fludioxonil are essential for maintaining healthy crops and reliable, high-quality yields. However, using these bioactive molecules poses environmental issues including mainly their leaching and migration in soils and groundwater. To circumvent these drawbacks, raw clays and clays modified with organic cations have been proposed as effective barriers to prevent the mobility of pesticides and fungicides and as slow release formulations of the active molecules.

In this work, a raw and an organically modified Patagonian montmorillonite were investigated as adsorbents for fludioxonil (4-(2,2-difluoro-1,3-benzodioxol-4-yl)-1H-pyrrole-3-carbonitrile). After treatment with octadecyltrimethylammonium cations ( $\text{C}_{18}\text{TMA}^+$ ), a  $d_{001}$  value of 2.00 nm was found for organically modified Patagonian montmorillonite, suggesting a pseudo-trilayer arrangement of the cations in the interlayer space. The integrity of the organic moieties was checked by IRTF. Information about the mobility of the organic chains was gathered by  $^{13}\text{C}$  solid state NMR, whereas the organic matter content was obtained by TGA. After contact between the samples and fludioxonil, no significant difference was observed by XRD; however, higher amounts of fludioxonil are adsorbed on organically modified montmorillonite.  $^{19}\text{F}$  solid state NMR revealed a structural change of fludioxonil in the presence of montmorillonite. Inverse Gas Chromatography at Infinite Dilution indicated that the ion exchange induced a decrease of the value of the dispersive component of the surface energy and that there are very strong polar interactions on raw Patagonian montmorillonite and raw Patagonian montmorillonite containing fludioxonil.



## Viability of bacteria in the presence of modified clay minerals: Perspective of polyaromatic hydrocarbon (PAH) biodegradation

Bhabananda Biswas<sup>1,2,4</sup>, Binoy Sarkar<sup>1,2</sup>, Asit Mandal<sup>1,3</sup>, Ravi Naidu<sup>1,2</sup>

<sup>1</sup>Centre for Environmental Risk Assessment and Remediation

University of South Australia, Mawson Lakes Campus, SA 5095, Australia

<sup>2</sup>Cooperative Research Centre for Contamination Assessment and Remediation of the Environment, P.O. Box 486, Salisbury, SA 5106, Australia

<sup>3</sup>Division of Soil Biology, Indian Institute of Soil Science, Bhopal, India

<sup>4</sup>Bhabananda.Biswas@mymail.unisa.edu.au

Polyaromatic hydrocarbons (PAHs) can potentially have negative impact on environmental quality and human health. Bioremediation through microbial degradation is considered as more cost effective and eco-friendly method than physiochemical strategies for PAH remediation. While low molecular weight PAHs (< 4 aromatic rings) are easily biodegraded, high molecular weight PAHs including 4 and 5 ring-compounds pose significant challenge, which is largely attributed to their toxicity to microorganisms and limited bioavailability. Biocompatible adsorbent particles can promote formation of biofilm and 'bacterial hutch' and keep PAHs in the proximity of microorganisms so that the compounds remain bioavailable. This can be a potential strategy for complete biodegradation of PAHs [1].

Modification of natural clay minerals (e.g., bentonite and palygorskite) with organic compounds (e.g., surfactants) can promote PAHs adsorption [2]. However, these modified clay minerals (organoclays) can be inhibitory to soil microbial functions [3]. Therefore, alternative clay adsorbents with different mode of modifications exerting better biocompatibility might assist in complete biodegradation. However, assessment of the viability and functionality of PAH degrading microbial species in the presence of those modified clay minerals is scant in the literature.

To this end, thermally treated and acid/alkali treated bentonite and palygorskite were tested in the current study for their effects to the viability of a PAH degrading bacterium (*Burkholderia sartisoli*). Both types of modifications resulted in a change of the surface area and charge properties of the clay minerals. Specially, increase in heating temperature had significantly impacted the fibrous structure and pore size distribution of palygorskite. The aggregation pattern of the modified clay minerals also considerably differed in aqueous suspension. How these physico-chemical changes would affect the bacterial cell adsorption, viability and degradability of phenanthrene is discussed by using *Burkholderia sartisoli* under batch experimental conditions.

**Keywords:** Clay-microbe interaction, modified clay minerals, PAH biodegradation.

[1] Lünsdorf, E. et al., 2000. Environ. Microbiol., 2: 161-168.

[2] Sarkar, B. et al., 2012. Crit. Rev. Environ. Sci. Technol., 42: 435-488.

[3] Sarkar, B. et al., 2010. J. Hazard. Mater., 184: 448-456.

## From spent clay minerals to functional materials

Runliang Zhu\*, Qingze Chen, Minwang Laipan, Tianyuan Xu, Hongping He

Guangzhou Institute of Geochemistry, Chinese Academy of Sciences, Guangzhou, 510640, China; zhurl@gig.ac.cn

Clay minerals and their modified derivatives have found potential applications in various pollution control areas. Proper disposal and recycling of the spent clay minerals are critical to their applications but have not been concerned yet. Here we report our recent studies in terms of using the spent clay minerals as precursors for synthesizing functional materials.

In the first study, the spent montmorillonite (Mt) after the adsorption of cationic dyes (e.g., crystal violet) were heated under the protection of  $N_2$ . The Mt layers functioned as a template and the cationic dyes were transformed into 2D carbon monolayers within the interlayer space of Mt. After removing Mt layers by acid washing, we obtained N-doped graphene-like carbon materials (Fig. 1), which showed efficient electrocatalytic activity for the oxygen reduction reaction. Using similar method, we reutilized the spent r Mg/Al layered double hydroxide (LDH) after the adsorption of anionic dyes (e.g., orange II), and the resulting carbon materials showed 3D porous structure with BET specific surface area over  $1400 \text{ m}^2/\text{g}$ . As such, the obtained materials can be effective adsorbents for organic contaminants.

The complex obtained by modifying Mt with hydroxyl-iron can effectively adsorb oxyanion contaminants (e.g., phosphate) from water. The spent clay minerals after the adsorption of phosphate were used as precursor and were impregnated with  $AgNO_3$  to obtain hydroxyl-iron and  $Ag_3PO_4$  co-modified Mt complex. The resulting complex showed excellent catalytic degradation capacity of organic contaminants under visible light irradiation.

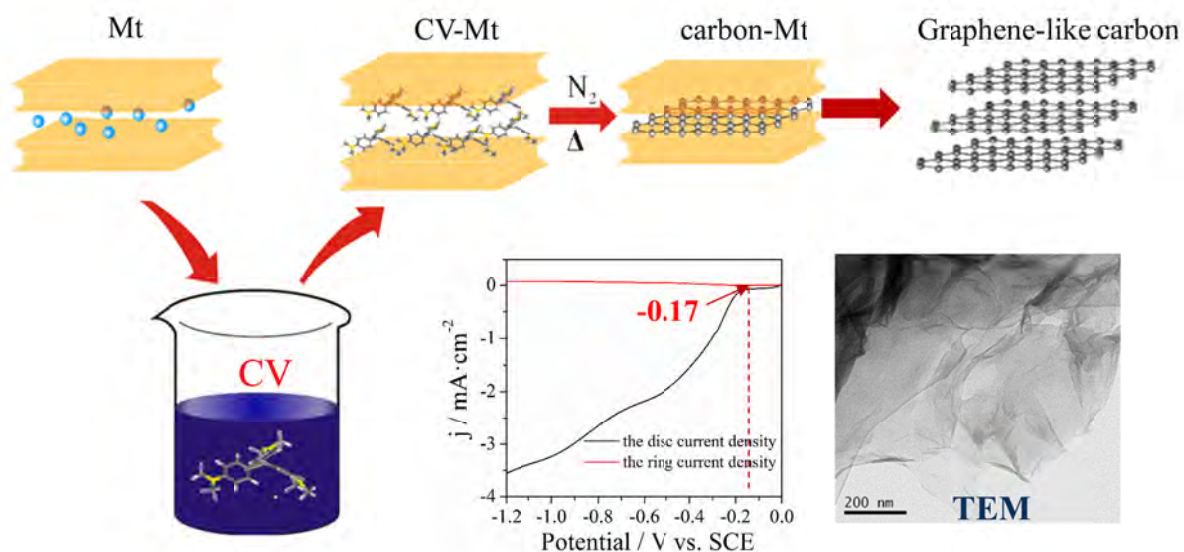


Fig 1 Templated synthesis of N-doped graphene-like carbon materials using the spent Mt after the adsorption of crystal violet

## **The effect of diatomite addition on the pore characteristics of a pyrophyllite-diatomite composite support layer**

Jang-Hoon Ha, Jongman Lee, and In-Hyuck Song

Powder and Ceramics Division, Korea Institute of Materials Science, 797 Changwondaero, Seongsan-gu, Changwon, Gyeongnam 642-831, Republic of Korea, hjhoon@kims.re.kr

Recently, porous ceramic membranes have become a subject of special interest due to their outstanding thermal and chemical stability. To alleviate the manufacturing cost issues of porous ceramic membranes, recent research is focused on the utilization of low cost natural materials. In this study, we introduced porous ceramic membranes prepared from pyrophyllite as a matrix and diatomite as a pore former, and both of them are low-cost natural materials. We report the results of our efforts to determine whether we could prepare a pyrophyllite-diatomite composite support layer that could control the largest pore size and permeability effectively. The pore characteristics of the sintered diatomite specimens were studied by scanning electron microscopy, mercury porosimetry, and capillary flow porosimetry.

## Biochar effects on nutrient leaching in soils

David Laird<sup>1</sup> and Natalia Rogovska<sup>1</sup>

<sup>1</sup>Department of Agronomy, Iowa State University, Ames Iowa, USA; dalaird@iastate.edu

Loss of nutrients by leaching from agricultural soils is a major cause of pollution in groundwater aquifers and both inland and coastal surface waters. Our group has been investigating mechanisms of interaction between nutrients and biochar surfaces, the effect of aging (surface oxidation) on biochar-nutrient interactions, and the impact of biochar soil amendments on nutrient leaching in laboratory, greenhouse and field studies.

Biochar can either increase or decrease nutrient leaching in agricultural soils depending on properties of the biochar, the soil, and the nutrient. Nutrients interact with biochar in soil environments through numerous different mechanisms illustrated in Figure 1. Biochar can increase soil water retention capacity and nutrients may be passively retained with the immobile water (A). Such physical retention of nutrients typically increases as biochars age (weather) in soil environments; on the other hand, fresh biochars may increase soil macro-porosity and hydraulic conductivity and thereby increase nutrient leaching. Biochars typically contribute significantly to the cation exchange capacity (CEC) of soil due to the presence of acidic organic functional groups on biochar surfaces, and leaching of cationic nutrients may be retarded by interaction with CEC sites (B). Our research shows that some biochars also have substantial anion exchange capacity (AEC) due to the presence of O and N heterocycles (oxonium and pyridinium groups, respectively) in the condensed aromatic carbon matrix. These AEC sites have the potential to directly retain anionic nutrients ( $\text{NO}_3^-$ ,  $\text{SO}_4^{2-}$  and  $\text{PO}_4^{3-}$ ) (C). The ash component, which is admixed with the aromatic C matrix of fresh biochars, is predominantly composed of carbonates and oxides. Dissolution of these carbonates in acidic soils releases cations ( $\text{Ca}^{2+}$ ,  $\text{K}^+$ ,  $\text{Mg}^{2+}$ , and  $\text{Na}^+$ ) from the biochar which contribute to the pool of potentially leachable nutrients in soils (D). The dissolution of carbonates raises soil pH, which is a major factor influencing the solubility and leachability of many nutrients (E). Biochars commonly have high surface area and an associated high capacity to adsorb nutrient containing organic molecules from the soil solution (F). Biochar provides a physical habitat for soil microorganisms and adsorbed organic compounds are a potential substrate for microorganisms, hence biochar amendments may enhance nutrient cycling (G). Some nutrients such as  $\text{PO}_4^{3-}$  may form sparingly soluble precipitates within biochar (H).

Most studies report that biochar amendments decrease nutrient leaching, however due to the complexity of nutrient-biochar interactions noted above, increases in nutrient leaching have also been reported. Evidence for the impact of biochar on nutrient cycling and nutrient use efficiently by crops is more equivocal.

Laird D.A. and N. Rogovska. 2015. Biochar effects on nutrient leaching. Ch. 19: in J. Lehmann and S. Joseph (eds.) Biochar for Environmental Management, Second Edition. Earthscan. London, UK.

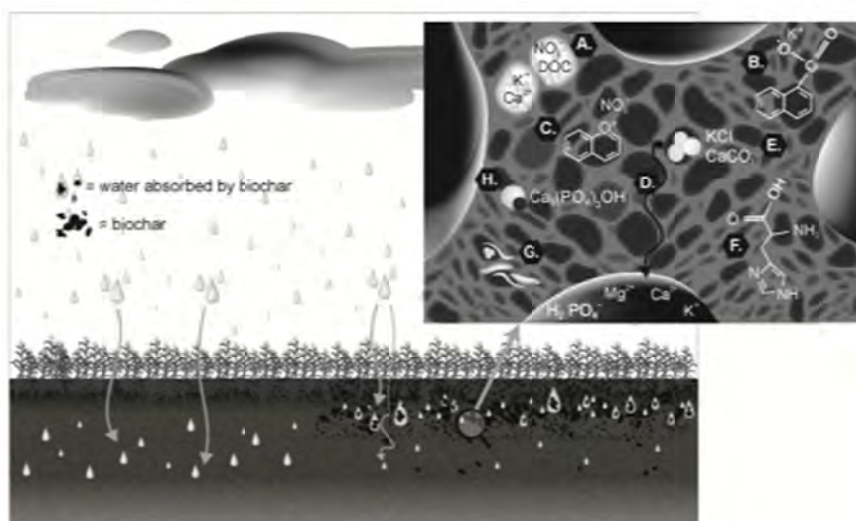


Figure 1: Major mechanisms of interactions between nutrients and biochar in soil environments (see text for explanation). Source: Laird and Rogovska, 2015.

Tuesday  
7<sup>th</sup> July

Lecture room 1  
Developments and  
applications of  
quantitative analysis to  
clay bearing materials  
incorporating The  
Reynolds Cup School

## The background, motivation and history of the Reynolds Cup

Jan Środoń

Institute of Geological Sciences, Polish Academy of Sciences, Research Centre in Kraków, Senacka St. 1, PL-31002  
Kraków, Poland

The Reynolds Cup is a success story. It started as a private initiative but became a permanent CMS institution, which deeply and positively affected the field of clay science and beyond. This success is rooted in failures and would not happen without the lessons learned from these failures. It also teaches us how fast the present becomes history: not an obvious observation in our busy lives.

The story goes back to 1998, when Dougal McCarty was hired by Texaco to run their XRD lab in Houston. We had met two years earlier in Boulder, where Victor Drits and I were working with Denny Eberl in his USGS lab on the crystal size distribution of illite and the techniques for measuring this property. Dougal very quickly found money to invite us to work with him in his lab and asked me what could we do, to – other than having fun of doing science together - be also useful for Texaco. I proposed quantitative mineral analysis, being aware of the importance of good quantitative data for the calibration of borehole geophysics. I had cooperated for many years in this field with my geophysicist friend Tomek Zorski, and he had never been happy with the quality of my analyses.

We came to Houston in the fall of 1998. Dougal and Victor started working on the effects of high pH on shales - a second topic, requested by the borehole stability specialists, and I started with the quantitative analysis, knowing from my past experience that I want to use natural standards, an internal standard, random powders, and mostly the 060 region to quantify clays. Victor Drits at that time was very sceptical about the use of Rietveld in quantitative mineral analysis, so he supported my approach. I was also lucky because the lab had a complementary knowledge: they knew already that the McCrone wet grinding was the only way to prepare powders adequately for the quantitative XRD.

After four months of hard work, half of it devoted to checking the purity of natural standards from the Texaco collection and those purchased for this project, the technique was ready in its original Excel spreadsheet version and tested on our artificial mixtures, mimicking the common sedimentary rock composition. I gave my Excel spreadsheet to Denny Eberl, who based his RockJock on it, and in 1999 my student Krzysztof Mystkowski turned my spreadsheet into a computer program employing genetic algorithms. The program was latter refined during our work for Texaco and is known today as QUANTA.

We were convinced that we have a technique which was quick and which generated much better data than those provided by service companies. But at Texaco every project manager was free to buy the analyses from both inside and outside the company. How to convince them to buy from the Texaco own Houston lab and not from the providers they had used for years? That is how the idea of organizing an open competition (which we hoped to win) came to our minds and that is how the rule of disclosing only the names of winners was born. We assumed that the commercial companies would only be attracted if we guaranteed that not so good results would remain anonymous, identifiable only to the competitor themselves.

We agreed quickly that the competition would be called the Reynolds Cup, to honour Bob Reynolds, our good friend and mentor, and that the results will be announced at the annual CMS meeting. We started calling around to find the organizer of the first event. This turned out to be a major problem: people realized how much work was involved. Only Dewey Moore agreed, but in the meantime he retired, so the failure was complete. Consequently the Texaco lab, which in the meantime became a Chevron lab, had to organize the first Reynolds Cup in 2002 and thus could not participate in it. This is how the key idea, which turned the Reynolds Cup into a permanent institution was born: we put into the rules that the winner organizes the next contest. Thanks to that insertion the Houston team was able to participate in 2004 in the contest organized by the first winner Reinhard Kleeberg, and came second.

In our today world of big projects, consortia, planning, reviewing and auditing this success story provides a reflection on financing research: are we indeed going in the right direction or perhaps we are on a wrong track?

## Preliminary results of an inter-laboratory study on quantitative phase analysis

M. Suárez, P. Aparicio, J. Fernández Barrenechea, J. Cuevas, R. Delgado, A.M. Fernández, F.J. Huertas, M.T. García-González, E. García-Romero, I. González, R. Fernández, L. León-Reina, A. López Galindo, J. Párraga, M. Pelayo, E. Pozo, M. Pozo, J.M. Martín-García, F. Nieto, A. Sánchez-Bellón, J. Santaren, A.I. Ruiz, E. and D. Terroso  
Sociedad Española de Arcillas. Avda. de las Palmeras, 4 - 18100 Armilla, Granada, Spain

Quantitative phase analysis (QPA) of clayey materials using X-Ray diffraction data has always been a challenge. While quantitative methods based on Rietveld analysis offer excellent results for non-clay minerals, they become problematic when high crystallochemical and order degree variations are present in the phases, as is the case of most clay minerals.

In the summer of 2014, the Spanish Clay Society (Sociedad Española de Arcillas, SEA) proposed a collective QPA experiment to its members. The aim was to compare the results obtained in different clay laboratories studying the same samples by X-Ray diffraction. This comparative study is a starting point for a long-term work focused on the development of an optimized QPA guide for clay minerals adapted to modern equipment and software.

The results presented in this talk are those from the 2014 preliminary study in which the 22 participant laboratories analyzed three samples following their own laboratory routines. The only condition was not to use other complementary techniques for the quantification (e.g. IR spectroscopy, thermal or chemical analysis). The samples were mixtures of nearly pure quartz, feldspar, calcite, alunite, and different clays. Clay minerals included two different smectites (with low and high crystallinity), sepiolite, kaolinite and palygorskite.

The set of procedures, technical characteristics of the equipment, and software used in each laboratory was very different and, as a consequence, comparison of the results is not straightforward. The results were classified into "Reflecting Powers Method" (RPM) and "Relative Intensity Ratio (RIR) – Rietveld methods" groups. As it is well known RPM is based on the peaks areas while RIR is based on the peak intensities. As expected, a high dispersion of the results was found both globally and per group. At first glance, RPM returned, on average, better approximations to the true composition of the samples. Interestingly that trend was clearer in samples with clay minerals having higher variability in crystallochemistry and crystalline range order.

## PyXRD; a FOSS model to quantify disordered, layered minerals using multi-specimen X-ray diffraction profile fitting

Mathijs Dumon and Eric Van Ranst

Department of Geology and Soil Science (WE13), Ghent University, Krijgslaan 281/S8, B-9000 Ghent, Belgium

We present a free and open-source model called PyXRD (short for Python X-ray diffraction) to improve the quantification of complex, poly-phasic mixed-layer phyllosilicate assemblages. The novelty of this model is the *ab initio* incorporation of the multi-specimen method, making it possible to share phases and a selection of their parameters across multiple specimens. To check the hypothesis that the multi-specimen set-up can improve automatic parameter refinement, we calculated X-ray diffraction patterns for four theoretical mineral assemblages. These calculated patterns were then used as an input for the model with and without a multi-specimen set-up. For all four of the assemblages, PyXRD is able to reproduce or approximate the input parameters using the multi-specimen approach. Divergent solutions only occur in single-pattern set-ups which do not contain enough information (e.g. patterns of heated samples) to discern all the different minerals. The obtained results suggest a good quantification can be obtained with just a single pattern. At this stage it is likely that these results do not extrapolate to all real life samples. Still, PyXRD has proven to be a very useful tool when modeling X-ray diffraction patterns for complex mineral assemblages containing mixed-layer phyllosilicates.

Keywords: quantitative, XRD, clay mineralogy, PyXRD, multi-specimen



## Geological interpretations of clay mineral content enhanced by discriminant function analysis (DFA)

Ray E. Ferrell<sup>1</sup>, George F. Hart<sup>1</sup>, and Mohamed Agha<sup>2</sup>

<sup>1</sup> Dept. of Geology & Geophysics, Louisiana State University, Baton Rouge, LA, 70803, USA, rayferrell@cox.net

<sup>2</sup> Department of Geology, Faculty of Science, Fayoum University, Egypt

Simple mineral ratios, i.e., QFL tri-plots, are used for correlation and the recognition of spatial and temporal variability due to provenance and sedimentary processes. More complex, multiple-variable datasets produced by QXRD can be simplified and interpreted objectively by discriminant function analysis (DFA). The analysis assesses subtle associations among large numbers of variables when the class is identified by the investigator. Discriminant equations separate the variability amongst the groups and allow unknown samples to be classified with respect to groups. Once the assignments have been established, unknown samples can be back-classified to establish the probability of their membership in one of the defined classes.

The QXRD employed RIR and reiterative whole pattern fitting techniques to estimate the weight percent of major minerals and total clay minerals. Mineral abundances in the clay fraction were measured with NEWMOD simulated patterns.

DFA of 69 of 107 samples from eight sub-environments of the Krishna Delta\* (lagoon, river mouth bar, mudflat, barrier island, mangrove swamp, foreshore, tidal creek, and channel) produced distinct criteria for the recognition of the facies. The classification was 100% successful when the whole sample results included estimates of ideal clay-mineral layer types and a loss-on-ignition estimate. The 38 additional samples were used as an overlay to provide a limited test of the canonical equations established by the first DFA analysis and also were 100% successful in the classification analysis. Most of the mineralogical changes can be attributed to grain-size sorting. The major factors contributing to the success of the analysis are associated with quartz enrichment within the marine-dominated part of the delta and smectite enrichment in the riverine-process-dominated sub-environments.

QXRD and DFA of 124 Paleogene and Neogene bentonitic clays from the northern Western Desert of Egypt\* grouped the samples at three distinctly recognizable, but partially overlapping, levels of classification, including geographic region, geologic age, and quarry. At the province level, the back-classification of the samples was successful 92% of the time at the highest probability level; or 100% if the first plus second probability results were utilized. For samples of the same age, 80% of the first-choice assignments were correct and >90% were correct when the second choice was included. At the quarry level, predictability ranged from 76 to >90%. Using both probability results, only seven of the samples were misclassified. In a blind test of quarry samples, the DFA assignment was 80% correct, confirming the objective reliability of the class assignments. Results can be used to classify new samples in future geologic investigations, such as economic exploration.

To conclude, mineralogical (and geochemical) datasets contain multiple, complexly related variables that are difficult to assign to classes or groups (i.e. based on age, environment, or location). DFA identifies those functions (a priori) that can be used to assign unknown samples to pre-existing classes thus using and testing what is known about the units. In contrast, principal component analysis (PCA), principal factor analysis (PFA), and various forms of cluster analysis seek to identify those variables that can be grouped into consistent classes that were not specified beforehand. DFA confirms whether the recognized classes exhibit unique mineralogical contents, the weighting of the variables used to calculate discrimination coefficients, and the functions used for separation. The DFA leads to a probabilistic based distinction of classes thus reducing the potential for subjective errors.

\*published previously.

## Quantitative clay mineralogy as provenance indicator for recent muds in the North Sea

Rieko Adriaens<sup>1</sup>, Edwin Zeelmaekers<sup>2</sup>, Michaël Fettweis<sup>3</sup>, Noël Vandenberghe<sup>1</sup> and Jan Elsen<sup>1</sup>

<sup>1</sup>Department Earth and Environmental Sciences, Celestijnenlaan 200E, 3001 Heverlee

<sup>2</sup>Shell International E&P INC., 3333 Highway 6 South, Houston, TX, 77082 USA

<sup>3</sup>BMM- KBIN, Gulledelle 100, 1200 Brussel

Recent fine-grained mud deposits were mapped residing in an overall high-energy environment controlled by clay-poor, coarse sands on the Belgian Continental Shelf (BCS). Several provenance sources were cited in literature in order to explain the origin of the muds. In the current research, the quantitative clay mineral composition of the muds was characterized and compared with the clay mineral composition of possible sources such as the present day marine environment, estuarine or fluvial discharges, local erosion etc.

Although seemingly contrasting with the present-day hydrodynamics of the area, the clay composition of the Scheldt estuary coincides with the BCS mud composition. As all other source areas have a significantly different clay composition, the Scheldt river system must be the main clay supplier of the BCS muds. Additional sampling was performed in the fluvial part of the Scheldt river system along different tributaries. Through analysis and recalculation of present-day clay composition, river flow rates and suspension concentrations of the different tributary rivers of the Scheldt system, it was proven that the clay composition presently discharged by the Scheldt river system is identical to that of the BCS muds.

Although hydrodynamic modeling shows that the Scheldt is presently not discharging fluvial mud to the BCS, the Scheldt must have been the source of a significant mud discharge in the past, most likely in the period before anthropogenic influence. The clay composition present on the BCS can be traced back to early-Holocene tidal deposits in the coastal plain but also to Weichselian (MIS-5d), Eemian (MIS-5e) and Saalian (MIS-7) deposits of dominantly fluvial origin. Logically, the clay composition was first introduced in the coastal plain when the paleo-Scheldt river system united all tributary rivers during which the current Scheldt river clay composition was formed for the first time. This most likely happened during the Elsterian when all tributary rivers merged into one river system. The Scheldt river system discharged from then on in westward direction, occupying the Flemish Valley. This most likely occurred around 450.000 years BP, during the Elsterian (~MIS12), after a proglacial breakthrough in the North Sea.

## In-situ XRD studies of the clay mineralogy of Gale Crater, Mars

David Bish<sup>1</sup> and Ralph Milliken<sup>2</sup>

1Department of Geological Sciences, Indiana University, Bloomington, IN 47401 USA; bish@indiana.edu

2Department of Earth, Environmental & Planetary Sciences, Brown University, Providence, RI 02912 USA

The past decade of Mars exploration has seen the detection of numerous clay mineral-bearing outcrops in the ancient heavily cratered crust of the red planet. Reflectance spectra acquired by orbital visible-near infrared imaging spectrometers have been interpreted to represent occurrences of kaolinite, serpentine, smectite, illite, and chlorite. The most common spectral signatures are considered to represent Fe/Mg-bearing smectites or mixed-layer chlorite/smectite; in some locations these are overlain by Al-bearing clays such as montmorillonite and kaolinite. Although orbital spectroscopy has suggested a diverse clay mineralogy on Mars, the origin, geological context, and age of these minerals have been difficult to constrain from satellite data alone. *In situ* observations and analyses by the Mars Science Laboratory Curiosity rover have allowed these issues to be addressed by providing a deeper understanding of the local geology and depositional context of orbitally detected clay minerals in Gale Crater.

The Curiosity rover landed in Gale Crater in 2012 and continues to conduct a variety of scientific studies along a traverse approaching 10 km. A suite of ten instruments on the rover includes CheMin, a miniaturized X-ray diffraction/X-ray fluorescence (XRD/XRF) instrument that uses Co radiation and transmission geometry to obtain powder XRD data from scooped and drilled samples. CheMin XRD data clarify for the first time the clay mineralogy of the Gale Crater area and provide ground truth for orbital detections of clay minerals. XRD analyses of one scooped and six drilled samples reveal a largely basaltic mineralogy, with significant amounts of amorphous component(s) and variable clay mineralogy. Locations known as John Klein and Cumberland contain one or more 2:1 phyllosilicates, with significant broad peaks at  $\sim 10.1\text{\AA}$  and  $\sim 14\text{\AA}$ , respectively. Other samples (e.g., Windjana) exhibit a weak broad peak at  $\sim 10\text{\AA}$ . The breadth of these low-angle peaks and lack of higher-order reflections likely rule out phyllosilicates such as micas, vermiculite, or chlorite, and the very broad low-angle peaks and 2-D diffraction bands suggest that they are disordered. The broad  $\sim 10.1\text{\AA}$  peaks may be due to a collapsed smectite, although illitic material cannot be excluded. Treatments used in laboratory XRD measurements to distinguish between clay minerals are unavailable on Mars, but it is possible to use the change in humidity from Mars ambient surface to inside the Curiosity rover (RH  $\ll 1\%$ ) as a proxy for drying. No collapse of the  $\sim 14\text{\AA}$  peak was seen after 150 Mars days within CheMin, suggesting that this mineral may be a smectite containing high hydration-energy interlayer cations (e.g., Ca or Mg) or that it is a partially chloritized smectite. As CheMin XRD data extend only to  $\sim 52^\circ 2\theta$  ( $\text{CoK}\alpha$ ,  $2.04\text{\AA}$ ), the  $06,33\ell$  band cannot be used to provide information on the di-trioctahedral nature of the phyllosilicate. Other 2-D diffraction bands can be used to infer the dimensions of the a-b plane, including the  $02,11\ell$  band, which appears in difference curves in Rietveld refinements for both John Klein and Cumberland at  $\sim 22.7^\circ$ . Together, the XRD data suggest the presence of a smectite (or chloritized smectite), most similar to nontronite, and the  $\sim 14\text{\AA}$  material may be similar to material seen on Earth in soils. The latter, in particular, is consistent with authigenic reactions at low temperatures in a "soil" environment.

## Quantitative mineralogy of clay-rich silicoclastic rocks by using XRD and XRD/XRF methods

M. Cesarano<sup>1</sup>, D.L. Bish<sup>2</sup>, P. Cappelletti<sup>1</sup>, C. Belviso<sup>3</sup>, F. Cavalcante<sup>3</sup> and S. Fiore<sup>3</sup>

1 DiSTAR, Università degli Studi di Napoli Federico II, 80134 Napoli, Italy, mara.cesarano@unina.it

2 Dept. of Geological Sciences, Indiana University, 47405 Bloomington - IN, USA

3 Institute of Methodologies for Environmental Analysis-CNR, 85050 Tito Scalo, Potenza, Italy

Quantitative mineralogical analysis of clay-bearing rocks is considered a not-easy-to-face problem, because clays can be characterized by complex structures, often affected by structural disorder and interstratification. Preparation of clay rich samples for mineralogical analyses can also affect the determined results (Ploetze 2014).

Traditional methods, (e.g. RIR and Rietveld) may not be able to provide accurate results. For this reason, in the present study, these methods have been combined with bulk rock chemical analyses using the Vb Affina software (Leoni et al., 2008) to obtain the quantitative mineralogical evaluation of clay-rich flyschoid materials from the silicoclastic sedimentary successions occurring in the Sorrento peninsula of southern Italy.

XRPD qualitative analyses have shown that the samples are mainly constituted by quartz, mica, feldspars and different types of clay minerals. Specific analysis on the clay fraction of the samples identified kaolinite, chlorite, mixed layer illite/smectite (I/S) and mixed layer chlorite/smectite (C/S).

XRPD quantitative analyses was firstly conducted by combining RIR and Rietveld methods, through the Bruker Topas software. An amount of 20 wt. % corundum was added to the samples as internal standard. It is well known that the Topas software usually gives the best results when it is used to evaluate materials made of crystalline mineralogical phases. We found that when investigating samples containing poorly crystalline phases such as clay minerals and mixed layer phyllosilicates the software was not able to produce a good fit between measured and calculated patterns.

The Vb Affina software recalculates the amounts of mineral phases, obtained by XRPD quantitative analysis, on the basis of chemical compositions of the samples (in this study chemical analyses were conducted by XRF method), following the procedure described by Leoni et al. (2008). The Vb Affina software separately evaluates the amounts of illite and smectite in mixed layer I/S, starting from the percentage of illite determined in the mixed layer illite/smectite using the approach taken by Moore and Reynolds, which considers the stacking order R parameter. In our study, the stacking order R of I/S is R0 and R1, and the amount of illite has a mean value of 56%, ranging between 21% and 83%.

The progressive matching of mineralogical and chemical compositions allowed workers to refine the quantitative evaluation of phases. For example the amount of mixed layer I/S, which represents the dominant phase, evaluated by using Vb Affina, is not as high as those detected by using Topas software (e.g. 52 wt% instead of 64.5 wt%).

Leoni L., Lezzerini M., Saitta M. (2008)- Calcolo computerizzato dell'analisi mineralogica quantitative di rocce e sedimenti argillosi basato sulla compinazione dei dati chimici e diffrattometrici. Atti Soc. tosc. Sci. nat., Mem., Serie A, 113, Pag. 63-69.

Ploetze M. (2014)-Quantitative mineral analysis of complex mineral assemblages- the Reynolds Cup round robins in clay analysis. 21<sup>st</sup> General Meeting of the International Mineralogical Association September 1-5 2014, Johannesburg (ZA) <http://www.ima2014.co.za/>.

## Quantification of Soil Mineralogy by X-ray Powder Diffraction (XRPD) Full Pattern Fitting

Helen A. Pendlowski<sup>1</sup> and Stephen Hillier<sup>1</sup>

<sup>1</sup>The James Hutton Institute, Craigiebuckler, Aberdeen AB15 8QH (helen.pendlowski@hutton.ac.uk)

The quantification of soil mineralogy by X-ray powder diffraction (XRPD) can be done by a number of methods (for example Rietveld, full pattern fitting). During the quantification of the minerals in soils a range of issues may arise and present problems with the final results. These include the presence within the soils of organic carbon, iron oxides and clay minerals. Not all methods of quantification allow for these issues to be overcome easily, however, the full pattern fitting method allows for all aspects of the soil to be fully quantified and is done without the need for an internal standard.

A small set of twelve samples obtained from the National Soils Archive of Scotland (NSIS) were used to illustrate the strength of the full pattern fitting method of quantification. These samples were chosen so that a range of potential issues would arise for quantification. The final quantification data obtained from XRPD was compared to a range of other data including XRF to show the accuracy that can be achieved using full pattern fitting and to illustrate how other properties of soil can be related to mineralogy.

The success of the full pattern fitting quantification of XRPD data is also highlighted by the repeated success in the biennial Reynolds Cup round robin competition. However, it is clear that any form of quantification relies on correct and appropriate sample preparation.

## Latest breakthrough of sub-micron SEM-EDS analysis discussed within the context of the 2014 Reynolds Cup participation

David Haberlah<sup>1</sup>, Dirk Sandmann<sup>2</sup> and Michael Owen<sup>1</sup>

<sup>1</sup> FEI Australia, 73 Northbourne Ave, Canberra ACT 2600, Australia

<sup>2</sup> Department of Mineralogy, TU Bergakademie Freiberg, Brennhaugasse 14, 09599 Freiberg, Germany

FEI Australia is developing next generation SEM-EDS (automated mineralogy) mineral mapping technology, with a particular focus on clay speciation and quantitative mineral analysis of fine-grained rocks. The new spectral analysis algorithm resolves individual X-ray spectra into multiple minerals, and incorporates mineralogical knowledge on solid solution series, cation exchanges, elemental ratios, and trace minerals. It also introduces uncertainty mapping based on spectral match quality.

Results of participating in the 2014 Reynolds Cup are discussed, highlighting strengths and limitations of this technology applied to samples RC 1-3. In addition, subsequent advances in resolving multiple minerals per pixel (representing the x-ray excitation volume), are highlighted. When applied to shale rocks such as the example in *Fig 1*, the impact of this novel approach on mineral ID is demonstrated for chemically similar minerals such as K-feldspar, illite and muscovite.

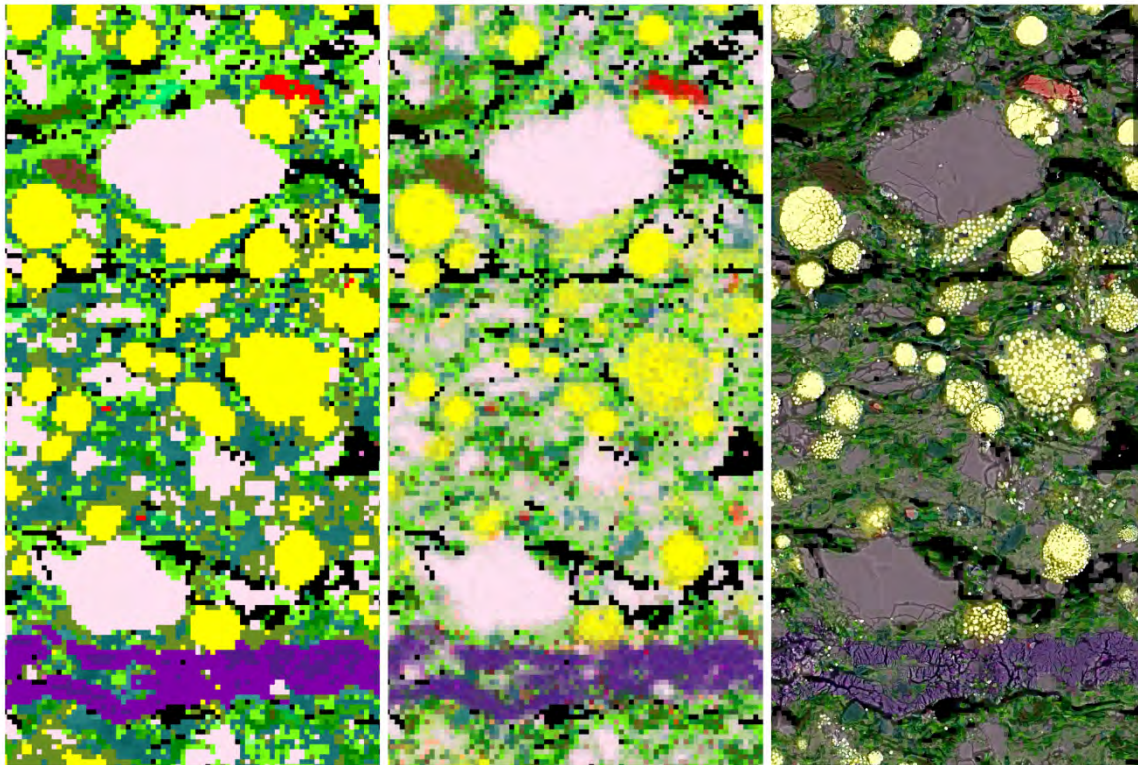


**Fig.1** 2015 results of the Spectral Analysis Engine (SAE) resolving EDX spectra into: **a)** dominant mineral per pixel (e-beam excitation volume); **b)** up to 3 minerals per pixel, and; **c)** overlay of EDX classification results on higher-resolution backscatter electron (BSE) image.

## Outcomes of 12 years of the Reynolds Cup quantitative mineral analysis round robin

Mark D Raven

CSIRO Land and Water, Waite Road, Urrbrae, South Australia, Mark.Raven@csiro.au

In 2000, the Clay Minerals Society established a biennial quantitative mineralogy round robin. The Reynolds Cup competition, as it is called, is named after Bob Reynolds for his pioneering work in quantitative clay mineralogy and exceptional contributions to clay science. The first contest was run in 2002 with 40 sets of 3 samples prepared and composed of mixtures of purified, natural and synthetic minerals commonly found in clay bearing rocks and soils that represent realistic mineral assemblages.

2014 marked the 7<sup>th</sup> Reynolds Cup quantitative mineralogy competition where a total of 81 sets of three samples were distributed to participants from 21 countries. Samples were made available to individuals in commercial, industrial, government, and academic laboratories. Any method or a combination of methods could be used to obtain the most accurate quantitative mineralogical analysis. X-ray diffraction is dominantly the method of choice for quantifying the mineralogy of the sample mixtures, however, a multitude of other techniques were also used to assist with phase identification and quantification.

The number of participants, and more importantly, the return rate has steadily increased since 2002 despite the highly complex mineral assemblages presented. The accuracy of a particular quantification is judged by calculating a "bias" for each mineral in an assemblage. Determining exactly the true amount of a mineral in the assemblage would give a bias of zero. Average biases per mineral phase for the winners of the first 4 contests between 2002 and 2008 remained relatively constant at a little under 1%. Since 2010 the contest was assessed in greater detail with the clay minerals in particular being judged to a higher level. For example, dioctahedral 2:1 clay minerals (muscovite, illite, illite-smectite and smectite) and trioctahedral 2:1 clays minerals (saponite, biotite and vermiculite) were grouped together prior to 2010 but were assessed separately from 2010 to 2014. As a result of this closer scrutiny the average bias per mineral phase for the winners of the 2010 contests initially doubled to ~2% but has since returned to 1% in the 2014 event.

Generally the higher placed participants correctly identified all or most of the mineral phases present. Conversely the worst performers failed to identify or misidentified phases. Several contestants reported a long list of minor exotic phases, likely reported by automated search/match programs but mineralogically unrealistic. Not surprisingly, clay minerals were the greatest source of error reported.

## Sample preparation suitable for quantitative XRD and procedures for identification of clay minerals

Michael Plötze

<sup>1</sup> ETH Zurich, IGT, Stefano-Francini-Platz 3, 8093 Zurich, Switzerland, ploetzel@ethz.ch

The Reynolds Cup competitions demonstrated the importance of XRD-based methods on quantitative analysis of clay-bearing materials. The strategy of the sample preparation for qualitative and quantitative phase analysis by XRD is often assumed to be a simple procedure. However, there is no “standard” way. The questions and goals as well as the sample composition determine the preparation procedure, e.g. in milling. Additionally, in bulk analysis clay minerals cannot be characterised in all their details. Therefore, beside other techniques, disaggregation and particle size separation is the most important technique for enrichment of clay minerals. Parameters like crystallite statistics, microabsorption and preferred orientation will be evaluated in their importance for sample preparation.

The XRD analysis of clay-bearing materials has to be carried out on powder specimen (<20 µm or fraction <2 µm) „without“ texture and on textured specimens. Procedures for their preparation will be evaluated in terms of their suitability and reproducibility (Gibbs 1965, Hillier 1999, Srodon et al. 2001, Kleeberg et al. 2008, Dohrmann et al. 2009).

The characteristic basal spacing (00l) of clay minerals in textured specimens is commonly used for qualitative X-ray diffraction analysis. Relative intensities and positions of the other, non-basal peaks (e.g. the 060 reflections) of randomly oriented powders were used e.g. to distinct dioctahedral and trioctahedral types as well as the determination of polytypes (MacEwan & Wilson 1980, Moore and Reynolds 1989). Diagnostic evaluation of the basal peaks were performed by a number of different cation saturation (e.g. Ca), solvations (e.g. ethylene glycol, formamide) and heating. The application of these procedures for the qualitative analysis of clay minerals will be demonstrated and evaluated for different samples from the Reynolds Cup.

Dohrmann, R. et al. (2009) Variation of preferred orientation in oriented clay mounts as a result of sample preparation and composition. *Clays and Clay Minerals*, v57, 686-694.

Gibbs, R.J. (1965) Error due to segregation in quantitative clay mineral X-ray diffraction mounting techniques. *American Mineralogist*, v50, 741-751.

Hillier, S. (1999) Use of an air-brush to spray dry samples for X-ray powder diffraction. *Clay Minerals*, v34, 127-135.

Kleeberg, R. et al. (2008) Preferred orientation of mineral grains in sample mounts for quantitative XRD measurements: How random are powder samples? *Clays and Clay Minerals*, v56, 404-415.

MacEwan D.M.C. & Wilson M.J. (1980) Interlayer and Intercalation Complexes of Clay Minerals. In: Brindley G.W. & Brown G. (eds.) *Crystal Structure of Clays and their X-ray Identification*. 1980, pp. 197-248, MSA.

Moore, D.M. and Reynolds R.C. (1989) *X-ray diffraction and the Identification and Analysis of Clay Minerals*. Oxford University Press, Oxford, New York 332 p.

Srodon, J, et al. (2001) Quantitative X-ray diffraction analysis of clay bearing rocks from random preparation. *Clays and Clay Minerals*, v49, 514-528.



## Multi-specimen computer modelling: Examples of illite-smectite mixed-layered structural characterization

Marek Szczerba<sup>1</sup> and Douglas K. McCarty<sup>2</sup>

<sup>1</sup> Institute of Geological Sciences, Polish Academy of Sciences, Kraków, Poland

<sup>2</sup> Chevron ETC, Houston, TX, United States

ndszczer@cyf-kr.edu.pl, mccarty@chevron.us

A comprehensive characterization of mixed-layered illite-smectite (I-S) includes an analysis of the composition and structure of the constituent illite fundamental particles, as well as the one-dimensional stacking sequence and distribution of illite and smectite interlayers. However, XRD is not very sensitive to variations in structural defects of these minerals. This can lead to equally good correspondence between experimental and theoretical patterns for substantially different structural models. In the case of illite-smectite, confidence in the actual mixed-layered structure is increased by obtaining close correspondence of calculated XRD patterns with corresponding experimental XRD patterns collected from air-dried (AD) and ethylene glycol (EG) solvated sample preparations. A reasonable structural interpretation is achieved when equivalent layer contents and probability parameters in the distribution of illite and smectite layers is achieved for both EG and AD experimental states. Theory and practical application of the method will be presented.

Examples of previous work, where analysis of XRD patterns of I-S from oriented sample preparations indicates that illitization of smectite is not a statistically homogeneous and continuous reaction with a progressive increase in illite layer content and degree of order in the layer-type stacking sequence will be presented. Early diagenesis in Oligocene Gulf sediment show that XRD patterns that are similar to ideal randomly interstratified I-S (R0 I-S), are actually a physical mixture of pure smectite and I-S with a 65:35 illite to smectite layer ratio. Additional results from a suite of I-S samples at the intermediate stage of diagenesis in a zoned K-bentonite from the Montana distributed belt have systematic structural trends in *cv* layer content and total expandability due to K and Mg metasomatism. I-S structure in the zoned bentonite was modelled as a physical mixture of an R0 I-S with constant high expandability (70 %S), coexisting with an ordered R1 I-S with a consistent illite to smectite layer ratio of 62:38, and only the relative proportion of the model structures varies with K and Mg content. The zonation of the I-S model structures, including chemistry and *cv/tv* layer profile, indicates there is strong structural control in illite fundamental particles during the conversion of volcanic ash, to smectite and then to I-S.

## X-ray powder diffraction full-pattern summation methods for quantitative analysis of clay bearing samples

Stephen Hillier<sup>1,2</sup>

<sup>1</sup>The James Hutton Institute, Craigiebuckler, Aberdeen, AB15 8QH stephen.hillier@hutton.ac.uk

<sup>2</sup> Department of Soil and Environment, Swedish University of Agricultural Sciences, Box 7014, Uppsala SE-750 07, Sweden

X-ray powder diffraction has long been the method of choice for the quantitative analysis of multiphase materials and the fundamental principles of performing it were worked out over more than 50 years ago. Until relatively recently (1980's), most implementations used single peak methods but the availability of computers has made it easy and practical to adopt full-pattern methods instead. The Rietveld method is one well known and very popular approach that can use the full diffraction pattern from some mixture of minerals (phases) to obtain a quantitative analysis in terms of the weight fractions of the minerals present. With the Rietveld approach the diffraction patterns for the component minerals are calculated on-the-fly and each can be refined to match in various details those present in the mixture, including their relative abundances. Clay minerals are amongst the most difficult minerals to include in a Rietveld quantification as the calculation of their diffraction patterns is not as straight forward as more 'conventional' minerals such as quartz and feldspars. Any full-pattern approach has a number of clear benefits over simpler single peak methods. One benefit is that peak overlaps between different minerals are explicitly accounted for; a second benefit is that the presence of initially unrecognized minerals becomes obvious as the analysis progresses, indeed the detection of trace phases can be greatly improved. An alternative to gain the benefits of the full-pattern approach but to avoid the skills required and the pitfalls that may abound when clay minerals are included in a Rietveld analysis is to use experimentally measured (or prior calculated) patterns for clay minerals along with all and any other minerals present in the mixture for which a quantitative analysis is required. The basic premise of this pattern summation method is that a diffraction pattern of a mixture of minerals can be simulated as a weighted sum of the diffraction patterns of its component minerals (Smith et al. 1987). In essence, this approach is like the Rietveld approach but without the refinement and solution of anything other than the proportions of the patterns required to model the unknown. One additional benefit is that the background can be included as data in a pattern summation approach and this is especially useful when dealing with X-ray amorphous phases and or poorly ordered phases, a description that applies to many clay minerals. There are various implementations of pattern summation methods, using various methods to obtain the fit of the experimental patterns to the unknown mixture, but the underlying principles that relate pattern proportions to quantitative mineral proportions are all fundamentally based on measuring a reference intensity ratio (RIR) of any given mineral, i.e. how well does one mineral diffract, with respect to another. Pattern summation methods are relatively easy to implement and do not require the level of crystallographic understanding for mastery of the Rietveld approach. Their main drawback is the time and effort required to set up a library of appropriate pure mineral patterns. Future developments are likely to include the incorporation of further constraints and restraints from complementary data including other pattern types, and perhaps calibration routines to assist in the transfer of libraries from lab to lab; but it is well to remember that appropriate sample preparation is the corner stone on which all of these procedures do, and will, continue to rely.

Smith, D. K., Johnson, G. G. Jr, Scheible, A., Wims, A. M., Johnson, J. L. & Ullmann, G. (1987). Quantitative X-ray powder diffraction method using the full diffraction pattern. *Powder Diffr.* 2, 73-77.

## The application of the Rietveld method in the Reynolds Cup contest

Kristian Ufer<sup>1</sup> and Mark Raven<sup>2</sup>

<sup>1</sup>Federal Institute for Geosciences and Natural Resources, Hannover, Germany, Kristian.ufer@bgr.de

<sup>2</sup>CSIRO Land and Water, Urrbrae, Australia

Although the Reynolds Cup round robin allows all possible analysis methods, X-ray diffraction is the most frequently used techniques. It is not only used for identification of components, but also for quantitative phase analysis. Several approaches allow the quantitative determination of mineral contents, among them the Rietveld method (Rietveld, 1967). The successful application of the Rietveld method for QPA requires the identification of all components and an appropriate description of their diffraction patterns, at best structurally based. In addition, the quality of a Rietveld quantification also depends on a suitable sample preparation and measurement conditions, as well as the correct description of instrument settings.

Almost all samples from the past Reynolds Cup samples contained minerals which are difficult to handle with the Rietveld method. Mixtures of minerals with similar structure and composition tend to correlations, e.g. kaolinite and halloysite. Other clay minerals contain stacking disordering, which is not describable within a traditional unit cell. Some components are difficult to describe in a structurally based way like amorphous phases and have to be quantified indirectly. Several Rietveld codes were so far applied in the Reynolds Cup. They differ in features like the description of peak broadening, correction of preferred orientation and the treatment of 'critical' components.

It came out that a satisfying quantification depends strongly on the user's skills. Although the refinement procedure itself is automatic and therefore user-independent, the result is strongly influenced by the choice of structural models, refineable parameters and limitations of these parameters. All refinement results, even if the result is statistically satisfying, need validation and – if necessary - correction with other methods. A choice of examples for successful applications of Rietveld refinements as well as limitations of the method will be discussed in this presentation.

## Supporting methods for mineral quantification in clay-bearing rocks

Arkadiusz Derkowski<sup>1</sup> and Stephan Kaufhold<sup>2</sup>

<sup>1</sup> Institute of Geological Sciences, Polish Academy of Sciences, Senacka 1, 31-002 Krakow, Poland  
ndderkow@cyf-kr.edu.pl

<sup>2</sup> BGR, Bundesanstalt für Geowissenschaften und Rohstoffe, Stilleweg 2, D-30655 Hannover, Germany

Mineral quantification tests applied during the famous Reynolds Cup (RC) unambiguously proved the importance and success of X-ray diffractometry (XRD)-based methods. However, additional methods can be used to both complement XRD data and validate quantitative XRD results.

Chemical composition is the primary verification of mineral quantification. A multiplication product of element concentration in minerals (assumed or average for a species) forming the sample and their quantities should return the value measured by chemical methods (*Controller* approach). Along with infrared spectroscopy (IR), this method is especially useful for amorphous phases. In the *BestRock* approach, quantitative mineral analysis and whole rock chemistry from sample aliquotes are optimized to obtain the chemical composition of the individual minerals present (McCarty *et al.*, 2015).

Because the RC is dedicated to clay-rich sedimentary rocks, clay minerals identification and quantification remains a crucial portion of the workflow. Accurate information about clays can be gained from both chemical- and CEC- based methods. Based on a set of suitable index cations quite accurate smectite contents can be calculated from CEC values based on assuming (or knowing) the variable charge, the layer charge density, and the molar mass of a formula unit (Kaufhold *et al.*, 2002).

In addition to XRD and chemical methods, IR provides quantitative information specific for certain minerals. Kaufhold *et al.* (2012) discussed different quantifications based on a pattern summation IR method. The accuracy of the results depends on the suitability of reference spectra (in how far do they actually represent the minerals present) and the reproducibility of the grinding which is known to be particularly important for quartz and/or feldspar. This method helped to quantify the mixture of halloysite and kaolinite in the RC7.

Precise thermogravimetry allows verifying the identification and quantification of minerals releasing volatile gasses (identifiable by mass spectrometry) upon heating including carbonates, sulphates and organic matter. Dehydroxylation of phyllosilicates helps in their quantification and in determining their structure (dioctahedral or trioctahedral, cis- and trans-vacant).

Kaufhold, S., Dohrmann, R., Ufer, K., Meyer, F.M., (2002) Comparison of methods for the quantification of montmorillonite in bentonites. *Applied Clay Science* 22, S. 145 – 151

Kaufhold, S., Hein, M., Dohrmann, R., Ufer, K. (2012) Quantification of the mineralogical composition of clays using FTIR spectroscopy. *Journal of Vibrational Spectroscopy*, 59, 29 - 39.

McCarty D.K., Theologou P.N., Fischer T.B., Derkowski A., Stokes M.R., and Ollila A. (2015) Mineral-chemistry quantification and petrophysical calibration for multi-mineral evaluations: The *BestRock™* Approach. *AAPG Bulletin*, in press.

**TUESDAY  
POSTER  
SESSION**

Title and authors	Page No.
<b>From microscopic pore structures to transport properties in shales (workshop follow on session)</b>	
On the use and abuse of N <sub>2</sub> physisorption for the characterization of the pore structure of shales <u>Pieter Bertier</u> , Kevin Schweinar, Helge Stanjek, Amin Ghanizadeh, Andreas Busch, Niko Kampman, Dirk Prinz, Alexandra Amann-Hildenbrand, Bernhard M. Krooss, Vitaliy Pipich and Zhenyu Di	183
Microstructure of clay assembly – from clay particles to shale <u>Wen-An Chiou</u> , Stephan Kaufhold and Reiner Dohrmann	184
Hydration of FEBEX-bentonite observed by Environmental Scanning Electron (ESEM) <u>Frank Friedrich</u> , Dieter Schild, Peter G. Weidler and Thorsten Schäfer	185
Comparison of methods for the determination of the pore system of a potential German gas shale <u>S. Kaufhold</u> , G. Grathoff, M. Halisch, M. Plötze, J. Kus, K. Ufer, R. Dohrmann, S. Ladage and Ch. Ostertag-Henning	186
Microstructural insights in petrophysical characteristics of indurated clays <u>P. Marschall</u> , L. Keller, S.B. Giger and J. Becker	187
Clay-based modelling approach for diffusion and sorption in the argillaceous rock from the Horonobe URL: application for Ni(II), Am(III) AND Se(IV) <u>Yukio Tachi</u> , Tadahiro Suyama, Kenji Yotsuji, Yasuo Ishii and Hiroaki Takahashi	188
Diffusion model in consideration of multiple pore structure in compacted bentonite <u>Kenji Yotsuji</u> , Yukio Tachi and Takahiro Ohkubo	189
The internal architecture and permeability structures of faults in shale formations <u>Pierre Dick</u> , Charles Wittebroodt, Christelle Courbet, Juuso Sammaljärvi, Imène Estève, Jean-Michel Matray, Marja Siitari-Kauppi, Miko Voutilainen and Alexandre Dauzères	190
Porosity evolution in the chalk: an example from the chalk-type source rocks of the Outer Carpathians (Poland) <u>Katarzyna Górniak</u>	191
Clay mineralogy and pore-scale characterization during and after CO <sub>2</sub> flow and saturation in the Mt. Simon Sandstone, Illinois Basin, USA <u>Jared T. Freiburg</u> , Peter M. Berger, Lois E. Yoksoolian, Shane K. Butler and Georg H. Grathoff	192
Hydration of smectite as a function of temperature and humidity: examples from natural fault rocks <u>Anja M. Schleicher</u> and Ben A. van der Pluijm	193
Characterizing the contents of nanopores in black shale using Nano-secondary ion mass spectrometry <u>Lynda B. Williams</u> and Maitrayee Bose	194
Edge structures of montmorillonite: A density functional theory study <u>Hiroshi Sakuma</u> , Yukio Tachi, Kenji Yotsuji and Katsuyuki Kawamura	195
Lithofacies and depositional environment of black shale in the Dniepr-Donets basin (Ukraine) <u>Eva Wegerer</u>	196
Microscale X-ray analysis of metal uptake by argillaceous rocks <u>Felician Gergely</u> , Janos Osan, Annamaria Keri, Rainer Dähn, Margit Fabian and Szabina Torok	197
<b>Asian Clay Minerals Group Research in Progress II</b>	
Adsorption and desorption of zearalenone by commercial and organophilic clays <u>Sumio Aisawa</u> , Hidetoshi Hirahara, Shota Endo, Mai Sekine, Eiichi Narita, Kazunori Sakao and Noriyuki Takahashi	198
Clay mineral composition and origin of Central Yellow Sea Mud (CYSM) in the Yellow Sea <u>Hyen Goo Cho</u> , Kyeong Yoon Kwak, Hunsoo Choi and Soo-Jae Lee	199
Preparation and evaluation of core-shell structured layered silicate and metal nanoparticles <u>Miharu Eguchi</u>	200
Aeolian contribution to volcanic soils, Mt. Daisen, Japan <u>W. Crawford Elliott</u> , Afshan Shaikh, Cyndi Jackson, J. Marion Wampler, Atsushi Nakao, and Junta Yanai	201

Natural extract incorporated nanoclays for antibacterial film additive <u>Hyoungh-Jun Kim</u> , Kang Koo, Sung-Woo Lee, Jin-Hee Lee, In-Kee Hong, Eun-Ji Kim, Soon-Seok Hwang and Jae-Min Oh	202
Isomorphous Co(II) incorporation into hydrotalcite type anionic clays via hydrothermal reaction <u>Tae-Hyun Kim</u> , Won-Jae Lee, Hyoungh-Mi Kim, Seung-Min Paek and Jae-Min Oh	203
Interaction between blood components and size/surface charge controlled anionic clays <u>Jae-Min Oh</u> , Hyoungh-Mi Kim, Sung Hoon Kim, Yoon Suk Kim	204
Generation of second stage structure in the alkylammonium cation and potassium sericite <u>Kenji Tamura</u> and Hiroshi Sakuma	205
The formation of smectite and its redox reaction in deep subsea floor sediment, South Pacific Gyre: IODP expedition 329 Kiho Yang, Toshihiro Kogure, Bryce Hoppie, Robert Harris, Hionsuck Baik, Hailiang Dong, IODP Expedition 329 shipboard scientists, and Jinwook Kim	206
Macroscopic orientation of Liquid crystalline fluorohectorite colloid by shear and electric field <u>Shohei Yoshimura</u> , Takumi Inadomi, and Nobuyoshi Miyamoto	207
Preparation of flame retardant expanded polystyrene (EPS) form using nanoclays <u>Minjae Kwon</u> and J. Yoon Choi	208
<b>Computational chemistry studies of clay minerals - bridging length and time-scales</b>	
Structural properties of montmorillonite intercalated with n-butylammonium cations (n= 1-4) – computational and experimental study <u>Eva Scholtzová</u> , Jana Madejová and Daniel Tunega	209
Performance of organic/inorganic force field combinations for molecular simulations of smectites intercalated with ethylene glycol evaluated by comparison with X-ray diffraction data <u>Marek Szczerba</u> and Andrey Kalinichev	210
Understanding the barrier properties of dry, clay-based coatings. A contribution from computational modelling <u>Nikita Siminel</u> , Chris Breen, Doug Cleaver, Francis Clegg	211
<b>Halloysite a unique, diverse and widely useful natural nanomaterial</b>	
Halloysite nanotubes from Burela, Spain. A preliminary study <u>Emilio Galán</u> , Patricia Aparicio and Marcial G. Márquez	212
Raw, acid activated and calcined halloysite for metals and metalloids adsorption: sorption capacity and mechanisms Paulina Maziarz, Anna Prokop and <u>Jakub Matusik</u>	213
Co-remediation method of nickel contaminated soil by halloysite and Indian mustard ( <i>Brassica juncea</i> L.) <u>Maja Radziemska</u> , Zbigniew Mazur, Joanna Fronczyk and Jakub Matusik	214
Interaction of isoniazid with halloysite as natural nanocarrier E. Carazo, A. Borrego, F. García-Villén, C. Aguzzi, P. Cerezo and <u>C. Viseras</u>	215
Effects of organo-modification of tubular halloysite on its performance as drug/agrochemical carrier <u>Peng Yuan</u> , Daoyong Tan, Faiza Annabi-Bergaya	216
<b>Natural zeolites environmental biomedical and industrial applications</b>	
Distribution of inorganic contaminants in a zeolite-sand reactive zone: laboratory column tests <u>Joanna Fronczyk</u> , Kazimierz Garbulewski and Maja Radziemska	217
Ion exchange on zeolitized geopolymers <u>David Kolousek</u> , Barbora Dousova, Miloslav Lhotka, Heinrich Jencus, Martina Urbanova, Libor Kobera and Roman Slavík	218
Characterization of CsAlSi <sub>5</sub> O <sub>12</sub> obtained by thermal treatment of Cs-clinoptilolite <u>Mariano Mercurio</u> , Antonio Brundu, Piergiulio Capelletti, Guido Cerri, Bruno de Gennaro, Mauro Farina, Patrizia Fumagalli, G. Diego Gatta and Lorenzo Guaschino	219

Temperature effects on cathodoluminescence of hydrous minerals <u>Hirotsugu Nishido</u>	220
Modification of Philippine natural zeolites by copper loading for <i>Escherichia coli</i> inactivation <u>Eleanor Olegario-Sanchez</u> , Michael Tan and Mary Donnabelle Balela	221
Long-term immobilization method for radioactive cesium-137 using hydrothermal synthesis of zeolite from coal fly ash <u>Yujiro Watanabe</u> , Koki Kitanaka, Kaoru Fujinaga, Syunichi Oshima, Hirohisa Yamada and Yu Komatsu	222
<b>Developments and applications of quantitative analysis to clay bearing materials incorporating The Reynolds Cup School</b>	
Quantitative modeling of XRD patterns of natural bentonites <u>Youjun Deng</u> and Ana L. Barrientos Velázquez	223
XRD at the Geological Survey of Norway – The BASE project <u>Jasmin Schönenberger</u> and Jochen Knies	224
Outcomes of 12 years of the Reynolds Cup quantitative mineral analysis round robin <u>Mark D Raven</u>	225
Sample preparation suitable for quantitative XRD and procedures for identification of clay minerals <u>Michael Plötze</u>	225
Multi-specimen computer modelling: Examples of illite-smectite mixed-layered structural characterization <u>Marek Szczerba</u> and Douglas K. McCarty	225
X-ray powder diffraction full-pattern summation methods for quantitative analysis of clay bearing samples <u>Stephen Hillier</u>	225
The application of the Rietveld method in the Reynolds Cup contest <u>Kristian Ufer</u> and Mark Raven	225
Supporting methods for mineral quantification in clay-bearing rocks <u>Arkadiusz Derkowski</u> and Stephan Kaufhold	225
<b>Clay and fine particle based materials for environmental technologies and clean up</b>	
Role of iron oxy-hydroxides on metal retention in marsh soils of the Domingo Rubio coastal wetland (SW Spain) <u>C. Barba-Brioso</u> , J.Delgado, J.C.Fernández-Caliani, A.Miras and E. Galán	226
Study of titanium-synthetic montmorillonite interactions by XRD, chemical analysis, solid state <sup>27</sup> Al, <sup>29</sup> Si and <sup>19</sup> F MAS NMR spectroscopy and synchrotron-based X-ray techniques <u>Jocelyne Brendlé</u> , Jeoffrey Huve, Daniel Grolimund, Paul Wersin, Leena Kiviranta and Margit Snellman	227
Comparing a modified low-value clay with commercial samples to remove pesticides from water M. Carmen Hermosín, Miguel Real, Esperanza Duran, Salvador Bueno, Lucia Cox, Rafael Celis, <u>Juan Cornejo</u>	228
Sorption of copper and nickel ions from solution with clay minerals <u>Ali Rıza Demirkiran</u> , Bilal Acemioğlu, Tuğba Gönen	229
Interaction of <i>Pseudoxanthomonas kaohsiungensis</i> with bentonite <u>Argha Chakraborty</u> , Binoy Sarkar, Bhabananda Biswas and Ravi Naidu	230
Combined fine-size substrates for remediation of highly acid mine drainages from the Puyango river watershed (El Oro, Ecuador) <u>J. Delgado</u> , D. Ayala, T. Boski, E. Calderón, F. López and C. Barba-Brioso	231
Dehydroxylation of I-S interstratifications: Implications for alkaline activated cements <u>Jan Dietel</u> , Annett Steudel, Laurence N. Warr and Katja Emmerich	232
The role of ceramic building materials for CO <sub>2</sub> sequestration. Preliminary results <u>Patricia Aparicio</u> , Emilio Galán, Domingo Martín, Adolfo Miras, Antonio Romero, Cinta Barba-Brioso	233



Diatomite-based porous materials and their performances for benzene adsorption <u>Peng Yuan</u> , Wenbin Yu, Weiwei Yuan, Dong Liu and Liangliang Deng	234
Assessing the redox reactivity of Fe(II)-reduced clay minerals <u>Katherine Ann Rothwell</u> and Anke Neumann	235
Flocculation of clay suspensions by model polyelectrolytes <u>Y. Sakhawoth</u> , L. Michot, P. Levitz and N. Malikova	236
Oil sorption by kaolinite and its potential role in the remediation of oil spillages <u>Ayodele A. Oyedeji</u> , A. R. Demirkiran, J. Kayode, L. Besenyei and M. A. Fullen	237
<b>Bioreactive clay minerals impacts on environmental and human health</b>	
Insights on anti-inflammatory, anti-bacterial, cytotoxic and oxidant activity, and oxidative stress inhibition by fibrous clays <u>Javiera Cervini-Silva</u> , Antonio-Nieto-Camacho, María Teresa Ramírez-Apan, Virginia Gómez-Vidales, Eduardo Palacios, Ascención Montoya and Elba Ronquillo de Jesús	238
Development and characterization of antibiotic-intercalated smectite <u>Donghoon Chung</u> , Yungoo Song, Il-mo Kang, YG Song and Woohyun Choi	239
Mineralogy and transformation trends of hard rocks from geophagic materials (South Africa) Georges-Ivo Ekosse, <u>Sofia Lessovaia</u> , Yury Polekhovskiy, Kirill Chistiakov, Elena Zelepukina, Alexey Filimonov, Natalia Andreeva, Anna Frolova, John Odiyo, Francis Mongogoa, Manneheng Raputhing, Nenita Bukalo, Johanna Molepo, Sally Ibeh, Jason Ogola, Elvis Fosso-Kankeu, Rachel Ravuluvulu and Valery Phakoago	240
Physical, chemical and thermal characteristics of Makirina bay peloids (N. Dalmatia, Republic of Croatia) <u>Darja Komar</u> , Petra Vrhovnik, Nastja Rogan Šmuc, Matej Dolenc, Tadej Dolenc, Sonja Lojen, Goran Kniewald, Živana Lambaša Belak, Sanja Slavica Matešić, Lourdes Mourelle and Carmen Gómez	241
Intercalation of pravastatin drug into LDH - molecular simulation study <u>Milan Pšenička</u>	242
Mineralogy and geochemical characteristics of some geophagic clays from southern Nigeria <u>Akinade S. Olatunji</u> and Jerry O. Olajide-Kayode	243
<b>Clay mineral indices in palaeo-geothermal studies hydrocarbon and geothermal prospection - third Frey-Kübler symposium</b>	
Chlorite geothermometer applied to the Patricia Zn-Pb-Ag epithermal deposit (Tarapacá-Andean Cordillera, Chile) <u>X. Arroyo</u> , D. Chinchilla, L. Ortega, R. Piña, F. Nieto and R. Lunar	244
Fluid-rock interaction in a fault-controlled geothermal system: the Pucuro Fault System in Central-Chile <u>Mercedes Vázquez</u> , Diego Morata, Leonardo Navarro, Fernando Nieto, Isabel Abad, Gloria Arancibia, Linda Daniele and Gert Heuser	245
Study of the low-grade thermal evolution of Wairarapa Area, North Island, New Zealand Pierre Malie, <u>Sébastien Potel</u> , Rafael Ferreira Mählmann, Julien Bailleul, Frank Chanier, Geoffroy Mahieux, Vincent Crombez and Brad Field	246
<b>General</b>	
Isotopic investigation of clay gouge from the central Alpine Fault, New Zealand: Testing the meteoric geofluid infiltration hypothesis <u>Austin Boles</u> and Ben van der Pluijm	247
Effect of process water circulation and stability of clay minerals in fluid fault zones: Tíscar active fault (Betic Cordillera, SE Spain) <u>Pilar Hernández Puentes</u> , Rosario Jiménez Espinosa and Juan Jiménez Millán	248
Phyllosilicates in the Alhama de Murcia fault zone and its influence in fault seismicity <u>C. Sanchez</u> , I. Abad, F. Nieto, J. Jimenez-Millan, D.R. Faulkner	249

Preferred orientation of talc in tectonites <u>J. Gómez-Barreiro</u> , J.M. Benítez Pérez, M. Suárez, E. García-Romero, M. Durán Oreja, M. Sánchez del Rio, O. Oriol Vallcorba Valls, H.-R. Wenk, J. García Rivas and B. Ouladdiaf	250
Na-bearing white micas from the Permo-Triassic Rocks of the Ghomaride Complex and Federico Units (Internal Zone of the Rif Chain, northern Morocco) <u>M.D. Rodríguez-Ruiz</u> , M.D. Ruiz-Cruz, C. Sanz de Galdeano and M.J. Bentabol-Manzanares	251
Key properties of selected organo-clay-polymer nanocomposites <u>Peter Komadel</u> , Jana Madejová, Ľuboš Jankovič, Valéria Bizovská, Lukáš Petra, Daniela Jochec-Mošková and Ivan Chodák	252
Weathering of glaciogene marine clays from West Greenland <u>Louise Josefine Belmonte</u> , Niels Foged and Thomas Ingeman-Nielsen	253
Sedimentology and mineralogy of paleosol and fluvio-lacustrine succession of the Late Miocene Bayramhacılı member, Cappadocian Volcanic Province, central Turkey: paleoenvironmental and paleoclimatic interpretation <u>Selahattin Kadir</u> and Ali Gürel	254
Salts present in the materials developed on marl in an area of badlands in Alicante (Spain) <u>Laura García-España</u> , <u>Maria Desamparados Soriano</u> and Anatonela Colica	255
Identification of the main parameters controlling the plasticity of ceramic pastes: The case study of the Marrakech region (Morocco) <u>Hicham El Boudour El Idrissi</u> , <u>Lahcen Daoudi</u> , <u>François Fontaine</u> , Frédéric Collin and Nathalie Fagel	256
Residual water in smectites <u>Artur Kuligiewicz</u> and Arkadiusz Derkowski	257
High-level waste and Spent fuel result from nuclear power generation <u>Ping Shen</u> and Nick Hankins	258
Validation of conventional K-Ar dating of single clay test portions <u>J. M. Wampler</u> and W. Crawford Elliott	259
Influence of clay mineralogy on shallow continental margin sediment shear strength <u>Joshua R. DeVore</u> and <u>Jeffrey R. Walker</u>	260
Chlorite nanocrystal formation from amphibolitic and dioritic rocks in Terphis' Serres, Greece <u>Paraskevi Lampropoulou</u> , Dimitrios Papoulis Eugenia Metaxa Konstantinos Hatzipanagiotou and Theophani Tzevelekou	261
Characterisation of Sotho pot clays using XRF, XRD and FTIR <u>Antoine F. Mulaba-Bafubiandi</u> and <u>Phindile Hlekane</u>	262
Analysis of water content in raw perlite samples <u>Helena Pálková</u> , Valéria Bizovská, Jana Madejová, Michal Slaný, Adriana Czímerová, Viktor Hronský, Peter Uhlík and Jaroslav Lexa	263

## On the use and abuse of N<sub>2</sub> physisorption for the characterization of the pore structure of shales

Pieter Bertier<sup>1</sup>, Kevin Schweinar<sup>1</sup>, Helge Stanjek<sup>1</sup>, Amin Ghanizadeh<sup>2</sup>, Andreas Busch<sup>3</sup>, Niko Kampman<sup>3</sup>, Dirk Prinz<sup>4</sup>, Alexandra Amann-Hildenbrand<sup>5</sup>, Bernhard M. Krooss<sup>5</sup>, Vitaliy Pipich<sup>6</sup> and Zhenyu Di<sup>6</sup>

<sup>1</sup>Clay and Interface Mineralogy, RWTH-Aachen University, Bunsenstr. 8, D-52072 Aachen, Germany

[Pieter.Bertier@emr.rwth-aachen.de](mailto:Pieter.Bertier@emr.rwth-aachen.de)

<sup>2</sup>Department of Geoscience, University of Calgary, Calgary, Canada

<sup>3</sup>Shell Global Solutions International, Kessler Park 1, 2288 GS Rijswijk, The Netherlands

<sup>4</sup>Dynchem, Saarstrasse 98, D-52062 Aachen, Germany

<sup>5</sup>Institute for Petroleum & Coal, RWTH-Aachen University, Lochnerstr. 2, D-52062 Aachen, Germany

<sup>6</sup>Jülich Centre for Neutron Science JCNS, MLZ Garching, Germany

This contribution aims to assess the use of N<sub>2</sub> physisorption for the characterization of the pore structure of shales. This will be done by addressing some common pitfalls and misconceptions related to the interpretation of physisorption data. In addition, N<sub>2</sub> physisorption will be compared to other methods used to characterize shales. For this purpose a set of pore structure and total porosity data from N<sub>2</sub> physisorption, He-pycnometry, Hg intrusion porosimetry (MIP), fluid saturation (Archimedes) methods and (ultra) small angle neutron scattering (SANS) will be used. This dataset was obtained from measurements on representative shales and mudrocks used in different applications, such as radioactive waste storage, geological storage of CO<sub>2</sub> and shale gas/oil production.

*Poster also presented at the workshop: 'Filling the gaps – from microscopic pore structures to transport properties in shales' held on Sunday 5<sup>th</sup> July 2015.*

## Microstructures of clay assemblies – from clay particles to shale

Wen-An Chiou<sup>1</sup>, Stephan Kaufhold<sup>2</sup> and Reiner Dohrmann<sup>2</sup>

<sup>1</sup> NISP Lab, Nanocenter, University of Maryland, College Park, MD 20742, USA, wachiou@umd.edu

<sup>2</sup> Federal Institute for Geosciences and Natural Resources, State Authority of Mining, Energy and Geology, GEOZENTRUM HANNOVER, Stilleweg 2, D-30655 Hannover, Germany

The spatial distribution, orientation, and particle-to-particle relationships of less than 4  $\mu\text{m}$  solid particles (mainly clay minerals) or as an assembly in fine-grained sediment determines the properties and behavior of sediments/soils, and provides pore space for interstitial water, gas, and organic matter in both living organisms and their products. Recent interest in oil shale due to energy needs and its enormous economic potential has spurred interest in the study of clay microstructure. However, advancements in this area of research have been slow due to the lack of a high resolution instrumentation. This paper introduces unique novel methods and technologies of studying individual clay particle assemblies and their applications to geological, mineralogical, biogeochemical, soil science, and civil engineering research.

High-resolution characterization of clay particle size, mineralogy, shape (morphology), and texture is important for understanding clay microstructure. Historical difficulties with measuring individual clay particles (domains/assemblies) due to minute size have been overcome by recent technological developments in electron and ion microscopy and microanalysis, such as high resolution scanning/transmission electron microscopy (S/TEM) with different analytical techniques, wet environmental TEM (WETEM) and focus ion beam (FIB). Other techniques, such as 3D SEM image reconstruction, 3D TEM tomography and 3D tomography using FIB have also recently provided excellent characterization of the fundamental characteristics of clay particles, small clay assemblages, and hard shale.

Samples from various depositional environments depicting individual clay particles have been studied. Traditionally, researchers believed that smectite was characterized by a platy fluffy morphology. Through WETEM, it was discovered that different shapes (spherical-like, platy, elongated rod-like, needle, triangular, and polygon shape) of nano-size clay particles exist. Recent studies revealed that almost all of smectite particles are < 500 nm in equivalent diameter with a mode between 30 to 125 nm and a mean between 90 to 180 nm regardless of the clay fraction obtained by settling method. The thinnest individual smectite particles range 4 to 10 nm with the mode of 5 to 6 nm. This thickness corresponds to  $\sim$  4 to 5 unit cell layers and is unique to the development of smectitic clay microstructure.

TEM observation of clay particles/assemblies in marine sediments from the Mississippi Delta, Middle-America Trench, Pacific Basin, California Continental Slope, and Baltic Sea reveals many characteristics of the depositional environment. Clay aggregates observed in both conventional TEM, WETEM, and SEM showed many interesting features. With advanced hard- and soft-ware, surface 3-D images and 3-D tomography can be constructed by images obtained from SEM, TEM and FIB. Using advanced FIB techniques and 3D tomography software, microstructure (such as particle orientation) of highly compacted shale, particle to particle relationships, and micropores can be clearly observed and volume fraction of pore space or solids and porosity can thus be calculated. The application of 3-D analysis of clays and its assembly promises to increase our understanding and improve the application of clays.

Depositional environment, pore water geochemistry, and biological/organic interactions play important roles in the formation and diagenesis of clay fabric and ultimately the fundamental sediment properties. Investigation of clay assembly and its microstructure synthesized in the laboratory contributes to the understanding of the developmental history of clay microstructure in natural environments, and also provides useful and important applications in materials science/engineering and related disciplines.

## Hydration of FEBEX-bentonite observed by Environmental Scanning Electron (ESEM)

Frank Friedrich<sup>1,\*</sup>, Dieter Schild<sup>1</sup>, Peter G. Weidler<sup>2</sup> and Thorsten Schäfer<sup>1</sup>

<sup>1</sup> Karlsruhe Institute of Technology, Institute for Nuclear Waste Disposal (INE), Hermann-von-Helmholtz-Platz 1, D-76344 Eggenstein-Leopoldshafen, Germany, \*frank.friedrich@kit.edu

<sup>2</sup> Karlsruhe Institute of Technology, Institute for Functional Interfaces (IFG), Hermann-von-Helmholtz-Platz 1, D-76344 Eggenstein-Leopoldshafen, Germany

An environmental scanning electron microscope was used to study the water sorption of FEBEX bentonite as a function of relative humidity (RH). The measured hydration isotherms had an exponential shape with strong swelling of the clay particles occurring especially at high RH above 85%. The two branches of the isotherm did not overlap and a hysteresis of type H3 was observed, which is typical for plate-like particles with slit shaped pores. Obviously the dehydration was hindered, which can be attributed mainly to geometrical factors. Hydration experiments with cation exchanged bentonite samples showed that the hydration behavior and swelling of the bentonite was controlled by the interlayer cations. In this bentonite the hydration behavior of the Na- and Sr-forms was very similar, but the Sr-form showed a significantly higher swelling already at low relative humidities. This can be explained by the much higher hydration energy of strontium in comparison to monovalent cations and thus its higher hydration force within the clay interlayer.

*Poster also presented at the workshop: 'Filling the gaps – from microscopic pore structures to transport properties in shales' held on Sunday 5<sup>th</sup> July 2015.*

## Comparison of methods for the determination of the pore system of a potential German gas shale

S. Kaufhold<sup>1</sup>, G. Grathoff<sup>2</sup>, M. Halisch<sup>3</sup>, M. Plötze<sup>4</sup>, J. Kus<sup>1</sup>, K. Ufer<sup>1</sup>, R. Dohrmann<sup>5</sup>, S. Ladage<sup>1</sup> and Ch. Ostertag-Henning<sup>1</sup>

<sup>1</sup>BGR, Bundesanstalt für Geowissenschaften und Rohstoffe, Stilleweg 2, D-30655 Hannover, Germany

<sup>2</sup>Ernst-Moritz-Arndt Universität Greifswald, Institute for Geography and Geology, Friedrich-Ludwig-Jahn-Str. 17a, D-17487 Greifswald, Germany

<sup>3</sup>Leibniz Institute for Applied Geophysics (LIAG), Stilleweg 2, 30655 Hannover, Germany

<sup>4</sup>ETH Zurich, Institute for Geotechnical Engineering, 8093 Zurich, Switzerland

<sup>5</sup>LBEG, Landesamt für Bergbau, Energie und Geologie, Stilleweg 2, D-30655 Hannover, Germany

**Keywords:** gas shale,  $\mu$ -CT, pore size distribution, FIB, Hg-intrusion, Posidonia shale

The aim of the present study was to investigate the porosity of the Posidonia shale as a potential gas shale and to compare the results with data published on gas shales known to be productive. The characterization of the porosity of clays and shales, however, is still an analytical challenge. Different methods were investigated based on a comparison of four different Posidonia shales with different maturity. Both direct microscopical methods, as well as indirect methods based on gas adsorption or Hg intrusion, were applied. Most of the pores of clays and shales were too small to be detected by any of the existing direct methods. About 80 % of the porosity was below 30 nm. The Posidonia shales, as with most shales, are dominated by mesoporosity (ranging from 20 – 50 nm<sup>3</sup>/g). The mesopore peak representing the average pore diameters could be resolved by Hg-intrusion and was found to decrease with increasing maturity, which may be explained by increased compaction and/or temperature. This relation, if applicable for the entire Posidonia shale at all, may be restricted to one sedimentary system (as a basin or a sequence) because other shales did not follow it. The results of the indirect methods (except for CO<sub>2</sub>-microporosity of course) were comparable which could be explained by the low macroporosity. The most important question concerning shale gas production and porosity relates to the diameter needed to provide gas migration. Natural gas in micropores may be bound too strongly to liberate it without low-pressure/vacuum. For gas production either meso- or macropores may be important. Notably all methods used for porosity characterization were performed on dry samples. A nm-scaled connectivity determined at an illite/smectite interfaced pore is not supposed to provide a gas pathway in the water saturated state. Therefore, the prediction of the gas production potential from porosity measurements is not possible yet. However, considering the organic carbon content, vitrinite reflection, and the comparison of the porosity with famous gas shales indicates a potential of the Posidonia shale which, of course, has to be proven by shale gas production tests.

*Poster also presented at the workshop: 'Filling the gaps – from microscopic pore structures to transport properties in shales' held on Sunday 5<sup>th</sup> July 2015.*

## Microstructural insights in petrophysical characteristics of indurated clays

P. Marschall<sup>1,\*</sup>, L. Keller<sup>2</sup>, S.B. Giger<sup>1</sup> and J. Becker<sup>1</sup>

<sup>1</sup> National Cooperative for the Disposal of Radioactive Waste, 5430 Wettingen, Switzerland

<sup>2</sup> ZHAW/ICP, Wildbachstrasse 21, 8401 Winterthur, Switzerland

\*paul.marschall@nagra.ch

Core samples from the Opalinus Clay, an indurated clay formation of Jurassic age, were subjected to comprehensive microstructural investigations, comprising Transmission Electron Microscopy (TEM), Focused Ion Beam nanotomography (FIB-nt) and Micro-X-ray tomography (Micro CT). Digital representations of the microstructure were derived from the tomographic images by segmentation and 3-D reconstruction of the geomaterial on a grid of regular voxel elements with a typical edge length as low as 10 nm and a maximum size in the order of 1000<sup>3</sup> voxels. Pertinent geotechnical properties were derived on the microscopic scale using state-of-the-art image processing procedures. The results were compared with results from geotechnical laboratory characterisation methods such as mercury intrusion porosimetry, BET, XRD and triaxial testing. Excellent agreement was achieved between microscopic and macroscopic characterisation methods. Furthermore, the macroscopic (poro-elastic) deformation behaviour of the Opalinus Clay was reproduced fairly well by geomechanical modelling on the microscopic scale, including the cross-anisotropic stiffness of the rock mass. In addition, new insight was gained with regard to the role of small mesopores (2 – 10 nm), essentially controlling the macroscopic deformation behaviour of indurated clays.

**Keywords:** Claystones, shales, Opalinus Clay, microstructural characterization, FIB, X-ray tomography, TEM, petrophysical properties, property scaling

*Poster also presented at the workshop: 'Filling the gaps – from microscopic pore structures to transport properties in shales' held on Sunday 5<sup>th</sup> July 2015.*

## Clay-based modelling approach for diffusion and sorption in the argillaceous rock from the Horonobe URL: application for Ni(II), Am(III) AND Se(IV)

Yukio Tachi\*, Tadahiro Suyama, Kenji Yotsuji, Yasuo Ishii and Hiroaki Takahashi  
Japan Atomic Energy Agency, Muramatsu 4-33, Tokai, Ibaraki, 319-1194, Japan  
\*tachi.yukio@jaea.go.jp

Sorption and diffusion of radionuclides in argillaceous rocks are key processes in safe geological disposal. The diffusion and sorption behavior of Ni(II), Am(III) and Se(IV) in mudstone from the Horonobe URL were investigated by experimental and modelling approaches. Effective diffusivities obtained by the through-diffusion experiments were in the sequence of  $Cs^+ > Ni^{2+} \approx HTO > I^- > Se (SeO_4^{2-}) > Am (Am(CO_3)_2^-)$  by comparison with the previous paper. The distribution coefficient values were consistent with those obtained by batch sorption tests. These results were interpreted by a clay-based modelling approach that coupled the thermodynamic sorption model, assuming key contributions of clays (smectite and illite), and the diffusion model, assuming the electric double layer theory and the simplified pore model with size distribution. This clay-based model could provide reasonable account of observed trends and could be basically applicable for various radionuclides.

**Keywords:** Diffusion, Sorption, Horonobe URL, Mudstone, Clay-based model

*Poster also presented at the workshop: 'Filling the gaps – from microscopic pore structures to transport properties in shales' held on Sunday 5<sup>th</sup> July 2015.*



## Diffusion modelling of multiple pore structure in compacted bentonite

Kenji Yotsuji<sup>1,\*</sup>, Yukio Tachi<sup>1</sup> and Takahiro Ohkubo<sup>2</sup>

<sup>1</sup>Japan Atomic Energy Agency, 4-33, Muramatsu, Tokai-mura, Ibaraki, 319-1194, Japan

<sup>2</sup>Chiba University, 1-33, Yayoi-cho, Inage-ku, Chiba, 263-8522 Japan

\*yotsuji.kenji@jaea.go.jp

The integrated sorption and diffusion (ISD) model has been developed to quantify radionuclide transport in compacted bentonite. The current ISD model, based on averaged pore aperture and the Gouy-Chapman electric double layer (EDL) theory, can quantitatively account for diffusion of monovalent cations and anions under a wide range of conditions (e.g., salinity, bentonite density). In this paper, to improve the applicability of the model, the modified ISD model considered multiple pore structure including interlayer and intraparticle pores. The model was developed and tested through the application of the current ISD model to multiple pore structure. In conclusion, even if we only consider inter-particle pore and averaged inter-layer pore in a heterogeneous pore model, the effects of heterogeneous pore structure are reflected well in the diffusion model.

**Keywords:** Compacted bentonite, Radionuclide migration, Diffusion model, Multiple pore model

*Poster also presented at the workshop: 'Filling the gaps – from microscopic pore structures to transport properties in shales' held on Sunday 5<sup>th</sup> July 2015.*

## The internal architecture and permeability structures of faults in shale formations

Pierre Dick<sup>1</sup>, Charles Wittebroodt<sup>1</sup>, Christelle Courbet<sup>1</sup>, Juuso Sammaljärvi<sup>2</sup>, Imène Estève<sup>3</sup>, Jean-Michel Matray<sup>1</sup>,  
Marja Siitari-Kauppi<sup>2</sup>, Miko Voutilainen<sup>2</sup> and Alexandre Dauzères<sup>1</sup>

<sup>1</sup> IRSN- Institut de Radioprotection et de Sûreté Nucléaire, BP 17, F-92262 Fontenay-aux-Roses, France

<sup>2</sup> Laboratory of Radiochemistry, Department of Chemistry, FI-00014 University of Helsinki, Finland

<sup>3</sup> Institut de Minéralogie et de Physique des Milieux Condensés (IMPMC), UMR 7590 CNRS-UPMC/Paris VI-IRD, Case  
115, 4 place Jussieu, 75252 Paris Cedex 05, France

\*pierre.dick@irsn.fr

This study focuses on the structural evolution within brittle to ductile shear zone in order to understand permeability enhancement and sealing processes affecting a strike-slip fault system from the Tournemire Underground Research Laboratory (URL), southern France. A combination of quantitative field measurements, laboratory and in situ experiments were used to estimate fluid flow properties of a fractured shale formation. Results indicate that microfractures govern the matrix porosity in the damage zone and exert an increasingly dominant role on fluid flow along the fault damage-core boundary. Such outcomes are important for the long-term performance assessment of radioactive waste repositories in shale formations and could be used to assess CO<sub>2</sub> storage security or the integrity of caprocks and reservoir capacity.

**Keywords:** Porosity, permeability, shale, in situ experiment, fault architecture, gouge

*Poster also presented at the workshop: 'Filling the gaps – from microscopic pore structures to transport properties in shales' held on Sunday 5<sup>th</sup> July 2015.*

## **Porosity evolution in the chalk: an example from the chalk-type source rocks of the outer Carpathians (Poland)**

Katarzyna Górniak

AGH University of Science and Technology, Faculty of Geology, Geophysics and Environmental Protection,  
al. Mickiewicza 30, Kraków, 30-059, Poland; \*gorniak@agh.edu.pl

A pore space evolution study by using high-resolution petrography techniques (FESEM/BS/CCI) was conducted on the Oligocene dirty chalk-type source rocks (Grybów Marls). These rocks are products of re-deposition of shelf sediments into deeper parts of the basin during the closure stage of the Outer Carpathian basin. The results show that the starting sediments for these rocks were clay-depleted, at least periodically and locally. Consequently, their diagenetic history was primarily similar in the way that the chalk was altered, and just after re-deposition the course of diagenesis was controlled by clay content. The tectonically-induced micro-cracks were mostly created in foraminiferal tests, because the majority of coccolith shields were protected against crushing due to the presence of clay cement, which, by stress, underwent the re-organization forming less porous lamellar aggregates. The timing of diagenetic processes revealed by microscopic images presented in this paper point out that the origin of clay and eogenetic overgrowth cementation influenced the pathway of burial diagenesis and pore space evolution in the dirty chalk.

**Keywords:** Dirty chalk, Diagenesis, Pore space evolution, Grybów Marls, Outer Carpathians

*Poster also presented at the workshop: 'Filling the gaps – from microscopic pore structures to transport properties in shales' held on Sunday 5<sup>th</sup> July 2015.*

## Clay mineralogy and pore-scale characterization during and after CO<sub>2</sub> flow and saturation in the Mt. Simon Sandstone, Illinois Basin, USA

Jared T. Freiburg<sup>1,2</sup>, Peter M. Berger<sup>2</sup>, Lois E. Yoksoulia<sup>2</sup>, Shane K. Butler<sup>2</sup> and Georg H. Grathoff<sup>1</sup>

<sup>1</sup>Institut für Geographie und Geologie, Ernst-Moritz-Arndt Universität Greifswald, Germany, freiburg@illinois.edu

<sup>2</sup>Illinois State Geological Survey, University of Illinois at Urbana-Champaign, Illinois, USA

The Cambrian-age Lower Mt. Simon Sandstone serves as the reservoir for the Illinois Basin - Decatur Project (IBDP), a 1 million tonne carbon capture and storage demonstration project located in Decatur, Illinois, USA. The Lower Mt. Simon Sandstone is dominantly composed of fluvial braided river deposited, moderately sorted, fine- to coarse-grained sub-arkose arenite. Reservoir properties include porosity up to 27% and permeability up to 1 Darcy. Both primary intergranular porosity and secondary dissolution porosity are prevalent. Secondary porosity is primarily the result of potassium feldspar dissolution and alteration to illite. Authigenic illite is the most prevalent clay mineral in the Mt. Simon and most commonly forms a thin coating over detrital quartz grains. This clay coating acted as a barrier to the early authigenic quartz precipitation that is abundant throughout the overlying Middle and Upper Mt. Simon. However, in the Lower Mt. Simon Sandstone, clay minerals variably clog pore throats decreasing reservoir permeability.

Previous laboratory-scale experiments helped understand the short-term geochemical and mineralogical reactions between synthetic brine, carbon dioxide (CO<sub>2</sub>), and the Mt. Simon Sandstone at reservoir temperature and pressure. Post-reaction analysis of rock samples using polarizing light and scanning electron microscopy (SEM) showed evidence of clay mineral dissolution and increased porosity. Clay mineral dissolution is further supported by post-experimental brine chemistry and geochemical modeling. However, the variability of mineralogy, porosity, and pore connectivity in thin-sections and the inability of traditional analytical methodology (polarized light microscopy, SEM, X-ray diffraction, and inductively coupled plasma mass spectrometry) to detect small changes pose a problem for quantifying diagenetic changes as a result of CO<sub>2</sub>-brine-rock interaction. To monitor and quantify in-situ changes to the rock resulting from CO<sub>2</sub> interaction, X-ray microtomography (micro-CT) was conducted. Micro-CT produced three-dimensional pore-scale maps of three Mt. Simon samples from the same reservoir facies. Map images include: (1) sample before CO<sub>2</sub> interaction; (2) sample during a laboratory CO<sub>2</sub> flow through experiment at reservoir pressure and temperature; and (3) sample extracted from the CO<sub>2</sub> reservoir approximately three years post-injection. Preliminary results suggest an increase in reservoir porosity and permeability as a result of clay mineral dissolution. Understanding the diagenetic effects of CO<sub>2</sub> injection in the Mt. Simon Sandstone is necessary for modeling the long-term implications of CO<sub>2</sub> storage. Furthermore, pore-scale mapping is essential to completing competent reservoir-scale models.

## Hydration of smectite as a function of temperature and humidity: examples from natural fault rocks

Anja M. Schleicher<sup>1,2</sup> and Ben A. van der Pluijm<sup>2</sup>

<sup>1</sup>Helmholtz-Zentrum Potsdam, GFZ Deutsches GeoForschungsZentrum, Telegrafenberg, D-14473 Potsdam, Germany, anja.schleicher@gfz-potsdam.de

<sup>2</sup>Department of Earth and Environmental Sciences, University of Michigan, 1100 North University Ave, Ann Arbor, MI 48109, USA

The hydration behavior of smectite clay minerals provides information about alteration processes and the temperature history in active, near-surface fault zones. We examined mudrock samples from different drill cores taken during IODP (International Ocean Discovery Program) Expedition 338/348 in the Nankai Trough subduction zone (Japan), and during Expedition 343 in the Japan Trench. Using both a humidity chamber and a high-temperature stage attached to an X-ray diffractometer, we examined the swelling characteristics of smectite formed between ~800-1600 mbsf. With the humidity chamber, we assessed the absorption of water onto and/or into the crystal structure of smectite by in-situ analysis of the hydration state at controlled humidity and temperature conditions. Based on experiments on the clay-rich fault gouge from the Nankai Trough accretionary prism, we showed that (i) smectite is abundant down to ~1600 mbsf, (ii) contains constant 2-3 water layers at temperatures of ~50°C and a relative humidity (RH) between 30-90% (the depth where the rocks were situated), and (iii) swelling is also not significantly affected up to 75°C/90°C with changing RH. This detailed characterization of the hydration state of smectite in its original setting is critical for the understanding of clay-fluid interaction and mechanical properties during crustal displacement. Using the high-temperature stage, we examined the hydration behavior of smectite during rapid (5 minutes) and extended (5 hours) heating sequences in the mudrock samples from a fault zone in the Japan Trench. Measurements were taken at 25°C pre-heating, at increasing maximum temperatures in the range between 50-220°C, and 25°C post-heating. We observe that (i) pelagic-sourced smectite is the most abundant clay mineral that is incorporated into the fault zone at ~820 mbsf, (ii) both slow and fast heating causes reduction of water interlayers in smectite between 50-200°C, (iii) smectite recovers more quickly to the original hydration state after rapid heating, and (iv) non-recoverable collapse of all smectite occurs at ~200°C. Our results show that the characterization of the hydration state of smectite in natural conditions is critical for our understanding of clay-fluid interaction processes. Beyond fault zone dynamics, our work also has implications for (nuclear) waste disposal, showing that temperature and humidity of smectitic clay minerals need careful study for storage site considerations.

## Characterizing the contents of nanopores in black shale using Nano-secondary ion mass spectrometry

Lynda B. Williams<sup>1</sup> and Maitrayee Bose<sup>2</sup>

<sup>1</sup>School of Earth & Space Exploration, Arizona State University, Tempe, AZ 85287-1404

<sup>2</sup>Dept. of Chemistry & Biochemistry, Arizona State University, Tempe, AZ 85287-1604

lynda.williams@asu.edu

Judicious use of energy resources requires decisions regarding optimal resource recovery with minimal environmental impact. Identifying productive intervals of black shale can be enhanced by characterization of the connectivity of nanopores that not only serve as channels for migrating oil and gas, but may also be filled with reserves of mature 'live-C'. To evaluate the contents of nanopores we studied Mississippian black shale from the Bakken Fm (North Dakota, USA) using a Cameca NanoSIMS 50L secondary ion mass spectrometer. Core samples were collected from the lower Bakken shale where total organic carbon is 10-20%.

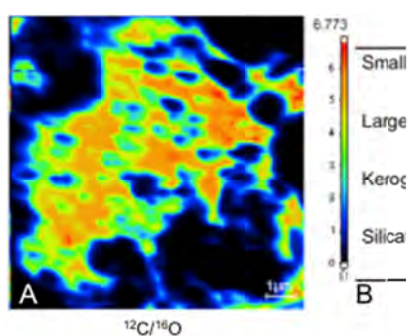


Fig. 1 (A) NanoSIMS map ( $10\ \mu\text{m}^2$ ) and (B) data summary of O/C and H/C composition in nanopores, kerogen and silicate in Bakken shale ( $R_o$  3%).

Samples were Ar-ion polished to reveal nanopores 2-200nm in diameter in kerogen. Imaging by high resolution scanning electron microscopy shows no pores in immature kerogen ( $R_o < 0.5\%$ ), but pores develop in mature kerogen ( $R_o$  1.0) and increase in diameter in overmature kerogen ( $R_o \sim 3.0\%$ ) as hydrocarbons leave the host organic matrix. NanoSIMS imaging measured C-H-O distributions in the kerogen vs. nanopores showing the different O/C and H/C ratios (Fig. 1) that could potentially be used as a hydrocarbon correlation tool. However, these major elements may not vary significantly between source rocks. Therefore, we focused on the abundance of trace elements boron and lithium that vary significantly with organic source maturity.

B and Li exist in kerogen because these trace elements are incorporated in the primary material (plant, plankton) that forms kerogen through burial. With increasing thermal maturity B and Li are released, increasing their concentrations (100's ppm) in oilfield brines (Collins, 1975). The thermal conditions of B and Li release from kerogen have not been documented, but their elevated concentration in oilfield brines suggests generation coincident with hydrocarbons. Kerogen is normally isolated from shale using concentrated HF-HCl to dissolve silicates, leaving the concentrated organic fraction. However, we found that this treatment also releases B and Li. NanoSIMS direct measurements on kerogen at high spatial resolution, avoiding silicates, gives higher ratios ( $B/C = 0.3207$ ;  $Li/C = 1.1564$ ) than measured in chemically isolated kerogen ( $B/C = 0.0022$ ;  $Li/C = 0.0555$ ). With increasing thermal maturity Bakken kerogen shows decreasing B-content (200 -100 ppm), while the clay increases in B (140-260 ppm), and extracted bitumen shows the highest B content (450 ppm) in mature shale ( $R_o$  1.0%). Li- shows similar trends, but lower Li contents (<100 ppm). Therefore, elevated concentrations of B and Li in shale nanopores may help to identify optimal targets for enhanced oil recovery.

Collins, A. G. (1975). *Geochemistry of Oilfield Waters*. New York, Elsevier. pp. 496.

## Edge structures of montmorillonite: A density functional theory study

Hiroshi Sakuma<sup>1</sup>, Yukio Tachi<sup>2</sup>, Kenji Yotsuji<sup>2</sup> and Katsuyuki Kawamura<sup>3</sup>

<sup>1</sup>National Institute for Materials Science, 1-1 Namiki, Tsukuba, Ibaraki 3050044, JAPAN

E-mail: sakuma.hiroshi@nims.go.jp

<sup>2</sup>Japan Atomic Energy Agency, 4-33, Muramatsu, Tokai-mura, Ibaraki, 319-1194, Japan

<sup>3</sup>Okayama University, 3-1-1, Tsushimanaka, Kita-ku, Okayama 7008530, Japan

Clay minerals are good adsorbents of many toxic elements and molecules in the natural environment, because of their large surface areas and their high affinity for organic and inorganic materials. Adsorption occurs on interlayer, surface and edge planes of layered clay minerals. The adsorption sites of ions and molecules on the basal planes can be estimated by experiments and computer simulations based on the simple surface structure. However, the adsorption of ions and molecules on the edge planes of clay minerals is poorly understood due to the absence of established model of the edge structures. Analysis of the edge structures based on crystal growth theory [1] proposed two plausible structures for dioctahedral clay minerals. Stability of edge planes of pyrophyllite based on the study was evaluated by the density functional theory (DFT) [2].

In this study, the edge structures of montmorillonite were examined by the first-principles calculations based on the DFT. One of calculated edges is shown in Figure 1. The effect of isomorphous substitution, layer charge, and positions of interlayer cations was evaluated for four different edge planes by calculating the surface energy. The acidity constant of the edges were calculated by an empirical method. We will discuss possible adsorption sites of cations on these edges.

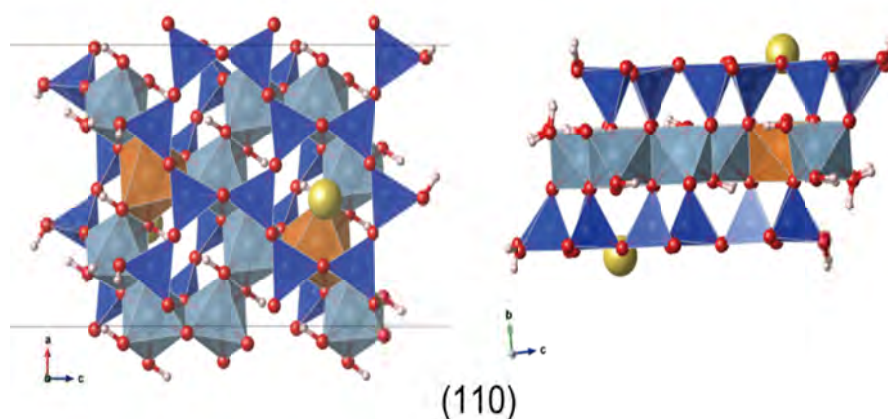


Figure 1. Edge structure of (110) plane of montmorillonite (Left: top view, right: side view). Edge planes are located at left and right.

[1] G.N. White and L.W. Zelazny, Analysis and implications of the edge structure of dioctahedral phyllosilicates, *Clays Clay Minerals* 1988, **36**, 141-146.

[2] S.V. Churakov, Ab initio study of sorption on pyrophyllite: Structure and acidity of the edge sites, *J. Phys. Chem. B* 2006, **110**, 4135-4146.

\*This study was partly conducted as “The project for validating assessment methodology in geological disposal system” funded by the Ministry of Economy, Trade and Industry of Japan

## Lithofacies and depositional environment of black shale in the Dniepr-Donets basin (Ukraine)

Eva Wegerer

University of Leoben, Chair of Petroleum Geology, Peter-Tunner-Strasse 5, A-8700 Leoben, eva.wegerer@unileoben.ac.at

A correlation between the variability of the lithofacial composition of Devonian to Upper Carbonian black shales and the depositional conditions of the Dniepr-Donets Basin took place. The mineralogical content, the amount and type of clay minerals, the percentage of clay minerals in relation to clay-size silica, carbonate particles and accessory components (e.g. pyrite and siderite) of the organic-matter-rich fine-grained rocks reflect the formation conditions of the basin. 107 bore core samples, especially originating from the area of the Srebren Depression, were determined by qualitative and quantitative XRD-analyses. The lithofacial classification by means of clay minerals took place primarily by mica-group minerals, kaolinite-group minerals, chlorites and expanded clay minerals. The results are validated by other investigation methods (e.g. calcite equivalent).

The Dniepr-Donets Basin represents a Devonian rift-structure within the East European Craton bounded by the Voronezh high of the Russian Craton (NE), the Ukrainian shield (SW), the Pripjat basin of Belarus which is separated by the Brag-Loev uplift (NW) and extends into the deformed Donbas fold belt (SE). The basement dips south-eastward with a maximum basin fill of about 18 km thickness. The late Palaeozoic to Cenozoic sedimentary successions comprise a Middle-Upper Devonian pre-rift platform, Upper Devonian syn-rift sediments characterized by a succession of volcanic rocks, sandstone, shale, carbonates and evaporites. The Carboniferous succession reflects fluvial and shallow marine depositions of transgressive and regressive cycles. The Permian period is characterized by salt-tectonics. Triassic to Cenozoic sediments built up the post-rift platform.

Devonian to Lower/Middle Carboniferous black shales reflect the positional environment related to the syn- and post-rift phases. In the northwestern area of the Srebren Depression the shale-cycles of the Devonian facies are characterized by a clay mineral content of approximately 50 to 85 %, primarily mica-group clays ( $2M_1$ ,  $1Md$ ,  $1M$ ) with an increasing content of glauconite in the lower part of the succession. The feldspar proportion, mainly plagioclase, ranges up to 20 %. Farther southeast the lower shale horizon of the Devonian sequence consists of approximately 50 % carbonate, traces of anhydrite and illite as predominate clay component. The transition to the post-rift phase in the Tournaisian stage is characterized by a high increase of kaolinite proportion. In the central part of the Srebren Depression the Tournaisian shales show an increasing amount of pyrite (potentially bacterial sulfate reduction) and siderite. The stratigraphic distribution of black shales in the Tournaisian to Visean succession is mainly controlled by eustatic sea-level rises and deeper marine conditions. Kaolinite-group minerals represent the main clay-components, followed by Mica-group clays (mainly  $2M_1$ ,  $1Md$ ). The percentage of calcite in the Tournaisian and early and late Visean cycles of sedimentation can be attributed to reef-bioherm bodies. The Serpukhovian succession is related to shallow non-marine environments with an increased occurrence of chlorite-group minerals and expanded clay minerals. Intercalations of coal appear in the Lower Serpukhovian shales.

Sachsenhofer R.F., Privalov V.I., Izart A., Elie M., Kortensky J., Panova E.A., Sotirov A., Zhykalyak, M.V., 2003. Petrography and geochemistry of Carboniferous coal seams in the Donets Basin (Ukraine): implications for paleoecology. *Int. J. Coal. Geol.* 55, 225-259.

Shymanovskyy V.A., Sachsenhofer R.F., Izart A., Li Y., 2004. Modelling of the thermal evolution of the northwestern Dniepr-Donets Basin (Ukraine). *Tectonophysics* 381, 61-79.

Ulmishek, G.F., Bogino, V.A., Keller, M.B., Poznyakevich, Z.L., 1994. Structure, stratigraphy, and petroleum geology of the Pripjat and Dniepr-Donets basins, Byelarus and Ukraine, in Landon, S.M., ed., *Interior rift basins: American Association of Petroleum Geologists Memoir* 59, 125-156.



## Microscale X-ray analysis of metal uptake by argillaceous rocks

Felician Gergely<sup>1</sup>, Janos Osan<sup>1</sup>, Annamaria Keri<sup>1,2</sup>, Rainer Dähn<sup>2</sup>, Margit Fabian<sup>1</sup> and Szabina Torok<sup>1</sup>

<sup>1</sup>HAS Centre for Energy Research, (MTA EK), H-1525, Budapest P.O. Box: 49, Budapest Hungary

<sup>2</sup>Laboratory for Waste Management (LES), Paul Scherrer Institute, 5232 Villigen PSI, Switzerland

Email address of the presenting author: gergely.felician@energia.mta.hu

The final disposal of high-level radioactive waste (HLW) was investigated in our research where the possible host rock formation was the Hungarian Boda Claystone Formation (BCF). In Hungary, two geological sites (Gorica Block and Boda Block) of the Boda Claystone Formation (BCF) have been selected for the study of potential host rocks for HLW.

In order to complete macroscopic and molecular scale sorption results, microspectrometry measurements are indispensable to characterize the radionuclide retention property of the selected possible host clay rock formations. The focus of the investigation was on the reactions between the radioactive cations (Cs(I), Ni(II), Nd(III) and U(VI)) and surface of the rock forming mineral phases. Inactive Cs(I), Ni(II), Nd(III) and natural U(VI) were selected for the experiments chemically representing key radionuclides. The loaded thin sections for the microspectrometry measurements were prepared on high-purity silicon wafers from geochemically characterized cores of Boda Claystone Formation, Hungary. Samples were subjected to 24-72-hour sorption experiments with one ion of interest added. The samples were investigated by laboratory scale and synchrotron radiation (SR) microscopic X-ray fluorescence ( $\mu$ -XRF) and electron probe X-ray microanalysis (EPMA) techniques. The laboratory  $\mu$ -XRF system is suitable to conduct point measurements, recording two-dimensional elemental maps at 20–100  $\mu$ m resolution. The obtained elemental maps indicate a correlation of Cs, Ni and with Fe- and K-rich regions, already indicating that the uptake is controlled to the clayey matrix. The laboratory scale  $\mu$ -XRF detection limits of caesium and nickel found to be sufficient to obtain information about the behaviour of these radionuclides. For Nd and U the laboratory scale  $\mu$ -XRF system is a suitable pre-selection tool for SR measurements. The solubility limits of these elements allowed a very low load on the thin sections requiring high sensitivity SR  $\mu$ -XRF. [1] SR  $\mu$ -XRF measurements were performed on thin sections subjected to uptake experiments using 1-5  $\mu$ m spatial resolution. EPMA was found to be a valuable tool for accurate microanalysis aiming major elemental composition of thin rock sections, complementing the laboratory and synchrotron based  $\mu$ -XRF investigations.

When multivariate data analysis is used for the processing of elemental maps, significant information can be obtained in most cases that can be related to the uptake of element by a particular mineral phase. U and Nd was found to be bound not only to the clayey matrix, but the cavity filling carbonate minerals also played important role in the uptake. [2,3] The uptake capacity of the different mineral phases could be quantified with additional mineralogical information [2] The multivariate approach based on  $\mu$ -XRF to identify the minerals was validated using microscopic X-ray diffraction.

[1] C. Walther, M.A. Denecke. Chemical Reviews 113 (2013) 995-1015.

[2] J. Osán, A. Kéri, D. Breitner, M. Fábrián, R. Dähn, R. Simon, S. Török. Spectrochimica Acta Part B 91 (2014) 12–23.

[3] D. Breitner, J. Osán, M. Fábrián, P. Zagyvai, C. Szabó, R. Dähn, M. Marques Fernandes, I.E. Sajó, Z. Máthé, S. Török. Submitted to Environmental Earth Sciences

## Adsorption and desorption of zearalenone by commercial and organophilic clays

Sumio Aisawa<sup>1</sup>, Hidetoshi Hirahara<sup>1</sup>, Shota Endo<sup>1</sup>, Mai Sekine<sup>1</sup>, Eiichi Narita<sup>1</sup>, Kazunori Sakao<sup>2</sup> and Noriyuki Takahashi<sup>2</sup>

<sup>1</sup> Department of Frontier Materials and Function Engineering,

Graduate School of Engineering, Iwate University, 4-3-5 Ueda, Morioka 020-8551, Japan

<sup>2</sup> R & D Department, Mizusawa Industrial Chemicals, Ltd., 1-1 Mizusawa-cho, Tainai 959-2638, Japan

Animal feeds are made from several grain sources such as wheat, barley, rice and corn *etc.*; however, they may be contaminated by various mycotoxins. Zearalenone (ZEN) is one of the mycotoxins produced by species of *Fusarium* and the major toxicity of ZEN is its estrogenic effect on farm animals. Various feed additives contain clays, activated carbon, and yeast that adsorb and remove of mycotoxins from animal feeds. We have previously reported the adsorption and desorption behavior of ZEN by commercial clay (CC) from ZEN solutions<sup>1,2</sup>. In this study, we report the adsorption and desorption behavior of ZEN by various CCs and synthesized organophilic CCs to develop high-performance feed additives.

The CC was provided by Mizusawa Industrial Chemicals, Ltd. for this study. The CC is mainly composed of montmorillonite and removes aflatoxin. The organophilic CC was synthesized by the ion-exchange method, whereby 200 cm<sup>3</sup> of alkyl cations solution, cetyltrimethyl-ammonium chloride (CTAC) or cetyltributylphosphonium bromide (CTPB), were placed in Erlenmeyer flask together with 0.5 g of CC, stirred at 25°C for 24 h. Adsorption experiments with ZEN involved agitating 125 mg of clays with 50 cm<sup>3</sup> of 1.0–10 ppm ZEN solution at 25°C for 2 h. ZEN solutions were separated by using a PTFE membrane filter (pore size 0.2 μm). The residual concentration of supernatant was measured by UV-Vis absorbance at 236 nm. ZEN adsorption was determined by the difference between the initial and residual concentrations of ZEN solutions.

From the results of XRD patterns, the  $d_{001}$ -value of organophilic CC was 1.97 nm for the CTA/CC and 2.76 nm for the CTP/CC as compared to the original CC which  $d_{001}$ -value is 1.57 nm. Both alkyl cations were intercalated into the interlayer space of CC, suggesting that the interlayer properties of the CC were modified from hydrophilic to hydrophobic. The amount of ZEN adsorption was 0.20 mg/g for the CC and 1.98 mg/g for the CTA/CC and CTP/CC, respectively. These results implied that ZEN adsorption for the CC was influenced by the hydrophobic interaction between ZEN and intercalated alkyl cations. The influence of thermal treatment temperature of CC on the adsorption of ZEN increased with increasing thermal treatment temperature. Maximum ZEN adsorption was 1.86 mg/g for the thermally treated CC. These adsorption properties indicated that the thermally treated CC has a hydrophobic phyllosilicate surface. We also found that the solvent, composed of a mixture of water/AcCN to dissolve ZEN, greatly affected ZEN adsorption. The CCs exhibited increased adsorption capacity when using a low proportion of the water/AcCN solvent.

1) S. Aisawa *et al.*, The 2nd Asian Clay Conference, Abstract Book, pp. 103-104 (2012)

2) T. Sasaki *et al.*, *Mycotoxin Res.*, **30**, 33-41 (2014)

## Clay mineral composition and origin of Central Yellow Sea Mud (CYSM) in the Yellow Sea

Hyen Goo Cho<sup>1</sup>, Kyeong Yoon Kwak<sup>1</sup>, Hunsoo Choi<sup>2</sup> and Soo-Jae Lee<sup>3</sup>

<sup>1</sup>Department of Earth and Environmental Sciences and Research Institute of Natural Science, Gyeongsang National University, Jinju 660-701, Korea, hgcho@gnu.ac.kr

<sup>2</sup>Petroleum and Marine Research Division, Korea Institute of Geoscience and Mineral Resources, Daejeon 305-350, Korea

<sup>3</sup>Environmental Policy Research Group, Korea Environment Institute, 370 Sicheong-daero, Sejong 339-007, Korea

The Central Yellow Sea Mud (CYSM), located in the Yellow Sea, is mainly composed of clayey silt and silty clay. The thickness of this mud is less than 5 m or as thick as 16 m and typically uniform. In this study, we investigated the relative composition of four major clay minerals and discuss the origin of fine-grained sediments in the CYSM by synoptic maps, using 67 surface sediments collected through KIOST (Korea Institute of Ocean Science and Technology) cruise. The clay mineral assemblages of the CYSM sediments are composed of illite (avg. 67.5%), chlorite (avg. 17.7%), kaolinite (avg. 12.6%), and smectite (avg. 2.2%). According to the distribution pattern, CYSM is divided into two zones: the central and marginal zones. The central zone is composed of higher content of illite and lower content of chlorite, kaolinite and smectite, but the marginal zone is composed of lower amounts of illite and more chlorite, kaolinite and smectite. Sediments distributed in the marginal zone of CYSM are mainly from the modern and old Huanghe, while sediments in central zone of CYSM are a complex mixture from the Changjiang and Korean rivers (Shi et al., 2011). The combination of cyclonic circulation and cold-water mass forms a low-energy, weakly dynamic sedimentary environment. The cyclonic eddy controls the transportation and deposition pattern of sediments in this region (Hu, 1994).

Hu, D.X. (1994) Upwelling and sedimentation dynamics. *Chinese J. Oceanol. Limnol.*, 2, 12-19.

Shi, X., Liu et al. (2012) Origin, transport processes and distribution of modern sediments in the Yellow Sea. In: Li, M.Z. et al. (eds) *Continental Shelf Sedimentology*, Wiley-Blackwell, 345-374.

## Preparation and evaluation of core-shell structured layered silicate and metal nanoparticles

Miharu Eguchi

National Institute for Materials Science (NIMS), 1-1 Namiki, Tsukuba, Ibaraki 305-0044, Japan, EGUCHI.Miharu@nims.go.jp

Metal nanoparticles are widely used in applications such as conductive ink, sensors, dyes, and catalysts. During

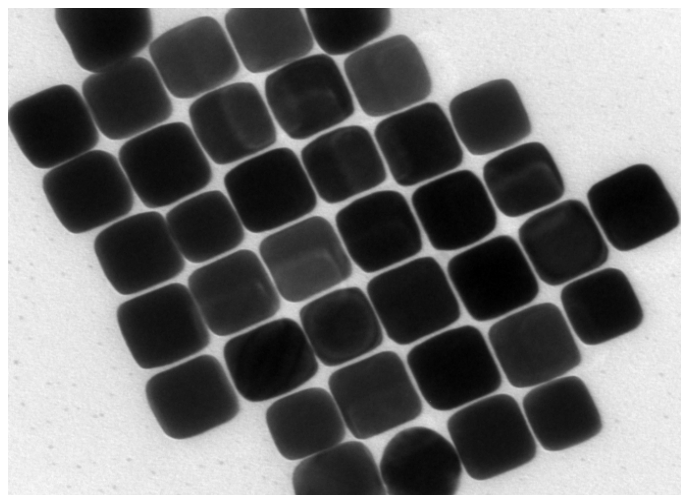


Figure 1. TEM image of obtained cubic gold nanoparticles

chemical preparation of nanoparticles, a surfactant needs to be added to stabilize the surface of the metal nanoparticles. The surfactant forms a bilayer at the nanoparticle surface with hydrophilic groups in contact with the nanoparticle and the surrounding solvent, so that the particles are stabilized in water.<sup>1</sup> Since the adsorptivity of surfactants on nanoparticles is limited, nanoparticles aggregate easily when the surfactant concentration in dispersion decreases during purification. In this study, it is aimed to produce a structure of nanoparticles that are stable in solution in the absence of extra surfactant by applying layered silicate.

A dispersion of cubic gold nanoparticles was prepared chemically by reducing chloroauric acid in the presence of a cationic surfactant, cetyltrimethylammonium chloride (CTAC)<sup>2</sup> (Figure 1). The  $\zeta$  potential of the colloidal solution was positive, which is attributed to the CTAC bilayer that forms at

the nanoparticle surface (Au-CTACs). Resultant Au-CTACs were combined with layered silicate (LS) in dispersion electrostatically and a composite of Au-CTACs with LS was formed. A core-shell structure consisting of gold nanoparticles wrapped with layered silicate was revealed by TEM. The efficient adsorption of LS to Au-CTACs was confirmed because of the negative  $\zeta$  potential of the composite, allowing its high dispersibility. A surface modification potential of the composite was also confirmed by adding cationic dye solution to the dispersion.<sup>3</sup> Complexes formed by such composites and cationic molecules are suitable for studying metal-molecule interactions since adsorption behavior of certain types of cationic molecules on LS are already known in detail.

[1] C. Zhu, H.-C. Peng, J. Zeng, J. Liu, Z. Gu, Y. Xia, *J. Am. Chem. Soc.* **2012**, *134*, 20234.

[2] M. Eguchi, D. Mitsui, H.-L. Wu, R. Sato, T. Teranishi, *Langmuir* **2012**, *28*, 9021.

[3] M. Eguchi, M. Ito, T. Ishibashi, *Chem. Lett.*, **2014**, *43*, 140.

## Aeolian contribution to volcanic soils, Mt. Daisen, Japan

W. Crawford Elliott<sup>1</sup>, Afshan Shaikh<sup>1</sup>, Cyndi Jackson<sup>1</sup>, J. Marion Wampler<sup>1</sup>, Atsushi Nakao<sup>2</sup>, and Junta Yanai<sup>2</sup>

<sup>1</sup> Department of Geosciences, Georgia State University, Atlanta, GA 30302-3965 USA; wce Elliott@gsu.edu

<sup>2</sup> Graduate School of Life and Environment, Kyoto Prefectural University, 1-5 Hangi-sho, Shimogamo, Sakyo-ku, Kyoto 0606-8522, Japan

A thick andisol located near Mt. Daisen was studied to understand the trends in chemistry and mineralogy. These soils are thought to contain materials from weathering of parent tephra and an aeolian component. The silicate fractions of the aeolian component within these volcanic soils in Japan contain primary rock-forming minerals and phyllosilicates (mica, illite, hydroxy-interlayered vermiculite). These phyllosilicates can sorb both naturally occurring stable Cs and radiocesium released from nuclear power reactors. Radiocesium released from reactors in the 2011 Fukushima-Daiichi accident have been fixed in the upper 5 cm of soil. This fixation is attributable to the presence of micaceous phyllosilicates (Nakao et al., 2015). The provenance of these phyllosilicates in volcanic soils is uncertain but an aeolian origin is proposed. Soil samples were collected at Mt. Daisen in SW Japan to test this idea on a preliminary basis. This soil is an andisol underlain by a geologically young dacite tephra whose age is < 1 Ma.

Throughout the Mt. Daisen profile, the soils are enriched in stable Cs relative to Cs content in the Upper Continental Crust. These soils were depleted in most of the alkaline metals (Ba, Rb, Sr, K, Ca, and Mg) relative to the Upper Continental Crust. Such enrichment of Cs and depletion of the other alkaline metals has been attributed to weathered micaceous phases in soil elsewhere (e.g. Zaunbrecher et al, 2015). An aeolian micaceous component might conceivably be responsible for the observed enrichment of Cs. The Chemical Index of Alteration values range from as low as 63 to as high as 76. The fine-silt fractions (5-20  $\mu\text{m}$ ) of the upper two soil samples (0-33 cm, 33-58 cm) are composed of K-feldspar, quartz, and trace amounts of 10 Å and 14 Å phases.

The K-Ar age of the fine-silt fraction is highest in the uppermost soil sample (61 $\pm$ 2 Ma). The measured age of the fine-silt fractions of two deeper soil samples (33-58 cm and 58-72 cm) are both about 30 Ma with relatively large uncertainties of  $\pm$ 3 Ma due to correction for large amounts of atmospheric Ar. These measured age values are clearly far greater than the < 1 Ma age of the dacite tephra, indicating that K-bearing minerals in fine-silt fractions of this volcanic soil are derived from materials other than the tephra. By comparison, measured K-Ar age values of dust collected at Kyoto Prefecture University are much greater (130 and 210 Ma). The lower, downward-decreasing age values found for the soil fine-silt fractions indicate increasing dilution of the aeolian component with very young K-bearing material (K-feldspar) from the tephra. The sources of the fine silt in the soil at Mt. Daisen are likely aeolian material, eluviated phases, and tephra.

Nakao, A., Takeda, A., Ogasawara, S., Yanai, J., Sano, O., Ito, T., 2015, Relationships between Paddy Soil Radiocesium Interception Potentials and Physiochemical Properties in Fukushima, Japan: *J. Environ. Qual.* doi: 10.2134/jeq2014.10.0423

Zaunbrecher, L.K., Elliott, W.C., Wampler, J.M., Perdrial, N., Kaplan, D.I., 2015, Enrichment of Cesium and Rubidium in Weathered Micaceous Materials at the Savannah River Site, South Carolina: *Environ. Sci. Technol.* doi: 10.1021/es5054682

## Natural extract incorporated nanoclays as antibacterial film additives

Hyoungh-Jun Kim<sup>1</sup>, Kang Koo<sup>2</sup>, Sung-Woo Lee<sup>2</sup>, Jin-Hee Lee<sup>2</sup>, In-Kee Hong<sup>3</sup>, Eun-Ji Kim<sup>3</sup>, Soon-Seok Hwang<sup>3</sup> and Jae-Min Oh<sup>1\*</sup>

<sup>1</sup>Department of Chemistry and medical chemistry, College of Science and Technology, Yonsei University, Wonju, Gangwondo, 220-710, Korea

<sup>2</sup>C&KPROPAC Co., 37, Gangnam-daero 162-gil, Gangnam-gu, Seoul, 135-888, Republic of Korea

<sup>3</sup>RADIANT INC, 1143, G-tech village, Geodu-ri, Dongnae-myeon, Chuncheon, Gangwondo, 200-883, Republic of Korea  
\*E-mail: jaemin.oh@yonsei.ac.kr

Antibacterial natural extracts obtained from *Paeonia suffruticosa* Andrews (PS), *Agrimonia pilosa* Ledeb (AP) and *Paeonia japonica* var. *pilosa* Nakai (PJ) were incorporated into pore-modified nanoclays, illite (IL), holrait (HO) and scoria (SC). Prior to natural extract loading, nanoclays were treated with 6 M HCl to enhance pore size, volume and specific surface area. Nanoclays and natural extracts were simply mixed in aqueous solution and incubated for 24 h to obtain antibacterial-clay hybrids. The power X-ray diffraction patterns, scanning electron microscopic images and zeta potential measurement suggested that chemical species in natural extracts were adsorbed on the surface of nanoclays. The combustion of organic moieties in hybrids was determined to occur at lower temperatures than those in natural extract powder itself, according to thermogravimetry and differential thermal analyses. This suggests that molecules rearranged on the surface of nanoclays diminish inter-molecular forces. The antibacterial activities of the hybrids were evaluated by the bacterial colony count method, and show similar or enhanced antibacterial activity for the hybrids compared with natural extracts alone. Prepared hybrids were then coated on polyethylene terephthalate (PET) film by a blade coating method with polyurethane. The coated film was determined to preserve transparency and to enhance antibacterial activity of PET film on *Escherichia coli*.

## Isomorphous Co(II) incorporation into hydrotalcite type anionic clays via hydrothermal reaction

Tae-Hyun Kim<sup>1</sup>, Won-Jae Lee<sup>2</sup>, Hyoung-Mi Kim<sup>1</sup>, Seung-Min Paek<sup>2</sup> and Jae-Min Oh<sup>1,\*</sup>

<sup>1</sup>Department of Chemistry and Medical Chemistry, College of Science and Technology, Yonsei University, Wonju, Gangwondo 220-710, Korea.

<sup>2</sup>Department of Chemistry, Kyungpook National University, Taegu 702-701, Korea.

\*E-mail:jaemin.oh@yonsei.ac.kr

We incorporated Co(II) ions into the lattice of hydrotalcite type anionic clays ( $\text{Mg}_{0.67}\text{Al}_{0.33}(\text{OH})_2(\text{CO}_3)_{0.16} \cdot m\text{H}_2\text{O}$ ) through isomorphous substitution. Pristine hydrotalcite was synthesized via a coprecipitation reaction followed by hydrothermal treatment, and were of uniform size (~ 250 nm) and hexagonal plate-like morphology. For Co(II) incorporation, hydrotalcite powder was dispersed into aqueous Co(II) solution and hydrothermally treated at 150 °C. Quantitative analyses revealed that Co(II) moved from solution to the hydrotalcite framework, in a time-dependent manner, corresponding with the release of Mg(II) from hydrotalcite to solution. The system was saturated in 12 h with final solutions displaying a Mg(II)/Co(II)/Al(III) ratio, as in hydrotalcite, of 1/1/1. From powder X-ray diffraction and scanning electron microscopy, we confirmed that the particle size, morphology and crystallinity of hydrotalcite did not change significantly upon Co(II) incorporation. The energy dispersive spectroscopic mapping results showed homogenous incorporation of Co(II) throughout the hydrotalcite lattice. We also carried out diffuse reflectance UV-vis and X-ray absorption spectroscopy and determined that the Co(II) was well stabilized in the octahedral site of hydrotalcite, which was previously occupied by Mg(II).

## Interaction between blood components and size/surface charge controlled anionic clays

Jae-Min Oh<sup>1,\*</sup>, Hyoung-Mi Kim<sup>1</sup>, Sung Hoon Kim<sup>2</sup>, Yoon Suk Kim<sup>2\*</sup>

<sup>1</sup>Department of Chemistry and Medical Chemistry, College of Science and Technology, Yonsei University, Wonju, Korea

<sup>2</sup>Department of biomedical laboratory science, College of Health Sciences, Yonsei University, Wonju, Korea

\*Email: jaemin.oh@yonsei.ac.kr

We evaluated the interaction between blood components and anionic clays with controlled size and surface charge. Four kinds of anionic clays ( $\text{Mg}_2\text{Al}(\text{OH})_6(\text{CO}_3)_{0.5}\cdot\text{mH}_2\text{O}$ ) were synthesized with controlled particle sizes of 100, 150, 350 and 2000 nm by carefully manipulating synthetic conditions. The surface charge of anionic clays was controlled by coating their surfaces with L-serine, succinate and citrate, respectively. Anionic clays were then treated with blood components such as blood cells and plasma proteins to investigate their potential blood toxicity and clay-bio interaction. In general, all of the anionic clays were blood-compatible in terms of red blood cell membrane disruption or cell death and flocculation of plasma proteins, regardless of size and surface charge. However, we found that size and surface charge of anionic clays influenced their biological behavior. Large particle size and negative surface charge tend to induce more disruption on red blood cell membrane and cell death, possibly by physical attack. In terms of plasma protein interaction, surface charge was determined to affect more than particle size. Proteins showed surface adsorption on anionic clays through electrostatic interaction, showing the highest adsorption with positively charged anionic clays.



## Generation of second stage structure in the alkylammonium cation and potassium sericite

Kenji Tamura\* and Hiroshi Sakuma

National Institute for Materials science, 1-1 Namiki, Tsukuba, Japan

\*TAMURA.Kenji@nims.go.jp

Layered inorganic materials such as clay minerals have been used to prepare nanoscale organic/inorganic layered complexes in efforts to develop new functional or high performance materials. In developing these new materials, it is essential to control the nanostructure of the complexes (the mode of the layer stacking), and also the orientation of incorporated organics in the interlayer space to fully utilize the features of each component. In the present study, the staging phenomenon was investigated for alkylammonium/sericite complexes. Sericite consists of negatively charged silicate layers with anhydrous potassium cations located at the interlayer space for charge compensation. Although the majority of research concerned with clay minerals has described the orientation of incorporated organic molecules, only a few cases of staging have been reported[1].

The potassium sericite (SE) used was FSP (Sanshin mine Ind. Co., Ltd), which was mined from a hydrothermal deposit in Aichi, Japan; its chemical formula is:  $(K_{0.7}Na_{0.08}Ca_{0.07})(Al_{1.77}Fe_{0.12}Mg_{0.08})(Si_{3.22}Al_{0.78})O_{10}(OH)_2$ . The powder sample was a  $2M_1$  sericite which had 7.8  $\mu m$  median particle diameter. The dehydrated sample was prepared by heating at 800 °C for 1 hour using an electric furnace, which was denoted by dhSE. Dodecylamine (DDA) hydrochloride was obtained from Wako Pure Chemical Industries, Japan. The DDA-SE was prepared by an ion exchange reaction between each of the SEs and DDA solutions of various initial concentrations (7.3, 21.9 and 73.3 mM, corresponding to  $DDA^+/K^+$  mole ratio = 1.0, 3.0 and 10.0, respectively). In a typical procedure, 0.3 g of SE powder was treated with 100 mL of a DDA solution and kept at 90 °C.

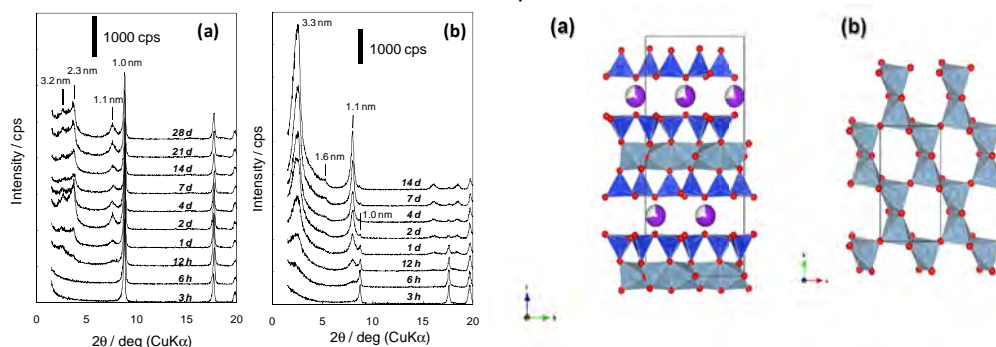


**Fig. 2.** XRD patterns of the complexes [(a) DDA-SE, (b) DDA-dhSE] treated with  $DDA^+/K^+$  mole ratio =1: for varying synthesis durations.

**Fig.2** Refined structure of the dhSE (heated at 800 °C): (a) TOT sheet and (b) octahedral sheet. The three-dimensional space-group symmetry of c2.

In the case of the SE complexes treated with  $DDA^+/K^+$  mole ratio = 1.0, two separated phases, 1.0 and 2.3 nm, were obtained. These were ascribed to the non-intercalated layers, and vertical (perpendicular to the layers) orientations of the incorporated DDA, respectively (Fig.1a). On the other hand, in the case of the dhSE complexes, a large basal spacing of 3.3 nm was observed (Fig.1b). The 3.3 nm basal spacing is close to the sum of the basal spacing for the vertical orientations and that for the non-intercalated layers. This is interpreted as a regular alternation of the 2.3 nm layer and the 1.0 nm layer, exhibiting  $c=3.3$  nm supercell ("1:1 ordered interstratifications" or "second-staging").

A structure of the dhSE refined by Rietveld analysis using powder X-ray diffraction was a pentacoordinated octahedral sheet (Fig. 2). In this paper, an overview of the intercalation behaviour in various conditions will be given, while examining the factors behind the structural change of the silicate sheet.

[1] J-Y. Chiou et al., *RSC Adv.*, 2013, **3**, 12847.

## The formation of smectite and its redox reactions in deep sub-seafloor sediment, South Pacific Gyre: IODP expedition 329

Kiho Yang<sup>1</sup>, Toshihiro Kogure<sup>2</sup>, Bryce Hoppie<sup>3</sup>, Robert Harris<sup>4</sup>, Hionsuck Baik<sup>5</sup>, Hailiang Dong<sup>6</sup>, IODP Expedition 329 shipboard scientists<sup>7</sup>, and Jinwook Kim<sup>1\*</sup>

<sup>1</sup>Department of Earth System Sciences, Yonsei University, Seoul, Korea;  
khyang@yonsei.ac.kr; \*Correspondence to jinwook@yonsei.ac.kr

<sup>2</sup>Department of Earth and Planetary Sciences, Graduate School of Science, The University of Tokyo, Tokyo, Japan;

<sup>3</sup>Department of Chemistry and Geology, Minnesota State University, Mankato, MN, USA;

<sup>4</sup>College of Oceanic and Atmospheric Sciences, Oregon State University, OR, USA;

<sup>5</sup>Korea Basic Science Institute (KBSI), Seoul, Korea;

<sup>6</sup>Department of Geology and Environmental Science, Miami University, Oxford, OH, USA;

<sup>7</sup>IODP Expedition 329 shipboard scientists

Sub-seafloor sediment from the South Pacific Gyre (SPG) was recovered for the first time by Integrated Ocean Drilling Program (IODP) Expedition 329 (2010.10.10-2010.12.13). Clay mineralogy from two sites (U1369 and U1365) was investigated. We compared clay mineralogy and formation conditions from sites U1365 (margin of SPG) and U1369 (center of SPG close to the East Pacific Rise). The sediment at the site U1369 has a young crustal age of 13.5 Ma compared with the site U1365 (84-120 Ma).

Fine clay fractions less than 1  $\mu\text{m}$  were analyzed by x-ray diffraction (XRD), transmission electron microscopy (TEM) with the selected area electron diffraction (SAED), and electron dispersive x-ray spectrometry (EDS). Saturation indices (SI) with respect to smectite were modeled based on the pore water chemistry.

The dominant clay minerals in the investigated sediments are smectite and illite. The ordering of illite polytypes ( $1M$ ,  $2M_1$ , and  $3T$ ) at U1369 is distinctive compared with disordered  $1M_d$  illite at U1365. This suggests that hydrothermal alteration influences the smectite mineral formation at U1369. The lower heat flow measurement comparing to the lithospheric cooling reference also supports the hypothesis of hydrothermal activity at U1369. Smectites of hydrothermal origin such as Al-rich beidellite, and saponite were observed at U1369, whereas Fe-rich montmorillonite, likely to be associated with the basalt-seawater interaction at ambient temperature, was dominant at U1365. Fe-rich smectite (nontronite) was detected at both sites. Saturation indices with respect to smectite and muscovite, using pore water chemistry, showed oversaturation. The Red-brown to yellow-brown Semiopaque Oxide minerals (RSO) were widely distributed with Fe-rich smectite near the basaltic crust at U1365. The presence of K-nontronite at the basalt-sediment interface at both sites indicates an oxidative basalt alteration. However, the variations in oxidation state of structural Fe in nontronite, measured by EELS, may indicate that the reductive environment may persist locally at the basalt/sediment interface.

## Macroscopic orientation of liquid crystalline fluorohectorite colloid by shear and electric field

Shohei Yoshimura<sup>1</sup>, Takumi Inadomi,<sup>1</sup> and Nobuyoshi Miyamoto<sup>1</sup>

<sup>1</sup>Graduate School of Fukuoka Institute of Technology, 3-30-1 Wajirohigashi, Higashiku, Fukuoka 811-0295, Japan;  
miyamoto@fit.ac.jp

**Introduction:** We recently reported the formation of a fluid liquid crystalline (LC) phase in the aqueous colloid of fluorohectorite (FHT).<sup>1)</sup> The inorganic LCs are applicable to many fields, which are not covered by conventional organic liquid crystals. For example, we have reported LC-FHT/polymer composite gel materials with anisotropic properties.<sup>2)</sup> However, further control of macroscopic orientation is required for detailed fundamental studies and applications. Here we demonstrate that the macroscopic orientation of the LC FHT colloid as controlled by both shear flow and alternative electric field and its fixation into an anisotropic gel by photo-polymerization.

**Experimental:** Fluorohectorite (Topy Industries Co.) purified by centrifugation was dispersed in water to form stable LC colloid. The colloid was added with *N*-isopropylacrylamide (monomer), *N,N*-methylenebisacrylamide (a crosslinking agent), and 2-hydroxy-2-methyl-propiophenone (a photoinitiator). The colloid was continuously injected with a peristaltic pump at into the fluid channel (100 mm long, 1mm thick, and 10 mm wide) made of silicone rubber and ITO glass, while alternative electric field is applied. After stopping the flow and the electric field, UV light is irradiated for 5 min to fix the structure by photo- polymerization. The gel is observed with a polarized microscopy (POM).

**Results and Discussion:** The gel synthesized with 1 wt% of FHT in the shear (19 mm/s) and electric field (10 V mm<sup>-1</sup>, 10kHz) was observed with POM from three orthogonal directions from the top, and sides. Strong birefringence was observed from all the directions, indicating macroscopic orientation of the FHT nanosheets along both the shear and electric field direction. In contrast, the orientation was imperfect if only the shear or the electric field is applied. The orientation order was affected by the voltage and flow speed: the above condition was found to be optimal. At higher FHT concentration, the colloid become more viscose so that electric field is not effective to control the orientation; however, we found that the simultaneous use of the electric field with shear improve this situation.

(1) N. Miyamoto, H. Iijima, H. Ohkubo, Y. Yamauchi, *Chem. Commun* **2010**, 46, 4166.

(2) N. Miyamoto, M. Shintate, Y. Hoshida, R. Motokawa, M. Annaka, *Chem. Commun.* **2013**, 49, 1082.; Inadomi, T., Ikeda, S., Okumura, Y., Kikuchi, H. & Miyamoto, N., *Macromol. Rapid Commun.* **2014**, 35, 1741.

## Preparation of flame retardant expanded polystyrene (EPS) form using nanoclays

Minjae Kwon and J. Yoon Choi\*

Fire & Safety Evaluation Technology Center, Korea Conformity Laboratories,  
73, Yangcheong 3-gil, Cheongwon-gu, Cheongju-si, Chungcheongbuk-do, 363-883, Korea, (mj.kwon@kcl.re.kr)

The sandwich panel comprises a three layer structure: a low density inner insulation core between two relatively thin metal sheets. Expanded polystyrene (EPS) has been used for the inner insulation core because it possesses exceptional thermal insulation properties and economic advantages.

In many countries, national regulations require intrinsically flammable EPS foams to meet obligatory fire safety levels when used for building elements. Generally brominated additives such as HBCD (Hexabromocyclododecane), PBB (Polybromobiphenyl) and PBDE (Polybromodiphenyl ether) have been added when producing PS pellets, which are later expanded to make the required shape. However, recently HBCD with 16 possible stereo-isomers has been classified as persistent, bioaccumulative, and toxic (PBT) chemical to be gradually phased out of usage[1].

As an attempt to increase fire safety, EPS forms were prepared by surface coating pre-expanded EPS beads using aqueous solution containing different types of nanoclays with synergetic agents such as expanded graphite and guanidine compounds[2,3]. Fire retardancy and mechanical properties were investigated using a cone calorimeter, UL94 test and universal tensiometer (UTM). Increased flame retardancy effects, such as the function of nanoclay contents, are discussed along with different synergetic agents.

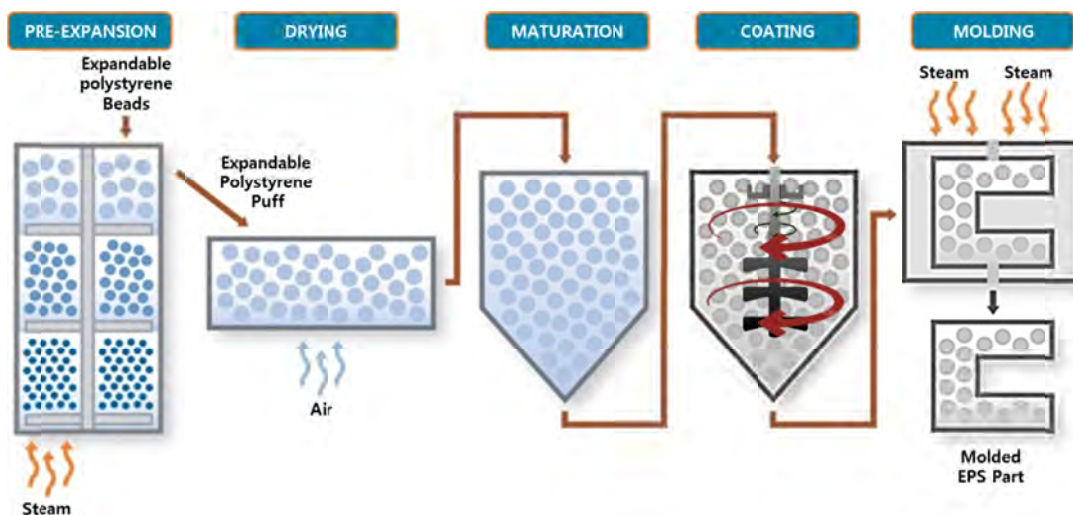


Figure. Manufacturing process of flame retardant EPS

J.L. Lyche et al. Human health risk associated with brominated flame-retardants (BFRs). *Environment International*. 74 (2015) 170–180.

K. Chrissafis et al. Can nanoparticles really enhance thermal stability of polymers? Part I: An overview on thermal decomposition of addition polymers. *Thermochimica Acta* 523 (2011) 1-24.

K. Chrissafis et al. Can nanoparticles really enhance thermal stability of polymers? Part II: An overview on thermal decomposition of polycondensation polymers. *Thermochimica Acta* 523 (2011) 25-45.

## Structural properties of montmorillonite intercalated with n-butylammonium cations (n= 1-4) – computational and experimental study

Eva Scholtzová<sup>1</sup>, Jana Madejová<sup>1</sup> and Daniel Tunega<sup>2</sup>

<sup>1</sup> Institute of Inorganic Chemistry of Slovak Academy of Sciences, Dúbravská cesta 9, 845 36 Bratislava, Slovakia

<sup>2</sup> Institute for Soil Science, University of Natural Resources and Life Sciences, Peter-Jordanstrasse 82, A-1190, Wien, Austria

A combined theoretical approach based on density functional theory (DFT) and infrared spectroscopy is performed to study the structure and properties of organoclays prepared from montmorillonite and mono-, di-, tri- and tetra-butyl ammonium (nBA; n= 1-4) cations. The difference in the interlayer arrangement of the cations is explained and types of the interactions between cations and layer surfaces are described. The FTIR spectra are collected for all four types of the organoclays. DFT-calculated vibrational spectra are used in the analysis and interpretation of experimental IR spectra, which have a complex structure with overlapping bands.

**Acknowledgement** Gratefully acknowledged is the financial support for this research by Slovak Grant Agency VEGA (Grant 2/0132/13).

## Performance of organic/inorganic force field combinations for molecular simulations of smectites intercalated with ethylene glycol evaluated by comparison with X-ray diffraction data

Marek Szczerba<sup>1</sup> and Andrey Kalinichev<sup>2</sup>

<sup>1</sup>Institute of Geological Sciences, Polish Academy of Sciences, Kraków, Poland, ndszczer@cyf-kr.edu.pl

<sup>2</sup>Laboratoire SUBATECH (UMR 6457), Ecole des Mines de Nantes, Nantes, France

Recent development of force fields for clay minerals and their subsequent modifications leave an open question: which of these inorganic force field parameterizations are best suited for the molecular modeling of interactions between clays and organic molecules in aqueous environment. The issue is further complicated by the availability of a large number of different force fields for the description of organic molecules. To quantitatively address this question we use a testing model of the structural description of a complex ethylene glycol (EG)-water-smectite. The intercalation of EG in hydrated smectites provides a stable interlayer complex with relatively constant basal spacing. These structures are also well characterized by having relatively constant numbers of EG and H<sub>2</sub>O molecules.

In this study, the simulations were performed for three smectites with substantially different layer charge and its distribution: SWy-1, SAz-1 and SbCa-1. Atoms of the smectites were described with the CLAYFF and INTERFACE force fields. GAFF, OPLS-aa, CGenFF and CVFF organic force fields were considered for EG, while the SPC model was assumed for water molecules. Additionally, in the original clay mineral force fields, the Lennard-Jones parameters for basal oxygens were also modified according to Ferrage et al. (2011) (CLAYFF-mod and INTERFACE-mod). These Lennard-Jones parameters were confirmed by comparison with the optimized interatomic distances obtained by *ab initio* calculations for a model cluster representing a fragment of the clay mineral structure interacting with one water molecule under MP2/6-311+G\* level of theory.

A set of different EG compositions around those of Reynolds (1965) – 1.7 EG per half unit cell (phuc) – was covered by our simulations to obtain the basal spacing closest to the experimentally observable. A constant number of interlayer water molecules – 0.8 H<sub>2</sub>O phuc – was assumed. For every structure, the atomic density distributions of the interlayer species as well as electronic density profiles along the direction perpendicular to the layer plane were calculated. For these structures X-ray diffraction data were calculated using the Sybilla code (Chevron proprietary). The values of  $T_{\text{mean}}$ ,  $d$ -spacing,  $\sigma^*$  and  $\Delta$ - $d$ -spacing were optimized automatically.

The results show large discrepancies in the final structures and basal spacings for different layer charges as well as for different combinations of force fields. For low charge montmorillonite (SWy-1) the results agree well with experiment for all clay mineral force fields, while there are some differences between the organic force fields used. However, for high charge montmorillonite (SAz-1) and beidellite (SbCa-1) the correction of Lennard-Jones basal oxygens parameters of clay mineral force field substantially improves the agreement between the theoretical and experimental diffractograms for all the organic force fields tested.

Generally, among the organic force fields the least accurate results are obtained for CGenFF. For unmodified CLAYFF, GAFF gives the best results, while the two other sets (OPLS-aa and CVFF) give the best results for CLAYFF-mod. Surprisingly, INTERFACE and INTERFACE-mod produce relatively poor results for high charge beidellite.

### Acknowledgement

The study was supported by a NCN grant 2012/05/B/ST10/01948.

Reynolds, R.C., 1965. An X-ray study of an ethylene glycol-montmorillonite complex. *Am. Mineral.*, **50**, 990-1001.

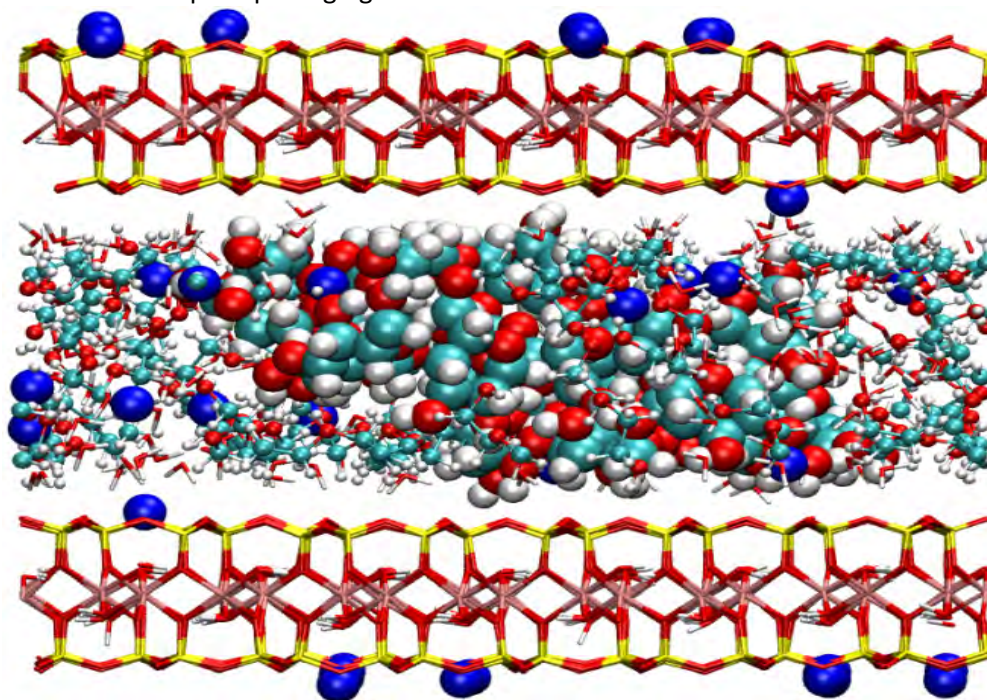
Ferrage E., Sakharov B.A., Michot L.J., Delville A., Bauer A., Lanson B., Grangeon S., Frapper G., Jimenez-Ruiz M., Cuello G.J., 2011. Hydration properties and interlayer organization of water and ions in synthetic Na-smectite with tetrahedral layer charge. Part 2. Toward a precise coupling between molecular simulations and diffraction data, *J. Phys. Chem. C*, **115**, 1867–1881.

## Understanding the barrier properties of dry, clay-based coatings. A contribution from computational modelling

Nikita Simine<sup>1</sup>, Chris Breen<sup>1</sup>, Doug Cleaver<sup>1</sup>, Francis Clegg<sup>1</sup>

<sup>1</sup> Materials and Engineering Research Institute, Sheffield Hallam University, Howard Street, Sheffield, S1 1WB, UK

Coatings with high barriers to gases, vapours and flavours find their major application in food packaging materials<sup>[1]</sup>. Taking into account the amount of food currently wasted every year, packaging that keeps it fresh for a longer time has an important role to play in reducing the amount of energy consumed during the food production and transport cycle. Moreover, the importance of using sustainable packaging materials has become apparent over recent decades. This can be achieved by replacing the petroleum-derived additives (e.g. plastics) used when coating paper and board packaging by greener alternatives that still deliver the barrier and other crucial properties needed for competitive, low carbon footprint packaging materials.



Driven by this inspiration, a recent experimental study<sup>[1]</sup> has demonstrated that naturally occurring swelling clay minerals (in particular the smectites) can when combined with starch and bio-based plasticisers, provide sustainable paper coatings which are competitive with oil-derived barrier coatings. Experimental characterization of the molecular-scale structure and dynamics within the interlayer space in these systems gives little information due to static and dynamic disorder. It can, however, be obtained via use of molecular dynamics (MD) simulation techniques based on classical force fields<sup>[2]</sup>.

To extend understanding of the roles played by clay, water and bio-polymers in these sustainable coatings and their respective impact on the resultant barrier properties, we have initially employed MD simulation to validate our models using experimental observations. Subsequently, the influence of clay charge location, cation exchange capacity, and interlayer cation on the equilibrated interlamellar arrangement in the clay-polymer composite was derived from the simulation study. With the combination of the results of the two methods, we can provide new insights for understanding the sorptive characteristics of the polymer-clay composites studied. Current work is supported by European project NewGenPak (Marie Curie International Training Network (ITN), FP-7-PEOPLE-2011, project number 290098)

C. Johansson, J. Bras et al. *Bioresources*, 7(2), 2506-2552 (2012)

R. Cygan, J. Liang, A. Kalinichev. *J. Phys. Chem. B*, 108, 1255-1266 (2004)

## Halloysite nanotubes from Burela, Spain. A preliminary study

Emilio Galán<sup>1</sup>, Patricia Aparicio<sup>1</sup> and Marcial G. Márquez<sup>1</sup>

Dpto. Cristalografía. Mineralogía y Q. Agrícola, University of Seville, Spain [egalan@us.es](mailto:egalan@us.es), [paparcicio@us.es](mailto:paparcicio@us.es),  
[amiras@us.es](mailto:amiras@us.es)

Halloysite is a high-value clay typically used in the manufacture of porcelain, bone china and fine china, and also for high-tech ceramic applications. But because halloysite shows a 1:1 nanotubular structure with some particular characteristics: nanoparticle size, high length-to-diameter ratio, relatively low hydroxyl group density on the surface, etc., numerous exciting applications have been discovered for this clay mineral, such as drug releasing agent, fabrication of polymer nanocomposites, additives in biocide, protective coatings, etc. Presently, the major source of high-grade, high aspect ratio halloysite nanotubes is a mine in Matauri Bay, New Zealand.

In Spain, as far as it is known, the only halloysite deposit is located at Burela in the Lugo province. This kaolin deposit is being mined for more than half a century to produce porcelain ware. Kaolin was mainly formed by the weathering alteration of felsic rocks.

It is of paramount importance in assessing the value of halloysite clay deposits to know the composition of the deposit itself in terms of the halloysite/kaolinite ratio, the crystal length as well as the aspect ratio (length to diameter). In this research the mineralogical composition of the raw material was mineralogically determined by XRD, as well as the halloysite/kaolinite ratio in the commercial fractions (<45  $\mu\text{m}$  and <2  $\mu\text{m}$ ), and the length of the nanotubes and the aspect ratio were measured by TEM and AFM.

Kaolin minerals in the raw material range between 27-74%, accompanied by quartz (16-31%), illite (from trace to 33%), feldspars and traces of smectite. For the < 45  $\mu\text{m}$  fractions the amount of kaolin minerals ranges from 61% to 90%, and in the <2  $\mu\text{m}$  fractions, the amount of kaolin minerals reached up to 92 %. Traces of allophone, gibbsite and chlorite were also detected. Halloysite accounts from 11 to 60%. The length of halloysite nanotubes ranges from 0.5-8 $\mu\text{m}$  (500-8000 nm), with an aspect ratio from 0.1 to 0.3. The specific surface area (BET) average is 16  $\text{m}^2/\text{g}$  and it ranges between 8 and 21  $\text{m}^2/\text{g}$ . Fractal dimension is also related with halloysite content.

Therefore, this Spanish halloysite could be used as nanotubes in different important applications, after a selective mining and appropriate processing. The method proposed in this paper for the quantification of halloysite vs. kaolinite would be suitable for halloysite control in the mining operations.



## Raw, acid activated and calcined halloysite for metals and metalloids adsorption: sorption capacity and mechanisms

Paulina Maziarz, Anna Prokop and Jakub Matusik\*

Department of Mineralogy, Petrography and Geochemistry, Faculty of Geology, Geophysics and Environmental Protection, AGH University of Science and Technology, al. Mickiewicza 30, Krakow, 30 059, Poland, \*e-mail: jakub\_matusik@wp.pl

Clay minerals are widely used as natural adsorbents of toxic and/or carcinogenic ionic species. Their specific structural features enable them to attract ions from aqueous solutions. Halloysite is a unique 1:1 layered mineral from the kaolin group which often exhibits tubular morphology. It was shown that chemical modifications may enhance its sorption properties [1,2]. In relation to that research the objective of the study was to examine the sorption affinity of commercial products: raw, acid activated and calcined halloysites toward Pb(II), Zn(II), Cd(II) and As(V). The primary goal was to investigate the adsorption mechanisms.

The halloysite sample (H) came from the Polish Dunino deposit located in Lower Silesia which is owned and exploited by the Intermark company. The halloysite is modified by the company on an industrial scale. The modification involves acid activation by sulfuric acid (HA sample) and calcination (HC sample). The sorption capacity was determined at room temperature in a broad concentration range (0.02-50.0 mmol/L) using 20 g/L suspension concentration at initial pH 5.

The XRD patterns of all samples revealed the presence of 7.2 Å peak corresponding to dehydrated halloysite-(7 Å). The calcination did not reveal any changes in the XRD pattern, while acid activation led to peak intensity decrease and changes in the 19-25°2θ region due to structural perturbations. In analogy, the FTIR spectra showed only differences for the HA sample where the bands in the 1300-1000 cm<sup>-1</sup> were significantly altered. The S<sub>BET</sub> and CEC were the following: H (49.5 m<sup>2</sup>/g) < HC (52.1 m<sup>2</sup>/g) < HA (171.6 m<sup>2</sup>/g) and HC (8.2 meq/ 100 g) < H (8.8 meq/100 g) < HA (10.7 meq/ 100 g). The sorption capacity for H sample reached 168.4 mmol As/kg, 37.2 mmol Pb/kg, 3.7 mmol Cd/kg, and 1.9 mmol Zn/kg. The sorption on HC sample was found to be the following: 219 mmol Pb/kg, 212 mmol Zn/kg, 134 mmol Cd/kg, and 103.0 mmol As/kg. For the HA sample the adsorption capacity reached 235 mmol Pb/kg and 66 mmol As/kg. The results obtained for Zn(II) and Cd(II) indicated no adsorption. Adsorption for raw halloysite can take place via ion-exchange and surface complexation through silanol Si-OH and aluminol Al-OH groups. In the case of cations, the sorption often correlates with cation hydrolysis constants. The Pb(II) ions are more likely to hydrolyze and create PbOH<sup>+</sup> forms, which may link to deprotonated groups. Thus, its sorption increased when structure was altered by calcination or acid treatment. Heavy metals such as Zn(II) and Cd(II) tend to adsorb through ion-exchange. However, their sorption increased only for the HC sample. In turn, for the HA sample the results indicated that acid activation hampered the ion-exchange of these metals. It is worthwhile to underline the highest As(V) adsorption capacity of H sample which is most likely due to surface complexation. The X-ray photoelectron (XPS) measurements suggested the possibility of As(V) to As(III) reduction in connection to Fe(II) to Fe(III) oxidation, especially for the H sample. The XPS analyses also indicated that calcination induced a partial halloysite dehydroxylation which explains its improved sorption capacity towards metals. The acid activation caused dealumination and formation of amorphous SiO<sub>2</sub>. The results proved that appropriate selection of a halloysite-based adsorbent is highly dependent on the type of pollutant.

This project was supported by the Polish National Science Centre under research project awarded by decision No. DEC-2011/01/D/ST10/06814.

[1] Matusik, J., Bajda, T., 2013. Journal of Colloid and Interface Science, 398, 74-81.

[2] Matusik, J., Wóscisło, W., 2014. Applied Clay Science, 100, 50-59.

## Co-remediation method of nickel contaminated soil by halloysite and Indian mustard (*Brassica juncea* L.)

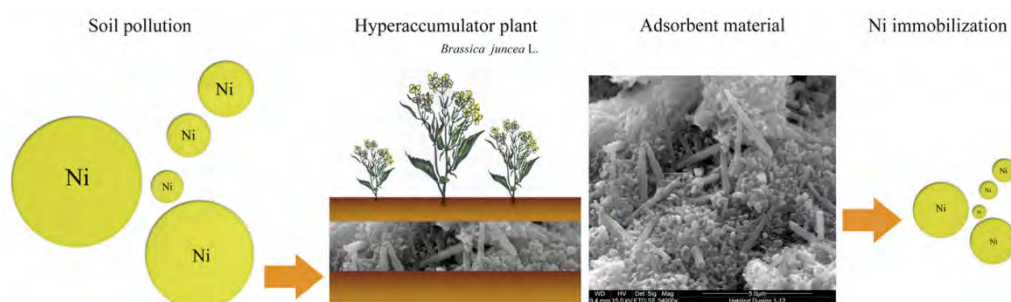
Maja Radziemska<sup>1</sup>, Zbigniew Mazur<sup>2</sup>, Joanna Fronczyk<sup>1</sup> and Jakub Matusik<sup>3</sup>

<sup>1</sup>Warsaw University of Life Sciences - SGGW, Faculty of Civil and Environmental Engineering, 159 Nowoursynowska Av., 02-773 Warsaw, Poland, e-mail: maja\_radziemska@sggw.pl

<sup>2</sup>University of Warmia and Mazury in Olsztyn, Faculty of Environmental Management and Agriculture, Pl. Łódzki 4, 10-727, Olsztyn, Poland

<sup>3</sup>AGH University of Science and Technology in Kraków, Faculty of Geology, Geophysics and Environmental Protection, 30 Mickiewicza Av., 30-059 Kraków, Poland

Phytoremediation methods of heavy metals persisting in the soil environment are a low-cost and environmentally compatible alternative to other techniques. However, these methods generally remove only a very small percentage of soil contaminants. Moreover, the low bioavailability of heavy metals in contaminated soil may also limit the efficiency of this process. In order to improve the immobilization efficiency phytoremediation methods can be applied with the combination of reactive materials such as mineral sorbents including halloysite and zeolites.



This research objective was to investigate the effect of adsorbents: raw halloysite (RH), modified halloysite (MH), and natural zeolite (NZ) on the efficiency of phytoremediation technique involving the use of *Brassica juncea* L. for nickel removal from soils.

The RH sample was a dehydrated halloysite-(7Å) which came from the Polish Dunino deposit located near Legnica (Lower Silesia region) which is owned and exploited by the Intermark company. The MH sample is produced by the company by calcination of the RH at 650°C. The RH and MH show different sorption properties towards heavy metals due to partial dehydroxylation of the MH as proved by other studies. The NZ sample came from a Slovak deposit located near Nižny Hrabovec.

The co-remediation experiment was conducted in a greenhouse by a random complete block design in four repetitions. The soil had the granulometric composition of light clay sand and was artificially spiked with nickel in the amount of 0, 80, 160, 240, and 320 mg kg<sup>-1</sup> introduced in the form of aqueous solutions of nickel sulphate heptahydrate. The metals concentrations were determined using flame atomic absorption spectroscopy (AAS) in extracts obtained after microwave digestion of the plant.

The results demonstrated that the heavy metals content in the *Brassica juncea* L. was influenced by the extent of Ni-contamination as well as the addition of RH, MH and NZ. The average accumulation of metals in *Brassica juncea* L. followed the sequence Mn>Zn>Cu>Ni>Pb>Cr, respectively. The soil contaminated with 320 mg Ni kg<sup>-1</sup> led to the highest increase in Ni, Cu and Mn content in the *Brassica juncea* L. Among the reactive materials the application of MH was shown to be the most effective. The application of NZ and RH for the soil with the highest contamination of Ni (320 mg kg<sup>-1</sup>) had a positive influence on the nickel content in *Brassica juncea* L.

## Interaction of isoniazid with halloysite as natural nanocarrier

E. Carazo<sup>1</sup>, A. Borrego<sup>1</sup>, F. García-Villén<sup>1</sup>, C. Aguzzi<sup>1</sup>, P. Cerezo<sup>1</sup> and C. Viseras<sup>1,2</sup>

<sup>1</sup> Department of Pharmacy and Pharmaceutical Technology, School of Pharmacy, University of Granada, Campus of Cartuja, 18071 s/n, Granada, Spain, ecarazogil@ugr.es

<sup>2</sup> Andalusian Institute of Earth Sciences, CSIC-University of Granada, Avda. de Las Palmeras 4, 18100, Armilla (Granada), Spain

Isoniazid (INH) is a widely used first line antimycobacterial agent for the therapy of tuberculosis. The drug is characterized by a short half-life (1-4 h), depending on the rate of metabolism. INH has a pronounced absorption from all the three sections of the small intestine (1). It is inactivated in the liver, mainly by acetylation and dehydrazination. However, long-term therapy with INH leads to hepatotoxicity and peripheral neuritis. It is the reason why it is important to have a drug formulation with controlled release of INH. Mineral nanotubes possess good biocompatibility, strong adsorption and ion exchange ability (2). Their characteristics are directly related to their colloidal size and crystalline structure, resulting in high specific surface, optimum rheological properties and/or excellent adsorptive capacity (3). With these premises, the aim of this work was to study the interaction between isoniazid and halloysite nanotubes, as first stage in the development of modified delivery systems of the drug.

**Methodology:** Isoniazid (INH) was purchased from Sigma Aldrich (Spain). Halloysite nanotubes of pharmaceutical grade (HLNT) were purchased from Sigma Aldrich (Spain). Known volumes of INH aqueous solution (100 g/L) and a known amount of nanotubes (0,1g) were put in contact for 24 hours using a multi-magnetic-stirrer (Velp Scientifica). Contact time was long enough to ensure equilibrium between drug adsorbed and drug in solution. The supernatant was recovered by centrifugation and the INH equilibrium concentration ( $C_{eq}$ ) was assessed by spectrophotometric measurements at 262 nm (UV-Vis spectrophotometer Lambda 25, Perkin Elmer, S). **Results and discussion:** The amount of INH retained per mg of HLNT was calculated from the difference between the initial ( $C_0$ ) and the equilibrium ( $C_{eq}$ ) concentration of the drug. Adsorption of INH by the HLNT occurs following an equilibrium process (4). The equilibrium isotherms of INH and the HLNT are plotted as amount of INH retained by the nanotubes (mg/mg) vs INH initial concentration (g/L) (Figure 1).

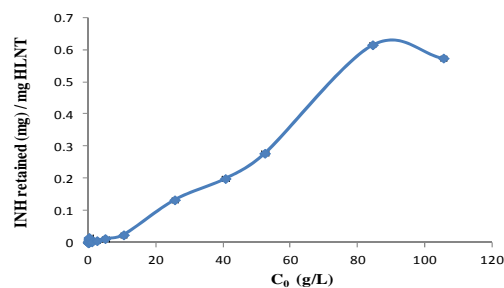


Fig 1. Equilibrium isotherms of INH and HLNT at 25°C. (mean values  $\pm$  s.d.;  $n = 3$ )

**Acknowledgements:** This study was supported by the Andalusian group CTS-946 and by the Ministry of Education, Culture and Sport of Spain (Predoctoral Grant FPU 13).

1) Mariappan TT, Singh S. Int. J. Tuberc. Lung Dis.7(8), 797-803 (2003).

2) Zhou, C.H., Keeling, J. Appl. Clay Sci. 74, 3-9 (2013).

3) Aguzzi, C., Cerezo, P., Viseras, C., Caramella. Appl. Clay Sci. 36, 1-3, 22-36 (2007).

4) Viseras, M.T., Aguzzi, C., Cerezo, P., Viseras, C., Valenzuela, C. Micropor. Mesopor. Mat., 112-116 (2008).

## Effects of organo-modification of tubular halloysite on its performance as drug/agrochemical carrier

Peng Yuan<sup>1</sup>, Daoyong Tan<sup>2</sup>, Faïza Annabi-Bergaya<sup>3</sup>

<sup>1</sup> CAS Key Laboratory of Mineralogy and Metallogeny, Guangzhou Institute of Geochemistry, Chinese Academy of Sciences, Guangzhou 510640, China, yuanpeng@gig.ac.cn

<sup>2</sup>Key Laboratory of Solid Waste Treatment and Resource Recycle, Ministry of Education, Southwest University of Science and Technology, Mianyang 621010, China

<sup>3</sup>ICMN, CNRS-Université d'Orléans, Orléans 45071, France

Tubular halloysite (Hal) is a naturally occurring porous material suitable for use as drugs or agrochemicals carrier because of its unique mesoporous (2-50 nm) or even macroporous (>50 nm) lumen and its excellent biocompatibility. Drugs are normally anchored onto the external surface and the lumen surface of Hal *via* weak interactions such as hydrogen-bond and van der Waals force, but are hard to be directly intercalated into the interlayer space of Hal. As a result, Hal exhibited a low loading capacity for drugs, and this drawback severely limits the applications of Hal as a carrier in the fields of pharmaceuticals. In this study, organo-modification was applied to enhance the capacity of Hal for the loading of drugs and agrochemicals, and the effects of modification showed three possible mechanisms, as revealed by the following examples.

(1) The lumen surface of Hal was grafted by 3-aminopropyltriethoxysilane (APTES). When Hal was used as the carrier for ibuprofen (IBU, anti-inflammatory drug), the carboxyl groups of IBU was electrostatically attracted with the aminopropyl groups of modified Hal. This strong affinity enhanced the loading content of IBU from 11.7 mass% (for unmodified Hal) to 14.8 mass% (APTES-modified Hal); moreover, it retarded the *in vitro* release of IBU, and changed the IBU release mechanism from Fickian diffusion (for unmodified Hal) to non-Fickian diffusion (APTES-modified Hal).

(2) The interlayer surface of Hal was grafted by methanol leading to an increase of the  $d_{001}$  value (0.85 nm). When Hal was used as the carrier for 5-fluorouracil (5FU, anti-cancer drug), 5FU was intercalated in the interlayer space of methoxy-modified Hal in a roughly vertical monolayer arrangement. The 5FU loading content in methoxy-modified Hal was 45.0 mass%, which was almost twice the loading in unmodified Hal. The intercalated 5FU was in amorphous state. It had a high thermal stability because of the protection of the lamellar structure of Hal. The diffusion limitation function of the lamellar structure also led to a slow release of the drug. Moreover, the 5FU release was prolonged in simulated colonic fluid at pH 5.5 and in simulated intestinal fluid at pH 6.8, but exhibited a fast release in simulated gastric fluid at pH 1.2.

(3) Methoxy-modification could also make the interlayer space of Hal and kaolinite (Kaol) an additional space for the loading of amitrole (AMT, a herbicide). The AMT loading content in methoxy-modified Hal was 30.5 mass%, which was greater than that in methoxy-modified Kaol (20.8 mass%). The high loading capacity of Hal is attributed to the significant loading of AMT in the lumen of Hal. However, the methoxy-modified Kaol exhibited a slower release of AMT in comparison with the methoxy-modified Hal due to i) the higher proportion of the intercalated AMT in methoxy-modified Kaol, the diffusion of which was restricted by the lamellar structure; and ii) the longer diffusion path of intercalated AMT because of the larger size of Kaol particles than Hal particles.

These experimental results demonstrated that the organo-modification significantly promoted the performance of Hal as carriers for drugs and agrochemicals. The modified Hal is a potentially versatile carrier/support material in the pharmaceuticals, agriculture, and biochemistry industries.

**Acknowledgement:** This study was financially supported by the National Natural Science Foundation of China (Grant No. 41472045).

## Distribution of inorganic contaminants in a zeolite-sand reactive zone: laboratory column tests

Joanna Fronczyk\*, Kazimierz Garbulewski and Maja Radziemska

Warsaw University of Life Sciences – SGGW, Faculty of Civil and Environmental Engineering,  
Nowoursynowska Av. 166, 02-776 Warsaw, Poland; \*joanna\_fronczyk@sggw.pl

In the last few decades human activity has caused a negative impact on the quality of the groundwater environment. The main sources of groundwater pollution include e.g.: municipal waste disposals, industrial plants, as well as petroleum infrastructure or highways. There are a lot of commonly implemented methods of active environmental remediation that are often successfully applied, such as 'pump&treat', air-sparging or biodegradation. An alternative technique is the technology of reactive zones known as permeable reactive barriers (PRB) that involves the reduction of contaminant concentrations by physical and chemical processes. In designing PRBs, the most important step is the modelling of contaminated groundwater flow through the sorption reactive zone where all remediation processes take place.

The purpose of our tests was to estimate, under laboratory conditions: (1) the distribution of inorganic contaminants (copper and ammonium ions) along the reactive zone; (2) the influence of competing ions on the contaminants distribution; and (3) the intensity of Na, Ca and Mg release to the solution as a result of ion exchange processes.

The column experiments were carried out in seven columns (length 0.8 m, inner diameter 0.1 m) using two mixtures of natural zeolite with 0.5–1.0 mm particles (Slovak tuff, Nižny Hrabovec) and Vistula sand (50–50% and 80–20% of the column volume). A multichannel peristaltic pump (ISMATEC) was used to transport the solution through the columns (bottom–top) at a constant flow rate ( $4.16E-08$  m<sup>3</sup>/s). The tests were performed for a one-component model solution (100 mgCu/L) and a four-component model solution (100 mgCu/L, 360 mgNH<sub>4</sub><sup>+</sup>/L, 100 mgCa/L and 200 mgMg/L). Contaminated liquid samples were taken from 6 sampling points located at 0.16, 0.24, 0.30, 0.38, 0.48 and 0.63 m from the influent point using a syringe with a long needle in appropriate intervals. The metals (Cu, Na, Mg, Ca) were analyzed using atomic adsorption spectroscopy (AAS) (ICE-3000, Thermo Scientific, USA) and ammonium analysed using photometric methods. Electrical conductivities and pH values were also measured.

The performed studies confirm that with the increase of the cumulative volume of the solution, the contaminant front moves upwards in the column. Copper transport along the reactive zone decreased by 14 times in the case of ions competing for free space on the surface of the material.

The Cu concentration of  $0.5C_0$  (50 mg/L) in the mid-length of the reactive zone (0.4 m) was reached with a cumulative flow equal to 35 L/kg and 15 L/kg in the 50–50% and 80–20% mixtures, respectively. In the case of conditions of competing ions (Ca, Mg, NH<sub>4</sub><sup>+</sup>), the values were achieved with cumulative flows of 2.5 L/kg and 0.9 L/kg. The NH<sub>4</sub><sup>+</sup> concentration of  $0.5C_0$  (150 mg/L) was achieved with cumulative flows of 7.9 L/kg (50–50% mixture) and 1.9 L/kg (80–20% mixture). During the test with single and multi-component solutions, the copper ions were observed to be retained by ion exchange with ions that follow the order: Na≈Ca>>Mg. The magnesium concentration in the solution ranged from 0 to 4 mg/L, and the calcium and sodium concentration – from 0 to 80 mg/L. It can be concluded that the solution content has a great impact on the treatment processes in the reactive zone and the by-products may in some cases pollute groundwater.

## Ion exchange on zeolitized geopolymers

David Koloušek<sup>1</sup>, Barbora Dousova<sup>1</sup>, Miloslav Lhotka<sup>1</sup>, Heinrich Jencus<sup>1</sup>, Martina Urbanova<sup>2</sup>, Libor Kobera<sup>2</sup>  
and Roman Slavík<sup>3</sup>

<sup>1</sup> University of Chemistry and Technology Prague, Technická 5, 166 28 Prague 6, Czech Republic,  
david.kolousek@vscht.cz

<sup>2</sup> Institute of Macromolecular Chemistry AS CR, Heyrovsky sq. 2, 162 06 Prague 6, Czech Republic

<sup>3</sup> Thomas Bata University in Zlín, Faculty of Technology, T. G. Masaryka square 275,  
762 72 Zlín, Czech Republic

The organisation of the Si-O-Al(Si) units in geopolymers is not random. These units can create porous systems with cavities resembling zeolites structures. Heating of prepared geopolymers with variable Si/Al ratio leads to a change from "amorphous" arrangements to formation of various zeolite structures such as analcime, chabazite, zeolite P, zeolite X, zeolite A or hydroxy sodalite. Ion exchange properties of these zeolitic products depend on the matrix ratio of Si/Al.

Fig.1 shows the results of an immediate reduction in the concentration of  $\text{NH}_4^+$  from 64 mg/l and 10 mg/l (S/L ratio) respectively by geopolymeric zeolite type A. Similar results of ion exchange with natural clinoptilolite (Nizny Hrabovec - SK) and pure commercial zeolite A (Silchem) are also given for comparison. X-ray results show that ammonium is removed from deeper bulk at the same S/L ratio by geopolymer zeolite as the content of the active zeolite A reaches a maximum around 50%.

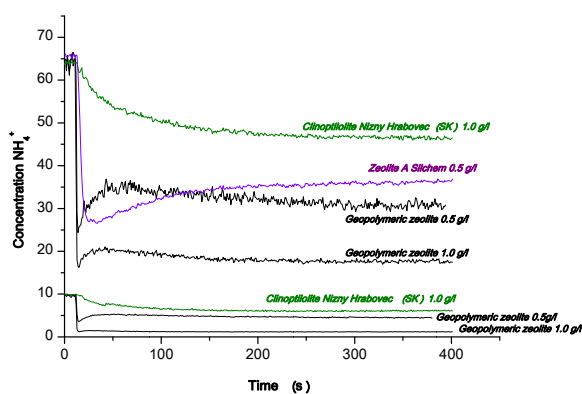


Fig. 1 – Kinetics of  $\text{NH}_4^+$  concentration changes in contact with geopolymeric zeolite, commercial zeolite A and natural zeolite clinoptilolite with various S/L ratio.

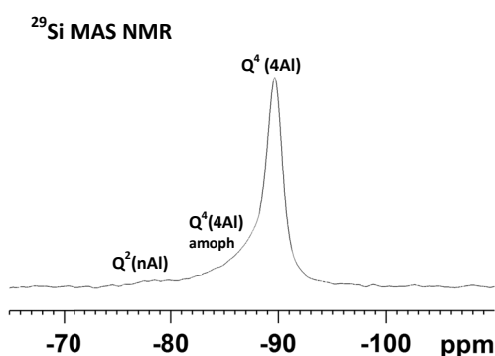


Fig. 2:  $^{29}\text{Si}$  MAS NMR spectrum of tested geopolymeric zeolite.

The explanation lies in the "arrangement" within the amorphous geopolymer phase as confirmed by  $^{29}\text{Si}$  MAS NMR measurements (Fig. 2). The composition of zeolite and amorphous phases is identical and corresponds to the ratio of Si/Al = 1, which corresponds to the homogeneous presence of Si (4Al) in both phases. Another parameter that facilitates an efficient ion exchange is the better accessibility of exchangeable positions in the more open geopolymer structure as compared to clinoptilolite or the commercial zeolite A.

**Acknowledgements:** This work was a part of project 13-24155S (Grant Agency of Czech Republic).

## Characterization of CsAlSi<sub>5</sub>O<sub>12</sub> obtained by thermal treatment of Cs-clinoptilolite

Mariano Mercurio<sup>1</sup>, Antonio Brundu<sup>2</sup>, Piergiulio Cappelletti<sup>3</sup>, Guido Cerri<sup>2</sup>, Bruno de Gennaro<sup>4</sup>, Mauro Farina<sup>2</sup>, Patrizia Fumagalli<sup>5</sup>, G. Diego Gatta<sup>5</sup> and Lorenzo Guaschino<sup>5</sup>

<sup>1</sup> Dipartimento di Scienze e Tecnologie, Università del Sannio, Via dei Mulini 59A, 82100 Benevento (Italy) – mariano.mercurio@unisannio.it

<sup>2</sup> Dipartimento di Scienze della Natura e del Territorio, Sassari University, Via Piandanna 4, 07100 Sassari (Italy)

<sup>3</sup> Dipartimento di Scienze della Terra, dell'Ambiente e delle Risorse, Università Federico II, Via Mezzocannone 8, 80134, Napoli (Italy)

<sup>4</sup> Dipartimento di Ingegneria chimica, dei Materiali e della Produzione Industriale, Università Federico II, Piazzale Tecchio 80, 80125, Napoli (Italy)

<sup>5</sup> Dipartimento di Scienze della Terra, Università di Milano, Via Botticelli 23, 20133 Milano (Italy)

Clinoptilolite is a zeolite employed for cesium decontamination. Thermal treatments are generally used to prevent Cs<sup>+</sup> release from spent clinoptilolite. Temperatures up to 1300-1500 K are required to attain an almost complete Cs immobilization in a glassy matrix [1]. The protocol to obtain crystalline CsAlSi<sub>5</sub>O<sub>12</sub> (CAS) by thermal treatment of Cs-clinoptilolite, as a potential host for radioactive cesium [2], was recently reported by Brundu and Cerri [3]. However, the structural refinement of the obtained compound (*i.e.*, CsAlSi<sub>5</sub>O<sub>12</sub>) was not performed, and its thermal and chemical stability were not studied. In this study, a Sardinian zeolite was used to prepare a clinoptilolite-rich powder by authogenous comminution, dry sieving and wet separations. The material (clinoptilolite ≈ 90 wt.%) was initially Na-, then Cs-exchanged, reaching a cesium content of 22.5 wt.%. Cs-aluminosilicate glass and a crystalline compound with chemical formula CsAlSi<sub>5</sub>O<sub>12</sub> were prepared by heating the Cs-clinoptilolite for 2h at 1323 K and 1473 K, respectively. Density increased from 2.57 to 2.85 g/cm<sup>3</sup> with the transformation Cs-clinoptilolite → CsAlSi<sub>5</sub>O<sub>12</sub>. Chemical analyses of CAS were also performed by SEM/EDS on polished thin sections, from epoxy resin-embedded samples, and the results gave average analyses of CAS with 25.8 % wt. Cs<sub>2</sub>O. Impurities of Ca-plagioclase were also detected.

Samples of Cs-aluminosilicate glass and CsAlSi<sub>5</sub>O<sub>12</sub> were subjected to release control tests (reverse exchange and availability AVA [1] test) in order to evaluate the effective immobilization of Cs. Reverse exchange tests showed that amorphous Cs-aluminosilicate glass released 1.10 mg/g of Cs, while CsAlSi<sub>5</sub>O<sub>12</sub> does not release any Cs (below L.O.Q). As far as AVA tests are concerned, the amorphous Cs-aluminosilicate glass releases 1.94 mg/g of Cs<sup>+</sup> and CAS displays a value of 0.05 mg/g.

For a structural characterization of CsAlSi<sub>5</sub>O<sub>12</sub>, synchrotron powder diffraction data were collected and the Rietveld refinement was performed (to  $wR_p = 0.05$  and  $R_f = 0.11$ ), proving that the material has the CAS-type structure as previously reported by Gatta et al. [2] (with  $a=16.775(1)$ ,  $b=13.8301(6)$ ,  $c=5.0548(2)$  Å, space group: *Ama2*). *In-situ* high-temperature powder diffraction data were collected up to 1700 K. The diffraction patterns showed that the crystallinity of this compound decreases at  $T>1400$  K and an irreversible amorphization occurs between 1600 and 1650 K.

One of the most important findings of this preliminary characterization is demonstrated by the minor amount of Cs released by the crystalline material compared to its amorphous counterpart.

[1] Cappelletti et al., J. Nucl. Mater., 414 (2011), 451-457. [2] Gatta et al., Phys. Chem. Miner., 35 (2008), 521-533. [3] Brundu and Cerri, Microporous Mesoporous Mater., 208 (2015), 44-49.

## Temperature effects on cathodoluminescence of hydrous minerals

Hirotsugu Nishido

Department of Bio-Geosphere Science, Okayama University of Science, Japan, nishdio@rins.ous.ac.jp

Cathodoluminescence (CL), the light emission induced by electron irradiation, has been widely applied in mineralogical and petrological investigations. The nature of a CL emission results from an intrinsic (lattice defects) and/or extrinsic (impurities) centers in the lattice of minerals. CL analytical methods enable observations of trace element distributions and defects in the lattice, which are difficult to detect with other techniques. Furthermore, luminescence emission depends on sample temperature, but the temperature effect on the CL of hydrous minerals including zeolites and clay minerals, has not been investigated so far. A scanning electron microscopy-CL (SEM-CL) instrument was used to collect CL spectral measurements of natural zeolites with high resolution at various temperatures. In this study, CL characterization of several zeolites and clay minerals has been conducted to clarify unusual effects of sample temperature on their CL emissions.

CL measurements have been performed for zeolites (bikitaite, brewsterite, erionite, ferrierite, gonnardite, harmotome and stilbite) and clay minerals (kaolinite and serpentine minerals). CL spectra and CL images were obtained employing a new system of CL-SEM, which comprises a SEM (Jeol JSM-5400) combined with an integral grating monochromator (Oxford Mono CL2) with high sensitivity and high spatial resolution over the wide wavelength range of 300 nm to 800 nm. The sample stage can be controlled at various temperatures from  $-194\text{ }^{\circ}\text{C}$  to  $400\text{ }^{\circ}\text{C}$  using a cryo-stage. The system was operated at 15 kV with 1 nA to 2 nA incident beam current in a scanning mode (X1000) to prevent the surface damage of the sample by electron bombardment. All CL spectra were corrected for the total instrumental response.

In general, luminescence efficiency decreases with rising temperature due to an increase in non-radiative transitions. This phenomenon has been recognized in a number of different materials as temperature quenching. Most of the hydrous minerals analysed here, however, show various responses of CL intensities to sample temperature depending on the minerals, which are inexplicable by temperature-quenching theory. Such phenomena have not been previously reported.

CL spectra of brewsterite, a Ba/Sr bearing zeolite, at around 500 nm indicate a notable reduction of CL intensity with a decrease in sample temperature, suggesting temperature sensitizing. The luminescent efficiencies at individual temperatures were quantitatively estimated from the integrated intensity calculated by a Gaussian fit. Arrhenius plots reveal two straight-line relationships indicating different kinds of temperature sensitizing mechanisms, which can be clearly explained on the basis of Mott-Seitz theory. The CL of this zeolite has two temperature sensitizing processes with a low activation energy of approximately 0.05 eV from  $-194\text{ }^{\circ}\text{C}$  to  $-50\text{ }^{\circ}\text{C}$  and a high activation energy of approximately 0.51 eV from  $-50\text{ }^{\circ}\text{C}$  to  $50\text{ }^{\circ}\text{C}$ . The former might be nearly the same order of energy related to an O-Si(Al)-O bending vibration, and the latter to an O-H stretching vibration. At lower temperatures the sensitizing energy for a radiative transition could be transferred from the lattice vibration in the T-O framework, and at higher temperatures pronounced sensitizing energy could come from water molecule vibrations in a channel.

Kaolinite, dickite and nacrite give CL emissions in the blue spectral region with a broad band peak at around 390 nm, which can be assigned to radiation induced defect centers (RID) presumed from EPR investigations. These minerals show almost the same degree of change in CL intensity against sample temperature. The intensity increased on heating above  $-50\text{ }^{\circ}\text{C}$ , and up to its maximum at  $40\sim 60\text{ }^{\circ}\text{C}$ , and then reduced on further heating. Arrhenius plots based on the Mott-Seitz model result in activation energy in a temperature-quenching process;  $0.50\sim 0.62\text{ eV}$  in the increasing process of CL intensity from  $-50$  to  $40\text{ }^{\circ}\text{C}$  and  $0.43\sim 0.66\text{ eV}$  in the diminishing process above  $60\text{ }^{\circ}\text{C}$ . The value of such energy profiles corresponds to that of the O-H stretching vibrations characteristic of kaolin group minerals, suggesting that the energy transfer as phonons occurs in a temperature quenching process above  $60\text{ }^{\circ}\text{C}$ . On the other hand, the same amount of energy in temperature sensitizing processes below  $60\text{ }^{\circ}\text{C}$  were induced by the lattice vibration.



## Modification of Philippine natural zeolites by copper loading for *Escherichia coli* inactivation

Eleanor Olegario-Sanchez<sup>1</sup>, Michael Tan<sup>2</sup> and Mary Donnabelle Balela<sup>3</sup>

<sup>1</sup>Department of Mining, Metallurgical, and Materials Engineering, University of the Philippines, Diliman, Quezon City, 1101, Philippines; <sup>1</sup>eleanor.olegario@gmail.com, <sup>2</sup>mikertan@gmail.com, <sup>3</sup>mdlbalela@gmail.com

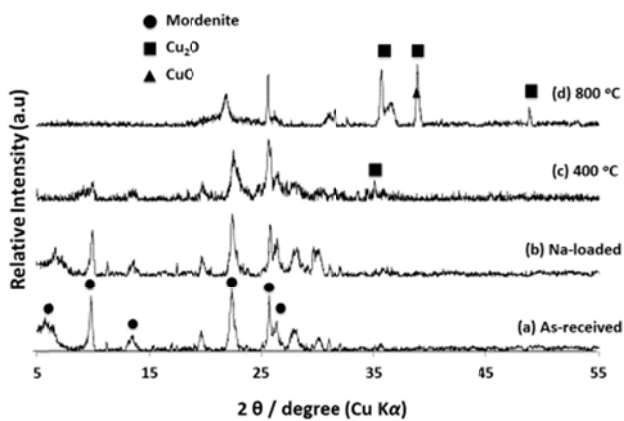


**Figure 1.** XRD pattern of the (a) as-received natural zeolite sample from Mangaterem, Pangasinan, (b) Na-loaded natural zeolite, (c) calcined Cu-loaded zeolite at 400°C and (d) calcined Cu-loaded zeolite at 800°C.

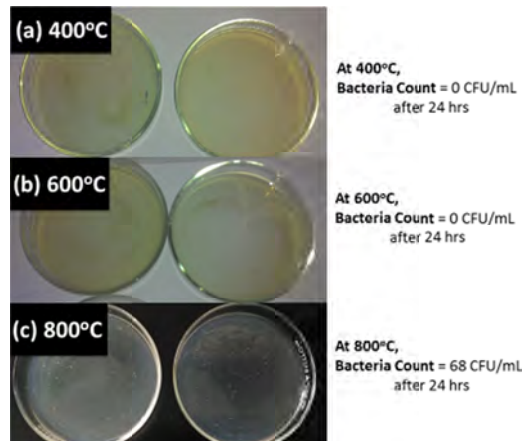


**Figure 2.** Swab inoculated samples using zeolite calcined at 400, 600, and 800°C showing bacterial growth in agar media of calcined zeolite and its serial dilutions (0.01, and 0.001 %) against *E. coli* after 24 h.

The antibacterial properties of copper have been widely reported and used as coatings in a variety of surfaces in such as medical devices, birth control devices, appliances, sanitation pipelines, and self-sterilizing packages [1-5]. However, one problem with copper in antibacterial applications such as filters is that it can easily leach out [6]. One way to address this problem is by using natural zeolites to act as cages for copper and locking it in place [7]. This study reports the modification of Philippine natural zeolites, sourced from Mangataram, Pangasinan, by copper doping and its use in *E. coli* inactivation. The effect of calcination temperature on the structure and its relation to the antibacterial properties is discussed.

Zeolite samples were de-aluminized by soaking in 1 M HCl for 24 h. The sample was washed several times until the pH of the supernatant became neutral. Then, the sample was soaked in 1 M NaOH for 24 h, washed thoroughly, and dried at 110 °C. Next, 100 g of zeolite was mixed in 1 L of deionized water containing 25 wt.% copper sulfate. The slurry was rotated gently and soaked for 12, 24, and 48 h. The samples were then calcined at 400, 600, and 800°C for 2 h.

The antimicrobial property of the samples was tested against *Escherichia coli* (*E. coli*) using an agar slurry test (ASTM E2180). First, a suspension of *E. coli* was prepared from a 24 hr old culture using 0.1% peptone water as diluent. Next, 0.25 g of each zeolite sample was added into 10 mL of the working suspension and was held for 24 h. After, the samples were plated in agar and bacterial growth was recorded.

Calcination at 400 and 600°C enhanced the stability of copper inside the zeolite, thereby effectively killing *E. coli* bacteria even at very low concentrations of 3 ppb. It is more economical to produce copper zeolite calcined at 400°C and might be beneficial to enhance inactivation of *E. coli* for various applications such as filter media, coatings on hard surfaces, and additives to plastics and textiles.

[1] X. Bilian, *Intrauterine devices*, Best Pract Res Clin Obstet Gynaecol 16: 155-68, 2002

[2] G. Borkow, J. Gabbay, *Putting copper into action: copper-impregnated products with potent biocidal activities*, Faseb J 18: 1728-30, 2004.

## Long-term immobilization method for radioactive cesium-137 using hydrothermal synthesis of zeolite from coal fly ash

Yujiro Watanabe<sup>1</sup>, Koki Kitanaka<sup>1</sup>, Kaoru Fujinaga<sup>1</sup>, Syunichi Oshima<sup>1</sup>, Hirohisa Yamada<sup>2</sup> and Yu Komatsu<sup>1</sup>

<sup>1</sup>Department of Applied Chemistry, College of Bioscience and Chemistry, Kanazawa Institute of Technology, 3-1 Yatsukaho, Hakusan, Ishikawa 924-0838, Japan

<sup>2</sup>Environmental Remediation Materials Unit, National Institute for Materials Science, 1-1 Namiki, Tsukuba, Ibaraki, 305-0044 Japan

As a result of the accident at the Fukushima Daiichi nuclear power plant following the 9.0 magnitude Tohoku earthquake and Tsunami disaster on 11 March 2011, radioactive substances, mainly cesium-137 and cesium-134 were released into the atmosphere and polluted urban areas, agriculture lands, forests, lakes and seawaters around the Tohoku area in Japan. The recovery and the long term storage of radioactive cesium-137 which has a long half-life of 30 years is of great importance for environmental remediation of the Tohoku area. Zeolites are porous aluminosilicates with high specific areas and ion-exchange abilities. Harmful cations and molecules can be absorbed into channels and cages in these materials. Synthesis of high-quality zeolites, such as NaP1 type zeolite, zeolite X, sodalite and analcime by hydrothermal treatment of various materials, such as coal fly ash<sup>1-2)</sup>, smectite, kaolinite, bentonite and natural zeolites, has been reported. Analcime is a well-known natural zeolite. It has the structure  $X_{16/m}(\text{Si}_{32}\text{Al}_{16}\text{O}_{96}) \cdot 16\text{H}_2\text{O}$ , where X is a cation and m is the charge number, of which the pore size is 0.24 nm. The pore size is smaller than a cesium ion diameter of 0.36 nm. Therefore the uptake of cesium ion using hydrothermal synthesis of analcime may be useful as barriers for the long term storage of cesium ions.

In this study, analcime, as a main component, was hydrothermally synthesized from coal fly ash in CsCl solution treated with  $1.0 \text{ mol}\cdot\text{dm}^{-3}$  NaOH at 200°C for 24 hours. The recovery of the cesium ion on the product was more than 85 %. The elution percentage of cesium ion on the product in pure water was less than 0.25%. These results are caused by the pore size of analcime being smaller than the cesium ion diameter. This method is very useful as one of the stabilization methods of the radioactive cesium-137.

**Acknowledgment:** This work supported by a Grant-in-Aid for Scientific Research (26820308) from the Japan Society for Promotion of Science.

[1] Okada Y, Synthesis of zeolite using fly ash on closed system. *Jpn. J. Soil Sci. Plant Nutr.* **62**, 1-6 (1991).

[2] Querol X, Plana F, Alastuey A, and Lopez A, Synthesis of Na-zeolites from fly ash. *Fuel.* **8**, 793-799 (1997).

## Quantitative modeling of XRD patterns of natural bentonites

Youjun Deng\*, and Ana L. Barrientos Velázquez

Department of Soil & Crop Sciences, Texas A&M University, College Station, Texas, USA: \*yjd@tamu.edu

Bentonites occur worldwide and are mined in at least 23 countries with an annual production of more than 14.4 million metric tons. They have a wide range of industrial, environmental, domestic, and agricultural applications including drilling fluid, pet litters, metal casting, pelletizing iron ore, civil engineering, waterproofing and sealing, animal feed, fillers and extenders, filtering and clarifying decolorizing, and detoxification. To better serve these diverse applications, quantifying mineral compositions of the bentonites is often required. With increasing popularity of the Rietveld method for mineral quantification, it is possible to quantify the highly crystalline phases such as quartz, gypsum, feldspars, mica in the bentonites with reasonable accuracy. Several articles have also reported incorporating simulated smectite models in Rietveld analysis. In addition to the contents of minerals, several other properties of smectites in bentonites can have determinative roles in the applications. These properties include the type of smectites in the clays, exchange cation composition, layer structural defects, layer stacking disordering, charge sources (tetrahedral vs. octahedral), octahedral sheet cation composition, interstratification with other 2:1 minerals. In theory, a successful modeling of the X-ray diffraction (XRD) pattern of a natural bentonite should yield all of these types of information. Yet, such modeling in routine mineral analysis is rarely conducted due to the lack of a robust mathematical method to describe the different smectites encountered in different bentonites. The objectives of this study are: 1) to summarize the major methods and programs used in modeling smectite minerals in bentonites reported in the literature, and 2) to select and modify the methods for quantitative mineral analysis based on frequent mineral assemblages found in natural bentonites.

Bentonites with a variety of smectite compositions, including low and high cation exchange capacity (CEC) montmorillonite, saponite, beidellite, hectorite, and nontronite, were selected in the study. The clay fractions of these samples were collected to concentrate the smectites for detailed characterization with chemical (CEC) and spectral and microscopic (FTIR and HRTEM) methods. These analyses offered the baseline structural information about the smectite minerals in the bentonites. Program NEWMOD was used to simulate the 1-D XRD patterns of the oriented clay films after Mg- and K-saturation, glycerol solvation, heating treatments to extract structural information of the smectite. We attempt to incorporate this baseline information in the structural models of smectites used in the Rietveld quantification.

The natural bentonites were spiked with known amounts (10% wt) of ZnO, micronized in 200 proof ethanol, spray dried at 130 °C to achieve uniform particle size and random orientation for quantitative XRD analysis. The Rietveld method will be used to simulate the experimental XRD patterns of the natural bentonites. Program TOPAS will be used in the Rietveld analysis. The smectite contents from Rietveld analysis will be compared with the contents obtained based on CEC and charge density of the smectites. Progress and challenges will be reported.

## **XRD at the Geological Survey of Norway – The BASE project**

Jasmin Schönenberger<sup>1</sup> and Jochen Knies<sup>1</sup>

<sup>1</sup>Geological Survey of Norway (NGU), Leiv Eirikssons Vei 39, 7040 Trondheim, Norway [jasmin.schoenenberger@ngu.no](mailto:jasmin.schoenenberger@ngu.no)

The analytical facilities at the Norwegian Geological Survey (NGU) comprise a suite of standard inorganic analytical techniques like XRF, SEM, (LA) ICP-MS, ICP-OES, AAS, IC along with CNS and grain size distribution analyses. Recently, NGU has acquired a new Bruker D8 Advance diffractometer with a LYNXEYE XE (1D) detector to enhance its capability to characterise different rock types and to quantify their mineralogical composition. The applications are manifold: they range from geological mapping, mineral resources and geohazards (e.g. quickly identifying clay occurrences) to the characterisation of carbonates. Analytical service is provided mainly for internal customers, but external enquiries are also handled.

A recently launched 4 year project is the BASE project that focuses on basement fracturing and weathering on- and offshore Norway. The main goal is to constrain the spatial and temporal evolution of fracturing, faulting, deep-weathering and saprolite genesis. This is particularly interesting for the oil industry as oil reservoirs have been discovered in such deeply weathered basement rocks and computer models aim to simulate hydrocarbon migration in such host rocks.

The new XRD will play a key-role in the characterisation of saprolite samples and the identification of illite polytypes. While 2M1 illites are commonly detrital in origin, 1Md polytypes are typically diagenetic (Bailey, 1966). Once the polytypes have successfully been identified in different grain size fractions, the newly established K/Ar dating facility will shed light on the temporal evolution of the fracturing history of the basement and will help to correlate weathering processes.

The poster presentation discusses first results of XRD analyses on weathered and fresh rock samples and will focus the combination of XRF and XRD analysis for better characterisation.

Bailey SW. 1966. The status of clay mineral structures. Proceedings of the 14th National Conference on Clays and Clay Minerals. New York: Pergamon Pr. p 1-23.

See abstracts by

Mark Raven

Michael Plötze

M. Szczerba and D. McCarty

S. Hillier

K. Ufer

A. Derkowski and Stefan Kaufhold

in the oral abstracts session, pp. **171–176**

## Role of iron oxy-hydroxides on metal retention in marsh soils of the Domingo Rubio coastal wetland (SW Spain)

C. Barba-Brioso<sup>1</sup>, J. Delgado<sup>2</sup>, J.C. Fernández-Caliani<sup>3</sup>, A. Miras<sup>1</sup> and E. Galán<sup>1</sup>

<sup>1</sup> Dpto. Cristalografía, Mineralogía y Química Agrícola. Faculty of Chemistry. University of Seville. 41072 Seville, Spain.  
cbarba@us.es

<sup>2</sup> CIMA Centro De Investigação Marinha e Ambiental. University of Algarve, 8005-139 Faro, Portugal.

<sup>3</sup> Dpto. Geología. University of Huelva. 21071 Huelva, Spain

Salt marsh soils (Salic fluvisols) developed in the tidal-affected area of the Domingo Rubio wetland (SW Spanish Atlantic coast) today preserve the effects of multi-source pollution problems derived from a variety of human activities, including intensive industrial, mining and smelting operations, and agricultural land uses (*Barba-Brioso et al. 2010*).

Fifteen randomly selected soils from the wetland were sampled at the surface and at 5cm depth. In addition one surficial bottom sediment sample from a lagoon was also taken. These materials were mineralogically and chemically analyzed by XRD, XRF, SEM-EDS, IC, and ICP-OES). The results showed that Fe compounds are abundant in the wetland soils, with a total Fe content of up to 13.1% expressed as Fe<sub>2</sub>O<sub>3</sub>. Elevated pseudo-total concentrations of Fe (up to 5.58%) and potentially toxic trace elements, notably As (up to 406 mg kg<sup>-1</sup>), Cd (up to 4.26 mg kg<sup>-1</sup>), Cu (up to 2160 mg kg<sup>-1</sup>), Pb (up to 591 mg kg<sup>-1</sup>), and Zn (up to 2048 mg kg<sup>-1</sup>) were also found.

A single extraction scheme was employed to investigate the selective leaching of trace metal/loids bound to the Fe oxy-hydroxides, using the combined action of 0.04M hydroxylamine hydrochloride (NH<sub>2</sub>OH.HCl) and 25% v/v glacial acetic acid (HOAc), at two different temperatures, 30°C and 96°C (*Fortin et al., 1993*). The extraction results revealed that all the analyzed trace elements, except Cd, are bonded to Fe oxy-hydroxides in proportions higher than 30% of the pseudototal Fe. Iron extracted from crystalline phases (hematite with minor goethite as inferred by XRD) accounted for 24.8 % of the total Fe, whereas a small proportion (8.5 %) was accounted by poorly crystalline or amorphous Fe.

Arsenic and Pb appear mainly associated with well-crystallized phases in all samples, as they were preferentially extracted with NH<sub>2</sub>OH.HCl+HOAc at 96°C. In contrast, the amorphous and/or poorly-crystallized Fe oxy-hydroxides seem to be efficient scavengers of Cu and Zn in the surface soil, because the largest proportions of such metals were extracted with the treatment performed at 30°C. Nevertheless, unlike Cu, in the subsurface soil samples Zn was rather retained in crystalline Fe oxy-hydroxides.

In conclusion, the Fe oxy-hydroxides play a significant role in controlling the mobility of potentially toxic trace elements in the wetland. Chemical partitioning of trace elements among the Fe compounds is critically dependent on whether the solid phase is amorphous or crystalline.

Barba-Brioso, C., Fernández-Caliani, J.C., Miras, A., Cornejo, J., Galán, E. (2010). Multi-source water pollution in a highly anthropized wetland system associated with the estuary of Huelva (SW Spain). *Marine Pollution Bulletin*, 60, 1259-1269.

Fortin, D., Leppard, G.G. and Tessier, A. (1993). Characteristics of lacustrine diagenetic iron oxyhydroxides. *Geochimica et Cosmochimica Acta*, 57, 4391-4404.

## Study of titanium-synthetic montmorillonite interactions by XRD, chemical analysis, solid state $^{27}\text{Al}$ , $^{29}\text{Si}$ and $^{19}\text{F}$ MAS NMR spectroscopy and synchrotron-based X-ray techniques

Jocelyne Brendlé<sup>1</sup>, Jeffrey Huve<sup>1</sup>, Daniel Grolimund<sup>2</sup>, Paul Wersin<sup>3</sup>, Leena Kiviranta<sup>4</sup> and Margit Snellman<sup>5</sup>

<sup>1</sup> Pôle Matériaux à Porosité Contrôlée, Institut de Science des Matériaux de Mulhouse, UMR CNRS 7361, Université de Strasbourg-Université de Haute-Alsace, 3b rue A. Werner, 68093 Mulhouse Cedex, France Jocelyne.Brendle@uha.fr

<sup>2</sup> Paul Scherrer Institute, CH-5232 Villigen, Switzerland

<sup>3</sup> University of Bern, Institute of Geological Sciences, CH-3012 Bern, Switzerland

<sup>4</sup> B+ Tech Oy, FIN-00420 Helsinki, Finland

<sup>5</sup> Saanio & Riekkola Oy, FIN-00420 Helsinki, Finland

Posiva, an expert organisation jointly owned by Finnish nuclear utilities Fortum and TVO, and SKB, the Swedish Nuclear Fuel and Waste Management Company are developing a method, termed KBS-3H, in which several spent nuclear fuel canisters are emplaced horizontally in deposition drifts (SKB/Posiva 2013). In this design, an assembly of a Cu-waste canister surrounded by bentonite blocks is placed in a perforated shell, a so-called supercontainer (SC), before emplacement in the deposition drift. The currently selected material for the SC is titanium. Ti-based materials display high strength and are known to behave chemically inert under a variety of conditions. This study addresses the suitability of titanium as supercontainer material with regard to the performance of the clay buffer. The aim is to determine how titanium (powder or foil) can interact with synthetic Ti-free montmorillonite and in particular whether Ti can be incorporated in the interlayer space, on the clay edges, or if it can be incorporated in the octahedral sheet of the clay layer. Experiments were conducted in 0.1 M NaCl solutions at different pH (2, 7 and 12) and temperature (80°C and 200°C) conditions. After different time intervals, Ti metal and clay materials were separated and analysed by wet chemistry and spectroscopic methods. In the case of montmorillonite and montmorillonite-titanium samples, X-ray diffraction was used to analyse the structure of the samples and the interlayer space between stacked clay platelets.  $^{27}\text{Al}$ ,  $^{29}\text{Si}$  and  $^{19}\text{F}$  MAS solid state NMR were used to investigate the solid samples prior and after experiments. It is worth notifying that the different treatments undergone by the montmorillonite, particularly in alkaline conditions, are the sources of various modifications of the clay structure. In alkaline conditions, a decrease in the amount of hexacoordinated aluminum as well as an increase of *tetracoordinated aluminum components were indeed evidenced by  $^{27}\text{Al}$  MAS NMR*. Scanning electron microscopy has provided information on the morphology of the clay, which seems to modify slightly with time and test conditions. Synchrotron-based X-ray techniques were employed to analyse the interaction of the released Ti with the clay material. First, X-ray Fluorescence (XRF) served to quantify the association of Ti with the clay. After measurable quantities being observed, X-ray Absorption Spectroscopy (XAS) techniques (XANES and EXAFS) were applied to obtain molecular-level information on the Ti reaction products. Findings from preliminary analysis are consistent with a structural incorporation of Ti into octahedral sites of the clay structure.

The employed innovative strategy allows the development of a molecular-level understanding of clay barrier modifications induced by the corrosive release of Ti.

## Comparing a modified low-value clay with commercial samples to remove pesticides from water

M. Carmen Hermosín, Miguel Real, Esperanza Duran, Salvador Bueno, Lucia Cox, Rafael Celis, [Juan Cornejo](mailto:cornejo@irnase.csic.es)  
(cornejo@irnase.csic.es)

<sup>1</sup>Instituto de Recursos Naturales y Agrobiología de Sevilla, CSIC (IRNAS-CSIC), Avda. Reina Mercedes 10, 41012 Seville, Spain; <sup>2</sup> Centro Tecnológico Innovarcilla

Clays, as natural materials or after diverse chemical modifications, have been widely studied in the last decades as possible adsorbents to remove pesticides or other organic contaminants from water<sup>1,2</sup>. The contamination of water, besides its scarcity, is encouraging research in water purification technologies. Rural environments suffer especially from water contamination because intensive crop management has increased the pesticide use, which then contaminate the surface and ground waters. Also, the after-crop processing industries produce waste water containing pesticides. This is a very serious concern in a region where a monoculture is established, as in Andalusia and many regions of the Mediterranean countries where hundreds of thousands of olives orchard are set up, causing contamination in their water bodies. These rural environments need the development of low-cost water purification technologies for small villages, scattered farmer houses or even small agro-industrial installations. This is the final target of our research, to look for low cost adsorbents to be used in filter systems for medium and small scale enterprises to remove pesticides from water.

Several commercial clays (Cloisites and Bentonites SD, >95% smectite content) were assayed together with a local clay sample of low value because of its low (30%) smectite content (CTI from Bailen, Jaen, Spain), which was increased up to 60% after carbonate removing (CTIwc). The CTIwc sample was saturated in Fe<sup>3+</sup>, hexadecyltrimethylammonium (CTI-Fe<sup>3+</sup> and CTI-HDTMA) and the polymer chitosan (CTI-CH4 and CTI-CH6). The clays assayed and their organic elemental analyses are summarized in TB1. The modified CTI clay was subjected to a granulation process with a natural polymer (carboxymethyl cellulose and wax) in order to get water resistance. The pesticides were selected as having a representative diverse chemical character as shown in TB2. The water was artificially contaminated with 1ppm of each compound and the adsorption measured using 20mg of clay in 8ml of water. The pesticides were analyzed by HPLC with diode-array detection.

TB1/Clay	C (%)	N(%)	H(%)
CTIwc	0.43	<0.05	0.81
CTI-HDTMA	8.49	0.5	1.95
CTI-Fe	-	-	-
CTI-CH4	7.65	1.28	1.93
CTI-CH6	19.63	3.64	3.79
Cloisite 15	33.87	1.08	6.31
Cloisite 20	28.41	0.93	5.36
Cloisite 30B	19.51	3.78	0.91
Bentonite SD1	37.70	1.12	6.4
Bentonite SD3	33.52	0.98	5.68
Bentonite EW	0.63	<0.05	0.89
Nanomer <sup>®</sup> Clay	28.85	1.35	-

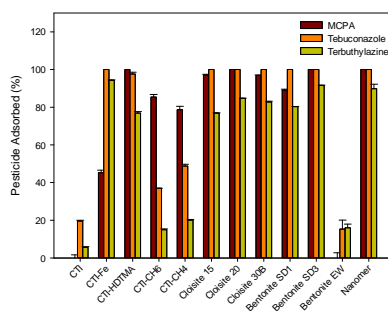


Figure 1. Simultaneous adsorption of the pesticides on the diverse clays from water.

TB2/Pesticide	pK <sub>a</sub>	Water Sol.(mg/l)
MCPA	3.7 Weak acid	293.9
Terbutylazine	1.9 Weak base	8.5
Tebuconazole	5.0 Weak base	36

The results show that the Fe<sup>3+</sup>- and HDTMA-CTI samples are as efficient for removing the assayed pesticides as the commercial clays. The initial granulation methods resulted in a small decrease in the pesticide sorption capacity, which ranged from 20% to 70%. Current trials with diverse polymers and composition ratios show that it is possible to reach a compromise between the water resistance and strength of the granules with an acceptable pesticide adsorption capacity. The results showed in this work open new possibilities for clay-polymer composites and at the same time that they offer potential practical solutions for applications in water purification.

**Acknowledgments:** Grants P11-07400 and AGR-264 by Junta de Andalucía, Contract RECUPERA2020 MINECO-CSIC and Grant AGL2011-23779 by MINECO, all of them cofinanced with EU FEDER-FSE funds.

<sup>1</sup>Cornejo et al. 2008. *Clay Minerals* 43, 155; <sup>2</sup>Unuabonah EI & Taubert A. 2014. *Appl. Clay Sci.* 99, 83.



## Sorption of copper and nickel ions from solution with clay minerals

Ali Rıza Demirkiran<sup>1,2</sup>, Bilal Acemioğlu, Tuğba Gönen<sup>4</sup>

<sup>1</sup> University of Bingol, Faculty of Agriculture, Department of Soil Science and Plant Nutrition Bingol, Turkey

<sup>2</sup> University of Wolverhampton, Faculty of Science and Technology, Wolverhampton WV1 1LY, UK

<sup>3</sup> Kilis 7 Aralık University, Faculty of Art and Science, Kilis, Turkey

<sup>4</sup> Agricultural Engineer, MSc, Kahramanmaraş, Turkey

In this study, the adsorption of Cu(II) and Ni(II) ions onto a white clay of the montmorillonite group obtained from the Kahramanmaraş Region was investigated. The effects of the amount of clay used, the initial metal ion concentrations, pH and temperature on sorption were studied. The results showed that increases in the clay amount, initial metal ion concentrations, pH and temperature led to the increases in the metal ion sorption. The competitive sorption of Cu(II) and Ni(II) ions was studied at various pH and temperature conditions and more Cu(II) ions were sorbed than Ni(II) ions. Thus, the clay had a high sorption capacity for metal ions. The sorption of Cu(II) and Ni(II) ions by the clay was in the range of 92.3–100% and 90.26–97.82% under all experimental conditions, respectively.

**Key words:** sorption, clay, copper, nickel.

## Interaction of *Pseudoxanthomonas kaohsiungensis* with bentonite

Argha Chakraborty<sup>1,2,3\*</sup>, Binoy Sarkar<sup>1,2§</sup>, Bhabananda Biswas<sup>1,2</sup> and Ravi Naidu<sup>1,2</sup>

<sup>1</sup> Center for Environmental Risk Assessment and Remediation, University of South Australia, Adelaide, 5095, Australia

<sup>2</sup> Cooperative Research Centre for Contamination Assessment and Remediation of the Environment, P.O. Box 486, Salisbury, SA 5106, Australia

<sup>3</sup> Renal Research Lab, Biomedical Research Centre, VIT University, Vellore 632014, Tamil Nadu, India

\*argha.chakra@gmail.com; §binoy.sarkar@unisa.edu.au

*Pseudoxanthomonas kaohsiungensis* is a biosurfactant producing bacteria capable of growing in highly oil contaminated areas [1]. The constituents of the biosurfactant include lipopeptide, glycolipid, polysaccharide-protein complex and fatty acid type compounds which can potentially enhance the bioavailability of organic contaminants in contaminated sites [2]. Such enhancement in bioavailability is likely to occur through a reduction in surface tension at the contaminant-mineral-water interface.

Clay minerals can influence the growth and functioning of bacteria by providing habitat support and nutrients [3]. Being an inexpensive and abundant resource, clay minerals can easily be used as a support material for increased biosurfactant production by bacteria, which may assist in the development of a stable biofilm and promote effective biodegradation of contaminants.

To this end, this research examines the growth and biosurfactant production ability of *Pseudoxanthomonas kaohsiungensis* in the presence of an Australian bentonite clay and characterises the clay-bacteria interaction through multiple techniques such as Scanning Electron Microscopy (SEM) coupled with Energy Dispersive X-Ray Spectroscopy (EDAX) analysis, X-ray Diffraction (XRD), Fourier Transformed Infrared (FTIR) spectroscopy, Thermogravimetric Analysis (TGA) and Inductively Coupled Plasma Mass Spectrometry (ICP-MS).

Presence of bentonite in the culture media increased the bacterial colony forming units (CFU) by 25% and thus contributed to enhanced biosurfactant production. Spherical shaped bacteria-clay agglomerates were observed under the SEM. Thermal characteristics confirmed the deposition of organic compounds on the bentonite surface. FTIR studies further indicated modifications of functional groups on the clay surface due to its interaction with the bacteria. XRD examination revealed a slight expansion (0.54Å) of the clay inter-layer following bacterial exposure. The interaction also indicated dislodging of structural elements (Si and Al) from bentonite in the bacterial growth media.

This study indicated enhanced growth and biosurfactant production by *Pseudoxanthomonas kaohsiungensis* in the presence of bentonite clay, which could be further explored in order to develop a clay minerals-assisted green technology for persistent organic contaminants remediation.

**Keywords:** Clay-bacteria interaction, biosurfactant, environmental remediation

[1] Chang, J.-S., et al., 2005, Systematic and Applied Microbiology 28: 137-144.

[2] Lai, C.-C., et al., 2009, Journal of Hazardous Materials 167: 609-614.

[3] Rogers, J.R. and P.C. Bennett., 2004, Chemical Geology 203: 91-108.

## Combined fine-size substrates for remediation of highly acid mine drainages from the Puyango river watershed (El Oro, Ecuador)

J. Delgado<sup>1</sup>, D. Ayala<sup>2</sup>, T. Boski<sup>1</sup>, E. Calderón<sup>2</sup>, F. López<sup>2</sup> and C. Barba-Brioso<sup>3</sup>

<sup>1</sup> CIMA Centro De Investigação Marinha e Ambiental. University of Algarve, 8005-139 Faro, Portugal. jdrodriguez@ualg.pt,

<sup>2</sup> INIGEMM Instituto Nacional de Investigación Geológico Minero Metalúrgico. Las Malvas E15-142 y de los Perales, Quito, Ecuador.

<sup>3</sup> Dpto. De Cristalografía, Mineralogía y Química Agrícola. University of Seville. 41072 Seville, Spain

Abandoned mine and uncontrolled tailing dumps cause tonnes of sulphide-rich wastes to be exposed to oxidation under atmospheric conditions, generating highly acid leachates (AMD) with extreme concentrations of metal-metalloids and sulphates. Nowadays, this problem is noticeable in the Portovelo-Zaruma mining district (South Ecuador), where several abandoned mines and uncontrolled environmental liabilities exist. During the last decades, passive treatment systems (PT) have been implemented to decontaminate AMD affected waters. In fluxes with high metal concentrations, the main PT systems tend to lose reactivity (*passivation* or *armoring*) or permeability (*clogging*) due to the formation of precipitates on the reactive surface/pore space of the system. To avoid these problems, Rötting et al. (2008) developed the *Dispersed Alkaline Substrate* (DAS), a reactive mixture of wood fragments, to create a more reactive and permeable layer (high porosity and specific surface area) improving the efficiency of the limestone sand

Here we have proposed a combination of a limestone-DAS (94% purity calcite sand, 0.1-2mm), which is suitable for trivalent metal removal (Fe, Al) with a MgO-DAS, which efficiently removes divalent metals (Zn, Mn, Cd, Co, and Ni). Two selected AMD-sources, *AMD-Buza* (liability) and *AMD-Torata* (mine shaft), were treated in experimental columns. Physical-chemical parameters, major and trace elements (Ca, Mg, Zn, Fe, Mn, Al, As, Ni, Cd, Co, Cr, Pb, Cu, Ag) and  $\text{SO}_4^{2-}$  were monitored for a total of 9 months.

The system showed iron, aluminium and copper removal rates around 100%, and highly efficient retention of divalent metals (Cd 89.9, Co 84.2, Cr 50.2, Ni 87.2, Pb 83.1, Zn 76.9 and Mn 80.0%), As (77.2%), and  $\text{SO}_4^{2-}$  (25%). These values support the usefulness of this new design of PT method to decontaminate AMD in equatorial mining areas. The preliminary observations of the different precipitated layers, showed the important role of Fe(III) precipitated in the first centimetres of the DAS-Ca column probably in form of low-crystalline oxyhydroxides such as *Schwertmannite*, which could be responsible for the removal of Cu and As from the solution, and later could evolve to *Goethite* during maturation processes, fixing this toxic elements. Aluminium is trapped deeper as hydroxysulfates, as well as gypsum (observed as green and white precipitates).

Rötting TS; Thomas RC; Ayora C; Carrera J. Passive treatment of acid mine drainage with high metal concentrations using dispersed alkaline substrate. J. Environ. Qual. 2008, 37: 1741–1751.

## Dehydroxylation of I-S interstratifications: Implications for alkaline activated cements

Jan Dietel<sup>1,2</sup>, Annett Steudel<sup>3</sup>, Laurence N. Warr<sup>1</sup> and Katja Emmerich<sup>3</sup>

<sup>1</sup>EMA-University Greifswald, Institute of Geography and Geology, Greifswald, Germany

<sup>2</sup>Current address: Federal Institute for Geosciences and Resources (BGR), Hannover, Germany

jandietel@gmx.de

<sup>3</sup>Competence Center for Material Moisture (CMM) and Institute for Functional Interfaces (IFG), Karlsruhe Institute of Technology (KIT), Eggenstein-Leopoldshafen, Germany

The dehydroxylation behaviour of several clay minerals such as kaolinite, smectites, or white mica has been extensively investigated. However, the dehydroxylation of interstratifications such as I-S seems to be more complex and less well known. The aim of this work is to characterise the dehydroxylation and structural breakdown of some I-S interstratifications as possible raw material for alkaline activated cements (e.g. geopolymers). Three different types of interstratifications were investigated: i) Friedland clay (R0 I(0.3)-S) as an irregular interstratification from Northern Germany, ii) rectorite as a regular interstratification from North Little Rock, Arkansas, U.S.A., and iii) "sárospatakite" (R3 I(0.84)-S) as a long-range ordered illite-rich interstratification from Korom Hill near Füzérradvány, Northern Hungary. The <0.1  $\mu\text{m}$  fraction of each clay was separated by centrifugation to concentrate the interstratification phases.

In-situ heating experiments were performed using Simultaneous Thermal Analysis coupled with a Mass Spectrometer (STA-MS) and temperature-dependent X-ray diffraction (TXRD) to investigate the behaviour of dehydroxylation, structural breakdown, and recrystallisation of the clay mineral phases present. Additionally,  $\text{N}_2$  adsorption (BET/BJH) and solid-state Nuclear Magnetic Resonance Spectroscopy (NMR) were applied to investigate the properties of heated samples such as specific surface area, pore size distribution, or the amount of 4-, 5-, and 6-fold coordinated Al. Based on these results, the suitability of these interstratifications in terms of usage as raw materials for alkaline activated cements, such as geopolymers, is discussed and the optimal heating temperature determined. The possible use of suitable additives is also considered.

It is commonly assumed that the amount of 5-fold coordinated Al strongly influences the reactivity of the dehydroxylated clay. Our results indicate that the amount of 5-fold coordinated Al is not the most important parameter, but instead the specific surface area of the dehydroxylated clay, as measured by BET, plays a key role in the successful alkali activation of binder materials to produce high compressive strength, low porosity, and low permeability cements.

## The role of ceramic building materials for CO<sub>2</sub> sequestration. Preliminary results

Patricia Aparicio, Emilio Galán, Domingo Martín, Adolfo Miras, Antonio Romero, Cinta Barba-Brioso  
Dpto. Cristalografía. Mineralogía y Q. Agrícola, University of Seville, Spain [paparcio@us.es](mailto:paparcio@us.es) [egalan@us.es](mailto:egalan@us.es),  
[dmartin5@us.es](mailto:dmartin5@us.es), [amiras@us.es](mailto:amiras@us.es), [aromero@us.es](mailto:aromero@us.es), [cbarba@us.es](mailto:cbarba@us.es)

The industrial development since the XIX Century has led to a huge increase in fossil fuel consumption and CO<sub>2</sub> emissions, causing a dramatic increase in atmospheric CO<sub>2</sub> concentration. The capture of CO<sub>2</sub> from the industries and the long-time storage is one of the options for reducing the CO<sub>2</sub> emissions and the concentration in the environment. This technology is named CCS (Carbon Capture Sequestration). The main obstacle to mineral carbonation is to do it economically in terms of both money and energy costs. This research explores the possibilities of CO<sub>2</sub> sequestration on ceramic building materials, in order to propose the injection of CO<sub>2</sub> in construction ceramic waste used for mining reclamation

Three types of bricks were selected for this research. The bricks are composed of quartz, feldspars, mica, gehlenite, wollastonite and kilchoanite. CaO ranges between 14 to 20 wt% and MgO from 2 to 4 wt%. The bricks were ground using a jaw crusher, and classified according to the particle size (>4mm, 4-2 mm, 2-1 mm, <1 mm). Grain size, temperature, CO<sub>2</sub> pressure, relative humidity and reaction time were the variables in the experimental alterations, which were conducted in a Parr reactor. The changes that occurred during the alteration experiments were monitored by XRD, BET, optical microscopy and SEM equipped with EDS. In addition the elemental carbon content was also measured using an elemental analyzer, DTA/TG and Bernard calcimeter.

A partial destruction of calcium silicates and the presence of calcite were detected by XRD. Calcite was also detected by DTA/TG. The BET-N<sub>2</sub> surface area of the altered bricks increased with the CO<sub>2</sub> treatments, possibly because the carbonic acid formed in the ambient led to the destruction of the calcium silicate structures. A layer of calcite was formed on the altered brick surface (Fig. 1a,c), and in addition, large crystals infilling the pores were also observed (Fig. 1b,d). The largest contents of carbonates were observed for experiment of 10 days, >4 mm fraction, 10 bar of CO<sub>2</sub> pressure.

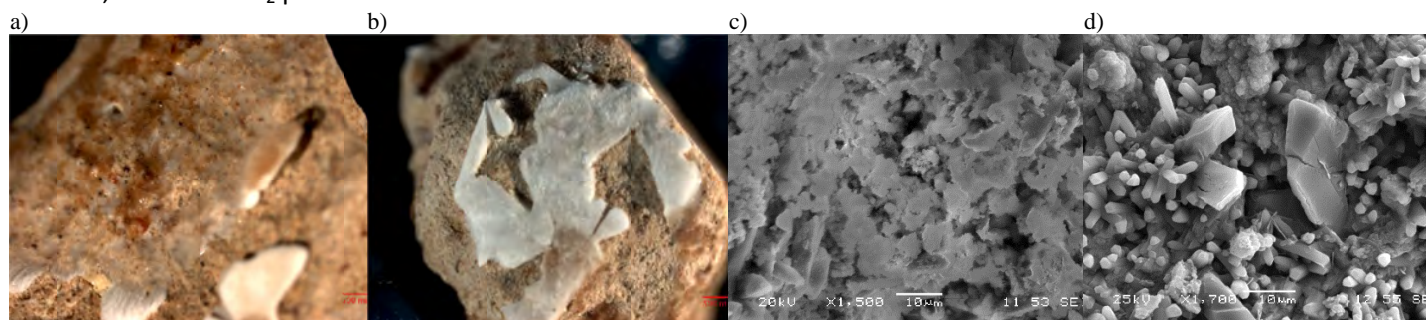


Figure 1. Carbonate crystals on the surface of brick, formed after CO<sub>2</sub> treatment. Observations by optical microscope (a, b) and SEM (c, d).

This research was financed by the Andalucía Government (RDCCO2 project, P12-RNM-568).

## Diatomite-based porous materials and their performances for benzene adsorption

Peng Yuan<sup>1</sup>, Wenbin Yu<sup>1,2</sup>, Weiwei Yuan<sup>1,2</sup>, Dong Liu<sup>1</sup> and Liangliang Deng<sup>1,2</sup>

<sup>1</sup>CAS Key Laboratory of Mineralogy and Metallogeny, Guangzhou Institute of Geochemistry, Chinese Academy of Sciences, Guangzhou 510640, China, yuanpeng@gig.ac.cn

<sup>2</sup>University of Chinese Academy of Sciences, Beijing 100049, China

Diatomite (Dt) is a natural biogenic mineral with unique macroporous and/or mesoporous structure. Dt has been widely used in the fields of adsorption and filtering because of its high porosity and large-sized diatom shells. However, Dt exhibits ordinary adsorption capacity for organic molecules. This is because the surface silanols of diatom shells do not possess a strong adsorption affinity for organics; moreover, the low specific surface area ( $S_{\text{BET}}$ ) of Dt is disadvantageous to adsorption. In this work, diatomite-based porous materials were prepared through the modification of Dt to improve the benzene adsorption performance of diatomite. The objectives of this study include: i) to improve the adsorption affinity between Dt and benzene through surface silylation; ii) to increase the  $S_{\text{BET}}$  value of Dt by preparation of diatomite/MFI-type zeolite (Dt/Z) composites and diatomite-based porous ceramic monoliths/silicalite-1 nanoparticles (Sil-PCS) composite.

In the case of surface silylation, Dt was functionalized with phenyltriethoxysilane (PTES). The hydrophobicity of Dt was significantly increased after silylation modification, with a water contact angle increase from  $0^\circ$  to  $120 \pm 1^\circ$ . The Langmuir adsorption capacity of benzene on the modified Dt is more than 4-fold greater than that on Dt, due to the strong  $\pi$ -system interactions between the phenyl groups and the benzene molecules.

Two routes were applied to prepare the above-mentioned Dt/Z composites: i) a hydrothermal method, in which a NaOH etching process was first performed to increase the pore size on diatom shells, followed by hydrothermal growth of a layer of MFI-type zeolite at the surface of the etched diatom shells already seeded with nanocrystalline silicalite-1 (Sil-1). The maximum  $S_{\text{BET}}$  of Dt/Z is  $325.4 \text{ m}^2/\text{g}$ , significantly larger than that of Dt ( $16.8 \text{ m}^2/\text{g}$ ). The Dt/Z composites exhibited higher benzene adsorption capacity per unit mass of zeolite and less mass transfer resistance than Sil-1; ii) a vapour-phase transport (VPT) method, in which the diatom shell was directly transformed into an MFI-type zeolite. A post-desilication treatment was applied to improve the structure of Dt/Z. The resulting Dt/Z composite exhibited hierarchical porosity, high surface area, and good performance for benzene adsorption. This performance is attributed to not only the mesopores created by desilication allowing for high accessibility during adsorption, but also that the terminal silanol formed on the newly developed mesopores after desilication having a high affinity for benzene molecules.

In the case of the Sil-PCS composite, porous ceramic supports with three-dimensional reticulated structures were first prepared using the polymeric sponge method in which diatomite was used as the ceramic framework and polyurethane foam as the sacrificial template, followed by a facile *in situ* homogeneous coating of Sil-1 on the surface of the ceramic supports. The  $S_{\text{BET}}$  of the Sil-PCS was as high as  $122.9 \text{ m}^2/\text{g}$ , with a zeolite loading of 32.4%. The Sil-PCS composite exhibited a high benzene adsorption capacity ( $133.3 \text{ mg/g(Sil-1)}$ ) compared with a commercial micron-sized ZSM-5 product ( $66.5 \text{ mg/g}$ ).

These results demonstrated that the surface silylation and the preparation of diatomite/zeolite composites and diatomite-based ceramic monoliths/zeolite composite are able to improve the benzene adsorption performance of diatomite, enabling the diatomite-based porous materials to be promising candidates for use in benzene emission control.

**Acknowledgement:** This study was financially supported by the Team Project of Natural Science Foundation of Guangdong Province (Grant No. S2013030014241).

## Assessing the redox reactivity of Fe(II)-reduced clay minerals

Katherine Ann Rothwell and Anke Neumann

<sup>1</sup>School of Civil Engineering and Geosciences, Cassie Building, Newcastle University, Newcastle upon Tyne, NE1 7RU, UK

Iron-bearing clay minerals are ubiquitously present within natural environments and structural Fe(III) within clay minerals is readily reduced by both abiotic and microbial mechanisms. The resulting structural Fe(II) is a major source of reduction equivalents capable of facilitating the reduction of a range of environmentally relevant contaminants, including nitroaromatic compounds, chlorinated aliphatics, radionuclides and heavy metals. Recently, it has been demonstrated that the reaction of Fe-bearing clay minerals with aqueous Fe(II) leads to interfacial electron transfer between sorbed Fe(II) and structural Fe(III)<sup>1</sup> resulting in structural Fe(III) reduction in the clay minerals as well as the formation of a solid phase Fe(III) oxidation product such as lepidocrocite<sup>2</sup>. It is, however, currently unknown how the presence of an *in situ* solid Fe(III) oxidation product will affect the reactivity of Fe(II)-containing clay minerals.

To assess the reactivity of Fe(II)-containing clay minerals, we used 2-acetylnitrobenzene as a reactive probe compound. We monitored reactive probe reduction in Fe(II)-reduced clay mineral systems and compared the reduction kinetics to 2-acetylnitrobenzene reduction in reactors containing dithionite reduced clay minerals with the same Fe(II)/Fe(III) ratio. To determine the effect of clay mineral properties such as iron content or location of excess charge on the reactivity of clay minerals, we investigated a variety of Fe-bearing clay minerals (smectites, chlorites). Mössbauer spectroscopy was used to monitor the (trans)formation of iron oxidation products and the clay mineral Fe(II)/Fe(III) ratio during probe molecule reduction. Results from our study will contribute to understanding the redox reactivity of complex, natural biogeochemical systems and to effective earth systems engineering for environmental clean up.

<sup>1</sup> Neumann A, Olson TL, Scherer MM. Spectroscopic evidence for Fe(II)-Fe(III) electron transfer at clay mineral edge and basal sites. *Environ Sci Technol* 2013; 47: 6969-77.

<sup>1</sup> Schaefer, M.V., Gorski, C.A. and Scherer, M.M. (2010) 'Spectroscopic evidence for interfacial Fe (II)– Fe (III) electron transfer in a clay mineral', *Environmental science & technology*, 45(2), pp. 540-545.

## Flocculation of clay suspensions by model polyelectrolytes

Y. Sakhawoth\*, L. Michot, P. Levitz and N. Malikova

Laboratory of Physical Chemistry of Electrolytes and Interfacial Nanosystems (PHENIX)

Sorbonne Universités, UPMC Univ Paris 06, CNRS, UMR 8234, F-75005, Paris, France

\*yasine.sakhawoth@upmc.fr

Flocculation is a key phenomenon used in many industrial processes such as water treatment, paper making and mineral processing<sup>1</sup>. Knowing its importance, we have been focussing on examining the mechanism of flocculation in a well-defined model system. We are studying flocculation in suspensions of smectite (montmorillonite) particles in water, induced by model polyelectrolytes<sup>2</sup>. For this purpose, quaternary ammonium based polyelectrolytes named ionenes are being used. Consisting of nitrogen atoms linked by simple hydrocarbon chains, ionene polyelectrolytes present several advantages over other systems: 1) charged centres are part of the polyelectrolyte backbone instead of a side group, 2) distance between the backbone charges is *regular and tuneable* by synthesis and 3) absence of bulky side groups. We possess extensive knowledge of ionene behaviour in aqueous solution from our recent neutron scattering and NMR studies<sup>3,4</sup>, as well as thermodynamic measurements<sup>5</sup>.

Firstly, conditions for optimal clay-ionene flocculation are established. Clay suspensions are flocculated using ionenes of three different charge densities and the turbidity of the supernatant liquid is studied by UV-VIS spectrometry. The established phase diagram of ionene-clay mixtures shows that the most pronounced flocculation (minimum in supernatant turbidity) arises at a ratio of positive and negative charge between polyelectrolytes and clay of 0.3-0.7. This is below the value of 1, based on simple electrostatic considerations. In addition, restabilisation of the suspensions is observed beyond this point of optimal flocculation.

As shown recently for the case of clay flocculation by inorganic ions<sup>6,7</sup>, X-ray scattering and imaging techniques are an ideal tool to probe the structure of clay aggregates formed in this process. The case of flocculation by polyelectrolytes adds complexity in terms of the different conformations of their chains between the clay particles. We intend to couple NMR spectroscopy to the above scattering and imaging techniques, in tackling this issue.

[1] G. Petzold and S. Schwarz, *Adv. Polym. Sci.*, 2014, 256, 25–66.

[2] B. Bolto and J. Gregory, *Water Research* **2007**, 41, pp. 2301-2324.

[3] N. Malikova, S. Cebasek, V. Glenisson, D. Bhowmik, G. Carrot, V. Vlachy, *Phys. Chem. Chem. Phys.* **2012**, 14, pp. 12898-12904.

[4] N. Malikova, A.-L. Rollet, S. Cebasek, M. Tomsic, V. Vlachy, *Phys. Chem. Chem. Phys.* **2015**, 17, 5650.

[5] S. Cebasek, M. Serucnik, V. Vlachy, *J. Phys. Chem. B*, **2013**, 117, 3682-3688.

[6] S. Brisard, R. S. Chae, I. Bihannic, L. Michot, P. Guttmann, J. Thieme, G. Schneider, P. J. M. Monteiro, P. Levitz, *Am. Mineralogist* **2012**, 97, pp. 480-483 ;

[7] L. J. Michot, I. Bihannic, F. Thomas, B. S. Lartiges, Y. Waldvogel, C. Caillet, J. Thieme, S. S. Funari, P. Levitz, *Langmuir* **2013**, 29, pp. 3500-3510.



## Oil sorption by kaolinite and its potential role in the remediation of oil spillages

Ayodele A. Oyedeji<sup>1,3\*</sup>, A. R. Demirkiran<sup>1,4</sup>, J. Kayode<sup>2</sup>, L. Besenyei<sup>1</sup> and M. A. Fullen<sup>1</sup>

<sup>1</sup>Faculty of Science and Engineering, University of Wolverhampton WV1 1LY, Wolverhampton, UK

<sup>2</sup>Department of Plant Science, Faculty of Science, Ekiti State University, Ado-Ekiti, Nigeria

<sup>3</sup>Department of Biological Sciences, Niger Delta University, Wilberforce Island, Nigeria

<sup>4</sup>Department of Soil Science and Plant Nutrition, University of Bingol, Bingol, Turkey

\*ayodele.oyedeji@yahoo.com

The efficacy of kaolinite (10 and 20 g samples) for the sorption of four different amounts of automobile oil (AO) (25, 50, 75 and 100 ml) representing low, moderate, high and very high spillages, respectively, was analysed. Kaolinite is the primary clay mineral in the kaolin mineral subgroup and it has many industrial uses, including the production of ceramics, sanitary ware, electrical porcelain and paint. The main use of kaolinite is in the paper industry, where it is utilized as a filler and coating agent. There is growing interest in the use of kaolinite as a combined source of silica and alumina for zeolite synthesis. There are large kaolinite (clay) resources in several countries, including Australia, Brazil, Ghana, Nigeria, the UK and USA.

In a laboratory experiment, 10 and 20 g kaolinite samples were tested for AO sorption in two separate experiments. Buchner funnels were lined with No 42 Whatman filter paper and an appropriate quantity of white superfine Australian kaolinite was added. Different amounts of AO (25, 50, 75 and 100 ml) were placed in separation funnels and allowed to drip slowly over 24 hours and soak into the 10 and 20 g kaolinite samples, with five replicates of each treatment. Excess AO was collected and measured. The results showed that 10 g kaolinite sorbed a mean of 75.28, 74.68, 61.52 and 60.80% of the 25, 50, 75 and 100 ml of AO treatment, respectively; while 20 g kaolinite sorbed a mean of 93.44, 87.04, 73.49 and 70.86% of 25, 50, 75 and 100 ml of AO treatment, respectively. AO contamination and oil sorption amounts in the 10 g and 20 g samples were strongly correlated ( $R^2 = 0.975$ ;  $n = 5$ ;  $P < 0.05$ ). The study provides evidence of the considerable potential of kaolinite to act as a natural cleaning agent and possibly as a soil amendment for partially alleviating oil spillages.

**Keywords:** automobile oil, environment, kaolinite, remediation, sorption, spillage.

## Insights on anti-inflammatory, anti-bacterial, cytotoxic and oxidant activity, and oxidative stress inhibition by fibrous clays

Javiera Cervini-Silva<sup>1</sup>, Antonio-Nieto-Camacho<sup>2</sup>, María Teresa Ramírez-Apan<sup>2</sup>, Virginia Gómez-Vidales<sup>3</sup>, Eduardo Palacios<sup>4</sup>, Ascención Montoya<sup>4</sup> and Elba Ronquillo de Jesús<sup>1</sup>

<sup>1</sup>Departamento de Procesos y Tecnología, Universidad Autónoma Metropolitana Unidad Cuajimalpa, México City, México; Av. Vasco de Quiroga 4871, Cuajimalpa de Morelos, Col. Santa Fe, México, D.F., México

<sup>2</sup>Laboratorio de Pruebas Biológicas, Instituto de Química, Universidad Nacional Autónoma de México, Ciudad Universitaria México City, México

<sup>3</sup>Laboratorio de Resonancia Paramagnética Electrónica, Instituto de Química, Universidad Nacional Autónoma de México, Ciudad Universitaria, México City, México

<sup>4</sup>Dirección de Investigación y Posgrado, Instituto Mexicano del Petróleo, Mexico  
jcervini@correo.cua.uam.mx

Produced worldwide at 1.2 m tons per year, fibrous clays are used in the production of pet litter, animal feed stuff to roof parcels, construction and rheological additives, and other applications needing to replace long-fibre length asbestos. To the authors' knowledge, however, information on the beneficial effects of fibrous clays on health remains scarce. This paper reports on the anti-inflammatory, anti-bacterial, and cytotoxic activity by sepiolite (Vallecas, Spain) and palygorskite (Torrejón El Rubio, Spain). Furthermore, this paper provides evidence to show that these materials inhibit effectively cell damage (*via* oxidative stress, determined as the progress of lipid peroxidation, LP). The anti-inflammatory activity was determined using the 12-O-tetradecanoylphorbol-13-acetate (TPA) and myeloperoxidase (MPO) methods. Histological cuts were obtained for quantifying leukocytes found in the epidermis. Thiobarbituric Acid Reactive Substances (TBARS) assay and Electron-Paramagnetic Resonance (EPR) analyses were conducted to study the role of these clays on LP and to quantify their oxidant activity, respectively.

Palygorskite and sepiolite caused edema inhibition and migration of neutrophils *ca.* 68.64 and 45.54%, and 80 and 65%, respectively. Fibrous clays yielded high rates of infiltration, explained by cleavage of polysomes and exposure of silanol groups. Also, fibrous clays showed high inhibition of myeloperoxidase contents shortly after exposure, but decreased sharply afterwards. In contrast, tubular clays caused an increasing inhibition of myeloperoxidase with time. Thus, clay structure restricted the kinetics and mechanism of myeloperoxidase inhibition. Fibrous clays were screened *in vitro* against 7 human cancer cell lines. Cytotoxicity was determined using the protein-binding dye sulforhodamine B (SRB). Exposing cancer human cells to sepiolite or palygorskite showed growth inhibition varying with cell line. This study shows that fibrous clays served as an effective anti-inflammatory, limited by chemical transfer and cellular-level signals responding exclusively to an early exposure to clay, and cell viability decreasing significantly only after exposure to high concentrations of sepiolite.

Sepiolite and palygorskite inhibited LP, with corresponding IC<sub>50</sub> values *ca.* 6557 ± 1024 and 4250 ± 289 µg mL<sup>-1</sup>. Dose-response experiments for palygorskite showed that LP inhibition was surface-controlled. Amongst all dispersions, only those containing high amounts of palygorskite (5,000 µg mL<sup>-1</sup>) showed oxidant activity *albeit* small, evidenced by the formation of HO<sup>•</sup> radicals. Overall, EPR results confirmed a lack of stabilization of HO<sup>•</sup> species by sepiolite and palygorskite surfaces. That is, LP inhibition by sepiolite and palygorskite surfaces related to a strong oxidant (or weak anti-oxidant) activity.

## Development and characterization of antibiotic-intercalated smectite

Donghoon Chung<sup>1</sup>, Yungoo Song<sup>1</sup>, Il-mo Kang<sup>2</sup>, YG Song<sup>3</sup> and Woohyun Choi<sup>1</sup>

<sup>1</sup>Yonsei Univ. BK21+ institute of earth.Atmosphere.Astronomy, Seoul, Korea.

<sup>2</sup>Korea institute of geoscience and mineral resources, Deajeon, Korea.

<sup>3</sup>Department of Internal Medicine, Yonsei University College of Medicine, Seoul, Korea.

dongh21@nate.com

Clay minerals have various usages in pharmaceutical ground both as excipients and active agents. Because of its swelling property and high cation exchange capacity (CEC), smectite is one of the pharmaceutical minerals for diarrhea. Needing safe and efficient drug dosage, smectite is suggested as one of the release control excipients based on their high retention capacities. In this study, we aimed to make efficient antibiotic-intercalated smectite for derivatives as new drug delivery systems. For the first goal of achievement, we defined the mineralogical characteristics of target smectite and performed the intercalation and preliminary releasing experiments. Firstly, we intercalated five selected antibiotics (Amoxicillin, Clarithromycin, Netilmicin, Tobramycin, and Gentamicin) into the interlayer of the smectite extracted from anti-diarrhotica. Secondly, we measured the maximum intercalated amount of Clarithromycin and Amoxicillin in equivalent per gram of smectite using equilibration with the different concentration solutions of antibiotics and Langmuir isotherm calculation. Thirdly, we setup the release test experimental apparatus and optimum conditions for the detail release test in the next step by using beforehand test with Clarithromycin intercalated smectite. In the intercalation experiments, we confirmed that antibiotics were intercalated into smectite by using XRD and SEM-EDS analysis, and 0.94 mmole/g of Amoxicillin and 0.81mmole/g of Clarithromycin were intercalated into smectite in maximum. In the preliminary release test, we observed that some of intercalated antibiotics were distinctly released out in pH 2 and 3 of physiological salt solution pH controlled by HCl and NaHCO<sub>3</sub>.

## Mineralogy and transformation trends of hard rocks from geophagic materials (South Africa)

Georges-Ivo Ekosse<sup>1</sup>, Sofia Lessovaia<sup>2</sup>, Yury Polekhovskiy<sup>2</sup>, Kirill Chistiakov<sup>2</sup>, Elena Zelepukina<sup>2</sup>, Alexey Filimonov<sup>3</sup>, Natalia Andreeva<sup>3</sup>, Anna Frolova<sup>2</sup>, John Odiyo<sup>1</sup>, Francis Mongogoa<sup>4</sup>, Manneheng Raputhing<sup>4</sup>, Nenita Bukalo<sup>1</sup>, Johanna Molepo<sup>1</sup>, Sally Ibeh<sup>1</sup>, Jason Ogola<sup>1</sup>, Elvis Fosso-Kankeu<sup>5</sup>, Rachel Ravuluvulu<sup>1</sup> and Valery Phakoago<sup>1</sup>

<sup>1</sup> University of Venda, P.O. Box Private Bag X5050 Thohoyandou 0950, South Africa

<sup>2</sup> St. Petersburg State University, 199178, V.O., 10 line, d.33, St. Petersburg, Russia

<sup>3</sup> St. Petersburg State Polytechnical University, 195251, 29 Politekhnicheskaya, St. Petersburg, Russia

<sup>4</sup> Central University of Technology, P. O. Box X20539 Bloemfontein, 9300 South Africa

<sup>5</sup> North West University Potchefstroom Campus, P/Bag X6001 Potchefstroom 2520 South Africa

lessovaia@yahoo.com

The study focused on investigating the transformation trends in the system hard rock – loose material of mineral associations in hard rocks sampled from geophagic soils and sediments. The materials are used in ethnomedicine based on historical and traditional motivations.

The studied samples were collected in Free State and Limpopo provinces of South Africa. Mineral association in the hard rocks, located in geophagic loose material, was studied by optical microscopy in thin sections. The mineralogical compositions of the <1 µm and <2 µm fractions separated from hard rocks and / or loose material were studied by X-ray diffractometry and FTIR spectroscopy. Two of studied sites were located in the area of Highveld (elevation ~ 1800m). The geophagic materials are represented by (i) clayish substrate accumulated between boulders of polymict sandstone and (ii) outcrops of arkosic sandstone. In polymict sandstone the grains of quartz, plagioclase, and “fresh” (unweathered) muscovite, and traces of metallic mineral were recognized. In the fine size fraction separated from clay and sandstone, kaolinite is predominant besides that smectite(s) and small proportion of mica were also present. The identities of the mineral associations confirm that sandstone is the source of clay minerals for the loose geophagic material. In arkosic sandstone, which is generally characterized by unsorted material and angularity of mineral grains, metallic mineral in rock’s cement and in the grains of the primary minerals were identified as well as high proportion of phyllosilicates in the rock cement. In fine size fraction mica and kaolinite with the predominance of smectite(s) were found.

Another two studied sites were located in the area of Low-veld (elevations ~ 800-900 m) in the stratal plains of midland depressions. The clayish oxidized tuff enriched by Fe-oxides was sampled (the first key plot in Low-veld). Chlorite, smectite(s) and mica were identified in the fine size fraction. In the last key study geophagic materials were sampled (i) in the alluvial valley and (ii) on the top of the hill (h ~ 100m) represented by residual outcrops of bedrocks. Despite the fact that loose material from alluvial valley is calcareous whereas from the top of the hill it is calcite free, their fine size fractions are characterized by the same association of phyllosilicates including mica and kaolinite with predominance of smectite(s). Thus, despite the differences in location and rock geneses the most common mineral in the geophagic materials is smectite(s). The hard rocks sampled from geophagic loose material are the source of phyllosilicates in the fine size fractions.

**Acknowledgement:** The work was supported by RFBR, N 14-05-93959 (RFBR-SA) and NRF UID 92199 project grants.

## Physical, chemical and thermal characteristics of Makirina bay peloids (N. Dalmatia, Republic of Croatia)

Darja Komar<sup>1</sup>, Petra Vrhovnik<sup>1</sup>, Nastja Rogan Šmuc<sup>1</sup>, Matej Dolenc<sup>1</sup>, Tadej Dolenc<sup>1</sup>, Sonja Lojen<sup>2</sup>, Goran Kniewald<sup>3</sup>, Živana Lambaša Belak<sup>4</sup>, Sanja Slavica Matešić<sup>4</sup>, Lourdes Mourelle<sup>5</sup> and Carmen Gómez<sup>5</sup>

<sup>1</sup>Dept of Geology, University of Ljubljana, Aškerčeva 12, 1000, Ljubljana, Slovenia

<sup>2</sup>Dept. of Environmental Sciences, Jožef Stefan Institute, Jamova cesta 39, 1000 Ljubljana, Slovenia

<sup>3</sup>Ruđer Bošković Institute, Bijenička 54, 10000 Zagreb, Croatia

<sup>4</sup>Dept. of the Environmental. Protection, Šibenik-Knin County, Trg Pavla Šubica I no. 2, 22000 Šibenik, Croatia

<sup>5</sup>Department of Applied Physics, University of Vigo, Lagoas-Marcosende s/n, 36310 Vigo, Spain

darja.komar@ntf.uni-lj.si

Makirina Bay (N Dalmatia, Republic of Croatia) represents one of the major and most important sites where organic-rich sediments accumulate along the eastern Adriatic coast. According to their organoleptic properties, these sediments (peloids) are suitable for application as a raw material for different therapeutic, cosmetic, and wellness-related purposes. In addition, Makirina Bay peloids are already frequently used by local people and tourists as pomades; peloids are collected in situ from the bay, applied directly on the skin, and sun dried.

Several characteristics of Makirina bay peloids were determined, including their granulometry, cation exchange capacity (CEC), mineral and elemental composition, potentially toxic elements (PTE) mobility/bioavailability and thermal properties (specific heat, thermal conductivity and thermal diffusivity) in order to evaluate the suitability of their application for medical/therapeutic purposes in balneotherapy and pelotherapy. Our results showed that Makirina bay peloids are represented mostly by sandy silt and have a relatively high CEC value (63.82 meq/100g). The mineral composition of peloids is dominated by dolomite and quartz, followed by illite/muscovite, aragonite, halite, calcite, and pyrite. Oriented preparations of the clay fraction revealed illite/muscovite, chlorite, and kaolinite as the dominant clay minerals. PTE concentrations in surficial (0-5 cm) peloids are [in mg/kg]: As (14.47), Cd (0.27), Cu (27.64), Mn (232.4), Mo (13.82), Ni (26.51), Pb (23.74) and Zn (47.67). The results of the sequential extraction procedure indicated that majority of PTE (except Cd, Mn and Mo) in Makirina bay peloids are not readily mobile or bioavailable since only a small percentage of PTE is extracted in the first two steps (e.g. water-soluble and exchangeable fraction). Thermal properties of Makirina bay peloids are as follows: specific heat 2050 J/kgK, thermal conductivity 0.99 W/mK and thermal diffusivity  $2.84 \cdot 10^{-7} \text{ m}^2/\text{s}$ .

## Intercalation of pravastatin drug into LDH - molecular simulation study

Milan Pšenička

Charles University in Prague, Faculty of Mathematics and Physics, Department of Chemical Physics and Optics, Ke Karlovu 3, 121 16 Prague 2, Czech Republic; milan.psenicka@matfyz.cz

Due to the constantly increasing demand for new multifunctional nanomaterials suitable for using in health care it is necessary to combine actual knowledge of the medical field and new approaches to the preparation of materials with desired physical and chemical properties. One of these unique materials are LDH that exhibit desired properties, which allows them to be suitable nanocarriers of synthetic or natural bioactive organic compounds. It was found that LDH are able to increase the chemical stability of the resulting intercalated material and allow its subsequent slow release in the body, or can restrict and eliminate undesirable side effects. We investigated LDH intercalated by pravastatin using molecular mechanics and classical molecular dynamics methods.

Statins are drugs used for reducing LDL cholesterol in the blood circulation and to prevent cardiovascular diseases. This drug typically contains 3-hydroxy-methylglutaryl coenzyme A reductase, which slows cholesterol biosynthesis. Several studies also showed the cardiovascular benefits of statins, which are associated with their anti-inflammatory effects, and which thus opens new possibilities for the use of statins in the treatment of chronic diseases such as e.g. Parkinson's or Alzheimer's disease. Therefore, LDH intercalated by pravastatin are very attractive systems for pharmaceutical industry.

Intercalation of pravastatin into LDH was performed in [1,2] by co-precipitation method. The experimentally obtained data from these two studies for pravastatin slightly differs. Likewise, data calculated using DFT methods do not correspond with experimental results appropriately. Due to the size of the system, ab-initio calculations and DFT calculations are a bit time inefficient. In contrast, the time efficiency of molecular simulation methods for solving the large systems is much higher.

On the basis of the experimentally obtained results [1,2] we created strategy and initial models for molecular modelling. Geometry of intercalated structures was optimized and calculated in Materials Studio2 and LAMMPS modelling environment. Resultant calculated structures with the best agreement with experimental data and interaction energies will be presented.

**Acknowledgement:** The study was supported by the Charles University in Prague, project GA UK No. 294215.

<sup>1</sup> PANDA, H. S., SRIVASTAVA, R., BAHADUR, D. In-vitro release kinetics and stability of anticardiovascular drugs-intercalated layered double hydroxide nanohybrids, *J. Phys. Chem. B*, 2009, vol. 113, p. 15090–15100.

<sup>2</sup> CUNHA, V., PETERSEN, P., GONCALVES, M., PETRILLI, H., TAVIOT-GUEHO, CH., LEROUX, F., TEMPERINI, M., CONSTANTINO, V. Structural, Spectroscopic (NMR, IR, and Raman), and DFT Investigation of the Self-Assembled Nanostructure of Pravastatin-LDH (Layered Double Hydroxides) Systems, *Chem. Mater.*, 2012, vol. 24, p. 1415–1425.

## Mineralogy and geochemical characteristics of some geophagic clays from southern Nigeria

Akinade S. Olatunji<sup>1</sup> and Jerry O. Olajide-Kayode<sup>2</sup>

<sup>1</sup> Department of Geology, University of Ibadan, Ibadan, Nigeria; akinadeshadrach@yahoo.com; as.olatunji@ui.edu.ng

<sup>2</sup> Department of Geology, University of Ibadan, Ibadan, Nigeria; jolugbn@yahoo.com

The mineralogy and geochemical characteristics of raw and processed geophagic clays from southern Nigeria were studied to determine their geophagic suitability, quality and the possible health effects of their consumption using XRD and ICP-MS.

The identified minerals in the clay samples were kaolinite (23.6-60.0%), montmorillonite (Nil - 6.2%), quartz (14.4-75.7%), and muscovite (Nil-3.3%). The results of the elemental composition of the consumed geophagic clays revealed that the concentration of essential micro-nutrients like Ca, P, Mg, Na and K are low while appreciable concentrations of Fe (0.49- 5.95%) and Al (7.58-14.46%) were observed. The processed clays have higher values for CaO, MgO and K<sub>2</sub>O while the value for the Al<sub>2</sub>O<sub>3</sub> are similar in both processed and unprocessed samples. The concentration of some Potentially Harmful Elements, PHEs are: Cu (9.1-23ppm), Pb (16.7-55.6ppm), Zn (13-148ppm), Ni (11.1-46.4ppm), Co (1.8-21.7ppm), Mn (16-338ppm), As (BDL-15ppm) and Cd (BDL-0.2ppm). These values were found to exceed the recommended dietary intake by humans in most of the samples (Table 1 & Fig.1).

Though the kaolinite present in the geophagic clays makes them suitable for use as traditional antacids, the toxic trace element concentrations and significant quartz content will most likely relegate such beneficial effects.

Table 1: Comparison of average concentration of trace elements in geophagic clays with recommended daily intakes

Element	Average for Nigerian Geophagic Clays (ppm)	ASC (ppm) <sup>1</sup>	Recommended daily intake (mg/day) <sup>2</sup>	ATSDR MRL (ppm/day) <sup>3</sup>
Cu	13.2	50	1.0-1.5	0.01
Pb	35.1	20	No safe threshold	No safe threshold
Zn	43.7	90	10-15	0.3
Ni	23.2	80	0.025-0.03	0.0002
Co	6.3	20	0.002-0.1	0.01
Mn	91.6	850	2-5	-
As	4.7	10	-	0.005
Cd	0.07	0.3	-	0.0005

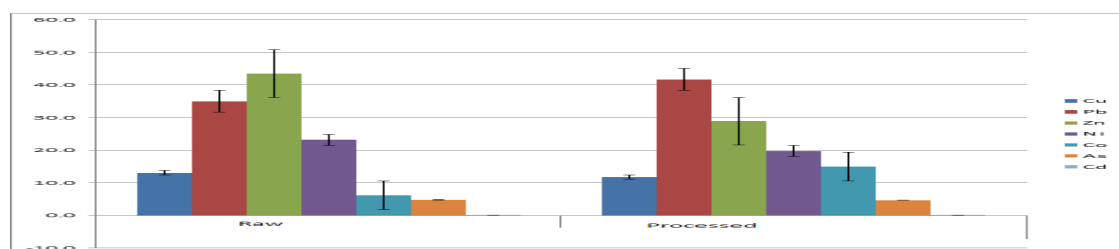


Figure 1: Average PHEs concentration in the clay samples

1 Turekian, K.K and Wedepohl, L.H. (1961) Distribution of elements in some major units of the Earth Crust. *Geological Society of America Bulletin*, **72**, 125.

2 Belitz, H.D., Grosch, W. and Schieberle, P. (2009) *Food Chemistry*. 425 p.

3 Agency for Toxic Substances and Disease Registry (ATSDR) (2012) Minimal Risk Levels.

## Chlorite geothermometer applied to the Patricia Zn-Pb-Ag epithermal deposit (Tarapacá-Andean Cordillera, Chile)

X. Arroyo<sup>1</sup>, D. Chinchilla<sup>2,3</sup>, L. Ortega<sup>2</sup>, R. Piña<sup>2</sup>, F. Nieto<sup>4</sup> and R. Lunar<sup>2,3</sup>

<sup>1</sup> CAI de Técnicas Geológicas, Facultad de CC. Geológicas (UCM), C/ José Antonio Nováis, 12, 28040, Madrid, Spain;

xarroyo@geo.ucm.es

<sup>2</sup> Departamento de Cristalografía y Mineralogía, Facultad de CC. Geológicas (UCM), C/ José Antonio Nováis, 12, 28040, Madrid, Spain

<sup>3</sup> Instituto de Geociencias (CSIC, UCM), Facultad de Ciencias Geológicas, Universidad Complutense de Madrid, Spain

<sup>4</sup> Departamento de Mineralogía y Petrología and Instituto Andaluz de Ciencias de la Tierra, Universidad de Granada-CSIC, Avenida Fuentenueva, 18002 Granada, Spain

The Patricia Zn-Pb-Ag deposit represents an example of base-metal and silver epithermal mineralization, unusual in northern Chile. The deposit is located within the Paguanta mining project, situated at the northern end of the Andean Oligocene Porphyry Copper Belt of Chile. The sulfide mineralization occurs as W-E oriented veins hosted in volcanic rocks, mainly andesite (pyroclastic, ash and lavas), of Upper Cretaceous to Middle Tertiary age. From petrographic studies, three stages of mineralization have been defined: (1) pre-ore stage, (2) base-metal and silver stage and (3) post-ore stage. The pre-ore stage is characterized by quartz, pyrite and arsenopyrite. The second main ore stage is characterized by sphalerite (6 to 15% mol. FeS), galena and minor amounts of Ag-bearing minerals, chalcopyrite and pyrrhotite. The post-ore stage is defined by late quartz, Mn-carbonates and minor sulfides (arsenopyrite, sphalerite, pyrite and galena). Two major types of hydrothermal alteration are observed in relationship to the mineralized veins within the host rock: chloritization and sericitization. Chlorite and micas also occur in the base-metal veins with chlorite as the most common phase.

The temperature of the hydrothermal system is an essential parameter to determine the ore-forming fluid that gave rise to the formation of the epithermal deposit. The aim of this study is to calculate the temperature using the Bourdelle chlorite geothermometer (Bourdelle *et al.*, 2013), as variations in the chemical composition of chlorite can provide useful information on the physicochemical conditions of its formation.

Representative samples ( $n = 32$ ) from different boreholes were chosen to be studied by X-ray diffraction (XRD), both in powder and oriented mounts, in order to further select samples for analysis by electron microprobe analysis (EPMA). The main clay minerals Fe-rich chlorite and mica and Fe-rich chlorite, the latter determined by the 002 reflection being more intense than the 001. Moreover, the complete absence of expandable layers, both as discrete phases and as I/S and C/S mixed-layers, has been confirmed by ethylene glycol solvation. EPMA preliminary results indicate chamosite-like chlorites. The calculated structural formulae indicate estimated formation temperatures between 350 to 150 °C, showing an evolution of decreasing (?) temperatures over time and indicates a similar process to those previously indicated from fluid inclusion analyses.

Bourdelle F., Parra T., Chopin C. and Beyssac O. (2013) A new chlorite geothermometer for diagenetic to low-grade metamorphic conditions. *Contributions to Mineralogy and Petrology*, 165(4), 723-735.



## Fluid-rock interaction in a fault-controlled geothermal system: the Pucuro Fault System in Central-Chile

Mercedes Vázquez<sup>1</sup>, Diego Morata<sup>1</sup>, Leonardo Navarro<sup>1</sup>, Fernando Nieto<sup>2</sup>, Isabel Abad<sup>3</sup>, Gloria Arancibia<sup>4</sup>, Linda Daniele<sup>1</sup> and Gert Heuser<sup>4</sup>

1. Department of Geology and Andean Geothermal Center of Excellence, Facultad de Ciencias Físicas y Matemáticas, Universidad de Chile, Santiago (Chile). mvazquez@ing.uchile.cl; dmorata@ing.uchile.cl;
2. Departamento de Mineralogía y Petrología and Instituto Andaluz de Ciencias de la Tierra, Universidad de Granada-CSIC. Granada (Spain). nieto@ugr.es
3. Departamento de Geología y CEACTierra, Unidad Asociada IACT (CSIC-UGR) Universidad de Jaén, 23071, Jaén, Spain miabad@ujaen.es
4. Departamento de Ing. Estructural y Geotécnica, Pontificia Universidad Católica Chile, and Andean Geothermal Center of Excellence, Santiago, Chile. garancibia@ing.puc.cl

Understanding the fluid flow behaviour in the most upper crust is becoming increasingly important due to the rising economic significance of geothermal systems and hydrocarbon storage. Geothermal manifestations frequently occur along faults, where the hydrothermal mineralization occurs according to the development and evolution of heat-fluid-rock interactions. Fluid flow drives a precipitation of mineral phases at low P-T conditions; consequently, the study of these new phases provides important information about the physical and chemical conditions of the fluids during hydrothermal process.

In this contribution we present a detailed mineralogical and petrological study (XRD, SEM/EDX and TEM/AEM methods) of hydrothermally altered Meso-Cenozoic volcanic and volcanoclastic rocks along the long-lived Pucuro Fault System in central Chile. Present-day fluid circulation along this fault system is evident by the presence of several low-temperature thermal springs, spatially related to this regional fault zone. Hydrothermal minerals from veins and host rocks have been used to reveal the physical and chemical evolution of the geothermal fluids that drove geothermal alteration during Cenozoic.

Calcite (the most abundant mineral), zeolites and phyllosilicates are the main minerals identified. Minor presence of other minerals such as epidote and titanite has also been detected. Laumontite is the most dominant zeolite, with wairakite, stilbite, epistilbite, yugawaralite, scolecite and analcime found only sporadically. Smectite is the most abundant phyllosilicate, but illite, chlorite, illite-smectite (I-S) R1, and chlorite-smectite (C-S) mixed layers were also identified. Chlorite thermometry (Bourdelle et al., 2013) indicates the chlorite formation temperature was around 220°C. Distribution of secondary mineralogy along the fault zone shows a clear zonation. Chlorite, illite, wairakite, yugawaralite, epidote and titanite appear in the core fault zone, where alteration is pervasive. Textural evidences show that wairakite and epidote crystallised before illite and smectite. On the other hand, in the damage zone, wairakite and laumontite appear exclusively in veins, while mixed layer clay minerals appear sporadically in the host rock.

Our results suggest high-T fluid-flow in the core fault zone, as indicated by the presence of high-T zeolites (yugawaralite, laumontite and wairakite), chlorite, illite and epidote. P-T conditions of these fluids would be around 220° C under hydrostatic pressure ( $P_{\text{fluid}}/P_{\text{total}}$  around 0.37). On the other hand, the presence of I-S R1 and C-S mixed layers in the damage zone would indicate lower temperatures (120-170°C) under similar fluid pressure. Pulses of hot fluids following permeable zones can explain the crystallisation of wairakite in the damaged zone at around 220-330°C. The hydrothermal mineralogy described in the Pucuro Fault System indicates long-lived geothermal activity, evolving from ancient high-T fluid circulation to present low-T thermal springs.

**Acknowledgements:** This research has been funded by Chilean Fondap-Conicyt 15090013 project “Andean Geothermal Center of Excellence (CEGA)” and the 1140629 Chilean Fondecyt Project.

Bourdelle et al. (2013). Contribution to Mineralogy and Petrology, 165, 723-735.

## Study of the low-grade thermal evolution of the Wairarapa area, North Island, New Zealand

Pierre Malie<sup>1</sup>, Sébastien Potel<sup>2</sup>, Rafael Ferreira Mählmann<sup>b</sup>, Julien Bailleul<sup>a</sup>, Frank Chanier<sup>c</sup>, Geoffroy Mahieux<sup>d</sup>, Vincent Crombez<sup>e</sup> and Brad Field<sup>f</sup>

<sup>1</sup> B2R, Institut Polytechnique LaSalle Beauvais, Geosciences Department, 19 Rue Pierre Waguet, F-60026 Beauvais, pierreromain.malie@gmail.com

(b) Technical and Low Temperature Petrology, Institut für Angewandte Geowissenschaften, Technische Universität Darmstadt, Schnittspahnstraße 9, D-64287 Darmstadt, Germany

(c) 8217-LOG, bâtiment SN5, University of Lille, Cité Scientifique, F-59650 Villeneuve d'Ascq, France

(d) University of Picardie Jules-Verne, Chemin du Thil, F-80000 Amiens, France

(e) IFP Energies nouvelles, Geosciences Division, 1 et 4 avenue de Bois-Préau, F-92852 Rueil-Malmaison Cedex, France

(f) GNS Science, 1 Fairway Ave, Lower Hutt, New Zealand

The thermal evolution of sedimentary basins in complex domains (i.e., orogenic wedges) is difficult to assess because of: 1) the low resolution of some thermo-barometric methods for low temperatures, 2) the absence of well constrained correlations between the different methods, and 3) the high number of geological parameters that may influence each individual determination (e.g., sedimentation and burial history, structural development of the orogenic wedge, faulting and associated fluid circulation, lithology). This is especially the case for accretionary prisms that are associated with very low heat flows and are generally submerged.

The Hikurangi prism in the North Island of New Zealand, which is generally considered to have developed during subduction of the Pacific plate under the Australian plate since 25 Ma, is partially emerged and therefore constitutes an excellent, accessible analogue. The highest part of the accretionary wedge outcrops in the Coastal Ranges, and permits high resolution sampling of Neogene trench slope basins and their Cretaceous to Oligocene basement. From previous work, there is a good understanding of the tectono-stratigraphic evolution of the Coastal Ranges and thus it is possible to present a preliminary thermobarometric data set, allowing comparisons between illite and chlorite "crystallinities" (Kübler and Árkai indices, respectively), and organic matter characterization (vitrinite reflection and  $T_{max}$ ). The resolution of our sampling enables the local importance of individual faults on exhumation rates and uplift to be tested. A particular focus of this study is to elucidate the influence of thrust-nappe emplacements.

## Isotopic investigation of clay gouge from the central Alpine Fault, New Zealand: Testing the meteoric geofluid infiltration hypothesis

Austin Boles<sup>1</sup> and Ben van der Pluijm<sup>1</sup>

<sup>1</sup>Department of Earth and Environmental Sciences, University of Michigan, 1100 North University Ave., Ann Arbor, MI, 48109, USA (aboles@umich.edu)

Recent work on clay-gouge bearing brittle fault zones from around the world has proved the viability of a new isotopic method that uses authigenic illite to constrain the source and timing of paleofluid activity in the earth's upper crust—illite uniquely lends itself to both hydrogen isotopic analysis and  $^{40}\text{Ar}/^{39}\text{Ar}$  geochronology. The method utilizes grain-size separation techniques and illite polytypism to generate size fractions with varying authigenic and detrital ratios, which in turn are used to extrapolate to true end-member values. Our hydrogen isotope approach has been adapted from Illite Age Analysis techniques. Together, these powerful methods can provide information about both the timing of neof ormation and the composition of the mineralizing fluid that produced a given population of clay minerals. The results have implications for fault mechanics, crustal-scale fluid circulation models, and economic deposit generation and exploration. In this study, an integrated XRD-isotopic method has been applied to a suite of gouge samples collected along the surface trace of the Alpine Fault of New Zealand. The suite includes samples from the principal slip zone, as well as subsidiary faults in both the hanging wall and footwall of the deformation zone. Preliminary X-ray characterization and polytype analysis indicates that some of the minor faults may be shallow in nature, without the displacement and exhumation needed to promote illite authigenesis. On the other hand, we expect that after X-ray characterization and isotopic investigation, samples from the principal slip zone will preserve neof ormed illite, testing our hypothesis of meteoric fluid infiltration at depths of several kilometers into the fault, similar to other continental strike-slip systems.

## Effect of process water circulation and stability of clay minerals in fluid fault zones: Tíscar active fault (Betic Cordillera, SE Spain)

Pilar Hernández Puentes<sup>1</sup>, Rosario Jiménez Espinosa<sup>2</sup> and Juan Jiménez Millán<sup>2</sup>

<sup>1-2</sup>Department of Geology, CEACTierra, IACT partner unit (CSIC-UGR), Faculty of Experimental Sciences, University of Jaén, Campus Las Lagunillas s / n, building B3, 23071 Jaén, Spain; ppuentes@ujaen.es

We have studied the effect of water flow processes and clay neof ormation in relation to the Tíscar active fault zone (Betic Cordillera, SE Spain) with the aim of obtaining data about the mechanical behaviour of these materials and their influence on the seismicity of the study area. The N130-150E strike-slip Tíscar fault is an important tectonic feature within the Betic External Zone, with a 6 km dextral translation and an extension of more than 20 km, and affected the Mesozoic and Tertiary cover detached from the Palaeozoic basement (Foucault 1971). These geological features will give this study area an important potential seismic hazard recently expressed by the earthquake of January 31<sup>st</sup>, 2012 in the Paleozoic basement (7 km), epicentre at W of Huesa and with a intensity of IV and a magnitude of 4.4 m<sub>bLg</sub>, 4.0M<sub>w</sub> ([www.ign.es](http://www.ign.es); Pérez-Valera et al. 2012).

Hydrogeochemical characterization indicates: (1) low conductivity waters (<840 µS/cm) and low mineralization (8 meq/l), with a Ca-Mg-HCO<sub>3</sub> type of hydrochemical facies; and (2) more salty waters (up to 3740 µS/cm) with a higher ionic content (up to 70 meq/l), and Ca-Mg-SO<sub>4</sub>-Cl facies. Alkaline waters, with temperatures below the hydrothermal limit (19 °C) were found, showing a surficial origin for them. Nevertheless, two samples with T >20°C and high boron contents (>0,3 ppm) have been identified, suggesting a deeper origin and a probable relationship with the fault activity.

Mineral stability plots have shown how groundwater in this area is in thermodynamic equilibrium with kaolinite for a group of samples and with smectite for another one. In this sense, the more stable minerals are smectite and kaolinite. Moreover, we have studied the internal microstructure of the fault rocks related to groundwater sites revealing deep water flow circulation and the presence of clays along weakness planes, with evidence of illite-rich levels, which promoted different slide surfaces, and calcite-rich levels with no deformation. Furthermore, smectite thin sheets are common throughout slide surfaces.

A multidisciplinary study of the Tíscar Fault Area including both the physico-chemical properties of the fluids circulating through fault planes and the characterization of rocks by SEM was carried out. This investigation has shown that during the faulting and fluid-rock interaction a significant growth of clay minerals took place in these rocks. Cataclasis and fluid infiltration during fault activity promoted the creation of microsites favourable for nucleation and neomineralization throughout the slide surfaces.

Financial support was provided by Andalusian Research Groups RNM-325 and by the Research Projects CGL2011-30153-C02-01 (Spanish Ministry of Economy and Competitiveness).

Foucault A (1971) Étude géologique des environs des sources du Guadalquivir (prov. Jaén et Granada, Espagne meridionale). Thèse de doctorat, Université de Paris VI, 633 p

Pérez-Valera F, Sánchez-Gómez M, Peláez JA, Pérez-Valera LA (2012) Fallas de edad Pleistoceno superior en el entorno del terremoto de Huesa, Jaén (4.4 m<sub>bLg</sub>, 31/01/2012): Implicaciones sismotectónicas. Geogaceta 52:25-28

## Phyllosilicates in the Alhama de Murcia fault zone and its influence in fault seismicity

C. Sanchez<sup>1</sup>, I. Abad<sup>1</sup>, F. Nieto<sup>3</sup>, J. Jimenez-Millan<sup>1</sup>, D.R. Faulkner<sup>2</sup>

<sup>1</sup> Departamento de Geología y CEA-Tierra, Unidad Asociada IACT (CSIC-UGR) Facultad de Ciencias Experimentales, Universidad de Jaén, Campus Las Lagunillas s/n 23071, Jaén, Spain

<sup>2</sup> Rock Deformation Laboratory, Department of Earth and Oceanic Sciences, University of Liverpool, 4 Brownlow Street, Liverpool L69 3GP, UK

<sup>3</sup> Departamento de Mineralogía y Petrología and IACT (CSIC-UGR), Facultad de Ciencias, Universidad de Granada, Avda. Fuentenueva s/n 18002, Granada, Spain

The collision of the Eurasian and the African plates keeps the southern Iberian Peninsula a tectonically active area. Many active faults are recognized in the area including the Carboneras, Baza, Galera, Alhama de Murcia and Palomares faults, some of which have been recently responsible for large magnitude earthquakes. The 5.1-magnitude Lorca Earthquake in May 2011 caused significant localized damage in the Murcia region leaving a total of nine deaths and an estimated four hundred injured. The aim of this study is to identify mineralization along the Alhama de Murcia's Fault plane, characterize them and evaluate the possible effects on the seismic activity of the fault.

The Alhama de Murcia Fault is a strike-slip fault located in the eastern Betic Cordillera, separating rocks from their internal zone. The fault is trending NE-SW and extends for 100 km. Samples were collected from three locations within the Lorca-Totana segment, directly from the fault plane of the Alhama de Murcia Fault, including a trench recently uncovered after the 2011 earthquake. A total of 27 samples were characterized by X-ray diffraction analyses of whole rock and clay fractions (<2µm). Analyses of the clay fractions show that all samples contain high amounts of K- and Na-dioctahedral micas, small amounts of quartz, carbonates, chlorite and haematite. There were no significant changes after ethylene glycol solvation, indicating the absence of expandable clays such as smectite except for minimal amounts in two samples. Meanwhile, kaolinite is present in all the samples. In addition to the fault gouges, apparent phyllites and schists were sampled near the fault. Polished thin sections were studied using a Merlin Carl Zeiss Scanning Electron Microscopy, showing that they are in fact microbreccias extremely deformed and very fine-grained, which confirms fault deformation by brittle fracturing. The textural and mineral characterization by SEM shows that the kaolinite crystals range in size from 40 µm to < 2 µm and are usually filling gaps in the rock structure and associated with K- and Na-micas, following their same orientation.

The high amounts of K and Na micas in the fault rocks is consistent with the mineralogy of the protolith characterized in detail for the area of Sierra Espuña by Abad et al. (2003). Nevertheless, kaolinite has not been described in any protolithic sample, which contrasts with its presence in all samples collected in or near the fault plane. The presence of kaolinite, the only authigenic mineral, in the fault rocks can have some consequences on the frictional stability of the Fault. Kaolinite has a friction coefficient of 0.40 dry and 0.29 wet (Behnsen and Faulkner, 2012), however its frictional behaviour is high when compared with the expandable clay minerals, 0.39 dry and 0.12 wet, which have often been related to fault stability as in the case of the central segment of the San Andreas Fault (Lockner et al., 2011). The general absence of expandable minerals could explain the fact that the fault is being controlled more by brittle mechanisms than plastic behaviours, especially since stronger minerals present in the fault, could trigger a more explosive release of elastic energy (Fagereng and Toy, 2014). The mineral characterization of other more seismically stable segments of the Alhama de Murcia Fault, will help to confirm the relevance of the kind of phyllosilicates present in faults.

Abad, I., Nieto, F., Peacor, D.R. and Velilla, N. (2003). *Clay Miner.*, 38, 1-23.

Fagereng, Å. and Toy, V.G. (2014). Geological Society, London, Special Publications 359 (1), 1-16.

Lockner, D.A., Morrow, C., Moore, D., Hickman, S. (2011) *Nature* 472, 82-85.

Behnsen, J. and Faulkner D.R., (2012) *Journal of Structural Geology* 42, 49-61.

## Preferred orientation of talc in tectonites

J. Gómez-Barreiro<sup>1</sup>, J.M. Benítez Pérez<sup>1</sup>, M. Suárez<sup>1</sup>, E. García-Romero<sup>2</sup>, M. Durán Oreja<sup>6</sup>,  
M. Sánchez del Río<sup>3</sup>, O. Oriol Vallcorba Valls<sup>4</sup>, H.-R. Wenk<sup>5</sup>, J. García Rivas<sup>1</sup> and B. Ouladdiaf<sup>5</sup>

<sup>1</sup> Departamento de Geología, Universidad de Salamanca, Salamanca, Spain

<sup>2</sup> Departamento de Mineralogía y Cristalografía, Universidad Complutense de Madrid, Madrid, Spain

<sup>3</sup> European Synchrotron Radiation Facility, Grenoble, France

<sup>4</sup> ALBA Synchrotron, Cerdanyola del Vallès, Spain

<sup>5</sup> Department of Earth and Planetary Science, University of California, Berkeley, California, USA

<sup>6</sup> Institut Laue-Langevin, Grenoble, France

Experimental and field observations indicate that fault rocks (mylonites) generated along the subduction channel determine the mechanical evolution of the system. Along the shallow portion of the subduction zone (above 100 km), the mylonites consist of a complex mixture of weak hydrous minerals, mainly serpentine (antigorite), talc and chlorite. All those phases are strongly anisotropic and should have a critical influence on the seismic anisotropy of the subduction zone. Beside, the abundance of those phases would favor slip along the subduction interface that causes 'silent earthquakes'. In spite of their geological relevance, little is known about the crystallographic preferred orientation of phases like antigorite and talc. The quantification of the preferred orientation of talc in polymineralic tectonites is a challenging task. A quantitative texture analysis based on the Rietveld method was applied to diffraction data of selected tectonites. Talc ODF data were used to evaluate elastic anisotropy of the polycrystals.

## Na-bearing white micas from the Permo-Triassic Rocks of the Ghomaride Complex and Federico Units (Internal Zone of the Rif Chain, northern Morocco)

M.D. Rodríguez-Ruiz<sup>1</sup>, M.D. Ruiz-Cruz<sup>1</sup>, C. Sanz de Galdeano<sup>2</sup> and M.J. Bentabol-Manzanares<sup>1</sup>

Departamento de Química Inorgánica, Cristalografía y Mineralogía, Facultad de Ciencias, Universidad de Málaga, Campus de Teatinos, 29071-Málaga, Spain

Instituto Andaluz de Ciencias de la Tierra, CSIC-Universidad de Granada, Facultad de Ciencias, 18071-Granada, Spain  
mdrodriguez@uma.es

K-white mica, white mica with intermediate Na-K composition, and paragonite from diagenetic to epizonal Permo-Triassic rocks of the Ghomaride complex and of the Federico units (Internal Zone of the Rif, North of Morocco) were studied by X-ray diffraction (XRD), Scanning Electron Microscopy/Energy Dispersive X-ray Spectroscopy (SEM/EDX) and Transmission/Analytical Electron Microscopy (TEM/AEM). The diagenetic-to-low anchizonal sandstones contain the assemblage K-illite + Na+K-illite + dickite + sudoite. The BSE images show that the dickite packets are replaced by K and Na+K illites. The Na/(Na+K) ratio determined in illite defines two populations with mean Na/(Na+K) ratios  $\sim 0.19$  and  $\sim 0.36$ , the second one clearly within the miscibility gap characteristic of low-temperature white mica (Chatterjee and Flux, 1986; Roux and Hovis, 1996). The lattice-fringe images of illite grains show intergrowths of packets of  $1M$  and  $2M_1$  polytypes, which correspond respectively to illite with the highest Na content and K-illite.

Under low anchizonal conditions, the mineral assemblage identified by SEM in sandstones and conglomerates is K-illite + pyrophyllite  $\pm$  dickite  $\pm$  Na+K illite  $\pm$  clinocllore. The EDX data show again two illite populations, with mean Na/(Na+K) ratios of  $\sim 0.50$  and  $\sim 0.17$ .

The high-anchizonal phyllites contain muscovite  $\pm$  paragonite  $\pm$  white mica with intermediate Na-K composition + clinocllore. The low-magnification TEM images of white mica grains show stacks of Na-K intermediate mica interleaved with sub-parallel packets of paragonite or muscovite. The lattice-fringe images of Na-K intermediate micas exhibit changes in crystal orientation and areas with 10 and 20 Å periodicities, the latter with wavy aspect. The SAED patterns show splitting along of the 00/ reflections of paragonite and muscovite and arcs perpendicular to  $c^*$ .

Under epizone conditions, fine-grained blue phyllites contain paragonite and muscovite also coexisting with white mica with Na-K intermediate composition, pyrophyllite and clinocllore. An increase in thickness of the mica packets relative to the high-anchizonal samples is observed at the TEM scale. The 00/ reflections of different white micas are distinguished.

Our data indicate that K- and Na-K illites formed from dickite under diagenetic and low anchizonal conditions. The entry of Na into the white mica structure appears to be related to the increase in temperature characterising the onset of the anchizone, with albite as the source of Na. Under high-anchizonal and epizonal conditions the TEM data suggest that white mica with intermediate Na+K composition represents a metastable phase in the formation of the Na end-member (paragonite).

Chatterjee, N.D. and Flux, S. (1986). Thermodynamic Mixing Properties of Muscovite-Paragonite Crystalline Solutions at High Temperatures and Pressures, and their Geological Applications. *Journal of Petrology*, 27, 677-693.

Roux, J. and Hovis, G.L. (1996). Thermodynamic Mixing Models for Muscovite-Paragonite Solutions Based on Solution Calorimetric and Phase Equilibrium Data. *Journal of Petrology*, 37, 1241-1254.

## Key properties of selected organo-clay-polymer nanocomposites

Peter Komadel<sup>1</sup>, Jana Madejová<sup>1</sup>, Ľuboš Jankovič<sup>1</sup>, Valéria Bizovská<sup>1</sup>, Lukáš Petra<sup>1</sup>, Daniela Joheč-Mošková<sup>2</sup> and Ivan Chodák<sup>2</sup>

<sup>1</sup>Institute of Inorganic Chemistry, Slovak Academy of Sciences, SK-845 36 Bratislava, Slovakia, peter.komadel@savba.sk

<sup>2</sup>Polymer Institute, Slovak Academy of Sciences, SK-845 41 Bratislava, Slovakia

Over the past decade the scientific community has largely focused on the preparation of polymer-clay nanocomposites (PCNs) in consequence of significant improvement in the resulting material properties by the addition of a tiny amount of these nano-dimensional particles. Continued progress in nanoscale controlling and an improved understanding of the physico-chemical phenomena at the nanometre scale have contributed to the rapid development of novel PCNs. Generally, the first step in the preparation of a PCN is in rendering the hydrophilic montmorillonite to a more organophilic using an ion exchange between naturally occurring alkali cations residing mostly between the aluminosilicate layers and alkyl ammonium surfactants to produce organo-modified clay. The selection of a suitable organo-clay is critical for producing nanocomposites with excellent exfoliation. Structural aspects of the surfactant like the number and length of alkyl tails, degree of saturation, etc., along with the amount of surfactant loading on the clay may significantly affect the degree of clay exfoliation. This abstract overviews the results gathered by Jankovič et al. (2011) and Madejová et al. (2011). In contrast to other studies investigating mainly long chain quaternary alkylammonium cations, they examined also ammonium cations containing different number of octyl chains.

Na-saturated montmorillonite Jelšovský Potok (Slovakia) and different surfactants containing octylammonium and/or hexadecylammonium chain(s) were used for organo-clay preparation. Four samples contained 1–4 octylammonium chains, from mono-octylammonium (1C8–JP) to tetra-octylammonium (4C8–JP). Two cations had chains with 16 carbons each, hexadecylammonium (1C16–JP) and dihexadecyldimethylammonium (2C16–JP). The  $d_{001}$  values depended on the size and structure of the organo-cation. The height of the interlayer space, obtained from the  $d_{001}$  by subtraction of the layer thickness of 0.96 nm, increased in the 1C8–4C8–JP series from 0.45 to 1.68 nm, and 0.84 – 2.20 nm for 1C16–JP and 2C16–JP. The 2C8 cation opened the interlayer space more than 1C16; 2C16 was more effective than 4C8. Infrared (IR) spectroscopy in the mid-IR (MIR) and near-IR (NIR) regions was used for organo-clay characterization. Infrared spectra were similar for 1C8–4C8–JP but different for the samples with 16 C and 32 C atoms due to altered ratios of CH<sub>3</sub> and CH<sub>2</sub> groups. Based on the stretching ( $\nu$ ) and bending ( $\delta$ ) vibrations in the middle IR (MIR) region, the first overtone (2 $\nu$ XH) and combination ( $\nu$ + $\delta$ )XH modes of XH groups (X = O, C, N) were discussed. The intensity of the ( $\nu$ + $\delta$ )H<sub>2</sub>O band decreased with the size of the organic cation reflecting increasing hydrophobicity of the montmorillonite surface. The NIR spectra were extremely useful in identification of NH<sub>2</sub><sup>+</sup> and, NH<sup>+</sup> groups, which were difficult to recognize in the MIR spectra of organo-clays due to their overlapping with other absorption bands.

The suitability of the prepared materials to be used as fillers for polymer nanocomposites was assessed by determining rheological data of dispersions in solvents selected according to solubility parameters. These should be the same or close to the values for a particular polymer intended to be used as potential matrix. The conclusions based on rheological measurements were confirmed by characterization of structure of composites of the organomodified clay in polyethylene, polycaprolactone, or polyamide matrices. Consequently the ultimate mechanical properties were determined. Strain at break and tensile strength differ significantly depending on the filler modification. Generally the positive effect was more pronounced for clay modified with larger cations.

Financial support from the Slovak Research and Development Agency, project APVV-0362-10, is acknowledged.

Jankovič L., Madejová J., Komadel P., Joheč-Mošková D. & Chodák I. (2011) Applied Clay Science 51: 438–444.

Madejová J., Jankovič L., Pentrák M., & Komadel P. (2011) Vibrational Spectroscopy 57: 8–14.



## Weathering of glaciogene marine clays from West Greenland

Louise Josefine Belmonte, Niels Foged and Thomas Ingeman-Nielsen

DTU Civil Engineering (Arctic Technology Centre), Brovej bygn. 118, 2800 Kgs. Lyngby, Denmark  
(email: lojon@byg.dtu.dk)

Deposits of fine-grained marine glaciogene sediments have been observed throughout the previously glaciated parts of the Northern hemisphere. Their particles were formed during glacial erosion of bedrock and deposited in marine environments during the retreating phases of the last glaciation. Although the sediments are distributed over a large geographical area, their overall grain size distributions and qualitative mineralogies are similar. They are dominated by the < 60  $\mu\text{m}$  fraction (clay and silt fractions) and contain only minor amount of the 60-2000  $\mu\text{m}$  fraction (sand fraction) (Belmonte et al., in prep.; Gillott, 1979; Pederstad and Jørgensen, 1985). Their chemical compositions are dominated by  $\text{SiO}_2$  (46-63 wt%),  $\text{Al}_2\text{O}_3$  (14-23 wt%) and  $\text{Fe}_2\text{O}_3$  (4-15 wt%) with an alkali-alkaline earth element content (i.e. the content of  $\text{K}_2\text{O}$ ,  $\text{Na}_2\text{O}$ ,  $\text{MgO}$  and  $\text{CaO}$ ) of 12-16 wt % (Bentley and Smalley, 1978; Gillott, 1971; Locat et al., 1984; Pederstad and Jørgensen, 1985; Roaldset, 1972). They often consist of feldspars, quartz, amphibole, mica/illite, chlorite, expandable clay minerals (e.g. smectite, vermiculite and mixed layer clays) and their < 2  $\mu\text{m}$  fraction (clay fraction) contain a high percentage of primary minerals such as quartz, feldspars and amphibole (Belmonte et al., in prep.; Foged, 1979; Bentley and Smalley, 1978; Gillott, 1971; Gillott, 1979; Locat, 1984; Pederstad and Jørgensen, 1985; Ramesh and d'Angeljan, 1995; Roaldset, 1972).

The presence of the expandable clay minerals raises the question of their origin, for which there are several possibilities. They could have resulted from pre-glacial or sub-glacial weathering of bedrock, weathering in the pro-glacial fluvial system, weathering under marine conditions or, for some, weathering after exposure to sub-aerial conditions.

In this study, marine sediments from West Greenland have been characterised according to their grain size, clay mineralogy, plastic properties and pore water chemistry. The samples were selected to represent environments above and below present day sea level, and with and without permafrost in order to investigate the influence of the different environments on the weathering properties. We argue that the content of expandable clay minerals in the clay fraction indicates that chemical weathering must have been an active process during glacial erosion of bedrock, in deposition in seawater and/or after subaerial exposure.

Belmonte, L.J., Foged, N.N. and Ingeman-Nielsen, T. (in prep) Characterisation and weathering properties of fine-grained marine sediments from West Greenland.

Bentley, S.P. and Smalley, I.J. (1978) Mineralogy of sensitive clays from Quebec. *Canadian Mineralogist*, 16, pp. 103-112.

Foged, N. (1979) Ingeniørgeologiske undersøgelser af kvartære marine leraflejringer på Vestgrønland, Licentiate (Ph.d.) dissertation, Technical University of Denmark, Lyngby, Denmark (in Danish).

Gillott, J.E. (1971) Mineralogy of Leda clay, *Canadian Mineralogist*, 10, pp. 767-811.

Gillott, J.E. (1979) Fabric, composition and properties of sensitive soils from Canada, Alaska and Norway. *Engineering geology*, 14, pp. 149-172.

Locat, J., Lefebvre, G. and Ballivy, G. (1984) Mineralogy, chemistry, and physical properties interrelationships of some sensitive clays from Eastern Canada. *Canadian Geotechnical Journal*, 21, pp. 530-540.

Pederstad, K. and Jørgensen, P. (1985) Weathering in a marine clay during postglacial time. *Clay minerals*, 20, pp. 477-491.

Ramesh, R., d'Anglejan, B. (1995) Mineralogy, Chemistry and particle size interrelationships in some Post-Glacial Marine Deposits of the St. Lawrence Lowlands. *Journal of Coastal Research*, 11 (4), pp. 1167-1179.

Roaldset, E. (1972) Mineralogy and geochemistry of Quaternary clays in the Numedal area, southern Norway, *Norsk Geologisk Tidsskrift* 52 (4), pp. 335-369.

## **Sedimentology and mineralogy of paleosol and fluvio-lacustrine succession of the Late Miocene Bayramhacılı member, Cappadocian Volcanic Province, central Turkey: paleoenvironmental and paleoclimatic interpretation**

Selahattin Kadir<sup>1</sup> and Ali Gürel<sup>2</sup>

<sup>1</sup> Eskisehir Osmangazi University, Department of Geological Engineering, TR-26480 Eskisehir, Turkey skadir.euroclay@gmail.com

<sup>2</sup> Niğde University, Department of Geological Engineering, TR-51200 Niğde, Turkey

The Late Miocene was characterized by high global temperatures (the Messinian salinity crisis). During this epoch the Mediterranean Sea went into a cycle of partly or nearly complete desiccation throughout the latter part of the Messinian age. The marine Mediterranean Sea area has been studied from widely different perspectives. Nevertheless, non-marine paleoenvironmental and paleoclimatic records of the Late Miocene surrounding the Mediterranean area are very limited in their spatial range. The paleosols and fluvio-lacustrine sedimentary rocks (limestone, marlstone and diatomite) of the Bayramhacılı member of the Ürgüp Formation were examined using polarized-light microscopy, X-ray diffractometry (XRD), and scanning-electron microscopy (SEM-EDX), as well as by chemical methods. Red colored paleosols formed within these terrestrial sedimentary rocks under near surface or surface conditions, and comprise predominantly of smectite  $\pm$  illite with feldspar, quartz, opal-CT, serpentine and amphibole. Micromorphological development of flaky smectite edges on illite and between devitrified volcanic glass and relict feldspar crystal reveals in-situ precipitation based on dissolution and precipitation mechanisms. The sedimentary rocks such as limestone, marlstone and diatomite formed in lacustrine environment. The alteration of the ignimbrites caused the depletion of Si, and increase of Al+Fe+Mg, Ti, and K (and related Ba+Sr) favored precipitation of smectite  $\pm$  illite in paleosols. The appearance of limestone, marlstone and diatomite from the upper profile level is suggestive of a shift to more arid or more seasonal conditions that is coincident with a prominent change in sediment provenance and these indicate decrease in sedimentation rate during the latter part of the Messinian age.

**Keywords:** Cappadocia, smectite $\pm$ illite, cyclic sedimentation, mineralogy, paleoclimate, paleoenvironment.

**Acknowledgments:** This study was financially supported by the Scientific and Technological Research Council of Turkey (TÜBİTAK) within the framework of Project No. 104Y070.

## Salts present in the materials developed on marl in an area of badlands in Alicante (Spain )

Laura García-España<sup>1</sup>, María Desamparados Soriano<sup>1</sup> and Anatonela Colica<sup>2</sup>

<sup>1</sup>School of Agricultural Engineering and Environment. Cami de Vera s/n. Politechnical University of Valencia. 46021, Valencia, Spain

<sup>2</sup>Department of Earth Sciences. University of Firenze. Piazzale delle Cacine 15 . 50147, Firenze, Italy  
asoriano@prv.upv.es

Saline materials present in an area of badlands have been studied using petrographic, geochemical and SEM-RX techniques. The geographical location of the studied system is located northwest of the province of Alicante (Spain), and corresponds to an area covered by sedimentary rocks of Cretaceous age with ???plenty of plasters??? and Quaternary sediments in high river terraces and infilling flat-bottomed valleys. The salts in this system are of  $Mg^{2+}$ ,  $Na^+$ ,  $SO_4^-$  type, and the main saline minerals are thenardite, halite and gypsum (IGME, 1978). The carbonate matrix is often dolomite formed in Holocene and Pleistocene inland lakes.

For the materials represented by eight samples (M1 to M8) (Fig. 1), the  $Ca^{2+}$ ,  $Mg^{2+}$ ,  $Na^+$ ,  $K^{2+}$ ,  $SO_4^-$ ,  $Cl^-$ , and  $HCO_3^-$  contents were determined to show the significant differences in the average  $Na^+$  contents of high (900 ppm) and  $Cl^-$  (300 to 3000 ppm) and in the values of  $pH > 8$ ,  $CE$  (2-8  $dS \cdot m^{-1}$ ), and density (between 1.02 to 1.40  $g/cc$ ), analyses confirmed by the X-ray diffraction (XRD) and scanning electron microscopy with X-ray analyzer (SEM- RX) salts with a composition shown halite, gypsum and thenardite, varying in proportion depending on the type of material, by studying morphological and chemical that this technique allows. DO NOT UNDERSTAND THIS VERY LONG SENTENCE In photomicrographs WHICH ONE?? thenardite mineral comprising sodium sulphate,  $Na_2(SO_4)$ , crystallized shown in the rhombic system, shaped and presents two pyramids light gray colors. The materials presented illite and kaolinite clays, with the presence of montmorillonite and accompanying minerals. THIS LAST PARA IS A NONSENSE!

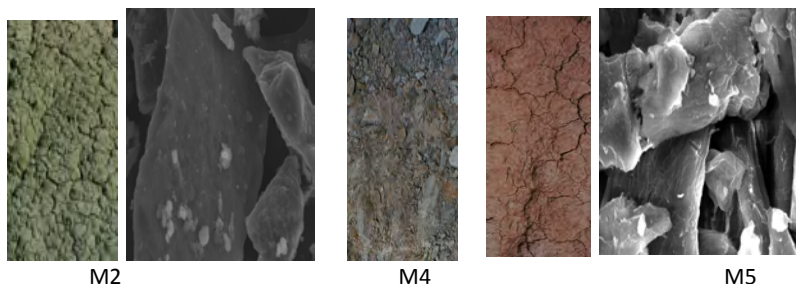


Figure 1. Materials of the study area . Electron microscopy of samples

## Identification of the main parameters controlling the plasticity of ceramic pastes: The case study of the Marrakech region (Morocco)

Hicham El Boudour El Idrissi<sup>1</sup>, Lahcen Daoudi<sup>2</sup>, François Fontaine<sup>1</sup>, Frédéric Collin<sup>3</sup> and Nathalie Fagel<sup>1</sup>

<sup>1</sup>UR Argile, Géochimie et Environnement sédimentaires (AGEs), Département de Géologie B.18, Sart-Tilman, Université de Liège, Liège, B-4000, Belgique; h.e.elidrissi@gmail.com

<sup>2</sup>Laboratoire de Géosciences et Environnement, Département de Géologie, Faculté des Sciences et Techniques, BP 549, Marrakech, Maroc.

<sup>3</sup>Laboratoire de Géotechnologies; Département Argenco, B52, Sart-Tilman, Université de Liège, Liège, B-4000, Belgique.

Numerous traditional ceramic workshops occur within a range of 10 to 80 km around the city of Marrakech. Our study aims to identify the main parameters controlling the plasticity of pastes used by the artisans. To reach this goal, we have characterized the local raw clay material by X-ray diffraction, granulometry and plasticity index (PI).

The investigation of 26 clay pastes shows the dominance of quartz (20 to 50%) and clay minerals (25 to 60%) with K-feldspar (2 to 17%), plagioclase (2 to 25%), calcite (0 to 18%), dolomite (0 to 15%), goethite (0 to 7%) and trace of hematite and anhydrite (< 3%). Amphibole occurs in trace (< 5%) but only in some samples. The clay minerals are diversified, including illite (10 to 40%), kaolinite (2 to 15%), mixed-layer (ML) (0 to 10%), smectite, vermiculite and chlorite (0 to 5%), and pyrophyllite-talc association (0 to 8%). Sepiolite (12%) is only present in one paste. The grain size is made by variable proportions of sand (5 to 65%), silt (12 to 53%) and clayey fraction (18 to 66%).

The Plasticity index (PI) indicates the presence of two principal groups of pastes. The first group is characterized by PI values ranging between 15 to 18. Their moderate plasticity behavior is related either to the low clay fraction and/or to the absence of plastic clays such as smectites and mixed layer smectitic clays.

The PI of the second group ranges between 20 to 32. The high plasticity values are influenced by the presence of specific clayey minerals like talc-pyrophyllite or sepiolite, or by the high content of smectite plus smectitic mixed-layers within the clay (< 2 micron) fraction. Only one sample without any of these plastic minerals but with a high clay fraction content is characterized by a high PI value (24).

We concluded that the workability of ceramic paste in Marrakech region is controlled by a combination of factors, dominated by the grain size distribution and the content of plastic clay minerals within the fine fraction.

## Residual water in smectites

Artur Kuligiewicz<sup>1,\*</sup> and Arkadiusz Derkowski<sup>1</sup>

Institute of Geological Sciences, Polish Academy of Sciences, ul. Senacka 1, 31-002 Krakow, Poland, ndkuligi@cyf-kr.edu.pl

Smectites and other minerals containing smectitic surfaces, including mixed layer illite-smectite, are capable of retaining molecular water after drying at temperatures above 100°C for prolonged time as was demonstrated by Środoń and McCarty (2008). This so called residual water can be present in smectites up to temperatures corresponding to the onset of dehydroxylation. A systematic quantification of residual water in smectites is absent, despite numerous works on smectite-water interactions.

The aim of this presentation is to summarize results of thermogravimetric (TG) studies performed on six natural smectite reference samples in four cationic forms (Cs, Na, Ca, Mg) representing highly variable hydration enthalpy. TG experiments involved multiple isothermal heating segments of increasing temperature, followed by a ramp heating to 1000°C. Residual water content was calculated by substitution of theoretical dehydroxylation mass loss of completely dry sample from actual mass loss measured during TG experiment. For chosen samples experiments were performed with four different heating rates between isothermal segments in order to determine activation energy ( $E_a$ ) of dehydration of residual water using model-independent isoconversional method.

Contents of residual water varied highly, decreasing with the hydration enthalpy of interlayer cation and drying temperature increase, as is shown on the example of Cheto montmorillonite (Table 1). Calculation of the  $E_a$  of dehydration produced values between 25.8 +/- 1.1 kcal/mol and 29.2 +/- 1.3 kcal/mol for Ca- and Na-Cheto montmorillonite. The calculation methodology was validated by calculating  $E_a$  values of water desorption at temperatures below 110°C that yielded values 16.5 +/- 1 and 10.2 +/- 0.6 kcal/mol for Ca- and Na-Cheto respectively, in accordance with data found in the literature.

Table 1. Residual water contents for Cheto montmorillonite in %<sub>wt</sub> normalized to the mass of the sample at the end of ramp heating.

Interlayer cation	Drying temperature		
	110°C	200°C	300°C
Mg	2.83	1.42	0.36
Ca	1.42	0.91	0.29
Na	0.97	0.66	0.26
Cs	0.86	0.57	0.18

The presented results show that for smectite, prolonged drying at temperatures above the boiling point of water may be too insufficient to reduce the amount of molecular water below the contents that can be neglected during calculation of bulk properties, such as effective porosity.

$E_a$  values of residual water dehydration calculated with isoconversional method are higher than data presented in the literature and are closer to the values of  $E_a$  of dehydroxylation (Drits et al. 2012).

## High-level waste and Spent fuel result from nuclear power generation

Ping Shen and Nick Hankins

University of Oxford, Lady Margaret Hall, Norham Gardens, Oxford OX2 6QA

To dispose of high –level nuclear waste material, the Nuclear Decommissioning Authority's Radioactive Waste Management Directorate (NDA RWMD) advises that it should be packed inside copper canisters, which will then be buried at approximately 650m below the earth's surface.

Multiple engineered barriers are recommended to prevent radioactive nuclide migration to the surrounding environment and groundwater system. An encapsulating layer of clay buffer forms an external barrier between the metal canister and the bedrock, and grouts are used to seal fractures in the bedrock to prevent ground water intrusion. The overall aim of the current research project is to evaluate the interfacial reaction between clay and grouts under the influence of groundwater at various chemical conditions, in order to provide an optimal fracture sealing strategy and prevent the leakage of radioactive nuclides into groundwater.

Three different brands of colloidal silica, namely, Cembinder U22, Eka EXP36 Equivalent and MEYCO MP320 were analysed and evaluated in terms of their buffering capacity, gelling time, gel strength as well as their interactions with bentonite clay.

## Validation of conventional K-Ar dating of single clay test portions

J. M. Wampler<sup>1</sup> and W. Crawford Elliott<sup>2</sup>

<sup>1</sup>Department of Geosciences, Georgia State University, Atlanta, Georgia 30302, USA, wamplerjm@earthlink.net

<sup>2</sup>Department of Geosciences, Georgia State University, Atlanta, Georgia 30302, USA, wcelliott@gsu.edu

Use of separate test portions in conventional K-Ar dating, one for potassium determination and one for extraction and isotopic analysis of argon, limits the accuracy of the age values in several ways. Error in weighing the test portions becomes part of the analytical error for the age value, and if an ordinary analytical balance is used the test portions must be much larger than those typically used in  $^{40}\text{Ar}/^{39}\text{Ar}$  dating of clay. In addition to instrumental error, possible differences in the state of hydration of the separate test portions must be considered in evaluating weighing error. Use of a single test portion for both argon and potassium measurements eliminates the effect of weighing error on the age value and also eliminates any effect of non-equivalence of separate test portions on the age value. Such non-equivalence may arise from inhomogeneity within samples of glauconitic pellets and in size-separated clay fractions that have not been mixed well after the separation process.

Because of the small size of clay particles and of effects of dehydroxylation, radiogenic argon is released virtually completely from phyllosilicate clay particles when they are heated under vacuum at 1000°C for a short time (10–20 minutes). There is no significant loss of potassium from the silicate material during such heating. Clay test portions encapsulated in copper foil may be recovered after heating at 1000°C because the copper does not melt at that temperature. The recovered test portions may then be used for potassium determination. This procedure has the potential to make conventional K-Ar dating competitive with the  $^{40}\text{Ar}/^{39}\text{Ar}$  method in respect to accuracy for dating clay samples.

To validate the procedure, it must be shown that, after the Ar extraction, any radiogenic Ar remaining in and any K lost from the residual solid are both negligible. To test the procedure, glauconitic pellets encapsulated in copper foil were placed within a fused-quartz tube segment having one end closed and having a diameter small enough that the entire tube segment could be inserted within a longer, larger diameter fused-quartz tube that was part of the Ar-extraction line. After evacuation of the line, each capsule in a set of six capsules, typically, was placed for heating in a position near the closed end of the fused-quartz tube segment and well away from other capsules not yet heated. Heating for Ar extraction was by a small, external electrical-resistance heater. Some capsules were heated a second time to see if any radiogenic Ar remained after the first heating. After Ar had been extracted from all the capsules, the fused-quartz tube segment was removed from the extraction line and the capsules were removed for K determination. The inside of the fused-quartz tube segment was then rinsed with a HF-HNO<sub>3</sub> solution to dissolve some evaporated copper and any K that had been lost from the capsules. The amount of K found in such rinse solutions was consistently less than 0.1% of the K remaining in the capsules. The amount of radiogenic Ar released in the second heating of some capsules was consistently less than 1% of the amount released in the first heating. A different approach was used to show that virtually all the radiogenic Ar in sedimentary illite is released by heating at 1000°C. Capsules recovered after Ar extraction from various sedimentary illite samples were not used for K determination. Instead, they were melted within an internal electrical-resistance heater in another part of the Ar-extraction line to show that virtually all of the radiogenic Ar had been released during the initial Ar extraction at 1000°C.

## Influence of clay mineralogy on shallow continental margin sediment shear strength

Joshua R. DeVore<sup>1</sup> and Jeffrey R. Walker<sup>2</sup>

<sup>1</sup>Ohio State University, School of Earth Sciences, 275 Mendenhall Laboratory, Columbus, OH 43210 devore.87@osu.edu

<sup>2</sup>Department of Earth Science and Geography, Vassar College, Poughkeepsie, NY 12604, USA; jewalker@vassar.edu

Shear strength of marine sediments are affected by numerous factors including, vertical effective stress conditions, grain size fraction, diagenesis, and burial history. Using the International Ocean Discovery Program (IODP) legacy data archive, we acquired core samples and pertinent moisture and density data from two off-shore sites with similar stress conditions, sedimentation history, and grain size fraction. We chose a site in the Nankai Trough (site C0001E) and in the Amazon Fan (site 942) in order to study the influences of clay mineralogy on sediment shear strength. Profiles of vertical effective stress versus shear strength show that samples from the Nankai Trough site have significantly higher shear strength than those from the Amazon Fan (Figure 1). X-ray diffraction analyses confirm that both sites contain illite, chlorite, and smectite, along with quartz and feldspar. The Nankai Trough samples contain significant and variable amounts of calcite, whereas the Amazon Fan samples contain a 7Å clay, presumably detrital kaolinite weathered from the Amazon Basin.

The differences in shear strength observed in this study may be influenced by clay mineral properties such as: 1) particle size distribution; 2) factors controlling the flocculation behavior of the clays including pH, valence of exchange cations, and the concentration of pore water electrolytes; or 3) the nature of interparticle and crystallographic bonding. Future work will focus on understanding these complex relationships.

### Increased Shear Strength at S. Japan Site

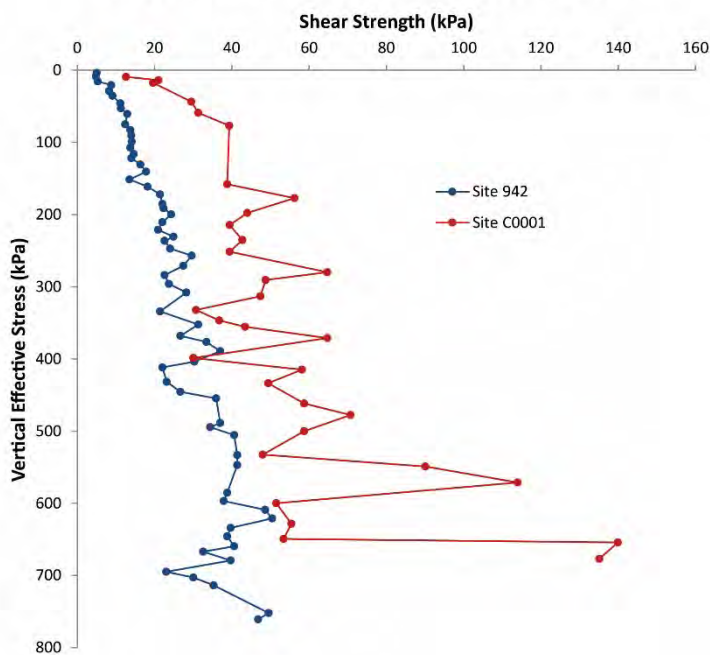


**Figure 1:** Shear strength versus vertical effective stress for site C0001E and 942 from IODP legacy data. Note the consistent increase in shear strength and the variability for site C0001E, trending to a possible merger with increased vertical effective stress. This may have implications for how clay mineralogy effects sediment compaction behavior in dilative versus contractive pore pressure regimes.



## Chlorite nanocrystal formation from amphibolitic and dioritic rocks in Terphis' Serres, Greece

Paraskevi Lampropoulou<sup>1</sup>, Dimitrios Papoulis<sup>2</sup> Eugenia Metaxa<sup>3</sup> Konstantinos Hatzipanagiotou<sup>4</sup> and Theophani Tzevelekou<sup>5</sup>

<sup>1</sup> Geology Department, University of Patras, 26504 p.lampropoulou@upatras.gr

<sup>2</sup> Geology Department, University of Patras, 26504 papoulis@upatras.gr

<sup>3</sup> Geology Department, University of Patras, 26504 eygenia.1990@hotmail.com

<sup>4</sup> Geology Department, University of Patras, 26504 K.Hatzipanagiotou@upatras.gr

<sup>5</sup> Hellenic Center of Metals Research S. A., Athens, 177 78 ftzevelekou@elkeme.vionet.gr

The occurrence of chlorite in metamorphic and igneous rocks of Terpnis' Serres of N. Greece, which are used as raw materials in stone wool production, has been studied. A relation of the distribution of chlorite in the microstructures, its origin and crystal forms, with the production procedure of stone wool was also investigated.

Selected epidote amphibolites and quartz diorite samples were analyzed by various methods and techniques including ICP, XRD, petrographic microscopy, SEM and SEM-EDS.

The epidote-amphibolites show evidences of both hydrothermal alteration and weathering leading to sericitic-saussuritized plagioclase crystals and secondary chlorite nanocrystals. Chlorite is expected to affect positively the grinding procedure and melting of raw materials under industrial conditions of stone wool production, due to its lower hardness and melting point than that of the primary hornblende.

The chemical and mineralogical compositions as well as the microstructure characteristics of the plutonic igneous rock samples (quartz diorite rocks) revealed the presence of some unaltered rocks as well as low to medium altered and completely altered samples affected by hydrothermal solutions but also weathering. Deficient secondary chlorite nanocrystals, smectite and cauliflower hematite are present in the slightly and medium altered rocks, whilst well formed chlorite nanocrystals occurs in the completely altered rocks. The presence of chlorite nanocrystals in both cases are anticipated to result in the easier grinding of the rocks.

## Characterisation of Sotho pot clays using XRF, XRD and FTIR

Antoine F. Mulaba-Bafubiandi and Phindile Hlekane

Mineral Processing and Technology Research Centre, Department of Metallurgy, School of Mining and Metallurgy and Chemical Engineering, Faculty of Engineering and The Built Environment, University of Johannesburg, amulaba@uj.ac.za

The investigation on pot clays used as raw materials for pottery in the Sotho tradition in QwaQwa (South Africa) requires an insight into the mineralogical composition, plasticity, shaping and firing process of the final product. This paper discusses the mineral composition of pot clay materials used in the Sotho culture. Clay pots are produced as a result of a set of indigenous knowledge specific processing procedures where the raw clays are shaped, sun dried, and oven fired using cow dung as fuel. The physical, chemical, and mineralogical characterizations of these pot clays were achieved by means of XRD, XRF and FTIR analysis. XRF results yielded chemical compositions of silica ( $\text{SiO}_2$ ) 62.16%; aluminium ( $\text{Al}_2\text{O}_3$ ) 23.68%; iron oxide ( $\text{Fe}_2\text{O}_3$ ) 6.21% and other oxides with minimal traces. Semi-quantitative XRD analysis shows 5% kaolinite, 16% montmorillonite, 75% quartz and 4% illite yielding a plasticity limit of 31.74 unlike a modern pot clay composed 25% native clay, 45% kaolin clay 10% river clay and 10% pyrophyllite and 10% feldspar. FTIR analyses of these clayey soils show the presence of weak M-OH type bands falling mostly within a wave number range of 680-880 ( $\text{cm}^{-1}$ ). Outcomes of the research presented in this paper provide information to help assess the availability of raw materials for pot making. Their characterisation was done with the view of validating and investigating the factors affecting the production of sealable and durable clay pots.

## Analysis of water content in raw perlite samples

Helena Pálková<sup>1</sup>, Valéria Bizovská<sup>1</sup>, Jana Madejová<sup>1</sup>, Michal Slaný<sup>1</sup>, Adriana Czímerová<sup>1</sup>, Viktor Hronský<sup>2</sup>, Peter Uhlík<sup>3</sup>  
and Jaroslav Lexa<sup>4</sup>

<sup>1</sup> Institute of Inorganic Chemistry, Slovak Academy of Sciences, Dúbravská cesta 9, 845 36 Bratislava, Slovakia, \* e-mail  
helena.palkova@savba.sk

<sup>2</sup> Department of Physics, Faculty of Electrical Engineering and Informatics, Technical University of Košice, Park Komenského 2,  
042 00 Košice, Slovakia

<sup>3</sup> Faculty of Natural Sciences, Comenius University, Mlynská dolina, 842 15 Bratislava, Slovakia

<sup>4</sup> Geological Institute, Slovak Academy of Sciences, Dúbravská cesta 9, 840 05 Bratislava, Slovakia

Perlite is a hydrated acid volcanic glass with wide industrial applications due to its remarkable properties. Perlites are often utilized in the form of expanded materials produced by rapid heating (900-1200°C). The quality of expanded perlite depends on the processing technology as well as on the qualitative parameters of raw perlite, including water content and its binding within the material. The purpose of this work is to characterize raw perlite samples taken from different parts (specified by GPS position) of Lehôtka pod Brehmi deposit (Slovakia) and to evaluate the ability of perlites to adsorb water. Thermal analysis (Fig. A) showed continuous mass loss between 2.5-4 % within the temperature range of 100 – 800°C attributed to the releasing of water molecules and/or dehydroxylation processes within the samples. The shape of the complex band observed in <sup>1</sup>H MAS NMR spectra reflected superposition of several signals (Fig. B). Chemical shifts at 1.7 and 3.4 ppm were attributed to hydrogen from OH groups attached predominantly to silicon in tetrahedral coordination while a sharp signal observable at 4.6 ppm in PL-6b and PL-6a was assigned to the hydrogen of physically bound water molecules. This resonance, very weak in PL-19, was not present in PL-24 and PL-29 (results based on deconvolution). The samples with pronounced signal of bound water showed also slightly higher mass loss in thermogravimetric profiles. The character of water molecules present in the perlite was examined also by NIR spectroscopy. The NIR spectra exhibited the band assigned to combination mode of stretching and bending vibration of H<sub>2</sub>O near 5246 cm<sup>-1</sup> (Fig C). Samples with the highest water content determined from TG profiles, *i.e.* PL-6a and PL-6b displayed broadening of this band towards lower wavenumbers compared to other samples due to the presence of a higher number of strongly H-bonded water molecules. The ability of perlites to adsorb water vapour at RH=100% was studied using of gravimetric analysis. Low amounts of adsorbed water reflected the relatively hydrophobic surface of perlite samples.

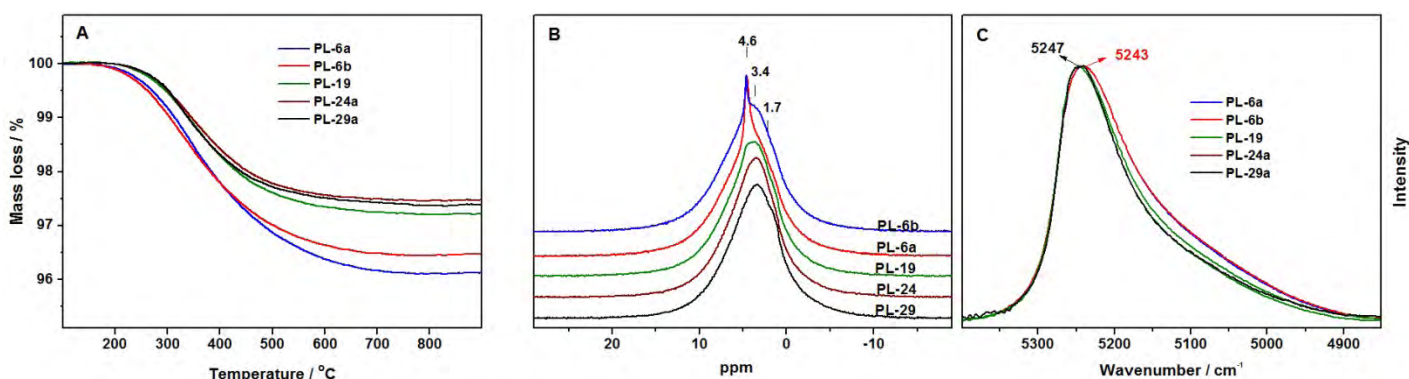


Fig. TG profiles (A), <sup>1</sup>H MAS NMR spectra (B) and NIR spectra (C) of the raw perlite samples

**Acknowledgment:** The authors gratefully acknowledge the financial support of the Slovak Research and Development Agency (contract No. APVV-0339-12).

**THURSDAY**

**ORAL**

**SESSIONS**

Time	Title + Authors	Page No.
08.30	<b>PLENARY:</b> Imperfect minerals can control soil fertility and geochemistry <u>Balwant Singh</u> ( <i>Marion L. and Chrystie M. Jackson Awardee of The Clay Minerals Society; George Brown Lecture of the Clay Minerals Group of the Mineralogical Society</i> ) Introduced by Prof. C. Johnston	271
	<b>Lecture room 5: The many faces of chlorite</b> <i>Session Chairs: Jeff Walker, Atsuyuki Inoue and Daniel Beaufort</i>	
09.10	Preliminary textural studies of the smectite to corrensite transition in the MH 2-B borehole, Snake River Plain, Idaho <u>Jeff Walker</u> , Sarah Perry and Anthony Walton	273
09.30	Mineralogical aspects of interstratified chlorite/smectite from hydrothermal ore veins: Implications for the environmental conditions of formation <u>T. Yoneda</u> and T. Watanabe	274
09.50	Dehydroxylation behavior of five chlorites of the solid solution series of chamosite-clinocllore <u>Annett Steudel</u> , Reinhard Kleeberg, Christian Bender Koch, Frank Friedrich and Katja Emmerich	275
10.10	An experimental study of talc-chlorite-serpentine behavior in a CO <sub>2</sub> ambient <u>Emilio Galán</u> , Inmaculada Macías, Patricia Aparicio and Domingo Martín	276
10.30	Laboratory studies of chloritization of smectite; applications to the clay mineralogy of Gale Crater, Mars <u>Anthony M. Frushour</u> and David L. Bish	277
10.50	<b>BREAK</b>	
11.10	A combined study by HRTEM and HAADF-STEM for Fe-rich berthierine and chlorite interstratified minerals <u>Sayako Inoué</u> and Toshihiro Kogure	278
11.30	<b>KEYNOTE:</b> What do chlorites and other phyllosilicates tell us about their conditions of formation? <u>O. Vidal</u>	279
12.00	Authigenic chlorite in Oligo-Miocene reservoir sandstones, Tapti Gas Fields, offshore western India <u>J. M. Huggett</u> , S.D. Burley and F.J. Longstaffe	280
12.20	Occurrence of tosudite in Guezouman, Tarat and Tchirezrine 2 formations, hosts of uranium deposits in Niger (Tim Mersoï basin) <u>Sophie Billon</u> , Patricia Patrier, Daniel Beaufort, Aurélia Wattinne and Grégoire André	281
12.40	Authigenic chlorite and chlorite-smectite mixed layer as indicator of increasing reducing condition in the Huincul Formation: Neuquén Basin, Argentina M.J. Pons, A. Rainoldi, <u>D. Beaufort</u> , P. Patrier, A. Impiccini and M.B. Franchini	282
13.00	<b>LUNCH</b>	

	<b>Lecture room 5: Structural characterization of lamellar compounds (1)</b> <i>Session Chairs: Douglas McCarty, Eric Ferrage and Vanessa Prevot</i>	
14.00	<b>KEYNOTE:</b> Crystal structures of defective lamellar compounds and their X-ray identification: insights into mineral reactions and material reactivity <u>Bruno Lanson</u>	284
14.30	Non classical crystal growth mechanism in clay minerals <u>E. García-Romero</u> and M. Suárez	285
14.50	Evolution of the configuration of tetrahedra with composition in 2:1 layer silicates <u>Jean-Louis Robert</u>	286
15.10	Influence of crystal structure defects on small-angle neutron scattering/diffraction patterns <u>Eric Ferrage</u> , Fabien Hubert, Emmanuel Tertre, Alain Baronnet, Alfred Delville, Laurent J. Michot & Pierre Levitz	287
15.30	<b>BREAK</b>	
15.50	Analysis of the diffraction pattern of materials with complex microstructure <u>Matteo Leoni</u>	288
16.10	Crystal structures of natural manganese oxide minerals <u>Jeffrey E Post</u> , <i>Peter J Heaney, Florence Ling, and Cara M. Santelli</i>	289
16.30	Water structure and dynamics in smectites: $^2\text{H}$ -NMR spectroscopy of Mg, Ca, Sr, Cs and Pb-hectorite <u>U. Venkateswara Reddy</u> , Geoffrey M. Bowers, Haley E. Argersinger, Brennan O. Ferguson and R. James Kirkpatrick	290
16.50	Stabilization of dyes on oxide surfaces Frédéric Fournier, Philippe Walter and <u>Maguy Jaber</u>	291

	<b>Lecture room 4: Industry perspectives in clay and fine-particle science (1)</b> <i>Session Chairs: Jon Phipps and Prakash Malla</i>	
09.10	<b>KEYNOTE</b> : Process selection heuristics in industrial mineral processing <u>Jarrold Hart</u>	293
09.40	Transition metal nanoparticles derived from phyllosilicates stabilized on SBA-15 mesoporous silica as efficient catalysts <u>C. Ciotonea, B. Drăgoi, A. Ungureanu, A. Chirieac, S. Petit, S. Royer and E. Dumitriu</u>	294
10.00	Silver bentonite complexes as antimicrobial additives in clay-starch based barrier coatings for sustainable packaging <u>Francis Clegg, Chris Breen, Peter Muranyi and Claudia Schönweitz</u>	295
10.20	Electrochemical synthesis of cobalt-containing layered hydroxides on stainless steel sieves: a way for obtaining supported catalysts <u>František Kovanda, Stanislava Krejčová, Daniel Bouša, Květa Jirátková and Lucie Obalová</u>	296
10.40	Influence of additives : boehmite and amorphous silica on geopolymer formulations <u>Lamyaa Laou, Sylvie Yotte, Sylvie Rossignol</u>	297
11.00	<b>BREAK</b>	
11.20	Effect of clay mineral type and associated iron phase on the strengthening of “geomimetic” materials <u>Gisèle L. Lecomte-Nana, Hervé Goure Doubi, Amina Mokrani, Benoît Nait-Ali, Agnès Smith, Léon Koffi Konan</u>	298
11.40	Feasibility of producing geopolymers materials from natural soil clays <u>Julie Peyne, Emmanuel Joussein, Sylvie Rossignol, Jérôme Gautron, Julie Doudeau</u>	299
12.00	Influence of clay mineralogy on the pozzolanic activity of lime treated soils <u>Enza Vitale, Dimitri Deneele and Giacomo Russo</u>	300
12.20	Facile fabrication of MgAl-LDH three-dimensional flower-like micro-nanostructures using surfactant as soft-template <u>Linjiang Wang, Jie Zhang, Xiangli Xie, Cunjun Li</u>	301
12.40	Surface chemistry and interaction of kaolinite particles in the presence of calcium rich alkaline solution <u>Yadeta C. Chemed, Dimitri Deneele, George E. Christidis and Guy Ouvrard</u>	302
13.00	<b>LUNCH</b>	
14.00	Ball clay ageing <u>Martyn Gadsdon and Laurence Boyer</u>	303
14.20	Application results for the quantum design SHGMS magnetic separator <u>Paul A. Beharrell</u>	304
14.40	A methodology to value reservoir sediment in fired-clay industry <u>Frédéric Haurine, Isabelle Cojan and Marie-Anne Bruneax</u>	305
15.00	Techniques for measuring the particle size and shape distribution of ultrafine industrial minerals – a user’s perspective <u>Jonathan Phipps</u>	306
15.20	<b>BREAK</b>	
15.40	Characterization of pH dependent colloidal behavior with respect to the arrangement of clay mineral particles in different arrested states <u>Müge Pilavtepe, Norbert Willenbacher, Annett Steudel, Rainer Schuhmann and Katja Emmerich</u>	307
16.00	The effect of K <sub>2</sub> CO <sub>3</sub> and Al addition on elastic modulus density and porosity of ceramic bodies derived from Westerwald ball clay <u>Aydın Aras</u>	308
16.20	Recycling of Rare Earth Elements from electronic wastes by selective adsorption and desorption on industrial clay minerals <u>Stefan Ginzl, Ralf Diedel, Michael Kunze, Rita Knodt, Caroline Volk, Joachim Scholz, Tobias Johann and Florian Geiger</u>	309

	<b>Lecture room 3: Bentonites: linking clay science with technology</b> <i>Session Chairs: Don Eisenhour, George Christidis and Stefan Kaufhold</i>	
09.10	Boron content and boron isotope composition of Na, Ca and Mg bentonites <u>Mathias H. Köster</u> , Lynda B. Williams, Petra Kudejova, Reiner Dohrmann and H. Albert Gilg	311
09.30	Mineralogy and Geochemistry of bentonites from the Western Thrace and the islands of Samos, Chios, Lesbos, and Limnos, East Aegean Greece <u>George E. Christidis</u> , Eleni Koutsopoulou and Ioannis Marantos	312
09.50	Explosive volcanic eruptions in the Upper Ordovician of the Siberian Platform <u>W.D. Huff</u> , A.V. Dronov, B. Sell, A.V. Kanygin, & T.V. Gonta	313
10.10	Bentonite composition and stratigraphy at Mawrth Vallis, Mars <u>Janice L. Bishop</u> and Christoph Gross	314
10.30	Geochemical properties and geologic significance of Devonian K-bentonites from northwestern Turkey <u>Asuman Günel Türkmenoğlu</u> , Ömer Bozkaya, Mehmet Cemal Göncüoğlu <sup>1</sup> , Özge Ünlüce, İsmail Ömer Yılmaz and Cengiz Okuyucu	315
10.50	<b>BREAK</b>	
11.20	A metamorphic geologist's perspective on clays: from protoliths with potential to essential components of nuclear waste disposal systems <u>Simon Harley</u> ( <i>Mineralogical Society–Schlumberger medallist of the Mineralogical Society</i> ) Introduced by F. Wall	316
11.40	Chemical alteration of bentonite in a radioactive waste repository – illitization of montmorillonite in 70°C by high pH solution <u>Satoru Miyoshi</u> , Yukinobu Kimura, Masahito Shibata, Takashi Sanbuichi and Tsutomu Sato	317
12.00	Effects of temperature, pressure, and brine composition on the interlayer spacing of montmorillonite at <i>in situ</i> conditions using CO <sub>2</sub> <u>Jacqueline Kowalik</u> , <u>Stephen Guggenheim</u> , and A.F. Koster van Groos	318
12.20	X-ray tomographic method for measuring 3D deformation and water content in swelling clays <u>Tero Harjupatana</u> , Jarno Alaraudanjoki and Markku Kataja	319
12.40	About the N <sub>2</sub> -BET-specific surface area of bentonites <u>S. Kaufhold</u> and R. Dohrmann	320
13.00	<b>LUNCH</b>	
13.40	Peculiarities of Cs adsorption on natural and acid modified montmorillonite <u>V. Krupskaya</u> , S. Zakusin, E. Tyupina, O. Dorzhieva and M. Chernov	321
14.00	Formation of four-water-layer hydrates in smectites with divalent interlayer cations - dependence of layer charge and temperature <u>Daniel Svensson</u> and Hansen, Staffan	322
14.20	<b>BREAK</b>	
14.40	<b>KEYNOTE:</b> Relevance of testing specifications for bentonites used in hydraulic barriers – can they be improved? <u>Will P. Gates</u>	323
15.10	Geochemical outcome of the dismantling of the engineering barrier experiment at Mont Terri (Switzerland) <u>Ana María Fernández</u> , D.M. Sánchez-Ledesma, A. Melón, M. Sánchez, P. Galán and J.C. Mayor	324
15.30	Gas migration in bentonite barriers <u>Patrik Sellin</u> , Antonín Vokál, Caroline Graham, Jiang Feng Liu, María Victoria Villar, Martin Birgersson and Robert Cuss	325
15.50	Effect of thermo-hydraulic gradients on the physical state and geochemistry of compacted bentonite <u>M.V. Villar</u> , F.J. Romero, R. Gómez-Espina, P.L. Martín, R.J. Iglesias	326
16.10	Removal of trichloroethylene (TCE) from contaminated soils by injection of nZVI-doped bentonite slurry <u>Andre Baldermann</u> , Stephan Kaufhold, Peter Freitag, Marcus Spitz, Claudia Nickel, Ilse Letofsky-Papst, Thomas G. Reichenauer and Martin Dietzel	327



	<b>Lecture room 2: Clay and fine particle based materials for environmental technologies and clean up (2)</b> <i>Session Chairs: Anke Neumann and Binoy Sarkar</i>	
09.10	Decomposition of hydrogen peroxide by Mg-Fe type layered double hydroxide (LDH) <u>Yoshikazu Kameshima</u> , Kana Nakamura, Shunsuke Nishimoto and Michihiro Miyake	329
09.30	Hexavalent chromium remediation by organic ligand-manganese-clay mineral system: A synchrotron based study <u>Binoy Sarkar</u> , Ravi Naidu, Avanthi Deshani Igalavithana and Yong Sik Ok	330
09.50	Spectroelectrochemical reduction of nontronite: A shifting mechanism Anna Weiss and <u>Alanah Fitch</u>	331
10.10	Characterisation of a stable clay-suspension with application to possible dewatering and reclamation of mine wastewater, Cullinan Diamond Mine, South Africa <u>Jessica Strydom</u> , Marthie Coetzee and Peter Wade	332
10.30	<b>BREAK</b>	
10.50	Development of chitosan-palygorskite composite as a sustainable material for heavy-metal removal from wastewater <u>Ruhaida Rusmin</u> , Binoy Sarkar , Yanju Liu, Ravi Naidu	333
11.10	Modification of clay minerals by chemical modification and graft polymerization <u>Juris Burlakovs</u> , Maris Klavins, Ruta Ozola and Juris Kostjukovs	334
11.30	Stability of tetrabutyl-phosphonium and -ammonium modified montmorillonite in inorganic acid <u>Helena Pálková</u> , Małgorzata Zimowska, Ľuboš Jankovič, Bogdan Sulikowski, Ewa Maria Serwicka and Jana Madejová	335
11.50	Application of Terahertz time domain spectroscopy for investigation of clays and clay mineral systems <u>M. Janek</u> , D. Zich, T. Zacher, M. Matejdes and M. Naftaly	336
12.10	Utilization of surfactant-modified zeolite for the treatment of coal fly ash leachate <u>Rona J. Donahoe</u> , Ghanashyam Neupane and Sidhartha Bhattacharyya	337
12.30	<b>LUNCH</b>	
13.30	Fluorescent lamp glass recycling in geopolymers and its use in dye removal <u>W. Hajjaji</u> , S. Andrejkovičová, V. Niknam, J.A Labrincha and F. Rocha	338
13.50	In-situ evidence of organic molecules trapping into hybrid metal-oxide nanotubes Mohamed Salah Amara, <u>Erwan Paineau</u> , Stéphan Rouzière, Antoine Thill and Pascale Launois	339
14.10	Environmental reactivity of iron oxide nanoparticles <u>Mikael Motelica-Heino</u> , Simona Iconaru, Régis Guégan and Daniela Predoi	340
14.30	Poorly crystalline nanoparticles formed in acid mine drainage (AMD) in a limestone environment <u>Youjun Deng</u> , L. Morgan, Roberta McClure, Maria Aurora Armienta, M. Newville, Shan-Li Wang, and T. Kogure	341

	<b>Lecture room 1: Clays in the Critical Zone soils, weathering and elemental cycling</b> <i>Session Chairs: Bruno Lanson, Jason Austin, Paul Schroeder and Steve Banwart</i>	
09.10	<b>KEYNOTE:</b> Critical Zone Science as the Earth Science for the Anthropocene <u>Daniel de B. Richter</u>	343
09.40	Dynamics of mineral recrystallization at the Earth's surface: Evidence from Ultisols, kaolins, and paleosols with implications for the "ages" of a rock <u>Paul A. Schroeder</u> and Jason C. Austin	344
10.00	C-14 age of the carbonate component of natural goethite (Fe(O,CO <sub>3</sub> )OH) from the Upper Ordovician Neda Fm., Neda, Wisconsin, USA <u>Jason C. Austin</u> and Paul A. Schroeder	345
10.20	Deeply buried Mesozoic weathering profiles from the Norwegian North Sea <u>Lars Riber</u> , Henning Dypvik, Ronald Sørli, Nikolas Oberhardt, Pingchuan Tan, Kristian Stangvik, Syed A. A. Naqvi, Paul A. Schroeder, Arlindo Begonha, and Ray E. Ferrell	346
10.40	<b>BREAK</b>	
11.00	Characteristics of early Earth's critical zone based on Devonian palaeosols properties (Voronezh Antecline, Russia) <u>T. Alekseeva</u> , P. Kabanov, A. Alekseev and P. Kalinin	347
11.20	Weathering intensity of a Pleistocene loess/paleosol sequence in Wels-Aschet (Upper Austria) indicated by clay minerals <u>Karin Wriessnig</u> , Franz Ottner and Birgit Terhorst	348
11.40	Formation of halloysite and kaolinite in tropical soil via sequential transformation of pedogenic smectite and kaolinite-smectite <u>Peter C. Ryan</u> and F. Javier Huertas	349
12.00	Identification of mixed layer minerals: implication for soil reactivity. <u>Fabien Hubert</u> , Jean Christophe Viennet, Emmanuel Tertre, Bruno Lanson and Eric Ferrage	350
12.20	<b>LUNCH</b>	
13.20	Influence of cropping practices on clay mineralogy: insights from the Morrow Plots experimental fields <u>Eleanor Bakker</u> , Bruno Lanson, Tauhid Belal Khan, Fabien Hubert, Nathaniel Findling, Camille Rivard, and Michelle M. Wander	351
13.40	A quantitative survey of sub-Saharan Africa soil mineralogy and its relationship to soil micronutrients <u>Mercy Nyambura</u> , Stephen Hillier, Keith D. Shepherd, Esala Martti and Michael Gatari	352
14.00	Are interlayered clay minerals important for phosphorus adsorption in agricultural soils? <u>Ann Kristin Eriksson</u> , Stephen Hillier, Dean Hesterberg, Magnus Simonsson and Jon Petter Gustafsson	353
14.20	Soils response to critical zone gradients at ecosystem scale: mineralogical and geochemical data <u>A.O. Alekseev</u> , T.V. Alekseeva, P.I. Kalinin and M. Hajnos	354
14.40	<b>BREAK</b>	
15.00	The search for soil hydroxy-interlayered vermiculites: A case for data stewardship <u>Carolyn Olson</u>	355
15.20	Reverse weathering in soils: a case study <u>Atsuyuki Inoue</u> , Minoru Utada, and Tamao Hatta	356
15.40	Influence of particle size on the experimental Al-hydroxylation of K-vermiculite <u>Jean-Christophe Viennet</u> , Fabien Hubert, Emmanuel Tertre, and Marie-Pierre Turpault	357
16.00	Textural and chemical controls in the formation of a clay-carbonate system in a volcanic soil <u>Javier Cuadros</u> , José L. Díaz-Hernández, Antonio Sánchez-Navas, Antonio García-Casco and Jorge Yepes	358
16.20	Opaline silica in cold climate <u>Elena Kuznetsova</u> and Motenko Rimma	359
16.40	Weathering and soil formation on ultramafic rock (Polar Ural, Russia) <u>Sofia Lessovaia</u> , Michael Plötze and Yury Polekhovsky	360

## **Imperfect minerals can control soil fertility and geochemistry**

Balwant Singh

Faculty of Agriculture and Environment, The University of Sydney, Eveleigh, NSW 2015, Australia

balwant.singh@sydney.edu.au

Soil mineral have a major bearing on the chemical and physical properties of soils and sediments derived from soils. Minerals in the clay fraction are particularly important in relation to soil fertility and geochemistry. There is a high variability in the clay mineral composition of soils depending on the soil parent material, extent of weathering and soil environmental conditions. Crystallographic and chemical properties of clay minerals in soils are also variable and often different from minerals derived from geological processes involving high temperature and/or pressure. Clay minerals in soils often have abundant structural defects and disorders, and their chemical composition is more variable than their geological counterparts. Examples of imperfect soil clay minerals and their possible effects on soil fertility and geochemistry will be discussed in this paper.

Thursday  
9<sup>th</sup> July

Lecture room 5

The many faces of chlorite

## Preliminary textural studies of the smectite to corrensite transition in the MH 2-B borehole, Snake River Plain, Idaho

Jeff Walker<sup>1</sup>, Sarah Perry<sup>2</sup> and Anthony Walton<sup>3</sup>

<sup>1</sup>Department of Earth Science and Geography, Vassar College, Poughkeepsie, NY 12604 jewalker@vassar.edu

<sup>2</sup>Department of Earth Science and Geography, Vassar College, Poughkeepsie, NY 12604

<sup>2</sup>Department of Geology, University of Kansas, Lawrence, KS 66044

The MH-2B borehole was drilled as a geothermal exploration well on the Mountain Home Air Force Base on the Snake River Plain southeast of Boise, Idaho. The borehole was part of Project Hotspot, a continental deep drilling project to study the path of the Yellowstone plume beneath the North American crust. Clay mineral analysis of core from the MH-2B borehole identified smectite below 750m depth in almost all samples. A restricted zone of corrensite crystallization was identified between 1730m and 1793m depth, below which the predominant clay mineral is again smectite. The boundaries between the corrensite zone and the surrounding rock appear to be sharp, and the top of the corrensite zone coincides with a zone of fracturing and flow of hot water (1745m; 145°C) under artesian pressure, a zone thought to represent a fault zone on the edge of a basement uplift. The bulk of the corrensite zone is not currently experiencing fluid flow.

Preliminary textural studies of the core samples in and around the corrensite zone of the MH-2B borehole suggest that many alteration textures are very similar in the rocks in and surrounding the corrensite zone. Alteration products outside the corrensite zone do not affect primary olivine (except for “iddingsite” along some fractures), pyroxene, plagioclase (lightly altered), or opaque minerals but primarily replace interstitial glass and fill vugs and veins with 2-3 episodes of material. Within the corrensite zone itself, the vug and vein filling textures are more complex than outside either boundary, showing up to 6 episodes of replacement. Many of the replacement products throughout the study are shades of brown, but in the corrensite zone there are also green products that may represent corrensite occurrences. Also, in the corrensite zone, plagioclase feldspar has a “moth-eaten” texture whereas feldspars outside the zone are lightly altered, and olivine appears to have been completely removed, and replaced by masses of clay minerals. Other alteration minerals in the corrensite zone include sulfides, calcite, laumontite, and possible analcime.

These textural differences suggest two episodes of alteration: 1) an earlier one that created the pervasive alteration seen throughout the depth range studied; and 2) a later episode related to the hydrothermal circulation that leached the plagioclase and dissolved the olivine, facilitating the conversion of smectite formed during the earlier episode to corrensite. Al<sup>3+</sup> from plagioclase leaching, along with Mg<sup>2+</sup> from olivine, possibly contributed ions to the formation of corrensite. No evidence has been found for randomly interstratified chlorite-smectite, and the conversion of smectite to corrensite in the MH-2B borehole is interpreted to be a discontinuous process forming corrensite as a discrete thermodynamic phase.

## Mineralogical aspects of interstratified chlorite/smectite from hydrothermal ore veins: Implications for the environmental conditions of formation

T. Yoneda<sup>1</sup> and T. Watanabe<sup>2</sup>

1: Hokkaido University, Sapporo, 060-8628, Japan, e-mail: yonet@eng.hokudai.ac.jp

2: Niigata College of Nursing, Joetsu, 943-0147 Japan

Interstratified chlorite/smectite minerals occur frequently as a common vein-mineral in some epithermal Au-Ag vein deposits in Japan. The interstratified chlorite/smectite minerals show banded or spotted aggregates in vein quartz, and are closely assembled with ore minerals such as Au-Ag minerals, Cu-Pb-Zn sulfides and Mn carbonate. The occurrence characteristics of the interstratified chlorite/smectite minerals in the hydrothermal ore veins may provide information to help understand their environmental conditions of formation. In this study the interstratification and chemical composition of the chlorite/smectite minerals occurring in two different ore veins (Chuetsu vein and Shuetsu vein) of the Todoroki deposit are described, and the environmental conditions of formation for the chlorite/smectite minerals is considered.

The interstratified chlorite/smectite minerals can be divided into four different types (I-IV) of interstratification based on comparison of measured XRD profiles with calculated ones. Type I is similar to a normal chlorite, occasionally with minor amounts of smectite layer; type II, with small amounts of smectite layers (10-20 %S), can be determined by the interstratification (Reichweite  $g=1$ ) of chlorite-chlorite layers and corrensite layers; the type III, with 20-45 %S, is a mixture of chlorite (type I) and corrensite (type IV), interpreted as a segregation structure; and the type IV, with about 50 %S, is corrensite. These types of interstratified chlorite/smectite minerals show an approximately continuous decrease in Al/Si atomic ratios, concordantly with an increase in %S. The chlorite/smectite minerals contain a variable amount of manganese in addition to Mg and Fe as the major octahedral cation. The chemical composition of the chlorite/smectite minerals correlate with their mineral assemblage and the chemistry of co-existing minerals. The Mn content of the chlorite/smectite minerals co-existing with rhodochrosite is relatively high. In addition the Mn/Fe ratios of the minerals vary over a wide range corresponding to the Mn/Fe ratios of co-existing sphalerite. This suggests that the interstratified chlorite/smectite minerals have primarily developed during vein formation, and the mineralogical properties of the minerals have been constrained by the hydrothermal conditions at the time, such as temperature, pressure, and chemistry of hydrothermal solution.

The type I-III interstratified chlorite/smectite minerals characteristically occur in the Shuetsu vein, whereas type IV commonly occurs in the Chuetsu vein, suggesting that differences in interstratification of the minerals may be constrained by the hydrothermal environment of vein formation. On the basis of the chemistry of co-existing minerals and the fluid inclusion thermometry of quartz, the type I-III minerals from the Shuetsu vein may have been formed at relatively high temperatures (150-240°C), whereas the type IV may have been formed at the lower end of this temperature range. In addition, the  $S_2$ -activity of the hydrothermal environment related to the ore formation of the Shuetsu vein may be higher than that of the Chuetsu vein, implying different redox environments for the type I-III and type IV minerals. A comparison of the chlorite-smectite minerals occurring in the two Au-Ag quartz veins shows that the hydrothermal environments of epithermal Au-Ag mineralization can provide a suitable hydrothermal environment of formation for interstratified chlorite/smectite minerals.

## Dehydroxylation behavior of five chlorites of the solid solution series of chamosite-clinocllore

Annett Steudel<sup>1</sup>, Reinhard Kleeberg<sup>2</sup>, Christian Bender Koch<sup>3</sup>, Frank Friedrich<sup>4</sup> and Katja Emmerich<sup>1</sup>

<sup>1</sup>Institute of Functional Interfaces (IFG) and Competence Center for Material Moisture (CMM), Karlsruhe Institute of Technology (KIT), Hermann-von-Helmholtz-Platz 1, D-76344 Eggenstein-Leopoldshafen, Germany annett.steudel@kit.edu

<sup>2</sup>Institute of Mineralogy, TU Bergakademie Freiberg, Brennhausgasse 14, D-09596 Freiberg, Germany

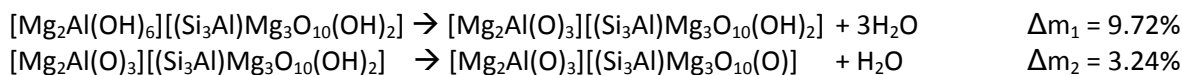
<sup>3</sup> Department of Chemistry, University of Copenhagen Universitetsparken 5, DK-2100 Copenhagen, Denmark

<sup>4</sup>Institute for Nuclear Waste Disposal (INE), Karlsruhe Institute of Technology (KIT), Hermann-von-Helmholtz-Platz 1, D-76344 Eggenstein-Leopoldshafen, Germany

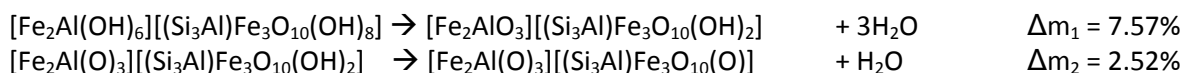
Chlorite minerals are found in different rocks and geological environments including sedimentary, low-grade metamorphic and hydrothermally altered rocks. Thus, chlorites display a wide range of chemical composition. Our study focuses on chlorites of the chamosite-clinocllore-series with trioctahedral octahedral sheets both in the 2:1 layer and in the interlayer hydroxide sheet. Si<sup>IV</sup> varies in the range between 2.34 and 3.45 eq/FU (Foster, 1962). Octahedral sites are usually occupied by Mg, Al, Fe(II) or Fe(III) but rarely by Cr, Mn, Ni, Zn or Li. Al<sup>VI</sup> is concentrated primarily in the interlayer hydroxide sheet (Wiewióra and Weiss, 1990). Octahedral vacancies are commonly between 0.0 and 0.3 positions (Foster, 1962).

Chemical variation strongly affects the dehydroxylation (DHX) behavior. Therefore thermal analysis is a powerful tool for the characterization of the chlorite group, if the influence of structural disorder and grain size is taken into account. DHX of the chlorite structure should occur in two steps: 1) DHX of the interlayer octahedral sheet ( $\Delta m_1$ ) between 400 and 700 °C and 2) DHX of the octahedral sheet of the 2:1 layers ( $\Delta m_2$ ) > 700 °C. The interlayer octahedral sheet of Fe-rich chlorites dehydroxylates at lower (about 150 and 200 K) temperatures than that of Mg-rich chlorites (Zhan and Guggenheim, 1995). The mass loss during both steps of DHX is calculated for the end members.

Clinocllore:



Chamosite:



However, sometimes non-stoichiometric DHX is reported for chlorites. The objective of the study was to investigate the DHX behavior of several chlorites in dependency of the composition systematically as the DHX process is not fully understood, yet. Five natural chlorite samples of the solid solution series of chamosite-clinocllore were investigated. Phase content, chemical composition, Fe<sup>2+</sup>/Fe<sup>3+</sup> content and thermal behavior were analyzed and structural formulae were calculated. The chemical analysis revealed SiO<sub>2</sub> between 28 - 47%, Al<sub>2</sub>O<sub>3</sub> between 7 - 23%, MgO between 2 - 41% and Fe<sub>2</sub>O<sub>3</sub>(t) between 3 - 38%. Mössbauer spectroscopy revealed Fe<sup>2+</sup> as FeO between 1.2 and 30% and Fe<sup>3+</sup> as Fe<sub>2</sub>O<sub>3</sub> between 0.6 – 6%. Mössbauer spectroscopy also demonstrate that for all samples Fe<sup>3+</sup> occurs in the 2:1 layers in the trans configuration (M1 sites) and Fe<sup>2+</sup> in the cis configuration (M2 sites). Additional Fe<sup>2+</sup> at either M1 or M3, and Fe<sup>3+</sup> at either M2 or M4 sites were observed. First results showed non-stoichiometric DHX for Fe-rich chlorites while Mg-rich chlorites dehydroxylate stoichiometrically. Detailed analysis of the correlation between content and position of Fe<sup>2+</sup>/Fe<sup>3+</sup> on DHX is under way.

Foster, M.D. (1962). U.S. Geological Survey professional paper, 414-A

Wiewióra, A. and Weiss, Z. (1990). Clay Minerals, 25, 83-92.

Zhan, W. and Guggenheim, S. (1995). Clay and Clay Minerals, 43, 622-629.

## An experimental study of talc-chlorite-serpentine behavior in a CO<sub>2</sub>-rich environment

Emilio Galán, Inmaculada Macías, Patricia Aparicio and Domingo Martín

Dpto. Cristalografía. Mineralogía y Q. Agrícola, University of Seville, Spain egalan@us.es, paparicio@us.es, dmartin5@us.es

A talc from the ultrabasic massif of the Serranía de Ronda (Betic Cordilleras, South Spain), mainly composed of talc, Mg-chlorite and serpentine (antigorite) was altered in an acid environment with CO<sub>2</sub>. Temperature, CO<sub>2</sub> pressure, relative humidity and reaction time were all varied during the experiments, which were conducted in a high-pressure and high-temperature Parr reactor. The raw material and its behavior after the alteration experiments were examined by XRD and SEM/TEM equipped with EDS. In addition the elemental carbon content was also measured using an elemental analyzer.

XRD analysis demonstrates that the talc content decreases in all the experiments carried out while serpentine and chlorite increase. In addition some carbon is retained in the material after the CO<sub>2</sub> attack, but no carbonate was detected by XRD, possibly due to the small quantity formed or because the carbon was physically trapped on the surface of minerals.

TEM and SEM studies show that talc has been transformed into fibrous serpentine. The talc laminae were dramatically changed, the edges were flaky and apparently some fibrous structures were formed (Figures 1a, b and c). On the other hand the carbon content increased respect to the starting material, from 0.06% to 0.10%.

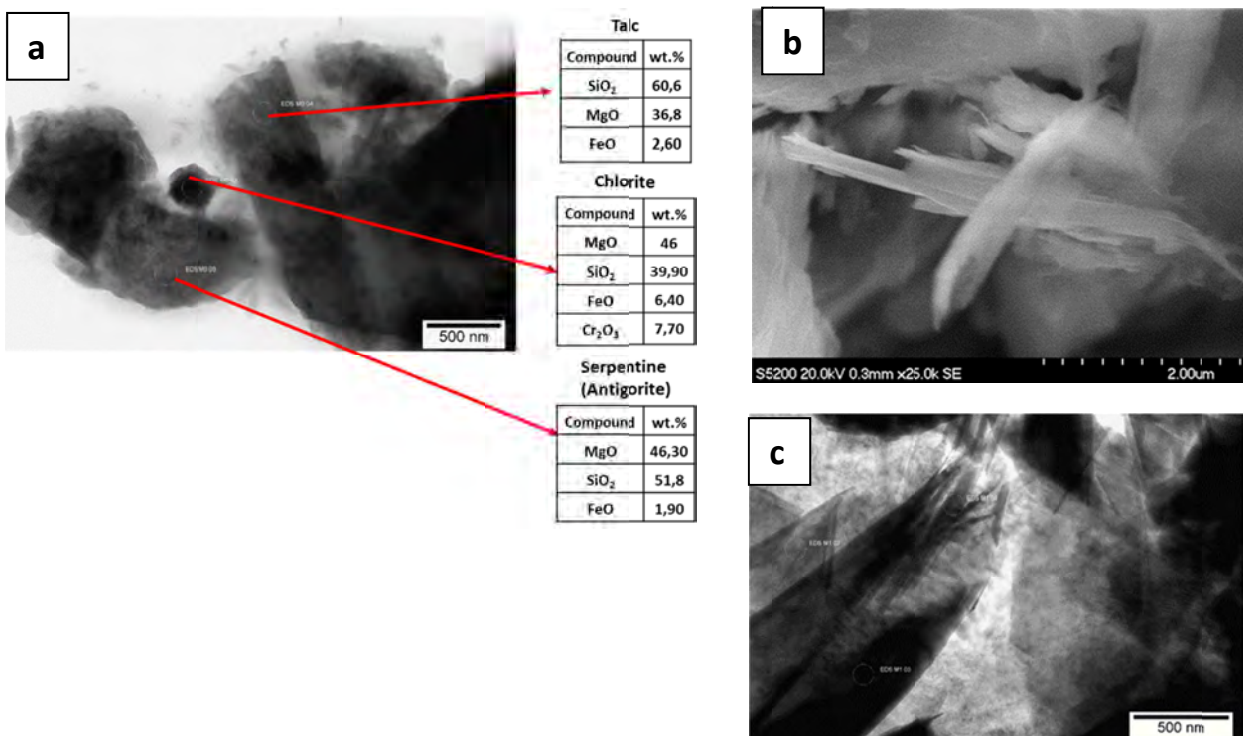


Figure 1. a) Association talc, chlorite and serpentine (antigorite) in original sample; b) Fibrous serpentine and chlorite layers after CO<sub>2</sub> treatment.; c) Morphological changes in the talc laminae which resulted in fibrous ending and curved edges after CO<sub>2</sub> treatment. The chemical analysis of these fibrous edges corresponds to that of the serpentine.

Therefore the talc transformation to fibrous serpentine is possible in an acid medium. In this transformation was the pressure the most important variable.



## Laboratory studies of chloritization of smectite; applications to the clay mineralogy of Gale Crater, Mars

Anthony M. Frushour and David L. Bish

Dept. of Geological Sciences, Indiana University, Bloomington, IN 47405, USA: afrushou@indiana.edu

The CheMin X-ray diffraction (XRD) instrument on the Mars Science Laboratory (MSL) Curiosity rover analyzed two mudstones, John Klein and Cumberland, at Yellowknife Bay, Gale Crater, Mars (Vaniman et al., 2014). The XRD data suggested the presence of clay minerals, based on the existence of broad 10Å and 13.2Å peaks. The position and breadth of the 10Å peak suggests a collapsed 2:1 phyllosilicate. The specific identity of the 13.2Å phase is unknown, although two explanations have been proposed, namely a smectite with partially hydrated Mg<sup>2+</sup> or Ca<sup>2+</sup> interlayer cations or a partially chloritized smectite. This study focused on the preparation and XRD analysis of synthetic chloritized smectite and Mg-exchanged smectite to clarify the nature of the 13.2Å phyllosilicate from Cumberland. Chloritized smectites were prepared by mixing SWy-1 montmorillonite with 0.5 M Mg(NO<sub>3</sub>)<sub>2</sub> and Al(NO<sub>3</sub>)<sub>3</sub> solutions in varying proportions to cation exchange the smectite. A 0.5 M NaOH solution was then added to the mixtures in an effort to produce Mg- and Al-hydroxy interlayers in the smectite. Synthesis products were analyzed on a Bruker D8 XRD instrument at 9-22% relative humidity (RH), after solvation with ethylene glycol, and after heating on Vycor from 100-400°C. Additional XRD measurements used an Anton-Paar TTK heating stage under roughing pump vacuum, from 22-250°C. Initial results show that at RH and temperatures comparable to CheMin analysis conditions, an Mg-pillared smectite had a 13.3Å basal reflection which did not collapse upon heating to 250°C (Fig. 1A). Mg-exchanged smectite partially collapsed to 11.9 Å under vacuum and collapsed to 10.1Å upon heating to 250°C under vacuum (Fig. 1B). XRD data for these exchanged and modified smectites reveal restricted collapse under vacuum and elevated-temperature conditions, and they suggest that partially chloritized smectite is a viable explanation for the expanded material seen by CheMin at Cumberland. The Mg-exchanged smectite is not a likely candidate based on its behavior under vacuum. As Curiosity continues to explore Gale Crater, XRD characterization of smectites will be an important aspect of understanding the geology of the region.

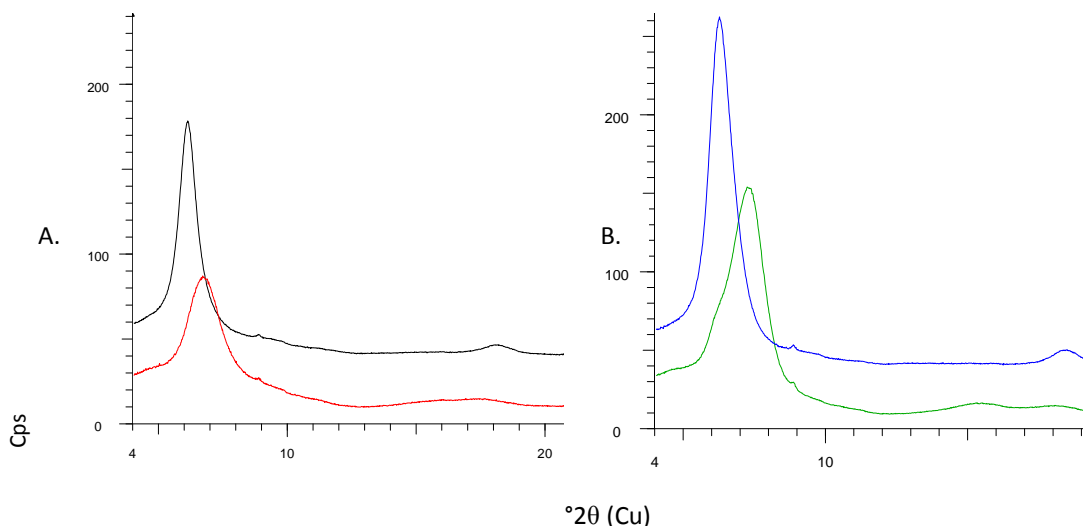


Figure 1. XRD patterns of (A) Mg-pillared SWy-1 at 22% RH (black, upper) and under vacuum at 22°C (red, lower), and (B) Mg-exchanged SWy-1 at 11% RH (blue, upper) and under vacuum at 22°C (green, lower).

Vaniman, D.T. et al. (2014) Mineralogy of a mudstone at Yellowknife Bay, Gale Crater, Mars. *Science*, **343**, 1243480.

## A combined study by HRTEM and HAADF-STEM for Fe-rich berthierine and chlorite interstratified minerals

Sayako Inoue<sup>1</sup> and Toshihiro Kogure<sup>2</sup>

<sup>1,2</sup>Department of Earth and Planetary Science, Graduate School of Science,  
The University of Tokyo, 7-3-1 Hongo, Bunkyo-ku, Tokyo 113-0033, Japan  
<sup>1</sup>sinoue@eps.s.u-tokyo.ac.jp

The crystal structure of Mg-chlorite like clinochore has been refined using X-ray diffraction (XRD) and nuclear magnetic resonance (NMR). The general structure is expressed as the alternation of 2:1 layer of  $\{M1(M2)_2[(T1)_2(T2)_2]O_{10}(OH)_2\}$  and the interlayer sheet of  $\{(M3)_2M4(OH)_6\}$ ; Al preferentially occupies M4 site in the interlayer sheet (e.g., Bailey, 1988). In contrast, there remains ambiguous in the structure of Fe-rich chlorite because of difficulty due to the fine grained-size and enriching Fe as a magnetic element. Recently, many nano-analytical and -spectroscopic techniques such as electron energy-loss spectroscopy (EELS) and high-angle annular dark field scanning transmission electron microscopy (HAADF-STEM) have been extensively applied to investigate the cation distribution in minerals. HAADF-STEM has the potential to directly identify the elemental distribution in Fe-rich chlorite. The contrast visible on a HAADF-STEM image is proportional to the square of the atomic number (Z). Hence, the distinct distribution of Fe, Al and/or vacancy occupying the octahedral sites of extremely Fe-rich chlorite and berthierine can be discriminated on HAADF-STEM images.

In this study, we undertook HAADF-STEM and high resolution TEM (HRTEM) studies in order to investigate the location of Al and/or vacancies in Fe-rich chlorites of hydrothermal origin. Samples observed by HRTEM contained two types of layer-stacks consisting of berthierine and berthierine-chlorite interstratified structures. HAADF-STEM studies indicate that either Al and/or vacancy in interlayering chlorite layers preferentially occupy M4 sites of the interlayer sheets. In addition, two types of octahedral sheets with different chemical compositions were recognized in berthierine layers. These combined studies using HAADF-STEM and HRTEM give crystallochemical constrains which will elucidate the transformation mechanisms between berthierine and chlorite which are commonly observed in diagenetic sandstones, metamorphosed serpentinites and massive sulfide ore deposits (e.g., Jiang et al., 1992; Xu and Veblen, 1996; Banfield and Bailey, 1996).

Bailey, S. W. (1988) *Rev. Mine.*, 347-403  
Banfield and Bailey (1996) *AM*, 79-91  
Jiang et al. (1992) *CCM*, 501-514  
Xu and Veblen (1996) *CMP*, 291-301

## What do chlorites and other phyllosilicates tell us about their conditions of formation?

O. Vidal

CNRS, Isterre, Université Grenoble, 1381 rue de la piscine, BP 53, 38041 Grenoble Cedex.  
olivier.vidal@ujf-grenoble.fr

Phyllosilicates are ubiquitous minerals, stable over a wide range of  $P$ ,  $T$ , fluid compositions and redox conditions. These minerals are present in most rocks from low-grade subsurface conditions to high pressures and temperatures prevailing in subduction zones. Numerous natural and experimental data show that the phase relations and compositional variations of phyllosilicates depend on the conditions at which they formed, and various approaches have been proposed to quantify the mineral composition- $T$ - $P$ -fluid activity relationships. In this context, chlorite is a pivotal mineral because its grain size is generally compatible with that of microprobe measurements and the structural interpretations of rock deformation. However the use of chlorite as a proxy for the conditions of crystallization and rock deformation requires a comprehensive analysis of: (1) its composition (including iron redox state); (2) the spatial variation of its composition; and (3) the influence of bulk-rock composition. This requires a thermodynamic modelling approach combining multi-equilibrium and energy minimizing approaches with experimental data to constrain the models. Numerous natural case studies, experimental studies and analytical developments have been conducted over the last 15 years which provide a solid framework with which to address these three points. The results and approaches developed for chlorite can be extended to smectite, serpentine and mica, which coexist with chlorite, or are its precursor or breakdown minerals.

## **Authigenic chlorite in Oligo-Miocene reservoir sandstones, Tapti Gas Fields, offshore western India**

J. M. Huggett<sup>1</sup>, S.D. Burley<sup>2,3</sup> and F.J. Longstaffe<sup>4</sup>

1. Petroclays, The Oast, Sandy Cross Lane, Heathfield, E Sussex, UK; info@petroclays.com
2. Basin Dynamics Research Group, School of Earth Sciences, The University of Keele, UK.
3. Murphy Exploration and Production Ltd, Petronas Towers, Kuala Lumpur 50088, Malaysia.
4. Department of Earth Sciences, The University of Western Ontario, London, N6A 5B7, Canada.

Reservoir sands of the Mid- and South Tapti fields have been investigated using a range of petrographic techniques, isotope geochemistry and basin modelling. Authigenic chlorite is abundant in the shallow-marine sandstones of the Miocene Mahim Formation, a major reservoir rock in the Mid and South Tapti gas fields in the Mumbai Offshore Basin, India. The sandstones are currently at burial depths of between ~1500 and 2800m. The authigenic chlorite has a significant impact on the resulting reservoir quality of the reservoirs and is interpreted to have originated as odinite clay that replaced faecal or pseudo-faecal pellets, and formed at the site of major riverine iron influx onto the shallow-marine shelf during periods of relatively low sea level. The high concentration of pelletal chlorite in the Mahim Formation sandstones suggests that climatic and sedimentological conditions were suitable for chlorite precursor mineral formation, though it is probable that intraformational reworking of pellets from low- to high-energy environments also took place during transgressions. Reservoir sandstones from similar depositional settings on the west coast of India or other sub-tropical settings are likely to exhibit comparable diagenetic effects on reservoir quality.

Compositionally the chlorite is chamosite. The authigenic chlorite occurs mainly as a replacement of pseudo-faecal pellets, together with volumetrically small but abundant grain coatings and grain rims. Pellets have been variably compacted to form pseudomatrix. Although textural relationships indicate that the rims and coatings formed after the pellets, replacement of the precursor pelletal clay by chlorite may have occurred at the same time as the chlorite rims precipitated. Oxygen isotope analyses of carbonate cements (calcite and siderite) in the Mahim Formation sandstones have provided an approximate temperature framework for diagenesis of the non-carbonate cements. Oxygen isotope results for the chlorite, however, suggest much higher temperatures than its position in the paragenetic sequence would warrant. These results suggest that the clay formed first as 1:1 layer clays, such as odinite or berthierine, which were then transformed to Fe-chlorite as burial depths and temperatures increased.

Reservoirs in the Mahim, Daman and Mahuva formation sandstones are variable and influenced by the diagenesis of authigenic chlorite and locally by the precipitation of carbonate cements. Reservoir quality is good where thick, continuous chlorite rim cements are present and where chlorite pellets are sufficiently indurated for them not to be compacted. Chlorite rim cements appear to have reduced the extent of quartz overgrowth cementation in the sandstones. Compaction of chlorite pellets is the principal mechanism for loss of reservoir quality, and the extent of chlorite pellet compaction may have been controlled by the rate of "verdinisation, ie replacement of precursor clays by the ferric-iron rich clay, odinite<sub>2</sub> during early diagenesis, as well as by the type of pellet-producing organism(s). Alternatively, the mineralogical maturity and hardness of the pellets may have been controlled by the time available for replacement of the clay by odinite. Where pellets remained soft at the onset of compaction they have been redistributed as pseudo-matrix, and intergranular porosity in these sandstones is consequently low. By contrast, pellets in matrix-supported sandstones were less susceptible to compaction and so these sandstones retain better reservoir quality.

## Occurrence of tosudite in Guezouman, Tarat and Tchirezrine 2 Formations, hosts of uranium deposits in Niger (Tim Mersoï Basin)

Sophie Billon<sup>1,2</sup>, Patricia Patrier<sup>2</sup>, Daniel Beaufort<sup>2</sup>, Aurélia Wattinne<sup>3</sup> and Grégoire André<sup>3</sup>

<sup>1</sup>Société ERM, rue Michel Brunet, Bat. 35, 86000 Poitiers, France

<sup>2</sup> Université de Poitiers, UMR 7285 CNRS, IC2MP, rue Michel Brunet, Bat. 35, 86073 Poitiers cedex 9, France

<sup>3</sup> AREVA, 1 place Jean Millier, 92084 Paris la Défense, France

Several uranium deposits have been discovered since 1958 in the Tim Mersoï Basin, near the major regional N-S fault of Arlit-In-Azawa. Both the Carboniferous Tarat and Guezouman Formations, deposited in a fluvial environment, host uranium deposits which are exploited respectively by the SOMAÏR and COMINAK mining companies. The yet to be exploited Imouraren deposit occurs in the fluvial Jurassic Tchirezrine 2 Formation. All these fluvial formations consist mostly of sandstones with a detrital mineralogy composed of quartz, microcline, orthose, albite and accessory minerals including muscovite and zircon.

In all these formations, siliciclastic diagenesis during burial results in the neoformation of Fe-rich chlorite from a berthierine precursor, quartz overgrowths due to pressure solution, kaolinite from the destabilization of detrital feldspars and, under deeper burial conditions, evidence of a kaolinite to dickite transformation. In addition, Carboniferous sandstones may also display early diagenetic dolomite cementation and the Jurassic formation shows the presence of analcime formed from destabilization of volcanic materials (ash), albite overgrowths and illite.

Subsequent to burial diagenesis the sandstones of the Guezouman, Tarat and Tchirezrine 2 Formations suffered a distinctive alteration as a consequence of regional fluid circulation, which resulted in partial dissolution of some pre-existing Al-bearing minerals and crystallization of secondary minerals (tosudite, montmorillonite, hematite, harmotome, calcite) and deposition of uranium in the form of uraninite, coffinite, uranophane and metatyuyamunite).

Tosudite, a regular interstratification of chlorite-smectite is one of the secondary minerals formed during this later alteration event from the destabilization of detrital feldspars, kaolins and chlorite. X-ray diffraction patterns of this mineral show a sharp superstructure at 29 to 29.6 Å (air-dried) which swells at 30.8 to 31.6 Å after ethylene glycol solvation. The 060 reflection at 1.507 Å indicates a dioctahedral behaviour and the very low coefficient of variation (0.03 to 0.13) for (00l) harmonic reflections confirms identification as tosudite. Chemical micro-analyses identifies a low-charge montmorillonite and a sudoite (di-trioctahedral chlorite) as the two components involved in the interstratification. Scanning electron microscopy demonstrates that the tosudite is closely associated with the uranium minerals and can be considered as a good marker of uranium deposition in the Tim Mersoï Basin.

## **Authigenic chlorite and chlorite-smectite mixed layers as an indicator of increasing reducing conditions in the Huincul Formation: Neuquén Basin, Argentina**

M.J. Pons<sup>1</sup>, A. Rainoldi<sup>2</sup>, D. Beaufort<sup>3</sup>, P. Patrier<sup>4</sup>, A. Impicini<sup>5</sup> and M.B. Franchini<sup>6</sup>

<sup>1</sup> josefina.pons074@gmail.com; <sup>2</sup> analaurarl@hotmail.com; <sup>3-4</sup> Université de Poitiers, IC2MP, CNRS-UMR 7285, Hydrasa, Bâtiment B08, Rue Albert Turpin, F-86022 Poitiers Cedex, France, <sup>3</sup> daniel.beaufort@univ-poitiers.fr; <sup>4</sup> patricia.patrier@univ-poitiers.fr; <sup>5</sup> aimpicc@gmail.com; <sup>6</sup> mfranchi@speedy.com.ar

The Huincul High (HH) and Dorso de los Chihuidos High (DCH) are two regional morpho-structures of the Neuquén Basin, characterized by the occurrence of hydrocarbon fields, regional structures at depth and the presence of solid hydrocarbons impregnating the foreland deposits of Cretaceous rocks (Neuquén Group). The Huincul Formation belongs to the fluvial and red-bed lake deposits of the Neuquén Group.

Some of the structures of HH and DCH were reactivated during the Tertiary Andean orogeny, and acted as vertical channels connecting the reservoir fluids with the sub-horizontal paleo-channel of the Huincul Formation. The circulation of these fluids in the clastic rocks is documented by the presence of bitumen associated with baroque calcite, pyrite and clay mineral rims (smectite, chlorite and chlorite-smectite mixed layers). The pervasively greenish gray clay coating is a common feature of the sandstones and conglomerate from the Huincul Formation. This presentation establishes the relationship between diagenetic processes, hydrocarbons migration and their role in controlling the composition of the clay coating.

During early diagenesis multiple episodes of clay infiltration into the unconfined meandering river deposits of the lower section of Huincul Formation resulted in the formation of thick (2-3  $\mu\text{m}$ ) clay coatings in some volcanic rich litharenite sandstones and conglomerates. Progressive burial caused the reddening of the whole Huincul Formation, whose mudstone and sandstone layers display a reddish brown or pink color due the presence of a hematite pigment. The hematite is derived from the infiltration of meteoric water following breakdown of ferromagnesian silicate minerals and iron bearing clay minerals.

Oil emplacement is demonstrated by the intense bitumen impregnation of sandstone and conglomerate and at micro scale via calcite and barite cements that host numerous organic rich fluid inclusions.

The greenish gray facies document hydrocarbon migrations in the Huincul Formation where previous kaolinite and hematite coatings were transformed to dioctahedral smectite, chlorite-smectite mixed layers or chlorite and pyrite. These changes from smectite to chlorite-smectite mixed layers or chlorite is interpreted as indicating increasingly reducing conditions. The direct transformation of smectite to chlorite in some of the greenish gray facies located in the lower part of the Huincul Formation, involved a fast rate of growth nucleation at the expense of previous smectite, suggesting a high fluid/rock ratio (Robinson et al., 2002). This condition prevailed in the permeable layers of the lower section of the sedimentary unit that yields a focused flow pathway. In the rest of the sedimentary unit, the presence of chlorite-smectite mixed-layers suggest chloritization of previous smectite. The partial transformation of dioctahedral smectite to chlorite-smectite mixed layers or trioctahedral chlorite produced an excess of silica resulting in the micro quartz precipitation (Mosser-Ruck et al., 2010). The addition of Mg is required to form chlorite-smectite mixed layers or chlorite from the dioctahedral smectite and this could be taken from the alteration of residual mafic minerals and/or Mg-rich formation water that migrated with the hydrocarbons.

Mosser-Ruck R., Cathelineau M., Guillaume D., Charpenetier D., Rousset D., Barres O., Michau N., 2010. Effects of temperature, pH, and iron clay and liquid/clay ratios on experimental conversion of dioctahedral smectite to berthierine, chlorite, vermiculite or saponite. *Clays and Clay Minerals*, Vol. 58, No. 2, 280–291.

Robinson D., Schmidt Th, de Zamora S., 2002. Reaction pathway and reaction progress for the smectite-to-chlorite transformation: evidence from hydrothermally altered metabasite. *Journal of Metamorphic Geology*, **20**, 167-174.

Thursday  
9<sup>th</sup> July

Lecture room 5

Structural characterization  
of lamellar compounds (1)

## **Crystal structures of defective lamellar compounds and their X-ray identification: insights into mineral reactions and material reactivity**

Bruno Lanson

ISTerre, CNRS – Univ. Grenoble Alpes, 38000 Grenoble, France – [bruno.lanson@ujf-grenoble.fr](mailto:bruno.lanson@ujf-grenoble.fr)

Layered minerals and materials are characterized by the frequent occurrence of stacking defects. In particular, interstratification (or mixed layering), which corresponds to the intimate intergrowth of layers differing by their layer thickness and/or internal structure, and stacking faults, both random and well-defined, are especially common. These defects strongly impact the reactivity of lamellar materials. They may also record the conditions of mineral (trans)formation.

Determining the nature, abundance, and possibly the distribution of stacking defects in layered structures is thus an essential step of their structural characterization in the scope of understanding their reactivity. Over the last decades, modelling of X-ray diffraction profiles has proved to be a unique and precious tool allowing such a detailed structural identification of defective lamellar structures. This presentation will outline how our understanding of defective structures and mixed layers has improved over the last decade or so and describe some of the new perspectives opened by this improvement.



## Non classical crystal growth mechanism in clay minerals

E. García-Romero<sup>1,2</sup> and M. Suárez<sup>3</sup>

<sup>1</sup>Dpto. Cristalografía y Mineralogía, Universidad Complutense. Madrid. 28040 Madrid, Spain.

<sup>2</sup>Instituto de Geociencias (UCM-CSIC), 28040 Madrid, Spain

<sup>3</sup>Dpto. Geología, Universidad de Salamanca, Plaza de la Merced s/n, 37008 Salamanca, Spain

Nowadays, nonclassical crystallization models are used to complement classical crystal growth theory. It describes processes which involve parallel multiple nucleation events that form nanoparticles that then form a superstructure (in stark contrast to a single nucleation event forming a single crystal) and the self-assembly of preformed nanoparticles to an ordered superstructure, which then can fuse to a single-crystalline structure. Nonclassical crystallization comprises oriented aggregation of nanoparticles and mesocrystal formation. "Oriented aggregation is a special case of aggregation that provides an important route by which nanocrystals grow, defects are formed, and unique, often symmetry-defying, crystal morphologies are produced" (Penn 2004). Mesocrystals are a nonclassical oriented aggregation consequence, built from crystallographically-oriented nanoparticles. They are one of the intermediate steps in which the primary units can still be identified (Cölfen and Antonietti 2008). Several papers provide examples of nonclassical crystallization of synthetic materials and growth in the laboratory (e.g. metal oxides, selenides, and sulfides) from initially homogeneous solutions (Penn and Banfield 1998; Penn 2004; Cölfen and Antonietti 2008), but are scarce in studies of natural materials. To the best of our knowledge, in natural environments, there are only studies examining the aggregation of framboidal pyrite, the formation and stacking of mica layers (Nespolo 2001; Meunier 2005; Eberl et al. 2011), or the fibrous clay minerals oriented aggregation (García-Romero and Suárez, 2014) which is in contrast with the preponderance of previous research that provides examples of synthetic materials. This work offers scanning electron microscopy (SEM-FEG) and transmission electron microscopy (TEM-HRTEM) evidences of oriented aggregation of natural clay minerals.

It is well known that the first stage in the formation of crystals from aqueous solution is nucleation (homogeneous or heterogeneous). The clusters that achieve critical nucleus size are stable and grow to form bigger crystals. In a saturated solution in equilibrium large crystals grow at the cost of smaller ones (Ostwald ripening process). Afterwards, the process of growth continues by aggregation and/or incorporation of ions at energetically favorable sites. As can be observed in electron microscopy images, clay nanoparticles can aggregate with each other and grow via a nonclassical crystal growth mechanism, which occurs via crystallographically oriented attachment, including rotation and oriented attachment. After the nucleation and their oriented aggregation, nanoparticles can continue growing in a much slower manner at the expense of the diffusion of molecular scale species throughout the solution. The more favorable growth directions depend on the periodic bond chain vectors (PBCs) which indicate the directions of strong bonding. The (00l) faces in laminar clay minerals and the (hk0) for sepiolite-palygorskite are F (flat) faces, without kinks, their attachment energy is very low and as a consequence, the addition of atoms in them is very difficult. However, the (hk0) faces in laminar clay minerals, or (00l), (h0l) and (0kl) for fibrous clay minerals are K (kinked) faces, where the attachment energy is very high. The energy of the K faces decreases greatly following the addition of atoms to complete their kinks, although immediately after this incorporation the energy returns to the same level as before the incorporation. As a consequence, clay minerals are greatly anisotropic (layers or fibers) where the more favorable growth mechanism should be by oriented aggregation and posterior growth by Oswald ripening processes.

Cölfen and Antonietti (2008) *Mesocrystals and Nonclassical Crystallization*, 276 pp. Wiley, Chichester, England.

Eberl, D.D., Blum, A.E., and Serravezza, M. (2011). *American Mineralogist*, 96, 586–593.

García-Romero, E., and Suárez, M. (2014). *American Mineralogist*, Volume 99, pages 1653–1661.

Meunier, A. (2005) *Clays*, 472 p. Springer, Berlin.

Nespolo, M. (2001) *Clays and Clay Minerals*, 40, 1–23. M

Penn, R.L. (2004). *Journal of Physical Chemistry B*, 108, 12707–12712.

Penn, R.L., and Banfield, J.F. (1998). *Science*, 281, 969–971

## Evolution of the configuration of tetrahedra with composition in 2:1 layer silicates

Jean-Louis Robert

Sorbonne Universités IMPMC (UMR 7590), Université Pierre et Marie Curie, CNRS, IRD, MNHM, 4 place Jussieu, 75252 Paris  
Cedex 05, France; jean-louis.robert@impmc.upmc.fr

An analysis of T-O distances in layer silicates shows that tetrahedra with ideal  $T_d$  symmetry are exceptional. Most of  $(TO_4)$  tetrahedra have much lower symmetry. A predictive model, based on bond valences is proposed. In willemseite, the Ni-talc, each  $(SiO_4)$  tetrahedron is adjacent to three identical  $(SiO_4)$  tetrahedra and to three octahedra occupied by  $Ni^{2+}$ . The charge balance on all oxygens is obeyed and does not require distortions of polyhedra. The  $(SiO_4)$  tetrahedron exhibits four equal Si-O bonds, 1.624 Å. This results in a single FTIR absorption band at  $1033\text{ cm}^{-1}$ , in the antisymmetric  $Si-O_b-Si_{as}$  (i.e.  $Si-O//$ ) and  $Si-O_{apical}$  (i.e.  $Si-O\perp$ ) region. This is surprisingly no longer observed in Mg-talc, where this band splits into two components, a low-intensity, high wavenumber band ( $1050\text{ cm}^{-1}$ ), corresponding to the  $Si-O_{apical}$  bond, which becomes shorter and a high-intensity, low wavenumber band due to  $Si-O-Si_{as}$  ( $Si-O//$ ) vibrations, at  $1020\text{ cm}^{-1}$ . This anisotropy of Si-O bond distances has never been detected by conventional XRD measurements because they remain within the uncertainties of measurements. In phyllosilicates with charge generated in octahedra only, like hectorites  $Na_x(Mg_{3-x}Li_x)Si_4O_{10}(OH,F)_2$ , the tetrasilicic magnesium mica  $K(Mg_{2.5}\square_{0.5})Si_4O_{10}(OH)_2$ , the tetrasilicic Li-micas tainiolite  $K(Mg_2Li)Si_4O_{10}(OH,F)_2$  and polyolithionite  $K(Li_2Al)Si_4O_{10}(OH,F)_2$ , the compensating cation induces a local charge excess on basal oxygens. The structure overcomes this charge imbalance by modifying the tetrahedral configuration, with three long  $Si-O_b$  ( $\approx 1.63\text{ Å}$ ) and a short  $Si-O_{apical}$  ( $\approx 1.60\text{ Å}$ ) bonds. This results in a huge splitting - much higher than in Mg-Talc- of Si-O bands into two groups: a low-intensity high-wavenumber band at  $\approx 1100\text{ cm}^{-1}$  due to  $Si-O_{apical}$  vibrations, and a high-intensity, low-wavenumber one at  $\approx 950\text{ cm}^{-1}$ . The intensity ratio of these bands is  $\approx 3/1$  and reflects the proportion of Si-O bond species. These bands are complex and can be decomposed in elementary Gaussians whose positions and intensities reflect local fluctuations of the octahedral composition. The introduction of  $Al^{3+}$ , or another low-charge cation, e.g.  $Be^{2+}$ ,  $Mg^{2+}$ ,  $Co^{2+}$  or  $Ni^{2+}$  in the tetrahedral layer provokes the opposite effect. The basal T- $O_b$  bonds become shorter and the T- $O_{apical}$  one increases in length. The tetrahedral regularity, initially observed in willemseite, is reached again for the composition  $A^+(Mg_{2.5}Al_{0.5})(Si_{2.5}Al_{1.5})O_{10}(OH)_2$ , with  $A^+ = Na^+$  or K, but the band position is shifted towards low-wavenumbers ( $35\text{ cm}^{-1}$ ). In more aluminous compositions, typically disilicic phases, like preiswerkite,  $Na(Mg_2Al)(Si_2Al_2)O_{10}(OH)_2$  or ephesite  $Na(Al_2Li)(Si_2Al_2)O_{10}(OH)_2$ , the trend continues, and basal T- $O_b$  bonds become shorter than the T- $O_{apical}$  one. In this case, the T- $O_{apical}$  stretching band is observed at a lower value, around  $900\text{ cm}^{-1}$ . On the whole, the shift of this band is considerable, from  $\approx 1100\text{ cm}^{-1}$  in tetrasilicic 2:1 layer silicates to  $\approx 900\text{ cm}^{-1}$  in disilicic ones. The use of FTIR data as fingerprints in the T-O stretching range is tricky in 2:1 phyllosilicates, but can provide useful compositional information, for example in remote sensing, provided that detailed factors influencing the band positions and intensities are taken into consideration.

## Influence of crystal structure defects on small-angle neutron scattering/diffraction patterns

Eric Ferrage<sup>1</sup>, Fabien Hubert<sup>1</sup>, Emmanuel Tertre<sup>1</sup>, Alain Baronnet<sup>2</sup>, Alfred Delville<sup>3</sup>, Laurent J. Michot<sup>4</sup> & Pierre Levitz<sup>4</sup>

<sup>1</sup> IC2MP-Hydrasa, UMR 7285 CNRS, Université de Poitiers, 86073 Poitiers, France, eric.ferrage@univ-poitiers.fr

<sup>2</sup> CINAM, UMR 7325 CNRS, Aix-Marseille Université, 13288 Marseille, France

<sup>3</sup> ICMN, UMR 7374 CNRS, Université d'Orléans, 45071 Orléans, France

<sup>4</sup> PHENIX, UMR 82324 CNRS, Université Pierre & Marie Curie, 72522 Paris, France

Small-angle (X-ray or neutron) scattering techniques are powerful methods to investigate large scale organization of clay porous media as information on the density contrast between clay material and the pore network can be obtained. At short spatial scales, the internal organization of clay grains is typically obtained from the analysis of *hkl* diffraction bands. However, it is well known that defects in the crystal structure of clay minerals (e.g., stacking faults, mixed-layering, etc...) control both position and intensity of experimental diffraction bands. Information on the influence of these structure defects on the experimental profiles in the small-angle region is thus crucial in order to provide a continuous description of the scattering properties of clay porous systems over spatial scales.

Recently, we have been interested in the characterization of different size fractions of vermiculite (i.e., 0.1-0.2, 1-2 and 10-20  $\mu\text{m}$ ) obtained by a sonication process (Reinholdt *et al.*, 2013). Using neutron scattering/diffraction method, the degree of anisotropy in particle orientation for the different porous media showed significant size-dependency (Hubert *et al.*, 2013). In parallel, representative 3D virtual porous media were obtained using a one-by-one particle deposition algorithm, similar to the one proposed by Coelho *et al.* (1997). The obtained results showed that the experimental data, such as the distribution of particle geometric factors (surface and aspect ratio) as well as particle orientation (rocking curves), were correctly reproduced for the three vermiculite size fractions.

Based on these virtual porous media, calculations of theoretical scattering/diffraction profiles are performed and compared to experimental ones. The comparison between experimental and calculated profiles provides sound constraints on the representativeness of the obtained virtual porous media. Moreover such close examination allows additional insights into the role played by crystal structure defects on the calculated intensities.

Coelho, D. et al. (1997). *Phys. Rev. E*, 55, 1959.

Hubert, F. et al. (2013) *Clays Clay. Miner.*, 61, 397.

Reinholdt, M.X. et al. (2013) *App. Clay Sci.*, 77-78, 18.

## Analysis of the diffraction pattern of materials with complex microstructure

Matteo Leoni

DICAM – University of Trento, via Mesiano, 77 – 38123 Trento (Italy)

The properties of most industrially-relevant materials are intimately related not just to the local atomic structure, but also to features such as, for example, the size of the grains or the presence and distribution of defects. This is especially valid for lamellar materials whose microstructure is notoriously complex. For a proper engineering of these materials it is necessary to quantitatively link properties/performance with structure and microstructure. Methods are thus needed to extract the structure and microstructure information in a fast and reliable way.

Transmission Electron Microscopy (TEM) is the usual first choice here. Any feature affecting the regular arrangement of the atoms can be easily spotted using a TEM, even if this occurs in a single grain. This is also one of the limits of the technique, as the retrieved information is not necessarily representative for the whole specimen. Diffraction, as a volume-sensitive technique, can complement the TEM as it can capture the disruptions in the periodicity of the atomic arrangement on large quantities of material, provided these effects alter a sufficiently large volume of specimen. Starting from the pioneering work of Scherrer [1], several techniques have been proposed to extract the microstructure information from a diffraction pattern. One of the current major limitations is however the impossibility of general, direct extraction of accurate microstructure information. Most of the available methods are based on pattern simulation and optimization of the corresponding parameters until a match is found between model and data. More and more flexible and accurate microstructure models are thus needed.

One of the complex cases, often met in real specimens and in particular in lamellar materials, is that of disorder in one or multiple directions. This case does not easily fall into the realm of modulated structures, as the periodicity broken by the disorder does not reappear in higher dimensional spaces. The defects and the corresponding configuration entropy must be described in a stochastic way, using a simple and compact representation, such as a Markov chain. The refinement of structure and microstructure of those materials pioneered by Leoni *et al.* in 2004 [1] has been recently generalised [2] to consider more accurate microstructure models [3]. Some results and a further extension are provided here to calculate the diffraction patterns of industrially relevant materials (such as for example clays and zeolites) with complex defect arrangement (including e.g. dislocations or mixed/variable layer character) and/or odd distribution of domain sizes and shapes.

Albeit quite powerful, the method is just a tool and as such is prone to fail. The availability of complementary information and the user intervention are still always the key to an accurate analysis compatible with all experimental evidence.

[1] M. Leoni, A. F. Gualtieri, N. Roveri, *J. Appl. Cryst.* 37 (2004) 166-173.

[2] R. J. Koch, M. Leoni, *Scientific Reports* (2015). Submitted.

[3] P. Scardi, M. Leoni, *Acta Crystallogr. A* 58 (2002) 190-200.

## Crystal structures of natural manganese oxide minerals

*Jeffrey E Post<sup>1</sup>, Peter J Heaney<sup>2</sup>, Florence Ling<sup>2</sup>, and Cara M. Santelli<sup>1</sup>*

*1Department of Mineral Sciences, Smithsonian Institution, Washington, DC 20560,  
United States; postj@si.edu*

*2Department of Geosciences, Penn State University, University Park, PA 16802, USA*

Manganese (Mn) oxide and hydroxide minerals are ubiquitous in aquatic and terrestrial environments and their presence can have sweeping environmental ramifications. They are highly reactive, often outcompeting co-existing Fe (hydr)oxide and clays as controls of metal cycling and redox state. Natural Mn oxide samples commonly occur as fine-grained masses and coatings, and determining the particular structure types or whether they are abiotic or biotic can be challenging. Most laboratory studies show that Mn-oxidizing bacteria and fungi primarily produce a poorly ordered, phyllo-manganate similar to synthetic  $\delta$ -MnO<sub>2</sub> or hexagonal birnessite [Webb et al. 2005, Santelli et al. 2011]. In only a few cases, however, have natural Mn oxides been extensively compared with these laboratory grown phases. We have assembled an unprecedented collection of well characterized, natural Mn oxides from a variety of geological settings, including cave deposits, streams, coal remediation sites, Mn mines, rock varnish, lake nodules, etc. We have characterized the structures and compositions of these samples using powder XRD, analytical SEM, and EXAFS/XANES and IR spectroscopies. For comparison, we also examined laboratory produced fungal Mn oxides. These spectroscopic methods, in particular, provide information about Mn oxidation state (XANES) and structural information for samples that typically are too poorly crystalline to yield useful powder diffraction patterns. Additionally, XAFS and XANES are powerful probes for characterizing Mn oxides that occur as thin coatings or are intimately mixed with other minerals. The study provides new insights into structural variations as functions of composition and formation environment.

A special emphasis of the study was on poorly crystalline Ca-rich phyllo-manganates; these are apparently predominant natural, terrestrial "biogenic" Mn oxide phases and yield typically poor X-ray diffraction patterns that resemble those from fungal and other biogenically produced samples. We compared laboratory produced Ca-rich phyllo-manganates and a variety of natural assumed biotic and abiotic samples. Spectroscopic data reveal similarities but also significant structural complexities that likely correlate with biotic/abiotic origins and local redox and other chemical conditions.

## Water structure and dynamics in smectites: $^2\text{H}$ -NMR spectroscopy of Mg, Ca, Sr, Cs and Pb-hectorite

U. Venkateswara Reddy<sup>1</sup>, Geoffrey M. Bowers<sup>2,3</sup>, Haley E. Argersinger<sup>2,3</sup>, Brennan O. Ferguson<sup>2,3</sup> and R. James Kirkpatrick<sup>4</sup>

<sup>1</sup>Department of Chemistry, Michigan State University, East Lansing, Michigan 48824, U.S.A. venkyreddy84@gmail.com

<sup>2</sup>Division of Chemistry, college of Liberal Arts and Sciences, Alfred University, Alfred, New York 14802, USA

<sup>3</sup>Department of Materials Engineering, Kazuo Inamori College of Engineering, Alfred University, Alfred, New York 14802, U.S.A

<sup>4</sup>College of Natural Science, Michigan State University, East Lansing, Michigan 48824, U.S.A.

$^2\text{H}$ -NMR spectra are uniquely sensitive to water dynamics in the  $10^2$  to  $10^4$  Hz frequency range, and for smectite minerals provide an otherwise unobtainable insight into the structure and dynamics of water in the interlayer galleries and on exterior surfaces. Static  $^2\text{H}$ -NMR data for the San Bernardino hectorite exchanged with a range of charge balancing metal cations shows that the structure and dynamics of interlayer water is greatly affected by the hydration energy and ionic radius of the cation. The spectra were collected at temperatures from 173K to 313K after equilibration at 43% relative humidity (RH) and as 1:1.5 hectorite: $^2\text{H}_2\text{O}$  (weight ratio) pastes. Similar data for  $\gamma\text{-Al}_2\text{O}_3$  and talc, which do not contain interlayer water, provide supporting results. The paste samples all show signals for the formation of bulk ice at approximately 193K. The dynamics of interlayer  $^2\text{H}_2\text{O}$  are similar in both Mg- and Pb-hectorite, in which we can discriminate between  $^2\text{H}_2\text{O}$  coordinated to metal cations and  $^2\text{H}_2\text{O}$  associated with only the basal smectite surface. The slow exchange between these sites is due to the high hydration energy of Mg and Pb ( $\Delta G = -1907$  KJ/mol for  $\text{Mg}^{2+}$  and  $1485$  KJ/mol for  $\text{Pb}^{2+}$ ). For the 43%RH samples the temperature at which the frequency of  $^2\text{H}_2\text{O}$  reorientation reaches the kHz range increases with increasing cation hydration energy from 183K to 193K to 213K for Sr, Ca, and Mg-hectorite, respectively. (Hydration energies of  $\Delta G = -1907$  KJ/mol,  $\Delta G = -1592$  KJ/mol and  $\Delta G = -1447$  KJ/mol and  $r = 86$  pm,  $r = 114$  pm and  $r = 133$  pm for  $\text{Mg}^{2+}$ ,  $\text{Ca}^{2+}$  and  $\text{Sr}^{2+}$ , respectively). In parallel, for paste samples the frequencies of interlayer  $^2\text{H}_2\text{O}$  dynamics are less than the kHz range below 213K for Mg-hectorite and 193K for Sr- and Ca-hectorite. The water dynamics in Cs-hectorite are quite different to those previously reported for Na and K-hectorite<sup>1,2</sup>, because of the small hydration energy of  $\text{Cs}^+$  (283KJ/mol) compared to  $\text{Na}^+$  (412KJ/mol) and  $\text{K}^+$  (338KJ/mol). For all samples at 173K, the  $^2\text{H}_2\text{O}$  reorientation frequencies are less than the kHz range. As a consequence, the  $^2\text{H}$  spectra show broad, ice-1h-like quadrupolar patterns<sup>3</sup>. For the 43% RH samples, the absence of well-defined singularities, however, suggests that although the strengths of the hydrogen bonds of the water molecules are similar to those in ice, their structural arrangement is disordered and not similar to that of ice-1h, in agreement with the results of computational Molecular Dynamics modeling<sup>4</sup>.

1. Bowers, G. M., Singer, J. W., Bish, D. L. & Kirkpatrick, R. J. Alkali Metal and H<sub>2</sub>O Dynamics at the Smectite/Water Interface. *J. Phys. Chem. C* **115**, 23395–23407 (2011).

2. Bowers, G. M., Bish, D. L. & Kirkpatrick, R. J. H<sub>2</sub>O and Cation Structure and Dynamics in Expandable Clays: 2H and 39K NMR Investigations of Hectorite. *J. Phys. Chem. C* **112**, 6430–6438 (2008).

3. Wittebort, R. J., Usha, M. G., Ruben, D. J., Wemmer, D. E. & Pines, A. Observation of molecular reorientation in ice by proton and deuterium magnetic resonance. *J. Am. Chem. Soc.* **110**, 5668–5671 (1988).

4. Morrow, C. P. *et al.* Structure, Energetics, and Dynamics of Smectite Clay Interlayer Hydration: Molecular Dynamics and Metadynamics Investigation of Na-Hectorite. *J. Phys. Chem. C* **117**, 5172–5187 (2013).

## Stabilization of dyes on oxide surfaces

Frédéric Fournier, Philippe Walter and Maguy Jaber

Sorbonnes Universités, UPMC Paris 06, CNRS UMR 8220, Laboratoire d'archéologie moléculaire et structurale, LAMS, F-75005, 4 place Jussieu, BP225, Paris, France  
maguy.jaber@upmc.fr

Historical paintings can be considered amongst the most precious parts of humanity's cultural heritage, since their physical aspects are deteriorating with age. A common phenomenon observed in these paintings is the photodegradation of dyes. It has been reported in several cases such as the "Eglise d'Auvers sur Oise" of Vincent van Gogh (fading of eosine) and the « *Bal du Moulin de la Galette* » of Auguste Renoir who has been surprised by the fading of the purple color and didn't recognize his own painting 20 years later (Figure 1).

Combining the color of natural or synthetic dyes and the resistance of inorganic structures, it is possible to produce hybrid materials with improved chemical properties and higher stability as in the case of the well-known example of "Maya Blue". Mayans had combined indigo, derived from the leaves of the local *añil* plant, with the clay mineral palygorskite, producing a hybrid compound that has conserved its color up to this day.

In this study, the stability of 3 organic dyes were investigated on different types of inorganic matrices including clay minerals. The hybrid materials were characterized by a combination of different techniques including thermal analysis, XRD, TEM, IR, UV-vis and solid state NMR in order to understand the mode of interaction between the organic moieties and the mineral matrix. The data unambiguously prove that an intimate interaction, when it occurs, between the host and the guest can stop the photodegradation of the dyes.

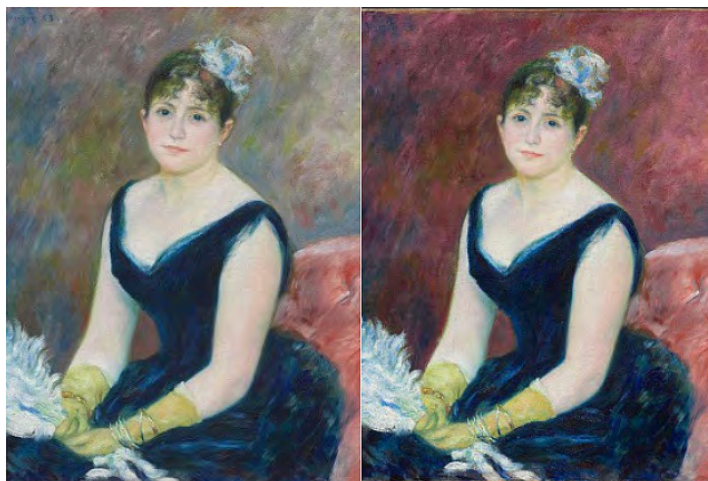


Figure 1 : Pierre-Auguste Renoir.

*Madame Léon Clapisson, 1883*

Thursday  
9<sup>th</sup> July

Lecture room 4

Industry perspectives in  
clay and fine-particle  
science (1)



## Process selection heuristics in industrial mineral processing

Jarrold Hart

Imerys, Par Moor Centre, Par Moor Road, Par PL24 2SQ, UK

Every mineral deposit is unique, and requires a unique process to exploit it with minimal environmental impact and maximal efficiency. The process engineer has a dizzying array of choices to make about extracting and concentrating the valuable ore, and the diversity of end-uses to which minerals are put increases this complexity exponentially. Where does one start?

In this talk, Jarrod Hart will lay out a practical framework to help narrow down these options with a focus on industrial minerals - he will review the concept of liberation size and then review how the fundamental properties of minerals may be exploited to effect beneficiation. The relative costs of popular techniques will then be considered and case studies visited to examine this decision making process in action.

## Transition metal nanoparticles derived from phyllosilicates stabilized on SBA-15 mesoporous silica as efficient catalysts

C. Ciotonea<sup>1,2</sup>, B. Drăgoi<sup>1</sup>, A. Ungureanu<sup>1</sup>, A. Chiriac<sup>1</sup>, S. Petit,<sup>2</sup> S. Royer<sup>2</sup> and E. Dumitriu<sup>1</sup>

<sup>1</sup>"Gheorghe Asachi" Technical University of Iasi, Faculty of Chemical Engineering and Environmental Protection, 73 Prof. D. Mangeron Blvd., 700050 Iasi, Romania, e-mail: carmen.ciotonea@univ-poitiers.fr

<sup>2</sup> Université de Poitiers, IC2MP, UMR 7285 CNRS, 4, Rue Michel Brunet, 86022 Poitiers Cedex, France

Nowadays, supported Transition Metal NanoParticles (TM-NPs) are widely studied due to their potential as catalysts, especially for hydrogenation reactions, the most frequent application in the manufacture of fine chemicals. Functional organic groups, anchored on the solid surface (*e.g.*, thiols, amines, surfactants, or even polymers), are frequently used to encourage dispersion of TM-NPs. However, the stability of NPs is still a challenging problem because upon thermal treatments (drying, calcination and/or reduction) at high temperature prior to reaction, sintering of NPs usually takes place. A valuable approach to preserve both the dispersion and stability of NPs consists of the stabilization of transition metals in phyllosilicates (PS) phases. In this work, we report the synthesis of transition metals (Co, Ni and Cu)-containing phyllosilicates supported over mesoporous silica (SBA-15), in order to obtain functional porous composites. The hydrogenation of cinnamaldehyde (CNA) was used as model reaction to illustrate the catalytic potential of these materials.

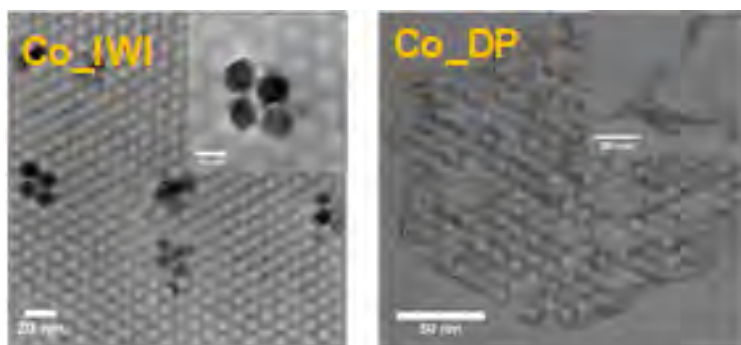


**Figure 1.** Example of phyllosilicate containing nanocomposite prepared by DP route by comparison with a sample obtained by IW. Ciotonea et al. Chem. Commun 49 (2013) 7665.

Synthesis of materials was carried out by an adapted *deposition-precipitation* method (DP) using urea. Metal nitrates were used as precursors. Oxide materials are denoted M\_DP, where M = Cu, Co, Ni. Samples were characterized by ICP-OES, XRD at low and high angles, N<sub>2</sub> physisorption, TEM/EDXS, and temperature-programmed reduction, and the results compared with those materials obtained by IW (incipient wetness impregnation, a classical route to prepare metal supported NPs). For the evaluation of their catalytic properties, the samples were subjected to reduction, under hydrogen flow (1 L h<sup>-1</sup>) for 10 h at 350 °C (Cu\_DP and Cu\_IWI) and 500 °C (Ni\_DP, Co\_DP and Co\_IWI).

X-ray diffraction patterns at low angles and N<sub>2</sub> adsorption/desorption isotherms for support were

typical for ordered hexagonal 2D structures of SBA-15-type. A significant alteration of the original mesostructure was noted after phyllosilicate formation, due to the silica dissolution and consumption under the slightly alkaline pH conditions. The XRD patterns at high angles show weak diffraction peaks assigned to PS phases. The intensity of these peaks depends on the nature of metal as follows: Ni\_DP > Co\_DP >> Cu\_DP. In addition, the formation of phyllosilicate-like phases is confirmed by FTIR analysis. TEM images have confirmed the XRD, N<sub>2</sub> physisorption and FTIR results, allowing us to observe: (i) the degradation of the mesoporous structure of SBA-15 and the formation of large pores in the silica grains, and (ii) the formation of fibrous PS particles highly dispersed in the porosity of SBA-15. The catalytic results show that the activity follows the order: Ni\_DP >> Cu\_DP > Co\_DP, consistent with literature data, but with significantly improved activity in this case. High selectivity levels to CNOL were obtained for Cu and Co-containing samples (*ca.* 50 mol%, at CNA conversion up to *ca.* 30 mole %). These interesting catalytic properties are obviously related to the high dispersion of the metallic phases derived from phyllosilicate-containing nanocomposites, as observed by TEM analysis after reduction and further confirmed by *in situ* XRD experiments.

**Keywords:** phyllosilicates, transition metal, nanocomposites, mesoporous support, heterogeneous catalysis.

**Acknowledgments:** The Romanian authors acknowledge the Romanian National Authority for Scientific Research, CNCS-UEFISCDI, through project numbers PN-II-ID-PCE-2011-3-0868 and PN-II-RU-TE-2012-3-0403. C. Ciotonea acknowledges Eiffel Excellence Fellowship for financial support.

## Silver bentonite complexes as antimicrobial additives in clay-starch-based barrier coatings for sustainable packaging

Francis Clegg<sup>1</sup>, Chris Breen<sup>1</sup>, Peter Muranyi<sup>2</sup> and Claudia Schönweitz<sup>2</sup>

<sup>1</sup>Materials and Engineering Research Institute, Sheffield Hallam University, City Campus, Howard Street, Sheffield, S1 1WB, U.K. E-mail: f.clegg@shu.ac.uk

<sup>2</sup>Fraunhofer Institute for Process Engineering and Packaging, Giggenhauser Straße 35, 85354 Freising, Germany

The incorporation of silver into polymer coatings, devices or products to impart antimicrobial activity is becoming increasingly popular. This trend is due to a need to control infectious diseases, in hospitals and communal environments, and in particular those that are becoming resistant to current antimicrobial treatments.

There are several types of silver that provide antimicrobial activity, including metallic, oxide and halide species and combined with a nanoparticle structure offering greatly enhanced surface areas their potency, which is partly governed by their release mechanisms/kinetics can be controlled. Clay minerals offer not only a substrate from which to reduce agglomeration of nano-sized particles, but additionally offer cation-exchange sites from which silver cations can be readily released to impart antimicrobial activity. Commercially, bentonites are the desired choice of clay mineral for such a silver-based antimicrobial because they are available in large quantities and are economically favourable.

The preparation of silver-exchanged bentonites wherein the silver is only present as exchangeable cations has been found to be complex and challenging due to the range of impurities and processing additives present. These challenges are discussed with reference to a range of silver-clay complexes, prepared by a number of different approaches, and their characterisation by x-ray fluorescence, x-ray diffraction and transmission electron microscopy.

The antimicrobial activity of the silver-exchanged bentonite complexes has also been assessed by their incorporation in a recently developed sustainable coating for packaging. They have shown to demonstrate very strong activity towards *Escherichia coli*, *Kocuria rhizophila* and *Aspergillus niger*. Incorporating just 0.03 wt% of a silver-exchanged bentonite complex produced a >4.4 log reduction against an initial loading of  $2.1 \times 10^5$  CFU/object for *E. coli*. Water vapour barrier properties of coatings prepared on paper and containing pre-determined quantities of silver clay, rather than sodium clay alone, were also unaffected since water vapour transmission rate values of ~20-40 g/m<sup>2</sup>.day (23 °C, 50% relative humidity) were maintained. The preservation of the barrier properties relies on clay dispersion, which was shown not to be adversely affected by the presence of silver-bentonite.

## Electrochemical synthesis of cobalt-containing layered hydroxides on stainless steel sieves: a way to obtain supported catalysts

František Kovanda<sup>1</sup>, Stanislava Krejčová<sup>1</sup>, Daniel Bouša<sup>2</sup>, Květa Jiráťová<sup>3</sup> and Lucie Obalová<sup>4</sup>

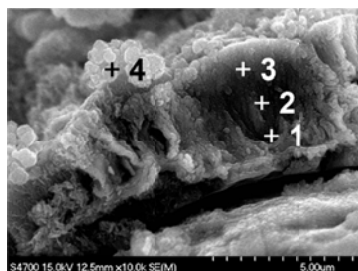
<sup>1</sup>Department of Solid State Chemistry, University of Chemistry and Technology, Prague, Technická 5, 166 28 Prague, Czech Republic, Frantisek.Kovanda@vscht.cz

<sup>2</sup>Department of Inorganic Chemistry, University of Chemistry and Technology, Prague

<sup>3</sup>Institute of Chemical Process Fundamentals of the CAS, Rozvojová 135, 165 02 Prague, Czech Republic

<sup>4</sup>VSB-Technical University of Ostrava, 17. listopadu 15, 708 33 Ostrava, Czech Republic

Oxide catalysts are often obtained by thermal decomposition of hydroxide precursors. In the catalysts prepared from powdered precursors formed into pellets, much of the catalyst grain volume is often not fully utilized. The effect of reactant diffusion in the fast reaction can be minimized, when the precursors are deposited in a thin layer on supporting material. The Co-Mn-Al mixed oxides prepared by calcination of layered double hydroxide (LDH) precursors showed high catalytic activity in total oxidation of volatile organic compounds and N<sub>2</sub>O decomposition. Recently we reported analogous catalysts deposited on anodized aluminum foils [1,2]. In the present work the Co-Mn-Al LDH precursors were prepared on the surface of stainless steel sieves. The electrochemical synthesis, consisting of cathodic reduction of Co, Mn and Al nitrates in aqueous solutions, was performed in potentiostatic mode and the reaction conditions were optimized to obtain the product with desired cation composition. Powder XRD showed phases with LDH structure but SEM images and microprobe analysis indicated non-homogeneous distribution of the metal cations. A surface layer, probably consisting of small LDH crystals with large amounts of Co and Mn, was formed on the support and aggregates observed over this surface layer were enriched with Al (Fig 1). The same procedure was used for electrochemical synthesis of cobalt hydroxide; a product with layered structure, probably the Co(II)-Co(III) layered hydroxide, was formed. The catalysts were obtained by heating the prepared samples at 500°C in air, when oxide phases with spinel structure were formed. The catalysts prepared contained large portions of easily reducible components. During testing in the total oxidation of ethanol and N<sub>2</sub>O decomposition, the catalysts deposited on stainless steel sieves showed less conversion compared to the grained oxides prepared from the precipitated precursors but their specific activity calculated per weight of the active components (Co and Mn) was considerably higher.



Point	Concentration / wt. %			
	Co	Mn	Al	O
1	16.8	9.0	13.3	60.3
2	18.0	9.5	11.6	60.4
3	18.2	8.2	13.0	60.1
4	9.6	3.4	25.4	59.4

Fig. 1: Profile of the mixed oxide layer deposited on stainless steel support and concentrations of elements determined by microprobe analysis

**Acknowledgements:** This work was supported by the Czech Science Foundation (project P106/14-13750S).

Kovanda F., Jiráťová K.: Supported layered double hydroxide-related mixed oxides and their application in the total oxidation of volatile organic compounds. *Appl. Clay Sci.* 53 (2011) 305-316.

Kovanda F., Jiráťová K., Ludvíková J., Raabová H.: Co-Mn-Al mixed oxides on anodized aluminum supports and their use as catalysts in the total oxidation of ethanol. *Appl. Catal. A* 464-465 (2013) 181-190.

## Influence of additives: boehmite and amorphous silica on geopolymer formulations

Lamyaa Laou<sup>1,2</sup>, Sylvie Yotte<sup>2</sup> and Sylvie Rossignol<sup>1</sup>

<sup>1</sup>SPCTS, 12 rue Atlantis, 87068 Limoges Cedex, France

<sup>2</sup>GEMH, boulevard Jacques Derche, 19300 Egletons, France

The field of building and construction is the world's largest consumer of energy. In order to fit into a perspective of sustainable development, it is necessary to think about eco-materials (wood and mudbrick). To ensure adhesion between these two materials, it is necessary to find a time-stable geopolymer binder to allow bonding between these materials and to prevent any eventual co-interaction which may induce interphase formation and thus, decreases the mechanical strength of the assembly.

This study aims to determine a suitable formulation for this type of application. For this, it was necessary to destabilize the composition to delay the binder setting by changing the chemical composition through incorporating additives. These formulations were synthesized in a restricted domain of the ternary diagram Al-Si-K/O. The physico-chemical properties of different geopolymer formulations were characterized by in-situ FTIR spectroscopy and pH value measurements.

The FTIR-spectroscopy results revealed that formulations synthesized either by adding boehmite or amorphous silica were obtained with different kinetics. Modifying the formulation tends to reduce Si-O-M (M= K, Si, Al) bridges' shift and slope. In the case of boehmite, a considerable deceleration of the polycondensation reaction was observed. However, adding amorphous silica to the reactive mixture led to the formation of a geopolymer network and a silicon-rich gel. Finally, the pH-measurements were found to be in good agreement with IR-spectroscopy results.

## Effect of clay mineral type and associated iron phase on the strengthening of “geomimetic” materials

Gisèle L. Lecomte-Nana<sup>1</sup>, Hervé Goure Doubi<sup>1</sup>, Amina Mokrani<sup>1</sup>, Benoît Nait-Ali<sup>1</sup>, Agnès Smith<sup>1</sup>, Léon Koffi Konan<sup>2</sup>

<sup>1</sup>Laboratoire Science des Procédés Céramiques et Traitements de Surface (SPCTS, UMR CNRS 7315), Ecole Nationale Supérieure de Céramique Industrielle(ENSCI), Centre Européen de la Céramique – 12, rue Atlantis – 87068 Limoges Cedex – France

<sup>2</sup>LCMI : Laboratoire de Chimie des Matériaux Inorganiques, Université Félix Houphouët-Boigny, 22 BP 582 Abidjan 22, Côte d’Ivoire

The main objective of the present work was to investigate the effect of the nature of clay minerals as well as the nature of associated iron phases on the processing and the properties of use of “geomimetic” products. In the context of sustainable development, economic and environmental issues there is an increasing promotion of development of local materials using original methods, mainly for building purpose. It is in this approach that a new type of product based on lateritic clay, denoted “geomimetic” products, or “eco-sustainable” materials, have been developed. The given name arises because these products were inspired by the process of formation of lateritic concretions, mechanically resistant in tropical soils. Their processing involves a 24-hour reaction of lateritic clay with a humic substance followed by a neutralization using lime ( $\text{Ca}(\text{OH})_2$ ), and a consolidation step of 18 days at 60°C under an atmosphere saturated with water. The influence of kaolinite, illite and smectite as major constituents was studied whereas goethite, hematite and ferrihydrite were tested as secondary phases. X-ray diffraction, thermal analyses and mechanical compressive strength were performed on the as-obtained samples.

It appears that the clay mineral type plays a determining role in the strengthening of “geomimetic” materials. Illite appears to be detrimental to the consolidation of manufactured samples, mainly because of the competitive adsorption of calcium ions onto illite. Furthermore, the presence of iron phases has an additional reinforcing role mostly with goethite. The consolidation mechanisms involved the pozzolanic reaction of lime with acid-activated clays and the formation of iron-organic-clay complexes. The mechanical properties of these materials are relevant with further application for building purpose. A significant improvement can be achieved by using a dry shaping process such as unidirectional pressing instead of conventional casting.

**Keywords:** kaolinite, 2:1 clay minerals, iron phases, “geomimetic” materials, strengthening, mechanical properties

## Feasibility of producing geopolymers materials from natural soil clays

Julie Peyne<sup>1,3</sup>, Emmanuel Joussein<sup>2</sup>, Sylvie Rossignol<sup>1</sup>, Jérôme Gautron<sup>3</sup>, Julie Doudeau<sup>4</sup>

<sup>1</sup> Science des Procédés Céramiques et de Traitements de Surface (SPCTS), Ecole Nationale Supérieure de Céramique Industrielle,  
12 rue Atlantis, 87068 Limoges Cedex, France

<sup>2</sup> Université de Limoges, GRESE EA 4330, 123 avenue Albert Thomas, 87060 Limoges, France

<sup>3</sup> Bouyer Leroux, L'établère, 49280 La Séguinière, France

<sup>4</sup> Bouyer Leroux Structure, 32 route d'Auch, 31770 Colomiers, France

Within the last two decades, the use of clays in the formation of geopolymer-type materials has been of significant interest. Clay materials are , abundant, low-cost natural minerals and don't require much in terms of preparation before use. Geopolymers have lots of advantages in industry because they are environmentally friendly and have several properties (mechanical, chemical and thermal) which are constant over time. They are used in numerous applications.

The aim of this work is to study the feasibility of producing geopolymers from natural untreated soil clays from France, which are currently used in brick production. This work is based firstly on the raw clay materials characterization and then in the investigation of the clay reactivity in geopolymer mixture. Physical and chemical clay characteristics were studied by specific surface and particle-size distribution measurement and by the cation exchange capacity determination. The main phases in the raw clays were examined using by X ray diffraction and FTIR. Several geopolymers (Na- and K-based) mixtures were tested in order to check the feasibility. Finally, the role of the clays in the formulation of the geopolymers was established.

## Influence of clay mineralogy on the pozzolanic activity of lime-treated soils

Enza Vitale<sup>1</sup>, Dimitri Deneele<sup>2</sup> and Giacomo Russo<sup>1</sup>

<sup>1</sup>University of Cassino and Southern Lazio, Via G. Di Biasio, 43 - 03043 Cassino(FR), Italy, e.vitale@unicas.it

<sup>2</sup>Institute of Material Jean Rouxel (IMN), University of Nantes, CNRS, 2 rue de la Houssinière, BP 32229, 44322 Nantes Cedex 3, France

The study of the physical-chemical mechanisms controlling the behaviour of lime-stabilised soils is relevant given the frequent use of this technique as an economical solution in geotechnical applications to reduce the consumption of natural resources. The use of stabilizing agents such as lime, cement and fly ash, has a significant impact on the physical and hydro-mechanical properties of soils as a results of the short- and long-term reactions which take place after the treatment.

In the present study, an investigation of the long-term interaction mechanisms of clay-lime systems has been performed. In order to understand the influence of clay mineralogy on the kinetics of pozzolanic reactions, an experimental testing program was carried out on two different soils: Speswhite kaolinite and Sardinian bentonite (mainly composed of montmorillonite), treated with different lime contents (1, 3 and 5% for kaolinite and 3, 5, 7, 10% for bentonite).

The mineralogical and fabric changes induced by lime addition were monitored at increasing curing time by means of X-ray diffraction (XRD), thermogravimetric analysis, <sup>29</sup>Si NMR spectroscopy, Scanning electron microscopy (SEM) and nitrogen adsorption/desorption measurements.

Test results indicated that the two clay minerals reacted differently with lime. Sardinian bentonite showed a high initial reactivity characterized by a rapid and total consumption of lime which promoted the formation of hydrated phases such as calcium silicate hydrates (C-S-H) and calcium aluminate hydrates (C-A-H), as a results of the hydrolysis of silicon and aluminum favoured by the high pH environment. The pozzolanic phases appeared to form after a long curing time ( $\geq 60$  days) in lime-treated kaolinite. The lower reactivity is reflected in a delay of the portlandite consumption and the formation of new phases (C-A-H, C-A-C-H). In addition, C-S-H was not detected after 60 days of curing, highlighting a different rate of dissolution of the silica and alumina layers of kaolinite.

In both cases the lime treatment strongly modified the clay fabric as shown by SEM images and nitrogen adsorption-desorption measurements.



## Facile fabrication of MgAl-LDH three-dimensional flower-like micro-nanostructures using surfactant as a soft-template

Linjiang Wang<sup>1,3</sup>, Jie Zhang<sup>1</sup>, Xiangli Xie<sup>2</sup>, Cunjun Li<sup>1</sup>

1. College of Materials Science and Engineering, Guilin University of Technology, Guilin 541004, China;

2. College of Chemistry and Bioengineering, Guilin University of Technology, Guilin 541004, China;

3. Ministry-province jointly-constructed cultivation base for state key laboratory of Processing for non-ferrous metal and featured materials, Guilin University of Technology, Guilin, 541004, China

E-mail: wlinjiang@163.com

Structure and morphology have significant effects on the physical and chemical properties of materials. Layered double hydroxides (LDHs) are a class of ionic lamellar compounds that consist of positively charged layers with an interlayer region containing charge compensating anions and solvent molecules. The morphology of a 'soft-template' is diverse and easily built. The simple process and mild conditions mean that the soft-template method is better in terms of the structure and diversity composition of composite materials.

In this work, three-dimensional (3D) flower-like micro-nanostructure MgAl layered double hydroxide (MgAl-LDH) with curved surfaces and crossed nanoplates were successfully synthesized via a facile template method using the anionic surfactant, sodium dodecyl sulfate (SDS) as the soft-template. Scanning electron microscopy (SEM), energy-dispersive X-ray spectrometry (EDS), X-ray diffraction (XRD), fourier transform infrared (FT-IR), thermogravimetric analysis (TGA) and the Brunauer-Emmett-Teller (BET) method were employed to characterize the products. The results revealed that the 3D flower-like structure MgAl-LDH consisted of numerous curved nanoplates on the surface. With increase of the crystallization temperature and time, the size of such 3D flower-like structure increased significantly and the dispersibility also improved noticeably. When the crystallization temperature was 160°C and crystallization time was 6 h, the product exhibited uniform flower-like nanosphere structure with the average diameter of 4 μm. The specific surface area of the materials with such flower-like nanosphere structure was 41.20 m<sup>2</sup>/g with a wide hierarchical distribution of pores. The pore diameter was 1.544 nm and the pore volume was 0.076 cm<sup>3</sup>/g. The 3D flower-like nanosphere structure also exhibited high thermal stability. Anionic surfactant in aqueous solutions might aggregate to form spherical micelles which can serve as template for inducing the crystal nucleation and growth. The flower-like nanosphere micro-nanostructures were formed from self-assembly of nanoplates in a spontaneous process in hydrothermal conditions.

## Surface chemistry and interaction of kaolinite particles in the presence of calcium-rich alkaline solution

Yadeta C. Chemed<sup>1,2</sup>, Dimitri Deneele<sup>1,2</sup>, George E. Christidis<sup>3</sup> and Guy Ouvrard<sup>1</sup>

<sup>1</sup>Institut des Matériaux Jean Rouxel (IMN), Université de Nantes, CNRS, 2 rue de la Houssinière, BP 32229, 44322 Nantes Cedex 3, France: Yadeta.Chemed@cnsr-imn.fr

<sup>2</sup>Institut Français des Sciences et des Technologies des Transports, de l'Aménagement et des Réseaux (IFSTTAR), BP 4129, route de Bouaye, 44332 Bouguenais, France

<sup>3</sup>Technical University of Crete, Department of Mineral Resources Engineering, 73100 Chania, Greece

From both environmental and economic points of view, there is a growing interest in using local material for construction works. However, the clayey soils that are commonly encountered in construction sites often do not meet the geotechnical requirement and need to be stabilized prior to use as a construction material. Lime is a widely used chemical additive in stabilization of such materials. However, the physico-chemical mechanisms involved (particularly in short-term), which are considered to be key parameters in soil stabilization, are still not well understood. Understanding the reaction mechanism is crucial for optimisation of the lime-treatment technique. In the present study, a pool of techniques was used in an attempt to understand the causes of short-term (i.e. prior to precipitation of calcium hydrates) improvement in the mechanical property of lime-treated clayey soil. Two kaolinites, namely KGa-2 (high defect) and KGa-1b (low defect) were used. The interfacial chemistry was analyzed with calcium adsorption and zeta-potential measurements while three kinds of rheological experiments (steady state rheometry, forced oscillatory shearing and creep-recovery) were conducted to examine the influence of hydrated lime solution on kaolinite particle interaction. The influence of other factors such as type of cation (Ca vs Na) and pH ( $\text{Ca(OH)}_2$  vs  $\text{CaCl}_2$ ) both on the interfacial chemistry and kaolinite particle interaction were also investigated. The results reveal that the nature (species) of calcium adsorbed at neutral (pH = 7) and alkaline (pH = 12) pH are different and have different effects on surface properties and interaction of kaolinite particles. In the non-linear viscoelastic region, where the gel structure is not stable and the particles are forced to move, the slurries in de-ionized water, calcium chloride solution ( $[\text{Ca}] = 22 \text{ mmol/l Ca}$ , pH < 7) and saturated lime solution ( $[\text{Ca}] = 22 \text{ mmol/l}$ , pH = 12) showed different behaviours in terms of width of strain hump, strain at maximum loss modulus and intensity of strain hardening, revealing difference in the microstructural organisation of clay particles. It appears that simultaneous occurrence of multivalent cations and alkaline pH is necessary for densely packed aggregation of clay particles. Calcium at lower pH (pH < 7) induces flocculation of clay particles, while at higher pH (pH > 10) it induces both flocculation and linkage between clay particles and provides the most efficient way to form dense and tightly packed flocs.

## Ball clay ageing

Martyn Gadsdon<sup>1</sup> and Laurence Boyer<sup>2</sup>

<sup>1</sup>Imerys Minerals Ltd, Higher Brocks Plantation, Newton Abbot TQ12 6QZ. martyn.gadsdon@imerys.com

<sup>2</sup>Imerys Minerals Ltd, Higher Brocks Plantation, Newton Abbot TQ12 6QZ. laurence.boyer@imerys.com

Ball clays are widely varying clay minerals primarily containing kaolinite, illite, and quartz. Other secondary minerals and materials may be present, including pyritic minerals and organic materials such as lignite. The behaviour of ball clays is known to change with time as a result of a process called ageing. This process is understood to be driven by oxidation reactions that generate an increase in soluble ionic species that are associated with some of the secondary materials; for example, the oxidation of insoluble iron pyrite to soluble ferrous iron sulphate. These species, along with others, are known to have a strong influence on the in-application performance of the ball clay – particularly rheology in the case of sanitaryware. Empirical evidence shows that, whether as an indicator or as the key driver, the concentration of soluble sulphate is correlated with this oxidation process. Imerys has recently developed a test to simulate and accelerate this ageing process ahead of time in order to highlight potentially abnormally ageing clays.

## Application results for the quantum design SHGMS magnetic separator

Paul A. Beharrell

Quantum Design Inc., 6325 Lusk Boulevard, San Diego, CA 92129, United States of America

paulb@qdusa.com

Quantum Design, Inc. has developed a high throughput, conduction-cooled, superconducting high-gradient magnetic separation system (SHGMS) for use in various industries and applications. The system operates at 5 tesla for high throughput and material selectivity and has a processing volume of 203mm x 406mm. Designed for modular deployment, the system is fully integrated, has a small footprint and low energy requirements. The system's superconducting magnet is supported at operating temperature by a single cryocooler, obviating the need for expensive and inconvenient liquid cryogenes.

The first system has been deployed at a customer site, a kaolin mine in Zhangzhou, China, and has been successfully utilized in the beneficiation of a number of china clays from the region. Results are presented for the brightness improvements to these clays which are used extensively in the ceramics industry and whose value depends on brightness. The system is capable of improving the brightness of these clays to values as high as 93 and in full production the system has a capacity in excess of 10,000 tonnes per year of dry material for these clays.

A second system is being constructed to enable testing to proceed for other applications. In addition to further application within the worldwide kaolin industry, magnetic measurements on bentonite samples from California have revealed color components whose targeted removal is possible via the magnetic separation technique.

Further R&D is being carried out in other industries such as oil and gas. Incorporating extensions to the magnetic separation technique developed at Quantum Design, the technology is ideally suited to the high volume recovery and reuse of catalysts in the post-reaction process streams in such applications as coal gas hydrogenation and the Fischer-Tropsch process for the production of liquid fuels from various sources including biomass.

## A methodology to value reservoir sediment in the fired-clay industry

Frédéric Haurine<sup>1,2</sup>, Isabelle Cojan<sup>2</sup> and Marie-Anne Bruneax<sup>1</sup>

<sup>1</sup>CTMNC Centre Technique de Matériaux Naturels de Construction, Service Céramique,  
17 rue Letellier 75015 PARIS - France - frederic.haurine@mines-paristech.fr

<sup>2</sup>MINES-ParisTech, PSL Research university, Centre de Géosciences,  
35 rue St Honoré 77305 Fontainebleau Cedex, France

Preservation of natural resources becomes an important issue in the general frame of European environmental policies. Clay deposits in rivers, in particular associated with hydraulic structures (dams, harbors, locks,...), constitute potential alternatives to the quarrying of geologic formations. Through the example of the Durance watershed, we present a methodology to recover sediments considered as waste by industrial operators by enhancing their value in the fired-clay industry.

The Durance River and its tributaries are characterized by an important flux of suspended particulate matter (SPM). A large part of these SPM (more than 1Mt/year) is trapped in the 17 reservoirs of hydropower dams built along the Durance watershed. Compared with the annual consumption of raw material by the French fired clay industry (7Mt/year), this flux is quite significant.

To assess the potential of reservoir sediment, an industrial referential has been established from a set of 35 industrial samples. It is based on grain size distribution, mineralogical content (bulk rock and clay minerals) and geochemical compositions. All reservoir sediments are analyzed according to this protocol. For samples within the appropriate values, tests specific of the fired clay industry (firing, drying, resistance ...) are conducted. When necessary, mixture with sand, calcined clay, other sediment or fossil material are prepared to reach characteristics similar to that of the industrial referential.

In the upper course of the Durance river (particularly in Serre Ponçon dam reservoir), the SPM contain large amounts of illite and chlorite and a coarse grain size distribution which do not favor direct use in the fired-clay industry. In the middle course, the smectite and kaolinite content increases in the SPM associated with a larger CaCO<sub>3</sub> content. SPM from Verdon River (main tributary of Durance) has similar mineralogical contents. This change in mineralogy is explained by the important contribution from sedimentary formations like the Jurassic marls. The large CaCO<sub>3</sub> content can create some defaults during shaping or firing as observed in the Verdon samples (Castillon dam reservoir). Downstream of the Durance-Verdon confluence (Cadarache dam reservoir), CaCO<sub>3</sub> content and clay\_mineral composition in SPM are close to expected values for use in the fired-clay industry, due to the mix of SPM from upper Durance and Verdon. All fired-clay laboratory tests could be performed on the Cadarache samples although the grain size distribution seems too fine for an industrial use. For better characteristics, mixtures were prepared by adding sand or calcined clay. Both the grain size distribution and geochemical composition were improved without significantly modifying their drying and firing properties. To value as much as possible reservoir sediments, other mixtures were successfully prepared, one with Cadarache and Serre Ponçon samples and another with a Cadarache sample and an industrial clay mixture.

These results for the Durance watershed reveals that substitution of clay from geologic formations by modern reservoir sediments is feasible and can represent a significant mass when compared to the French fired-clay industry consumption. It also reveals that mixtures of reservoir sediment with waste from the fired-clay industry or industrial clay, make suitable some reservoir sediments that were not suitable based on their mineralogical compositions. This type of incorporation of "waste reservoir sediment" in the fired-clay industrial process will allow to reduce the consumption of non-renewable raw material and to extend the extraction duration of quarries.

## Techniques for measuring the particle size and shape distribution of ultrafine industrial minerals – a user's perspective

Jonathan Phipps

Imerys Minerals Ltd, Par Moor Centre, Par, Cornwall, UK, PL24 2SQ. jon.phipps@imerys.com

Fine particulate industrial minerals are used as fillers and additives in a wide range of applications, in which their performance is determined as much by the size and shape distribution of the particles as by their mineralogy. For many minerals consisting of anisotropic particles (e.g. kaolin, talc and halloysite), particle aspect ratio is critical to their suitability for those applications. Therefore it is important for the suppliers and users of industrial minerals to be able to characterise them as fully as possible. In recent years, growing interest in nanotechnology and nanoparticles, not least from a regulatory standpoint, has brought the need to measure ever smaller particles which may be beyond the accepted range of conventional sizing techniques.

For non-spherical particles, the definition of particle size itself is not straightforward. The two measurement techniques most commonly used are laser diffraction and sedimentation, which represent size in terms of an equivalent spherical diameter. The relationship between this diameter and the actual particle dimensions depends upon the shape of the particle and the technique itself; this was addressed theoretically many years ago but is not commonly used to help interpret measurements.

Many different commercial instruments are available which can measure size distributions of micron-sized particles and smaller, though none can specifically measure shape or aspect ratio. As a result, in the 1990s Imerys developed an instrument in which the conductivity of a suspension of particles in both quiescent and laminar flow conditions is measured, and a value for the mean aspect ratio is derived from the difference between them. This instrument is still in routine use today.

In this presentation we examine the assumptions behind the main techniques, the limitations of the methods and how best to interpret the particle size data. Methods for combining techniques to give shape information across the distribution will be evaluated, and results compared with similar measurements made on fractionated versions of the same materials, as well as with the conductivity technique.

## Characterization of pH dependent colloidal behavior with respect to the arrangement of clay mineral particles in different arrested states

Müge Pilavtepe<sup>1</sup>, Norbert Willenbacher<sup>1</sup>, Annett Steudel<sup>2</sup>, Rainer Schuhmann<sup>2</sup> and Katja Emmerich<sup>2</sup>  
muege.pilavtepe@kit.edu

<sup>1</sup> Karlsruhe Institute of Technology, Institute for Mechanical Process Engineering and Mechanics, 76131 Karlsruhe, Germany

<sup>2</sup> Karlsruhe Institute of Technology, Competence Center for Material Moisture and Institute of Functional Interface, 76344 Karlsruhe, Germany

Colloidal clay mineral suspensions consist of plate-like particles having charges at the edges and on the surfaces based on morphological substitutions within the clay mineral. If these particles are dispersed in electrolyte solutions, from the competing attractive and repulsive interactions between particles different states with structural features resulted. The orientation of the particles to each other is influenced by the pH of the suspension, as the charge of the edge is pH dependent. At high pH values, where the edges and surfaces are negatively charged, a parallel and partially overlapped (PPO) band structure is formed. At low pH values attractive electrostatic interaction between the positively charged edges and negatively charged areas is possible, thus resulting in a so-called house of cards (HOC) structure of the aggregates [1].

In this study we use ultrasonic velocity measurements to characterize the differences between these particle orientations. The adsorption and bonding of water on the clay mineral particle surface depends on the relative orientation of adjacent particles and has a strong effect on compressibility of the aqueous phase and hence the ultrasonic velocity. For this purpose, dispersions are produced with clay mineral contents 1-5 wt. % (depending on the material), ion concentrations between  $10^{-2}$  and  $10^{-5}$  M as well as pH values varying from 8.5 to 12. For the HOC structure formed at lower pH the ultrasonic velocity was found lower than for the PPO structure, since HOC structure has more active surface area for bonding water. This feature is used for pharmaceutical and paint formulations [2, 3]. Synthetic and natural clay minerals, i.e. Laponite® (*registered trademark of BYK Additives*), hectorite (0.2  $\mu\text{m}$  fraction of SHCa-1 Source Clay) and montmorillonite (0.2  $\mu\text{m}$  fraction of Volclay) with different particle diameters of 20, 50 and 200 nm, respectively, have been used to determine the effect of particle size on the formation of the band or house of cards structures.

Concurrently, the mechanical strength of clay mineral dispersion is related to the formation of particles networks in which individual clay particles are in contact with others. The sol-gel transition of natural clay suspensions depends heavily on the surface-charge distribution of the respective clay particles, which depends not only on the type of clay, but also varies with pH as well as concentration of the electrolyte in the liquid phase. Time dependent effects during gelation and degree of aging of clay suspension at different pH values were investigated by classical rotational rheometry with small-amplitude oscillatory shear measurement. After destroying the gel-like structure the change in the ratio  $G'/G''$  is much more rapid for dispersions with HOC structure than with PPO structure, whereas they have the same mechanical strength after the complete restructuring of the particle network.

[1] Tombacz, E., Szekeres, M., Applied Clay Science, 27, 75-94, (2004).

[2] Rice, Z., Bergkvist, M., Journal of Colloid and Interface Science 335, 189–195, (2009).

[3] Elaziouti, A., Laouedj, N., Ahmed, B., J. Chem. Eng. Process Technology, 2, 113, (2011).

## The effect of $K_2CO_3$ and Al addition on elastic modulus density and porosity of ceramic bodies derived from Westerwald ball clay

Aydın Aras

Yuzuncu Yil University, Engineering and Architecture Faculty, Geological Engineering Department, 65080 Van /Turkey

This study aims to investigate the effect aqueous  $K_2CO_3$  and Al addition on some physical properties of ceramic bodies derived from Westerwald ball clay HB (WBC-HB). The geological-mineralogical properties of the clays of the Westerwald area described in a large number of studies of Rohstoffmerkbblätter der DKG(1). This integrative work is a follow up of the investigation of the K and Na-Ca feldspar effect on phase change in ceramic bodies derived from WBC-HB(2) and  $K_2CO_3$  (K) and alumina (Al) effect on phase change of ceramic bodies derived from WBC-HB clay (3)(4). Six wet mixtures were prepared by adding 20, 40 or 60 wt.% Al to the WBC-HB clay and by adding 5 wt.% K to WBC-HB containing 20, 40 or 60 wt % Al. These six mixtures were also wet milled for 4 h and 8 h. The elastic modulus (E), density and porosity of these 36 ceramic bodies derived from original and 2 h and 8 h wet milled mixtures fired at 1200°C and 1400°C were evaluated. The measured and calculated properties of bodies derived from original mixture were compared with the results of bodies derived from 4 h and 8 h wet-milled mixtures (Fig. 1). The E modulus decreases with increasing Al addition from 20 to 60% in the bodies without 5% K, but increases with increasing Al from 20 to 60% in the bodies with 5% K. Smaller decreases and increases were observed in intermediate bodies (40% Al) and the difference between the measured E modulus of bodies milled for 20 h and 40 h and 60% Al bodies of 8 h were less than those measured in bodies derived from bodies milled for 0 h and 4 h. The maximum elastic modulus, 258 GPa, was measured from the body derived from original mixture containing 60% Al and 5% K fired at 1400°C and caused by a maximum Al content (60 wt.% Al) and complete dissolution of detrimental quartz. The addition of 5 wt.% K inhibited cristobalite formation and also reduced the amount of mullite and preserved the amorphous phase to higher temperature; later it produced fusions that resulted in a glassy phase in the body (4). The measured E modulus and density were controlled predominantly by porosity, crystal/glass ratio, crystal size and type of crystal. The fired ceramic bodies offer an exceptional opportunity for investigating the interdependence of these factors: (i) measured and calculated true, open and closed porosity; (ii) quartz-mullite-corundum at 1200°C, mullite-corundum(1400°C, 0–4h milled) and corundum (1400°C, 8 h milled) bodies. The maximum measured E modulus confirmed the optimum 60 wt.% Al addition, along with original particle size of Al ( $D_{50}$  40 $\mu$ ). On the other hand, in WBC-HB Al<sub>60</sub> K<sub>5</sub> and unmilled body, the size of mullite needles and the amount of mullite in the microstructure was at a minimum in favor a maximum amount of corundum(3).

1-Kromer, H., 1980. Tertiary clays in the Westerwald area. Geol. Jb. D. Rhei D Hanover, 69–84 (Ton HB no 105 Ber. dt. keram. Ges., 55, 7)

2-Aras, A., " The change of phase composition in ceramic bodies in kaolinite-and illite-rich clay-based ceramic bodies" Applied Clay Science 24 257-269 (2004)

3-Aras A, Madai, V, Kristally, F., Effect of  $K_2CO_3$  and  $Na_2CO_3$  and  $CaCO_3$  on cristobalite and mullite formations in the Al oxide –kaolinite and Al oxide –illite ceramic bodies European Clay Conference Euroclay-2011 26-June 01 July 2011 Antalya /Turkey

4-Aras, İ, A., K, Ca-Na feldspar, firing schedule and mixing type effects on cristobalite formation in kaolinitic and illitic clays from the Westerwald Mid European Clay Conference 16-19 September 2014 Dresden Germany



## Recycling of Rare Earth Elements from electronic wastes by selective adsorption and desorption on industrial clay minerals

Stefan Ginzel<sup>1</sup>, Ralf Diedel<sup>1</sup>, Michael Kunze<sup>2</sup>, Rita Knodt<sup>1</sup>, Caroline Volk<sup>1</sup>, Joachim Scholz<sup>2</sup>, Tobias Johann<sup>2</sup> and Florian Geiger<sup>2</sup>

<sup>1</sup> FGK Höhr-Grenzhausen, Research Institute of inorganic materials - Glass and Ceramic, 56203 Höhr-Grenzhausen, Germany, Stefan.Ginzel@fgk-keramik.de

<sup>2</sup> Department of inorganic Chemistry, Institute of Science, University Koblenz – Landau, 56070 Koblenz, Germany

The development and production of new climate- and environmentally friendly so called “green technologies” depend heavily on *REE* supply from China. The worldwide demand for *REE* is constantly increasing leading to higher prices and resource exploration projects. At the same time many authors and institutions describe the supply situation as critical. In contrast <1% of the *REE* are recycled from end-of-life products. The conventional *REE* recycling approaches need a high input of chemicals and energy and focus on materials with high *REE* concentrations like Nd-magnets and *REE*-bearing batteries. In order to extend the recycling spectrum of *REE* containing products, especially for materials with low concentrations, adsorption and desorption processes of  $\text{Ln}^{3+}$  on clay minerals were tested. The principle is given by a naturally occurring *REE* deposit type in southern China. The deeply weathered lateritic *REE* ion-adsorption clay deposits provide a significant amount of the *HREE* production. *REE* remain in the lateritic horizons while other elements are leached and washed out by weathering fluids. Most of the *REE* are adsorbed by the residual clay fraction.

The naturally occurring cation exchange capacity (CEC) and negative surface charge of clay minerals were used as an example to recover free  $\text{Ln}^{3+}$  from standardized solutions. The adsorption of  $\text{Ln}^{3+}$  on industrial clays was investigated by bringing a known amount of  $\text{Ln}^{3+}$  in acid standard solutions with suspended clay. Due to the adsorption of the  $\text{Ln}^{3+}$  on dispersed clay particles, their concentration in the solution decreases after 2 hours at experimental determined pH-values. It was also recognized that trivalent ions like  $\text{Fe}^{3+}$  and  $\text{Al}^{3+}$  in the solution constrain the adsorption of  $\text{Ln}^{3+}$ . At a later stage the selective desorption of  $\text{Ln}^{3+}$  can be controlled by the pH-value.

Typical electronic waste was also brought to solution, their  $\text{Ln}^{3+}$  concentration was measured and the clay adsorption effect was tested. Different clay minerals were characterized and their chemical and mineralogical composition where analyzed. The specific surface area and CEC were measured before and after acid bleaching of selected clays. The result was a shortened screening method for the applied adsorption on raw material. In addition, different solvents were tested to leach the metals out of electronic wastes, to reduce the environmental impact of solvent use.

Due to the rising *REE* recycling potential, because of the accumulation of electronic equipment, batteries and installed wind turbines, there is a need to develop new methods that have the potential to be integrated in existing recycling flows. The approach provides a new potential recycling method and a further application of industrial clay minerals. The method also might be a *REE* recycling opportunity for materials with lower concentrations as in typical electronic waste or slags.

Thursday  
9<sup>th</sup> July

Lecture room 3

Bentonites: linking clay  
science with technology

## Boron content and boron isotope composition of Na, Ca and Mg bentonites

Mathias H. Köster<sup>1</sup>, Lynda B. Williams<sup>2</sup>, Petra Kudejova<sup>3</sup>, Reiner Dohrmann<sup>4</sup> and H. Albert Gilg<sup>1</sup>

<sup>1</sup>Lehrstuhl für Ingenieurgeologie, Technische Universität München, Arcisstr. 21, D-80333 Munich, Germany.

mathias.koester@tum.de

<sup>2</sup>School of Earth and Space Exploration, Arizona State University, Tempe, United States of America

Heinz Maier-Leibnitz Zentrum, Technische Universität München, Garching, Germany

<sup>4</sup>Bundesanstalt für Geowissenschaften und Rohstoffe, Landesamt für Bergbau, Energie und Geologie, Hannover, Germany

The natural interlayer cation composition of smectites allows a classification of economic bentonites into fully expandable and often more valuable Na bentonites and the more common Ca or Mg bentonites that require Na activation for use in specific applications. The origin of natural Na bentonites has often been attributed to formation by interaction of seawater with volcanic protoliths. However, their genesis remains enigmatic, as conflicting stable H-O-isotope evidence exists regarding the fluids involved in the formation of Na bentonites of Wyoming and Montana. Some Ca and Mg bentonites probably formed in marine settings, and post-formational cation exchange cannot be excluded.

We, therefore, applied a new approach using the trace element boron(B) located in the tetrahedral site of smectite substituting for silicon. The structural B was removed using mannitol washing and cation exchange. Boron is considered an excellent tool to trace paleosalinity and/or fluid origin related to clay mineral formation, but has not yet been systematically applied to bentonites. We studied the concentration and isotope composition of B in 18 smectite separates (<0.2  $\mu\text{m}$  fractions) from a variety of bentonite deposits in marine and terrestrial settings using prompt gamma neutron activation analysis (PGAA) and secondary ion mass spectrometry (SIMS). Additionally, we measured the stable C and O isotope compositions of carbonates present in the coarser fraction of some samples.

Smectites from Ca and Mg bentonites have low B concentrations of up to a few tens of ppm, with the lowest value in a lateritic bentonite formed from Precambrian gneisses in Bahia, Brazil. Smectites from Na bentonites have higher B contents with values in the low hundred ppm range indicating their formation in B containing salt-rich fluids. In the majority of samples, neither the removal of ancillary Feoxides using the acid ammonium oxalate method nor cation exchange with ammonium acetate had notable influence on B contents. Smectites show a wide range of  $\delta^{11}\text{B}$  values relative to NBS SRM 951 with values ranging from -22.0 to +27.2 ‰. The bentonites formed in a purely terrestrial environment exhibited negative  $\delta^{11}\text{B}$  values. In contrast, Na bentonites from marine depositional settings revealed highly variable B and C and O isotope values similar to associated carbonates. Our results indicate that both marine and non-marine B-rich fluids are involved in the formation of natural Na bentonites.

## Mineralogy and geochemistry of bentonites from the western Thrace and the islands of Samos, Chios, Lesvos, and Limnos, East Aegean Greece

George E. Christidis<sup>1</sup>, Eleni Koutsopoulou<sup>2</sup> and Ioannis Marantos<sup>2</sup>

<sup>1</sup>Technical University of Crete, School of Mineral Resources Engineering Chania, 73100, Greece  
christid@mred.tuc.gr

<sup>2</sup>Institute of Geological and Mineral Exploration (IGME), Spyrou Loui 1, 13677 Acharnes, Greece

Greece is the second largest bentonite producer in the world with Milos Island being one of the largest mining bentonite centers worldwide. Bentonite was also mined periodically until recently in Kimolos Island. In addition to these well-known deposits, bentonites also exist in the islands of Chios, Samos, Lesvos, Limnos and Chios Eastern Aegean and in some areas of Thrace in the mainland NE Greece. These bentonites are associated with volcanic activity and their age ranges from Lower Oligocene in Thrace, to Lower-Middle Miocene in Lesvos, Limnos and Chios and finally to Upper Miocene in Samos. Although some of these materials have been utilized since the ancient times (e.g. the Lemnian Earth), but these bentonites have been mined only at a local scale. Also, with one exception (Christidis et al. 1999) there is not published information available on the bentonites. The aim of the present study was to evaluate the mineralogical and geochemical characteristics of these bentonites.

The Samos bentonites crop out in the SE margin of the Karlovasi Basin formed at the expense of acidic pyroclastic flows mainly in subaerial-lacustrine environment. They consist mainly of Ca-rich dioctahedral smectite, opal-CT and sanidine with minor quartz and locally mordenite. These bentonites are medium-low grade with smectite content 30-60%, that is similar to the bentonites from Komia area, Milos (Christidis et al., 1995). The Chios bentonites have formed at the expense of trachyandesitic tuffs in a lacustrine environment, they crop out in the Neogene Basin at the SE part of the island. Mineralogy of these bentonites consists mainly of Ca-rich dioctahedral smectite and opal-CT, with minor amounts of plagioclase chlorite, plagioclase and carbonates (dolomite, calcite, aragonite) and traces of talc and serpentine. The smectite content is 50-80%, but the materials have inferior foundry, rheological and swelling properties. Nevertheless after acid activation, smectite acquires very good bleaching properties.

The Lesvos bentonites have formed at the expense of acidic-intermediate pyroclastic rocks. The bentonites consists of Ca-rich dioctahedral smectite, with minor quartz, opal-CT, plagioclase and K-feldspar and in places illite. The Limnos bentonites consist of Ca-rich dioctahedral smectite and quartz as major phases, and minor intermediate-basic plagioclase, chlorite, illite and in places calcite. In general, the calcite-rich bentonites are poorer in smectite with few exceptions to this trend. They are low-medium grade materials with 30-60% smectite. Finally in Thrace, there are several basins of Lower Oligocene age in which pyroclastic flows, tuffs and lavas of acidic-intermediate composition were altered to zeolites and bentonites. The most significant bentonite beds occur in the area of Pefkos in which pyroclastic rocks of intermediate composition were altered to Ca-rich and in places Na-rich dioctahedral smectite with minor opal-CT, mordenite, quartz, plagioclase and in places illite. The materials are medium-high grade, with smectite content locally exceeding 85%.

In conclusion, the bentonites of Eastern and NE Greece are associated with alteration of acidic-intermediate pyroclastic rocks, mainly pyroclastic flows. Although most of them are of low-medium quality, the bentonites from Thrace and Chios Island are promising for further exploration.

Christidis, G., Scott, P. W., Markopoulos, Th., (1995). Origin of the Bentonite Deposits of Eastern Milos, Aegean, Greece: Geological, Mineralogical and Geochemical Evidence. *Clays and Clay Minerals*, 43, 63-77.

Christidis G.E., Markopoulos Th., Foscolos A., (1999). Origin, and Physical Properties of a Bentonite Deposit of Chios Island, Eastern Aegean, Greece. Proceedings of the 11<sup>th</sup> International Clay Conference Ottawa, Canada, 75-82.

The study is based on the results of the research project: "Evaluation of Industrial Minerals for production of nanocomposites for new industrial applications" part of the Project "EXPLORATION AND EVALUATION OF SELECTED INDIGENOUS NON-ENERGY MINERAL RAW MATERIALS AIMING AT SUSTAINABLE OPERATION OF THE EXTRACTIVE INDUSTRY" funded by the NATIONAL STRATEGIC REFERENCE FRAMEWORK ESPA 2007-2013.

## Explosive volcanic eruptions in the Upper Ordovician of the Siberian Platform

W.D. Huff<sup>1</sup>, A.V. Dronov<sup>2</sup>, B. Sell<sup>3</sup>, A.V. Kanygin<sup>4</sup>, & T.V. Gonta<sup>4</sup>

<sup>1</sup>Department of Geology, University of Cincinnati, OH 45221-0013, USA. e-mail: huffwd@ucmail.uc.edu

<sup>2</sup>Geological Institute, Russian Academy of Sciences. Pyzhevsky per.7, 119017, Moscow, Russia. e-mail: dronov@ginras.ru

<sup>3</sup> Earth and Environmental Sciences, University of Michigan, Ann Arbor, Michigan 48109, USA, e-mail: bksell@umich.edu

<sup>4</sup>Trofimuk Institute of Petroleum Geology and Geophysics, Siberian Branch of Russian Academy of Sciences. Acad. Koptyug 3, 630090, Novosibirsk, Russia. e-mail: kanyginav@ipgg.sbras.ru

Eight K-bentonite beds have been discovered in the Upper Ordovician of the Tungus basin on the Siberian Platform. All the beds were identified in the outcrops of the Baksian, Dolborian and Burian regional stages, which correspond roughly to the Upper Sandbian, Katian and probably lowermost Hirnantian Global Stages. The 4 lower most beds are represented by thin beds (1-2 cm) of soapy light gray or yellowish plastic clays and usually easily identifiable in the outcrops. The beds were traced in the outcrops over a distance of more than 60 km along the Podkamennaya Tunguska River valley. Modeling of the XRD tracings showed the samples consist of R3 ordered illite-smectite with 80% illite and 20% smectite plus a small amount of corrensite, which is a regularly interstratified chlorite-smectite. The K-bentonites provide evidence of intensive explosive volcanism on or near the western margin of the Siberian craton in Late Ordovician time.

The K-bentonite beds from the Baksian and Dolborian regional stages (Katian) of the southwestern part of the Tungus basin in Siberia are thus derived from the alteration of volcanic ash falls. All four beds contain volcanogenic euhedral zircon and apatite phenocrysts. Zircon crystals from the uppermost K-bentonite bed within the Baksian regional stage provide a  $^{206}\text{Pb}/^{238}\text{U}$  age of  $450.58 \pm 0.27$  Ma. The timing of volcanism is surprisingly close to the period of volcanic activity of the Taconic arc near the eastern margin of Laurentia and it appears that the Taconic arc has its continuation along the western continental margin of Siberia. This contradicts popular palaeogeographic interpretations and points to the position of a subduction zone along the western but not the eastern margin of the Siberian palaeocontinent at this time.

## Bentonite composition and stratigraphy at Mawrth Vallis, Mars

Janice L. Bishop<sup>1,2</sup> and Christoph Gross<sup>2</sup>

<sup>1</sup>SETI Institute, 189 Bernardo Ave., Mountain View, CA 94043, USA (JBISHOP@SETI.ORG)

<sup>2</sup>Institute of Geological Sciences, Freie Universität Berlin, Berlin, Germany

Fe- and Mg-rich smectites are the most prevalent phyllosilicates on the surface of Mars (Murchie et al. 2009) and a region called Mawrth Vallis contains one of the richest phyllosilicate-bearing outcrops (Bishop et al., 2008). This study investigated the composition and stratigraphy of these Fe/Mg-smectites and their accompanying clay units at this site on Mars. Recent studies have documented the presence of allophane and poorly ordered aluminosilicates at the upper stratigraphy of the clay deposits at Mawrth Vallis (Bishop et al., 2014) and acid alteration of smectites at an intermediate stratigraphy (Bishop et al., 2015). We are building on these results to map the stratigraphy of multiple clay units at Mawrth Vallis and investigate changes in the geochemical environment. We observe Fe- and Mg-rich smectites in the lower clay unit, covered by chlorite, then acid-treated smectites and sulfates, followed by montmorillonite and opal, with allophane and related materials at the top of the clay profile. These clay minerals were identified by the OH spectral features near 2.15-2.45  $\mu\text{m}$ , a bound  $\text{H}_2\text{O}$  band near 1.9  $\mu\text{m}$  and a broad  $\text{Fe}^{2+}$  feature from 1.2-1.8  $\mu\text{m}$ . Changes in clay chemistry and composition can be observed through orbital spectral imagery of Mars at scales of 100 m or less. The variations in bentonite composition detected through the clay profile are consistent with neutral or mildly basic conditions in the ancient Fe/Mg-smectites-bearing rocks, followed by strongly acidic conditions to form sulfates and acid-treated smectites, then mildly acidic conditions to form Al-rich phyllosilicates and opal, and a well-drained environment at the top of the clay profile where the allophane and poorly crystalline aluminosilicates are most prevalent.

Our analyses involve coordinating composition and stratigraphy through the use of orbital instruments at Mars. The Compact Reconnaissance Imaging Spectrometer for Mars (CRISM) imager on board NASA's MRO orbiter provides hyperspectral visible/near-infrared data that enables documentation of specific types of clay minerals on Mars at a resolution of 18 m/pixel (1). The High Resolution Stereo Camera (HRSC) on board the European Mars Express orbiter allows for 3D views of the surface at a resolution of  $\sim 12$  m/pixel (Neukum et al., 2004).

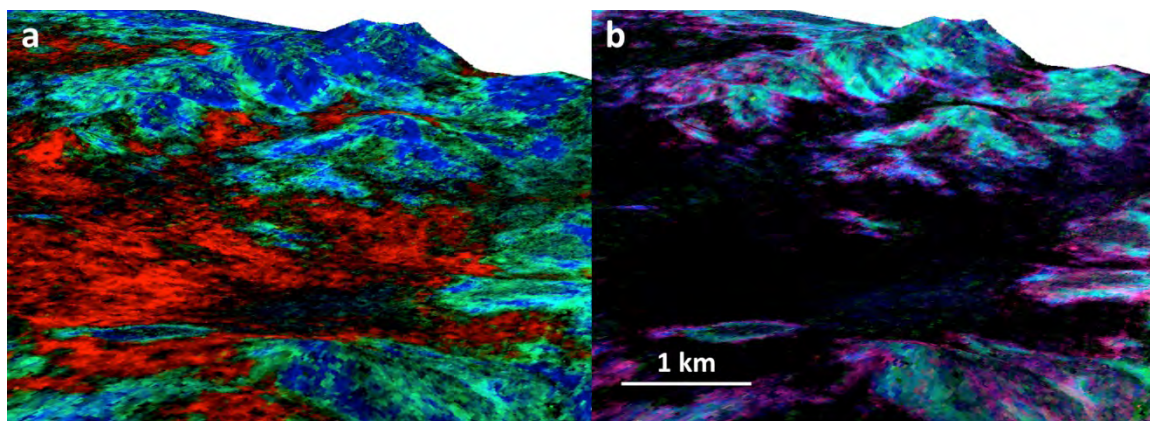


Figure 1. Map of bentonite units in a region of Mawrth Vallis Mars illustrating variable clay stratigraphy in CRISM image FRT0000AA7D. The clay units are mapped as Fe/Mg-smectite in red, acid alteration products in green, and Al-phyllosilicates, opal and allophane in blue on the left (a) and as acid alteration products in pink, Al-phyllosilicates and opal in blue, and allophane and poorly crystalline aluminosilicates in green on the right (b).

Murchie, S.L., et al. (2009) A synthesis of Martian aqueous mineralogy after 1 Mars year of observations from the Mars Reconnaissance Orbiter. *Journal of Geophysical Research* 114, doi:10.1029/2009JE003342.

Bishop, J.L. et al. (2008) Phyllosilicate diversity and past aqueous activity revealed at Mawrth Vallis, Mars. *Science*, 321, 830-833.

Bishop, J.L. and Rampe, E.B. (2014) The presence of nanophase Al-Si-Fe components at Mawrth Vallis indicate varying environmental conditions. *8th Intl. Conf. Mars*, abs. #1265.

Bishop, J.L. Gross C., Wray J.J., Horgan B., Viviano-Beck C.E., and Seelos F.P. (2015) Acid-alteration at Mawrth Vallis between the older Fe/Mg-rich clays and the younger Al/Si-rich clays. *LPSC*, abs. #1455.

Neukum, G. et al. (2004) Recent and episodic volcanic and glacial activity on Mars revealed by the High Resolution Stereo Camera. *Nature*, 432, 971-979.

## Geochemical properties and geologic significance of Devonian K-bentonites from northwestern Turkey

Asuman Günel Türkmenoğlu<sup>1</sup>, Ömer Bozkaya<sup>2</sup>, Mehmet Cemal Göncüoğlu<sup>1</sup>, Özge Ünlüce<sup>1</sup>, İsmail Ömer Yılmaz<sup>1</sup> and Cengiz Okuyucu<sup>3</sup>

<sup>1</sup>Middle East Technical University, Department of Geological Engineering, 06800 Çankaya-Ankara/TURKEY  
asumant@metu.edu.tr

<sup>2</sup>Pamukkale University, Department of Geological Engineering, Gümüşler Kampusu 114 Denizli/TURKEY

<sup>3</sup>Selçuk University, Department of Geological Engineering, 42030 Karatay-Konya/TURKEY

Two sets of thin K-bentonite beds occur in the Middle Devonian-Lower Carboniferous age Yılanlı Formation exposed at two different areas, namely Bartın and Şapcı areas, in the Western Black Sea region of Turkey. They belong to stratigraphically different levels of the Formation and are suggested to correlate with Kellwasser Event at the Frasnian-Famennian Boundry and the Hangenberg Events at the close of the Devonian.

Major, trace and REE geochemical parameters of the K-bentonite samples distinguish two different precursor ash compositions for the stratigraphically different K-bentonite zones. The lower Kellwasser zone is the product of an alkali-basaltic eruption whereas the upper Hangenberg Event related zone was originated from a trachytic volcanism. The geochemical fingerprints indicate backarc extensional basin and within plate-alkaline continental rift types of tectono-magmatic settings for these volcanic eruptions, respectively. These two compositionally different precursor ashes evolved through diagenesis and illitization processes into geologically significant K-bentonites of regional significance.

The worldwide correlation of the studied K-bentonite zones is not yet recognized. However, the lower zone may be the coeval occurrences of the Late Devonian K-bentonites from southern Urals and rift related alkali basalts within the Donbas basin on the East margin of the East European Craton as suggested recently by Türkmenoğlu et. al. (2015). On the other hand, the K-bentonites from the upper zone are thought to be the products of volcanic eruptions having yet unknown source and distance during the close of Devonian.

This research is supported by TÜBİTAK Project No.110Y272.

Türkmenoğlu, A.G., Bozkaya, Ö., Göncüoğlu, M.C., Ünlüce, Ö., Yılmaz, İ.Ö., Okuyucu, C. (2015). Clay Mineralogy Chemistry and Diagenesis of Late Devonian K-Bentonite Occurrences in Northwestern Turkey, *Turkish Journal of Earth Sciences*, in Press.

## A metamorphic geologist's perspective on clays: from protoliths with potential to essential components of nuclear waste disposal systems

Simon Harley

The University of Edinburgh, Grant Institute of GeoSciences, James Hutton Road, Edinburgh EH9 3FE  
(Simon.Harley@ed.ac.uk)

As a metamorphic petrologist working on high- and ultrahigh-temperature rocks, in much of my previous research I have considered claystones and bentonites only from the perspective of their importance as distinctive protoliths giving rise to excellent metamorphic schists and gneisses. Indeed, the high-T metamorphism of claystones produces a variety of spectacular aluminous mineral assemblages involving combinations of cordierite, sillimanite, sapphirine, spinel, osumilite, feldspars and corundum that can be of great use in constraining metamorphic conditions. Some remarkable examples of such 'schist from clay' will be illustrated in the first part of this presentation.

A recent research focus, complementary to that on granulites and UHT metamorphic rocks, has been on developing mineralogical methods for remotely and passively monitoring the evolution of the bentonite-based Engineered Barrier System (EBS) typical of a number of geological disposal concepts for the management of nuclear waste. In particular, the reaction and corrosion of NEO-magnets ( $\text{Nd}_2\text{Fe}_{14}\text{B}$ ) in response to groundwater chemistry within a bentonite-buffered EBS system has been investigated experimentally (at 70-100°C) in order to determine how time-resolved variation in magnetic properties can be used to monitor the system. In a series of batch experiments sealed inert containers have been loaded with grains of selected magnetic materials along with known quantities of fluids with defined initial compositions (neutral, elevated pH, low- or higher-salinity, oxidizing) either with bentonite or without bentonite. These single-step sealed experiments are then run in an oven for several months and observed at various times throughout the experiment.

In the presence of bentonite under saline, alkaline and oxidising conditions the corrosion and alteration of NEO-magnets is intense, with the magnets disaggregating and hence decreasing in their overall magnetic moment. The reaction is characterised by the precipitation of oxyhydroxides and hydroxides [ $\text{Nd}(\text{OH})_3$ ] onto clay surfaces. Fe is incorporated into the octahedral site of the bentonite, leading to its nontronitization or vermiculitization, which fortunately does not have an influence on the overall swelling behaviour of the clay matrix. NEO-magnets reacted in water only show much less intense alteration, indicated by the presence of oxidation rims and precipitates of black oxy-hydroxides at the magnet/water interface.

Bentonite is demonstrated under these static experimental conditions to have a dramatic effect on NEO-magnet corrosion in the presence of saline waters. The presence of bentonite facilitates the development of two electrical double layers with opposite polarity (one generated by the clay and the other by the corrosion on the magnet surface), which causes enhanced corrosion of the magnets compared with the corrosion of the magnets in water alone. Thus, NEO-magnets embedded systematically in bentonite buffer material in the EBS of a geological disposal facility (GDF) for high level waste are likely to show pronounced changes in their magnetic moment /intensity as the GDF re-saturates and then evolves in the presence of saline groundwaters. It is proposed that these changes could be used to monitor GDF re-saturation and bentonite buffering over significant timescales.



## Chemical alteration of bentonite in a radioactive waste repository – illitization of montmorillonite in 70°C by high pH solution

Satoru Miyoshi<sup>1</sup>, Yukinobu Kimura<sup>1</sup>, Masahito Shibata<sup>2</sup>, Takashi Sanbuichi<sup>3</sup> and Tsutomu Sato<sup>3</sup>

<sup>1</sup>Obayashi Corp., Shimo-kiyoto 4-640, Kiyose-shi, Tokyo 204-8558, Japan miyoshi.satoru@obayashi.co.jp

<sup>2</sup>Taiheiyo Consultant, Daisaku 2-4-2, Sakura-shi, Chiba 285-8655, Japan

<sup>3</sup>Hokkaido University, Kita 13jo Nishi 8chome, Kita-ku, Sapporo-shi, Hokkaido 060-8628, Japan

In geological repositories of radioactive waste, bentonite buffer is planned to be used as one of the multiple-layered barriers. In some concepts, the layer of bentonite-containing material is placed next to the layer of cementitious material such as ordinary portland cement (OPC). There is the scenario for the performance assessment of repositories that the ability of bentonite to delay the transport of nuclides could decrease by the chemical effects of the alkaline solution leached out from the cementitious materials. In the case that OPC is used, the leachate solution in the first stage contains  $K^+$  and  $Na^+$  ions as well as  $Ca^{2+}$  ions and its pH is greater than 13. There are three major effects of the alkaline solution on bentonite: the exchange of the inter-layer cation, the dissolution of mineral crystals, and the precipitation of secondary minerals.

In the present study, the effects of potassium hydroxide on the compacted bentonite, Kunigel V1 (Kunimine Corp.) from Japan was tested. Kunigel V1 is composed mainly of sodium montmorillonite and silica minerals. First Kunigel V1 was treated with potassium chloride solution to exchange the interlayer cations with  $K^+$  ions. The  $K^+$  saturated Kunigel V1 was compacted in the three column-type cells with diameter and thickness of 60 mm and 5 mm, respectively. The dry density was  $1.6 \text{ g/cm}^3$ . Three different solutions were injected to the cells: deionized water for Case 1, and 0.3 and 1.0 M potassium hydroxide solutions for Case 2 and Case 3, respectively. The experimental temperature was maintained at  $70 \pm 0.2^\circ\text{C}$ .

The change of hydraulic conductivity is shown in Fig. 1. While the hydraulic conductivity in Case1 remained constant, in Case 3 the value suddenly increased around  $1,000 \text{ cm}^3$ . After injection, the materials were analyzed using EPMA, AFM, XRD, and MIT. The charts of oriented XRD of the materials treated with ethylene glycol for Case2 and Case3 show the feature of I/S mixed layers (Fig. 2).

We conclude illitization of montmorillonite in compacted bentonite at pH 13.5-14.0 and  $70^\circ\text{C}$ . Illitization of montmorillonite in compacted bentonite caused an increase in its permeability.

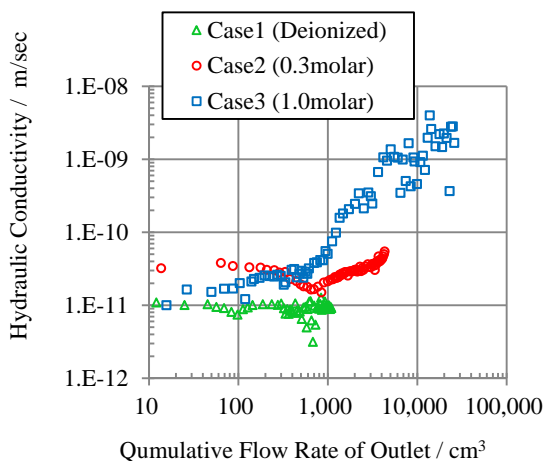


Fig. 1 Change of hydraulic conductivity

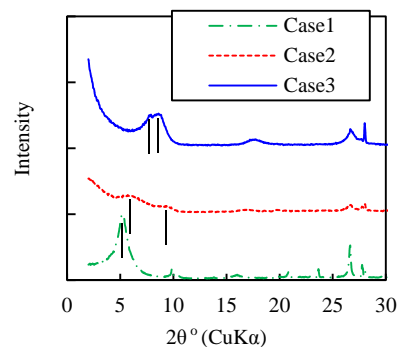


Fig. 2 Charts of Oriented XRD

## Effects of temperature, pressure, and brine composition on the interlayer spacing of montmorillonite at *in situ* conditions using CO<sub>2</sub>

Jacqueline Kowalik, Stephen Guggenheim, and A.F. Koster van Groos

Department of Earth and Environmental Sciences, University of Illinois at Chicago, 845 W. Taylor St., Chicago, Illinois 60607, U.S.A.; e-mail: xtal@uic.edu

A high-pressure environmental chamber (HPEC) was used to study the effect of temperature ( $T$ ), pressure ( $P$ ), and NaCl brines on the  $d(001)$  values of Na-rich montmorillonite clay (Clay Minerals Society Source Clay SWy-2). In the HPEC, the brine and the sample in suspension were pressurized using either CO<sub>2</sub> or He to 500 bars and examined by X-ray diffraction at  $T$  to 150° C. The clay particles were allowed to move freely within the liquid, establishing steady state conditions during the illumination by the Mo ( $\lambda = 0.7107 \text{ \AA}$ ) X-ray beam.

At  $P(\text{CO}_2) = 0$  bar and  $T = \sim 30^\circ \text{ C}$ , a change in brine composition from 0.17 M to 5.99 M resulted in  $d(001)$  values decreasing from 20.44 Å to 15.67 Å (25%). Increasing  $P(\text{CO}_2)$  from 0 to 500 b at  $T = \sim 30^\circ \text{ C}$  resulted in a decrease in  $d(001)$  values, with pressure having greater effects on lower salinity brines. With increasing pressure to  $P(\text{CO}_2) = 500$  b at  $T = \sim 30^\circ \text{ C}$ ,  $d(001)$  values of the clay in 0.68 M brine decreased from 19.71 Å to 18.96 Å (4%), whereas  $d(001)$  values of the 5.99 M brine declined from 15.67 Å to 15.50 Å (1%). Increasing  $T$  from  $\sim 30$  to 150° C at  $P(\text{CO}_2) = 500$  b resulted in a decrease in  $d(001)$  values with temperature having greater effects on lower salinity brines. With increasing  $T$  from  $\sim 30$  to 150° C at  $P(\text{CO}_2) = 500$  b,  $d(001)$  values of montmorillonite in 0.17 M brine decreased from 19.56 Å to 18.97 Å (3%), whereas  $d(001)$  values of clay in 5.99 M brine decreased from 15.71 Å to 15.52 Å (1%). The greatest decrease in  $d(001)$  values with increasing  $T$  at  $P(\text{CO}_2) = 500$  b occurred for brine compositions of 1.37 M and 1.71 M. For the  $T$  interval from  $T = 100$  to 150° C,  $d(001)$  values declined from 18.89 Å to 17.26 Å (9%) for the clay in the brine of 1.37 M NaCl brine. In a 1.71 M NaCl brine and with an increase from  $T = 50$  to 150° C,  $d(001)$  values declined by 16% (18.58 to 15.70 Å). Results with He were identical, within error, to the CO<sub>2</sub> results.

The results extend our knowledge of interlayer spacings as a function of  $T$ ,  $P$ , and brine compositions under *in situ* conditions. In previous work, it was found that less than fully hydrated cation-exchanged montmorillonite clay exposed to super critical CO<sub>2</sub> (scCO<sub>2</sub>) at  $P$  of 50 to 640 bars and  $T$  to 50° C may result in expansion of the interlayer owing to the intercalation of the CO<sub>2</sub> into the interlayer. The results of the present study are consistent with the earlier work in that the lack of expansion in the  $d(001)$  values in the present work can be attributed to the fully hydrated state of the clay at the time of exposure to scCO<sub>2</sub>.

## X-ray tomographic method for measuring 3D deformation and water content in swelling clays

Tero Harjupatana<sup>1</sup>, Jarno Alaraudanjoki<sup>1</sup> and Markku Kataja<sup>1</sup>

<sup>1</sup>Department of Physics, University of Jyväskylä, Finland.

Email: tero.t.harjupatana@jyu.fi

A non-invasive method for measuring the three-dimensional displacement field and water content distribution in a wetting and swelling clay using X-ray tomographic (CT) imaging is introduced. The method is based on comparison of X-ray tomographic images of the clay sample in the reference state and in the wetted and deformed state. Deformation field can be measured for clays that contain sufficient amount of details visible in tomographic images so as to allow tracking by a 3D image correlation algorithm. The water content distribution can be determined from the difference tomographic image between the wetted state and the reference state. The results of deformation analysis and of water content analysis based on the CT-method were compared with those from numerical solution for an axially compressed cylindrical rubber sample, and from gravimetric measurements of sliced samples, respectively. In both cases, the results given by the CT-method are in close agreement with those obtained by the reference methods.

The method has been applied here for monitoring the evolution of 3D deformation and water content distributions in cylindrical bentonite samples wetted in a constant volume (4D study). The measurements were carried out using a high-resolution microtomographic device (SkyScan 1172) and image voxel size 24  $\mu\text{m}$ . The results can be utilized in developing and validating hydromechanical material models for bentonite clay, planned to be used as buffer material in nuclear waste deposition sites.

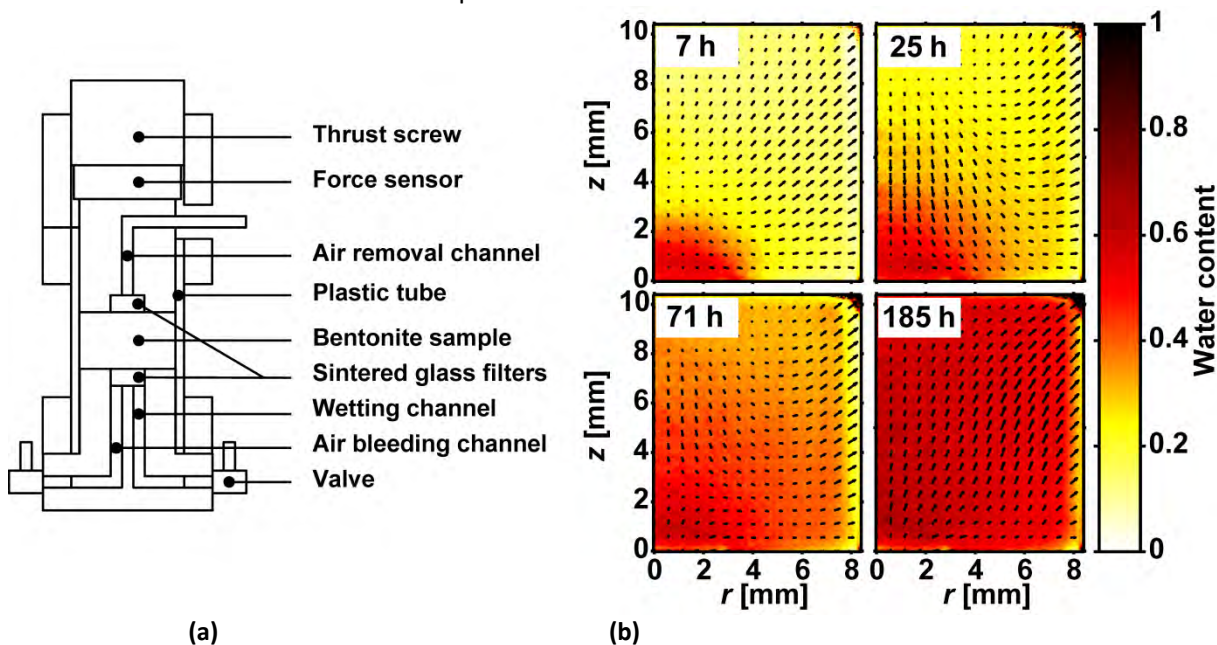


Figure 1: Schematic cross-section image of the sample holder used in bentonite clay measurements (a). Measured displacement field (scaled by factor 5) and water content distribution in a cylindrical bentonite sample at various times of wetting, and averaged over azimuthal angle (b).

## About the N<sub>2</sub>-BET-specific surface area of bentonites

S. Kaufhold and R. Dohrmann

The total surface area of bentonites may reach 800 m<sup>2</sup>/g and mainly depends on the smectite content, because most of the surface area results from the interlayer of the swelling clay minerals. For all processes taking place at the outer surfaces, the outer surface may be even more important despite being much smaller than the inner surface area. The outer surface area is commonly measured by nitrogen gas adsorption using the BET-equation ( $SSA_{N_2BET}$ , Brunauer et al., 1938). The comparison of the  $SSA_{N_2BET}$  of 36 different bentonites from all over the world showed that Ca/Mg-bentonites have larger values compared with Na-bentonites. In a suspension state Na-smectites tend to delaminate and thus the outer surface area of Na-bentonites is much larger compared with Ca-bentonites.  $SSA_{N_2BET}$  is measured in a dry state, Ca/Mg-bentonites show larger values than Na-bentonites. The study was conducted to explain this difference (Kaufhold et al., 2010). Valuable information was gained from measuring the  $SSA_{N_2BET}$  of the same bentonites after Cu-trien exchange which hydrophobizes the interlayer and fixes the interlayer distance to about 13 Å (Kaufhold et al., 2011). After Cu-trien exchange, larger  $SSA_{N_2BET}$  values were found for low charged smectites compared with high charged ones. This result could be explained by the larger space between the Cu-trien molecules in the interlayer of low charged smectites and the fact that the interlayer does not collapse upon dehydration. This result suggests that a similar mechanism may explain the different  $SSA_{N_2BET}$  values of Ca/Mg- and Na-bentonites. Complete dehydration followed by interlayer collapse of Ca/Mg-bentonites is more difficult to achieve compared with Na-bentonites. In addition, Ca/Mg-bentonites only contain 50 % of the number of interlayer cations compared with Na-bentonites hence leaving more space between the charges/cations. The difference of the  $SSA_{N_2BET}$  values of Ca/Mg-bentonites and Na-bentonite, therefore, can probably be explained by the different accessibility of the outer part of the interlayer resulting in different microporosity which in turn is known to affect the  $SSA_{N_2BET}$ .

Brunauer, S., Emmett, P. H., Teller, E. (1938) Adsorption of Gases in Multimolecular Layers. - *Journal of the American Chemical Society*, 60, 309. doi:10.1021/ja01269a023

Kaufhold, S., Dohrmann, R., Klinkenberg, M., Siegesmund, S., Ufer, K. (2010) N<sub>2</sub>-BET specific surface area of bentonites. *Journal of Colloid and Interface Science*, 349, 275–282.

Kaufhold, S., Dohrmann, R., Ufer, K., Kleeberg, R., Stanjek, H. (2011) Cu trien exchange to improve the analytical understanding of smectites. – *Clay Minerals*, 46, 411 – 420.

## Peculiarities of Cs adsorption on natural and acid modified montmorillonite

V. Krupskaya<sup>1,2</sup>, S. Zakusin<sup>1,2</sup>, E. Tyupina<sup>3</sup>, O. Dorzhieva<sup>1,4</sup> and M. Chernov<sup>2</sup>

1 Institute of Ore Deposits, Mineralogy, Petrography and Geochemistry, Russian Academy of Science (IGEM RAS), Russia, 119017, Moscow, Staromonetny per., 35, krupskaya@ruclay.com

2 Lomonosov Moscow State University, Moscow

3 D. Mendeleev University of Chemical Technology of Russia, Moscow

4 Geological Institute, Russian Academy of Sciences, Moscow

Montmorillonite is the main component of bentonite clays, which have a number of useful properties such as high adsorption capacity and low permeability. Bentonites are used in various sectors of the economy, including the removing radioactive waste contaminants from lubricating oil and as engineered barriers in the disposal of high level radioactive waste. Acid modified bentonite is preferably used for the removing radioactive waste contaminants from lubricating oil. Modification increases specific surface area, micro- and meso-pores volume and the number of micropores. Engineered barriers can be affected by radioactive solutions due to leaking of nuclear waste storage canisters in the case of contact with pore water and obviously the buffer must maintain the stability of its properties for many hundreds and thousands of years.

Samples for this study were collected from several Russian deposits with a minimum montmorillonite content of 70-80%. Raw and modified samples were studied with X-ray diffraction, infrared spectroscopy, scanning electron microscopy. Acid modification was performed by treating with 10 M HNO<sub>3</sub> at 90°C for different duration. Saturation of raw and acid modified montmorillonites with Cs<sup>+</sup> was carried out by treatment with a CsNO<sub>3</sub> solution, at a set of Cs<sup>+</sup> concentrations to obtain a full isotherm. The differences in adsorption capacities between natural, acid-modified and Cs-forms were revealed by comparing the results of cation exchange capacity determination, Cs<sup>+</sup> adsorption capacity (including the total capacity determination using Cs-137 radiolabel), specific surface area, textural characteristics. Acid treatment causes modification of the structure. Octahedral cations removal and partial protonation of the interlayer space resulted in the formation of micro- and meso-porous structure with an increase of the adsorption capacity. A certain degree of modification was achieved after 0.5-1 hour of treatment in montmorillonite of different bentonites. After 5 hours of treatment, the structural changes of montmorillonite became significant (Fig.1a). Molecular dynamics simulation showed that Cs<sup>+</sup> in the interlayer space was coordinated to Al that substitutes Si in the tetrahedral sheet. However, more preferable position for Cs<sup>+</sup> was in holes in tetrahedral rings. Changes of interlayer occupation, its protonation and / or substitution with Cs<sup>+</sup>, a decrease of octahedral sites occupation results in changes in charge redistribution between the edges and basal surfaces. The interaction between the particles and changes in this interaction with the modification of the montmorillonite structure can be observed in details with electron microscopy of freeze-dried suspensions (Fig. 1b,c).

Structural and textural properties, and Cs<sup>+</sup> adsorption behaviour of montmorillonites change after acid treatment of bentonites. The results from this study can be used in modeling of buffer stability of bentonites in the disposal of high level radioactive waste.

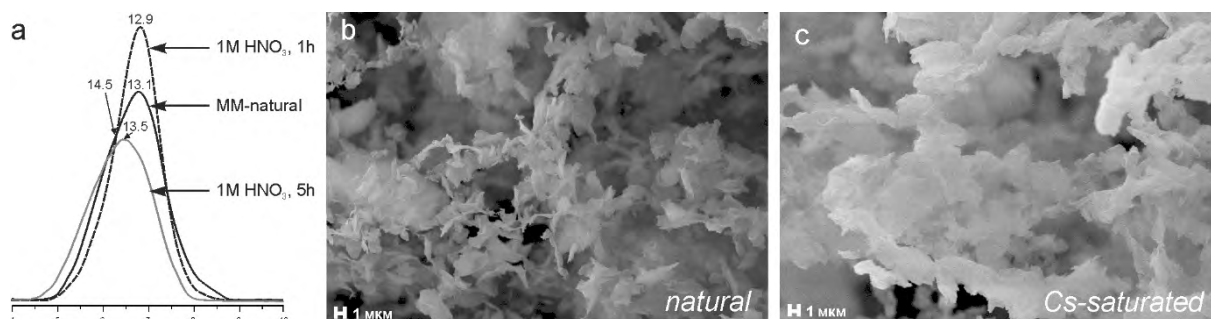


Fig 1. Natural and acid modified montmorillonite (001) reflection profiles (a) and changes of particles interaction and consolidation of micro-aggregates due to Cs<sup>+</sup> saturation (b – natural montmorillonite, c – Cs<sup>+</sup>-saturated).

## Formation of four-water-layer hydrates in smectites with divalent interlayer cations - dependence of layer charge and temperature

Daniel Svensson<sup>1</sup> and Hansen, Staffan<sup>2</sup>

<sup>1</sup>Äspö Hard Rock Laboratory, SKB, P.O. Box 929, SE-57229, Oskarshamn, Sweden; daniel.svensson@skb.se

<sup>2</sup>Centre for Analysis and Synthesis, Department of Chemistry, Lund University, P.O. Box 124, SE-22100, Lund, Sweden

Most divalent smectites such as Ca-smectite are known to form a 19 Å basal spacing (three-water-layers; W3) when placed into water. It has been observed that during cooling of Wyoming Ca-montmorillonite in water, a four-water-layer hydrate (W4) partly form with a basal spacing of 21 Å (Svensson and Hansen, 2010). The current study was aimed at investigating this effect further using synchrotron X-ray diffraction and smectites with different layer charges (origin), ion-exchanged with divalent Ca, Cu, Mg, Sr, and Zn (Wyoming, USA) or with Ca, Mg, and Zn (Milos, Greece; Kutch, India). The temperature was typically cycled between +20 and -50 °C, and the solid/water mass ratio was kept constant at 30 wt.% solid. It was observed that Ca and Sr Wyoming montmorillonite formed W4 in a similar way during cooling while Mg, Cu and Zn Wyoming montmorillonite formed W4 already at 20 °C, and by lowering the temperature the hydration and the W4/W3 intensity ratio increased further until ice was formed. After ice formation the smectites were dehydrated to 16 Å (W2). Neither the Milos nor Kutch smectites (Ca, Mg, Zn) were found to form the W4 phase during cooling. Factors found to affect the crystalline swelling and W4 formation was found to be the layer charge (total charge and/or location of the charge), temperature and interlayer cation. Lower charged smectite (Wyoming) expanded further compared to smectites with higher charge (Milos and Kutch). Lower temperature expanded the smectites further until ice was formed, and with higher Gibbs hydration energy of the interlayer cation further hydration (expansion) was observed (Sr < Ca < Mg < Zn < Cu). The results contribute to improving the understanding of the swelling behavior of smectites in complex applications.

Svensson, P. D., Hansen, S. (2010) Freezing and thawing of montmorillonite - a time-resolved synchrotron X-ray diffraction study. *Applied Clay Science*, 49, 127-134.

## Relevance of testing specifications for bentonites used in hydraulic barriers – can they be improved?

Will P. Gates

SmecTech Research Consulting, 24 Chapel Road Moorabbin, VIC, Australia 3189  
gateswp@smectech.com.au

Geosynthetic clay liners (GCLs) often serve to replace compacted clay liners as secondary hydraulic barriers in municipal solid waste containment facilities. Within the past decade however, GCLs have become increasingly assessed for suitability in industrial and mining applications. Typical scenarios include primary or secondary barriers for permanent or temporary storage of process waters, permanent disposal of tailings and as short-term barriers beneath heap leach pads. In each case, GCLs would be subjected to loads, hydraulic heads and leachate chemistries outside normal conditions for which they were designed. Performance of GCLs is traditionally assessed through a series of index tests, but adaptation of new specification criteria for the bentonite component in GCLs has often lagged behind these new applications.

This paper considers the importance of recent limited research on compatibility assessment of GCLs to leachates having extreme chemistry, here defined as strongly alkaline ( $\text{pH} > 12$ ), strongly acidic ( $\text{pH} < 3$ ), hyper-saline ( $> 1 \text{ M}$ ) or containing one or more contaminants at concentrations exceeding safe limits. Based on the limited research available, GCLs cannot be expected to perform for the long-term (i.e.  $> 20$  years) when in contact with strongly acidic leachates, whereas many GCLs can achieve long-term performance objectives for strongly alkaline leachates, where there exists the possibility of inducing conditions for pore clogging. In both extreme pH ranges, leachate ionic strength and the potential for cation exchange have the greatest immediate negative effects on bentonite swelling and GCL hydraulic conductivity. Different products are already available that purport to enhance GCL performance when exposed to hyper-salinity, some of which are proving to be highly effective. Future developments toward improving bentonite resistance to leachates having extreme chemistry should focus on improving the short- to mid-term performance of GCLs, and undertake to evaluate, as far as possible, changes in leachate chemistry and bentonite mineralogy involved in loss of field performance. Armed with this information, engineers are better able to design effective barrier systems with appropriate performance life-times for applications in mining and mineral processing industries.

## Geochemical outcome of the dismantling of the engineering barrier experiment at Mont Terri (Switzerland)

Ana María Fernández<sup>1</sup>, D.M. Sánchez-Ledesma<sup>1</sup>, A. Melón<sup>1</sup>, M. Sánchez<sup>1</sup>, P. Galán and J.C. Mayor<sup>2</sup>

<sup>1</sup> CIEMAT, Dpto. Medio Ambiente, Madrid, Spain; anamaria.fernandez@ciemat.es

<sup>2</sup> ENRESA, C/ Emilio Vargas, 7, 28043, Madrid, Spain

Bentonites are one of the more important industrial raw materials, widely used for different technological applications, such as catalysis, environmental remediation and engineering. This is because they are composed of smectites comprising outstanding physical and chemical properties: swelling capacity, low permeability and large sorption capacity.

About 40 years ago few commercial high quality bentonites were acquired for the study of bentonites as buffer and backfill materials in the construction of engineering barrier systems (EBS) for the isolation of high-level radioactive waste (e.g., MX-80, Calcigel, etc.). The selected natural bentonites are industrially processed to fabricate highly compacted bentonite blocks, which have been used in different *in situ* large-scale EBS experiments (e.g., FEBEX-*in situ*, LOT, Prototype, TBT) and Mock-Up tests. The aim is to analyze the properties, manufacturing, handling and long-term performance of the buffer. However, new reference designs for the EBS consists on compacted blocks and pellets for filling the gap between the bentonite compacted blocks and the host-rock.

The Engineered Barrier Emplacement Experiment (EB Experiment) was designed to demonstrate the feasibility of granular bentonite material (GBM) as alternative buffer in horizontal drift (6 m long gallery) excavated in the Opalinus Clay at Mont Terri Rock Laboratory. The test consisted on a real scale isothermal simulation (16 °C) using two types of FEBEX bentonite material. A lower bed made of compacted bentonite (1.69 g/cm<sup>3</sup>, 14% w.c.), constructed to emplace a dummy canister; and a bentonite pelletized material (2.12 g/cm<sup>3</sup>, 3.5% w.c.) filling the remaining space (final average GBM dry density of 1.36 g/cm<sup>3</sup> in the test section). The drift was sealed with a 2 m-long concrete plug and the whole system was artificially hydrated with saline Opalinus Clay pore water (0.3 M). After 10.5 years of operation the test was dismantled, and bentonite properties were analysed (HM and G).

At the end of the test, both bentonite materials (GBM and blocks) showed a relative homogenous distribution. The buffer was practically fully saturated ( $S_r=96\%$ , w.c.=36%,  $\rho_d=1.34$  g/cm<sup>3</sup>); preserving the low hydraulic conductivity properties (Mayor and Velasco, 2014). However, different mineralogical, geochemical and pore water composition characteristics were observed in both types of materials after dismantling. Lower CEC, slightly lower  $d(001)$  values after EG solvation, lower total surface area and higher pore water salinity were observed in the pellets compared to the compacted blocks (Fig. 1), which may be related to the initial fabrication process of the pellets, due to the FEBEX bentonite powder was pre-heated at 120°C prior to compaction. Furthermore, other mineralogical and bio-geochemical processes related to the saturation process were found.

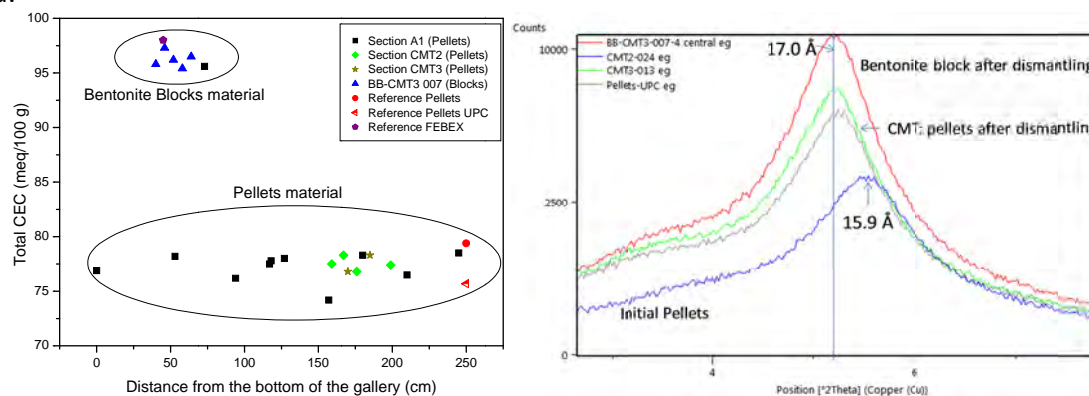


Figure 1. CEC values and EG-solvation  $d(001)$  values for pellets and blocks after dismantling the EB experiment

Mayor, J.C., Velasco, M., 2014. EB dismantling. Synthesis Report. PEBS Project. Deliverable D2.1-8, 49 pp.



## Gas migration in bentonite barriers

Patrik Sellin<sup>1</sup>, Antonín Vokál<sup>2</sup>, Caroline Graham<sup>3</sup>, Jiang Feng Liu<sup>4</sup>, María Victoria Villar<sup>5</sup>, Martin Birgersson<sup>6</sup> and Robert Cuss<sup>3</sup>

Svensk Kärnbränslehantering AB, Box 250, 101 24 Stockholm, Sweden

SÚRAO, Dlážděná 6, 110 00 Praha 1, Czech Republic

British Geological Survey, Keyworth Nottingham NG12 5GG, United Kingdom

Ecole Centrale de Lille – LML, UMR CNRS 8107, France

CIEMAT, Av Complutense, 40, 28040 Madrid

Clay Technology, AB Delta 6, IDEON Science Park S-223 70 Lund, Sweden

The multiple barrier concept is the cornerstone of all proposed schemes for underground disposal of radioactive wastes. The concept invokes a series of barriers, both engineered and natural, between the waste and the surface. Gas generation from either the waste form or the engineered barriers is an unavoidable but generally undesired effect in most European repository concepts for radioactive waste. Gas generation and migration can potentially alter the hydraulic and mechanical properties of the repository. The purpose of this work was to investigate gas migration processes and the consequences of gas migration in the Engineered Barrier Systems (EBS) of the repositories. A detailed series of laboratory and field scale experiments were undertaken to provide new fundamental insights into the processes and consequences of gas migration through the engineered barrier and seals of repositories. In an unsaturated or partially saturated bentonite there is a linear dependence between gas flow rate and pressure gradient, which indicates that two-phase flow is the dominating transport mechanism. This may also be the case for saturated sand-bentonite mixtures if the sand content is sufficiently high. At a degree of saturation of ~80-90% or higher the behaviour changes entirely. No flow of gas will take place in the bentonite unless the applied pressure is equal to or higher than the total stress. The only transport mechanism is the omnipresent diffusion of dissolved gas. Diffusion has not been a key issue, but evaluated diffusivities are well in line with what has been presented elsewhere. If the gas pressure reaches a higher value than that the pressure in the bentonite a mechanical interaction will occur. This will lead to either: Consolidation of the bentonite, and/or Formation of dilatant pathways.

Consolidation means that a gas volume will be formed within the clay that and that the clay is compressed. This increases the clay density closest to the gas volume and the local swelling pressure is increased to balance the gas pressure. There is however a limit to the extent of consolidation. At some critical pressure, pathways will be formed and the gas will become mobile. The pathways are characterized by a strong coupling between total stress ( $\sigma$ ), swelling pressure ( $\Pi$ ) and pore pressure ( $p_w$ ), localised changes in  $\sigma$ ,  $\Pi$  and  $p_w$ , unstable flow, exhibiting spatio-temporal evolution, localised outflows during gas breakthrough and no measurable desaturation in any test samples. It is still unclear when consolidation ends and pathway formation starts. In some tests, pathways form when the gas pressure reaches the sample pressure. An example of this is the full scale Lasgit test. Other tests show pathway formation at an overpressure at about 20-30%, while there also are tests where breakthrough occurs at pressures 2-3 times higher than the sample pressure. The effect is clearly geometry dependent, but other factors may be involved as well. However, it is clear that classical two-phase flow models cannot correctly represent gas migration in a compacted saturated bentonite.

## Effect of thermo-hydraulic gradients on the physical state and geochemistry of compacted bentonite

M.V. Villar, F.J. Romero, R. Gómez-Espina, P.L. Martín, R.J. Iglesias  
CIEMAT, Avd. Complutense 40, 28040 Madrid, mv.villar@ciemat.es

Two 40-cm long columns of compacted FEBEX bentonite were tested for 12 years in cylindrical cells. Water was supplied through the top surface of the columns and in one of them a heater was placed at the base and set to 100°C (Fig. 1). The purpose of these tests was to simulate the behaviour of an engineered barrier in a radioactive waste repository and investigate the effect of the thermal gradient on the bentonite modifications. To manufacture the columns the bentonite was compacted to 1.65 g/cm<sup>3</sup> with its hygroscopic water content, which was 13.1% (Villar & Gómez-Espina 2009).

Upon dismantling of the cells it was observed that the gravimetric water content along the columns was not homogeneous, and it ranged from 35% at the top in both columns, to 23% at the bottom in the isothermal test (test I40) and to 3% near the heater in the column subjected to thermal gradient (test GT40). The dry densities had changed according to the swelling caused by hydration (Villar et al. 2014).

The changes of mineralogy and geochemistry of the bentonite along the columns have been analysed. In particular, the composition of the pore water was determined by means of aqueous extracts of solid:liquid ratio 1:8. In the two tests the salinity of the top of the column considerably decreased due to the increase in water content, as the electric conductivity of the aqueous extracts shows (Fig. 1). The concentration of most soluble species increased towards the base of the column, particularly in test GT40, since it seems that the thermal gradient favoured the movement of ions such as sodium and chloride. The composition of the cation exchange complex changed along the columns, not only as a consequence of hydration, but also of the thermal gradient.

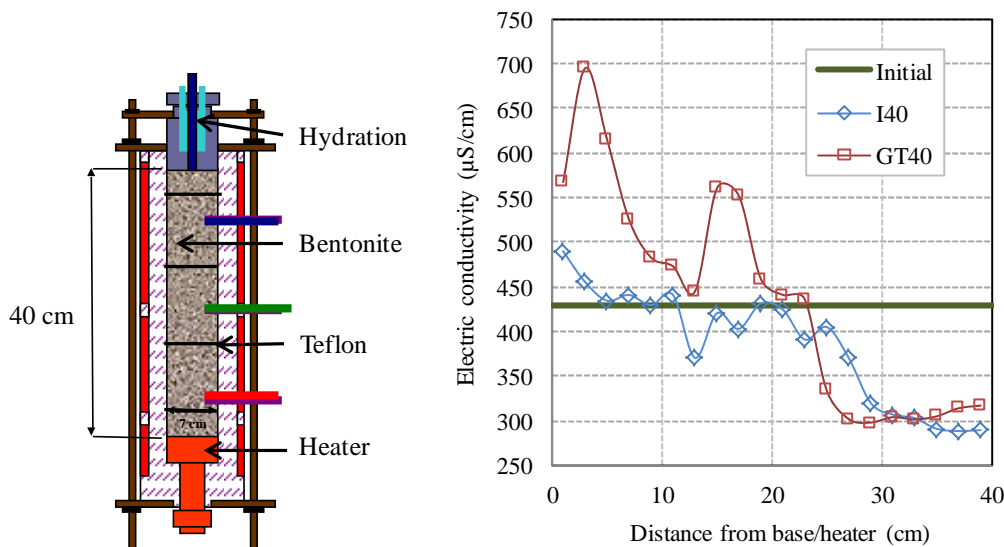


Figure 4: Schematic design of the cells and electric conductivity of bentonite aqueous extracts at the end of the tests

Villar, M.V. & Gómez-Espina, R. (2009): Report on thermo-hydro-mechanical laboratory tests performed by CIEMAT on FEBEX bentonite 2004-2008. Informes Técnicos CIEMAT 1178, Madrid, 67 pp.

Villar, M.V.; Gómez-Espina, R.; Martín, P.L.; Romero, F.J. & Iglesias, R.J. 2014. Efecto del gradiente termo-hidráulico sobre el estado físico de bentonita compactada. XXIII Reunión SEA 2014, Libro de resúmenes pp. 79-80.

## Removal of trichloroethylene (TCE) from contaminated soils by injection of nZVI-doped bentonite slurry

Andre Baldermann<sup>1</sup>, Stephan Kaufhold<sup>2</sup>, Peter Freitag<sup>3</sup>, Marcus Spitz<sup>1</sup>, Claudia Nickel<sup>4</sup>, Ilse Letofsky-Papst<sup>5</sup>, Thomas G. Reichenauer<sup>6</sup> and Martin Dietzel<sup>1</sup>

<sup>1</sup>Institute of Applied Geosciences, Graz University of Technology, Rechbauerstraße 12, A-8010 Graz, Austria;  
baldermann@tugraz.at

<sup>2</sup>BGR, Bundesanstalt für Geowissenschaften und Rohstoffe, Stilleweg 2, D-30655 Hannover, Germany

<sup>3</sup>Keller Grundbau Ges.mbH, Mariahilferstraße 127A, 1150 Wien, Austria

<sup>4</sup>Institute of Technology and Testing of Building Materials, Graz University of Technology, Inffeldgasse 24, A-8010 Graz, Austria

<sup>5</sup>Institute of Electron Microscopy and Nanoanalysis, Graz University of Technology, Steyrergasse 17, A-8010 Graz, Austria

<sup>6</sup>AIT, Austrian Institute of Technology GmbH, Konrad-Lorenz-Straße 24, A-3430 Tulln, Austria

The industrial application of trichloroethylene (TCE) as a cleaning and degreasing agent in built-up areas in Austria, especially from the 1920s to 1970s, resulted in locally severe pollution of soils and surrounding groundwater with cancerogenic and non-biodegradable TCE. The *in-situ* remediation of TCE contaminated soils and groundwater by reduction with nanoscale zero-valent iron (nZVI) additives into non-toxic and de-chlorinated hydrocarbons such as ethane and ethane has been recently introduced as an ecologically sustainable countermeasure (Arnold & Roberts, 2000). In the course of the HaloCrete research project one aim was to increase the physical mixing of nZVI and TCE in subsoils utilizing the jet grouting technique. In order to apply this technique in built up areas, where a system-inherent reduction of the bearing capacity of the soil has to be minimized, additional geotechnical binders such as bentonite clay have to be used in conjunction. The physicochemical interaction mechanisms between nZVI aggregates and commercial IBECO bentonite (70±5 wt.% of Na-montmorillonite) are still to question and hence their effects on the kinetics of TCE degradation remain uncertain.

In the present study a series of batch experiments were performed, in which groundwater contaminated with TCE was reacted with a nZVI-bearing bentonite slurry for 1.5 and 96 hours at 22±3°C in incubation reactors. The mineralogical and geochemical modifications of the bentonite clay as well as the progress of TCE degradation during the experiments were monitored by transmission electron microscopy, X-ray diffraction analyses, infra-red spectroscopy and gas chromatography. Our data reveal that the TCE has been completely converted into ethane and ethane after 48 hours of reaction time, which clearly demonstrates the high efficiency of nZVI particles as catalysts, and clay mineral additives, on the TCE reduction rates. Goethite and ferrihydrite were identified as the main oxidative weathering products of nZVI nano-particles. However, we also observed a strong increase of ~130% in the Fe(III) content in Na-montmorillonite, from initial 5.7 atom% to 13.0 atom% after only 96 hours of nZVI-bentonite interaction, as evidenced by combined nanoscale Fe distribution maps and electron energy-loss spectroscopy data. These results suggest intense modifications of the original bentonite clay due to rapid formation into nontronitic domains. Therefore, the oxidative alteration of nZVI particles and accompanying formation of highly labile Fe-oxyhydroxides and nontronite could affect a variety of biogeochemical processes involved in soil environments.

Arnold, W. and Roberts, L. (2000). Pathways and kinetics of chlorinated ethylene and chlorinated acetylene reaction with Fe(O) particles. *Environmental Science & Technology* **34**(9), 1794–1805.

Thursday  
9<sup>th</sup> July

Lecture room 2

Clay and fine particle  
based materials for  
environmental  
technologies and clean up  
(2)

## Decomposition of hydrogen peroxide by Mg-Fe layered double hydroxides (LDHs)

Yoshikazu Kameshima, Kana Nakamura, Shunsuke Nishimoto and Michihiro Miyake

Department of Material and Energy Science, Graduate School of Environmental and Life Science, Okayama University, 3-1-1 Tsushima-naka, Kita-ku, Okayama 700-8530, Japan

E-mail: ykameshi@cc.okayama-u.ac.jp

Manganese dioxide ( $\text{MnO}_2$ ) is well known as an inorganic catalyst that catalyzes the decomposition of hydrogen peroxide into oxygen and water. Hydrogen peroxide ( $\text{H}_2\text{O}_2$ ) is used in various industrial processes, and it is necessary to be decomposed after use. Although  $\text{MnO}_2$  is useful for the decomposition of  $\text{H}_2\text{O}_2$ , a material which is less toxic is desirable from the point of view on the environment and safety. In this study, we have found that Mg-Fe layered double hydroxides (LDHs) decomposed  $\text{H}_2\text{O}_2$  by oxidation-reduction reaction of the Fe ions in the LDH host layer.

LDHs containing  $\text{Fe}^{3+}$  in the host layer were prepared by the co-precipitation method. The obtained Mg-Fe type LDHs were characterized by XRD, FT-IR and SEM-EDS. The sample was dispersed in  $\text{H}_2\text{O}_2$  aqueous solutions of 1.0 M. The generated gas was collected by the downward displacement of water and the volume of the generated gas was measured. Additionally, the sample was dispersed in  $\text{H}_2\text{O}_2$  aqueous solutions of 50 mM. The solution was sampled at a regular interval and an amount of residual  $\text{H}_2\text{O}_2$  was measured by UV-vis spectroscopy.

The generated gas was identified as oxygen ( $\text{O}_2$ ) by an analysis of gas chromatography. The amount of the generated  $\text{O}_2$  against for reaction time was shown in Fig.1. It was shown that Mg-Fe LDHs had high activity to decompose  $\text{H}_2\text{O}_2$ . Rate of  $\text{O}_2$  generation for the LDH of Mg/Fe=2 and Mg/Fe=3 were 0.14 mol/h and 0.09 mol/h, respectively. These rates were same order as the rate 0.19 mol/h of  $\text{MnO}_2$ . It is considered that Mg-Fe LDHs decomposed  $\text{H}_2\text{O}_2$  by the same mechanism as  $\text{MnO}_2$ .

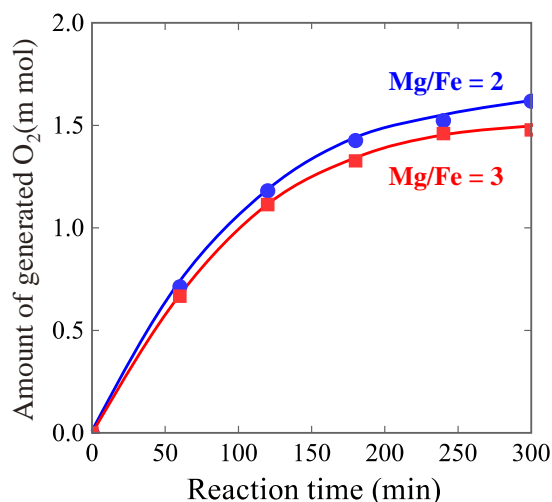


Fig.1 The amount of generated oxygen by Mg-Fe LDHs.

## Hexavalent chromium remediation by organic ligand-manganese-clay mineral system: A synchrotron based study

Binoy Sarkar<sup>1,2\*</sup>, Ravi Naidu<sup>1,2</sup>, Avanthi Deshani Igalavithana<sup>3</sup> and Yong Sik Ok<sup>3</sup>

<sup>1</sup>Centre for Environmental Risk Assessment and Remediation (CERAR), University of South Australia, Mawson Lakes Campus, SA 5095, Australia

<sup>2</sup>Cooperative Research Centre for Contamination Assessment and Remediation of the Environment (CRC CARE), P.O. Box 486, Salisbury, SA 5106, Australia

<sup>3</sup>Korea Biochar Research Centre and Department of Biological Environment, Kangwon National University, Chuncheon 200-701, Republic of Korea

\*binoy.sarkar.clay@gmail.com; binoy.sarkar@unisa.edu.au

Hexavalent chromium (Cr(VI)) is a highly toxic environmental contaminant. Due to its adverse environmental effects, stringent health guidelines, and limited cost effective remedial options, there is a need of alternate strategies for remediation. It undergoes complex electron transfer redox reactions involving electron acceptors, such as lower valent metals (iron and manganese) and low molecular weight organic ligands in soils [1-3]. Conversion of Cr(VI) to trivalent form (Cr(III)) via a reduction reaction is seen as a remediation strategy for this toxic pollutant. However, the mechanisms of such process occurring in soils, especially involving divalent manganese (Mn(II)) and clay minerals, are not clear yet. This study explores such a reaction mechanism through the solution-based measurements of Cr and Mn, as well as their X-ray absorption near edge structure (XANES) based speciation on clay surfaces, following the experiments conducted in the presence of citrate under simulated soil environmental conditions.

We found that citrate reduced Cr(VI) in the presence of Mn(II) as a catalyst, which is assisted by montmorillonite [1]. The solution chemistry and X-ray photoelectron spectroscopy (XPS) results indicated that Cr(III) were deposited on montmorillonite surface following the reduction. However, evidence of oxidised species of Mn (Mn(III and IV)) on mineral surface was lacking, due to limited instrumental sensitivity. We proposed a multi-step mechanism as follows: in the first step, citrate forms a complex with Mn(II), which triggers the reduction reaction in the aqueous phase. This is followed with adsorption of Cr(III) by clay mineral surface [1]. A Mn-citrate complex reacting with Cr(VI) would form an ester-like species, which upon decomposition converts Cr(VI) to Cr(III) [1].

Through a synchrotron based XANES study, we further revealed the following: (a) oxidation of Mn(II) during the reaction and deposition of the oxidised species occurred on the clay surfaces (specially on montmorillonite); (b) Mn(II)-citrate complex attaching to the clay surfaces (both montmorillonite and kaolinite) also contributed to the reduction reaction; and (c) clay minerals (montmorillonite and kaolinite) acted as a sink for both Cr and Mn following the reaction. However, deposition of Cr(III) was more obvious on kaolinite than montmorillonite surface. Therefore, the reactions in soil involving Cr(VI), organic ligand, manganese, and clay minerals are highly complex in Nature. While citrate was the key reductant, Mn(II) also enhanced the reaction rate by donating electrons. Surfaces of clay minerals further increased the reaction rates. This implied that Mn dominated soil should be abundant in organic ligands in order to prevent the re-oxidation of Cr(III) to Cr(VI). Knowledge generated in this study will contribute to better management and remediation of Cr(VI) in soil environments.

**Keywords:** Hexavalent chromium, Clay minerals, XANES, Remediation

[1] Sarkar, B., et al., 2013, Environ. Sci. Technol. 47 (23), 13629-13636.

[2] Buerge, I.J. and Hug, S.J., 1999, Environ. Sci. Technol. 33 (23), 4285-4291.

[3] Lan, Y. et al., 2008, Chemosphere 71 (4), 781-787.

## Spectroelectrochemical reduction of nontronite: A shifting mechanism

Anna Weiss and Alanah Fitch\*

Department of Chemistry and Biochemistry, Loyola University Chicago, Chicago, IL, USA.

AQDS (anthraquinone 2,6-disulfonate) is used as a mediator for the quantitative reduction of nontronite (NAU2). The extent of reduction is monitored both by the total charge passed and by optical changes in AQDS on reduction. Concentrations of the mediator from 0.5 to 12.5 times the calculated amount of iron present were used to reduce a fixed amount of clay. Assuming all electrons could be transferred, the iron should have been reduced by 0.5 mole fraction as AQDS is a 2 electron transfer agent. A linear relationship indicating a  $2e^-$  transfer was observed up to ca. 30% of the reducible clay present. Beyond that point  $4e^-$  were required for subsequent iron reduction, suggesting that a AQDS dimer (observed spectroscopically) supplied the dominate electron transfer route. The change in mechanism at ca. 30% is interesting particularly with respect to other mechanistic studies which suggest that only fractional reduction of iron is present. Those other studies suggest that fractional reduction is related to structural identity of the iron present. The data presented indicates very complex and variable mechanisms related to dimerization of the mediator, and, possibly, concerted electron proton transfer is necessary for reduction.

## **Characterisation of a stable clay-suspension with application to possible dewatering and reclamation of mine wastewater, Cullinan Diamond Mine, South Africa**

Jessica Strydom, Marthie Coetzee and Peter Wade

North-West University, Potchefstroom, South Africa; 21212627@nwu.ac.za

More than a century of mining of the Cullinan kimberlite pipe has resulted in the accumulation of a significant amount of waste water. The unique location of the waste-water dam constrains further mine development, while poor water quality in the dam increases the risk of potential environmental contamination from seepages and spillages. Dam water currently exhibits elevated levels of pH, dissolved salt content, density, and extreme turbidity that originates from dispersed colloidal clay as a natural weathering product of the ore. Turbidity is the principal factor hindering dewatering operations. Flocculation of the dispersed clay particles will enable (a) effective and efficient separation of the clay material from the waste water and (b) cost-effective water treatment options. Thorough characterization of the individual components was performed to further understanding of the dynamics of the water-salts-clays system in the context of dewatering options. A conceptual system dynamics model of the dam water was initially developed, upon which the design of the experimental regime was based. Suspended clay particles and associated aqueous solutions were characterised by physical and chemical methods. X-Ray Diffraction, X-Ray Fluorescence and electron microscopy were used to determine the bulk mineralogy of the clay suspension. The turbidity results from dispersion of colloidal chlorite, saponite, nontronite and mixed layer microaggregates. The shapes of the colloid particles were found to contribute significantly to the non-settlement of the solids. Chemical characterisation of the system components included standard water quality analysis, electrophoretic mobility tests and chemical speciation calculations. Interpretation of the combined physical and chemical data explained the observed stability of the clay suspension and yielded valuable information for remediation options. Subsequent laboratory chemical investigations revealed that the system characteristics could be adjusted for sufficient interparticular attraction to reach the critical coagulation point ( $c_K$ ). At this point the solids rapidly coagulated and separated from the solution. Based on the derived characteristics of the clay-salt-water system, an industrial chemical flocculation process was proposed for complete effective and efficient sedimentation of the clay material.



## Development of chitosan-palygorskite composite as a sustainable material for heavy-metal removal from wastewater

Ruhaida Rusmin<sup>1,2,\*</sup>, Binoy Sarkar<sup>1,3</sup>, Yanju Liu<sup>1,3</sup>, Ravi Naidu<sup>3</sup>

<sup>1</sup>CERAR – Centre for Environmental Risk Assessment and Remediation, Building X, University of South Australia, Mawson Lakes, SA, 5095, Australia

<sup>2</sup>Faculty of Applied Science, Universiti Teknologi MARA Negeri Sembilan, Kuala Pilah 72000, Malaysia

<sup>3</sup>CRC CARE – Cooperative Research Centre for Contamination Assessment and Remediation of the Environment, P.O. Box 486, Salisbury, SA, 5106, Australia

\*[ruhaida.rusmin@mymail.unisa.edu.au](mailto:ruhaida.rusmin@mymail.unisa.edu.au)

Despite considerable efforts are in place for remediating toxic heavy metals by using suitable adsorbents, challenges still occur to produce material which is cost effective, highly stable and environmentally safe by not introducing any secondary pollutant. Chitosan, which is a natural polymer and low cost material, is manufactured by deacetylation of chitin extracted from shellfish waste. Having metal chelating properties by virtue of its reactive functional groups, chitosan can serve as an effective adsorbent in heavy metal remediation. Over the last decade, composites of chitosan and natural aluminosilicate minerals, especially clay minerals, have been studied as potential materials for environmental clean-up [1]. Research showed that chitosan-clay composites could improve mechanical properties of the materials [2, 3] and significantly enhance the adsorption capacity as compared to the pristine material [4]. Montmorillonite and bentonite were commonly used for the preparation of chitosan-clay nanocomposites, but little attention was given to fibrous clay mineral like palygorskite. Palygorskite has moderate surface area and reactive silanol groups that can also participate in toxic cation removal from wastewater. Thus, it is expected that a composite of chitosan and palygorskite could have synergic effects towards adsorption of toxic metals. In this preliminary study, the preparation of chitosan-palygorskite composite through solvent method was developed and optimised. The structural characteristics of the composite were investigated through Scanning Electron Microscopy (SEM), X-Ray Diffraction (XRD), and Fourier Transform Infrared Spectroscopy (FTIR), while the surface area analysis was performed through N<sub>2</sub> adsorption-desorption experiments. Performance of the composite in lead (Pb<sup>2+</sup>) removal from water was evaluated through batch adsorption experiments. It is expected that the outcome of this research will help to develop a green adsorbent effective for environmental remediation.

[1] Alcântara et Al., Applied Clay Science, 96 (2014) 2-8.

[2] Lewandowska et al., International Journal of Biological Macromolecules, 65 (2014) 534-541.

[3] Xu et al., Journal of Applied Polymer Science, 99 (2006) 1684-1691.

[4] Tirtom et al., Chemical Engineering Journal, 197 (2012) 379-386.

## Modification of clay minerals by chemical modification and graft polymerization

Juris Burlakovs, Maris Klavins, Ruta Ozola and Juris Kostjukovs

Faculty of Geographical and Earth Sciences, University of Latvia, Rainis Blvd. 19, LV 1586, Riga, Latvia

e-mail: juris@geo-it.lv

Clay properties can be significantly modified using different approaches to obtain materials with new areas of application. Considering highly hydrophilic properties of clay minerals, one of the major aims of such modification is their hydrophobization in order to improve interaction with low polarity organic molecules - a common group of materials in this respect are organoclays. However, intercalation and binding by ionic bonds of organic modifiers, does not prevent their leakage during application of such materials, especially if they have some degree of biological activity, toxicity.

The aim of the study was to develop method of synthesis and test application possibilities of clays modified chemically with different functional groups as well as to study graft polymerization possibilities onto clays.

Chemical modification was achieved by using derivatives of trimethoxysilanes, containing, for example, aminopropyl -, glycidyl- or thiol- functional groups. The derivatization reaction is fast, and it ensures possibilities to obtain materials with a high derivatization degree, but the desired functional groups are attached to the surface of clay minerals with covalent bonds. The introduced functional groups are able to interact with organic molecules of differing polarity.

Graft polymerization was done using polymerization of acrylic (methacrylic) acid derivatives with radical initiation onto clay surface. This approach helps to cover clay surface with a layer of polymeric chains, thus significantly changing the properties of the obtained materials.

Obtained modified clay materials were characterized using granulometric analysis, BET surface area was estimated, FTIR and XRD spectra were obtained and sorption pattern was characterized.

This study was supported by the project "Res Prod".

## Stability of tetrabutyl-phosphonium and -ammonium modified montmorillonite in inorganic acid

Helena Pálková<sup>1</sup>, Małgorzata Zimowska<sup>2</sup>, Ľuboš Jankovič<sup>1</sup>, Bogdan Sulikowski<sup>2</sup>, Ewa Maria Serwicka<sup>2</sup> and Jana Madejová<sup>1</sup>

<sup>1</sup> Institute of Inorganic Chemistry, SAS, Dúbravská cesta 9, 845 36 Bratislava, Slovakia, helena.palkova@savba.sk

<sup>2</sup> Jerzy Haber Institute of Catalysis and Surface Chemistry, PAS, Niezapominajek 8, 30-239 Krakow, Poland

The stability of Na-SAz-1 montmorillonite (Na-S), and SAz-1 intercalated with two quaternary organic cations, in hydrochloric acid was studied. Tetrabutylammonium ( $\text{Bu}_4\text{N}^+$ ) and tetrabutylphosphonium ( $\text{Bu}_4\text{P}^+$ ) cations, *i.e.* cations with the same length and number of alkyl chains but comprising different central atoms bearing positive charge, were used for organoclays preparation. The samples were treated with 6 M HCl at 80°C for 1/2-12 h and solid products obtained after reaction were characterized using various methods. Elemental analysis revealed only negligible content of octahedral Mg and/or Al in the solid reaction products after 8 h treatment of Na-S indicating almost completely decomposed montmorillonite. The  $\text{Bu}_4\text{P-S}$  and  $\text{Bu}_4\text{N-S}$  revealed higher resistance to the acid; more than one half of the initial Mg and Al content remained undissolved after 8 h treatment. The infrared spectra showed decreasing intensities of the absorption bands attributed to  $\text{CH}_3$  and  $\text{CH}_2$  groups confirming diminishing amount of organic surfactants with the enhanced acid treatment. In addition, the positions of the bands were shifted by about  $4\text{cm}^{-1}$  to lower wavenumbers for samples treated for 12 h. A shift of  $\nu_{\text{Si-O}}$  band to higher wavenumbers after 8 h treatment reflected the formation of a reaction product - amorphous silica phase. This change was more pronounced for Na-S ( $\Delta\nu_{\text{SiO}}=60\text{ cm}^{-1}$ ) than for  $\text{Bu}_4\text{N-S}$  ( $\Delta\nu_{\text{SiO}}=12\text{ cm}^{-1}$ ) and  $\text{Bu}_4\text{P-S}$  ( $\Delta\nu_{\text{SiO}}=20\text{ cm}^{-1}$ ). Moreover, a bit broader  $\nu_{\text{Si-O}}$  band of  $\text{Bu}_4\text{P-S}$  indicated slightly higher extent of  $\text{Bu}_4\text{P-S}$  decomposition than  $\text{Bu}_4\text{N-S}$ . Formation of acid sites during HCl treatment was investigated via pyridine adsorption. The IR bands of pyridine adsorbed on acid-treated samples confirmed the presence of Brønsted acid sites, able to resist heating of the samples at 230°C. The results proved that modification of montmorillonite with both organic cations imparted higher resistance of the layers to decomposition upon acid treatment in comparison to the unmodified natural sample.

**Acknowledgments:** The authors gratefully acknowledge the financial support from the Slovak Research and Development Agency (contract No. APVV-0362-10) and the Polish-Slovak joint Project 2013-2015. We are also grateful to the Polish Ministry of Science and Higher Education for the NMR 500 MHz spectrometer investment grant (project No. 75/E-68/S/2008-2).

## Application of Terahertz time domain spectroscopy for investigation of clays and clay mineral systems

M. Janek<sup>1,\*</sup>, D. Zich<sup>2</sup>, T. Zacher<sup>2,3</sup>, M. Matejdes<sup>2,4</sup> and M. Naftaly<sup>5</sup>

<sup>1,\*</sup>Slovak University of Technology, Radlinského 9, SK-81237 Bratislava, Slovakia; \* marian.janek@stuba.sk

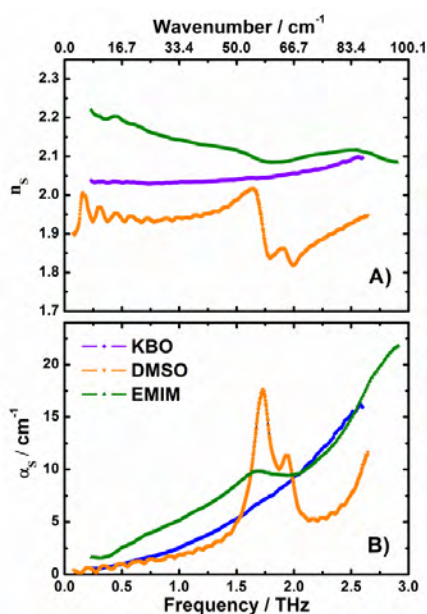
<sup>2</sup>Comenius University, Faculty of Natural Sciences, Mlynská dolina CH1, SK-84215 Bratislava, Slovakia

<sup>3</sup>Slovak Institute of Metrology, Department of Chemistry, Karloveská 63, SK-84255 Bratislava, Slovakia

<sup>4</sup>Institute of Inorganic Chemistry, Slovak Academy of Sciences, Dúbravská cesta 9, 845 36 Bratislava, Slovakia

<sup>5</sup>National Physical Laboratory, Hampton Rd, Teddington, Middlesex, TW11 0LW, UK

Terahertz time domain spectroscopy (THz-TDS) was recently successfully used for the investigation of layered clay minerals in the far-infrared region<sup>i,ii,iii</sup>. This technique enables measurement with high signal sensitivity and phase information, enabling rich spectroscopic and dielectric analysis in the frequency range of about 0.1–3.0 THz in the transmission mode. The details of THz-TDS measurements can be found elsewhere<sup>iv,v</sup>. In short, the measurements were carried out using laboratory build equipment with a standard configuration based on a femtosecond-laser driven photoconductive emitter and electro-optic detection. The values of the frequency dependent complex refractive index were calculated from the transmission data as  $\tilde{n}_S = n_S - i\kappa_S$ , where  $n_S$  is the real refractive index and  $\kappa_S$  is absorption. The power absorption coefficient  $\kappa_S$  of the samples was calculated from  $\alpha_S = 2\kappa_S\omega/c$ ; where  $\omega$  is the angular frequency and  $c$  the speed of light in vacuum, representing sample spectral response in far-infrared region. Because organic quarternary cations can be adsorbed on negatively charged surfaces of layered clay minerals via very strong non-covalent interaction, the adsorption of organic cationic species is an experimentally straightforward task, useful for specific surface modification.<sup>1</sup> In our experiments were used Kaolinite (KBO) from a primary deposit in Bayern-Oberpfalz, hectorite (HSH) and montmorillonite (M48) received from current Clariant International Ltd. (Germany). The selection of investigated clay mineral samples was done in accordance with significant differences in their chemical composition, allowing their comparison after chemical modification. The measurements revealed sample specific spectral response after their modification, which may shed more light on the processes involved during their physical-chemical modification. The frequency dependence of the refractive index  $n_S$  and absorption coefficient  $\alpha_S$  of parent and modified KBO in the range of  $\sim 3 - 100 \text{ cm}^{-1}$  as determined by THz-TDS are shown in Figure 1. Interesting differences were observed in the frequency dependence of absorption coefficient  $\alpha_S$  among all studied samples. The steepest rise of absorption coefficient with frequency was detected for parent HSH ( $72 \text{ cm}^{-1}$  @ 1THz) and M48 ( $78 \text{ cm}^{-1}$  @ 1THz), while the weakest was shown by KBO ( $2.5 \text{ cm}^{-1}$  @ 1THz). This behavior may be connected to water content present as hydration water of exchangeable cations in HSH and M48 samples, or to the differences in the chemical composition of selected samples. While kaolinite retains its



Dependence of refractive index  $n_S$  and power absorption coefficient  $\alpha_S$  of Dimethylsulfoxide (DMSO), 1-ethyl-3-metylimidazolium ethyl-sulphate (EMIM) of kaolinite KBO.

absorption coefficient in the range of pristine KBO even after chemical modification by either neutral molecule such as dimethylsulfoxide ( $1.9 \text{ cm}^{-1}$  @ 1THz) or amino acid modified KBO ( $2.0 \text{ cm}^{-1}$  @ 1THz) or HSH ( $21.4 \text{ cm}^{-1}$  @ 1THz). This behavior indicates the effect of water content reduction in clay minerals, because CTA acts as a surface hydrophobising agent upon adsorption on clay particles. It was demonstrated that organic molecules such as amines and amino acids change the refraction and absorption properties of modified clay minerals upon their adsorption; furthermore, it was shown that THz-TDS is sufficiently sensitive for investigation of these species, despite the high absorption coefficient of the parent clay samples at the level of about  $100 \text{ cm}^{-1}$ .

**Acknowledgements:** The financial support of the Comenius University for supporting of the D. Zich PhD. work with the UK Grants No. 309/2010, 338/2011, 298/2012 is greatly acknowledged. The financial support of the Slovak Grant Agency for Science VEGA (grant No. 1/0943/13), of the Slovak Research and Development Agency APVV (grant APVV-0291-11) and work support at NPL by the National Measurement Office of the U.K. is greatly appreciated.

<sup>i</sup> M. Janek, I. Bugár, D. Lorenc, V. Szöcs, D. Velic, D. Chorvát (2009) *Clays Clay Miner.* 57, 416–424.

<sup>ii</sup> M. Janek, M. Matejdes, V. Szöcs, I. Bugár, A. Gaál, D. Velic, J. Darmo (2010) *Philos. Mag.* 90, 2399–2413.

<sup>iii</sup> Wilke, V. Ramanathan, J. LaChance, A. Tamalonis, M. Aldersley, P.C. Joshi, J. Ferris (2014) *Appl. Clay Sci.* 87, 61–65.

<sup>iv</sup> D. Zich, T. Zacher, J. Darmo, V. Szöcs, D. Lorenc, M. Janek (2013) *Vibr. Spectr.* 69, 1–7.

<sup>v</sup> M. Janek, D. Zich, M. Naftaly (2014) *Mat. Chem. Phys.* 145(3), 278–287.

<sup>vi</sup> M. Janek, G. Lagaly (2003) *Colloid Polym. Sci.* 281(4), 293

## Utilization of surfactant-modified zeolite for the treatment of coal fly ash leachate

Rona J. Donahoe<sup>1</sup>, Ghanashyam Neupane<sup>2</sup> and Sidhartha Bhattacharyya<sup>1</sup>

<sup>1</sup>Dept. of Geological Sciences, University of Alabama, Tuscaloosa, AL 35487-0338, USA, rdonahoe@ua.edu

<sup>2</sup>Idaho National Laboratory, EES&T, Idaho Falls, ID 83415, USA

The majority of fly ash and other coal combustion residuals (CCRs) in the United States are disposed of in landfills and surface impoundments. The December 2008 Kingston Plant coal ash spill in Tennessee prompted the US EPA to intensify its review of the 1980 RCRA Amendments which excluded CCRs from Subtitle C hazardous waste requirements. Among other provisions, the resulting December 2014 Disposal of Coal Combustion Residuals from Electric Utilities final rule regulates the disposal of CCRs under Subtitle D of RCRA and mandates the monitoring of groundwater near coal ash disposal facilities. Coal fly ash leachate contains elevated levels of several potentially hazardous trace elements such as As, B, Cr, Mo, Ni, Se, Sr and V, many of which exist in the environment as highly mobile oxyanions. Effective treatment technologies are needed to limit the mobility of toxic trace elements in the ash disposal environment.

In this study, laboratory batch leaching and column experiments were performed to assess the utility of surfactant-modified zeolite for the treatment of leachate generated from acidic and alkaline fly ash samples. Natural zeolite (74% clinoptilolite) was treated with HDTMA-Br to produce a positively charged, surfactant bi-layer on the external surfaces, while retaining the intrinsic cation exchange capacity within the internal channels. Batch experiments were conducted in duplicate using fly ash leachate and either 1%, 5%, 10%, 15%, or 20% SMZ. The SMZ treatments successfully reduced the concentrations of A, Cr, Mo, Ni, Sr and V, but had little to no effect on B. No improvement in removal of As, Se, and V was observed for SMZ greater than 10%.

Column experiments were conducted to investigate the effectiveness of SMZ as a permeable reactive barrier (PRB) material at ash disposal facilities. Columns were dry-packed using a 17.5 cm thick ash layer at the top and a 17.5 cm thick underlying soil layer, with one of the duplicate columns having a 5 cm thick layer of SMZ at the bottom to mimic the disposal environment with an installed PRB. The packed columns were then leached with a synthetic acid rain (SAR) solution at ~1.3 ml/min. At the end of the column experiment, the SMZ layer was recovered and air dried, and then subjected to sequential batch leaching at a 1:15 SMZ:SAR ratio. The simulated SMZ PRB decreased the concentrations of several cationic and anionic trace elements in the column effluent solutions, but was generally more effective for treating the acidic fly ash leachate. Effectiveness decreased with time, as SMZ sorption sites became saturated. Regeneration of the reacted SMZ would increase the lifetime of the PRB. Sequential SAR leaching of the reacted PRB material showed only minor mobilization of the adsorbed trace elements, indicating that SMZ should be considered a good candidate material for PRB treatment of coal fly ash leachate at disposal sites.

## Fluorescent lamp glass recycling in geopolymers and its use in dye removal

W. Hajjaji<sup>1</sup>, S. Andrejkovičová<sup>1</sup>, V. Niknam<sup>1</sup>, J.A. Labrincha<sup>2</sup> and F. Rocha<sup>1</sup>

<sup>1</sup> Geobiotec, Geosciences Dept, University of Aveiro.3810-193 Aveiro. Portugal

<sup>2</sup> Materials and Ceramic Engineering Dept & CICECO. University of Aveiro.3810-193 Aveiro. Portugal

Geopolymers, a class of largely amorphous aluminosilicate binder materials, have been studied extensively over the past several decades. New metakaolin based geopolymer formulations were elaborated by addition of fluorescent lamp glass through sodium silicate/NaOH activation. The influence on the microstructure and mechanical properties of compositional variation with partial replacement of metakaolin by lamp waste glass (0, 25, 50 and 75 %) and Si/Al ratio (3, 3.5 and 4) were studied. From 1 to 7 days curing, the combination of these two amorphous materials (metakaolin and glass) exhibited suitable compressive strength values reaching 16 MPa and 12 MPa for glass addition of 25 and 50 %, respectively. At higher percentage of waste (25% metakaolin 75% glass), the mechanical resistance tends to decrease due to the higher reactivity of metakaolin with alkaline solution. This behavior is also observed when more curing time is applied to the studied geopolymers (28 days). Nevertheless, the mechanical properties of glass based geopolymers at different Si/Al ratio remain superior to metakaolin based one (around 4 MPa).

The methylene blue adsorption tests using the confectioned geopolymers show an important decrease of the dye concentration; visible after 10 min. Indeed a quick uptake reaching up to 95% is reported when fluorescent lamp glass based geopolymers are used as adsorbent. In case for metakaolin products, lower removal rate has occurred. These disparities in initial formulations, inducing different degrees of geopolymerization reactivity, were reflected in porosity and adsorption behavior.

**Keywords:** Geopolymers, metakaolin, fluorescent lamp glass, compressive strength, adsorption.

## In-situ evidence of organic molecules trapping into hybrid metal-oxide nanotubes

Mohamed Salah Amara,<sup>1</sup> Erwan Paineau,<sup>1</sup> Stéphan Rouzière,<sup>1</sup> Antoine Thill,<sup>2</sup> Pascale Launois,<sup>1</sup>

<sup>1</sup> Laboratoire de Physique des Solides, Bât. 510, Université Paris Sud, 91405 Orsay, France

erwan-nicolas.paineau@u-psud.fr

<sup>2</sup> Laboratoire Interdisciplinaire sur l'Organisation Nanométrique et Supramoléculaire, IRAMIS/NIMBE/CEA, 91191 Gif sur Yvette, France

Nanotubes are ultimate one-dimensional nanochannels for molecular confinement. A key point is the control of their diameter and surface properties, to adjust their interactions with the molecules to be confined. *Normal* imogolite nanotubes *n*-INT  $(\text{OH})_3\text{Al}_2\text{O}_3\text{Si}_x\text{Ge}_{(1-x)}(\text{OH})$  are hydrophilic metal-oxide nanotubes covered with hydroxyl groups [1], which appear as promising building blocks for water sorption and anti-dewing material [2].

We synthesized *modified* imogolite nanotubes *m*-INT  $(\text{OH})_3\text{Al}_2\text{O}_3\text{Si}_x\text{Ge}_{(1-x)}(\text{CH}_3)$ , where hydroxyl groups on the inner surface are replaced with methyl groups through water-based chemistry under mild condition. Herewith, we present a detailed X-ray scattering (XRS) analysis of hybrid organic-inorganic imogolite nanotubes, from the determination of their dimension to their capability in terms of organic molecules trapping (figure) [3]. The as-synthesized nanotubes are found to have well-defined inner and outer diameters, shaped at the level of the angstrom thanks to the control of their Ge/Si content (internal diameter vary from 24.6 to 18.4 Å for *x* varying from 0 to 1). The water density inside methylated nanotubes is reduced by a factor of 3 in *m*-INT compared to *n*-INT, due to their newly internal hydrophobic character. The capacity of those nanotubes to capture organic molecules is demonstrated in-situ, for bromopropanol molecules added into a solution (Figure 1). These new members of imogolite family may open up possibilities for water filtration or water decontamination.

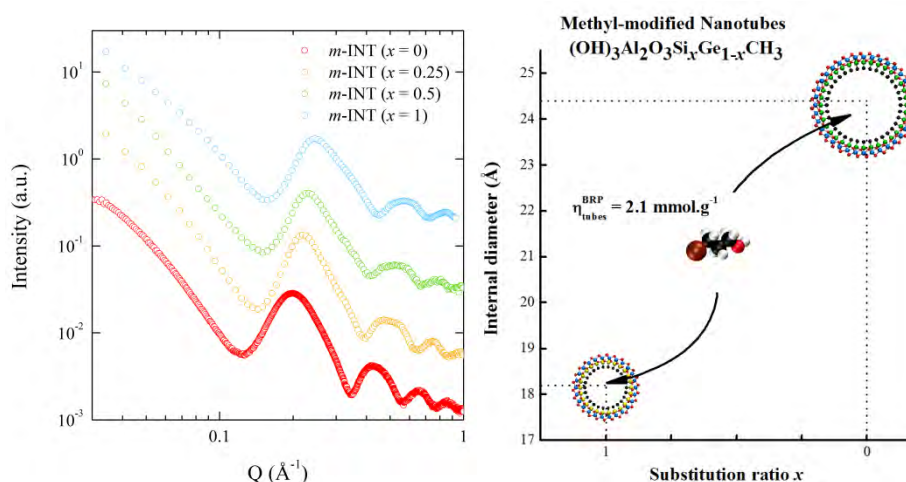


**Figure 1.** Methyl-modified imogolite nanotubes (*m*-INT) for organic molecules confinement. (Left) XRS diagrams of *m*-INT at different  $x = [\text{Si}]/([\text{Si}]+[\text{Ge}])$  ratios. (Right) Atomic structure and internal diameter of *m*-INT for  $x = 0$  and  $x = 1$ .

[1] Cradwick, P.D.G.; Farmer, V.C.; Russell, J.D.; Masson, C.R.; Wada, K.; Yoshinaga, N. *Nature Phys. Sci.* **1972**, 240, 187

[2] Suzuki, M. & Inukai, K. *Inorganic and Metallic Nanotubular Materials*, Springer, **2010**, 159

[3] Amara, M.S.; Paineau, E.; Rouzière, S.; Guiose, B.; Krapf, M.E.M.; Taché, O.; Launois, P.; Thill, A. *Chem. Mater.*, **2015**, accepted for publication

## Environmental reactivity of iron oxide nanoparticles

Mikael Motelica-Heino<sup>1</sup>, Simona Iconaru<sup>2</sup>, Régis Guégan<sup>1</sup> and Daniela Predoi<sup>2</sup>

<sup>1</sup>ISTO UMR 7327 CNRS Université d'Orléans, Orléans, France mikael.motelica@univ-orleans.fr

<sup>2</sup>3National Institute of Materials Physics, Bucuresti-Magurel, Romania

The remediation of soils contaminated with disperse and low levels of problematic trace elements (TE), metals and metalloids, calls for the applications of technologies that are effective, safe and cost-competitive [1]. Nanoscience and nanotechnology are an ever increasing field of multidisciplinary research and development growing on all continents [2] and the market for soil and groundwater remediation by nanoparticles is expected to keep growing fast in the coming years. Soil remediation with engineered nanoparticles promises more effective and cheaper technologies than conventional approaches due to the increased specificity and reactivity of the manufactured nanoparticles [3]. Among them magnetite and maghemite, the most common iron oxide nanoparticles, has been the subject of intensive studies because at nanometric scale they exhibit unique physical and chemical particularities [4, 5].

The aim of this study was to determine and optimize the reactivity of the geoengineered nanoparticles of iron oxide for TE for environmental remediation.

Iron oxide based magnetic nanoparticles were synthesized by co-precipitation of Fe<sup>3+</sup> and Fe<sup>2+</sup> ions.

At the stoichiometry Fe<sup>2+</sup>/Fe<sup>3+</sup> = 0.5 crystallization of magnetite (Fe<sub>3</sub>O<sub>4</sub>) with an inverse spinel phase is quasi-immediate at room temperature. Then, because of their high instability against oxidation, the magnetite nanoparticles are transformed into maghemite (γFe<sub>2</sub>O<sub>3</sub>) by desorption of Fe<sup>2+</sup> ions and creation of vacancies.

Physical, structural and morphological characterization at the nanoscale of the nanoparticles has been performed. The obtained materials will be characterized by a suite of physico-chemical techniques such as: X-ray diffraction (XRD), X-ray Photoelectron Spectroscopy (XPS), infrared spectroscopy (FT-IR), thermal analysis (ATG and ATD), chemical and elemental analysis, determination of specific surface area (BET method), porosity studies using ultrasounds, scanning electron microscopy coupled with a Raman spectrometer (FEG-SEM/Raman), transmission electron microscopy (TEM) and electron tomography, Raman spectroscopy, photoluminescence, UV-Visible spectroscopy.

The adsorption of TE such as As and Cu at the surface of iron oxide nanoparticles has also been investigated. The surface reactivity was correlated with the size of magnetite and maghemite nanoparticles. Adsorption isotherms of the iron oxide samples after adsorption of TE on their surface using a Langmuir model was calculated in order to highlight the connection between the surface area and the adsorption of TE.

Collectively our results suggest that iron oxide nanoparticles have a potential for removal and/or immobilisation of TE in contaminated soils.

[1] S.J.T. Pollard, A. Brookes, N. Earl, J. Lowe, T. Kearney, C.P. Nathanail, Integrating decision tools for the sustainable management of land contamination, *Science of the Total Environment*, 325 (2004) 15–28.

[2] Nicoara G, Fratiloiu D., Nogues M, Dormann JL, Vasiliu F: Ni-Zn ferrite nanoparticles prepared by ball milling. *Mater Sci Forum* 1997,235:145-150.

[3] B. Nowack, T.D. Bucheli, Occurrence, behavior and effects of nanoparticles in the environment, *Environmental Pollution*, 150 (2007) 5-22.

[4] Xiong Y, Ye J, Gu X, Chen Q: Synthesis and magnetic properties of iron oxide nanoparticles/C and a-Fe/iron oxide nanoparticles/C composites. *J Magn Magn Mater* 2008, 320:107–112.

[5] A.F. Ngomsik, A. Bee, M. Draye et al., Magnetic nano- and microparticles for metal removal and environmental applications: a review, *Comptes Rendus Chimie*, 8 (2005) 963-970.



## Poorly crystalline nanoparticles formed in acid mine drainage (AMD) in a limestone environment

Youjun Deng<sup>1,\*</sup>, L. Morgan<sup>1</sup>, Roberta McClure<sup>1</sup>, Maria Aurora Armienta<sup>2</sup>, M. Newville<sup>3</sup>, Shan-Li Wang<sup>4</sup>, and T. Kogure<sup>5</sup>

<sup>1</sup>Department of Soil & Crop Sciences, Texas A&M University, College Station, Texas, USA: \*yjd@tamu.edu;

<sup>2</sup>Universidad Nacional Autónoma de México, Instituto de Geofísica, Circuito Exterior, C.U., Mexico DF 04510

<sup>3</sup>Center for Advanced Radiation Sources, Advanced Photon Source, University of Chicago, USA

<sup>4</sup>Department of Agricultural Chemistry, National Taiwan University, Taipei, Taiwan;

<sup>5</sup>Department of Earth and Planetary Science, The University of Tokyo, 7-3-1 Hongo, Bunkyo-ku, Tokyo 113-0033, Japan

Arsenic, zinc, lead, copper, nickel and many other heavy metals are the major concerns of acid mine drainage (AMD) resulting from the oxidation of sulfide minerals exposed to air. In theory, acid mine drainage and heavy metal contamination should not be problems in limestone areas due to the abundance of carbonate minerals that can neutralize the acidity. Poorly crystalline nanoparticles such as various iron oxides, silica, and the oxides of heavy metals are the most reactive compounds in regulating the heavy metals. Unfortunately, our knowledge on these reactive particles in the limestone environment or the liming reclamation areas is limited due to the difficulties in characterizing these materials with common methods and instruments. The objectives of our study were to: 1) characterize on an atomic scale low-crystallinity nanoparticles and colloids generated in AMD and examine their transformations in a limestone environment, and 2) characterize As speciation in each associated solid phase and quantify the mobilization and transformation of As and the heavy metals associated with the mineral phase conversions.

The mine tailings and streams in Zimapán, Mexico offer an excellent model to systematically investigate the geochemical processes of the heavy metals and metalloid. Mineralogical analyses, physico-chemical parameters, inverse geochemical modeling and isotopic determinations showed that As is released from arsenopyrite oxidation and, in some locations, also by scorodite dissolution. Arsenopyrite oxidizes releasing As that is further retained through sorption on ferric oxyhydroxides and clays, and also by the formation of secondary As-bearing minerals like beudantite and jarosite. Our preliminary analysis indicated that, in addition to calcite in the limestone and the tailings, silicate minerals such as amphiboles, pyroxenes, pyroxenoids (wollastonite), mica (biotite), and clay minerals (illite and smectites) in the mine tailings are also involved in the acidity neutralization. Both Fe-containing silica nanoparticles and Si-containing Fe oxides have been observed in the oxidized tailings under TEM. Both amorphous silica (biotic origin?) and poorly crystalline iron oxide nanoparticles formed in an oxidized Zimapán mine tailing. It appears that the silica particles were coated with Fe and other elements. Similarly, the Fe oxides particles were coated with silicate compounds. Trace amounts of As could be found in these nanoparticles. In an oxidized stratum of the tailing (sample 4L), several Fe, Si, As, and heavy metal containing nanoparticles were identified. The energy dispersive spectroscopy patterns suggested the goethite contained more As than the jarosite did and that Si was associated with both goethite and jarosite particles. The acicular goethite nano-crystallite showed ca. 0.5 nm fringes which correspond to 020 lattices in goethite. Goethite crystals had a crystal habit elongation along the *c*-axis. The selected area electron diffraction intensity distribution in the diffraction rings was not circumferentially uniform but had roughly six maxima. The electron diffraction pattern changes suggested that this As-containing goethite nanoparticle was not stable to electron beam radiation, which is rare in pure or larger goethite particles. Bulk and micro-XANES and EXAFS and XRF mapping have been conducted on unoxidized and oxidized samples. The arsenic showed distinct valence changes under different environment as suggested by the XANES data, yet the EXAFS spectra are far more diverse and complex than the reference samples. In the oxidized tailing, As occur mainly as As(V). No As(III) signals were detected with the X-ray absorbance analysis. It appears that the As(VI) were associated with either different minerals or colloids phases as an incorporated structural component, or adsorbed on the surfaces. We are analyzing the EXAFS data to extract more structural information, yet, it requires more well defined reference EXAFS spectra for good linear combination analysis.

Our investigations on colloids and nanoparticles in the oxidized tailings have shown a complex arsenic-mineral interaction mechanism. The iron oxyhydroxides may have deviated from the ideal structures due to the small size and incorporation of various anions and heavy metals.

Thursday  
9<sup>th</sup> July

Lecture room 1

Clays in the Critical Zone  
soils, weathering and  
elemental cycling

## Critical Zone Science as the Earth Science for the Anthropocene

Daniel de B. Richter

Professor of Soils, Duke University, Durham, NC 27708 USA [drichter@duke.edu](mailto:drichter@duke.edu)

Integrative concepts of the biosphere, ecosystem, biogeocenosis and, recently, Earth's critical zone embrace scientific disciplines that link matter, energy, organisms, including clay minerals, in a systems-level understanding of our remarkable planet.

Earth's critical zones are highly diverse and they range across spatial scales from vegetation-clad weathering profiles and hillslopes, small catchments, landscapes, river basins, continents, to the terrestrial Earth itself. What may be less obvious are the vertical dimensions. The depth of Earth's critical zone is determined by others as depth of weathering, total depth of active water cycling, seismic velocity of competent rock, or total depth of biological activity, but here we use soil respiration, and ecosystem energy flow and metabolism to argue that the full accounting of photosynthetically-fixed carbon must include respiratory CO<sub>2</sub> that propagates to the base of the critical zone itself. Though soil respiratory CO<sub>2</sub> exits quickly back to the atmosphere, downward diffusion of CO<sub>2</sub> helps determine rates of mineral weathering and soil formation and, ultimately, ecosystem evolution and resilience. Because plant life perched in upper portions of ecosystems significantly affects biogeochemistry throughout weathering profiles, soils and terrestrial ecosystems have historically been demarcated at depths too shallow to permit complete understanding of soil and the structure and function of the subsurface environment. Opportunities abound to explore connections between upper and lower components of critical-zone ecosystems, between deep soil profiles and streams in watersheds, and between plant-derived CO<sub>2</sub> and deep microbial communities and mineral weathering.

## Dynamics of mineral recrystallization at the Earth's surface: Evidence from Ultisols, kaolins, and paleosols with implications for the "ages" of a rock

Paul A. Schroeder<sup>1,2</sup> and Jason C. Austin<sup>1</sup>

<sup>1</sup>Department of Geology, University of Georgia, Athens, GA 30602-2501, USA schroe@uga.edu

<sup>2</sup>Department of Geological Engineering, Istanbul Technical University, Maslak 34469, Istanbul, Turkey

The age of a rock is generally considered in the context of its relative position within a stratigraphic sequence and/or by a numeric time as determined by geochronology. These two tenets (i.e., stratigraphic superposition and radiometric dating), along with the founding principle of evolutionary faunal succession have guided the field of Earth history for over a century. Inherent in the majority of geologic studies is the idea that metastability of a rock's mineral composition is long-lasting once re-exposed at the Earth's surface. In other words, a rock's texture and composition retain information about original facies conditions and subsequent time/temperature/compositional changes after its burial diagenesis, metamorphism, or crystallization. In the case of paleosols, overprinting textural features (e.g., peds, redoximorphic mottles, clay horizons) and elemental trends (e.g., chemical alteration indices) support the notion of an older preexisting weathering surface. It has been often assumed that if a paleo-solum is preserved back into the deep subsurface then paleoenvironmental properties of the weathering event are preserved.

Crystal-chemical and stable/cosmogenic isotopic study of modern Ultisols and kaolins in the southeastern United States supports a hypothesis that minerals undergo multiple generations of recrystallization at the surface and deep (i.e., 80+ meters) below the surface. Validating evidence includes these observations: 1) Increases in Al substitution and coherent scattering domain disorder in goethite close to the surface in Ultisols, which suggests a tertiary generation mineral assemblage is established as weathering fronts propagate downward; 2) Stable carbon and oxygen isotope signatures from gibbsite in Ultisol depth profiles, which suggest a dynamic exchange between long term atmospheric and soil gas effluxes; 3) Hydrogen isotopic compositions of Eocene kaolins, which become enriched in an up dip trend as overburden thin and meteoric water influences are greater in rocks nearer to the surface; and 4) Detection of modern cosmogenic carbon in goethites found in Ordovician Neda Formation paleosols (Austin and Schroeder, 2015), which suggests that millennial-scale recrystallization surface weathering processes have the potential to overprint the "age" and therefore skew paleoenvironmental information preserved in rock exposed at the Earth's surface.

We support a modified paradigm for the concept of a weathering age of a rock (as noted by Fitzpatrick, 1963). Criteria would use traditional quantitative constraints as determined by elemental, mineral, textural, and color measures, but also employ cosmogenic nuclides, other chronological techniques, and isotopic studies. We should continue with the understanding that the age of a rock is defined by its complex assemblage of components, which may include more newly formed minerals mediated by hydrolysis and/or redox reactions to extremely old mineral such detrital zircons that formed billion of years ago. The question about "how old is that rock?" for the purpose of discovering Earth history remains to be challenge and the answer(s) could be "one or many ages", depending upon what part of the rock is being considered.

Austin, Jason C. and Schroeder, Paul A. (2015). C-14 age of the carbonate component in natural goethite ((Fe(O,CO<sub>3</sub>)OH) from the Upper Ordovician Neda Fm., Neda Wisconsin, USA. EuroClay 2015, abstracts with program (this volume), Edinburgh, Scotland.

Fitzpatrick, E.A. (1963). Deeply weathered rocks in Scotland, Its occurrence, age, and contribution to soil. *European Journal of Soil Science*, 14 (1), 33-38.

## **C-14 age of the carbonate component of natural goethite (Fe(O,CO<sub>3</sub>)OH) from the Upper Ordovician Neda Fm., Neda, Wisconsin, USA**

Jason C. Austin<sup>1</sup> and Paul A. Schroeder<sup>1,2</sup>

<sup>1</sup>Department of Geology, University of Georgia, Athens, GA 30602-2501, US [austinj1@uga.edu](mailto:austinj1@uga.edu)

<sup>2</sup>Department of Geological Engineering, Istanbul Technical University, Maslak 34469, Istanbul, Turkey

Measured C-14 ages of carbon collected during the step-wise dehydration / decarbonation of natural goethite from the Upper Ordovician Neda Fm., Neda, WI, indicate a model age of 13 to 20 thousand years. This finding suggests the carbonate component of natural goethite undergoes exchange with the environment after burial, potentially invalidating the use of the stable isotope composition of this carbon as a proxy for the partial pressure of CO<sub>2</sub> in the Ordovician atmosphere. Agreement of the measured stable isotope ratios of the collected CO<sub>2</sub> between two independent labs and the published values from this locality suggest that the results are valid. These findings are contrary to the conclusions from short-term exchange experiments conducted previously (Yapp and Poths, 1993) and suggest that exchange occurs over thousands of years. The measured age of the carbon coincides generally with the retreat of the Laurentian Ice Sheet from Wisconsin. This suggests that weathering of the Neda formation during this time caused exchange of the carbonate component of the goethite. Care should be taken to ensure that similar post-burial isotope exchange does not occur in other paleo-climate proxies that utilize carbon isotopes from pedogenic minerals in paleosols.

Yapp, C.J. and Poths, H. (1993). Geochemistry of goethite ( $\alpha$ -FeOOH) in ironstone of the Upper Ordovician Neda Formation, Wisconsin, USA: Implications for early Paleozoic continental environments. *Geochimica Et Cosmochimica Acta*, 57, 2599-2611.

## Deeply buried Mesozoic weathering profiles from the Norwegian North Sea

Lars Riber<sup>1</sup>, Henning Dypvik<sup>1</sup>, Ronald Sørli<sup>2</sup>, Nikolas Oberhardt<sup>1</sup>, Pingchuan Tan<sup>1</sup>, Kristian Stangvik<sup>1</sup>, Syed A. A. Naqvi<sup>3</sup>, Paul A. Schroeder<sup>4</sup>, Arlindo Begonha<sup>5</sup>, and Ray E. Ferrell<sup>6</sup>

<sup>1</sup>Department of Geosciences, University of Oslo, P.O. Box 1047, Blindern, NO-0316 Oslo, Norway lars.riber@geo.uio.no

<sup>2</sup>Lundin Norway AS, Strandveien 50D, NO-1366 Lysaker, Norway

<sup>3</sup>Volcanic Basin Petroleum Research, Gaustadalléen 21, NO-0349 Oslo, Norway

<sup>4</sup>Department of Geology, University of Georgia, 210 Field St., Athens, GA 30602-2501, USA

<sup>5</sup>Faculdade de Engenharia da Universidade do Porto, Rua Dr. Roberto Frias, s/n, 4200-465 Porto, Portugal

<sup>6</sup>Department of Geology & Geophysics, Louisiana State University, Baton Rouge, LA, 70803, USA

For the first time on the Norwegian Continental Shelf, altered and fractured basement rocks have been shown to act as reservoirs and possible migration pathways for commercial hydrocarbon deposits. Following recent discoveries on the Utsira High (Edvard Grieg and Johan Sverdrup fields), good reservoir properties have been observed in parts of the altered basement underlying the main Cretaceous, Jurassic and Triassic reservoir rocks.

In the present study, eighteen basement cores were made available by the Norwegian Petroleum Directorate and Lundin Norway AS. Two well-developed weathering profiles were identified in two cores (16/3-4, 16/1-15) based on an upwards increase in disintegration of the rock associated with an increase of clay minerals. The clay mineral assemblages developed from interstratified illite/smectite at the base to kaolinite towards the top, at the expense of plagioclase and biotite.

Earlier onshore Scandinavian studies revealed that deep weathering took place from Mid/Late Triassic through Jurassic. In the onshore cores, the late Jurassic/early Cretaceous age of overlying sediments indicates that the offshore profiles are contemporaneous with the onshore weathering.

In the two profiles, evidence of multiple stages of alteration was observed. Before exposure and weathering the basement experienced retrograde metamorphism, typically manifested by chloritisation of biotite, sericitisation of plagioclase, and precipitation of secondary phases such as TiO<sub>x</sub>, secondary K-feldspars and secondary quartz. During subaerial exposure deep weathering occurred. Argillisation was observed in one of the cores (well 16/3-4), represented by >15 wt% kaolinite in the most severely altered upper interval and accompanied by the leaching of mobile elements such as K, Na and Ca. The core of well 16/1-15 exhibited a different set of features. In this profile the total clay content was less than 2 wt% and dominated by interstratified illite/smectite and chlorite/7 Å. The mixed layered phase was thought to represent the weathering of plagioclase and biotite. The chlorite/7 Å most likely originates from diagenetic processes during post-exposure burial.

Limited lateral resolution in cores made the interpretation of weathering profiles difficult due to their heterogeneity. In this study, time-equivalent onshore weathering from Bornholm (Denmark) and Ivö Klack (Sweden) displayed comparable argillisation to 16/3-4. In Braga, northern Portugal, recent weathering of the Braga granite in a temperate and humid climate resulted in the disintegration of the granite, but the clay content was low, similar to what was observed in 16/1-15. In fractures, where the fluid flow was high, extreme weathering took place resulting in the formation of gibbsite, which was not observed in the offshore profiles. In Georgia (USA) two profiles from the Keystone and Sparta granites were analyzed. These profiles represent modern weathering in a subtropical and humid climate, with a development comparable to that observed in 16/3-4.

## Characteristics of early Earth's critical zone based on Devonian palaeosols properties (Voronezh Antecline, Russia)

T. Alekseeva<sup>1</sup>, P. Kabanov<sup>2</sup>, A. Alekseev<sup>1</sup> and P. Kalinin<sup>1</sup>

1 - Institute of Physical, Chemical, and Biological Problems of Soil Science, Russian Academy of Sciences, Pushchino, Russia;  
alekseeva@issp.serpukhov.su

2 - Geological Survey of Canada, Calgary

The Devonian (Givetian – Frasnian) pedocomplex was discovered in Pavlovsk granite quarry (Voronezh region, Russia) in 2010. Devonian deposits on the northern slope of the Voronezh Antecline are known as “Central Devonian Field”. This territory during Middle - Late Devonian was greatly affected by volcanism. The volcanic rocks have intermediate and mafic compositions providing the palaeosols by iron. The pedocomplex is underlined by Devonian marine clay deposits interstratified with siderite layers and overlapped by Cretaceous deposits. Palaeosols (PSs) are located on a top and a slope of the pronounced palaeorelief. They are characterized by good preservation of profiles (sometimes – unique), contain *in situ* roots and inborn flora. The multidisciplinary mineralogical and geochemical study (XRD, XRF, SEM, FT-IR, magnetic susceptibility, Mass spectrometry, <sup>13</sup>C - NMR), palaeobotanical and topographic investigations gave us the rare opportunity to characterize the Devonian - early Earth's critical zone developed with a participation of vascular plants. The pedocomplex consists from 7 PSs with the whole thickness of about 9 m. PSs are developed from terrigenous non-marine deposits: argillites in the lower part of pedocomplex and tuff – sandstones – in the upper. Lower 3 PSs are semi-hydromorphous soils with stages when oxidizing conditions prevailed. The upper 4 PSs are Andosols of different degree of development. PS profiles demonstrate several common characteristics: eluvial - illuvial redistribution of clay; presence of Fe- carbonate nodules; the enhance values of MnO /Al<sub>2</sub>O<sub>3</sub> (intensity of pedogenesis) and Fe<sub>2</sub>O<sub>3</sub>+MnO /Al<sub>2</sub>O<sub>3</sub> (degree of oxidation); *in-situ* roots. The main mineral component of clay fractions in all palaeosols is kaolinite. Clay fractions from some horizons are *monomineral* (100 % kaolinitic), others additionally contain goethite. The latter is the most common in the root containing horizons. Stable isotope analysis of C of siderite nodules shows the δ<sup>13</sup>C values between -10 and -11 ‰, indicating their pedogenic origin. Micromorphological study of nodules shows that many of them consist from degraded roots with the preserved concentric structure. Besides goethite some horizons additionally may contain ilmenite, pyrite and other Fe-bearing minerals. Their joint presence testifies the diverse and complicated paleoecological environments accompanied pedogenesis which were determined by palaeorelief, active volcanism and tectonics. The important unit of some PS profiles is the red hematite - rich layer in the bottom which sharply marks the individual PS profiles within pedocomplex. It developed at different soil depths and has the different thicknesses. We regard such a layer as the marker of wetted depth by oxygenic waters. The most pronounced hematitic layer is in the bottom of pedocomplex at the boundary with marine deposits which marks the bottom of the whole visual critical zone. The imprint of vegetation is exhibited by *in-situ* individual roots and rooting systems, coaly plant debris, well preserved spores and fragments of rhyniophytes, lycopsides, progymnospermous plants - *Svalbardia*, *Tanaitis*, *Callixylon* – *Archaeopteris* et al. Roots are of different shape, size and preservation. Most of the time they preserve their concentric structure; are substituted by goethite, siderite or rare - by pyrite. The obtained PSs characteristics suggest warm – wet with temporally arid palaeoclimate. Calculated precipitation is around 1000 mm y<sup>-1</sup>. Discovered Middle - Late Devonian landscape was characterized by large biodiversity, in many respects – unique.

## **Weathering intensity of a Pleistocene loess/paleosol sequence in Wels-Aschet (Upper Austria) indicated by clay minerals**

Karin Wriessnig<sup>1</sup>, Franz Ottner<sup>1</sup> and Birgit Terhorst<sup>2</sup>

<sup>1</sup>Institute of Applied Geology, University of Natural Resources and Life Sciences, Vienna. karin.wriessnig@boku.ac.at

<sup>2</sup>Institute of Geography, University of Würzburg, Am Hubland, D-97074 Würzburg

A complex loess/paleosol sequence on a fluvio-glacial terrace near Wels/Aschet, classified as a classical Günz unit, has been investigated. Sedimentological and mineralogical analyses were carried out on the basis of paleopedological field data. The results show that in terms of mineralogical composition, the paleosols can clearly be differentiated from loess layers. Bulk mineralogical as well as clay mineralogical data allow a ranking of weathering intensity based on indicator minerals.

From the bulk mineralogical point of view, slightly weathered loess still contains carbonate minerals and primary chlorite whereas the intensely weathered soil horizons are characterized by the total absence of carbonate minerals and primary chlorite and a very low content of micas and feldspars. Regarding the clay minerals in the fraction <2 $\mu$ m, chlorite and the relation of 14Å- and 18Å-vermiculites, as well as mixed layer minerals, play an important role to determine the weathering level. Primary chlorite can be present in less weathered loess loams, and vermiculite 14Å is dominant there (level 1 and 2). From weathering level 3 onwards, the amount of vermiculite 18Å increases considerably and dominates the following level 4. Moreover, intensive weathering causes the absence of illite (level 5). Generally, the studied paleosols are classified at least as level 3.

With the applied methods, four interglacial paleosols as well as a highly weathered paleosol within the terrace gravels of the Günz in Wels-Aschet have been identified. The characterization of weathering intensity using these mineralogical data was compared with indices based on grain size ( $K_d$ -Index) and geochemical data (Chemical Index of Alteration, CIA).



## Formation of halloysite and kaolinite in tropical soil via sequential transformation of pedogenic smectite and kaolinite-smectite

Peter C. Ryan<sup>1,2</sup> and F. Javier Huertas<sup>2</sup>

<sup>1</sup> Geology Department, Middlebury College, Middlebury, Vermont, 05753 USA

<sup>2</sup> Instituto Andaluz de Ciencias de la Tierra (CSIC-UGR), 18100 Armilla, Granada, Spain

Halloysite (both spherical and tubular) and platy Fe-rich kaolinite in moist tropical soils (Costa Rica) are derived from precursor smectite and interstratified kaolin-smectite (K-S). Iron-rich smectite ( $13.2 \pm 1.6\%$  Fe<sub>2</sub>O<sub>3</sub>, anhydrous basis) is the dominant mineral in Holocene soils (1 – 10 ka); it forms during early stage pedogenesis from precursor sediments rich in plagioclase and augite with accessory quartz and, in some localities, volcanic glass, heulandite or calcite (shell fragments). Over time spans of 10 to 50 ka, pedogenic smectite evolves to interstratified K-S that inherits flaky smectite crystal form. In late Pleistocene (40 - 80 ka) soils, K-S is the dominant soil mineral, comprising ~ 90 % of soil clay in the C-horizon of 50 ka terrace soils. The oldest soils in the chronosequence (120 ka) are dominated by subequal amounts of Fe-kaolinite and halloysite (4.9 % Fe<sub>2</sub>O<sub>3</sub>) and K-S only comprises 5 – 10 % of these evolved soils.

K-S was identified in XRD analyses by asymmetric 001 peak at 16 Å (ethylene glycol-solvated) and irrational 00l peaks (7.6, 3.52 Å) that exhibit Méring-like behavior. TEM-AEM images and elemental analyses document flaky-to-platy single crystals of K-S with compositions intermediate to those of end-member smectite and kaolinite. Changes in the compositions of tetrahedral and octahedral sheets, notably decreases in octahedral Fe and Mg and increases in Al, indicate that the smectite to K-S reaction is accompanied by localized dissolution of smectite 2:1 layers that likely proceeds laterally along the 2:1 layers. TEM, FTIR and XRD confirm the presence both forms of halloysite and platy Fe-kaolinite, and XRD (e.g. incomplete expansion and collapse) and DTA indicate the development of Al-hydroxy-interlayers in K-S with time. B-horizons of 120 ka soils contain small amounts of hexagonal kaolinite with low iron content (< 3 % Fe<sub>2</sub>O<sub>3</sub>), suggesting that formation of this type of kaolinite requires  $\geq 100$  ka in tropical soil.

Changes in crystal chemistry (decreasing Fe and Mg, increasing Al) over time likely reflect two reaction mechanisms. The first is layer-by-layer, cell-preserved reaction of smectite layers to kaolin layers that accompanies conversion of smectite to K-S and eventually kaolinite — this mechanism results in the formation of platy Fe-rich kaolinites and eventually hexagonal, low-Fe kaolinites. The second mechanism involves dissolution of K-S crystals followed by crystallization of tubular and spheroidal halloysite. The likely sequences of transformations, based on the changes in chemistry, are as follows: (A) smectite → K-S → Fe-kaolinite (solid state, cell-preserved), simultaneous with (B) smectite → K-S → spheroidal halloysite → tubular halloysite. The origin of halloysite and disordered Fe-bearing kaolinite from smectite (via K-S) has potentially important implications for clay mineral reactions and elemental cycling in tropical soils.

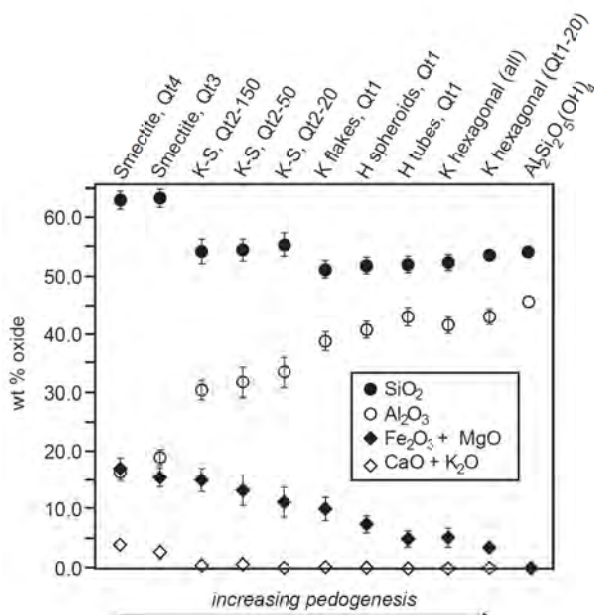


Figure 2. Changes in crystal chemistry from TEM-AEM analysis. Data are arranged from youngest soil (left) to oldest (right), with idealized end-member kaolinite on far right.

## Identification of mixed layer minerals: implication for soil reactivity.

Fabien Hubert<sup>1</sup>, Jean Christophe Viennet<sup>1</sup>, Emmanuel Tertre<sup>1</sup>, Bruno Lanson<sup>2</sup> and Eric Ferrage<sup>1</sup>

<sup>1</sup> HydrASA, IC2MP, Université de Poitiers – CNRS, F-86022 Poitiers, France. fabien.hubert@univ-poitiers.fr

<sup>2</sup> ISTerre, Université Grenoble 1 – CNRS, F-38041 Grenoble, France.

In most soils, the clay fraction (<2 µm) contains several types of discrete clay minerals and mixed layer minerals (MLMs). The reactivity of these MLMs in soils is difficult to assess because of the difficulty in their identification. Using X-ray diffraction (XRD) analysis of oriented sample, this identification is classically based on the different behaviours of their clay crystal structures submitted to various treatments. Because of both the different origins of clay minerals and the rapid changes of the weathering conditions in soils, several MLMs commonly coexist in the soil clay fraction and their irrational series of broad reflections most often overlap. Moreover, due to the wide range of particle sizes in the soil clay fraction (from ~50 nm to ~5 µm), the low peak intensities of the most defective MLMs can be easily hidden by the diffraction maxima of the less defective clay minerals such as discrete clays.

This work aims at showing that the XRD profile modelling approach applied on various sub-fractions (<0.05, 0.05-0.1, 0.1-0.2 and 0.2-2 µm) of the clay fraction allows to improve the identification of MLMs from soils (Hubert et al., 2012, Viennet et al., 2015). The results obtained from different soils (Cambisol, Acrisol) show that the finest and most reactive particles are not visible on the experimental XRD profile of the clay fraction whereas their relative proportion range from about 15 to 33 wt.% of the clay fraction. The finest sub-fractions (<0.05, 0.05-0.1 µm) are mainly composed by MLMs with low coherent scattering domain size and MLMs are also the dominant clay minerals of the clay fraction. In addition, the increase proportion of swelling layers in MLMs with the decrease in their particle size leads to a large increase of the cationic exchange capacity (from 21 cmol<sub>c</sub> kg<sup>-1</sup> for 0.2-2 µm fraction to 51 cmol<sub>c</sub> kg<sup>-1</sup> for <0.05 µm fraction of the Acrisol). Based on the relative contribution and the crystal structure of the different clay phases, the key role plays by MLMs in soils can be assessed.

Hubert, F., Caner, L., Meunier, A. & Ferrage, E. 2012. Unraveling complex <2 µm clay mineralogy from soils using X-ray diffraction profile modelling on particle-size sub-fractions: implications for soil pedogenesis and reactivity. *American Mineralogist*, 97, 384–398.

Viennet, J.-C., Hubert, F., Ferrage, E., Tertre, E., Legout, A., Turpault, M.-P., 2015. Investigation of clay mineralogy in a temperate acidic soil of a forest using X-ray diffraction profile modeling: beyond the HIS and HIV description. *Geoderma*, 241–242, 75–86.

## **Influence of cropping practices on clay mineralogy: insights from the Morrow Plots experimental fields**

Eleanor Bakker<sup>1</sup>, Bruno Lanson<sup>1</sup>, Tauhid Belal Khan<sup>1</sup>, Fabien Hubert<sup>2</sup>, Nathaniel Findling<sup>1</sup>, Camille Rivard<sup>3</sup>, and Michelle M. Wander<sup>4</sup>

<sup>1</sup>ISTerre, CNRS – Univ. Grenoble Alpes, 38000 Grenoble, France – eleanor.bakker@ujf-grenoble.fr;

<sup>2</sup>IC2MP, CNRS – Univ. Poitiers, 86000 Poitiers, France;

<sup>3</sup>European Synchrotron Radiation Facility, 38000 Grenoble, France;

<sup>4</sup>Natural Resources and Environmental Sciences, Univ. of Illinois, Urbana, IL, 61801, USA

The Morrow Plots were established at the University of Illinois in 1876 to answer agricultural questions. They are the oldest agronomic experiment fields in the US with a recorded history of cropping practices. The exceptional series of samples thus represent a unique opportunity to investigate both short- and long-term influence of cropping practices on the status of potassium, an essential plant nutrient. As clay minerals, together with K-feldspars and micas, represent a major K reservoir for plants their mineralogy is likely to be impacted by K uptake during plant growth.

In 2012, top soils were sampled from four plots representing continuous corn crops (CC) and corn-oats-fodder rotations (CR), both with and without fertilization. 2.0-0.2  $\mu\text{m}$ , 0.2-0.05  $\mu\text{m}$ , <0.05  $\mu\text{m}$  sub-fractions were separated and X-rayed in their Ca-saturated form. X-ray diffraction patterns were simulated using a trial-and-error approach to determine structure models for discrete and mixed layer contributions and to quantify their relative contributions.

Discrete chlorite, kaolinite, and chlorite are present in all samples together with randomly interstratified illite-expandable (ill-exp), kaolinite-expandable (kaol-exp), and chlorite-expandable (chl-exp). The relative content of discrete minerals decreases with decreasing size fraction. In all samples, illite and ill-exp dominate the 2.0-0.2  $\mu\text{m}$  fraction, the global proportion of these two contributions decreasing with decreasing size fraction, whereas the relative proportion of kaol-exp increases.

The behavior of illite and ill-exp contributions is most relevant with respect to the fate of K in these soils. When considered globally these two contributions are similar for each fraction of the different samples. The 2.0-0.2  $\mu\text{m}$  fraction of the CR samples is dominated by illite, however, whereas ill-exp dominates in CC samples. The contrast between CC and CR samples is less pronounced for finer fractions.

Illite thus appears most degraded, and possibly transformed to ill-exp, in CC plots compared to CR ones. This effect is enhanced when size fraction is decreased likely owing to the increased specific surface areas of the finest fraction which promotes K uptake by plants. Formation of kaol-exp appears as a major process in these soils and kaol-exp dominates the finest fractions of all samples.

Further sampling of the same plots in 2013 and 2014 has provided samples over the complete crop-rotation cycle, thus allowing the short-term effects due to the different crops to be investigated using the same method of trial-and-error simulation of X-ray diffraction patterns obtained from Ca-saturated clay subfractions.

## **A quantitative survey of sub-Saharan Africa soil mineralogy and its relationship to soil micronutrients**

Mercy Nyambura<sup>1,\*</sup>, Stephen Hillier<sup>2</sup>, Keith D. Shepherd<sup>1</sup>, Esala Martti<sup>4</sup> and Michael Gatari<sup>3</sup>

<sup>1</sup>World Agroforestry Centre (ICRAF), United Nations, Nairobi, Kenya.

<sup>2</sup>The James Hutton Institute, Aberdeen, Scotland.

<sup>3</sup>Institute of Nuclear Science, College of Architecture and Engineering, University of Nairobi, Nairobi, Kenya

<sup>4</sup>Natural Resources Institute Finland (Luke)

\*m.nyambura@cgiar.org

Soil micronutrients are primarily made available through geochemical and pedochemical weathering processes of parent materials, and their total contents in soils usually reflect the composition of materials from which they have been derived. In Africa, there is a wide variety of soils ranging from old, highly weathered soils and aeolian sands with an inherently low fertility to more recent soils formed from volcanic and tectonic rejuvenation with larger nutrient capital reserves. This study aims to establish the prevalence of low soil micronutrient levels in Africa soils and test whether levels are associated with distinct clusters associated with soil mineralogy. Mineral composition was determined at a semi-quantitative level on 1,300 samples from 55 randomly located sentinel sites, covering 21 countries. Natural clustering of mineralogy and their relationships with available micronutrient contents are explored.

## Are interlayered clay minerals important for phosphorus adsorption in agricultural soils?

Ann Kristin Eriksson<sup>1</sup>, Stephen Hillier<sup>2</sup>, Dean Hesterberg<sup>3</sup>, Magnus Simonsson<sup>1</sup> and Jon Petter Gustafsson<sup>1,4</sup>

<sup>1</sup>Department of Soil and Environment, Swedish University of Agricultural Sciences, Uppsala, Sweden

<sup>2</sup>Environmental and Biochemical Sciences, The James Hutton Institute, Aberdeen, Scotland

<sup>3</sup>Department of Soil Science, North Carolina State University, Raleigh, U.S.

<sup>4</sup>Department of Land and Water Resources Engineering, Royal Institute of Technology, Stockholm, Sweden

Email: ann.kristin.eriksson@slu.se

Phosphorus (P) is an essential nutrient for crop production, but too much P may promote eutrophication. Therefore, P sorption reactions in soil are of great environmental significance. Possible sorbents in soils include hydroxy-Al-interlayered clay minerals. The aims of this study were; (1) to investigate P speciation in the clay fraction from agricultural soils; and (2) to develop a method to quantify the amount of hydroxy interlayering in the clay minerals of the soil.

The soils included in this investigation originate from six different sites used for long-term field experiments in Sweden. From each site, clay fractions from two different fertilization treatments were analysed: one with no fertilization and one in which 30 kg P ha<sup>-1</sup> yr<sup>-1</sup> had been added.

To investigate the P speciation of the clay fraction P K-edge X-ray absorption near edge structure (XANES) spectroscopy was used. Linear combination fitting was used on the XANES results to estimate the relative contribution of different phases. In those unfertilized soil that had a high ratio of oxalate extractable Al to Fe, P was mostly adsorbed to Al-hydroxides in the clay fraction. Further, the XANES results showed that in most of the soils, the P added by fertilization had predominantly been adsorbed to Al-hydroxides.

To investigate the extent of hydroxy interlayering in the clay minerals, four different interlayering indices were evaluated using clay fractions of the mentioned soils and synthetically interlayered trioctahedral vermiculite that was prepared in the laboratory. All indices were based on X-ray diffraction (XRD) patterns obtained after different treatments of the sample. The measurements included; (1) the center of gravity (COG) of diffracted intensity along the axis of *d*-spacing determined in K-saturated samples heated to 300°C; (2) the change in COG upon K-saturation compared to the Mg-saturated samples (Esser, 1990); (3) the intensity ratios of Mg- and K-saturated, where the change in intensity of the 14 Å peak compared to the sum of the 10 Å and 14 Å peaks was evaluated (Matsue and Wada, 1988); and (4) the change in COG during in situ heating between 250°C and 450°C, where the COG at 450°C may serve as an estimate of the stability of the interlayers. The measurements involving COG were made in the range 9.5-15.5 Å. All the investigated indices were able to point out the same soils as having the largest amount of hydroxy interlayering, but varied in their ranking of the remaining soils.

Another tested method, to quantify the amount of hydroxy interlayers, was oxalate extraction of the clay fraction under UV irradiation. However, the XRD pattern of oxalate-extracted clay fractions did not differ noticeably from the unextracted ones. Clay fractions with high amounts of hydroxy interlayers according to XRD also had higher amounts of oxalate extractable Al in the clay fraction. This result indicated that clay fractions with high amounts of hydroxy interlayers also may contain significant amounts of free Al-hydroxides. It remains to clarify whether P-sorption to Al-hydroxy minerals primary takes place in Al-hydroxy interlayers of clay minerals or on free Al-hydroxides in the clay fraction.

Esser, K.B., 1990. X-ray-diffraction indexes for relative quantification of interlayering in phyllosilicates. *Soil Science Society of America Journal*, 54, 923-926.

Matsue, N., Wada, K., 1988. Interlayer minerals of partially interlayered vermiculites in dystrochrepts derived from tertiary sediments. *Journal of Soil Science*, 39, 155-162.

## Soils response to critical zone gradients at ecosystem scale: mineralogical and geochemical data

A.O. Alekseev<sup>1</sup>, T.V. Alekseeva<sup>1</sup>, P.I. Kalinin<sup>1</sup> and M. Hajnos<sup>2</sup>

<sup>1</sup> Institute of Physical, Chemical, and Biological Problems of Soil Science, Russian Academy of Sciences, Pushchino, Russia, (alekseev@issp.serpukhov.su)

<sup>2</sup> Institute of Agrophysics, Polish Academy of Science, Lublin, Poland

The complex investigation of soils from two bioclimatic zone of Russia (Moscow region) were determined with the main goal to investigate the role of the mineralogical composition in the transformation and fractionation of soil organic matter and study weathering processes in soils along global gradients of environmental change; e.g. in land use and climate. First is the Southern taiga subzone (Prioksko-Terrasny Biospheric National Reserve) with two sod-weakly podzolic soils (Albeluvisol Umbric, ST profiles) under mature deciduous forest and grassland. The second set with tree grey forest soils (Phaeozem Luvic, DF profiles) under secondary deciduous forest, grassland and cropland. Detailed measurements of mineralogy and chemistry (XRD, XRF and FTIR), surface area, porosity, organic matter, carbon/microbial biomass, moisture content, monitoring of total soil respiration (CO<sub>2</sub> emission from soil surface) are executed.

Grey forest soils (Phaeozem Luvic) are loamy textured. The maximum OC concentration (3.63%) was obtained for the top layer of DF-1 (under forest) followed by the grassland (DF-2) where value was 2.60 %, and the least OC concentration (1.16%) occurred in the cropland (DF-3). Granulometric sub-fractions analysis data show that the maximal concentrations of OC and N are in 2 sub-fractions, i.e. > 100 µm and the clay fraction (< 2 µm). The main minerals in bulk mineralogical composition of soil samples are: quartz (30-40 %), two kinds of feldspars (K- feldspar and plagioclase (20-33 % and upto 15 % respectively) and 2: 1 layer silicates (smectites and mica) – 20-30 %. All tree profiles are developed from the parent material with the similar mineralogical composition where the low-charged dioctahedral smectite – montmorillonite (51-56 %) The second mineral phase is dioctahedral hydromica (28-32 %), additionally clay fractions contain kaolinite and vermiculite. In the upper 1 m of the studied soil profiles smectite concentration is reducing and reaches 22-31 % in topsoils being the largest in DF-1 and the smallest in DF-3. In this part of the profile, smectite is the component of the irregular-interstratified mica-smectite phase. Simultaneously with the decreasing of smectites in the upper parts of profiles the increasing of mica content takes place and reaches 49-53 % in A-horizons. The intensity of the given process is increasing as the following: DF-1 < DF-2 < DF-3. The specific feature of the vermiculite from DF-1 profile (under forest) is its HIV nature - the development of the hydroxyl-interlayers. This process takes place within the upper 80 cm of this profile and has not observed in other two profiles: DF-2 and DF-3.

The content of clay fractions in all studied soils is relatively low - 3-20 %, being the largest in the DF and smallest in ST profiles. As the general found trend, we can conclude that clay fractions in a comparison with bulk soils samples are enriched in both OC and N. Minimal OC and N is in 10-100 µm fraction. The stable large values were for clay fractions, for which all values are within the small range: 4-6 % OC and 0.4-0.8 % for N. For all studied soils C/N values are the smallest for clay fractions and are increasing with the increasing of the particle size. Large N concentrations and small C/N values found for clay fractions (natural organo-minerals complexes) from all studied soils can be explained by the large affinity of N-compounds (amino acids, amino-sugars etc.) towards the surfaces of clay minerals.

Statistical relationship of the soil mineralogy, geochemistry, porosity, soil organic matter, total soil respiration, along gradients at ecosystem scale will be discussed.

## The search for soil hydroxy-interlayered vermiculites: A case for data stewardship

Carolyn Olson

USDA-OCE-Climate Change Program Office, Washington, DC, USA, colson@oce.usda.gov

Data stewardship includes all aspects of information management that preserves data, improves data quality and provides long-term accessibility to data element content and to metadata. Today this would include an electronic metadata storage library for instrumentation, analytical techniques, and modeling. Why is data stewardship so important to scientists? Field data collection and subsequent laboratory analyses are two of the most expensive aspects of research. In the earth sciences, there is the potential for collection site depletion, site contamination, and access denial due to liability and other landowner concerns.

Years ago, I attempted to understand why so few instances of hydroxy-interlayer vermiculite had been reported in the literature. After searching published papers on hydroxy-interlayer vermiculite to find parameters in common, a few facts emerged. Studies reporting the mineral were largely related to weathered materials, particularly acidic soils. Aluminum seemed to play a role. Beyond that, paper after paper yielded various factors about the mineral but not enough comparable information to systematically eliminate or confirm a natural physio-chemical environment responsible for formation, or in some cases, whether authors were even reporting on the same mineral. Many of the missing parameters should have been known to the authors but were not recorded in the journal article or available elsewhere. Undoubtedly, a great deal of data was collected in every one of those early research projects. “Big data” became smaller and smaller sets of data as I applied my requirements for my investigations to the available literature. My questions could not be answered in a statistical manner.

In some ways, we are in a much better position today to record and preserve valuable data sets than years ago. Our computing systems and data storage capacities are exponentially better equipped to preserve data in so many different formats and those systems are improving daily. However, a new problem has developed. Researchers are struggling with the massive amount of information available and the need to synthesize that data to understand what has been accomplished and where the gaps lie. The issues today are not so much can we preserve the data, but can we must track what we have collected in a systematic way with standard sets of requirements to preserve and aggregate *quality* data sets for future use. Decreasing research funding makes this critically important because we will find it necessary to use data sets to their fullest. In the future, we may not have the luxury to collect and analyze materials ourselves but only to rely on existing data sets. We also cannot predict new uses or technology that may be on the horizon needing irreplaceable data collected in the past. But we can begin with systematic reviews that follow strict standards for evaluating and combining data sets from different studies on a particular topic. Including meta-analyses applying statistical relations to the data gathered during the review process would add new dimensions to the process. This is not a simple literature review of research to which we’re all accustomed. This is a new direction for organizing data for the future.

## Reverse weathering in soils: a case study

Atsuyuki Inoue, Minoru UTADA<sup>2,\*</sup>, and Tamao HATTA<sup>3</sup>

<sup>1</sup>Department of Earth Sciences, Chiba University, Chiba 263-8522, Japan; atsuyuki\_inoue@faculty.chiba-u.jp

<sup>2</sup>Futo Onoma 912-14, Ito 413-0231, Japan; \*deceased

<sup>3</sup>Japan International Research Center for Agricultural Science, Tsukuba 305-8686, Japan

Weathering is the result of water-rock interactions in open system under the Earth's surface conditions. With progressing water-rock interaction primary minerals of rocks decompose while specific clays and other particulate minerals like (oxy-) hydroxides and oxides form newly. Elemental redistribution is concomitant with mineral alteration; mobile elements like alkali and alkaline earth elements are removed from the system, whereas immobile (or inert) elements (e.g., Al, Fe, Ti) are left to accommodate into (oxy-) hydroxide and oxide minerals. As a consequence, vertical zonal distribution of minerals and elements is established in the weathering crust which covers on the primary rocks. Soil is defined as a horizon that occupies on the uppermost part of developing weathering crust. Soils are ecologically important not only for plants, insect, and animals but also for humankind because the soil is situated at an active interface which faces directly our living sphere. In general, primary minerals of rocks alter to secondary ones with progressing water-rock interactions in the following order: mica, feldspar → illite, I-V, I-S interstratified minerals, vermiculite, smectite → kaolinite → gibbsite. The order is characterized by desilicification series. On the other hand illite, hydroxyl interlayered vermiculite (HIV), and/or smectite (HIS) are often found in the uppermost horizons of mature soils. They are not relics. The occurrence of such minerals is apparently inconsistent with the above weathering trend through water-rock interaction. This results from the reverse weathering which was derived by interactions between biocycling system and clay minerals in the uppermost horizon of soils (Velde and Barré, 2010).

In the present communication, we describe the occurrence of HIV in the uppermost part of weathering crust which developed in metamorphic, granitic, and sedimentary rocks in the southwestern area of Japan. We recognized two types of weathering series of primary minerals, i.e., from feldspar to halloysite and from micas to regularly interstratified I-V or I-S, finally to dioctahedral vermiculite, the two series which are considered as products of usual water-rock interactions. The minerals distribute regularly following the different altitudes of eroded surfaces with low relief. HIV minerals of interest appear characteristically in the mostly weathered soil horizons associated with dissolving halloysite and concentrating K<sub>2</sub>O and SiO<sub>2</sub> in bulk composition. This suggests that halloysite which formed from feldspars is further dissolved by continuing water-rock interactions in the uppermost part of soil, while micas and/or HIV are neoformed or at least the weathering is retarded by bio-clay minerals interaction.

Velde B. and Barré P. (2010). *Soils, Plants and Clay Minerals*. Springer.



## Influence of particle size on the experimental Al-hydroxylation of K-vermiculite

Jean-Christophe Viennet<sup>1,2</sup>, Fabien Hubert<sup>1</sup>, Emmanuel Tertre, and Marie-Pierre Turpault<sup>2</sup>

<sup>1</sup> IC2MP-HydrASA, Bât B8. - TSA 51106, 5, rue Albert Turpain, 86073, Poitiers Cedex 9, France

<sup>2</sup> INRA, UR 1138 « Biogéochimie des écosystèmes forestiers », centre INRA de Nancy 54280 Champenoux, France,  
jean.christophe.viennet@univ-poitiers.fr

In acidic soils, the Al-hydroxylation process is most often described as resulting from the adsorption of aluminium and its subsequent polymerization in the interlayer of swelling clay minerals. Formation of these hydroxy-interlayered (HI) layers leads to a decrease of the cation exchange capacity of the soil.

Recently, X-ray diffraction profile modelling technique has been used to characterize the amount of HI layers and their distribution in the different sub-fractions (<0.05, 0.05-0.1, 0.1-0.2, 0.2-2 µm) of the bulk <2 µm fraction from the surface horizon of a forest Aluminic Cambisol (Viennet et al, 2015). The results showed that the amount of HI layers decreases with the size of particles. Moreover HI layers were shown to be distributed among complex illite-HI-expandable layer mixed layer minerals (MLMs).

In order to provide additional information on the formation mechanism of such complex HI-MLMs, an experimental auto-aluminisation study was undertaken. Three size fractions of K-saturated Santa Olalla vermiculite (0.1-0.2, 1-2 and 10-20 µm) were submitted to dissolution in a flow-through trough reactor in HCl at pH = 3. The degree of mineral transformation as a function of time was followed from both the chemical analysis of solutions and solid characterization using X-ray diffraction.

The results showed that K-vermiculite transforms into MLM constituted by original K-vermiculite layers, together with HI and expandable layers. The extent of transformation increases when the particle size decreases leading to the same general trend as observed previously in natural media.

Viennet J.-C., Hubert F., Ferrage E., Tertre E., Legout A. and Turpault M.-P. (2015). Investigation of clay mineralogy in a temperate acidic soil of a forest using X-ray diffraction profile modeling: Beyond the HIS and HIV description. *Geoderma*, **241–242**, 75–86.

## Textural and chemical controls in the formation of a clay-carbonate system in a volcanic soil

Javier Cuadros<sup>1</sup>, José L. Díaz-Hernández<sup>2</sup>, Antonio Sánchez-Navas<sup>3</sup>, Antonio García-Casco<sup>3</sup> and Jorge Yepes<sup>4</sup>

<sup>1</sup>Department of Earth Sciences, Natural History Museum, Cromwell Road, London SW7 5BD, United Kingdom,  
j.cuadros@nhm.ac.uk

<sup>2</sup>IFAPA, Área de Recursos Naturales, Consejería de Agricultura, Pesca y Medio Ambiente, Junta de Andalucía, 18080 Granada,  
Spain

<sup>3</sup>Departamento de Mineralogía y Petrología-IACT, Universidad de Granada-CISC, 18071 Granada, Spain

<sup>4</sup>Departamento de Ingeniería Civil, Universidad de las Palmas de Gran Canaria, 35017, Las Palmas de GC, Spain

Weathering of basaltic tephra under arid-semiarid conditions in the Gran Canaria island (Canary Islands) produced soils containing sepiolite, palygorskite and quartz together with large amounts of calcite and calcian dolomite. There is a marked sequence of mineral abundance, with sepiolite and calcite forming in the upper soil horizons and palygorskite and dolomite occurring in the lower levels. Smectite also occurs in the lowest soil levels. Carbonate formation was due to biological activity and secretion of CO<sub>2</sub>. Textural, mineralogical and chemical analyses of the soil profile indicate that sepiolite and calcite precipitated within the interstitial space between altered tephra grains, consuming Si, Ca and Mg from both the surrounding dissolving tephra and percolating water run-off. Palygorskite, smectite and dolomite formed within tephra grains, although dolomite crystals grew down in the soil profile until dolomite became by far the most abundant mineral phase. The study shows the chemical and textural control on clay and carbonate formation at micro-metric scale with great resolution and is relevant to the “dolomite problem”, i.e., to the low levels of dolomite formation in recent systems as compared to ancient environments.

## Opaline silica in cold climate

Elena Kuznetsova<sup>1</sup> and Motenko Rimma<sup>2</sup>

<sup>1</sup>Norwegian University of Science and Technology (NTNU), Trondheim, Norway, Elena.kuznetsova@ntnu.no

<sup>2</sup>Lomonosov Moscow State University, Moscow, Russia

Laminar opaline silica with a typical disc shape was discovered for the first time in the volcanic soils developed less than 500 years ago at Hokkaido, Japan. This opal was mostly found in the 0.2-5  $\mu\text{m}$  fractions and had a pedogenic origin. Laminar opaline silica has also been found in volcanic soils at Tohoku, Kanto and Kyushu, Japan; Papua New Guinea; Oregon, USA; and in New Zealand. Henmi and Parfitt (1980) concluded that opaline silica is characteristic of the early stages of weathering of volcanic ash in the humid temperate climatic zone. Our observations of volcanic tephra show that cold humid climates and permafrost can preserve opaline silica.

The volcanic tephra used in our investigation was preserved in cold and humid climate of Kamchatka, Far-East of Russia, in the area where permafrost and periglacial processes are widespread. Volcanic ash was erupted mostly in the Quaternary and the upper part of the early Pleistocene. IR analysis showed the presence of opaline silica in all samples.

Opaline silica was present as very fine particles and these could only be seen clearly at high magnification using transmission electron microscopy (TEM). TEM micrographs showed that the opaline silica particles are spherical in form and are closely packed in microaggregates (Fig. 1). The forces and processes involved in the aggregation of the particles are not entirely understood, but there are suggestions that the long range electrostatic repulsion force and the short range van der Waal's forces are the major forces that predetermined the configuration of the aggregate made up of spheres. The opaline silica particles are extremely small; the size of each particle can be up to 10-20 nm.

Some TEM images showed a corroded edge of the opaline silica around glass particle which suggests that dissolution occurs during weathering. The completely altered soft zone is filled with spherical bodies and these are characteristic of opaline silica (Figure 1). These particles differ from glass fragments which are more angular and larger. The elemental composition of the opaline silica showed the chemistry of opals linked it to that of the host volcanic rock, even if modified by weathering processes. Opal is not a pure form of silica, as it contains water as a component and various impurities and trace elements can also enter its structure. The most common impurity in our samples was Al, which substitutes for Si, as well as Ca, K, Mg, Fe and Na were also presented. The most common trace element was Ti.

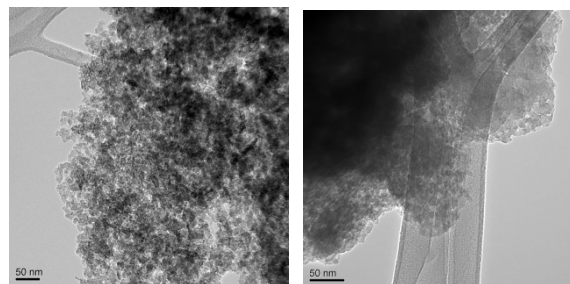


Figure 1. Opaline silica

Henmi T. and Parfitt R.L. (1980). Laminar opaline silica from some volcanic ash soils in New Zealand. *Clays and Clay Minerals*, 28, 57-60.

## Weathering and soil formation on ultramafic rock (Polar Ural, Russia)

Sofia Lessovaia<sup>1</sup>, Michael Plötze<sup>2</sup> and Yury Polekhovsky<sup>1</sup>

<sup>1</sup> St. Petersburg State University, Institute of Earth Sciences, 199178, V.O., 10 line, d.33, St. Petersburg, Russia,  
lessovaia@yahoo.com

<sup>2</sup> ETH Zurich, Institute for Geotechnical Engineering, CH-8093 Zurich, Switzerland

The identification of mineral associations as either inherited from parent substrate, or newly formed in soil, or as result of primary mineral transformation affected by pedogenesis is one of the problems of modern soil mineralogy. This problem was investigated on: (i) permafrost affected soils - mature profile of Haplic Cryosol (Reductaquic) and (ii) weakly developed Haplic Regosols (Eutric) in the Rai-Iz massif that is made up of ultramafic rocks. Both study plots were located in the mountainous tundra of the Polar Urals (Russia). The mature profile was found on the flat summit where soil fine earth has accumulated upon blocks of serpentinous dunite that behave as aquifuges. The weakly developed soil has formed on the slope covered by colluvial blocks of this serpentinous dunite.

Mineral association of the rock fragments from soil horizons and blocks on the surface were studied in thin sections by optical microscopy. The mineralogical composition of the rocks and the soil was determined by X-ray diffraction with subsequent Rietveld analysis and FTIR spectroscopy.

As expected, olivine is the predominant (almost 40 wt.%) mineral in serpentinous dunite. The proportion (almost 30 wt.%) of the serpentine identified as antigorite reflects the serpentinization of the rock. Besides these minerals talc, chlorite, amphibole, and traces of pyroxenes, magnetite, and quartz were determined. Serpentinous dunite is one of the most weatherable rocks. It's weathering is reflected by reddening of the rock due to the formation of X-ray amorphous Fe-oxides (approx. 10 wt.%) in the micro-cracks in the olivine, serpentine, and chlorite.

Chlorite, talc, and serpentine minerals were found in the fine size fractions of the soil profiles have inherited from the ultramafic substrate. The significant proportion of quartz in the fine size fractions of soils, although only traces were found in the rock as well as the presence of micas illustrate the influence of allochthonous material. Besides these minerals, vermiculite and smectite(s) were found in the soil but are absent in the rock. The vermiculite, which occurs in the upper horizon of the mature profile, is most probably a result of the chlorite transformation affected by pedogenesis. Distribution of smectite(s) in soil profiles as a result of soil formation is usually more pronounced in mature profile. The appearance of this mineral in the weakly developed soil profile illustrates the soil formation from "mature" fine earth from weathering of high sensitive rock.

The work was supported by RFBR (project N 14-04-00327) and St. Petersburg State University

**THURSDAY  
POSTER  
SESSION**

POSTERS SESSION: THURSDAY + FRIDAY, 9th–10th July

Title and authors	Page no.
<b>Clays in the Critical Zone soils, weathering and elemental cycling</b>	
The use of the clay mineralogy as a paleoclimate tool: An example of the kaolinite rich-Weald facies in the Iberian Chains (NE Spain) <u>Blanca Bauluz</u> , Alfonso Yuste and María José Mayayo	366
Effect of peptides and amino acid adsorption on montmorillonite, illite and illite-smectite mixed layer clays <u>Karin A. Block</u> , Al Katz, Paul Gottlieb and Jeffrey LeBlanc	367
Land erosion and associated evolution of clay minerals assemblages in Mediterranean region (Southern Turkey): Amik Lake <u>Meriam El Ouahabi</u> , Aurélia Hubert-Ferrari, Helene Le Beau, Nathalie Fagel and Volcan Karabacak	368
Reactivity of Vertic dark soil towards applications of pesticides cocktails E. Dumas, Zemelka, G., T. Alekseeva, Y. Kolyagin, M. Sancelme, <u>C. Forano</u> and P. Besse-Hoggan	369
Warm kaolins in Scotland Adrian M. Hall, <u>H. Albert Gilg</u> , Anthony E. Fallick, and Jon W. Merritt	370
How elements, including heavy metals, behave during weathering in tropical climate? The case of Cretaceous and Messinian palaeosoils of Sardinia, western Mediterranean (Italy) <u>Paola Mamelì</u> , Giovanni Mongelli, Rosa Sinisi and Giacomo Oggiano	371
Particle-lacing in an Alpine stream <u>Michael Plötze</u> , Daniela König and Gerhard Furrer	372
<b>Clay and fine particle based materials for environmental technologies and clean up</b>	
Competitive adsorption of mixed contaminants on metal-immobilising organoclay (MIOC): Implication in the biodegradation of polyaromatic hydrocarbons (PAHs) <u>Bhabananda Biswas</u> , Binoy Sarkar, Asit Mandal, Ravi Naidu	373
Hydration properties of a montmorillonite saturated with octylammonium cations: Effect of the alkyl-chains number and surfactant concentration <u>Valéria Bizovská</u> , Ľuboš Jankovič and Jana Madejová	374
Photoactive hybrid material based on kaolinite grafted with a reactive laser dye Samuel Sas, Martin Danko and <u>Juraj Bujdák</u>	375
Natural and synthetic modified clays as perspective soil amendments for remediation of soil contaminated with metals <u>Juris Burlakovs</u> , Ruta Ozola, Zane Vincevica-Gaile and Karina Stankevica	376
Ordered Functional Heterostructures via Simple Intercalation Reactions <u>Christoph Habel</u> , Matthias Stöter, Bernhard Biersack, Rainer Schobert and Josef Breu	377
Dye solution discoloration by Fe-loaded Bustos clay catalyst <u>W. Hajjaji</u> , S. Andrejkovičová, D.M. Tobaldi, J. A. Labrincha and F. Rocha	378
Smectite-fungicide complex as a potential smart delivery system for slow release formulation: Environmental advantages Inés M. Aguilar, Rafael Celis, Juan Cornejo, <u>M. Carmen Hermosín</u>	379
Synthesis and modification of layered double hydroxides (LDHs) as mycotoxin binders <u>Chun-Chun Hsu</u> and Youjun Deng	380
Molecular modelling of CdS-CTA <sup>+</sup> -MMT nanoparticles <u>M. Pospíšil</u> , M. Pšenička, P. Kovář and P. Praus	381
MOPS – A New Class of Functional Hybrid Materials <u>Martin A. Rieß</u> , Markus M. Herling, Mathias Schwedes, Hussein Kalo, Rainer Schobert, Josef Breu	382
Synthesis of surfactant-modified montmorillonites for adsorption of perchlorate Wuhui Luo and <u>Keiko Sasaki</u>	383
Clay-based nanocomposite coating for flexible optoelectronics applying commercial polymers <u>Jasmin Schmid</u> , Daniel A. Kunz, Patrick Feicht, J. Erath, A. Fery, Josef Breu	384

POSTERS SESSION: THURSDAY + FRIDAY, 9th–10th July

H <sub>2</sub> S fixation at mineral surfaces under supercritical CO <sub>2</sub> conditions in aqueous and quasi-dry systems <u>Theodor Alpermann</u> and Christian Ostertag-Henning	385
The water purification program using the redox properties of green rusts related minerals, fougérite and trébeurdenite <u>Jean-Marie R. Génin</u> , Georges Ona-Nguema, Christian Ruby and Stuart Mills	386
<b>Bentonites linking clay science with technology</b>	
Thin bentonite beds in Neogene lakes/lagoons, northern Israel – effects of detritus and early diagenesis <u>Amir Sandler</u> , Alexis G. Rozenbaum, George Christidis and Pagona Makri	387
Mineralogical and smectite layer charge systematics in a bentonite profile from Milos Island, Greece Pagona Makri and <u>George. E. Christidis</u>	388
Evaluation of bentonites of Turkey and an investigation of their utilization in ceramic tile manufacturing <u>Cengiz Ozgur</u>	389
10 years of exploitation: still the same Kopernica bentonite? <u>Renata Adamcova</u> , Franz Ottner, Karin Wriessnig and Jana Deliova	390
EPSP – Experimental Pressure and Sealing Plug as part of the European DOPAS project <u>Irena Hanusová</u> , Jiří Svoboda and Petr Večerník	391
Alteration and mechanical behavior of bentonite immersed in NaOH and Ca(OH) <sub>2</sub> solutions <u>Yasutaka Watanabe</u> and Shingo Yokoyama	392
A non-linear elastic approach to modelling the hydro-mechanical behaviour of the SEALEX laboratory tests on compacted MX-80 bentonite <u>Andrew Fraser Harris</u> , Chris McDermott, Alex Bond, Kate Thatcher and Simon Norris	393
Mineralogy and chemistry of illites in Late Devonian K-bentonites, NW Turkey Ömer Bozkaya, <u>Asuman Günal-Türkmenoğlu</u> , M. Cemal Göncüoğlu <u>Özge Ünlüce</u> , İsmail Ömer Yılmaz	394
Physico-chemical properties of bentonite from Rokle deposit (Czech Republic) in temperature range of 20-95 °C <u>Petra Fůrychová</u> , Miroslav Honty, Tomáš Kuchovský, Marek Osacký, Dana Kuchovská and Arno Grade	395
Structural Incorporation of Al into Diatomite and Its Influence on the Surface Solid Acidity of Diatomite <u>Dong Liu</u>	396
Elaboration and characterization of materials obtained by pressing of vermiculite without binder addition <u>L. Duclaux</u> , A-N. Nguyen, F. Balima, L. Reinert, F. Muller, S. Le Floch, V. Pischedda, A. San Miguel	397
Fines from aggregate quarrying and its influence on frost protection in roads <u>Elena Kuznetsova</u> and Svein Willy Danielsen	398
Natural zeolite as filler for metakaolin geopolymers <u>Slávka Andrejkovičová</u> , Walid Hajjaji and <u>Fernando Rocha</u>	399
REE recovery from kaolinite-rich saprolite and a clayish horizon related to the Serra Dourada granite, Brazil: potential for ion-adsorption type deposits <u>Igor V. Santana</u> , Frances Wall and Nilson F. Botelho	400
Production of refractory aggregates from waste chamotte and industrial clays Stavroula Kavouri, <u>Michael G. Stamatakis</u> and Efthimios Kagiaras	401
Solid State NMR study of multiple extra-frameworks cationic sites in hybrid geopolymer systems <u>Martina Urbanova</u> , Libor Kobera, Barbora Dousova and Jiri Brus	402
Effect of temperature on surface properties of rehydrated metakaolinites <u>Miloslav Lhotka</u> , Barbora Doušová, Vladimír Machovič and Libor Kobera	403
<b>The many faces of chlorite</b>	
Chlorites from the Faina and Serra de Santa Rita greenstone belts (Goias, Brazil) <u>Raquel Guimarães da Silva</u> , Edi Mendes Guimarães, Caio Aguiar, Jérémie Garnier, Adalene Moreira Silva, and Catarina Labouré Bemfica Toledo	404

POSTERS SESSION: THURSDAY + FRIDAY, 9th–10th July

Oscillatory chemical zoned chlorite from a hydrothermal vein, Pic-de-Port-Vieux thrust, Pyrenees, Spain Vincent Trincal, Pierre Lanari, <u>Martine Buatier</u> , Brice Lacroix, Delphine Charpentier, Pierre Labaume and Manuel Muñoz	405
Measurement of Fe oxidation state in chlorite by electron energy-loss spectroscopy <u>Takeshi Kasama</u> , Sayako Inoue and Toshihiro Kogure	406
<i>Pietra ollare</i> (chlorite-schist) artefacts from Červar Porat (Istria, Croatia) – comparison with possible source rocks <u>Darko Tibljaš</u> , Balen Dražen, Maja Vučković and Zrinka Šimić-Kanaet	407
The role of clays and carbonates in the palaeoenvironmental reconstruction of Miocene deposits in the Daroca Basin (Spain) <u>Manuel Pozo</u> , José Pedro Calvo, Juan Emilio Herranz and Pablo Peláez-Campomanes	408
Authigenic Mg-sudoite and Mg trioctahedral chlorite in Permian reservoir red-beds, SW Poland <u>Julita Biernacka</u>	409
Authigenic chlorite and chlorite-smectite mixed layer as indicator of increasing reducing condition in the Huincul Formation: Neuquén Basin, Argentina M.J. Pons, A. Rainoldi, <u>D. Beaufort</u> , P. Patrier, A. Impiccini and M.B. Franchini	410
<b>Structural characterization of lamellar compounds</b>	
Natural Zn clay mineral characterization combining XRD, SEM and TEM-EDS analyses <u>Martine Buatier</u> and Flavien Choulet	411
Synthesis and crystal structure refinement of one- and two-layer hydrate of sodium-fluorohectorite <u>Matthias Daab</u> , Hussein Kalo, Wolfgang Milius and Josef Breu	412
Nanocage structures derived from cyclodextrin-intercalated layered double hydroxides and their inclusion properties for HAP and phenol compounds <u>Arnaud Di Bitetto</u> , Gwendal Kervern and Cédric Carteret	413
Deciphering the vibrational signature of layered double hydroxides through a joint experimental and theoretical approach <u>Erwan André</u> , Jean Fahel, Arnaud Di Bitetto and Cédric Carteret	414
Insight into the structure of layered zinc hydroxide salts intercalated with dodecyl sulfate anions <u>Petr Kovář</u> , Jan Demel, Jan Hynek, Yan Dai, Christine Taviot-Guého, Ondřej Demel, Miroslav Pospíšil and Kamil Lang	415
Non-ideal stacking in layered systems: contributions to the X-ray powder diffraction profiles of kaolinite <u>A. Leonardi</u> and D. Bish	416
Effect of hydrous perturbation and the soil-pH on the adsorption of etracycline onto Na-montmorillonite <u>Walid Queslati</u>	417
Ordered and disordered carbon from pyrolysed clay-organic intercalates C. Breen, F. Clegg, J. Hrachová, <u>L. Petra</u> and P. Komadel	418
The origin of Al-O-Al defects in Zn-Al layered double hydroxides studied by solid state NMR spectroscopy <u>Suraj S. C. Pushparaj</u> , Andrew S. Lipton, Vanessa Prevot, Claude Forano and Ulla Gro Nielsen	419
Comparison of inverse microemulsion method and conventional pillaring in synthesis of transition metal oxide/montmorillonite nanocomposites <u>Melania Rogowska</u> , Alicja Michalik-Zym, Elżbieta Bielańska, Roman Dula, Daria Napruszewska, Paweł Nowak, Ewa M. Serwicka, Adam Gaweł and Krzysztof Bahranowski	420
XPS and FTIR studies combined with MD simulations of clays and organo-clays <u>B. Schampera</u> , D. Tunega, R. Solc, S. Dultz, S.K. Woche and R. Mikutta	421
Synthesis of saponite with different Si/Al using a heterogeneous hydrothermal method <u>Qi Tao</u> , Dan Zhang, Hongping He, Manyou Chen, Shichao Ji and Tian Li	422
Crystal chemistry of natural Mg-Al-CO <sub>3</sub> layered double hydroxides with variable interlayer spacing <u>Elena S. Zhitova</u> , Sergey V. Krivovichev, Victor N. Yakovenchuk and Igor V. Pekov	423
Physicochemical and catalytic properties of the tin-doped porous clay heterostructures <u>Małgorzata Zimowska</u> , Joanna Olszówka, Jacek Gurgul, Kazimierz Łątka and Ewa Maria Serwicka	424



POSTERS SESSION: THURSDAY + FRIDAY, 9th–10th July

<b>Clay minerals in the oil and gas industry</b>	
Impacts of altered volcanic ash on oil and gas production <u>Christina Calvin</u> and Helena Gamero Diaz	425
Kinetics and geochemical equilibria in the oil window: Concomitant mineralogical and organic geochemical changes in hydrous pyrolysis experiments <u>Christian Ostertag-Henning</u> , Thomas Weger, Kristian Ufer and Stephan Kaufhold	426
Understanding the surface chemistry of oil sands clay minerals: implications for improved extraction and management of tailings. <u>Cliff T. Johnston</u>	427
Complex thermal history reconstruction of the Carboniferous rocks from the Fore-Sudetic Monocline (Poland) - application in a tight gas exploration <u>Sylwia Kowalska</u> , Krzysztof Wolański, Dariusz Botor, Istvan Dunkl, Artur Wójtowicz and Urszula Jonkis	428
Mineralogical and chemical variations in clay minerals as key to decipher hydrocarbon migration in siliciclastic rocks, Neuquén Basin (Argentina) A. Rainoldi, D. Beaufort, <u>P. Patrier</u> , M. Franchini, M.J. Pons and A. Impiccini	429
Effects of clay minerals on the catalytic pyrolysis of amino acids Hongmei Liu, <u>Xiang Zhou</u> , Dong Liu and Peng Yuan	430
<b>Beyond smectite-based nanocomposites</b>	
Photo-oxidative degradation of injection molded polyamide66/sepiolite nanocomposites <u>A. Yebra-Rodríguez</u> , C. Fernandez-Barranco, M.D. La Rubia, A. Yebra, A.E. Koziol and J. Jimenez-Millan	431
Study of spatial distribution of sepiolite in polyamide 66/sepiolite nanocomposites <u>C. Fernández-Barranco</u> , A.E. Koziol, K. Skrzypiec, M. Rawski, M. Drewniak and A. Yebra-Rodríguez	432
Design of novel biocatalysis microreactor based on hierarchical structuration of enzyme/layered double hydroxide/polysaccharide beads Rima Mahdi, Philippe Michaud, Christine Hélaïne, <u>Vanessa Prevot</u> , Céline Laroche, Marielle Lemaire and Claude Forano	433
Urea intercalation of kaolin and bentonite focusing ceramic applications Sahar Seifi, Marthe Tatiana Diatta, Sabine Petit, Philippe Blanchart, <u>Gisèle L. Lecomte-Nana</u>	434
Intercalation into fine crystallites of a layered silicate on monodisperse spherical colloidal silica particles <u>Tomohiko Okada</u> , and Asuka Suzuki	435
Modification of the properties of organophilic-clay by the pretreatment of raw material using a jet mil <u>Makoto Ogawa</u> , Takayuki Hayakawa, Mitsuru Oya, Makoto Minase, Ken-ichi Fujita	436

## The use of the clay mineralogy as a paleoclimate tool: An example of the kaolinite rich-Weald facies in the Iberian Chains (NE Spain)

Blanca Bauluz<sup>1</sup>, Alfonso Yuste<sup>2</sup> and María José Mayayo<sup>3</sup>

Department of Earth Sciences. University of Zaragoza. Pedro Cerbuna 12, 50.009 Zaragoza (Spain). bauluz@unizar.es

Department of Earth Sciences. University of Zaragoza. Pedro Cerbuna 12, 50.009 Zaragoza (Spain). alfon@unizar.es

Department of Earth Sciences. University of Zaragoza. Pedro Cerbuna 12, 50.009 Zaragoza (Spain). mayayo@unizar.es

Clay mineralogy is widely considered to be a powerful tool for interpreting weathering and palaeoclimate (Ruffell et al., 2002; Raucskik and Varga, 2008, and references therein). Palaeoclimatic interpretations based on sedimentary clay assemblages are rooted in the correlation between climate, weathering, and soil formation. However, in old sedimentary series, special care has to be taken because sediment reworking or diagenesis may transform the primary composition and alter the palaeoclimatic signal (Thiry, 2000; Bauluz et al., 2014). Nevertheless, once these effects have been estimated and differentiated, clay minerals such as kaolinite and/or smectite can be successfully used as indicators of humid versus arid conditions for the Mesozoic period (Ruffell et al., 2002; Raucsik and Varga, 2008).

In this research, we have investigated kaolinite-rich clays of the Weald facies (Barremiense, Lower Cretaceous) in the Iberian Chains (NE, Spain) with the aim of determining the origin of the abundant kaolinitic clays and their relationship to the sedimentary environment, palaeoclimate and diagenetic processes. The samples were examined by X-ray diffraction and scanning and transmission electron microscopy, with special emphasis on clay-mineral characterization. The combination of these techniques has allowed determination of the mineral associations, crystal chemical parameters of clays, textural relations and chemical compositions.

The analyzed materials are a mixture of detrital (quartz, micas, and K-feldspars) and authigenic phases (kaolinite, Fe-oxides, gibbsite, dickite, and calcite). Therefore, the mineralogy of the rocks reflects the source area, the sedimentary conditions, and the diagenetic evolution. The most abundant authigenic phases are kaolinites. The combination of XRD and electron microscopy shows that the kaolinites are well crystallized and have as high a degree of ordering as those formed by weathering in palaeosols; this clay formed in the rock matrix, as intergrowths with muscovite, and as vermicular booklets that replaced detrital silicates (eg. K feldspar and quartz) as a consequence of intense dissolution processes. The diagenetic processes have recrystallized kaolinites in the sandstones, producing larger crystallinity indices along with dickite. In contrast, kaolinites from the finer lithologies (claystones and siltstones) probably reflect formation by weathering. The kaolinitization process described, associated with the crystallization of gibbsite and iron oxides, is in agreement with the relatively warm and humid conditions described for the Iberian Range basin in the Early Barremian.

**Acknowledgements:** This research has been funded by the Spanish Ministerio de Economía y Competitividad (CGL2013-16169-C2-1-P), the University of Zaragoza (UZ2012-CIE-05), and the Gobierno de Aragón and the European Social Fund ("Grupos Consolidados").

Bauluz et al. (2014). *Cretaceous Research*, 50, 214-227.

Raucsik & Varga, A (2008). *Paeleogeography Paleoclimatology Paleoeology*, 265, 1-13.

Ruffell et al., (2002). *Philosophical Transactions of the Royal Society of London*, A 360, 675-693.

Thiry (2000). *Earth Sciences Review*, 49, 201-221.

## Effect of peptides and amino acid adsorption on montmorillonite, illite and illite-smectite mixed layer clays

Karin A. Block<sup>1</sup>, Al Katz<sup>2</sup>, Paul Gottlieb<sup>3</sup> and Jeffrey LeBlanc<sup>4</sup>

<sup>1</sup> Department of Earth and Atmospheric Sciences, City College of New York, 160 Convent Avenue, New York, NY 10031 United States

<sup>2</sup> Department of Physics, City College of New York, 160 Convent Avenue, New York, NY 10031 United States

<sup>3</sup> Sophie Davis School of Biomedical Education, 160 Convent Avenue City College of New York, New York, NY 10031 United States

<sup>4</sup> Department of Chemical Engineering, Grove School of Engineering, City College of New York, 160 Convent Avenue, New York, NY 10031 United States

Recent reviews addressing knowledge gaps in how mineral soils stabilize organic matter highlight the need to achieve a better understanding of how mineral composition affects mean residence time of carbon and nitrogen in soils. The discipline's movement away from treatment of organic matter under the catch-all term "humus" stresses the need to document how specific organic compounds interact with clay minerals and which functional groups result in the strongest bonds. This study extends recent work on the interaction between a suite of peptides derived from a casein digest (tryptone) and montmorillonite clay to examine how amino acids interact with illites and illite-smectite mixed layer clays. X-ray diffraction, thermogravimetric analysis and high-resolution transmission electron microscopy revealed that the interaction results in exfoliation of the montmorillonite and shorter range of crystallite domains after adsorption. Our results indicate that the nature of adsorption (intercalation vs. surface adsorption) is concentration-dependent (Block et al. 2015). More surprisingly, the adsorption regime corresponds to an onion-layer scheme where surface-adsorption mediates intercalation and corresponds to a finite amount, approximately 16 wt. %. We also report on similar experiments using peptides and amino acids as employed in the montmorillonite experiments, but utilizing illite and a 70-30 illite-smectite mixed layer clay mineral. We predict that hydrophobic amino acids will intercalate the montmorillonite and illite-smectite mixed-layer clay, and that charged amino acids will strongly adsorb to the surface of the clay.

Block, K. A., Trusiak, A., Katz, A., Gottlieb, P., Wei, H., Alimova, A., Steiner, J. C. "Exfoliation and intercalation of montmorillonite by small peptides". *Applied Clay Sciences*; 107: 173-181. doi: 10.1016/j.clay.2015.01.021

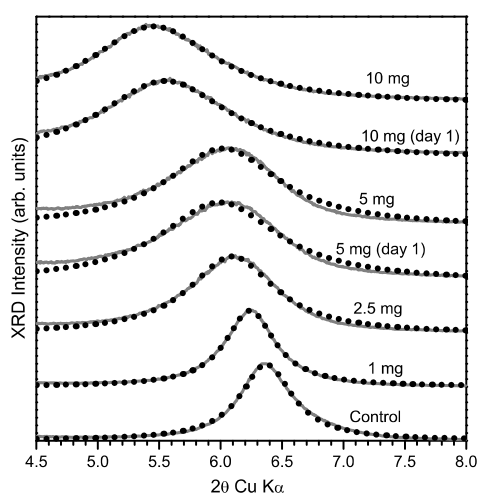


**Fig. 1.** XRD  $d_{001}$  reflections and single-peak Lorentzian least-square fits from montmorillonite reacted with various concentrations of tryptone. Tryptone and montmorillonite were allowed to mix for 3 days except as noted.

## Land erosion and associated evolution of clay minerals assemblages in Mediterranean region (Southern Turkey): Amik Lake

Meriam El Ouahabi<sup>1</sup>, Aurélia Hubert-Ferrari<sup>2</sup>, Helene Le Beau<sup>3</sup>, Nathalie Fagel<sup>4</sup> and Volcan Karabacak<sup>5</sup>

<sup>1,4</sup>University of Liège, Department of Geology, Liège, Belgium, Meriam.elouahabi@ulg.ac.be

<sup>2</sup>University of Liège, Department of Geography, Liège, Belgium

<sup>3</sup>Eskisehir Osmangazi University, Department of Geological Engineering, Eskisehir, Turkey

<sup>4</sup>University of Cologne, Institute of Physical Geography, Germany

In the Mediterranean region, continuous human occupation is recorded in the Amik Basin (southern Turkey) since 6000-7000 BC. The Basin also is crossed by The Dead Sea Fault (DSF), a major neotectonic structure in the Middle East extending from the Red Sea in the south to the East Anatolian Fault Zone in the north. The study focuses on the mineralogy and clay mineralogy record of Amik Lake, which occupies the central part of the Basin. Our objective is to constrain major mineralogical and clay mineral evolution in the area over the last 4000 years and assess how soil formation is related to possible human impact.

Sediments were collected at 1 to 2 cm intervals in core sediments up to a depth of 6 meters in the clay deposits. Geochemistry (XRF), mineralogy (XRD) and clay mineralogy were applied to study the sediment records. The age of the record was constrained by combined radionuclide and radiocarbon dating.

Chemical and mineralogical composition of the sediments is quite diverse reflecting the significant geological variation of drainage basins. Abundant mixed-layer and partly disordered minerals characterize different soil levels recorded in those sediments. Levels relatively rich in chlorite, illite and quartz are interpreted as corresponding to relatively dry periods, while more humid periods lead to more intensive weathering and consequently to the dominance of clay minerals more advanced on the relative stability scale, such as kaolinite. Smectite is taken to indicate a climate with contrasting seasons and a pronounced dry season.

The sedimentary record clearly shows two periods indicating strong soil erosion in the Lake catchment. The most recent erosion phase is modern. The oldest one would have occurred during the late Bronze period. The first older period is attributed to a strong aggradation period linked to a major increase in erosion. Our study shows that this episode has specific characteristics: mixed-layer clay mineral, high percentages of Ni, Cr and Mg coupled with significant amount of organic matter of terrestrial origin. Ni and Mg most probably come from the Amanos Mountains ophiolite belt indicating intensive upland cultivation and possible exploitation of its mineral resources. The second period is attributed to the modern period. The signature of the increase in erosion is different, because most of the soil cover has already been eroded. Only a patchy thin and immature soil cover exists since the Late Roman time. Erosion is associated with a marked increase of smectite-illite interstratified clay, and with goethite and hematite found in the deep soil horizons. Moreover, a marked increase in Cr is seen and is probably related to an enhanced exploitation of its mineral resources.

## Reactivity of Vertic dark soil towards applications of pesticide cocktails

E. Dumas<sup>1</sup>, Zemelka, G.<sup>1</sup>, T. Alekseeva<sup>2</sup>, Y. Kolyagin<sup>3</sup>, M. Sancelme<sup>1</sup>, C. Forano<sup>1</sup> and P. Besse-Hoggan<sup>1</sup>

<sup>1</sup> Université Clermont Auvergne, Université Blaise Pascal, Institut de Chimie de Clermont-Ferrand, CNRS, UMR 6296, BP 80026, F-63171 Aubière, France; claude.forano@univ-bpclermont.fr

<sup>2</sup> Institute of Physical Chemical and Biological Problems of Soil Science. Russian Academy of Sciences, Institutskaya ul., 2,142290 Pushchino, Russia

<sup>3</sup> Moscow State University, Chemistry Dept., Leninskie gori, GSP-2 ,1/3, 119991, Moscow, Russia

Application of herbicide mixtures to enhance their individual efficiency is now a common practice in agriculture. It broadens the range of weeds treated and limits the agronomic dose applied for each herbicide. Nevertheless the presence of multiple contaminants in the soil can affect the behaviour of individual components and only a few studies have dealt with this phenomenon. The objectives of our study were to explore the sorption processes of herbicides belonging to various chemical families, applied alone or in cocktails, on bulk soil and fine clay fraction of a vertic dark soil from a sedimentary valley (Limagne valley, center France). The sorption process governs not only the transport of the xenobiotic substance into the water but also its bioavailability. Competitive effects of molecules belonging to various chemical families are addressed in this work. Cocktails are composed of one of the triketone herbicide (sulcotrione, mesotrione or tembotrione) and S-metolachlor (chloroacetamide) and nicosulfuron (sulfonylurea) (Figure 1).

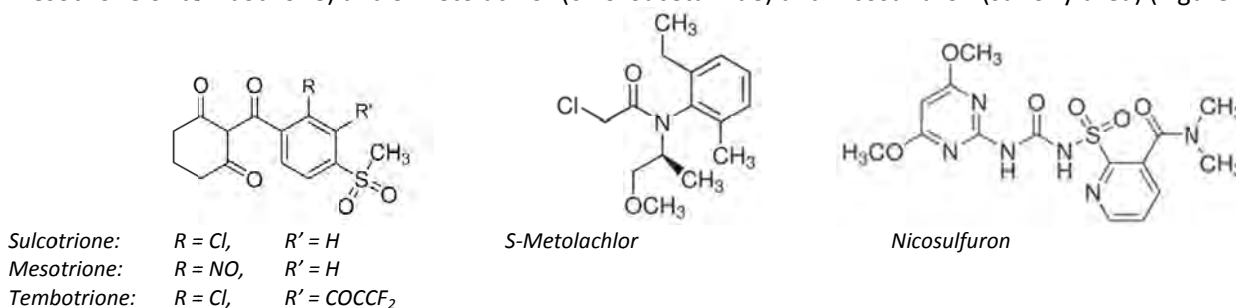


Figure 1: Molecular structures of the herbicides studied

The agricultural alkaline soil (pH = 8.2) was fully characterized as a black soil with Vertic trends. The clay fraction of the soil is 43% (mainly montmorillonite) and a high organic matter content (1.70%) is strongly linked to the clay. This soil is very fertile due to the swelling clays which are rich in exchangeable cations available for plants. The properties of all soil constituents were studied using MEB, XRD, FT-IR, <sup>13</sup>C-SSNMR.

Adsorption kinetics and isotherms of each pesticide, alone or in mixtures, with the various soil fractions were determined to quantify the soil response to pesticide contamination. The effect of organic matter on sulcotrione immobilization was also studied by working with hydrogen peroxide treated soil, which contains less organic matter. Adsorption isotherms were fitted according to the Freundlich model, and behaviours of soils fractions are compared and discussed. Adsorption of the herbicides by corn crops in this vertic black soil show no limit, it is a physical phenomenon. The equilibrium between soil and water compartment can lead to leaching of pesticides if the water is renewed in the soil, as indicated by literature on leaching studies for short and long time periods<sup>1,2</sup>.

<sup>1</sup> Cherrier R, Perrin-Ganier C, Schiavon M (2004). Degradation of sulcotrione in a brown soil amended with various organic matters. *Agronomie* 24:29-33.

<sup>2</sup> Chaabane H, Cooper J-F, Azouzi L, Coste C-M (2005). Influence of soil properties on the adsorption-desorption of sulcotrione and its hydrolysis metabolites on various soils. *J. Agric. Food Chem.* 53:4091-4095.

## Warm kaolins in Scotland

Adrian M. Hall<sup>1</sup>, H. Albert Gilg<sup>2</sup>, Anthony E. Fallick<sup>3</sup>, and Jon W. Merritt<sup>4</sup>

<sup>1</sup>Department of Physical Geography and Quaternary Geology, Stockholm University, S-106 91 Stockholm, Sweden

<sup>2</sup>Lehrstuhl für Ingenieurgeologie, Technische Universität München, Arcisstr. 21, D-80333 Munich, Germany. agilg@tum.de

<sup>3</sup>Scottish Universities Environmental Research Centre, East Kilbride, Glasgow G75 0QF, Scotland, UK

<sup>4</sup>British Geological Survey, Murchison House, West Mains Road, Edinburgh EH9 3LA, Scotland, UK

Stable isotope ratios can provide important evidence for estimating groundwater temperatures during the formation of clay minerals in response to chemical weathering of rocks at the landsurface. Here, we investigate weathering kaolins found in Buchan, NE Scotland. Stable oxygen and hydrogen isotopes for kaolins from weathered clasts in post-Cretaceous fluvial gravels and from clay-rich saprolites developed in Dalradian metamorphic and Caledonian igneous rocks indicate weathering under warm groundwater temperatures of  $23 \pm 5$  °C. Comparisons with Cenozoic palaeotemperatures derived from North Sea sediments indicate that weathering took place under humid tropical climates of the Palaeocene-Eocene.

The >25 m deep weathering profiles in the Buchan Gravels indicate that these coarse, quartzite- and flint-bearing gravels are older than previously thought and were likely deposited by rivers which also fed thick Palaeocene-Early Eocene deepwater sand fans in the western North Sea basin. A later phase of kaolin weathering at lower temperatures of  $15 \pm 5$  °C took place in the Middle Miocene. Kaolinitic weathering remnants are largely confined to elevations of >100 m in eastern Buchan and define a well-preserved, deeply weathered Cenozoic landscape in north-east Scotland.

## How do elements, including heavy metals, behave during weathering in tropical climates? The case of Cretaceous and Messinian palaeosoils of Sardinia, western Mediterranean (Italy)

Paola Mameli<sup>1</sup>, Giovanni Mongelli<sup>2</sup>, Rosa Sinisi<sup>2</sup> and Giacomo Oggiano<sup>1</sup>

<sup>1</sup> Dipartimento di Scienze della Natura e del Territorio - Università di Sassari (Italy). mamelip@uniss.it

<sup>2</sup> Dipartimento di Scienze - Università della Basilicata (Italy)

The breakdown of rock at the Earth's surface produces a thin, porous covering, recently labeled the Critical Zone (NRC, 2001), which displays tremendous heterogeneity both vertically, manifested in distinguishable layers of weathered rocks, regolith, and soil, and laterally, by the diversity of landscapes and the distribution of soils across them (Anderson et al., 2007).

The aim of this work is to assess the behavior of elements, including heavy metals, in relation to climate forcing during weathering processes. Two case studies were chosen in the post-Variscan covers of north Sardinia (Italy), both represented by alterites lying on Mesozoic carbonate rocks. These two alterites were generated in different chronostratigraphic and palaeogeographic contexts. The older alterite rests below - and grades into - a horizon of karstic bauxite of mid-Cretaceous age, whereas the younger is assigned to Messinian time and occurs within alluvial deposits. The Cretaceous alterites are thought to be precursors of the overlying bauxite and were affected by partial lateritic processes under monsoonal climate, mostly at the expense of sediments of uncertain provenance (Purbeckian marlstone and allochthonous alluvium). Conversely, the Messinian alterites were unmistakably derived from phyllites of the metamorphic Variscan basement. They consist of alluvial clayey deposits with interbedded palaeosoils and were tentatively ascribed to a climatic stage characterized by alternating dry and wet phases, typical of savannah regions (Mongelli et al., 2012).

Mineralogical and chemical analyses were performed on 42 representative samples, collected from vertical loglines along profiles and single spots from both the deposits. The mineralogy of bulk samples was obtained by X-Ray Diffraction, using a Siemens D5000 diffractometer (CuK $\alpha$  radiation, at 40 kV and 30 mA). Major, trace elements and rare earth elements (REE) were obtained by ICP/MS at Activation Laboratories (Ancaster, Canada).

The Cretaceous alterites are mostly composed of kaolinite with subordinate illite, minor Fe-oxyhydroxide, and rare boehmite or gibbsite. The Messinian alterites are composed of illite and kaolinite in equal proportion with minor amounts of Fe-oxyhydroxide and slight proportion of gibbsite.

Chemical data have been normalized to the Gloss standard (Plank & Langmuir, 1998) in order to stress their features relative to the average composition of the upper continental crust. As for major elements, both alterites are enriched, even if at different extents, in Ti, Al and Fe (1.5-4 x Gloss Cretaceous; 1.5-2.5 x Gloss Messinian) and depleted (<1 x Gloss) in Si and especially in Mn, Ca, Na, and P. Though the general behaviour of trace elements in both alterites is similar, some metals, including Sc, V, Cr and Pb, and some high field strength elements, including, Zr, Nb, Th and U, are enriched in Cretaceous set, whereas the Messinian set has contents only slightly higher or close to Gloss. Rb and Cs are manifestly related to K abundance hence they are enriched in the relatively illite-rich Messinian set. Chondrite-normalized REE (Taylor & McLennan, 1985) in the Cretaceous set show fractionation effects likely due to a more intense weathering, in agreement with higher CIA average values (84 vs 74) and A-CN-K ternary plot, whereas Messinian patterns are more homogeneous.

Anderson S.P., von Blanckenburg F., White A.F. (2007) - Physical and chemical controls on the Critical Zone. *Elements*, 3, 315-319.

Mongelli G., Mameli P., Oggiano G., Sinisi R. (2012) - Messinian palaeoclimate and palaeo-environment in the western Mediterranean realm: insights from the geochemistry of continental deposits of NW Sardinia (Italy). *International Geology Review*, 54, 8, 971-990.

NRC (National Research Council) (2001) - Basic Research Opportunities in Earth Science. National Academy Press, Washington, 154 pp.

Plank T., Langmuir C.H., (1998) - The chemical composition of subducting sediment and its composition for the crust and mantle. *Chemical Geology*, 145, 325-394.

Taylor S. R. and McLennan S. M. (1985) - *The Continental Crust: Its Composition and Evolution*. Blackwell, Oxford, 312 pp.

## Particle-lacing in an Alpine stream

Michael Plötze<sup>1</sup>, Daniela König<sup>2</sup> and Gerhard Furrer<sup>2</sup>

<sup>1</sup>ETH Zurich, IGT, Stefano-Franscini-Platz 3, 8093 Zurich, Switzerland, ploetzel@ethz.ch

<sup>2</sup>ETH Zurich, IBP, Universitätstrasse 16, 8092 Zurich, Switzerland

A beautiful flow pattern caused by a particle-rich suspension in the Aua da Tiral stream underneath Piz Tasna, a mountain peak in the Engadine Alps north of Scuol, Switzerland, was observed in 2012 (Fig. 1).



Fig. 1: Flow pattern in the Aua da Tiral stream (Photo G. Furrer 17 Aug 2012).

Similar looking artificial suspensions, so-called 'rheoscopic fluids' are used in fluid mechanics experiments or art installations to visualize flow patterns even though the underlying mechanisms of these fluids are not yet fully understood. An important environmental aspect is the potential colmation of the stream bed by such particles if present at high density. Colmation within the porous structure of a stream bed is promoted by high particle concentrations, as the fine material is more likely to settle in large numbers than in low particle concentration.

To investigate the shiny flow patterns and the impact of factors such as particle concentration and mineral composition, suspensions of various particle numbers were produced using the original particle suspension, sediment samples from the stream and four separate minerals. The minerals were chosen either due to their presence in the original suspension (muscovite, quartz, illite) or because of their flaky shape (kaolinite), since flaky particles and their distinct orientation within the stream's suspension can contribute to the optical effect. The minerals and a sediment sample were split into three particle sizes. The visibility of the pattern was quantified by measuring the contrast between the bright and dark streaks.

The ability of muscovite and kaolinite to evoke a similar pattern indicates that flaky particles might be crucial for the phenomenon. Additionally, a material-dependent 'optimum number' of particles in suspension seems to be relevant.



## Competitive adsorption of mixed contaminants on metal-immobilising organoclay (MIOC): Implication in the biodegradation of polyaromatic hydrocarbons (PAHs)

Bhabananda Biswas<sup>1,2,\*</sup>, Binoy Sarkar<sup>1,2</sup>, Asit Mandal<sup>1,3</sup>, Ravi Naidu<sup>1,2</sup>

<sup>1</sup>Centre for Environmental Risk Assessment and Remediation

University of South Australia, Mawson Lakes Campus, SA 5095, Australia

<sup>2</sup>Cooperative Research Centre for Contamination Assessment and Remediation of the Environment, P.O. Box 486, Salisbury, SA 5106, Australia

<sup>3</sup>Division of Soil Biology, Indian Institute of Soil Science, Bhopal, India

\*Bhabananda.Biswas@mymail.unisa.edu.au

In a mixed-contaminated soil containing polyaromatic hydrocarbons (PAHs) and heavy metals, the latter may pose a serious toxic stress to native PAH-degrading microorganisms. Such toxicity can be reduced through immobilising the metals on adsorptive materials, such as clays and modified clay minerals. However, in a mixed-contaminant situation, this adsorption can be unspecific and can bind PAHs too, making them unavailable to microorganisms. Therefore, an adsorption process more specific to the metal without affecting the bioavailability of PAHs is needed for an effective degradation. In the current study, a metal-immobilising organoclay (Arquad® 2HT-75-bentonite treated with palmitic acid) (MIOC) was developed, and tested for a competitive adsorption of a metal (cadmium (Cd)) in the presence of PAH (phenanthrene) in aqueous suspension. The MIOC was then applied to a mixed-contaminated soil containing the above contaminants. The MIOC (ABP) differed considerably from the parent clay for its metal immobilising capacity (ABP > unmodified bentonite (B) > Arquad-bentonite (AB)). The MIOC also improved the bacterial colony forming units (CFU) (up to 10–43%), and enzymatic (dehydrogenase) activity (up to 68%) in soil through alleviating Cd toxicity (Fig. 1). Simultaneously, the MIOC maintained phenanthrene in bioavailable form in the mixed-contaminated soil. This study may find application in the MIOC-assisted bioremediation for PAHs in mixed-contaminated situation.

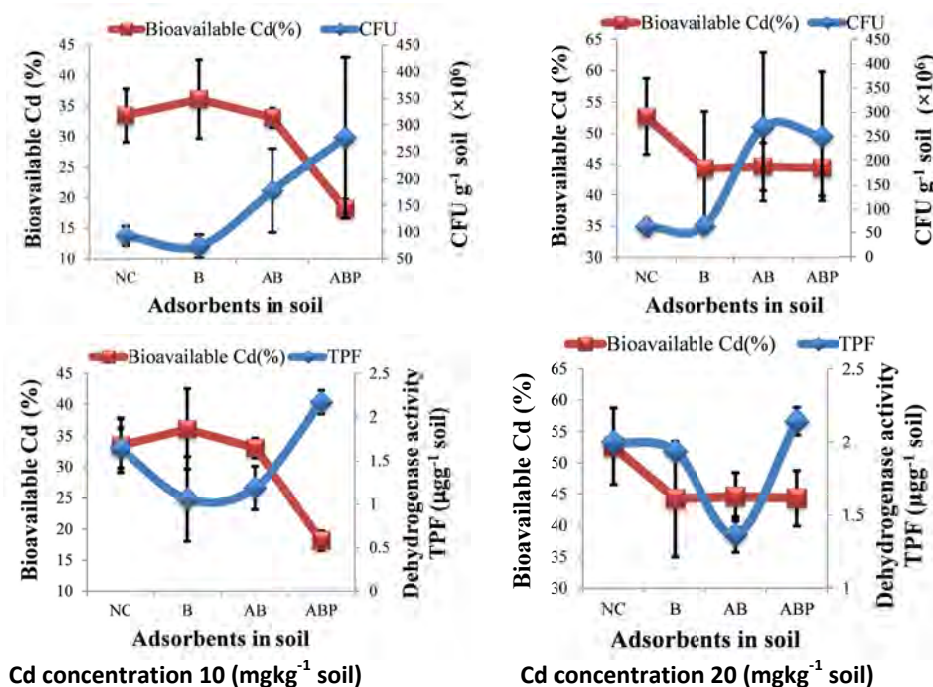


**Fig. 1.** Microbial responses (CFU and dehydrogenase activity) to bioavailable Cd in clay and modified clay-amended soil at different Cd concentrations

## Hydration properties of a montmorillonite saturated with octylammonium cations: Effect of the alkyl-chains number and surfactant concentration

Valéria Bizovská, Ľuboš Jankovič and Jana Madejová

Institute of Inorganic Chemistry, Slovak Academy of Sciences, Dúbravská cesta 9,  
SK-845 36 Bratislava, Slovakia, e-mail: valeria.bizovska@savba.sk

The modification of montmorillonites (MMT) with cationic surfactants is an important subject in current research since various organoclays are widely used in different industrial and environmental applications. Understanding the microstructure and hydration potential of organo-montmorillonites is of high importance in clarifying their adsorption characteristics towards different organic compounds. The objective of the present work was to examine the effect of loading amount of mono- (1C8), di- (2C8), tri- (3C8) and tetra- (4C8) octylammonium cations on their arrangement within the montmorillonite interlayers and to record the hydration properties of prepared organo-montmorillonites. The montmorillonite from Jelšový Potok, Slovakia (JP) and organic salts in the loading concentration range of 0.2 - 2.0 mmol.g<sup>-1</sup> (corresponding to 20 - 200 % of the CEC of JP) were used for organoclays preparation. Carbon analysis, XRD, and IR spectroscopy were used for the samples characterization. The degree of surfactant adsorption calculated from measured carbon content was 93% of CEC for 1C8, while 172 %, 180% and 196 % saturation of CEC was determined for 2C8, 3C8 and 4C8, respectively, at 2.0 mmol.g<sup>-1</sup> of the organo-cation used for the preparation. It is assumed that in addition to 2C8, 3C8 and 4C8 cations the organic salts were co-adsorbed to MMT interlayers and/or outer surfaces. The  $d_{001}$  value of 1C8-JP showed creation of monolayers while for 2C8-, 3C8- and 4C8-JP formation of monolayers, bilayers and paraffin arrangement was confirmed depending on the number of alkyl chains and the loading amount. The bands related to CH<sub>2</sub> stretching (3000-2800 cm<sup>-1</sup>) and the first overtone (near 5800 cm<sup>-1</sup>) modes were used to probe the ordering of the intercalated cations. With growing amount of 2C8, 3C8 and 4C8 surfactant the bands were shifted from the position characteristic for disordered *gauche* conformers to lower wavenumbers indicating increasing number of ordered *all-trans* conformers. The hydration properties of the samples were investigated by NIR spectroscopy and gravimetry. Difference in the area of the H<sub>2</sub>O combination band near 5250 cm<sup>-1</sup> at 100% and 0% relative humidity reflected the quantity of adsorbed water. The spectra showed decreasing content of water with growing amount of surfactants and octyl chains number. The NIR results correlated very well with the values obtained from gravimetric analysis. Almost linear decrease of water content from 9.4 to 5.0 mass % for 1C8, from 8.1 to 1.8 mass % for 2C8, from 7.2 to 1.1 mass % for 3C8 and from 7.0 to 1.0 mass % for 4C8 was observed with increasing cation loading content from 0.2 to 1.0 mmol.g<sup>-1</sup>. Further increase of the cation adsorption content reduced the amount of water only negligibly. Both methods demonstrated the effect of the amount of adsorbed and/or intercalated cations and number of alkyl chains on the hydration of montmorillonite.

**Acknowledgment:** This work is the result of the project Competence center for new materials, advanced technologies and energy ITMS 26240220073, supported by the Research and Development Operational Program funded by the European Regional Development Fund.

## Photoactive hybrid material based on kaolinite grafted with a reactive laser dye

Samuel Sas<sup>1</sup>, Martin Danko<sup>2</sup> and Juraj Bujdák<sup>1,3</sup>

<sup>1</sup>Institute of Inorganic Chemistry, Slovak Academy of Sciences, Bratislava, Slovakia, bujdak@fns.uniba.sk

<sup>2</sup>Polymer Institute, Slovak Academy of Sciences, Bratislava, Slovakia

<sup>3</sup>Department of Physical and Theoretical Chemistry, Faculty of Natural Sciences, Comenius University, Bratislava, Slovakia

The main strategies for the preparation of organoclays were mostly based on reactions of expandable clay minerals. Ion exchange reactions with large organic cations or intercalation of various molecules in smectites led to the development of organoclays with variable properties and functionalities. Hybrid materials and organoclays bearing photoactive molecules represent perspective optical materials for various applications, such as photocatalysts, sensors, photosensitizers, solid luminescent materials, etc. In contrast to smectites, kaolinites do not readily expand under mild conditions and the formation of their hybrids requires special procedures, or is limited to specific molecules.

New luminescent material based on a laser xanthene dye covalently linked to the surface of kaolinite particles was developed in this work. Molecules of common laser dyes of any type do not irreversibly intercalate or adsorb onto kaolinite surface. Therefore, our strategy was to prepare a reactive precursor, i.e. dye derivative, which would exhibit strong affinity to bind covalently to the surface of octahedrons via the condensation reaction with Al-OH groups. The reactive dye was synthesized by the reaction of rhodamine with (3-aminopropyl) triethoxysilane molecule. The mineral was pre-expanded with dimethyl sulfoxide in order to enable the penetration of the reactive dye molecules between kaolinite layers and to make a large fraction of mineral surface accessible for the modification. The swelling of kaolinite, its intercalation and surface modification with the dye were investigated by X-ray diffraction and infrared spectroscopy. The intercalation of the reactive dye into the interlayer spaces of the mineral specimen pre-treated with DMSO led only to slight additional expansion but was accompanied with significant disordering of kaolinite structure. Intercalated laser dye molecules exhibited a high degree of photoactivity and were resistant to a mild thermal treatment. Optical properties of the hybrids were studied by means of absorption, steady-state, and time-resolved fluorescence spectroscopy in a visible spectral region. Low concentrations of the dye had to be used to prevent molecular aggregation and fluorescence quenching. Fluorescence quantum yield of the hybrid material was only slightly below the parameters found for the solutions of a dye precursor.

Similar hybrid materials based on kaolinite and other photoactive molecules could be prepared by the strategy developed in this work. Such materials can expand the range of mineral applications. They might be applied as photoactive components for the materials developed for paper and pharmaceutical industries, in sensors, in paints, polymer nanocomposites, etc.

**Acknowledgement:** This work was supported by the Slovak Research and Development Agency under the contract No. APVV-0291-11 and Grant Agency VEGA (2/0107/13, 1/0943/13).

## Natural and synthetic modified clays as prospective soil amendments for remediation of soil contaminated with metals

Juris Burlakovs, Ruta Ozola, Zane Vincevica-Gaile and Karina Stankevica  
Faculty of Geographical and Earth Sciences, University of Latvia, Rainis Blvd. 19, LV 1586, Riga, Latvia  
e-mail: juris@geo-it.lv

Soil contamination by heavy metals is a major problem in brownfields, dumpsites, former and active military and industrial sites as well as areas contaminated naturally. Pollution of soil is induced by many sources such as application of fertilizers in agriculture, air pollution from industry and transport, as well as point sources, e.g., wastewater streams. Immobilization of heavy metals in such polluted soil can be accomplished by *in situ* treatment technologies, and soil amendments are a potential solution. Modified clay sorbents have broad prospects for immobilization of lead, zinc, copper and other heavy elements. Performance of innovative sorbents for heavy metal remediation in aqueous and dispersed solid media is important as the environmental clean-up industry demands materials that are highly efficient, recyclable and sustainable.

The aim of this work included elaboration and testing of prospective soil amendments for potential *gentle* remediation applicability.

A series of metal speciation and immobilization efficiency experiments were performed for natural and synthetic modified clays by adding in one case amorphous iron oxyhydroxides and in another - monopotassium phosphate and calcium chloride. Clay sorbents modified with iron oxyhydroxide and oxyapatite achieved improved beneficial properties for specific remedial applications.

Innovative materials were characterized using texture and PXRD mineralogical analysis, SEM images, BET surface area measurements and FTIR spectra. The sorption pattern and amount of exchangeable fraction for immobilized metals were determined. The results revealed broader prospects for the use of local resources in *gentle* remediation by soil amendments for heavy metal contaminated soils.

This study was supported by the European Social Fund Project "Interdisciplinary Team of Young Scientists for Assessment and Restoration of Soil Quality and Usage Potential in Latvia" No.2013/0020/1DP/1.1.1.2.0/13/APIA/VIAA/066.

## Ordered Functional Heterostructures via Simple Intercalation Reactions

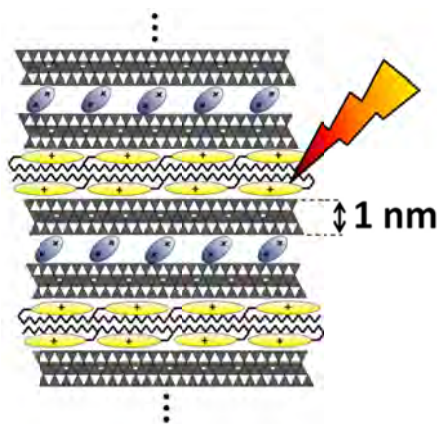
Christoph Habel<sup>1</sup>, Matthias Stöter<sup>1</sup>, Bernhard Biersack<sup>2</sup>, Rainer Schobert<sup>2</sup> and Josef Breu<sup>1</sup>

<sup>1</sup> Department of Inorganic Chemistry I, University of Bayreuth, Universitätsstraße 30, 95440 Bayreuth, Germany; Josef.Breu@uni-bayreuth.de

<sup>2</sup> Department of Organic Chemistry I, University of Bayreuth, Universitätsstraße 30, 95440 Bayreuth, Germany

Because of their large interface area, materials with alternating functional layered nanostructures have shown great potential for energy and electron transfer, sensing, and catalysis.<sup>[1]</sup> Such materials are usually made by bottom up processing like layer by layer assembly. We established a generally applicable alternative process for the synthesis of such nanostructures based on a simple partial ion exchange into every other interlayer of a synthetic clay. The driving force for the formation of such one-dimensionally ordered interstratified nanostructures was found to be a charge density of exchanged, densely packed interlayers (e.g. N-Hexadecyl-4-(3,4,5-trimethoxystyryl)-pyridinium) deviating from the density of the host clay. This mechanism requires a perfectly homogenous charge density of the host which is only provided by clays synthesized from a melt.<sup>[2]</sup> The heterostructure may be further functionalized by selective exchange of the remaining sodium cations with any other functional molecule, for instance with the pillar 1,4-dimethyl-1,4-diazoniabicyclo[2.2.2]octane (Figure 1).<sup>[3]</sup> Consequently, any combination of two different, strictly alternating functionalities will be accessible offering great potential for instance in size and shape selective photochemistry.

Figure 1. Scheme of the one-dimensionally ordered functional heterostructure.



[1] K. Ariga, Q.M. Ji, J.P. Hill, Y. Bando, M. Aono, *NPG Asia Mater* **2012**, 4, e17.

[2] M. Stöter, D.A. Kunz, M. Schmidt, D. Hirsemann, H. Kalo, B. Putz, J. Senker, J. Breu, *Langmuir* **2013**, 29, 1280-1285.

[3] M. Stöter, B. Biersack, N. Reimer, M. Herling, N. Stock, R. Schobert, J. Breu, *Chem. Mater.* **2014**, 26, 5412-5419.

## Dye solution discoloration by Fe-loaded Bustos clay catalyst

W. Hajjaji<sup>1</sup>, S. Andrejkovičová<sup>1</sup>, D.M. Tobaldi<sup>2</sup>, J.A. Labrincha<sup>2</sup> and F. Rocha<sup>1</sup>

<sup>1</sup> Geobiotec, Geosciences Dept, University of Aveiro.3810-193 Aveiro. Portugal

<sup>2</sup> Materials and Ceramic Engineering Dept & CICECO. University of Aveiro.3810-193 Aveiro. Portugal

Using the proposed photo-Fenton method in the present study, Bustos (central Portugal) illite-kaolinite clays were modified by pillaring small amount of stabilized iron. The Fe-clay catalyst has been prepared and tested for Orange II oxidation with H<sub>2</sub>O<sub>2</sub> in aqueous solution. The reaction is carried out in a batch reactor, using different catalyst and dye concentrations, a wide range of contact time and UV/visible exposure.

By combination of various photo-Fenton process parameters, the application of UV in the presence H<sub>2</sub>O<sub>2</sub> recorded a degradation rate of 34% in 480 min. This suggests a generation of the HO• achieved via photolysis of H<sub>2</sub>O<sub>2</sub>. The discoloration of Orange II dye improved with Fenton like process (Fe-Clay and H<sub>2</sub>O<sub>2</sub>) reached 92% after 480 min, confirming the higher catalytic activity of the Fe-rich clay. This increase was due to the combined role of adsorptive capacity of the clay, with photolysis of H<sub>2</sub>O<sub>2</sub> and probably also with the partial generation of HO• from the presence of iron at surface of clay particles. An optimum degradation efficiency (98%) was obtained under UV light irradiation. This excellent level of removal, achieved after 250 min testing, shows the high catalytic activity in a photo-Fenton reaction of the pillared clay.

**Keywords:** Clay, orange II dye, photo-Fenton, degradation.

## Smectite-fungicide complex as a potential smart delivery system for slow release formulation: Environmental advantages

Inés M. Aguilar, Rafael Celis, Juan Cornejo, M. Carmen Hermosín (mchermosin@irnase.csic.es)

*Instituto de Recursos Naturales y Agrobiología de Sevilla, CSIC (IRNAS-CSIC), Avda. Reina Mercedes 10, 41012 Seville, Spain*

Clays as carriers for slow release formulations (SRF) have been widely studied in the last 15 years because they have the advantage of being natural soil components and hence they do not represent an added environmental problem. Nanopesticide technology is an increasing research trend<sup>1-3</sup>, even with the associated risk of confusion or perception that this word may suppose<sup>2-3</sup>. The term *nanopesticide* most widely accepted<sup>2,3</sup> deals with those pesticide formulations including at least one nanosized component. The nanosize structure of smectites, in addition to their surface availability due to their layer charge and the flexibility of their exchangeable cation, makes them attractive candidates as a carrier or smart delivery system for herbicides application<sup>1-3</sup>. The systemic fungicides are suitable compounds to investigate for possible advantages of smart and located delivery of the active ingredient (AI), since they are absorbed by plant roots or leaves, and once they enter in plant tissues, exert their action inside the plant body. However, the most valuable advantage of a SRF is to show less environmental risk than formulations available in the market. We present here the environmental advantages that smectite-fungicide complexes display as compared with the commercial formulations of two systemic fungicides. Two standard smectites (SWy and SH from the Clay Minerals Repository) saturated with diverse cations ( $\text{Fe}^{3+}$ , Chytosan CH and Octadecylammonium C18) were assayed for the fungicides metalaxyl (polar and water soluble) and tebuconazole (protonable and poorly water soluble). The adsorption and preparation of the fungicide-clay complex were characterized by XRD and FTIR spectroscopy. These complexes were assayed also for the release of fungicides in water and for soil leaching through hand-packed soil columns.

A preliminary adsorption at two fungicide concentrations (1 and 3 ppm) allowed the selection of 4-5 adsorbents showing medium-high sorption capacity. The adsorption of both herbicides was extremely high in  $\text{Fe}^{3+}$  smectites, with tebuconazole having the highest sorption in  $\text{Fe}^{3+}$ -SW. Protonation of tebuconazole molecules, once adsorbed in the interlayer, enlarged the total amount adsorbed in this clay. Metalaxyl only adsorbed through polar attraction, associating with and/or replacing the water molecules in the cation hydration sphere; however, its hydrophilic character rendered higher fungicide adsorption possible by all assayed clays, with the consistent exception of SHC18. The adsorbent with lower adsorption capacity for both fungicides was SHC18, and the interaction in this case was mainly hydrophobic. The bionanocomposite SWCH showed an intermediate behavior. The fungicide-clay mix (HM or hand milling) and complexes (SC and WC in methanol) loaded at 4 and 20% of active ingredient were examined by FTIR and XRD, showing interlayer adsorption, clearly evident at high loading. All the fungicide-clay mixes or complexes assayed showed a SRF release profile, although some of them rendered very low release after 100h. The fungicide release rate from the clay-fungicide complexes was closely related to the strength of fungicide-clay interaction. Fungicide-SHC18 complexes displayed the best performance as SRF suggesting both: a) an important decrease in fungicide soil losses by leaching and b) an important increase of the fungicide remaining in soil-target location thus suggesting they could be incorporated in SRF as nanopesticides.

**Acknowledgments:** Grants P11-07400 and AGR-264 by Junta de Andalucía, Contract RECUPERA2020 MINECO-CSIC and Grant AGL2011-23779 by MINECO, all of them cofinanced with EU FEDER-FSE funds.

(1) Pérez-de-Luque A. & Hermosín M.C. 2013. In *Bio-Nanotechnology: A Revolution in Food, Biomedical and Health Sciences*. Wiley-Blackwell, Oxford (UK), pp.:383-398. (2) Kah M. et al. 2013. *Critical Reviews in Environmental Science and Technology*, pg.:43. (3) Kah M. et al. 2014. *Environment International* 63, 224

## Synthesis and modification of layered double hydroxides (LDHs) as mycotoxin binders

Chun-Chun Hsu\* and Youjun Deng

Department of Soil & Crop Sciences, Texas A&M University, College Station, Texas, USA: \*chunchunhsu@tamu.edu

Fumonisin (FB), ochratoxin A (OTA), deoxynivalenol (DON), and zearalenone (ZEN) are the four major groups of agriculturally important mycotoxins produced by molds *Fusarium*, *Aspergillus*, and *Penicillium*. They are naturally occurring mycotoxins and are frequently found on corn, wheat, barley, oat, tree nuts, rice, peanut, sorghum, hay, fruits, and other crops. Contamination of food and feedstuff by mycotoxins is a worldwide problem and unavoidable despite significant progress in preventing the growth of the fungi, developing more resistant crops, and implementing biological control measurements. Preventing the health risks and economic losses from mycotoxin contamination are crucial issues.

Layered double hydroxides (LDHs) are known as anionic clays or hydrotalcite-like compounds. The isomorphous substitution of divalent cations by trivalent cations in the hydroxide layers results in excess positive charges within the layers. The chemical compositions of LDHs is generally expressed as  $[M_{1-x}^{2+}M_x^{3+}(\text{OH})_2]^{x+}X_{x/m}^{m-} \cdot n\text{H}_2\text{O}$ . LDHs have high specific surface area (20-120 m<sup>2</sup>/g) and high anion exchange capacity (200-500 cmol(-)/kg) and are widely used as anionic pollutant adsorbents. Inspired by reported high adsorption capacity of LDHs for many anionic contaminants, we are making efforts to synthesize LDHs to detoxify/decontaminate mycotoxins by adsorption. The objective of this study is to evaluate the adsorption efficiency of Mg/Al-LDH with 1) different layer charge density, 2) different interlayer exchange anion type, and 3) different solution pH.

We used three approaches to modify the Mg/Al-LDH: 1) changing the layer charge density by using different Al<sup>3+</sup>/ (Al<sup>3+</sup>+Mg<sup>2+</sup>) molar ratio in synthesis process, 2) replacing exchange anions with different size and valences, and 3) adjusting the solution pH to allow the mycotoxins to occur as anionic species.

Experimental results indicated that Mg/Al-LDH with Al<sup>3+</sup>/ (Al<sup>3+</sup>+Mg<sup>2+</sup>) molar ratio of 0.33 showed various adsorption capacities. In unadjusted pH solution, the adsorption capacities were 0.029 mol/kg (0.76 % by weight) and 0.078 mol/kg (1.74 % by weight) for ZEN and DON, respectively. In pH-adjusted solution, the mycotoxins were anionic and the adsorption capacities doubled, i.e. 0.056 mol/kg for ZEN and 0.193 mol/kg for DON.

Overall, the preliminary results indicated that the mycotoxin adsorption capacity can be enhanced by increasing pH. This is more likely related to the anionic exchange capacity of Mg/Al-LDH. Yet, the results also suggested that it is possible to enhance the adsorption by modifying the layer charge density of Mg/Al-LDH. The optimal charge density, exchange anion type, and adsorption condition will be evaluated.



## Molecular modelling of CdS-CTA<sup>+</sup>-MMT nanoparticles

M. Pospíšil<sup>1</sup>, M. Pšenička<sup>1</sup>, P. Kovář<sup>1</sup> and P. Praus<sup>2</sup>

<sup>1</sup> Charles University in Prague, Faculty of Mathematics and Physics, Department of Chemical Physics and Optics, Ke Karlovu 3, 121 16 Prague 2, Czech Republic, pospasil@karlov.mff.cuni.cz

<sup>2</sup>VŠB-Technical University of Ostrava, Department of Analytical Chemistry and Material Testing, 17. listopadu 15, 70833 Ostrava-Poruba, CZ

Cadmium sulphide is a very good photo catalyst and semiconductor with wide direct band-gap energy of about 2.5 eV. CdS nanoparticles were precipitated by reaction of cadmium acetate and sodium sulphide in aqueous dispersions of cationic surfactant cetyltrimethylammonium bromide (CTAB). The 5 nm sphere radii of CdS nanoparticles were determined from TEM and by calculation. The CTA concentration in final dispersion was about 4 mmol L<sup>-1</sup>[1].

CdS particles with radii 5 nm were used for calculations and were surrounded with various amounts of CTA<sup>+</sup> cations. In most cases minimization pushed CTAs further from CdS surface but all stayed in (i) perpendicular positions (10 to 100 CTA<sup>+</sup>, step 10 in monolayer and bilayer arrangement) with respect to CdS surface or (ii) parallel arrangement with respect to surface for small amount CTA<sup>+</sup> up to 10 molecules per one nanoparticle. Perpendicular arrangement is strongly preferred with respect to other positions of CTA<sup>+</sup>. Simulations show that at the higher CTAs concentrations, CdS nanoparticles were surrounded by CTA<sup>+</sup> bilayers forming positively charged micelles.

Five different sets of models were created on the base of experimental data: (i) CdS nanoparticles adsorbed on montmorillonite (MMT), (ii) CdS nanoparticle covered with CTA<sup>+</sup> cations, (iii) CdS nanoparticle covered with CTA<sup>+</sup> cations immersed among water molecules, (iv) CdS nanoparticles covered with CTA<sup>+</sup> cations adsorbed on MMT surface, and (v) CdS nanoparticle covered with CTA<sup>+</sup> cations absorbed on MMT surface and immersed among water molecules. All variations of models were calculated for Hawleyite and Greenockite crystal structure. Molecular simulations were applied in Material Studio modelling environment.

[1] P. Praus *et al.*, *J. Col. Int. Sci.* **360**, 574-579 (2011).

## MOPS – A New Class of Functional Hybrid Materials

Martin A. Rieß<sup>1</sup>, Markus M. Herling<sup>1</sup>, Mathias Schwedes<sup>2</sup>, Hussein Kalo<sup>1</sup>, Rainer Schobert<sup>2</sup>, Josef Breu<sup>1</sup>

<sup>1</sup> Department of Inorganic Chemistry I, University of Bayreuth, Universitätsstraße 30, 95440 Bayreuth, Germany; josef.breu@uni-bayreuth.de

<sup>2</sup> Department of Organic Chemistry I, University of Bayreuth, Universitätsstraße 30, 95440 Bayreuth, Germany;

Synthetic layered silicates with high layer-charge homogeneity and excellent intracrystalline reactivity were pillared with organic and metal organic cations of different charge, size and shape. This new class of Microporous Organically Pillared Layered Silicates (MOPS) is exhibiting a plethora of possible applications like stereo- and size discrimination (Fig. 1.).

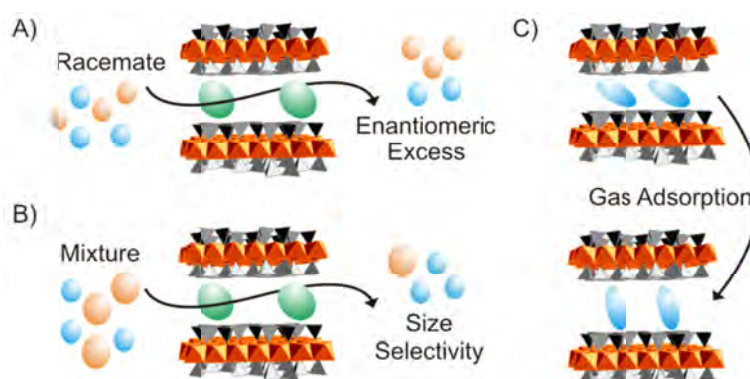


Figure 1. Features of MOPS, A) Stereodiscrimination, B) Size Selectivity and C) Flexible Pore System

Recent progress allows fine-tuning the charge density of the host lattice *post synthesis*. Such deliberate and fine-graded alteration of the pillar density in turn permits adjusting the pore size in steps as small as 0.1 Å to a given adsorbate and thus will pave the way to maximize adsorption enthalpies and to improve selectivity. Rational design of microporous hybrid materials with full control over size, shape, and chemical nature of micropores certainly represents the strength and great potential of the pillaring approach.<sup>[1]</sup>

Herein we present different MOPS with features like stereo-/size-discrimination and flexible pore system.<sup>[2,3]</sup>

**Keywords:** Microporous, Stereodiscrimination, Size selectivity, breathing system

[1] M. M. Herling, J. Breu, *Z. anorg. allg. Chem.* **2014**, *640*, 547-560.

[2] M. M. Herling, M. Schwedes, S. Seibt, H. Kalo, U. Lacher, R. Schobert, J. Breu, to be submitted.

[3] M. M. Herling, R. Matsuda, H. Sato, L. Li, H. Kalo, , S. Kitagawa, J. Breu, to be submitted.

## Synthesis of surfactant-modified montmorillonites for adsorption of perchlorate

Wuhui Luo and Keiko Sasaki\*

Department of Earth Resources Engineering, Kyushu University, Fukuoka, 819-0395, Japan

\*keikos@mine.kyushu-u.ac.jp

Perchlorate ( $\text{ClO}_4^-$ ) has been used in the production of solid propellants for rockets and missiles, and of matches, fireworks, and roadside flares, because of its properties as a strong oxidant. It has emerged as a widespread contaminant in groundwater and surface water, and aroused across extensive concern because of its negative health effect. Although some commercial ion-exchange resins have been employed to remove  $\text{ClO}_4^-$ , development of cost-effective adsorbents is still imperative. Montmorillonite (MMT) is one of the most abundant naturally-occurred clay minerals and has been widely used for environmental remediation because it is a cation exchanger with high surface areas. Quaternary ammonium salts are known to be effective modifiers for MMT creating a strong affinity for  $\text{ClO}_4^-$ . Modification of MMT can be conducted by anchoring the quaternary ammonium ions of the cationic surfactants to the surface of MMT layer without counter ions (e.g.,  $\text{Cl}^-$  or  $\text{Br}^-$ ) through electrostatic force, and then capturing the ion-paired type through hydrophobic interaction with the polar head facing to the bulk solution. Based on an ion-exchange between the  $\text{ClO}_4^-$  ion and a paired anion, the removal of  $\text{ClO}_4^-$  is governed by the amount of ion-paired surfactant, which is affected by alkyl chain lengths and head groups including quaternary ammonium ions in the structure of surfactants. Thus, a series of surfactants with different structures in terms of alkyl chain lengths and head groups, were deliberately selected to modify MMT, and the resultant surfactant-modified MMT were tested to investigate their performances on removal of  $\text{ClO}_4^-$ . The longer alkyl-chain length gave rise to a higher loading of surfactant in the final composites in association with greater adsorption capacity and higher selectivity of  $\text{ClO}_4^-$  over coexisting anions. In structures with identical alkyl-chain length, the head group of benzyl dimethyl ammonium showed greater  $\text{ClO}_4^-$  adsorption density than that of trimethyl ammonium and pyridinium. It is proposed that the diverse adsorption features of  $\text{ClO}_4^-$  on surfactant-modified MMTs are likely to be caused by the swelling properties of composites which are influenced by the chemical structure of surfactants.

## Clay-based nanocomposite coating for flexible optoelectronics applying commercial polymers

Jasmin Schmid<sup>1</sup>, Daniel A. Kunz<sup>1</sup>, Patrick Feicht<sup>1</sup>, J. Erath<sup>2</sup>, A. Fery<sup>2</sup>, Josef Breu<sup>1</sup>

<sup>1</sup> Department of Inorganic Chemistry I, University of Bayreuth, Universitätsstraße 30, 95440 Bayreuth, Germany; Josef.Breu@uni-bayreuth.de

<sup>2</sup> Department of Physical Chemistry II, University of Bayreuth, Universitätsstraße 30, 95440 Bayreuth, Germany

Transparency, flexibility, and especially ultralow oxygen (OTR) and water vapor (WVTR) transmission rates are the key issue to be addressed for packaging of flexible organic photovoltaics and organic light emitting diodes. Concomitant optimization of all essential features is still a big challenge. Here we present a thin (1.5  $\mu\text{m}$ ), highly transparent, and at the same time flexible nanocomposite coating with an exceptionally low OTR and WVTR ( $1.0 \times 10^{-2} \text{ cm}^3 \text{ m}^{-2} \text{ day}^{-1} \text{ bar}^{-1}$  and  $<0.005 \text{ g m}^{-2} \text{ day}^{-1}$  at 50% RH, respectively).<sup>[1]</sup>



A commercially available polyurethane (Desmodur N 3600 and Desmophen 670 BA, Bayer MaterialScience AG) was filled with a delaminated synthetic layered silicate exhibiting huge aspect ratios of about 25 000.<sup>[2]</sup> Functional films were prepared by simple doctor-blading a suspension of the matrix and the organophilized clay. This preparation procedure is technically benign, is easy to scale up, and may be applied readily for encapsulation of sensitive flexible electronics.

[1] D.A. Kunz, J. Schmid, P. Feicht, J. Erath, A. Fery, J. Breu, *ACS Nano* **2013**, 7 4275-4280.

[2] M. Stöter, D.A. Kunz, M. Schmidt, D. Hirsemann, H. Kalo, B. Putz, J. Senker, J. Breu, *Langmuir* **2013**, 29 1280-1285.

## H<sub>2</sub>S fixation at mineral surfaces under supercritical CO<sub>2</sub> conditions in aqueous and quasi-dry systems

Theodor Alpermann and Christian Ostertag-Henning

Federal Institute for Geosciences and Natural Resources, Stilleweg 2, 30655 Hannover, Germany, theodor.alpermann@bgr.de

In this study, geochemical interactions of different minerals (illite, montmorillonite, hematite and dolomite) with a CO<sub>2</sub>/H<sub>2</sub>S 9:1 mixture were investigated in aqueous and quasi-dry systems under conditions similar to those of acid gas storage operations in deep strata. Acid gas mixtures composed of predominantly CO<sub>2</sub> and H<sub>2</sub>S which derive from sour gas processing, have been injected into several deep carbonate or sandstone formations in Canada since 1989 [1]. Despite obvious similarities with the *carbon capture and storage* (CCS) technology, the reactivity of the co-injected H<sub>2</sub>S may significantly influence the geochemical processes occurring under geologic storage conditions of acid gases. In order to detect geochemical reactions of an acid gas mixture with potentially reactive minerals of both cap rock and reservoir rock, experiments with gas-mineral mixtures in the presence and absence of water were conducted under near *in-situ* reservoir conditions (120°C, 120 bar). Extensive chemisorption of H<sub>2</sub>S by illite, montmorillonite and hematite was observed in both aqueous and quasi-dry systems while dolomite was virtually inert towards CO<sub>2</sub>/H<sub>2</sub>S under the reaction conditions. SEM-EDX, bulk sulfur analysis and DTA-MS characterization of dry altered illite and hematite indicate different H<sub>2</sub>S fixation mechanisms like e.g. secondary mineral formation in the course of the reaction as shown for hematite in Fig.1. The observed heterogeneous gas-solid reactions may constitute a significant alteration process of clay minerals in cap rocks above pore-space storage for natural gas or H<sub>2</sub>S-containing CO<sub>2</sub>. Besides, the observed extensive alteration of hematite which is an important constituent of sandstone formations implies a significant alteration of the pore space volume and distribution in such formations under geologic acid gas conditions, even in the desiccated zone around the injection well.

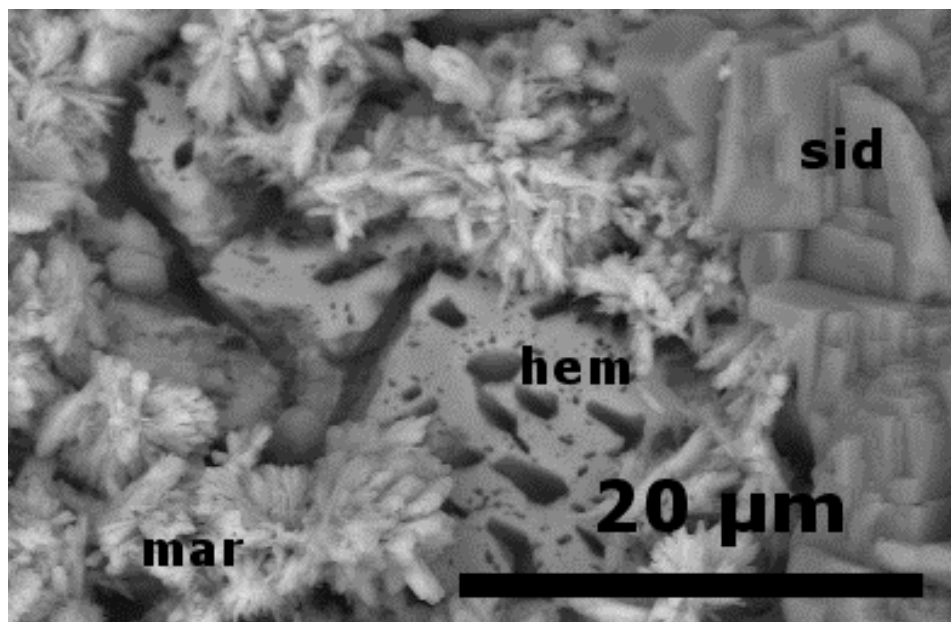


Fig.1: SEM image of the secondary minerals siderite (*sid*) and marcasite (*mar*) generated during the alteration of hematite (*hem*) in a dry reaction system

[1] Bachu, Gunter (2004), *Geological Society Special Publications* 233, 225-234.

## The water purification program using the redox properties of green rusts-related minerals, fougèrite and trébeurdenite

Jean-Marie R. Génin<sup>1</sup>, Georges Ona-Nguema<sup>2</sup>, Christian Ruby<sup>1</sup> and Stuart Mills<sup>3</sup>

<sup>1</sup> Institut Jean Barriol (FR2843), ESSTIN-Université de Lorraine

<sup>2</sup> rue Jean Lamour, 54500 Vandoeuvre lès Nancy

<sup>2</sup> Institut de Minéralogie & Physique des Milieux Condensés, Université Pierre et Marie Curie, F75252 Paris, France

<sup>3</sup> Geosciences, Museum Victoria, GPO Box 666, Melbourne 3001, Australia

Fe<sup>II-III</sup> hydroxysalts, originally studied for understanding the corrosion of iron-based materials and steels, form between metallic iron and ferric oxyhydroxide orange rusts; they are commonly called green rusts because of their color. They belong to the layered double hydroxide family (LDH) and have undoubted redox properties where both divalent and trivalent cations come from the same iron element; thus, Mössbauer spectroscopy can determine very easily the molar ferric ratio  $x = \{[Fe^{III}] / ([Fe^{II}] + [Fe^{III}])\}$ . Green rust-related minerals of the “fougèrite group” discovered in the gleys of hydromorphic soils of aquifers [1,2] opened a new field of water purification since synthetic green rusts are able to reduce oxidized pollutants.

An explanation of what occurs in the field was found by oxidizing carbonated green rust with H<sub>2</sub>O<sub>2</sub> as demonstrated by Mössbauer spectroscopy. The oxidation proceeded by *in situ* deprotonation of OH<sup>-</sup> ions making us think that a phase Fe<sup>II-III</sup> oxyhydroxycarbonate with formula Fe<sup>II</sup><sub>6(1-x)</sub>Fe<sup>III</sup><sub>6x</sub>O<sub>12</sub>H<sub>2(7-3x)}</sub>CO<sub>3</sub>·3H<sub>2</sub>O does exist instead of dissolving in solution for precipitating a usual ferric oxyhydroxide FeOOH as it does with oxygen [3]. Any average value of x ratio comes from mixing domains of the “fougèrite group” that transform topotactically during the redox reaction as explained elsewhere (cf. Génin *et al.*).

By comparing the E<sub>h</sub>-pH diagrams between the dissolution-precipitation oxidation and the *in situ* deprotonation modes, the remarkable properties of weathering (CORTEN®) steels which were discovered empirically in the 1960s are explained; the protection of these steels comes from the *in situ* deprotonation of the layer that forms ferric mössbauerite at the steel surface.

Another development is being currently investigated; the minerals found in gleysols of characteristic bluish-green shade come from the bacterial reduction of natural ferric oxyhydroxides in anoxic conditions under the water table of aquifers. Results from the development of a tertiary treatment for waste water denitrification by reed bed filter plants will be presented. Finally, the landscaping of “watered areas with reinforced iron purification” (WARIP) which is starting in Brittany for large scale treatment in the field will be discussed. This development is intended to solve the long term the devastating proliferation of algae at the mouth of coastal rivers and beaches due to intense agricultural activity. Similar developments are envisioned for fighting algal bloom of the river Murray (Australia).

[1] Génin, J.-M. R., Mills, S. J., Christy, A. G., Guérin, O., Herbillon, A. J., Kuzman, E., Morin, G., Ona-Nguema, G.,

Ruby, C. Upadhyay, C. (2014) Mössbauerite, Fe<sup>3+</sup><sub>6</sub>O<sub>4</sub>(OH)<sub>8</sub>CO<sub>3</sub>·3H<sub>2</sub>O, the first fully oxidised “green rust” mineral from Mont Saint-Michel Bay, France. *Mineralogical Magazine*, **78(2)**, 447–465.

[2] Mills, S. J., Christy, A. G., Génin, J.-M. R., Kameda, T. Colombo, F. (2012) Nomenclature of the hydrotalcite supergroup: natural layered double hydroxides. *Mineralogical Magazine*, **76(5)**, 1289–1336.

[3] Génin J.-M. R., Ruby C. and Upadhyay C. (2006) Structure and thermodynamics of ferrous, stoichiometric and ferric oxyhydroxycarbonate green rusts; redox flexibility and fougèrite mineral. *Solid State Science*, **8**, 1330-1343

## Thin bentonite beds in Neogene lakes/lagoons, northern Israel – effects of detritus and early diagenesis

Amir Sandler<sup>1</sup>, Alexis G. Rozenbaum<sup>1,2</sup>, George Christidis<sup>3</sup> and Pagona Makri<sup>3</sup>

<sup>1</sup> Geological Survey of Israel, 30 Malkhe Israel St, Jerusalem, 95501

<sup>2</sup> Institute of Earth Sciences, The Hebrew University of Jerusalem, Jerusalem 91904, Israel

<sup>3</sup> School of Mineral Resources Engineering, Technical University of Crete,  
73100 Chania, Greece. christid@mred.tuc.gr

Studies on bentonite formation are usually focused on large bodies adjacent to volcanic centers in which the source material is altered to smectites in subaqueous, mostly marine environments, at ambient or elevated temperatures. Deeply-buried bentonite beds of older ages are subjected to illitization, whereby smectite absorb potassium and transform into random and/or ordered mixed layer illite-smectite (K-bentonite) and finally to illite. Here, we present a case of thin bentonite beds, mm's to cm's thick, formed in continental basins with repeated short marine invasions that experienced evaporation and fluctuating salinity. Mineralogical composition of bulk and clay fractions, and chemical composition, including trace elements, were determined on bentonite samples and a few associated single pyroclasts, pyroclastic beds and basaltic soils, and chemical composition was compared to published data of related basalts.

Abundant greenish-gray clay layers occur in the aquatic sedimentary sequence that was deposited between the top of the thick Middle Miocene Lower Basalt and the base of the Early Pliocene Cover Basalt in the northern valleys of Israel. The sequence is well-bedded or laminated and consists of soft dolostone, limestone, marl, with accessory gypsum. In some sections most beds (up to 85%) include pyroclasts with silt to fine sand and occasionally larger grain sizes. A concurrent upward increase of pyroclastic material and greenish-gray clay layers is evident in some of these sections. In certain beds larger pyroclasts have been weathered in situ into clays, which might have been washed away to leave a unique "cell limestone" structure. The appearance and the association with the pyroclasts suggest that the clayey beds are weathered fine volcanic material rich in smectite and hence they should be defined as bentonites.

The bulk mineralogical composition consists of 65 - 86% phyllosilicates, 0 - 25% dolomite, 1 - 15% quartz, and 0 - 10% calcite. Calcite and dolomite occurrence indicates mixing with bottom carbonates or precipitation from infiltrated pore waters of overlying carbonate sediments. Quartz and kaolinite in the clay fraction indicated occasional detrital contribution, probably from airborne dust.

Mixed-layer R0 illite-smectite (IS) is the dominant phase in the clay fraction, with a large compositional range of 55 - 99% expandability. Palygorskite and kaolinite are abundant with amounts of 0 - 35% and 0 - 25%, respectively. High palygorskite amounts occur along IS of low expandability. Early diagenesis in evaporitic environments enabled dolomite and palygorskite precipitation, along with a variable illitization of original discrete smectite. Trace element patterns indicate a complex situation that reflects volcanic origin as well as additions from sediments. Palygorskite associated with bentonite of basic volcanic rocks from different environmental settings has been documented in the past. However, formation of K-bentonites in non-buried strata, is apparently described for the first time.

## Mineralogical and smectite layer charge systematics in a bentonite profile from Milos Island, Greece.

Pagona Makri<sup>1</sup> and George. E. Christidis<sup>1</sup>

<sup>1</sup>Technical University of Crete, School of Mineral Resources Engineering, 73100 Chania, Greece  
christid@mred.tuc.gr

Milos Island, Aegean Greece is well known for world-class bentonite deposits with more than 80 million tonnes of proven reserves. The deposits formed from hydrothermal alteration of pyroclastic flows and to a lesser degree of lavas of dacitic-andesitic to rhyolitic composition in a submarine environment. In this presentation we present layer charge and mineralogical systematics of a well-exposed bentonite 130 x 25 m profile in Eastern Milos. The bentonite formed at the expense of a dacitic lava flow. For this purpose 75 samples were collected in a 12 x 3.5 m grid. Quantitative XRD mineralogical analysis was performed on random powders (side loading method) by the Autoquan code, using ZnO as internal standard. Mineral textures were studied by SEM-EDS. Layer charge and charge distribution of smectites in the two profiles was determined according to the method of Christidis & Eberl (2003), which is based on the comparison of XRD patterns of K-saturated, ethylene-glycol solvated smectites with calculated XRD-patterns for three-component interlayering (fully expandable 17.1 Å layers, partially expandable, 13.5 Å layers and non-expandable 9.98 Å layers). Measurement of layer charge and charge distribution is possible by means of the LayerCharge program.

Diocahedral Ca-smectite is the most abundant mineral with quartz, opal-CT, calcite, kaolinite, K-feldspar, plagioclase, dolomite and trace brookite and pyrite being present as accessory phases. Smectite morphology is uniform, characterized by typical wavy flakes. The quantitative mineralogical analysis showed that opal-CT is distributed in two steep linear sub-parallel zones, whereas igneous plagioclase of intermediate composition is distributed in a sub-parallel zone mainly in the higher sectors of the profile. The remaining minerals display a less well defined distribution. The profile is characterized by gradual increase of layer charge towards the surface and is considered to reflect the geochemical-hydrological conditions prevailing during the bentonite formation, in a hydrothermal system. Application of the Green–Kelly test showed that the proportion of beidellitic layers increases towards the top of the profile.

The observed variations are cryptic, i.e. they are not visible macroscopically, within the bentonite profile. The distribution of authigenic minerals and tetrahedral charge strongly suggest that bentonite formation is related to fluid flow in a hydrothermal system. This flow was directed along sub-vertical channels and facilitated redistribution of Si by precipitation as opal-CT in linear structures and formation of beidellitic layers towards the top of the profile.

Christidis G.E., Eberl D.D, (2003). Determination of layer-charge characteristics of smectites. *Clays and Clay Minerals*, 51, 644-655.



## Evaluation of bentonites of Turkey and an investigation of their utilization in ceramic tile manufacturing

Ozgur Cengiz

Afyon Kocatepe University, Faculty of Fine Arts, Department of Ceramics, 03200, Afyonkarahisar, Turkey  
ocengiz@aku.edu.tr

In this present work, different bentonite deposits from Mid-Anatolia and Western Anatolia (Turkey) were investigated. Mineralogical, chemical and thermogravimetric analyses were carried out by XRD, XRF and TGA, respectively. Based on the chemical compositions of the bentonites, five samples were chosen from the studied locations- Artvin, Konya, Tokat, Trabzon and Edirne in order to prepare ceramic tile compositions to assess their potential in the ceramic industry. Several formulations incorporating different amounts of bentonites were prepared and the effect of bentonite content on the body, on physical and the mechanical properties, and on the firing temperature was investigated. The results indicated that bentonite could be sufficient in certain amounts in ceramic wall and floor tile production.

**Keywords:** Bentonite, applied mineralogy, ceramic tile

## 10 years of exploitation: still the same Kopernica bentonite?

Renata Adamcova<sup>1</sup>, Franz Ottner<sup>2</sup>, Karin Wriessnig<sup>2</sup> and Jana Deliova<sup>1</sup>

<sup>1</sup>Comenius University in Bratislava, Faculty of Natural Sciences, Mlynska dolina, 842 15 Bratislava, Slovakia, adamcova@fns.uniba.sk

<sup>2</sup>BOKU – University of Natural Resources and Life Sciences, Institute of Applied Geology, Peter-Jordan-Str. 70, 1190 Vienna, Austria

A special application-focused investigation of Slovak bentonites considered for technical barriers in the future deep geological repository (DGR) of radioactive waste was started in 2003. Bentonite K45 from Kopernica (Central Slovakia) was one of the five studied types. A large amount of information was collected about this material through interdisciplinary cooperation, whereby all participating scientists worked with the same material provided by a commercial supplier in the beginning of the project which was finished in 2005 (Adamcova, Frankovska & Durmekova, 2009; Galambos et al., 2011). At the end, all of the supplied bentonite was used up. A new DGR-related project started 10 years later (Adamcova et al., 2013). The bentonite K45 from Kopernica was selected for those tests as it seemed to be the most suitable one for the bentonite barrier around the canisters. However, the former supplier was not able to provide the same bentonite. Mining moved to another site (not defined) and the designation of the commercial product changed to BKT with the description “bentonite of Kopernica type”, instead of “bentonite from Kopernica”. It was necessary to compare at least some basic properties of those two materials to be sure that former knowledge about K45 can be applied to BKT and used in the interpretation of tests resulting from the recent project. Those principal properties are mineral composition and plasticity, represented by the Atterberg liquid limit  $w_L$  (%). This is the soil moisture when soil consistency changes from plastic to liquid. Former results confirmed that it is a very good indicator of the swelling and sealing potential. A comparative qualitative mineral analysis of bulk samples and of the clay fraction (<0.002 mm) was done by X-ray diffraction (XRD) and by simultaneous thermal analysis (STA), consisting of thermogravimetric (TG) and differential scanning calorimetry (DSC). Casagrande method and the cone penetration method were used for tests on the liquid limit. Results showed that the mineral composition is nearly identical, with only minor (but interesting) changes in the thermal behaviour. Certain differences in the liquid limit might be of subjective character, because personal influence is not negligible in these standard test procedures. Based on these results, it seems to be really the same type of bentonite even after 10 years of exploitation.

**Acknowledgment:** We acknowledge the Scientific Granting Agency of the Ministry of Education, Science, Research and Sport of the Slovak Republic for funding the project VEGA 1/0828/13.

Adamcova R., Frankovska J. & Durmekova T.: Engineering geological clay research for a radioactive waste repository in Slovakia. AGEOS (2009), 1, 2: 71 – 82.

Adamcova R., Galambos M., Durmekova T., Rosskopfova O., Krajnak A. & Ekkertova P.: Pilot research on diffusion parameters of U235 fission products. Proceed. Of the XV International Clay Conference, Rio de Janeiro, Brazil, July 7-11, 2013.

Galambos M., Rosskopfova O., Kufcakova J. & Rajec P.: Utilization of Slovak bentonites in deposition of high-level radioactive waste and spent nuclear fuel. J Radioanal Nucl Chem (2011) 288:765–777

## EPSP – Experimental Pressure and Sealing Plug as part of the European DOPAS project

Irena Hanusová<sup>1</sup>, Jiří Svoboda<sup>2</sup> and Petr Večerník<sup>3</sup>

<sup>1</sup>Dlážděná 6, Prague 1, 110 00 Czech Republic; hanusova@surao.cz

<sup>2</sup>CTU in Prague, Thákurova 7, 166 29 Prague 6, Czech Republic; jiri.svoboda@seznam.cz

<sup>3</sup>ÚJV Řež, a. s., Hlavní 130, 25068 Husinec-Řež, Czech Republic; petr.vecernik@ujv.cz

The international DOPAS (Full-Scale Demonstration of Plug and Seals) project involves research into, and the development of, different types of plugs and sealing materials for use in the construction of radioactive waste repositories.

The project was initiated by the IGD-TP and is being subsidised from European RTD project resources. Fourteen organisations from a total of eight European countries are involved in the project, the planned duration of which is four years (09/2012 – 08/2016). Financial support is provided by Euroatom's Seventh Framework Programme.

Several different types of plugs are proposed in the Czech Deep Geological Repository concept. Their purpose is to safely and securely seal and close individual parts of the repository during the operational stage of the facility, i.e. up to 150 years.

The Czech part of the DOPAS project - Experimental Pressure and Sealing Plug (EPSP) is being conducted by a 3-member Czech consortium (SÚRAO, CTU, ÚJV) at the Josef Underground Research Centre (located close to the town of Dobříš) in the Čelina – Mokrsko Au-bearing section of the facility.

The EPSP experiment concept is based primarily on the use of Czech materials (low pH concrete, Ca/Mg bentonite) and technologies (shotcreting, the shotclay technique and compaction of bentonite pellets) available in the Czech Republic. The construction of the plug (Fig. 1) was designed at the Centre of Experimental Geotechnics of the Czech Technical University in Prague. The plug consists of a concrete segment made of low pH cement and a layer of compressed bentonite pellets. The pellets are of Ca/Mg bentonite with the industrial designation Bentonite 75 from the Rokle/Černý Vrch deposit. The plug is closed by a second concrete layer (see Fig. 1).

The EPSP experimental plug itself which will be completed and put into operation in 2<sup>nd</sup> Q of 2015 is currently under construction. The continuous monitoring is running and will be carried out through the whole lifetime of the project. The data obtained will subsequently be used for the construction of mathematical models and for safety analysis purposes.

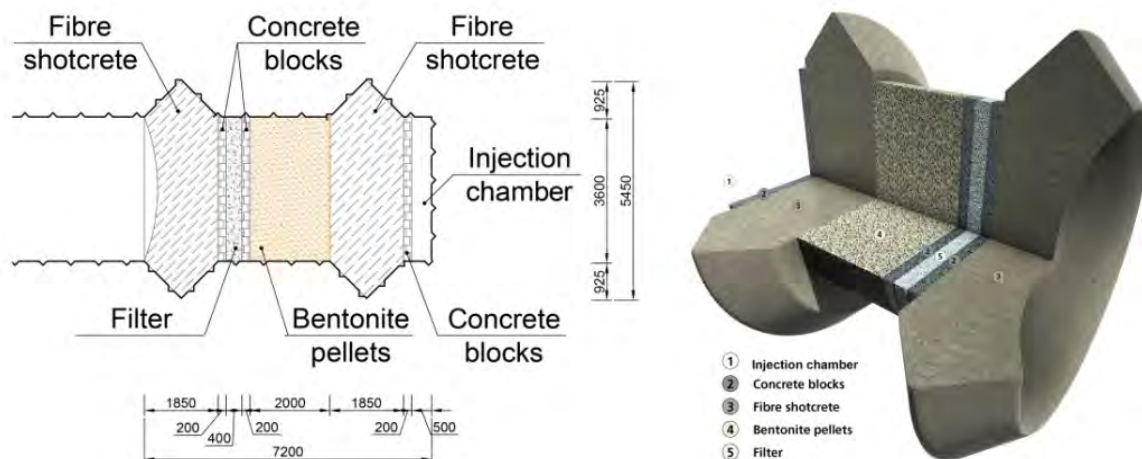


Fig. 1 Structural plug design and cross-section through the EPSP plug

## Alteration and mechanical behavior of bentonite immersed in NaOH and Ca(OH)<sub>2</sub> solutions

Yasutaka Watanabe<sup>1</sup> and Shingo Yokoyama<sup>2</sup>

<sup>1</sup>Central Research Institute of Electric Power Industry, 1646 Abiko, Abiko-shi, Chiba-ken 270-1194 Japan, yasutaka@criepi.denken.or.jp

<sup>2</sup>Central Research Institute of Electric Power Industry, 1646 Abiko, Abiko-shi, Chiba-ken 270-1194 Japan, shingo@criepi.denken.or.jp

**Introduction:** Bentonite will be used in radioactive waste disposal facilities as a part of the engineered barrier. It is expected that the bentonite will be exposed to alkaline solutions from leaching of cementitious materials. Under alkaline conditions, dissolution of minerals composing the bentonite and precipitation of secondary materials would occur. Since the alteration would change hydraulic conductivity and mechanical properties of the bentonite, it is important to evaluate the change in engineering properties to model the long-term stability of the engineered barrier. Therefore, the alteration and shear characteristics of the bentonite immersed in NaOH and Ca(OH)<sub>2</sub> solutions has been investigated, and effects of the alteration on the mechanical behavior of the bentonite has been evaluated.

**Experimental procedure:** Ca-type bentonite was used. Montmorillonite content of the bentonite was estimated approximately 88 % by methylene blue absorption. Compacted bentonite was immersed in 0.1 mol/L-NaOH and 5 mmol/L-Ca(OH)<sub>2</sub> solutions, and stored at 40 degrees Celsius. pH and chemical composition of immersion solutions were measured intermittently. Triaxial compression tests in un-drained condition were executed using the immersed specimens. Mineral compositions, leacheable cations, and the nature of the montmorillonite were investigated after the triaxial compression tests.

**Experimental results and discussion:** In the immersion tests for 711 days at most, leaching of Si ion was observed, while Al ion was not detected in both reactive solutions. Methylene blue absorbed of the immersed bentonite did not decrease. Therefore, montmorillonite in the bentonite might not be dissolved. According to X-ray diffraction pattern, it is plausible that cristobalite was dissolved. Mean layer charge of montmorillonite remained constant. In the case of the NaOH solution, the cation exchange reaction progressed only slightly; a small amount of exchangeable Ca ion from the bentonite has exchanged by Na ion. Observation by SEM-EDX and EPMA showed higher Ca concentration at the edge of the specimens, interpreted to be the new precipitate. In the triaxial compression tests, shear strength drastically increased, and brittle failure was observed after immersion. In the specimen immersed in Ca(OH)<sub>2</sub> solution, cohesion increased, and friction angle at failure was barely changed. In the case of NaOH solution, only the friction angle of the specimen was changed. The experimental results imply that precipitates in the case of Ca(OH)<sub>2</sub> solution act as a bonding material between soil particles. It is concluded that the change of shear characteristics of the bentonite depends on variations in precipitation and chemical conditions.

## A non-linear elastic approach to modelling the hydro-mechanical behaviour of the SEALEX laboratory tests on compacted MX-80 bentonite

Andrew Fraser Harris<sup>1</sup>, Chris McDermott<sup>1</sup>, Alex Bond<sup>2</sup>, Kate Thatcher<sup>2</sup> and Simon Norris<sup>3</sup>

<sup>1</sup> School of Geosciences, University of Edinburgh, The Grant Institute, James Hutton Rd, Edinburgh. EH9 3FE, UK. <sup>2</sup> Quintessa Ltd, 633/635 Birchwood Boulevard, Birchwood, Warrington. WA3 7QU, UK

<sup>3</sup> Radioactive Waste Management Limited, Building 587, Curie Avenue, Didcot, UK.

Email: a.p.fraser-harris@ed.ac.uk

Bentonite is commonly proposed as an important component of engineered barrier systems in High Level Radioactive Waste disposal concepts. The complex behaviour of bentonite must be well understood and predicted in order to provide a scientific basis for disposal safety case and licence applications. The SEALEX experiments conducted by IRSN at the Tournamire underground rock laboratory, France, are designed to test the sealing potential of compacted bentonite blocks with specific emphasis on long-term hydraulic performance, intra-core geometry of the bentonite block, and changes in external confining conditions e.g. concrete plug failure (Barnichon et al. 2012). The experiments comprise both laboratory tests and *in situ* experiments, and as such, provide a good case study for model development. As a result, these experiments have been chosen to form Task A of the coupled process modelling collaboration DECOVALEX-2015 ([www.decovallex.org](http://www.decovallex.org)). This work forms the initial model development for a non-linear elastic approach to modelling the SEALEX Laboratory tests and has been completed by a team working for Radioactive Waste Management Limited (RWM).

The laboratory tests can be broken down into two modelling steps. The first stage comprises oedometer consolidation tests at different induced suctions, and a constant volume infiltration test. A strain dependent non-linear elastic mechanical model was calibrated to the consolidation tests and coupled to a pressure-based Richards flow simulation to model the infiltration test. The second modelling step is a 1/10<sup>th</sup> scale mock-up test which includes a symmetrical technological void around the circumference of the sample which causes complex hydro-mechanical behaviour (Wang et al 2012). The non-linear elastic approach is able to reproduce the general trends of the behaviour, but does not capture the plastic collapse in the early stages.

Model development is still ongoing but the initial results indicate the applicability of the approach. While this model currently does not recreate all aspects of the experimental data, it requires few calibration parameters to recreate the general trends and can serve as a comparison to more complex model approaches.

Barnichon J.D., Dick P., Bauer, C. 2012. The SEALEX *in situ* experiments: Performance tests of repository seals. In *Harmonising Rock Engineering and the Environment*. ISBN-97804158448

Wang, Q., Tang, A.M., Cui, Y-J., Delage P., Barnichon, J.D., Ye, W.M., 2012. The effects of technological voids on the hydro-mechanical behaviour of compacted bentonite-sand mixture. *Soils and Foundations*. **53**. 2.

## Mineralogy and chemistry of illites in Late Devonian K-bentonites, NW Turkey

Ömer Bozkaya<sup>1</sup>, Asuman Günel-Türkmenoğlu<sup>2</sup>, M. Cemal Göncüoğlu<sup>2</sup>, Özge Ünlüce, İsmail Ömer Yılmaz  
<sup>1</sup>Department of Geological Engineering, Pamukkale University, Denizli, Turkey, bozkaya66@gmail.com  
<sup>2</sup>Department of Geological Engineering, Middle East Technical University, 06800 Çankaya-Ankara, Turkey  
asumant@metu.edu.tr

K-bentonite (tephra) layers are exposed as thin beds within the Late Devonian carbonate rocks of the Yılanlı formation at three different limestone/dolomitic limestone quarries, Gavurpinari, Yılanlı Burnu and Sapca Cimsir Cukurlari, in northwestern Turkey. The mineral composition of K-bentonite layers consists mainly of illite and illite-smectite (I-S) with subordinate kaolinite, dolomite, calcite, quartz, feldspar, and gypsum. K-bentonite whole rocks and pure illites, separated from K-bentonites, were analyzed by X-ray diffraction, scanning and high-resolution transmission electron microscopy, and inductive coupled plasma-mass spectrometry methods. Illite is the major clay mineral in the Gavurpinari and Yılanlı Burnu quarries, but I-S (R3 type, I 92%, S 8%) in Sapca Cimsir Cukurlari quarry. Platy illites of Gavurpinari and Yılanlı Burnu quarries have regular stacking sequences with the crystallite sizes of 15-20 nm. Illite Kübler index (KI,  $\Delta^{\circ}2\theta$ ),  $d_{060}$  values (Å) and polytype data of illites do not exhibit significant variations in Gavurpinari (0.69-0.77, average 0.72  $\Delta^{\circ}2\theta$ ; 1.4991-1.5015, average 1.5000 Å;  $2M_1/(2M_1+1M_d)=30\%$ ) and Yılanlı Burnu (0.47-0.93, average 0.71  $\Delta^{\circ}2\theta$ ; 1.4992-1.5039, average 1.5015 Å;  $2M_1/(2M_1+1M_d)=25\%$ ) quarries, but are fairly different in Sapca Cimsir Cukurlari quarry (1.47-1.50, average 1.48  $\Delta^{\circ}2\theta$ ; 1.4967-1.4972, average 1.4970 Å;  $1M/(1M+1M_d)=30\%$ ). The crystal-chemical data of illites and I-S indicate high-grade diagenesis for the Gavurpinari and Yılanlı Burnu quarries, and low-grade diagenesis for the Sapca Cimsir Cukurlari quarry. The relatively higher  $d_{060}$  values in the Yılanlı Burnu quarry seem to be related to Mg diffusion from dolomitic limestone host-rocks. Major, trace element compositions of illites from Sapca Cimsir Cukurlari quarry are different from the other two locations. FeO, Na<sub>2</sub>O and P<sub>2</sub>O<sub>5</sub> (wt %) are lower, whereas Sn, W, Be, Rb, Nb, Zr, Th and U (ppm) have higher values for Sapca Cimsir Cukurlari quarry. Illites have phengitic compositions for Gavurpinari and Yılanlı Burnu quarries, but muscovitic compositions for Sapca Cimsir Cukurlari quarry. Chondrite-normalized REE patterns are somewhat similar for Gavurpinari and Yılanlı Burnu quarries, but are relatively higher for Sapca Cimsir Cukurlari quarry. Mineralogical and chemical data indicate the existence of two different K-bentonite occurrences as (1) Gavurpinari and Yılanlı Burnu quarries, and (2) Sapca Cimsir Cukurlari quarry. The first group originated from alkali basaltic volcanism and was illitized under high-grade diagenetic conditions, whereas the second group was derived from trachytic volcanism and evolved under low-grade diagenetic conditions.

This research study is supported by TÜBİTAK Project No: 110Y272.

## Physico-chemical properties of bentonite from Rokle deposit (Czech Republic) in temperature range of 20-95 °C

Petra Fůrychová<sup>1</sup>, Miroslav Honty<sup>2</sup>, Tomáš Kuchovský<sup>1</sup>, Marek Osacký<sup>3</sup>, Dana Kuchovská<sup>1</sup> and Arno Grade<sup>2</sup>

<sup>1</sup> Department of Geological Sciences, Faculty of Science, Masaryk University, Kotlářská 2, 611 37 Brno, Czech Republic, petra.furychova@mail.muni.cz

<sup>2</sup>SCK-CEN, Waste and Disposal Research Group, Boeretang 200, B-2400 Mol, Belgium

<sup>3</sup>Department of Geology of Mineral Deposits, Comenius University, Mlynská Dolina, 842 15 Bratislava, Slovak Republic

In the Czech Republic, natural raw Mg-Ca bentonite from Rokle deposit (B75 bentonite) is widely used in industry, and is also considered as a potential buffer material for deep geological repository. In this context, study of its hydraulic properties, and mineralogical and geochemical stability under heat exposure is important for many applications. Here, we present a comparison of basic characteristics of B75 bentonite with bentonite samples exposed to temperatures of between 27-95 °C for over 4 years (CZ Mock-Up: Pacovský et al., 2007).

Hydraulic conductivity of B75 bentonite was measured for different densities (1.3; 1.5; 1.7 g cm<sup>-3</sup>) at 20°C in permeameter cells by the constant-head method. With increasing dry density, hydraulic conductivity decreases from 1.27×10<sup>-12</sup> to 3.29×10<sup>-13</sup> to 1.18×10<sup>-13</sup> m.s<sup>-1</sup> in the most compacted sample. The mineralogical composition of raw B75 bentonite (bulk and <2 μm) was determined by XRD analysis. B75 bentonite consists mainly of montmorillonite, illite, kaolinite, quartz, calcite and anatase. Cation exchange capacities (CEC) measured by the Cu(II)-triethylenetetramine method are 74.9±1.1 and 98.3±2.4 mEq/100 g for bulk and <2 μm size fractions, respectively. The specific surface area (SSA) of raw B75 bentonite measured by the Brunauer Emmett Teller (BET) N<sub>2</sub> adsorption method is 78.1±0.1 m<sup>2</sup>/g.

For B75 bentonite exposed to a temperature of 80°C, hydraulic conductivity increased in comparison with the values measured at 20°C. With increasing dry densities (mentioned above), the corresponding values are 3.07×10<sup>-12</sup>; 8.54×10<sup>-13</sup>, and 3.67×10<sup>-13</sup> m.s<sup>-1</sup>.

No significant changes in mineralogy were observed for samples exposed to 20–95°C for >4 years. Only slight changes were found in the position of 001 smectite reflection between the samples from coldest and warmest part. The Bertaut Warren Averbach (BWA) analysis results show no effect of temperature on the smectite mean crystallite thicknesses. Thus, the slight changes in 001 smectite reflection are likely not due to changes in the mean crystallite thickness of smectites. For reacted bulk and <2 μm samples, the CECs range from 59.0 ±1.3 to 69.8 ±1.1 mEq/100 g and from 93.0 ±3.5 to 105.2 ±3.0 mEq/100 g, respectively. However, the results show no effect of temperature on the CEC values of reacted bulk and <2 μm samples. The most pronounced changes for samples exposed to 20–95°C for >4 years were observed in the SSA values. Generally, the SSA values for reacted bulk samples from colder parts (~30 °C) were greater (75.6 ±0.2–81.7 ±2.2 m<sup>2</sup>/g) than those from warmer parts (80-90°C) (68.9 ±0.5–74.8 ±0.2 m<sup>2</sup>/g). A similar trend in the SSA values was observed for the corresponding <2 μm size fractions after the same experiment (colder parts, 113.6±0.8–118.3±0.3 m<sup>2</sup>/g versus warmer parts 96.7–112.7 ±1.1 m<sup>2</sup>/g).

Overall, the preliminary results indicate that the experimental conditions affected the surface properties (mainly SSA) rather than mineralogy of the studied samples. The mercury intrusion porosimetry measurements are on-going to further investigate this phenomenon on a meso scale.

Pacovský, J., Svoboda, J., Zapletal, L.(2007): Saturation development in the bentonite barrier of the Mock-Up-CZ geotechnical experiment. Physics and Chemistry of the Earth 32, 767-779.

## Structural incorporation of Al into diatomite and its influence on the surface solid acidity of diatomite

Dong Liu<sup>1</sup>, Liangliang Deng<sup>1,2</sup>, Weiwei Yuan<sup>1,2</sup> and Peng Yuan<sup>1</sup>

<sup>1</sup>CAS Key Laboratory of Mineralogy and Metallogeny, Guangzhou Institute of Geochemistry, Chinese Academy of Sciences, Guangzhou 510640, China, liudong@gig.ac.cn

<sup>2</sup>University of Chinese Academy of Sciences, Beijing 100049, China

Diatomite is sourced from deposits of diatom frustules which are mainly composed of amorphous hydrated silica ( $\text{SiO}_2 \cdot n\text{H}_2\text{O}$ ). Aluminum (Al) is the dominant element in diatomite besides major elements of silicon (Si) and oxygen (O). Existence of Al in the structure of diatomite is demonstrated to effectively lower the solubility of diatomaceous silica and is beneficial to the preservation of diatomite. Moreover, existence of Al affects the structure and surface properties of diatomite, such as the size of nano silica balls, which are the basic component of diatom shells, the surface charge and solid acidity. However, the mechanism of Al-incorporation and its influence on diatomite have not been investigated until now.

In this study, hydroxyl aluminum polymer was loading on the surface of diatomite and then the obtained composition was heated in various temperatures to incorporate Al into the structure of diatomaceous silica. The structural incorporation of Al into diatomite is investigated by preparing Al-diatomite composites, during which loading of Al precursor, hydroxyl aluminum polymer ( $\text{Al}_{13}$ ) on the surface of diatomite and subsequent heating at various temperatures were carried out. Incorporation possibility and mechanism were estimated by  $^{29}\text{Si}$  MAS NMR spectra and Fourier transform infrared spectrum (FTIR).

The results show that Al was incorporated with diatomite and implanted into the structure of diatomite by the condensation reaction of the hydroxyl groups of  $\text{Al}_{13}$  and diatomite, and the Si-O-Al(OH) groups were formed during the condensation reaction. Al incorporation by the condensation reaction of hydroxyl groups of  $\text{Al}_{13}$  with single silanols of diatomite was easier than that with germinal silanols. Al incorporation influenced the solid acidity of diatomite. Solid acid sites of diatomite increased after Al incorporation. And the improvement of acidity for different types of acid sites depended on the heating temperature of Al-incorporated diatomite preparation: the Brønsted (B) and Lewis (L) acid sites increased greatly after heating at 250 and 350 °C for the appearance of the Si-O-Al(OH) groups sourced from the condensation reaction; but only L acidity significantly improved after heating at 500 °C because of dehydroxylation of the Si-O-Al(OH) groups on the surface of diatomite and thus formation of unsaturated  $\text{Al}^{3+}$  ions with L acidity. These results firstly demonstrate that the structural incorporation of  $\text{Al}^{3+}$  ions into diatomite can occur by the condensation reaction of hydroxyl groups of Al precursors and diatomite. Moreover, the rich solid acid sites of Al-incorporated diatomite show promising application as a solid acid catalyst.

**Acknowledgment:** This study was financially supported by the National Natural Science Foundation of China (Grant No. 41202024).



## Elaboration and characterization of materials obtained by pressing of vermiculite without binder addition

L. Duclaux<sup>1</sup>, A-N. Nguyen<sup>1,2</sup>, F. Balima<sup>2</sup>, L. Reinert<sup>1</sup>, F. Muller<sup>3</sup>, S. Le Floch<sup>2</sup>, V. Pishedda<sup>2</sup>, A. San Miguel<sup>2</sup>

<sup>1</sup> Univ. Savoie Mont Blanc, LCME, F-73000 Chambéry, France, laurent.duclaux@univ-savoie.fr

<sup>2</sup> Institut Lumière Matière, Université Lyon 1-CNRS, Université de Lyon 69622 Villeurbanne, France.

<sup>3</sup> ISTO, 1A Rue de la Férollerie, 42071 Orléans Cedex 2, France

Vermiculite materials were obtained by uniaxial pressing of potassic vermiculite powders obtained by sonication without any binder addition. The vermiculite powders, made of aggregates of particles with nanometric thickness and micrometric in plane dimension, were pressed in the range 17.7-80 MPa at room temperature and 200°C, and further annealed in the range 400-800°C. Pressing powders at 200°C instead of 25°C allowed the slight increase of the density of the formed materials (from 1.9 to 2) due to the desorption of the water molecules from the interaggregate and interparticle spaces, allowing a higher densification. The density was also increased by tailoring the particle size distribution. The pressed materials were formed of oriented arrangement of vermiculite aggregates. The porous structure, characterized by mercury porosimetry, scanning electron microscopy, and small angle X-ray scattering, was modelled by oriented oblate spheroidal pores formed in the voids between the stacked aggregates organised in a structure possessing a cylindrical symmetry. The porous structure was found to vary with the pressure and the annealing temperature.

## Fines from aggregate quarrying and its influence on frost protection in roads

Elena Kuznetsova<sup>1</sup> and Svein Willy Danielsen<sup>2</sup>

<sup>1</sup>Norwegian University of Science and Technology (NTNU), Trondheim, Norway, Elena.kuznetsova@ntnu.no

<sup>2</sup>Independent Geomaterials Consultant, Trondheim, Norway, swdanielsen@gmail.com

With natural (fluvial, glaciofluvial) sand/gravel resources being rapidly depleted in many countries, the last decade has seen a significant trend towards using more alternative materials for construction purpose. In Norway the development and implementation of crushed aggregate technology has been the most important way to get around the problem of increased resource scarcity. Today Norway is one of the European countries with the highest percentage of crushed/manufactured aggregates. A crushed product will reveal a different particle size distribution, a sharper, more angular particle shape, and not least – a significantly different mineral composition. The latter may often be characterised by more polymineral composition, and it will also depend much more on the local bedrock. When handled with care and knowledge, these differences can give the user a lot of new opportunities relating to materials design.

In Norway, research is currently being undertaken to study the properties of crushed aggregates for road construction – specifically relating to frost heave protection and the development of new guidelines for this purpose. During spring 2014 The Norwegian Public Roads Administration introduced a new handbook with requirements for roads construction in Norway, including new specifications for the frost protection layer. When pavements are constructed over moist and/or frost susceptible soils in cold and humid environments, the frost protection layer also becomes a very important part of the road system. According to new specification, the allowed amount of fines content (<0.063 mm) was increased to 15% (calculated for the material less than 22.4 mm).

Analysing these new requirements, two questions arise. First of all how this materials size will affect heat exchange in the layer? Secondly – if the allowable fines content will make the materials frost susceptible?

Various publications emphasise the outstanding effect of the mineral content of fine grains on the frost susceptibility of soils. But detailed quantitative information with regard to the allowable contents of fine grains and specific (clay) minerals in order to provide a certain degree of safety against freeze-thaw damage on roads, highways, railways, airfields, etc., is rarely available.

The study presented here is part of a larger research program to investigate the properties of crushed rock materials in relation to frost heaving in the frost protection layer. An important issue will be the resistivity for frost penetration due to presence of water and fine particles. Due to new requirements for allowed fines content, it is essential to investigate if increased amount of fines <0.063 mm together with increased water content in the frost protection layer, will not lead to more frost heave problems.

Novel research as well as innovative industrial development relating to manufactured (crushed) aggregates has involved technologies to control even the particle size distribution of the fines. The industrial perspective to be followed up is to tailor-make not only the sand grading and fines content, but also the grading curve of the finest fractions (crusher fines as well as industry fillers), to meet requirements designed by the frost properties research. Also – since the mineral composition of the fines influences the properties – a part of the industrial perspective will also be to do the necessary mineralogical analyses in order to choose the rock, and to design the fines grading and amount in relation to the mineral composition.

## Natural zeolite as filler for metakaolin geopolymers

Slávka Andrejkovičová, Walid Hajjaji and Fernando Rocha

Geosciences Department, Geobiotec Research Unit, University of Aveiro, Campus Universitário de Santiago, 3810-193 Aveiro, Portugal, tavares.rocha@ua.pt

The aim of this work is to investigate the effect of natural zeolite as filler on the mechanical performance and on the adsorption capacity of geopolymers products.

Four different types of geopolymers were prepared, in which metakaolin was replaced by 25, 50 and 75% of natural zeolite. The geopolymerization mixtures were designed by using metakaolin 1200S (MK) (AGS Mineraux, France) and natural zeolite (Zeocem, Nižný Hrabovec, Slovakia).

In water medium, alkaline activators NaOH (ACS AR Analytical Reagent Grade Pellets) and hydrated sodium silicate (Merck, Germany) were used to dissolve aluminosilicates. The target was the following molar oxide ratios:  $\text{SiO}_2/\text{Al}_2\text{O}_3 = 1$ ,  $\text{Na}_2\text{O}/\text{Al}_2\text{O}_3 = 1$ . The water content for all the samples was kept constant with a molar ratio of  $\text{H}_2\text{O}/\text{Na}_2\text{O} = 17$ . The mixing of the blends was carried out by a laboratory stirrer at two different speeds; 100 rpm for 2 min and 200 rpm for 4 min, to insure their homogeneity and avoid bubbles and agglomeration into the sample. The pastes were immediately poured into 20 x 20 x 20 mm cubic molds and placed in oven at 50 °C for 24 h and thereafter left at room temperature for 1 day. Curing was carried out by keeping the geopolymer cubic specimens in distilled water from 1, 7, 14 and up to 28 days.

Geopolymeric products were characterized by XRD, NMR and SEM analysis. Mechanical resistance of geopolymers was determined by measuring their compressive strength. The results showed that at early ages of curing, all geopolymers containing zeolite provided higher compressive strengths compared to reference metakaolin geopolymer. Already after 1 day of curing, geopolymer containing 50% of natural zeolite provided a rise of 450 % of compressive strength compared to the reference (2 MPa). At 28 days of curing, increased compressive strength values were determined for all geopolymers containing zeolite compared to metakaolin.

Based on water absorption data it was observed that the values are comparable for all geopolymers, with the best result provided by geopolymer without zeolite.

## REE recovery from kaolinite-rich saprolite and a clayish horizon related to the Serra Dourada granite, Brazil: potential for ion-adsorption type deposits

Igor V. Santana<sup>1</sup>, Frances Wall<sup>1</sup> and Nilson F. Botelho<sup>2</sup>

<sup>1</sup>Camborne School of Mines, University of Exeter, Penryn Campus, TR10 9FE, UK.

igorunesp@gmail.com; F.Wall@exeter.ac.uk

<sup>2</sup>Instituto de Geociências, Universidade de Brasília, 70910-900, Brazil. nilsonfb@unb.br

The Serra Dourada granite is located in Goiás/Tocantins state, central Brazil, and thus exposed to a tropical warm climate with alternating dry and wet seasons. The main lithology consists in a medium-coarse grained biotite granite, with other more evolved facies such as muscovite-biotite granite, granitic pegmatite, albitite, and biotitite occurring locally. Whole-rock analyses in the biotite granite yield high REE contents of 800 ppm on average, made up mainly by primary accessory minerals such as allanite, apatite, monazite-(Ce), xenotime-(Y), zircon, fluocerite and bastnäesite-group minerals. Parts of the granite are well known for hosting placer deposits of monazite-(Ce) and xenotime-(Y). However, during the weathering of this granite, the soluble accessory minerals may be broken down, releasing REE cations that will eventually adsorb onto clay minerals formed at the expense of plagioclase. As a consequence, a progressive REE enrichment in the alteration products of the granite is observed, especially in the saprolite and in clayish-rich horizons, both of which possess abundant kaolinite-group minerals. This model of REE mineralization is known as ion-adsorption type, currently the major source in China of the 'critical' heavy REE (Eu-Lu+Y). In order to be considered an ion-adsorption ore, one of the essential conditions is that a substantial proportion of REE in the alteration products must be present as exchangeable cations. We carried out a pilot test in one saprolite and one clayish horizon following step one of the procedure of Sanematsu et al. (2013). This consists of the extraction of exchangeable REE ions adsorbed on clay minerals and analysis by ICP-MS. The concentration of REE (including Y) recovered from the saprolite after the test was around 397 ppm, which corresponds to approximately 18% of its original REE content of 2162 ppm. The chondrite-normalized pattern is enriched in the light REE,  $(La/Yb)_N = 77$ , with strong negative Ce and Eu anomalies. The REE extraction from the clayish horizon yielded better results. The REE recovered were 562 ppm, which corresponds to approximately 49% of the original content of 1126 ppm. The chondrite-normalized pattern is still light REE-enriched but less steep,  $(La/Yb)_N = 21$ , with lower negative Ce and Eu anomalies. In terms of grades, Bao and Zhao (2008) state that weathering profiles containing more than 500 ppm of exchangeable REE can be considered as ore, which allow comparison of this study with other ion-adsorption deposits from southern China.

Bao, Z., & Zhao, Z. (2008). Geochemistry of mineralization with exchangeable REY in the weathering crusts of granitic rocks in South China. *Ore Geology Reviews*, 33(3), 519-535.

Sanematsu, K., Kon, Y., Imai, A., Watanabe, K., & Watanabe, Y. (2013). Geochemical and mineralogical characteristics of ion-adsorption type REE mineralization in Phuket, Thailand. *Mineralium Deposita*, 48(4), 437-451.

## Production of refractory aggregates from waste chamotte and industrial clays

Stavroula Kavouri<sup>1</sup>, Michael G. Stamatakis<sup>1</sup> and Efthimios Kagiara<sup>2</sup>

<sup>1</sup>University of Athens, Panepistimiopolis, Ano Ilissia, Athens, Greece, [stamatakis@geol.uoa.gr](mailto:stamatakis@geol.uoa.gr)

<sup>2</sup>Mathios Refractories S.A., 5, Epidavrou St., 18233 Rentis, Greece

Following current trends in the recycling of waste and the development of innovative green materials, waste chamotte and industrial clays were evaluated and tested for the development of refractory pellets. Pelletization with the addition of clay materials is a widely used process for the recycling of inorganic waste materials. Pellets that come off the process have a large range of application mainly in the construction industry.

The objective of the research is the recycling of chamotte resulting as waste from the production process of a Greek refractory industry. Several compositions of chamotte and industrial clays were tested for the production of fire resistant aggregates applied in refractory mortars.

Spherical artificial aggregates [green pellets], were produced by mixing chamotte with three types of binding agents [5% w/w], namely bentonite [commercial Greek product], clayey diatomite [lignite overburden], and fire clay [commercial clay consisted mainly of quartz and kaolinite]. Sawdust as combustible material was added [5-7,5% w/w].

Chamotte is a sintered material mainly composed of mullite, quartz, cristobalite and corundum, which contribute to high compressive and flexural strength values of the end-product. The three binding clayey materials tested contain, besides clay minerals, quartz, micas, feldspar and biogenic opal-A, and they are added to improve plasticity and cohesion during pelletizing.

Green pellets were sintered in a laboratory kiln at temperatures ranging between 800-1300°C, in order to utilize them in applications in fire-resistant end-products. The optimum product concerning its composition, time and temperature of sintering was estimated based on the physical and mechanical properties of the pellets. Characteristic physical and mechanical properties were tested and evaluated based on international standards, regulations and technical instructions. Additionally, the transformation of crystalline phases at elevated temperatures was studied, from the ambient conditions of the raw materials up to the application temperature of refractory mortars.

Test results of physical and mechanical properties revealed that pellets produced with chamotte and bentonite presented higher porosity and lower apparent density, whereas pellets produced with chamotte and clayey diatomite presented better mechanical properties. Pellets produced with fire clay presented intermediate properties. Favorable sintering temperature for pellets of all composition is between 1100-1200°C.

Furthermore, refractory mortars produced by mixing of the newly formed refractory aggregates compared with others of conventional lightweight aggregates were examined and evaluated. Substitution of conventional lightweight aggregates with the laboratory refractory pellets resulted in final products resistant to higher temperature application and to improvement of their mechanical properties. On the other hand, the increase in permanent linear change and density is estimated as unfavorable.

In this study, it was proven that pelletization is a favorable technique for recycling of industrial waste materials and production of end-products that can find application in the refractory and construction industry.

## Solid State NMR study of multiple extra-frameworks cationic sites in hybrid geopolymer systems

Martina Urbanova<sup>1</sup>, Libor Kobera<sup>1</sup>, Barbora Dousova<sup>2</sup> and Jiri Brus<sup>1</sup>

1 Institute of Macromolecular Chemistry of AS CR, Heyrovsky sq.2, Prague, Czech Republic, urbanova@imc.cas.cz

2 Institute of Chemical Technology Prague, Technicka 5, Prague, Czech Republic

Nanostructured materials generally offer enhanced physicochemical properties because of the large interfacial area. In this contribution we present novel preparation procedure and characterization of hybrid inorganic-organic geopolymers with controllable amounts of in-situ synthesized zeolites. The inorganic amorphous Al-O-Si framework is formed by geopolymerization reactions of metakaolin with alkali activated sodium metasilicate. Simultaneous polymerization of organic co-monomers then creates a polymeric network that is covalently bound to the aluminosilicate matrix via the co-condensation of silanol groups. The extent of amorphous phase transformation and subsequent zeolite growth is controlled by two separate steps. Formation of crystallization centers is controlled by the initial sol-gel activation periods, while the propagation of phase transformation and zeolites growth at the submicrometer scale is driven by hydrothermal treatment. It has been established that the prepared hybrids exhibit considerably enhanced sorption capacity towards  $Pb^{2+}$  ions. Moreover, the in-situ formed polymeric network enhances not only the durability and mechanical integrity of the resulting geopolymer systems but also introduces additional acidic and basic units, providing the framework sites accessible for coordination of sodium ions. In this respect multiple sodium site occupation was evidenced by the novel experimental approach based on the 2D  $^{23}Na$ - $^{23}Na$  double-quantum (DQ) NMR spectroscopy allowing detection of sodium sites that otherwise were below the resolution limits. Consequently the  $^{23}Na$ - $^{23}Na$  DQ experimentation opened a new way for understanding the role of  $Na^+$  ions in geopolymers and related inorganic-organic hybrids.

**Acknowledgments:** The authors thank Czech Science Foundation (Grant No. GA13-24155S) for financial support.

## Effect of temperature on surface properties of rehydrated metakaolinites

Miloslav Lhotka<sup>1</sup>, Barbora Doušová<sup>3</sup>, Vladimír Machovič<sup>2,4</sup> and Libor Kobera<sup>5</sup>

<sup>1</sup> Department of Inorganic Technology, University of Chemistry and Technology, Technická 5, 166 28, Prague, Czech Republic, miloslav.lhotka@vscht.cz

<sup>2</sup> Laboratory of Molecular Spectroscopy, University of Chemistry and Technology, Prague, Czech Republic

<sup>3</sup> Department of Solid State Chemistry, University of Chemistry and Technology, Prague, Czech Republic

<sup>4</sup> Institute of Rock Structure and Mechanism v.v.i., ASCR, Prague, Czech Republic

<sup>5</sup> Institute of Macromolecular Chemistry v.v.i., ASCR, Prague, Czech Republic

This work is focused on the effect of different temperatures on the rehydration process, surface and physical properties of a kaolinite-based rehydrated metakaolinite. Rehydration of metakaolinite was studied from 150 to 250°C under autogenous pressures. A natural kaolinite was calcined to metakaolinite and then rehydrated at different temperatures to a highly porous kaolinite. The influence of different temperatures (within the range 150 to 250 °C) was studied systematically by means of Fourier transform infrared spectroscopy (FTIR), Scanning electron microscopy (SEM), Nuclear magnetic resonance spectroscopy (NMR), X-ray diffraction (XRD) and Thermogravimetric analysis (TGA). The surface area and pore distribution of new phases were also assigned. Equilibrium adsorption isotherms of nitrogen were measured at 77 K using static volumetric adsorption systems (ASAP 2020 analyser, Micromeritics). The adsorption isotherms were fitted to produce the Brunauer-Emmett-Teller method (BET) surface area, the micropore volume was derived by the t-plot method and the pore size distribution by the Barret-Joyner-Halenda method (BJH) and Density Functional Theory method (DFT). The results showed the existence of an optimum temperature at which the rehydrated metakaolinite provided a high specific surface area and high amount crystalline phase- kaolinite. The surface area of the newly prepared kaolinites was much larger than the raw kaolinite and metakaolinite (from 15.8 to ~103.1 m<sup>2</sup> g<sup>-1</sup>). The volume of pores increased with reaction time of rehydration at temperatures of 150 and 175°C. The porous structures of new kaolinites were not fully developed at a rehydration temperature of 150°C. In the kaolinites prepared at 175°C, the volume of pores was at a maximum, while the volume of pores was lower in samples prepared at 200 and 250°C. From the IR spectra of samples treated at 175°C the characteristic kaolinite bands have been developed. The Al - OH stretching (3800 - 3500 cm<sup>-1</sup>) and bending modes (940 and 910 cm<sup>-1</sup>), along with Al-O<sub>6</sub> stretching, were useful for monitoring kaolinite rehydroxylation. In our study the intensities of the Al-O<sub>6</sub> stretching band at 523 cm<sup>-1</sup> were used as a check on the rehydration process. Since the tetrahedral deformation of the Si-O-Si band near 460 cm<sup>-1</sup> did not shift significantly throughout the rehydration process, it can be used as a semi-quantitative internal standard for comparison purposes. The rehydration of metakaolinite to kaolinite strongly depended on the temperature and time of hydrothermal process. The optimum transformation from the point of view of the surface properties was observed after longer-term autoclaving (4-7 days) at 175°C, when the specific surface area S<sub>BET</sub> of raw kaolinite increased more than three times.

[1] Rocha J., Klinowski J. (1991): The Rehydration of Metakaoline to Kaoline. J. Chem. Soc., Chem. Commun., 582-584.

[2] Lhotka, M., Doušová, B., & Machovič, V. (2012): Preparation of modified sorbents from rehydrated clay minerals. *Clay Miner.* 47: 251-258.

## Chlorites from the Faina and Serra de Santa Rita greenstone belts (Goias, Brazil)

Raquel Guimarães da Silva<sup>1</sup>, Edi Mendes Guimarães<sup>1</sup>, Caio Aguiar<sup>1</sup>, Jérémie Garnier<sup>1</sup>, Adalene Moreira Silva<sup>1</sup>, and Catarina Labouré Bemfica Toledo<sup>1</sup>

<sup>1</sup>Instituto de Geociências, Universidade de Brasília, Brasília-DF, Brazil 70910-900; raquelguimaraes123@gmail.com

<sup>1</sup>Instituto de Geociências, Universidade de Brasília, Brasília-DF, Brazil 70910-900

The Faina and Serra de Santa Rita *Greenstone Belt* (GBF), in the southern Goiás Archean Block, consist of mafic to ultramafic terms (metabasalts and metakomatiites) overlaid by a sedimentary sequence (orthoquartzites, metapelites, carbonaceous schists, marbles and iron formations), affected by low-grade metamorphism. Regional faults and thrusts juxtaposed different lithotypes, hindering stratigraphic understanding of the area and the correlations among these sequences. The present study aims to compare the structure and composition of chlorites from different rocks belonging to mafic, ultramafic and sedimentary sequences of the GBF. Characterizing chlorites from each of the lithotypes will contribute to better establish the stratigraphic correlations in tectonically deformed zones. Chlorites have been studied by means of petrographic analysis, geochemistry, x-ray diffraction (XRD) and microprobe (EPMA), carried out in the laboratories of the Geosciences Institute - Universidade de Brasília. Diffraction analyzes were made on a Rigaku Ultima IV diffractometer operating with Cu tube and Ni filter, under voltage of 35 kV and 15 mA, scanning speed of 2°/min, and 2 $\theta$  to 80° 2 $\theta$ . The diffractograms were interpreted with MDI JADE 9.4, with the PDF database. The microprobe analyses were performed with JEOL JXA-8230 equipment under voltage of 15kV and current of 1.5 mA; 10 counting time to 20 seconds and focus of 1  $\mu$ m. The elements measured were Si, Ti, Al, Fe, Mg, Mn, Cr, Ni, Ca, Na and K, iron being assumed as Fe<sup>2+</sup>, with all the results in percentage by weight of oxides. The results in wt.% were then rearranged to chlorite structural formulae assuming 56 negative charges. In thin section chlorites are identified by green to gray pleochroism, as very fine grained masses or fibrous to lamellar habit grains, sometimes accompanying the rock's fracture planes and mineral cleavages, and combined with other phyllosilicates. By total rock composition XRD analysis, different mineral associations could be observed. Exclusively chlorite is observed in chloritite (TF - 199), chlorite + albite + amphibole + quartz in metamafic rocks (TF - 178), chlorite + talc + magnetite in the metaultramafic rock (TF - koma) and chlorite + muscovite + quartz in the metasedimentary rock (TF - 043). The diffractograms show narrow symmetrical chlorite reflections around  $d \sim 14, 7, 4.7$  and  $3.6$  (Å). The ratio of the intensities of (001) and (002) reflections varies, indicating that chlorites in samples TF - 199 and TF - 043 are the most magnesian and most ferrous ones respectively; others samples have intermediate composition. The microprobe analyses show typical chlorites, with total alkalis less than 0.01 and Si values around 5.2 to 5.7. The sum of the octahedral cations is close to 12 atoms and Al content varies between 2.2 and 2.8. The nature of magnesian TF - 199, is confirmed by Mg higher than 8 and Fe less than 2 with Fe/(Fe+Mg) close to 0.17. TF - 043 contains a ferrous chlorite with values of Mg and Fe less than 4 and greater than 5, respectively along with Fe/(Fe+Mg) ratio greater than 0.55. The TF - 178 sample is slightly magnesian with a Fe/(Fe+Mg) ratio around 0.3. According to the diffractograms and mineral chemistry analyses, a direct relationship between the reflection intensities and the chemical composition of chlorites can be made. These features can be helpful when identifying stratigraphic units in tectonically deformed zones and to aid a better understanding the geology of the Faina and Serra de Santa Rita Greenstone Belts.



## Oscillatory chemical zoned chlorite from a hydrothermal vein, Pic-de-Port-Vieux thrust, Pyrenees, Spain

Vincent Trincal<sup>1,2</sup>, Pierre Lanari<sup>3</sup>, Martine Buatier<sup>1</sup>, Brice Lacroix<sup>4</sup>, Delphine Charpentier<sup>1</sup>, Pierre Labaume<sup>5</sup> and Manuel Muñoz<sup>6</sup>

<sup>1</sup>Université de Franche-Comte, Laboratoire Chrono-Environnement, Besançon, France - vincenttrincal@gmail.com

<sup>2</sup> Université de Lorraine, GéoRessources - ENSG, Vandoeuvre-lès-Nancy, France

<sup>3</sup>Institute of Earth Sciences, University of Bern, Bern, Switzerland

<sup>4</sup>Department of Earth and Environmental Sciences, University of Michigan, Ann Arbor, United States

<sup>5</sup>Géosciences Montpellier, UMR 5243, Montpellier, France

<sup>6</sup>Laboratoire ISTerre, Université Joseph Fourier, Grenoble, France

Oscillatory compositional zoning in minerals is commonly attributed to chemical or physical cyclical changes during crystal growth and has been observed in hydrothermal, magmatic and metamorphic environments. Chemical zoning is a common feature of solid solutions (e.g. for garnets), it has however been rarely reported in phyllosilicates. In this study, an oscillatory zoning pattern in chlorite is described in quartz-chlorite shear veins from the pelitic Pic-de-Port-Vieux thrust sheet (Central Pyrenees, Spain). These chlorites occur as pseudo-uniaxial plates arranged in rosette-shaped aggregates which appear to have been developed as a result of radial growth of the chlorite platelets.

Oscillatory zoning in chlorite has been imaged by backscattered scanning electron microscopy (Figure 1) and by X-ray quantitative micro-mapping and corresponds to alternating iron-rich and magnesium-rich bands. Its chemical composition ranges from an Fe-rich pole ( $[\text{Si}_{2.62}\text{Al}_{1.38}\text{O}_{10}](\text{Al}_{1.47}\text{Fe}_{1.87}\text{Mg}_{2.61})(\text{OH})_8$ ) to a Mg-rich pole ( $[\text{Si}_{2.68}\text{Al}_{1.31}\text{O}_{10}](\text{Al}_{1.45}\text{Fe}_{1.41}\text{Mg}_{3.06})(\text{OH})_8$ ).  $\text{XFe}^{3+}$  values were directly measured in each chlorite band using  $\mu\text{XANES}$  spot analyses; they vary from 0.23 to 0.44. Temperature maps, built from standardized microprobe X-ray images and redox state using the program XMAPTOOLS, indicate oscillatory variations from about 310 to  $400\pm 50^\circ\text{C}$  throughout the chlorite crystallization. The highest values are in the Fe-rich area.

Temperature variations during chlorite crystallization are correlated with a  $\text{Fe}^{3+}/\Sigma\text{Fe}$  variation by  $\text{Al}^{3+}\text{Fe}^{3+}_{-1}$  and dioctahedral substitutions highlighted by Mg and  $\text{Fe}_{\text{Tot}}$  contents (Fe-Mg zoning). Chemical variation could then be explained by alternation of cooling times and cyclical pulses of a fluid hotter than the host rock. It is, however, not excluded that kinetic effects influence the incorporation of Mg or Fe during chlorite crystallization.

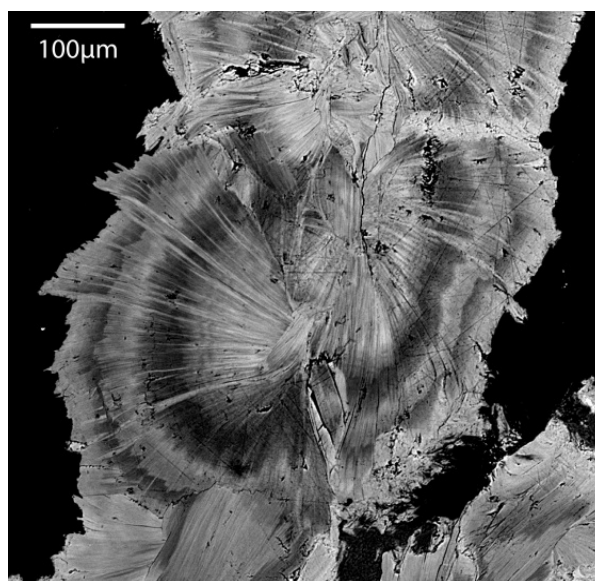


Figure 1. SEM image of an oscillatory zoning pattern chlorite, from a hydrothermal quartz-chlorite vein.

## Measurement of Fe oxidation state in chlorite by electron energy-loss spectroscopy

Takeshi Kasama<sup>1,\*</sup>, Sayako Inoue<sup>2</sup> and Toshihiro Kogure<sup>2</sup>

<sup>1</sup> Center for Electron Nanoscopy, Technical Univ. of Denmark, Denmark; \*tk@cen.dtu.dk

<sup>2</sup> Dept. of Earth & Planetary Sciences, Univ. of Tokyo, Japan

Determination of  $\text{Fe}^{3+}/\Sigma\text{Fe}$  is one of the lasting subjects in mineralogy since the measurement can be used to study past redox states in the environment where the growth of crystals has occurred, e.g. for the estimation of P-T conditions in igneous and metamorphic rocks and the determination of oxygen fugacity in the mantle. Chlorite, which is known as an iron-containing layered silicate mineral, has been extensively studied for use as a geothermometer/geobarometer because of its sensitivity to growth conditions such as temperature and pressure and ubiquitous existence in most diagenetic and metamorphic rocks [1]. Some of the methods proposed for geothermometry require knowledge of  $\text{Fe}^{3+}/\Sigma\text{Fe}$  at relatively high spatial resolution [2].

Electron energy-loss spectroscopy (EELS), as a transmission electron microscopy (TEM) technique, has been proven to be a powerful tool to study oxidation states in minerals quantitatively at the nanometer scale. However, layered silicates containing OH are sensitive to the electron beam and can be altered structurally and chemically during the TEM observation. Garvie et al. [3] has reported that the Fe oxidation state in cronstedtite varies considerably with electron irradiation.

Here we use EELS to understand the effect of electron beam irradiation of chlorite towards developing quantitative measurement of  $\text{Fe}^{3+}/\Sigma\text{Fe}$  for chlorite. The Fe-L<sub>2,3</sub> core-loss edge EELS spectra of four different samples were acquired in TEM diffraction mode using an FEI Titan 80-300ST TEM equipped with a monochromator and a Tridiem Gatan imaging filter. In all the EELS measurements, the beam size and dose rate used were around 350 nm in diameter and  $1.6 \times 10^5$  e/nm<sup>2</sup>/sec, respectively. Following light crushing, the samples were mounted on holey carbon TEM grids.

Time-dependent EELS spectra were acquired every 5 sec, typically for 2 min in total from the same regions with a dwell time of 5 sec (i.e. the EELS spectra were being acquired *continuously*) to investigate  $\text{Fe}^{3+}/\Sigma\text{Fe}$  changes induced by the electron beam. In all the samples measured in this study, the  $\text{Fe}^{3+}/\Sigma\text{Fe}$  increased significantly with an increase in the electron dose, which is the opposite behaviour to cronstedtite [3], suggesting that  $\text{Fe}^{2+}$  ions in chlorite were oxidised at the present conditions along with amorphitisation of chlorite. It was found that no significant influence on the oxidation was observed with different accelerating voltage or specimen temperature. The original  $\text{Fe}^{3+}/\Sigma\text{Fe}$  values, i.e. 'damage-free ratios' were estimated by extrapolation from their oxidation rate. The calculated values are rather scattered even in the same samples, which probably results from too aggressive experimental conditions for chlorite, passive surface oxidation after crushing the samples, or the presence of chlorite grains that have different origins of the growth. A monochromator that improves the energy resolution in the EELS and different calculation methods [4,5] to obtain  $\text{Fe}^{3+}/\Sigma\text{Fe}$  were also employed to improve the accuracy of the quantification.

[1] Bourdelle et al., Contrib. Miner. Petrol. 165, 723 (2013).

[2] Inoue et al., Clay Clay Miner 57, 371 (2009).

[3] Garvie et al., Amer. Miner. 89, 1610 (2004).

[4] Garvie & Buseck, Nature 396, 667 (1998).

[5] van Aken & Liebscher, Phys. Chem. Miner. 29, 188, (2002).

[6] We thank Shima Kadkhodazadeh for valuable discussion.

## ***Pietra ollare* (chlorite-schist) artefacts from Červar Porat (Istria, Croatia) – comparison with possible source rocks**

**Darko Tibljaš<sup>1</sup>, Balen Dražen<sup>1</sup>, Maja Vučković<sup>1</sup> and Zrinka Šimić-Kanaet<sup>2</sup>**

<sup>1</sup>University of Zagreb, Faculty of Science, Department of Geology, Horvatovac 95, HR-10000, Zagreb, Croatia;  
dtibljias@geol.pmf.hr

<sup>2</sup>University of Zagreb, Faculty of Philosophy, Department of Archaeology, Ivana Lučića 3, HR-10000, Zagreb, Croatia

During archaeological excavations performed between 1976 and 1980 at a Roman villa rustica in Červar Porat located close to the town Poreč (Istria peninsula, Croatia), among other Late Antique period fragments (glass, metal, ceramics), fourteen peculiar stone vessel fragments were discovered. They show characteristic tracks of the manufacturing by means of a lathe. Vessels made by an analogous process from similar materials have already been found at several localities along the Croatian Adriatic coast, but no systematic mineralogical study on this kind of material was performed so far.

Two of these vessel fragments were investigated by Tibljaš et al. (2006). X-ray powder diffraction revealed that the only constituent of the first, greenish-grey fragment (inv. no. 7912) is a chlorite group mineral. The mineral composition together with visible schistosity indicated that the source material was chlorite-schist, a low-grade metamorphic rock. Such material is one of a number of different lithologies included in the Italian term *pietra ollare* and German *Lavez*.

The other fragment (inv. no. 7907) is dark greenish-grey on the fresh broken surface and brownish on the outer and inner vessel surfaces. Distinctive bronze coloured flakes can be seen in some parts. The fact that the XRD pattern of the second fragment was similar to the XRD pattern recorded on the material from the first fragment after heating to 1100°C indicates that the second vessel was most probably used for cooking, and during that process it was exposed to elevated temperatures.

In order to determine the possible origin of the analysed fragments recent investigations (including X-ray powder diffraction, FTIR-spectroscopy, and chemical analyses) were performed on samples collected from localities in the Italian Alps known as ancient production centers of *pietra ollare* vessels. Mineral and chemical characteristics of artefacts from Červar Porat were compared with those recorded for samples from Valli di Lanzo, Valle d'Aosta, Valchiavenna, and Valmalenco as well as with literature data for *pietra ollare* (Antonelli et al., 2006, Santi et al., 2005; 2009).

Antonelli, F., Santi, P., Renzulli, A., Bonazza, A. (2006): Petrographic features and thermal behaviour of the historically known „*pietra ollare*“ from the Italian Central Alps (Valchiavenna and Valmalenco). In: Maggeti, M., Messiga, B. (Eds.), *Geomaterials in Cultural Heritage*. Geological Society of London Special Publication, 257, 229-239.

Santi, P., Antonelli, F., Renzulli, A. (2005): Provenance of Medieval *pietra ollare* artefacts found in archeological sites of Central-Eastern Italy: insight into the Alpine soapstone trade. *Archeometry* 47, 253-264. Special issue: the linking role of the Alps in past cultures: an archaeometric approach.

Santi, P., Renzulli, A., Antonelli, F., Alberti, A. (2009): Classification and provenance of soapstones and garnet chlorite schist artifacts from Medieval sites of Tuscany (Central Italy): insights into the Tyrrhenian and Adriatic trade *Journal of Archaeological Science*, 36, 2493-2051.

Tibljaš, D., Balen, D., Šimić-Kanaet, Z. (2006): *Pietra ollare* artefact from Červar Porat (Istria, Croatia). 15th Slovenian-Croatian Crystallographic Meeting, Book of abstracts, 25, Jezersko.

## The role of clays and carbonates in the palaeoenvironmental reconstruction of Miocene deposits in the Daroca Basin (Spain)

Manuel Pozo<sup>1</sup>, José Pedro Calvo<sup>2</sup>, Juan Emilio Herranz<sup>1</sup> and Pablo Peláez-Campomanes<sup>3</sup>

<sup>1</sup> Department of Geology and Geochemistry. Universidad Autónoma de Madrid. Spain. manuel.pozo@uam.es

<sup>2</sup> Department of Petrology and Geochemistry. Universidad Complutense de Madrid. Spain

<sup>3</sup> Department of Palaeobiology. National Museum of Natural Sciences. Madrid, Spain

In the Daroca Basin the Aragonian-Vallesian deposits were accumulated in alluvial fan to shallow lake environments surrounded mainly by quartzite and slate formations of Palaeozoic age. The sedimentary deposits were subdivided into four lithostratigraphic units named: Valdemoros-Vargas, Las Umbrías, Las Planas and Nombrevilla. The distribution of the sedimentary deposits characterising the four units indicates an initial stage dominated by clastic deposition in an alluvial fan environment punctuated by very shallow carbonate lakes, followed by the installation of shallow lakes and marshes with abundant organic matter, then evolving to deposition in distal alluvial fan environments and shallow carbonate lakes sometimes with the presence of evaporites (gypsum). The occurrence and evolution of abundant micromammal communities suggest palaeoclimatic changes that can be tested by means of clay minerals assemblages and supported by isotopic compositions and textures of associated carbonates.

The analysis of clay lithofacies indicates a bulk-sample assemblage composed of phyllosilicates, calcite, quartz, potassium feldspar and plagioclase. Within phyllosilicates mica is common but also clay minerals. Clay mineralogy consists of dioctahedral smectite, illite, kaolinite and chlorite, arranged in two clay mineral assemblages. The associated carbonates are mostly calcite (LMC) showing palustrine-lacustrine textures with common pedogenic features and locally channeled tuffa deposits. The isotopic analysis indicate poorly evaporated waters ( $\delta^{18}\text{O} = -5,41$  a  $-8,10$  ‰) and variable biological contribution ( $\delta^{13}\text{C} = -5,42$  a  $-8,85$  ‰).

The study of the clay mineral associations, which are mainly detrital with minor change upwards in the section, and the stable isotopic composition of the carbonate deposits in the Daroca Basin does not provide clear evidence for palaeoclimatic changes thus behaving as 'blind indicators' for the palaeoenvironmental reconstruction of the area. Our conclusion is that in some continental basins major external/global signatures can be hidden in the sediments because of local depositional conditions, in particular the hydrogeological framework and the source rocks bounding the basin. These facts can explain the absence of authigenic clays (commonly Mg-clays) such as those reported in many other lacustrine-palustrine palaeoenvironments.

**Acknowledgements:** The work has been financed by Project CGL2011-28877, and is part of the scientific activities of Research Groups UCM-910607 and UAM-144.

## **Authigenic Mg-sudoite and Mg trioctahedral chlorite in Permian reservoir red-beds, SW Poland**

Julita Biernacka<sup>1</sup>

<sup>1</sup> Institute of Geology, University of Poznan, Makow Polnych 16, 61-606 Poznan, PL;  
julbier@amu.edu.pl

Authigenic grain-coating chlorite occurring in sandstones deserved much attention in the last three decades because of its potential to preserve high porosity in deeply buried reservoirs. A rare variety of such grain coating/pore lining mineral is magnesium-rich trioctahedral chlorite, known primarily from two prominent examples of reservoir aeolian sandstones, the Jurassic Norphlet formation in the USA and the Permian Hannover and Slochteren formations in Germany. The origin of this Mg-chlorite has been interpreted as a deep burial transformation of early diagenetic Mg-smectite (saponite). This contribution concerns Permian aeolian sandstones which were deposited concomitantly with the German Slochteren Fm., in a similar palaeogeographical setting, further to the east of the Southern Permian Basin in Europe. Paradoxically, the major pore-lining mineral is Mg-sudoite, whereas Mg trioctahedral chlorite is a minor component. This raises the question about the commonness of the association of aluminium chlorite (tosudite, sudoite) and red beds (Hillier, 2003), as well as a possible link between diagenetic Mg-chlorite and Mg-sudoite.

Fifty Permian (Rotliegend) sandstone samples taken from boreholes drilled by the Polish Oil and Gas Company in the Fore-Sudetic Monocline, SW Poland, were studied by means of XRD, SEM, and electron microprobe. The reconstructed maximum burial of the sandstones varied from ca. 3 to 5 km. Sudoite was identified by its characteristic XRD pattern and the 060 reflection of a dioctahedral mineral. It occurs commonly as a pore-lining mineral in porous subarkosic arenites, in the ~200 m thick upper part of the Rotliegend section, below the Upper Permian (Zechstein) marine Cu-bearing shale (Kupferschiefer). The occurrence of sudoite broadly coincides with the occurrence of Lower Permian volcanic rocks either in the basement or in the vicinity. Additionally, sudoite was recognized as a local alteration phase in the basement volcanic rocks. Sudoite forms a honeycomb texture highly resembling that of various smectite-rich clay minerals. The average chemical composition of this mineral was specified as  $(Al_{2.4}Mg_{2.5}Fe_{0.2})_{\Sigma 5.1}(Si_{3.2}Al_{0.8})_{\Sigma 4}O_{10}(OH)_8$ , with less octahedral vacancies and more (Mg+Fe) and silica than in ideal sudoite  $(Al_3Mg_2)(Si_3Al)O_{10}(OH)_8$ . The excess of silica probably reflects minor smectite (tosudite) interlayers, suggested also by wide XRD peaks. In turn, Mg-chlorite was recorded only in the deeper part of a few Rotliegend sections. It forms larger crystals with platy habits and more random orientation. The edges of the crystals are nucleation sites for fibrous illite. The 'crystallinity' of Mg-chlorite (expressed as FWHM values) is always better than that of sudoite. The average chemical composition of the Mg-chlorite,  $(Al_{1.7}Mg_{3.1}Fe_{0.8})_{\Sigma 5.6}(Si_3Al)_{\Sigma 4}O_{10}(OH)_8$ , indicates some octahedral vacancies, and suggests either a dioctahedral component or it is a result of a physical mixture of Mg-chlorite and fine sudoite unrecognized during analyses.

It is suggested that sudoite crystallized at the expense of early diagenetic dioctahedral smectite under the influence of hot, Mg-rich, oxidised fluids, which migrated from a basement upward through permeable aeolian sandstones. Mg-chlorite could form coincidentally at a higher temperature if there is access to enough magnesium in the system.

Hillier S. (2003) Chlorite in sediments. Pp. 123–127 in: *Encyclopedia of sediments and sedimentary rocks* (G.V. Middleton, M.J. Church, M. Coniglio, L.A. Hardie & F.J. Longstaffe, editors). Kluwer Academic Publishers, Dordrecht.

## **Authigenic chlorite and chlorite-smectite mixed layer as indicator of increasing reducing condition in the Huincul Formation: Neuquén Basin, Argentina**

M.J. Pons<sup>1</sup>, A. Rainoldi<sup>2</sup>, D. Beaufort<sup>3</sup>, P. Patrier<sup>4</sup>, A. Impiccini<sup>5</sup> and M.B. Franchini<sup>6</sup>

<sup>1</sup> josefina.pons074@gmail.com; <sup>2</sup> analaurarl@hotmail.com; <sup>3-4</sup> Université de Poitiers, IC2MP, CNRS-UMR 7285, Hydrasa, Bâtiment B08, Rue Albert Turpin, F-86022 Poitiers Cedex, France, <sup>3</sup> daniel.beaufort@univ-poitiers.fr; <sup>4</sup> patricia.patrier@univ-poitiers.fr; <sup>5</sup> aimpicc@gmail.com; <sup>6</sup> mfranchi@speedy.com.ar

The Huincul High (HH) and Dorso de los Chihuidos High (DCH) are two regional morpho-structures of the Neuquén Basin, characterized by the occurrence of hydrocarbon fields, regional structures at depth and the presence of solid hydrocarbons impregnating the foreland deposits of Cretaceous rocks (Neuquén Group). Huincul Formation belongs to the fluvial and lake red-bed deposits of the Neuquén Group.

Some of the structures of HH and DCH were reactivated during the Tertiary Andean orogeny, and acted as vertical channels connecting the reservoir fluids with the sub-horizontal paleo-channel of the Huincul Formation. The circulation of these fluids in the clastic rocks is documented by the presence of bitumen associated with baroque calcite, pyrite and clay minerals rims (smectite, chlorite and chlorite-smectite mixed layer). The pervasively greenish gray clay coating is a common feature of the sandstones and conglomerate from the Huincul Formation. This presentation establishes the relationship between diagenetic processes, hydrocarbons migration and their implication in the composition of clay coating precipitation.

During the early diagenesis stage, multiple episodes of clay infiltration into the unconfined meandering river deposits of the lower section of Huincul Formation resulted in the thick (2-3  $\mu\text{m}$ ) clay coating present in some volcanic rich litharenite sandstone and conglomerate. Progressive burial caused the reddening of the whole Huincul Formation, documented in the reddish brown and pink color of the mudstone and sandstone layers due to the presence of hematite pigment. This hematite derived from infiltration of meteoric water following breakdown of ferromagnesian silicate minerals and iron bearing clay mineral.

The oil emplacement is documented in the intense bitumen impregnation of sandstone and conglomerate and at micro scale in calcite and barite cements that host numerous organic rich fluid inclusions.

The greenish gray facies documents hydrocarbon migrations in the Huincul Formation where previous kaolinite and hematite coating were transformed to dioctahedral smectite, chlorite-smectite mixed layer or chlorite and pyrite, respectively. These changes from smectite to chlorite-smectite mixed layer or chlorite are interpreted as a signature of increasing reducing conditions. The direct transformation of smectite to chlorite in some of the greenish gray facies located at the lower part of the Huincul Formation, involved a fast rate of growth nucleation at the expense of previous smectite suggesting a high fluid/rock ratio (Robinson et al., 2002). This condition prevailed in the permeable layers of the lower section of the sedimentary unit that yields a focused flow pathway. In the rest of the sedimentary unit, the presence of chlorite-smectite mixed-layer suggests chloritization of previous smectite. The partial transformation of dioctahedral smectite to chlorite-smectite mixed layer or trioctahedral chlorite produced an excess of silica resulting in micro quartz precipitation (Mosser-Ruck et al., 2010). Addition of Mg is required to form chlorite-smectite mixed layer or chlorite from the dioctahedral smectite and could be taken from the alteration of detrital mafic minerals and/or Mg-rich water formation that migrate with hydrocarbons.

Mosser-Ruck R., Cathelineau M., Guillaume D., Charpenetier D., Rousset D., Barres O., Michau N., 2010. Effects of temperature, pH, and iron clay and liquid/clay ratios on experimental conversion of dioctahedral smectite to berthierine, chlorite, vermiculite or saponite, *Clays and Clay Minerals*, Vol. 58, No. 2, 280–291.

Robinson D., Schmidt Th, de Zamora S., 2002. Reaction pathway and reaction progress for the smectite-to-chlorite transformation: evidence from hydrothermally altered metabasite. *Journal of Metamorphic Geology* 20, 167-174.

## Natural Zn clay mineral characterization combining XRD, SEM and TEM-EDS analyses

Martine Buatier and Flavien Choulet

Chrono-Environnement, UFR Sciences et Technique, Université de Franche Comté, 13 Route de Gray Besançon,  
France

Zn-clay minerals have been found in the non-sulphide deposits of Bou Arhous (High Atlas, Morocco). They occur as white or ochre clays embedding willemite mineralizations and are commonly associated with red detrital clays in karstic cavities. Scanning electron microscopy (SEM), X-ray diffraction (XRD) and Transmission Electron microscopy (TEM) with energy dispersive X (EDX) analyses were combined in order to characterize this clay mineral and to determine the mechanism of its formation.

XRD patterns of the  $<2\mu\text{m}$  fraction of the white clays display two major reflections at 7.25 Å and 3.61 Å that move to 7.39 Å and 3.53 Å, respectively after Ethylene Glycol treatment. The best Newmod simulation to describe the XRD patterns is obtained for a R0 mixed layer with 80% of TO clay mineral) and 20% of smectite

Scanning Electron Microscopic observation (back-scattered electron mode) shows that Zn clays are closely associated to willemite ( $\text{Zn}_2\text{SiO}_4$ ); euhedral willemite crystals present evidence of partial dissolution that preferentially affects edges or sites of crystalline defect. Zn clays are also present as aggregates of about 50 microns filling the porosity or pervading the detrital clays. Intimate mixtures of Zn clays with detrital micas can also be observed.

TEM-EDX analyses were made on clay separates but also on TEM foil prepared with focused ion beam (FIB) microscope directly on the thin section. Low and high resolution transmission electron microscopic images were realized on selected areas preserving the texture of the sample. Two types of textural sites were selected: the Zn clay aggregates filling the porosity, and the detrital clays partially replaced by Zn clay minerals.

STEM EDS maps and point analyses confirmed the WDS microprobe analyses. Individual particles of clay minerals with about 10% of Zn were analysed. Structural formulae calculation revealed the occurrence of trioctahedral TO (Fraipontite, a Zn berthierine) and TOT Zn clay minerals (sauconite, a Zn trioctahedral smectite).

TEM images and SAED patterns on the Zn clay aggregates confirmed the occurrence of fraipontite. In the analysed aggregates, the clays are composed of crystals of about 0.5-1  $\mu\text{m}$  in diameter and 10 to 100 nm in thickness. At high magnification, the 0.7 nm layer periodicity was clearly imaged and confirmed by the SAED patterns. Double layer periodicity is also common. In some fraipontite crystals, a few intercalations with 1 nm layer were imaged.

Based on the TEM and SEM observations at various scales, we discuss the formation mechanism of this rarely described Zn clay mineral. The nature of the precursor will also be particularly discussed.

## Synthesis and crystal structure refinement of one- and two-layer hydrate of sodium-fluorohectorite

Matthias Daab<sup>1</sup>, Hussein Kalo<sup>1</sup>, Wolfgang Milius<sup>1</sup> and Josef Brey<sup>\*1</sup>

<sup>1</sup> Department of Inorganic Chemistry I, University of Bayreuth, Universitätsstraße 30, 95440 Bayreuth, Germany;  
josef.brey@uni-bayreuth.de

The crystal structures of one- and two-layer hydrates (1WL, 2WL) of sodium fluorohectorite (Na-hect)  $\text{Na}_{0.7}[\text{Mg}_{2.3}\text{Li}_{0.7}]<\text{Si}_4>\text{O}_{10}\text{F}_2$  were refined. The swelling Na-hect from melt synthesis<sup>[1]</sup> converts upon hydration to semi-ordered (1WL) and ordered (2WL) hydrates. The significant reduction of stacking faults in these synthetic hydrates allowed for the first time to solve the structure of the one-layer hydrate. The interlayer cations reside in the central plane in a 9-fold coordination of 6 basal oxygen atoms and three water molecules. The stacking order is determined by hydrogen bonding of the latter to the second tetrahedral sheet. For the two-layer hydrate, structures proposed for vermiculites in the literature were in large confirmed.<sup>[2]</sup> However, modifications in details like ordering of alternative sites for  $[\text{Na}(\text{H}_2\text{O})_6]^+$  were suggested.

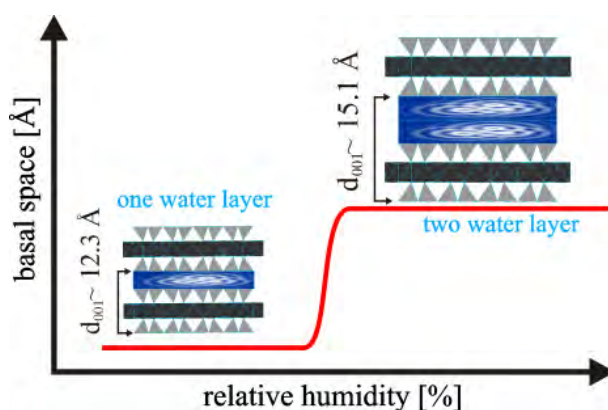


**Figure 1** Different hydration states of sodium fluorohectorite at different relative humidities

**Keywords:** swelling clay, crystal structure, stacking order/disorder.

[1] H. Kalo, M. W. Möller, M. Ziadeh, D. Dolej, J. Brey, *Appl. Clay Sci.* **2010**, *48*, 39.

[2] P. G. Slade, P. A. Stone, E. W. Radoslovich, *Clays Clay Miner.* **1985**, *33*, 51.



## Nanocage structures derived from cyclodextrin-intercalated layered double hydroxides and their inclusion properties for HAP and phenol compounds

Arnaud Di Bitetto<sup>1,2\*</sup>, Gwendal Kervern<sup>2</sup> and Cédric Carteret<sup>1</sup>

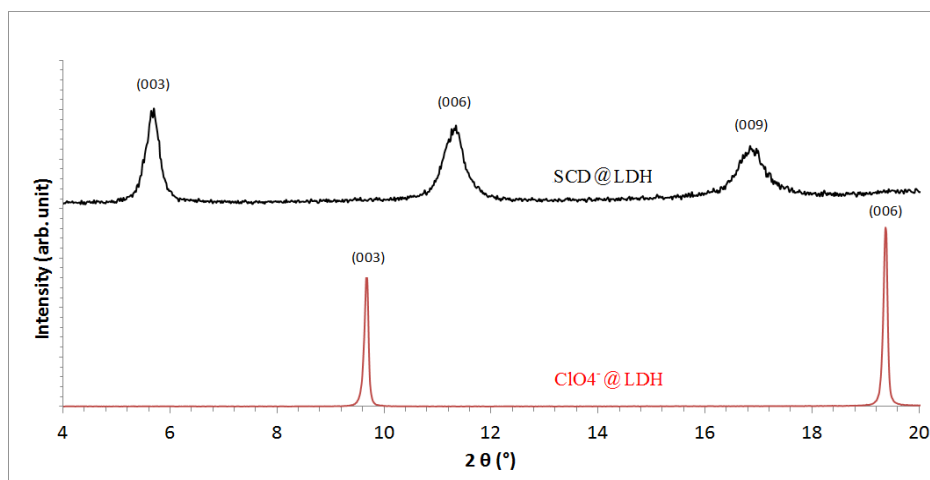
<sup>1</sup> Lorraine University-CNRS, LCPME UMR 7564, 405 rue de Vandoeuvre 54602 Villers-lès-Nancy, France.

<sup>2</sup> Lorraine University-CNRS, CRM2 UMR 7036, Faculté des Sciences et Technologies, Boulevard des Aiguillettes, BP 239, 54506 Vandoeuvre-lès-Nancy Cedex, France ; \*arnaud.di-bitetto@univ-lorraine.fr

Layered double hydroxides (LDH) are of considerable geological and chemical relevance because of their anion exchange capacity. In particular, there is a growing interest in the synthesis of hybrid organic-inorganic LDH. In that context, we chemically modified our LDH by intercalating cyclodextrins, characterized by a hydrophobic cavity in order to trap neutral pollutants.

In our work, nanocage structures derived from sulfonated  $\beta$ -cyclodextrin (SCD), carboxymethyl  $\beta$ -cyclodextrin (CMCD) and carboxyethyl  $\beta$ -cyclodextrin (CECD) intercalated in LDH based on Zn/Al and Mg/Al cationic couples were prepared through anion exchange. The SCD-LDH, CMCD-LDH and CECD-LDH hybrids were fully analyzed by elemental analysis, Raman spectroscopy, Infrared spectroscopy, solid state NMR, XRD, and structural models were proposed for each material. *In situ* infrared measurements revealed the high thermal stability of the intercalated cyclodextrins.

The inclusion property of the CD-LDH hybrids for HAP and phenol compounds was thoroughly investigated. Neutral aromatic molecules have been included within the functionalized solid by driving the hydrophobic aromatic molecules from a polar solvent into the less polar interior of the anchored cyclodextrin cavities by a partitioning process. The sorption results at 25°C showed that SCD-LDH gave low adsorption capacity whereas the CMCD and CECD-LDH could retain a much higher quantity for all the organic compounds studied. The sorption affinity for organic compounds was positively related to their hydrophobicities. The best capacity was obtained for cyclodextrins intercalated in MgAl LDH.



XRD patterns of R=2 ZnAl LDH showing the exchange between  $\text{ClO}_4^-$  and sulfonated  $\beta$ -cyclodextrin (SCD)

## Deciphering the vibrational signature of layered double hydroxides through a joint experimental and theoretical approach

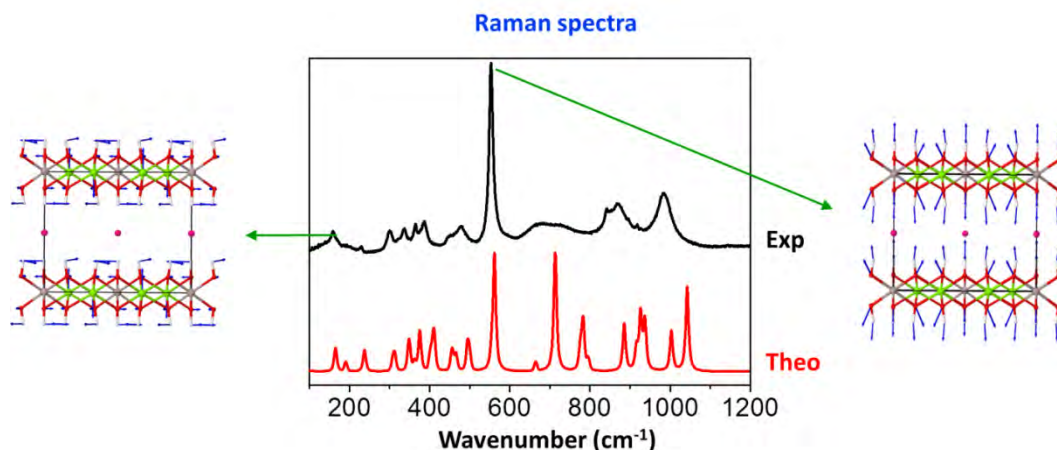
Erwan André<sup>1</sup>, Jean Fabel<sup>1</sup>, Arnaud Di Bitetto<sup>1</sup> and Cédric Carteret<sup>1</sup>

<sup>1</sup> erwan.andre@univ-lorraine.fr, Lorraine University-CNRS, UMR 7564 LCPME, 405 rue de Vandoeuvre  
54602 Villers-lès-Nancy, France

Layered Double Hydroxides (LDH) are well known for their properties of anion exchanger, pollutant scavenger, or catalyst precursors [1]. Such properties are closely related to the interactions between the different parts of these chemical systems: The composition of the layers, the stacking sequence or the structuration of the interlayer domain. While the X-Ray Diffraction technique (XRD) is commonly used to characterize the structural properties of these materials at the crystal scale (stacking sequence, interlayer spacing...), vibrational spectroscopies (Infrared and Raman) can give access to in-situ information, at molecular scale, of both the anionic and cationic parts of these systems and of their interactions.

The aim of this work is to show how quantum mechanical calculations, realized on periodic systems at DFT level, can be used in synergy with experimental data to validate a model structure, to assign the experimental spectra and to give access to various properties related to the electronic distribution.

To illustrate this methodology, a focus will be made on  $[M_2Al(OH)_6]^+ \cdot A^-$  (with  $A^- = F^-, Cl^-, Br^-, I^-$  and  $M = Mg^{2+}$  or  $Zn^{2+}$ ). As they do not possess any internal vibration modes, they are good probes of the layer vibrational signatures. In a second part, by changing the nature of the divalent cation (from  $Mg^{2+}$  to  $Zn^{2+}$ ) we will show how the layer's vibrational fingerprint is influenced by the cationic couple. Finally, a few examples will be given for more complex systems ( $A^- = NO_3^-, \frac{1}{2} CO_3^{2-}, R-COO^-$ ), where the anions possess internal vibration modes. The influence of the confined environment of the interlayer domain on their vibrational signature will emphasize the versatility of the host-guest interactions.



Comparison between experimental and calculated Raman spectra of  $[Mg_2Al(OH)_6]^+ \cdot Cl^-$  along with vibration modes of characteristic peaks.

[1] Rives, V. Layered Double Hydroxides: Present and Future, Nova Publishers (2001).

## Insight into the structure of layered zinc hydroxide salts intercalated with dodecyl sulfate anions

Petr Kovář<sup>1</sup>, Jan Demel<sup>2</sup>, Jan Hynek<sup>2</sup>, Yan Dai<sup>3</sup>, Christine Taviot-Guého<sup>3</sup>, Ondřej Demel<sup>4</sup>, Miroslav Pospíšil<sup>1</sup> and Kamil Lang<sup>2</sup>

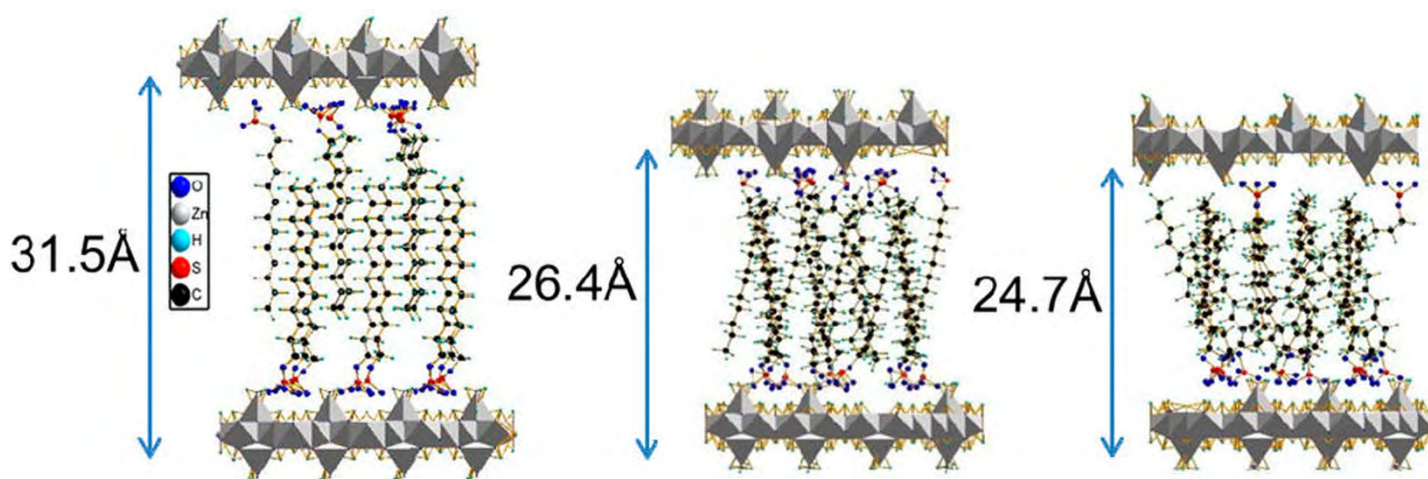
<sup>1</sup>Faculty of Mathematics and Physics, Charles University in Prague, Ke Karlovu 3, 121 16 Praha, Czech Republic, kovar@karlov.mff.cuni.cz

<sup>2</sup>Institute of Inorganic Chemistry of the Academy of Sciences of the Czech Republic, v.v.i., Husinec-Řež 1001, 250 68 Řež, Czech Republic

<sup>3</sup>Institut de Chimie de Clermont-Ferrand, UMR-CNRS no. 6296, Université Blaise Pascal, BP 80026, 63177 Aubiere Cedex, France

<sup>4</sup>J. Heyrovský Institute of Physical Chemistry of the Academy of Sciences of the Czech Republic, v.v.i., Dolejškova 3, 182 23 Praha, Czech Republic

We describe the systematic experimental and theoretical investigation of the structural arrangements of dodecyl sulfate (DS) anions in the interlayer space of layered zinc hydroxide salts (LZH-DS) and of the structure of zinc hydroxide layers, with a detailed description of the zinc ions' coordination environment. As-prepared, well-crystalline LZH-DS has a basal spacing of 31.5 Å. After treatment with methanol at room temperature, zinc hydroxide layers shrank to form two new layered phases with basal spacings of 26.4 and 24.7 Å. The shrinking was accompanied by a decrease in the content of DS anions in the interlayer space, indicating a change in the alignment of the intercalated anions and a decrease in the charge density of the zinc hydroxide layers. The latter effect was assessed by the atomic pair distribution function (PDF) analysis of powder X-ray diffraction patterns, revealing the successive removal of Zn ion tetrahedra from the hydroxide layers, with the octahedrally coordinated Zn ions left unaffected. The interlayer space of all three phases was modelled by molecular dynamics, and the models were validated by the comparison of modelled and experimental powder XRD patterns and one-dimensional electron density maps. The arrangement of DS anions in the interlayer space of LZH-DS also depended on temperature. Remarkably, the basal spacing was considerably increased at 55 °C, which was explained by the formation of a second-staging heterostructure with the regular alternation of layers with two basal spacings, 31.5 and 34.2 Å. This is the first reported interstratification phenomenon in layered hydroxides intercalated with aliphatic molecules. Our results provide insight into the great variability of layered hydroxide structures controlled by external stimuli.



## Non-ideal stacking in layered systems: contributions to the X-ray powder diffraction profiles of kaolinite

A. Leonard<sup>1</sup> and D. Bish

<sup>1</sup>Department of Geological Sciences, Indiana University, Bloomington, Indiana 47405, U.S.A.  
alby\_leo@yahoo.it

The X-ray powder diffraction line profiles of turbostratically stacked layer configurations of kaolinite nanocrystals were investigated using the Debye scattering equation, with no approximations. X-ray powder diffraction patterns of a large collection of numerical models of different kaolinite microstructures were simulated to evaluate the effects of various types of disorder (Fig. 1). Line profile features corresponding to variable misorientation and shift (in or out of the 2-D plane) of stacked layers were investigated (Fig. 2), and these simulations were compared with experimental X-ray diffraction patterns. Changes in line broadening and relative peak intensities are a function of the particular statistical layer stacking arrangement (Fig. 1a), from perfect to uniformly random (i.e., from single-crystal to ideally-turbostratic). The  $00l$  peaks shift and broaden, depending on the spacing and degree of overlap of the stacked layers. Moreover, the layer misorientation directly affects the relative intensity sequence of the  $hkl$  peaks, which can potentially be used to interpret observed diffraction patterns (Fig. 1b).

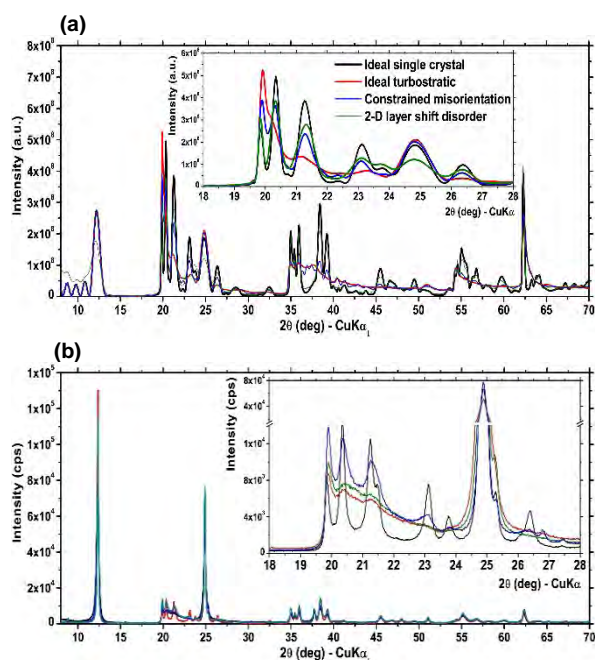


Figure 1. Debye (a) and Experimental (b) XRD profiles.

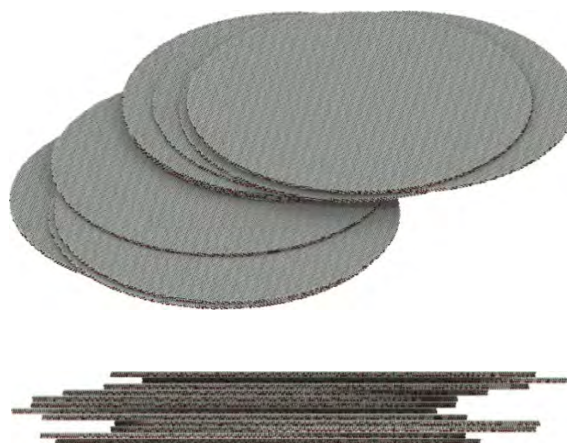


Figure 2. 3D and front view of a microstructure model. (The green line in Fig. 1a shows the simulated XRD profile)

## Effect of hydrous perturbation and the soil-pH on the adsorption of tetracycline onto Na-montmorillonite

Walid Oueslati<sup>1,2</sup>

<sup>1</sup>Faculté des Sciences de Bizerte, 7021 Zarzouna, Tunisia

<sup>2</sup>General Studies Department, College of Electronics & Communications, Technical and Vocational Training Corporation, TV Street, Jeddah, Saudi Arabia

The adsorption of tetracycline (TC) on a Na-montmorillonite (Swy-Na) is studied as a function of the swelling behaviour of clayey entity and the pH of the surrounding soil solution. The variation of the hydration amounts is performed by several in situ hydration dehydration sequences (i.e. variation of relative humidity conditions). The effect of the humic acid (HA) character of the soil solution is investigated (i.e. the pH range from 3 to 9). These aims are achieved using the XRD and FTIR measurement. The XRD profile modelling approach consists of the comparison of the experimental patterns to calculated ones obtained from theoretical models. This indirect method allows defining the organization/position of interlamellar compounds / species and the water molecules along  $c^*$  axis . The FTIR technic is used in order to investigate the band changes of amide carbonyl and amino groups in tricarbonyl methane group and the carbonyl group in phenolic deketone group. Results showed that pH had great effect on the TC adsorption and acidic condition is more favoured. The materials hydration history showed very different effects on the TC adsorption onto Swy-Na . The FTIR spectra of TC equilibrated with Swy-Na confirmed that TC was adsorbed via the ion exchange process and surface complexation.

## Ordered and disordered carbon from pyrolysed clay-organic intercalates

C. Breen<sup>1</sup>, F. Clegg<sup>1</sup>, J. Hrachová<sup>2</sup>, L. Petra<sup>2</sup> and P. Komadel<sup>2</sup>

<sup>1</sup>Materials and Engineering Research Institute, Sheffield Hallam University, Sheffield S1 1WB, United Kingdom

<sup>2</sup>Institute of Inorganic Chemistry, Slovak Academy of Sciences, Dúbravská cesta 9, SK-845 36 Bratislava, Slovakia

The preparation and characterisation of the pyrolysis products obtained from clay-organic intercalates has become popular once again due to the worldwide interest in graphene and, to a lesser extent, graphene oxides. In this contribution, the influence of the elemental composition of bentonite used, the bentonite-organic ratio, the mixing procedures, and the pyrolysis conditions have been evaluated. Preliminary studies of the effect of exchange cation and added acid will also be presented.

The pyrolysis precursors and the pyrolysed products have been characterised using X-ray diffraction, thermal analysis, vibrational spectroscopy and BET surface area analysis.

The products prepared in the absence of acids were characterised by low nitrogen surface areas ( $8 - 30 \text{ m}^2 \text{ g}^{-1}$ ) and the combination of the bentonite and exchange cation used exerted a notable influence on the ordering of the clay-carbon product as determined using x-ray diffraction. The d-spacing of these well-ordered clay-carbon products ( $13.4 \text{ \AA}$ ) were commensurate with a single layer of carbon in the interlayer space.

The surface area of the carbosils produced ( $215 \pm 15 \text{ m}^2 \text{ g}^{-1}$ ) could be optimised by the amount of acid added. The contribution of the  $13.4 \text{ \AA}$  interlayer spacing to the diffraction pattern of the carbosils was significantly lower than that observed for the samples prepared without acid. The identity of the gas(es) released during the decomposition of the acid, which helped generate the larger surface area products, was confirmed using TG-MS.

## The origin of Al-O-Al defects in Zn-Al layered double hydroxides studied by solid state NMR spectroscopy

Suraj S. C. Pushparaj<sup>1</sup>, Andrew S. Lipton<sup>2</sup>, Vanessa Prevot<sup>3</sup>, Claude Forano<sup>3</sup> and Ulla Gro Nielsen<sup>1</sup>

<sup>1</sup> Dept. of Physics, Chemistry and Pharmacy, Univ. Southern Denmark, Campusvej 55, 5230 Odense M, Denmark

<sup>2</sup> Biological Science Division, Pacific Northwest National Laboratory, 902 Battelle Boulevard, Richland, WA 99354

<sup>3</sup> Université Clermont Auvergne, Université Blaise Pascal, Institut de Chimie de Clermont-Ferrand, CNRS, UMR 6296, BP 80026, F-63171 Aubière, France; <sup>1</sup>email: shiv@sdu.dk

The anion exchange properties of Layered Double Hydroxides (LDHs) have been exploited for various interesting, innovative applications in the field of material and nanoscience. The charge density distribution (cation ordering) within the metal hydroxide sheets ( $MO_6$ ) in this material remains an active area of research. Recently, direct evidence of local ordering of the cations was confirmed for Mg-Al<sup>1,2</sup> and Mg-Ga<sup>3</sup> LDHs using Solid State NMR (SSNMR) spectroscopy. Neighboring M(III)-O- M(III) octahedra inside the LDH structure (Figure 1) would affect the material performance in e.g. catalysis. Reports of Al-O-Al defects were observed in Mg-Al LDHs<sup>4</sup>. Synthesis parameters such as pH have been shown to affect the end product composition for Mg-Ga LDHs<sup>3</sup>. However a link between the effect of synthetic procedures on LDH phase e.g. composition, cation ordering and M(III)-O- M(III) defects is still missing. Moreover, only Mg-Al and Mg-Ga LDHs have been studied thoroughly by SSNMR. Thus, we report a detailed <sup>1</sup>H, <sup>27</sup>Al, <sup>67</sup>Zn SSNMR investigation of Zn-Al LDH having theoretical formula of  $Zn_{0.67}Al_{0.33}(OH)_2(CO_3^{2-}, NO_3^-).nH_2O$ , i.e., a Zn:Al ratio of 2:1. Our results evidently suggest that experimental parameters (e.g. methodology, synthesis pH, and temperature and post synthesis treatment) have a dramatic impact on LDHs properties such as crystallinity, purity and defect concentration. In addition, SSNMR unambiguously identifies Al-O-Al defects inside the Zn-Al LDHs and provides detailed insight into their origin. Thus, SSNMR studies in combination pXRD, TEM and micro-Raman spectroscopy links the synthetic parameters to the quality of LDH obtained.

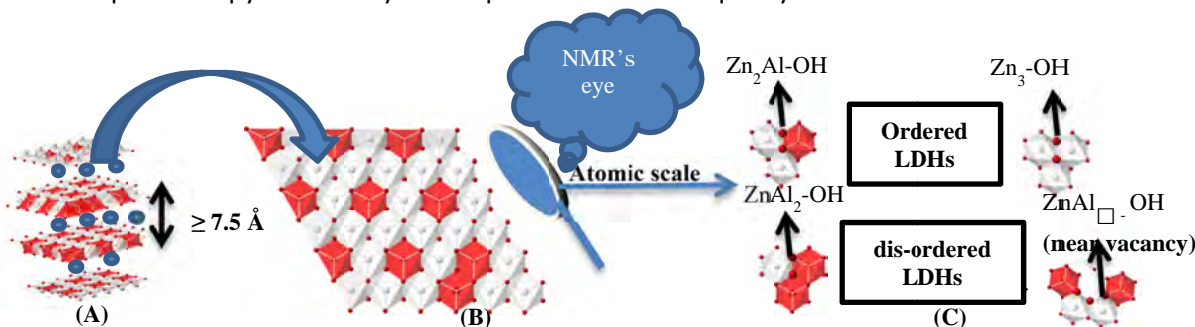


Figure 1, A) Model structure of Zn-Al LDH showing octahedral Zn, Al and anions (spheres) respectively in grey, red and blue color B) Single layer metal hydroxide sheet seen along "c" axis C) Different local environments studied by <sup>1</sup>H NMR.

- (1) Sideris, P. J.; Nielsen, U. G.; Gan, Z.; Grey, C. P. *Science* **2008**, *321*, 113–117.
- (2) Sideris, P. J.; Blanc, F.; Gan, Z.; Grey, C. P. *Chem. Mater.* **2012**, *24*, 2449–2461.
- (3) Petersen, L. B.; Lipton, A. S.; Zorin, V.; Nielsen, U. G. *J. Solid State Chem.* **2014**, *219*, 242–246.
- (4) Cadars, S.; Layrac, G.; Gérardin, C.; Deschamps, M.; Yates, J. R.; Tichit, D.; Massiot, D. *Chem. Mater.* **2011**, *23*, 2821–2831.

## Comparison of inverse microemulsion method and conventional pillaring in synthesis of transition metal oxide/montmorillonite nanocomposites

Melania Rogowska<sup>1</sup>, Alicja Michalik-Zym<sup>1</sup>, Elżbieta Bielańska<sup>1</sup>, Roman Dula<sup>1</sup>, Daria Napruszewska<sup>1</sup>, Paweł Nowak<sup>1</sup>, Ewa M. Serwicka<sup>1</sup>, Adam Gawel<sup>2</sup> and Krzysztof Bahranowski<sup>2</sup>

<sup>1</sup> Jerzy Haber Institute of Catalysis and Surface Chemistry, PAS, Niezapominajek 8, 30-239 Krakow, Poland  
melania.rogowska@gmail.com

<sup>2</sup> AGH University of Science and Technology, Faculty of Geology, Geophysics and Environmental Protection, al. Mickiewicza 30, 30-059 Krakow, Poland

In the field of catalysis transition metal intercalated montmorillonites belong to the most studied clay based nanocomposites. The materials find application as catalysts, photocatalysts and catalyst supports. In the present work we investigated the properties of TiO<sub>2</sub>/montmorillonite composites obtained by two different methods: conventional pillaring and a novel approach, involving an inverse microemulsion method. In the first case, titania nanoclusters were introduced between the clay layers by means of cation exchange with Ti oligocations, resulting in a Ti-pillared interlayered clay (Ti-PILC); in the second, titania nanoclusters formed by inverse microemulsion method were intermixed with an exfoliated organoderivative of montmorillonite (Ti-IMEC). Ti-PILC was synthesized from the sodium form of montmorillonite (Na-mt) and TiCl<sub>4</sub> as a source of pillaring agent. Ti-IMEC sample was prepared from a HDTMA-form of montmorillonite exfoliated in hexanol, and inverse microemulsion prepared from TiCl<sub>4</sub>, HDTMABr and hexanol. The content of TiO<sub>2</sub> was 17-40 wt.%. The materials were characterized with XRD, XRF, SEM, TEM/HRTEM, XPS and Raman spectroscopies, N<sub>2</sub> adsorption/desorption at -196 °C, NH<sub>3</sub> TPD-MS, and FTIR of pyridine adsorption.

XRD analysis demonstrated that the basal spacing observed for Ti-IMEC material was much larger than that characteristic of Ti-PILC (Fig. 1). In addition, XRD analysis suggested that depending on the method of preparation, titania nanoparticles tend to crystallize in different modifications: rutile in Ti-IMEC and anatase in Ti-PILC. This finding was confirmed by Raman spectroscopy study.

The materials were tested for their photocatalytic activity in degradation of cationic (rhodamine B) and anionic (methyl orange) organic dyes, and, after doping with Cu and/or Mn, for catalytic activity in combustion of toluene. The catalytic data are discussed in terms of the physico-chemical characteristics of the solids.

**Acknowledgments:** The authors gratefully acknowledge the financial support from the National Science Center Poland, project OPUS 2013/09/B/ST5/00983.

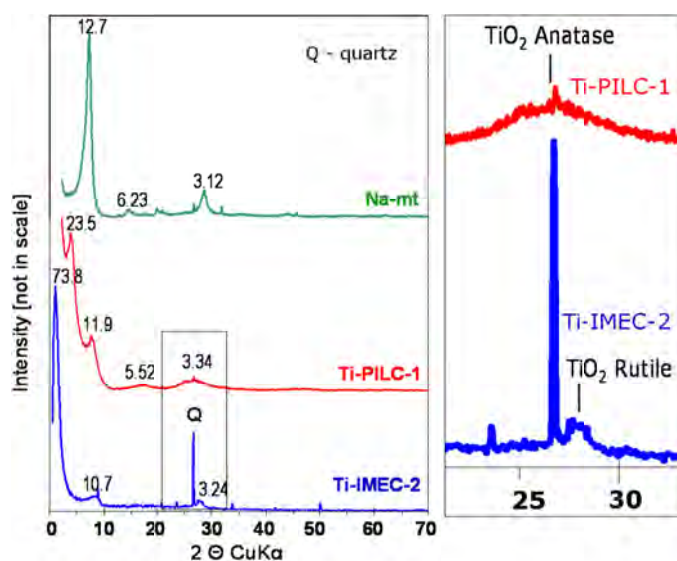


Fig. 1 XRD patterns of Na-mt, Ti-PILC and Ti-IMEC



## XPS and FTIR studies combined with MD simulations of clays and organo-clays

B. Schampera<sup>1</sup>, D. Tunega<sup>2</sup>, R. Solc<sup>2</sup>, S. Dultz<sup>1</sup>, S.K. Woche<sup>1</sup> and R. Mikutta<sup>1</sup>

<sup>1</sup> Institute of Soil Science, Leibniz Universität Hannover, Germany; schampera@ifbk.uni-hannover.de

<sup>2</sup> Institute for Soil Research, University of Natural Resources and Life Sciences (BOKU), Austria

Clays and clay minerals in natural or engineered barriers prevent migration of toxic species to the environment. Especially bentonites, predominantly consisting of montmorillonite, are examined for their use in barrier systems to reduce pollutant discharge due to low permeability as well as high ductility and cation exchange capacity (CEC). Moreover, an improvement of low retardation capacity with respect to a certain chemical species can be achieved by clay modification with specific organic cations. Chemical modification induces changes of clay properties including their surface characteristics. As transport mechanisms at the solid-liquid interface are generally affected by surface properties, knowledge on altered clay surfaces is required. Little is known about the modification of physicochemical properties such as surface charge, wettability, or cation arrangement on the external clay surfaces.

The effect of increasing loadings (up to 4.0 times of the CEC) of two organic cations [hexadecylpyridinium- (HDPyCl) and hexadecyltrimethylammoniumchlorid (HDTMACl)] on the basal external montmorillonite surface has been investigated. A detailed insight onto surface coverage, distribution, and orientation of organic cations on external clay surfaces was provided by a combination of X-ray photoelectron spectroscopy (XPS) and classical molecular dynamics (MD) simulations. To examine changing transport properties, diffusion experiments on conservative solutes, anions, cations, and non-polar compounds were conducted using ATR-FTIR spectroscopy [1] and MD simulations.

Quantification of XPS spectra showed an increasing coverage of the external surface by organic cations. Classical force-field MD simulations were performed on organo-clay-water slab models with a surface coverage by organic cations ranging from 33 to 400% of the CEC of the clay. The calculations were performed using the LAMMPS package [2]. Interactions between surface, organic cations, and chloride anions were described using CLAYFF [3] and OPLS-AA [4] force fields. Findings by XPS and MD confirmed the formation of mono- to bilayers parallel or in an angled arrangement of the cations on the basal external clay surface. This was supported by a variation of surface charge with applied organic cations (-119 to +182 mmol<sub>e</sub>/kg) and shifts in wettability (hydrophilic to hydrophobic; 49°-106°). The arrangement of the organic cations at the surface differed from that in the interlayer space. In the interlayer, e.g. bilayers, could be ascertained at an applied amount >80 %, while a second layer on the external surface arranged only at amounts >200 % of the CEC.

MD simulations provided comparable results and trends for diffusion. For example, the diffusion coefficient for the NO<sub>3</sub><sup>-</sup> anion in the water solution was 1.17 x 10<sup>-9</sup> m<sup>2</sup>/s (diffusion-experiment) and 1.5 x 10<sup>-9</sup> m<sup>2</sup>/s (MD simulation), respectively. Experimental apparent diffusion decreased for the NO<sub>3</sub><sup>-</sup> solution with increasing amounts of organic cations due to charge reversal. High retention of conservative solutes was observed for the natural clay and organo-clays (except hydrophobic HDPy<sup>+</sup>-montmorillonite). Further, the natural clay exhibited low retardation for monovalent anions and hydrophobic HDTMA<sup>+</sup>-montmorillonite samples for bivalent anions. The lowest retention for cations prevailed for the hydrophobic HDPy<sup>+</sup>-montmorillonite and the largest for non-polar compounds was analyzed for the hydrophobic HDTMA<sup>+</sup>-montmorillonite.

The presented work showed that the combined experimental and MD studies proved to be powerful tools in the characterization of the arrangement of organic cations on the external clay surfaces as well as in the determination of diffusion and transport processes at the solid-liquid interface of organo-clays.

[1] Schampera, B., Dultz, S. *Clay Min.* (2009) **44**, 249-266.

[2] Plimpton, S. J. *Comp. Phys.* (1995) **117**, 1-19.

[3] Cygan, R.T., Liang, J.J., Kalinichev, A.G. *J. Phys. Chem. B* (2004) **108**, 1255-1266.

[4] Jorgensen, W.L., Maxwell, D.S., Tirado-Rives, J. *J. Am. Chem. Soc.* (1996) **118**, 11225-11236.

## Synthesis of saponite with different Si/Al using a heterogeneous hydrothermal method

Qi Tao<sup>1,2\*</sup>, Dan Zhang<sup>1,2,3</sup>, Hongping He<sup>1,2</sup>, Manyou Chen<sup>1,2,3</sup>, Shichao Ji<sup>1,2,3</sup> and Tian Li<sup>1</sup>

<sup>1</sup> Key Laboratory of Mineralogy and Metallogeny, Guangzhou Institute of Geochemistry, Chinese Academy of Sciences, Guangzhou 510640, P. R. China

<sup>2</sup> Guangdong Provincial Key Laboratory of Mineral Physics and Materials, Guangzhou 510640, P. R. China

<sup>3</sup> Graduate School of Chinese Academy of Sciences, Beijing 100049, P. R. China

Saponite is a 2:1 type trioctahedral phyllosilicate of the smectite group of clay minerals. Its octahedral sheet sites are occupied by brucite-like  $[\text{Mg}_3(\text{OH})_6]$  units, in which four out of six  $\text{OH}^-$  groups are replaced by oxygen atoms. These oxygen atoms are connected to two  $\text{Si}^{4+}\text{-O}^{2-}$  tetrahedral sheets, sandwiching the octahedral sheet. The ideal formula of saponite can be presented as  $\text{M}^{\text{x+}}[\text{Mg}_3][\text{Si}_{4-x}\text{Al}_x]\text{O}_{10}(\text{OH})_2 \cdot n\text{H}_2\text{O}$ , where M is the exchangeable interlayer cation, and x is the fraction of Al in tetrahedral sheet. Hydrothermal synthesis (HT), especially the homogeneous HT, is a convenient and easy controlled approach to rapid synthesis of pure saponite with a good crystallinity. Therefore, HT method is much more suitable to obtain saponite products for the purpose of industry applications. Compared with homogeneous HT, heterogeneous HT procedure is more similar to the "water-rock" reaction as occurs in nature to a certain extent. Furthermore, it can also promote the nucleation and subsequently accelerate the growth of secondary minerals, by providing a local environment with super-saturation of ion concentration and a relatively lower energy barrier. In the present study, a series of samples were synthesized using heterogeneous HT method, in which brucite was used as the Mg source, by altering Si/Al ratio (fixing the  $\text{Mg}:(\text{Si}+\text{Al}) = 3:4$ ), reaction temperature and time. Characteristic reflections of phyllosilicate were recorded in XRD patterns of the resulting products with  $d_{(060)} \geq 0.153$  nm, indicating a successful synthesis of saponite. The well-crystallized saponite was obtained in the initial Si/Al ratio range of 5.43–7.89, and their crystallinity was increased by raising reaction temperature and extending duration. In the cases of 160°C, brucite and analcime formed as impurity minerals, resulting from the low dissolution ability of brucite and the excess of  $\text{Si}^{4+}$  and  $\text{Al}^{3+}$  in the solution. Both of them disappeared with the extension of reaction time. In the cases of 300°C, a small amount of chrysotile formed, corresponding to the rapid release of  $\text{Mg}^{2+}$ .

## Crystal chemistry of natural Mg-Al-CO<sub>3</sub> layered double hydroxides with variable interlayer spacing

Elena S. Zhitova<sup>1,4</sup>, Sergey V. Krivovichev<sup>1,2</sup>, Victor N. Yakovenchuk<sup>2</sup> and Igor V. Pekov<sup>3</sup>

<sup>1</sup> St. Petersburg, University emb. 7/9, 199034, zhitova\_es@mail.ru

<sup>2</sup> Apatity, Fersman st., 14, 184209

<sup>3</sup> Moscow, Leninskie Gory, 1, 119991

<sup>4</sup> Petropavlovsk-Kamchatski, Piip blvd., 9, 683006

Layered Double Hydroxides (LDHs) is a class of natural and synthetic materials that are characterized by crystal structures based upon brucite-type octahedral sheets. In LDHs some of the M<sup>2+</sup> cations are replaced by M<sup>3+</sup> cations forming a net of positive charge. This charge is compensated by anionic groups in the interlayer galleries (Duan and Evans 2006). These compounds have found different applications in modern industry and have been extensively studied. The fact that the thickness of the interlayer space depends on the nature of the intercalated anion is already common knowledge. For example, carbonate-bearing LDHs are considered to have layer spacing of ~ 7.8 Å, SO<sub>4</sub>-LDHs of ~ 8.9 Å, LDHs containing [Sb(OH)<sub>6</sub>]<sup>-</sup> complexes (cualstibite, zinalstibite, omsite) have *d* ~ 9.7 Å, natural LDHs with cation and anion in the interlayer space (wermlandite group) have *d* ~ 11 Å (Mills *et al.*, 2012). Nevertheless, the influence of M<sup>2+</sup>:M<sup>3+</sup> on the *d* spacing has not been studied in detail.

The extensive single crystal XRD study of natural layered double hydroxides from various localities revealed a high prevalence of the Mg<sub>2</sub>AlCO<sub>3</sub> LDHs (mineral quintinite) described in Kovdor massif (Kola pen., Russia), Bazhenovo and Mariinsk deposits (Middle Urals, Russia), Rudnogorsk deposit (Eastern Siberia, Russia), Zeilberg quarry (Bavaria, Germany), Frankline mine (New Jersey, USA), and Jacupiranga mine (San Paulo, Brazil)). These Mg<sub>2</sub>AlCO<sub>3</sub> LDHs were found in five polytypic modifications: 6R, 2T, 2H, 3R and 1M, the last one was found the most often (Krivovichev *et al.*, 2010a,b; Zhitova *et al.*, 2010). Generally, the interlayer spacing of quintinite is fairly well sustained and equal to 7.56 Å. The same value has been reported for quintinites from the central pre-Caspian depression (Middle Asia, USSR) by Drits *et al.*, 1997; Stradner Kogel (Steiermark, Austria) by Alker *et al.*, 1981; Mont Saint Hilaire (Quebec, Canada) by Chao and Gault, 1997 and some other localities.

Single crystal and powder XRD of Mg-Al-CO<sub>3</sub> LDHs also have revealed species with interlayer spacing ~ of 7.78 Å from Snarum (Norway), Zelentsovskaya pit (Southern Urals, Russia), Talnakh deposit (Taimyr pen., Russia) and St. Lawrence (New York, USA). Interim species with *d* ~ 7.65 Å were registered in Kovdor massif (Kola pen., Russia) and Tayozhnoe deposit (Yakutia, Russia).

The observed distinction in the interlayer *d* spacing can be explained by different M<sup>2+</sup>:M<sup>3+</sup> cation ratios (the higher ratio corresponds to the smaller interlayer spacing). Therefore, the observed *d* spacing can be considered as an indicator of the charge of the brucite-like layer and the M<sup>2+</sup>:M<sup>3+</sup> ratio in particular.

The XRD studies have been performed at the X-ray Diffraction Centre of St. Petersburg State University. This work was supported by the Russian Foundation for Basic Research (project no.14-05-31229) and StSPbU internal grant No 3.37.222.2015 and Special Rector StSPbU scholarship.

1. Alker A., Golob P., Postl W. und Waltiger H. Mitt.-Bl. ABT. Miner. Landesmuseum Joanneum. 1981. 41. P. 279-291.
2. Chao G.Y. and Gault R.A. The Canadian Mineralogist. 1997. 35. P. 1541-1549.
3. Duan X., Evans G.D. Springer, Berlin. 2006.
4. Drits V.A., Sokolova T.N., Sokolova G.V., Cherkashin V.I. Clay and Ckay minerals. 1987. 35/6. 401-417.
5. Krivovichev S.V., Yakovenchuk V.N., Zhitova E.S., Zolotarev, A.A., Pakhomovsky Ya.A., Ivanyuk G.Yu. Mineralogical Magazine. 2010. 74(5). P. 821-832(a), P. 833-840(b).
7. Mills, S.J., Christy, A.G., Génin, J-M. R., Kameda, T., Colombo, F. Mineralogical Magazine. 2012. 76. P. 1289-1336.
8. Zhitova, E.S., Yakovenchuk, V.N., Krivovichev, S.V., Zolotarev, A.A., Pakhomovsky, Ya.A., Ivanyuk, G.Yu. Mineralogical Magazine. 2010. 74(5). P. 841-848.

## Physicochemical and catalytic properties of the tin-doped porous clay heterostructures

Małgorzata Zimowska<sup>1</sup>, Joanna Olszówka<sup>1</sup>, Jacek Gurgul<sup>1</sup>, Kazimierz Łątka<sup>2</sup> and Ewa Maria Serwicka<sup>1</sup>

<sup>1</sup> Jerzy Haber Institute of Catalysis and Surface Chemistry, PAS, Niezapominajek 8, 30-239 Krakow, Poland  
nczimows@cyf-kr.edu.pl

<sup>2</sup> Marian Smoluchowski Institute of Physics, Jagiellonian University, Reymonta 4, 30-059 Kraków, Poland

The impact of porous clay heterostructures (PCH) composite doping by tetravalent ( $\text{Sn}^{4+}$ ) cations on the physicochemical and catalytic properties was investigated. PCHs have been prepared through the surfactant directed assembly of organosilica in the galleries of the synthetic layered hydrous magnesium silicate Laponite® (*registered trademark of BYK Additives*). The resulting crystalline-amorphous composite was doped by a post-synthesis impregnation with tin chloride pentahydrate to obtain samples with Si/Sn = 10, 40 and 60. The influence of the physicochemical properties of the synthesised materials on the catalytic activity was tested in Baeyer-Villiger oxidation of cyclohexanone to  $\epsilon$ -Caprolactone using hydrogen peroxide as benign oxidant.

For comparison purposes a Sn-Lap sample, obtained by ion exchange of Na<sup>+</sup> cations presented between the layers of Laponite® (*registered trademark of BYK Additives*) into Sn<sup>4+</sup> ions and Sn-Lap-550 obtained by calcination of Sn-Lap at 550° C were also examined.

Elemental XRF and EDS analysis revealed incorporation of Sn into the composite structure. Impregnation of the PCH with tin resulted in a decrease of BET specific surface area from 667 m<sup>2</sup>/g (PCH) to 515 m<sup>2</sup>/g (Sn-PCH-10) and decrease of pore volume, while retaining both the nature of the nitrogen adsorption isotherm, as well as high quality pores formed during the synthesis of the PCH composite.

With the increase of Si/Sn ratio gradual segregation of Sn at the edges of grains was detected. In the sample with the highest tin content (Sn-PCH-10) XRD analysis revealed the presence of a SnO<sub>2</sub> phase (~100 nm crystallites).

<sup>119</sup>Sn Mössbauer spectroscopy indicated the quantitative distribution of the tetravalent ( $\text{Sn}^{4+}$ ) cations in the PCH structure. In Sn-PCH-10 about 30 % of tin corresponded to the Sn atoms incorporated into the silica structure, whereas the rest had parameters characteristic for SnO<sub>2</sub>. This indicates that wet impregnation of PCH structure with tin (IV) chloride pentahydrate and further calcination resulted in the introduction of only a small part of tin atoms into the network of PCH structure while the majority leaves as some extra lattice tin species.

The NIR infrared spectra showed increasing intensities of the absorption bands at 7316 cm<sup>-1</sup> attributed to the first overtone of Si-OH groups when PCH was subsidized with tin. As most SiOH groups are formed as an integral part of the TEOS-derived silica network during PCH synthesis, the increase of the intensity of Si-OH upon Sn doping indicates creation of new Si-OH bands of amorphous silica. This is a result of certain, shore-grain amorphization/decomposition of clay component during impregnation of PCH with SnCl<sub>4</sub>·5H<sub>2</sub>O in acidic (pH=1.7) environment.

PCH composites revealed high activity in cyclohexanone oxidation when hydrogen peroxide was used as oxidant. The addition of tin improves the catalytic properties of PCH. Despite improving both the selectivity and yield to  $\epsilon$ -caprolactone after calcination of Sn-Lap, the highest activity and yield was observed for the Sn-PCH-40 sample.

**Acknowledgments:** The authors gratefully acknowledge the financial support from the Polish-Norwegian RP operated by the National Centre for R&D under the Norwegian Financial Mechanism 2009-2014 PC No Pol-Nor/210445/53/2013.

## Impacts of altered volcanic ash on oil and gas production

Christina Calvin<sup>1</sup> and Helena Gamero Diaz<sup>2</sup>

<sup>1</sup> 1325 South Dairy Ashford, Houston TX, 77077 US; ccalvin@slb.com

<sup>2</sup> 3011 Internet Blvd, Suite 200, Frisco TX, 75034 US; gamero1@exchange.slb.com

Oil and gas production of mudstone plays can be impacted by the presence of ash beds that are interbedded between the mudstone layers. These ash layers undergo alteration to a wide variety of mineralogic compositions and textures based on their initial grain size and composition as well as their diagenetic history. Evaluating the variability of altered ash within a basin has become critical to mapping the best zones for completion as well as predicting the best ways to complete the well. This paper highlights some of the variations in the mineralogy of diagenetically modified ash within the Eagle Ford basin.

The following images (Figure A and B) represent two different ash beds within the same well. While they both contain significant quantities of kaolinite, they have variable amounts of iron-bearing sulfides, quartz, and dolomite. The variation in diagenetic grain size and distribution leads to differences in the mechanical behavior of the rock as well as porosity and permeability. Characterization of these ash beds can lead to better completions within wells. However, understanding how these ash beds evolve during diagenesis can allow better prediction of the impact the ash beds have laterally within the basin.

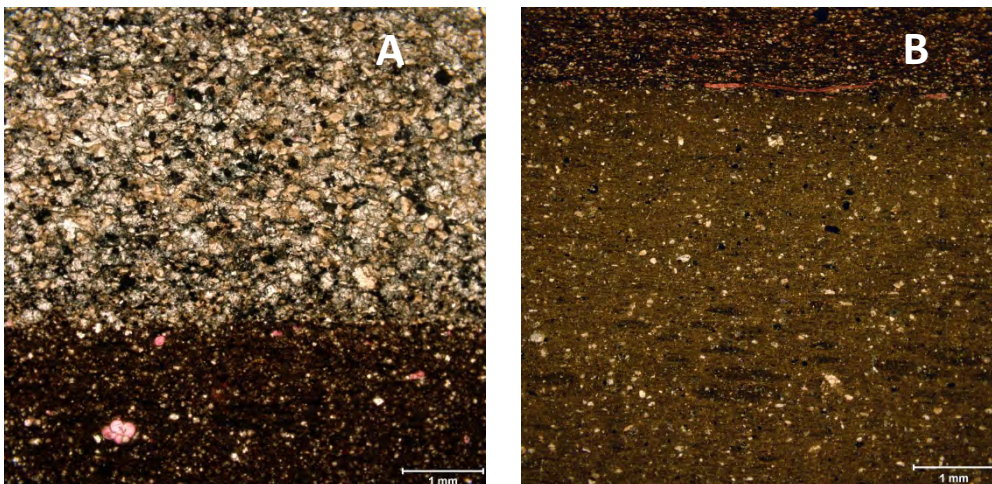


**Figure A** (left) contains a weather ash bed (top) overlying a calcite-rich mudstone. The calcite-rich mudstone contains foraminifera fossils that have been stained pink. The ash bed contains a mixture of diagenetic kaolinite, dolomite and quartz. Some of the quartz is microcrystalline. Opaque minerals within the ash bed are a mixture of titanium, sulfur, and iron. **Figure B** (right) contains a fine-grained ash bed that has altered to kaolinite. White minerals are outlines of the original volcanic phenocrysts that have since been altered to dolomite. At the top of the image, a thin bed of calcite-rich mudstone containing calcareous fossils (pink) overlies the ash.

This paper will examine the factors that impact the diagenetic changes within Eagle Ford ash beds as they evolve from the initial ash deposit to kaolinite- and smectite-rich deposits. Examples will be shown from several wells in different parts of the basin that have different mineralogies and textures to show the impact of the different diagenetic pathways on practical applications for oil and gas exploration.

## Kinetics and geochemical equilibria in the oil window: Concomitant mineralogical and organic geochemical changes in hydrous pyrolysis experiments

Christian Ostertag-Henning<sup>1</sup>, Thomas Weger<sup>1</sup>, Kristian Ufer<sup>1</sup> and Stephan Kaufhold<sup>1</sup>

<sup>1</sup>Federal Institute for Geosciences and Natural Resources (BGR), Stilleweg 2, D-30655 Hannover, Germany.  
christian.ostertag-henning@bgr.de

For decades petroleum geochemists have investigated the thermal breakdown of macromolecular organic matter (kerogen) to oil and gas as a series of kinetically controlled processes, while the minerals in the source rocks were only considered to be the boundary of the available pore space. In contrast, clay mineralogists most often studied the clay-mineral transformation with respect to changing pore-water–mineral equilibria in subsiding sedimentary basins. These two schools of thought have been bridged sporadically by e.g. the pioneering works of Helgeson (1991) or Seewald (1994) in the geochemical realm. Both authors stressed the importance of organic–inorganic reactions for metastable equilibria in sedimentary rock systems evolving in subsiding basins. In the chemical world of surface catalysis, clay minerals or similar structures are of prime importance for the effective transformation of organic compounds, but this seldom is taken into account in studies on natural oil and gas formation.

In a series of hydrous pyrolysis experiments with a clay-rich, initially immature hydrocarbon source rock (Posidonia shale, Germany) the transformation of the organic matter, the formation of oil and gas, changes in pore-water chemistry and the concomitant mineralogical changes have been investigated. The results clearly identify the dependence of organic and inorganic parts of the system: the redox conditions are buffered by the pyrite-pyrrhotite-magnetite system as evidenced by the fugacities of H<sub>2</sub> and H<sub>2</sub>S. This resulted e.g. in metastable equilibria of H<sub>2</sub>S, small organo-sulfur compounds (alkanethiols and thiophenes), and of small hydrocarbon compounds during the formation of oil and gas from the kerogen in the experiment. Small parts of the pyrite were dissolved. In addition, it affected the chemical pathways of hydrocarbon (fragments) towards more oxidized organic compounds like ketones, carbonic acids, and CO<sub>2</sub> in the system. The pH of the system was buffered over the long term mainly by the dissolution and precipitation of carbonates, evidenced by dissolution of dolomite and ankerite and precipitation of calcite as well as the stable carbon isotopic composition of CO<sub>2</sub> in the system. The transformation of clay minerals (e.g. the complete dissolution of kaolinite) and partial dissolution of other silicates (e.g. quartz) resulted in precipitation of secondary phases as zeolithes. (Clay) mineral surface reactions might have influenced the ratios of branched to linear saturated hydrocarbons and catalysed saturation and aromatization reactions of hydrocarbons. The porosity of the rock chips was increased significantly – mainly due to expulsion of oil and gas and volume reduction of kerogen, but this new pore space is less accessible.

The implications of these observations – and the quantitative treatment of the organic and inorganic parts of the system investigated – clearly call for a combined assessment of inorganic and organic geochemical reactions in petroleum-system modelling with respect to metastable equilibria and kinetics. This is necessary to better predict the quality of hydrocarbons in petroleum systems, especially shale oil and shale gas reservoirs, as well as the evolution of the porespace by mineralogical transformations influenced by (organic) products of the petroleum formation.

Helgeson (1991): Organic/inorganic reactions in metamorphic processes. – Can. Min. 29: 707-739.

Seewald, J.S. (1994): Organic-inorganic interactions in petroleum-producing sedimentary basins. – Nature 370: 285-287.

## **Understanding the surface chemistry of oil sands clay minerals: implications for improved extraction and management of tailings**

Cliff T. Johnston<sup>1</sup>

<sup>1</sup>Purdue University, Bindley Bioscience Center, Enhanced Oil Recovery Laboratory, West Lafayette, IN 47907, USA

The oil sand ores of northern Alberta are currently being mined at a rate of  $10^5$  tons per hour which provides a significant portion of the overall energy portfolio for North America. Surprisingly, it is the presence of nano-sized clay minerals that play a defining role both in the extraction of bitumen and in tailings management. Although seemingly insignificant in size, naturally occurring clay minerals present in the oil sand ores of northern Alberta create significant challenges in all aspects of bitumen extraction and recovery, processing of oil sand ores, and management of tailings. Although a significant body of knowledge exists on the characterization of 'oil sands clay minerals', much of this work has focused on the identification of the clay minerals present and not on their respective surface chemistries. This talk will focus on some of the unique structural features of the clay minerals found in the oil sands and their respective surface chemistries. To better understand the surface chemistry of these important mineral phases, we will report on their hydrophilic and hydrophobic nature as determined using a suite of molecular probes.

## Complex thermal history reconstruction of the Carboniferous rocks from the Fore-Sudetic Monocline (Poland) – application in a tight gas exploration

Sylwia Kowalska<sup>1</sup>, Krzysztof Wolański<sup>2</sup>, Dariusz Botor<sup>3</sup>, Istvan Dunkl<sup>4</sup>, Artur Wójtowicz<sup>5</sup> and Urszula Jonkis<sup>1</sup>

<sup>1</sup> Oil and Gas Institute, Lubicz St. 25A, 31-503 Kraków, Poland, e-mail: kowalska@inig.pl

<sup>2</sup> Polish Oil and Gas Company, Zielona Góra Branch, ul. Bohaterów Westerplatte 15, 65-034 Zielona Góra, Poland

<sup>3</sup> AGH University of Science and Technology, al. Mickiewicza 30, 30-059 Kraków, Poland

<sup>4</sup> Sedimentology & Environmental Geology, Geoscience Center, University of Göttingen, Goldschmidtstr. 3, Göttingen, D-37077 Germany

<sup>5</sup> Maria Curie Skłodowska University, Plac Marii Curie-Skłodowskiej 5, 20-031 Lublin, Poland

The Carboniferous rocks of the Fore-Sudetic Monocline (SW, Poland) are treated as a source rocks for the conventional gas accumulation in the Rotliegendes Sandstones. They are part of the European Variscan orogen extending across Europe. In the near future, the more sandy parts of profiles could also become one of the most important targets for prospecting of the tight gas deposits in Poland. The present-day organic carbon content in shales reaches 5% in some places. Until now, the thermal maturity was determined on the basis of vitrinite reflectance. Values obtained vary widely from 1.0 to 5.0%, indicating the phase of thermogenic dry gas generation.

The aim of the project was reconstruction of the thermal history of Carboniferous rocks and distinguishing the tectonic blocks with different degree of thermodiagenesis. The results obtained were correlated with areas of already known gas deposits. The maximum paleotemperatures of thermodiagenesis were estimated using the illite-smectite paleothermometer (also with the Kübler index) and Raman microscopy. The results achieved were compared with vitrinite reflectance. The time constraints of diagenesis were determined using K-Ar dating on bentonites samples (the maximum paleotemperatures) and (U-Th)/He thermochronology applied to zircon (the cooling time below ~170°C).

On the basis of the results obtained the maximum paleotemperatures of diagenesis for the Carboniferous rocks were estimated to be between 130–150°C and 250–260°C, which corresponds to late diagenetic to anchimetamorphic conditions; the whole study area was divided into several tectonic units. The anchimetamorphic rocks were recognized in two regions: the Wolsztyn-Leszno high and in the most eastern part of the Fore-Sudetic Monocline.

The K-Ar ages of the maximum paleotemperatures obtained, ~221–259 Ma, are consistent with presence of the discontinuity in the diagenetic profiles (within the Upper–Lower Triassic strata) which was found in five different boreholes from that region: Zakrzyń IG-1, Kalisz IG-1, Marcinki IG-1, Objezierze IG-1 and Września IG-1. The similar age of thermal reset was also indicated by (U-Th)/He (ZHe) thermochronology – 221–254 Ma. Therefore, a good coincidence of the dates obtained by the K-Ar method for bentonites and by the (U-Th)/He method for zircons could suggest a very quick reduction in the paleotemperatures, which could be a result of the rapid change of the temperature paleogradient or very rapid exhumation.

The Triassic thermal event could have occurred in the whole western part of Poland, west of the Teisseyre-Tornquist zone. The same situation as on the Fore-Sudetic Monocline took place in the Koszalin-chojnice zone - the diagenetic “jump” is clearly visible in the Triassic strata in the borehole Jamno IG-1 and Karsin-1 and the K-Ar dating of the maximum paleotemperatures for the Ordovician bentonite from the borehole Bydgoszcz-1 gave a date of 235 Ma (Środoń and Clauer, 2001).

The maximum paleotemperatures for the Carboniferous rocks which were attained during the Triassic period offer the best potential for the preservation of deposits. Gas generation occurred under the cover of the Zechstein and Triassic strata which became the natural seal for the traps created in the porous and permeable Rotliegendes and in the tight Carboniferous sandstones.



## Mineralogical and chemical variations in clay minerals as key to decipher hydrocarbon migration in siliciclastic rocks, Neuquén Basin (Argentina)

A. Rainoldi<sup>1</sup>, D. Beaufort<sup>2</sup>, P. Patrier<sup>3</sup>, M. Franchini<sup>4</sup>, M.J. Pons<sup>5</sup> and A. Impiccini<sup>6</sup>

<sup>1</sup>Centro Patagónico de Estudios Metalogenéticos, CONICET, Argentina ; [analaurl@hotmail.com](mailto:analaurl@hotmail.com),

<sup>4</sup>[mfranchi@speedy.com.ar](mailto:mfranchi@speedy.com.ar), <sup>5</sup>[josefina.pons074@gmail.com](mailto:josefina.pons074@gmail.com), <sup>6</sup>[aimpicc@gmail.com](mailto:aimpicc@gmail.com)

<sup>2</sup>IC2MP, CNRS-UMR 7285, Hydrasa, Bâtiment B08, Rue Albert Turpin, F-86022 Poitiers Cedex, France; [daniel.beaufort@univ-poitiers.fr](mailto:daniel.beaufort@univ-poitiers.fr), <sup>3</sup>[patricia.patrier@univ-poitiers.fr](mailto:patricia.patrier@univ-poitiers.fr)

The Neuquén Basin, represents the main gas and the second oil-producing basin in Argentina with 2075.5 million barrels of oil and 17 tcf (trillion cubic feet) of gas of discovered resources (Giusiano *et al.*, 2011). Hydrocarbons are produced in conventional and unconventional reservoirs ranging from Late Triassic to Tertiary in age. The Late Cretaceous (Cenomanian-Campanian) deposits of the Neuquén Group comprises a thick continental red-bed sequence, which is an important reservoir for hydrocarbons in the northern part of the Neuquén Basin. Along the Los Chihuidos and Huincul highs, two of the most important morphostructural units of the basin, the red-bed sequence is bleached and the clay mineralogy is further modified where the hydrocarbons have passed through. The objective of this contribution is to decipher the clay variations, including mineralogy and chemical transformations, after the circulation of hydrocarbons.

The Neuquén Group consists of seven formations; in this case we focus on the basal Candeleros and Huincul Formations. The Candeleros Formation, deposited in fluvial and swamp environments, contains Na-rich corrensite whereas the Huincul Formation deposited in meandering and braided fluvial systems, under more humid and acidic conditions than the Candeleros Formation, lacks corrensite and in some places contains well-ordered authigenic kaolinite. Both formations were deposited under oxidizing conditions and contain hematite coatings also, giving the red coloration to the sedimentary sequence.

In the areas affected by the paleo-migrations of the hydrocarbons, the sandstones are pervasively bleached and contain bitumen impregnations. In the Candeleros Formation, corrensite is partially dissolved and its interlayer charge is satisfied by Ca instead of by Na as in corrensite from the red sandstones; in the Huincul Formation, kaolinite is partially dissolved and smectite (montmorillonite) and randomly interstratified chlorite-smectite mixed layer have precipitated. In the bleached sandstones, Ca-rich corrensite, montmorillonite and chlorite-smectite mixed-layer contain minor amounts of Cu; V has also been measured in montmorillonite and in randomly interstratified chlorite-smectite mixed layer.

The arrival of hydrocarbons and their associated reducing fluids generated cation exchange between the infiltrated extraformational fluids (Ca-rich) and the earlier corrensite (Na-rich) whereas, in the Huincul Formation new additional authigenic minerals were precipitated including montmorillonite and mixed-layer chlorite-smectite; mixed-layer chlorite-smectite probably precipitated from an incipient chloritization process of previous montmorillonite in response to more reducing local conditions. Bleaching of the sandstones is due to the redox reactions between hematite and the reducing waters associated with hydrocarbons where the hematite is reduced and the Fe<sup>2+</sup> produced is fixed in iron sulfides or removed, promoting the bleaching of the sandstone. V is commonly related to the hydrocarbons whereas Cu seems to be incorporated in the clay minerals after its precipitation.

The behavior of clay minerals plays an important role in the study of the hydrocarbon paleo-migrations. The complex clay mineral paragenesis, contemporaneous with bleaching of the red beds, can potentially be used to provide evidence for hydrocarbons migration, including in those cases where early hematite is not present or where the original red color has been removed completely, making it more difficult to recognize the passage of the hydrocarbons.

Giusiano, A., Mendiberri, H., and Carbone, O., 2011, Introducción a los Recursos Hidrocarburíferos, in Leanza, H. A., Arregui, C., Carbone, O., Danieli, J.C., and Vallés, J.M., eds., Geología y Recursos Naturales de la Provincia de Neuquén: XVIII Congreso Geológico Argentino, p. 639-644.

## Effects of clay minerals on the catalytic pyrolysis of amino acids

Hongmei Liu<sup>1</sup>, [Xiang Zhou](#)<sup>1,2</sup>, Dong Liu<sup>1</sup> and Peng Yuan<sup>1,\*</sup>

<sup>1</sup>CAS Key Laboratory of Mineralogy and Metallogeny, Guangzhou Institute of Geochemistry, Chinese Academy of Sciences, Guangzhou 510640, China.

<sup>2</sup>University of Chinese Academy of Sciences, Beijing 100049, China; \*[yuanpeng@gig.ac.cn](mailto:yuanpeng@gig.ac.cn)

A large number of field observations and simulation experiments confirm that clay minerals have a catalytic pyrolysis effect on hydrocarbon-generation material. In hydrocarbon-generation experiments, kerogen, asphaltenes, fatty acids and their derivatives are usually chosen as the hydrocarbon-generation material.

In the stratum, amino acids are the common organic matter. However, the amino acids are not easy to retain in the stratum due to bacterial decomposition. Therefore, there are few reports about the simulation studies on hydrocarbon generation by using the amino acid.

Recent studies have found that the oil and gas of the biological-thermal catalytic transitional zone is the product of the transition phase, which has basically ended the biochemical decomposition, though not yet produced large amount of liquid hydrocarbons via thermal catalytic reaction. At this time, although the primitive amino acids in the shallow strata have been decomposed by the microbe, most of the early generated biological macromolecule organic matter (such as the lipids and proteins) have also been decomposed to large amounts of fatty acid and amino acids. During the diagenetic evolution, these acids transform into hydrocarbons with small molecules after decarboxylation and deamination. Finally, these hydrocarbons become the important source of oil and gas in the transition zone. The hydrocarbon generation of amino acids is the essential procedure of the generation of oil and gas in the biological-thermal catalytic transitional zone. It is of great significance to study this procedure, especially for the procedure which was catalyzed by the solid acid sites of clay minerals.

The effects of different types of clay minerals and their solid acidity on the thermal decomposition of amino acids were investigated in this study. The experiment method was as follows: two different long-chain amino acids, DL-Leucine (LEU) and 12-aminolauic acid (ALA), were chosen as the model of organic matter, and four types of clay minerals: Ca-montmorillonite (denoted as Ca-Mt), Na-montmorillonite (denoted as Na-Mt), rectorite (denoted as Rt, on behalf of the mixed layered illite-smectite), and illite (denoted as Ill) were used as model minerals.

The amino acid and clay mineral were firstly well mixed, and the resulting complexes were denoted as ALA-clay or LEU-clay: *e.g.* the ALA-Mt (Ca) was referred to the complexes of 12-aminolauic acid and the Ca-montmorillonite. Then these amino acid-clay complexes were decomposed using a Netzsch 449C thermogravimetry (TG) instrument to study the thermal decomposition behaviors of amino acids in the presence of clay minerals. Samples were heated from 30 to 1000°C at a heating rate of 10°C min<sup>-1</sup>. The amount of inherent solid acid sites in the clay minerals was determined by using n-Butylamine titration method. The total amount of solid acid sites of samples were as follows: 0.80 mmol g<sup>-1</sup> for Ca-Mt, 0.30 mmol g<sup>-1</sup> for Na-Mt, 0.25 mmol g<sup>-1</sup> for Rt, 0.03mmol g<sup>-1</sup> for Ill.

Thermal decomposition results of LEU-clay showed a remarkable decrease in terms of the decomposition temperature of LEU in the LEU-clay samples compared to the LEU itself (310°C). The decomposition temperature of LEU in LEU-Mt (Ca), LEU-Mt (Na), LEU-Rt, and LEU-Ill occurred at 234°C, 257°C, 262°C and 275°C, respectively. Obviously, the decomposition temperature of LEU in LEU-Mt was the lowest. This suggested that montmorillonite has the most catalytic effect on LEU pyrolysis. A similar result was obtained in ALA-clay samples: the decomposition temperature of pure ALA was 464°C, and the decomposition ALA in ALA-Mt(Ca), ALA-Mt(Na), ALA-Rt, ALA-Ill occurred at 400°C, 397°C, 417°C and 452°C, respectively.

The effect of different types of clay minerals on promoting amino acids decomposition in this study decreased as follows: Mt > Rt > Ill. Apparently, a positive correlation existed between the decomposition temperature and the amount of solid acid sites. Similar catalytic effect of Ca-Mt and Na-Mt was observed in the samples containing ALA, even though the amounts of their solid acid sites varied widely. This may be related to the fact that the montmorillonite endures high temperatures during the decomposition. It was reported that after heating at 400°C, Ca-Mt and Na-Mt possessed similar amounts of the solid acid sites. These preliminary results show that the solid acidity of the clay minerals has a catalytic effect on the amino acid thermal decomposition, and the clay mineral can significantly decrease the decomposition temperature of the amino acid. Nevertheless, the specific catalytic mechanisms of the clay minerals is not clear, *e.g.* it's not known which types of acid sites works and how it affects the product of the pyrolysis. On these issues, further investigation should be performed.

## Photo-oxidative degradation of injection-molded polyamide66/sepiolite nanocomposites

A. Yebra-Rodríguez<sup>1</sup>, C. Fernandez-Barranco<sup>1</sup>, M.D. La Rubia<sup>2</sup>, A. Yebra<sup>3</sup>, A.E. Koziol<sup>4</sup> and J. Jimenez-Millan<sup>1</sup>

<sup>1</sup> Dept. of Geology and CEACTierra, University of Jaen, Campus Las Lagunillas s/n, 23071 Jaen, Spain  
e-mail: ayebra@ujaen.es

<sup>2</sup> Department of Chemical, Environmental and Materials Engineering, EPS, University of Jaen, Campus Las Lagunillas s/n, 23071 Jaen, Spain

<sup>3</sup> Dept. Optics, University of Granada, Campus Fuentenueva s/n, 18071 Granada, Spain

<sup>4</sup> Dept. Crystallography, Maria Curie-Sklodowska University, Maria Curie Sklodowska Square 3, Lublin 20-031, Poland

The usefulness of clay/polymer nanocomposites (CPNs) depends on their durability in a particular environment or their interaction with environmental factors (Okada and Usuki, 2006). CPNs degrade when exposed to extreme conditions of temperature or UV radiation which, in the presence of atmospheric oxygen, affect their properties (Bussi ere et al., 2013). Studying the degradation and stability of these materials is thus an issue of great interest from scientific and industrial points of view, as better knowledge of the degradation mechanisms will enable greater time of service for these products. The aim of this work is to establish the effect of UV exposure on the mechanical, optical and crystallographic properties of polyamide66/sepiolite nanocomposites.

Nanocomposite pellets of neat polyamide66 and reinforced nanocomposites were manufactured as described elsewhere (Yebra-Rodr iguez et al., 2009). The pellets were injected (BABYPLAST 6/10, CRONOPLAST) into a specific mold (UNE-EN ISO 527-2). After UV exposure (UNE-EN-ISO 4892-1) the following analyses were carried out: mechanical properties (Universal Testing Machine MTS Insight<sup>TM</sup>, UNE-EN ISO 527-1), transparency (SpectraScan PR-704 spectroradiometer, Photo Research, Chatsworth, USA), infrared spectroscopic analyses (FT-IR Bruker Tensor 27, ATR mode), Differential Scanning Calorimetry (DSC 822e, Mettler Toledo) and X-Ray Diffraction (X-Ray Empyrean diffractometer with the PIXcel-3D detector, PANalytical, The Netherlands). Additionally, the Structural Chemical Analyzer (SCA) technique (Renishaw plc., Gloucestershire, U.K.) was applied to characterize the fresh and UV damage nanocomposites. This novel technique combines Raman spectroscopy and SEM-EDX in a hyphenated instrument: the SEM-SCA system.

Tensile tests show a reduction in the ductility and an embrittlement after the degradation process. In addition, the transparency of the samples increases with the UV exposure. The degradation was quantified by a Yellowness Index (YI) and a Carbonyl Index (CI) from spectroscopic data. The CI in reinforced samples is lower than in neat PA66 whereas the YI is not affected by degradation. Sepiolite has an inhibitor effect on the formation of C=O bonds. These results indicate that the breaking of the polyamide66 chains start in the amorphous region and that is lower in nanocomposite samples due to the low diffusion of oxygen. This affirmation is corroborated by the obtained diffraction patterns.

**Acknowledgements:** Financial support was provided by the CEACTierra (University of Jaen, Spain), Andalusian Research Groups RNM-325, TEP-138 and Spanish Research Project EXPOAIR (P12-FQM-1889). The authors thank CICT (University of Jaen, Spain), CIC (University of Granada, Spain) and the technicians for data collection.

Bussi ere PO, Peyrouz J, Chadeyron G (2013). *Polym Degrad Stabil* 98, 2411-2418.

Okada A, Usuki A (2006). *Macromol Mater Eng* 291, 1449-1476.

Yebra-Rodr iguez A, Alvarez-Lloret P, Cardell C, Rodr iguez-Navarro AB (2009). *Appl Clay Sci* 43, 91-97.

## Study of spatial distribution of sepiolite in polyamide 66/sepiolite nanocomposites

C. Fernández-Barranco<sup>1</sup>, A.E. Koziol<sup>2</sup>, K. Skrzypiec<sup>2</sup>, M. Rawski<sup>2</sup>, M. Drewniak<sup>2</sup> and A. Yebra-Rodríguez<sup>1</sup>

<sup>1</sup> Dept. of Geology and CEACTierra, University of Jaen, Campus Las Lagunillas s/n, 23071 Jaen, Spain  
e-mail: cfernand@ujaen.es

<sup>2</sup> Dept. of Crystallography, Maria Curie-Sklodowska University, Maria Curie Sklodowska Square 3, Lublin 20-031, Poland

Polymer/clay nanocomposites (PCN) are new industrial materials in which the hybrid material exhibits enhanced properties with respect to the counterparts (Okada and Usuki, 2006). The amount of clay as reinforcement and the homogeneity and dispersion of the filler within the polymer matrix are crucial for their effectiveness and therefore the enhancement of the technical properties is highly dependent on the extent of exfoliation of the clay filler into their primary nanometer scale size (Silva *et al.*, 2011).

In this work we studied samples of pure polyamide 66 (PA66) and reinforced PA66 with 1, 3, 5, 7 and 9 wt.% of sepiolite, that were described by Fernández-Barranco *et al.* (2014). The samples have been analysed qualitatively with different microscopy techniques (confocal microscope Nikon D-ECLIPSE C1; Scanning Electron Microscope Quanta 3D FEG; Transmission Electron Microscope, TEM JEOL JEM-1010) and with X-Ray diffraction (X-Ray Empyrean Diffractometer with PIXcel-3D detector, PANalytical, The Netherlands) and scattering techniques (SWAXS optical system of HECUSMBRAUN, Austria).

The XRD patterns of neat polyamide and PCN samples reveal that some peaks correspond to the microstructure of the hybrid (at 8.70°, 17.55°, 26.03° and 32.86 °2θ). These peaks are more intense as the percentage of reinforcement increases. The images obtained by confocal microscopy show that the sepiolite is distributed homogeneously in the PA66 matrix. The micrographs taken using scanning electron microscopy (SEM) and transmission electron microscopy (TEM) show that sepiolite fibers are oriented and equidistantly distributed even in the samples with high percentages of sepiolite. TEM images revealed the absence of clusters of sepiolite and good dispersion of the reinforcement within the matrix.

The quantification of the dispersion, calculated from the results of Small Angle X-Ray Scattering (SAXS) following the method described by Lee and Phillips (2007), indicates that the polymer chains are expanded due to the arrangement of sepiolite within the PA66 matrix and that the clay is properly exfoliated in the polymer.

**Acknowledgements:** Financial support was provided by the CEACTierra (University of Jaen, Spain) and Andalusian Research Group RNM-325. The authors thank CICT (University of Jaen, Spain) and the technicians for data collection.

Fernández-Barranco C, Yebra-Rodríguez A, La Rubia-García MD, Navas-Martos FJ, Álvarez-Lloret P (2014). Polym Composite. In press.

Lee SS, Phillips PJ (2007). Eur Polym J, 43, 1933-1951.

Okada A, Usuki A (2006). Macromol Mater Eng 291, 1449-1476.

Silva AA, Dahmouche K, Soares BG (2011). Appli Clay Sci, 54, 151-158.

## Design of novel biocatalysis microreactor based on hierarchical structuration of enzyme/layered double hydroxide/polysaccharide beads

Rima Mahdi<sup>1</sup>, Philippe Michaud<sup>2</sup>, Christine hélaine<sup>1</sup>, Vanessa Prevot<sup>1</sup>, Céline Laroche<sup>2</sup>, Marielle Lemaire<sup>1</sup> and Claude Forano<sup>1</sup>

<sup>1</sup> Clermont Auvergne University, Université Blaise Pascal, Institut de Chimie de Clermont-Ferrand, CNRS, UMR 6296, ICCF, BP 80026, France, F-63171 AUBIERE, France ; vanessa.prevot@univ-bpclermont.fr

<sup>2</sup> Clermont Université, Université Blaise Pascal, Institut Pascal, CNRS, UMR 6602, IP, BP 10448, France, F-63171 Aubière, France

The potential of aldolases as biocatalysts for the formation of C-C bonds with the desired chirality has been reported widely as a relevant alternative to classical aldol reactions in the synthesis of complex polyhydroxylated molecules [1]. In the past decade, fructose-6-phosphate aldolase from *Escherichia coli* has attracted considerable interest [2] due to its catalytic potential as a non-phosphorylated donor-dependent aldolase. FSA was found to catalyze stereoselectively aldol condensation of dihydroxyacetone (DHA), hydroxyacetone (HA) hydroxybutanone (HB) and also glycolaldehyde (GA) on a variety of aldehydes to form sugars with 3*S*,4*R* configuration. Thus, FSA has proven to be a useful tool for asymmetric synthesis of polyhydroxylated compounds such as iminocyclitols and carbohydrates [3].

To improve the catalytic activity and stability, to facilitate their re-use and reduce the costs of using enzymes in organic synthesis, the enzyme immobilization remains one of the main challenges for industrial applications [4]. A general method adaptable for all enzymes remains to be discovered. Encapsulation of enzyme inside a semi-permeable network matrix such polysaccharide microsphere demonstrates a particular interest and has been investigated extensively. Recently, the fuculose-1-phosphate aldolase was immobilized on glyoxal-agarose gels, and applied in synthesis on an example [5]. However, this biotechnology suffers from partial enzyme release and loss of activity in time.

Recently, a suitable approach was offered by using Mg<sub>2</sub>Al-NO<sub>3</sub> layered double hydroxide (LDH) as an original, easily produced and low-cost inorganic support to design novel enzyme based biohybrid nanomaterials[6]. Indeed, LDH display surface and anionic exchange properties which favour enzyme immobilization. Preparation by a soft chemistry method, structural and textural characterization and bioactivity of FSA@Mg-Al LDH biohybrids will be presented and discussed. The nanomaterials keep the same activity as the free enzyme.

Encapsulation of FSA and FSA@LDH in various polysaccharides beads has been performed. Biocatalytic activity of the bionanocomposites is strongly dependent on both the FSA interactions at the molecular level and the Enzyme/LDH/Polysaccharides nanoscale structuration. FSA activity will be discussed in relation to the entrapment system.

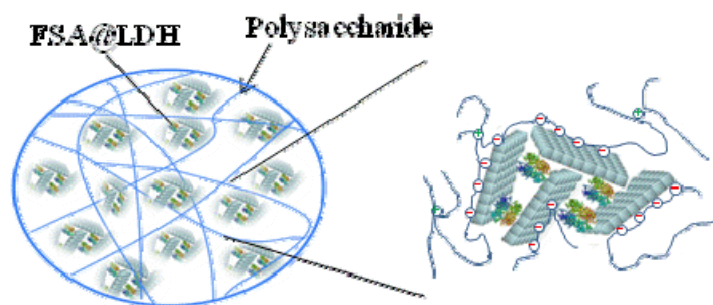


Figure 1: Schematic representation of the FSA@LDH microreactor.

- [1] P. Clapes, W.-D. Fessner, G. A. Sprenger and A. K. Samland, *Curr. Opin. Chem. Biol.*, 2010, **14**, 154-167.  
[2] X. Garrabou, J. A. Castillo, C. Guerard-Helaine, T. Parella, J. Joglar, M. Lemaire and P. Clapes, *Angew. Chem., Int. Ed.*, 2009, **48**, 5521-5525;  
[3] A. L. Concia, C. Lozano, J. A. Castillo, T. Parella, J. Joglar and P. Clapes, *Chem. Eur. J.*, 2009, **15**, 3808-3816  
[4] D. Brady, J. Jordan., *Biotechnology Letters* **2009**, **31**, 1639-1650.  
[5] T. Suau, G. Alvaro, M. D. Benaiges and J. Lopez-Santin, *Biocatal. Biotransform.*, 2009, **27**, 136-142.  
[6] C. Guérard-Hélaine, B. Legeret, C. Fernandes, V. Prevot, C. Forano, M. Lemaire *New J. Chem.* 2011, **35**, 776-779

## Urea intercalation of kaolin and bentonite focusing on ceramic applications

Sahar Seifi<sup>1,2</sup>, Marthe Tatiana Diatta<sup>1,3</sup>, Sabine Petit<sup>2</sup>, Philippe Blanchart<sup>1</sup>, Gisèle L. Lecomte-Nana<sup>1</sup>

<sup>1</sup> Laboratoire Science des Procédés Céramiques et Traitements de Surface (SPCTS, UMR CNRS 7315), Ecole Nationale Supérieure de Céramique Industrielle(ENSCI), Centre Européen de la Céramique – 12, rue Atlantis – 87068 Limoges Cedex – France

<sup>2</sup> Institut de Chimie des Milieux et Matériaux de Poitiers (IC2MP), UMR 7285 CNRS - Université de Poitiers – SFA, 4, rue Michel Brunet (Bât B27), TSA 51106, 86073 Poitiers cedex 9 France

<sup>3</sup> Laboratoire de Chimie et Physique des matériaux (LCPM), Université Assane SECK de Ziguinchor B.P 523, Senegal

The main objective of the present work was firstly preparing intercalated kaolinite-urea complexes using KGa-1b kaolin by means of two techniques, ball milling and mixing at room temperature in water. Secondly, the most straightforward method was applied for the processing of urea-intercalated smectite using a commercial bentonite. These urea-clay complexes have potential application in the ceramics industry, as the chemical and thermal behaviors of the as-obtained products are significantly modified. X-ray diffraction, IR spectroscopy and thermal analyses (TG, DTA and dilatometry) were performed on the different starting and intercalated samples.

XRD patterns confirmed the intercalation of urea into kaolinite by the expansion of the basal spacing of kaolinite from 0.715 nm to 1.069 nm. Moreover, the presence of urea in to kaolinite interlayers was confirmed by the occurrence of hydrogen bonding between urea and kaolinite as identified by infrared spectroscopy. The intercalation degree of KGa-1b kaolin was found to be 72% and 69% when using mixing and ball milling methods respectively. The intercalation of bentonite was more or less complete due to the disappearance of the basal peak of montmorillonite and the occurrence of a new peak as seen in the XRD patterns. The study of the sintering behavior of intercalated kaolinite pointed out a decrease in the densification temperature. This result is promising for the development of less energy consuming ceramics based on the use of such urea-intercalated clays.

**Keywords:** kaolinite, bentonite, Urea-intercalation, sintering, ceramics

## Intercalation into fine crystallites of a layered silicate on monodisperse spherical colloidal silica particles

Tomohiko Okada, and Asuka Suzuki

Department of Chemistry and Material Engineering, Shinshu University, Wakasato 4-17-1, Nagano 380-8553, Japan  
(tomohiko@shinshu-u.ac.jp)

Cation-exchange reactions of the interlayer cations in a smectite group of layered clay minerals are well known, and are used in such applications as modifying surfaces, and producing hydrophobic and microporous inorganic-organic hybrids for the uptake of a specific molecule, producing controlled release materials and achieving efficient photo-induced processes (Okada et al., 2012a; 2014). The shapes required have been produced through the bottom-up self-assembly of silicate layers by freeze-drying hydrogels, and using optically transparent films fabricated by various techniques (including deposition of the smectite suspensions on a substrate, Langmuir–Blodgett technique from exfoliated the platelets, and layer-by-layer deposition technique). The deposition of smectite silicate layers on different particles using an alternate adsorption technique has recently allowed another class of multifunctional materials with hierarchical hybridization to be produced (Hickey et al., 2011). We have described the *in situ* crystallization of a smectite on spherical silica particles. In that process the silica particles were found to be consumed through hydrothermal reactions without losing the silica morphology (Okada et al., 2012b). The core-shell hybridization is not like the *papier mâché* method (the so-called sacrificial template or self-template method), and it is possible to avoid flakes falling off the silica particles even in aqueous media. The monodisperse core-shell particles produced using the sacrificial template method could be used as host materials and/or building units in future separation, sensor, optics and electronic applications, because the periodic arrangement of smectite (or a related layered solid) particles with defined shapes is key to achieving more sophisticated functional materials.

Here we present the crystal growth of a hectorite-like layered silicate on monodisperse spherical silica particles with diameter of 1.0  $\mu\text{m}$  and the intercalation behavior. Fine crystals were formed by reacting spherical silica particles in a colloidal suspension with Li and Mg ions under alkaline conditions at 373 K in a rotating Teflon-lined autoclave. Core-shell particles with a uniform grain size were produced because the heterogeneous nucleation reaction rate was higher than the homogeneous nucleation reaction rate. The cation-exchange capacity, which correlates the negative layer charge density of the layered silicate, varied depending on the amounts of Li and Mg ions that were present in the initial mixture (which ranged from 0.11 to 0.21 mmol/g). In some cases, we found that the intercalation of dioctadecyldimethylammonium ions through cation-exchange reactions expand the interlayer space, topochemically increasing the grain size without any change occurring in the shapes of the core-shell particles.

Hickey, J., Burke, N. A. D. and Stöver, H. D. H. (2011): J. Membr. Sci., 369, 68.

Okada, T., Ide, Y. and Ogawa, M. (2012a): Chem. Asian-J., 7, 1980.

Okada, T., Seki, Y. and Ogawa, M. (2014): J. Nanosci. Nanotechnol., 14, 2121.

Okada, T., Yoshido, S., Miura, H., Yamakami, T., Sakai, T. and Mishima, S. (2012b): J. Phys. Chem. C, 116, 21864.

## Modification of the properties of organophilic clay by the pretreatment of raw material using a jet mill

Makoto Ogawa<sup>1,2\*</sup>, Takayuki Hayakawa,<sup>1</sup> Mitsuru Oya,<sup>1</sup> Makoto Minase<sup>1</sup>, Ken-ichi Fujita<sup>1</sup>

<sup>1</sup> Laboratory of Applied Clay Technology, Hojun Co., Ltd., An-naka, Gunma 379-0133, Japan.  
(waseda.ogawa@gmail.com)

<sup>2</sup> Vidyasirimedhi Institute of Science and Technology, Rayong 21210, Thailand.

Layered solids have been used as functional materials for a wide range of application including energy, environment, and health problems<sup>[1-4]</sup>. In addition to the nanostructural design, particle morphology of layered materials is a key issue to optimize the performance. Accordingly, morphosyntheses of such layered materials as layered double hydroxides and transition metal oxides toward controlled particle size and particle size distribution have been reported recently<sup>[5,6]</sup>. As for smectites, which have been used extensively as functional materials, the morphosynthesis is difficult; the purification of bentonite has been examined using a dispersion-sedimentation method, therefore. In the present study, we examined effects of the sample pre-treatment for the modification of the properties of bentonite and their derivatives.

The bentonite suspension was classified with liquid cyclone and, then, was re-dispersed into water using a wet type super atomizer. Then, the suspension was classified again to obtain a suspension of purified bentonite. In order to demonstrate the positive effects of our pre-treatment, organic modification was done using dimethyldioctadecylammonium chloride<sup>[7-10]</sup> by a conventional ion-exchange procedure, because dimethyldioctadecylammonium-exchanged montmorillonite has been commercialized and advanced materials' application reported. Organic modification of raw bentonite without purification was also carried out for comparison. The careful classification followed by the ion exchange with dimethyldioctadecylammonium ion resulted in the organophilic clay with improved viscosity and transparency of the suspension in toluene if compared with those observed for the organophilic clay prepared without the present bentonite purification process.

1. T. Okada, Y. Ide, M. Ogawa, Organic-inorganic hybrids based on ultrathin oxide layers - Designed nanostructures for molecular recognition, *Chem. Asian J.* **7** (2012) 1980-1992.

2. T. Okada, Y. Seki, M. Ogawa, Designed nanostructures of clay for controlled adsorption of organic compounds, *J. Nanosci. Nanotech.* **14** (2014) 2121-2134.

3. M. Ogawa, K. Saito, M. Sohmiya, A controlled spatial distribution of functional units in the two dimensional nanospace of layered silicates and titanates, *Dalton Trans.* **43** (2014) 10340-10354.

4. G. Lagaly, M. Ogawa and I. Dekany, Clay-organic interaction, in F. Bergaya, B. K. G. Theng and G. Lagaly (Editors), *Handbook of Clay Science*, Elsevier Science, Amsterdam (2006).

5. M. Ogawa, M. Morita, S. Igarashi, S. Sato, Green synthesis of a layered titanate, potassium lithium titanate; lower temperature solid-state reaction and improved materials performance, *J. Solid State Chem.*, **206** (2013) 9-13.

6. M. Ogawa, K. Inomata, Preparation of layered double hydroxides, *Clay Sci.*, **15** (2011) 131-137.

7. M. Ogawa, T. Matsutomo, T. Okada, Preparation of hectorite-like swelling silicate with controlled layer charge density, *J. Ceram. Soc. Jpn.*, **116** (2008) 1309-1313. (2008).

8. M. Ogawa, T. Matsutomo, T. Okada, Preparation of iron containing hectorite-like swelling silicate, *Bull. Chem. Soc. Jpn.*, **82** (2009) 408-412.

9. M. Ogawa, T. Aono, K. Kuroda, C. Kato, Photophysical probe study of alkylammonium-montmorillonites" *Langmuir*, **9** (1993) 1529-1533.

10. M. Ogawa, M. Hama, K. Kuroda, Photochromism of azobenzene in the hydrophobic interlayer spaces of dialkyldimethylammonium-fluor-tetrasilicic micas, *Clay Miner.*, **34** (1999) 213-220.



**FRIDAY  
ORAL  
SESSIONS**

Time	Title + Authors	Page No.
	<b>Lecture room 5: Structural characterization of lamellar compounds (2)</b> <i>Session Chairs: Douglas McCarty, Eric Ferrage and Vanessa Prevot</i>	
08.40	What happens during the talc synthesis? From nucleation to crystal growth: a study by XRD, FTIR, EXAFS and <sup>29</sup> Si NMR <u>Angela Dumas</u> , Martin Mizrahi, François Martin and Felix Requejo	445
09.00	Formation and restacking of disordered smectite osmotic hydrates <u>Benjamin Gilbert</u> , Luis Comolli, Ruth Tinnacher, Martin Kunz and Jillian F. Banfield	446
09.20	Hydration and dehydration of a Na <sup>+</sup> -exchanged smectite – a temperature-dependent infrared spectroscopy study <u>Florian Schnetzer</u> , Peter Thissen and Katja Emmerich	447
09.40	Crystal-chemical controls on smectite hydration Baptiste Dazas, <u>Bruno Lanson</u> , Eric Ferrage and Alfred Delville	448
10.00	Mixed-layered structure formation and analysis during illite dehydroxylation <u>Douglas K. McCarty</u> , Victor A. Drits, and Arkadiusz Derkowski	449
10.20	<b>BREAK</b>	
10.40	From crystalline hydrates to osmotic swelling and lyotropic liquid-crystalline phases Sabine Rosenfeldt, Matthias Stöter, Thomas Weiß, Stephan Förster and <u>Josef Breu</u>	450
11.00	Microscopic structure and permittivity of interlayer water in Na-saturated montmorillonite <u>Katja Emmerich</u> , Heike Kaden, Franz Königer and Peter Thissen	451
11.20	Systematics of Li <sup>+</sup> fixation in reduced-charge montmorillonite <u>Georgios D. Chryssikos</u> , Vassilis Gionis and George E. Christidis	452
11.40	Cs-sorption in weathered biotite from Fukushima granitic soils <u>Ryosuke Kikuchi</u> , Hiroki Mukai, Chisaki Kuramata and Toshihiro Kogure	453
12.00	Use of the pair distribution function technique for the development of detailed structure/property correlations in layered double hydroxides (LDH) <u>C. Taviot-Guého</u> , P. Vialat, A. Faour, V. Prévot, C. Mousty and F. Leroux	454
12.20	<b>LUNCH</b>	
14.10	Local environment in layered double hydroxides probed by solid state NMR spectroscopy <u>Ulla Gro Nielsen</u> , Line B. Petersen, Suraj Charan, Nicolai D. Jensen, Claude Forano, Vanessa Prevot, and Andrew S. Lipton	455
14.30	NMR study of structure and dynamics in Mg/Al layered double hydroxides <u>Arnaud Di Bitetto</u> , Gwendal Kervern and Cédric Carteret	456
14.50	The structure and stability of layered double hydroxides with various Ca(II) : Fe(III) ratio : a dissolution-reprecipitation mechanism to explain very high phosphate removal efficiency <u>M. Al-Jaberi</u> , S. Naille, G. Medjahdi and C. Ruby	457
15.10	Structure and reactivity of intercalated amino-acids into layered double hydroxides <u>Jean Fahl</u> , Erwan André and Cédric Carteret	458
15.30	Structure of the new “green rust” related minerals: fougèrite, trébeurdenite and mössbauerite; some occurrences <u>J.-M. R. Génin</u> , A. G. Christy, O. Guérin, A. Herbillon, E. Kuzmann, C. Ruby, H. Shcherbakova, C. Upadhyay and S. J. Mills	459
15.50	<b>PLENARY:</b> Hydrotalcites, water purification and carbon sequestration <u>Stuart Mills</u> ( <i>Max Hey Medallist of the Mineralogical Society</i> ) Introduced by F. Wall	460

Friday, 10th July

<b>Lecture room 5: General (4)</b> <i>Session Chair: F. Wall</i>		
16.30	<b>LECTURE ROOM 5: KEYNOTE:</b> The roles of chance and necessity in the diversification of minerals: is Earth's continental crust unique? <u>Edward S. Grew (<i>Collins Medallist of the Mineralogical Society</i>)</u> Introduced by F. Wall	462
16.50	<b>Awards and closing</b>	

	<b>Lecture room 4: Clays in the Critical Zone soils, weathering and elemental cycling (2)</b> <i>Session Chairs: Bruno Lanson, Jason Austin, Paul Schroeder and Steve Banwart</i>	
09.00	Is solution chemistry responsible for clay particle mobility through soil pores in lessivage process? <u>Jerome Labille</u> , Romain Van den Bogaert and Sophie Cornu	464
09.20	Effects of iron electron transfer on clay mineral stability and redox reactivity <u>Anke Neumann</u> , Drew E. Latta, W.A.P.J. Premaratne, Tyler L. Olson, Luiza Notini de Andrade, and Michelle M. Scherer	465
09.40	Nature of sites involved in Cs <sup>+</sup> desorption from vermiculite <u>Liva Dzene</u> , Emmanuel Tertre, Eric Ferrage and Fabien Hubert	466
10.00	Influence of the clay content as variable charge sites in the adsorption/desorption of explosives from soils <u>Rosalina Gonzalez</u> , Herb Allen and Dominic Di Toro	467
10.20	Dissolution of beidellite in acidic solutions: New insights on smectite interface reactions and effect of crystal chemistry on dissolution rates <u>Valentin Robin</u> , Emmanuel Tertre, Olivier Regnault and Michael Descostes	468

	<b>Lecture room 3: Beyond smectite-based nanocomposites</b> <i>Session Chairs: Pilar Aranda and Christian Detellier</i>	
08.50	<b>KEYNOTE:</b> Fibrous vs. layered clays in nanocomposites <u>Eduardo Ruiz-Hitzky</u>	470
09.20	Stimuli-responsive hydrogels formed by the rigid cylindrical clay mineral “Imogolite” <u>Kazuhiro Shikinaka</u> , Keisuke Kaneda, Tei Maki, Hiroyasu Masunaga, Yoshihito Osada, and Kiyotaka Shigehara	471
09.40	Photo-induced anisotropic deformation of poly( <i>N</i> -Isopropylacrylamide) gel hybridized with an inorganic nanosheet liquid crystal aligned by electric field <u>Nobuyoshi Miyamoto</u> and Takumi Inadomi	472
10.00	Chitosan-vermiculite bionanocomposite foams as biosorbents for the removal of cadmium(II) ions <u>Érika Padilla-Ortega</u> , <u>Margarita Darder</u> , Pilar Aranda, Roberto Leyva-Ramos and Eduardo Ruiz-Hitzky	473
10.20	Hydro-mechanical properties of clay-polymer composites for application in geotechnical engineering <u>Hanna Haase</u> and Tom Schanz	474
10.40	<b>BREAK</b>	
11.00	Beyond homopolymers: kaolinite functionalized with a block co-polymer <u>Jonathan Fafard</u> and Christian Detellier	475
11.20	Functional nanohybrid materials derived from kaolinite <u>Christian Detellier</u> and Gustave Kenne Dedzo	476
11.40	Two-photon absorption properties of acetylenic and diacetylenic compounds in the interlayer space of smectite <u>Yasutaka Suzuki</u> , Hiroyuki Sugihara, Shuhei Mochida, Koichiro Satomi, Jun Kawamata	477
12.00	Elaboration of nanocomposite latexes containing Layered Double Hydroxides by macroRAFT-mediated encapsulating emulsion polymerization <u>Vanessa Prévot</u> , Samuel Pearson, Ana Maria Cenacchi Pereira, Fabrice Leroux, Christine Taviot-Guého, Franck D’Agosto, Muriel Lansalot, Elodie Bourgeat-Lami	478
12.20	<b>KEYNOTE:</b> Emerging nano convergence science: clay based drug delivery system <u>Jin-Ho Choy</u>	479
12.50	<b>LUNCH</b>	
13.50	<b>Martin Vivaldi Award:</b> Clay-lipid nanohybrids: Toward influenza vaccines and beyond <u>Bernd Wicklein</u> , Margarita Darder, Pilar Aranda, Eduardo Ruiz-Hitzky	480
14.10	Easily processable polymer-clay hydrogels for biomedical applications <u>Chris Breen</u> , Chris Sammon, Victoria Boyes, Christine Le Maitre and Jonathan Foulkes	481
14.30	Immobilization of proteins in ultrathin clay films via layer-by-layer self-assembly <u>Tamás Szabó</u> , Raluca Mitea, Márta Szekeres, Imre Dékány and Robert A. Schoonheydt	482
14.50	Hierarchical “nano-to-macro” organization of oxide nanosheets based on their colloidal liquid crystalline behavior <u>Teruyuki Nakato</u> , Yoshihiro Nono and Emiko Mouri	483
15.10	Layered double hydroxide/sepiolite heterostructured materials <u>Almudena Gómez-Avilés</u> , <u>Pilar Aranda</u> and Eduardo Ruiz-Hitzky	484

	<b>Lecture room 2: Industry perspectives in clay and fine-particle science (2)</b> <i>Session Chairs: Jon Phipps and Prakash Malla</i>	
09.10	Room temperature and high temperature sealing properties and compression properties of compressive gaskets made of micrometric vermiculite particles <u>L. Duclaux</u> , L. Reinert, A.N. Nguyen, L. Mirabel, JF Juliaa and A. Beziat	486
09.30	Nature and origin of zinc clays in supergene non-sulphide ore deposits <u>Flavien Choulet</u> , Martine Buatier, Luc Barbanson, Régis Guégan and Aomar Ennaciri	487
09.50	Influence of some clays on cement hydration <u>D. Deneele</u> , M. Paris and I. Serclerat	488
10.10	Influence of swelling clay content when using additives in ternary systems: gypsum, water & impurities <u>Annette Quetscher</u> , Albrecht Wolter and Jazmín Aboytes-McNeela	489
10.30	Upgrading Philippine pottery clay into nanoclay-grade material through super-centrifugation for advanced applications <u>Johanna Michelle S. Ambait</u> and Leslie Joy L. Diaz	490
10.50	<b>BREAK</b>	
11.10	Use of glaciogene marine clays for brick production in the Arctic <u>Louise Josefine Belmonte</u> and Lisbeth Ottosen	491
11.30	Clay mineralogy for geometallurgy of Cu-Mo ores. Challenges in university and professional training in Chile <u>Ursula Kelm</u> and Oscar Jerez	492
11.50	An experimental study of CO <sub>2</sub> -H <sub>2</sub> O-listwanite-based reactions using serpentine from the Ahırözü kaolin deposits, Eskişehir-Mihalıççık, Turkey <u>İşıl Ömeroğlu</u> , Stephen Guggenheim, Asuman Günel Türkmenoğlu, A. F. Koster van Groos, and Şih Ali Sayın	493

	<b>Lecture room 1: Clay minerals in the oil and gas industry</b> <i>Session Chairs: Edwin Zeelmaekers and Ruairri Day Stirrat</i>	
08.30	<b>KEYNOTE:</b> Reconstructing basin burial and thermal history using shale seismic properties, reservoir fluid inclusions, and advanced modal analysis methods in the Arctic Barents Sea <u>Paul Nadeau</u> , <u>TineStraaso</u> , <u>Theis Solling</u> , <u>Xiomara Marquez</u> , <u>Lothar Schulte</u>	495
09.00	Diagenesis of silica and clay minerals – Field observations and pyrolysis experiments <u>Elen Roaldset</u>	496
09.20	A 2-stage model for growth of fibrous illite in oilfield sandstones <u>Mark Wilkinson</u>	497
09.40	A clay mineralogy study of the Shurijeh Sandstone Reservoir, Kopet Dagh sedimentary basin, NE Iran <u>Golnaz Jozanikohan</u> , <u>Gholam Hossain Norouzi</u> , <u>Fereydoun Sahabi</u> and <u>Quentin Fisher</u>	498
10.00	Tracing hydrocarbons in gas shale using lithium and boron isotopes: Denver Basin USA, Wattenberg Gas Field <u>W. Crawford Elliott</u> , <u>Lynda B. Williams</u> and <u>Richard L. Hervig</u>	499
10.20	<b>BREAK</b>	
10.40	Crystal-chemical evolution of clay minerals with depth in the Vaca Muerta Formation: Impact on the evaluation of total clay content <u>Claire I. Fialips</u> , <u>Ahmed Abd Elmola</u> , <u>Daniel Beaufort</u> , <u>Jean-Paul Laurent</u> , <u>Bernard Labeyrie</u> and <u>François Umbhauer</u>	500
11.00	Further insight into the depositional environment of the Holywell Shale (Carboniferous, northeast Wales) <u>Leo P. Newport</u> , <u>H. Chris Greenwell</u> , <u>Andrew C. Aplin</u> , <u>Jon G. Gluyas</u> and <u>Darren R. Gröcke</u>	501
11.20	Stratigraphic controls on clay minerals in the McMurray Formation <u>Ruairi J Day-Stirrat</u> , <u>Ronny Hofmann</u> , <u>Anton Nikitin</u> , <u>Robert Mahood</u> , <u>Stephen Hillier</u> and <u>Gilles Mertens</u>	502
11.40	Moss and peat as monitors of past, present, and future rates of atmospheric dust deposition <u>Gillian Mullan-Boudreau</u> and <u>William Shotyk</u>	503
12.00	Wettability of Smectites: effect of exchangeable ions and surface roughness <u>J. Ballah</u> , <u>M. Chamerois</u> , <u>G. Hamon</u> , <u>P. Levitz</u> and <u>L. Michot</u>	504
12.20	<b>LUNCH</b>	
13.30	Gaining insight into of oil-brine-clay mineral interactions through core- to nanoscale experimental and computational studies <u>Chris Greenwell</u> , <u>Pablo Cubillas</u> , <u>Rikan Kareem</u> , <u>Valentina Erastova</u> and <u>Thomas Underwood</u>	505
13.50	Towards a nanoscopic understanding of oil-clay mineral wettability: implications for enhanced oil recovery <u>Pablo Cubillas</u> , <u>Rikan Kareem</u> and <u>Chris Greenwell</u>	506
14.00	The kaolinite - water interface: Insight from the electrical double layer <u>N. Bovet</u> , <u>S. Jelavic</u> , <u>T. Clausen</u> and <u>S.L.S. Stipp</u>	507
14.30	A cryogenic X-ray photoelectron spectroscopy (cryo-XPS) study of illite and clinocllore control on low salinity enhanced oil recovery <u>S. Jelavić</u> , <u>N. Bovet</u> , <u>A. Rath Nielsen</u> and <u>S.L.S. Stipp</u>	508
14.50	The effect of the water boundary layer on clay properties in shales in oil reservoirs <u>Lyudmyla Wilson</u> and <u>M. J. Wilson</u>	509
15.10	Swelling of clay minerals: from micro to macro scales. <u>Radhika Patel</u> , <u>Neal Skipper</u> and <u>Chris Greenwell</u>	510
15.30	Shale - drilling mud interactions tested in Flysch reservoirs <u>Andrea Schicker</u> and <u>Susanne Gier</u>	511

Friday  
10<sup>th</sup> July

Lecture room 5

Structural characterization  
of lamellar compounds (2)



## What happens during the talc synthesis? From nucleation to crystal growth: a study by XRD, FTIR, EXAFS and $^{29}\text{Si}$ NMR

Angela Dumas<sup>1,2</sup>, Martin Mizrahi<sup>2</sup>, François Martin<sup>1</sup> and Felix Requejo<sup>2</sup>

<sup>1</sup> ERT 1074 "Géomatériaux", GET (Géosciences Environnement Toulouse), UMR 5563 (UPS-CNRS-IRD-CNES), 14 Avenue Edouard Belin, 31400 Toulouse, France dumangela@hotmail.fr

<sup>2</sup> Instituto de Investigaciones Fisicoquímicas Teóricas y Aplicadas, INIFTA (CONICET-UNLP), diag. 113 y calle 64, 1900 La Plata, Argentina

Synthetic talc ( $\text{Mg}_3\text{Si}_4\text{O}_{10}(\text{OH})_2$ ) appeared ten years ago as a technical solution to perform new lubricant composite materials [1]. In collaboration with industrial partners, synthesis processes were recently revised and improved [2,3] to obtain an economically viable process. Nowadays, synthetic talc appears in various industrial sectors as a competitive and original fillers [4,5]. While synthetic talc is a well-documented product [6-7], very few information is available about the early stages of its formation. However, understanding talc crystallogenesi mechanisms is of primordial importance before scaling-up syntheses processes.

In the aim to study what happens during the talc synthesis, we prepared two series of samples (Ni-talc and Mg-talc) composed by the talc precursor sample (PT) obtained at room temperature, and by talc samples (T) synthesized at 100, 200 and 300 °C during 1 or 6 hours. Then, samples were characterized by XRD, FTIR and EXAFS at the Ni K edge or  $^{29}\text{Si}$  NMR. While X-ray diffraction (XRD) data inform about the crystalline long-range order, Fourier Transformed Infrared spectroscopy (FTIR), X-ray absorption spectroscopy (XAS) and  $^{29}\text{Si}$  NMR provide details about the local structure.

The EXAFS data of the talc precursor give information about the average composition of the talc growth unit: 2 to 3 Ni-octahedra distanced from each other by 3.07 Å and 3 to 4 Si-tetraedra distributed on the top and bottom of the octahedral "sheet" and distanced from Ni by 3.29 Å. With synthesis temperature, the octahedral sheet is growing: it is visible both in the local order (increase of the coordination number Ni-Ni; increase in the intensity of  $\nu\text{Mg}_3\text{OH}$ ) and in the long range order (increase in intensity of the 06l-33l peak). Simultaneously, the tetrahedral sheet is also expanding.  $^{29}\text{Si}$  NMR data evidence the role of the hydrothermal temperature on the transformation of Q1 into Q2 environments (Q means that the Si atom is bonded to four oxygen atoms and the associated number is related to the number of Si neighbors). Nevertheless, temperatures higher than 180°C are necessary to transform Q2 into Q3 environments. Then, at 300°C, the hydrothermal synthesis time has only an influence on particle growth.

These new insights into the mechanisms of the transformation of the talc precursor into crystalline talc will help to fine tune the talc synthesis process.

[1] Martin et al. International patent: WO 2009081046 A9 2008

[2] Dumas et al. International patent: WO 2013004979 A1 2013

[3] Dumas et al. Applied Clay Science 2013; 85:8–18

[4] Yousfi et al. Journal of Colloid and Interface Science 2013; 403:29–42

[5] Yousfi et al. Journal of Applied Polymer Science 2014; 131.

[6] Dumas et al. Physics and Chemistry of Minerals 2013; 40:361–73

[7] Dumas A. PhD thesis UPS, 2013

## Formation and restacking of disordered smectite osmotic hydrates

Benjamin Gilbert<sup>1</sup>, Luis Comolli<sup>2</sup>, Ruth Tinnacher<sup>1</sup>, Martin Kunz<sup>3</sup> and Jillian F. Banfield<sup>1,4</sup>

<sup>1</sup> Earth Sciences Division, Lawrence Berkeley National Laboratory, Berkeley, CA 94720

<sup>2</sup> Life Sciences Division, Lawrence Berkeley National Laboratory, Berkeley, CA 94720

<sup>3</sup> Advanced Light Source, Lawrence Berkeley National Laboratory, Berkeley, CA 94720

<sup>4</sup> Earth and Planetary Science, University of California – Berkeley, Berkeley, CA 94720

Clay swelling, an important phenomenon in natural systems, can dramatically affect the properties of soils and sediments. Of particular interest in low salinity, saturated systems are osmotic hydrates, forms of smectite in which the layer separation greatly exceeds the layer thickness due to the intercalation of water. *In situ* X-ray diffraction studies have shown a strong link between ionic strength and average interlayer spacing in osmotic hydrates, but the nature and origin of disorder in them has not been fully described. Here, we investigated the structural state of expanded smectite in sodium chloride solutions by combining very low electron dose, high-resolution cryogenic-transmission electron microscopy (HRCTEM) observations with X-ray diffraction experiments. Standard Wyoming smectite (SWy-2) was embedded in vitreous ice to evaluate clay structure *in aqua*. Lattice fringe images show that smectite equilibrated in aqueous, low ionic strength solutions exists as individual smectite layers and osmotic hydrates. We found no evidence for alternative modes of clay aggregation, such as edge to sheet configurations, but observed significant variability in interlayer spacing. We investigated whether this variation could be explained by a dependence of the magnitude of long-range cohesive (van der Waals) forces on the number of layers. Calculations of the Hamaker constant for layer-layer interactions showed that van der Waals forces span at least five layers and the intervening water and confirmed that forces vary with layer number. Variation in spacings and other disorder in osmotic hydrates probably also arise from short-range compositional heterogeneity. Drying of the disordered osmotic hydrates induced re-aggregation of the smectite to form particles that exhibited interparticle diffraction. Clay disaggregation and restacking may be considered as an example of oriented attachment, with the unusual distinction that the process is reversible.

## Hydration and dehydration of a Na<sup>+</sup>-exchanged smectite – a temperature-dependent infrared spectroscopy study

Florian Schnetzer<sup>1,2\*</sup>, Peter Thissen<sup>1</sup> and Katja Emmerich<sup>1,2</sup>

<sup>1</sup> Karlsruhe Institute of Technology, Institute of Functional Interfaces, Hermann-von-Helmholtz-Platz 1, 76344 Eggenstein-Leopoldshafen, Germany \*corresponding author: florian.schnetzer@kit.edu

<sup>2</sup> Karlsruhe Institute of Technology, Competence Center for Material Moisture, Hermann-von-Helmholtz-Platz 1, 76344 Eggenstein-Leopoldshafen, Germany

Hydration and dehydration are the most important reactions of swellable 2:1 layer silicates. To investigate the microscopic structure of water adsorption and desorption, a well characterized Na<sup>+</sup>-exchanged dioctahedral smectite (BV-M0.2Na) with a low layer charge (0.26/formula unit) is studied by *in situ* transmission Fourier Transform Infrared Spectroscopy (FTIR) in the middle-IR (MIR) region (4000 – 550 cm<sup>-1</sup>). For this, a silicon wafer (thickness 500 μm) of 3 cm × 1 cm, cut parallel to (111), was cleaned with piranha solution (1:3 30% H<sub>2</sub>O<sub>2</sub>: 18 M H<sub>2</sub>SO<sub>4</sub> for 30 min at 80 °C), thoroughly rinsed with deionized water and dried in a stream of N<sub>2</sub>. The clean silicon wafer was measured as reference. Afterwards, the silicon wafer was immersed in a dispersion of BV-M0.2Na with a solid content of 6 × 10<sup>-3</sup>%. The dispersion was heated at 105 °C until complete evaporation (~12 h) of the liquid and the clay mineral particles covered both sides of the wafer surface (T-BAG method, Hanson et al., 2003, Vega et al., 2012). The sample was stored in a desiccator at 53% relative humidity (r. h.) to reach a defined water content. FTIR measurements were done with a custom-made, heatable sample holder in an oxygen free atmosphere under N<sub>2</sub> purging.

In the course of this study, we describe different states of dehydration of BV-M0.2Na up to 500 °C. Moreover, we also consider the dissociation of water.

At low temperatures (25 – 200 °C), we observed broad OH stretching vibrations  $\nu(\text{OH})$  between 3710 and 3000 cm<sup>-1</sup> and a weak  $\nu(\text{OH})$  band at 3620 cm<sup>-1</sup>, which became sharper as the temperature increased. H-O-H bending vibrations  $\delta(\text{H-O-H})$  at 1642 cm<sup>-1</sup> were observed. A similar ratio of  $\nu(\text{OH})$  to  $\delta(\text{H-O-H})$  (~ 1:1) can be detected. At higher temperatures (250 – 400 °C), the  $\nu(\text{OH})$  at 3620 cm<sup>-1</sup> shifted to 3640 cm<sup>-1</sup>. This shift was accompanied by an occurrence of the Si-O-Si bending vibration  $\delta(\text{Si-O-Si})$  at 630 cm<sup>-1</sup>. In addition, an increased ratio of  $\nu(\text{OH})$  to  $\delta(\text{H-O-H})$  (~ 5:1) indicates (1) a predominant 1W state at the beginning and (2) the release of the weakly bound water. These results are in accordance with the theoretical work of EMMERICH ET AL. (2015).

In the area of the Si-O stretching vibrations  $\nu(\text{SiO})$  we observed two prominent absorption bands at 1085 and 1050 cm<sup>-1</sup> for the sample equilibrated at 53% r.h.. With increasing temperature, the two  $\nu(\text{SiO})$  vibrations shifted closer together as the dehydration process continued. Finally, we detected only one Si-O stretching vibration at 1064 cm<sup>-1</sup>.

In the differential spectra of 500/400 °C only  $\nu(\text{OH})$  and no more  $\delta(\text{H-O-H})$  were observed. Together with newly formed  $\nu(\text{SiO})$  at 1250 and 1190 cm<sup>-1</sup> as well as an increase of intensity of  $\delta(\text{Si-O-Si})$  indicated the dissociation of water.

Emmerich, K. et al., (2015). J. Colloid Interface Sci. 448, 24-31

Hanson, E. et al., (2003). J. Am. Chem. Soc. 125, 16074–16080,

Vega, A. et al. (2012). Langmuir 28, 8046-8051

## Crystal-chemical controls on smectite hydration

Baptiste Dazas<sup>1</sup>, Bruno Lanson<sup>1</sup>, Eric Ferrage<sup>2</sup> and Alfred Delville<sup>3</sup>

<sup>1</sup>ISTerre, CNRS – Univ. Grenoble Alpes, 38000 Grenoble, France – [bruno.lanson@ujf-grenoble.fr](mailto:bruno.lanson@ujf-grenoble.fr);

<sup>2</sup>IC2MP, CNRS – Univ. Poitiers, 86000 Poitiers, France;

<sup>3</sup>CRMD, CNRS – Univ. Orléans, 45000 Orléans, France;

Swelling clay minerals such as smectites are ubiquitous at the Earth surface and possess major hydration ability and contaminant uptake/retention capacity. As a consequence smectites exert a pivotal influence on elemental transfers in surficial environments. These properties are especially relevant also when smectites are used as sealant in engineered or geological barriers for waste disposal facilities. As interlayer H<sub>2</sub>O molecules account for more than 80% of smectite water in undersaturated conditions, characterization of H<sub>2</sub>O organization and dynamics in smectites interlayers is essential to determining the geometrical and dynamical properties of clay barriers for waste disposal and to predicting the mobility of contaminant whose principal vector is water.

Within this general framework, the main goal of the present talk is to review the influence of structural parameters such as the amount and location of layer charge deficit and the chemical composition (and more especially the presence of structural fluorine/hydroxyl) on smectite hydration properties. A set of samples covering the whole compositional range of swelling phyllosilicates has thus been synthesized and characterized chemically and structurally. Special attention was paid to determining the amount (water vapor sorption isotherms) and the distribution (X-ray diffraction) of interlayer water.

## Mixed-layered structure formation and analysis during illite dehydroxylation

Douglas K. McCarty<sup>1\*</sup>, Victor A. Drits<sup>2</sup>, and Arkadiusz Derkowski<sup>3</sup>

<sup>1</sup>Chevron ETC, 3901 Briarpark, Houston, Texas 77042, U.S.A. dmccarty@chevron.com

<sup>1</sup>Geological Institute of the Russian Academy of Science, Pyzhevsky per. 7, 119017 Moscow, Russia.

<sup>3</sup>Institute of Geological Sciences, Polish Academy of Sciences, Research Centre in Kraków, Senacka 1, PL-31002 Kraków, Poland

The < 1 $\mu$ m fraction of a trans-vacant 1M illite (RM30) was studied by conventional and synchrotron X-ray diffraction (XRD) techniques, and thermogravimetric methods to investigate structural transformation of illite at different temperatures and degrees of dehydroxylation ( $D_T$ ). Non-dehydroxylated structures in oriented specimens are represented by preheating at 300 °C ( $D_T = 0$ ) and the completely dehydroxylated 1M illite structures at 680°C ( $D_T = 100\%$ ). Deviation of the basal reflection positions from rationality, expressed by the coefficient of variation of  $d(00l)$  values, which express deviation from rationality, progressively increase from 0.05 at  $D_T = 4\%$ , to 0.14 at  $D_T = 51\%$ , and then decrease to 0.06 at  $D_T = 95\%$ . A similar trend occurs with the full width at half-maximum (FWHM) with increasing preheating temperature. Both of these features are characteristic for mixed-layered structures.

The experimental profiles of 00l reflections from the oriented partially dehydroxylated specimens perfectly matched calculated XRD patterns of mixed-layered structures where non-dehydroxylated (ND) and completely dehydroxylated (CD) illite layers are interstratified with a tendency toward segregation. The CD layer content in the modeled mixed-layered structures of the preheated specimens have a significant linear correlation with corresponding  $D_T$  values ( $R^2=0.99$ ).

Random powder XRD patterns collected with synchrotron radiation show a distinctive trend in the unit cell parameters in the preheated specimens. However, the accuracy of the lattice parameters at first decreases up to  $D_T = 61\%$  and then increases with a further increase in  $D_T$ . This unexpected evolution of the unit cell parameters during progressive dehydroxylation is explained by the interstratification of ND and CD layers in illite.

The formation of the mixed-layered structures during Al-rich 1M illite dehydroxylation agrees with a kinetic model prediction where dehydroxylation of each portion of the initial OH groups corresponds to a zero-order reaction that is independent of the structural and chemical composition. The reaction is homogeneous and during partial dehydroxylation of the illite structure, ND layers transform into the CD layers without formation of an intermediate phase. A layer-by-layer dehydroxylation mechanism is suggested for thermally induced illite structural transformation.

## From crystalline hydrates to osmotic swelling and lyotropic liquid-crystalline phases

Sabine Rosenfeldt,<sup>1</sup> Matthias Stöter<sup>2</sup>, Thomas Weiß<sup>1</sup>, Stephan Förster<sup>1</sup> and Josef Breu<sup>2,\*</sup>  
<sup>1</sup> Physical Chemistry I and <sup>2</sup> Inorganic Chemistry I, University of Bayreuth, Universitätsstrasse 30,  
95440 Bayreuth, Germany, Josef.breu@uni-bayreuth.de

The tendency of interlayer cations to solvate cause clay minerals to expand the interlayer space and to accommodate water molecules. Two swelling regimes can be identified. At low water concentration, a series of discrete hydration steps is realized. This swelling regime is referred to as crystalline swelling. Under certain circumstances, crystalline swelling may be followed by osmotic swelling, in which continuum electrostatic forces govern the interactions between adjacent layers. Osmotic swelling was first observed for graphite oxide in 1932<sup>i</sup> and was shortly thereafter confirmed for **montmorillonite**. Osmotic swelling represents the most gentle, cheap, and scalable route to obtain perfectly delaminated clay platelets of uniform thickness of 1 nm. Such perfectly delaminated clays have great potential in gas barrier coatings<sup>ii</sup>.

The swelling phenomenon of natural clay minerals is always masked by charge density heterogeneities inherent in the material that modulate intracrystalline reactivity. Synthetic **hectorites** synthesized from the melt at temperatures well above 1,000 K now allow for a more detailed look at osmotic swelling. When various amounts of water are added to synthetic  $[\text{Na}_{0.5}]^{\text{inter}}[\text{Mg}_{2.5}\text{Li}_{0.5}]^{\text{oct}}[\text{Si}_4]_{\text{tet}}\text{O}_{10}\text{F}_2$  it swells osmotically, and gel formation is observed<sup>iv</sup>. Below the Debye length, the separation is driven by the electrostatic repulsion and initially a single phase of a highly ordered lamellar liquid crystalline phase (Wigner crystal) with basal distances from 1 – 20 nm depending only on water/clay ratio is formed. For instance, for 17-wt% hectorite a perfectly rational 00 $l$  series with a  $d$  spacing of 147 Å, as indicated by SAXS, is observed. The liquid crystalline phase then melts at a volume fraction of 0.02 %, where the interlamellar distance is equal to the Debye-length. In the melt the layers fill space homogeneously but have gained mutual torsional and translational freedom. At this point, the suspension may be regarded as delaminated although adjacent platelets still cannot freely rotate due to the huge lateral extension ( $\approx 25 \mu\text{m}$ ) and can still easily be oriented by shear.

<sup>i</sup> Hofmann U. (1932) *Kolloid Z.* 61:297–304; Hofmann U, Kurd E, Diederich W. (1933) *Z. Kristallogr.* 86:340–48.

<sup>ii</sup> Möller MW, Kunz DA, Lunkenbein T, Sommer S, Nennemann A, Breu J. (2012) *Adv. Mater.* 24:2142-47; Kunz DA, Schmid J, Feicht P, Erath J, Fery A, Breu J. (2013) *ACS Nano* 7:4275-80.

<sup>iii</sup> Stöter M, Kunz DA, Schmidt M, Hirsemann D, Kalo H, et al. (2013) *Langmuir* 29:1280-85.

<sup>iv</sup> Stöter M, Rosenfeldt S, Breu J. (2015) *Annu. Rev. Mater. Res.* 45: DOI 10.1146/annurev-matsci-070214-020830.

## Microscopic structure and permittivity of interlayer water in Na-saturated montmorillonite

Katja Emmerich<sup>1</sup>, Heike Kaden<sup>1,2</sup>, Franz Königer<sup>1,2</sup> and Peter Thissen<sup>2</sup>

<sup>1</sup>Competence Center for Material Moisture (CMM), Karlsruhe Institute of Technology (KIT), Hermann-von-Helmholtz-Platz 1, 76344 Eggenstein-Leopoldshafen, Germany

katja.emmerich@kit.edu.

<sup>2</sup>Institute of Functional Interfaces (IFG) Karlsruhe Institute of Technology (KIT), Hermann-von-Helmholtz-Platz 1, 76344 Eggenstein-Leopoldshafen, Germany

A large surface area and a high water binding capacity characterize clay minerals. Water uptake of clay minerals is even amplified for swellable clay minerals by hydration of interlayer cations. A high clay content in soft rocks and soils together with the presence of smectites plays an important role for the moisture balance of soils e.g. for agriculture and in the Earth's climate. Water uptake, swelling and low permeability of smectites is also utilized in hydraulic barriers built of bentonites that separate underground mines or that will be part of the geotechnical barriers in radioactive waste deposits.

Hence, monitoring and precise determination of in-situ water content is required, but the water binding mechanisms are complex in clay minerals and calibration of dielectric spectroscopy data still lacks reliable permittivity of bound water related to the clay minerals structure.

The Na-saturated montmorillonite / water interface was investigated in the present work within the density functional theory (DFT). A large structural variety and a broad range of layer charge between 0.4 and 1.2 eq/unit cell characterize dioctahedral smectites of the montmorillonite beidellite series. Therefore, the adsorption process in the presence of water is described by first principles calculations for two different surface charge densities, namely -0.086 and -0.172 C/m<sup>2</sup>.

Results were compared to experimental results from homoionic Na-saturated natural montmorillonites. A fairly good agreement was found between calculated permittivity of bound water in smectites and experimental data. The bound water permittivity for a Na-saturated montmorillonite with the structural formula [Na<sub>1.04</sub>(Si<sub>15.88</sub>Al<sub>0.12</sub>)(Al<sub>6.36</sub>Fe<sub>0.72</sub>Mg<sub>0.92</sub>)O<sub>40</sub>(OH)<sub>8</sub>] was determined to be  $\epsilon W1 \approx \epsilon W2 \approx \epsilon W3 = 22$  in the range of gravimetric water content between 6.4 and 28.9% related to the dry weight of the material. Data were obtained from fitting of measured bulk permittivity at 1 GHz by a semi-empirical mixing law (Emmerich et al., 2015).

Emmerich et al., 2015: JCIS <http://dx.doi.org/10.1016/j.jcis.2015.01.087>

## Systematics of Li<sup>+</sup> fixation in reduced-charge montmorillonite

Georgios D. Chryssikos<sup>1</sup>, Vassilis Gionis<sup>1</sup> and George E. Christidis<sup>2</sup>

<sup>1</sup>Theoretical and Physical Chemistry Institute, National Hellenic Research Foundation, 48 Vass. Constantinou Ave., Athens, Greece 11635 gdchryss@eie.gr

<sup>2</sup>Technical University of Crete, Department of Mineral Resources Engineering, Chania, Greece 73100

A recent study of Li-SA<sub>z</sub>-1 montmorillonite (Skoubris et al. 2013) has indicated that Li<sup>+</sup> fixation and the concomitant reduction of layer charge is operating via a single structural mechanism in the 60-300 °C range. This mechanism was manifested in the infrared spectra by the progressive appearance of well defined doublets of structural OH stretching, combination and overtone modes (best observed by the 2<sup>nd</sup> derivative), suggesting the simultaneous formation of two new OH species. It was further argued that this spectral signature of Li<sup>+</sup> fixation is specific to the thermally induced occupancy of *tv* rather than the expected *cv* sites.

This paper extends the aforementioned study of reduced-charge Li-SA<sub>z</sub>-1 by comparing the near-infrared vibrational spectra of a broader montmorillonite sample set, subjected to Li-exchange and heating at 300 °C. The selected montmorillonite samples from various localities represent a broad range of layer charge (~0.35-0.55 phuc), variable charge location and Fe-content. They also exhibit different dehydroxylation temperature profiles, suggesting a representative gamut of variable % *tv-cv* character on the basis of Drits et al. (1995) and Wolters & Emmerich (2007).

The structural variability of the montmorillonite sample set is reflected, as expected, in the positions and relative intensities of infrared bands in the spectra of the unheated Li-samples. Heating results, on the contrary, in the uniform appearance of the doublet structural OH bands (2ν: 7171.0±1.5 and 7114±3 cm<sup>-1</sup>; ν+δ: 4534±3 and 4467±3 cm<sup>-1</sup>), as in SA<sub>z</sub>-1. It is therefore concluded that the Li<sup>+</sup> fixation mechanism previously identified in SA<sub>z</sub>-1 is also operating in all montmorillonite samples investigated despite their structural differences and, especially, regardless of their % *tv-cv* character that was estimated from TGA measurements.

Research at NHRF was supported in part by project Nanomacro-Kripis 447963 (GSRT-Greece). The expert technical assistance of C. Tsiantos (NHRF) and P. Makri (TUC) is gratefully acknowledged.

Drits, V.A., Besson, G., and Muller, F. (1995). An improved model for structural transformations of heat-treated aluminous dioctahedral 2:1 layer silicates. *Clays and Clay Minerals*, 43, 718-731.

Skoubris, E.N., Chryssikos, G.D., Christidis, G.E., and Gionis, V. (2013). Structural characterization of reduced-charge montmorillonites. Evidence based on FTIR spectroscopy, thermal behavior, and layer-charge systematics. *Clays and Clay Minerals*, 61, 83-97.

Wolters, F. and Emmerich, K. (2007) Thermal reactions of smectites - Relation of dehydroxylation temperature to octahedral structure. *Thermochimica Acta*, 462, 80-88.



## Cs-sorption in weathered biotite from Fukushima granitic soils

Ryosuke Kikuchi<sup>1</sup>, Hiroki Mukai<sup>1</sup>, Chisaki Kuramata<sup>1</sup> and Toshihiro Kogure<sup>1</sup>

<sup>1</sup>Department of Earth and Planetary Science, Graduate School of Science, The University of Tokyo, 7-3-1 Hongo, Bunkyo-ku, Tokyo, 113-0033, Japan  
rkikuchi@eps.s.u-tokyo.ac.jp

The sorption of cesium (Cs) ions into weathered biotite with biotite-vermiculite interstratification collected from weathered granodiorite in Fukushima Prefecture, Japan has been investigated. Both single crystals and crushed powder forms of the weathered biotite were experimentally reacted with 20–2000 ppm CsCl aqueous solutions, and analyzed by powder X-ray diffraction (XRD), scanning electron microscopy (SEM) and scanning transmission electron microscopy (STEM) to examine the distribution of Cs inside the crystals. From the XRD pattern, the proportion of vermiculite unit layers in the weathered biotite was estimated at ca. 12%, with a tendency for segregation, and the whole XRD pattern was explained by the coexistence of biotite and vermiculite packets as well as the interstratified regions. Powder XRD of Cs-sorbed specimens showed that the 14.9 Å peak of the vermiculite packets was weakened at a low Cs concentration in the solution or with a short immersion time. Single crystals of the weathered biotite with a polished edge-surface were immersed in the CsCl solutions and examined using SEM and high-angular annular dark field (HAADF) imaging in STEM. Cs was not only incorporated in the vicinity of the exposed surface but also penetrated deeply inside the crystals. These analyses and observations revealed the Cs-sorption process in weathered biotite. At first, Cs preferentially replaced specific vermiculite interlayers in the vermiculite packets. As the reaction proceeded or with a higher Cs concentration in the solution, the Cs-substituted vermiculite interlayers increased in the vermiculite packets, and vermiculite layers interstratified in biotite also incorporated Cs.

## Use of the pair distribution function technique for the development of detailed structure/property correlations in layered double hydroxides (LDH)

C. Taviot-Guého, P. Vialat, A. Faour, V. Prévot, C. Mousty and F. Leroux

Clermont Université, Université Blaise Pascal, Institut de Chimie de Clermont-Ferrand, BP 10448, F-63000  
CLERMONT-FERRAND- CNRS,

UMR6296, ICCF, BP 80026, F-63171 Aubiere, France; \*[christine.taviot-gueho@univ-bpclermont.fr](mailto:christine.taviot-gueho@univ-bpclermont.fr)

As highly flexible compounds in terms of chemical compositions, LDH materials have been studied widely in the literature in recent years. In particular, the chemistry of the interlayer region endows these materials with many interesting properties which allow their use for numerous applications such as anionic exchange resins, sensors or biosensors, drug delivery systems and more recently as filler in polymers.

Owing to the low crystallinity of hybrid LDHs, establishing the structure-property relationship for these materials is not an easy task. Indeed, these materials contain many defects attributed to mismatches in the geometry/charge density of the host layers and guest anions, preventing an ideal packing of the slabs and also inhibiting crystal growth. Yet, the structure-property control is essential if one wants to tailor and fine-tune properties (optical, thermal, chemical) in very broad ranges and to design advanced hybrid LDH for specific applications.

Both experimental and theoretical approaches have been developed in our research group for investigating LDH structure and microstructure and their influence on properties [1, 2, 3]. Traditional crystallographic methods provide depictions of structure that are most sensitive either to short-range order (X-ray absorption) or long-range periodicity (X-ray diffraction or electron diffraction). Recently, we have investigated pair distribution function (PDF) analysis using high-energy X-ray total diffraction to probe the LDH structure. In addition to the Bragg peaks, information contained in the diffuse scattering of the X-ray diffraction patterns is particularly valuable when dealing with disordered materials such as LDH. The interest of PDF in describing the local structure of LDH will be discussed through two studies we have been conducting:

-Insights into the role of the structural (2H1 versus 3R1 polytype) and microstructural (coherent domains) parameters in determining the electrochemical properties of Ni<sub>2</sub>Al-CO<sub>3</sub> LDHs as alkaline secondary batteries materials [4].

-Investigation of the distribution of CoII and CoIII cations and its modification during electrochemical treatment in monometallic CoII/CoIII-CO<sub>3</sub> LDH as a super capacitor materials [5].

**Keywords:** pair distribution function (PDF), layered double hydroxides (LDH).

[1] C. Taviot-Guého, Y.J. Feng, A. Faour, F. Leroux *Dalton. Trans.*, **39**, 5994-6005 (2010)

[2] J. Pisson, N. Morel-Desrosiers, J.P. Morel, A. de Roy, F. Leroux, C. Taviot-Guého, P. Malfreyt *Chem. Mater.*, **23**,1482–1490 (2011)

[3] L. Aimoz, C. Taviot-Guého, S. V. Churakov, M. Chukalina, R. Dähn, E. Curti, P. Bordet, M. Vespa *J. Phys. Chem. C*, **116**, 5460–5475 (2012).

[4] A. Faour, C. Mousty, V. Prevot, B. Devouard, A. De Roy, P. Bordet, E. Elkaim, and C. Taviot-Gueho *J. Phys. Chem. C*, **116**, 15646–15659 (2012)

[5] P. Vialat, C. Mousty, C. Taviot-Gueho, G. Renaudin, H. Martinez, J.-C. Dupin, E. Elkaim, F. Leroux *Adv. Funct. Mater.* *accepted*

## Local environment in layered double hydroxides probed by solid state NMR spectroscopy

Ulla Gro Nielsen<sup>1</sup>, Line B. Petersen<sup>1</sup>, Suraj Charan<sup>1</sup>, Nicholai D. Jensen<sup>1</sup>, Claude Forano<sup>2</sup>, Vanessa Prevot<sup>2</sup>, and Andrew S. Lipton<sup>3</sup>

<sup>1</sup> Department of Physics, Chemistry, and Pharmacy, University of Southern Denmark, 5230 Odense M, Denmark; [ugn@sdu.dk](mailto:ugn@sdu.dk)

<sup>2</sup> Université Clermont Auvergne, Université Blaise Pascal, Institut de Chimie de Clermont-Ferrand, CNRS, UMR 6296, BP 80026, F-63171 Aubièrre, France

<sup>3</sup> Environmental Molecular Sciences Laboratory, Pacific Northwest National Laboratory, 902 Battelle Boulevard, Richland, WA 99354, USA

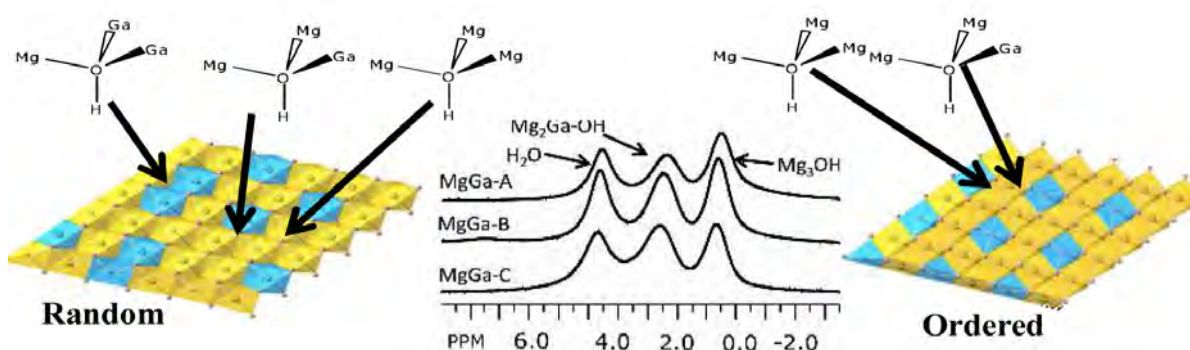


Figure 1. Random and ordered LDHs can be distinguished by  $^1\text{H}$  MAS NMR [1] as illustrated for a MgGa LDH with a 3:1 Mg:Ga ratio. Ordered LDHs will only have two different local  $\text{M}_3\text{-OH}$  groups due to M(III) avoidance whereas four different  $\text{-OH}$  groups are expected for a random M(III) distribution.  $^1\text{H}$  SSNMR shows that MgGa LDHs are ordered [2].

Layered double hydroxides, LDHs,  $(\text{M}(\text{II})_{1-x}\text{M}(\text{III})_x\text{AnH}_2\text{O})$  have a wide range of applications including environmental remediation, catalysis, electrochemistry, and drug delivery. The design of efficient materials require a detailed understanding of the molecular level structure of the LDHs. However, low crystallinity, stacking disorder, and impurities render characterization challenging.

Recently, it has been demonstrated that Solid-State NMR spectroscopy (SSNMR) provides detailed information about ordering in the cation layer, which allows for the determination of the M(II):M(III) ratio and the presence of structural defects [1–4]. Generally, cation ordering is observed, although there have been indications of both Al-rich and Mg defects in some MgAl LDHs [3, 4].

We have investigated several different types of LDH's including MgAl, ZnAl, and MgGa LDH's to determine how the synthesis method and the choice of anion affects the local structure and purity of the LDH product. Detailed information about the cation layer including structural defects is obtained from  $^1\text{H}$ ,  $^{27}\text{Al}$ ,  $^{25}\text{Mg}$ ,  $^{67}\text{Zn}$ , and  $^{71}\text{Ga}$  SSNMR single and double resonance experiments, which are further supported by powder X-ray diffraction, SEM, micro-Raman spectroscopy, TEM and elemental analysis providing a detailed picture of the local environment including defects in the cation layer. These studies show that several techniques must be combined in order to obtain reliable structural information.

[1] P.J. Sideris, U.G. Nielsen, Z.H. Gan, C.P. Grey, *Science* 321 (2008) 113-117.

[2] L.B. Petersen, A.S. Lipton, V. Zorin, U.G. Nielsen, *J. Solid State Chem.* 219 (2014) 242-246.

[3] S. Cadars, G. Layrac, C. Gérardin, M. Deschamps, J.R. Yates, D. Tichit, D. Massiot, *Chem. Mater* 23 (2011) 2821-2831.

[4] P.J. Sideris, F. Blanc, Z. Gan, C.P. Grey, *Chem. Mater.* 24 (2012) 2449-2461.

## NMR study of structure and dynamics in Mg/Al layered double hydroxides

Arnaud Di Bitetto<sup>1,2</sup>\*, Gwendal Kervern<sup>2</sup> and Cédric Carteret<sup>1</sup>

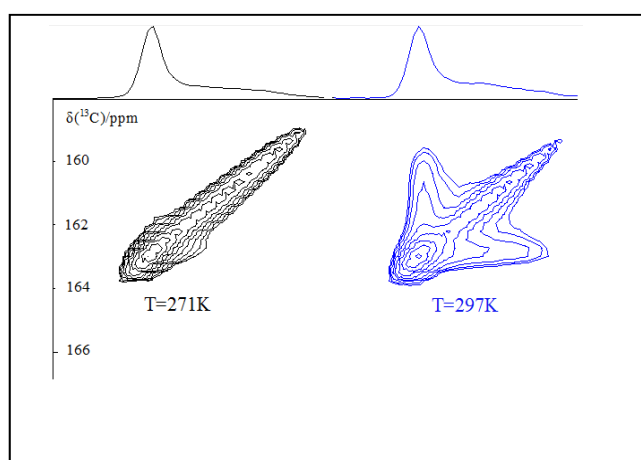
<sup>1</sup> Lorraine University-CNRS, LCPME UMR 7564, 405 rue de Vandoeuvre 54602 Villers-lès-Nancy, France.

<sup>2</sup> Lorraine University-CNRS, CRM2 UMR 7036, Faculté des Sciences et Technologies, Boulevard des Aiguillettes, BP 239, 54506 Vandoeuvre-lès-Nancy Cedex, France; \*arnaud.di-bitetto@univ-lorraine.fr

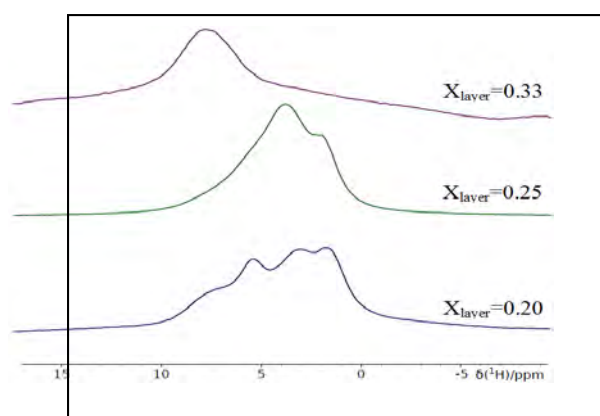
The term layered double hydroxide (LDH) is used to designate synthetic or natural lamellar hydroxides with brucitic sheets holding two types of metallic cations and a hydrated interlayer domain containing anionic species. These materials are characterised by the charge of the layer  $x_{layer}$ , which represents the  $M^{III}/(M^{III}+M^{II})$  molar fraction, and by the nature of intercalated anions which can vary greatly from small inorganic anions ( $Cl^-$ ,  $CO_3^{2-}$ ,  $NO_3^-$ ...) to organic species of various size (from carboxylic acids to DNA). While their anion exchange capacity is employed for various applications, the role of the natural LDH in the sequestration of  $CO_2$  is subject to environmental interests.

A recent work realized by Ishihara et al. [1] highlighted a dynamic exchange between intercalated carbonate and atmospheric carbon dioxide. Likewise, many recent solid-state NMR studies have presented various results on structural and dynamic aspects in the chemistry of such materials. Some of the most recent investigations based on modern innovations revealed deep insights in the structure of the cationic part of Mg/Al-based LDH materials, as well as the layer/interlayer interface [2-4].

In our study, we synthesized different Mg/Al LDH by varying the charge of the layers ( $x_{layer} = 0.2, 0.25$  and  $0.33$ ) and the intercalated anions ( $CO_3^{2-}$ ,  $NO_3^-$ ,  $Cl^-$ ...), and we focused on the structural and dynamic features of these materials with various characterization techniques, including Infrared and Raman Spectroscopy, XRD, and solid-state NMR. In particular, we studied the influence of the layers' charge and of the intercalated anions on the cationic order of the sheets. We finally focused on carbonate-containing LDH: we showed the coexistence of bicarbonate and carbonate, and highlighted the dynamical exchange between these anions with  $^{13}C$ - $^{13}C$  EXSY, and its dependence on the layers' charge, the temperature and the hydration state (i.e. relative humidity RH).



a)  $^{13}C$ - $^{13}C$  EXSY (no recoupling in the mixing time) spectra at various temperatures of Mg/Al- $CO_3^{2-}$  LDH,  $x_{layer}=0.25$ , 0%RH



b)  $^1H$  MAS (30kHz) spectra of Mg/Al- $NO_3^-$  LDH with various layer charges ( $x_{layer}$ )

[1] S. Ishihara et al., J. Am. Chem. Soc., 135 (2013), 18040-18043.

[2] P. J. Sideris, U. G. Nielsen, Z. Gan, and C. P. Grey. Science, 321 (2008), 113-117.

[3] S. Cadars et al., Chem. Mater., 23 (2011), 2821-2831.

[4] P. J. Sideris, F. Blanc, Z. Gan, and C. P. Grey. Chem. Mater., 24 (2012), 2449-2461.

## The structure and stability of layered double hydroxides with various Ca(II) : Fe(III) ratio : a dissolution-precipitation mechanism to explain very high phosphate removal efficiency

M. Al-Jaberi\*,<sup>1</sup>, S. Naille<sup>1</sup>, G. Medjahdi<sup>2</sup> and C. Ruby<sup>1</sup>

<sup>1</sup> Université de Lorraine-CNRS, Laboratoire de Chimie Physique et Microbiologie pour l'Environnement  
UMR7564, 405, rue de Vandoeuvre 54600 Villers-lès-Nancy, France

<sup>2</sup> Université de Lorraine-CNRS, Institut Jean Lamour, Centre de Compétences X-Gamma, Parc de Saurupt, France  
CS 50840 54011 Nancy cedex, France; \* muayad.al-jaberi@univ-lorraine.fr

The chloride and nitrate form of CaFe-layered double hydroxides (CaFe-LDH) were prepared *via* three ways of coprecipitation method. The effects of the Ca(II) : Fe(III) molar ratio varying from 2 : 1 to 4 : 1 on the structure of the selected LDHs have been studied. For characterization, powder x-ray diffraction (XRD), BET surface area determination and Raman spectroscopy were applied. The XRD patterns and Raman analysis of the samples at all Ca(II) : Fe(III) ratios exhibited reflections corresponding to CaFe-LDH. Above the Ca(II) : Fe(III) ratio of 2 : 1, the reflections of Ca(OH)<sub>2</sub> compound also appeared. This phase was found to stabilize the LDH as already observed by Sipiczki et al. [1]. The resulting LDHs were studied for their performance in removing phosphate from aqueous test solution. For the same LDH's dose, more phosphate was removed by CaFe-LDH intercalating chloride anions than CaFe-LDH intercalating nitrate anions. Removal experiments were carried out as a function of contact time, initial phosphate concentration, and initial pH of phosphate solution. The experimental data showed a good compliance with the pseudo-second-order kinetic model. The Freundlich model described the removal isotherm data well. The analytical and spectroscopic analyses indicated that the dissolution-precipitation mechanism was mainly responsible for phosphate removal by CaFe-LDH. The CaFe-LDH with Ca (II) : Fe(III) ratio of 3 : 1 showed higher removal capacity compared to other Ca(II) : Fe(III) ratios. The removal rates of phosphate onto CaFe-LDH-Cl and CaFe-LDH-NO<sub>3</sub> at this ratio were 570 mg PO<sub>4</sub> g<sup>-1</sup> and 480 mg PO<sub>4</sub> g<sup>-1</sup> respectively, suggesting that CaFe-LDHs were excellent minerals for phosphate removal from aqueous solution. Indeed, this value is between 6 times and 10 times higher than the adsorption capacity of ferrihydrite and mössbauerite, both compounds being the best phosphate adsorbents among the iron oxyhydroxides family [2].

[1] M. Sipiczki, E. Kuzmann, Z. Homonnay, J. Megyeri, I. Palinko, P. Sipos, The structure and stability of CaFe layered double hydroxides with various Ca:Fe ratios by Mossbauer spectroscopy, X-ray diffractometry and microscopic analysis, J. Mol. St., 1044 (2013) 116-120

[2] K. Barthélémy, S. Naille, C. Despas, C. Ruby, M. Mallet, Carbonated ferric green rust as a new material for efficient phosphate removal F.M. Lastname, J. Colloid and Interf. Sci., 384 (2012) 121-127.

## Structure and reactivity of intercalated amino-acids into layered double hydroxides

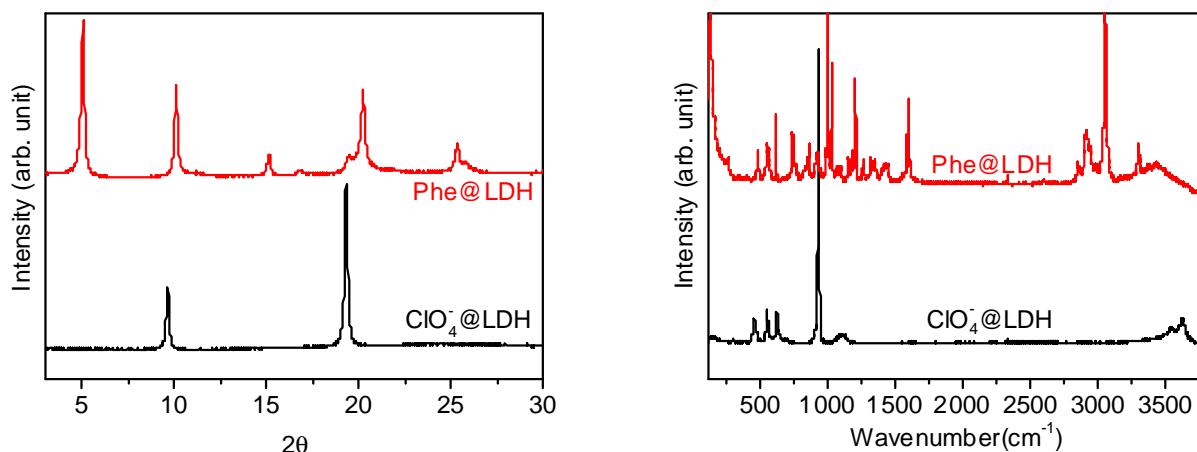
Jean Fabel<sup>1</sup>, Erwan André and Cédric Carteret

<sup>1</sup> Lorraine University-CNRS, UMR 7564 LCPME, 405 rue de Vandoeuvre  
54602 Villers-lès-Nancy, France; jean.fabel@univ-lorraine.fr,

As a layered material, LDH possess the capacity to trap reversely a wide array of negatively charged species regardless of their size or chemical nature. In particular, over the last few years, there has been a growing interest for Hybrid organic-inorganic LDH [1].

This work is focused on a new family of Inorganic-Organic hybrid materials where amino acids have been intercalated into LDH. Our goal is to explore the peculiar reactivity induced by the confinement of the interlayer domain (ordered water, high concentrations, reaction selectivity). To do so, the structure and the reactivity of the hybrids have been studied through a complementary approach combining experimental technics such as Infra-red and Raman spectroscopies, solid state NMR or XRD, to theoretical data obtained with DFT simulations in a periodic approach.

We will present the synthesis of nanohybrids obtained from the 21 standard amino acids. Different groups can be identified from the competition with the carbonate anion which highlights the characteristics ruling the intercalation process. To illustrate the molecule-host interactions, the question of the amino acid's orientation within the interlayer domain will be discussed and put in relation with the layer charge and the hydration state of the material. We will show an example of the confinement effects by monitoring the thermal decomposition of these materials under different conditions (in-situ thermo-Infra-red and thermos-Raman spectroscopies). Finally, we will show their potentialities as materials for the carbon (CO<sub>2</sub>) capture and storage.



XRD patterns: (a) and Raman spectra (b) of R2MgAl LDH showing exchange between ClO<sub>4</sub><sup>-</sup> and phenylalanine.

[1] M. Wei, Q. Yuan, D.G. Evans, Z. Wang, X. Duan, J. Mater. Chem. 15 (2005) 1197–1203.

## Structure of the new “green rust” related minerals: fougèrite, trébeurdenite and mössbauerite; some occurrences

J.-M. R. Génin<sup>1</sup>, A. G. Christy<sup>2</sup>, O. Guérin<sup>3</sup>, A. Herbillon<sup>4</sup>, E. Kuzmann<sup>5</sup>, C. Ruby<sup>1</sup>, H. Shcherbakova<sup>6</sup>, C. Upadhyay<sup>7</sup> and S. J. Mills<sup>8</sup>

<sup>1</sup> Inst Jean Barriol, CNRS-Université de Lorraine, ESSTIN, 2 rue Jean Lamour, F-54500 Vandoeuvre-lès-Nancy, France

<sup>2</sup> Centre Advanced Microscopy, Sullivans Creek Road, Australian National University, Canberra 0200, ACT, Australia

<sup>3</sup> Lab. géomorphologie, Ecole Pratique des Hautes Etudes, 15 bd de la mer, F-35800 Dinard, France

<sup>4</sup> Unité des Sciences du Sol, Université Catholique de Louvain, B-1348 Louvain-la-Neuve, Belgium

<sup>5</sup> Department of Chemistry, Eötvös Lorand University, Pazmany Peter setany, H1117, Budapest, Hungary

<sup>6</sup> Institute of Mineralogy, Urals division, Russian Academy of Sciences, Miass, 453618, Russia

<sup>7</sup> School of Materials Science & Technology, IT-Banaras Hindu University, 221005 Varanasi, India

<sup>8</sup> Geosciences, Museum Victoria, GPO Box 666, Melbourne 3001, Australia

“Green rusts” Fe<sup>II</sup>–III compounds were initially studied to explain the corrosion of steels within E<sub>h</sub>-pH diagrams. They present outstanding redox properties since, as a member of layered double hydroxides family (LDH), divalent and trivalent cations belong to the same iron element. Therefore, they consist of the stacking of [Fe<sub>(1-x)</sub>Fe<sup>III</sup><sub>x</sub>(OH)<sub>2</sub>]<sup>x+</sup> layers and [(x/n)A<sup>n-</sup>.m(H<sub>2</sub>O)]<sup>x-</sup> interlayers as characterized by X-ray diffraction (XRD) whereas Mössbauer spectroscopy determines the ferric ionic ratio  $x = \{[Fe^{III}]/Fe_{total}\}$ , which lies within the [1/4, 1/3] range. Quadrupole doublets, D1 and D2, which have large splitting, are attributed to Fe<sup>II</sup> ions among which those of D<sub>2</sub> lie in register to an anion; doublet D3, which has small splitting is attributed to Fe<sup>III</sup> ions. Each Fe<sup>III</sup> is surrounded by six Fe<sup>II</sup> ions giving rise to a 2D cation order for x values of 1/4, 2/7 and 1/3 that depends on the charge, size and shape of the anions in interlayers as demonstrated for chloride, carbonate, oxalate and methanoate [1].

Mössbauer spectroscopy showed that the mineral responsible for the bluish color of gleys in samples from Fougères (Brittany) is similar to “green rusts” where CO<sub>3</sub><sup>2-</sup> ions are intercalated [2]; it was then named “fougèrite” displaying an x ratio in the range [1/3, 2/3], whereas the synthetic sample had a ratio strictly equal to 1/3. Any “green rust” displays two modes of oxidation: (i) it dissolves classically precipitating an orange-brownish ferric oxyhydroxide; (ii) it is oxidized *in situ* by deprotonation in conditions such as fast oxidation... that keeps its global structure unchanged [3]. Moreover, a product where  $x > 1/3$  is obtained by bacterial reduction of ferric oxyhydroxide in anoxic conditions. Later, gleys extracted from maritime marshes in Trébeurden (Brittany) and Mont-Saint Michel bay showed x ratio in the [2/3, 1] range [4] as well as gleys from Takul lake (Urals).

The formula Fe<sup>II</sup><sub>6(1-x)</sub>Fe<sup>III</sup><sub>6x</sub>O<sub>12</sub>H<sub>2(7-3x)</sub>CO<sub>3</sub>·3H<sub>2</sub>O does not lead to a solid solution but a mixture of distinct minerals with different cation order and topotactical relationship; thus IMA accepted them as fougèrite, trébeurdenite and mössbauerite for x values of 1/3, 2/3 and 1, respectively. The minerals of the “fougèrite group” have a global unchanged structure with differences due to the deprotonation of OH<sup>-</sup> ions at the apices of octahedrons occupied by cations and Fe<sup>II</sup> become Fe<sup>III</sup>. The centred rectangular mesh that comprises four CO<sub>3</sub><sup>2-</sup> ions in configurations  $\Delta$  and  $\nabla$  presents a 2D long range-order with identical primitive rhombic mesh  $\sqrt{12} \times \sqrt{12}$ ; synchrotron XRD patterns display different stacking sequences in mössbauerite and fougèrite where polytypes are compatible with short range coupling [4,5].

[1] Génin J.-M. R. and Ruby C. (2008) Composition and anion ordering in some Fe<sup>II</sup>-III hydroxysalt green rusts (carbonate, oxalate, methanoate); the fougèrite mineral. *Solid State Science*, **10**, 244-259.

[2] Génin J.-M. R., Bourrié G., Trolard F., Abdelmoula M., Jaffrezic A., Refait, Ph., Maître V., Humberts B., Herbillon A.J. (1998) Thermodynamic equilibrium in aqueous suspensions of synthetic and natural Fe<sup>II</sup>-Fe<sup>III</sup> green rusts : occurrences of the mineral in hydromorphic soils. *Environ. Sci. Technol.*, **32**, 1058-1068.

[3] Génin J.-M. R., Aïssa R., Géhin A., Abdelmoula M., Benali O., Ernstsén V., Ona-Nguema G., Upadhyay C. and Ruby, C. (2005) Fougèrite and Fe<sup>II</sup>-III hydroxycarbonate green rust: ordering, deprotonation and/or cation substitution; structure of hydrotalcite-like compounds and myctosic ferrous hydroxide Fe(OH)<sub>(2+x)</sub>. *Solid State Sciences*, **7**, 545-572.

[3] Génin J.-M. R., Ruby C. and Upadhyay C. (2006) Structure and thermodynamics of ferrous, stoichiometric and ferric oxyhydroxycarbonate green rusts; redox flexibility and fougèrite mineral. *Solid State Science*, **8**, 1330-1343.

[4] Génin, J.-M. R., Mills, S. J., Christy, A. G., Guérin, O., Herbillon, A. J., Kuzman, E., Morin, G., Ona-Nguema, G., Ruby, C. Upadhyay, C. (2014) Mössbauerite, Fe<sub>3+6</sub>O<sub>4</sub>(OH)<sub>8</sub>CO<sub>3</sub> · 3H<sub>2</sub>O, the first fully oxidised “green rust” mineral from Mont Saint-Michel Bay, France. *Mineralogical Magazine*, **78(2)**, 447–465.

[5] Mills, S. J., Christy, A. G., Génin, J.-M. R., Kameda, T. Colombo, F. (2012) Nomenclature of the hydrotalcite supergroup: natural layered double hydroxides. *Mineralogical Magazine*, **76(5)**, 1289–1336.

## Hydrotalcites, water purification and carbon sequestration

S. J. Mills<sup>1</sup>, A. G. Christy<sup>2</sup> and J.-M. R. Génin<sup>3</sup>,

<sup>1</sup>Geosciences, Museum Victoria, GPO Box 666, Melbourne 3001, Australia

<sup>2</sup>Centre for Advanced Microscopy, Sullivans Creek Road, Australian National University, Canberra 0200, ACT, Australia

<sup>3</sup>Institut Jean Barriol FR2843 CNRS-Université de Lorraine, ESSTIN, 2 rue Jean Lamour, F-54500 Vandoeuvre-Lès-Nancy, France

The layered double hydroxides (LDHs) are a large class of natural and synthetic compounds whose layered structure is derived from that of brucite,  $\text{Mg}(\text{OH})_2$ . In LDHs, two cations of different charge substitute on the sites corresponding to Mg in brucite, to give an overall positive charge to the hydroxide layer, which is balanced by monatomic or small complex anions intercalated between the layers. To date, 44 minerals have been described as being natural examples of LDH phases or, as they are commonly known to mineralogists, the “hydrotalcite supergroup” of minerals. These species exhibit polytypic stacking variation. A number of mineral examples exist where distinct names have been used historically for different polytypes of the same compound, although the nomenclature has recently been rationalised (Mills *et al.*, 2012).

In addition to streamlining the nomenclature for the hydrotalcite supergroup, we have over the past few years devised a classification scheme, and have discovered a number of new polytypes (Mills *et al.*, 2012a,b; Génin *et al.*, 2014). We have also been looking at ways the LDH structure type can incorporate interlayer ions from the environment, and show that different minerals in the group can contribute to sequestering carbon from mine tailings and the environment, while other members (‘green rusts’) can catalyse nitrate reduction, thus preventing agricultural runoff from triggering algal blooms. Future research will be concerned with locking up toxic elements within the interlayer of the LDH structure type, using organic molecules such as cyclotricatechylene as custom sequestrants for specific applications.

Mills, S. J., Christy, A. G., Génin, J.-M. R., Kameda, T. & Colombo, F. (2012) Nomenclature of the hydrotalcite supergroup: natural layered double hydroxides. *Mineralogical Magazine*, **76(5)**, 1289–1336.

Mills, S. J., Christy, A. G., Kampf, A. R., Housley, R. M., Favreau, G., Boulliard, J.-C. & Bourgoïn, V. (2012) Zincalstibite-9R: the first 9-layer polytype with the layered double hydroxide structure-type. *Mineralogical Magazine*, **76(5)**, 1337–1345.

Génin, J.-M. R., Mills, S. J., Christy, A. G., Guérin, O., Herbillon, A. J., Kuzman, E., Morin, G., Ona-Nguema, G., Ruby, C. & Upadhyay, C. (2014) Mössbauerite,  $\text{Fe}^{3+}_6\text{O}_4(\text{OH})_8\text{CO}_3 \cdot 3\text{H}_2\text{O}$ , the first fully oxidised “green rust” mineral from Mont Saint-Michel Bay, France. *Mineralogical Magazine*, **78(2)**, 447–465.



Friday  
10<sup>th</sup> July

Lecture room 5

General (4)

## The roles of chance and necessity in the diversification of minerals: is Earth's continental crust unique?

Edward S. Grew<sup>1</sup> and Robert M. Hazen<sup>2</sup>

<sup>1</sup>School of Earth and Climate Sciences, University of Maine, Orono, Maine 04469, U.S.A. esgrew@maine.edu

<sup>2</sup>Geophysical Laboratory, Carnegie Institution of Washington, Washington, DC 20015, U.S.A.

Mineral ecology addresses a new set of questions related to the relative roles of chance and necessity in the diversification of minerals—questions that were first raised by Grew and Hazen (2014) in considering the evolution of beryllium minerals. Hazen et al. (2015) examined these questions in greater detail and applied statistical methods to calculate the reproducibility of Earth's crustal mineralogy. They identified several factors involving both chance and necessity in the diversification of minerals in the Earth's upper continental crust, including crystal chemical characteristics and the probability of occurrence for rare minerals. Stellar and planetary stoichiometries must also be considered in order to extend this treatment to other terrestrial planets and moons as stars can differ significantly from one another in relative element abundances.

In order to evaluate the role of crystal chemistry, Hazen et al. (2015) plotted the number of mineral species in which an element is essential ( $N_E$ ) versus the abundance of that element in Earth's upper continental crust ( $C_E$ ), which gave the following relationship:

$$\text{Log}(N_E) = 0.22\text{Log}(C_E) + 1.70 \quad (R^2 = 0.34) \quad (4861 \text{ minerals, } 72 \text{ elements}).$$

Elements that plot significantly below this trend (e.g., Ga, Hf, and Rb) have chemical properties similar to those of more abundant elements (Al, Zr, K, respectively) and thus are less likely to form their own species. In contrast, elements that plot significantly above the trend (e.g., Ag, As, Cu, Pb, S, and U) are characterized by multiple coordination and oxidation states, concentration in ore-forming fluids, and/or frequent occurrence with a large number of other constituents, all factors that increase the diversity of minerals containing such elements. Hazen et al. (2015) reported a parallel trend for the Moon:

$$\text{Log}(N_M) = 0.19\text{Log}(C_M) + 0.23 \quad (R^2 = 0.68) \quad (63 \text{ minerals, } 24 \text{ elements})$$

That is, the increase in mineral diversity with element abundance could be a deterministic aspect of planetary mineral diversity, as are the crystal chemical reasons for deviation from the trend.

Though based on a very few samples, the Moon's observed mineralogical diversity could approach the minimum for a rocky planet or moon comparable in size and thus serve as a baseline for considering diversity of other terrestrial bodies. Mineral-forming processes on the Moon are limited to igneous activity, meteor impacts, and the solar wind, none of which yielded a clay mineral, whereas the great diversity of clay minerals in Earth's upper continental crust attest to the myriad of physical, chemical, and biological processes that have increased mineral diversity since Hadean times (Hazen et al. 2013).

Of 4933 mineral species approved by the IMA as of 1 June 2014, Hazen et al. (2015) found that 34% are reported from only 1 or 2 localities, and over 50% from 5 or fewer localities. Their statistical analysis of this frequency distribution suggests that thousands of other plausible rare mineral species await discovery or could have existed at some point in Earth's history, only to be subsequently lost; i.e., chance plays the leading role in which rare minerals contribute to overall diversity. Were Earth's history to be replayed, and the same number of mineral species discovered, it is probable that many of these minerals would differ from species known today; an extrasolar Earth-like planet is even more likely to have a different suite.

Grew, E.S., Hazen, R.M. (2014) Beryllium mineral evolution. *American Mineralogist*, **99**, 999-1021

Hazen, R.M., Sverjensky, D.A., Azzolini, D., Bish, D.L., Elmore, S.C., Hinnov, L., Milliken, R.E. (2013) Clay mineral evolution. *American Mineralogist*, **98**, 2007-2029

Hazen, R.M., Grew, E.S., Downs, R.T., Golden, J., Hystad, G. (2015) Mineral ecology: chance and necessity in the mineral diversity of terrestrial planets. *Canadian Mineralogist*, **53**, in press

Friday  
10<sup>th</sup> July

Lecture room 4

Clays in the Critical Zone  
soils, weathering and  
elemental cycling (2)

## Is solution chemistry responsible for clay particle mobility through soil pores in lessivage process?

Jerome Labille<sup>1</sup>, Romain Van den Bogaert<sup>1,2</sup> and Sophie Cornu<sup>2</sup>  
<sup>1</sup> Aix-Marseille Université, CNRS, IRD, CEREGE UM 34, F-13545 Aix en Provence  
<sup>2</sup> INRA, UR 1119 Géochimie des Sols et des Eaux, F-13100 Aix en Provence, France  
email: labille@cerege.fr

Clay particle mobility in soil is responsible for the preferential transfer of various contaminants and for the soil textural differentiation at the pedological time scale. The aggregation and dispersion mechanisms of clay particles are expected to play a major role in this transfer. In this work, we studied the respective impacts of pH and salt concentration on the colloidal behavior of pedogenetic smectite particles. Both static and dynamic approaches were used considering (i) a time lapse of 1 to 5 hours that corresponds to the duration of a physico-chemical perturbation caused by infiltration of gravitational water from a rain event; (ii) a pH range of 4 to 8; and (iii) CaCl<sub>2</sub> concentration range from 10<sup>-5</sup> to 10<sup>-3</sup> M, in order to be representative for the conditions encountered in the soil solution. Aggregation and dispersion kinetics were measured by time resolved laser diffraction, complemented with electrophoretic mobility analyses. The structural organization of clay particles and aggregates was studied using X-ray diffraction, cryogenic SEM and static light scattering. Finally, percolation experiments through saturated diffusion columns were attempted to estimate the role of these physico-chemical reactions on the behavior of clay particles at the scale of the porous medium.

Based on these experiments, we have drawn a phase diagram for soil clay as a function of pH and calcium concentration, and identified the mechanisms and kinetics associated with the formation of the respective states. We have showed that the behaviour of pedogenetic smectite in suspension is similar to that recorded for model clays such as pure and well crystalized montmorillonite; and that the aggregation and dispersion mechanisms related to pH and/or calcium modification are rapid enough to occur through the time scale of gravitational water, and thus within soil porosity.

**Funding program:** ANR 10 Blanc 605 – Agriped

Van den Bogaert et al., (2014) Soil Sci. Soc. Am. J. 79:43–54

## Effects of iron electron transfer on clay mineral stability and redox reactivity

Anke Neumann<sup>1</sup>, Drew E. Latta<sup>2</sup>, W.A.P.J. Premaratne<sup>3</sup>, Tyler L. Olson<sup>2</sup>, Luiza Notini de Andrade<sup>4</sup>, and Michelle M. Scherer<sup>2</sup>

<sup>1</sup> School of Civil Engineering and Geosciences, Newcastle University, Newcastle upon Tyne, UK,  
anke.neumann@ncl.ac.uk

<sup>2</sup> Department of Civil and Environmental Engineering, The University of Iowa, Iowa City, IA, USA

<sup>3</sup> Department of Chemistry, University of Kelaniya, Kelaniya, Sri Lanka

<sup>4</sup> Department of Sanitary and Environmental Engineering, Universidade Federal de Minas Gerais, Belo Horizonte, Brazil

Iron in clay minerals is a major source of redox reactivity in the critical zone. Microorganisms were found to reduce ferric iron (Fe(III)) in the structure of clay minerals to the ferrous form (Fe(II)), which in turn, can reduce organic and inorganic compounds, including nutrients and contaminants. Microbial activity in subsurface freshwater environments also leads to the ubiquitous occurrence of aqueous Fe(II), which can sorb to iron-bearing clay minerals and transfer electrons to structural Fe(III); a reaction that we have recently demonstrated using <sup>57</sup>Fe Mössbauer spectroscopy [1,2]. We also used an enriched isotope tracer approach to determine whether the interfacial electron transfer leads to Fe atom exchange between structural and dissolved Fe, as observed for Fe oxides and oxyhydroxides. We indeed observed up to 20% of Fe atom exchange for clay mineral NAu-2 at pH 7.5, and lower, yet significant Fe atom exchange at pH 6.0 for the clay minerals SWa-1 and NAu-1 [3]. We estimated that for the extent of Fe atom exchange to occur, Fe atoms in at least 2-3 unit cells inward need to take part in the reaction, indicating a surprisingly highly mobile Fe fraction in clay minerals.

To determine whether the observed mobility of Fe in clay minerals is an inherent property of Fe-bearing clay minerals or only due to the reaction with aqueous Fe(II), we additionally carried out sequential extractions on non-reduced, partly reduced, completely reduced, and reduced-reoxidized clay minerals. We found negligible amounts of extractable Fe in non-reduced and reduced-reoxidized clay minerals but up to 20% of structural Fe(III) could be extracted in partly reduced clay minerals NAu-1 and NAu-2, suggesting that interfacial electron transfer mobilized a significant portion of structural Fe in clay minerals. Interestingly, the observed extent of mobilization was similar for partial reduction with Fe(II) and with dithionite, indicating that structural Fe mobilization is a function of structural Fe reduction. To test this hypothesis further, we used dithionite to reduce all structural Fe in clay minerals NAu-1 and NAu-2 and found that 80-95% of structural Fe could be extracted and only 3-13% were recovered in the HF digestion. Mössbauer spectroscopic data on extracted samples was consistent with reversible electron transfer between aqueous Fe(II) and clay mineral Fe(III) during reduction and extraction. Furthermore, Mössbauer spectra indicated that structural Fe(III) was mobilized, which was not accessible for sequential extraction before reaction with either aqueous Fe(II) or dithionite.

To test whether the observed mobilization had an effect on the redox reactivity of Fe-bearing clay minerals, we carried out experiments with model contaminants. Preliminary data showed that nitroaromatic compounds were reduced with Fe(II)-reduced clay minerals, yet with slower reduction kinetics compared to dithionite reduced clay minerals with the same Fe(II)/Fe(III) ratio. Further experiments are underway to investigate Fe-bearing clay mineral properties to explain the observed difference in reactivity.

1 Neumann, A., Olson, T. L., Scherer, M. M., *Environ Sci Technol*, 2013. **47**(13), 6969-6977.

2 Schaefer, M.V., Gorski, C. A., Scherer, M. M., *Environ Sci Technol*, 2011. **45**(2), 540-545.

3 Neumann A., Wu, L., Li, W., Beard, B. L., Johnson, C. M., Rosso, K. M., Frierdich, A. J., Scherer, M. M., *Environ Sci Technol*, 2015. **49**(5), 2786-2795.

## Nature of sites involved in Cs<sup>+</sup> desorption from vermiculite

Liva Dzene<sup>1</sup>, Emmanuel Tertre<sup>1</sup>, Eric Ferrage<sup>1</sup> and Fabien Hubert<sup>1</sup>

<sup>1</sup> IC2MP, Université de Poitiers-CNRS, 4, rue Michel Brunet (B27) - TSA 51106 - 86073 Poitiers cedex 9, France Email:  
liva.dzene@univ-poitiers.fr

Caesium pollution in the environment can occur from the accidents in nuclear power plants as in Chernobyl (Ukraine) in 1986 or in Fukushima (Japan) in 2011. Once released in the environment, this element is known to be trapped in soils, especially by sorption onto swelling clay minerals. Then, information about adsorption and desorption processes of caesium (Cs<sup>+</sup>) on these minerals is of prime interest to constrain reactive transport models, predicting the mobility of Cs<sup>+</sup> in natural environments.

In our study, we used three distinct particle size fractions of vermiculite (10-20, 1-2 and 0.1-0.2 μm), a common swelling clay mineral in soils, to assess the effect of particle morphology on Cs<sup>+</sup> desorption processes. A previous study (Reinholdt et al., 2013) showed that these three size fractions were characterized by the same chemistry and crystal structure and differed only by the ratio of the external sorption sites (basal + edge) over the total number of sites (basal + edge + interlayer).

For the same chemical composition of the solution in equilibrium with vermiculite particles, our results show that the finest particles (0.1-0.2 μm) desorb more Cs<sup>+</sup> compared to the larger ones (10-20 μm). Regardless of the size fraction investigated and for an initial concentration of Cs<sup>+</sup> higher than 8×10<sup>-3</sup> mol/L, the amount of desorbed Cs<sup>+</sup> with ammonium (NH<sub>4</sub><sup>+</sup>) corresponds to the amount of external sites. In addition, the strong fixation of Cs<sup>+</sup> in the interlayer sorption sites is attributed to the collapse of the interlayer space during the adsorption process, as evidenced by in situ XRD analysis of the crystal structure of the clay particles in water saturated conditions.

Our findings show that thermodynamic formalisms describing reversible sorption of Cs<sup>+</sup> onto high charge swelling clay minerals, such as vermiculite, could only be applied for external sorption sites of the particles. Such results imply that characterization of both the mineralogy and the morphology of clay particles found in soils have to be performed in order to constrain reactive transport models dealing with reversible sorption of Cs<sup>+</sup> in these environments.

Reinholdt, M. X. et al. (2013). *App. Clay Sci.* **77-78**, 18–32.

## Influence of clay content as variable charge sites in the adsorption/desorption of explosives from soils

Rosalina Gonzalez<sup>1,2</sup>, Herb Allen<sup>2</sup> and Dominic Di Toro<sup>3</sup>

<sup>1</sup> La Salle University Carrera 2 # 10-70 Bogotá, Colombia. Environmental Engineering Program, University of Delaware  
rogonzalez@unisalle.edu.co

<sup>2</sup> University of Delaware Newark, Delaware 19716, USA allen@udel.edu

<sup>3</sup> University of Delaware Newark, Delaware 19716, USA ditoro@udel.edu

Multiple research studies have demonstrated that soil clay content is a key parameter in the fate of explosives in the environment. In this study we have demonstrated that the adsorption and desorption of explosive materials can be successfully predicted using the variable charge sites of clay instead of clay content. To do this, we used a modified and refined version of the Anderson and Sposito method [1], developed in 1991, to measure the contribution of permanent and variable surface-charge sites to the net surface charge density in clays, based upon the strong preference of permanent-charge sites and low affinity of most variable-charge sites for cesium. This information was used with organic carbon content to determine the fate of explosives in soils in a model. The experiment involved batch experiments containing near 1:1 soil to solution ratios reflecting field conditions and using a mix of HMX, RDX, nitroglycerine (NG), nitroguanidine (NQ), TNT and 2,4-dinitrotoluene. We used twenty-five soils composed of 5 to 40% clay and 0.04 to 18% total carbon in an experiment that involved 2 days of adsorption followed by four consecutive desorption steps. The most important observation was that for each explosive, even if they were in a mixture, we successfully predicted the fate of explosive in the environment using the charge cesium data rather than the clay size data (Figure 1.)

**Key Words:** Charge Sites, Munitions Constituents, Cesium

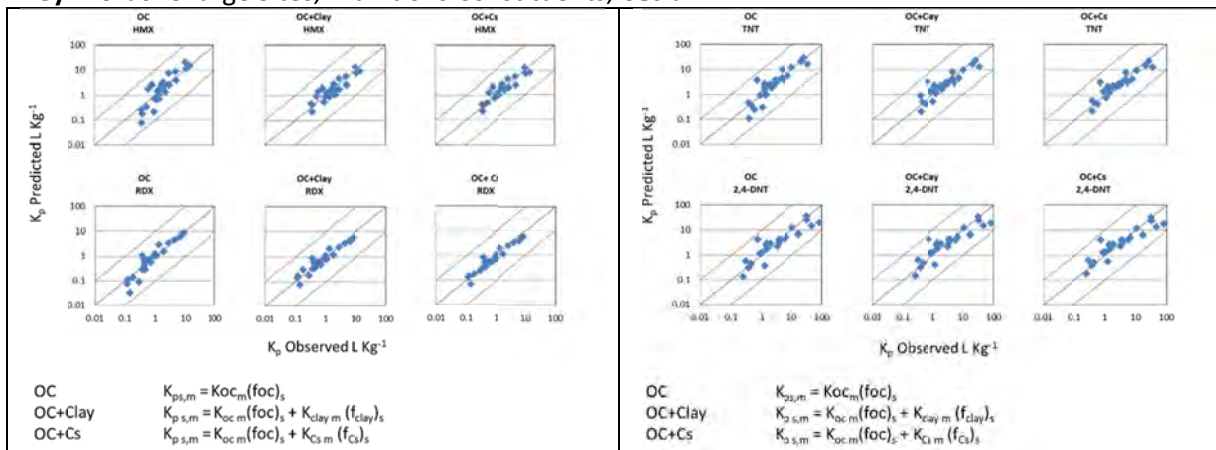


Figure 1. Relationship between  $K_p$  for HMX, RDX, TNT and 2,4DNT calculated with the equations shown in the figure. OC (organic carbon model), OC+Clay (clay size model) and OC+Cs (charge sites model and measured values of  $K_p$ ). The solid line represents the 1:1 ratio, and the dashed lines bracket at 1 log unit above and below the 1:1 line.

[1] Anderson SJ, Sposito G. 1991. Cesium-adsorption method for measuring accessible structural surface-charge. *Soil Science Society of America Journal* 55:1569-1576.

## Dissolution of beidellite in acidic solutions: New insights on smectite interface reactions and effect of crystal chemistry on dissolution rates

Valentin Robin<sup>1,2</sup>, Emmanuel Tertre<sup>1</sup>, Olivier Regnault<sup>2</sup> and Michael Descostes<sup>2</sup>

<sup>1</sup> Université de Poitiers/CNRS, UMR 7285 IC2MP, équipe HydrASA, Bat. B8 rue Albert TURPAIN, TSA 51106 - 86073 Poitiers CEDEX 9, France; valentin.robin@univ-poitiers.fr

<sup>2</sup> AREVA, Business Group Mines, Research and Development Department. Tour AREVA, 1, place Jean Millier 92084 Paris La Défense Cedex, France

Clay minerals in soils and sediments, and in particular smectites, play a significant role in the mobility of pollutants due to their sorption properties. As smectites can be dissolved in acidic conditions, the preservation or not of their sorption properties has to be assessed, in particular by the study of mechanisms occurring at the clay/water interface at low pH. If dissolution kinetics of montmorillonites (di-octahedral smectites with octahedral charge) has been widely studied, the effect of the crystal chemistry of di-octahedral smectites on their reactivity has been poorly discussed.

To understand this problem, this study aims to obtain dissolution rates for beidellite (Al-rich di-octahedral smectite with tetrahedral charge), a common swelling clay mineral in surface and subsurface natural environment. The <0.3 μm size fraction of the SBId1 beidellite ( $(\text{Si}_{7.148}\text{Al}_{0.852})(\text{Al}_{3.624}\text{Mg}_{0.18}\text{Fe}^{3+}_{0.224})\text{O}_{20}(\text{OH})_4\text{M}^{+}_{0.948}$ ) from the Clay Mineral Society was used as starting material, and experiments were performed at 25°C far from equilibrium conditions using stirred flow through reactors and HCl solutions with pH ranging from 1 to 3. Several hydrodynamic conditions were tested using different flow rates with stirred and unstirred particles. Aqueous Al/Si ratios measured at the outlet of the reactor were measured as a function of time, and compared to solid stoichiometry values in order to assess the mechanisms occurring at the solid/solution interface.  $\text{Al}^{3+}$  reversible sorption in the smectite interlayer space was evidenced for pH>1, and the presence of an amorphous Si-enriched layer can be reasonably assumed in some cases from interpretation of aqueous concentrations and the characterization of the solid phase (X-ray diffraction and FTIR spectroscopy measurements). Beidellite dissolution rates normalized to the sample mass ( $\text{mol}\cdot\text{g}^{-1}\cdot\text{s}^{-1}$ ) were obtained from Si and Al concentrations at steady state dissolution conditions. Calculated rates were compared with those previously obtained on montmorillonite and reported from several published works. It appears that the beidellite dissolution rates are on average ten times lower than montmorillonite ones, although the mean size of the beidellite particles used in this present study was lower than that of the montmorillonite particles used in literature. This observation implies that the smectite crystal chemistry (i.e., amount of  $\text{Al}^{3+}$  versus  $\text{Mg}^{2+}$  or  $\text{Fe}^{3+}$  substitution in the structure) has a strong effect of its stability, and should be considered in reactive transport models in which dissolution properties of smectites are taken into account.



Friday  
10<sup>th</sup> July

Lecture room 3

Beyond smectite-based  
nanocomposites

## Fibrous vs. layered clays in nanocomposites

Eduardo Ruiz-Hitzky

Materials Science Institute of Madrid, CSIC, C/ Sor Juana Inés de la Cruz 3, 28049 Madrid (Spain), e-mail: eduardo@icmm.csic.es

Since the seminal work chiefly developed by Fukushima and other researchers at the Toyota Central Laboratories three decades ago (1), natural and synthetic smectites such as montmorillonites, saponites and hectorites, have been widely studied and effectively used as nanofillers in numerous polymer matrices to produce polymer-clay nanocomposites (PCNs). As it is well known, delamination or exfoliation of these clay minerals modified or not by intercalation of cationic organic species, afford to the PCNs key properties such as improvement of mechanical behaviour, barrier properties, thermal stability and flame retardancy (2).

More recently, clay minerals showing non-lamellar structure such as nanotubular halloysite and imogolite, and more frequently sepiolite and palygorskite fibrous clays, have been investigated as alternative nanosize fillers for many diverse polymers. Although the use of this type of nanofillers is still rare it has attracted researchers in Academia and Industry pointing out to novel and advantageous applications compared to "conventional" PCNs based on layered clays.

This communication intends to introduce a comparative study of layered vs. fibrous clays based nanocomposites regarding synthetic approaches, surface clay modifications, mechanism of interactions, physical-chemistry properties and potential applications. In particular it consider and discuss various examples of sepiolite-based PCNs obtained in our Laboratory emphasizing on *green nanocomposites* related to the assembling of biopolymers to both types of clays (bionanocomposites) (3-5).

**Acknowledgements:** CICYT (Spain, project MAT2012-31759) and the EU COST Action MP1202.

1. Y. Fukushima, A. Okada, M. Kawasumi, T. Karauchi, O. Kamigaito, "Swelling behaviour of montmorillonite by poly-6-amide" Clay Miner. 23, 27-34 (1988).

2. E. Ruiz-Hitzky & A. Van Meerbeek, "Clay Mineral-and Organoclay-Polymer nanocomposites" Development in Clay Science: Chapter 10.3 in Handbook of Clay Science. Bergaya F., Theng B.K.G., Lagaly G., eds. Elsevier, pp. 583-621 (2006)

3. E. Ruiz Hitzky, M. Darder, P. Aranda, K. Ariga, "Advances in Biomimetic and Nanostructured Biohybrid Materials", Adv. Mater. 22, 323-336 (2010)

4. E. Ruiz-Hitzky, M. Darder, F.M. Fernandes, B. Wicklein, A.C.S. Alcântara, P. Aranda, "Bionanocomposites based on fibrous clays", Progr. Polym. Sci. 38, 1392-1414 (2013)

5. E. Ruiz-Hitzky, M. Darder, B. Wicklein, A.C.S. Alcântara, P. Aranda, "Recent advances of fibrous clay-based nanocomposites" Adv. Polym. Sci. 267, 39-86 (2015)

## Stimuli-responsive hydrogels formed by the rigid cylindrical clay mineral “Imogolite”

Kazuhiro Shikinaka<sup>1</sup>, Keisuke Kaneda<sup>1</sup>, Tei Maki<sup>1,2</sup>, Hiroyasu Masunaga<sup>3</sup>, Yoshihito Osada,<sup>4</sup> and Kiyotaka Shigehara<sup>1</sup>

<sup>1</sup> Graduate School of Engineering, Tokyo University of Agriculture and Technology  
2-24-16, Naka-cho, Koganei, Tokyo, 184-8588, Japan, k-shiki@cc.tuat.ac.jp

<sup>2</sup> JEOL Ltd. 3-1-2, Musashino, Akishima, Tokyo, 196-8558, Japan

<sup>3</sup> Experimental Research Division, SPring-8, Japan Synchrotron Radiation Research Institute  
1-1-1, Kouto, Sayo-cho, Hyogo, 679-5198, Japan

<sup>4</sup>RIKEN 2-1, Hirosawa, Wako, Saitama, 351-0198, Japan

Imogolite (IG) is a single-walled alumino-silicate type rigid cylindrical clay mineral with the formula  $(\text{HO})_3\text{Al}_2\text{O}_3\text{SiOH}$  and a well defined size.<sup>[1]</sup> The external and internal diameters are  $\sim 2$  and  $\sim 1$  nm, respectively. In contrast, their length ranges from several tens of nm to several  $\mu\text{m}$ . The outer and inner surfaces of IG are covered with aluminol and silanol groups, respectively, where protonation–deprotonation equilibria such as [outer surface]  $\text{Al}(\text{OH})_2 + \text{H}^+ \rightleftharpoons \text{Al}(\text{OH})\text{O}^+\text{H}_2$  and [inner surface]  $\text{Si}-\text{OH} \rightleftharpoons \text{Si}-\text{O}^- + \text{H}^+$  occur. Because of these protonation–deprotonation behaviors, the dispersibility of IG in water strongly depends on the pH and ionic strength. That is, when dissolved in neutral to acidic and relatively low-ionic strength aqueous media, IG gives transparent or opaque solutions containing mono-disperse nanotubes or thin bundles.<sup>[2]</sup>

In this presentation, stimuli-responsive hydrogels prepared from IG nanotube and dicarboxylic acids (DAs) will be described.<sup>[3]</sup> Due to the network structure of IGs connected by DAs, the hydrogel exhibited thixotropy in response to mechanical shock that could be liquefied and re-solidified reversibly by shaking and standing, respectively, within subseconds. After flow-orienting and subsequent standing of the sol-state mixture, the uniaxial alignments of IGs with centimeter scale were realized in the recovered gel. The self-standing interpenetrated network gels were also prepared by the in situ polymerization of the uniaxially oriented gels that were pre-impregnated by a vinyl monomer and a cross-linker. The confinement of the IGs with the uniaxial orientation induced some anisotropic physical properties to the gels such as anisotropic birefringence and mechanical strength. Furthermore, using the latest structural/rheological characterization techniques, the relationship between the structural transition processes and the fast thixotropy was estimated. The evidence obtained by the experiments revealed the direct relationship between the microscopic structural change and the macroscopic thixotropic behavior. The thixotropic hydrogel has the hierarchical architecture in the combination of IG and dicarboxylic acid, *i.e.*, sheathed nanotubes/hydroclusters of cross-bridged nanotubes/frameworks. The formation and disintegration of the network structure upon resting and agitating, respectively, were the origin of gel/sol transition (thixotropy), although the hydroclusters of crossbridged nanotubes were maintained throughout the transition.

[1] Donkai, N.; Inagaki, H.; Kajiwar, K.; Urakawa, H.; Schmidt, M. *Makromol. Chem.* **1985**, *186*, 2623.

[2] Shikinaka, K.; Koizumi, Y.; Kaneda, K.; Osada, Y.; Masunaga, H.; Shigehara, K. *Polymer* **2013**, *54*, 2489.

[3] Shikinaka, K.; Kaneda, K.; Mori, S.; Maki, T.; Masunaga, H.; Osada, Y.; Shigehara, K. *Small* **2014**, *10*, 1813.

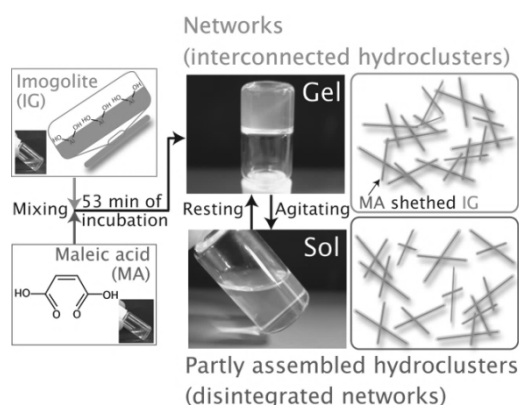


Figure Thixotropic gel consisted of IG and DA

## Photo-induced anisotropic deformation of poly(*N*-Isopropylacrylamide) gel hybridized with an inorganic nanosheet liquid crystal aligned by electric field

Nobuyoshi Miyamoto and Takumi Inadomi

<sup>1</sup>Graduate School of Fukuoka Institute of Technology, 3-30-1 Wajirohigashi, Higashiku, Fukuoka 811-0295, Japan;  
miyamoto@fit.ac.jp

**Introduction:** Recently, lyotropic LCs of inorganic nanosheets[1] are emerging as new-type LC materials. We have reported the utilization of inorganic nanosheet LCs to facilitate synthesis of hydrogels with anisotropic structures and anisotropic properties.[2] Here, we demonstrate electric field assisted synthesis of a cm-scale monodomain gel of exfoliated LC clay/ polymer composite. The gel is printable with a dye and the colored gel shows a photo-induced anomalous deformation behavior. [3]

**Experimental:** The nanosheet LCs were obtained by exfoliation of purified synthetic fluorohectorite clay.[1] The gels were synthesized by photo-polymerization of *N*-isopropylacrylamide (NIPA) dissolved in the nanosheet LCs in a 1 mm-thick cell made of ITO glass and silicone rubber spacer.[2] The alignment of the nanosheet LC at the cm-scale is achieved by the application of an in-plane or out-of-plane AC electric field during photo-polymerization.

**Results and Discussion:** When the LC clay/pNIPA hybrid gel is observed between crossed polarizers, it showed a uniform interference color due to birefringence over the entire gel of several cm length, indicating the formation of the large oriented monodomain (Fig. 1). A photoresponsive pattern is printable onto the gel with  $\mu\text{m}$ -scale resolution by adsorption of the dye through a pattern-holed silicone rubber. When the gel is irradiated with light, only the colored part is photothermally deformed; the deformation is anisotropic due to the oriented nanosheets in the gel. Interestingly, the photo-irradiated gel shows temporal expansion along one direction followed by anisotropic shrinkage, which is an anomalous behavior for a conventional PNIPA gel.

(1) N. Miyamoto, H. Iijima, H. Ohkubo, Y. Yamauchi, *Chem. Commun.* **2010**, 46, 4166.

(2) N. Miyamoto, M. Shintate, Y. Hoshida, R. Motokawa, M. Annaka, *Chem. Commun.* **2013**, 49, 1082.

(3) Inadomi, T., Ikeda, S., Okumura, Y., Kikuchi, H. & Miyamoto, N., *Macromol. Rapid Commun.* **2014**, 35, 1741.

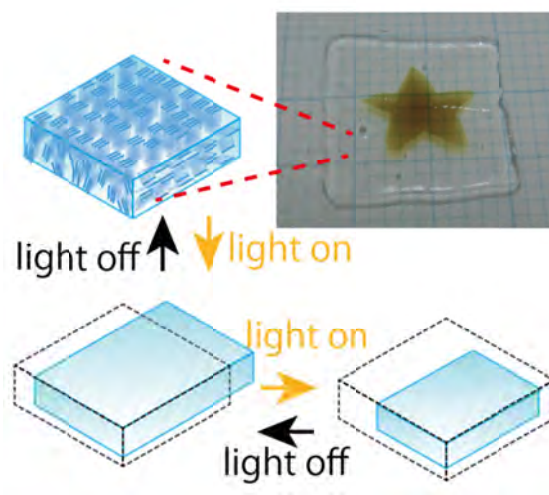


Fig.1 The photograph and schematic model of the monodomain anisotropic gel of clay/PNIPA composite colored with a dye in a star-pattern, which show photo-induced anisotropic deformation.

## Chitosan-vermiculite bionanocomposite foams as biosorbents for the removal of cadmium(II) ions

Érika Padilla-Ortega<sup>1,2</sup>, Margarita Darder<sup>1</sup>, Pilar Aranda<sup>1</sup>, Roberto Leyva-Ramos<sup>2</sup> and Eduardo Ruiz-Hitzky<sup>1</sup>

<sup>1</sup> Instituto de Ciencia de Materiales de Madrid, CSIC, Cantoblanco, 28049, Madrid (Spain)

e-mail: darder@icmm.csic.es

<sup>2</sup> Centro de Investigación y Estudios de Posgrado, Universidad Autónoma de San Luis Potosí, 78810, San Luis Potosí (Mexico)

Bionanocomposites have emerged in the last decade as nanostructured hybrid materials with new structural and functional properties through the combination of natural polymers (biopolymers) and inorganic solids, with at least one dimension at the nanometer scale (1). These new ecofriendly materials are being addressed to a wide range of applications including food packaging, biomedical purposes or environmental remediation (2). Chitosan, prepared by basic deacetylation of chitin, has been extensively used in the synthesis of bionanocomposites due to its great abundance and interesting properties. Smectites and fibrous clays, such as sepiolite, have been combined with this polysaccharide to produce bionanocomposites for various applications (3-5), but analogous materials based on vermiculite have been less explored, probably due to the difficulty of polymers to penetrate the interlayer space of this clay.

The aim of this work was to optimize the preparation of bionanocomposites based on chitosan and vermiculite from Louisiana (USA), pristine or modified with hexadecyltrimethylammonium cations, using ultrasound irradiation, followed by the processing of the resulting materials as low density macroporous foams by means of freeze-drying. Physicochemical characterization by means of elemental analysis, X-ray diffraction, infrared spectroscopy, thermal analysis and scanning and transmission electron microscopy confirmed the intercalation of chitosan into the interlayer space of vermiculite, reaching the exfoliation of the clay layers under certain conditions. These bionanocomposite foams were applied in the removal of Cd(II) from aqueous solutions. The adsorption data were evaluated with the Langmuir, Freundlich and Prausnitz-Radke (P-R) isotherm models, and the P-R isotherm best fitted the experimental data. The adsorption capacity of these bionanocomposites was proven to be remarkably high, and at least three times higher than pristine vermiculite and chitosan applied separately.

**Acknowledgements:** CICYT (Spain, project MAT2012-31759) and the EU COST Action MP1202.

1. Ruiz-Hitzky, E., Aranda, P. and Darder, M., 2008, in Kirk-Othmer Encyclopedia of Chemical Technology, John Wiley & Sons, Inc, Hoboken, N.J
2. Darder, M., Aranda, P. and Ruiz-Hitzky, E., 2007. Bionanocomposites: a new concept of ecological, bioinspired and functional hybrid materials. *Advanced Materials* 19, 1309–1319
3. Darder, M., Colilla, M. and Ruiz-Hitzky, E., 2003. Biopolymer-clay nanocomposites based on chitosan intercalated in montmorillonite. *Chemistry of Materials* 15, 3774–3780.
4. Wang, S.F., Shen, L., Tong, Y.J., Chen, L., Phang, I.Y., Lim, P.Q. and Liu, T.X., 2005. Biopolymer chitosan/montmorillonite nanocomposites: Preparation and characterization. *Polymer Degradation and Stability* 90, 123–131
5. Darder, M., López-Blanco, M., Aranda, P., Aznar, A.J., Bravo, J. and Ruiz-Hitzky, E., 2006. Microfibrous chitosan-sepiolite nanocomposites. *Chemistry of Materials* 18, 1602–1610.

## Hydro-mechanical properties of clay-polymer composites for application in geotechnical engineering

Hanna Haase and Tom Schanz

Ruhr-Universität Bochum, Universitätsstraße 150, 44780 Bochum, hanna.haase@rub.de

In recent years, composite materials based on clay-polymer complex formation has become of great interest. With its origin in fields of material science focusing, e.g., mechanical improvement of polymeric materials (Fu & Qutubuddin 2001), beneficial composite properties have also been found with respect to geotechnical applications, e.g., enhanced barrier performance of bentonites in landfill lining (Scalia et al. 2014), volume stabilization of expansive soils (Inyang et al. 2007) and reduction of clogging potential in tunneling (Zumsteg et al. 2013). However, also several limitations and failure conditions of composite performance have been observed (e.g., Ashmawy et al. 2002). To date, there is a lack in analyzing and understanding these inconsistencies in material performance and thus, general findings on the relationship between composition and the resulting micro- and macroscopic composite properties with relevance in geotechnical engineering.

Therefore, in the present study clay-polymer composites varying systematically in composition have been investigated in terms of their macroscopic hydro-mechanical properties as well as their microstructure under varying loading conditions. Three types of natural clays, i.e., Spergau kaolin, Calcigel bentonite and MX 80 bentonite, have been used to form composites with polyacrylamides (nonionic in a homopolymer form as well as cationic and anionic in a co-polymer form). Adsorption isotherms were determined in order to quantify complex formation depending on the type of clay and polymer. Composites were prepared to their individual maximum adsorption capacity using the solution intercalation method. Subsequently, they were classified in terms of plasticity and experiments were performed on their volumetric behaviour under mechanical loading conditions and hydraulic permeability at various void ratios. Additionally, environmental scanning electron microscopy was performed to characterize the composite microstructure.

The results indicate that with varying clay and polymer characteristics significant changes can be observed in composite microstructure and the resulting macroscopic composite performance. It was concluded that at low stresses long range interparticle bridging due to polymer adsorption plays a major role, whereas with increasing stress level clay particle association, i.e., preferred face-to-face aggregation and edge-to-face flocculation dominate macroscopic behaviour.

Ashmawy, A. K., El-Hajji, D., Sotelo, N. & Muhammad, N. (2002), 'Hydraulic Performance of Untreated and Polymer-treated Bentonite in Inorganic Landfill Leachates', *Clays and Clay Minerals* **50**(5), 546-552.

Fu, M. & Qutubuddin, S. (2001), 'Polymer-clay nanocomposites: exfoliation of organophilic montmorillonite nanolayers in polystyrene', *Polymer* **42**, 807-813.

Inyang, H. I., Mbamalu, G. & Park, S.-W. (2007), 'Aqueous Polymer Effects on Volumetric Swelling of Na-Montmorillonite', *Journal of Materials in Civil Engineering* **19**(1), 84-90.

Scalia, J., Benson, C., Bohnhoff, G., Edil, T. & Shackelford, C. (2014), 'Long-Term Hydraulic Conductivity of a Bentonite-Polymer Composite Permeated with Aggressive Inorganic Solutions', *Journal of Geotechnical and Geoenvironmental Engineering* **140**(3).

Zumsteg, R., Plötze, M. & Puzrin, A. (2013), 'Reduction of the clogging potential of clays: new chemical applications and novel quantification approaches', *Géotechnique* **63**(4), 276-286.

## Beyond homopolymers: kaolinite functionalized with a block co-polymer

Jonathan Fafard and Christian Detellier

Center for Catalysis Research and Innovation and Department of Chemistry, University of Ottawa, Ottawa, ON K1N 6N5, Canada

Kaolin clays, despite their abundance, are rarely used in the preparation of polymer clay nanocomposite materials. Unlike smectitic clays, their minimal capacity for cation exchange and their non-swelling, 1:1 layered structure make their use in the preparation of functionalized materials a significant challenge. Nevertheless, kaolinite functionalization can be achieved using displacement strategies: where small molecules with strong dipolar moments such as dimethylsulfoxide, urea, N-methylformamide, potassium acetate or hydrazine are intercalated to open up the clay interlayer and be subsequently displaced by the desired guest molecules to be used for functionalization. This strategy has been used to prepare a variety of polymer functionalized kaolinites through in-situ polymerization as well as using melts or saturated solutions of the polymer. However, these have been limited to linear homopolymers and literature on kaolinite functionalization with more complex polymer architectures has been largely absent. Here we demonstrate what is to the best of our knowledge, the first successful intercalation of a block co-polymer, polyethylene-*block*-poly(ethylene glycol) by the displacement of a dimethylsulfoxide pre-intercalate. Powder x-ray diffraction gives a 3.87Å d-spacing increase compared to the unmodified clay which remains after washing in water. Thermal gravimetric analysis and nuclear magnetic resonance confirm the presence of the polymer in the prepared material. Dipolar dephasing nuclear magnetic resonance experiments confirm a loss of mobility in functional groups present in both blocks of the co-polymer, a defining characteristic in intercalated materials. Functionalization of kaolinite with the highly hydrophobic polyethylene blocks is expected to favour the retention or sequestration of hydrophobic species, which could be of interest in controlled release applications.

## Functional nanohybrid materials derived from kaolinite

Christian Detellier and Gustave Kenne Dedzo

Department of Chemistry and Center for Catalysis Research and Innovation, University of Ottawa, 10, Marie-Curie, Ottawa (Ont) K1N6N5 Canada; dete@uottawa.ca

Nanoscale chemical modification of inorganic materials by functional organic compounds affords robust and efficient structures that can be used in environments unsuitable for organic compounds. Mesoporous silica compounds are so far the most popular inorganic materials used for this purpose, because of their structure which can be easily tuned and functionalized by various organosilanes. Clay minerals, abundant natural materials, find applications in this type of materials, with the advantage of being inexpensive. Kaolinite, a 1:1 layered clay mineral, despite its relative abundance, is less used than clay minerals of the smectite family, largely because of a low reactivity which is related to its particular structure. Kaolinite is a non-swelling clay mineral with low layer charge. The reactive chemical functions of this clay mineral (hydroxyl groups of the aluminol surface) are protected in the non-swelling interlayer. However, some salts and polar molecules can be intercalated in one step with substantial expansion of the interlayer<sup>1</sup>. Using these pre-intercalates as starting materials, the successful grafting of various organic compounds in the interlayer of kaolinite was reported, with a subsequent increase of the basal spacing. These grafted compounds include amino alcohols, organosilanes and ionic liquids<sup>2,3</sup>. Used as electrode modifiers for the preparation of electrochemical sensors, these materials showed excellent behavior for the electrochemical detection of various compounds. They have also found applications in the environmental field through their ability to adsorb organic pollutants. More recently, such materials could be used for the sequestration and control release of molecules with biomedical interest<sup>4</sup>. Grafted kaolinites are also good candidates for the preparation of nanocomposites by facilitating the dispersion of individual clay layers in polymer matrices, with a subsequent improvement of the native polymer properties. Recent results in our group show that the grafting can be tuned and controlled, with promising applications in catalysis and in the building of nano-reactors.

**Keywords:** Kaolinite, grafting, intercalation, nanohybrid material, ionic liquid.

1- S. Olejnik, A.M. Posner, J.P. Quirk, The intercalation of polar organic compounds into kaolinite, *Clay Miner.*, 1970, 8 421–434.

2- S. Letaief, C. Detellier, Functionalized nanohybrid materials obtained from the interlayer grafting of aminoalcohols on kaolinite, *Chem. Commun.*, 2007, 2613–2615.

3- G.K., Dedzo, S. Letaief, and C. Detellier, Kaolinite–ionic liquid nanohybrid materials as electrochemical sensors for size-selective detection of anions, *J. Mater. Chem*, 2012, 22, 20593-20601.

4- G.K., Dedzo, C., Detellier, Intercalation of two phenolic acids in an ionic liquid–kaolinite nanohybrid material and desorption studies, *Appl. Clay. Sci.*, 2014, 97–98, 153-159.



## Two-photon absorption properties of acetylenic and diacetylenic compounds in the interlayer space of smectite

Yasutaka Suzuki<sup>1</sup>, Hiroyuki Sugihara<sup>2</sup>, Shuhei Mochida<sup>2</sup>, Koichiro Satomi<sup>1</sup>, Jun Kawamata<sup>1</sup>

<sup>1</sup>Graduate School of Medicine, Yamaguchi University, 1677-1, Yoshida, Yamaguchi, Japan, ysuzuki@yamaguchi-u.ac.jp

<sup>2</sup>Graduate School of Science and Engineering, 1677-1, Yamaguchi University, Yoshida, Yamaguchi, Japan

Two-photon absorption (TPA) is a most attractive nonlinear optical phenomenon of which a material absorbs two photons simultaneously to create a excited state. The TPA rate increases quadratically with increasing excitation intensity. Consequently, by using a focused laser beam as excitation light source, the excitation can occur only at a focal point. For this characteristic, 3D optical data storage, two-photon excited microscopy, 3D microfabrication and optical limiting has been demonstrated [1]. To realize such applications, intense laser light is typically required due to low TPA efficiencies of conventional materials. Efficient TPA materials open a way to utilizing TPA applications more easily. We reported that TPA cross-section, efficiency of TPA, of some of organic compound were enhanced considerably by intercalation into smectite compared to that in the solution state [2]. In this study, we focused on acetylenic compounds as guest of smectite.

Synthetic saponite (Smecton SA (SSA)) purchased from the Clay Science Society of Japan was used in this study as a host clay mineral. The chemical structure of acetylenic compounds synthesized for this study is shown in fig.1. Clay-organic hybrids were prepared by ion exchange reaction as previously reported [3].

The TPA cross-section of Ac in dimethylsulfoxide (DMSO) and in hybrid were 135 and 213 GM ( $1 \text{ GM} = 1 \times 10^{-50} \text{ cm}^4 \text{ s}^{-1} \text{ photon}^{-1} \text{ molecule}^{-1}$ ), respectively. The TPA cross-section of Ac in hybrid was 1.6 times larger than that in DMSO. This enhancement was attributed to improved molecular orientation; the  $\pi$ -plane of the molecules and the incident electric field lie in the same plane, and thus the probability of light absorption is higher than in the isotropic solution. On the other hand, further enhancement of TPA cross-section by hybridization was seen in the diacetylenic compound. The TPA cross-section of 1Diac in DMSO and in hybrid were 75 and 544 GM, and the TPA cross-section of 2Diac in DMSO and in hybrid were 102 and 1380 GM, respectively. The TPA cross-section of 1Diac and 2Diac in hybrid was 7.3 and 13.5 times greater than that in the DMSO solution. This enhancement was attributed to improved molecular orientation and extension of  $\pi$ -electron system due to the enhanced planarity.

Although, acetylenic compounds demonstrated in this study possessed simple acceptor (A)-p-A intramolecular charge transfer, the observed TPA cross-section of those in hybrids were significantly high. Employment of diacetylenic compounds having strong intramolecular charge transfer should produce much more efficient TPA materials. Thus, it is concluded that confinement of diacetylenic compounds in an interlayer space of a clay mineral should be an effective strategy for obtaining an efficient TPA material.

[1] M. Pawlicki, *et. al.*, *J. Angew. Chem. Int. Ed.*, **48**, (2009) 3244.

[2] Y. Suzuki, *et. al.*, *J. Phys. Chem. C*, **115** (2011) 20653.

[3] Y. Suzuki, *et al.*, *Appl. Clay Sci.*, **94** (2014) 116.

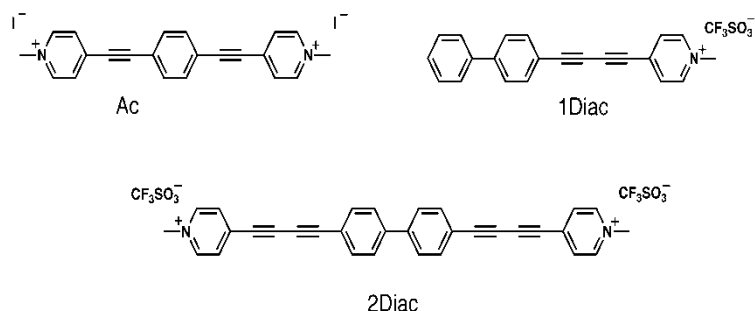


Fig. 1 Chemical structure of acetylenic compounds (Ac), monocationic diacetylenic compound (1Diac) and dicationic diacetylenic compound (2Diac)

## Elaboration of nanocomposite latexes containing Layered Double Hydroxides by macroRAFT-mediated encapsulating emulsion polymerization

Vanessa Prévot<sup>1</sup>, Samuel Pearson<sup>1,2</sup>, Ana Maria Cenacchi Pereira<sup>2</sup>, Fabrice Leroux<sup>1</sup>, Christine Taviot-Guého<sup>1</sup>, Franck D'Agosto<sup>2</sup>, Muriel Lansalot<sup>2</sup>, Elodie Bourgeat-Lami<sup>2</sup>

<sup>1</sup> Université Clermont Auvergne, Université Blaise Pascal, Institut de Chimie de Clermont-Ferrand, CNRS, UMR 6296, BP 80026, F-63171 Aubière, France ; vanessa.prevot@univ-bpclermont.fr

<sup>2</sup> Université de Lyon 1, CPE Lyon, CNRS, UMR 5265, Laboratoire de Chimie, Catalyse, Polymères et Procédés (C2P2), LCPP group, F-69616 Villeurbanne, France

Layered double hydroxides (LDH)<sup>1</sup> are two-dimensional mineral nanoparticles displaying promise in drug delivery, adsorption, catalysis and nanocomposite applications. In nanocomposite field, the addition of anisotropic nanoparticles such as LDH platelets acting as fillers in a polymeric matrix can induce a drastic improvement in properties including mechanical strength, toughness and gas permeation<sup>2</sup>. The use of polymer latex particles-encapsulated anisotropic nanofillers appears as an efficient approach to achieve spatial organization of inorganic particles into latex films<sup>3</sup>. In this work, elaboration of organic/inorganic latexes encapsulating LDH nanoparticles was investigated using a generic synthetic reversible addition-fragmentation chain transfer (RAFT)-based emulsion polymerization process. To this end, LDH were chemically modified by an appropriate macroRAFT agent carrying suitable carboxylic groups typically a random copolymer of acrylic acid (AA) and n-butyl acrylate (BA). The interaction between the macroRAFT agents and the LDH surface was investigated. Adsorption isotherms demonstrate >95% macroRAFT adsorption up to the charge neutralisation point, after which the adsorbed polymer amount plateaus dramatically. The influence of the LDH composition, concentration and length of macroRAFT agent on the colloidal stability of the aqueous dispersion of LDH particles was investigated as well as the inorganic particle modifications by X-ray diffraction, Infra-red spectroscopy and dynamic light scattering. MacroRAFT agent-modified LDH nanoparticles were then used in the emulsion polymerization of hydrophobic monomers (a mixture of methyl acrylate (MA) and BA) in order to form the encapsulating shell. The quantity of free macroRAFT in the polymerisation solution strongly influences stability and latex morphology, with higher concentrations encouraging secondary nucleation and lower concentrations compromising stability (**Fig. 1**). The morphology of the nanocomposite latex particles was characterized by (cryo-) TEM and correlated with the surface modification.

In summary, we report here the successful incorporation of carbonate intercalated LDH into the core of poly(MA-co-BA) latex particles by adsorbing short statistical RAFT copolymers of acrylic acid and butyl acrylate on the positively-charged LDH surface and polymerising MA/BA and MMA/BA mixtures under starved-feed conditions.

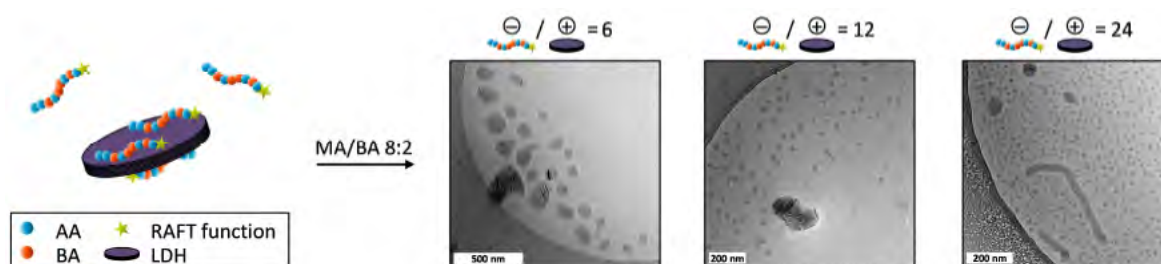


Figure 1: Latex morphologies (cryoTEM) as a function of poly(AA17-st-BA17) concentration, defined in terms of charge ratio between negative polymer and positive LDH surface.

<sup>1</sup> Forano, C.; Costantino, U.; Prevot, V.; Taviot-Gueho, C., In *Handbook of Clay Science, Second Edition Part A*, Bergaya, F.; Lagaly, G., Eds. Elsevier: **2013**; pp 745.

<sup>2</sup> Costantino, U.; Leroux, F.; Nocchetti, M.; Mousty, C., *Handbook of Clay Science, Second Edition Part B.*; Faiza, B.; Gerhard, L., Eds. Elsevier: **2013**; pp 765.

<sup>3</sup> Nguyen, D.; Zondanos, H. S.; Farrugia, J. M.; Serelis, A. K.; Such, C. H.; Hawket, B. S., *Langmuir* **2008**, 24 (5), 2140-2150; Zgheib, N.; Putaux, J.-L.; Thill, A.; Bourgeat-Lami, E.; D'Agosto, F.; Lansalot, M., *Polym. Chem.* **2013**, 4 (3), 607-614

## Emerging nano convergence science: clay-based drug delivery system

Jin-Ho Choy

Center for Intelligent Nano-Bio Materials (CINBM), Department of Chemistry and Nano Science,  
Ewha Womans University, Seoul 120-750, Korea

The purpose of this presentation is not to provide the definition of convergence in terms of various science and technology disciplines, but to help audiences understand what the hybrid materials are, and how to design and synthesize novel 2-dimensional clay hybrid materials, to induce their synergetic effects, and eventually to apply them for nanomedicine.

A novel concept of clay nano-bio hybrids with imaging, targeting and drug delivery functions will be proposed to get breakthroughs in gene and drug delivery research. In order to examine 2d-clay as a nanovehicle for gene and drug delivery, an attempt has been made to prepare host-guest interaction mediated nanohybrid assemblies by the coprecipitation and/or ion-exchange type reactions, where guest biomolecules [antisense and siRNA] or anticancer drugs [Methotrexate and Pemetrexed (Alimta)] could be immobilized in the interlayer space of the host layered clay. And thus encased guest drug molecules could also be slowly released out in a body fluid depending upon the chemical design of the host 2-d clay.

According to the intercellular uptake experiments for clay nanoparticles, we found for the first time that drugs or genes in clay were effectively permeated inside the cell by clathrin-mediated endocytosis. Since clay nanoparticles are partially soluble in cytosol, the drug concentration in the cell increases and as a consequence, the drug efficacy is maximized. More recently, the intracellular trafficking pathways of clay nanoparticles, depending on particle sizes, were clearly demonstrated on the basis of quantitative immunofluorescence microscopy and confocal laser scanning microscopy analyses.

It is, therefore, concluded that the present multifunctional nano-bio hybrid drug delivery system could provide a promising integrative therapeutic action in chemo- and gene therapy.

## Clay-lipid nanohybrids: Toward influenza vaccines and beyond

Bernd Wicklein, Margarita Darder, Pilar Aranda, Eduardo Ruiz-Hitzky

Instituto de Ciencia de Materiales de Madrid, CSIC, C/ Sor Juana Inés de la Cruz 3, 28049 Madrid (Spain), e-mail:

bernd@icmm.csic.es

The design of nanostructured materials based on natural components, as it is the case of clay minerals, offers new solutions to biomedical challenges such as more efficient and storage stable influenza vaccines. The influenza A virus is a periodically recurring threat to public health and has caused several pandemics, the last one in 2009. Vaccines have proved to be a good means to fight this disease but storage related vaccine degradation and low potency are still unresolved problems and require novel and improved vaccine formulations. At the same time nanostructured hybrid materials have gained importance in biomedicine in recent years due to a better understanding of the control and design of their structural and functional properties.<sup>1</sup>

Here, we present clay-lipid hybrid materials as adjuvants in influenza vaccines and with a possible projection to leishmaniasis and other vaccines. Self-assembly of phospholipid molecules on the surface of microfibrillar sepiolite clay and lamellar Mg/Al layered double hydroxide renders a biocompatible lipid bilayer membrane that ensures non-degrading immobilization of proteins and other biological species including viral particles and DNA.<sup>2,3</sup> Immunization tests in mice showed the superior immunogenicity of clay-lipid supported virus in comparison to a commercial aluminum hydroxide adjuvant.<sup>4</sup> Furthermore, the clay-lipid hybrids demonstrated their potential suitability in advanced sub-unit vaccines and as transfection agent in DNA vaccines for leishmaniasis.<sup>5</sup>

**Acknowledgements:** CICYT (Spain, project MAT2012-31759) and the EU COST Action MP1202.

1. Ruiz-Hitzky, Aranda, Darder, Ogawa, *Chemical Society Reviews* **2011**, *40*, 801.

2. Wicklein, Darder, Aranda, Ruiz-Hitzky, *Langmuir* **2010**, *26*, 5217.

3. Wicklein, Darder, Aranda, Ruiz-Hitzky, *ACS Applied Materials & Interfaces* **2011**, *3*, 4339.

4. Wicklein, Martín del Burgo, Yuste, Darder, Escrig, Aranda, Ortin, del Real, Ruiz-Hitzky, *European Journal of Inorganic Chemistry* **2012**, *2012*, 5186.

5. Gomez, Wicklein, Darder, Aranda, Esteban, Ruiz-Hitzky, *in preparation*.

## Easily processable polymer-clay hydrogels for biomedical applications

Chris Breen<sup>1</sup>, Chris Sammon<sup>1</sup>, Victoria Boyes<sup>1</sup>, Christine Le Maitre<sup>2</sup> and Jonathan Foulkes<sup>3</sup>

<sup>1</sup>Materials and Engineering Research Institute, Sheffield Hallam University, Howard St,  
Sheffield, S1 1WB, UK. Email: c.breen@shu.ac.uk

<sup>2</sup>Biomedical Research Centre, Sheffield Hallam University, Howard St, Sheffield, S1 1WB, UK

<sup>3</sup>Smith and Nephew Extruded Films Ltd, Gateway Business Park, Gilberdyke, HU15 2TD, UK

Polymer hydrogels are cross-linked three dimensional polymer networks containing large amounts of water that are used in a wide variety of applications due to their physical and chemical characteristics. In the field of regenerative medicine, they show great potential as scaffolds and stem cell delivery vehicles. It is difficult to process such cross-linked materials and workers have looked at *in situ* polymerisation or stimuli responsive gelation to overcome this. This contribution highlights the development and application of a series of N-isopropylacrylamide (NIPAM) based hydrogels<sup>#</sup> containing 1 to 10 wt% of the synthetic hectorite, Laponite<sup>®</sup> (*registered trademark of BYK Additives*). These NIPAM/Laponite<sup>®</sup> hydrogels remain liquid indefinitely until they are cooled at a predetermined temperature, whereupon they form a hydrogel that does not melt upon re-heating. The facile use of casting, extruding, injecting and electrospinning elegantly demonstrates the high processability of these materials and the excellent biocompatibility is proven by the cell viability studies.

The hydrogels were synthesised via free radical polymerization, in aqueous solution using a thermal initiator as described in reference 1. The resulting hydrogel precursor was maintained at temperatures above 50 °C prior to processing.

Human mesenchymal stem cells (MSCs) were labelled with a green fluorescent membrane dye to enable visualisation prior to culture within or on hydrogel systems. Effects on cell viability, migration characteristics, matrix production and differentiation capacity of MSCs were investigated. Moreover, the feasibility of injection through thin bore needles into a model degenerate intervertebral disc (IVD) was investigated.

The initial biocompatibility studies have proven extremely successful; MSCs readily proliferate and produce matrix in the presence of the set hydrogels and, perhaps more importantly, the MSCs can be pre-mixed into the hydrogel precursor and subsequently injected into cadaver without any detriment to the ability of the cells to proliferate.

**Acknowledgement.** The authors would like to thank Smith and Nephew Extruded Films Ltd, the Materials and Engineering Research Institute, METRC (M9027), EPSRC grant (EP/H000275/1) and EPSRC grant (EP/I016473/1) for financial support

<sup>#</sup> Great Britain Patent Application GB1114446.6

## Immobilization of proteins in ultrathin clay films via layer-by-layer self-assembly

Tamás Szabó<sup>1</sup>, Raluca Mitea<sup>2</sup>, Márta Szekeres<sup>1</sup>, Imre Dékány<sup>1</sup> and Robert A. Schoonheydt<sup>2</sup>

<sup>1</sup>Department of Physical Chemistry and Materials Science, University of Szeged, Aradi vértanúk tere 1 Szeged, Hungary; E-mail: sztamás@chem.u-szeged.hu

<sup>2</sup>Centrum voor Oppervlaktechemie en Katalyse, K. U. Leuven, Kasteelpark Arenberg 23, Leuven, Belgium

Construction of proteins or protein systems immobilized on various supports is an important research target in biorelated chemistry and in biotechnology. Although adsorption of proteins onto various surfaces has been known for a long time, Lvov et al. demonstrated in their pioneering work (1) that it is possible to adopt the layer-by-layer self-assembly technique for the deposition of polymer/protein films in a predetermined way on a molecular or nanometric scale. The as-obtained biomolecular architecture consisting of alternating multilayers is especially interesting because they may carry out complex enzymic reactions. However, the proteins may easily lose their biological activity while immobilization due to conformational changes.

Protein films were deposited by self-assembly which we have successfully applied before for clays and other charged colloids (2-4). We have used two proteins with biological activity: protamine, which is a small nuclear protein and papain, which acts as a proteolytic enzyme, both positively charged in a wide pH range. Multilayer films from these biomolecules and negatively charged clay (saponite) particles were deposited at pH = 4 and 8 with and without cationic polyelectrolyte (PDDA) support layers. The effect of the pH and the presence of polymer on the structure and thickness of nanofilms as well as the conformation of immobilized proteins were investigated by means of UV-spectroscopy, X-ray diffraction, atomic force microscopy and ATR-FTIR, respectively. It was shown that protein/saponite multilayers can be built up without applying any charged polymers which, according to Lvov et al., was considered to act as electrostatic glue and thought to be necessary for multilayer film formation.

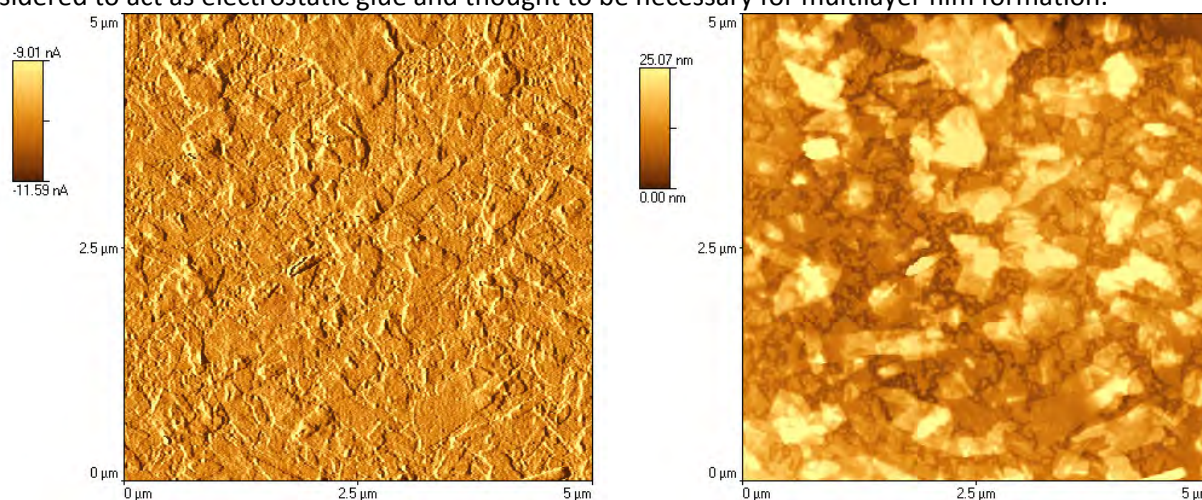


Fig.1 AFM images of PDDA/Saponite/Papain film deposited on glass. Left: cantilever deflection signal image, right: topographical image. In case of layer-by-layer self-assembly, the clay particles are randomly oriented and overlap each other considerably.

1. Y. Lvov, K. Ariga, I. Ichinose, T. Kunitake, J Am Chem Soc, 1995, 117: 6117
2. N.A. Kotov, I. Dékány, J.H. Fendler, J. Phys Chem, 1995, 99: 13065.
3. I. Dékány, T. Haraszti, Coll Surf A, 1997, 123-124: 391.
4. B. van Duffel, R.A. Schoonheydt, C.P.M. Grim, F.C. de Schryver, Langmuir, 1999, 15: 7520.

## Hierarchical “nano-to-macro” organization of oxide nanosheets based on their colloidal liquid crystalline behavior

Teruyuki Nakato, Yoshihiro Nono and Emiko Mouri

Department of Applied Chemistry, Kyushu Institute of Technology, 1-1 Sensui-cho, Tobata-ku, Kitakyushu, Fukuoka 804-8550, Japan. E-mail: nakato@che.kyutech.ac.jp

Layered solid materials exemplified by smectite-type clay minerals and various layered oxides can be converted to colloidal liquid crystals (LCs) through exfoliation into inorganic nanosheets. Such LCs, called “nanosheet LCs” hereafter, are important as a rare example of LCs consisting of inorganic building blocks. In the nanosheet LCs, colloidal nanosheets with a constant thickness of ca. 1 nm and lateral dimension up to micrometers are orientationally ordered in solvents. Utilization of the large size and the collective behavior of the nanosheets in the LC state, we may obtain macroscopic colloidal structures of the nanosheets controlled over all length-scale from micro-, meso-, to macroscopic hierarchies. Such structures are different from conventional intercalation-based nanocomposites, colloidal crystals, and organic molecular assemblies because of their softness of colloidal state, anisotropy of the nanosheets, and robustness of the inorganic building blocks. In the present study, we have hierarchically organized macroscopic structures with characteristic lengths up to millimeters from a nanosheet LCs. We employed layered niobium oxide as the mother layered crystal of the nanosheets [1].

The macroscopic organization is attained through a two-stage process that is the growth of LC domains as the secondary building blocks followed by orientational change of the domains under controlled application of external fields, as schematically shown in Figure 1 [2]. The LC domains are grown by incubation of the LCs at room temperature. The grown domains are then assembled to higher-order structures with characteristic length of sub-mm to mm under the simultaneous application of an AC electric field and gravity, whose directions determine the final textural motif of the macroscopic structures. Application of the electric field in the direction perpendicular to gravity yields a stripe texture. In this structure, the nanosheets are unidirectionally aligned over mm-length (indicated schematically in Figure 1). A net-like texture is observed when the electric and gravitational forces are applied from the same direction. The use of well-grown domains is the key to the macroscopic structural control. The final structures of the nanosheet LCs are influenced by both of the area and thickness of the domains.

[1] N. Miyamoto and T. Nakato, *J. Phys. Chem. B*, **2004**, *108*, 6152.

[2] T. Nakato, Y. Nono, E. Mouri, and M. Nakata, *Phys. Chem. Chem. Phys.*, **2014**, *14*, 955–962.

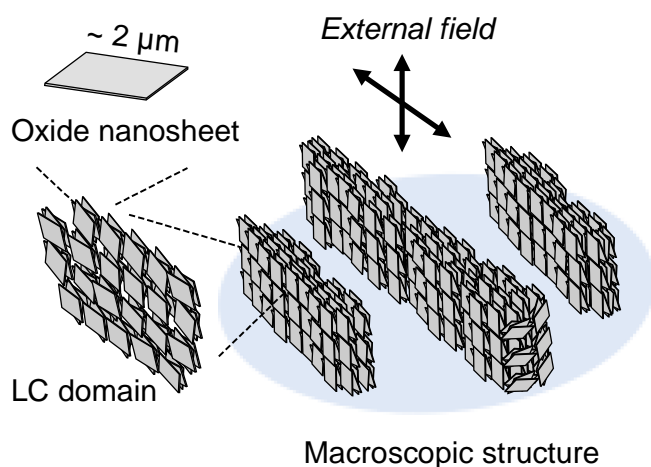


Figure 1. Schematic representation of a macroscopic structure hierarchically organized by a nanosheet LC, in which the LC domains constructed by assembly of the mesogenic inorganic nanosheets work as the secondary building blocks.

## Layered double hydroxide/sepiolite heterostructured materials

Almudena Gómez-Avilés, Pilar Aranda and Eduardo Ruiz-Hitzky

Instituto de Ciencia de Materiales de Madrid, CSIC, C/ Sor Juana Inés de la Cruz 3, 28049 Madrid (Spain), e-mail:

pilar.aranda@csic.es

Smectites and other layered clay minerals have been largely used for developing diverse nanostructured porous materials by generation of metal oxide nanoparticles in their interlayer region (e.g., pillared clays). Sepiolite and palygorskite fibrous clay minerals present a relatively large external surface area which also offers interesting opportunities for assembling diverse type of nanoparticles. In this sense, various methodologies for producing nanostructured materials based on the assembly of diverse type of nanoparticles to fibrous clays have been reported. For instance, the sol-gel approach combined with organosepiolites has been used to build nanostructured porous functional materials (1), treatment with ferrofluids can be applied to produce superparamagnetic adsorbents and catalysts (2), and more recently it has been reported the *in situ* generation of more complex crystalline nanoparticles, such as zeolites, in the presence of the fibrous clay (3). In this communication a new type of heterostructured materials will be introduced in which layered double hydroxides (LDH) are assembled to sepiolite fibrous clay (4). In this way, Mg-Al and Zn-Al LDH were assembled to sepiolite nanofibres by following two procedures of synthesis: i) coprecipitation of the LDH at the convenient pH from chloride precursors in the presence of a water dispersion of the clay; and ii) LDH reconstruction from the corresponding layered double oxide (LDO) also in the presence of a aqueous suspension of the clay. The resulting LDH/sepiolite heterostructures were characterized by diverse physicochemical techniques (XRD, TG-DTA, FTIR, <sup>29</sup>Si NMR, SEM, TEM), revealing the interaction of the generated LDH with sepiolite through the silanol groups at the external surface of the silicate. The N<sub>2</sub> adsorption-desorption isotherms provide evidence the effect of the sepiolite in providing a stable support for dispersing the LDH particles, resulting in materials with a relatively high external surface area and microporosity which depends on the relatively ratio sepiolite: LDH in the final heterostructure. Thus, for instance, the MgAl-LDH/sepiolite heterostructure with a LDH:clay ratio of 0.1:1 shows even a greater micropore volume than the starting sepiolite. Adsorption properties of the resulting materials refer to those of both types of inorganic components with the possibility of adsorbing both cationic and anionic species. Moreover, the LDH can be transformed in the corresponding oxide by thermal treatment giving rise to nanoparticles that remain bonded onto the sepiolite fibers, which could be of interest in applying this methodology to the preparation of highly disperse oxide catalysts supported on sepiolite by first generating the LDH of interest.

**Acknowledgements:** CICYT (Spain, project MAT2012-31759) and the EU COST Action MP1202.

1. E. Ruiz-Hitzky, P. Aranda, "Novel architectures in porous materials based on clays", *J. Sol-Gel Sci. Technol.* 70, 307–316 (2014)
2. Y. González-Alfaro, P. Aranda, F.M. Fernandes, B. Wicklein, M. Darder, E. Ruiz-Hitzky, "Multifunctional porous materials through ferrofluids" *Adv. Mater.* 23, 5224–5228 (2011)
3. A. Gómez-Avilés, C. Belver, P. Aranda, E. Ruiz-Hitzky, M.A. Cambor, Zeolite–sepiolite nanoheterostructures, *J. Nanostruct. Chem.* (2014) 4:90 (14 March 2014) DOI 10.1007/s40097-014-0090-5
4. E. Ruiz Hitzky, P. Aranda, A. Gómez-Avilés, "Micro- and nano-structured composite materials based on laminar double hydroxides of hydrotalcite type and silicates of the clay family", Patente, N. WO2010072870, 2008



Friday  
10<sup>th</sup> July

Lecture room 2

Industry perspectives in  
clay and fine-particle  
science (2)

## Room temperature and high temperature sealing properties and compression properties of compressive gaskets made of micrometric vermiculite particles

L. Duclaux<sup>1</sup>, L. Reinert<sup>1</sup>, A.N. Nguyen<sup>1,2</sup>, L. Mirabel<sup>2</sup>, JF Juliaa<sup>2,3</sup> and A. Beziat<sup>3</sup>

<sup>1</sup> Univ. Savoie Mont Blanc, LCME, F-73000 Chambéry, France, laurent.duclaux@univ-savoie.fr

<sup>2</sup> CEA/DEN/DTEC Laboratoire Maestral F30207 Bagnols sur Cèze, France

<sup>3</sup> Technetics Group France, 90 Rue de la roche du geai 42029 Saint-Etienne, France

Vermiculite gaskets were obtained by pressing vermiculite sonicated powders in the range 17.7-80 MPa [1]. They were studied for their sealing (leak rate measurements) and compressive properties (compressibility and resiliency). The *in plane* permeability at room temperature was found to decrease strongly through increasing elaboration pressure, that reduced both the median pore radius (<30 nm) and the macropore volume fraction (< 45%), measured by mercury intrusion. After annealing at temperature up to 600°C, the *out of plane* permeability (measured at room temperature) increased from  $\sim 10^{-20}$  (at 200°C) to  $\sim 10^{-24}$  due to the increase in anisotropy related to the densification and the formation of interlayer bonds. The global leak rate was found to be determined exclusively by the contact leak rate and independent of the materials permeability. The leak rates measured at room temperature were also found to be dependent on the gaskets resiliency values. The global helium leak rate ( $2.5 \times 10^{-2}$  atm.cm<sup>3</sup>.s<sup>-1</sup>.m<sup>-1</sup>, for 35 MPa working pressure, under 5 bar helium pressure) neither relied on the working temperature (25°C to 800°C) nor the materials porosity for gaskets pressed at 200°C and 80 MPa. The resiliency ( $\sim 5\%$ ) and compressibility (9%) values of these gaskets were reduced after heating the materials to 800°C due to the densification induced both by pressure and temperature, increasing their rigidity.

[1] Nguyen, A.N., Balima, F., Penhoud, P., Duclaux, L., Mirabel, L., Reinert, L., Muller, F., Le Floch, S., Pischedda, V., San Miguel, A., Beziat, A., Dehaut, P., Juliaa, J-F. 2014. Elaboration and characterization of materials obtained by pressing of vermiculite without binder addition. Appl. Clay Sci. 101, 409–418.

## Nature and origin of zinc clays in supergene non-sulphide ore deposits

Flavien Choulet<sup>1</sup>, Martine Buatier<sup>1</sup>, Luc Barbanson<sup>2</sup>, Régis Guégan<sup>2</sup> and Aomar Ennaciri<sup>3</sup>

<sup>1</sup> Chrono-Environnement, Université de Franche-Comté/CNRS, Besançon flavien.choulet@univ-fcomte.fr

<sup>2</sup> Institut des Sciences de la Terre d'Orléans, Université d'Orléans/CNRS/BRGM, Orléans

<sup>3</sup> Groupe Managem, Casablanca

The occurrence of clays associated with ores is often considered to be an intricate challenge for mineral processing requiring de-sliming. The difficulty increases when clay minerals contain a noteworthy content of the commodity, as exemplified by zinc clays in non-sulphide Zn-Pb ore deposits. Such unconventional deposits have been reappraised since the early 2000's, but the nature and the origin of the zinc clay minerals remain poorly understood. Based on the example of the Bou Arhous Zn-Pb ore deposit in the Moroccan High Atlas, we present new advances for the characterization of the barren and mineralised clays associated with the zinc ore.

In the field, two types of clay-rich material have been identified. White to ochre granular clays are closely associated with willemite (zinc silicate), the main Zn ore mineral, whilst red smooth clays fill karst-related cavities cutting across the non-sulphide mineralized bodies. The red smooth clays present evidence of stratification that reflects internal sedimentation processes during karst evolution. Bulk chemical analyses reveal that the Zn content is highly variable in all clayey samples and can reach up to 30 wt% in the white clays. This enrichment may be due to fine inclusions of zinc silicate or carbonate in the clayey material, or to the occurrence of zinc clay minerals.

The mineralogy of the clays and associated minerals in bulk powders and in <2µm oriented fractions from the two types of clay deposits has been investigated. X-ray diffraction (XRD) analyses complemented by Scanning Electron Microscope (SEM) observations, have allowed us to identify the nature of the clay minerals and to characterize the textural relationships between clay minerals and other ore minerals. The red clays contain kaolinite, chlorite, illite, and illite/smectite mixed layers. In a few samples of white clays with high zinc content (>5 wt%), bulk XRD analyses do not reveal the occurrence of zinc sulphides, carbonates or silicates, suggesting that zinc is associated with clay minerals. XRD results indicate that the <2µm fraction is mainly composed of a 7Å-clay mineral/smectite irregular mixed layers with less than 20% of smectite layers; pure smectite, illite and chlorite. On the other hand, SEM observations demonstrated that willemite crystals are partially dissolved and are surrounded by authigenic zinc clay minerals. Microprobe (EPMA) analyses on newly formed clay aggregates have revealed that this mixed layered mineral is composed by fraipontite (a zinc berthierine) and sauconite (a zinc saponite). Cation-exchange capacity measurements on the clay mineral fractions support that zinc is only located within the octahedral sheets.

Beyond characterizing Zn speciation in these supergene deposits, these new results enable us to propose the following processes accounting for the origin of zinc clays with: 1) dissolution of willemite, leading to the release of Si and Zn in meteoric waters, 2) interactions between Zn-Si rich solutions and residual clays originated from the dissolution of limestone-dominated host rocks, 3) neogenesis of zinc clays in the form of mixed-layered clay minerals that grow from detrital micas, which represent the source for Al. This study also has important implications for mineral processing of zinc non- sulphide ore. Despite the economic potential of this clayey material with high Zn content, leaching techniques would be necessary for zinc recovery and special attention should be paid to the frequent association of zinc clays with barren clays.

## Influence of some clays on cement hydration

D. Deneele<sup>1,2</sup>, M. Paris<sup>1</sup> and I. Serclerat<sup>3</sup>

<sup>1</sup>Université de Nantes, CNRS, UMR 6502, IMN, 2 rue de la Houssinière, BP 32229, F-44322 Nantes, France

<sup>2</sup>LUNAM Université, IFSTTAR, GERS, TC, F-44340 Bouguenais, France

<sup>3</sup>Lafarge Research Center, 95 rue de Montmurier, BP 15, 38291 Saint Quentin Fallavier Cedex, France

Supplementary cementing materials are often added to cement or concrete to make mixtures more economical and to reduce the carbon footprint of the cement industry. Blended cements have been successfully used, incorporating amorphous and cryptocrystalline industrial by-products and natural calcined resources in ordinary cement. The results have been satisfactory to date. However, to further cut down carbon emission, an approach using natural blends was recently introduced.

This study deals with the use of natural kaolinite and montmorillonite samples along with white Portland cement (WPC) to study the effects of the respective natural clays on cement hydration. 20% wt/wt kaolinite and montmorillonite cement blends were prepared and studied by using XRD, IR, TGA and NMR. The results show that both clay minerals have an initial accelerating effect on the hydration of silicates and aluminates in WPC. The main consequence is an increase of the amount of CSH in the blends, with different characteristics to the CSH formed in the pure cement. Kaolinite blend influences the conversion of ettringite to monosulphate promoting the stabilization of the AFm phase. In both blends, the dissolution of the clay is reduced and we think that the montmorillonite contributes to the pozzolanic reaction. In terms of macroscopic behaviour, if the accelerating effect of both the clays increases the amount of CSH, the resistance of the blends decreases with time.

## Influence of swelling clay content when using additives in ternary systems: gypsum, water & impurities

Annette Quetscher<sup>1</sup>, Albrecht Wolter<sup>1</sup> and Jazmín Aboytes-McNeela<sup>2</sup>

<sup>1</sup>TU Clausthal, Institute of Non-Metallic Materials, Zehntnerstr. 2A, D - 38678 Clausthal-Zellerfeld, Germany  
annette.quetscher@tu-clausthal.de

<sup>2</sup>Bergheimer Str. 87b, D - 69115 Heidelberg, Germany, aboytesjazmin@gmail.com

The optimization of the manufacture of gypsum wallboard is a major target for the building materials industry. Admixtures, such as PCEs, are widely used as additives to decrease the water demand without affecting the workability of the cementitious and gypsum systems. The limiting factors for the use of PCEs in the manufacture of gypsum-based products are impurities of the raw materials. The presence of certain impurities, such as swelling clays, could result in an incompatibility with the admixtures, which directly affects the workability. Aboytes [1] investigated the fundamental mechanisms in the interaction of methoxypoly(ethylene-glycol)methacrylate type comb polycarboxylate-based superplasticizers by:

- (1) the influence of the raw material,
- (2) the influence of the PCE structure and
- (3) the influence of the bentonite as an impurity.

Two model systems were considered: natural beta-hemihydrate and natural beta-hemihydrate with bentonite as a contaminant. The decrease of the PCE performance as an effect of impurities in natural hemihydrate was determined by the decrease of the workability of the slurry and the adsorption of the PCE in raw materials. To understand the influence of the PCE structure, three main areas were analyzed as follows:

- Effect of the side chain lengths of the polycarboxylates on the workability of the slurry.
- Influence of the backbone type of these copolymers on workability and hydration of the hemihydrate slurry.
- Effect of the side chain density of the polycarboxylate copolymers on their adsorption-workability behavior.

The investigation revealed how the polymer consumption is dependent on the side chain length and backbone type, in correlation with the bentonite contamination.

In the current investigations the aim is to find an analytical method to determine and qualify even the smallest amounts of swelling clay minerals in natural gypsum or limestone. Different methods e.g. separation by gravity or by dissolving the gypsum or limestone are tested to concentrate the clay minerals extracted from contaminated gypsum or limestone samples without changing their chemistry. The analyses of the extracted clay samples are performed using STA, XRD and CEC.

The method of a two-step process first involving a substance that hinders the PCE from interacting with the swelling clays and afterwards, the addition of the PCE to achieve a better workability of the slurry is under investigation.

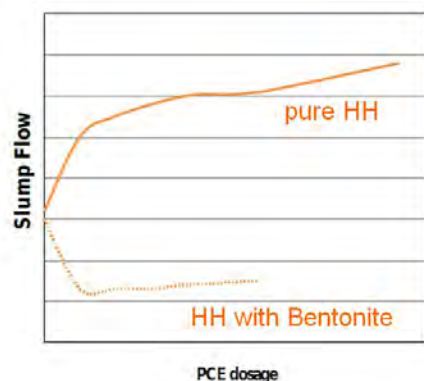


Figure 3: Influence of smallest amounts of bentonite on the PCE consumption and the slump flow. (From [1])

[1] Aboytes, J.: Multi-method approach to study the influence of additives in ternary systems: gypsum, water and impurities. Dissertation, Clausthal, 2014.

## Upgrading Philippine pottery clay into nanoclay-grade material through super-centrifugation for advanced applications

Johanna Michelle S. Ambait<sup>1,\*</sup> and Leslie Joy L. Diaz<sup>1</sup>

<sup>1</sup>Department of Mining, Metallurgical, and Materials Engineering,  
University of the Philippines, Diliman, Quezon City, 1101, Philippines

\*ambait.jm@gmail.com and lesliejoy.diaz@coe.upd.edu.ph

Clay is commonly used as a pottery material in the Philippines, particularly in San Nicolas, Ilocos Norte. However, recent developments in technology have positioned clay as a potential advance material. Clay, particularly nanoclay, has been used in different industries as drug carriers and fillers in cosmetics, an adsorbent for waste water treatment and a nanocomposite for energy storage applications – to name some of the advance applications.

In order to add value to the country's clay usage, this study aims to recover nanoclay from the raw material used in the San Nicolas pottery. Separation of nanoclay from accompanying minerals in the raw clay was investigated by using super-centrifugation. A 2<sup>2</sup> factorial experiment was used to assess effects of the material and equipment settings on the quality of the upgraded nanoclay. A clay slurry was prepared that was initially subjected to wet sieving to remove particle sizes greater than the nozzle size of the super-centrifuge. Large particle sizes were subjected to size reduction and mixed back into the slurry prior to super-centrifugation.

The material property factors that were explored are percent solid loading and particle size while the equipment properties were speed and nozzle size. Significant factors were evaluated through the use of statistical techniques for the analysis of variance of the quality of the product determined using X-ray diffraction analysis, i.e. using mineral intensity factor.

On average, San Nicolas raw clay contained about 18.3% smectite, 10.7% kaolinite and 70.9% non-clay soil minerals. After one cycle of super-centrifugation, the highest average nanoclay yield was 6.55% from a 0.50% slurry, which was determined to be upgraded to 71.07% nanoclay, i.e. mixture of smectite and kaolinite minerals, with 41.4% smectite and 29.6% kaolinite.

## Use of glaciogenic marine clays for brick production in the Arctic

Louise Josefine Belmonte and Lisbeth Ottosen

DTU Civil Engineering (Arctic Technology Centre), Brovej bygn. 118, 2800 Kgs. Lyngby, Denmark

lojon@byg.dtu.dk

Large occurrences of fine-grained glaciogenic marine sediments (clays and silts) were deposited after the last glaciation and some later uplifted above sea level due to isostatic movements. Today, they are found all over the formerly glaciated regions of the northern hemisphere, such as Canada, northern Scandinavia and Greenland (Belmonte et al., in prep.; Foged, 1979; Gillott, 1979; Locat et al., 1984; Ramesh and d'Angeljan, 1995; Roaldset, 1972). Research world-wide has established that marine sediments can be suitable as primary and secondary resources in the production of clay ceramics, such as bricks (Baruzzo et al., 2006; Hamer and Karius, 2002; Mezencevova et al., 2012).

Today, bricks are not commonly used nor produced in Greenland, where building materials such as wood and concrete are favoured (Bjarløv and Vladykova, 2011; Garcia; 2012). However, as most of the construction materials used in the country, are imported, it is of great importance to investigate the potential for local production.

In this study, a representative clay occurrence from Ilulissat, West Greenland was investigated as a potential resource for local brick production. The study comprised of three parts: 1) raw material characterisation based on grain size distribution, major element chemistry including total carbon, sulphur and chloride concentrations, mineralogy, morphology and Atterberg limits 2) production of test bricks and 3) testing of the bricks based on total shrinkage, water absorption, hygroscopic adsorption, open porosity, bulk density, compressive strength, freeze-thaw resistance and mineralogy. The bricks produced proved to have excellent compressive strengths, low open porosity and low water absorption. In conjunction with some of the other investigated properties, this indicates that this type of clay is highly suitable as a resource for bricks, which could be used in the Arctic climate.

Baruzzo, D., Minichelli, D., Bruckner, S., Fedrizzi, L., Bachiorrini, A. and Maschio, S. (2006) Possible production of ceramic tiles from marine dredging spoils alone and mixed with other waste materials. *Journal of hazardous materials*, B134, pp. 202-210.

Belmonte, L.J., Foged, N.N. and Ingeman-Nielsen, T. (in prep) Characterisation and weathering properties of fine-grained marine sediments from West Greenland.

Bentley, S.P. and Smalley, I.J. (1978) Mineralogy of sensitive clays from Quebec. *Canadian Mineralogist*, 16, pp. 103-112.

Bjarløv, S. P. and Vladykova, P. (2011) The potential need for energy saving in standard family detached and semi-detached wooden houses in arctic Greenland. *Building and Environment*, 46, pp. 1525-1536.

Foged, N. (1979) Ingeniørgeologiske undersøgelser af kvartære marine leraflejringer på Vestgrønland, Licentiate (Ph.d.) dissertation, Technical University of Denmark, Lyngby, Denmark (in Danish).

Garcia, D. (2012) View from Nuuk, Greenland. *The Architectural Review*, 27th March.

Gillott, J.E. (1979) Fabric, composition and properties of sensitive soils from Canada, Alaska and Norway. *Engineering geology*, 14, pp. 149-172.

Hamer, K. and Karius, V. (2002) Brick production with dredged harbour sediments. An industrial-scale experiment. *Waste Management*, 22, pp. 521-530.

Locat, J., Lefebvre, G. and Ballivy, G. (1984) Mineralogy, chemistry, and physical properties interrelationships of some sensitive clays from Eastern Canada. *Canadian Geotechnical Journal*, 21, pp. 530-540.

Mezencevova, A., Yeboah, N. N., Burns, S. E., Kahn, L. F. and Kurtis, K. E. (2012) Utilization of Savannah Harbor river sediments as the primary raw material in production of bricks. *Journal of Environmental Management*, 113, pp. 128-136.

Ramesh, R., d'Angeljan, B. (1995) Mineralogy, Chemistry and particle size interrelationships in some Post-Glacial Marine Deposits of the St. Lawrence Lowlands. *Journal of Coastal Research*, 11 (4), pp. 1167-1179.

Roaldset, E. (1972) Mineralogy and geochemistry of Quaternary clays in the Numedal area, southern Norway, *Norsk Geologisk Tidsskrift* 52 (4), pp. 335-369.

## Clay mineralogy for geometallurgy of Cu-Mo ores. Challenges in university and professional training in Chile

Ursula Kelm and Oscar Jerez

Instituto de Geología Económica Aplicada (GEA), Universidad de Concepción, Concepción, Chile. ukelm@udec.cl

Some of the world's largest Cu-Mo-(Au) porphyry copper deposits are located in the Chilean and southern Peruvian Andes. The associated propylitic, sericitic, intermediary and advanced argillic alterations include a wide range of di- and trioctahedral micas, smectites (including regular mixed layered phases) and kaolinites in terms of composition and crystallinity which directly affect the efficiency of ore processing at the stages of comminution, flotation or heap leaching, process water recovery and final tailings disposal. Key tools to adequately control the incidence of gangue on ore processing are the use of automated mineral analysis, (semi) quantitative X-ray diffraction or field- based IR methods.

A judicious use of these and further auxiliary techniques requires a solid training in basic mineralogy and in particular clay mineralogy, a requirement difficult to be fulfilled by mining company staff and associated consulting companies. Among the reasons for this situation are: (1) a lack of non-metallic – in particular clay – tradition that is viewed as a potential employment option by geo- and mineral processing professionals. Existing operations favour chemical control over mineralogical monitoring. In the metal mining sector staff rotation at all levels is high, even more so during boom periods for Cu and Mo commodities. (2) Pressure on universities to reduce the duration of undergraduate programs, at the expense of “theoretical subjects” like mineralogy and enhanced focus on the use of modelling software. A traditional rigidity of curricula leaves clay minerals sidelined as voluntary subjects. (3) Lack or closure of R & D departments within mining companies generates starter careers with only limited need for direct mineralogical analysis, as most analytical work is subcontracted, but company geologists or mineral processing engineers are expected to interpret the data received and supervise their quality. Here, shortcomings with respect to clay phases is a frequent lack of understanding of analytical techniques from sample preparation, instrumental resolution to the detail of mineralogical information required for a specific application.

Due to limited curricular space for the introduction of clay mineralogy beyond the very basics at an undergraduate stage, efforts by universities are directed at professional training programs, such as diplomas or professional masters, in particular taking advantage of the knowledge on rock textures already acquired by the professionals and then contextualizing it within traditional clay mineral analysis and the options to apply more automated analytical procedures. Furthermore, the substitution of mineralogical analysis by routine and easy to perform rock compartment tests (often mine-specific developments) rely on staff with technical rather than university training. In addition, involvement with clays and mining related projects is offered at undergraduate level to chemistry and physics students thus widening future career options.



## An experimental study of CO<sub>2</sub>-H<sub>2</sub>O-listwanite-based reactions using serpentine from the Ahırözü kaolin deposits, Eskişehir-Mihalıççık, Turkey

İşıl Ömeroğlu<sup>1</sup>, Stephen Guggenheim<sup>2</sup>, Asuman Günel Türkmenoğlu<sup>1</sup>, A. F. Koster van Groos<sup>2</sup>, and Şih Ali Sayın<sup>3</sup>

<sup>1</sup>Middle East Technical University, Department of Geological Engineering, 06800 Çankaya-Ankara, Turkey  
isilom@metu.edu.tr, asumant@metu.edu.tr

<sup>2</sup>Department of Earth and Environmental Sciences, University of Illinois at Chicago, Chicago, IL 60607-7059, USA; xtal@uic.edu,  
kvg@uic.edu

<sup>3</sup>Aldridge Minerals Inc., Ankara, Turkey

Fresh ultramafic rock samples were acquired from drill cores from the Kavak chromite mine at Eskişehir-Mihalıççık, Turkey in 2014 to study rock-water-CO<sub>2</sub> interactions of listwanite, a carbonate-altered serpentinite. In the study area, the listwanite occurs in a serpentinite - granite contact zone. The granite is strongly altered and forms kaolin-rich hydrothermal deposits (Ömeroğlu et al. 2013a, b; Sincan, 1979). Chemical analyses of these rocks show a high percentage of SiO<sub>2</sub> (app. 60%), and the X-ray analysis shows the presence of kaolin, potassium-rich feldspar, and quartz (Ömeroğlu et al. 2013a, b). Fluid inclusion analysis of samples from the kaolin-rich deposits indicated that these kaolins were formed from 126°C to 365°C. The associated listwanite is plagioclase-rich, but no quartz was found. The listwanite contains ~ 300 ppm nickel (Ömeroğlu et al. 2013b). The serpentine mineral present in the listwanite rock is mostly lizardite.

Lizardite starting material was obtained from drill cores, and ground to pass 325 to 200 mesh sieves. Experiments were made in a rotating titanium vessel with a bore of 2 cm diameter and 20 cm long. Each sample was comprised of 2.5 g lizardite and 20 ml water. In addition, three 1.3-mm ceramic balls were added to the sample to prevent particles being coated with reaction products during the experiment. The vessels were pressurized with CO<sub>2</sub>, placed in an oven, and rotated at one rotation per minute.

Experiments were performed at 25 °C and 80 °C with P (CO<sub>2</sub>) = 110 to 130 bar. The reaction products were analyzed by X-ray diffraction and a quantitative analysis was performed using FullPat (Chipera and Bish, 2002). In the experiments at 80 °C, the reaction products included magnesite. In addition, the co-existing aqueous liquids, upon evaporation, formed nesquehonite (MgCO<sub>3</sub>·3H<sub>2</sub>O). At 25 °C, the reaction products contained nesquehonite, but magnesite was not produced in any of the experiments at this temperature. The results of a further series of experiments using olivine under the same conditions will be discussed.

This study was performed with the support of a TÜBİTAK 2214-A Scholarship.

Chipera, S.J. and Bish, D.L. (2002) FULLPAT: a full-pattern quantitative analysis program for X-ray powder diffraction using measured and calculated patterns. *J. Applied Cryst.*, 35, 744-749.

<sup>a</sup>Ömeroğlu, I., Türkmenoğlu, A.G., Sayın, A., Ahırözü (Mihalıççık-Eskişehir) Dolaylarındaki Kaolen Yataklarının İncelenmesi, 66. Türkiye Jeoloji Kurultayı-Ankara, p.216-217, April 1<sup>st</sup>-5<sup>th</sup> 2013

<sup>b</sup>Ömeroğlu, I., Türkmenoğlu, A.G., Sayın, Ş., A., Investigation of the Genesis of Ahırözü Kaolin Deposits (Eskişehir, Turkey) Using Mineralogical, Petrographical and Geochemical Analyses, 50th Anniversary of Clay Minerals Society-Illinois/USA, p.188, October 6<sup>th</sup>-10<sup>th</sup> 2013

Sincan, M., 1979, Eskişehir Mihalıççık Kaolen Etüt Report, MTA, Ankara/Turkey

Friday  
10<sup>th</sup> July

Lecture room 1

Clay minerals in the oil  
and gas industry

## Reconstructing basin burial and thermal history using shale seismic properties, reservoir fluid inclusions, and advanced modal analysis methods in the Arctic Barents Sea

Paul Nadeau<sup>1</sup>, TineStraaso<sup>1</sup>, Theis Solling<sup>2</sup>, Xiomara Marquez<sup>2</sup>, Lothar Schulte<sup>3</sup>

<sup>1</sup> Maersk Oil Norway, Stavanger, Norway

<sup>2</sup> Maersk Oil Research and Technology Centre, Doha, Qatar; <sup>3</sup> Schlumberger SIS, Stavanger, Norway

Evaluation of the petroleum potential of sedimentary basins which have undergone significant amounts of inversion and erosion requires that particular attention be paid to the reconstruction of their burial and thermal histories. Resolving these issues in terms of magnitude and timing is particularly challenging in the structurally complex Arctic Barents Sea.

Prior work has demonstrated that trap preservation with respect to timing of hydrocarbon charge and seal integrity is a major risk factor with increasing amounts of erosion. Here we present methods that convert shale sonic velocities and seismic interval transit times into erosion estimates, facilitating regional 2D mapping, as well as higher resolution characterization of traps/structures on 3D data. These data were integrated with burial depths estimated from reservoir fluid inclusion trapping temperatures and pressures for key wells to reconstruct basin configuration, structural relationships and trap geometries at the time of oil migration and charge.

By combining these data sets with quantitative electron microscopy of shale composition and properties in terms of porosity and preferred grain orientation, an overall assessment of mechanical and chemical compaction, burial and thermal history for individual play fairways can be undertaken. This is particularly important for evaluating data from different shale units in terms of age, depositional environment, and mineralogy. These studies support prospective volume estimates for basin, play, and prospect levels.

Applying this methodology with models for oil entrapment efficiency (Nadeau *et al.*, 2005) to the Barents Sea, a clear preferential depth/thermal interval can be identified, which includes the bulk of recently discovered resources.

Nadeau, P.H., Bjørkum, P.A. & Walderhaug, O., 2005. Petroleum system analysis: Impact of shale diagenesis on reservoir fluid pressure, hydrocarbon migration and biodegradation risks. In: Doré, A. G. & Vining, B. (eds) *Petroleum Geology: North-West Europe and Global Perspectives – Proceedings of the 6th Petroleum Geology Conference, 1267-1274*. Petroleum Geology Conferences Ltd., Published by the Geological Society, London.

## Diagenesis of silica and clay minerals – Field observations and pyrolysis experiments

Elen Roaldset

Natural History Museum, University of Oslo, P.O.Box 1172 Blindern, 0318 Oslo  
elen.roaldset@nhm.uio.no

Diagenetic mineral transformations and reactions can significantly affect the properties of source and reservoir rocks including porosity, permeability, and rock mechanical properties.

The presentation will focus on the diagenetic reactions associated with quartz and the clay minerals kaolinite, smectite, and illite. Special attention will be paid to the transformations from smectite to illite, kaolinite to illite, and amorphous/biogenic silica through cristobalite/tridymite to quartz. These reactions have been experimentally studied by hydrous pyrolysis by the author and coworkers, with subsequent kinetic modelling of mineral transformations to geological depths and temperatures. The results from these studies will be reported.

In reservoir sandstones the illitization of kaolinite has received much attention, due to its devastating effect on reservoir permeability. On the contrary, the transformation of kaolinite to its diagenetic polymorphs dickite and nacrite, has so far hardly been noticed. In certain cases these transformations may also influence the petrophysical properties of the source and reservoir rocks. The formation of illite from smectite via a mixed layer illite-smectite (I-S) intermediate, is a typical diagenetic reaction in claystones, but may also occur in sandstones. By experimental pyrolysis it has been demonstrated that temperature, time, fluid composition (in particular the  $K^+$  content), and initial composition of clay materials, affect the rate and extent of illitization. Pyrolysis experiments also demonstrate that the transformation of opaline silica to quartz is controlled by temperature, and that the temperature range for the transformation, to some extent is related to geologic time. A quantitative kinetic model has been developed based on the hydrous pyrolysis experiments for biogenic silica and smectite that has been successfully extrapolated to geological time.

Although the variations in physical properties of sediments are complicated by many factors, the pyrolysis experiments may provide a useful tool for linking geological age, palaeotemperature, mineralogy, physical and associated acoustic properties to burial history and time.

Better understanding of diagenesis and petrophysical properties in future exploration and production can be achieved by combination of detailed observations of texture and mineralogy combined with experimental pyrolysis and modelling.

## A 2-stage model for growth of fibrous illite in oilfield sandstones

Mark Wilkinson

School of GeoSciences, University of Edinburgh, Grant Institute, The King's Buildings, James Hutton Road, Edinburgh EH9 3FE

Illite crystals are limited in size to a few 10's microns in length and a few microns in width and are in turn composed of large numbers of fundamental particles (FP's). To precipitate 1% illite in a sandstone requires huge numbers of new FPs to nucleate ( $\sim 10^{13}$ ), a kinetically difficult process. Illite crystals (FPs) do not enlarge to sizes typical of other authigenic minerals, or even other clay mineral crystals, because of strain inherent in the illite lattice. A two stage model for the growth of fibrous illite in oilfield sandstones is proposed: an initial growth 'event' controlled largely by the kinetics of nucleation, forming thin and low-K fundamental particles; slow thickening of the fundamental particles during subsequent burial, leading to a progressive increase in potassium content.

Because the first stage of growth is controlled by the kinetically-difficult nucleation of FP's, growth only occurs under unusual geological conditions. This is triggered by 'events' of relatively short duration compared to the age of a host sandstone, such as fluid flow associated with fault movement, oil charging of the reservoir, or an influx of carboxylic acids also associated with oil charging. Once the 'event' is over, the conditions within a reservoir sandstone are not conducive to the nucleation of significant numbers of new FP's. The lack of 'zero-age' illite within the North Sea, a basin currently at its maximum depth of burial (and likely maximum temperature) could be a result of a lack of recent triggering events due to tectonic quiescence and largely already mature source rocks. The fibrous nature of the illite may reflect this rapid growth event, though may also be the result of selective poisoning of crystal faces.

The slow increase in potassium and the thickness of the FP's with subsequent burial has been documented from the North Sea (Wilkinson et al., 2014). It is suggested that the rate of illite precipitation controls the rate of feldspar dissolution (Wilkinson, 2015), a potentially important reaction that generates secondary porosity of economic importance in many petroleum reservoirs. Feldspars can potentially dissolve rapidly (on geological timescales) but are sparingly soluble, so that illite precipitation must occur for dissolution to proceed.

The model may explain why secondary porosity can form in shale-free deeply buried sandstones that would be expected to be geochemical closed systems. The illite FP's (neo-formed and possibly detrital) thicken to absorb solutes from dissolving feldspars, resulting in a decrease in micro-porosity within clay rims and aggregates, but not impinging on open porosity as much as continued neof ormation of fibrous, pore-filling fibres which would involve the kinetically difficult nucleation stage of growth.

Wilkinson, M. (2015) Does the nucleation of illite control the rate of diagenesis in deeply buried sandstones? *Clay Minerals*, **in press**.

Wilkinson, M., Haszeldine, R.S. & Fallick, A.E. (2014) Authigenic illite within northern and central North Sea oilfield sandstones: evidence for post-growth alteration. *Clay Minerals*, **49**, 229 – 246.

## A clay mineralogy study of the Shurijeh Sandstone Reservoir, Kopet Dagh sedimentary basin, NE Iran

Golnaz Jozanikohan<sup>1</sup>, Gholam Hossain Norouzi<sup>1</sup>, Fereydoun Sahabi<sup>1</sup> and Quentin Fisher<sup>2</sup>

<sup>1</sup> School of Mining Engineering, University of Tehran, Tehran, Iran, E-mail: gjkohan@ut.ac.ir

<sup>2</sup> The Centre for Integrated Petroleum Engineering and Geoscience (CiPEG), University of Leeds, UK

Determining the clay mineralogy of hydrocarbon-bearing clastic reservoirs is an important step in the overall reservoir characterization workflow as the clay minerals control many petrophysical properties. In addition, clay minerals may react with injected fluids, so knowledge of clay mineralogy is crucial for planning secondary and tertiary recovery. The Shurijeh Formation, represented by sandstones of Late Jurassic-Early Cretaceous age, is the main reservoir rock in the eastern Kopet-Dagh region, NE Iran. This paper utilizes powder X-ray diffraction (PXRD), wavelength dispersive X-ray fluorescence (WDXRF), and scanning electron microscopy (SEM/EDX) techniques to characterize the clay minerals in 76 representative core samples from the Shurijeh Formation, obtained from a gas production well and a non-producing well. The results of WDXRF analysis showed high percentages of silicon and moderate to low percentages of aluminium, sulphur, calcium, potassium, sodium, magnesium, and iron in the both wells. The PXRD analysis indicated that the above elements were concentrated in quartz, plagioclase, anhydrite, dolomite, calcite, K-feldspars, hematite and the clay minerals. Further XRD examination of the clay fraction, revealed that illite, chlorite, and kaolinite were the major types of clay mineral present. Glauconite, smectite, and mixed layer illite-smectite and chlorite-smectite were only observed in a few samples. The percentages of individual clay minerals were determined, using external standard calibration curves and successfully validated by a system of simultaneous linear equations, acquired from detailed elemental information based on XRF analysis. Quantitative mineralogies generated from the WDXRF data, showed that each of the Shurijeh wells exhibited moderate to high amounts of clay minerals, typically up to 32.5%. The amount of illite, the most dominant clay mineral, reached a maximum of 18.3%, while the other clay types were significantly smaller. The most common clay minerals with clear authigenic origin in the Shurijeh Formation were pore-bridging illite, pore-lining aggregates of magnesium-rich chlorite, and booklet-like aggregates of pore-filling kaolinite. Discrete smectite and mixed layer clay minerals were very rare in the Shurijeh reservoir sandstones. The clay minerals distribution pattern in the production well was structural and dispersed (pore-filling and pore lining) and in the non-producing well was structural, dispersed (pore-filling, pore lining and pore bridging) and laminar. Only small amounts of dispersed authigenic clay minerals were found in the producing well. However, far larger concentrations were found in the non-producing well and it is likely that this is the main reason for the poor reservoir quality.

**Keywords:** Clay minerals, Powder X-ray diffraction, Wavelength dispersive X-Ray fluorescence, Quantitative mineralogical analysis

## Tracing hydrocarbons in gas shale using lithium and boron isotopes: Denver Basin USA, Wattenberg Gas Field

<sup>1</sup>W. Crawford Elliott, <sup>2</sup>Lynda B. Williams and <sup>2</sup>Richard L. Hervig

<sup>1</sup>Department of Geosciences, Georgia State University, Atlanta, GA 30302-3965

<sup>2</sup> School of Earth & Space Exploration, Arizona State University, Tempe, AZ 85287-1404:

wcelliott@gsu.edu

Bentonites are altered volcanic ash layers commonly used as marker beds in sedimentary basins. Alteration of the ash produces diagenetic smectite and illite-smectite (I-S) which incorporate trace elements (Li and B), thus recording the altering paleofluid compositions. Organic macerals can be a source of Li and B generated during thermal maturation, producing distinctly light B and Li isotopic compositions in fluids related to hydrocarbon generation compared to most surface and groundwaters.

We examined Li and B contents and their isotopic compositions in different crystal size fractions of I-S separated from Cretaceous bentonites from core samples of the Wattenberg Gas Field (WGF), and elsewhere in the Denver Basin, Colorado (USA). Outside of the WGF, the  $\delta^7\text{Li}$  of I-S in outcrops range from  $-7$  to  $+4\text{‰}$ . Within the WGF, I-S ranges from  $-4$  to  $-18\text{‰}$ . A key sample from the highly thermally mature region, where vitrinite reflectance values (Ro) reach 1.2-1.5%, showed  $\delta^7\text{Li} = +12\text{‰}$  in the  $<0.1\mu\text{m}$  I-S clay fraction while the 0.1-2.0  $\mu\text{m}$  fraction of the same sample shows the lowest  $\delta^7\text{Li}$  value of  $-18\text{‰}$ . This sample has a K-Ar date of  $60\pm 3$  Ma, prior to Colorado Mineral Belt (CMB)-related igneous activity. Assuming that the finest fraction contains the first nucleated illite, the 30‰ decrease in  $\delta^7\text{Li}$  between these two size fractions within the same sample indicates influx of  $^6\text{Li}$  dominated fluid related to oil and gas generation, *after illitization began*. This signature developed coincident to the time of foreland basin development. B-isotopes ranged from  $-7$  to  $-15\text{‰}$  showing no significant trend, however the B-content reached 180 ppm in the WGF, decreasing to 64-105 ppm at the margins. Thus, high concentrations of isotopically light Li and high B in diagenetic illite reflect the influx of hydrocarbon related fluids formed during the earliest stages of oil generation in the WGF. These data do not discount the possibility of later thermal maturation caused by a secondary heating event related to CMB igneous activity (Higley et al., 2003). However if the proposed igneous related heating at 40-20Ma occurred, then it was not high enough to reset illite K-Ar ages, or increase percentage of illite layers formed in I-S.

Higley, D.K., Cox, D.O., Weimer, R.J., 2003, Petroleum system and production characteristics of the Muddy (J) Sandstone (Lower Cretaceous) Wattenberg continuous gas field, Denver basin, Colorado: AAPG Bulletin, v. 87, p. 15-37.

## Crystal-chemical evolution of clay minerals with depth in the Vaca Muerta Formation: Impact on the evaluation of total clay content

Claire I. Fialips<sup>1</sup>, Ahmed Abd Elmola<sup>2</sup>, Daniel Beaufort<sup>2</sup>, Jean-Paul Laurent<sup>1</sup>, Bernard Labeyrie<sup>1</sup> and François Umbhauer<sup>1</sup>

<sup>1</sup>Total S.A., Exploration-Production, Technical Center CSTJF, avenue Larribau, 64018 Pau, FRANCE: Claire.Fialips@Total.com

<sup>2</sup>University of Poitiers, CNRS UMR 7285, IC2MP, HydrASA, rue Albert Turpain, 86022 Poitiers, FRANCE

Accurate quantification of total clay content of a statistically representative set of core samples is essential for reliable interpretation and calibration of well logs in shale intervals. Our in-house approach to quantitative mineralogy, called QM, integrates standard X-ray diffraction (XRD) analyses of bulk powders and extracted fine fractions with a large suite of additional chemical and physical measurements on the same samples. It has been developed over the last decade to optimize accuracy and robustness but it remains complex in that it requires some knowledge of the elemental composition of individual mineral components. As a first approximation, an average chemical formula determined by  $\mu$ -X-Ray Fluorescence ( $\mu$ -XRF) is used for each Fe- and/or Mg-bearing carbonate and for each clay mineral, regardless of burial depth within the same formation. Crystal-chemical variability of individual mineral components over the short depth intervals being studied (generally <160m) would be minor and would not therefore have a significant impact on our quantification of total clay content.

In the present study, a series of 19 core samples from two depth intervals of the Upper-Jurassic Vaca Muerta Formation in the Neuquen Basin of Argentina, which had already been analyzed using the QM approach in 2013, were re-analyzed in more detail to further evaluate crystal-chemical variability of clay minerals with depth. The samples were analyzed by XRD, Fourier Transformed Infrared Spectroscopy (FTIR) and Scanning Electron Microscopy (SEM) with Energy Dispersive X-ray Spectroscopy (EDX).

Results confirmed that the clay minerals present in the samples are mainly composed of interstratified illite-smectite (I/S) with more than 85% illitic component (type R3). The presence of chlorite and detrital muscovite was also confirmed. Observed variations in the chemical composition of I/S phases determined by EDX do not show any systematic evolution with depth. Their Mg, Fe, octahedral Al, Ca and Na contents per  $O_{10}(OH)_2$  are particularly stable (<0.03 stdev). A marked anti-correlation does however appear between their K and Si contents, indicating that the observed variability in K content (from 0.4 to 0.8K per  $O_{10}(OH)_2$ ) is mostly correlated to tetrahedral substitutions. FTIR analyses of few samples also revealed the presence of non-exchangeable  $NH_4^+$  in the I/S. Its actual proportion could not be quantified based on the available data. However, it is likely to range between 0 and 0.3  $NH_4^+$  per  $O_{10}(OH)_2$  based on the very poor swelling behaviour of the I/S, which suggests a rather high charge (>0.7 per  $O_{10}(OH)_2$ ), while the measured Na, Ca and K contents only account for a charge of 0.5 to 0.9 per  $O_{10}(OH)_2$ . Tobelite-like layers may have formed through fixation of ammonium released during oil and gas generation as already reported in early-Ordovician Alum shales in the Baltic area (cf. Lindgreen et al., 2000).

Re-interpretation of the quantitative mineralogy analysis of the 19 core samples using the individual chemical formulae of the I/S and chlorite obtained by EDX instead of average formulae led to a modification of the initially evaluated total clay+mica contents by less than 4 mass% (1 mass% on average). Highest deviations are observed for the samples presenting a chemical formula of I/S with the lowest and highest K contents (0.4 and 0.8K per  $O_{10}(OH)_2$ ), therefore deviating the most from the average formula used in the initial MQ analysis. This study is therefore validating our initial hypothesis: the use of average structural formula for the clay minerals in our MQ approach over the whole interval of Vaca Muerta Formation (~159m) is appropriate as the fairly minor crystal-chemical variability of I/S and chlorite does not have a significant impact on our quantification of total clay content.

Lindgreen, H., Drits, V.A., Sakharov, B.A., Salyn, A.L., Wrang, P., Dainyak, L.G. (2000) Illite-smectite structural changes during metamorphism in black Cambrian Alum Shales from the Baltic area. *American Mineralogist* 85, 1223-1238.



## Further insight into the depositional environment of the Holywell Shale (Carboniferous, northeast Wales)

Leo P. Newport\*, H. Chris Greenwell, Andrew C. Aplin, Jon G. Gluyas and Darren R. Gröcke  
Durham University, Department of Earth Sciences, Science Labs, Durham, DH1 3LE, UK  
\*leo.newport@durham.ac.uk

The Carboniferous Bowland Shale Formation of northwest England has been identified as one of the largest potential shale gas targets in the UK. The Holywell Shale is part of the Bowland Shale Formation and represents a succession of marine, brackish and non-marine mudstones at the southwest edge of the Pennine Basin. Five outcrop locations of the Holywell Shale across northeast Wales were sampled to investigate variations in mudstone deposition and organic matter input/ preservation throughout the Namurian (326.4 - 313 Ma). A multidisciplinary approach was adopted relating organic and inorganic geochemistry, petrographic imaging, and SEM imaging of micro-scale fabrics to determine the range of depositional environments and organic matter types which occur within the Holywell Shale.

At outcrop, the Holywell Shale is immature to early oil mature and has organic matter contents (TOC) ranging from 0.12 wt % to 10.31 wt %. Carbon and nitrogen isotopic data combined with RockEval<sup>TM</sup> analyses indicate that the organic matter ranges from type II/III kerogen in the lower Holywell Shale to type III kerogens in the middle and upper shale. This can be related to a temporal shift in the source of organic matter, from a more marine influenced signature to a more terrestrial influenced signature. There is only a weak relationship between the quality and quantity of organic matter, suggesting quite complex controls on organic matter supply and preservation. Similarly, there is a broad range of mineralogies and depositional fabrics at a wide range of spatial scales. In the context of a potential shale gas reservoir, these data indicate that the Holywell Shale has highly variable reservoir quality. The identification of "sweet spots" will have to be underpinned by detailed geological investigations.

## Stratigraphic controls on clay minerals in the McMurray Formation

Ruarri J Day-Stirrat<sup>1</sup>, Ronny Hofmann<sup>1</sup>, Anton Nikitin<sup>1</sup>, Robert Mahood<sup>2</sup>, Stephen Hillier<sup>3</sup> and Gilles Mertens<sup>4</sup>

<sup>1</sup> Shell International Exploration and Production Inc., STCH, 3333 Highway 6 South, Houston, Texas, 77082,  
Ruarri.Day-Stirrat@Shell.com

<sup>2</sup> Shell Canada, Shell Technology Center Calgary, 3655 36st. N.W., Calgary, Alberta, T2L 1Y8

<sup>3</sup>The James Hutton Institute, Craigiebuckler, Aberdeen, AB15 8QH, UK

<sup>4</sup>Qmineral bvba, Gaston Geenslaan 1, B-3001 Heverlee, Belgium

Clay mineral diversity in the McMurray Formation has been recently explored by Shell in the context of stratigraphic occurrence by bulk X-ray diffraction (XRD), cation exchange capacity (CEC) measurements, X-ray fluorescence (XRF), clay size fraction (<2 micrometer) XRD analysis, reflected light microscopy, and cryogenic-scanning electron microscopy (cryo-SEM).

Imaging of Lower McMurray Formation fluvial channel sands shows clay minerals to be infiltrated into the channel sands at the time of deposition and their location to be adjacent to quartz particles. This was confirmed in cryo-SEM where bitumen was not removed from the sample and aluminum gathered from energy dispersive spectra was used as a proxy for clay minerals.

Throughout the McMurray Formation discrete clay minerals (chlorite, muscovite, and kaolinite) were quantified in both bulk and clay size XRD. In addition, mixed-layered illite-smectite (I-S) was also quantified. Lower and Middle McMurray Formation sediments were dominated by I-S with a low expandability (smectite content). Expandability was estimated to be 20-30%. Upper McMurray Formation sediments by contrast had higher expandability (60-70%). Concomitantly, CEC values increased five times from the Lower/Middle McMurray Formation to the Upper McMurray Formation in response to the increase in expandable layers.

In flood plain sediments of the Lower McMurray Formation an additional mixed-layer mineral has been variably identified and quantified as kaolinite-smectite (K-S), or in some cases kaolinite-vermiculite (K-V) with a high smectite or vermiculite content. The associated CEC values of this phase are 10 times the baseline for the McMurray Formation. K-S or K-V appears to be reworked in the Middle McMurray Formation but is generally absent in the Upper McMurray Formation. K-V formation appears to be related to soil forming processes and has a complex internal structure of either hydrated cations or hydroxyl sheets that manifest as a variable CEC both in response to the vermiculite structure and interstratification with kaolinite.

Identification and characterization of the highly charged mixed-layer clay phases in the McMurray Formation can lead to both an improved understanding of clay interaction in bitumen processing as well as tailings settling behavior, and eventually an evaluation of how to best capture this data for mine and tailings models.

## Moss and peat as monitors of past, present, and future rates of atmospheric dust deposition

Gillian Mullan-Boudreau and William Shotyk

531 South Academic Building, University of Alberta, Edmonton, Alberta, Canada mullanbo@ualberta.ca

348 South Academic Building, University of Alberta, Edmonton, Alberta, Canada

Open pit mining of the Athabasca bituminous sands generates enormous quantities of mineral dusts. One measure of the success of reclamation in this area will be the reduction of dust emissions to pre-mining, or natural “background” levels. Mining is by no means the only industry with anthropogenic emissions of atmospheric dusts: forest-clearing (agriculture and forestry) and construction (airports, roads, towns and other infrastructure) also contribute to the burden. In the pre-anthropogenic period, dust deposition was primarily affected by climate change with some periodic volcanic inputs, indicating that northern Alberta may have considerable variation in the rates and sources of dust deposition throughout time. The purpose of this research is to reconstruct present and past rates of atmospheric dust deposition, using moss and peat, to identify the natural “background” rates for which future reclamation practices shall strive to achieve.

Present-day rates of dust deposition are being obtained by ashing Sphagnum moss from ombrotrophic bogs surrounding the bituminous sands region. The plants growing in ombrotrophic bogs receive all their nutrients and water from the atmosphere, making any dusts a key component in mineral uptake. The concentrations of acid-insoluble ash (AIA) combined with surrogates of mineral matter concentrations, namely Al, Ba, Sc, Ti and Th, are then analyzed. Past rates of dust deposition are being obtained using the same techniques, except applied to peat cores from the bituminous sands region, which have been age-dated using  $^{210}\text{Pb}$  and  $^{14}\text{C}$ . Electrical conductivity and pH were also measured from the porewater of the peat cores to establish the thickness of the ombrotrophic layers. Finally, the morphologies of the mineral particles are also being studied using scanning electron microscopy imaging and chemical composition analysis.

Results from moss samples show a wide range of dust particle morphology and size that tends toward larger particles, e.g. 8-100  $\mu\text{m}$ , which indicates localized deposition. The electrical conductivity and pH of the peat cores reveal ombrotrophic layers ranging from 18 to over 100 cm. Chemical analyses of the particles using the X-ray fluorescence spectrometer of the SEM will help to identify the predominant dust sources. Particle size analyses will also be performed on the AIA fraction of the moss and peat.

## Wettability of Smectites: effect of exchangeable ions and surface roughness

J.Ballah<sup>1,2</sup>, M.Chamerois<sup>3</sup>, G.Hamon<sup>3</sup>, P.Levitz<sup>1</sup> and L.Michot<sup>1</sup>

<sup>1</sup> PHENIX-CNRS-UPMC, 4 place Jussieu, 75005 Paris Cedex, France.

<sup>2</sup> jamoowantee.ballah@upmc.fr

<sup>3</sup> TOTAL E&P, Avenue Larribau, 64018, Pau Cedex, France

Enhanced oil recovery processes, EOR, attempt to recover residual oils trapped in petroleum reservoirs. So far, after early evidence of the benefits of low salinity waterflooding, some controversial results emerged, particularly about amount and type of clay present in the reservoir. It thus appears crucial to have a thorough understanding of the wettability of clays as the reservoir is a porous medium in which solid and fluid phases coexist as a result of the complex triple phase “rock-brine-oil” interaction.

The wettability of three swelling aluminosilicate clays (beidelite, nontronite and montmorillonite) have been investigated as a function of different interlayer cations,  $\text{Li}^+$ ,  $\text{Na}^+$ ,  $\text{K}^+$  and  $\text{Ca}^{2+}$  by using the static sessile drop method. The results show that water contact angles on the different clay films vary as a function of the different interlayer ions with a specific behaviour of  $\text{K}^+$ -exchanged clay.

During the study, the effect of parameters influencing contact angle measurements such as surface roughness and relative humidity have been examined. In the former case, clay films have been probed by Atomic Force Microscopy, AFM and surface roughness correlated to the corresponding contact angles. The results show that in the order of decreasing surface roughness are the films of  $\text{Li}^+$ ,  $\text{Na}^+$ ,  $\text{K}^+$  and  $\text{Ca}^{2+}$ . In a first approximation, it appears that surface roughness is directly linked to the interlayer cation and hence to contact angles. The specific behaviour of  $\text{K}^+$ -exchanged clays are confirmed since AFM measurements have revealed that their films are among the flat ones. In the latter case, comparison between contact angles measured at the time of drop deposit at a relative humidity of 46 (ambient conditions), 84 and 100% do not show any significant change but stabilisation of the drops have been observed.

[1]: J.Shang, M.Flury, J.Harsh, R.Zollars, J.Colloid Interface Sci. 328 (2008) 299-307

[2]: S.Boussour, M.Cissokho, P.Cordelier, H.Bertin, G.Hamon, Paper SPE 124277, (2009)

[3]: J.Shang, M.Flury, J.Harsh, R.Zollars, Colloids and Surfaces A: Physicochem. Eng. Aspects 353 (2010) 1–9

## Gaining insight into oil-brine-clay mineral interactions through core-nanoscale experimental and computational studies

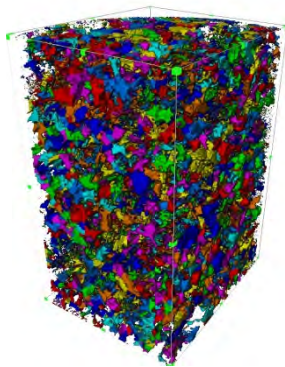
Chris Greenwell\*, Pablo Cubillas, Rikan Kareem, Valentina Erastova and Thomas Underwood

Department of Earth Sciences, Durham University, Science Site, Durham, DH1 3LE, UK.

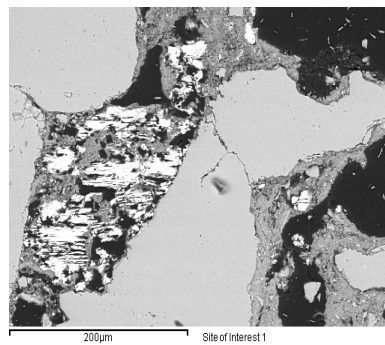
\*Presenting author e-mail: chris.greenwell@durham.ac.uk

Low salinity water floods have been found to be effective in enabling enhanced oil recovery (EOR) operations to extend oil production in sandstone reservoirs. The reservoir-rock wettability is thought to be a key controlling parameter, and understanding of the change in wettability as an effect of flood water composition is critical. This study brings together a number of strands of investigation, starting with a multi-scale characterisation of Berea sandstone using petrography, X-ray micro-computer tomography ( $\mu$ CT) and field emission gun scanning electron microscopy (FEG-SEM). It is shown that although pore-coating clay minerals form a small fraction by weight in Berea sandstone, their role in determining pore-oil-brine interactions is likely to be significant (Figure a). Nanoscale analysis shows clay minerals are present in a number of morphologies and settings (Figure b and c), alongside other fine particles and surface coatings.

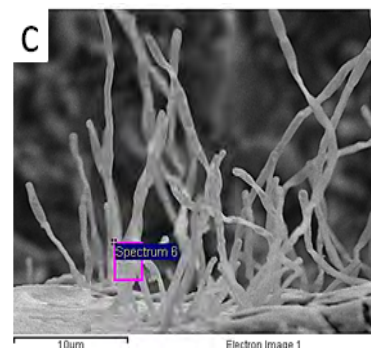
As well as understanding structure, wetting processes at the nanoscale-microscale are probed using environmental scanning electron microscopy (d) where the mineral surfaces are successively wetted whilst being imaged to understand how contact angles vary as a function of mineralogy, oil wetness and salinity. Finally, the adhesion of polar and non-polar hydrocarbon molecules at the clay-brine surface is explored at the nanoscale using chemical force microscopy (CFM), as shown in (e) with insight added at atomic resolution through coupled molecular dynamics computational simulations (Figure f).



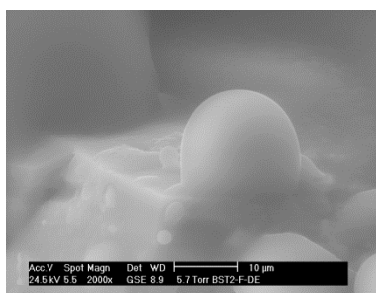
(a)



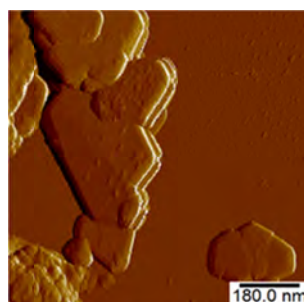
(b)



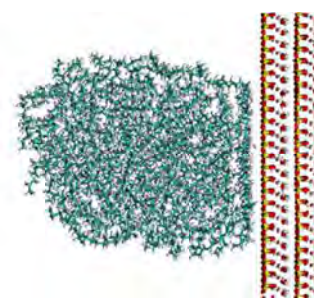
(c)



(d)



(e)



(f)

## Towards a nanoscopic understanding of oil-clay mineral wettability: implications for enhanced oil recovery

Pablo Cubillas<sup>\*</sup>, Rikan Kareem and Chris Greenwell

Department of Earth Sciences, Durham University, Science Site, Durham, DH1 3LE, UK.

<sup>\*</sup>Presenting author e-mail: pablo.cubillas@durham.ac.uk

Due to the continuous rise in the demand of oil across the globe and diminishing availability of conventional sources, enhanced oil recovery (EOR) operations are increasingly deployed to extend crude production. In most cases EOR involves injecting low salinity water (diluted seawater or brine) into the reservoir (waterflooding). Therefore, reservoir-rock wettability is thought to be a key controlling parameter along with water composition. In this regard, understanding the fundamental chemical controls of oil/water wettability on clay mineral surfaces is critical. This is because clay particles are present, in large quantities, on pore surfaces and pore openings of most sandstones; even though they are a minor component (by weight) of the rock. Although a few studies have looked at oil interaction with mica minerals, these materials do not represent the best analogue for clay minerals.

In this study, kaolinite and nacrite crystals were studied by means of atomic force/chemical force microscopy (AFM/CFM). Measurements were carried out using OH, COOH, NH<sub>2</sub> and CH<sub>3</sub> functionalised probes, and were taken in the presence of solutions with different compositions (NaCl -0.01M and 1M, CaCl<sub>2</sub> -0.01M and 1M) and 2 different pHs (4 and 6). The main results of the study are:

OH functionalised tips: Measured adhesion in kaolinite crystals indicate an increase in adhesion when increasing the concentration of either NaCl or CaCl<sub>2</sub> (from 0.01 to 1 M in both cases). CaCl<sub>2</sub> experiments showed a higher adhesion compared to those performed in NaCl.

COOH functionalised tips: Experiments performed in kaolinite show a slight increase in the adhesion when the concentration of CaCl<sub>2</sub> is increased from 0.01M to 1M. The same result was observed in the nacrite experiments. Nevertheless the biggest change in adhesion is observed when decreasing the pH of the solution from 6 to 4. This resulted in the doubling of the measured adhesion.

CH<sub>3</sub> functionalised tips: experiments performed with these tips show an increase in the measured adhesion when increasing the CaCl<sub>2</sub> concentration from 0.01 M to 1 M.

NH<sub>2</sub> tips: results show that this terminal group has very low affinity for the kaolinite surfaces under neutral pH conditions and at all brine concentrations, with adhesion just reaching 100 pN at most. Nevertheless, low pH conditions (pH = 4) increased the adhesion considerably.

## The kaolinite - water interface: Insight from the electrical double layer

N. Bovet, S. Jelavic, T. Clausen and S.L.S. Stipp

Nano-Science Center, Department of Chemistry, University of Copenhagen

bovet@nano.ku.dk

One of the methods for enhancing oil recovery (EOR) relies on flooding reservoirs with low salinity water. This can increase oil recovery from sandstone by 5% to 40% compared with standard methods where pressure is maintained in the reservoir by flooding with sea water or formation water. The effect has been explained by changes in wettability of the pore surfaces, resulting from a decrease in concentration of the divalent cations in the low salinity water. Several explanations have been proposed but the exact mechanism is still not well understood, especially at the molecular scale.

The presence of clays, particularly kaolinite, is known to influence the extent of the low salinity response and the presence of divalent cations in the formation water is essential. We have therefore studied the behaviour of kaolinite (standard KGa1-b) at the molecular level during contact with solutions of various salinities, containing  $\text{Ca}^{2+}$ ,  $\text{Mg}^{2+}$  and  $\text{Na}^+$  cations with  $\text{Cl}^-$  and propionate [ $\text{C}_2\text{H}_5\text{COO}^-$ ] as a counter anions.

To observe the surface chemical composition of kaolinite and its change as a function of solution change, we used cryogenic X-ray photoelectron spectroscopy (cryo-XPS), which provides information about the composition of the mineral-fluid interface. XPS requires ultrahigh vacuum but when the solution is vitrified, the concentration in the near surface fluid, i.e. the portion of the solution that includes the electric double layer, is preserved. The analysis depth of this technique (10 nm) means that it can probe the ion concentrations in the fluid that was at equilibrium with the kaolinite surface at the instant it solidified.

The results demonstrate that the relative ion concentration near the surface is different than in the bulk, consistent with electrical double layer theory. Of particular interest is that when the salinity of  $\text{CaCl}_2$  solution in contact with kaolinite decreases below 12 mM, the ratio of Cl:Ca also decreases, meaning that the surface loses its negative charge to a greater extent than its positive charge. Our experiment was designed to model negatively charged species, such as the oil components that are attached to pore surfaces, so the relative loss of negatively charged adsorbed molecules during exposure to low salinity solutions would mean oil release in the reservoir.

The ability of cryo-XPS to probe the electrical double layer at the kaolinite-water interface provides insight into the mechanism of the low salinity effect at the molecular level, which provides a better picture for the processes governing surface-fluid behaviour.

## A cryogenic X-ray photoelectron spectroscopy (cryo-XPS) study of illite and clinocllore control on low salinity enhanced oil recovery

S. Jelavić, N. Bovet, A. Rath Nielsen and S.L.S. Stipp

Nano-Science Center, Department of Chemistry, University of Copenhagen, Denmark  
stanislav.jelavic@nano.ku.dk

Illite and chlorite are common and important clay minerals in oil-bearing rocks. They can act as cements, reducing the flow rates of the pore fluids, preserve porosity during diagenetic alteration and they are very reactive, as a consequence of their high surface area and surface charge density. Skovbjerg et al. [1] showed that the presence of clay minerals can alter the wettability of the pore surfaces in reservoir rocks by selectively adsorbing some components from the oil and the water used to push oil to the production well. Understanding the mechanisms of adsorption of common cations and anions, found in formation waters and brines, on clay minerals is essential for predicting the response of oil reservoirs during low salinity water flooding for oil recovery.

We investigated the adsorption preference of Ca-Cl and Na-Cl pairs for illite and chlorite. Cryo-XPS was used to obtain the chemical composition and the bonding environment from the topmost layers of atoms at the solid-solution interface from fast frozen (i.e. vitrified) samples [2, 3]. We prepared and equilibrated illite (standard IMt-1, fraction <2 µm separated by centrifugation) and clinocllore (CCa2, Mg-rich chlorite, hand ground and passed through a 50 µm sieve) in CaCl<sub>2</sub> and NaCl solutions at a range of concentrations (1-125 mM) in batch experiments. Samples were fast frozen by placing the centrifuged wet paste directly on a precooled sample holder in the spectrometer antechamber, using a liquid nitrogen cooled stage (-170 °C). The difference in Cl 2p electron binding energy for the fast frozen specimens and those dried under ultrahigh vacuum demonstrates that the electrical double layer (EDL) is preserved by the fast freezing. The surface excess of Ca<sup>2+</sup>, Na<sup>+</sup> and Cl<sup>-</sup> was measured and the organisation of cations and anions in the electrical double layer could be observed. Both illite and chlorite have higher preference for Ca<sup>2+</sup> than Na<sup>+</sup>, because of the higher ionic charge density of Ca<sup>2+</sup>. Decreasing the bulk solution concentration of CaCl<sub>2</sub> induced expansion of the electrical double layer on both minerals and caused a rapid decrease in the concentration of negative charges (Cl<sup>-</sup>) close to the surface. The bulk solution concentration, below which the surface ratio of Cl:Ca<sup>2+</sup> drops below 1 is lower for chlorite (12-18 mM) than illite (75-100 mM). This trend is not seen for the NaCl solutions. Instead, an increase in Cl<sup>-</sup> surface excess with decrease of the bulk solution concentration is observed.

This study shows how clay mineral type can affect the distribution of positive and negative charges in the oil reservoir pores. The mineral phase controls the thickness of the EDL as bulk solution concentrations vary and the cation valence controls the behaviour of anions at low bulk solution concentrations when the EDL is expanded. This is important for low salinity EOR because it demonstrates the necessity for thorough characterisation of the clays and understanding about clay mineral surface behaviour if predictions of the low salinity response in reservoir rock are to be reliable.

[1] Skovbjerg, L.L., Hassenkam, T., Makovicky, E., Hem, C.P., Yang, M., Bovet, N., Stipp, S.L.S. (2012), *Geochimica et Cosmochimica Acta*, **99**, 57-70

[2] Shchukarev, A., Sjöberg, S. (2005), *Surface Science*, **584**, 106-112

[3] Shchukarev, A., Boily, J.-F., Felmy, A.R. (2007), *Journal of Physical Chemistry C*, **111**, 18307-18316



## The effect of the water boundary layer on clay properties in shales in oil reservoirs

Lyudmyla Wilson<sup>1</sup> and Michael J. Wilson<sup>2</sup>

<sup>1</sup> Corex Ltd, Units B1-B3, Howe Moss Drive, Airport Industrial Park, Dyce, Aberdeen, UK, lwilson@corex.co.uk

<sup>2</sup> James Hutton Institute, Craigiebuckler, Aberdeen Jeff.Wilson@hutton.ac.uk

The instability of shales in drilled formations often leads to operational problems with economic consequences for petroleum exploration and production. It is known that the nature of the clay minerals in shale formations is a primary causative factor leading to their instability, although the exact mechanism involved is more debateable. The majority of publications claim that volume expansion, following the osmotic swelling of Na-smectite, is the principal cause of shale instability. However, the nature of instability in shales containing illitic and kaolinitic clays is not clearly understood, as in these instances interlayer expansion cannot be considered as the causative mechanism of the instability.

Illite, mixed-layer illite-smectite (I/S) and kaolinite are often associated with shale instability when they are present in shales as major clay minerals. This paper considers the evaluation of the boundary water layer on clay surfaces in the double electric layer (DEL) of kaolinite and illite, both being representative of non-swelling clays [Alekseyev et al., 2003]. It is found from the literature that the thickness of the diffuse double layer (DDL) of the aqueous solutions associated with the charged external surfaces of clay minerals is probably of the same order or even thicker than the sizes of a significant proportion of the pores found in shales. In these circumstances, overlap of the DDLs associated with exposed outer surfaces of clay minerals on opposing sides of micropores (<2 nm in diameter) and mesopores (2-50 nm in diameter) in a lithostatically compressed shale would bring about electrostatic repulsion and lead to increased pore/hydration pressure in smectitic, illitic and even kaolinitic shales. This pressure could be inhibited by the use of more concentrated K-based fluids which effectively shrink the thickness of the DDL towards the clay mineral surfaces in the pore walls. The use of soluble polymers would also encapsulate these clay mineral surfaces and so inhibit their hydration. In this scenario, the locus of action with respect to shale instability and its inhibition is moved from the interlamellar space of the smectitic clays to the charged external surfaces of the various clay minerals bounding the walls of the shale pores [Wilson & Wilson, 2014].

Alekseyev O L, Bojko Yu P and Pavlova L A (2003) Electroosmosis in concentrated colloids and the structure of the double electric layer, *Colloids and Surfaces A: Physico-chem and Engin Asp.*, 222, pp. 27-34.

Wilson M J and Wilson L (2014) Clay mineralogy and shale instability: an alternative conceptual analysis, *Clay Minerals*, 49, pp. 127-145.

## Swelling of clay minerals: from micro to macro scales.

Radhika Patel<sup>1</sup>, Neal Skipper<sup>2</sup> and Chris Greenwell<sup>3</sup>

<sup>1,2</sup>Dept Physics and Astronomy, University College London, Gower St, London, WC1E 6BT

<sup>3</sup>Dept Earth Sciences, Durham University, Science Site, South Rd. DH1 3LY

Organo-amine and ammonium compounds are particularly useful for the oil and gas exploration sector as they aid in the inhibition of swelling in clay mineral-rich shale formations which are encountered whilst drilling for oil. Shale swelling inhibition is required due to the increased use of water-based drilling fluids which have adverse effects on drilling operations leading to a loss of production costs estimated as greater than \$500 M per annum. Fundamental knowledge about how these compounds work is still lacking, making optimisation of swelling inhibition difficult.

The swelling of tetramethylammonium (TMA)-intercalated vermiculite clays are investigated using neutron scattering techniques for microscopic measurements of  $d$ -spacing. Here we studied the change in  $d$ -spacing in response to added external pressures and temperatures. Also investigated, is the macroscopic swelling behaviour of TMA-intercalated vermiculite using a custom built constant humidity cell and non-contact linear displacement sensors.

The dry  $d$ -spacing of the TMA-exchanged Eucatex vermiculite is measured at 13.66 Å which increases to 14.03 Å with the addition of D<sub>2</sub>O. Beyond this, there is no change in  $d$ -spacing with increasing pressure and temperature indicating the strength of the TMA ions binding to the clay interlayers and therefore its performance as a clay-swelling inhibitor.

Also presented is the design and measurement of macroscopic swelling of compacted clay pellets and the comparison between what is observed microscopically to that which is observed macroscopically.

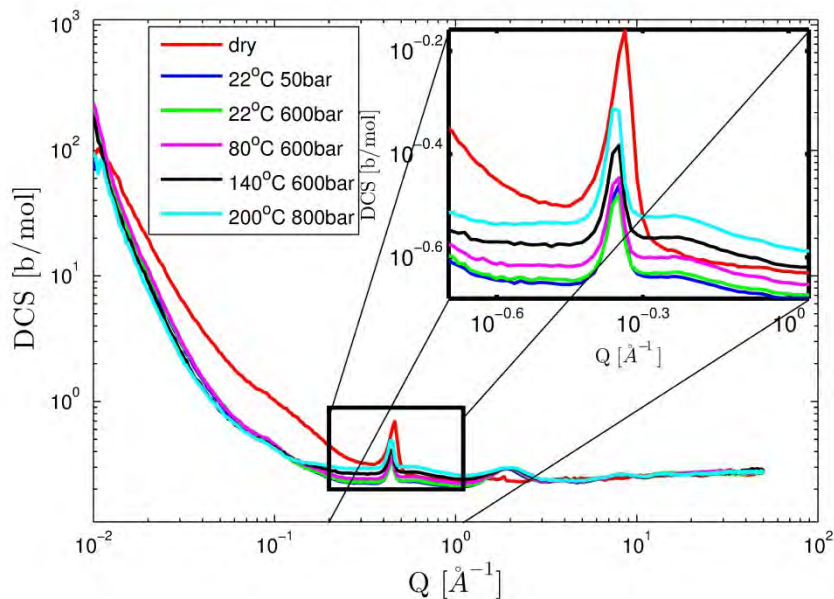


Fig.1 Change in  $d$  spacing of TMA intercalated vermiculite with increasing  $T$  &  $P$ .

## Shale - drilling mud interactions tested in Flysch reservoirs

Andrea Schicker<sup>1</sup> and Susanne Gier<sup>1,\*</sup>

<sup>1</sup>Department for Geodynamics and Sedimentology, University of Vienna, Althanstrasse 14, 1090 Vienna, Austria;  
\*susanne.gier@univie.ac.at

Interlayered shales in deepwater flysch sediments can cause problems during drilling because of the reaction of expandable clay minerals with the drilling mud. Amongst other problems, borehole stability is directly affected by clay swelling. Knowing the composition and the properties of the clay fraction is crucial when using water based drilling muds.

In this study the bulk and clay mineralogy of 13 samples from exploration wells were characterized and their reaction with drilling mud tested. In contact with fresh water the samples immediately disintegrate. Different methods, such as cation exchange capacity (CEC), methylene blue method (MB), zeta potential measurements and swelling tests were applied to understand the interaction between the samples from wells and the drilling mud and to characterize the swelling capacity of the shales.

The bulk samples contain large amounts of clay minerals together with quartz, calcite, ankerite, pyrite, K-feldspar and plagioclase. The clay mineralogy is dominated by illite, chlorite, kaolinite and up to 26% smectite in the bulk samples. The highest CEC (25.1 mmol/100g clay) and MB (17.6 g MB/100g) values correlate with samples with the highest smectite content. The zeta potentials of the samples range between -383.4 to -218.4 mV.

Potassium in the form of  $K_2CO_3$  was added to the drilling mud. Swelling tests on a smectite-rich sample showed that this potassium entered the smectite interlayer and thus prohibited further swelling (Fig.1).

By combining all information gathered from the different methods it can be stated, that the tested drilling mud meets the requirements and prevents the shale samples from the flysch units from swelling.

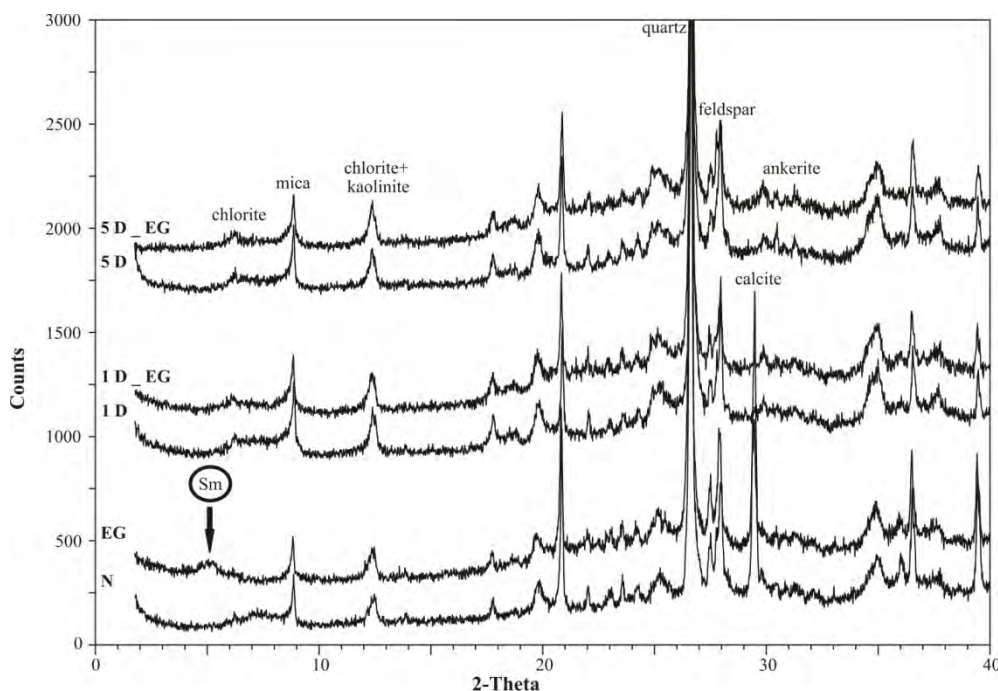


Fig.1: X-ray diffraction patterns of a shale sample, depth 996m. Patterns N, EG (base) are samples measured natural and saturated with ethylene glycol; patterns 1D, 1D\_EG (middle) and 5D, 5D\_EG are the samples after shaking in drilling mud for 1 day respectively 5 days and saturated with ethylene glycol. After one day contact with the drilling mud the smectite (Sm) does not expand anymore.

## DELEGATE LIST

**A**

Adamcova, Renata, Comenius University in Bratislava, Faculty of Natural Sciences, Mlynska dolina, Bratislava, 842 15, Slovakia, [adamcova@fns.uniba.sk](mailto:adamcova@fns.uniba.sk)

Adriaens, Rieko, KULeuven, Celestijnenlaan 200E, Heverlee, 3001, Belgium, [rieko.adriaens@ees.kuleuven.be](mailto:rieko.adriaens@ees.kuleuven.be)

Aisawa, Sumio, Iwate University, 4-3-5 Ueda, Morioka, 208551, Japan, [aisawa@iwate-u.ac.jp](mailto:aisawa@iwate-u.ac.jp)

Alam, Sabrina, Texas A&M University, 404 D, Wellborn Road, North, College station, 77840, USA, [ssalam@tamu.edu](mailto:ssalam@tamu.edu)

Alekseeva, Tatiana, Russian Academy of Sciences, Institutskaya ul., 2, Pushchino, 142290, Russia, [alekseeva@issp.serpukhov.su](mailto:alekseeva@issp.serpukhov.su)

Al-Jaberi, Muayad, University of Lorraine, 405, rue de Vandoeuvre, Villers-Les-Nancy, 54602, France, [muayad.al-jaberi@univ-lorraine.fr](mailto:muayad.al-jaberi@univ-lorraine.fr)

Alpermann, Theodor, Federal Institute for Geosciences and Natural Resources, Stilleweg 2, Hannover, 30655, Germany, [Theodor.Alpermann@bgr.de](mailto:Theodor.Alpermann@bgr.de)

Ambait, Johanna Michelle, University of the Philippines, Department of Mining, Metallurgical, and Materials Engineering, Velasquez St corner C P Garcia, UP Diliman, Quezon City, 1101, Philippines, [ambait.jm@gmail.com](mailto:ambait.jm@gmail.com)

Aparicio, Patricia, University of Sevilla, Dpto. Cristalografía, Mineralogía y Q. A., Facultad de Química, C/ Prof. García González nº1, Sevilla, 41012, Spain, [paparicio@us.es](mailto:paparicio@us.es)

Aplin, Andrew, Durham University, Department of Earth Sciences, Durham, DH1 3LE, United Kingdom, [a.c.aplin@durham.ac.uk](mailto:a.c.aplin@durham.ac.uk)

Aranda, Pilar, ICMM-CSIC, C/ Sor Juana Inés de la Cruz 3, Madrid, 28049, Spain, [pilar.aranda@csic.es](mailto:pilar.aranda@csic.es)

Aras, Ismail Aydin, Yuzuncu Yil university (YYU), Engineering Fac Geological Engineer Dep, Van, 65080, Turkey, [aras5549@yahoo.com](mailto:aras5549@yahoo.com)

Armbruster, Thomas, University of Bern, Inst. Geol. Sciences, Freie Str. 3, Bern, CH-3012, Switzerland, [armbruster@krist.unibe.ch](mailto:armbruster@krist.unibe.ch)

Arroyo, Xabier, Complutense University of Madrid, Jose Antonio Novais, 12, Madrid, 28040, Spain, [xarroyo@geo.ucm.es](mailto:xarroyo@geo.ucm.es)

Austin, Jason, University of Georgia, 210 Field Street, Geology Dept., Athens, 30602, USA, [jaycaustin@live.com](mailto:jaycaustin@live.com)

Aygor, Tugce

**B**

Bacle, Pauline, Université Pierre et Marie Curie, 4 Place Jussieu, Bat. F, 7eme etage, Paris, 75005, France, [pauline.bacle@upmc.fr](mailto:pauline.bacle@upmc.fr)

Bain, Derek, The James Hutton Institute, Craigiebuckler, AB15 8QH, Scotland, [derek.bain@hutton.ac.uk](mailto:derek.bain@hutton.ac.uk)

Bakker, Eleanor, Institut des Sciences de la Terre, 1381, rue de la Piscine, BP 53, Grenoble, 38041, France, [eleanor.bakker@ujf-grenoble.fr](mailto:eleanor.bakker@ujf-grenoble.fr)

Baldermann, Andre, Graz University of Technology, Institute of Applied Geosciences, Rechbauerstraße 12, Graz, 8010, Austria, [baldermann@tugraz.at](mailto:baldermann@tugraz.at)

Ballah, Jamoowantee, CNRS/UPMC UMR8234, 4, Place Jussieu, Paris Cedex 5, Case Courrier 51, Paris, 75252, France, [jamoowantee.ballah@upmc.fr](mailto:jamoowantee.ballah@upmc.fr)

Banwart, Steven, The University of Sheffield, Krotto Research Building, North Campus, Broad Lane, Sheffield, S3 7HQ, United Kingdom, [s.a.banwart@sheffield.ac.uk](mailto:s.a.banwart@sheffield.ac.uk)

Barba-Brioso, Cinta, University of Seville, Profesor García González, Dpto. Cristalografía, Mineralogía y Química Agrícola, Campus Reina Mercedes, Faculty of Chemistry, Seville, 41012, Spain, [cbarba@us.es](mailto:cbarba@us.es)

Baron, Fabien, Université de Poitiers, IC2MP-UMR 7285, 4 rue Michel Brunet, TSA 51106, Poitiers Cedex 9, 86073, France, [fabien.baron@univ-poitiers.fr](mailto:fabien.baron@univ-poitiers.fr)

Bauluz, Blanca, University of Zaragoza, Departamento de Ciencias de la Tierra, Pedro Cerbuna 12, Zaragoza, 50010, Spain, [bauluz@unizar.es](mailto:bauluz@unizar.es)

Beaufort, Daniel, University of Poitiers CNRS, IC2MP UMR 7285, 4 rue Michel Brunet TSA 51106, Bat B 27, Poitiers Cedex 9, 86073, France, [daniel.beaufort@univ-poitiers.fr](mailto:daniel.beaufort@univ-poitiers.fr)

Beharrell, Paul, Quantum Design Inc., 6325 Lusk Blvd, San Diego, 92121, USA, [paulb@qdusa.com](mailto:paulb@qdusa.com)

Bellezza, Marco, Laviosa Chimica Mineraria Spa, Via L. da Vinci 21, Livorno, 57123, Italy, [marco.bellezza@laviosa.com](mailto:marco.bellezza@laviosa.com)

Belmonte, Louise Josefine, DTU, Brovej bygn. 118, Kgs. Lyngby, 2800, Denmark, [lojon@byg.dtu.dk](mailto:lojon@byg.dtu.dk)

Bender Koch, Christian, University of Copenhagen, Department of Chemistry, Universitetsparken 5, Copenhagen, 2100, Denmark, [cbk@chem.ku.dk](mailto:cbk@chem.ku.dk)

Benitez Perez, Jose Manuel, Geology - University of Salamanca, Fac. Ciencias, Pza de los Caidos s/n, Salamanca, 37008, Spain, [jgbckp1@gmail.com](mailto:jgbckp1@gmail.com)

Bergaya, Faiza, CNRS, 1B Rue de la férollerie, Orleans, 45100, France, [f.bergaya@cnrs-orleans.fr](mailto:f.bergaya@cnrs-orleans.fr)

Berti, Debora, Texas A&M University, 4304 Odell Lane, College Station, 77845, USA, [debora-berti@email.tamu.edu](mailto:debora-berti@email.tamu.edu)

Bertier, Pieter, RWTH-Aachen University, Clay and interface Mineralogy, Bunsenstrasse 8, Aachen, 52072, Germany, [Pieter.Bertier@emr.rwth-aachen.de](mailto:Pieter.Bertier@emr.rwth-aachen.de)

Bertolino, Silvana, IFEG-CONICET, Cordoba, 4036, Argentina, [silvanarbertolino@gmail.com](mailto:silvanarbertolino@gmail.com)

Betulius, Joe, Profile Products LLC, 750 Lake Cook Road, Suite 440, Buffalo Grove, 60089, USA, [jbetulius@profileproducts.com](mailto:jbetulius@profileproducts.com)

Biasci, Andrea, Laviosa Chimica Mineraria Spa, Via L. da Vinci 21, Livorno, 57123, Italy, [andrea.biasci@laviosa.com](mailto:andrea.biasci@laviosa.com)

Biernacka, Julita, University of Poznan, Institute of Geology, Makow Polnych 16, Poznan, 61-606, Poland, [julbier@amu.edu.pl](mailto:julbier@amu.edu.pl)

Billon, Sophie, Université de Poitiers, rue Michel Brunet, Batiment 35, Poitiers, 86000, France, [sophie.billon@univ-poitiers.fr](mailto:sophie.billon@univ-poitiers.fr)

## DELEGATE LIST

- Bish, David, Indiana University, Department of Geological Sciences, 1001 E. 10th St., Bloomington, 47401, USA, [bish@indiana.edu](mailto:bish@indiana.edu)
- Bishop, Janice, SETI Institute, 189 Bernardo Avenue, Mountain View, 94043, USA, [jbishop@seti.org](mailto:jbishop@seti.org)
- Bisset, Yvonne, Core Specialist Services Ltd, Brathens Eco Business Park, Glassel, Aberdeenshire, AB31 4BW, United Kingdom, [accounts@core-specialist-services.com](mailto:accounts@core-specialist-services.com)
- Biwswas, Bhabananda, CERAR/University of South Australia, Building X, CERAR, University Parade, Mawson Lakes, 5095, Australia, [bhabananda.biswas@mymail.unisa.edu.au](mailto:bhabananda.biswas@mymail.unisa.edu.au)
- Bizovská, Valéria, Institute of Inorganic Chemistry, Slovak Academy of Sciences, Dúbravská cesta 9, Bratislava, 84536, Slovakia, [valeria.bizovska@savba.sk](mailto:valeria.bizovska@savba.sk)
- Black, Tim, Sietronics Pty Ltd, 11 Cheney Place, Mitchell ACT, Canberra, 2911, Australia, [tim.black@sietronics.com.au](mailto:tim.black@sietronics.com.au)
- Blackbourn, Graham, Blackbourn Geoconsulting, 26 East Pier Street, Bo'ness, EH51 9SN, United Kingdom, [graham@blackbourn.co.uk](mailto:graham@blackbourn.co.uk)
- Block, Karin, City College of New York, Earth and Atmospheric Sciences, 160 Convent Avenue, New York, 10031, USA, [kblock@ccny.cuny.edu](mailto:kblock@ccny.cuny.edu)
- Boek, Edo, Department of Chemical Engineering, Imperial College London, London SW7 2AZ, UK, [e.boek@imperial.ac.uk](mailto:e.boek@imperial.ac.uk)
- Boles, Austin, University of Michigan, Ann Arbor, 1100 North University Ave., Ann Arbor, 48109, USA, [aboles@umich.edu](mailto:aboles@umich.edu)
- Bosshardt, Darryl, Redmond, 475 W 910 S, Herber City, 84032, USA, [darrylb@realsalt.com](mailto:darrylb@realsalt.com)
- Bovet, Nicolas, University of Copenhagen, Universitetsparken, 5, Nano-Science Center, Copenhagen, 2100, Denmark, [bovet@nano.ku.dk](mailto:bovet@nano.ku.dk)
- Bower, William, University of Manchester, Research Centre for Radwaste Disposal, Williamson Building, School of Earth Science, Oxford Road, Manchester, M13 9PL, United Kingdom, [william.bower@postgrad.manchester.ac.uk](mailto:william.bower@postgrad.manchester.ac.uk)
- Boyer, Laurence, Imerys Mineral Limited, Higher Brocks Plantation, Old Newton Road, Newton Abbot, TQ12 6QZ, United Kingdom, [laurence.boyer@imerys.com](mailto:laurence.boyer@imerys.com)
- Breen, Chris, Sheffield Hallam University, City Campus, Howard Street, Sheffield, S1 1WB, United Kingdom, [c.breen@shu.ac.uk](mailto:c.breen@shu.ac.uk)
- Brendle, Jocelyne, Pôle Matériaux à Porosité Contrôlée, Institut de Science des Matériaux de Mulhouse, UMR CNRS 7361, Université de Strasbourg-Université de Mulhouse, 15 rue Jean Stracky, Mulhouse, 680057, France, [jocelyne.brendle@uha.fr](mailto:jocelyne.brendle@uha.fr)
- Breu, Josef, University of Bayreuth, Inorganic Chemistry, Universitätsstr. 30, Bayreuth, 95440, Germany, [josef.breu@uni-bayreuth.de](mailto:josef.breu@uni-bayreuth.de)
- Buatier, Martine, ChronoEnvironnement Université de Franche Comté, 13 Route de Gray, Besançon, 25030, France, [martine.buatier@univ-fcomte.fr](mailto:martine.buatier@univ-fcomte.fr)
- Bujdák, Juraj, Institute of Inorganic Chemistry, Slovak Academy of Sciences, Dúbravská cesta 9, Bratislava, 84536, Slovakia, [bujdak@fns.uniba.sk](mailto:bujdak@fns.uniba.sk)
- Burlakovs, Juris, University of Latvia, Prusu str 22/4-9, Riga, LV-1057, Latvia, [juris@geo-it.lv](mailto:juris@geo-it.lv)
- ### C
- Cai, Yuanfeng, Nanjing University, School of Earth Sciences and Engineering, Nanjing, 210046, China, [caiyf@nju.edu.cn](mailto:caiyf@nju.edu.cn)
- Calvin, Chistina, Schlumberger, 1325 S Dairy Ashford, Houston, 77057, USA, [ccalvin@slb.com](mailto:ccalvin@slb.com)
- Campbell, Linda S., University of Manchester, School of Earth, Atmospheric & Environmental Sciences, Oxford Road, Manchester, M13 9PL, United Kingdom, [Linda.Campbell@manchester.ac.uk](mailto:Linda.Campbell@manchester.ac.uk)
- Canico, Ana, Geobiotec Research Centre, Univ. Aveiro, Campo de Santiago, Aveiro, 3810-193, Portugal, [canico.ana@ugmail.com](mailto:canico.ana@ugmail.com)
- Cappelletti, Piergiulio, Università Federico II di Napoli, Dipartimento de Scienze della Terra, Dell' Ambiente e delle Risorse, Via Mezzocannone 8, I-80138, Italy, [piergiulio.cappelletti@unina.it](mailto:piergiulio.cappelletti@unina.it)
- Celejewski, Magda, University of New Brunswick, Department of Earth Sciences, Rm. 112, Bailey Dr., Fredericton, NB, E3B 1W4, Canada, [m.celejewski@unb.ca](mailto:m.celejewski@unb.ca)
- Cengiz, Ozgur, Afyon Kocatepe University, ANS Kampus Faculty of Fine Arts Dept. of Ceramics, Zafer Mah Levent Sok No:22/3 03100, Afyonkarahisar, 03200, Turkey, [ocengiz1@gmail.com](mailto:ocengiz1@gmail.com)
- Cervini-Silva, Javiera, Universidad Autonoma Metropolitana, Av. Vasco de Quiroga 4871, Col. Santa Fe, Del. Cuajimalpa, Ciudad de Mexico, 5348, Mexico, [icervini@correo.cua.uam.mx](mailto:icervini@correo.cua.uam.mx)
- Cesarano, Mara, Università degli Studi di Napoli Federico II, Via Mezzocannone 8, 80134, Italy, [mara.cesarano@unina.it](mailto:mara.cesarano@unina.it)
- Chakraborty, Argha, University of South Australia, 362 Nayabad, North Jadavpur, Kolkata, 700094, India, [argha.chakra@gmail.com](mailto:argha.chakra@gmail.com)
- Chemeda, Yadeta, IMN- IFSTTAR, 2 rue de la Houssiniere, Nantes, 44322, France, [yadeta.chemeda@cirs-irn.fr](mailto:yadeta.chemeda@cirs-irn.fr)
- Chiou, Wen-An, University of Maryland, NISP Lab, NanoCenter, 1234 Kim Building, College Park, 20742-2831, USA, [wachiou@umd.edu](mailto:wachiou@umd.edu)
- Chlimintzas, Georgios, OTM S.A. Engineering Consulting Co., Koumarianou 6-8, off Plapouta Str., Athens, 11473, Greece, [gchlimintzas@tee.gr](mailto:gchlimintzas@tee.gr)
- Cho, Hyen Goo, Gyeongsang National University, 500-1 Jinjudaero, room 204 Building 354, Jinju, 660-701, Republic of Korea, [hgcho@gsnu.ac.kr](mailto:hgcho@gsnu.ac.kr)
- Choi, J. Yoon, Korea Conformity Laboratories, 73 Yangcheon 3-gil, Cheongwon-gu, 363-883, Korea, [j.yoon.choi@kcl.re.kr](mailto:j.yoon.choi@kcl.re.kr)
- Choi, Woohyun, Yonsei University, 173 Baekryeonsan-ro, 501 Seoan ACE apt, Seoul, 122-906, Korea, [choi1005414@naver.com](mailto:choi1005414@naver.com)
- Choulet, Flavien, Université de Franche-Comté, 16 route de Gray, Besançon, 25030, France, [flavien.choulet@univ-fcomte.fr](mailto:flavien.choulet@univ-fcomte.fr)

## DELEGATE LIST

- Choy, Jin-Ho, Center for Intelligent Nano-Bio Materials (CINBM), Department of Chemistry and Nano Science, EWHA WOMANS UNIVERSITY, 52, Ewhayeoadae-gil, Seodaemun-gu, Seoul, 120-750, South Korea, [jhchoy@ewha.ac.kr](mailto:jhchoy@ewha.ac.kr)
- Christidis, George, Technical University of Crete, School of Minerals Resources Engineering, University Campus, Chania, 73100, Greece, [christid@mred.tuc.gr](mailto:christid@mred.tuc.gr)
- Chryssikos, Georgios D., National Hellenic Research Foundation, 48, Vass Constantinou Ave, Athens, 11635, Greece, [gdchryss@eie.gr](mailto:gdchryss@eie.gr)
- Chung, Dong Hun, Yonsei Univ, Seoul, 120-749, Korea, [dongh21@nate.com](mailto:dongh21@nate.com)
- Ciotonea, Carmen, University of Poitiers / CNRS IC2MP, UMR 7285 IC2MP, B27 4 rue Michel BRUNET, TSA 51106, Poitiers, 86073, France, [carmen.ciotonea@univ-poitiers.fr](mailto:carmen.ciotonea@univ-poitiers.fr)
- Clarkson, Christopher R., University of Calgary, 2500 University Drive Northwest Calgary, Alberta, T2N 1N4, Canada, [clarksoc@ucalgary.ca](mailto:clarksoc@ucalgary.ca)
- Claudio, Geloni, San Donato Milanese, Via Maritano 26, Milan, 20097, Italy, [claudio.geloni@eni.com](mailto:claudio.geloni@eni.com)
- Clegg, Francis, Sheffield Hallam University, Howard Street, Sheffield, S1 1WB, United Kingdom, [f.clegg@shu.ac.uk](mailto:f.clegg@shu.ac.uk)
- Colmenero, Francisco, CSIC, C/Serrano 113 Bis, Madrid, 28006, Spain, [francisco.colmenero@iem.cfmac.csic.es](mailto:francisco.colmenero@iem.cfmac.csic.es)
- Cornejo, Juan, Real Academia Sevillana de Ciencias, Ed. Jose Manuel Lara 1-1ªA, Sevilla, 41013, Spain, [cornejo@irnase.csic.es](mailto:cornejo@irnase.csic.es)
- Coveney, Peter, University College London, 20 Gordon Street, London, WC1H 0AJ, United Kingdom, [p.v.coveney@ucl.ac.uk](mailto:p.v.coveney@ucl.ac.uk)
- Cuadros, Javier, Natural History Museum, London, Cromwell Road, London, SW7 5BD, United Kingdom, [j.cuadros@nhm.ac.uk](mailto:j.cuadros@nhm.ac.uk)
- Cubillas, Pablo, Durham University, Department of Earth Sciences, Mountjoy Site, South Road, Durham, DH1 3LE, United Kingdom, [pablo.cubillas@durham.ac.uk](mailto:pablo.cubillas@durham.ac.uk)
- Cygan, Randall, Sandia National Laboratories, Department of Geochemistry, P O BOX 5800, New Mexico, Albuquerque, 87185-0754, USA, [rtcyan@sandia.gov](mailto:rtcyan@sandia.gov)
- D**
- Daab, Matthias, University of Bayreuth, Department of Anorganic Chemistry I, Universitätsstr.30, Bayreuth, 95447, Germany, [matthiasdaab@web.de](mailto:matthiasdaab@web.de)
- Darder, Margarita, ICMM-CSIC, C/ Sor Juana Inés de la Cruz 3, Madrid, 28049, Spain, [darder@icmm.csic.es](mailto:darder@icmm.csic.es)
- Dathe, Wilfried, Heck Bio-Pharma GmbH, Hegelstraße 73, Halle (Saale), 6114, Germany, [daweidoc@gmx.de](mailto:daweidoc@gmx.de)
- Day-Stirrat, Ruarri, Shell International E&P Inc, STCH, 3333 Highway 6 South, R1004b, Houston, 77082, USA, [ruarri.day-stirrat@shell.com](mailto:ruarri.day-stirrat@shell.com)
- Delgado, Joaquín, CIMA. University of Algarve, Edifício 7, Campus Universitário de Gambelas, Faro, 8005-139, Portugal, [jdrodriguez@ualg.pt](mailto:jdrodriguez@ualg.pt)
- Demirkiran, Ali R., Univ of Bingol/Univ of Wolverhampton, Faculty of Agriculture, Department of Soil Science and Plant Nutrition, Bingol, Turkey, [ademirkiran2000@gmail.com](mailto:ademirkiran2000@gmail.com)
- Deneele, Dimitrios, IMN- IFSTTAR, 2 rue de la Houssiniere, Nantes, 44322, France, [dimitri.deneele@cnrs-imn.fr](mailto:dimitri.deneele@cnrs-imn.fr)
- Deng, Youjun, Texas A&M University, Department of Soil and Crop Sciences, College Station, Texas, 77843-2474, USA, [yjd@tamu.edu](mailto:yjd@tamu.edu)
- Derkowski, Arkadiusz (Arek), Institute of Geological Sciences Polish Academy of Sciences, Senacka 1, Krakow, 31-002, Poland, [ndderkow@cyf-kr.edu.pl](mailto:ndderkow@cyf-kr.edu.pl)
- Detellier, Christian, University of Ottawa, Department of Chemistry, 10 Marie-Curie, Ottawa, Ontario, K1N 6NS, Canada, [dete@uottawa.ca](mailto:dete@uottawa.ca)
- Di Bitetto, Arnaud, Lorraine University/L.C.P.M.E., 405 rue de Vandoeuvre, Villers-les-Nancy, 54602, France, [arnaud.di-bitetto@univ-lorraine.fr](mailto:arnaud.di-bitetto@univ-lorraine.fr)
- Di Leo, Paola, Institute for Environmental Analyses, National Research Council, Via S. Loja, Zona Ind.le, Tito Scalo (PZ), 85050, Italy, [pdileo@imaa.cnr.it](mailto:pdileo@imaa.cnr.it)
- Dick, Pierre, IRSN, BP 17, Fontenay-aux-Roses, 92262, France, [pierre.dick@irsn.fr](mailto:pierre.dick@irsn.fr)
- Diedel, Ralf, Research Institute of inorganic Materials - Glass/Ceramics, Heinrich-Meister-Str.2, Höhr-Grnezhhausen, 56203, Germany, [ralf.diedel@fgk-keramik.de](mailto:ralf.diedel@fgk-keramik.de)
- Dietel, Jan, BGR Hannover, Stilleweg 2, Hannover, 30655, Germany, [jandietel@gmx.de](mailto:jandietel@gmx.de)
- Dohrmann, Reiner, LBEG/BGR, Stilleweg 2, Hannover, 30655, Germany, [Reiner.Dohrmann@lbeg.niedersachsen.de](mailto:Reiner.Dohrmann@lbeg.niedersachsen.de)
- Donahoe, Rona, University of Alabama, Dept. of Geological Sciences, 2003 Bevill Building, Tuscaloosa, 35487-0338, USA, [rdonahoe@ua.edu](mailto:rdonahoe@ua.edu)
- Dondi, Michele, CNR-ISTEC, Via Granarolo 64, Faenza, 48018, Italy, [michele.dondi@istec.cnr.it](mailto:michele.dondi@istec.cnr.it)
- Dong, Tian, University of Alberta, Department of Earth and Atmospheric Sciences, Edmonton, T6E 2N1, Canada, [td2@ualberta.ca](mailto:td2@ualberta.ca)
- Dorn, Alevtina, Ichron (part of the RPS Group), Century House, Gadbrook Business Centre, Northwich, CW9 7TL, United Kingdom, [alevtina.dorn@rpsgroup.com](mailto:alevtina.dorn@rpsgroup.com)
- dos Santos Guimarães, Vanessa, Geobiotec, Departamento de Geociências da Universidade de Aveiro, Campus de Santiago, Aveiro, 3810-193, Portugal, [quimavs@gmail.com](mailto:quimavs@gmail.com)
- Dousova, Barbara, University of Chemistry and Technology Prague, Technicka 5, Prauge 6, 166 28, Czech Republic, [Barbora.Dousova@vscht.cz](mailto:Barbora.Dousova@vscht.cz)
- Duclaux, Laurent, University Savoie Mont Blanc, LCME, Campus de Savoie Technolac, Le Bourget du Lac, 73376, France, [laurent.duclaux@univ-savoie.fr](mailto:laurent.duclaux@univ-savoie.fr)
- Dumas, Angela, GET- Université Paul Sabatier, 3 rue Milhes, Toulouse, 31300, France, [dumangela@hotmail.fr](mailto:dumangela@hotmail.fr)
- Dumon, Mathijs, Ghent University, Krijgslaan 281/S8 WE13, Gent, 9000, Belgium, [mathijs.dumon@ugent.be](mailto:mathijs.dumon@ugent.be)
- Dzene, Liva, University of Poitiers / CNRS IC2MP, 5 rue Albert Turpain, Bât. B8, TSA 51106, Poitiers, 86073, France, [liva.dzene@univ-poitiers.fr](mailto:liva.dzene@univ-poitiers.fr)
- Eguchi, Miharuru, National Institute for Materials Science, 1-1 Namiki, Tsukuba, Ibaraki, 305-0044, Japan, [EGUCHI.Miharuru@nims.go.jp](mailto:EGUCHI.Miharuru@nims.go.jp)

## DELEGATE LIST

El Ouahabi, Meriam, University of Liège, Department of Geology, Bat. 18., Boulevard de Rectorat, Allée du 6 Aout, Sart-Tilman, 4000, Belgium, [Meriam.elouahabi@ulg.ac.be](mailto:Meriam.elouahabi@ulg.ac.be)

### E

Elliott, Crawford, Georgia State University, Geosciences, Atlanta, 30302, USA, [wcelliott@gsu.edu](mailto:wcelliott@gsu.edu)

Elmi, Chiara, viale del Sagittario Trav. G51, Modena, 41126, Italy, [chiara.elmi@alice.it](mailto:chiara.elmi@alice.it)

Emmerich, Katja, Karlsruhe Institute of Technology, H.v Helmholtz Platz 1, Eggenstein, Leopoldshafen, 76344, Germany, [katja.emmerich@kit.edu](mailto:katja.emmerich@kit.edu)

Erastova, Valentina, Durham University, Department of Earth Sciences, Mountjoy Site, South Road, Durham, DH1 3LE, United Kingdom, [valentina.erastova@durham.ac.uk](mailto:valentina.erastova@durham.ac.uk)

Eriksson, Ann Kristin, Swedish University of Agricultural Sciences, Dep. soil and environment, Box 7014, Uppsala, S-750 07, Sweden, [ann.kristin.eriksson@slu.se](mailto:ann.kristin.eriksson@slu.se)

Erkoyun, Hülya, Eskişehir Osmangazi University, Department of Geological Engineering, Eskişehir, TR-26480, Turkey, [herkoyun@ogu.edu.tr](mailto:herkoyun@ogu.edu.tr)

Ernich, Martin, X-Ray Laboratory, Am Kandelborn 7, Reinheim, D-64354, Germany, [roentgenlabor-dr.ernich@t-online.de](mailto:roentgenlabor-dr.ernich@t-online.de)

### F

Fafard, Jonathan, University of Ottawa, 10 Marie Curie, Ottawa, K1N 6N5, Canada, [jfafard.uottawa@gmail.com](mailto:jfafard.uottawa@gmail.com)

Fahel, Jean, Lorraine university/L.C.P.M.E, 405 rue de vandoeuvre, Villers-Les-Nancy, 54600, France, [jean.fahel@univ-lorraine.fr](mailto:jean.fahel@univ-lorraine.fr)

Fernández Díaz, Ana María, CIEMAT, CIEMAT. Ed. 19., Avda./ Complutense 40, Madrid, 28040, Spain, [anamaria.fernandez@ciemat.es](mailto:anamaria.fernandez@ciemat.es)

Fernández-Barranco, Cristina, University of Jaén and CEACTierra, University of Jaen, Campus Las Lagunillas s/n, Jaén, 23071, Spain, [cfernand@ujaen.es](mailto:cfernand@ujaen.es)

Ferrage, Eric, University of Poitiers / CNRS IC2MP, UMR 7285 IC2MP, B27 4 rue Michel BRUNET, TSA 51106, Poitiers, 86073, France, [eric.ferrage@univ-poitiers.fr](mailto:eric.ferrage@univ-poitiers.fr)

Ferrell, Ray, LSU, Geology and Geophysics, 595 Maxine Drive, Baton Rouge, Louisiana, 70808, USA, [rayferrell@cox.net](mailto:rayferrell@cox.net)

Fialips, Claire, Total.S.A, CSTJF, Avenue Larribau, Pau, 64018, France, [claire.fialips@total.com](mailto:claire.fialips@total.com)

Fiore, Saverio, Institute of Methodologies for Environmental Analysis, C.da S. Loja, Potenza, 85050, Italy, [saverio.fiore@cnr.it](mailto:saverio.fiore@cnr.it)

Fitch, Alanah, Loyola University, Department of Chemistry, 1032 W.Sheridan Road, Chicago, 60626, USA, [afitch@luc.edu](mailto:afitch@luc.edu)

Fleury, Marc, IFPEN, 1 avenue de Bois-Preau, Rueil Malmaison, 92851, France, [marc.fleury@ifpen.fr](mailto:marc.fleury@ifpen.fr)

Fontaine, Francois, Ulg, rue basse, 122, 5020, Belgium, [f.fontaine@ulg.ac.be](mailto:f.fontaine@ulg.ac.be)

Forano, Claude, Institute of Chemistry of Clermont-ferrand - CNRS - BlaisePascal University, Campus des Cézeaux, 24 Avenue des Landais, BP 80026, Aubiere, 63171, France, [claude.forano@univ-bpclermont.fr](mailto:claude.forano@univ-bpclermont.fr)

Fraser Harris, Andrew, University of Edinburgh, School of Geosciences, The Grant Institute, James Hutton Road, Edinburgh, EH9 3FE, United Kingdom, [a.p.fraser-harris@ed.ac.uk](mailto:a.p.fraser-harris@ed.ac.uk)

Fraser, Donald G., University of Oxford, Department of Earth Sciences, South Parks Road, Oxford, OX1 3PR, United Kingdom, [don@earth.ox.ac.uk](mailto:don@earth.ox.ac.uk)

Freiburg, Jared, Illinois State University, 615 E.Peabody Dr, Champaign, 61820-6918, USA, [freiburg@illinois.edu](mailto:freiburg@illinois.edu)

Friedrich, Frank, Karlsruhe Institute of Technology, Hermann-von-Helmholtz-Platz 1, Eggenstein-Leopoldshafen, 76344, Germany, [frank.friedrich@kit.edu](mailto:frank.friedrich@kit.edu)

Fronczyk, Joanna, Warsaw University of Life Science - SGGW, Nowoursynowska 166, Warsaw, 02-787, Poland, [joanna\\_fronczyk@sggw.pl](mailto:joanna_fronczyk@sggw.pl)

Frushour, Anthony, Indiana University - Bloomington, Geological Sciences, 1001 East 10th Street, Bloomington, 47405, USA, [afrushou@indiana.edu](mailto:afrushou@indiana.edu)

Fujii, Kazuko, 1-1 Namiki, Tsukuba, 305-0044, Japan, [fujii.kazuko@nims.go.jp](mailto:fujii.kazuko@nims.go.jp)

Fürychová, Petra, Department of Geological Sciences, Masaryk university, Kotlářská 2, Brno, 61137, Czech Republic, [326141@mail.muni.cz](mailto:326141@mail.muni.cz)

### G

Gadsdon, Martyn, Imerys Mineral Limited, Higher Brocks Plantation, Teigngrace, Newton Abbot, TQ12 6QZ, United Kingdom, [martyn.gadsdon@imerys.com](mailto:martyn.gadsdon@imerys.com)

Galán, Emilio, University of Seville, Dpto. Cristalografía, Mineralogía y Q. A., Facultad de Química, C/Prof. García González nº1, Sevilla, 41012, Spain, [egalan@us.es](mailto:egalan@us.es)

Gao, Jun, China University of Geosciences, School of Water Resources and Environment, 29 Xueyuan Road, Haidian District, Beijing, 100083, China, [gjun@cugb.edu.cn](mailto:gjun@cugb.edu.cn)

García-Romero, Emilia, Universidad Complutense, C/ Jose Antonio Novais, 12, Madrid, 28040, Spain, [mromero@ucm.es](mailto:mromero@ucm.es)

Gatari Gichuru, Michael, University of Nairobi, Institute of Nuclear Science and Technology, P O BOX 30197-00100, Nairobi, 00100, Kenya, [gatarimj@gmail.com](mailto:gatarimj@gmail.com)

Gates, Will, SmecTech Research Consulting, 24 Chapel road, Moorabin, Victoria, Australia, [gateswp@smectech.com.au](mailto:gateswp@smectech.com.au)

Genin, Jean-Marie, ESSTIN - Université de Lorraine, 2 rue Jean Lamour, Vandoeuvre les Nancy, 54500, France, [jean-marie.genin@univ-lorraine.fr](mailto:jean-marie.genin@univ-lorraine.fr)

Gergely, Felician, Konkaly-Thege Street 29-33, H-1211, Hungary, [gergely.felician@energia.mta.hu](mailto:gergely.felician@energia.mta.hu)

Gier, Susanne, University of Vienna, Althanstrasse 14, Vienna, 1090, Austria, [susanne.gier@univie.ac.at](mailto:susanne.gier@univie.ac.at)

Gilbert, Benjamin, Lawrence Berkeley National Laboratory, 1 Cyclotron Road, MS 74R314C, Berkeley, 94720, USA, [bgilbert@lbl.gov](mailto:bgilbert@lbl.gov)

## DELEGATE LIST

- Gilg, H. Albert, Technische Universität München, Lehrstuhl für Ingenieurgeologie, Arcisstr. 21, Munich, 80333, Germany, [agilg@tum.de](mailto:agilg@tum.de)
- Gilkes, Bob, University of Western Australia, School of Earth and Environment, Stirling Highway, Nedlands, 6009, Australia, [bob.gilkes@uwa.edu.au](mailto:bob.gilkes@uwa.edu.au)
- Ginzel, Stefan, Research Institute of inorganic Materials - Glass/Ceramics, Heinrich-Meister-Str.2, Höhr-Gmezhhausen, 56203, Germany, [stefan.ginzel@fgk-keramik.de](mailto:stefan.ginzel@fgk-keramik.de)
- Gionis, Vassilis, National Hellenic Research Foundation / Theoretical & Physical Chemistry Institute, 48, Vas. Constantinou Ave., Athens, 11635, Greece, [vgionis@eie.gr](mailto:vgionis@eie.gr)
- Glasmann, Reed, Willamette Geological Service, 31191 Peterson Road, Philomath, 97370, USA, [wgsclays@yahoo.com](mailto:wgsclays@yahoo.com)
- Goh, Tee Boon, University of Manitoba, Dept. of Soil Science, Winnipeg, R3T 2N2, Canada, [gohtb@umanitoba.ca](mailto:gohtb@umanitoba.ca)
- Gonzalez, Rosalina, La Salle University, Carrera 2 # 10-70, Bogotá, 1100821, Colombia, [rogonzalez@unisalle.edu.co](mailto:rogonzalez@unisalle.edu.co)
- Gorniak, Katarzyna, [gorniak@agh.edu.pl](mailto:gorniak@agh.edu.pl)
- Grathoff, Georg, University of Greifswald, I. Geologie, FL Jahnstr. 17a, Greifswald, D17489, Germany, [Grathoff@uni-greifswald.de](mailto:Grathoff@uni-greifswald.de)
- Gray, Mary, Clay Minerals Society America, 13802 Laurel Rock Ct, Clifton, Virginia, 20124, USA, [cms@clays.org](mailto:cms@clays.org)
- Gray, Nia, The James Hutton Institute, Craigiebuckler, Aberdeen, AB15 8QH, United Kingdom, [nia.gray@hutton.ac.uk](mailto:nia.gray@hutton.ac.uk)
- Gray, Nia, The James Hutton Institute, Craigiebuckler, Aberdeen, AB15 8QH, United Kingdom, [Nia.Gray@hutton.ac.uk](mailto:Nia.Gray@hutton.ac.uk)
- Greathouse, Jeffery, Sandia National Laboratories, Geochemistry Department, PO Box 5800, MS 0754, Albuquerque, 87185-0754, USA, [jagreat@sandia.gov](mailto:jagreat@sandia.gov)
- Greenwell, Chris, Durham University, Department of Earth Sciences, Mountjoy Site, South Road, Durham, DH1 3LE, United Kingdom, [chris.greenwell@durham.ac.uk](mailto:chris.greenwell@durham.ac.uk)
- Grew, Edward, University of Maine, School of Earth and Climate Sciences, 5790 Bryand Global Science Centre, Orono, 04469, USA, [esgrew@maine.edu](mailto:esgrew@maine.edu)
- Grew, Priscilla, University of Nebraska-Lincoln, 307 Morrill Hall, State Museum UNL, Lincoln, 68588-0338, USA, [pgrew1@unl.edu](mailto:pgrew1@unl.edu)
- Grings Cedeño, Daniel, UFRGS-Universidade Federal do Rio Grande do Sul, Fernandes Vieira St., 370, Ap. 202, Porto Alegre, 90035090, Brazil, [daniel.gringscedeno@gmail.com](mailto:daniel.gringscedeno@gmail.com)
- Grolimund, Daniel, Paul Scherrer Institute, Swiss Light Source, microXAS Beamline Project, Villigen PSI, CH-5232, Switzerland, [daniel.grolimund@psi.ch](mailto:daniel.grolimund@psi.ch)
- Guggenheim, Stephen, Univ. of Illinois at Chicago, Dept. of Earth & Environmental Sciences, 845 W. Taylor St, m/c 186, Chicago, IL, 60607-7056, USA, [xtal@uic.edu](mailto:xtal@uic.edu)
- Guimarães da Silva, Raquel, Universidade de Brasília, SHIN QI 13 cj 01 casa 08, Brasília, 71535-010, Brazil, [raquelguimaraes123@gmail.com](mailto:raquelguimaraes123@gmail.com)
- Guimarães, Edi, Universidade de Brasília, SHIN QI 13 cj 01 casa 08, Instituto Geociências UnB Campus Darcy Ribeiro, Brasília, 71535-010, Brazil, [rxedi@unb.br](mailto:rxedi@unb.br)
- ### H
- Ha, Jang-Hoon, Korea Institute of Materials Science, 797 Changwondaero, Seongsan-gu, Changwon, 642-831, Republic of Korea, [hjhoon@kims.re.kr](mailto:hjhoon@kims.re.kr)
- Haase, Hanna, Ruhr-Universität Bochum, Universitätsstraße 150, Bochum, 44780, Germany, [hanna.haase@rub.de](mailto:hanna.haase@rub.de)
- Habel, Christoph, Department of Anorganic Chemistry I, Universitätsstr.30, Bayreuth, 95447, Germany, [christophhabel20@googlemail.com](mailto:christophhabel20@googlemail.com)
- Haberlah, David, FEI Australia, 73 Northbourne Avenue, Canberra, 2600, Australia, [david.haberlah@fei.com](mailto:david.haberlah@fei.com)
- Haidon, Cheryl, University of Leicester, Bennett Building, University Road, Leicester, LE1 7RH, United Kingdom, [ch230@le.ac.uk](mailto:ch230@le.ac.uk)
- Hajjaji, Walid, Geobiotec Research Centre, Univ. Aveiro, Campo de Santiago, Aveiro, 3810-193, Portugal, [w.hajjaji@ua.pt](mailto:w.hajjaji@ua.pt)
- Hanusová, Irena, SÚRAO (Radioactive Waste Repository Authority), Dlážděná 6, Prague, 110 00, Czech Republic, [hanusova@suraoc.cz](mailto:hanusova@suraoc.cz)
- Harjupatana, Tero, University of Jyväskylä, Department of Physics, P.O. Box 35, FI-40014, Finland, [tero.t.harjupatana@jyu.fi](mailto:tero.t.harjupatana@jyu.fi)
- Harley, Simon, University of Edinburgh, School of Geosciences, Grant Institute, James Hutton Road, Edinburgh, EH9 3FE, United Kingdom, [simon.harley@ed.ac.uk](mailto:simon.harley@ed.ac.uk)
- Hart, Jarrod, Imerys, Par Moor Centre, Par Moor Road, Cornwall, PL25 2SQ, United Kingdom, [jarrod.hart@imerys.com](mailto:jarrod.hart@imerys.com)
- Hashizume, Hideo, National Institute for Materials Science, 1-1 Namiki, Tsukuba, 305-0044, Japan, [HASHIZUME.Hideo@nims.go.jp](mailto:HASHIZUME.Hideo@nims.go.jp)
- Haurine, Frederic, CTMNC, 17 rue Letellier, Service Ceramique, Paris, 75015, France, [frederic.haurine@mines-paristech.fr](mailto:frederic.haurine@mines-paristech.fr)
- Haynes, Haydn, University of Manchester, 39 Landcross Road, Fallowfield, Manchester, M14 6LZ, United Kingdom, [haydn.haynes@postgrad.manchester.ac.uk](mailto:haydn.haynes@postgrad.manchester.ac.uk)
- Hermosin, M. Carmen, IRNAS-CSIC, Instituto de Recursos Naturales y Agrobiología de Sevilla, Consejo Superior de Investigaciones Científicas, Avda. Reina Mercedes Nº 10, Sevilla, 41012, Spain, [mchermosin@irnase.csic.es](mailto:mchermosin@irnase.csic.es)
- Hernández Puentes, Pilar, University of Jaén, Department of Geology. CEACTierra., IACT partner unit (CSIC-UGR). Faculty of Experimental Sciences, Campus Las Lagunillas s / n, building B3, Jaén, 23071, Spain, [ppuentes@ujaen.es](mailto:ppuentes@ujaen.es)
- Hertam, Anke, TU Bergakademie Freiberg, Leipziger Strasse 29, Freiberg, 9599, Germany, [anke.hertam@chemie.tu-freiberg.de](mailto:anke.hertam@chemie.tu-freiberg.de)
- Hillier, Stephen, The James Hutton Institute, Craigiebuckler, Aberdeen, AB15 8QH, United Kingdom, [stephen.hillier@hutton.ac.uk](mailto:stephen.hillier@hutton.ac.uk)



## DELEGATE LIST

Hlekane, Phindile, University of Johannesburg, Department of Metallurgy, School of Mining, Metallurgy and Chemical Engineering, Faculty of Engineering and Built Environment, Johannesburg, South Africa, [p.hlekane@gmail.com](mailto:p.hlekane@gmail.com)

Hohmann, Marc, Weimar, Cranachstr. 12, Weimar, 99423, Germany, [hohmann-weimar@t-online.de](mailto:hohmann-weimar@t-online.de)

Holbeche, Georgina, University of Western Australia, 187A Thomas Street, Subiaco, Perth, 6008, Australia, [georgina.holbeche@uwa.edu.au](mailto:georgina.holbeche@uwa.edu.au)

Honty, Miroslav, SCK.CEN, Av Hermann Debroux 40, Brussels, 1160, Belgium, [mhonty@sckcen.be](mailto:mhonty@sckcen.be)

Houben, Maartje, Utrecht University, Budapestlaan 4, 3584 CD, The Netherlands, [m.e.houben@uu.nl](mailto:m.e.houben@uu.nl)

Hsu, Chun-Chun, Texas A&M University, 370 Olsen Blvd, TAMU MS 2474, College Station, TX, 77843-2474, USA, [chunchunhsu@tamu.edu](mailto:chunchunhsu@tamu.edu)

Hubert, Fabien, University of Poitiers / CNRS IC2MP, UMR 7285 IC2MP, B27 4 rue Michel BRUNET, TSA 51106, Poitiers, 86073, France, [fabien.hubert@univ-poitiers.fr](mailto:fabien.hubert@univ-poitiers.fr)

Huertas, F. Javier, CSIC-Univ. Granada, Instituto Andaluz de Ciencias de la Tierra, Avad. de las Palmeras 4, Armilla (Granada), E-18100, Spain, [javierhuertas@ugr.es](mailto:javierhuertas@ugr.es)

Huff, Anezka, [warren.huff@uc.edu](mailto:warren.huff@uc.edu)

Huff, Warren, University of Cincinnati, Department of Geology, 345 Clifton Court, Cincinnati, 45221, USA, [warren.huff@uc.edu](mailto:warren.huff@uc.edu)

Huggett, Jenny, Petroclays Ltd, The Oast, Sandy Cross, Heathfield, TN21 8QP, United Kingdom, [info@petroclays.com](mailto:info@petroclays.com)

Hughes, Martin, The Mineralogical Society, 12 Baylis Mews, Amyand Park Road, Twickenham, TW1 3HQ, United Kingdom, [admin@minersoc.org](mailto:admin@minersoc.org)

### I

Ide, Yusuke, National Institute for Materials Science, 1-1 Namiki, Tsukuba, 305-0044, Japan, [IDE.Yusuke@nims.go.jp](mailto:IDE.Yusuke@nims.go.jp)

Inoue, Atsuyuki, Chiba University, Department of Earth Sciences, 1-33, Yayoi-cho, Inage-ku, [atsuyuki\\_inoue@faculty.chiba-u.jp](mailto:atsuyuki_inoue@faculty.chiba-u.jp)

Isik, Eren, Dumlupinar University, Geological Engineering Depat, 43000, Turkey, [eren.isik@dpu.edu.tr](mailto:eren.isik@dpu.edu.tr)

Ito, Kenichi, University of Miyazaki, Center for International Relations, 1-1, Gakuenkibanadai-Nishi, Miyazaki, Miyazai, 889-2192, Japan, [itoken@cc.miyazaki-u.ac.jp](mailto:itoken@cc.miyazaki-u.ac.jp)

### J

Jaber, Maguy, Sorbonnes Universités, Univ Pierre et Marie Curie, Laboratoire d'Archéologie Moléculaire et Structurale, 4 place jussieu, Paris, 75005, France, [maguy.jaber@upmc.fr](mailto:maguy.jaber@upmc.fr)

Jackson, Cynthia, Georgia State University, 405 4th Street NE Apt 5, Atlanta, 30308, USA, [cynDIMJ@gmail.com](mailto:cynDIMJ@gmail.com)

Jacquet, Alain, Lafarge Centre de Recherche, 95 Rue du Montmurier, Saint Quentin Fallavier, 01600, France, [alain.jacquet@lafarge.com](mailto:alain.jacquet@lafarge.com)

Janek, Marián, Comenius University, Mlynská dolina Ch-1, SK-842 15, Slovakia, [marian.janek@fns.uniba.sk](mailto:marian.janek@fns.uniba.sk)

Janosik, Michal, Comenius University in Bratislava, Faculty of Natural Sciences, Department of Geology

of Mineral Deposits, Mlynská dolina, Bratislava, 84215, Slovakia, [mjanosik1@gmail.com](mailto:mjanosik1@gmail.com)

Jeans, Christopher, University of Cambridge, 10 Adams Road, Cambridge, CB3 9AD, United Kingdom, [cj302@cam.ac.uk](mailto:cj302@cam.ac.uk)

Jelavic, Stanislav, University of Copenhagen, Nano-Science Center, Universtitesparken, 5, C108, Copenhagen, 2100, Denmark, [stanislav.jelavic@nano.ku.dk](mailto:stanislav.jelavic@nano.ku.dk)

Johnston, Cliff, Purdue University, 915 W. State St, West Lafayette, IN, 47906, USA, [cliffjohnston@purdue.edu](mailto:cliffjohnston@purdue.edu)

Jones, Stacie, Ichron (part of the RPS Group), Century House, Gadbrook Business Centre, Northwich, CW9 7TL, United Kingdom, [stacie.jones@rpsgroup.com](mailto:stacie.jones@rpsgroup.com)

Jones, Stephen, X-ray Mineral Services Ltd, 1 Claughton Road, Colwyn Bay, LL29 7EF, United Kingdom, [steve@xrayminerals.co.uk](mailto:steve@xrayminerals.co.uk)

Jones, Timothy, Cardiff University, School of Earth and Ocean Sciences, Main Building, Park Place, Cardiff, CF10 3YE, United Kingdom, [jonestp@cf.ac.uk](mailto:jonestp@cf.ac.uk)

Jonkis, Urszula, Oil and Gas Institute; National Research Institute, 25A Lubicz St, Kraków, 31-503, Poland, [jonkis@inig.pl](mailto:jonkis@inig.pl)

Jozanikohan, Golnaz, University of Leeds, no 25 Skelton Terrace, Leeds, LS9 9ES, United Kingdom, [eej@leeds.ac.uk](mailto:eej@leeds.ac.uk)

### K

Kadir, Selahattin, Eskişehir Osmangazi University, Department of Geological Engineering, Meşelik, Eskişehir, TR-26480, Turkey, [skadir.euroclay@gmail.com](mailto:skadir.euroclay@gmail.com)

Kalinichev, Andrey, Ecole des Mines de Nantes - Laboratoire SUBATECH, 4 rue Alfred Kastler, La Chantrerie BP 20722, Nantes, 44307, France, [kalinich@subatech.in2p3.fr](mailto:kalinich@subatech.in2p3.fr)

Kameshima, Yoshikazu, Okayama University, 3-1-1 Tsushima-naka, Kita-ku, Okayama, 700-8530, Japan, [ykameshi@cc.okayama-u.ac.jp](mailto:ykameshi@cc.okayama-u.ac.jp)

Karan, Birgul, Hacettepe University, Department of Chemistry, Beytepe Campus, Ankara, 06800, Turkey, [bkaran@hacettepe.edu.tr](mailto:bkaran@hacettepe.edu.tr)

Kasama, Takeshi, Technical University of Denmark, Center for Electron Nanoscopy, Fysikvej, Kongens Lyngby, 2800, Denmark, [tk@cen.dtu.dk](mailto:tk@cen.dtu.dk)

Kaufhold, Stephan, BGR, Stilleweg 2, Stilleweg 2, Hanover, 30655, Germany, [s.kaufhold@bgr.de](mailto:s.kaufhold@bgr.de)

Kawamata, Jun, Yamaguchi University, Yoshida, Yamaguchi, 7538512, Japan, [j\\_kawa@yamaguchi-u.ac.jp](mailto:j_kawa@yamaguchi-u.ac.jp)

Kelm, Ursula, Universidad de Concepcion, GEA, Cabina 2, Barrio Universitario s/n, Concepcion, 0, Chile, [ukelm@udec.cl](mailto:ukelm@udec.cl)

Kemp, Simon, British Geological Survey, Environmental Science Centre, Keyworth, Nottingham, NG12 5GG, United Kingdom, [sjk@bgs.ac.uk](mailto:sjk@bgs.ac.uk)

Kenworthy, Sarah, The University of Manchester, 1.46 Williamson Building, SEAES, Oxford Road, Manchester, M13 9PL, United Kingdom, [sarah.kenworthy@postgrad.manchester.ac.uk](mailto:sarah.kenworthy@postgrad.manchester.ac.uk)

## DELEGATE LIST

- Kikuchi, Ryosuke, The University of Tokyo, 7-3-1 Hongo Bunkyo-ku, Tokyo, 113-0033, Japan, [rkikuchi@eps.s.u-tokyo.ac.jp](mailto:rkikuchi@eps.s.u-tokyo.ac.jp)
- Kim, Hyoung-Jun, Yonsei University, #327, Changjohall, Wonju, 220710, Korea, [hjun.kim@yonsei.ac.kr](mailto:hjun.kim@yonsei.ac.kr)
- Kim, Hyoung-Mi, Yonsei University, #327, Changjohall, Yonseidae-gil1, Heoungup-meon, Gangwon-do, Wonju-si, 220-710, Republic of Korea, [annabb@hanmail.net](mailto:annabb@hanmail.net)
- Kim, Jin-Wook, Yonsei University, 134 Shinchon-dong, Seodaemun-Gu, Seoul, 120-749, Republic of Korea, [jinwook@yonsei.ac.kr](mailto:jinwook@yonsei.ac.kr)
- Kirkpatrick, James, Michigan State University, Natural History Building, East Lansing, Michigan, 48864, USA, [rjkirk@msu.edu](mailto:rjkirk@msu.edu)
- Klaver, Jop, RWTH Aachen University, Geologie-Endogene Dynamik, Energy & Mineral Resources Group, Lochnerstrasse 4-20, Aachen, 52056, Germany, [jop.klaver@emr.rwth-aachen.de](mailto:jop.klaver@emr.rwth-aachen.de)
- Kleeberg, Reinhard, TU Bergakademie Freiberg, Brennhausgasse 14, Freiberg, D-09596, Germany, [kleeberg@mineral.tu-freiberg.de](mailto:kleeberg@mineral.tu-freiberg.de)
- Klinkenberg, Martina, Forschungszentrum Julich, Wilhelm-Johnen-Str, Julich, 52425, Germany, [m.klinkenberg@fz-juelich.de](mailto:m.klinkenberg@fz-juelich.de)
- Kogure, Toshihiro, University of Tokyo, 7-3-1 Hongo, Bunkyo-ku, Tokyo, 113-0033, Japan, [kogure@eps.s.u-tokyo.ac.jp](mailto:kogure@eps.s.u-tokyo.ac.jp)
- Kolousek, David, UCT Prague, Technická 5, Prauge 6, 166 28, Czech Republic, [koloused@vscht.cz](mailto:koloused@vscht.cz)
- Komadel, Peter, Institute of Inorganic Chemistry, Slovak Academy of Sciences, Dúbravská cesta 9, Bratislava, 84536, Slovakia, [peter.komadel@savba.sk](mailto:peter.komadel@savba.sk)
- Komar, Darja, University of Ljubljana, Faculty of Natural Sciences and Engineering, Aškerčeva 12, Ljubljana, 1000, Slovenia, [komar.darja@gmail.com](mailto:komar.darja@gmail.com)
- Koo, Tae-Hee, Yonsei University, 134 Shinchon-dong, Seodaemun-gu, Seoul, 120-749, Republic of Korea, [ktaehee@yonsei.ac.kr](mailto:ktaehee@yonsei.ac.kr)
- Köster, Mathias H., Technische Universität München, Lehrstuhl f. Ingenieurgeologie, Arcisstr. 21, Munich, 80333, Germany, [mathias.koester@tum.de](mailto:mathias.koester@tum.de)
- Koteja, Anna, AGH University of Science and Technology, ul. Mickiewicza 30, Krakow, 30059, Poland, [anna.koteja@gmail.com](mailto:anna.koteja@gmail.com)
- Kovanda, František, University of Chemistry and Technology, Prague, Technická 5, Prague, 166 28, Czech Republic, [Frantisek.Kovanda@vscht.cz](mailto:Frantisek.Kovanda@vscht.cz)
- Kovář, Petr, Charles University in Prague, Ke Karlovu 3, Prague, 12116, Czech Republic, [kovar@karlov.mff.cuni.cz](mailto:kovar@karlov.mff.cuni.cz)
- Kowalska, Sylwia, Oil and Gas Institute; National Research Institute, 25A Lubicz St, Kraków, 31-503, Poland, [kowalska@inig.pl](mailto:kowalska@inig.pl)
- Kralj, Polona, Geological Survey of Slovenia, Dimiceva 14, Ljubljana, 1500, Slovenia, [polona.kralj@geo-zs.si](mailto:polona.kralj@geo-zs.si)
- Krupskaya, Victoria, Staromonetnyi per., 35, Moscow, 119017, Russian Federation, [krupskaya@ruclay.com](mailto:krupskaya@ruclay.com)
- Kuligiewicz, Artur, Institute of Geological Sciences, Polish Academy of Sciences, Senacka 1, Krakow, 31-002, Poland, [ndkuligi@cyf-kr.edu.pl](mailto:ndkuligi@cyf-kr.edu.pl)
- Kumar, Vinay, Federal Institute for Geosciences and Natural Resources, Stilleweg 2, Hannover, 30453, Germany, [vinay.kumar@bgr.de](mailto:vinay.kumar@bgr.de)
- Kutlu, Sena Zeynep
- Kuznetsova, Elena, NTNU (Norwegian University of Science and Technology), Høgskoleringen 7A, Trondheim, NO-7465, Norway, [elena.kuznetsova@ntnu.no](mailto:elena.kuznetsova@ntnu.no)
- Kwon, Minjae, Korea Conformity Laboratories, 73 Yangcheong 3-gil, Cheongwon-gu, 363-883, Korea, [mj.kwon@kcl.re.kr](mailto:mj.kwon@kcl.re.kr)
- ### L
- Labille, Jérôme, CNRS/CEREGE, Europole Méditerranéen de l'Arbois, BP80, Aix en Provence, 13545, France, [labille@cerege.fr](mailto:labille@cerege.fr)
- Laine, Maxime, CEA/Saclay, DSM/IRAMIS/NIMBE/LIONS UMR 3685, Gif sur Yvette, Cedex, F-91191, France, [maxime.laine@cea.fr](mailto:maxime.laine@cea.fr)
- Laird, David, Iowa State University, 2505 Agronomy Hall, Department of Agronomy, Ames, Iowa, 50011, USA, [dalaird@iastate.edu](mailto:dalaird@iastate.edu)
- Lakhane, Madhuri, University of Maribor, Faculty of Mechanical Engineering, Smetanova Ulica-17, Maribor, 2000, Slovenia, [madhurilakhane@gmail.com](mailto:madhurilakhane@gmail.com)
- Lampropoulou, Paraskevi, University of Patras, Rion Patras, Patras, 26504, Greece, [p.lampropoulou@upatras.gr](mailto:p.lampropoulou@upatras.gr)
- Lamyaa, Laou, SPCTS, Centre Européen de la céramique, 12 rue Atlantis, Limoges Cedex, 87068, France, [lamyaa.laou@etu.unilim.fr](mailto:lamyaa.laou@etu.unilim.fr)
- Langella, Alessio, University of Sannio, Via dei Mulini 59/A, Benevento, I-82100, Italy, [langella@unisannio.it](mailto:langella@unisannio.it)
- Lanson, Bruno, ISTERre, CNRS – Univ. Grenoble, ISTERre OSUG, Grenoble cedex 9, F-38042, France, [bruno.lanson@ujf-grenoble.fr](mailto:bruno.lanson@ujf-grenoble.fr)
- Lanzirotti, Antonio, The University of Chicago, 9700 S. Cass Ave, Bldg.434A, Argonne National Lab, Argonne, IL, 60565, USA, [lanzirotti@uchicago.edu](mailto:lanzirotti@uchicago.edu)
- Latrille, Christelle, CEA, DEN/DANS/DPC/SECR/L3MR, bat 450 CEA Saclay, Gif sur Yvette, 91191, France, [christelle.latrille@cea.fr](mailto:christelle.latrille@cea.fr)
- Launois, Pascale, CNRS, Laboratoire de Physique des Solides, Bât. 510, Université Paris Sud, Orsay, 91405, France, [pascale.launois@u-psud.fr](mailto:pascale.launois@u-psud.fr)
- Lazzara, Giuseppe, University of Palermo, viale delle Scienze ed 17, Palermo, 90124, Italy, [giuseppe.lazzara@unipa.it](mailto:giuseppe.lazzara@unipa.it)
- Lecomte, Gisele, ENSCI, 12 rue Atlantis, Limoges, Cedex, 87068, France, [gisele.lecomte@unilim.fr](mailto:gisele.lecomte@unilim.fr)
- Leggo, Peter, University of Cambridge, Department of Earth Sciences, Downing Street, Cambridge, CB2 3EQ, United Kingdom, [pjl46@cam.ac.uk](mailto:pjl46@cam.ac.uk)
- Leonardi, Alberto, Indiana University, Department of Geological Sciences, 1001 East 10th Street, Indiana, 47405-1405, USA, [alby\\_leo@yahoo.it](mailto:alby_leo@yahoo.it)
- Leoni, Matteo, University of Trento, via mesiano, 77, Trento, 38123, Italy, [matteo.leoni@unitn.it](mailto:matteo.leoni@unitn.it)
- Leporatti, Stefano, NNL-Istituto di Nanotecnologia CNR, Via Arnesano 16, Lecce, 73100, Italy, [stefano.leporatti@nano.cnr.it](mailto:stefano.leporatti@nano.cnr.it)

## DELEGATE LIST

- Lessovaia, Sofia N., St. Petersburg State University, V.O. 10 line d.33, St. Petersburg, 199178, Russia, [lessovaia@yahoo.com](mailto:lessovaia@yahoo.com)
- Leyva-Ramos, Roberto, Universidad Autonoma de San Luis Potosi, Alvaro Obregon No. 64, Zona Centro, San Luis Potosi, 78000, Mexico, [rlr@uaslp.mx](mailto:rlr@uaslp.mx)
- Lhotka, Miloslav, University of Chemistry and Technology Prague, Department of Inorganic Technology, Technická 5, Prauge 6, 166 28, Czech Republic, [miloslav.lhotka@vscht.cz](mailto:miloslav.lhotka@vscht.cz)
- Lindsay, Craig, Core Specialist Services Ltd, Brathens Eco Business Park, Glassel, Aberdeenshire, AB31 4BW, United Kingdom, [craig.lindsay@core-specialist-services.com](mailto:craig.lindsay@core-specialist-services.com)
- Liu, Dong, Guangzhou Institute of Geochemistry, Chinese Academy of Sciences, 511 Kehua Street, Wushan, Tianhe District, Guangzhou, Guangdong province, 510640, China, [liudong@gig.ac.cn](mailto:liudong@gig.ac.cn)
- Liu, Mingxian, Jinan University, 601 Huangpu Avenue West, Guangzhou, 510632, China, [liumx@jnu.edu.cn](mailto:liumx@jnu.edu.cn)
- Liu, Zhifei, State Key Laboratory of Marine Geology, Tongji University, 1239 Siping Road, Shanghai, 200092, China, [lzhifei@tongji.edu.cn](mailto:lzhifei@tongji.edu.cn)
- Lofts, Anna, The Mineralogical Society, 12 Baylis Mews, Amyand Park Road, Twickenham, TW1 3HQ, United Kingdom, [admin@minersoc.org](mailto:admin@minersoc.org)
- Loganathan, Narasimhan, Michigan State University, 578, S Shaw Lane, East Lansing, 48824, USA, [naresh20@msu.edu](mailto:naresh20@msu.edu)
- López Galindo, Alberto, CSIC-Univ. Granada, Instituto Andaluz de Ciencias de la Tierra, Avad. de las Palmeras 4, Armilla (Granada), E-18100, Spain, [alberto@ugr.es](mailto:alberto@ugr.es)
- M**
- Madejová, Jana, Institute of Inorganic Chemistry, Slovak Academy of Sciences, Dúbravská cesta 9, Bratislava, 84536, Slovakia, [jana.madejova@savba.sk](mailto:jana.madejova@savba.sk)
- Maes, André, KU Leuven, Kasteelpark Arenberg 23 - bus 2461, Heverlee, 3001, Belgium, [Andre.Maes@biw.kuleuven.be](mailto:Andre.Maes@biw.kuleuven.be)
- Mahlmann, Rafael Ferreira, Technische Universität Darmstadt, Institute of Applied Geosciences, Technical Petrology, Darmstadt, 64287, Germany, [ferreiro@geo.tu-darmstadt.de](mailto:ferreiro@geo.tu-darmstadt.de)
- Malan, Paul, Redmond, 475 W 910 S, Herber City, 84032, USA, [paulm@redmondinc.com](mailto:paulm@redmondinc.com)
- Malla, Prakash, Thiele Kaolin Co, Research and Development, 520 Kaolin Road, Andersville, Georgia, 31082, USA, [prakash.malla@thielekaolin.com](mailto:prakash.malla@thielekaolin.com)
- Mameli, Paola, University of Sassari, Via Piandanna 4, Sassari, 07100, Italy, [mamelip@uniss.it](mailto:mamelip@uniss.it)
- Marchel, Christian, Dea-Group, Industriestrasse 2, Wietze, 29323, Germany, [christian.marchel@dea-group.com](mailto:christian.marchel@dea-group.com)
- Marschall, Paul, National Cooperative for the Disposal of Radioactive Waste, Hardstrasse 73, Wettingen, 5430, Switzerland, [marschall@nagra.ch](mailto:marschall@nagra.ch)
- Matusik, Jakub, AGH University of Science and Technology, ul. Mickiewicza 30, Krakow, 30059, Poland, [jakub.matusik@wp.pl](mailto:jakub.matusik@wp.pl)
- Mazurek, Martin, University of Bern, Baltzerstr.3, Bern, 3012, Switzerland, [mazurek@geo.unibe.ch](mailto:mazurek@geo.unibe.ch)
- McCabe, Richard, The Mineralogical Society, 12 Baylis Mews, Amyand Park Road, Twickenham, TW1 3HQ, United Kingdom, [richard@minersoc.org](mailto:richard@minersoc.org)
- McCarthy, Douglas, Chevron ETC, 3901 Briarpark Dr., Houston, TX, 77042, USA, [dmccarty@chevron.com](mailto:dmccarty@chevron.com)
- Menicagli, Elena, Laviosa Chimica Mienraria Spa, Via L. da Vinci 21, Livorno, 57123, Italy, [elena.menicagli@laviosa.com](mailto:elena.menicagli@laviosa.com)
- Mercurio, Mariano, University of Sannio, Department of Science and Technology, Via dei Mulini 59/A, Benevento, I-82100, Italy, [mariano.mercurio@unisannio.it](mailto:mariano.mercurio@unisannio.it)
- Mercurio, Mariano, University of Sannio, Via dei Mulini 59/A, Benevento, 82100, Italy, [mariano.mercurio@unisannio.it](mailto:mariano.mercurio@unisannio.it)
- Merten, Giles, Q Mineral, Gaston Geenslaan 1, Heverlee, 3001, Belgium, [gmertens@qmineral.com](mailto:gmertens@qmineral.com)
- Meyer, Uwe, BGR, Stilleweg 2, Hannover, 30655, Germany, [uwe.meyer@bgr.de](mailto:uwe.meyer@bgr.de)
- Michau, Nicolas, ANDRA, 1-7 Rue Jean Monnet, Châtenay-Malabry, 92298, France, [nicolas.michau@gmail.com](mailto:nicolas.michau@gmail.com)
- Michot, Laurent, CNRS/UPMC UMR8234, 5, Place Jussieu, Paris, 75005, France, [laurent.michot@upmc.fr](mailto:laurent.michot@upmc.fr)
- Midtbo, Ruth Elin, Statoil ASA, Sandslivieien 90, Bergen, 5254, Norway, [rumid@statoil.com](mailto:rumid@statoil.com)
- Mills, Stuart, Museum Victoria, GPO 666, Melbourne, Victoria, 3001, Australia, [smills@museum.vic.gov.au](mailto:smills@museum.vic.gov.au)
- Miyamoto, Nobuyoshi, 3-30-1, Wajirohigashi, Higashiku, Fukuoka, 8110295, Japan, [miyamoto@fit.ac.jp](mailto:miyamoto@fit.ac.jp)
- Miyoshi, Satoru, Obayashi Corporation, Shimo-kiyoto 4-640, Kiyose-shi, Tokyo, 204-8558, Japan, [miyoshi.satoru@obayashi.co.jp](mailto:miyoshi.satoru@obayashi.co.jp)
- Morrison, Keith, Arizona State University, ASU School of Earth and Space Exploration, PO Box 871404, Tempe, AZ, 85287-1404, USA, [keith.morrison@asu.edu](mailto:keith.morrison@asu.edu)
- Mosselmans, Fred, Diamond Light Source, Diamond House, Harwell Campus, Didcot, OX11 0DE, United Kingdom, [fred.mosselmans@diamond.ac.uk](mailto:fred.mosselmans@diamond.ac.uk)
- Motelica-Heino, Mikael, ISTO UMR 7327 CNRS-Université d'Orléans, 1A rue de la Férollerie, Orléans, 45071, France, [mikael.motelica@univ-orleans.fr](mailto:mikael.motelica@univ-orleans.fr)
- Mullan-Boudreau, Gillian, University of Alberta, 8910 Windsor Rd NW, Edmonton, T6G 2A2, Canada, [mullanbo@ualberta.ca](mailto:mullanbo@ualberta.ca)
- Mullis, Josef, University of Basel, Bernoullistrasse 30, Basel, 4056, Switzerland, [josef.mullis@unibas.ch](mailto:josef.mullis@unibas.ch)
- Murphy, Kevin, The Mineralogical Society, 12 Baylis Mews, Amyand Park Road, Twickenham, TW1 3HQ, United Kingdom, [kevin@minersoc.org](mailto:kevin@minersoc.org)
- Murray, Roseanne, University of Durham, 108 Park Avenue, Coxhoe, Durham, DH6 4JN, United Kingdom, [rosanne.murray@durham.ac.uk](mailto:rosanne.murray@durham.ac.uk)
- Müthing, Nina, Ruhr-Universität Bochum, Universitätsstr. 150, Bochum, 44780, Germany, [nina.muething@rub.de](mailto:nina.muething@rub.de)

## DELEGATE LIST

### N

Nadeau, Christina, University of Aberdeen, Nadlandsberget 6C, Stavanger, 4034, Norway, [phnad1@gmail.com](mailto:phnad1@gmail.com)

Nadeau, Paul, Univ. Stavanger, Nadlandsberget 6C, Stavanger, 4034, Norway, [paul.h.nadeau@uis.no](mailto:paul.h.nadeau@uis.no)

Nakato, Teruyuki, Kyushu Institute of Technology, 1-1 Sensui-cho, Tobata-ku, Kitakyushu, 804-8550, Japan, [nakato@che.kyutech.ac.jp](mailto:nakato@che.kyutech.ac.jp)

Nash, Tyler, BYK Additives Limited, 501 Mussey Road, Dripping Springs, Texas, 78620, USA, [tyler.nash@atlanta.com](mailto:tyler.nash@atlanta.com)

Neumann, Anke, Newcastle University, School of Civil Engineering and Geosciences, Claremont Road, Newcastle upon Tyne, NE1 7RU, United Kingdom, [anke.neumann@ncl.ac.uk](mailto:anke.neumann@ncl.ac.uk)

Newport, Leo, Durham University, Department of Earth Sciences, Mountjoy Site, South Road, Durham, DL12 8GP, United Kingdom, [leo.newport@durham.ac.uk](mailto:leo.newport@durham.ac.uk)

Nielsen, Ulla Gro, University of Southern Denmark, Department of Physics, Chemistry and Pharmacy, Campusvej 55, Odense M, 5230, Denmark, [ugn@sdu.dk](mailto:ugn@sdu.dk)

Nieto, Fernando, Univ. Granada, Facultad de Ciencias, Av. Fuentenueva s/n, Granada, 18014, Spain, [nieto@ugr.es](mailto:nieto@ugr.es)

Nishido, Hirotugu, Okayama University of Science, 1-1 Ridaicho, Kitaku, Okayama, 700-0005, Japan, [nishido@rins.ous.ac.jp](mailto:nishido@rins.ous.ac.jp)

Norris, Simon, Radioactive Waste Management Ltd, 587 Curie Avenue, Harwell, Didcot, OX11 0RH, United Kingdom, [simon.norris@nda.gov.uk](mailto:simon.norris@nda.gov.uk)

Nyambura, Mercy, World agroforestry Centre, P.O. Box 30677, Nairobi, 00100, Kenya, [m.nyambura@cgiar.org](mailto:m.nyambura@cgiar.org)

### O

Ogawa, Makoto, Hojun Co. Ltd., An-naka, Gunma, 379-0133, Japan, [waseda.ogawa@gmail.com](mailto:waseda.ogawa@gmail.com)

Oh, Jae-Min, Yonsei University, #327, Changjohall, Wonju, 220710, Korea, [jaemin.oh@yonsei.ac.kr](mailto:jaemin.oh@yonsei.ac.kr)

Okada, Tomohiko, Shinshu University, Wakasato 4-17-1, Nagano, 380-8553, Japan, [tomohiko@shinshu-u.ac.jp](mailto:tomohiko@shinshu-u.ac.jp)

Olegario, Eleanor, University of the Philippines, Dept of Mining, Metallurgy and Materials, Diliman, Quezon City, 1101, Philippines, [eleanor.olegario@gmail.com](mailto:eleanor.olegario@gmail.com)

Olson, Carolyn, USDA-OCE-CCPO, 14th & Independence SW, Washington DC, 20250, USA, [colson@oce.usda.gov](mailto:colson@oce.usda.gov)

O'Meara, Paul, PANalytical, 7310 Cambridge Research Park, Waterbeach, CB25 9AY, United Kingdom, [paul.omeara@panalytical.com](mailto:paul.omeara@panalytical.com)

Omeroglu, Isil, Middleast Technical University, Department of Geological Engineering, Cankaya, Ankara, 06800, Turkey, [isilom@metu.edu.tr](mailto:isilom@metu.edu.tr)

Ostertag-Henning, Christian, Federal Institute for Geosciences and Natural Resources, Stilleweg 1, Hannover, 30655, Germany, [christian.ostertag-henning@bgr.de](mailto:christian.ostertag-henning@bgr.de)

Ottner, Franz, University of Natural Resources and Life Sciences, Vienna, Peter Jordan Strasse 70, Vienna, 1190, Austria, [franz.ottner@boku.ac.at](mailto:franz.ottner@boku.ac.at)

Oueslati, Walid, Université de Carthage, Département de physique, faculté des sciences de Bizerte, Zarzouna, 7021, Tunisia, [walioueslati@ymail.com](mailto:walioueslati@ymail.com)

Oyedele, Ayodele, University of Wolverhampton, Faculty of Science and Engineering, Wolverhampton, WV1 1LY, United Kingdom, [ayodele.oyedele@yahoo.com](mailto:ayodele.oyedele@yahoo.com)

Ozdilek, Cihan

Ozen, Sevgi, Recep Tayyip Erdogan University, Faculty of Engineering Fener, Rize, 53000, Turkey, [sevgi.ozen@erdogan.edu.tr](mailto:sevgi.ozen@erdogan.edu.tr)

Ozturk, Ufuk, Gordes Zeolit Madencilik San. ve Tic. A.S., Ankara Caddesi, NO: 81, Bayrakli Tower, Kat: 18, Daire: 123, Bayrakli, Izmir, Turkey, [ufukozturk1971@me.com](mailto:ufukozturk1971@me.com)

### P

Paineau, Erwan, LPS/CNRS, Laboratoire de Physique des Solides, BAT 510, Université Paris-Sud, Orsay, 91405, France, [erwan-nicolas.paineau@u-psud.fr](mailto:erwan-nicolas.paineau@u-psud.fr)

Pálková, Helen, Institute of Inorganic Chemistry, Slovak Academy of Sciences, Dúbravská cesta 9, Bratislava, 84536, Slovakia, [helena.palkova@savba.sk](mailto:helena.palkova@savba.sk)

Papoulis, Dimitrios, University of Patras, Dept of Geology, 26504 Rio, Patras, 26504, Greece, [papoulis@upatras.gr](mailto:papoulis@upatras.gr)

Parker, Ben, LOT-QuantumDesign Ltd, 1 Mole Business Park, KT22 7BA, United Kingdom, [angela@lot-qd.co.uk](mailto:angela@lot-qd.co.uk)

Pasbakhsh, Pooria, Monash University Malaysia, School of Engineering, 5 Level 4 Room 3, Jalan Lagoon Selatan, Bandar Sunway, 47500, Malaysia, [pooria.pasbakhsh@monash.edu](mailto:pooria.pasbakhsh@monash.edu)

Patel, Radhika, University College London, Gower Street, London, WC1E 6BT, United Kingdom, [radhika.patel@ucl.ac.uk](mailto:radhika.patel@ucl.ac.uk)

Patrier, Patricia, Univ Poitiers, IC2MP - HYDRASA, 5 rue Albert Turpain - B8, TSA 51106, Poitiers Cedex 9, 86073, France, [patricia.patrier@univ-poitiers.fr](mailto:patricia.patrier@univ-poitiers.fr)

Pendrowski, Helen, The James Hutton Institute, Macaulay Drive, Craigiebuckler, Aberdeen, AB15 8QH, United Kingdom, [helen.pendrowski@hutton.ac.uk](mailto:helen.pendrowski@hutton.ac.uk)

Perry, Sarah, Vassar College, 124 Raymond Avenue, Box 2186, New York, 12604, USA, [sarperry@vassar.edu](mailto:sarperry@vassar.edu)

Petit, Sabine, Université de Poitiers / CNRS IC2MP, UMR 7285 IC2MP, B27 4 rue Michel Brunet, TSA 51106, Poitiers cedex 9, 86073, France, [sabine.petit@univ-poitiers.fr](mailto:sabine.petit@univ-poitiers.fr)

Petra, Lukáš, Institute of Inorganic Chemistry, Slovak Academy of Sciences, Dúbravská cesta 9, Bratislava, 84536, Slovakia, [lukas.petra@savba.sk](mailto:lukas.petra@savba.sk)

Peyne, Julie, SPCTS, Centre Européen de la céramique, 12 rue Atlantis, Limoges Cedex, 87068, France, [julie.peyne@etu.unilim.fr](mailto:julie.peyne@etu.unilim.fr)

Phipps, Jonathan, Imerys, Par Moor Centre, Par Moor Road, Par, PL24 2SQ, United Kingdom, [jon.phipps@imerys.com](mailto:jon.phipps@imerys.com)

Pilavtepe, Müge, Karlsruhe Institute of Technology, Gotthard-Franz-Straße 3, Geb. 50.31, Karlsruhe, 76131, Germany, [muege.pilavtepe@kit.edu](mailto:muege.pilavtepe@kit.edu)

## DELEGATE LIST

- Ploetze, Michael, ETH Zurich, IGT, Stefano-Francini-Platz 3, Zurich, 8093, Switzerland, [ploetzel@ethz.ch](mailto:ploetzel@ethz.ch)
- Po-Hsiang, Chang, National Cheng Kung University, No.1, University Road, Tainan City, 70101, Taiwan, [tectonicion@yahoo.com.tw](mailto:tectonicion@yahoo.com.tw)
- Polubesova, Tamara, The Hebrew University of Jerusalem, Faculty of Agriculture, Food and Environment, Rehovot, 76100, Israel, [tamara.polubesova@mail.huji.ac.il](mailto:tamara.polubesova@mail.huji.ac.il)
- Pospíšil, Miroslav, Charles University in Prague, Ke Karlovu 3, Prague, 12116, Czech Republic, [pospisil@karlov.mff.cuni.cz](mailto:pospisil@karlov.mff.cuni.cz)
- Post, Jeffery, Smithsonian, PO Box 37012, MRC 0119, Washington, 20013, USA, [postj@si.edu](mailto:postj@si.edu)
- Potel, Sébastien, Institut Polytechnique LaSalle Beauvais, 19 rue Pierre Wagué, Beauvais, 60026, France, [sebastien.potel@lasalle-beauvais.fr](mailto:sebastien.potel@lasalle-beauvais.fr)
- Pourtabib, Kristina, University of Idaho, 235 N. Home St., Moscow, 83843, USA, [pour1824@vandals.uidaho.edu](mailto:pour1824@vandals.uidaho.edu)
- Pouvreau, Maxime, Subatech, 4 rue Alfred Kastler, La Chantrerie, BP20722, Nantes, 44307 Cedex 3, France, [Maxime.Pouvreau@subatech.in2p3.fr](mailto:Maxime.Pouvreau@subatech.in2p3.fr)
- Pozo, Manuel, Universidad Autónoma de Madrid, Department of Geology and Geochemistry, Faculty of Sciences, Madrid, 28049, Spain, [manuel.pozo@uam.es](mailto:manuel.pozo@uam.es)
- Previde Massara, Elisabetta, Eni, Via F. Maritano, 26, San Donato Milanese, 20097, Italy, [elisabetta.previde@eni.com](mailto:elisabetta.previde@eni.com)
- Prevot, Vanessa, CNRS, 24 Avenue des Landais, Campus les Cezeaux, Aubière, 63170, France, [vanessa.prevot@univ-bpclermont.fr](mailto:vanessa.prevot@univ-bpclermont.fr)
- Pšenička, Milan, Charles University in Prague, Ke Karlovu 3, Prague, 12116, Czech Republic, [milan.psenicka@matfyz.cz](mailto:milan.psenicka@matfyz.cz)
- Pushparaj, Suraj Shiv Charan, University of Southern Denmark, Department of Physics, Chemistry and Pharmacy, Campusvej 55, Odense, 5320, Denmark, [shiv@sdu.dk](mailto:shiv@sdu.dk)
- Q**
- Quetscher, Annette, TU Clausthal, Institute of Non-Metallic Materials, Zehntnerstrasse 2a, Clausthal - Zellerfeld, 38678, Germany, [annette.quetscher@tu-clausthal.de](mailto:annette.quetscher@tu-clausthal.de)
- R**
- Radziemska, Maja, Warsaw University of Life Science - SGGW, Nowoursynowska 166, Warsaw, 02-787, Poland, [maja\\_radziemska@sggw.pl](mailto:maja_radziemska@sggw.pl)
- Raftery, Tony, Queensland University of Technology, Institute for Future Environments, GPO BOX 2434, Brisbane, 4000, Australia, [ife.travel@qut.edu.au](mailto:ife.travel@qut.edu.au)
- Rajendra, Russell, The Mineralogical Society, 12 Baylis Mews, Amyand Park Road, Twickenham, TW1 3HQ, United Kingdom, [russell@minersoc.org](mailto:russell@minersoc.org)
- Rasamimanana, Sabrina, CEA Saclay, CEA, DEN, DPC, L3MR, Bat. 450, Pièce 76, Gif-Sur-Yvette, 91191, France, [sabrina.rasamimanana@cea.fr](mailto:sabrina.rasamimanana@cea.fr)
- Raven, Mark, CSIRO Land and Water, Waite Rd, Urrbrae, 5064, Australia, [Mark.Raven@csiro.au](mailto:Mark.Raven@csiro.au)
- Reddy uddigiri, Venkateswara, Michigan State University, 578 S Shaw In, East Lansing, 48824, USA, [venkyreddy84@gmail.com](mailto:venkyreddy84@gmail.com)
- Riber, Lars, University of Oslo, Skogliveien 59A, Drammen, 3047, Norway, [lars.riber@geo.uio.no](mailto:lars.riber@geo.uio.no)
- Richter, Daniel, Duke University, Nicholas School of the Environment, Box 98328, Durham, NC, 27708, USA, [drichter@duke.edu](mailto:drichter@duke.edu)
- Rickertsen, Nils, Stephan Schmidt KG, Bahnhofstr.92, Langendernbach, 65599, Germany, [nils.rickertsen@schmidt-tone.de](mailto:nils.rickertsen@schmidt-tone.de)
- Rieß, Martin, University of Bayreuth, Department of Anorganic Chemistry I, Universitätsstr.30, Bayreuth, 95447, Germany, [martin\\_riess@t-online.de](mailto:martin_riess@t-online.de)
- Rigonat, Nicola, University of Edinburgh, Grant Institute of Geosciences, James Hutton Road, Edinburgh, EH9 3FE, United Kingdom, [nicola.rigonat@ed.ac.uk](mailto:nicola.rigonat@ed.ac.uk)
- Roadset, Elen, University of Oslo, Natural History Museum, P.O.Box 1172 Blindern, Oslo, 0318, Norway, [roadset@online.no](mailto:roadset@online.no)
- Robert, Jean-Louis, Université Pierre et Marie Curie, IMPMC, UPMC, Case courrier 115, 4 place Jussieu, Paris, 75252, France, [jean-louis.robert@impmc.upmc.fr](mailto:jean-louis.robert@impmc.upmc.fr)
- Robeson, Michael, Profile Products LLC, 2029 Majestic Ct, Fort Collins, CO, USA, [mrobeson@profileproducts.com](mailto:mrobeson@profileproducts.com)
- Robin, Valentin, University of Poitiers / CNRS IC2MP, UMR 7285 IC2MP, B27 4 rue Michel BRUNET, TSA 51106, Poitiers, 86073, France, [valentin.robin@univ-poitiers.fr](mailto:valentin.robin@univ-poitiers.fr)
- Robinet, Jean-Charles, Andra, 1-7 Rue Jean Monnet, Chatenay-Malabry, 92298, France, [jean-charles.robinet@andra.fr](mailto:jean-charles.robinet@andra.fr)
- Rocha, Fernando, Geobiotec Research Centre, Univ. Aveiro, Campo de Santiago, Aveiro, 3810-193, Portugal, [tavares.rocha@ua.pt](mailto:tavares.rocha@ua.pt)
- Rodríguez Ruiz, María Dolores, Málaga University, Departamento de Química Inorgánica, Cristalografía y Mineralogía, Facultad de Ciencias, Campus de Teatinos s/n, Málaga, 29071, Spain, [mdrodriguez@uma.es](mailto:mdrodriguez@uma.es)
- Rogowska, Melania, Jerzy Haber Institute of Catalysis and Surface Chemistry Polish Academy of Sciences, Niezapominajek 8, Kraków, 30-239, Poland, [melania.rogowska@gmail.com](mailto:melania.rogowska@gmail.com)
- Rossignol, Sylvie, Limoges, 12 rue Atlantis, Limoges, 87570, France, [sylvie.rossignol@unilim.fr](mailto:sylvie.rossignol@unilim.fr)
- Rotenberg, Benjamin, CNRS, Laboratoire PHENIX, CC 51, UPMC, 4 place Jussieu, Paris Cedex 05, 75252, France, [benjamin.rotenberg@upmc.fr](mailto:benjamin.rotenberg@upmc.fr)
- Rothwell, Katherine, Newcastle University, School of Civil Engineering and Geosciences, Cassie Building, Newcastle Upon Tyne, NE1 7RU, United Kingdom, [k.rothwell@newcastle.ac.uk](mailto:k.rothwell@newcastle.ac.uk)
- Ruiz-Hitzky, Eduardo, ICMM-CSIC, C/ Sor Juana Inés de la Cruz 3, Madrid, 28049, Spain, [eduardo@icmm.csic.es](mailto:eduardo@icmm.csic.es)
- Rusmin, Ruhaida, University of South Australia, Centre for Environmental Risk Assessment and Remediation, Building X, University Boulevard, Mawson Lakes, South Australia, 5095, Australia, [ruhaida.rusmin@mymail.unisa.edu.au](mailto:ruhaida.rusmin@mymail.unisa.edu.au)
- Ryan, Peter, Middlebury College, 276 Bicentennial Way, Geology Dept, Middlebury, 5753, USA, [pryan@middlebury.edu](mailto:pryan@middlebury.edu)

## DELEGATE LIST

Rytwo, Giora, MIGAL/Tel Hai, Israel, Environmental Physical Chemistry Laboratory, POB 831, Kiryat Shmona, 11015, Israel, [rytwo@telhai.ac.il](mailto:rytwo@telhai.ac.il)

### S

Sainz-Díaz, C. Ignacio, Instituto Andaluz de Ciencias de la Tierra (CSIC-UGR), Av. de las Palmeras, 4, Armilla, Granada, 18100, Spain,

[ignacio.sainz@iact.ugr-csic.es](mailto:ignacio.sainz@iact.ugr-csic.es)

Sakhawoth, Yasmine, Université Pierre et Marie Curie, 4 Place Jussieu, Paris Cedex 5, Case Courrier 51, Paris, 75252, France, [yasmine.sakhawoth@upmc.fr](mailto:yasmine.sakhawoth@upmc.fr)

Sakuma, Hiroshi, National Institute for Materials Science, 1-1 Namiki, Tsukuba, 3050044, Japan, [SAKUMA.Hiroshi@nims.go.jp](mailto:SAKUMA.Hiroshi@nims.go.jp)

Sanchez, Catalina, Universidad de Jaen, Campus las Lagunillas, s/n, Edificio B3-336, Jaen, 23071, Spain, [catasroa@gmail.com](mailto:catasroa@gmail.com)

Sanchez, Jose Francisco, Mapua Institute of Technology, 17 Cavite Street, Bonifacio Village, Pasong Tamo, 1107, Philippines, [eleanor.olegario@gmail.com](mailto:eleanor.olegario@gmail.com)

Santana, Igor Vasconcelos, University of Exeter, Camborne School of Mines, 9 Raleigh Place, Falmouth, TR11 3QJ, United Kingdom, [igorunesp@gmail.com](mailto:igorunesp@gmail.com)

Sardisco, Lorenza, X-ray Mineral Services Ltd, 1 Claughton Road, Colwyn Bay, LL29 7EF, United Kingdom, [lorenza@xrayminerals.co.uk](mailto:lorenza@xrayminerals.co.uk)

Sarkar, Binoy, CRC CARE & University of South Australia, X2-02- C01, University Boulevard, Mawson Lakes, South Australia, 5095, Australia, [binoy.sarkar.clay@gmail.com](mailto:binoy.sarkar.clay@gmail.com)

Sasaki, Keiko, Kyushu University, Motooka 744, Fukuoka, 8190395, Japan, [keikos@mine.kyushu-u.ac.jp](mailto:keikos@mine.kyushu-u.ac.jp)

Sato, Tsutomu, Hokkaido University, Faculty of Engineering, Hokkaido University, Kita 13 Nishi 8, Kita-Ku, Sapporo, 060-8628, Japan, [tomsato@eng.hokudai.ac.jp](mailto:tomsato@eng.hokudai.ac.jp)

Schafer, Thorsten, Karlsruhe Institute of Technology, P O BOX 3640, 76021, Germany, [thorsten.schaefer@kit.edu](mailto:thorsten.schaefer@kit.edu)

Schampera, Birgit, Leibniz Universität Hannover/ Institute of Soil Science, Herrenhäuser Str.2, Hannover, 30419, Germany, [schampera@ifbk.uni-hannover.de](mailto:schampera@ifbk.uni-hannover.de)

Schleicher, Anja, Helmholtz-Zentrum Potsdam, Deutsches GeoForschungsZentrum GFZ, Telegrafenberg, Potsdam, 14473, Germany, [aschleic@gfz-potsdam.de](mailto:aschleic@gfz-potsdam.de)

Schmid, Jasmin, University of Bayreuth, Department of Anorganic Chemistry I, Universitätsstr.30, Bayreuth, 95447, Germany, [jasmin.schmid@uni-bayreuth.de](mailto:jasmin.schmid@uni-bayreuth.de)

Schmidt, Susanne Th, Uni Genève, Rue des Maraîchers 13, Genève, 1205, Switzerland, [susanne.schmidt@unige.ch](mailto:susanne.schmidt@unige.ch)

Schnetzer, Florian, Karlsruhe Institute of Technology (KIT), Hermann-von-Helmholtz-Platz 1, Eggenstein-Leopoldshafen, 76344, Germany, [florian.schnetzer@kit.edu](mailto:florian.schnetzer@kit.edu)

Schoenenberger, Jasmin, Norwegian Geological Survey, Leiv Eirikssons vei 39, Trondheim, 7040, Norway, [jasmin.schoenenberger@ngu.no](mailto:jasmin.schoenenberger@ngu.no)

Scholtzová, Eva, Institute of Inorganic Chemistry, Slovak Academy of Sciences, Dúbravská cesta 9, Bratislava, 84536, Slovakia, [eva.scholtzova@savba.sk](mailto:eva.scholtzova@savba.sk)

Schoonheydt, Robert, KU Leuven, COK, Kasteelpark Arenberg 23, Leuven, 3001, Belgium, [robert.schoonheydt@biw.kuleuven.be](mailto:robert.schoonheydt@biw.kuleuven.be)

Schroeder, Paul, University of Georgia, Department of Geology, 210 Field Street, Athens, 30602-2501, USA, [schroe@uga.edu](mailto:schroe@uga.edu)

Schurig, Christian, Technische Universität München, Chair of Soil Science, Emil-Ramann-Str. 2, Freising-Weihenstephan, 85354, Germany, [christian.schurig@wzw.tum.de](mailto:christian.schurig@wzw.tum.de)

Seiffarth, Torsten, Weimar, Meyerstr. 26, Weimar, 99423, Germany, [torsten.seiffarth@uni-weimar.de](mailto:torsten.seiffarth@uni-weimar.de)

Sellin, Patrik, SKB, BOX 250, Stockholm, 10124, Sweden, [patrik.sellin@skb.se](mailto:patrik.sellin@skb.se)

Selvam, Thangaraj, University of Erlangen-Nuremberg, Egerlandstr. 3, Erlangen, 91058, Germany, [thangaraj.selvam@cbi.uni-erlangen.de](mailto:thangaraj.selvam@cbi.uni-erlangen.de)

Shaw, David, BYK Additives Limited, Moorfield Road, Widnes, WA8 3AA, United Kingdom, [david.shaw@altana.com](mailto:david.shaw@altana.com)

Shaw, Harry, Imperial College London, Rivendell, Malt row, Cupar, KY15 7SY, United Kingdom, [harry.shaw1@btinternet.com](mailto:harry.shaw1@btinternet.com)

Shen, Ping, University of Oxford, Lady Margaret Hall, Norham Gardens, Oxford, OX2 6QA, United Kingdom, [pingqian.shen@eng.ox.ac.uk](mailto:pingqian.shen@eng.ox.ac.uk)

Shikinaka, Kazuhiro, Tokyo University of Agriculture and Technology, 2-24-16, Naka-cho, Koganei, 184-8588, Japan, [k-shiki@cc.tuat.ac.jp](mailto:k-shiki@cc.tuat.ac.jp)

Shin, Koichi, Central Research Institute of Electric Power Industry, Abiko 1646, Abiko city, Chiba prefecture, 270-1194, Japan, [shin@criepi.denken.or.jp](mailto:shin@criepi.denken.or.jp)

Shohei, Yoshimura, Graduate school of Fukuoka Institute, Department of Life, Environment, and Materials Science, 3-30-1, Wajiro-higashi, Higashi-ku, Fukuoka, 811-0295, Japan, [mbm14017@bene.fit.ac.jp](mailto:mbm14017@bene.fit.ac.jp)

Sims, Adam, University of Manchester, 35 Filey Road, Manchester, M14 6GG, United Kingdom, [adam.sims@postgrad.manchester.ac.uk](mailto:adam.sims@postgrad.manchester.ac.uk)

Singh, Balwant, University of Sydney, Faculty of Agriculture and Environment, 1 Central Ave, Australian Technology Park, Eveleigh, NSW, 2015, Australia, [balwant.singh@sydney.edu.au](mailto:balwant.singh@sydney.edu.au)

Sitnikova, Maria, BGR, Stilleweg 2, Hannover, 30655, Germany, [maria.sitnikova@bgr.de](mailto:maria.sitnikova@bgr.de)

Smoliga, John, Boehringer Ingelheim Pharmaceuticals, 900 Ridgebury Rd., Ridgefield, 6877, USA, [john.smoliga@boehringer-ingelheim.com](mailto:john.smoliga@boehringer-ingelheim.com)

Soriano, Maria, University of Valencia, Cami de Vera s/n, Valencia, 46021, Spain, [asoriano@prv.upv.es](mailto:asoriano@prv.upv.es)

Spratt, Henry, Queensland University of Technology, Institute for Future Environments, GPO BOX 2434, Brisbane, 4000, Australia, [ife.travel@qut.edu.au](mailto:ife.travel@qut.edu.au)

Środoń, Jan, Inst. of Geological Sciences PAN, Senacka 1, Kraków, 31-002, Poland, [ndsrodon@cyf-kr.edu.pl](mailto:ndsrodon@cyf-kr.edu.pl)

Stamatakis, Michael G., University of Athens, Department of Geology & Geoenvironment, Panepistimiopolis, Zografou, Athens, 15784, Greece, [stamatakis@geol.uoa.gr](mailto:stamatakis@geol.uoa.gr)

## DELEGATE LIST

- Stanjek, Helge, RWTH Aachen University, Bunsenstr. 8, Aachen, 52070, Germany, [helge.stanjek@cim.rwth-aachen.de](mailto:helge.stanjek@cim.rwth-aachen.de)
- Stedel, Annett, Karlsruhe Institute of Technology, Hermann-von-Helmholtz-Platz 1, Eggenstein-Leopoldshafen, 76344, Germany, [annett.stedel@kit.edu](mailto:annett.stedel@kit.edu)
- Strydom, Jessica, North-West University, 11 Hoffman street, E4-G44, Potchefstroom, 2531, South Africa, [21212627@nwu.ac.za](mailto:21212627@nwu.ac.za)
- Suarez, Mercedes, Universidad de Salamanca, Departamento de Geología, Facultad de ciencias, plaza de la Merced, Salamanca, 37008, Spain, [msuarez@usal.es](mailto:msuarez@usal.es)
- Süssenberger, Annette, Département des Sciences de la Terre Université de Genève, 13, Rue des Maraichers, Genève, 1205, Switzerland, [annette.suessenberger@unige.ch](mailto:annette.suessenberger@unige.ch)
- Süssenberger, Annette, Uni Genève, Rue des Maraichers 13, Geneva, 1205, Switzerland, [annette.suessenberger@unige.ch](mailto:annette.suessenberger@unige.ch)
- Suzuki, Noriko, Showa Pharmaceutical University, 3-3165, Higashitamagawagakuen, Machida, Tokyo, 194-8543, Japan, [n-suzuki@ac.shoyaku.ac.jp](mailto:n-suzuki@ac.shoyaku.ac.jp)
- Suzuki, Yasutaka, Yamaguchi University, 1677-1, Yoshida, Yamaguchi, 753-8512, Japan, [ysuzuki@yamaguchi-u.ac.jp](mailto:ysuzuki@yamaguchi-u.ac.jp)
- Svensson, Daniel, Swedish Nuclear Fuel and Waste Management Co (SKB), Äspö Hard Rock Laboratory, Långö 300, Figeholm, 572 95, Sweden, [daniel.svensson@skb.se](mailto:daniel.svensson@skb.se)
- Szabo, Tamas, University of Szeged, Department of Physical Chemistry and Materials Science, Aradi vertanuk tere 1, Szeged, H-6720, Hungary, [sztamas@chem.u-szeged.hu](mailto:sztamas@chem.u-szeged.hu)
- Szczerba, Marek, Institute of Geological Sciences, Polish Academy of Sciences, Senacka 1, Kraków, 31-002, Poland, [ndszczer@cyf-kr.edu.pl](mailto:ndszczer@cyf-kr.edu.pl)
- Szilagyi, Istvan, University of Geneva, 30 Quai Ernest-Ansermet, Geneva, 1205, Switzerland, [istvan.szilagyi@unige.ch](mailto:istvan.szilagyi@unige.ch)
- T**
- Taitel-Goldman, Nurit, The Open University of Israel, 1 University road, Raanana, 4353701, Israel, [nuritg@openu.ac.il](mailto:nuritg@openu.ac.il)
- Tamura, Kenji, National Institute for Materials Science, 1-1 Namiki, Tsukuba, 305-0044, Japan, [TAMURA.Kenji@nims.go.jp](mailto:TAMURA.Kenji@nims.go.jp)
- Tanner, James, Profile Products LLC, 750 Lake Cook Road, Buffalo Grove, 60089, USA, [jtanner@profileproducts.com](mailto:jtanner@profileproducts.com)
- Tao, Qi, Guangzhou Institute of Geochemistry, Chinese Academy of Sciences, 511 Kehua St, Guangzhou, 510640, China, [taoqi@gig.ac.cn](mailto:taoqi@gig.ac.cn)
- Taviot-Gueho, Christine, Blaise Pascal University, ICCF UMR 6296, 24 avenue des Landais, BP8002, Aubiere Cedex, 63171, France, [Christine.TAVIOT-GUEHO@univ-bpclermont.fr](mailto:Christine.TAVIOT-GUEHO@univ-bpclermont.fr)
- Tertre, Emmanuel, University of Poitiers / CNRS IC2MP, UMR 7285 IC2MP, B27 4 rue Michel BRUNET, TSA 51106, Poitiers, 86073, France, [emmanuel.tertre@univ-poitiers.fr](mailto:emmanuel.tertre@univ-poitiers.fr)
- Tesson, Stephane, Université Pierre et Marie Curie, 4 Place Jussieu, Bat. F, 7eme etage, Paris, 75005, France, [stephane.tesson@upmc.fr](mailto:stephane.tesson@upmc.fr)
- Theng, Benny, Landcare Research, Private Bag 11052, Manawatu Mail Centre, Palmerston North, 4442, New Zealand, [Thengb@landcareresearch.co.nz](mailto:Thengb@landcareresearch.co.nz)
- Tibljias, Darko, University of Zagreb, Miner.-petro. Zavod, PMF, Horvatovac 95, Zagreb, HR-10000, Croatia, [dtibljias@geol.pmf.hr](mailto:dtibljias@geol.pmf.hr)
- Tominaga, Makoto, Yamaguchi University, 1677-1, Yoshida, Yamaguchi, 753-8512, Japan, [t030uh@yamaguchi-u.ac.jp](mailto:t030uh@yamaguchi-u.ac.jp)
- Torber, Philip, University of Greifswald, F.L Jahn strasse 17A, Greifswald, D-17487, Germany, [warr@uni-greifswald.de](mailto:warr@uni-greifswald.de)
- Torrez, Gerardo, Weatherford Laboratories, 5200 N Sam Houston Pkwy W, Ste 500, Houston, TX, 77086, USA, [gerardo.torrez@weatherfordlabs.com](mailto:gerardo.torrez@weatherfordlabs.com)
- Tosca, Nicholas, University of Oxford, Department of Earth Sciences, South Parks Road, Oxford, OX1 3AN, United Kingdom, [nickt@earth.ox.ac.uk](mailto:nickt@earth.ox.ac.uk)
- Tournassat, Christophe, BRGM, 3, av. Claude Guillemin, Orleans, 45060, France, [c.tournassat@brgm.fr](mailto:c.tournassat@brgm.fr)
- Traber, Daniel, Nagra, Hardstrasse 73, Wettingen, 5430, Switzerland, [daniel.traber@nagra.ch](mailto:daniel.traber@nagra.ch)
- Tulunay, Cagatay, Gordes Zeolit Madencilik San. ve Tic. A.S., Ankara Caddesi, NO: 81, Bayrakli Tower, Kat: 18, Daire: 123, Bayrakli, Izmir, Turkey, [CagatayTulunay@gordeszeolite.com](mailto:CagatayTulunay@gordeszeolite.com)
- Türkmenoğlu, Asuman Günal, Middle East Technical University, Department of Geological Engineering, Dumlupınar Bulv. No.1, Ankara, 6800, Turkey, [asumant@metu.edu.tr](mailto:asumant@metu.edu.tr)
- U**
- Ufer, Kristian, Federal Institute for Geosciences and Natural Resources, Geozentrum Hannover, Stilleweg 2, Hannover, 30655, Germany, [kristian.ufer@bgr.de](mailto:kristian.ufer@bgr.de)
- Umemura, Yasushi, National Defence Academy, Hashirimizu 1-10-20, Kanagawa Prefecture, Yokosuka, 239-8686, Japan, [umemura@nda.ac.jp](mailto:umemura@nda.ac.jp)
- Umemura, Yasushi, National Defence Academy, Hashirimizu 1-10-20, Kanagawa Prefecture, Yokosuka, 239-8686, Japan, [umemura@nda.ac.jp](mailto:umemura@nda.ac.jp)
- Underwood, Thomas, Durham University, Department of Earth Sciences, Mountjoy Site, South Road, Durham, DH1 3LE, United Kingdom, [thomas.underwood@durham.ac.uk](mailto:thomas.underwood@durham.ac.uk)
- Urbanova, Martina Cubova, Institute of Macromolecular Chemistry AS CR, v.v.i., Heyrovsky sq.2, Prague 6, 16200, Czech Republic, [urbanova@imc.cas.cz](mailto:urbanova@imc.cas.cz)
- Utley, James, University of Liverpool, 4 Brownlow Street, Liverpool, L69 3GP, United Kingdom, [etrsi2@liv.ac.uk](mailto:etrsi2@liv.ac.uk)
- Uysal, I. Tonguç, Hacettepe University, Department of Geological Engineering, Beytepe, Ankara, 06800, Turkey, [t.uysal@uq.edu.au](mailto:t.uysal@uq.edu.au)
- V**
- Vandenbergh, Noel, KU Leuven, Geo Institut, Celestijnenlaan 200E, Heverlee, BE-3001, Belgium, [noel.vandenbergh@ees.kuleuven.be](mailto:noel.vandenbergh@ees.kuleuven.be)
- Vangdal, Brita, Statoil ASA, Sandslivieien 90, Bergen, 5254, Norway, [briv@statoil.com](mailto:briv@statoil.com)

## DELEGATE LIST

Vázquez-Vilchez, Mercedes, Andean Geothermal Centre of Excellence/ Chile University, Plaza Ercilla 803, Santiago, 803, Chile, [mvazquez@ing.uchile.cl](mailto:mvazquez@ing.uchile.cl)

Velbel, Michael, Michigan State University, Department of Geological Sciences, 288 Farm Lane, 206 Natural Sciences Building, East Lansing, 48824, USA, [velbel@msu.edu](mailto:velbel@msu.edu)

Viennet, Jean-Christophe, University of Poitiers, IC2MP-HydrASA Bât B8. - TSA 51106 5, rue Albert Turpain, Poitiers, 86073, France, [jean.christophe.viennet@univ-poitiers.fr](mailto:jean.christophe.viennet@univ-poitiers.fr)

Viggiani, Cino, Civil Engineering at Université Joseph Fourier, Laboratoire 3S-R (Sols, Solides, Structures – Risques), BP 53 38041 Grenoble, France, [cino.viggiani@hmg.inpg.fr](mailto:cino.viggiani@hmg.inpg.fr)

Villa, Maria Victoria, CIEMAT, Avd Complutense 40, Madrid, 28040, Spain, [mv.villar@ciemat.es](mailto:mv.villar@ciemat.es)

Viseras, César, University of Granada, Andalusian Institute of Earth Sciences, Avenida de las Palmeras 4, Granada, 18100, Spain, [cviseras@ugr.es](mailto:cviseras@ugr.es)

Vitale, Enza, University of Cassino and Southern Lazio, Via G. Di Biasio, 43, Cassino (FR), 3043, Italy, [e.vitale@unicas.it](mailto:e.vitale@unicas.it)

### W

Wagner, Jean-Frank, Trier University, Geology Dept., Cmapus II, Behringstrasse, Trier, 54296, Germany, [wagnerf@uni-trier.de](mailto:wagnerf@uni-trier.de)

Walker, Jeffrey, Vassar College, 124 Raymond Avenue, Poughkeepsie, 12603, USA, [jewalker@vassar.edu](mailto:jewalker@vassar.edu)

Wall, Frances, University of Exeter (Camborne School of Mines), Penryn Campus, Penryn, TR10 9FE, United Kingdom, [f.wall@exeter.ac.uk](mailto:f.wall@exeter.ac.uk)

Wampler, J.M., Georgia State University, 4053 Commodore Dr, Chamblee, 30341, USA, [wamplerjm@earthlink.net](mailto:wamplerjm@earthlink.net)

Wang, Linjiang, Guilin University of Technology, 12 Jiangan Road, Guilin, 541004, China, [wlinjiang@163.com](mailto:wlinjiang@163.com)

Watanabe, Yasutaka, Central Research Institute of Electric Power Industry, 1646 Abiko, Abiko-shi, Chiba-ken, 270-1194, Japan, [yasutaka@criepi.denken.or.jp](mailto:yasutaka@criepi.denken.or.jp)

Watanabe, Yujiro, Kanazawa Institute of Technology, 3-1 Yatsukaho Hakusan, Ishikawa, 9240838, Japan, [yujiro@neptune.kanazawa-it.ac.jp](mailto:yujiro@neptune.kanazawa-it.ac.jp)

Webb, Nigel, Amcol Minerals Europe Ltd., Weaver Valley Road, Winsford, Cheshire, CW7 3BU, United Kingdom, [nigel.webb@amcol.com](mailto:nigel.webb@amcol.com)

Wegerer, Eva, University of Leoben, Chair of Petroleum Geology, Peter-Tunner-Strasse 5, Leoben, 8700, Austria

Wicklein, Bernd, ICMM-CSIC, C/ Sor Juana Inés de la Cruz 3, Madrid, 28049, Spain, [bernd@icmm.csic.es](mailto:bernd@icmm.csic.es)

Wilkinson, Mark, University of Edinburgh, 30 Galt Crescent, Musselburgh, EH21 8HE, United Kingdom, [mark.wilkinson@ed.ac.uk](mailto:mark.wilkinson@ed.ac.uk)

Will, Patrizia, Technische Universität München, Lehrstuhl für Ingenieurgeologie, Arcisstr. 21, München, 80333, Germany, [patrizia.will@mytum.de](mailto:patrizia.will@mytum.de)

Williams, Lynda, Arizona State University, Physical Science F-686, 550 E.Tyler Mall, Tempe, Arizona, 85287-1404, USA, [lynda.williams@asu.edu](mailto:lynda.williams@asu.edu)

Wilson, Ian, Withielgoose Farmhouse, Withiel, Bodmin, Cornwall, PL30 5NW, United Kingdom, [ian.r.wilson@btinternet.com](mailto:ian.r.wilson@btinternet.com)

Wilson, Jeff, The James Hutton Institute, Craigiebuckler, Aberdeen, AB15 8QH, United Kingdom, [jeff.wilson@hutton.ac.uk](mailto:jeff.wilson@hutton.ac.uk)

Wilson, Lyudmyla, Corex UK Ltd, Units B1-B3, Airport Industrial Park, Howe Moss Drive, Dyce, Aberdeen, AB21 0GL, United Kingdom, [lwilson@corex.co.uk](mailto:lwilson@corex.co.uk)

Wittebroodt, Charles, IRSN, BP 17, Fontenay-aux-Roses, 92262, France, [Charles.wittebroodt@irsn.fr](mailto:Charles.wittebroodt@irsn.fr)

Wray, David, University of Greenwich, Science Departments, Pembroke, Chatam Maritime, ME4 4TB, United Kingdom, [d.wray@gre.ac.uk](mailto:d.wray@gre.ac.uk)

Wriessnig, Karin, University of Natural Resources and Life Sciences, Vienna, Peter Jordan Strasse 70, Vienna, A-1190, Austria, [karin.wriessnig@boku.ac.at](mailto:karin.wriessnig@boku.ac.at)

### Y

Yang, Kiho, Yonsei University, #237, Biogeochemistry Lab., Science Hall, Shinchon-dong, Seodaemun-gu, Seoul, 120-749, Korea, [kyang@yonsei.ac.kr](mailto:kyang@yonsei.ac.kr)

Yazaydin, Ozgur, University College London, Department of Chemical Engineering, Torrington Place, London, WC1E 7JE, United Kingdom, [ozgur.yazaydin@ucl.ac.uk](mailto:ozgur.yazaydin@ucl.ac.uk)

Yebrá-Rodríguez, Africa, University of Jaen, Department of Geology, Faculty of Experimental Sciences, Campus Las Lagunillas s/n, Jaen, 23071, Spain, [ayebrá@ujaen.es](mailto:ayebrá@ujaen.es)

Yoneda, Tetsuro, Hokkaido University, Chuou-ku, Miyanomori, 1-11-4-11, Sapporo, 064-0951, Japan, [yonet@eng.hokudai.ac.jp](mailto:yonet@eng.hokudai.ac.jp)

Yoruk, Aysegul, Gordes Zeolit Madencilik San. ve Tic. A.S., Ankara Caddesi, NO: 81, Bayrakli Tower, Kat: 18, Daire: 123, Bayrakli, Izmir, Turkey

Yotsuji, Kenji, Japan Atomic Energy agency, 4-33 Muramatsu, Ibaraki, 319-1194, Japan, [yotsuji.kenji@jaea.go.jp](mailto:yotsuji.kenji@jaea.go.jp)

Yu, Wenbin, Guangzhou Institute of Geochemistry, Chinese Academy of Sciences, 511 Kehua Street, Wushan, Tianhe District, Guangzhou city, Guangdong province, 510640, China, [yuwenbin@gig.ac.cn](mailto:yuwenbin@gig.ac.cn)

Yuan, Peng, Guangzhou Institute of Geochemistry, Chinese Academy of Sciences, 511 Kehua Street, Wushan, Tianhe District, Guangzhou, 510640, China, [yuanpeng@gig.ac.cn](mailto:yuanpeng@gig.ac.cn)

### Z

Zeelmaekers, Edwin, Shell, Carel van Bylandtlaan 30, 2596HR, The Netherlands, [edwin.zeelmaekers@shell.com](mailto:edwin.zeelmaekers@shell.com)

Zhitova, Elena, St. Petersburg State University, University emb. 7/9, St. Petersburg, 199034, Russia, [zhitova\\_es@mail.ru](mailto:zhitova_es@mail.ru)

Zhou, Xiang, Guangzhou Institute of Geochemistry, Chinese Academy of Sciences, 511 Kehua Street, Wushan, Tianhe District, Guangzhou, GD, Guangdong province, 510640, China, [196037545@qq.com](mailto:196037545@qq.com)

Zhu, Runliang, Guangzhou Institute of Geochemistry, Chinese Academy of Sciences, 511 Kehua Street,



## DELEGATE LIST

Tianhe District, Guangzhou, 510640, China,  
[zhurl@gig.ac.cn](mailto:zhurl@gig.ac.cn)

Zimowska, Małgorzata, Jerzy Haber Institute of  
Catalysis and Surface Chemistry Polish Academy of  
Sciences, Niezapominajek 8, Kraków, 30-239,  
Poland, [nczimows@cyf-kr.edu](mailto:nczimows@cyf-kr.edu)

## AUTHOR INDEX

Presenting authors have page numbers in **bold****A**

Abad, I., 245, 249  
 Abd Elmola, Ahmed, 500  
 Aboytes-McNeela, Jazmín, 489  
 Acemioğlu, Bilal, 229  
 Adamcova, Renata, **390**  
 Adams, Rachel, 137  
 Adriaens, Rieko, **166**  
 Agha, Mohamed, 165  
 Aguiar, Caio, 404  
 Aguilar, Inés M., 379  
 Aguzzi, C., 215  
 Aisawa, Sumio, **134, 198**  
 Al, Tom, 80  
 Alaraudanjoki, Jarno, 319  
 Albrecht, Wolter, 489  
 Alekseev, A., 347, **354**  
 Alekseeva, T., **347**, 354, 369  
 Algarra, Manuel, 153  
 Al-Jaberi, M., **457**  
 Allen, Herb, 467  
 Almeida, S., 136  
 Alpermann, Theodor, **385**  
 Amann-Hildenbrand, Alexandra, 183  
 Amano, Yuri, 46  
 Amara, M.S., 71  
 Ambait, Johanna Michelle S., **490**  
 Ammar, Marwa, 26  
 Anczkiewicz, Aneta A., 121  
 Andersson, Ulf B., 127  
 Ando, Toshihiro, 38  
 André, Erwan, **414**, 458  
 André, Grégoire, 281  
 Andreeva, Natalia, 240  
 Andrejkovičová, S., 338, 378, 399  
 Annabi-Bergaya, Faïza, 216  
 Aparicio, Patricia., 163, 212, **233**, 276  
 Aplin, Andrew C., 501  
 Arancibia, Gloria, 130  
 Arancibia, Gloria, 245  
 Aranda, Pilar, 473, 480, **484**  
 Aras, Aydin, **308**  
 Argersinger, Haley E., 290  
 Armienta, Maria Aurora, 341  
 Arroyo, X., **244**  
 Austin, Jason C., 344, **345**  
 Ayala, D., 231

**B**

Bacle, Pauline, **59**  
 Bahranowski, Krzysztof, 420  
 Baik, Hionsuck, 48, 206  
 Bailleul, Julien, 246  
 Bakker, Eleanor, **351**  
 Baldermann, Andre, **327**

Balela, Mary Donnabelle, 221  
 Balima, F., 397  
 Ballah, J., **504**  
 Banaś, Michał, 121  
 Banfield, Jillian F., 446  
 Barba-Brioso, C., **226**, 231, 233  
 Barbanson, Luc, 487  
 Barnhoorn, A., 85  
 Baron, Fabien, **104**, 109  
 Baronnet, Alain, 287  
 Barrientos Velázquez, Ana L., 223  
 Bauluz, Blanca, **126, 366**  
 Baum, Richard P., 33  
 Beaucaire, Catherine, 154  
 Beaufort, Daniel, 129, 281, **282**, **410**, 429, 500  
 Becker, J., 187  
 Begonha, Arlindo, 346  
 Beharrell, Paul A., **304**  
 Belal Khan, Tauhid, 351  
 Belmonte, Louise Josefine, **253**, **491**  
 Belviso, C., 168  
 Bemfica Toledo, Catarina Labouré, 404  
 Bender Koch, Christian, **105**, 275  
 Benítez Pérez, J.M., 250  
 Bentabol-Manzanares, M.J., 251  
 Berger, Peter M., 192  
 Bernini, Fabrizio, 62  
 Bertier, Pieter, **183**  
 BeruBe, Kelly, 137  
 Besenyi, L., 237  
 Besse-Hoggan, P., 369  
 Beziat, A., 486  
 Bhabananda Biswas, **157**  
 Bhattacharyya, Sidhartha, 337  
 Bielańska, Elżbieta, 420  
 Biernacka, Julita, **409**  
 Biersack, Bernhard, 377  
 Billon, Sophie, **281**  
 Birgersson, Martin, 325  
 Bíroň, Andrej, 91  
 Bish, D., **167**, 168, 227, 416  
 Bishop, Janice L., **314**  
 Biswas, Bhabananda, 230, **373**  
 Bizovská, Valéria, 252, 263, **374**  
 Blackbourn, Graham, **116**  
 Blanchart, Philippe, 434  
 Block, Karin A., **367**  
 Bobos, Iuliu, 153  
 Boles, Austin, **89**, **247**  
 Bond, Alex, 393  
 Borrego, A., 215  
 Borsari, Marco, 62  
 Bose, Maitrayee, 194  
 Boski, T., 231

Botelho, Nilson F., 400  
 Botor, Dariusz, 428  
 Bourgeat-Lami, Elodie, 478  
 Bouša, Daniel, 296  
 Bovet, N., **507**, 508  
 Bowers, Geoffrey M., 53, 55, 290  
 Boyer, Laurence, 303  
 Boyes, Victoria, 481  
 Bozkaya, Ömer, 315, 394  
 Brčeková, Jana, 91  
 Breen, C., 211, 295, 418, **481**  
 Brendlé, Eric, 156  
 Brendlé, Jocelyne, **156, 227**  
 Breu, Josef, 377, 382, 384, 412, **450**  
 Brigatti, M. Franca, 62  
 Brown, Alastair, 116  
 Brundu, Antonio, 219  
 Bruneax, Marie-Anne, 305  
 Brus, Jiri, 402  
 Buatier, Martine, **405, 411**, 487  
 Bueno, Salvador, 228  
 Bujdák, Juraj T., **149, 375**  
 Bukalo, Nenita, 240  
 Burlakovs, Juris, **334, 376**  
 Burley, S.D., 280  
 Busch, Andreas, 183  
 Butler, Shane K., 192

**C**

Cai, Y., **108**  
 Calderón, E., 231  
 Calvin, Christina, **425**  
 Calvo, José Pedro, 408  
 Caniço, Ana, **115**  
 Cappelletti, Piergiulio, 168, 219, **28**  
 Carazo, E., 215  
 Carmen Hermosín, M., 228, **379**  
 Carniel, Larissa C., 106  
 Carteret, Cédric, 413, 414, 456, 458  
 Castellini, Elena, 62  
 Cavalcante, F., 168  
 Cavallaro, Giuseppe, 69  
 Celejewski, Magda, **80**  
 Celis, Rafael, 228, 379  
 Cemal Göncüoğlu, M., 394  
 Cenacchi Pereira, Ana Maria, 478  
 Cerezo, P., 215  
 Cerri, Guido, 219  
 Cervini-Silva, Javiera, **140, 238**  
 Cesarano, M., **168**  
 Chakraborty, Argha, **230**  
 Chamerois, M., 504  
 Chang, Po-Hsiang, **150**  
 Chanier, Frank, 246

## AUTHOR INDEX

Charan, Suraj, 142, 455  
 Charpentier, Delphine, 405  
 Chefetz, Benny, 43  
 Chemedá, Yadeta C., **302**  
 Chen, Manyou, 422  
 Chen, Qingze, 158  
 Chen, Zongyuan, 51  
 Chernov, M., 321  
 Chikuma, Toshiyuki, 46  
 Chinchilla, D., 244  
 Chiou, Wen-An, 87, 184  
 Chirieac, A., 294  
 Chistiakov, Kirill, 240  
 Chodák, Ivan, 252  
 Choi, Hunsoo, 199  
 Choi, J. Yoon, 208  
 Choi, Woohyun, 239  
 Chorfi, Nejmeddine, 26  
 Choulet, Flavien, 411, **487**  
 Choy Jin-Ho, 49, **479**  
 Christidis, George E., 302, **312**,  
 387, **388**, 452  
 Christy, A. G., 459  
 Chryssikos, Georgios D., 452  
 Chung, Donghoon, **239**  
 Churchman, Jock, 68, 75  
 Ciotonea, C., **294**  
 Clark, Ian, 80  
 Clausen, T., 507  
 Cleaver, Doug, 211  
 Clegg, F., 211, **295**, 418  
 Coetzee, Marthie, 332  
 Cojan, Isabelle, 305  
 Colella, C., 32  
 Colica, Anatonela, 255  
 Colin, Christophe, 42  
 Collin, Frédéric, 256  
 Comolli, Luis, 446  
 Conceição, Rommulo Vieira, 106  
 Cornejo, Juan, **228**, 379  
 Cornu, Sophie, 464  
 Courbet, Christelle, 190  
 Coveney, Peter, **61**  
 Cox, Lucia, 228  
 Crawford Elliott, W., **201**, 259, **499**  
 Crombez, Vincent, 246  
 Cuadros, Javier, 358  
 Cubillas, Pablo, 64, 505, **506**  
 Cuevas, J., 163  
 Cuss, Robert, 325  
 Cygan, Randall T., 55, **58**, 63  
 Czimerová, Adriana, 263

**D**  
 D'Agosto, Franck, 478  
 da Silva, Raquel Guimarães, **404**  
 Daab, Matthias, **412**  
 Dagnelie, R., 155  
 Dähn, Rainer, 197  
 Dai, Yan, 415  
 Daniele, Linda, 245  
 Danko, Martin, 375  
 Daoudi, Lahcen, 256

Darder, Margarita, **473**, 480  
 Dathe, Wilfried, **33**  
 Dauzères, Alexandre, 190  
 Day-Stirrat, Ruarri J, **502**  
 Dazas, Baptiste, 448  
 de B. Richter, Daniel, **343**  
 de Gennaro Bruno, 28, 32, 219  
 de Jesús, Elba Ronquillo, 140, 238  
 De Silva, Rohan, 116  
 de Souza, Márcio R. W., 106  
 Dékány, Imre, 482  
 del Angel, Paz, 140  
 Delay, Frederick, 79  
 Delbos, Evelyne, 70  
 Delgado, J., 226, **231**  
 Delgado, R., 163  
 Deliova, Jana, 390  
 Delville, Alfred, 52, 79, 287, 448  
 Demel, Jan, 415  
 Demel, Ondřej, 415  
 Demirkiran, Ali. Rıza, **31**, **229**, 237  
 Deneele, Dimitri, 300, 302. **488**  
 Deng, Liangliang, 234  
 Deng, Youjun, **223**, **341**, 380  
 Derkowski, Arkadius, **81**, **176**, **225**,  
 257, 449  
 Desamparados Soriano, Maria,  
**255**  
 Desbois, Guillaume, 86  
 Descostes, Michael, 468  
 Detellier, Christian, 475, **476**  
 DeVore, Joshua R., 260  
 Di Bitetto, Arnaud, **413**, 414, **456**  
 Di Toro, Dominic, 467  
 Di, Zhenyu, 183  
 Diatta, Marthe Tatiana, 434  
 Diaz, Leslie Joy L., 490  
 Díaz-Hernández, José L., 358  
 Dick, Pierre, **190**  
 Diedel, Ralf, 309  
 Dietel, Jan, **232**  
 Dietzel, Martin, 327  
 Dionisi, Chiara, 66  
 Dohrmann, R., 87, 184, 186, 311,  
 320  
 Dolenc, Matej, 241  
 Dolenc, Tadej, 241  
 Donahoe, Rona J., **337**  
 Dong, Hailiang, 48, 206  
 Dorzhieva, O., 321  
 Doublie, Michael-Patrick, 125  
 Doudeau, Julie, 299  
 Doušová, Barbora, **152**, 218, 402,  
 403  
 Drăgoi, B., 294  
 Drakou, Foteini, 34  
 Dražen, Balen, 407  
 Drewniak, M., 432  
 Drits, Victor A., 74, 449  
 Dronov, A.V., 313  
 Drury, M.R., 85  
 Duarte, Luís Vitor, 115  
 Duclaux, L., **397**, **486**

Dufrêche, Jean-François, 59  
 Dula, Roman, 420  
 Dultz, S., 421  
 Dumas, Angela, **445**  
 Dumas, E., **369**  
 Dumitriu, E., 294  
 Dumon, Mathijs, **164**  
 Dunkl, István, 121, 428  
 Durán Oreja, M., 250  
 Duran, Esperanza, 228  
 Dypvik, Henning, 346  
 Dzene, Liva, **466**

**E**  
 Eberl, Dennis D., 138  
 Eguchi, Miharuru, **200**  
 Ekosse, Georges-Ivo, 240  
 El Boudour El Idrissi, Hicham, 256  
 El Ouahabi, Meriam' **368**  
 Elena, Kuznetsova, 398  
 Elsen, Jan, 166  
 Emmerich, Katja, 232, 275, 307,  
 447, **451**  
 Ennaciri, Aomar, 487  
 Enza Vitale, **300**  
 Erastova, Valentina, **60**, 64, 505  
 Erath, J., 384  
 Eren, Muhsin, 114  
 Eriksson, Ann Kristin, **353**  
 Erkoyun, Hülya, **113**, 114  
 Estève, Imène, 190  
 Ezersky, Vladimir, 110

**F**  
 Fabian, Margit, 197  
 Fafard, Jonathan, **475**  
 Fagel, Nathalie, 256, 368  
 Fahel, Jean, 414, **458**  
 Fallick, Anthony E., 127, 370  
 Faour, A., 454  
 Farina, Mauro, 219  
 Faulkner, D.R., 249  
 Feicht, Patrick, 384  
 Ferguson, Brennan O., 290  
 Fernández Barrenechea, J., 163  
 Fernández, Ana María, 163, **324**  
 Fernández, R., 163  
 Fernandez-Barranco, C., 431, **432**  
 Fernández-Caliani, J.C., 226  
 Ferrage, Eric, 52, 79, **287**, 350,  
 448, 466  
 Ferrell, Ray E., **165**, 346  
 Fery, A., 384  
 Fettweis, Michaël, 166  
 Fialips, Claire I., **500**  
 Field, Brad, 246  
 Filimonov, Alexey, 240  
 Findling, Nathaniel, 351  
 Fiore, S., 168  
 Fisher, Quentin, 498  
 Fitch, Alanah, **331**  
 Fjuita, Ken-ichi, 24  
 Flores, Federico Manuel, 156

## AUTHOR INDEX

Foged, Niels, 253  
 Fontaine, François, **256**  
 Forano, Claude., **142**, 369, 419, 433, 455  
 Forro, Laszlo, 25  
 Förster, Stephan, 450  
 Fosso-Kankeu, Elvis, 240  
 Foulkes, Jonathan, 481  
 Fournier, Frédéric, 291  
 Franchini, M.B., 282, 410, 429  
 Fraser Harris, Andrew, **393**  
 Fraser, Donald G., **141**  
 Fraser, Tony, 70  
 Freiburg, Jared T., **192**  
 Freitag, Peter, 327  
 Friedrich, Frank, 107, 127, 185, 275  
 Frolova, Anna, 240  
 Fronczyk, Joanna, 214, **217**  
 Frushour, Anthony M., **277**  
 Fujii, Kazuko, **38**  
 Fujinaga, Kaoru, 222  
 Fujit, Masahiko, 146  
 Fujita, Ken-ichi, 436  
 Fullen, Michael A., 237, 31  
 Fumagalli, Patrizia, 219  
 Furnival, Steve, 116  
 Furrer, Gerhard, 372  
 Fůrychová, Petra, **395**

### G

Gadsdon, Martyn, **303**  
 Galán, Emilio, **212**, 226, 233  
 Galán, P., **276**, 324  
 Gamero Diaz, Helena, 425  
 Garbulewski, Kazimierz, 217  
 García Rivas, J., 250  
 García-Casco, Antonio, 358  
 García-España, Laura, 255  
 García-González, M.T., 163  
 García-Romero, E., 163, 250, **285**  
 García-Villén, F., 215  
 Garnier, Jérémie, 404  
 Gatari, Michael, 352  
 Gates, Will P., **323**  
 Gatta, G. Diego, 219, 32  
 Gautron, Jérôme, 299  
 Gawel, Adam, 420  
 Geatches, Dawn L., 63  
 Geese, Gill, 41  
 Geiger, Florian, 309  
 Génin, J.-M. R., **386**, **459**  
 Gergely, Felician, **197**  
 Gervilla, Fernando, 90  
 Ghanizadeh, Amin, 183  
 Giannatou, Spiridoula, 34  
 Gier, Susanne, 187, **511**  
 Gilbert, Benjamin, **446**  
 Gilg, H. Albert, 107, **127**, 311, 370  
 Gilkes, Robert, 112  
 Ginzel, Stefan, **309**  
 Gionis, Vassilis, 452  
 Giora Rytwo, **148**

Gluyas, Jon G., 501  
 Gómez, Carmen, 241  
 Gómez-Avilés, Almudena, 484  
 Gómez-Barreiro, J., **250**  
 Gómez-Espina, R., 326  
 Gómez-Vidales, Virginia, 140, 238  
 Göncüoğlu, Mehmet Cemal, 32, 315  
 Gönen, Tuğba, 229  
 Gonta, T.V., 313  
 González, I., 163  
 Gonzalez, Rosalina, **467**  
 Goo Cho, Hyen, **199**  
 Górniak, Katarzyna, **83**, **191**  
 Gottlieb, Paul, 367  
 Goure Doubi, Hervé, 298  
 Grade, Arno, 395  
 Graham, Caroline, 325  
 Grathoff, Georg H., 84, 107, 186, 192  
 Gray, Nia, 70, **73**  
 Greathouse, Jeffery A., **55**, 63  
 Greenwell, Chris, 60, 63, 64, 141, 501, **505**, 506, 510  
 Gregoire, Brian, 141  
 Grew, E.S., **462**  
 Grings Cedeño, Daniel, **106**  
 Gröcke, Darren R., 501  
 Grolimund, Daniel, 227  
 Gross, Christoph, 314  
 Guaschino, Lorenzo, 219  
 Guégan, Régis, 340, 487  
 Guérard-Hélaine, Christine, 142  
 Guérin, O., 459  
 Guggenheim, Stephen, **318**, 493  
 Guimarães, Vanessa, **153**  
 Guisseau, Delphine, 129  
 Günal-Türkmenoğlu, Asuman, **394**  
 Gunter, Mickey, 29  
 Gürel, Ali, 254  
 Gurgul, Jacek, 424  
 Gustafsson, Jon Petter, 353

### H

Ha, Jang-Hoon, **159**  
 Haase, Hanna, **474**  
 Habel, Christoph, **377**  
 Haberlah, David, **170**  
 Hajjaji, W., **338**, **378**, 399  
 Hajnos, M., 354  
 Halisch, M., 186  
 Hall, Adrian M., 127, **370**  
 Hamon, G., 504  
 Hanafy, Nemany A.N., 66  
 Hankins, Nick, 258  
 Hansen, Staffan, 322  
 Hanusová, Irena, **391**  
 Harjupatana, Tero, **319**  
 Harley, Simon, 316  
 Harris, Robert, 48, 206  
 Hart, David B., 55  
 Hart, George F., 165  
 Hart, Jarrod, **293**

Hashizume, Hideo, 38, **143**  
 Hassan, Yusuf, 137  
 Hatta, Tamao, 39, 356  
 Hatzipanagiotou, Konstantinos, 261  
 Haurine, Frédéric, **305**  
 Hayakawa, Takayuki, 24, 436  
 He, Hongping, 158, 422  
 He, Rui, 72  
*Heaney, Peter J.*, 289  
 Hee Jung, Da, 41  
 Hélaine, Christine, 433  
 Herbillon, A., 459  
 Herling, Markus M., 382  
 Herranz, Juan Emilio, 408  
 Hervig, Richard L., 499  
 Hesterberg, Dean, 353  
 Heuser, Gert, 245  
 Hillier, Stephen, **70**, 73, 169, **174**, 225, 352, 353, 502  
 Hirahara, Hidetoshi, 134, 198  
 Hirajima, Tsuyoshi, 44  
 Hlekane, Phindile, 262  
 Hochleitner, Rupert, 107  
 Hofmann, Ronny, 502  
 Holbeche, Georgina, **112**  
 Holcova, Lenka, 152  
 Hong, In-Kee, 202  
 Honty, Miroslav, 395  
 Hoppie, Bryce, 48, 206  
 Horvath, Endre, 25  
 Houben, M.E., **85**  
 Hrachová, J., 418  
 Hronský, Viktor, 263  
 Hsu, Chun-Chun, **380**  
 Hubert, Fabien, 79, 287, **350**, 351, 357, 466  
 Hubert-Ferrari, Aurélia, 368  
 Huertas, F. Javier, **90**, 349  
 Huertas, F.J., 163  
 Huff, W.D., **313**  
 Huggett, J. M., **280**  
 Huve, Jeoffrey, 227  
 Hwang, Soon-Seok, 202  
 Hynek, Jan, 415

### I

Ibeh, Sally, 240  
 Iconaru, Simona, 340  
 Ide, Yusuke, **145**  
 Igalavithana, Avanthi Deshani, 330  
 Iglesias, R.J., 326  
 Iiyama, Taku, 146  
 Impiccini, A., 282, 410, 429  
 Inadomi, Takumi, 207, 472  
 Ingeman-Nielsen, Thomas, 253  
 Inoue, Atsuyuki, **356**  
 Inoué, Sayako, **278**, 406  
 Ishii, Yasuo, 188  
 Ito, Kenichi, **39**  
 Iucolano, F., 32

## AUTHOR INDEX

### J

Jaber, Maguy, **291**  
 Jackson, Cyndi, 201  
 Janek, M., **336**  
 Jankovič, Ľuboš, 22, 252, 335, 374  
 Jánošík, Michal, **91**  
 Jean, Jiin-Shuh, 150  
 Jeans, Christopher, **117**  
 Jelavic, S., 507, **508**  
 Jencus, Heinrich, 218  
 Jensen, Nicholai D., 455  
 Jerez, Oscar, 492  
 Ji, Shichao, 422  
 Jiang, Wei-Teh, 150  
 Jiménez Espinosa, Rosario, 248  
 Jiménez Millán, Juan, 248, 249, 431  
 Jimenez-Ruiz, Monica, 52  
 Jiráťová, Květa, 296  
 Jochec-Mošková, Daniela, 252  
 Johann, Tobias, 309  
 Johnston, Cliff T., **63, 427**  
 Jones, Timothy, **137**  
 Jonkis, Urszula, 428  
 Joussein, Emmanuel, 299  
 Jozanikohan, Golnaz, **498**  
 Juárez-Carbajal, Esmeralda, 140  
 Juliaa, JF, 486  
 Jun, Gao, **82**

### K

Kabanov, P., 347  
 Kaden, Heike, 451  
 Kadir, Selahattin, 113, **114, 254**  
 Kagiaras, Efthimios, 401  
 Kalinichev, Andrey G., **51, 53, 56, 210**  
 Kalinin, P.I., 347, 354  
 Kalo, Hussein, 382, 412  
 Kampman, Niko, 183  
 Kaneda, Keisuke, 471  
 Kang, Il-mo, 239  
 Kanygin, A.V., 313  
 Karabacak, Volcan, 368  
 Kareem, Rikan, 505, 506  
 Kasama, Takeshi, 105, **406**  
 Kataja, Markku, 319  
 Katz, Al, 367  
 Kaufhold, S., 84, 87, 140, 184, 225, 327, 426, 186, **320**  
 Kavouri, Stavroula, 401  
 Kawamata, Jun, 47, 477  
 Kawamura, Katsuyuki, 195  
 Kawiak, Tadeusz, 121  
 Kayode, J., 237  
 Keller, L., 187  
 Kelm, Ursula, **492**  
 Kenne Dedzo, Gustave, 476  
 Keppert, Martin, 152  
 Keri, Annamaria, 197  
 Kervern, Gwendal, 413, 456  
 Khairnar, Rajendra, 35  
 Khunová, Viera, **76**

Kikuchi, Ryosuke, **453**  
 Kim, Eun-Ji, 202  
 Kim, Hyoung-Jun, **202**  
 Kim, Hyoung-Mi, 203, 204, **40**  
 Kim, Hyun-Joong, 49  
 Kim, Jee-Young, 41  
 Kim, Jinwook, 41, 48, 206  
 Kim, Sung Hoon, 204  
 Kim, Tae-Hyun, **203**  
 Kim, Yoon Suk, 204  
 Kimura, Yukinobu, 317  
 Kirkpatrick, R. James, **18, 53, 55, 290**  
 Kitanaka, Koki, 222  
 Kiviranta, Leena, 227  
 Klaver, J., **86**  
 Klavins, Maris, 334  
 Kleeberg, Reinhard, 275  
 Knies, Jochen, 224  
 Kniewald, Goran, 241  
 Knodt, Rita, 309  
 Kobera, Libor, 218, 402, 403  
 Koděra, Peter, 91  
 Koffi Konan, Léon, 298  
 Kogure, Toshihiro, 48, **50, 74, 206, 278, 341, 406, 453**  
 Koilraj, Paulmanickam, 44  
 Kokol, Vanja, 35  
 Kolousek, David, 152, **218**  
 Kolyagin, Y., 369  
 Komadel, Peter, **252, 418**  
 Komar, Darja, **241**  
 Komatsu, Yu, 222  
 König, Daniela, 372  
 Königer, Franz, 451  
 Koo, Kang, 202  
 Koo, Tae-hee, **41**  
 Kornaros, Michalis, 133  
 Koster van Groos, A. F., 318, 493  
 Köster, Mathias H., **311**  
 Kostjukovs, Juris, 334  
 Koteja, Anna, **20, 24**  
 Koutra, Eleni, 133  
 Koutsopoulou, Eleni, 312  
 Kovanda, František, **296**  
 Kovář, Petr, 381, 415  
 Kowalik, Jacqueline, 318  
 Kowalska, Sylwia, **428**  
 Koziol, A.E., 431, 432  
 Kralj, Polona, **128**  
 Krejčová, Stanislava, 296  
 Krivovichev, Sergey V., **36, 423**  
 Krooss, Bernhard M., 183  
 Krupskaya, V., **321**  
 Kuchovská, Dana, 395  
 Kuchovský, Tomáš, 395  
 Kudejova, Petra, 311  
 Külah, Tacit, 113  
 Kuligiewicz, Artur, **257**  
 Kunz, Daniel A., 384  
 Kunz, Martin, 446  
 Kunze, Michael, 309  
 Kuramata, Chisaki, 453

Kus, J., 186  
 Kuzmann, E., 459  
 Kuznetsova, Elena, **359**  
 Kwak, Kyeong Yoon, 199  
 Kwon, Minjae, 49, **208**

### L

La Rubia, M.D., 431  
 Labaume, Pierre, 405  
 Labeyrie, Bernard, 500  
 Labille, Jerome, **464**  
 Labrincha, J.A., 338, 378  
 Lacroix, Brice, 405  
 Ladage, S., 186  
 Laipan, Minwang, 158  
 Laird, David, **160**  
 Lakhane, Madhuri, **35**  
 Lambaša Belak, Živana, 241  
 Lamprompti, Giulio L., 30, 117  
 Lampropoulou, Paraskevi, **261**  
 Lanari, Pierre, 405  
 Lang, Kamil, 415  
 Langella, Alessio, 28  
 Lansalot, Muriel, 478  
 Lanson, Bruno, **284, 350, 351, 448**  
 Laou, Lamyaa, **297**  
 Laroche, Céline, 433  
 Łątka, Kazimierz, 424  
 Latrille, Christelle, **154**  
 Latta, Drew E., 465  
 Launois, Pascale, **71, 339**  
 Laurent, Jean-Paul, 500  
 Lazzara, Giuseppe, **69**  
 Le Beau, Helene, 368  
 Le Floch, S., 397  
 Le Maitre, Christine, 481  
 LeBlanc, Jeffrey, 367  
 Lecomte-Nana, Gisèle L., **298, 434**  
 Lee, Jin-Hee, 202  
 Lee, Ji-Yeong, 40  
 Lee, Jongman, 159  
 Lee, Soo-Jae, 199  
 Lee, Sung-Woo, 202  
 Lee, Won-Jae, 203  
 Lefèvre, G., 155  
 Leggo, Peter J., **30**  
 Lemaire, Marielle, 142, 433  
 Leonardi, A., **416**  
 Leoni, Matteo, **288**  
 León-Reina, L., 163  
 Leporatti, Stefano, **66**  
 Leroux, Fabrice, 454, 478  
 Lessovaia, Sofia, **240, 360**  
 Letofsky-Papst, Ilse, 327  
 Levitz, P., 236, 287, 504  
 Lexa, Jaroslav, 263  
 Leyva-Ramos, Roberto, **21, 473**  
 Lhotka, Miloslav, 152, 218, **403**  
 Li, Cunjun, 301  
 Li, Tian, 422  
 Li, Xijiang, 42  
 Li, Zhaohui, 150  
 Lie-A-Fat, J., 85

## AUTHOR INDEX

- Lieske, Wolfgang, 101  
 Liguori, B., 32  
*Ling, Florence*, 289  
 Lipton, Andrew S., 419, 455  
 Liu, Dong, 234, **396**, 430  
 Liu, Hongmei, 430  
 Liu, Jiang Feng, 325  
 Liu, Mingxian, **72**  
 Liu, Yanju, 333  
 Liu, Zhifei, **42**  
 Loganathan, Narasimhan, 51, **53**  
 Lojen, Sonja, 241  
 Longstaffe, F.J., 280  
 López Galindo, A., 163  
 López, F., 231  
 Lowe, David, 68  
 Lu, Xia, 82  
 Lumsdon, David, 73  
 Lunar, R., 244  
 Luo, Wuhui, 383  
 Lvov, Yuri M., 66
- M**  
 Machovic, Vladimír, 403  
 Macías, Inmaculada, 276  
 Madejová, Jana, **22**, 209, 252, 263, 335, 374  
 Mahabole, Megha, 35  
 Mahdi, Rima, 142, 433  
 Mahieux, Geoffroy, 246  
 Mählmann, Rafael Ferreira, **123**, 125, 124, 246  
 Mahood, Robert, 502  
 Maierdan, T., 108  
 Maillet, Marine, 125  
 Maison, Tatiana, 125  
 Maki, Tei, 471  
 Makri, Pagona, 387, 388  
 Malie, Pierre, 246  
 Malikova, N., 236  
 Mameli, Paola, **371**  
 Mandal, Asit, 157, 373  
 Marantos, Ioannis, 312  
 Marion Wampler, J., 201  
 Márquez, Marcial G., 212  
 Marquez, Xiomara, 495  
 Marry, V., 57  
 Marry, Virginie, 59  
 Marschall, P., 187  
 Martín, Domingo, 233, 276  
 Martin, François, 445  
 Martín, P.L., 326  
 Martínez-Costa, Jesus I., 21  
 Martín-García, J.M., 163  
 Martti, Esala, 352  
 Marynowski, Leszek, 81  
 Mas, Antoine, 129  
 Masunaga, Hiroyasu, 471  
 Matejdes, M., 336  
 Matešić, Sanja Slavica, 241  
 Matray, Jean-Michel, 190  
 Matsuda, Tatsuro, 39  
 Matusik, Jakub, 20, **23**, **213**, 214
- Mayayo, María José, 366  
 Mayor, J.C., 323  
 Maziarz, Paulina, 213  
 Mazur, Zbigniew, 214  
 McCarty, Douglas K., 173, 225, **449**  
 McClure, Roberta, 341  
 McDermott, Chris, 393  
 Medjahdi, G., 457  
 Meidina, N., 108  
 Melón, A., 324  
 Mendes Guimarães, Edi, 404  
 Mercurio, Mariano, 28, **219**  
 Merritt, Jon W., 370  
 Mertens, Gilles, 502  
 Metaxa, Eugenia, 261  
 Michalik-Zym, Alicja, 420  
 Michaud, Philippe, 433  
 Michot, Laurent J., **52**, 236, 287, 504  
 Mikutta, R., 421  
 Milioto, Stefana, 69  
 Milius, Wolfgang, 412  
 Milliken, Ralph, 167  
 Mills, S. J., 386, 459, **460**  
 Minase, Makoto, 24, 436  
 Mirabel, L., 486  
 Miras, A., 226  
 Miras, Adolfo, 233  
 Mitea, Raluca, 482  
 Mitsis, Ioannis, 34  
 Miyake, Michihiro, 329  
 Miyamoto, Nobuyoshi, **472**  
 Miyamoto, Nobuyoshi, 207  
 Miyoshi, Satoru, **317**  
 Mizrahi, Martin, 445  
 Mochida, Shuhei, 477  
 Mogilyanski, Dmitry, 110  
 Mokrani, Amina, 298  
 Molepo, Johanna, 240  
 Mongelli, Giovanni, 371  
 Mongogoa, Francis, 240  
 Montavon, Gilles, 51  
 Montoya, Ascención, 140  
 Montoya, Ascención, 238  
 Morata, Diego, 126  
 Morata, Diego, 130  
 Morata, Diego, 245  
 Moreira Silva, Adalene, 404  
 Morgan, L., 341  
 Morrison, Keith D., 138, **139**  
 Motelica-Heino, Mikael, **340**  
 Mourelle, Lourdes, 241  
 Mouri, Emiko, 483  
 Mousty, C., 454  
 Mukai, Hiroki, 453  
 Mulaba-Bafubiandi, Antoine F., **262**  
 Mullan-Boudreau, Gillian, **503**  
 Muller, F., 397  
 Mullis, Josef, **124**  
 Muñoz, Manuel, 405  
 Muranyi, Peter, 295
- Müthing, Nina, **101**
- N**  
 Nadeau, Paul, **495**  
 Naftaly, M., 336  
 Naidu, Ravi, 157, 230, 330, 333, 373  
 Naille, S., 457  
 Nait-Ali, Bénéît, 298  
 Nakamura, Kana, 329  
 Nakao, Atsushi, 201  
 Nakato, Teruyuki, **483**  
 Napruszewska, Daria, 420  
 Naqvi, Syed A. A., 346  
 Narita, Eiichi, 134, 198  
 Navarro, Leonardo, 245  
 Neumann, Anke, 235, **465**  
 Neupane, Ghanashyam, 337  
 Newport, Leo P., **501**  
 Newville, M., 341  
 Ngouana Wakou, Brice F., 51  
 Nguyen, A.N., 397, 486  
 Nickel, Claudia, 327  
 Nielsen, Ulla Gro, 142, 419, **455**  
 Nieto, Fernando, 126, 130, 163, 244, 245, 249,  
 Nieto-Camacho, Antonio, 140, 238  
 Nikitin, Anton, 502  
 Niknam, V., 338  
 Nishido, Hirotsugu, **220**  
 Nishimoto, Shunsuke, 329  
 Nono, Yoshihiro, 483  
 Norouzi, Gholam Hossain, 498  
 Norris, Simon, 393  
 Notini de Andrade, Luiza, 465  
 Nowak, Paweł  
 Nyambura, Mercy, **352**
- O**  
 Obalová, Lucie, 296  
 Oberhardt, Nikolas, 346  
 Ochi, Kotaro, 46  
 Oda, Chie, 45  
 Odiyo, John, 240  
 Ogawa, Makoto, **24**, **436**  
 Oggiano, Giacomo, 371  
 Ogola, Jason, 240  
 Oguchi, Junpei, 146  
 Oh, Jae-Min, 40, 202, 203, **204**  
 Ohkubo, Takahiro, 189  
 Okada, Tomohiko, **146**, **435**  
 Okuyucu, Cengiz, 315  
 Olajide-Kayode, Jerry O., 243  
 Olatunji, Akinade S., **243**  
 Olegario-Sanchez, Eleanor, **221**  
 Olson, Carolyn, **355**  
 Olson, Tyler L., 465  
 Olszówka, Joanna, 424  
 Ömeroğlu, İşıl **493**  
 Önalgil, Nergis, 114  
 Ona-Nguema, Georges, 386  
 Oniki, Yudai, 47  
 Ortega, L., 244

## AUTHOR INDEX

Osacký, Marek, 395  
 Osada, Yoshihito, 471  
 Osan, Janos, 197  
 Oshima, Syunichi, 222  
 Ostertag-Henning, Christian, 186, 385, **426**  
 Ottner, Franz, 348, 390  
 Ottosen, Lisbeth, 491  
 Oueslati, Walid, **26, 417**  
 Ouladdiaf, B., 250  
 Ouvrard, Guy, 302  
 Owen, Michael, 170  
 Oya, Mitsuru, 436  
 Oyedeji, Ayodele A., 237  
 Ozen, S., **32**  
 Ozgur, Cengiz, **389**  
 Ozola, Ruta, 334, 376

### P

Pabakhsh, Pooria, **68**  
 Padilla-Ortega, Érika, 473  
 Paek, Seung-Min, 203  
 Paineau, Erwan, 71, **339**  
 Palacios, Eduardo, 140, 238  
 Pálková, Helena, **263, 335**  
 Pan, Y., 108  
 Panagiotaras, Dionisios, 133  
 Papapanagiotou, Photinie, 129  
 Papoulis, Dimitrios, **133, 261**  
 Paris, M., 488  
 Parisi, Filippo, 69  
 Park, Kyong Ryang, 41  
 Párraga, J., 163  
 Pasbakhsh, Pooria, **75**  
 Passey, Simon R., 30  
 Patel, Radhika, **510**  
 Patrier, P., **129, 281, 282, 410, 429**  
 Peach, C.J., 85  
 Pearson, Samuel, 478  
 Pekov, Igor V., 423  
 Peláez-Campomanes, Pablo, 408  
 Pelayo, M., 163  
 Peltz, Markus, 84  
 Pendlowski, Helen A., 70, **169**  
 Pentrak, Martin, 140  
 Pentrakova, Linda, 140  
 Perry, Sarah, 273  
 Petersen, Line B., 455  
 Petit, Sabine, 104, **109, 294, 434**  
 Petra, Lukáš, 252, **418**  
 Payne, Julie, **299**  
 Phakoago, Valery, 240  
 Phillips, Ian, 70  
 Phipps, Jonathan, **306**  
 Pike, Darin Q., 63  
 Pilavtepe, Müge, **307**  
 Piña, R., 244  
 Pipich, Vitaliy, 183  
 Pishedda, V., 397  
 Plötze, M., **172, 186, 225, 360, 372**  
 Polekhovsky, Yury, 240, 360  
 Polubesova, Tamara, **43**  
 Pons, M.J., 282, 410, 429

Pospíšil, Miroslav, **381, 415**  
 Post, Jeffrey E, **289**  
 Potel, Sébastien, **125, 246**  
 Potter, Stephen, 137  
 Pourtabib, Kristina, **29**  
 Pouvreau, Maxime, **56**  
 Pozo, E., 163, **408**  
 Praus, P., 381  
 Predoi, Daniela, 340  
 Premaratne, W.A.P.J., 465  
 Prêt, Dimitri, 79  
 Prévot, Vanessa, 142, 25, 419, **433, 454, 455, 478**  
 Prinz, Dirk, 183  
 Prokop, Anna, 213  
 Prytherch, Zoe, 137  
 Pšenička, Milan, 381, **242**  
 Puentes, Pilar Hernández, **248**  
 Pushparaj, Suraj S. C., **419**  
 Puškelová, Ľubica, 91

### Q

Qingchun, Yu, 82  
 Quetscher, Annette, **489**  
 Quintela, A., 136

### R

Radziemska, Maja, **214, 217**  
 Rainoldi, A., 282, 410, 429  
 Ramírez-Apán, María Teresa, 140, 238  
 Rapsomanikis, Andreas, 133  
 Raputhing, Manneheng, 240  
 Rasamimanana, Sabrina, **155**  
 Rath Nielsen, A., 508  
 Raven, Mark D, **171, 175, 225**  
 Ravenstein, T., 85  
 Ravuluvulu, Rachel, 240  
 Rawski, M., 432  
 Real, Miguel, 228  
 Regnault, Olivier, 468  
 Reich, Martin, 130  
 Reichenauer, Thomas G., 327  
 Reinert, L., 397, 486  
 Reolid, Matías, 115  
 Requejo, Felix, 445  
 Riber, Lars, **346**  
 Rieß, Martin A., **382**  
 Rigolet, Séverinne, 156  
 Rimma, Motenko, 359  
 Rivard, Camille, 351  
 Roaldset, Elen, **496**  
 Robert, Jean-Louis, **286**  
 Robertson, Jean, 70  
 Robin, Valentin, **468**  
 Rocha, F., **136**  
 Rocha, Fernando, 115, 153, 338, 378, **399**  
 Rodríguez-Castellón, Enrique, 153  
 Rodríguez-Ruiz, M.D., **251**  
 Rogan Šmuc, Nastja, 241  
 Rogovska, Natalia, 160

Rogowska, Melania, **420**  
 Romero, Antonio, 233  
 Romero, F.J., 326  
 Rosenfeldt, Sabine, 450  
 Rossignol, Sylvie, 297, 299  
 Rotenberg, Benjamin, 57, 59  
 Rothwell, Katherine Ann, **235**  
 Rouzière, Stéphan, 71, 339  
 Rowbotham, Peter, 116  
 Royer, S., 294  
 Rozenbaum, Alexis G., 387  
 Ruby, Christian, 386, 457, 459  
 Ruiz, A.I., 163  
 Ruiz-Cruz, M.D., 251  
 Ruiz-Hitzky, Eduardo, **470, 473, 480, 484**  
 Rusmin, Ruhaida, **333**  
 Russo, Giacomo, 300  
 Ryan, Peter C., **349**

### S

Šafařík, Ivo, 76  
 Sahabi, Fereydoun, 498  
 Sainz-Díaz, C. Ignacio, **62**  
 Sakao, Kazunori, 198  
 Sakhawoth, Y., **236**  
 Sakuma, Hiroshi, **195, 205**  
 Salah Amara, Mohamed, 339  
 Salanne, M., 57  
 Sammaljärvi, Juuso, 190  
 Sammon, Chris, 481  
 San Miguel, A., 397  
 Sanbuichi, Takashi, 317  
 Sancelme, M., 369  
 Sánchez del Rio, M., 250  
 Sanchez, C., **249**  
 Sánchez, M., 324  
 Sánchez, Pablo, 130  
 Sánchez-Bellón, A., 163  
 Sánchez-Ledesma, D.M., 324  
 Sánchez-Navas, Antonio, 358  
 Sandler, Amir, **387**  
 Sandmann, Dirk, 170  
 Sano, Tsuneji, 145  
 Santana, Igor V., **400**  
 Santaren, J., 163  
 Santelli, Cara M., 289  
 Santin, Alessandro, 151  
 Sanz de Galdeano, C., 251  
 Sarkar, Binoy, 157, 230, **330, 333, 373**  
 Sarr, Anta-Clarisse, 125  
 Sas, Samuel, 375  
 Sasaki, Keiko, **44, 383**  
 Sato, Tsugio, 134  
 Sato, Tsutomu, **45, 317**  
 Satomi, Koichiro, 477  
 Sayın, Şih Ali, 493  
 Schäfer, Thorsten, **78, 185**  
 Schampera, B., **421**  
 Schanz, Tom, 101, 474  
 Scherer, Michelle M., 465  
 Schicker, Andrea, 511

## AUTHOR INDEX

- Schild, Dieter, 185  
 Schleicher, Anja M., **193**  
 Schmid, Jasmin, **384**  
 Schmidt, Susanne Th., **120**, 122  
 Schnetzer, Florian, **447**  
 Schobert, Rainer, 377, 382  
 Scholtzová, Eva, **209**  
 Scholz, Joachim, 309  
 Schönenberger, Jasmin, 224  
 Schönweitz, Claudia, 295  
 Schoonheydt, Robert A., 63, 482  
 Schroeder, Paul A., **344**, 345, 346  
 Schuhmann, Rainer, 307  
 Schulte, Lothar, 495  
 Schwarz, Jens-Oliver, 86  
 Schwedes, Mathias, 382  
 Schweinar, Kevin, 183  
 Schwieger, Wilhelm, 33  
 Seifi, Sahar, 434  
 Sekeráková, Ludmila, 22  
 Sekine, Mai, 198  
 Sell, B., 313  
 Sellin, Patrik, **325**  
 Selvam, Thangaraj, 33  
 Serclerat, I., 488  
 Serwicka, Ewa Maria, 335, 420, 424  
 Shaikh, Afshan, 201  
 Shcherbakova, H., 459  
 Shen, Ping, **258**  
 Shepherd, Keith D., 352  
 Shibata, Masahito, 317  
 Shigehara, Kiyotaka, 471  
 Shikinaka, Kazuhiro, **471**  
 Shimomura, Shuichi, 38  
 Shin, Koichi, 102  
 Shinohara, Satsuki, 134  
 Shiono, Takashi, 146  
 Shota, Endo, 198  
 Shotyk, William, 503  
 Siitari-Kauppi, Marja, 190  
 Sik Ok, Yong, 330  
 Šimić-Kanaet, Zrinka, 407  
 Siminel, Nikita, **211**  
 Simonsson, Magnus, 353  
 Singh, Balwant, 271  
 Sinisi, Rosa, 371  
 Skipper, Neal, **110**, 510  
 Škrátek, Martin, 76  
 Skrzypiec, K., 432  
 Slaný, Michal, 263  
 Slavík, Roman, 218  
 Smith, Agnès, 298  
 Smoliga, John A., **132**  
 Snellman, Margit, 227  
 Solc, R., 421  
 Solling, Theis, 495  
 Song, In-Hyuck, 159  
 Song, Y.G., 239  
 Song, Yungoo, 239  
 Sørli, Ronald, 346  
 Spitz, Marcus, 327  
 Środoń, Jan, **121**, **162**
- Stamataki, Stefania, 34  
 Stamatakis, Michael G., **34**, **401**  
 Stangvik, Kristian, 346  
 Stanjek, Helge, 183  
 Stankevica, Karina, 376  
 Stathatos, Elias, 133  
 Stattegger, Karl, 42  
 Steudel, Annett, 232, **275**, 307  
 Stipp, S.L.S., 507, 508  
 Stöter, Matthias, 377, 450  
 Straaso, Tine, 495  
 Strydom, Jessica, **332**  
 Stucki, Joseph W., 140  
 Suárez, M., **163**, 250, 285  
 Sugihara, Hiroyuki, 477  
 Suizuki, Noriko, **46**  
 Sulikowski, Bogdan, 335  
 Süssenberger, Annette, **122**  
 Suyama, Tadahiro, 188  
 Suzuki, Asuka, 435  
 Suzuki, Masaya, 39  
 Suzuki, Yasutaka, 47, **477**  
 Svein Willy, Danielsen, 398  
 Svensson, Daniel, **322**  
 Svoboda, Jiří, 391  
 Szabó, Tamás, **482**  
 Szczerba, Marek, **173**, **210**, 225  
 Szekeres, Márta, 482  
 Szilagyi, Istvan, **25**
- Tachi, Yukio, 188, 189, 195  
 Taitel-Goldman, Nurit, **110**  
 Takahashi, Hiroaki, 188  
 Takahashi, Noriyuki, 198  
 Takaki, Yu, 44  
 Tamura, Kenji, **205**  
 Tan, Daoyong, 216  
 Tan, Michael, 221  
 Tan, Pingchuan, 346  
 Tao, Qi, **422**  
 Taviot-Guého, Christine, 415, **454**, 478  
 Tazi, S., 57  
 Tenney, Craig M., 58  
 Terhorst, Birgit, 348  
 Terres, Eduardo, 140  
 Terroso, Denise, 115, 136  
 Terroso, E. D., 163  
 Tertre, Emmanuel, **79**, 287, 350, 357, 466, 468  
 Tesson, S., **57**  
 Thatcher, Kate, 393  
 Theng, Benny K.G., 68, 140, 143  
 Thill, Antoine, 339  
 Thissen, Peter, 447, 451  
 Tibljaš, Darko, **407**  
 Timea Baranyaiová, 149  
 Tinnacher, Ruth, 446  
 Tobaldi, D.M., 378  
 Tomanová, Katarína, 76  
 Tominaga, Makoto, **47**  
 Tomljenović, Bruno, 121  
 Torii, Masato, 145
- Torok, Szabina, 197  
 Torres Sanchez, Rosa Maria, 156  
 Trincal, Vincent, 405  
 Tsuyoshi Yaita, 50  
 Tunega, Daniel, 209, 421  
 Türkmenoğlu, Asuman Günel, **315**, 493  
 Turpault, Marie-Pierre, 357  
 Tyupina, E., 321  
 Tzevelekou, Theophani, 261
- U
- Üfer, Kristian, 140, **175**, 186, 225, 426  
 Uhlík, Peter, 91, 263  
 Umbhauer, François, 500  
 Underwood, Thomas, **64**, 505  
 Ungureanu, A., 294  
 Ünlüce, Özge, 315, 394  
 Upadhyay, C., 459  
 Urai, Janos L., 86  
 Urbanova, Martina, 218, **402**  
 Utada, Minoru, 356  
 Uysal, Tonguç, **119**
- V
- Vallcorba Valls, O. Oriol, 250  
 Van den Bogaert, Romain, 464  
 van der Gaast, Sjerry, 143  
 van der Pluijm, Ben A., 89, 193, 247  
 Van Ranst, Eric, 164  
 Vandenberghe, Noël, 166  
 Vasilatos, Charalampos, 34  
 Vazquez, Mercedes, 126, **130**, **245**  
 Večerník, Petr, 391  
 Velić, Ivo, 121  
 Venkateswara Reddy, U., **290**  
 Vergaro, Viviana, 66  
 Vialat, P., 454  
 Vidal, O., **279**  
 Viennet, Jean Christophe, 350, **357**  
 Villar, María Victoria, 325, **326**  
 Vincevica-Gaile, Zane, 376  
 Viseras, C., **135**, **215**  
 Vlahović, Igor, 121  
 Vokál, Antonín, 325  
 Volk, Caroline, 309  
 von Eynatten, Hilmar, 121  
 Voutilainen, Miko, 190  
 Vrhovnik, Petra, 241  
 Vučković, Maja, 407
- W
- Wade, Peter, 332  
 Wagner, Jean-Frank, **151**  
 Walker, Jeff, **260**, **273**
- Wall, Frances, 400  
 Walter, Philippe, 291  
 Walton, Anthony, 273  
 Wampler, J. M., **259**



## AUTHOR INDEX

Wander, Michelle, M., 351  
 Wang, H., 108  
 Wang, Linjiang, **301**  
 Wang, Shan-Li, 341  
 Warr, Laurence N., 232  
 Watanabe, T., 274  
 Watanabe, Yasutaka, **392**  
 Watanabe, Yujiro, **222**  
 Wattinne, Aurélia, 281  
 Weger, Thomas, 426  
 Wegerer, Eva, **196**  
 Weidler, Peter G., 185  
 Weiss, Anna, 331  
 Weiß, Thomas, 450  
 Wemmer, Klaus, 120  
 Wenk, H.-R., 250  
 Wersin, Paul, 227  
 Wicklein, Bernd, **480**  
 Wiesner, Martin G., 42  
 Wilcox, Jennifer, 63  
 Wilkinson, Mark, 497  
 Will, Patrizia, 107  
 Willenbacher, Norbert, 307  
 Williams, Craig D., 31  
 Williams, Lynda B., **138, 139, 194,**  
 311, 499  
 Williams, Stanley N., 138  
 Wilson, Ian, **67, 70**  
 Wilson, Lyudmyla, **509**  
 Wilson, M. Jeff, 103, 509  
 Wissocq, Aubéry, 154  
 Wittebroodt, Charles, 190  
 Włodarczyk, Anna, 137  
 Woche, S.K., 421  
 Wójtowicz, Artur, 428  
 Wolański, Krzysztof, 428  
 Wolf, Monika, 124  
 Wriessnig, Karin, **348, 390**  
 Wright, Iulia, 116

### X

Xie, Xiangli, 301  
 Xinou, Katerina, 34  
 Xu, Tianyuan, 158

### Y

Yakovenchuk, Victor N., 423  
 Yamada, Hirohisa, 39, 222  
 Yamamoto, Ken-ichiro, 146  
 Yanai, Junta, 201  
 Yang, Jae-Hun, 49  
 Yang, Jing, 72  
 Yang, Kiho, **206**  
 Yang, Kiho, **48**  
 Yazaydin, A. Ozgur, 53  
 Yebra, A., 431  
 Yebra-Rodriguez, A., **431, 432**  
 Yepes, Jorge, 358  
 Yılmaz, İsmail Ömer, 315, 394  
 Yingjie, Li, 82  
 Yokoyama, Shingo, 392  
 Yoksoulian, Lois E., 192  
 Yoneda, T., **274**

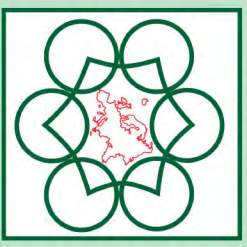
Yoon Choi, J., **49**  
 Yoshikazu Kameshima, **329**  
 Yoshimura, Shohei, **207**  
 Yotsuji, Kenji, 188, 189, 195  
 Yotte, Sylvie, 297  
 Yu, Wenbin, 234  
 Yuan, Peng, **216, 234, 430**  
 Yuan, Weiwei, 234  
 Yuste, Alfonso, 366

### Z

Zacher, T., 336  
 Zakusin, S., 321  
 Zeelmaekers, Edwin, 166  
 Zelepukina, Elena, 240  
 Zemelka, G., 369  
 Zhang, Dan, 422  
 Zhang, Jie, 301  
 Zhang, Yanwei, 42  
 Zhao, Yulong, 42  
 Zhitova, Elena S., **423**  
 Zhou, Changren, 72  
 Zhou, Xiang, **430**  
 Zhu, Ruanliang, **158**  
 Zich, D. 336  
 Zimowska, Małgorzata, 335, **424**



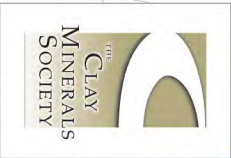
# Euroclay Quadrennial Meetings



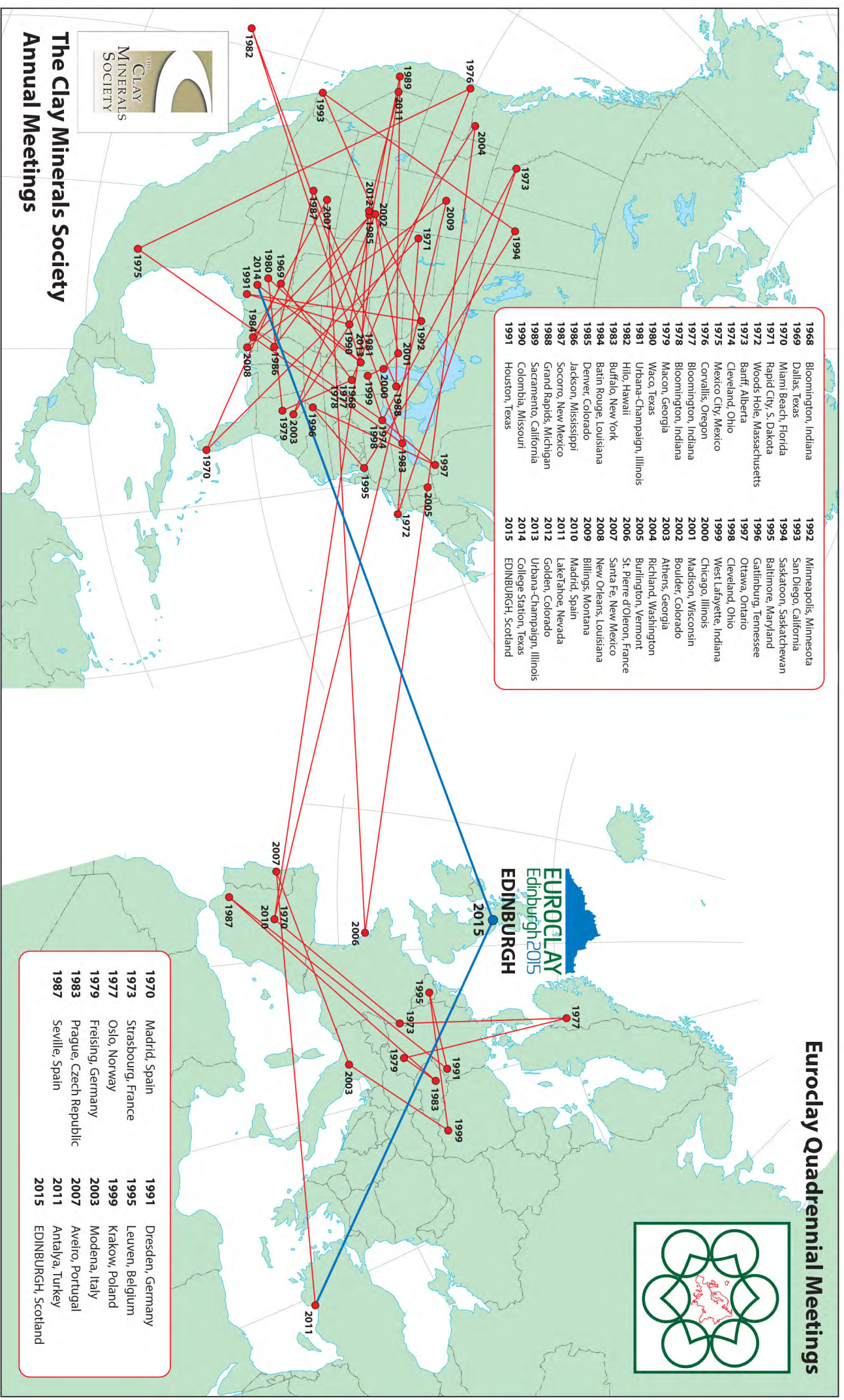
**EUROCLAY**  
Edinburgh 2015  
**EDINBURGH**

- |      |                        |      |                     |
|------|------------------------|------|---------------------|
| 1970 | Madrid, Spain          | 1991 | Dresden, Germany    |
| 1973 | Strasbourg, France     | 1995 | Leuven, Belgium     |
| 1977 | Oslo, Norway           | 1999 | Krakow, Poland      |
| 1979 | Freising, Germany      | 2003 | Modena, Italy       |
| 1983 | Prague, Czech Republic | 2007 | Aveiro, Portugal    |
| 1987 | Seville, Spain         | 2011 | Antalya, Turkey     |
|      |                        | 2015 | EDINBURGH, Scotland |

# The Clay Minerals Society Annual Meetings



- |      |                            |      |                             |
|------|----------------------------|------|-----------------------------|
| 1968 | Bloomington, Indiana       | 1992 | Minneapolis, Minnesota      |
| 1969 | Dallas, Texas              | 1993 | San Diego, California       |
| 1970 | Miami Beach, Florida       | 1994 | Saskatoon, Saskatchewan     |
| 1971 | Rapid City, S. Dakota      | 1995 | Baltimore, Maryland         |
| 1972 | Woods Hole, Massachusetts  | 1996 | Gatlinburg, Tennessee       |
| 1973 | Banff, Alberta             | 1997 | Ottawa, Ontario             |
| 1974 | Cleveland, Ohio            | 1998 | Cleveland, Ohio             |
| 1975 | Mexico City, Mexico        | 1999 | West Lafayette, Indiana     |
| 1976 | Corvallis, Oregon          | 2000 | Chicago, Illinois           |
| 1977 | Bloomington, Indiana       | 2001 | Madison, Wisconsin          |
| 1978 | Bloomington, Indiana       | 2002 | Boulder, Colorado           |
| 1979 | Waco, Georgia              | 2003 | Athens, Georgia             |
| 1980 | Waco, Texas                | 2004 | Richland, Washington        |
| 1981 | Urbana-Champaign, Illinois | 2005 | Burlington, Vermont         |
| 1982 | Hilo, Hawaii               | 2006 | St. Pierre d'Oleron, France |
| 1983 | Buffalo, New York          | 2007 | Santa Fe, New Mexico        |
| 1984 | Batn Rouge, Louisiana      | 2008 | New Orleans, Louisiana      |
| 1985 | Denver, Colorado           | 2009 | Billings, Montana           |
| 1986 | Jackson, Mississippi       | 2010 | Madrid, Spain               |
| 1987 | Socorro, New Mexico        | 2011 | Lake Tahoe, Nevada          |
| 1988 | Grand Rapids, Michigan     | 2012 | Golden, Colorado            |
| 1989 | Sacramento, California     | 2013 | Urbana-Champaign, Illinois  |
| 1990 | Colombia, Missouri         | 2014 | College Station, Texas      |
| 1991 | Houston, Texas             | 2015 | EDINBURGH, Scotland         |





53RD ANNUAL MEETING OF THE CLAY MINERALS SOCIETY  
Atlanta | June 5-8, 2016

**Place: Georgia Tech Conference Center and Hotel**

**Short Course: Industrial Applications of Clay Minerals**

**Field Trip: Georgia Kaolins**

**Tentative Technical Sessions (Poster and Oral):**

**Origin of Kaolins, Beneficiation, and Uses of Kaolins and other Industrial Clays  
(a session in Honor of Prof. Haydn Murray)**

**Contaminant sorption by clays**

**Nano-clay mineralogy techniques, Simulations, and Modelling**

**Critical Zone Clay minerals**

**Engineering Applications of Clay Minerals**

**Impact of clays on pore development and hydraulic fracturing of tight shales**

**Clay Minerals and Health**

**Intercalation and Nanocomposites**

**Extraterrestrial Clays**

**General Session Structure and Properties on Clays**

**Comments and Suggestions: Please contact Organizing Committee.**

Organizing Committee:

W. Crawford Elliott (co-Chair), Georgia State University  
(wcelliot@gsu.edu) Prakash Malla (co-Chair), Thiele Kaolin Company  
(Prakash.malla@thielekaolin.com) Robert J. Pruett (Program Committee),  
IMERYS Corporation (bob.pruett@imerys.com)  
Paul A. Schroeder (Field Trips), University of Georgia (schroe@uga.edu)  
Yuanzhi Tang (Program Committee), Georgia Institute of Technology  
(yuanzhi.tang@eas.gatech.edu)